Proceedings of the first *fib* Congress 2002

fib 2002
Osaka Congress

fib
CEB-FIP

Concrete Structures in the 21st Century

Volume 1

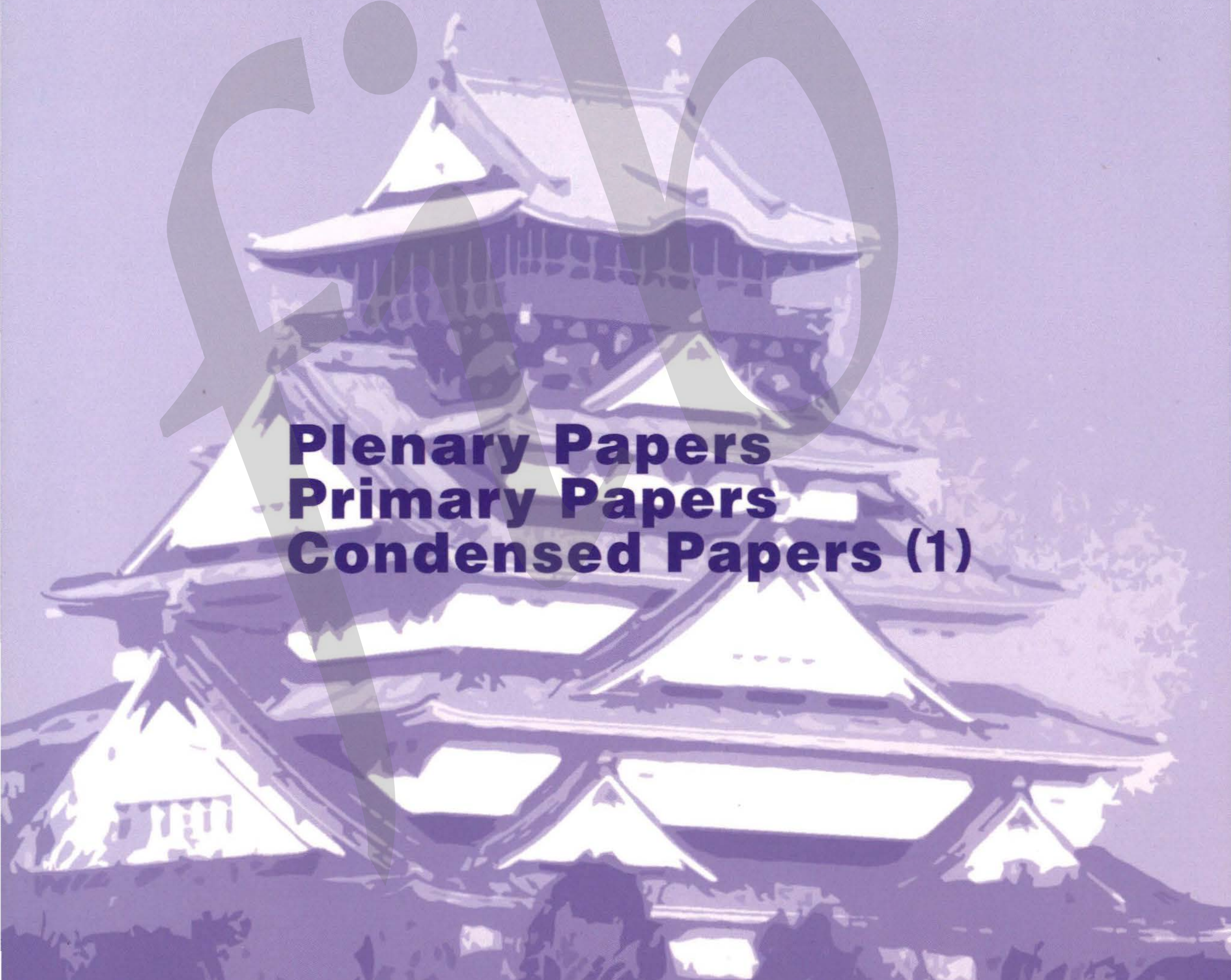

Plenary Papers
Primary Papers
Condensed Papers (1)

Organized by
Japan Prestressed Concrete Engineering Association
Japan Concrete Institute

Corrections

<Vol.1>

Table of Contents

Session1 P.1 Title:Advanced Structure For → Of

Session2 P.7 Title:Sant nigawa Bridge → Sntanigawa Bridge(CD-ROM)

Session6 P.99 Title:Building Structure of Chernobyl NPP Shelter Object→ Building Structures of Chornobyl NPP Shelter Object

<Vol.2>

Session7 P.109 Title: Ductal R → Ductal® (CD-ROM)

Session8 P.89 Name:Hiroshi Yokoyama/Shigeharu Takano/Hideaki Sakai

→Hiroshi Yokoyama/Shigeharu Takano/Hideaki Sakai/Ryutaro Furukawa/Yujiro Wasa

Session9 P.55 Name:Maya Sule → M.Sule

Session13 P.33 Title:C0 → C°

<Author Index>

Abe, T → Abe,Tadashi

Ayabe,Kenzi → Ayabe,Kenji

Breugel,Klaas van → Breugel,K van

Fischer, Gregorr → Fischer, Gregor

Furuichi,Kosuke Furuichi → Furuichi,Kosuke(CD-ROM)

Gardner,M,J → Gardner,N,J(CD-ROM)

Hikone,Shiger → Hikone,Shigeru(CD-ROM)

Hiroyuki Ikeda,Hiroyuki → Ikeda,Hiroyuki(CD-ROM)

Ikeda,Kenji Ikeda → Ikeda,Kenji

Katumi Kondo,Katumi → Kondo,K(CD-ROM)

Kitagima,Yasumi → Kitajima,Yasumi

Komuro,Mitsumaru → Komuro,Mitsuharu(CD-ROM)

Rokugo,Keitesu → Rokugo,Keitetsu

Kouichirou → Shito,K(CD-ROM)

,Matthew Stanton → Hoehler, Matthew(CD-ROM)

Shindoh,Takahumi → Shindoh,Takefumi

Shindoh,Takehumi → Shindoh,Takefumi(CD-ROM)

Tanabe,Tadaaki → T.Tanabe

Tsuka,T → Tsuka,Toshihiko

g,Jiandong → Zang,Jiandong

Session 9

P.19→P.17, P.43→P.47, P.45→P.49, P.67→P.69, P.47→51P, P.49→P.53, P.51→P.55, P.53→P.57,P.61→P.19, P.63→P.65, P.65→P.67, P.67→P.69, P.69→P.71, P.71→P.73, P.73→P.75, P.75→P.77,P.77→P.79, P.79→P.81, P.81→P.83, P.83→P.85, P.85→P.61

Corrections

CD-ROM
Table of Contents
<Plenary>

Title:5000 Years of Architecture and the Civilization of 21 st Century →Architecture of Five Thousand Years and The 21st Century

<Primary>

Title:The Capacity Design and Assessment of Reinforced Concrete Structures for Earthquqkes

→ Capacity Design and Assessment of Reinforced Concrete Structures for Earthquake Resistance

Title:Expressions of the Concrete Construction of the Past, the Present, and the Future →Past Present, and Future of Concrete

<Session 1>

Title:The Kiso-gawa Riger ~ → The Kiso-gawa River ~

<Session 3>

Title:Sotto Mayor Palace? Design ~ → Sotto Mayor Palace-Design ~

<Session 4>

The Seismic Reinforcement By Using Precast Panels to Piers Water

Name:Tomonori Kato → Kenji Noda(Author Index)

<Session 6>

Name:Fastenings to Concrete for Use in Seismically Active Regions

Name:Matthew Stanton Hoehler → Matthew Hoehler

Name:Susumu Kono/Bechtoula Hakim/Fumio Watanabe →Susumu Kono/Yusaku Arai/Bechtoula Hakim/Fumio Watanabe

Title:Seismicity in Ukraine and Seismic Resistance Evalution of Building Constructions of the "Shelter"Object Chernobyl NPP

→ Seismicity in Ukraine and Evalution of Seismic Resistance of Building Structures of Chornobyl NPP Shelter Object

Name:Ryoji Kinoshita/Yasuhiro Ohtani/Kazuaki Miyagawa/Kazuyoshi Fujisawa/Katsuhiko Imai/

→ Ryoji Kinoshita/Kazuaki Miyagawa/ManabuHaginoya/Kazuyoshi Fujisawa/Katsuhiko Imai/Yasuhiro Ohtani/Isao Mitani

Title:Construction of Seismic Retrofit of University ~ →Construction of Seismic Retrofit of Old University ~

Title:Performance of Statically Indeterminate Force in the Ultimate State → Performance of Statically Indeterminate Forces Under the Ultimate State

Name:Shin Yanaka → Makoto Yanaka(Author Index)

Name:M.J.Gardner →N.J.Gardner

<Session 7>

Title:~Mixture Proporting~ → ~Mixture Proportioning~

Name:Yoshihiro Tana →Yoshihiro Tanaka

Title:Devepomment of Ultra Fat PC Stand → Development of Ultra Fat PC Strand

Name:Andrei Zvezdov/Yuri Volkov →A.I.Zvezdov Y.S.Volkov

<Session 8>

Title:Countermeasures for Chloride-Induced~ → Countermeasures against Chloride-Induced~

Name:Ziduan Shang/Zhenbao Li/Wenying Li → Ziduan Shang/Yoshiteru Ohno/Zhenbao Li/Wenying Li

< on 10>

Proposed Requirements of Molten Slag Aggregates Produced from Minicipal → Municipal

<Session 11>

Title:New Plastic Design Model of Hyperstatic ~ →Indeterminate

Name:Naohiro Nakamura/Yasumi Kitajima/Makoto Fuji/Masahiro Sugata/Atsushi Kambayashi/Naoto Yabushita

→ Naohiro Nakamura/Yasumi Kitajima/Masashi Goto/Masahiro Sugata/Atsushi Kambayashi/Naoto Yabushita

<Session 12>

Inquiry and Analysis Regardning the Technical Lebel → Level

<Session 13>

Analysis of Slab-column Connections Using°C → C°

Pretest and Posttest Analysis → Analyses

<Session 14>

Aesthetics of Concrete → Comfortable and Beauty in Small Architecture

<Session 15>

Name:Sunaryo Sumitoro →Sunaryo Sumitro

Title:Evaluation of Grouting Condition in Tendon Ducts of Prestressed Concrete Members by Impact →IMPCT

Title:Inspection Based Health Monitoring of Prestressed Concrete Bridge in Michigan

→Inspection Based Health Monitoring of Prestressed Concrete Bridge

Name:Peter Schissl →Peter Schießl

<Author Index>

El-Salakawy,Ehab	Please look at Disc B Table of Contents Session 7
El-Wafa,Mahmound Abo	Please look at Disc B Table of Contents Session 7
Enomoto,Tsuyoshi	Please look at Disc B Table of Contents Session 7
Esaki,Mamoru	Please look at Disc B Table of Contents Session 7
Kadotani,Tsutomu Disc A→	Please look at Disc A Plenary

Antonios,Panagiotakos →Antonis J. Kosmopulos

Fujii,Makoto →Goto,Masashi,

Konig Gert →Koenig Gert

Mizug,Yoshiharu →Mizugami,Yoshiharu

Nakano,Masahumi →Nakano,Masafumi

Nemchynov,Yuriy Ivanovich →Nemchynov Yu.I

Nickas,William N → Nickas,William

Ogata,Jyunji →Ogata,Junji

O'Regan,Bill →Oregan,Bill

Takao Takashima,Takao →Takashima,Takao

Telemachos,Fardis → Telemachos B.Panagiotakos

N.,Michael → Fardis,Michael N.

Proceedings of the first *fib* Congress 2002

fib 2002 Osaka Congress

Concrete Structures in the 21st Century

Volume 1

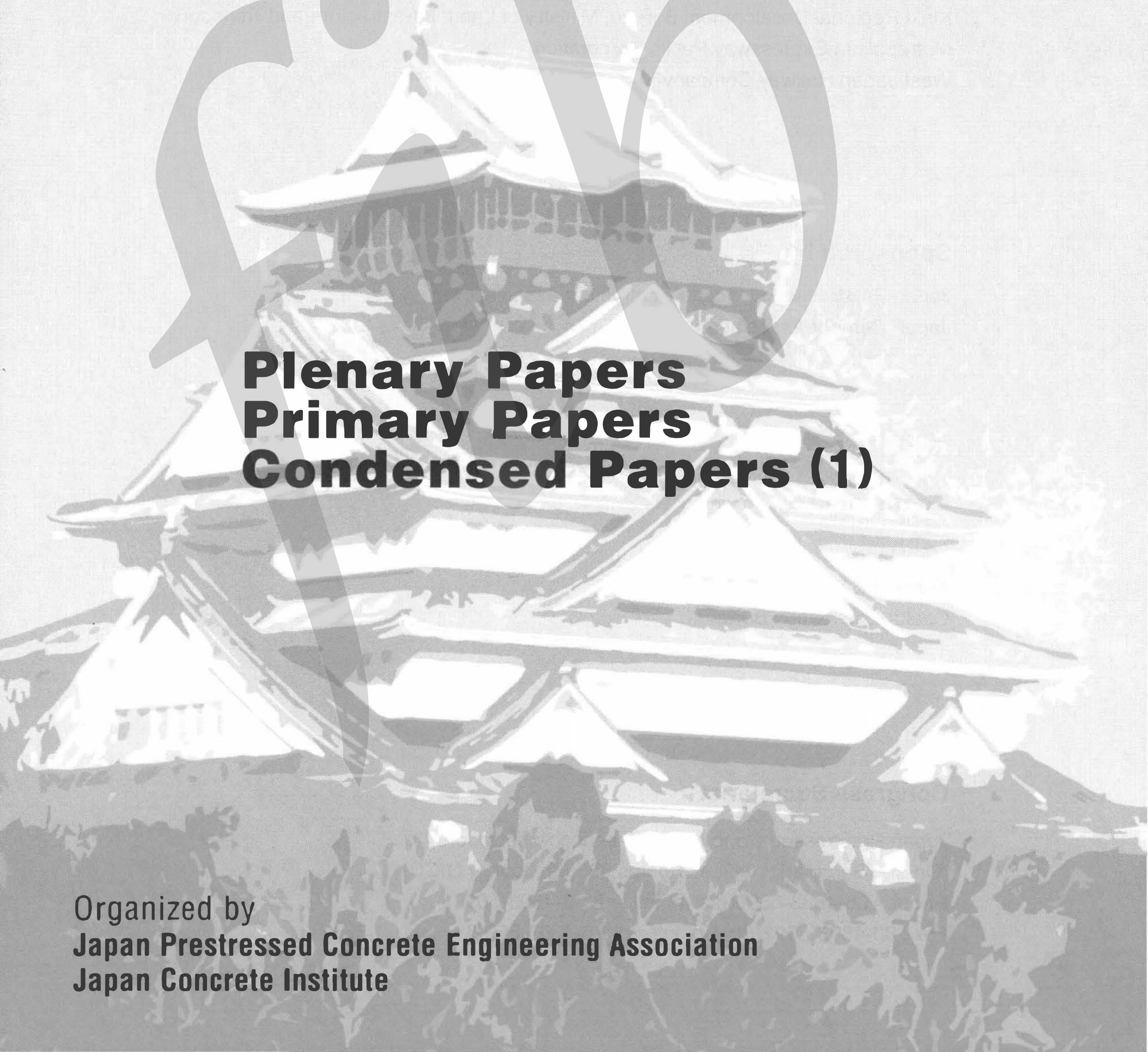

Plenary Papers
Primary Papers
Condensed Papers (1)

Organized by
Japan Prestressed Concrete Engineering Association
Japan Concrete Institute

Officially Supported by

Ministry of land, Infrastructure and Transport, Japan
Osaka Prefectural Government
Osaka City

Supported by

Hanshin Expressway Public Corporation
Honshu-Shikoku Bridge Authority
Japan Highway Public Corporation
The Kansai Electric Power Co., Inc
Kinki Regional Development Bureau, Ministry of Land, Infrastructure and Transport
Metropolitan Expressway Public Corporation
West Japan Railway Company

Sponsored by

Japan Prestressed Concrete Contractors Association
Japan Cement Association

Contributed by

The Maeda Engineering Foundation
March 8 Symposium
Osaka Convention Bureau

Congress Secretariat

Japan Prestressed Concrete Engineering Association
On-site Secretariat Office : Rooms 805(8th floor of OICC)
Phone : 06-4803-5590(dial in, Intl : +81-6-4803-5590)
Fax : 06-4803-5592((dial in, Intl : +81-6-4803-5592)

Table of Contents

Plenary 82 pp

Primary 64 pp ~~8~~

Session 1 120 pp 57 papers in 2p-abstracts

Session 2 156 pp 75 ~~pp~~ abstr.

Session 3 36 pp 17 abstr.

Session 4 26 pp 12 abstr.

Session 5 134 pp 64 abstr.

Session 6 194 pp 93 abstr.

Σ = 318 two page abstracts

ARCHITECTURE OF FIVE THOUSAND YEARS AND THE 21ST CENTURY

Juko Ito
Assoc. Prof., Graduate School of Science and Technology,
Kumamoto University, Japan

Keywords: architecture, monument, history,

1. INTRODUCTION

Human beings created many great masterpieces of architecture in the history of thousands of years. The men were not satisfied even at the primitive stage of the history with the buildings for only practical purposes. They started to build monuments like tombs to keep dead people in memory and temples to house their cult images. The word 'monument' is derived of an ancient Greek word 'mnemeia' which means memory. Thus, the great architectural works should be strong enough to last many centuries to keep the persons, historical events, etc. in memory.

Passion for power, religious dream, symbol of political system, etc., whatever they are, these motivated to create architectural splendor and inspired architects' imaginations. In this short article, the author reviews briefly the history of great monuments and discusses the problems of modern architecture and the prospect of architecture in the future. He concentrates on some epoch making masterpieces in Europe and west Asia, comparing them with some Japanese monuments.

2. ARCHITECTURE AS 'MASS' IN ANCIENT EGYPT AND MESOPOTAMIA

The ancient civilizations were born in the areas on the big rivers of the Eurasian continent together with the development of agriculture. Developed agricultural production and stock of provisions created great powers to rule the people and agricultural production system. This so-called agricultural revolution made it possible for human beings to bring much extraordinary wealth and to create magnificent architecture. The great architecture of this period expressed radical desires of men to be great. To make a large solid mass was the simplest and strongest way to express this desire at the early stage of the civilizations. It was as if a child makes a sandpile on beach. It expressed simplest and strongest will and power of rulers. Their forms must have been simple and stable.

The pyramids were the best examples of this kind of architecture. The three great pyramids at Gizah were built between 2545 and 2450 B.C. during the time of the third Dynasty. Among the three, the First Pyramid, which was dedicated to Khoufou, was the largest. Its four sides are 230.364 m in average, the present height 137.18 m, and the slope 51° 52'. The simple form of the pyramids required the strict accuracy of the dimensions, because small dimensional errors at initial stage cause indispensable results in the construction of the later stages. The First Pyramid is extraordinary in its accuracy of measurements. The errors of the side dimensions are 111 mm at maximum and 7 mm at minimum to the average length

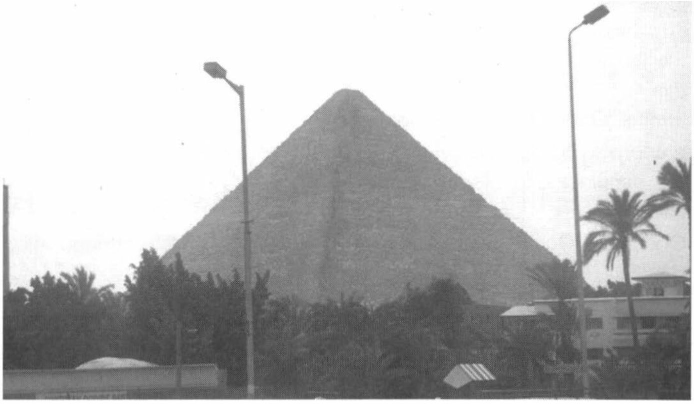

Fig. 1 The Great Pyramid at Gizah, 2545 and 2450 B.C.

of the sides. This error is less than 1 to 2000. The difference of level on its four sides is 0.021 m at maximum. The First Pyramid was oriented precisely to the cardinal direction and the average error of angulation is only 0° 3' 6". It is so gigantic that occupies 53,000 m² in plan, and the volume is 2,500,000 m³. The size of the blocks is approximately 1 m³, thus the approximate number of blocks are 2,500,000. If, as Herodotos, a Greek historian, wrote in his book, it took 20 years to be completed, 342 blocks must have been quarried everyday, then carried to the site, shaped up, pulled up and placed at their right positions, and finished with the surfaces. All of these construction processes must have been continued everyday without intermission until it reached to its top. All these works were certainly done by man power. Even for modern engineers, this big project would be a work of great wonder.

The ziggurats in Mesopotamia were of another type of architecture of mass in antiquity. Although built, not of stone but of bricks, they are comparable to the pyramids as mass architecture. They were less durable compared with pyramids due to their materials. Indeed, most of the ziggurats are not preserved very well. The origin of ziggurat is not very certain, but the temple platform from the 27th century B.C. which was excavated at Khafajah, 25 x 30 m in plan and 2.7 m high, is thought to be an origin of the ziggurats. The tradition of ziggurat architecture had lasted more than two thousand years in Mesopotamia, in contrast to the pyramids which had lasted only several centuries. The best preserved example is that of Ur. The present architectural remains of the ziggurat are from the 21st century B.C., although the original temple underneath is thought to date back to the 30th century. The ziggurat at Ur consists of four terraces. The first terrace is 62.5 x 43.0 m in plan and 11.0 m high, and the second 38.2 x 26.4 m and 5.7 m. The third and fourth terraces have not been preserved.

The ziggurats had become much larger as the time passed. The ziggurat at Babylon, which was reconstructed by Nebukadnezar in the 6th century B.C., is thought as a model of the famous Tower of Babel. Although almost no trace of the ziggurat remains now, we can conjecture its size and form according to the ancient records as that it had a plan of 90 x 90 m and was 90 m high, forming seven terraces. The top terrace was the temple itself of 24 x 21 m and 15 m high.

Historically, the pyramids were built in the 3rd millennium B.C., and the ziggurats lasted to be built from the 3rd to 1st millennium B.C. The pyramids and ziggurats are of simple solid masses and almost no void space was built inside. This kind of mass architecture in the ancient civilizations shows pure architectural powers in their simplest and strongest forms. Mass is the radical expression of human power and it was realized as architectural forms at the initial stage of our history. In the Far East, huge tumuli for emperors were constructed, although they were not very dominating as pyramids and ziggurats. For example, the Great Tumulus of the emperor Nintoku in Japan is the world largest earthen mound in plan. It has a keyhole plan with their front round and the back rectangular. Also, in China this kind of huge hill-like imperial tumuli was constructed for ancient emperors. To be massive and large is the simplest expression of powers at the early historical stage in both the Orient and Occident.

Fig. 2 The ziggurat at Ur, the 21st century B.C.

3. ORDERS IN CLASSICAL ANTIQUITY

After the centuries of simple mass architecture as pyramids and ziggurats in West Asia, another type of more sophisticated architecture had prevailed at the end of the Mediterranean antiquity. The building and design techniques developed much more, and the basic principles of architecture were proposed. It was the Greeks who created the new principles for their temples, although they were influenced by Egyptians at the beginning. The new principles of architecture are called Orders, i.e., Doric, Ionic and Corinthian, which are series of architectural compositions of members and ornaments. Then the Romans followed them and applied the principles even for civic architecture. With the expansion of the Hellenistic kingdoms and Roman Empire, the principles spread all around the Mediterranean area. Thus, the three Orders became the origin of the western architecture.

Among many Greek temples, the Parthenon must be the greatest. The construction of the Parthenon started in 490 B.C. after the First Persian War to honor their victory against Persians at Marathon. But the first Parthenon was destroyed by the Persians at the time of the 2nd Persian War. The building of the new Parthenon started in 447 B.C. after more than 30 years, when there was no menace of Persia. It was Pericles, a great Athenian statesman for democracy, who organized the construction of the new Parthenon and the Acropolis. The director of the construction was Phidias, a great sculptor and a friend of Pericles.

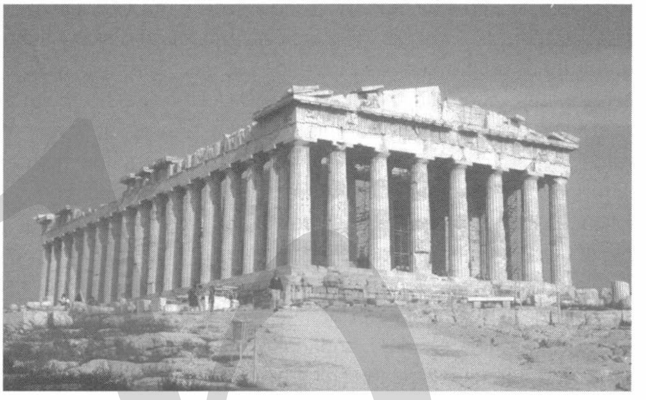

Fig. 3 The Parthenon at Athens, 447 – 432 B.C.

The temple was in Doric style which, after the development of a few centuries, reached its apogee in the Parthenon. The stylobate or the platform of the temple is 30.88 m wide and 69.50 m long with 8 columns on the ends and 17 on the sides. The column diameter is 1.90 m and the height 10.43 m. All the blocks are of shining Pentelic marble. With its detailed ornaments painted red, blue and gold, it looked quite differently compared with the present one. The shining beauty was observed on the Acropolis, and the splendor of the temple must have been incomparable. Another big feature is subtle curvature which is used in every part of the temple. For example, the temple platform is curved upward about 10 cm in the middles of sides and ends. This curvature continues to the beams and even to the eaves. The columns do not stand vertically but incline 6 cm inward at the top. Thus, the bottom drums are not uniform. The exterior lines of the columns are not straight but curve outward slightly, which we call 'enthasis'. The building work is extremely elaborate and shows full conscience of the architects. It must have been the final goal of architectural aesthetics which the Greeks achieved. Phidias made a 12 m-high statue of Athena of gold and ivory. It was extraordinarily expensive and twice as costly as the building cost itself.

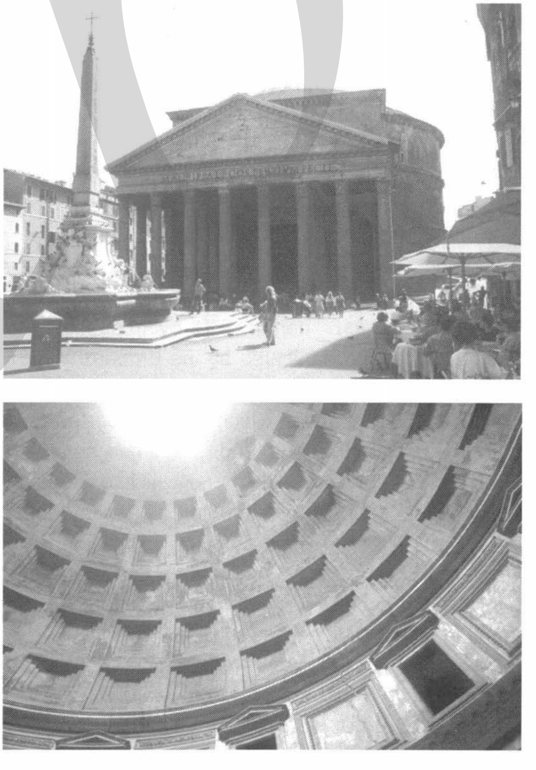

Fig. 4, 5 The Pantheon at Rome, 118 – 128 A.D., The Exterior and Interior.

In contrast to the Parthenon, the Pantheon was built with quite different concept. The present Pantheon was built around in 118 – 128 during the reign of the emperor Hadrian. It is told that the Pantheon was designed by the emperor himself. It has a Corinthian façade with 8 columns in front. Its granite columns are 14.14 m high and the diameter is 1.48 m. The most important part of the Pantheon is its interior space. It is a huge hemispherical dome supported by a cylindrical wall with a thickness of 6.05 m. The wall was separated into two courses with classical Corinthian order. The interior diameter of the wall is 42.98 m which is identical to the height of the dome. In other words, the Pantheon contains a huge void sphere in its building. The concept of the Pantheon was to create this huge void, but not to reproduce the Greek Order. Certainly, the Romans respected the Greeks as great creators of architectural principles and learned many things from them. But, the Romans did not repeat them as they learned from the Greeks. The huge void interior space was the very creation of the Romans, although they used the Order of Greek architecture. Walls and columns were only to create this interior space and this was the Romans' discovery. When we stand in this huge dome and watch the sunny circle which sun beam casts on the floor and wall, we realize the presence of astronomical space and the movement of the globe. Everybody must be moved by the grandeur of the hollow space which expressed the Roman world at the moment when he enters into the dome. The role of the Pantheon in the architectural history was to let us realize the presence of the interior space.

The Parthenon and Pantheon, two great masterpieces of architecture in classical antiquity, showed the new foresight of architecture in the history of architecture. The theme of the Parthenon was how its exterior looked, and that of the Pantheon how its interior did. Thus, these two continued to inspire later architects as the spiritual and practical origin of the Western architecture.

In Japan, the architecture of the second historical stage appears as Buddhist temples. The temple comparable to the Parthenon must be the Horyuji Temple which was built of wood in the 6th century A.D. in Nara. It consists of the central gate, five storied pagoda, prayer hall, and lecture hall, being encircled by the colonnades. The style and layout were transmitted from China, but its layout was transformed as asymmetrical in Japanese way. The temple is certainly quite different from the Greek temple, but shares common senses for formal balance and asymmetrical layout in the sanctuary.

4. AGES OF INTERIOR SPACE

With the rise of Christianity after the fall of the Roman Empire, the interior space became more important as the place of prayer. The architectural energy of Christians emerged as the form of great cathedrals. The first great monument was the Saint Sophia in Istanbul, built in the 6th century A.D. by architects Isidoros and Anthemios and dedicated by the Emperor Justinian. The interior volume exceeded that of the Pantheon with a central pendentive dome which was supported by two half domes at both ends and the other smaller half domes. There was no such dome which exceeded the Saint Sophia in space volume for next one thousand years. The top of the main dome is 55 m high and the diameter is 31 m. Its new spatial form and the structural technique was a creation at the end of antiquity or at the beginning of the Middle Ages.

Christianity spread all over Europe in the Middle Ages and it took several hundred years for Europe to create its own architecture; that is Gothic cathedrals. The Gothic architects or masons created new interior space which was suitable for the place of prayer. It originated in basilica of the Roman architecture. They developed the

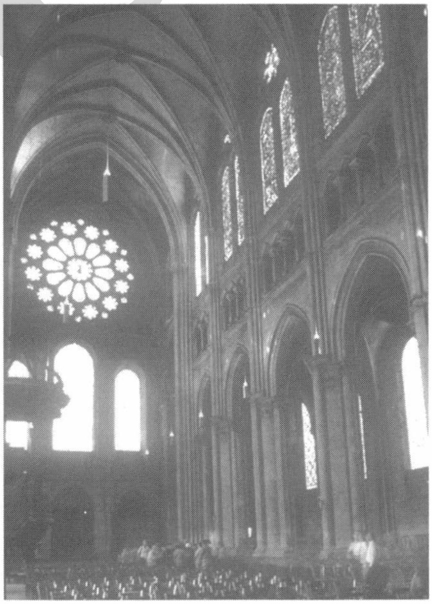

Fig. 6 The Cathedral at Chaltres, the 13th century.

basilica style church by roofing with cross-vault, ribs set along its edge to support the load of the roofs efficiently, and flying buttresses which support its thrust from outside.

The style became very popular to admire the glory of the divine kingdom. The Gothic cathedrals started to be built at Paris, Laon, Amiens, Reims, Beauvais, etc. in France and continued to be built for a following few centuries in all over Europe. The architects competed for their architectural magnificence, especially, for their height as skyscrapers in New York. Thus, the roof attained to the remarkable height of 48 m at Beauvais. Here, I should mention the Cathedral at Chartres not only for its height but also for its magnificence due to its incomparable beauty of stained glasses. It was built in the 13th century. The interior space was roofed with cross-vault of stone as a typical Gothic cathedral. But the splendor of the interior is further emphasized with its stained glasses in the rose window with the diameter of 13 m and the high windows all around the nave. They tell biblical stories and cast its soft lights of blue, red, yellow on its floor.

It was the interior spaces that were most important as places of prayer for the cathedrals in the Middle Ages. The exterior was the only means to materialize the interior space. The interior space which was 'discovered' in the Pantheon by the Romans was succeeded to the Saint Sophia in Byzantine Empire and to the cathedrals in medieval Europe. The development of their richer interior space can be reasonably explained from functional viewpoint but it was also the consequential development in architectural history of thousands of years.

5. NEW CHALLENGE IN THE AGES OF HUMANISM

Among many architectural great works in the second half of the second millennium A.D before the age of modernism, the author mentions here the Dome of the Santa Maria del Fiore at Florence for its creativity and the Versailles Palace for its strong influence upon the later architecture. I also mention the Himeji Castle as a comparable Japanese architecture of this period.

Fig. 7 The Dome of Santa Maria del Fiore, Florence, 1430

The dome at Florence was designed in 1418 by Brunelleschi who won the competition and was dedicated in 1430 after ten years of construction. It was the first dome after centuries of intermission since the Saint Sophia at Istanbul. The diameter of the dome is 43 m which is equivalent to that of the Pantheon. The dome itself starts to rise at a height of 55 m on the cylindrical walls and crowns the lantern on its top, attaining to a height of 120 m. Its double dome was octagonal and supported by ribs as Gothic cross-vault. The bottom of the dome was reinforced by a 'tension-ring' to prevent a thrust caused by the dome. The ring consists of 60 wooden beams, 3 m long and 30 cm square in section, fastened with iron bands and bolts. Its huge and dominant dome is one of the greatest works in architectural history, and its structural challenge was an annunciation of a new will of the architect.

The Versailles Palace also shows a new challenge for grandeur of vista and geometrical layout of the palace and garden. Louis XIV started to renew his fathers' small villa and enlarged it quite extensively. The main part of the palace building is 425 m long. Together with the annexed buildings it attained to more than 900 m long and more than 10 thousands people were working. Especially, its garden occupies enormous area around the palace. All the buildings, paths, canals were laid geometrically around an axis as if everything was laid in one order. The Hall of Mirrors or the main hall, the king's bed room, and, most surprisingly, even his bed, were laid exactly on this axis. He slept everyday in the center of the world. It is quite evident that the Versailles Palace shows the dignity and power of the absolutism with its axial plan. That is why it influenced strongly as a prototype on the later European palaces in 17th and 18th centuries.

The use of tension-ring in the dome at Florence shows a pioneering thinking that suggests an idea of reinforced concrete of modern architecture. Also, the axial and geometrical plan of the Versailles Palace shows the perspective view for which the Renaissance and later architects developed drawing method. At any rate, these two architectural works show humanism based on rationalism which formed the basic thinking in the western world.

As Japanese architecture comparable to these, I mention the Himeji Castle near Osaka. It was built in the 17th century as a castle of a local lord and was a symbol of feudalism. Its dominant appearance seems to share its architectural idea and political meaning with the dome at Florence, although their forms are quite different. The Japanese garden of the Imperial Villa Katsura in Kyoto is an antipole of the Versailles Palace for its asymmetrical and freehand plan. The difference of two gardens is very conspicuous, and interesting from the viewpoint of comparative studies.

6. SUMMING UP: MODERN ARCHITECTURE AND ITS FUTURE

From the late 19th century on, there was a drastic change in architecture with the development of modern civilization. Architecture with Greek order was not built any more. Citizens replaced the kings and aristocrats as new clients. The great architects like Le Corbusier, Mies van der Rohe, Frank Lloyd Wright, etc proposed new principles as 'modernism' and created the innovative works. The principle of the modernism is based on the rationalism and humanism which derives of the ancient Greek philosophy. Thus, the role of modern architecture was to provide everyone with buildings of good function and convenience at reasonable price. The citizens became incomparably richer and they enjoy greatly their lives also in architecture.

The form of architecture is going to be much freer in the future. With the rapid development of information technology, all the building processes from the design to construction is going to be controlled by a unified system of computers. This technology will make it possible to create new form of architecture in the future. Indeed, the trial has already begun as we see in the Guggenheim Museum, Bilbao, Spain, which was designed by Frank Gehry in 1997. Its extraordinarily free form in plan and elevation, and in exterior and interior, seems to predict the prospect of architecture in the future. This tendency of architecture will be accelerated and the freeness will liberate the human spirits. However, at the same time, we will also lose the human skills for architecture.

Reviewing briefly the history of architectural monuments in this short article, we wonder which monument will survive in the new millennium. Most of the historic monuments described above will probably be able to survive. At least, the Pyramids at Gizah will definitely do. For the architecture of modernism in the 20th century, there is no hope that they will survive until 3000 even apart from the demolition by wars, terrorisms or natural disasters. Reinforced concrete will destroy itself by rusting its steel bars. Thus, we can expect nothing about the durability of modern architecture for many centuries As far as we continue to build in the same way, there will be no remain of modern architecture in the 30th century and they would say that the 20th century was a dark age without any civilization. Here, we should reconsider what we should create and transmit to our descendants.

REFERENCES SELECTED

1. I. E. S. Edwards: The Pyramids of Egypt, London, 1961
2. Sir L. Wooly: Ur Excavations, Vol. V, Ziggurat and Surroundings, 1939
3. A. K. Orlandos: The Architecture of the Parthenon, Athens, 1949 (in Greek)
4. K. de Fine Licht: The Rotunda in Rome, Copenhagen, 1969
5. G. Henderson: Chartres, R. Merlet: La Cathédrale de Chartres, Paris, 1960
6. H. Zaalman: Filippo Brunelleschi; The Cupola of Santa Maria del Fiore, London, 1980

DESIGN AND DESIGNERS

by Michel VIRLOGEUX

fib Honorary President

Summary: Engineers have lost a great part of their influence on large projects, and even bridge design – the essence of structural engineering – is more and more attributed to architects. In this situation it is important to remind what is the real field of structural engineering, and to show that progress and architectural achievements in this field are due to great engineers who also were frequently great characters.

1. INTRODUCTION

1.1. In the last ten or fifteen years the design of more and more bridges has been given to architects with very diverse results. In most cases – specially after a design competition limited to architects – the bridge concept has been developed without any consideration for structural aspects; even the balance of loads and the flow of forces have been ignored, not speaking of erection techniques.

This resulted in major construction problems, with high costs for owners and contractors who had to suffer enormous losses. When more delicate problems, occured, involving dynamics or aerodynamic stability, it could even result in a serious misbehaviour. Everybody knows that two pedestrian bridges, one in Paris and one in London, had to suffer from some Parkinson decease due to a very low rigidity (at least in some direction) which favoured vibrations induced by what Jörg Schlaich calls the sailor's walk; a third one – in Paris again, but still a paper work – might suffer even more severe dynamic effects.

Some of these architects are really gifted sculptors and produce nice shapes despite the structural non-sense of the concept and the high cost. They are the more dangerous for structural engineering as their shapes can be considered attractive and some might think them worth the corresponding cost; we have to fight them to promote structural logics, structural ethics, and also to prove that elegance and beauty can be produced at reasonable and sometimes low cost.

But the majority of architects are not so gifted, and this policy produced ridiculous structures,. pretentious bridges and sometimes very ugly ones.

Even more, a design created by an engineer is frequently attributed to the architect who had been associated to the project – and who in some cases improved it significantly –, a situation which is unacceptable from a simple ethical point of view. It happens to me more and more frequently: I am not always cited as the designer of the Normandie Bridge, even in specialized books, and practically nowhere I am recognized as the designer of the Millau Viaduct to take only these two examples.

1.2. The reason of this incredible situation is partly due to the evolution of our society, which is sensible to mediatic impact more than to real facts. Words and show-off have more influence than real work and competence. But engineers also have a great responsibility in it:

- too many of us are only interested in computations, in cost, and in construction details. Of course cost, construction aspects, analyses… have a great importance, but they have to come after the development of a good concept, structurally intelligent and efficient, elegant and well integrated in the landscape; a poor design produced by an engineer is not better than a poor design produced by an architect, even if the bad aspects are generally different.

- Owners – who frequently are engineers – consider more attractive to show an architect than a designer. This is a direct result of the greater influence of media and communication, but also of the fact that even the best of engineers are not known outside their circle.

- Engineers and engineering associations frequently work against their own interest, placing the architects in the front row, sometimes because they are jealous of their colleagues who are more famous or because they don't want to cite some engineers. Since many years – 20, 30 perhaps – the leitmotiv is that a design is developed by a team; clearly, a good team is needed to develop a good project; but any team has a team leader and we shall see that in design the major progress came from individuals more than from teams. This "team policy", strongly promoted by large companies – administrations, design offices and contractors –, prevented the best engineers to receive some recognition outside their circle and helped the pre-eminence of architects – in a domain where they are not qualified – when personalisation, the "star system", is of major importance.

- But also we must recognize that many engineers have a limited interest for culture and beauty; even if once a philosopher told me that the notion of beauty is highly questionable. If we look back to the 18th century, engineers learnt at school some architecture; at the Ecole des Ponts des Chaussées they had to produce a project of bridge decoration and even to present the map of an imaginary country. Architecture, imagination, arts in all aspects were their concern. All of them did not become great designers, far from it, but the best of them received an education much more favourable than now.

1.3. I should like adding some words about the "academic style"; more and more scientific and technical journals adopt this convention. To be very clear the reason for this evolution is the promotion system in universities : to develop a "neutral" promotion system, professors and researchers are mainly evaluated through their publications in journals with a scientific publication committee. This is progressively transforming journals from an information system into an academic promotion channel, with very severe drawbacks.

I have been said frequently by reviewers: take out all personal names and names of companies, and give references in a bibliography. No ! Life cannot be reduced to academic literature. Facts and truth are not limited to references; companies might develop ideas and techniques and deserve being cited; those who design structures are not always those who write papers; some who gave good ideas or took part in a design or in a research, and are not authors, deserve being cited for their participation... The academic presentation might lead to real spoliation when a paper describes ideas or structures which are not from the author but from somebody else who never published; and it happens rather frequently in the construction industry.

Some might also express their doubts on a theory or on some specific problem without being able to give scientific evidences or demonstrations.

But the most severe drawback is the loss in free expression, in direct and personal thoughts. We are human beings, each with some personality, and cannot be reduced to formal and rigid literature. This is in my opinion an important factor in the de-personalisation of our profession.

And the last word will be the strongest: the industry and the profession are not to serve universities and academicians, but universities and academicians are to serve the industry and the profession. The goal is not to publish, not even to teach nor to research: the goal is to build in the best way; teaching, researching is only a way – a good way – to improve construction, but not the goal.

2. FROM SCIENCES TO ARCHITECTURE

A designer has to master a very wide domain, from sciences to architecture, to be able to develop a really good design; of course with his team, including specialists, architects, landscape architects etc... He cannot be a specialist in each field, but he has to master all of them to really master the design; in opposition to the idea which exists in some countries that a design has to be developed by a commission. As frequently reminded by René Walther, a camel is a horse designed by a commission.

2.1. Sciences are more important than codes; codes are only practical and legal ways to base projects on construction sciences. But for very large projects – as well as for a good understanding of any construction – we have to go back to the sciences themselves.

- A good example is given with seismic designs. Due to the large development of softwares, very sophisticated analyses can be performed and they help designing structures which can resist to extreme earthquakes. Japanese bridges are a good illustration in the domain, as well as the Rion-Antirion Bridge with its deck totally suspended to four pylons installed on large offshore structures.

- Aerodynamic stability and resistance to turbulent winds is now very well mastered, and extremely efficient structures can be designed, like the Normandie and Tatara bridges.

- Cable-vibration is another domain, not yet as well mastered. Many phenomena can induce cable-vibrations: direct vortex shedding; wake effects from pylons or other cables; aerodynamic instability produced by ice deposits in Winter, by helical stranding in lock-coil cables, or by the action of rain flowing along the cable-stays; parametric excitation coming from the structure vibrations… In fact we are more able to prevent or eliminate undesired cable-vibrations than to predict them, or even sometimes to prove their precise origin.

Finally, we have to be conscious that we are asking more and more from designers: the development of computers and softwares have considerably simplified analyses as well as the production of drawings; but in the same time the demand is higher and higher. The public now considers that construction can and must be totally mastered, and does not accept accidents or even operation limitations. Under this pressure codes are more and more demanding and the volume of computations increases year after year… not always for higher quality and safety.

But it is clear that if projects are more and more ambitious – as shown by the fantastic progress in span length for each bridge type or in the size of structures –, this is due to a much better understanding of physical phenomena and to the development of computational capacities; in fact to the scientific progress.

2.2. Construction techniques

It is unserious to design a bridge without an analysis of its construction steps; the poet Paul Valery wrote that he cannot separate a structure from its erection, a sentence placed by Jacques Mathivat at the front of his book devoted to the balanced cantilever method, though its real meaning was not exactly the one desired[1].

If classical erection techniques are very well known – and sometimes have been used centuries ago in very similar conditions for other types of structures –, there is a permanent evolution, specially for the construction equipment. The most recent evolution came with the development of heavy prefabrication initiated by the Japanese steel industry and by Ballast Nedam for concrete structures. Large concrete bridge elements – up to about 7 000 metric tons – have been lifted, moved and installed by a specific ship, Swanen, for the Storebelt western bridge, the Confederation Bridge and the Oresund; the lighter Rambiz was used for the Vasco de Gama Bridge…

We can also evoke the increasing use of computation, information and automation techniques. Computers have been first used to analyse structures, but progressively computers entered fabrication shops, specially in the steel industry. We are not very far to day of computer-aided-fabrication: the designer prepares drawings, and the computer prepares the steel procurement, optimises the division of steel plates in elements, and drives practically all shop works, tracing, cutting, handling, welding…

Sites and constructions are levelled with the help of satellites, and geometry adjusted and controlled with the same type of equipment; datas are directly sent from sites to design offices, from

[1] Je ne sépare plus l'idée d'un temple de celle de son édification.

computer to computer… In a forty years time, construction has completely changed, from man power to a very advanced technology.

2.3. Materials

If main construction techniques have been developed long ago, the major progress is due to the evolution of materials.

Steel strength and quality have been increased gradually since the middle of the nineteenth century, from "mild" iron to high tensile steel. Thermomechanical steel with a yield stress of 460 MPa is now currently used, easing welding on site; steel plates of variable depth help limiting welds…

As regards concrete, the recent progress is even more surprising. If a strength of 50 to 60 MPa could be obtained in the fifties by some contractors – like Freyssinet –, the classical value was reduced to 35 or 40 MPa during the sixties and seventies. But with the development of high performance concrete – in the USA, in Norway, in Japan, in France … - a strength of 80 or 100 MPa is now almost classical. And some special concretes – ultra-high-strength concrete – can reach a strength of 150 or 200 MPa. But special concretes can also have other goals than strength: high compactness (for durability), high resistance to abrasion, low shrinkage… Concrete can now be specifically designed, as well as structures.

2.4. Technology

Technology keeps a great importance: bearings, joints, need a specific design when loads and length variations reach high values, not forgetting the conditions of a possible replacement.

But cable-stays give a very good example of the influence of technology on design. We cannot speak any more of cables, but of cable-systems ; with the cable itself, the anchorages, the protective envelope, the devices to limit wind effects – such as dampers –, and all provisions to provide a high protection against corrosion (and vandalism) and to allow for cable adjustment and replacement. Much has changed during the last twenty years, when we progressively passed from lock-coil cables to parallel wires, and now to parallel individually protected strands. Just some more work is needed for a greater elegance of anchorages and additional devices.

2.5. And finally architecture

Those who are recognized as great engineers attached a major importance to bridge architecture.

Once I gave a lecture on bridge architecture, Fritz Leonhardt – who was attending the conference – told me that I made a mistake. He told me that we have to speak of bridge aesthetics, not of architecture, since politicians and the public might think that we need to give the design to architects if we speak of bridge architecture. But for once I shall not follow him, and I prefer to refer to Luigi Nervi and his "structural architecture", and to David Billington and his "structural art".

Structural architecture is the architecture of structural engineers, who alone can create logical, efficient and elegant shapes, mastering all conceptual aspects, from sciences to construction, materials and technology; the most gifted of them can also produce an elegant architecture.

This is exactly the goal of this lecture, and in addition we shall show that developing new concepts and new structures elegantly also calls for a very strong character. Great engineers are very often great characters, since they have to fight for their ideas, and sometimes to resist to adversity when they happen – as everybody – to make an error or have to pass hard times.

3. GREAT ENGINEERS

I have selected some famous engineers, from the 18th century to the present time, to support these ideas and to show that the major progress in our domain and the most elegant constructions are due to individuals, to their creativity and character.

Louis Alexandre de Cessart (1719-1806)

I desired beginning with a French engineer of the 18th century directly connected with the Ecole des Ponts et Chaussées, founded in 1747 and considered as the first place where a rational education in civil engineering was given. I could have selected Jean Rodolphe Perronet, its first director who kept this position until his death in 1794. But I prefer Louis Alexandre de Cessart for his greater originality.

He began as soldier during the war in Flanders, and took part in the famous battle at Fontenoy. Due to his health he had to resign and he entered the Ecole des Ponts et Chaussées the year it was created, in 1747. Sent as engineer at Tours he built the Saumur bridge over the river Loire, using for the first time in France wooden caissons for the foundations; he developed a special saw to cut wooden piles below water, after they have been driven. He then passed to Alençon and later to Rouen where he devoted most of this time to marine constructions, adapting the caisson concept to the erection of embankments and locks.

His most famous project is the erection of the Cherbourg dike, built to protect the military harbour form the English fleets. He designed a dike 4000 metres long, made of 90 enormous wooden cones, built on-shore and then shipped and sunk on the sea bed to be filled with stones. These cones were 50 metres in diameter and 20 to 24 metres high, a prefiguration of our modern heavy prefabrication and of off-shore structures. Erection began in 1783, but heavy tides and tempests damaged some of the first cones; other marine engineers altered the project by increasing the distance between cones; high costs produced delays and the dike was not finished when the revolution came, and the project could not be completed.

Cessart was of course extremely disappointed, but he had a last occasion to evidence his creativity when Bonaparte decided to erect a cast-iron bride to follow the new technique developed in England, and entrusted him with the design of the famous Passerelle des Arts in Paris; a pedestrian bridge which has been unfortunately destroyed in the seventies, after two ship collisions, and replaced by a copy which slightly longer spans.

Thomas Telford (1757-1834)

If the 18th century has certainly been dominated by French engineers and the creation of the Ecole des Ponts et Chaussées, the first half of the 19th century is without any doubt English, and the most famous engineer Thomas Telford.

In fact, everything began in the last decades of the 18th century with the erection of the Coalbrookdale bridge by Abraham Darby III (1779). Cast-iron and iron then became construction materials with a very rapid development, and were soon used for the erection of suspension bridges. To be honest, suspension bridges had already been built for many centuries in Tibet and China, but this was ignored in the western World.

The great step forward is due to Thomas Telford who designed the Menai Bridge, in Wales, built between 1819 and 1826 with a main span 177 metres long. The suspension was made of a series of the so-called eye-bars, based on an invention by Hawks (1805) and Brown (1808 – 1818).

Thomas Telford was the son of a Scottish shepherd and began his carrier as stone-cutter. In 1780 he works as such at the erection of large buildings in Edinburgh, and of Somerset House in London. Between 1784 and 1786 he works as architect for the construction of a house and for the rehabilitation of Shrewsbury castle; very soon recognized he becomes in charge of larger and larger projects such as the Ellesmere canal (1793) and the Caledonian canal (1803), and is even consultant for the Gotha canal in Sweden (1808-1822).

From 1803 to his death, he directed the erection of more than 1000 bridges, 1920 kilometres of roads; numerous harbours, churches and docks. During his life he had very diverse activities : he developed a kind of standardization of arch bridges in cast-iron, building them from standard truss panels ; he participated in the drainage of marshes, in the improvement of river navigation and in the development of water supply in London, Liverpool, Glasgow and Edinburgh.

Finally, he has been one of the founders of the Institution of Civil Engineers of which he became the first President, and received many honors, the greatest of all being to have been buried in Westminster Abbey. Later he gave his name to the publishing company of the Institution of Civil Engineers, which is the editor of our Journal.

Isambard Kingdom Brunel (1806-1859)

I could have selected Robert Stephenson (1803 – 1859) who erected the famous Britannia tubular bridge in 1850, after the Conwy tubular bridge (1848). Or later Sir John Fowler and Benjamin Baker who built one of the most famous bridges in the world, the great tubular bridge which crosses the Firth of Forth. But I prefer Isambard Kingdom Brunel.

Isambard is the single son of Marc Isambard Brunel, a famous French engineer who settled in Great Britain in 1799. Isambard is sent to France in 1820 to complete his education, and when back to London in 1824 he works with his father for the construction of the famous tunnel under the river Thames.

Very soon he designs the Clifton suspension bridge above the river Avon, near Bristol, which would have been the world record if the construction had not been delayed after his death (1860-1864), with some alteration of his project. We can note – in the line of this presentation – that he choose a long suspended span, with the chains directly anchored in the rock on each side, to eliminate any pier in the gorge for the preservation of the site.

Becoming the engineer of a railway company – the Great Western Railway – he selects a specific width for the track (2,10 metres in place of 1,45), limits the slopes to increase speed, designs large wheels for the travelers comfort and specific engines; then he turns to ship construction, with the SS Great Western, then the SS Great Britain – with a steel hull and one propeller, a very new solution –, and finally the Great Western with a double steel hull, a ship six times bigger than any other ship at her time.

He designed many bridges, basing his approach on empirism and tests, avoiding cast iron which is too brittle and developing the use of puddled iron. But he also used stone and timber.

He is one of the best examples of engineering creativity and innovation; his ideas have not been always successful, sometimes because he was too much in advance on his time, but he was respected and honoured as one of the men who produced the fantastic development of engineering and construction in Great Britain and the world.

Gustave Eiffel (1832-1923)

Gustave Eiffel is one of the rare French who could make a name in steel construction when it was dominated by English engineers. More than an engineer he was a contractor, creating his own company when he was 32 years old. He is famous for his tower (1889), but – as well as Cessart, Telford and Brunel – he worked in many very different domains.

He erected the central part of the main gallery for the world exhibition in Paris in 1867, churches, factories in Paris area; a series of small railway bridges, and two large viaducts across the river Sioule, at Rouzat and Neuvial. Due to his reputation and activity he obtains contracts all over Europe, being a real pioneer at a time when contractors were limited to their own countries: he built bridges in Romania, Spain, Portugal (the famous bridge over the river Douro in Porto), Peru and Bolivia.

He is then very successful, erecting many buildings, including the steel structure of the Statue of Liberty in New York, the famous Garabit viaduct over the river Truyère and the Tower.

Just the same year he takes part in the adventure of the Panama canal with Ferdinand de Lesseps, which ends with a financial collapse and a political scandal which stopped his contractor's career.

Eiffel never used steel, which appeared and developed progressively during his life, and preferred iron which he considered safer due to its greater ductility. He created a system of "transportable" bridges, fabricated in elements to be exported and erected far away; the company which kept his name maintained this system very lately, even after the Second World War when the development of local companies gave an end to this activity.

After the Panama scandal he devoted his time to sciences and research, mainly to preserve the Eiffel Tower which was supposed to be dismantled after 20 years. The three domains in which he was interested were all related to the Tower : aerodynamics and meteorology, in direct relation with his passed construction activity, and radiotelegraphy. He built in 1911 the first French wind tunnel, at Auteuil, which still exists and was used mainly for the development of aeronautics. And this is not a hazard if the Eiffel Tower is now used as a meteorological station, and that the first television emission was made from it in 1934.

The Roebling family: John Augustus (1806-1869), Washington Augustus (1837-1926) and Emily Warren-Roebling (1844-1903).

This is now the right time to cross the Ocean to the United States and John Roebling.

But in this case it will be more attractive to refer to the family, wholly involved in the erection of the Brooklyn bridge.

John Roebling was German, born in Mühlhausen and educated at the Royal Polytechnic Institute in Berlin where he was graduated in 1826. He also studied there philosophy under Hegel, who considered him as one of his best students. He settles in the United States as farmer in 1831, in Pennsylvania, but he soon accepts to become engineer in the State administration. He works on roads and canals, and from this experience decides in 1841 to create a small factory at Saxonburg, producing cables from iron wires to ease handling ships and wagons. In 1848, the success is so large that he moves his factory to Trenton, New Jersey.

His engineering activity begins in 1844, when he designs a suspension bridge to carry the Allegheny river above the Pennsylvania canal. The structure is made of timber, and the suspension cables of high strength parallel wires; his technique is fixed already in this first application, with a wire wrapped around the circular section for corrosion protection. Several other bridges follow, the most important ones being the Niagara bridge – the single suspension bridge to carry a railway line at the time – and the Cincinnati bridge over the river Ohio. In 1857-1860 he builds a new bridge in Pittsburgh across the Allegheny river, associating for the first time his son Washington to his work.

But of course he is mainly famous for his design of the Brooklyn bridge. Unfortunately his leg is pounded in an accident during preliminary works, and he dies from tetanus in 1869 before the real beginning of the bridge erection.

Logically, his son Washington is named chief engineer to follow him. But he had to suffer from two severe accidents: in December, 1870, fire started in the Brooklyn pneumatic caisson and after a hard night to fight fire, he collapsed and had to be taken home; in May, 1871, he collapsed again, in the New York pneumatic caisson, this time after a series of accidents who produced the death of several workers. This second accident was more serious, and he has lain near death for days; he returned to work for a time but never recovered and had to take a leave of absence in December, 1872. He travelled to Germany for six months, then directed construction from his Trenton house, and from 1876 watched erection form the window of his house on Columbia Heights; but during all these years until the inauguration, on 24 May, 1883, he has been strongly supported by his wife, Emily, who received no engineering education but revealed able to grasp her husband's ideas and instructions to his assistants, and visited the site twice of three times a day to check details. An editorial of a New York journal called her the "Chief engineer of the work", and she has been admired and respected by anyone, including assistant engineers, bridge trustees and local politicians, a very unique example in the construction history.

Othmar H. Ammann (1879-1965)

Othmar H. Ammann is the successor of Roebling in the great history of suspension bridges. Born in Schaffhouse, in Switzerland, he is graduated in 1908 at the Swiss Federal Polytechnic Institute in Zurich; after a short stay in Germany, he settles in the United States in 1904 and becomes an American citizen in 1924.

From 1904 to 1914, he works with several famous American designers – Mayer, Modjeski, Kunz and Lindenthal – before joining the Swiss army when it was feared that Germany pass the border, leaving to David Steinman his place of chief assistant to Lindenthal. But three months later, as war did not erupt on the Swiss border, he came back and Lidenthal immediately reinstalled him, creating the bitter rivalry between Ammann and Steinman which lasted during all their lives.

Ammann was deeply associated in the erection of the Hell Gate bridge (1917) designed by Lidenthal, and after some time spent outside the office worked on the later's project to cross the Hudson river. But this project was too ambitious with 12 railway lines and 16 road lanes; convinced that it was hopeless, Ammann decided to develop his own project and settles as independent designer in 1923. His project was unveiled in 1924 and immediately received strong supports, including the support of the governor George Silzer. The project was finally accepted and was about to be built by the Port of New York Authority, leaving Ammann jobless. Silzer remedied the situation by encouraging the Authority to establish the position of bridge engineer and to name Ammann at the post, so that Ammann has been civil servant during 15 years, from 1925 to 1939.

Everybody knows the story. He built his Hudson bridge, the George Washington Bridge (1931), the first modern suspension bridge with a main span 1000 metres long, doubling the previous record. Then he multiplies his achievements with the Bayonne bridge (1931) to cross the Kill van Kull, the famous arch bridge competing with the Sydney Harbour bridge for the world record (504 metres) which he brought back to the USA; with the Lincoln tunnel, but also with a series of suspension bridges: the Triborough bridge and the Bronx Whitestone bridge (1939).

Ammann then leaves the civil service and settles a new design office in 1946 with Charles Whitney, Ammann and Whitney. This is within his office that he builds the Verrazano bridge (1963), regaining his world record (1298 metres) taken by Joseph Strauss in 1937 with the erection of the famous Golden Gate bridge (1281 metres).

From this rapid evocation it is clear that Ammann gave us a fantastic example of creativity and innovation, but also of persistency and of political perspicacity. I have been specially interested, when reading his history, by the fact that he never worked according to his positions, but selected his positions to the work he desired.

It is also interesting to note the connections which existed between the engineers of the American school of the time: Modjeski, Lindenthal, Ammann, Steinman, Strauss – who began with Modjeski – and Moisseiff, the unfortunate designer of the Tacoma bridge. It would be worth spending some time on the development of knowledge and theories on aerodynamic stability, as well as it would be worth to evoke in more details Strauss and Steinman, the first engineer to design a suspension bridge, over the Mackinac straights, after the collapse of the Tacoma bridge.

Robert Maillart (1872-1940)

But we have to pass from steel to concrete, and back to Europe with one of the most famous of engineers, Robert Maillart. When the journal Bridge made an enquiry among engineers and architects to know which is the most famous bridge of the 20th century, a majority selected the Salgina bridge in the Swiss Alps.

Maillart's father was Belgian, but his mother Swiss. He has been graduated at the Swiss Federal Polytechnic Institute in 1894. He began his career in a contracting company, built a bridge in Zurich and then worked with a designer to erect the Zug bridge, the first concrete box-girder. In 1902 Maillart settles his company to design and built concrete structures and is immediately successful. In 1902 he builds the largest concrete water tank in the world, in 1905 an arch bridge with a box-girder structure, and the first slab structures which he patents in 1909. In 1912 he wins several design competitions and becomes very famous, extending his activities to Spain and Russia.

In 1914 he travels to Russia for Summer vacation and is trapped there by the war and the revolution. He can escape only at the end of 1918, and when he comes back to Switzerland he is ruined.

He then writes many technical papers and progressively recovers his reputation and success. In 1924 he erects the first arch bridge in which the arch is stiffened by the deck, the Valtschielbach bridge. In 1928 he wins the competition for the Salgina bridge which is completed in 1931. Then bridges are built one after another, all with an extreme structural efficiency and a great elegance.

At the end of his life, he builds a concrete roof, a very thin shell for the national exhibition in Zurich (1939).

During his last years he publishes many papers on “structural architecture”. Due to his constructions and his papers, he is considered as much as an artist as an engineer, and famous authors devoted papers and books to his works such as Siegfried Giedion, Max Bill and David Billington.

<u>Albert Caquot (1881-1976)</u>

Concrete has been very successful in France where some major progress took place, and of course everybody knows Eugène Freyssinet who developed the concept and the technology of prestressing. His life and his strong character are so well known that I prefer concentrating on another engineer, Albert Caquot, who had a fantastic career;

Graduated the same year as Freyssinet at the Ecole des Ponts et Chaussèes, he is nominated at Troyes, a very unhealthy city at the time. He strongly encourages the construction of sewers and drains which rapidly improve the situation and help limiting the effects of the large flood in 1910. But he loses interest in administrative work and joins Armand Considère – a pioneer of reinforced concrete – to settle a design office, in association with Considère's son-in-law after Considère's death in 1914. They design concrete dams, bow-strings and other structures.

During the first World War he designs observation balloons which are extremely stable, even under rather high winds, taking a major part in the supremacy of the allied artillery. After the war, he designs and erects many structures, like the les Usses arch bridge or the Saint-Nazaire dry dock, and develops some erection techniques.

In the same time he is named general director of the new Aviation Ministry and he tries to develop a modern aviation. Disappointed by the lack of funds he resigns in 1933, and is nominated again in 1938 without more success.

After the second World War he comes back to structural engineering, erects the la Girotte dam and the Donzère-canal cable-stayed bridge (1952), a pioneer concrete cable-stayed bridge which is often forgotten in the construction history, and he takes part in the erection of the tide-dam on the river Rance (1966).

He received almost all possible honours: the highest level of the French Legion d'honneur – the great cross – as well as many decorations from the allied countries during the first World War ; he has been member of the French Academy of Sciences, even becoming its president in 1952.

Caquot has certainly not paid very much attention to aesthetics, as Maillart did for example, but the diversity of his career is very unique in the modern times. He has also associated very closely theory and practical applications in structures as well as in soil mechanics, evidencing a very universal spirit.

Fritz Leonhardt (1909-1999)

If it had been possible, I should have evoked Nicolas Esquillan, one of the greatest French engineers of the 20th century, respected worldwide including by Fritz Leonhardt who admired him for his works and also for his modesty and personal character. But it is better to concentrate on Leonhardt himself who can be considered as the master of the second half of the century.

Graduated at the Stuttgart University in 1931 he travels to the United States in 1932-1933 on occasion of a students programme. In 1934 he has a technical position in the administration in charge of the motorway programme, and he works there in close cooperation with two architects, Paul Bonatz and Friedrich Tamms; this has been for him a very important experience which explains his dedication to structural elegance. Between 1938 and 1941, he designs and builds the Kölhn-Rodenkirschen suspension bridge which is – with his main span of 378 metres – the longest in Europe at the time, far behind the American bridges.

After the war he takes a decisive part in reconstruction, developing new systems for buildings and improving bridge construction techniques. His major achievements are the Köhln-Deutz bridge (1948), a light and elegant composite bridge, the three famous cable-stayed bridges over the river Rhine in Kölhn, with Tamms, and the Kochertal bridge; he developed the concept of a suspension with a unique axial cable, patented in 1953, with unsuccessful projects proposed in 1955 (for the Tancarville bridge) and 1961 (for the first Tagus bridge in Lisbon).

Leonhardt has also built many towers such as the pioneer one, the Stuttgart television tower in 1955, with a concrete core supporting the floors, a model which has been reproduced many times later. He also built shells, cable-supported roofs such as for the Munich Olympic stadium.

In addition to this important activity of designer – through his office, Leonhardt and Andrä – Leonhardt has been professor during twenty years at the Stuttgart University (1953-1973). As such he publishes his famous red books which have long been the bible for reinforced and prestressed concrete structures, and he wrote many technical papers, for an example on cable-stayed bridges. But his major influence, world wide, came with his two books, Bridges and Towers, in which in addition to historical and technical information he gave his views on structural architecture, on aesthetics and beauty.

Honoured by almost all international awards in structural engineering, he had a direct or indirect influence on all living designers.

Riccardo Morandi (1902-1989)

It is surprising to pass from Leonhardt to Morandi since they are very different and have built very different structures. But I have a very special appreciation of Riccardo Morandi who developed his own structural philosophy without any relation with the international trends.

His most famous construction is the Maracaibo bridge in Venezuela (1962) which I consider as one of the major ones in the world, together with the Brooklyn Bridge, the bridge across the Firth of Forth, the Washington bridge and the Golden Gate bridge. This is one of the largest constructions of the time, one of the first large concrete constructions built with heavy equipment. It is remarkable that, like the bridge above the Firth of Forth, this is a hopeless solution : the gigantic truss of the Firth of Forth was overpassed by suspension bridges, lighter and much cheaper to erect, more elegant also;

and the Morandi's system for cable-stayed bridges was overpassed by the design of the German cable-stayed bridges, with flexible pylons and deck; lighter, at much lower cost and finally more elegant. But what a strength in these two designs, the Firth of Forth and Maracaibo ! How evident is the flow of forces, even if not the most logical ! This is not a surprise if these two bridges, two deadlocks, are highly appreciated by architects and the public ; they express their strength and their behaviour.

Morandi kept the same line during all his career, mainly inspired by the architecture and the art of the twenties and thirties ; priviledging assemblies of beams and slabs.

He graduated in 1927 at the Scuola di Applicazione per Ingegneri and begins his career in Calabria to rebuilt in reinforced concrete churches destroyed after an earthquake. In 1931 he settles the Studio Morandi, mainly to work with a contracting company. He builds habitation buildings in reinforced concrete, large cinemas in Rome, churches, factories, schools; all with his specific style.

He develops his prestressing systems (1949) and a new technique to erect arches : each half-arch is built almost vertical inside a scaffolding, and then rotated with the help of maintaining cables to take its final position ; the Lussia pedestrian bridge (1954) and the Storms river bridge in South Africa (1954) are built that way.

And then he begins building his cable-stayed bridges : the Maracaibo bridge (1962), the Polcevera viaduct in Genoa (1964) and the Wadi-kuff bridge in Lybia (1971) with the same design ; and some more recent with amended solutions, tending to the international way. But he also builds cable-supported roofs for Alitalia in the Fiumicino airport and a very large arch bridge, the Fiumarella bridge with the same design philosophy.

A rather rare example of a man who followed his own way with no relation with the international trends and fashion.

Christian Menn (born 1927)

Christian Menn is certainly another example. Perhaps some will be surprised that I present living engineers, two in fact. But as my goal is to evidence the continuity in engineering and the influence of great engineers on our profession, it would be counterproductive to stop my list here and to leave the impression that there are no more great engineers today. At least there is a strong criterion : a book has been already published on the works of Christian Menn and of Jörg Schlaich.

Christian Menn has been graduated at the Zurich ETH in 1950, and in 1953 he became assistant to professor Lardy to receive his PhD in 1956. Working with Dumez in Paris he takes part in the erection of the Unesco building designed by Pier Luigi Nervi, and in 1957 he opens his own office in Switzerland.

His first constructions are very much inspired from Maillart, and he developed Maillart's concepts to the extreme, designing very light arches with light decks : the Crestawald bridge (1958), the Averserrhein bridge at Cröt (1959), the Grüne bridge (1961), the Valserrhein bridge (1962), the Rhine bridge at Reichenau (1964) and the two bridges at the San Bernardino pass (1967) – the Nanin and Cascella bridges – are among the most elegant arches built in the world.

Menn has also built more classical bridges – for modern times, since no other structure can be as classical as an arch –, but with extremely elegant shapes. The Felsenau bridge (1975) is one of these examples.

But Menn proved his originality when he designed the Ganter bridge, with a structure which can be compared to no other one at the time : the box-girder deck is supported not by cable-stays, but by prestressed concrete walls. This design has been reproduced by some other designers – in Mexico with the Papagayo bridge, in the USA with the Barton creek bridge, in Portugal with the Socoridos bridge and in Bahrain –, and inspired what is now called extradossed bridges following the name given by Jacques Mathivat when he developed an unsuccessful design for the Arrêt Darré viaduct. These extradossed bridges received many applications in Japan – some very elegant like the Odawara Blue Bridge –, but the most elegant has been recently designed and built by Christian Menn himself, the Sunniberg bridge.

Christian Menn followed his own way, his own philosophy. To evidence his strong character I shall just evoke his accident: when skiing alone he broke his leg ; as no help could come, he crawled on the snow on a long distance with his broken leg to be rescued.

In parallel with his professional activity, following the German and Swiss tradition he has been professor at the Zurich ETH from 1971 to 1992, influencing generations of Swiss engineers; but also engineers all over the world who have been impressed by the elegance of his constructions.

Jörg Schlaich (born 1934)

I should have liked to present René Greisch, a Belgian designer who worked as architect for buildings – including in own office in Liège – and as engineer for the erection of a series of elegant bridges, specially across the Albert canal, but due to the limits I have to conclude with Jörg Schlaich.

He studied in Stuttgart, Berlin and Cleveland at the Case institute (1960). He enters Leonhardt's office of which he becomes an associate in 1974. There he takes part in many major projects, mainly for light structures: concrete television towers, the suspended roof of the Munich Stadium for the Olympic Games, the Munich ice-stadium and the cooling tower of the Schmehausen nuclear plant (1974). He progressively develops from Otto Frei's theories a concept of light roofs, a cable net supporting glass or plastic membranes.

In 1972 he becomes the successor of Leonhardt at the Stuttgart University, as professor of concrete structures : but in 1980 he leaves Leonhardt's office to create his own, Schlaich-Bergermann and Partners. From his own office he develops his activities in light structures, such as for the fixed or mobile roofs of the Hamburg History Museum, the stadiums in Saragossa, Stuttgart, Hamburg and Oldenburg, for the Nimes roman arena or the Montreal stadium for which the roof could not have been installed in 1972.

He also designs bridges; some more or less classical, like the Hooghly bridge in Calcutta, a composite structure which would have taken the world record if construction had not been so slow (1978-1993), and more original ones, like the Evripos cable-stayed bridge in Greece, a simple prestressed concrete slab with a span of 210 metres inspired from the ideas of Ulrich Finsterwalder and René Walther, who pioneered the domain and had also passed in Leonahrdt's office. But from his experience in light roofs, Schlaich developed a very personal design of suspended and cable-stayed pedestrian bridges, extremely light and elegant; structures with very simple elements associated to produce an extremely efficient structure. More recently, he designed structures made form steel tubes, pedestrian bridges – arches for example, with a very light upper slab – and road bridges, mainly in Stuttgart area.

His structural capacities made possible the development of light bridges in any condition, like for a semi-circular pedestrian bridge in Kelheim where he took advantage of the curvature itself in the design. He also developed new ideas for mobile bridges, sometimes having a hard time to make them work.

He is an unpredictable designer, because each time he looks for a new idea, a new solution; this is also why I don't like all his structures, but I am always astonished by his creativity.

Being strongly engaged in sustainable development, he worked on the structural aspects of renewable energies, like for dish concentrators of solar receivers, or solar chimneys to create energy from the induced updraugth wind.

As a conclusion he is a fantastic example of creativity and imagination, and as many of his predecessors, other great engineers, he has a very universal activity. Among many deserved honours he received two exceptional ones: an excellent book by Alan Holgate recognizing his career, and having been black-listed by the German administration for his strong positions against an official recommendation about internal and external prestressing.

4. CONCLUSION

I regret that I could not evoke many other names of great engineers, like Paul Séjourné, Franz Dischinger, Ulrich Finsterwalder, Carlos Fernandez Casado, or more recently Hans Wittfoht, Javier Manterola, Armando Rito, Jean Muller, Jiri Strasky as well as those who inspired me more directly like Jacques Mathivat and René Walther.

There cannot be any conclusion after my presentation. I just hope that I could show the importance of great engineers in the development of modern civil engineering, and of the example given by their careers. Ours associations, *fib* and IABSE, certainly have to make some efforts to have them more recognized in the society.

I am more optimistic than I was some years ago : even if the title of the series might be considered as a problem, if taken in the wrong direction – the engineer's contribution to contemporary architecture – it is a good sign that Thomas Telford issues a series of books on great engineers like Peter Rice and Heinz Isler. As well as we all appreciate that the journal Bridge published a series of papers on engineers in activity: Fritz Leonhardt just before his death, T.Y. Lin, Jörg Schlaich and many others.

But we have to do more to have them recognized outside the small professional circle of engineers, through specific actions like biographies, exhibitions and a greater attention to our image in the society.

Bibliography

L.T.C. Rolt. Isambard Kingdom Brunel, engineer, visionary and magnetic personality, he transformed the face of England. Penguin books, 1957 (re-edition, 1989).

Giorgio Boaga and Benito Boni. The concrete architecture of Riccardo Morandi. Alec Tiranti. London, 1965.

Max Bill. Robert Maillart. Les Editions d'architecture (Artemis), Zurich, 1969.

Jean Kerisel. Albert Caquot, créateur et précurseur. Eyrolles, Paris, 1978.

Jacques Mathivat. Construction par encorbellement des ponts en béton précontraint. Eyrolles, Paris, 1979.

David Billington. Robert Maillart's bridges, the art of engineering. Princeton university press, 1979.

Richard Dillon, Thomas Moulin and Don DeNevi. High steel building, the bridges across San Fransico bay. Celestial Arts, Berkeley, California, 1979.

The development of long-span bridge building (Tom F. Peter and als). ETH Zurich August 1979.

Sylvie Deswarte and Bertrand Lemoine. L'architecture et les ingénieurs. Le Moniteur. December 1979.

Jose A. Fernandez Ordonez . Eugène Freyssinet. Societad Cooperation Industrial de Trabajo Associado, grupo 2C, 1979.

Mary J. Shapiro. A picture history of the Brooklyn bridge. Dover publications inc., New York 1983.

David P. Billington. The tower and the bridge, the new art of structural engineering. Princeton University Press, Princeton 1985.

Antoine Picon and Michel Yvon. L'ingénieur artiste. Presse des Ponts et Chaussées. Paris, 1989.

Sheila Mackay. The Forth Bridge, a picture history. HMSO publications, Edimburgh, 1990.

Riccardo Morandi, Innovazione, technologia, progetto (under the direction of Giuseppe Imbesi, Maurizio Morandi and Franseco Moschini). Gangeni, 1991.

Bernard Marrey. Nicolas Esquillan, un ingénieur d'entreprise. Picard. Paris, 1992.

Sylvie Deswarte and Bertrand Lemoine. L'architecture et les ingénieurs. Le Moniteur. Paris, 1997.

250 ans de l'Ecole des Ponts en cent portraits (under the direction of Guy Coronio). Presse des Ponts et Chaussées, Paris, 1997.

L'art de l'ingénieur (under the direction of Antoine Picon). Centre Georges Pompidou. Le Moniteur. Paris, June 1997.

Christian Menn, Brückenbauer (under the direction of Heinrich Figi and als). Birkhaüser Verlag, Basel. Boston. Berlin, 1997.

Alan Holgate. The work of Jörg Schlaich and his team, the art of structural engineering. Edition Axel Menges, Stuttgart. London, 1997.

Bridge. Interviews in each issue since Second quarter 1998, with T.Y. Lin. Route one publishing.

Bridge, design and engineering. Fourth quarter 1999. The most beautiful bridge of the 20th century (editorial, p.5 and p. 36-42) Route one publishing.

John Chilton. Heinz Isler (the Engineer's contribution to contemporary architecture). Riba publications. Thomas Telford, London, 2000.

Darl Rastorfer. Six bridges, the legacy of Othmar H. Ammann. Yale University Press. New Haven and London, 2000.

THE SUCCESS AND FAILURE OF TECHNOLOGY IN SOCIETY

Charles W. Dolan
H. T. Person Professor of Engineering, University of Wyoming
USA

Keywords: concrete, technology, acceptance, history

1. ABSTRACT

New technologies are constantly being introduced into society. Some succeed; others fail. An examination of the concrete and masonry industries explores the basic applications, associated technologies, economic benefits, government policy and societal impacts concerning the success and failure of new products and ideas. Examples of technological success include prestressed concrete and cable-stayed bridges. Other examples demonstrate that technology alone is not sufficient to assure success, and that a technologically sophisticated delivery system is required. Public acceptance of technology can lead to delegation of acceptance or rejection of new technologies.

2. INTRODUCTION

Countless researchers and engineers have puzzled at the prospect of a "brilliant idea" that fails to gain public acceptance. In the civil engineering community, the fickleness of success or failure of a technological advances is particularly perplexing. Ideas that, to the developer, have clear technological advantages and excellent economics do not always succeed. In exploring why success or failure occurs, it is easy to suggest that the convergence of technologies, the assessment of technological risk, the instability of the marketplace or lack of "management support" are the net drivers of technological advancement. Yet, the interaction of these drivers is not obvious.

The past decade of research into composite materials for concrete and current initiatives in adapting concrete structures for housing leads to the question of why some innovations succeed and others fail. Composite reinforcement has clear benefits for corrosion resistant applications, yet the industry is foundering. Thomas Edison designed reinforced concrete houses at the turn of the last century, yet they remain a rarity today.

Understanding the success of technological advancement is more complicated than the economics of first cost. Before developing case studies of technological successes and failures, it is necessary to examine the roles of the political economy, the decision process, and complexity in decision-making. The interplay between each of these elements provides an insight to fundamentals of technological success. Understanding the interactions gives the engineer background needed to achieve success beyond the technological innovation.

3. POLITICAL ECONOMY

The basic assumption for success is: if a technological innovation increases efficiency and profits, it will be successful. This is a marketplace model and is based on a theory that the marketplace is efficient. Improvements in efficiency are the only elements needed for innovation to be adopted. The model assumes the market is driven by a decentralized decision making process. The driver in the decentralized decision making process is the consumer.

Joel Mokyr points out that there are significant non-consumer, non-market institutional restraints affecting this decision process[1]. Most importantly, he identifies the need for an *imprimatur* to be in place before technologies can proceed. In our society, the *imprimatur* takes several forms. First, the technology should be available directly or by inference in the "building codes". Second, the innovation must be endorsed by an "expert," typically the engineer sealing the drawings. Third, it must be accepted by the "establishment," such as the local building authority. Depending on the particular project or concept, any or all of these restraints must be overcome before a technology can advance.

Mokyr expands constraints on technology by investigating the impact of systemic resistance to introduction of new technology. This resistance may develop at the production, marketing or regulatory level. Just as the lack of an *imprimatur* in a building code may be an impediment, the lack of quality control/quality assurance standards in the national reference standards such as ASTM, RILEM, CSA or DIN provide clients the needed excuse to discard innovation.

4. DECISION PROCESS

Even at the simplest operational level, e.g., a small consulting firm, inertial systemic resistance may inhibit innovation. The decision process involves four steps. First, postulate a decision. Second, reflect on the outcomes of the decision. Third, ask questions about both the impact and consequences of the decision. Fourth, "take the decision." Most often, the process begins with "taking a decision" and the reflection and questioning occurs later. The reflection involves an assessment of risk taking and consequences. Fear of disappointment or failure to understand the complexities of the problem lead to a rejection of the decision that is contrary to established practice. Keeping with established practice minimized the need to reexamine consequences.

A classic example is found in H. Ross Perot's endeavor to build the EDS Corporation[2]. IBM elected not to provide software for their mainframe computers. Perot not only provided the software but also soon became IBM's largest customer. Perot made a decision assessed the complexity, followed through to a successful conclusion.

A more difficult example follows the actions surrounding the disaster at the Chernobyl nuclear site. The power plant was undergoing routine maintenance when a series of small failures began to accumulate into larger problems. As control rods were pulled, the lack of communication led to a positive feedback loop and eventually to massive overheating of the reactor core[3]. Here the decision process failed through the lack of timely information.

The EDS example illustrates a beneficial or detrimental decision process depending on whether you were involved with EDS or the IBM. The Chernobyl decisions led to disastrous consequences on a multitude of levels. Not only were the environmental and human losses significant, but also the uncertainty surrounding the use of nuclear power was severely increased in the public sector. Even though the Chernobyl plant safety features were unique and not replicated in other plants worldwide, a major consequence of Chernobyl was a virtual shutdown of curtailment of nuclear power generation, especially in the USA.

The public decision process for major projects involves a number of independent decisions, not all of which are made on a technological level. Table 1 examines the decision makers, their motives and their roles. While somewhat simplified, the most significant observation concerning the role of the decision makers is the lack of motivation to accept risk and new technology. The range of motivations and decision basis make rapid adoption of a new technology very difficult.

TABLE 1 DECISION MAKERS AND INFLUENCE

Decision Maker	Motive	Decision Basis
Private Owner	Financial gain	Economic risk assessment, can accept technical risk if it is well described
Public Owner	Use of public funds	Prudent use of Public trust
Code Writers	Protection of public life safety	Technical maturity, competency, and safety without consideration of cost. Provides *imprimatur*
Designer	Recognition as innovator and client satisfaction	Creative ability to compete the project and client directives
Building Official	Protection of public life safety	Availability of *imprimatur* to validate decision - Limited risk taking
Standards Organizations	Technical competency	Assessment of maturity of given technology – provides *imprimatur*.
Contractor	Financial Gain	Overall corporate risk assessment of ability to complete task.

5. COMPLEXITY AND DECISION MAKING

Technical complexity has increased exponentially over the past century. The proliferation of low cost computing power has accelerated both the complexity and the speed of decision-making. For virtually every engineering endeavor, especially in the realm of concrete construction, the design and construction process may be simulated by computer models. Acceleration of computer based design and its inclusion in undergraduate education creates a generation of designers who may place considerable faith placed in outcomes of computer simulations. The need for physical validation of computer modeling is addressed elsewhere in this congress[a]. The critical point is assumptions are made in the computer simulations in addition to the designers judgment. Not all of these decisions are apparent. Some may include critical flaws that are not manifest unless sophisticated modeling is undertaken.

A second element of complexity involves the interaction between variables. A century ago, structures were designed for static and gravity loads. Today's building codes carefully interleave structural systems, loadings, and structural responses. This places an exceptional burden on the principal designer to select the appropriate framing systems, and then to assure that the system is not compromised during the design details. The classic example of failure in this area is the Hyatt Regency Hotel walkway collapse in Kansas City, Kansas. A relatively minor change in detailing violated the original design concepts and resulted in the death of over 100 individuals.

The third element of complexity is the presence of contradictory goals. Engineers are classically trained to find a single optimum solution. Major research initiatives in the late 70's and early 80's geared at "optimization" eventually discovered that optimization algorithms were far more complex than originally envisioned. Optimization programs that minimized material content in buildings were in conflict with construction optimization of similarity of construction. As the complexity of the programming increased, the value of the optimization effort faltered.

The combination of the complexity elements affects the method in which work is executed and the way acceptance criteria are satisfied. First, the interwoven design elements affect the method in which the design process is delegated. Design teams require a high level of communication. Reviewing agencies need to understand the basic assumptions of the design. Contractors must be able to execute both the details and the overall concept of the project.

The design and decision process have adapted technology to address complexity. It is common for the project documents to exist in electronic format. Drawing layering allows key concepts to be preserved as subconsultants and the delegated design squad members execute their respective

[a] Dr. Catherine W. French, Plenary Session 2

work. While not assuring that designs are error free, the electronic transfer helps assure commonality of design intent. Building officials, on the other hand, typically do not have access to the electronic format of the contract drawings and therefore rely on descriptions of framing systems included on the project documents for understanding. The contract is yet another step removed from the creative development process.

The technical competence required to assess the validity of complex project documents is not generally available in the public sector. Therefore, the public delegates the responsibility for project conformance to their proxy agents. The agent is typically the building department for public dwellings and commercial space, departments of transportation, or special use districts such a port authorities. Each of these agents is free to execute its mission unless the public revokes the charter. One case where the public revoked its delegation of authority is in nuclear power, which is discussed later.

6. CASE STUDIES

6.1 The Dome of Santa Maria del Fiore

In 1418, the Opera del Duomo announced a competition for the construction of what would become the largest masonry dome in the world[4]. The Cathedral in Florence Italy had been under construction for over a century. The base of the dome was constructed in an octagonal plan and the dome would complete the structures. The design-construct competition allowed and even encouraged innovation by requiring the completed project and a description of the methods and means to be supplied by the winning entry. Filippo Brunellshi's winning submittal provided few of the required technical details, but promised an innovative design. Among the features of Brunellshi's dome were construction without centering, safe working conditions and highly imaginative construction equipment. The Opera del Duomo functioned as both the technical *imprimatur* for the project and the competent public agent. The Opera monitored the technical issues and controlled the finances of the projects. Thus, all of the ingredients were present for successful introduction of new technologies.

6.2 Interstate Highway System

President Dwight Eisenhower inaugurated the Interstate Highway System in the late 1950s. The program was to develop a national road system connecting all states and providing military transport routes across the continent. The initiation of this major effort was extremely fortuitous for the prestressed concrete industry.

Eugene Freyssinet demonstrated prestressed concrete principles in the late 1930's. World War II significantly impacted the implementation of prestressed concrete through the 1940s. In 1949, the first prestressed concrete bridge in the United States was constructed at Walnut Lane in Philadelphia. The Walnut Lane Bridge was instrumented and monitored for a short time following its construction to validate design precepts. This follow-up monitoring provided the technical assurance that was impossible to demonstrate on a theoretical level.

As with the Dome in Florence, Italy, all key elements for a major technological advance were in place. The government provided sustained funding for the project. The scale of the project warranted investment in capital facilities needed to produce prestressed concrete bridge girders. A cadre of technically sophisticated engineers in the state highway departments and the US Department of Transportation were managing the program. Public support for the systems was generally favorable. The majority of the opposition that did exist dealt with routing the Interstate System outside towns rather than using existing services. Opposition on technical grounds was negligible. The economic recovery immediately following WWII placed heavy demands on the steel industry to supply needs for building construction thereby providing an economic advantage to prestressed concrete.

From the early 1950s to the mid 1970s, prestressed concrete production grew at an exponential rate. The growth was due initially to the market created by the interstate highway project and then the penetration into the traditional steel bridge fabrication. The success of prestressed concrete bridges led an overall credibility to the material and the migration into building structures followed. The initial capital investments provided the platform for this expansion. The economic downturn in the mid 70s coupled with the transition of prestressed concrete from a specialty item to a commodity product eventually slowed the industry growth. Nonetheless, new products and innovation based on a quarter decade of success allowed slow but continued growth in the industry.

6.3 Concrete Admixtures

Concrete admixtures, especially the water reducers, were a technology that has a huge impact on the concrete industry, yet one that developed "under the radar" of normal technological implementation. While research on water-reducing admixtures had been ongoing for several years, the oil embargo of the early 1970s created an opportunity for this technology not present before. The sudden and dramatic price increase in oil affected the cost of cement and correspondingly all types of concrete. The water reducing admixtures provided an immediate resolution of conflicting goals. They allowed the amount of cement in a mix to be reduced while maintaining the workability of the mix. The cost of the admixture was nearly prohibitive prior to the oil embargo, but was now economical.

The economic pressures to constrain the price of concrete welcomed the introduction of these admixtures. Sufficient technical information was available to suggest that durability and performance would not be compromised and the admixtures were adopted quickly. The migration through the industry varied depending on the application. Departments of Transportation tended to examine the rheology of wet concrete and the properties of hardened concrete systematically. The building community, examining only the 28-day strength, adopted the materials even more quickly. Once the admixture base was established, incremental improvements became easier. Newer admixtures such as high range water reducers were more readily accepted based on success of water reduction admixtures.

6.4 Segmental and Cable Stayed Bridges

Segmental bridges grew out of the prestressed concrete industry with a helping hand from external societal inputs. The environmental movement placed restrictions on construction in environmentally sensitive areas. These restraints had a major impact on bridge construction. Bridges in Europe and the USA began to be designed by segmental cantilever construction methods. The segmental construction may be either cast-in-place or precast, but the construction methods required minimal ground access and reduced environmental disruption. Glenwood Canyon in Colorado is often cited in the USA as a premier environmentally sensitive solution to highway construction.

Cantilever bridge development is the beneficiary of new technologies and a source for later cable-stayed bridge technology. The computational effort to design a cantilever bridge is far more complex than traditional bridges. Not only do the deflections have to be carefully controlled, but also the material properties need to be known to a much higher level than normal construction. This results in the need to understand short-term time predictions of concrete movements as the bridge construction advances. Computer software and the reduction in cost of computation efforts directly assisted the advancement of this type of construction. The development of the computational tools and material properties to support cantilever construction laid a portion of the groundwork for cable-stayed bridges. Without this background, the engineering effort to design and construct a cable stayed bridge is likely prohibitive.

Cable stayed bridge construction is even more computationally intensive than cantilever construction. The high redundancy of the stays requires multiple computations. Redistribution of stresses due to volume changes requires both computational rigor and a solid understanding of material behavior. A half-century ago, cable stayed bridges could at best be executed on a small scale.

Another shift in construction technology occurred in the cantilever and cable stayed bridge arena. The prestress and precast concrete industry, with nearly a quarter century of developmental work, is virtually excluded from this development. Bridge contractors set up their own casting sites for the manufacture of the large bridge segments. In many cases, there was no direct teaming with precast concrete producers. Thus, a new technology emerged that was grounded in the precast industry, but not tied to it.

6.5 Failures

Not all new technologies are successes. Lack of an *imprimatur*, lack of public endorsement, or lack of an authorized public representative have impacted advances in concrete design and construction. Two of these failures occurred in the housing area. Patented flat slab and joist systems were introduced in the USA in the early part of the 20th century. The efficiency of these systems was virtually ignored by designers and contractors as long as the patents were in effect. Once the patents expired, there was a rapid expansion in the use of these systems. The patent holders restraint on the use of the systems affected the economical viability and the corresponding public availability. Only after the proprietary restraints were removed did the technology advance.

Concrete use for residential housing is another area where early attempts were successful, but economic and social constraints severely impacted the technological advances. Thomas Edison designed reinforced concrete houses in the early 1900s. Low labor costs and economical timber moved the housing industry to frame construction even though durability and fire resistance were low. Moshe Safdie's Habitat, designed for the Montreal World's Fair in the 1960s, was to be the beginning of a new form of residential construction. The high costs of the initial construction were not defrayed through additional projects and the experiment was not repeated. Inability of the precast industry to provide more variation in form limited application. By 1990, the precast concrete industry was capable of providing both variations in style and shape but the economic considerations were not sufficient for the advancement of the technology.

In late 1947, President Harry Truman announced a major national initiative into residential housing. Dormant during the Eisenhower and Kennedy presidencies, the program was rejuvenated with Presidents Johnson's "War on Poverty." The US Department of Housing and Urban Development provided a major impetus for new housing construction. Though millions of dollars were spent on research, development, and on some major construction, there was no corresponding technological breakthrough as there was with the interstate highway system.

Many of the major housing projects from the 1960s are now in major disrepair and disrepute. The concrete industry was unable to capitalize on this initiative because several of the key elements for technology advancement were missing. There was no central technical advocate to steer the projects. The spending was conducted with no clear understanding of the complexities of housing goals, design objectives, long-term use, and social pressures on the tenants. While high funding rates were committed to the effort, no common agency similar to the state DOTs were in place to oversee construction. Drug use, lack of maintenance, security and other societal constraints were not included in the developmental process. With no one entity in charge of the larger pictures and no technological representative, the concrete industry was reduced to responding to requests for proposals, providing minimum cost solutions to flawed guidelines.

6.6 Nuclear Power

Nuclear power is another area where the concrete industry is an important but nearly inconsequential player. Failures at Three Mile Island and Chernobyl led the public to withdraw the authority of the Nuclear Regulatory agencies to issue new construction permits. Even though the shielding at Three Mile Island worked as designed, the near miss, coupled with the lack of understanding of the complexity of nuclear power and the complete failure at Chernobyl lead to a nearly complete elimination of the technology.

7. OBSERVATIONS ON NATIONAL PRACTICE

A cursory examination of national practice as it relates to acceptance of new technologies offers additional insight into the interaction of the issues addressed above. North American practice typically involves a separation of the design and construction practice. Under this constraint, the designer contracts with the owner to develop the plans and specifications for the project. In some cases, for example, the departments of transportation, the owner and the designer may be a single entity. In this scenario, the lack of an *imprimatur* can significantly restrain the introduction of new technology.

A classical case is in the area of transportation systems. Several years ago, the City of Dallas, Texas was considering construction of new transit systems. Initial proposals were presented for an elevated monorail structure. The concept would have been provided on a design-build basis. The project was eventually configured as a traditional light rail system. The major arguments against the monorail were the lack of national standards – an *imprimatur* – and the sole source supply of the vehicles. A secondary factor was that the influence of traditional transportation consultants was initially eliminated, thus the traditional decision-making process was disrupted. Inertial effects led to a conventional solution.

Overall, the fragmentation of research and development in the USA does not allow the various elements of innovation to be rapidly integrated. Once a concept is presented, there are often no resources to move the technology forward for code acceptance or introduction into the mainstream decision process.

Europe has an established history of design-build competitions. Design-build offers an opportunity to circumvent the *imprimatur* restraint because the design and construction company have the opportunity to making critical decisions regarding the introduction of technology. The established history of innovation is of critical importance. European design-build is not merely an aberration of normal construction practice, but rather an opportunity to introduce and display new technologies. In a more restrictive design-build environment, the external constraints on selection of method and means of project development still restrain innovation.

The Japanese national initiative for the development of FRP materials for concrete construction presents yet another approach to solve both the decision process and the approval process. By creating a multidisciplinary national effort, researches, designers, building officials and contractors are all involved in the development process. The development effort is sometimes much longer as each entity participates in the "buy-in" process. The end result, however, contains acceptance by all parties and, once accepted, implementation is accelerated.

With the creation of the European Union, new multi-national initiatives research efforts have begun. These initiatives offer the opportunity for round robin testing and transfer of technologies between countries. As a minimum, the "not invented here" syndrome may be circumvented. Coupled with the possibility rapid introduction in the design-build arena, technological innovation may accelerate rapidly. While it is too soon to assess the full impact of these efforts, the promise is large.

8. CONCLUSIONS

Four items must be present for a new technology to succeed. First, the technology must have an overall advantage compared to existing technologies. An economic advantage is desirable, but not necessary as anyone with digital satellite TV can attest. Second, the technology must be approved by an industry *imprimatur*. The approval can be done at a local level, but is far more successful at the national level so industries are justified in capital expenses to support the technology. Third, if the technology is particularly complex, the infrastructure for evaluation of the technology must be present. This may take the form of building officials, state agencies or national agencies. Agencies must be competent and not politically motivated. Lastly, the technology must be sufficiently well described that the public can assess and accept the risk and delegate authority for acceptance to its public agent.

These lessons need to be examined as the concrete industry again looks to enter the residential housing market. Modular construction dates back to before the Second World War. Concrete provides a superior product in terms of durability, use of environmental resources and fire protection. Yet, the solution is unlikely to be a success unless there is a broader understanding of the public's role in acceptance of the product. This will involve establishing the same infrastructure of a code *imprimatur,* establishment of planning and engineering approvals, identification of public agents to accept work, and an economic structure that rewards or at least recognized the benefits of superior technology. Similarly, fiber reinforced polymer technology is partially comatose in North America because major acceptance components are missing.

REFERENCES

1 Mokyr, Joel, "The Political Economy of Technological Change: Resistance and Innovation in Economic History," **Technological Revolution in Europe, Historical Perspectives**, M. Berg and K. Bruland, eds., Edward Elgar, Northampton MA, 1998.

2 Follett, Ken, **On Wings of Eagles**, William Morrow, New York, 1983.

3 Dörner, Dietrich, **The Logic of Failure,** Perseus Books, Cambridge Massachusetts, 1997

4 King, Ross, **Brunelleschi's Dome,** Walker and Company, New York, 2000

LIGHTING DESIGN FOR BRIDGES

Motoko Ishii
Lighting Designer, JAPAN

Fellow of the Illuminating Engineering Society of Japan
Member of the Japan Lighting Committee
Representative of Inter Light Forum, Japan
Member of the Illuminating Engineering Society of North America
Fellow of the International Association of Lighting Designers

1 INTRODUCTION

When evening comes and twilight gradually falls, a different expression appears on the face of the city. At about the time that street lamps begin to light here and there and neon signs show brightly, all the ugliness sinks into darkness. Like a picture on the black canvas, lights and bright objects alone create the city. The buildings and structures clearly seen during daylight disappear into the darkness of night and only lights appear, creating a completely different city as in the positive and negative images of a photograph.

The monotonous sameness of nightscapes of the Japanese archipelago, whether large or small, has changed in the last few years; there is now a feeling of individual character. This is the result of more people becoming aware of the relationship between cities and light.

The movement toward the application of light to create individual city nightscapes has become more widespread. Changing the daytime appearance of a city would require a long period of time and tremendous cost. In comparison, it is easy to create a new nightscape.

The application of light, not only to existing landmarks, but to newly constructed landmarks as well, answers the demand by local citizens for invigoration of the neighborhood.

When new roads are constructed across seas and rivers, new bridges are built. Among these, some bridges are intended to become new city landmarks from the planning stages. In other cases, local citizens, seeing the bridge under construction, are increasingly voicing their desire to see the bridge illuminated. The light from a bridge clothed in new lighting against the background of the dark sea reflects off the water's surface.

There is a pleasant flickering interplay of water and light. As dusk falls, people gather at the waterfront to look at the bridge. A new time is born and new places are built in the surrounding areas.

Fortunately, I have been carrying out many lighting design for bridges up to this time, not only designed lighting for new, large-scale bridges, but also for the rejuvenation of old bridges. I would like to introduce my representative projects among them.

The following seven examples indicate my approach to the lighting of bridges.

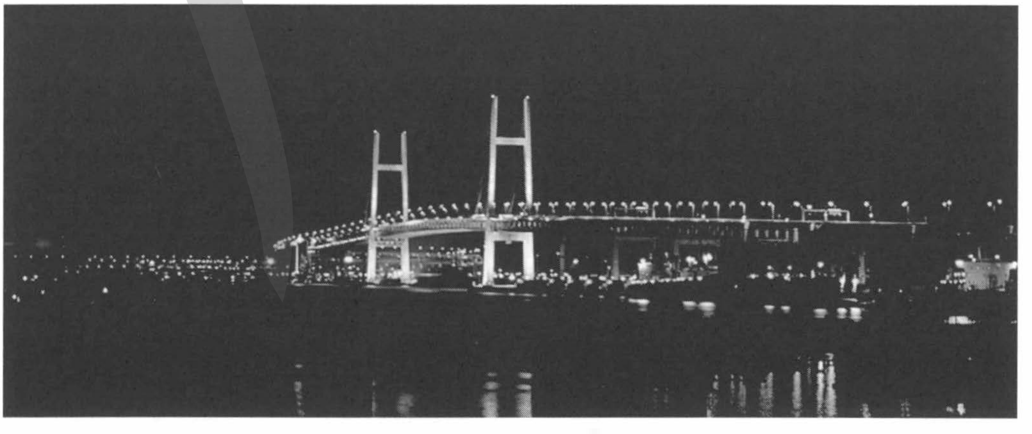

Photo 1 Yokohama Bay Bridge

2 REPRESENTATIVE WORKS

2.1 Yokohama Bay Bridge

The Yokohama Bay Bridge, spanning the entrance to Yokohama Bay between Honmoku and Daikoku Piers, ranks among the world's largest cable suspension bridges. The main tower stands 172m tall and the suspended roadway is 860m long.

The city of Yokohama, with its long history as a seaport, is currently holding several events including "Minato Mirai 21" as part of its development plan for the future and to emphasize the special characteristics of the city. Among these is the beautiful Yokohama Bay Bridge which has become an important city landmark. Bearing this in mind, the main goal of this lighting plan was to dramatize the grand scale and splender of the bridge. Three points -appearance, selection and emphasis-formed the basis for blending and enhancing the particular features of the bridge to create the attractive nighttime illumination.

In addition to overall floodlighting, the tops of the main towers of this bridge are lit up in blue. The blue lighting is set to go on at fifteen minutes before each hour and to go off on the hour.

While providing a time signal, it also adds a slowly varying color to the bridge, shining brightly against the background of the sea; one of my goals was to express the passage of time in lighting design.

Before deciding the color of the lighting, on-site experiments were carried out using various colors. We also asked the Tokyo Metropolitan Expressway Public Corporation and Yokohama City for their suggestions.

The bridge lighting was turned on in fall, 1989, during the period in which the Yokohama Exotic Showcase was being held. Since then, the bridge has continued to gain popularity as a new Yokohama landmark.

2.2 Millennium Light Up of Yokohama Bay Bridge

Bay Bridge, which acts as a gateway to Yokohama Port, completely changed its appearance from the familiar white and blue light up, to the brilliant color of dawn with an image of the dawn of the 21st century. It was enough to make viewers imagine the visit of the dawn of a new era in the city of Yokohama which has always been ahead of its time.

2.3 The Eitai Bashi Bridge, Tokyo

The Sumida River has been an important part of history since Tokyo was known as Edo.

The bridges spanning this river play an important role from the points of view of traffic, industries and people's daily lives. Recently, Tokyo has again begun to pay more attention to the upgrading of these bridges, with the goal of creating a better atmosphere for people.

Work on the bridges and surrounding parks included in this project has been progressing, and special lighting comprises one of the important aspects of work on the bridges.

The special lighting for Eitai Bashi is a first for a bridge spanning the Sumida River.

Its beautiful arch is enhanced by the placement of 40W fluorescent lamps as interval lighting of blue color. 100W self-ballasted mercury lamps set on the railing provide continuous lighting in combination with the arch lighting.

In addition, wide-angle HQI 150 and 250 uplights enhance the diagonal view of the bridge supports and the view from the roadway.

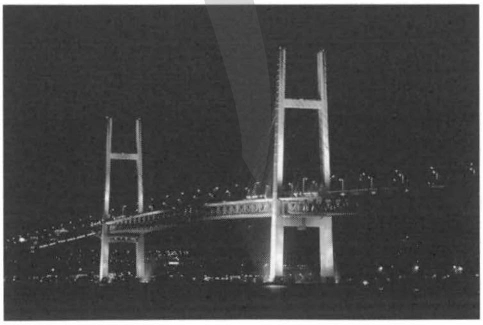

Photo 2 Millennium Light Up of Yokohama Bay Bridge

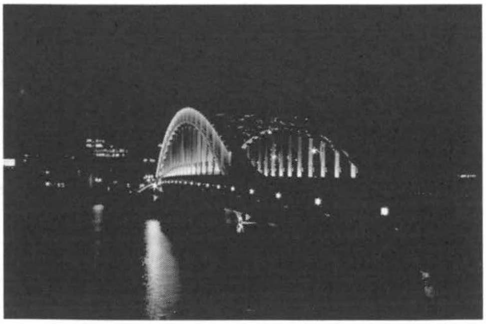

Photo 3T he Eitai Bashi Bridge, Tokyo

2.4 Rainbow Bridge, Tokyo

Completed in summer 1993, Rainbow Bridge spanning in Tokyo Bay is expected to ease traffic congestion in Tokyo by becoming a trunk access to the coastal heart of metropolitan "Tokyo Teleport town." The beautiful white structure adds an effective but useful accent to the Tokyo Water Front scenery. It became also popular as a new Tokyo Landmark.

The view was considered from the initial stage of the project, and lighting was a part of the master plan. Following studies conducted over several years, the bridge was completed. Lighting for the bridge comprises four elements: towers, cables, girders and anchorage.

These elements harmonize beautifully to form a single entity, while still maintaining their individual character. Lighting is varied with season, day and time to produce a complex spectacle, which is also effective from the point of view of ecological balance. Main tower lighting color is slightly varied for the seasons (white in summer, a warmer white in winter) but the effect is more psychological than visual.

This cable suspension bridge is more than 800m length. Special feature of this bridge is the illumination installed at the cable.

Cables are lighted using three different-colored 18W non-electrode lamps per unit: white, a neutral public color; green, the image color of Tokyo symbolizing the waterfront; and coral, symbolizing the dawn of the 21st century. The lighting pattern was designed to suit day, time and specific event. Special consideration was also given to energy saving and the environment, resulting in the use of solar batteries to generate 40% of the power used for cable lighting and the development of a floodlight with high-precision light distribution and minimal leakage of light to the sky.

2.5 Millennium Light Up of Rainbow Bridge

To produce scenery with a strong impact symbolic of the beginning of the year 2000, a simple, safe and highly effective dramatic light-up was implemented by temporarily adding special filters to existing floodlights used for the normal lightup of Rainbow Bridge, which spans Tokyo Bay. The bridge towers were tinted in the colors of the rainbow, as its name indicates, and illumination of the cables brilliantly decorated the moment of the countdown of the century.

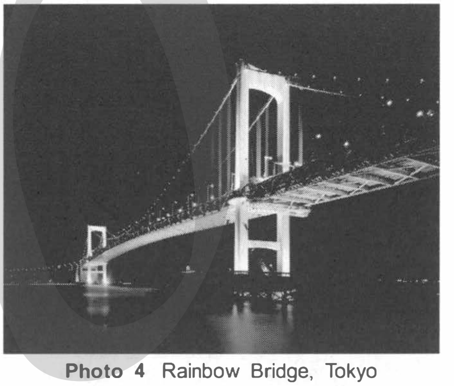

Photo 4 Rainbow Bridge, Tokyo

2.6 Kaita Bridge, Hiroshima

In response to the huge Torii gate for the Itsukushima Shrine, which is located in the ocean west of Hiroshima, lighting for the Kaita Bridge was planned as another gate for the port in the east.

Blue-filtered floodlights installed in bridge footings, two green-filtered floodlights on the underside of the span and indirect lighting provided by fluorescent lamps installed on girders provide dramatic lighting for this bridge. Intensity decreases gradually from the center, making the ends of the bridge seem to disappear into the darkness.

Construction took three years. The basic design was made in the first year, on-site lighting tests carried out in the second and, using the data obtained from these tests, the final design was executed and completed during the third year.

A committee was formed to confirm navigational safety and local citizens' opinions were gathered. Completion coincided with the holding of the Asian Games in summer, 1994, and the bridge has been lit until midnight every day since then.

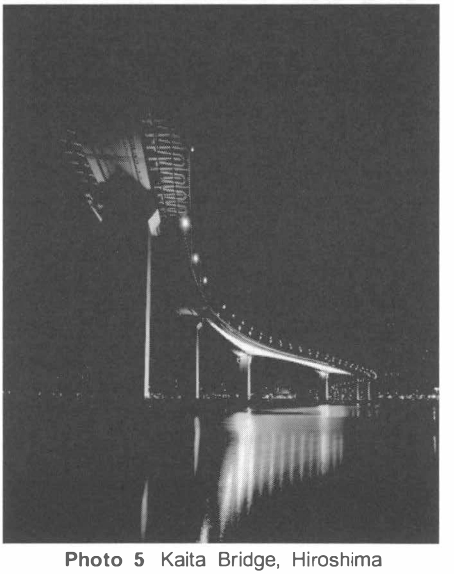

Photo 5 Kaita Bridge, Hiroshima

2.7 Sakuranomiya Bridge, Osaka

Sakuranomiya Bridge, called the "Silver Bridge," has the heavy, classical form typical of the early 20th century. The characteristic truss arch is emphasized by horizontal floodlighting.

The curved arch is floodlit and new bracket lights in the image of the original cast-iron fixtures on pillars provide vertical illuminance. Warm light for both the inside and outside the guard box gives the feeling that someone is standing watch. In addition to the regular floodlighting, festive light patterns are preset for the Tenjin Festival and others, when gold lights shine on the center and end hinges of the arch and colored foodlights light up the upper truss. Due to restrictions on the placement of fixtures, repeated on-site studies and tests were carried out to position lights and original louvers were designed to minimize blare affecting drivers. Through the application of various technological innovations, the historical bridge shines as if awakened, creating a panoramic scenic continuity with the neighboring Sakuranomiya Park representative of Osaka, the "City of Water."

2.8 Meiko Triton (Ise Bay Highway), Nagoya

Opened in March, 1998, the Meiko East, Central and West Bridges spanning Ise Bay in Nagoya are each one-kilometer long cable suspension bridges. The white central span seems to stretch its wings to the blue east and red west spans which provide a colorful accent to the scenery; the three spans are collectively called the Meiko Triton. For the light up, consideration was given to marine safety and the environment: light dispersion was controlled, energy requirements were kept low and existing fixtures were used; the colors and shapes of each span were considered and the lighting designed to give the impression of continuity.

Lighting for the Meiko Central Bridge enhances its beautiful shape and white color, which extends even to its cables. Basic white lighting gives the impression of a pair of which wings. Seasonal lighting shines inside the towers every hour for 10 minutes: forest green in spring, sea/sky blue in summer, yellow-green of leaves in fall and red of fire in winter, giving the bridge a changing expression against the brilliant whiteness of the basic white lighting.

Along with the color combination and gradations adjusted though repeated experiments, five special light-up programs, i.e. red and green for Christmas blue for Ocean Day etc., were set up emphasizing the presence of Nagoya's new landmark. Lighting for Meiko Central Bridge received the Paul Waterbury Award for Outdoor Lighting, Special Citation from the Illuminating Engineering Society of North America, in 1998.

Photo 6 Meiko Triton (Ise Bay Highway), Nagoya

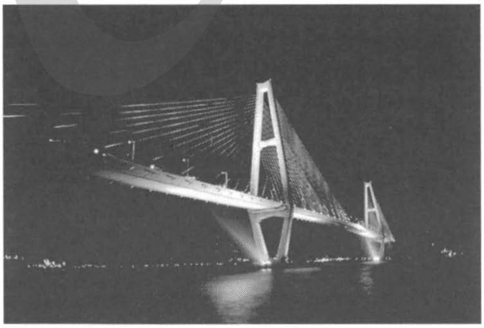

Photo 7 Meiko Central Bridge (Ise Bay Highway)

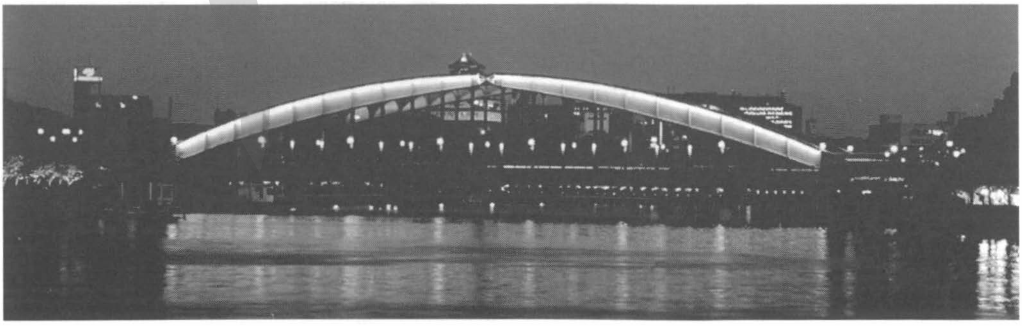

Photo 8 Sakuranomiya Bridge, Osaka

2.9 Akashi Kaikyo Bridge, Hyogo

To create a world-class nightscape for this, lighting was looked at from various points of view such as symbolism, internationality and universality. The four-kilometer length of the bridge and the height of the towers (taller than Tokyo Tower) were emphasized and made to stand out against the night sky.

After five years of planning, we decided to use high-illuminance, long-life induction lamps, which would be maintenance-free for 20 years, for the main cable and installed an exclusive system to provide stepless variation in color and light patterns.

As benefits its name, "Pearl Bridge," the white lighting is given slightly different hues for the seasons (peal pink, pearl yellow, etc.). On the hour, a rainbow pattern decorates the night sky, while a different birth stone indicates each half hour. There are a total of 28 light patterns with a variety of preset programs for regular days, holidays and other special occasions. The green-gray main towers are lit up in a refreshing white color; louvers are provided on all fixtures to adjust the light for marine workers and the environment.

Thus the illumination for the world's longest suspension bridge was born in consideration of peaceful coexistence with nature and the area. The new night scene is receiving wide acclaim.

This area is also very famous for fishery. So we carefully planned to keep natural environment not to brighten too much the sea. And also consideration was given to ships passing below.

The lighting for the Akashi Kaikyo Bridge received the Paul Waterbury Award for Outdoor Lighting, Award of Excellence from the Illuminating Engineering Society of North America, in 1998.

2.10 Bridge of Light

Bridges are not only practical. They also link different fields. Linking one thing with another reminds us of a bridge. Time passes and a bridge spans the eras. A bridge spanning several hundred years of time-space links us with the structures built during that age. Cultural properties from another time, when bathed in light, are linked with the present via the Bridge of Light. This is when the great power of light can really be sensed.

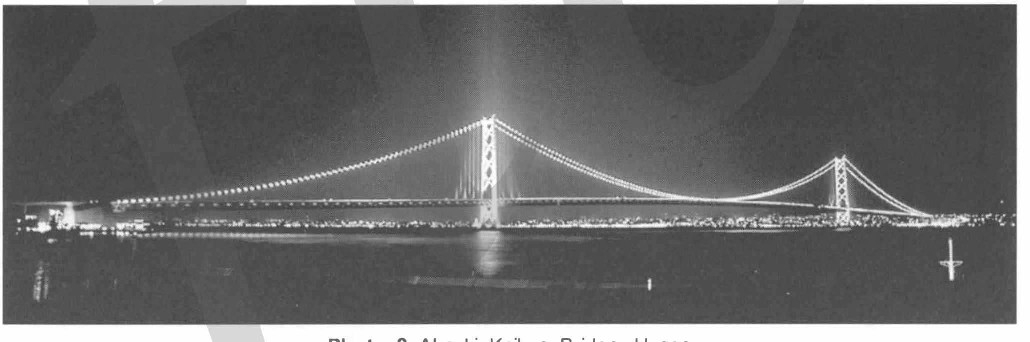

Photo 9 Akashi Kaikyo Bridge, Hyogo

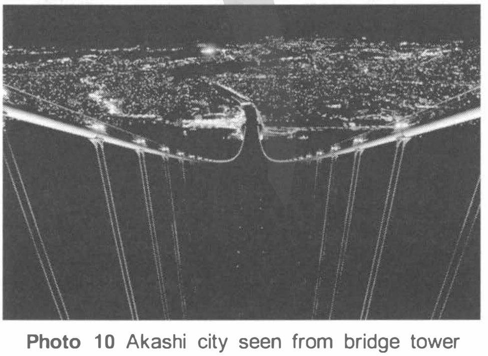

Photo 10 Akashi city seen from bridge tower

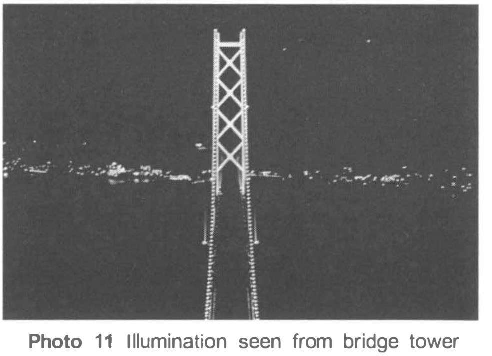

Photo 11 Illumination seen from bridge tower

Photo 12 Rainbow Bridge, 21st Century Special Light Up

As in the previous year, we held a light-up event at Tokyo Bay's Rainbow Bridge to celebrate the new year. To create bright rainbow colors suitable to raise the curtain on the 21st century, we increased the lighting and rethought light sources, to achieve a more effective result than last year. Further, to permit people to enjoy the cable illumination at once, we specially changed the program so all patterns would be displayed in 13 minutes, rather than once a day, painting a brilliant curtain raiser for the new century.

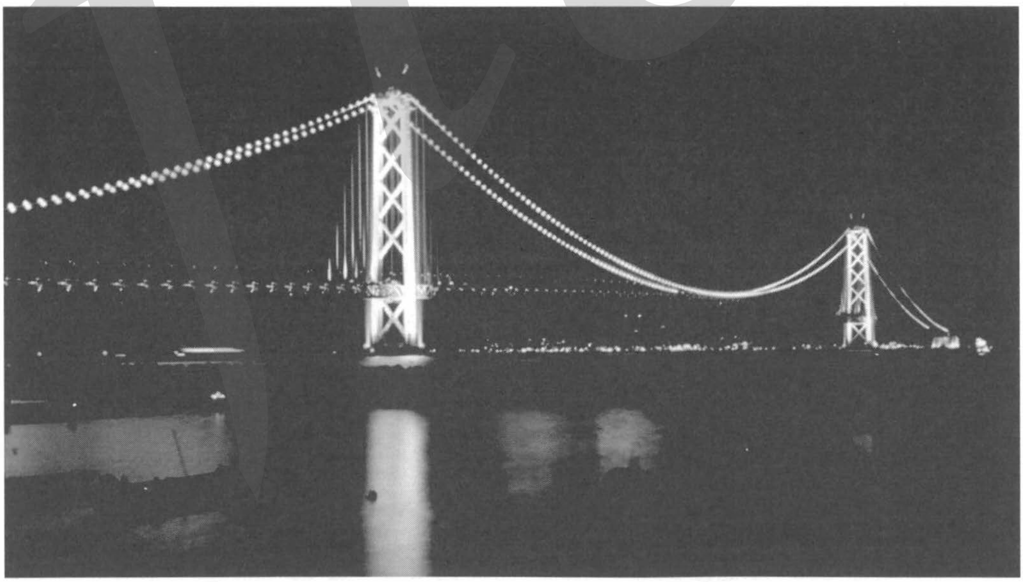

Photo 13 Akashi kaikyo Bridge, Rainbow pattern

THE INNOVATED TECHNOLOGY ON PRESTRESSING SYSTEM DEVELOPED BY JAPAN HIGHWAY PUBLIC CORPORATION

Tsutomu Kadotani
Japan Highway Public Corporation

Keywords: transparent sheath, pre-grouted internal tendon, innovated anchorage and coupler corrugated steel web

1. INTRODUCTION

There exist many corrosion problems caused by the improper grouting in prestressing tendons and they are very serious all over the world.

Japan Highway Public Corporation (JH) has developed the innovative technology for both internal and external tendons to overcome the problems and to improve the durability of the prestressed concrete structures. We call it JSAS system.

2. INNOVATED TECHNOLOGY ON THE PRESTRESSING CABLE SYSTEM

The innovated technology is shown in Fig.2, in comparison with the conventional method (Fig.1).

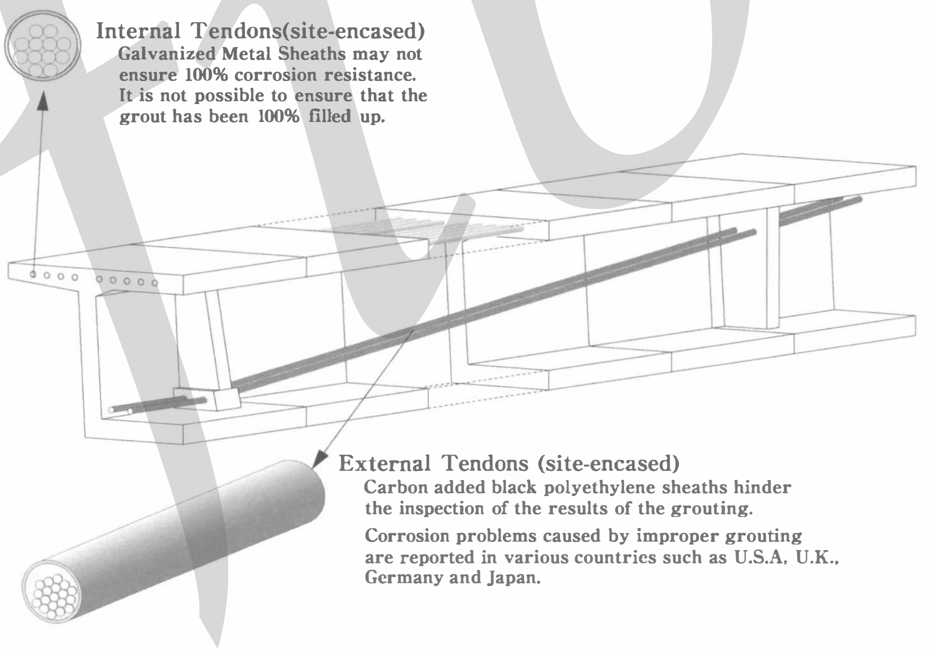

Fig.1 Conventional tendon layouts

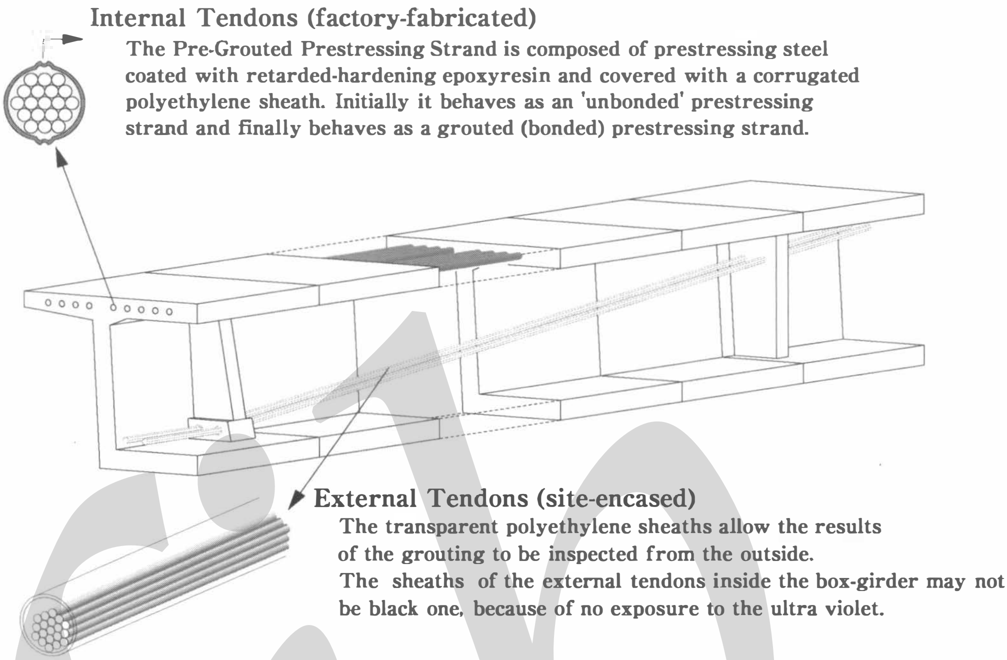

Fig.2 Innovated technology on the prestressing cable system

2.1 The transparent sheath

The transparent sheath is made from ethylene-based copolymers and allows the results of the grouting to be inspected from the outside. It is ensured that the strength is capable of withstanding bearing pressure due to deviation, in the same manner as conventional carbon added black polyethylene sheath. (Fig.3) Also, just in case air voids are formed in the sheath, they can readily be reinjected as shown in Fig.4. Fig.5 shows an example of applying the transparent sheath.

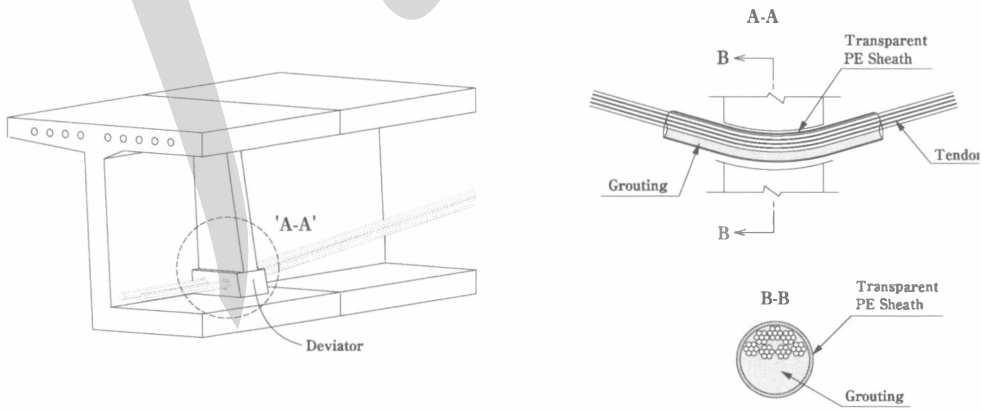

Fig.3 Deviator

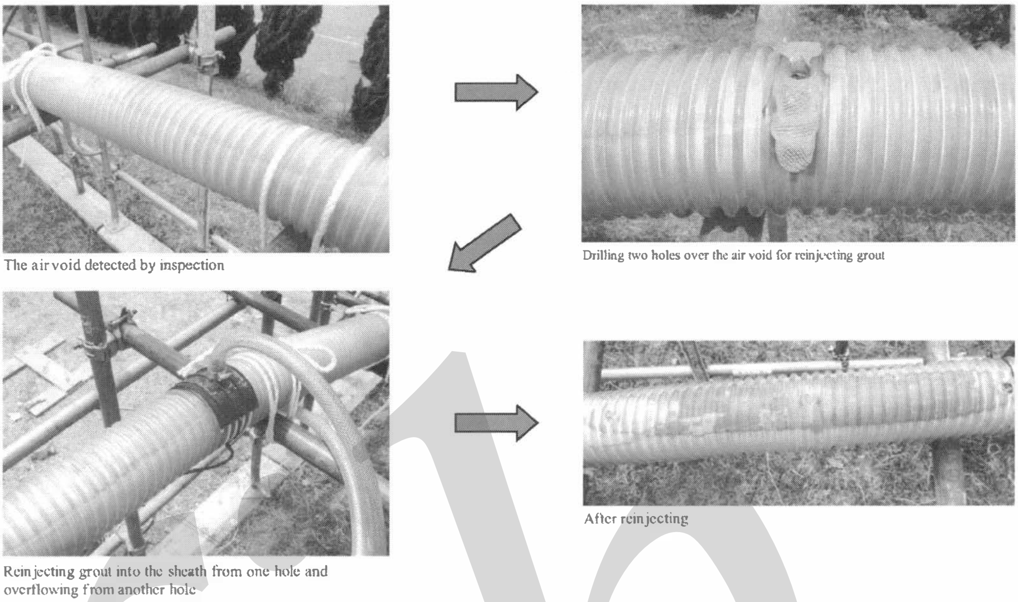

The air void detected by inspection

Drilling two holes over the air void for reinjecting grout

Reinjecting grout into the sheath from one hole and overflowing from another hole

After reinjecting

Fig.4 How to reinject grout into the air void in the transparent sheath

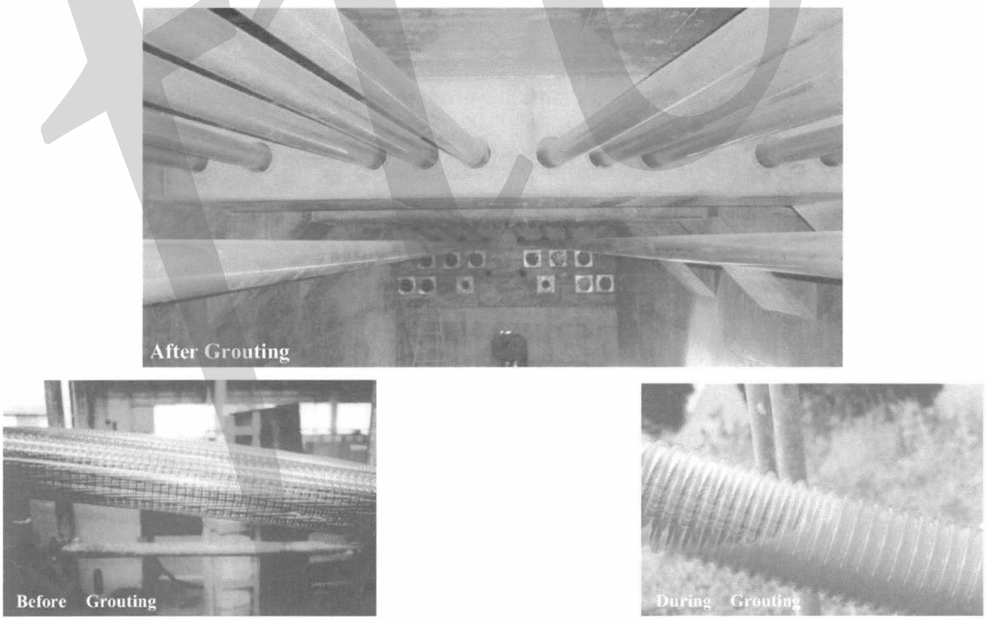

Fig.5 Example of applying the transparent sheath

2.2 Pre-grouted internal tendon

The pre-grouted internal tendon is applied as shown in Fig. 6. It is composed of prestressing steel strand coated with special epoxy resin and covered with a corrugated polyethylene sheath. (Fig.7) The advantages of the pre-grouted internal tendon are shown in the following;

- 100% grouting
- No grouting process at site
- Double corrosion protection by sheath and epoxy resin
- Stronger bond performance with concrete than conventional cement grout
- Lower and stabler friction during prestressing

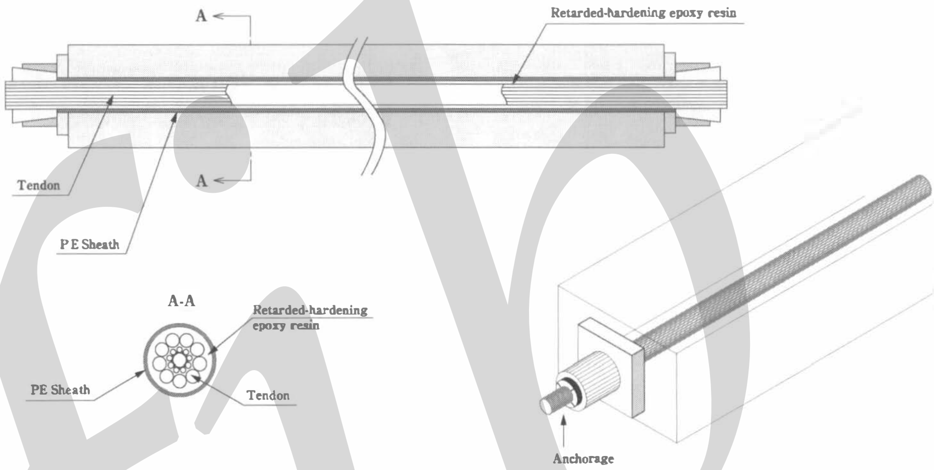

Fig.6 Internal tendons using pre-grouted prestressing strands

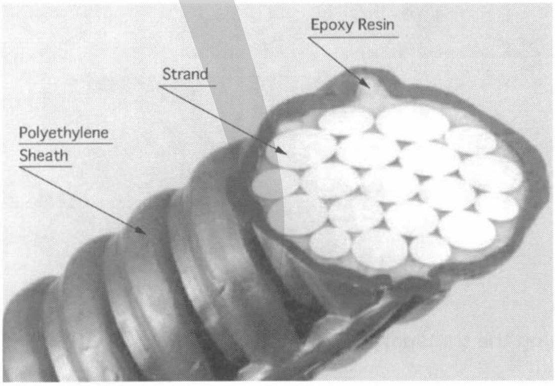

Fig.7 Pre-grouted prestressing strand

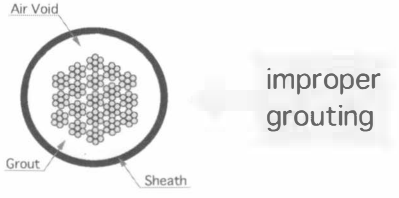

(The disadvantage of conventional grouted tendon)

2.3 Innovated anchorage and coupler

The innovated anchorage and coupler system has been developed for the pre-grouted internal tendons, and is shown in Fig.8.

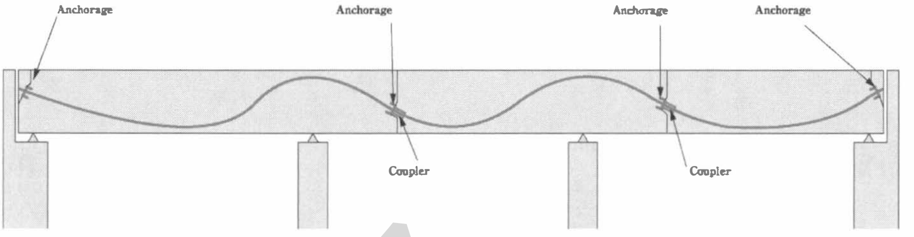

Anchorages

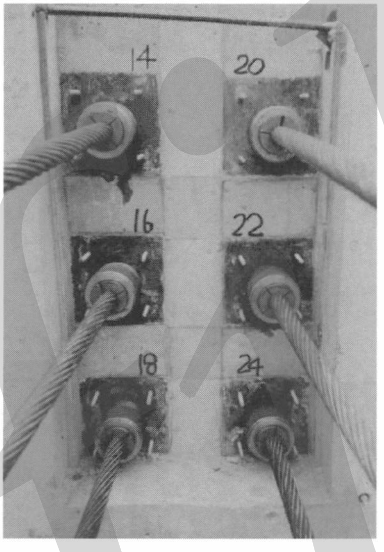

Couplers

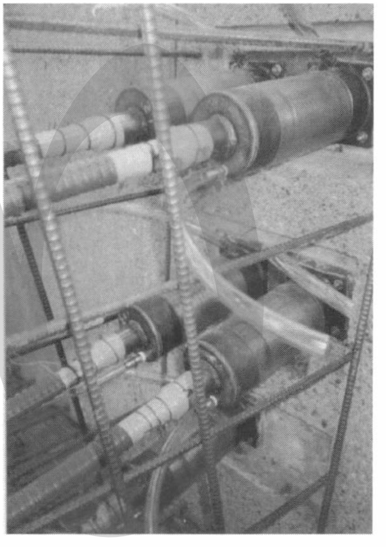

Fig.8 Innovated anchorage and coupler

2.4 Corrugated steel web

Advantages of corrugated steel web are shown in the following;

- Economical superstructures and substructures due to smaller dead load than conventional concrete webbed box girder
- Effective prestressing force to the slabs due to the accordion effect of corrugated web
- Enhanced capacity against buckling

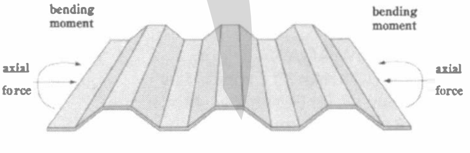

accordion effect

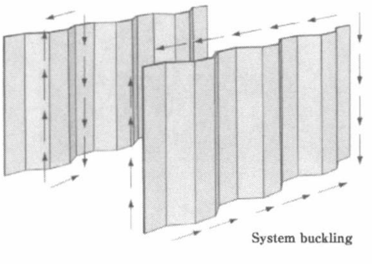

enhanced capacity against buckling

3. APPLICATION OF INNOVATED TECHNOLOGY

3.1 Application of pre-grouted internal tendons

(1) For hollow slab type structure constructed on stationary falsework

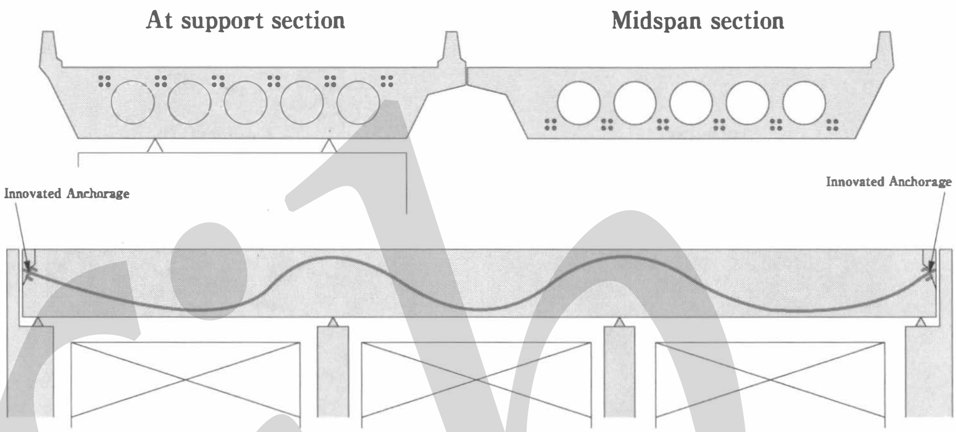

Unreeler for Pre-Grouted prestressing strand

NAME: JUGOSAWAGAWA Bridge
-The HOKKAIDO Expressway-
TYPE: 3-Continuous PC hollow-slab Bridge
SPAN: 23.6+32.5+25.3m
LOCATION: HOKKAIDO Pref. JAPAN

(2) For viaduct structure constructed by formwork launching girder

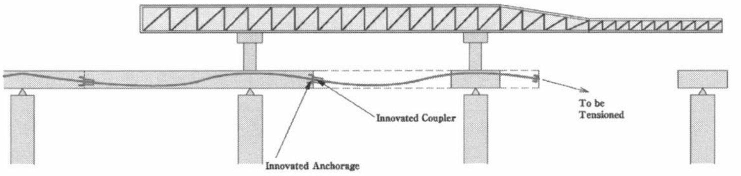

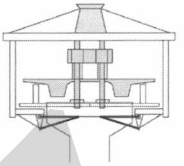

NAME: SHIKIJI Viaduct – The Second TOMEI expressway –
TYPE: 12-Continuous PC hollow-slab Bridge SPAN: 26+9@28.5+2@25.5
LOCATION: SHIZUOKA Pref. JAPAN

3.2 Application of pre-grouted internal tendons and transparent PE sheathed external tendons

(1) For cantilever-constructed bridge

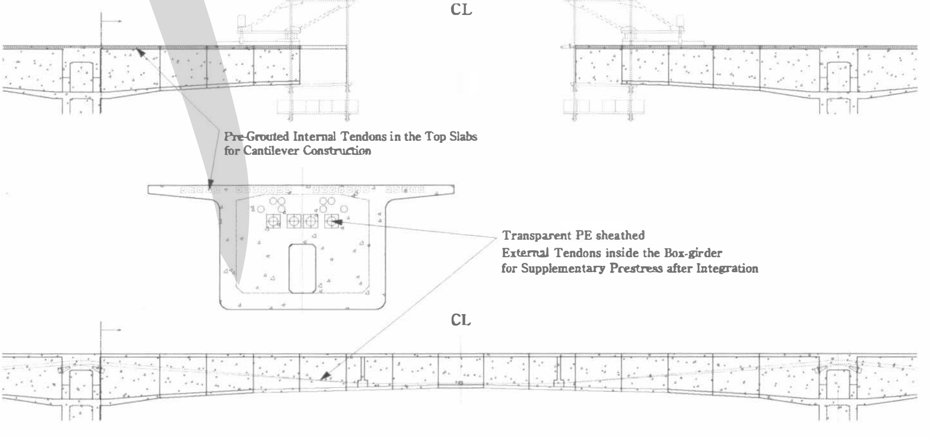

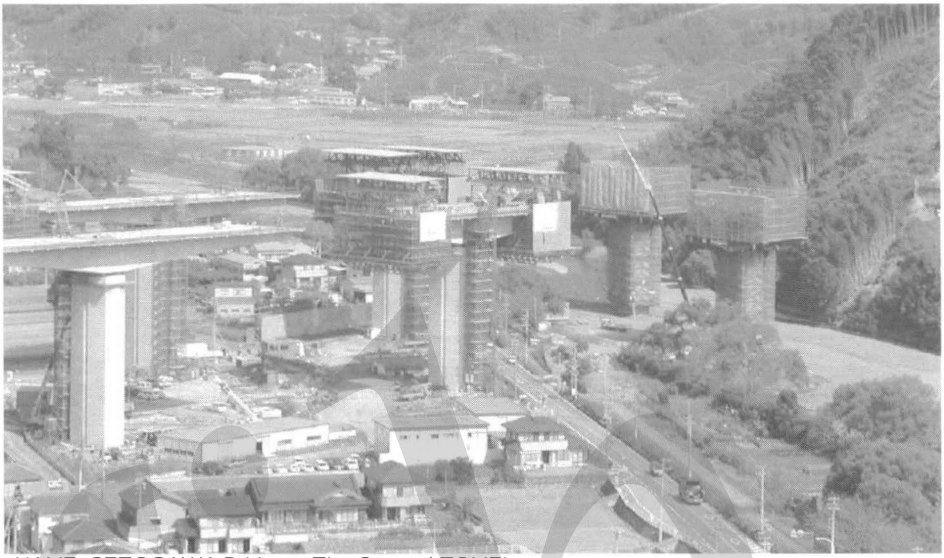

NAME: SETOGAWA Bridge – The Second TOMEI expressway –
TYPE: 11-Continuous PC box girder Bridge
SPAN: A Line 40.4+6@44.5+2@73.5+86+88.3m B Line 42.4+2@44.0+54.5+93.0+97.0+85.8m
LOCATION: SHIZUOKA Pref. JAPAN

NAME: TENRYUGAWA Bridge – The Second TOMEI expressway –
TYPE: 23-Continuous PC box girder Bridge
SPAN: 35.6+3@43+60+92+12@85.5+64.5+3@45+41.1m
LOCATION: SHIZUOKA Pref. JAPAN

(2) For corrugated steel webbed box girder

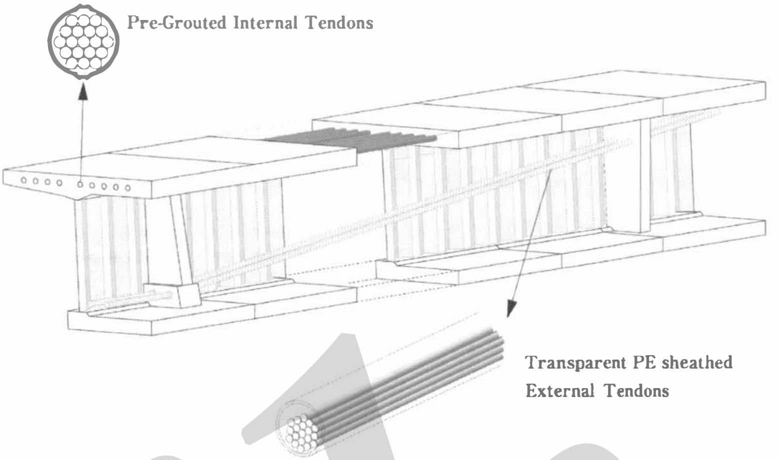

NAME: The second OHUCHIYAMAGAWA Bridge
-The KINKI Expressway-

TYPE: 7-Continuous PC Rigid frame Bridge
with corrugated steel web
SPAN: 49+2@66+120+57+43+34m
LOCATION: MIE Pref. JAPAN

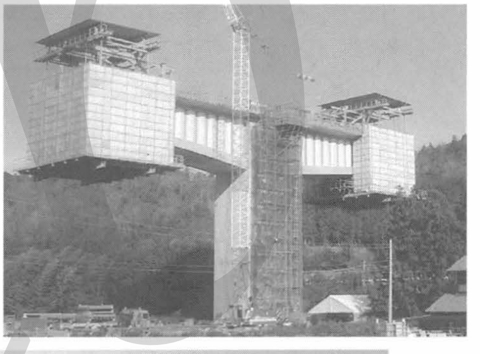

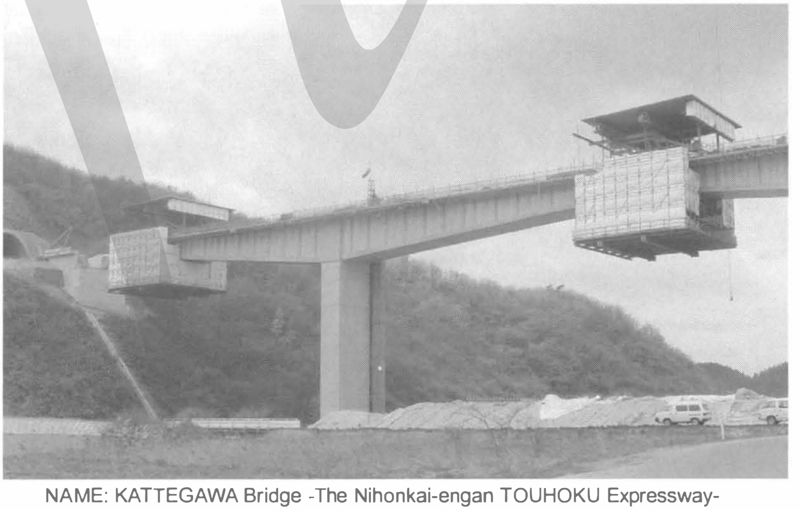

NAME: KATTEGAWA Bridge -The Nihonkai-engan TOUHOKU Expressway-
TYPE: 3-Continuous PC Rigid frame Bridge with corrugated steel web
SPAN: 59.3+96.5+69.8m
LOCATION: AKITA Pref. JAPAN

(3) For extradosed PC bridge with corrugated steel webbed

General view

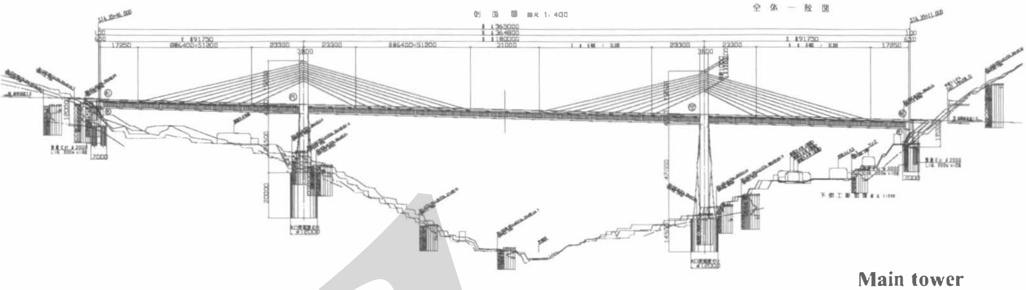

Main tower

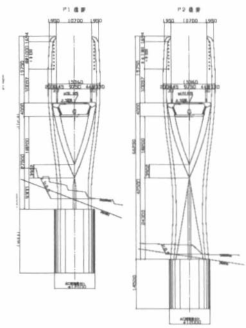

Cross section

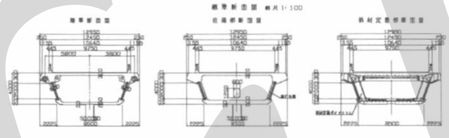

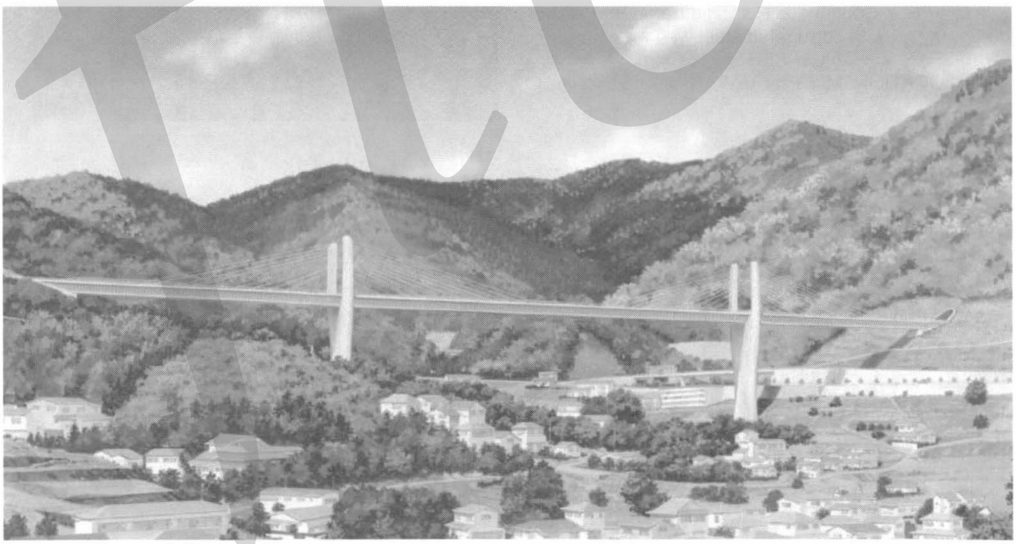

NAME: HIMI Bridge – The NAGASAKI expressway –
TYPE: Extradosed PC bridge with Corrugated Steel Webbed
SPAN: 91.75+180.0+91.75m
LOCATION: NAGASAKI Pref. JAPAN

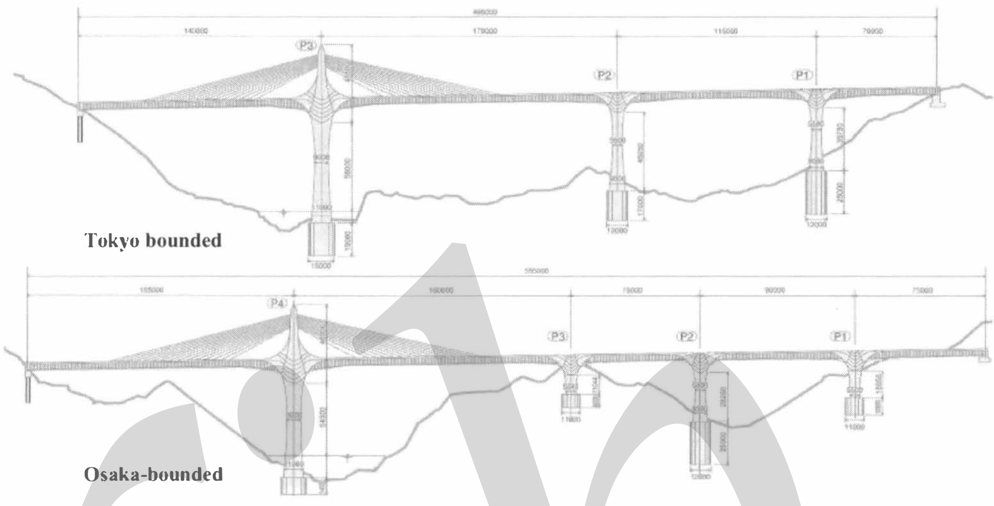

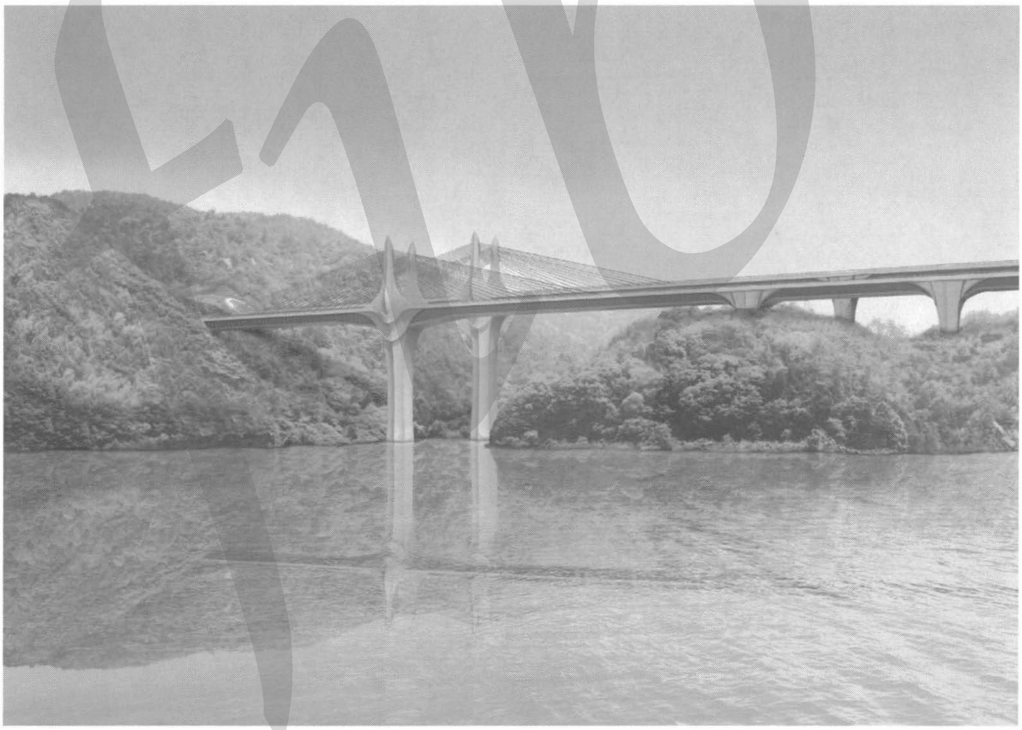

NAME: RITTOH Bridge – The second MEISHIN expressway –
TYPE: Extradosed PC bridge with Corrugated Steel Webbed
SPAN: Tokyo-bounded 140+170+115+70m
Osaka- bounded 155+160+75+90+75m
LOCATION: SHIGA Pref. JAPAN

(4) For cable stayed PC bridge with corrugated steel webbed

General view

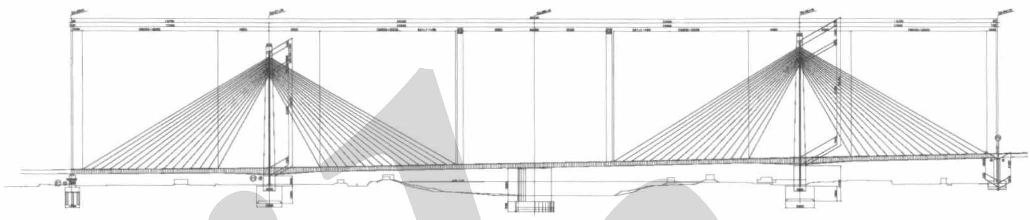

Cross Section at PC Grider — Midspan section | at support section

Cross Section at M Grider — Midspan section | at support section

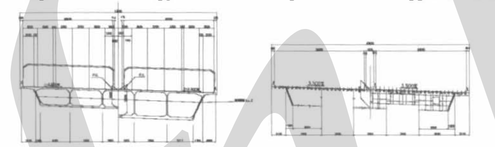

P2

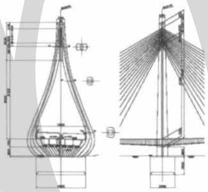

P4

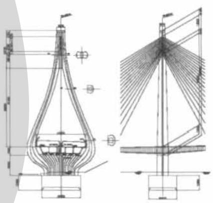

NAME: YAHAGIGAWA Bridge – The second TOMEI expressway –
TYPE: Cable stayed PC bridge with Corrugated Steel Webbed
SPAN: 174.7+2@235.0+174.7m
LOCATION: AICHI Pref. JAPAN

FUTURE OF EXPERIMENTATION AND SIMULATION IN REINFORCED CONCRETE RESEARCH

Catherine French
Department of Civil Engineering
University of Minnesota
U.S.A.

Keywords: reinforced concrete, seismic, experimentation, simulation, database

ABSTRACT:

Historically experimentation has been a cornerstone to the advancement of our knowledge of the behavior of reinforced concrete structural systems. Simulation integrated with experimentation has provided researchers with the ability to extend those experimental results to a broad range of applications. This paper will present an overview of some of the key advancements that have been made through this integrated approach to research. A perspective will be provided regarding the potential impact of programs such as the George E. Brown, Jr., Network for Earthquake Engineering Simulation (NEES) on the transformation of future research. This program represents an $82 Million investment in networked research equipment infrastructure that will be available as an international resource.

1 INTRODUCTION

The paper begins with a brief overview of the history of code development for reinforced concrete structural systems and integrated research efforts primarily between the United States and Japan that have been undertaken over the years to investigate the behavior of reinforced concrete structural systems in seismic regions. It also summarizes the development of experimental techniques that have been used and continue to be further developed including quasi-static cyclic testing, shake table testing, pseudo-dynamic testing techniques, effective force testing and hybrid methods to investigate structural behavior. Finally, a description is provided of the National Science Foundation (NSF) George E. Brown, Jr., Network for Earthquake Engineering Simulation (NEES) program that is intended to transform research into an integrated collaborative approach of experimentation combined with simulation.

2 BACKGROUND OF CODE DEVELOPMENT FOR REINFORCED CONCRETE STRUCTURAL SYSTEMS IN SEISMIC REGIONS

Although the San Francisco earthquake of 1906 produced devastating structural damage, it was not until 1927, following the 1925 Santa Barbara Earthquake, that the first explicit seismic provisions were introduced in the United States when the Pacific Coast Building Officials Conference, predecessor to the International Conference of Building Officials (ICBO), developed non-mandatory provisions in an appendix to the first edition of the *Uniform Building Code* (UBC). In parallel, several California municipalities adopted a range of mandatory earthquake provisions in their building codes. It was not until the early 1960's that seismic design recommendations became more or less standardized in the United States when the Structural Engineers Association of California (SEAOC) incorporated recommendations from the Seismology Committee into its building code, followed by adoption by the in the Uniform Building Code (UBC) in 1961 [1]. In 1961, the Portland Cement Association published a landmark publication by J.A. Blume, N.M. Newmark, and L.H. Corning, *Design of Multi-story Reinforced Concrete Buildings for Earthquake Motions* [2], which provided additional momentum for the construction of multi-story reinforced concrete buildings in regions of high seismicity.

Special provisions for earthquake resistant design of reinforced concrete structures were first introduced into the *American Concrete Institute Building Code Requirements for Reinforced Concrete (ACI-318)* in 1971 in an appendix. These original provisions were intended to apply to reinforced concrete structures in regions of high seismicity with substantial reduction in total lateral seismic force (compared with that calculated assuming elastic response) in anticipation of inelastic behavior. In conjunction with the addition of the appendix, changes were incorporated into the main body of the code to improve toughness and to increase resistance to ensure structural integrity in regions where there is likelihood of only light or moderate earthquake damage. The 1983 edition of ACI 318 was extensively updated to include current knowledge and requirements for special detailing were added for frames of moderate seismic risk. The appendix was moved to the main body of the code in 1989 as Chapter 21. Since that time, additional provisions have been added to address special reinforced concrete structural walls, coupling beams, and foundations. In 2002, provisions were added to address precast concrete structures in regions of moderate or high seismic risk. Types of precast systems included in the 2002 edition [3] include special moment frames, special structural walls, and intermediate walls. The design provisions for precast moment resisting frames are intended to result in structural systems, which emulate reinforced concrete special moment resisting frames. The precast frames may be designed with either "strong" connections, which remain elastic while adjoining members develop plastic hinges, or "ductile" connections, which undergo yielding within the connection elements, as a result of the design displacements. In the case of strong connections, capacity design concepts, first introduced in New Zealand [4,5], are used to ensure the connection remains elastic as the plastic hinges develop in selected regions of the structure. Precast frame systems which do not fall under either of these categories are required to be validated by laboratory testing and numerical analyses following the protocol of ACI T1.1-01 [6], where it must be demonstrated that the proposed system has strength and toughness equal or exceeding that of a comparable monolithic frame.

Across, the Pacific, Japan first introduced the concept of seismic design in 1924 following the Kanto earthquake of 1923 [7]. One of the eminent engineers of Japan, Dr. Tachu Naito, Professor of Architecture at Waseda University in Tokyo, had designed several buildings to withstand a lateral force equal to 1/15th of their weight, including the Kabuki Theater in Tokyo, which came through the Kanto earthquake undamaged. Dr. Naito was a proponent of designing stiff, braced structural systems to keep their natural period short and out of resonance with the ground motion. He indicated that the building should have a complete closed rectangular shape in plan, that rigid walls should be used abundantly, placed symmetrically in plan and continuous over the height of the structure; and that lateral forces should be assigned to the bents of the building in accordance with the rigidity of the elements. In 1933, the Architectural Institute of Japan (AIJ) published the *AIJ Standard for Structural Calculation of Reinforced Concrete Structures*. The building Standard Law Enforcement Order in Japan was revised and put in force from June 1981, which resulted in a significant change in the earthquake resistant design of reinforced concrete structures by introducing the concept of ductility design in Japan. In Japan, there are two-levels of earthquakes that must be considered in design. Allowable stress design is used for low-level earthquake loading, whereas ultimate strength is used in evaluating the collapse mechanism for extreme events. The 1990 edition of the AIJ *Design Guidelines for Earthquake Resistant Reinforced Concrete Buildings Based on the Ultimate Strength Concept* and 1991 edition of the AIJ *Standard for Structural Calculation of Reinforced Concrete Structures*, were translated into English in 1994 [8]. A brief history of the development of Japanese seismic design requirements can also be found in Reference [9].

3 DEVELOPMENT OF AN INTEGRATED RESEARCH EFFORT TO INVESTIGATE THE BEHAVIOR OF REINFORCED CONCRETE STRUCTURAL SYSTEMS

The need for coordinated international research programs for the investigation of the behavior of structural systems was identified more than a quarter century ago by the U.S.-Japan Panel of Wind and Seismic Effects, United States-Japan National Resources (U.J.N.R.) Program, which adopted the following resolution at the conclusion of their sixth joint meeting held in Washington, D.C., during 15-17 May 1974:

"...increased effort should be made in the near future to encourage joint research programs, especially in the area of mutual utilization of research facilities and the exchange of researchers."

A planning group was organized in 1977 to develop recommendations for a U.S.-Japan cooperative research program utilizing large-scale testing facilities to improve seismic safety practices. The reasoning and efforts behind the creation of the U.S.-Japan Cooperative Earthquake Engineering Research Program on the seismic performance of building structures is described in a paper by J. Penzien, H. Uemura, M. Watabe, and R. Hanson, entitled, "Introduction to U.S.-Japan Cooperative Earthquake Engineering Program," found in the American Concrete Institute Special Publication, ACI SP-84, *Earthquake Effects on Reinforced Concrete Structures – U.S.-Japan Research* [10]. The Joint Technical Coordinating Committee (JTCC) conducted the coordination for the program. Joseph Penzien and H. Umemura co-chaired the JTCC committee that coordinated Phase 1 – *Reinforced Concrete Structures* that featured the one of the first applications of large-scale pseudo-dynamic testing applied to a multi-degree of freedom structural system. Members of the JTCC for this project included V.V. Bertero, W.G. Corley, H.J. Degenkolb, R.D. Hanson, P.C. Jennings, J.O. Jirsa, R.C. Johnston, L.W. Lu, S. A. Mahin, J. Penzien, D. Rea, R.L. Sharpe, M.A. Sozen, J.K. Wight from the United States, and H. Aoyama, T. Hisada, B. Kato, M. Kasajima, Y. Mastsusima, T. Okada, M. Okamatsu, T. Okubo, M. Ozaki, S. Tani, H. Umemura, and M. Watabe from Japan.

The large-scale pseudo-dynamic test of the seven-story reinforced concrete frame-wall structure performed at the Building Research Institute, in Tsukuba, Japan, represented a design compromise between U.S. and Japanese building codes. The test was accompanied by complementary tests in Japan and the United States, which included quasi-static cyclic tests on beam-column joint subassemblages at the University of Texas at Austin, wall components at the Construction Technology Laboratories in Skokie, Illinois, shake table studies on 1/5th, 1/10th, and 1/12.5-scale models at the University of California at Berkeley, University of Illinois at Urbana-Champaign, and Stanford University, respectively.

One of the important outcomes of this test series was the identification of a flaw in planar analysis of frame-wall structural systems [11,12]. Conventional planar analysis led to a significant underestimation of the base shear strength of the structural system due to the unexpected contribution of the floor slab reinforcement to the flexural tensile strength of the longitudinal beams and due to the three-dimensional effects created by wall rocking. Design code modifications have been implemented to consider the effect of the additional tensile reinforcement in the slab when determining the relative ratio of column to girder flexural capacity.

This joint research program was followed up by several coordinated research projects focused on other types of building systems including the testing of a six-story steel braced frame structure, a masonry structure, and a composite steel/concrete hybrid system. In 1990, the coordinated research program returned its focus to concrete, with the initiation of the U.S.-Japan Precast Seismic Structural Systems (PRESSS) research program that consisted of three phases [13]. The first phase included a review of existing test data and the classification of connections based on type and function; the development of design concepts for structural systems; and the further development of inelastic time history analyses to numerically model the seismic response of precast systems. The second phase included tests on connections for precast beam-column frame systems and wall panel systems, followed by shake table studies, culminating in the test of a five-story precast test building at the University of California at San Diego during Phase III [14].

The results of this study included the classification of connection concepts and the development of connection details including new systems that take advantage of the jointed nature of precast concrete [15-17]. The investigation precipitated the development of design recommendations for precast concrete, recently incorporated in the 2002 edition of ACI 318 as discussed above [18].

In addition to the coordinated research efforts initiated by the UJNR Panel on Wind and Seismic Effects, researchers from a number of other countries have joined forces to further the understanding of reinforced concrete structural systems in seismic regions. In 1984, researchers from the United States, Japan, and New Zealand, met following the Eighth World Conference on Earthquake Engineering, to resolve differences in design approaches and test interpretations. The group conducted a coordinated series of tests on beam-column joints for which the joints were designed according to the provisions of the individual countries and subjected to a common bi-directional load history [19]. Researchers at Tongji University in China, followed suit with a test program that followed the objectives of the coordinated effort. In total, over forty participants were involved in four related meetings led by organizers, J.O. Jirsa, R. Park, H. Aoyama, and S. Otani.

The exchange of information among the countries has continued through joint workshops resulting in joint technical publications such as the report on high-strength concrete in seismic regions with contributions from researchers from the United States, New Zealand, Japan, Canada, and Australia [20]. One of the most recent coordinated efforts is the State-of-the-Art Report on the Seismic Design of Precast Concrete Building Structures, by the Task Group of Commission 7 of the International Federation of Structural Concrete (*fib*) nearing completion. Professor P. Pinto serves as the chair of Commission 7, with the Task Group co-convened by Deputy Chair, R. Park (New Zealand), and F. Watanabe (Japan), with additional contributors from Canada, Chile, Italy, Indonesia, Japan, Mexico, New Zealand, and the United States.

4 DEVELOPMENT OF EXPERIMENTAL TEST METHODS

Since the initiation of the U.S.-Japan Cooperative Research Program with the coordinated tests on the 7-story reinforced concrete frame-wall structure, some of the experimental test methods employed have undergone further development and improvement [21,22]. In addition, new test methods have been developed and are in implementation stages, and hybrid test methods have been proposed. The following is a brief summary of five test methods to investigate the effects of seismic loading on structural systems: quasi-static cyclic testing, shake table testing, pseudo-dynamic testing, effective force testing, and hybrid testing. In addition, where appropriate, a brief description of some of the capabilities of the experimental facilities being constructed as part of the National Science Foundation George E. Brown, Jr., Network for Earthquake Engineering Simulation (NEES) program is provided. Further discussion of the overall NEES research vision is discussed in Section 6.

4.1 Quasi-static cyclic testing typically involves the testing of a structural subassemblage such as a beam-column joint, wall, or portion of a multi-bay frame. The subassemblage is typically subjected to a load history consisting of a number of repeated cycles of increasing displacement amplitude that first characterize the structural response in the elastic range, and eventually take the structure into the inelastic range to drift ratios (where drift is the ratio of the lateral displacement to story height) exceeding three to four percent, or until failure.

Quasi-static cyclic testing can be used to investigate the behavior of existing structural systems, retrofit techniques, and new structural concepts. It is particularly useful for investigating the behavior of structural detailing such as beam-column joint reinforcement and anchorage requirements.

Typical tests are conducted unidirectionally. Multi-directional tests have consisted of a clover-leaf pattern of displacement (i.e., displace the structure in one direction and hold that displacement while subsequently displacing the structure in the orthogonal direction) due to the complex interaction of specifying the position of multiple actuators.

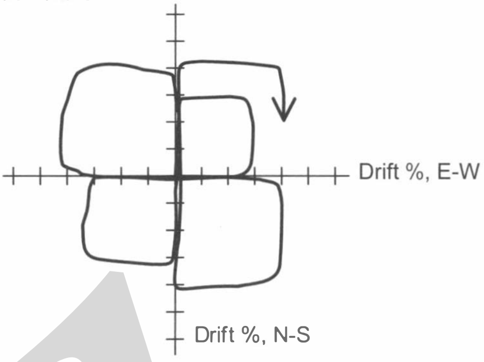

Fig. 1 Clover-leaf biaxial load history

As part of the NSF NEES program, a new laboratory is being constructed at the University of Minnesota to house a Multi-Axial Subassemblage Testing (MAST) system. The MAST system enables multi-axial cyclic static tests of large-scale structural subassemblages including portions of beam-column frame systems, walls, and bridge piers. The MAST system concept, employing a six-degree-of-freedom controller, can be used to apply realistic states of deformations and loading in a straightforward and reproducible manner.

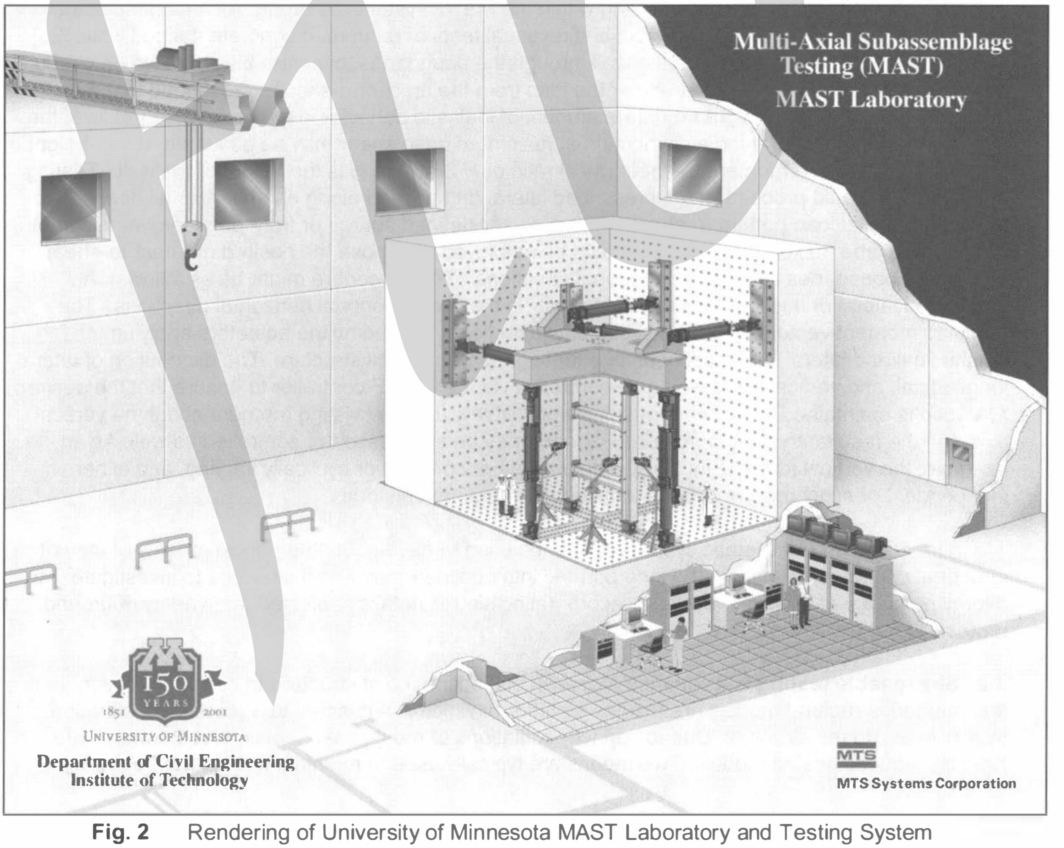

Fig. 2 Rendering of University of Minnesota MAST Laboratory and Testing System

The MAST system, shown schematically in Fig. 2, employs a stiff steel crosshead in the shape of a cruciform, which will be controlled with six-degree-of-freedom (6-DOF) control technology. Two sets of actuator pairs with strokes of ±400 mm will provide lateral loads up to ±3910 kN in the orthogonal directions. These actuator pairs will be secured to an L-shaped strong wall with universal swivels. Four ±1470 kN vertical actuators, capable of applying a total force of ±5870 kN with strokes of ±510 mm, will connect the crosshead and the strong floor. Horizontal clear distance between the vertical actuators can accommodate specimens up to approximately 6.1 m in length in the two primary orthogonal directions. The vertical clearance extends up to approximately 7.6 m.

Control of six degrees-of-freedom will enable application of complex biaxial load histories on subassemblages via control of the crosshead. Any degree-of-freedom may be programmed in either displacement control or load control, and degrees-of-freedom may be constrained in a master-slave relation to be a linear combination of the values of other degrees-of-freedom. For example, using the mixed-mode control capabilities of the MAST, it is possible to program any lateral displacement history, and at the same time specify overturning moment as a constant times the lateral force, while simultaneously maintaining an independent history of axial load on the test specimen. An advantage of the MAST system is that it controls a plane in space rather than just a point in space, which enables application of pure planar translations, as well as the possibility of applying gradients to simulate overturning (e.g., axial load gradient in the columns of a multi-bay frame, or wall rocking). The system also enables mode switching between DOF displacement and load control during testing.

The system will be equipped with four ±980 kN ancillary actuators with strokes of ±400 mm that can be used to apply simulated gravity loading, lateral displacements (or loads) to intermediate stories of multi-story subassemblages, or beam end boundary conditions at assumed inflection points.

The possibilities for structural testing within the MAST system are broad. As an example, the MAST system could be used to conduct bi-directional tests of reinforced concrete flanged walls [23]. To control the loading imposed on the wall through the boundaries, concrete blocks could be cast on the top and bottom of the wall to transfer the load from the cruciform-shaped crosshead to the flanged wall cross section. Assuming a moderate amount of inelastic behavior in the prototype structure, the centroid of the total lateral force distribution at maximum base shear may be assumed at mid-height of the wall, resulting in a moment-to-shear (M/V) ratio of $H/2$, where H is the height of the wall. Testing of this system could proceed with a prescribed lateral drift applied along each horizontal direction to define the biaxial load pattern (e.g., either from a user-defined source or from pseudo-dynamic input). At the same time, mixed-mode control could be employed to impose the desired moment-to-shear ratio at the boundaries in the two orthogonal directions. The procedure might be as follows: A prescribed lateral drift is imposed simultaneously in the two orthogonal horizontal directions. The resulting moment vectors in the two orthogonal directions, caused by the actuators applying longitudinal and lateral loads, apply an overturning moment to the structure. The distribution of lateral, longitudinal, and vertical loads would be controlled via the 6-DOF controller to ensure that the desired M/V ratio is maintained. The two remaining world DOF's (e.g., a twisting moment about the vertical axis and the resultant vertical force or axial load) may be suppressed or controlled as well. As an example, the vertical force might be specified as either constant or cyclically varying, and either independent or synchronous with the longitudinal/lateral drift histories.

The results of quasi-static cyclic tests can be used to develop mathematical models of the critical structural components that can be incorporated into nonlinear numerical analyses to investigate the overall response of structural systems incorporating similar details subjected to a variety of ground motions.

4.2 Shake table testing is a dynamic means of subjecting a test structure to a ground motion. In this test method, structural models are fixed to a platform, which is subjected to a ground acceleration history to excite the structure. Due to capacity limitations of most shake tables, test structures are typically reduced scaled models. Two means are typically used to maintain the natural frequency range of the test structure to the frequency range of interest of the ground motion: 1) the time-scale of the earthquake record can be compressed to modify the frequency range of the ground motion; 2) additional mass can be added to the test structure to scale its natural frequency; or combinations of these two means can be employed. Both means of have an impact on the structural response. Compressing the time-scale will result in increased apparent strengths due to strain rate effects on the structural response, and adding mass will have an impact on the moment-curvature response of the columns.

Due to the need to reduce the scale of the test structure to accommodate the capacity of the shake table, microconcrete and wires may be required to construct small-scale reinforced concrete models. This makes it difficult to model certain types of behavior, such as cracking and bond. Stub beams and columns are sometimes used to ensure the reinforcement is well-anchored.

Shake table studies do provide an excellent means to investigate the overall dynamic response of test structures. Many shake tables available today feature multi-degree of freedom capabilities. In addition, some laboratories are equipped with multiple tables that can be programmed to induce spatial and temporal effects of ground motion on structural systems which can be important for long span structures such as bridges. There are two such systems featured as part of the suite of experimental facilities available through the NEES program. One of them, the system at the University of Nevada at Reno (UNR), is shown in Fig. 3; the other, under construction at the State University of New York (SUNY) Buffalo is included in the discussion of hybrid test methods.

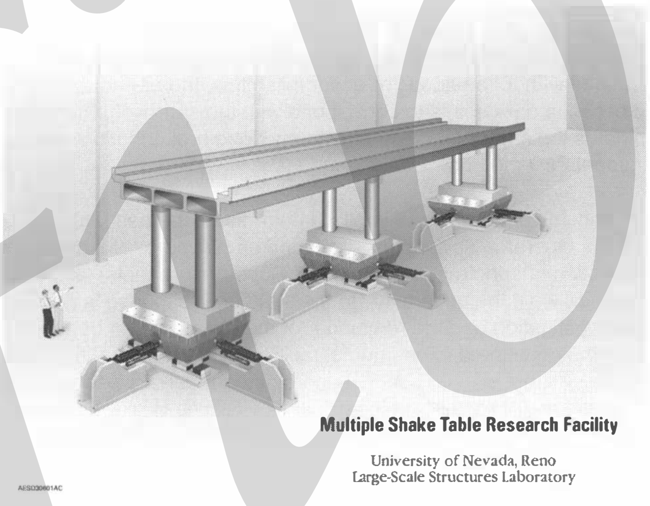

Fig. 3 Multiple Shake Table Research Facility featured at the University of Nevada at Reno

Features of the three UNR bi-axial shake tables include the ability to host specimens up to 1.35 MN. The tables are moveable and may be configured to act as a single shake table to test a single large structure, or may be configured to simulate the spatial and temporal differences in ground motion applied to piers of long-span bridge structures.

The size and multi-directional capabilities of shake tables has been increasing over the years. The year 2005 is the planned completion date for the world's largest shake table to be located in Miki City, north of Kobe City, in Japan. The construction of the this shake table is sponsored by the National Research Institute for Earth Science and Disaster Prevention (NIED), Science and Technology Agency of Japan. The table features a 20m by 15m platform designed to test a full-scale four-story reinforced concrete structure subjected to three-dimensional ground motions with up to 0.9g orthogonal horizontal components and 1.5g vertical.

The larger-scale systems remove the barriers to investigation of local effects such as structural details. In addition, they can be used to investigate systems for earthquake hazard mitigation including base isolation systems and energy dissipation devices such as velocity-dependent dampers.

4.3 Pseudo-dynamic testing (PsD) enables the testing of large-scale structural systems subjected to deformation histories that would be expected from an earthquake [24]. With this test method, the structure must be able to be idealized as a lumped mass system. The test structure is fixed to the laboratory floor and the deformations are imposed at the lumped masses (i.e., story heights) via a system of actuators. The deformations to be imposed at each story level are determined by solving the equations of motion using analytically determined inertial and damping forces and incorporating measured restoring forces determined in applying the required story displacements. Thus the deformations to be imposed depend upon the measured response of the test structure. Conducting the pseudo-dynamic test quasi-statically greatly reduces the actuator flow demands in comparison with similar scale shake table studies and enables visualization of damage as it develops in the structure. The resulting quasi-statically applied deformations represent those the structure would have experienced had it been subjected to the earthquake ground excitation.

The development of a continuous pseudo-dynamic test method (Continuous PsD) is underway at the European Laboratory for Structural Assessment (ELSA) of the Joint Research Centre (JRC) in Ispra, Italy, which eliminates the hold period by directing the actuator to a target displacement [25]. In the case of Continuous PsD, rather than pausing the test at the target displacement to determine the restoring force and solve the equations of motion to determine the next target displacement as is the case for conventional PsD, the restoring force is read at the sampling rate of the controller and the equations of motion are integrated on the fly without a hold period. In this way the next target displacement is determined without a pause. To accomplish this, the earthquake ground acceleration record is interpolated between data points to correspond with the sampling rate of the controller. The Continuous PsD eliminates the structural creep effects and load redistribution that develops during the pauses of the conventional PsD method.

The development and implementation of implicit integration schemes [26] such as the α-method of Hilber et al. [27] and the Operator-Splitting (OS)-method employed by Nakashima et al. [28] have facilitated the implementation of substructure PsD tests. Substructure tests can be accommodated at individual experimental facilities if the uncertainty in the structural response is primarily confined to the subassemblage under investigation and the remainder of the structure can be reasonably modeled numerically. A benefit of the networked experimental facilities with NEES, is that it will be possible to couple tests at multiple equipment sites to conduct coordinated multi-site pseudodynamic subassemblage tests. In such a case, tests at individual NEES sites might represent different representative components of a larger structural system, which can be numerically modeled at one of the NEES sites directly involved in the experimentation or at a remote site.

Other enhancements that have been made to the pseudo-dynamic test method include the development of real-time pseudo-dynamic testing [29-31]. Issues that must be considered in this application include the development of real inertial and damping forces that are numerically modeled in the traditional pseudodynamic test method. In addition, as the flow demands of the actuator increase, the nonlinearities of the servovalve system have an impact on the performance (discussed further relative to Effective Force Testing method in Section 4.4) [32]. NEES equipment sites that plan to feature real-time pseudo-dynamic test capabilities include the Large-Scale Structural Testing Facility at SUNY-Buffalo, the Reconfigurable Reaction Wall-Based Earthquake Simulation Facility at the University of California at Berkeley (UCB), and the Fast Hybrid Test System under development at the University of Colorado at Boulder.

4.4 Effective force testing (EFT), originally described in a number of papers associated with pseudo-dynamic testing [33-35], has been under development and implementation at the University of Minnesota [32,36,37] over the last ten years. As is the case for the pseudo-dynamic test method, the structure must be idealized as a lumped mass system for effective force testing. The basic test setup is similar to that of the pseudo-dynamic test method in that the structure is fixed at the base to the laboratory floor and loaded with actuators at the story levels. The difference between the two methods is that the pseudo-dynamic test method is displacement-controlled, whereas the effective force testing method is force-controlled. With the pseudo-dynamic test method, the imposed displacements are calculated during the test based on the measured structural response (restoring force). For the case of the effective force testing method, the effective forces (P_{eff}) to be applied at each story level are equal to the mass of the respective story level multiplied by the ground acceleration record as indicated in Fig. 4. As such, the forces to be applied are known a priori; they are not affected by the response of the test structure.

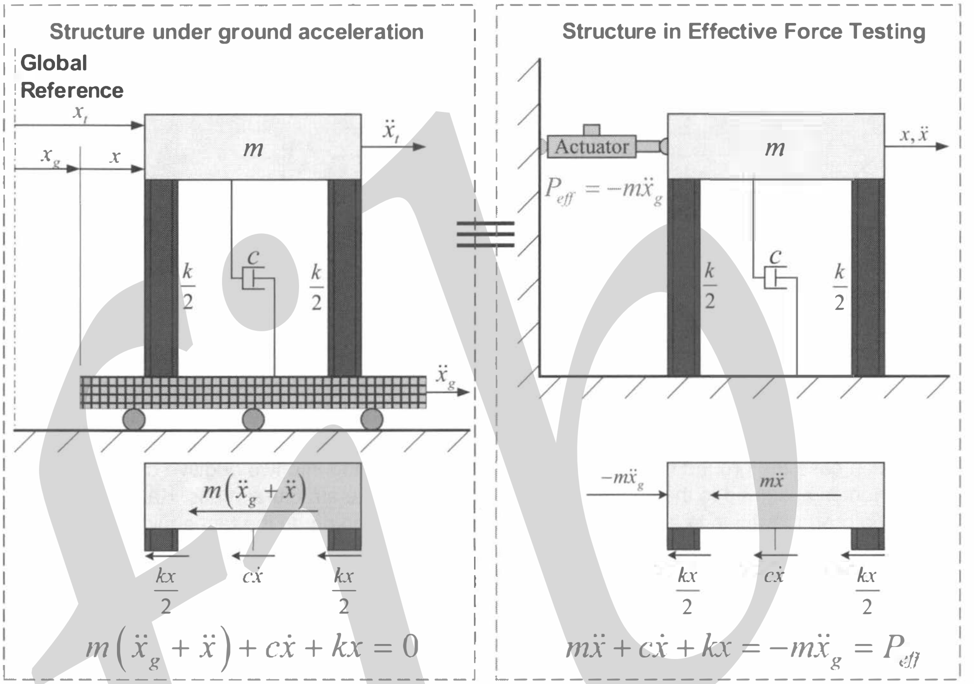

Fig. 4 Comparison of Shake Table (or ground excitation) System to Effective Force Testing

In the implementation of the EFT method [36,37], it was been determined that a direct application of the method is not feasible due to the natural velocity feedback phenomena which impairs the ability of the actuator to apply forces near the resonant frequency of the test structure.

Researchers at the University of Minnesota have developed control algorithms demonstrated to be effective in implementing the effective force testing technique. The implementation requires the measurement of the velocity of the piston or test structure to which it is attached. This information is then used to determine the increased flow required in the actuator to compensate for the velocity feedback phenomena by determining a modified command signal to account for these effects. The test method is shown schematically in Fig. 5 with the algorithm used to compensate for the velocity feedback. As noted in the figure, because the velocity feedback is compensated at the command signal to the servovalve, information regarding modeling of the actuator servovalve must be incorporated into the feedback correction loop along with phase compensation. The initial implementation was conducted assuming that the servovalve characteristics could be linearized. This was shown to be successful as long as the flow demands are not high. Two major types of nonlinearities of the servo-system, *nonlinear flow property* of the servovalve and *load pressure influence* on the actuator performance, have been identified. New velocity feedback compensation schemes have been developed featuring nonlinear velocity feedback compensation implemented with a digital signal processing (DSP) board. Experimental results of this implementation have indicated promising performance of the EFT method in situations of high flow demands when the nonlinearities become significant [31].

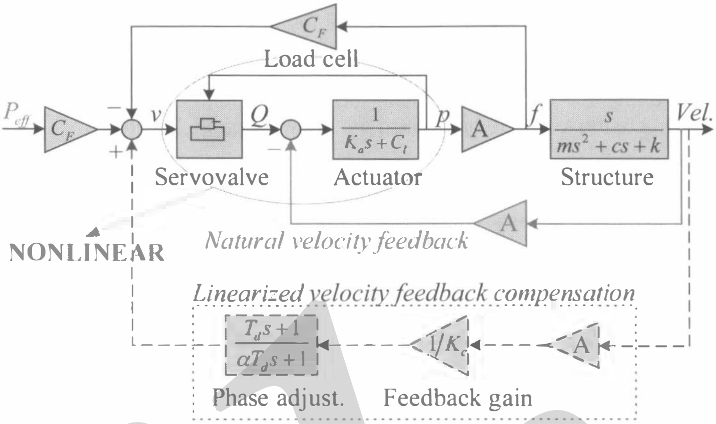

Fig. 5 Model of Force-Controlled Testing System Incorporating Linearized Velocity Feedback Correction

4.5 Hybrid test methods

Hybrid test methods have been proposed by researchers such as Kausel [38] who have suggested combining experimental test methods such as shake table testing with effective force testing in which case the ground motion is proposed to be separated into two additive components. One component is assigned to the shake table and the other to the structural mass. Kausel proposes separating the ground motion in a number of different ways depending on the test equipment and the type of test envisioned. Examples include separating the ground motion into low- and high-frequency components. If the low frequency components are assigned to the table it might simplify the design of the bearing mechanisms of the table, or vice versa, the shake table could be subjected to the high-frequency components to minimize the required stroke of the table. Other suggested alternatives include using the actuators applied to the story masses to increase the number of degrees of freedom that can be tested by a uni- or bi-directional shake table. The implementation of this hybrid test method, incorporating EFT, will have the same implementation issues as discovered by Zhao et al. [32], Dimig et al. [36], and Shield et al. [37] that will need to be addressed.

Fig. 6 shows the Real-Time Dynamic Hybrid Testing System under development at SUNY-Buffalo as part of the NEES program. The system incorporates two shake tables in combination with a series of actuators, resisted by a reaction wall, which can be used to apply forces or deformations to portions of the test structure.

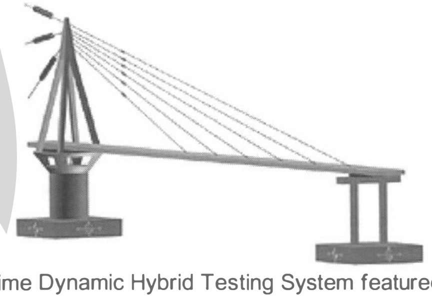

Fig. 6 Real-time Dynamic Hybrid Testing System featured at SUNY-Buffalo

5 DEVELOPMENT OF SIMULATION TOOLS AND THEIR APPLICATIONS

In parallel with experimentation, simulation tools have been under development to better understand the nonlinear behavior of reinforced concrete structural systems. As mentioned above, the first phase of the U.S.-Japan Precast Seismic Structural Systems (PRESSS) research program [13] included further development of inelastic time history analyses to numerically model the seismic response of precast systems, at that time DRAIN-2DX [39] was the platform that was utilized for the investigation. In this research effort, numerical models of the critical regions of precast structural systems were generated based on the experimental test data obtained from the isolated subassemblage tests. These models were then implemented into numerical models of entire precast structural systems of five- and fifteen-stories subjected to different ground motions to investigate the overall system response of structures incorporating the various types of connection details tested.

Other popular tools under continued development for seismic analysis of inelastic structural systems include IDARC [40], which was originally developed in 1987 to analyze multistory reinforced concrete structures subjected to earthquake loadings. This program is currently being extended to investigate three-dimensional structural response. As found in the testing of the seven-story reinforced concrete frame-wall structure as part of Phase 1 of the U.S.-Japan Cooperative Research Program in the mid 1980's, three-dimensional structural interaction (e.g. wall rocking and floor diaphragm effects) can have a significant impact on the structural response [11,12]. The investigation of other effects, such as torsion and degradation due to out-of-plane structural damage, will also be facilitated by the development of such three-dimensional structural analysis tools.

The Pacific Earthquake Engineering Research (PEER) Center has been sponsoring the development of an object-oriented code, *Open System for Earthquake Engineering Simulation* (OpenSees) [41], to conduct nonlinear seismic analyses. One of the important features under development in OpenSees is the ability to conduct finite element reliability analyses, which is a tool designed to meet one of the objectives of the PEER center which is the development of performance based earthquake engineering technologies for the economic and safety needs of society. Devastating economic losses that have resulted from many recent earthquakes have given engineers motivation for the development of a performance-based design approach in which case owners of structural systems may be able to choose levels of structural performance (e.g., fully operational, operational, life safe, near collapse) relative to the probability of occurrence of specific levels of seismic events (e.g. frequent, occasional, rare, very rare events) [42]. An example of a specified performance objective would be to tie more restrictive levels of performance criteria (e.g., fully operational) to levels of seismic events expected to occur more frequently, and to limit the near collapse performance level to seismic events that have an extremely low probability of occurrence. The use of tools such as OpenSees to conduct finite element reliability analyses enables the determination of probabilities of exceeding user-specified performance criteria, which is an essential feature for the development of performance based engineering, and can facilitate the construction of reinforced concrete structural systems that may exhibit improved performance under more frequent seismic events.

6 NETWORK FOR EARTHQUAKE ENGINEERING SIMULATION (NEES) PROGRAM

The need for coordinated research programs with mutual utilization of research facilities and exchange of researchers identified more than a quarter century ago by the U.S.-Japan Panel of Wind and Seismic Effects to mitigate the seismic hazard is continuing toward further fruition with the assistance of advanced technology in the George E. Brown, Jr. Network for Earthquake Engineering Simulation (NEES). The objective of this program, initiated by the National Science Foundation (NSF) in October of 1999, is to develop a network of advanced integrated and interconnected facilities that will transform earthquake engineering research so that it relies on the integration and coordination of experimentation, computation, and model-based simulation in a collaborative environment.

The development of the network of integrated NEES research facilities is being funded through a five-year, $82 Million Major Research Equipment (MRE) program. Comparable programs in the past have funded single major scientific equipment sites including the South Pole Station and the Kitt Peak Telescope. The NEES program represents NSF's first large investment in the engineering field, and the first major MRE funded as a distributed network of facilities. Approximately sixteen equipment facilities will be constructed within the United States, funded through two phases of program solicitations. The NEES network of facilities will be run as a consortium from October 1, 2004 through September 30, 2014 serving as both a national and international resource. It is envisioned that, in addition to the initial equipment sites funded through the NSF program solicitations, other globally significant earthquake engineering research facilities will participate in NEES.

There are three critical aspects to the development of the NEES research collaboratory over the next few years. They are: 1) Equipment Sites - the development, construction, implementation, and operation of the new unique experimental resources at the individual equipment sites awarded through the NEES program; 2) System Integration - the development of NEESgrid, which is the system that serves as the backbone to network the experimental and computational resources with the earthquake engineering research community and the public; and 3) Consortium Development - the development of the consortium which will manage the NEES research collaboratory, including the development of the vision for the collaboratory, organizational structure, operational procedures for shared use, and training, with input from the broader earthquake engineering community.

To date, eleven NEES equipment sites have been awarded during Phase 1. They cover experimental resources in five different categories, including four large-scale structural testing facilities, two shake tables, two geotechnical centrifuges, one tsunami wave tank, and two field equipment sites, some of which were described in Section 4. Fig. 7 shows a brief description and the geographical distribution of each of the eleven sites, including the University of Illinois at Urbana-Champaign, which is the location of the National Center for Supercomputing Applications (NCSA), coordinating the System Integration aspect of the NEES project. The Consortium of Universities for Research in Earthquake Engineering (CUREE), in conjunction with the American Society of Civil Engineers (ASCE) and the Earthquake Engineering Research Institute (EERI), are developing the NEES consortium.

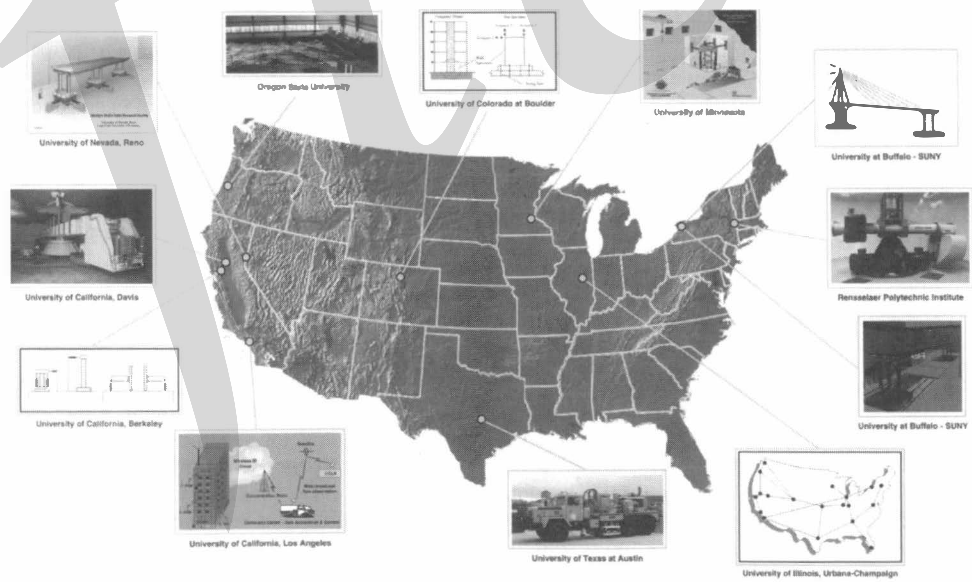

Fig. 7 Description and Geographical Distribution of Eleven NEES Phase I Equipment Sites [44]

There are several key aspects that make NEES unique in addition to the experimental facilities themselves. One of the aspects is that through NEESgrid researchers and the public will have the capability of remote access to the experimental facilities. Fig. 9 shows an example schematic of the data collection and telepresence infrastructure for one of the equipment sites described in Reference 44. The lower right hand quadrant of the figure below represents the NEESgrid with a remote research collaborator identified as a *private client* and a general public participant identified as a *public client* who may have some limited capabilities (e.g., lab sweep and communication devices). Key aspects to remote research collaboration include the ability to have video-teleconferencing capabilities, remote control of telepresence capabilities, immediate access to the data including the ability to playback portions of the test on demand and at least limited remote control of the experimental equipment.

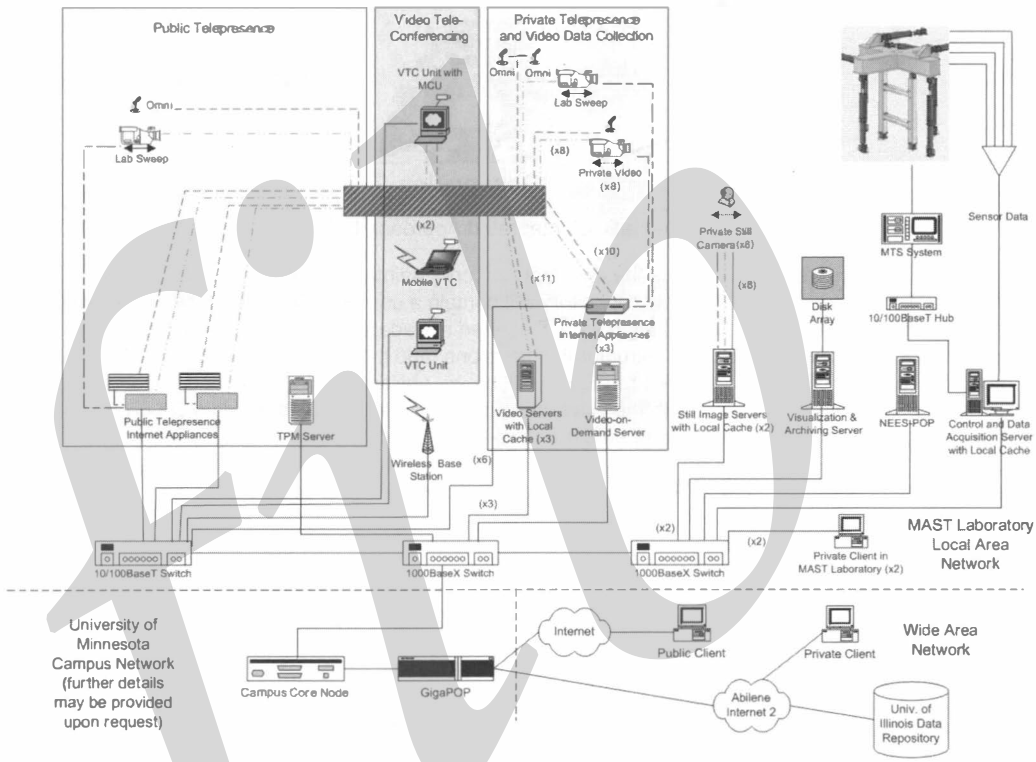

Fig. 8 Schematic of Data Collection and Telepresence Infrastructure for NEES MAST Site

The web-based telepresence features of NEES will facilitate integrated tests among multiple collaborators across the globe and at multiple experimental NEES facilities. As described in Section 4.3, it will be possible to integrate the simulation and testing of multiple reinforced concrete subassemblages tested simultaneously at a number of equipment sites. Fig. 9 shows a schematic of this integrated approach to research. A prototype structural system may be selected for investigation. Integrated simulation and experimentation such as the pseudo-dynamic test method might be employed at a remote site with the critical subassemblage or set of subassemblages tested experimentally at one or more of the networked NEES equipment sites. The results of the simulation drive the experiment(s), and the feedback from the experiment(s) continuously updates the structural model in the simulation. At the same time, additional remote participants including the public can participate in the experiment with various levels of access depending on the authorization-level of the participant. The collaborators will have immediate access to the visual and sensor data, as well as the simulation results.

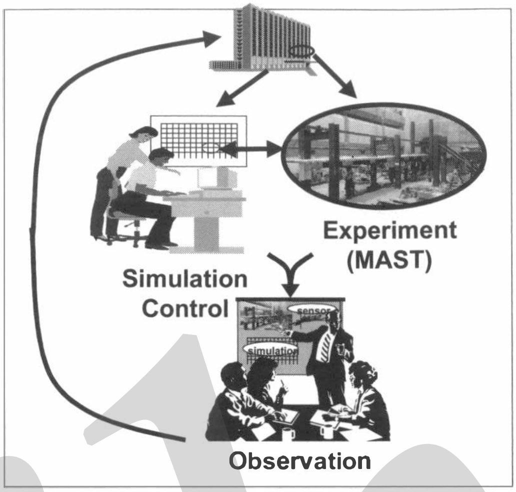

Fig. 9 Schematic of Integrated Approach to Research

Another key feature of NEES is the development and maintenance of a national curated searchable data repository. The data repository will contain a complete archive of the visual (video and still images), sensor, and simulation data. Required metadata to describe the information must include sensor types and locations, structural dimensions, and material properties. One of the most powerful features of the curated data repository will be the ability to replay tests and to couple the experimental sensor responses with the visual data and computer simulations. It is envisioned that in addition to the numerical data, a geometric framework may be developed to graphically associate dimensions and sensor locations on a model that can be used for visualization of the results as well as for numerical simulation (Fig. 10). The curated databank will also serve as a repository for software simulation tools.

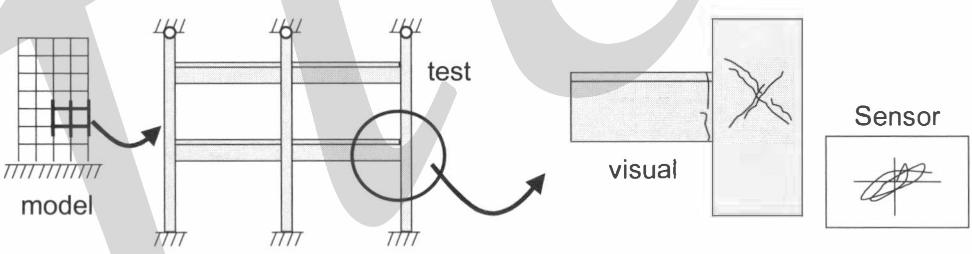

Fig. 10 Schematic of possible framework for control, archival, and replay

This feature of NEES, the curated data repository, may be one of the single greatest outcomes of the NEES program besides the facilitation of collaborative research. The experimental database will be invaluable for the life of the curated data repository as past experimental results will always be useful in the validation of new numerical models for structural systems. Subsequently, the numerical models validated and archived with the database may assist practitioners in the implementation of performance based design principles. The database might also be useful in justifying new types of structural systems and implementing them in practice, as an example, the archived information might be used to satisfy code requirements of experimental testing of precast frame systems that do not fall under the reinforced concrete emulation category [6]. The searchable features of the database will be particularly useful in code development, as it will be possible to call out all applicable test series in assessing the performance of models used in design codes as well as simulations. Types of information that might be evaluated for reinforced concrete structural systems are limitless, they include information for assessing joint shear models, assessment of the integrity of gravity load bearing columns that must go along for the ride with the lateral resisting system, effects of three-dimensional loading, etc. The searchable features of the database will make it possible to screen the information to meet explicit criteria for evaluation of models. As an example, it may be of interest to select only those data obtained from spirally reinforced columns for a specific comparison or only data from experiments within a specific range of concrete strength.

The value of a high-quality experimental database has had a long and significant history in code development from the implementation of shear models to the determination of development length requirements for reinforcement embedded in concrete. It is expected that the NEES curated database will continue that history for the improved performance of reinforced concrete structural systems in seismic regions.

7 SUMMARY AND CONCLUSIONS

Historically experimentation has been a cornerstone to the advancement of our knowledge of the behavior of reinforced concrete structural systems. Simulation integrated with experimentation has provided researchers with the ability to extend those experimental results to a broad range of applications. This paper has presented an overview of some of the key advancements that have been made through this integrated approach to research. In addition, it has been shown that multi-investigator international collaborative research programs have greatly benefited the understanding of the behavior of reinforced concrete structural systems in seismic regions. The NSF George E. Brown, Jr., Network for Earthquake Engineering Simulation (NEES) program will greatly facilitate continued efforts in this regard by making available a unique suite of networked experimental facilities as a national and international resource, with a vision for integrating other global resources in the future. A key feature of the NEES program is the development of a searchable archived database which will serve the research and practitioner communities by enabling continued calibration/validation of new numerical models, facilitation of the development of performance-based design methodologies, and means to improve design codes through an increased inventory of experimental results.

REFERENCES

[1] Berg, Glenn V. (1982). "*Seismic Design Codes and Procedures.*" *Engineering Monographs of Earthquake Criteria, Structural Design, and Strong Motion Records,* Agbabian, M. S. (ed.), Earthquake Engineering Research Institute Monograph Series, 119 pp.

[2] Blume, J.A., Newmark, N.M., and Corning, L.H. (1961). *Design of Multistory Reinforced Concrete Buildings for Earthquake Motions.* Portland Cement Association, 318 pp.

[3] ACI Committee 318 (2002). *Building Code Provisions for Structural Concrete*. American Concrete Institute, Farmington Hills, MI, 443 pp.

[4] Paulay, T. and Priestley, M.J.N, (1992). *Seismic Design of Reinforced Concrete and Masonry Buildings.* John Wiley and Sons, Inc., New York, 744 pp.

[5] Park, R. and Paulay, T., (1975). *Reinforced Concrete Structures*. John Wiley and Sons, New York, 769 pp.

[6] ACI Innovation Task Group 1 and Collaborators, (2001). *ACI T1.1-01: Acceptance Criteria for Moment Frames Based on Structural Testing.* American Concrete Institute, Farmington Hills, MI, 3pp.

[7] Aoyama, H., (1981). Outline of Earthquake Provisions in the Recently Revised Japanese Building Code. *Bulletin of the New Zealand National Society for Earthquake Engineering*, 14(2).

[8] Architectural Institute of Japan, (1994). *AIJ Structural Design Guidelines for Reinforced Concrete Buildings*. 207 pp.

[9] Otani, Shunsuke, (1995). "Brief History of Japanese Seismic Design Requirements. *Concrete International*, 17(12), 46-53.

[10] Penzien, J. ,Uemura, H., Watabe, M., and Hanson, R., (1985). Introduction to U.S.-Japan Cooperative Earthquake Engineering Program. ACI SP-84, *Earthquake Effects on Reinforced Concrete Structures – U.S.-Japan Research*, 1-10.

[11] Wolfgram, C., Rothe, D., Wilson, P., and Sozen, M. (1985). "Earthquake Simulation Tests of Three One-Tenth Scale Models," ACI SP-84, *Earthquake Effects on Reinforced Concrete Structures – U.S.-Japan Research*, 347-374.

[12] French, C.W., and Moehle, J.P, (1991). Effect of Floor Slab on Behavior of Slab-Beam-Column Connections. *Design of Beam-Column Joints for Seismic Resistance*, ACI SP-123, 225-258.

[13] Priestley, M.J.N., (1991). Overview of PRESSS Research Program. *PCI Journal*, 36(4), 50-57.

[14] Nakaki, S.D., Stanton, J.F., and Sritharan, S., (1999). "An Overview of the PRESSS Five-Story Precast Test Building," *PCI Journal*, 44(2), 26-39.

[15] Priestley, M. J. N., and Tao, J. R., (1993). Seismic Response of Precast Prestressed Concrete Frames with Partially Debonded Tendons. *PCI Journal*, 38(1), 58-59.

[16] Palmieri, L., Sagan, E., French, C., and Kreger, M. (1997). Ductile Connections for Precast Concrete Frame Systems. *Mete A. Sozen Symposium*, ACI SP-162, American Concrete Institute, Farmington Hills, MI, 313-355.

[17] Schultz, A.E., and Magana, R. A., (1996). Seismic Behavior of Connections in Precast Concrete Walls. *Mete A. Sozen Symposium*, ACI SP-162, American Concrete Institute, Farmington Hills, MI, 273-311.

[18] Ghosh, S.K., and Hawkins, N.M., (2002). Seismic Design Provisions for Precast Concrete Structures in ACI 318. *PCI Journal*, 46(1), 28-33.

[19] Jirsa, J. (editor), (1991). *Design of Beam-Column Joints for Seismic Resistance*, ACI SP-123, American Concrete Institute, Farmington Hills, MI, 518 pp.

[20] French, C.W., and Kreger, M.K. (editors), (1998). *High-Strength Concrete in Seismic Regions*, ACI SP-176, American Concrete Institute, Farmington Hills, MI, 471 pp.

[21] Moehle, J. (ed.) (1996). Theme Issue: Experimental Methods. *Earthquake Spectra*, (12)1, 183 pp.

[22] Clark, A., French, C.W., and Leon, R., (1989). Earthquake Testing Methods for Structures—Examples of Current Practice and Future Directions. *Earthquake Resistant Construction and Design*, Savidis, S.A. (ed.), Proceedings of the International Conference on Earthquake Resistant Construction and Design, Berlin, 13-16 June 1989.

[23] French, C.W., Schultz, A.E., Hajjar, J.F., Shield, C.K., Ernie, D.W., Dexter, R.J., Du., D.H.-C., and Bergson, P.M. (2002). "A System for Multi-Axial Subassemblage Testing (MAST): Design Concepts and Capabilities," Paper No. NS-1a, *Proceedings of the Seventh National Conference on Earthquake Engineering*, Boston, Massachusetts, July 21-25, 2002, Earthquake Engineering Research Institute, Oakland, California.

[24] Shing, P.S. and Mahin, S.A., (1984). *Pseudodynamic Test Method for Seismic Performance Evaluation: Theory and Implementation*, Report No. UCB/EERC-84/01, Earthquake Engineering Research Center, University of California, Berkeley.

[25] Magonette, G. (2001)."Development and Application of Large-Scale Continuous Pseudo-Dynamic Testing Techniques." *Philosophical Transactions of the Royal Society: Special Issue on Dynamic Testing of Structures*, **359**, 1771-1779.

[26] Shing, P.B., Nakashima, M. and Bursi, O.S., (1996). Application of Pseudodynamic Test Method to Structural Research. *Earthquake Spectra*, (12)1, 29-56.

[27] Hilber, H.M., Hughes, T.J.R., and Taylor, R.L., (1977). Improved Numerical Dissipation for Time Integration Algorithms in Structural Dynamics. *Earthquake Engineering and Structural Dynamics*, 5, 283-292.

[28] Nakashima, M., Kaminosono, T., Ishida, M. and Ando, K. (1990). Integration Techniques for Substructure Pseudo Dynamic Test. *Proceedings, Fourth National Conference on Earthquake Engineering*, EERI, Palm Springs, California, Vol. 2, 515-524.

[29] Nakashima, M., (2001). "Development, Potential, and Limitations of Real-Time Online (Pseudo-dynamic) Test," *Philosophical Transactions of the Royal Society: Special Issue on Dynamic Testing of Structures*, **359**, 1851-1868.

[30] Nakashima, M. and Masaoka, N. (1998). "Real-Time On-Line Test Method for MDOF Systems." *Earthquake Engineering and Structural Dynamics*, **28**, 393-420.

[31] Horiuchi, T., Inoue, M., Konno, T. and Namita, Y. (1998). "Real-Time Hybrid Experimental System with Actuator Delay Compensation and Its Application to a Piping System with Energy Absorber." *Earthquake Engineering and Structural Dynamics*, **28**, 1121-1141.

[32] Zhao, J., French, C., Shield, C. and Posbergh, T., (2002). Considerations for the Development of Real-Time Dynamic Testing using Servo-Hydraulic Actuation. *Submitted to the* …. A. Chopra (ed.).

[33] Mahin, S.A., and Shing, P.B. (1985). "Pseudodynamic Method for Seismic Testing." *Journal of Structural Engineering*, ASCE, 111(7), 1482-1503.

[34] Mahin, S.A., Shing, P.B., Thewalt, C.R., and Hanson, R.D. (1989). "Pseudodynamic Test Method—Current Status and Future Directions." *Journal of Structural Engineering*, ASCE, 115(8), 2113-2128.

[35] Thewalt, C.R., and Mahin, S.A. (1987). *Hybrid solution techniques for generalized pseudodynamic testing*. Report No. UCB/EERC-87/09, Earthquake Engineering Research Center, University of California, Berkeley.

[36] Dimig, J., Shield, C., French, C., Bailey, F. and Clark, A. (1999). "Effective Force Testing: A Method of Seismic Simulation for Structural Testing." *Journal of Structural Engineering*, ASCE, 125(9), 1028-1037.

[37] Shield, C.K., French, C.W., and Timm, J. (2001)."Development and Implementation of the Effective Force Testing Method for Seismic Simulation of Large-Scale Structures." *Philosophical Transactions of the Royal Society: Special Issue on Dynamic Testing of Structures*, **359**, 1911-1929.

[38] Kausel, E. (1998). "New Seismic Testing Method. 1: Fundamental Concepts." *Journal of Engineering Mechanics*, ASCE, (124)5, 565-570.

[39] Prakash, V., Powell, G., and Campbell, S. (1993). "DRAIN-2DX Base Program Description and User Guide: Version 1.10," Research Report No. UCB/SEMM-93/17&18, Structural Engineering Mechanics and Materials, Department of Civil Engineering, University of California, Berkeley.

[40] Reinhorn, A.M., Valles-Mattox, R., Kunnath, S., (2002). Website: http://civil.eng.buffalo.edu/idarc2d50

[41] McKenna, F., Fenves, G.L., Filippou, F.C., Scott, M., Mazzoni, S., Law, K., Deierlein, G., Peng, J., Kaul, R., Altoontash, A., and Turkiyyah, G., (2002). Website: http://opensees.berkeley.edu/OpenSees/developmentTeam.html

[42] FEMA 273. Structural Engineers Association of California (SEAOC), Vision 2000 Committee. (1995). *Performance Based Seismic Engineering of Buildings.* J. Soulages, (ed.), Sacramento, California, 2 vols.

[43] Website: http://www.nees.org

[44] Daugherty, D.J., Hajjar, J.F., Ernie, D.W., Du, D.H.-C., Shield, C.K., Beyer, J.C., and Polley, C. (2002). "Multi-Axial Subassemblage Testing (MAST) Data Collection and Telepresence Systems Specification." MAST Laboratory Report No. MAST-02-01, Department of Civil Engineering, University of Minnesota.

ARCHI-NEERING AND CONCRETE

Prof. Dr. Werner SOBEK
Werner Sobec Ingenieurre GmbH

Keywords: perception, schape, surface, colour, light

1 INTRODUCTION

An architecture and an engineering, which claim to formulate a mindset appropriate to our time as well as to future generations, cannot take shape through the use of traditional forms and materials. They rather have to develop on the basis of integral processes of planning that take into consideration present and future forms of human life. The question is not "How did we live and work until now?" but rather "How are we going to live and work in the future?" The search for an answer to this question might not always be easy and the answer itself might not always prove perfectly true. But with respect to intellectual tenability, seeking this answer is the only way.

For the author, the term "engineering" never meant the simple follow-up of an architect's thoughts and the analysis of what somebody else has sketched before. Engineering means to bring in all the ingenuity of a multi-discipline team also into the conceptual phase of the planning process. From it's very beginning. Engineering means creativity. Engineering means to work with all the materials available in such a way that each of them is used in an appropriate manner and as an integral part of the design idea. Engineering means to take advantage of all the methods developed in mechanics, mathematics and other related fields. But engineering never means to explain how the existing things function: Engineering means to create the new on the basis of the known.

Architecture cannot reach the realm of an answer to our future needs and dreams without being combined with an engineering that is more than it is nowadays and in the past. And engineering finally will not reach the realm of the art of building if it does not understand that the design of the environment needs more than technical correctness and economic competence. If we focus on concrete as the most used building material on our planet and as one of the most wonderful and chanceful materials we have to design the built environment, it becomes obvious that both disciplines, architecture and engineering, were not able to establish a satisfying state of the art of building with concrete beyond technical correctness. It does not need an explanation why concrete is a building material neither liked nor preferred by people. But it needs an explanation why architects and engineers failed to create a way to work with concrete as a material that is and that has to be more than a load bearing element. The problem is that science and industry have developed a material to a very high level but that most of the clients do not really like it. Not because of its technical or cost but because of its aesthetical qualities. So this is what architects and engineers have to overcome in the future.

2 PERCEPTION

People, mean the non-professionals or the "normal" users perceive a built structure not by its load bearing characteristics. Because no normal user is educated to understand why a moment loading requires other sections than an axial loading etc. The normal user perceives the entity of a structure as an assemblage of elements the shape, the surface qualities and the colour of which determine the quality of the seen. The perception of shape is a combination of the perception of the overall and of the detail. The perception of surface qualities is a combination of the perception of the macro- and the micro surface qualities. The perception of colour is, as the perception of surface qualities, strongly influenced by the natural and the artificial lighting.

3 SHAPE

The question of "How should one shape a structural element?" is as old as architecture and engineering. If one asks the question "How can we shape a structural element made out of concrete?" the answer would be: In any shape, because concrete is the only building material which can be brought into any shape and which, at the same time, is still cost effective and of a high load bearing capacity. But forming the concrete means solving the formwork-problem: With a few exceptions, there is no reason at all to poor concrete into a formwork, which shows plane surfaces

only. But the fact that nearly no non-planar formwork-technique has been developed limits the shaping of concrete to something, which reflects more, the constraints and the nature of the formwork than the nature of the concrete itself. In the worlds of technique and art, this is something really unique.
The search for the shape brings up a couple of fundamental questions: what is the function of the element and is there a classic, a natural or another somehow evident solution which fully fulfils this function and which is the one and only truth? (Figs. 1,2). Does a FRP-beam have the same shape as a concrete beam? How does the character of the material used influence the shape? Knowing that anything always has different functions like bearing of loads, defining of space, evoking of feelings etc.: Is there a hierarchy of functions and what position does the function of load bearing take?

It is obvious that there is no classic shape in the sense of the one-and-only-solution if there is a non-constant multifunctional set of demands and requirements to an element. This yields to the question of style.

4 STYLE

Style is in the very positive understanding of one out of several ways of how to design something in a consequent way. It is interesting that the term of style never played any role in the literature of conceptual design in structural engineering. This is only possible if there is either the conviction that there is only one solution possible and therefore the discussion of a variety is senseless or that there is a fundamental lack in the basic understanding of how things have to be formed. The latter one is unfortunately the true.

There are only a few names in the world of engineering, which are strongly linked to a certain style. (Fig.3). The buildings of all of them carry an identifiable "trademark" and show, interestingly, a wide acceptance also by the so-called normal users, which also means that even the un-educated or non-professionals have an understanding for quality.

Establishing a style is essential for a designer in order to achieve quality in design. Style means a constant, consequent and identifiable interpretation of the multi-level functions of a product and the transformation of those functions into a built structure or product. Style implicates objectivity as well as subjectivity in the interpretation and the ranking of certain demands and requirements and it implicates, of course, subjectivity in the interpretation of what the nature or the soul of the things might be or should be. But, and this is important, it never allows for any arbitrariness.

5 SURFACE

It is obvious that the surface qualities strongly determine the quality of the perceived. This has been realized before. (Fig.4). It yielded to a couple of techniques of structuring the plane formwork like e.g. the use of wooden planks in different states of treatments and outlining, plastic formwork inlays or sand blasting resp. water jet treatment of the concrete surface. A few of these techniques create macro- as well as microstructures in the surface. Wooden planks e.g. do so by defining a macrostructure by their joints and a microstructure, which can be seen from close distance only, by the ornaments in the planks their selves. Other techniques like steel formwork try to avoid any structuring of the concrete's surface.

The problem is that most of the surface treatments used today do not create enough quality within the surface itself and that they often enough do not give any scaling to the element in total. However, to achieve this it needs a very intense planning of what has to be done. This intense work often exceeds the content of the standard planning process. But the creation of the surface quality is an essential. Is it really right to give concrete the appearance of wooden planks, just with another colour? It is of course not the understanding of the designer that he wants to show which material has been used for the formwork. It is more a helpless trial adding a positive aspect to something, which is typically perceived with negative feelings.

The technique to put a somehow artificial layer with positively associated characteristics onto a surface with qualities typically associated with negative feelings is a technique, which is used in the treatment of the colouring of concrete too. Coming back to surface of concrete elements, the question is whether there is a natural, a self-evident type of surface for concrete.

6 COLOUR

The "famous" grey. The concrete's natural colour which varies from a very bright grey, nearly to white, if one uses white cement and white aggregates to the dark grey as it is found e.g. for ultra high strength concrete. Again, the natural appearance is not linked to strictly positive feelings. But painting the members and thus completely hiding or even denying their basic materiality is unacceptable because of its, if one is on the search for the truth, decorative quality.

Is there a natural colour of concrete? Is it the grey, which comes up if one mixes the ingredients technically needed, or is there an allowance for more? Pigments, coloured aggregates, glass powder etc.? Is the natural also the pure? Is there a need and logic to produce a homogeneous colour all over the elements or is it the irregularity one should go for? Is it allowable to cover the surface with a coloured but partially transparent glaze? Where is the transition between the raw and the glaze, where between the glaze and the paint?

7 LIGHT

The natural light in its variations during the day and the year as well as artificial lighting finally strongly influence the appearance and thus the perception of the built. Light in different intensities, with brightness and shadow evokes different appearances and different colour temperatures. It is somehow trivial to mention this but the fact that the connection between shapes, surface, colour and lighting is mastered, even considered so seldom justifies this remark.

It is essential to consider the effect of light and to design for the action of light. (Fig.5). Nearly every car-body is a masterpiece with respect to the shaping of a structure in such a way that the light is supporting, sometimes emphasizing the shape and reducing the optical weight of parts considered to be less important or of parts which should not be noticed as dominant. The same thoughts and techniques have to be introduced now to the design of concrete.

8 PATINA OR GETTING OLDER

The effect of aging of the surface's appearance is of fundamental influence to the perception of a structure. There are techniques, which prevent aging, like putting a transparent glaze-type coating onto the surface. The old then looks always new whereas anti-aging concepts fresh up the surfaces from time to time. Hydro jet treatment etc. stands for the techniques used here. Allowing for the aging sounds probably to be the most simple, is on the other hand the most complicated way a designer can take because the way the surface changes has to be anticipated. The effects of rainwater action, that of pollution, settlement of dirt and dust into the microstructure of the surface have to be considered as well as the growing of lichens und moss.

9 FUTURE NEEDS

Designing a building as a part of the built environment means to consider more than the fulfilling of primary functions like load bearing qualities. Because people do, can and must expect a quality of the built environment which is beyond technical correctness or even perfectionism. This all means that architects and engineers, especially the latter ones, consider that a building, independent from whether it is a bridge, a high-rise, an industrial building or a retaining wall has to fulfil a wide range of aesthetical demands. This necessitates an education in our teams and at our universities that is far away from what is usual. It necessitates the understanding and the mastering of the connection and interrelation between material, shape, surface, colour and light. (Fig.6). In our work with concrete, this must be the next step.

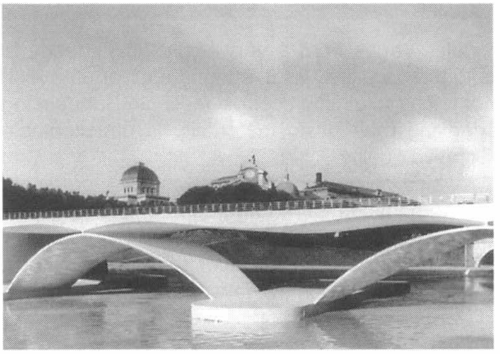
Fig.1 Design for the Garibaldi-Bridge over the river Tiber in Rome by Myron Goldsmith

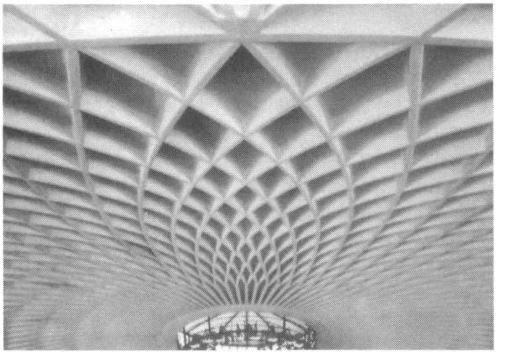
Fig.2 Palazetto dello Sport, one of the ribbed structures by Nervi.

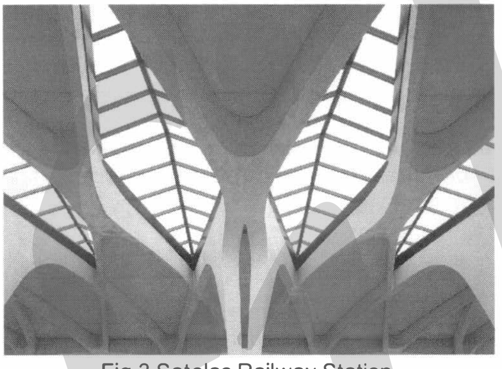
Fig.3 Satolas Railway Station by Santiago Calatrava

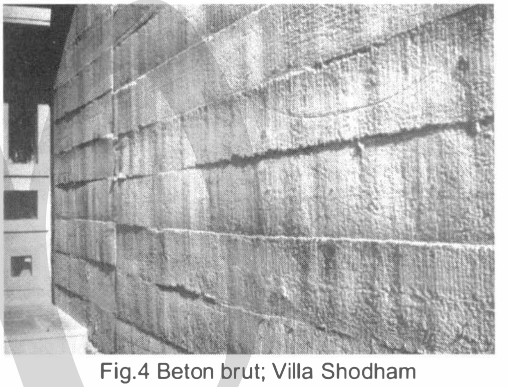
Fig.4 Beton brut; Villa Shodham by Le Corbusier

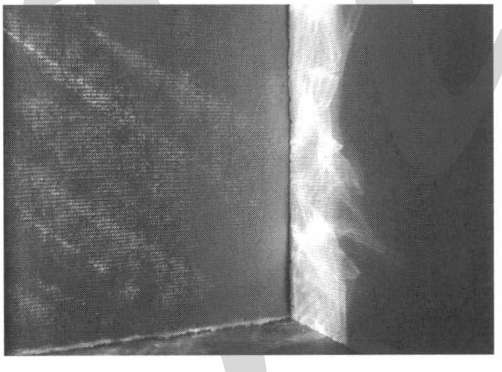
Fig.5 Action of light falling tangential onto a structured concrete surface. Diploma thesis at the authors institute by Jan-Christoph Diebel


Fig.6 Cutting of a painting of Anselm Kiefer. Setting the materiality, structuring of the surface and setting of colours

THE POWER OF PRESTRESSING

Jiri Strasky

Technical University of Brno, Czech Republic & Strasky Husty and Partners,
Consulting Engineers, Brno, Czech Republic and Greenbrae, CA, USA

Keywords: prestressing, load balancing, tension stiffening, internal and external post-tensioning.

Science, not Intuition, is the tool of creativity

1 INTRODUCTION

The idea of prestressing, a product of the twentieth century, has announced the single most significant new direction in structural engineering of any period in history. It put into the hands of the designer an ability to control structural behavior at the same time it enabled him - *or forced him* - to think more deeply about the construction. Moreover, the idea of prestressing opened up new possibilities for a form that influence the general culture.

To focus on that fact and to narrow my scope, I shall consider here only bridges, even though we all know that prestressing has broad applications to all kinds of buildings. Still the idea of prestressing arose out of bridge design and its most impressive forms, from a purely engineering viewpoint, have appeared in bridges.

While reinforced concrete combines concrete and steel bars by simply putting them together and letting them act together as they may wish, prestressed concrete combines high-strength concrete with high-strength steel in *an active* manner. The prestressing allows us to balance the load, change boundary conditions and create supports within the structure. Prestressing is really a revolution, prestressing is a radical step from passive reinforcement to creative thinking and development.

Modern concrete structures combine reinforced concrete with different level of post-tensioning to obtain the most appropriate behavior of structures both for service and ultimate load. In this way so-called 'Structural Concrete' is developed.

By post-tensioning of structures we can redistribute internal forces within the structure and achieve any stage of stresses. But we have to be careful. On the contrary to steel structures the chosen stage of stresses is redistributed in time by creep of concrete to the natural stage of concrete structures. And, of course, the alignment of prestressing tendons is influenced by the requirements on the ultimate capacity and ductility of the structures.

In this paper I would like to focus on some problems that are connected with finding the correct structural solution and corresponding arrangement of prestressing steel. On examples of several structures I would like to present possibilities of post-tensioning. I would like to remind you several outstanding structures that use prestressing in a non-tradition way.

I hope I will be forgiven for presenting some structures on whose design I had an opportunity to work on. I wanted to present my approach to designing of structures that is developed from my attempt to understand the structural behavior and trying to find the most appropriate solution.

2 LOAD BALANCING

Designing of structures is based on the full understanding of the function of the post-tensioning both during the post-tensioning, service and in the ultimate limit state. During the post-tensioning the structure is loaded by equilibrium of forces. Due to creep of concrete the original stage of stresses can significantly change in time. The importance of this phenomena is presented on the following example.

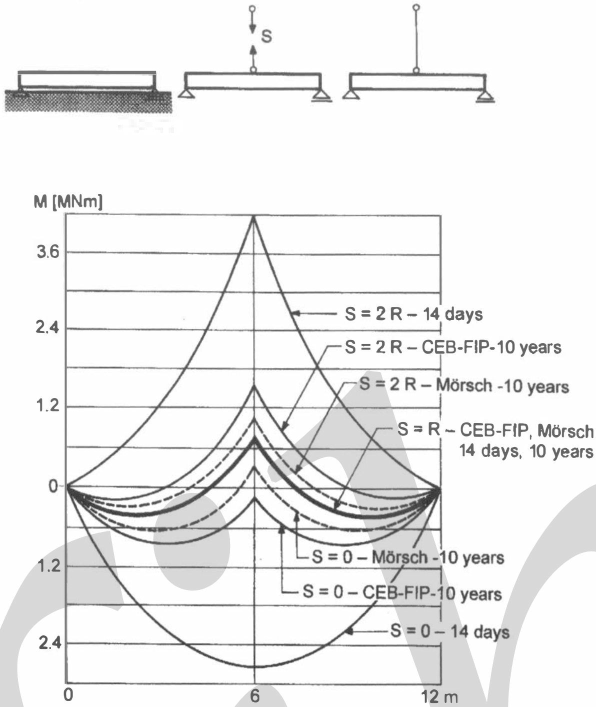

Fig.1

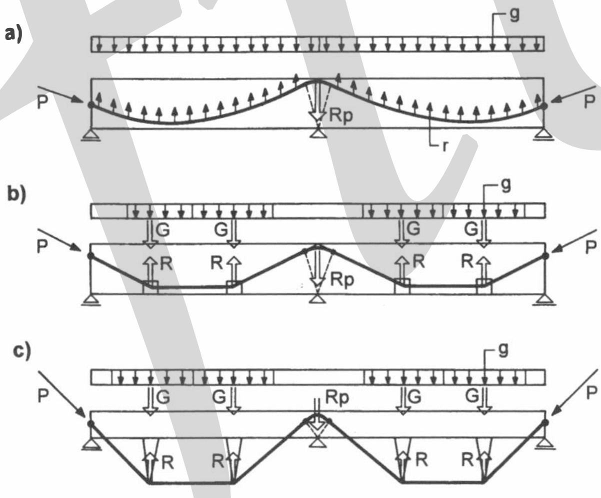

Fig.2

Fig.1 shows a simple beam of a span length of 12 m, which was after 14 days of curing, suspended at mid-span on a very stiff stay cable (EA = ∞). Before suspending a force S was created at the cable. The value of force S was S=0, S=R and S=2R, where R is a reaction at intermediate support of a continuous beam of two spans 2 x 6 m.

The time dependent analysis was performed for the old Mörch and CEB-FIP creep function. In the course of time a significant redistribution of bending moments has occurred for S=0 and S=2R. The course of bending moments is changing towards the course of the bending moments of two span beam. Concrete is natural material and therefore the structure tries to behave naturally – as a continuous beam. In this case a redistribution of stresses is larger for the old Mörch creep function.

It is important to realize that for the force S=R there is no redistribution of stresses in time for both creep functions. The structure keeps its shape and the stresses are constant in time. Their values do not depend on the adopted creep function.

Since it is difficult to design a structure in which the stresses are changing in time, it is very important to design an initial stage in such a way that the redistribution of stresses is minimum.

That means that the geometry and forces in the internal prestressing tendons or external cables (situated inside or outside of perimeter of the deck) have to be determined in such a way that their effects together with dead load create zero deflection at deviators - see Fig.2. It means that that the dead load should be balanced by prestressing. Then the structure that is loaded only by a normal force keeps its shape in time. This approach that was developed by professors F. Leonhardt and T.Y.Lin simply guides us to use partial, limited or full prestressing.

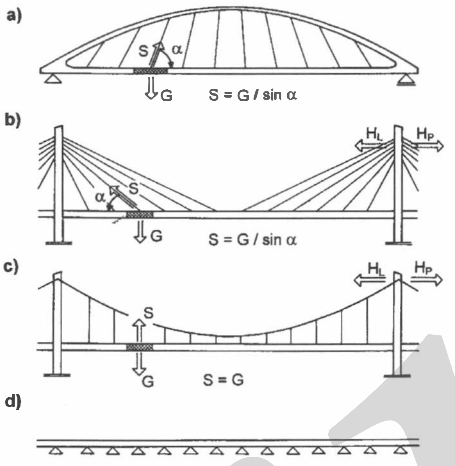

Fig.3

In case the deck is suspended on arches or pylons the initial forces in the stay or suspension cables have to determine from the condition of zero deflection of the deck at anchor points – see Fig.3.

The attempt to limit the redistribution of stresses caused by creep of concrete force us to design correct structural system and save us from designing fancy structures that are so common in steel at present. In contrast to steel structures we are not able to design the structures in which a beam is suspended on stay cables stressed to small or to large force and create an unnatural structural system developed by an architect.

In the following I would like to demonstrate how the full understanding of prestressing enables us to solve the problems of finding the best structural solution that is inherent in the site and which best fulfills the function of bridging the site.

HOECHST BRIDGE, FRANKFURT, GERMANY

The Hoechst Bridge that was designed and built by Dywidag is one of the first modern concrete cable-stayed bridge – see Fig.4. It was built across the river Main close to Frankfurt and carries a railway and a highway. The deck, which is formed by a box girder with large overhangs, is suspended on single pylon situated on one bank of the river and it is stiffened by a low concrete wall situated above the pier situated on the other bank. A hinge is created between these two parts of the deck – see Fig.4.

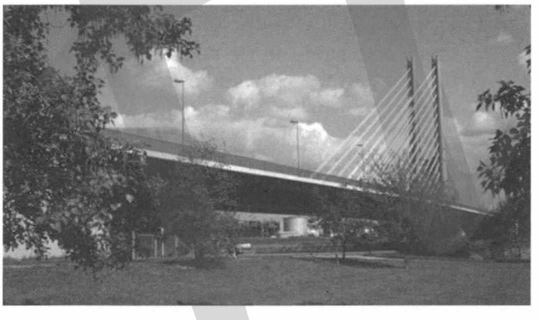

Fig.4

The forces in the stay cables are designed in such a way that exactly balance the dead load of the deck in the length between the neighboring stays. Similarly, prestressing of the wall is designed in such a way that balanced the dead load – see Fig.5. By a clever combination of the external prestressing created by stay cables and internal prestressing of the wall it was possible to reduce the length of the suspended portion of the deck and the height of the pylon. The solution opened the view on the river and created an impressive structure that fits into nice surroundings.

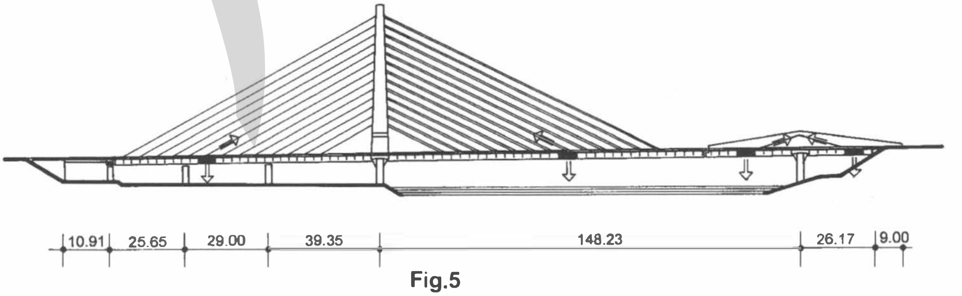

Fig.5

VIADUCT NEAR SHOPPING CENTER TESCO IN HRADEC KRALOVE, CZECH REPUBLIC

Fig.6

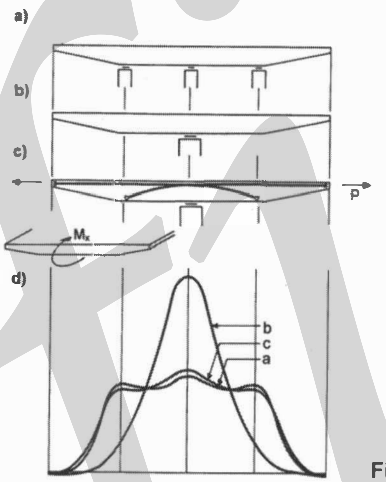

Fig.7

Swiss engineers have developed a strip post-tensioning of flat slabs. The prestressing tendons that are arranged in the support strips create support strips of zero deflection in the structure. Similar approach can be used in bridges, too. An advantage of this arrangement is demonstrated on an example of a recently completed bridge built in the Czech republic.

The bridge of the total length of 238.0 m is formed by a continuous deck slab of 13 spans of length from 12.00 to 19.00 m. The deck slab of the depth of 0.90 m and variable width from 12.30 to 14.30 m is supported by two pot bearings situated on narrow piers – see Fig.6.

Due to the difficulties with obtaining the building permission the bridge had to be designed and built within 15 weeks. Therefore a traditional span-by-span construction that requires progressive casting and post-tensioning of each span was impossible. The deck had to be cast only in few steps and progressive longitudinal post-tensioning of the deck had to be substituted by reinforcement by reinforcing bars.

To allow a very simple reinforcement formed by uniformly distributed straight rebars and stirrups a transverse post-tensioning of the structure above piers was designed. The idea of the transverse post-tensioning came from the idea of post-tensioning of flat slab. Transverse post-tensioning was created in such a way that there is no deformation in the transverse strips above support. From Fig.7 it is evident that the transverse post-tensioning can create a similar distribution of longitudinal bending moments as it is in the structure supported by several bearings.

SUNNIBERG BRIDGE, SWITZERLAND

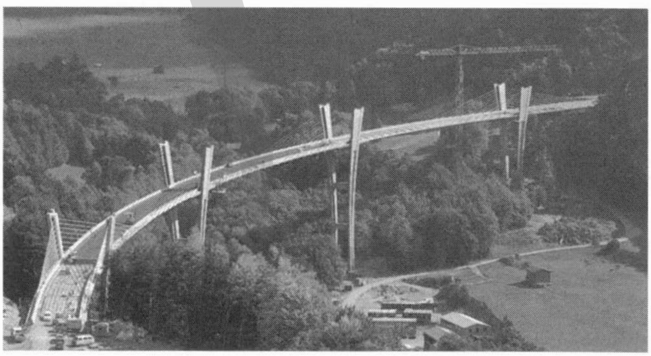

Fig.8

Sunniberg Bridge, whose concept was developed by Prof.Menn, is – according to my opinion - one of the most clever structures ever built. The bridge that has five spans of length from 59 to 134 m is in the plan curvature with radius R= 503 m – see Fig.8 and 9b. The slender deck running at sixty meters above grade is suspended on pylons protruding 15 m above the deck.

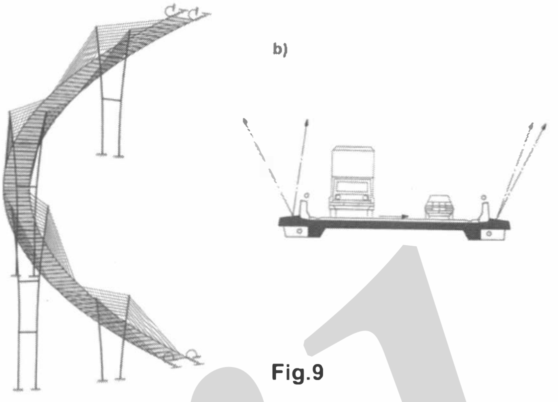

Fig.9

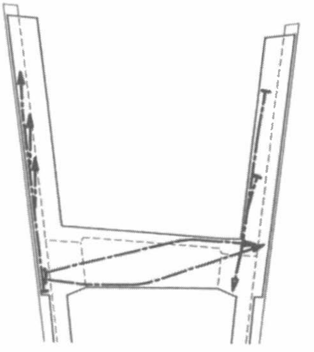

Fig.10

The stiffness of the structure comes from the plan curvature of the deck that is fixed at the abutments - see Fig.9. While in the traditional multi-span cable supported structures vertical deflection of the deck has to be controlled by intermediate anchor piers or by bending stiffness of the deck, in this bridge the vertical deformation of the deck is controlled by the transverse stiffness of the curved deck. Any vertical load causes the horizontal movement of the deck that acts in the horizontal plane as an arch. The transverse movement of the deck creates a significant transverse moments in the piers forming transverse frames – see Fig.11c. Non-traditional post-tensioning of the pylon legs and diaphragms (see Fig.10) eliminate these stresses.

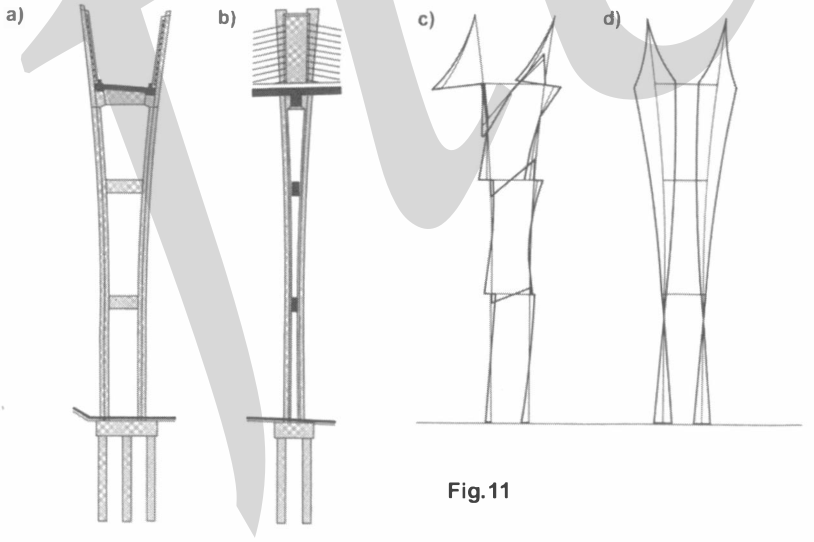

Fig.11

VRANOV LAKE PEDESTRIAN BRIDGE, CZECH REPUBLIC

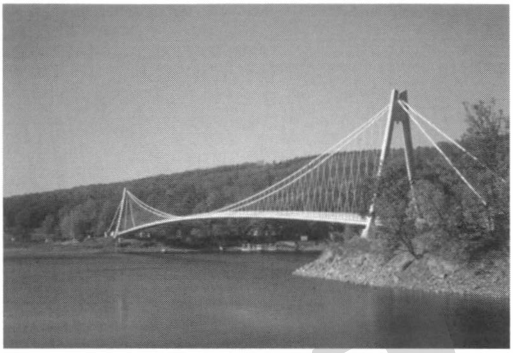

Fig.12

The deck of the suspension pedestrian bridge across the Swiss Bay of the Vranov Lake of the length of 252 m is suspended on suspension cables that are supported by A shaped concrete pylons – see Fig.12. To visually soften the structure the pylons have slightly curved legs.

The pylons were cast horizontally and then lifted into the design position. To resist significant bending stresses that originate in the pylon's legs during its lifting it was necessary to post-tension them. This post-tensioning was utilized in the completed structure too. The layout of the prestressing tendons was designed in such a way that exactly balanced the bending moment due to the dead load – see Fig.13

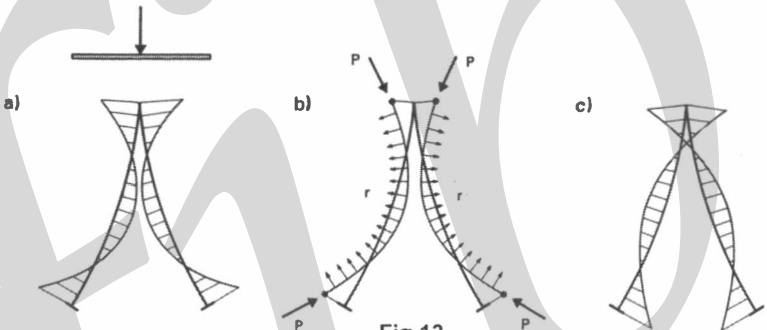

Fig.13

BRIDGES ACROSS THE RIVER ELBE AND VRSOVICE RAILWAY STATION, CZECH REPUBLIC

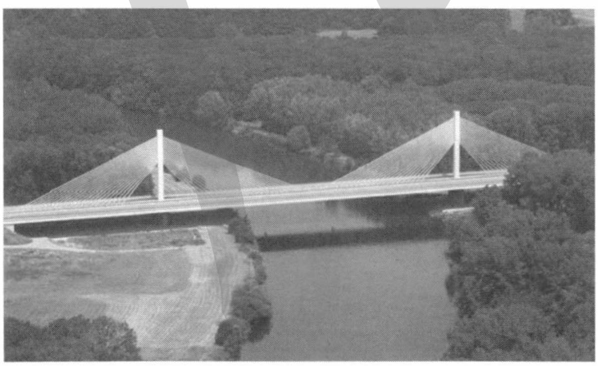

Fig.14

The cable stayed bridge across the river Elbe (see Fig.14) has three spans of length 61.60 +123.20 + 61.60 m, the cable stayed bridge across the Vrsovice railway station has 9 spans of length 26.40 + 4x35.00 + 44.00 + 101.20 + 48.40 + 33.00 m. The last three spans are suspended on one single pylon. Single piers situated in the bridge axis support the approach spans - see Fig.15.

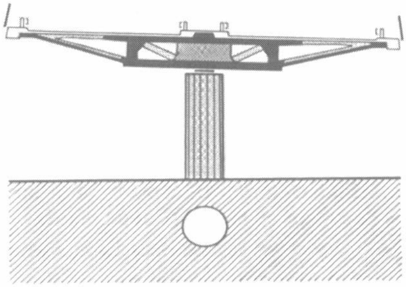

Fig.15

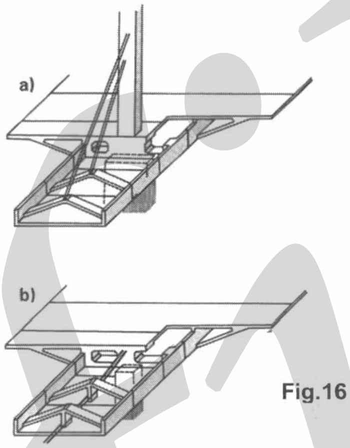

Fig.16

Both bridges have similar deck formed by a spine box girder and additionally cast overhangs that are supported by precast struts. The load from the girder's webs is transferred to the stay cables situated in the bridge axis by internal ties formed by prestressed concrete members – see Fig. 16a. This arrangement, which was developed by a French engineer in the design of the Broton Bridge, allows transferring of the dead load shear directly into the pylon. However in the non-suspended part of the structure the shear has to be resisted by webs.

In case of our first cable-stayed bridge across the River Elbe the bending moments in the non-suspended portion of the deck was balanced by short straight cables situated at the top slab. The shear was resisted by the shear capacity of the widened webs – see Fig.17a.

In case of the Vrsovice Bridge the shear in non-suspended parts of the deck (close to the pylon and in the approaches) is transferred into the pylon or single supports directly by external cables situated like the stay cables in the bridge axis. These cables are draped in blisters situated at bottom slab. The vertical component of the prestressing force balances the shear forces that are transferred into the middle of the top slab by ties - see Fig16b.The middles of the top and slabs are connected by short compression struts.

Recently, a similar structural arrangement and similar layout of external cables was used in the construction of the Santarem cable stayed bridge that was built in Portugal.

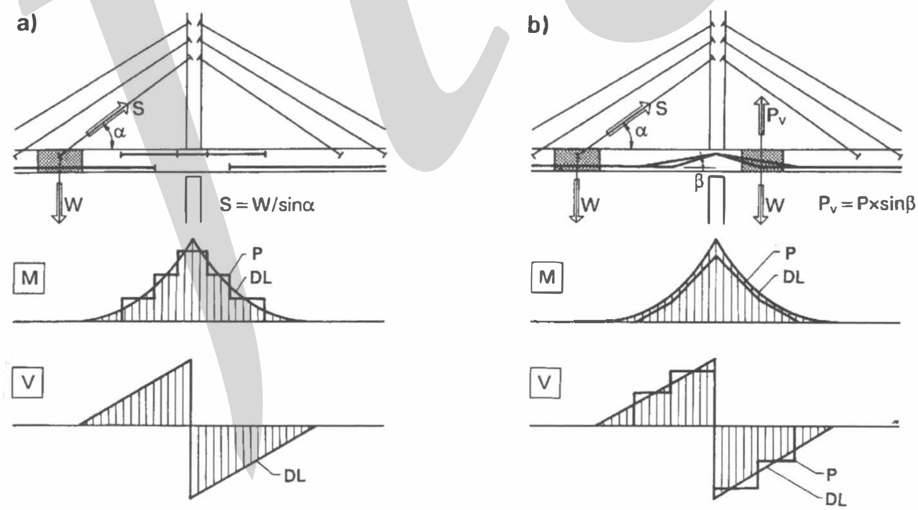

Fig.17

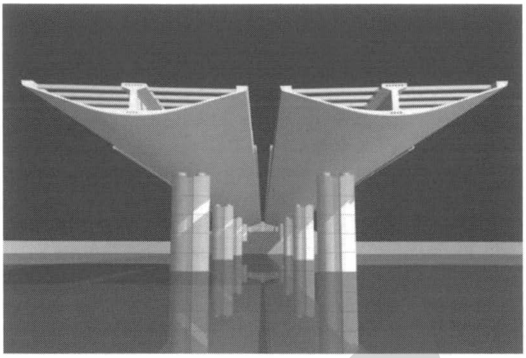

Fig.18

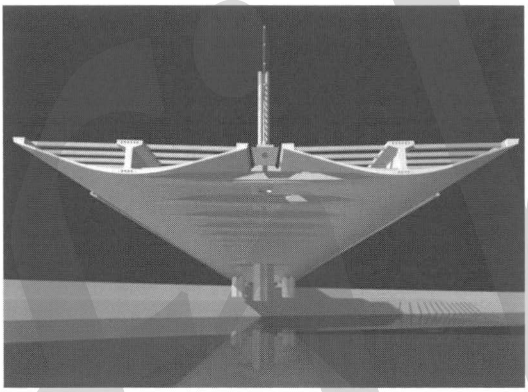

Fig.19

At present many clients prefer freeway bridges in which there is an independent structure for each direction of the freeway to easy repair works if needed by transferring the whole traffic onto one structure when repairing the other. The presented structure shows the possible solution for cable-supported bridge.

The designed freeway D47 crosses the river Odra and Antosovice lake on the bridge of the total length of 589 m. The span across the river Odra is suspended on a single pylon situated in the bridge axis – see Fig.19. The deck of each structure is formed by a continuous box girder. The girders of depth of 2.20 m are assembled of precast match-cast segments and additionally cast top slab – see Figs.18 and 19. The segments have an open cross section formed by central web and curved bottom slab. The segments together with the top slab form two cell box girders without traditional overhangs.

In the suspended spans the segments are mutually connected by a continuous deck slab and by single precast struts erected between the segments. These struts are fabricated together with stay anchor blocks – see Fig.19.

The transverse connection of the segments is relatively simple and creates a clear truss structural system. The shear forces from the central webs are transferred by post-tensioned inclined webs into the stay cable's anchor blocks. The transverse bending of the structure is resisted by a tension capacity of the transversally prestressed deck and by a compression capacity of the struts – see Fig.20.

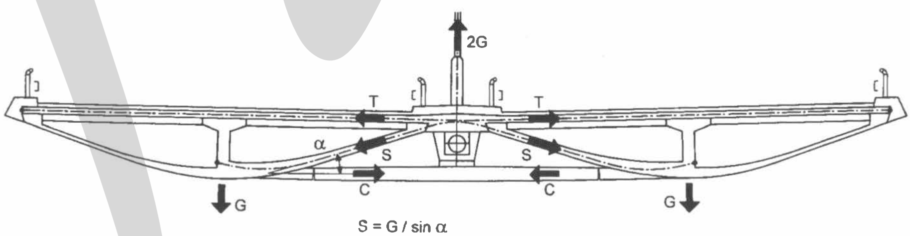

Fig.20

Similar arrangement can be easily used in design of an arch or suspension structure.

BRIDGE ACROSS THE RIVER SVRATKA, CZECH REPUBLIC

Fig.21

A relatively small cable stayed bridge with a span length of 50.00 m has been built across the river Svratka in a small city of Zidlochovice. The adjacent roads left little space on the banks; therefore the deck is suspended on one side by an inclined pylon – see Fig.21. The deck of the bridge, 18.60 m wide and only 0.70 m deep, is formed by two longitudinal precast edge girders and transverse solid slab members connected by longitudinal and transverse post-tensioning – see Fig.22.

The structure was erected progressively – see Fig.22. At first the edge girders were erected and

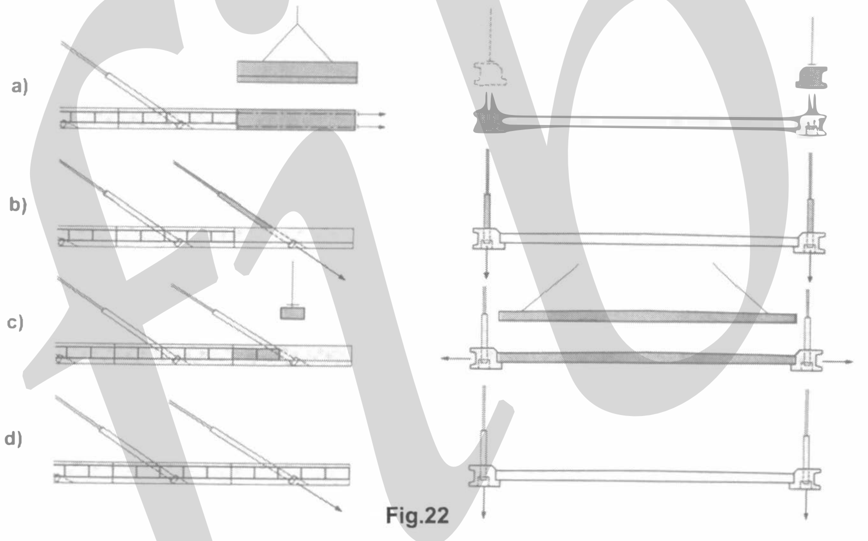

Fig.22

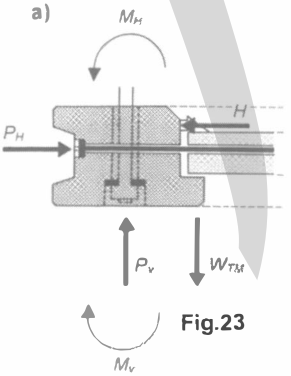

Fig.23

suspended on the stay cables – see Fig.22a, b, then the transverse solid members were placed on the edge girders - see Fig.22c. To eliminate the torsion of the longitudinal girders caused by their eccentric loading by transverse members an eccentric transverse post-tensioning was created – see Fig.23.

The transverse members were provided with steel brackets with nuts and screws located on the surface close to their ends. After transverse members were erected, the screws were drawn until their heads touched the longitudinal girders. Then, the post-tensioning bars were partially tensioned. The force couple acting on the girder (under the screw's head and the bar's anchor) created a moment that balanced the torsion.

RUCK A CHUCKY BRIDGE, CALIFORNIA

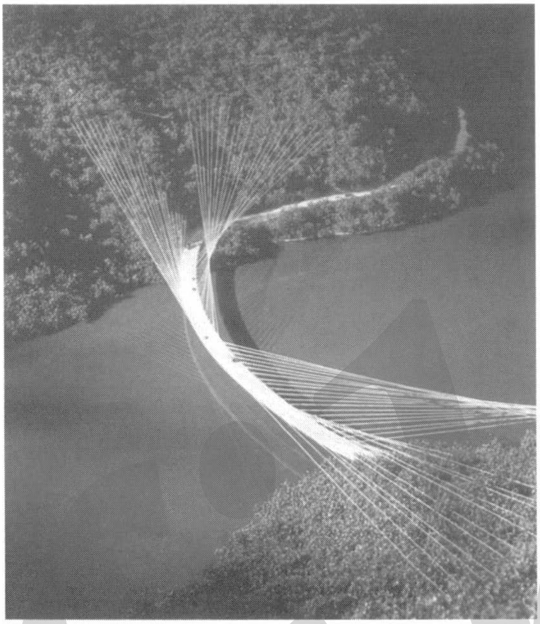

Fig.24

Excellent example of load balancing represents a design of the Ruck a Chucky Bridge performed by T.Y.Lin International. Although this bridge has not been built, its design clearly demonstrates how all internal forces can be balanced by an external prestressing – by the arrangement of stay cables.

The bridge with the span of 396.24 m crosses the reservoir in the plan curvature of 628.00 m - see Fig.24. The deck is suspended on the stay cables arranged in hyperbolic paraboloid formation to create an array of tensile forces, which produce pure axial compression in the curved deck. The vertical-force components of the cables balance the weight of the deck – see Fig.25a. The horizontal components are designed to reduce the horizontal bending moments at critical points to zero – see Fig.25b.

The design demonstrates how pure engineering approach can create a structure of an unbelievable beauty and elegance.

a)

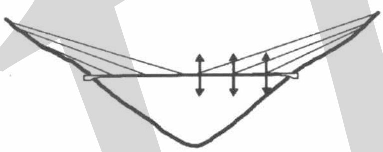

b)

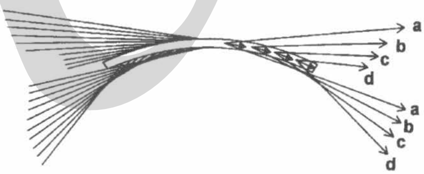

Fig.25

PEDESTRIAN BRIDGE IN KELHEIM, GERMANY

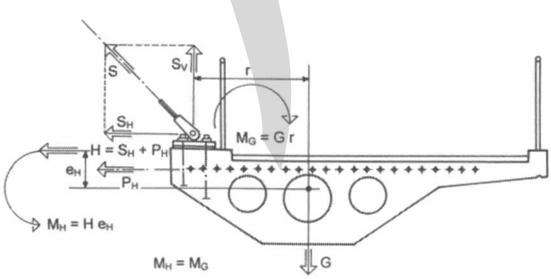

Fig.27

A design of the pedestrian bridge, which was built in a small city of Kelheim, clearly proves that *science, not intuition, is the tool of creativity*. The structural solution was developed from deep understanding of behavior of curved structures. The design was performed by Prof.Schlaich from Stuttgart.

The bridge crosses the canal Mohan – Danube in smooth curves naturally connecting the pedestrian traffic on both banks – see Fig.26. The deck, which is in the

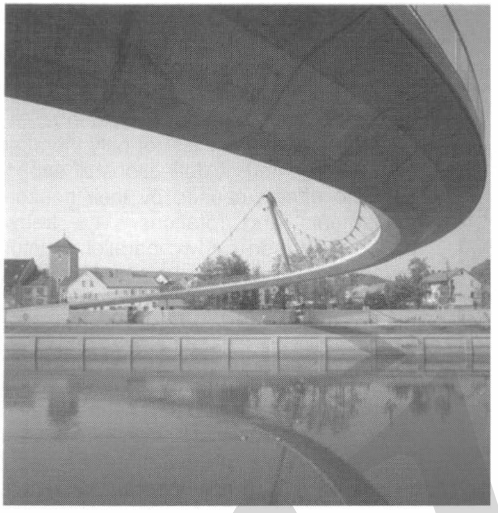

Fig.26

plan curvature with radius from 18.89 to 37.79 m, is suspended on one suspension cable situated inside of the plan curvature. Two inclined pylons situated on both banks support the suspension cables with hangers. The geometry and initial stresses in the cables were designed in such a way that vertical components of the hangers forces balance the dead load – see Fig.27. The horizontal components of the hanger force together with the radial forces from prestressing cables situated close to top fibre of the cross section create a moment that balance a torsional moment caused by vertical forces.

By full understanding of the prestressing and clever arrangement of the suspension cables a true structure was developed. Again the design demonstrates how pure engineering approach can create a structure of unbelievable beauty and elegance.

BRIDGE ACROSS THE VLTAVA RIVER NEAR PRAGUE, CZECH REPUBLIC

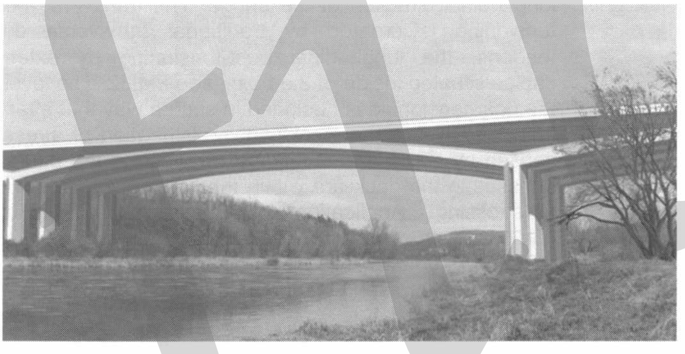

Fig.28

At present, cantilever structures are being designed for longer and longer spans. The sections above piers create unnatural barriers in the countryside. A proposed bridge across the river Vltava tries to solve this problem by creating light and transparent structure – see Fig.28.

The bridge is formed by a self anchored arch in which a horizontal force due to the dead load is resisted by external cables. The structure has three spans of length of 64 + 114 + 64 m. The arch is erected in symmetrical cantilevers starting from the piers using a temporary pylon and stays – see Fig.29. After erection of the arches the central joint is cast and the external cables are post-tensioned. Then the portion of the deck above the piers is cast and post-tensioned. Although the arches can be designed as traditional reinforced concrete members, they call for taking an advantage of high strength concrete.

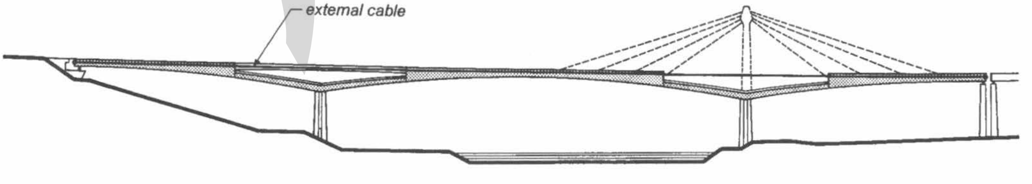

Fig.29

BRIDGE ACROSS THE ODRA RIVER, CZECH REPUBLIC

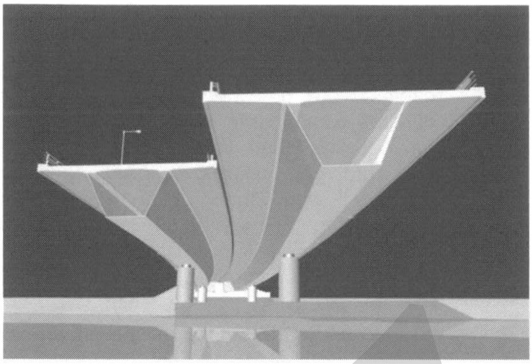

Fig.30

The bridge of the total length of 402 m is being built in the area influenced by the effects of the mining subsidence. The structures have to resist not only the effects caused by different deflections of supports but also effects caused by their horizontal movements and rotations. The freeway bridge is formed by two parallel structures formed by composite box girders of four spans of the length from 49 to 102 m – see Fig.30.

The design of the bridge was influenced by two opposing requirements. On the one hand the structure had to be sufficiently stiff to be able to resist the designed load, on the other hand the structure had to be sufficiently flexible to be able to resists the effects of the subsidence. Since the relative different rotations of supports decrease with the length of the bridge, the points where rotations are transferred into the deck was designed at the longest possible distance – at the abutments. On all intermediate supports the deck is supported by single bearings situated in the bridge axis.

The deck slab is stressed not only by bending and shear stresses caused by a local load but also by significant membrane stresses caused by global bending and torsion – see Fig.31. Since the composite deck slab guarantees the integrity of the structure we tried to eliminate the cracks. Therefore the deck is post-tensioned both in the transverse and longitudinal direction of the bridge. The transverse post-tensioning is created by traditional transverse deck tendons, the longitudinal post-tensioning by external cables situated inside of the box – see Fig.32. The level of the post-tensioning is designed in such a way that after all losses and after the significant redistribution of stresses caused by creep and shrinkage of concrete the principal stresses in the deck are within the limits given for limited prestressing. Application of post-tensioning in the composite structure allows us to design a very simple and clear continuous bridge structure in the area where only statically determined structures have been built so far.

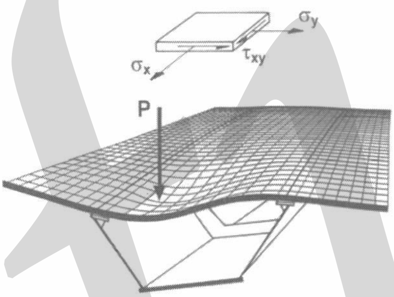

Fig.31

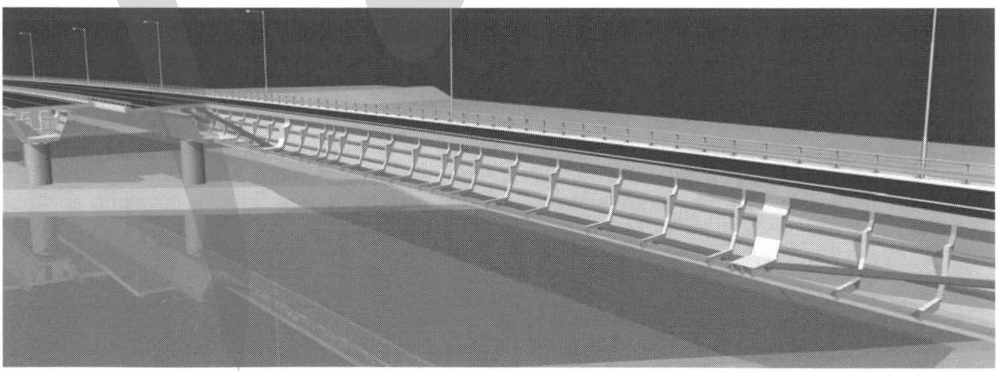

Fig.32

3 STRUCTURES USING TENSION STIFFENING

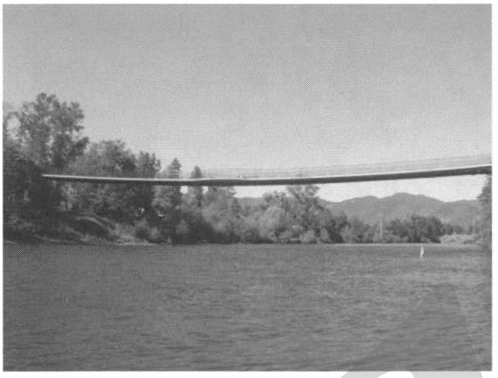

Fig.33

Fig.34

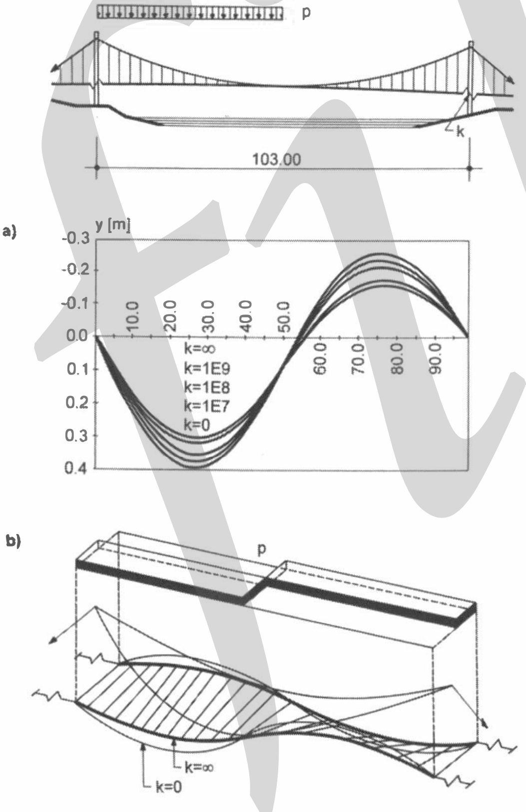

Fig.35

Our experience with the design of stress ribbon (see Fig.33) and suspension structures (see Fig.34) has confirmed that the static and dynamic response of the prestressed concrete deck can be significantly reduced by preventing of the horizontal movement of the deck at supports. Fig.35a shows vertical deformations of the deck of the central span of the Willamette River Bridge (see Fig.34), which was recently completed in Eugene, Oregon, for loading situated on one half of the main span and for different values of the horizontal springs modeling the flexible fixing of the deck. Although a tension force stresses the horizontally fixed deck, the resultant normal stresses are much smaller than the stresses in the structure with movable supports are.

Similar reduction of the deflection and stresses is for the load situated in the main span in a check board pattern that caused maximum distortions of the deck – see Fig.33b. It explains a very good behavior of stress ribbon and suspension structures with prestressed concrete deck for wind and pedestrian loading.

Since the segments of the stress ribbon and suspension structures are suspended on the bearing cables before the casting of the joints between them (Fig.36 and 37), the dead load of the structures is always balanced by the forces in the cables.

Fig.36

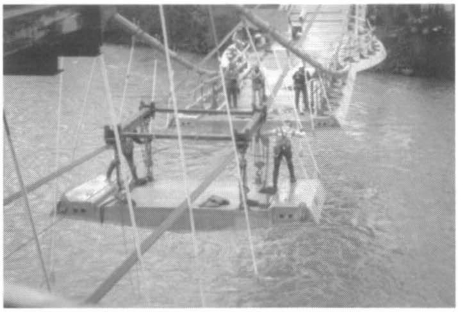

Fig.37

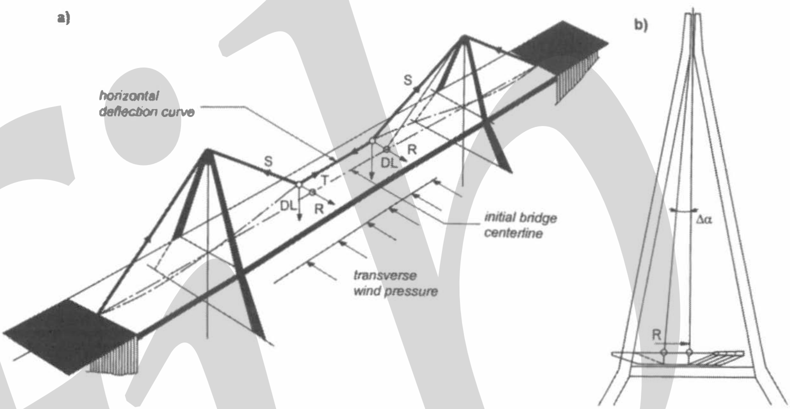

Fig.38

Tension stiffening of the deck was also utilized by Jean Muller in his proposal for long span cable - stayed structures that he calls *Bi-Stayed Bridges*. The longest back stays are anchored in abutments that serve as anchor blocks too. In this way the longest stays anchored in the main span create a tension force in the deck and stabilize it – see Fig.38.

It is well known that cables can stabilize mats, pylons and arches. Stabilizing effect of the cables for the seismic load is proposed by Prof.Ikeda from Japan. The cables are tension in such a way that they behave elastically for seismic load. Tension force in the cables – similarly to stay cables - stabilizes the columns.

4 CONCLUSIONS

Presented structures clearly demonstrate the power of prestressing. The prestressing allows us to balance the load, change boundary conditions, and create supports within the structures. Prestressing is really a revolution, prestressing is a radical step from passive to creative thinking and development.

The prestressing allows creating the structures of a high architectural value that have a minimum impact on environment. It is our responsibility to utilize prestressing and to provide our cultures with reasonable structures of architectural elegance, beauty, and charm.

The paper was prepared in a support of the research project MSM 261100007 'Theory, reliability and mechanism of failure of statically and dynamically stressed structures'.

****

The views expressed, or conclusion reached, are entirely those of the author.

SOME SPECIAL FEATURES IN MEDIUM SPAN CONCRETE CABLE-STAYED BRIDGES

Leonardo Fernández Troyano
Carlos Fernández Casado S.L.
Ph. D. Civl Eng.
Grijalba, 9, 28006 Madrid
Spain
cfcsl@cfcsl.com

Keywords: bridges, cable-stayed bridges, stays, arch bridges.

I.- INTRODUCTION

I.a.- Bridges at the present moment

Since the end of the 18th century, when metallic bridges first began to be built, up to the second half of the 20th century, bridges have always been in the process of constant and rapid development.

There were times when the development was basically due to the types of structures that appeared in modern bridges, and then there were other times when it was due to new materials. When referring to new materials here I mean different resistant systems made by combining various basic materials such as reinforced concrete, prestressed concrete or composite structures. To this development of structures and materials we must also add the theoretical knowledge of structures, and procedures of analysis for determining the safety of bridges that came about during the same period.

All the new techniques that have been coming out in construction in general and particularly in bridges have followed similar paths in their development. This development can be divided into two more or less differentiated stages:

The first stage, which could be called youth, begins with the discovery of a new technique, may it be a new type of bridge, a new material or a new construction procedure. In this first stage the evolution is fast, significant advances come one after another whenever a new bridge is built. The progress is quick until the new technique is almost completely mastered. This is when the stage we have called youth ends and the next, mature, one begins.

In the mature stage the advances are smaller and less frequent; the differences between the works that mark the progress consist of small steps. This does not mean that in the mature stage the evolution and progress are over, because the development of engineering continues. Yet it is rather due to the evolution of bridge techniques in general than to a better understanding of the specific technique being studied.

The constant development of bridges in the period was therefore motivated by consecutive partial developments:

As we have said, at the second half of the 18th century (1779), the first metallic bridge was built. It was the Coalbrookdale arch bridge made of cast iron elements. This bridge marked the beginning of the development of cast iron bridges which took place in the first half of the 19th century; in the second quarter of that century, metallic arches and suspension bridges had already become widespread and were replacing stone bridges to a great extent. By mid-19th century, before cast iron bridges even reached their mature stage, wrought iron appeared, which gave rise to the hot rolling of profiles and plates, elements which changed significantly the technology of metallic bridges. The second half of the 19th century is when great lattice-beam bridges were built on railroads.

Modern suspension bridges were first built at the beginning of the 19th century, in the United States, by J. Finley, using cables and chains. These bridges soon spread to Europe as well. In 1882 M. Seguin began building suspension bridges made with wire cables, and from then on, both systems were used in parallel.

In mid-19th century suspension bridges were questioned in Europe owing to various disasters that took place. As a result, their development continued only in the United States, until the end of the century.

At the end of the 19th century, steel appeared in construction, which brought about a significant change in the quality and regularity of the material used to build bridges.

Reinforced concrete was first used at the end of the 19th century and developed further at the beginning of the 20th century. It soon spread around the world, and became the most suitable material for small and mid-span bridges which are the most frequent ones.

In mid-20th century, when we could say that reinforced concrete bridges reached its mature stage, prestressed concrete came out. This system turned out to be better and resisting bending moments than reinforced concrete. Prestressed concrete underwent spectacular development after the Second World War and it made it possible to build concrete girder bridges as long as 301 m, one meter longer than metallic plate girder bridges.

Before the Second World War the welded joint appeared in metallic structures but it initially had many problems; it developed after the War and this brought about a further development of metallic bridges. Welded plate girder bridges developed very fast, as well as prestressed concrete bridges.

In the second quarter of the 20th century the behaviour/performance of composite structures began to be studied and bridges started to be built using this system. However, like the previous techniques, they only became widespread after the Second World War and they fully developed in the third quarter of the 20th century:

In mid 20th century as well, as we have seen, cable-stayed bridges appeared. This technique is the only one which was still going through its youthful stage during the second half of the 20th century and it stayed in this phase until the end of the century. That is why in the last quarter of the 20th engineers dedicated their greatest efforts to this type of bridge both in projects and in theoretical studies and related techniques such as stay cables. An endless number of books and publications were dedicated to cable-stayed bridges because there was a chance to make a contribution to a developing technique. It is the quintessential bridge in this part of the century.

With the above summary we wished to point out that from the 18th century until the end of the 20th, there always existed techniques of bridge construction which going through their youthful stages; however, at the end of the 20th century, the different bridge techniques entered the mature stage and there is no one technique in an initial stage. This is why the technological development of bridges has slowed down, which does not mean to say that it has come to a complete halt since techniques will always continue to evolve.

To this mature stage of the bridge techniques we must add the remarkable development of the computer aided methods of analysis, which changed substantially the possibilities of studying all kinds of structures. We can also consider the theoretical and practical knowledge of structures to have reached its maturity.

The present-day situation in bridges we have described has created among engineers a different kind of attitude from that which have had all the way through the evolution of the modern bridge. Engineers are innovators in their essence, and if technologies offer few possibilities for innovation, then they will explore other paths.

The maturity of these techniques, which really means their mastery, has made it possible to widen the field of possible solutions, retrieving almost abandoned techniques, such as lattice beams, that have turned up again after nearly disappearing altogether.

Another tendency that sprang up from this maturation is one we consider negative. It consists of the search for shape as the primary element in bridge design, sometimes even in an exclusive way: the bridge becomes an object of mere design, which must then be given a structure.

Due to all the reasons we have stated so far, we can talk about a certain eclecticism at the current moment in bridges, which exists in architecture as well. There exist all kinds of bridges, made of different materials (in the wide sense we defined earlier) and we can even talk about different styles. The current moment in bridges can be defined as having a limitated technological evolution while undergoing a wide use and exploration of diverse solutions.

I.b.- Medium span cable-stayed bridges

The bridges we are about to present can serve, in our opinion, as examples of the above exposition. They are cable-stayed bridges whose spans belong to the lower length range for this type of bridges. In other words, their spans are among the lower ones for which the cable-stayed solution is justified.

This condition of reduced spans allowed a greater freedom of design which enabled us to look for unique solutions with a minimum additional cost. The emphasis was on different expressions in each of them; in some it was placed on the stay cables, in others on the towers and in yet others on the bridge as a whole.

The unique structures of these bridges called for special solutions for some of the technical problems that came up. Some of these problems are of a technical nature and affect the whole or the important parts of the structure; others have to do with details, generally speaking with the stay cables.

Flaubert's phrase *"God lives in the details"* often quoted by Mies Van Der Rohe, is far too often forgotten by engineers. At other times the engineer is rendered virtually impotent by the determinism imposed by present-day construction systems and patents on many details of a bridge. There are many elements of the stay-anchorage mechanism, which are a part of approved systems patented to the stay cables systems on the market. The official approval and therefore obligatory use, of some of these elements is justified, but in others this is not quite the case and they should adaptable to each particular project. However, generally speaking the standard elements of the systems are imposed no matter whether their use is justified or not.

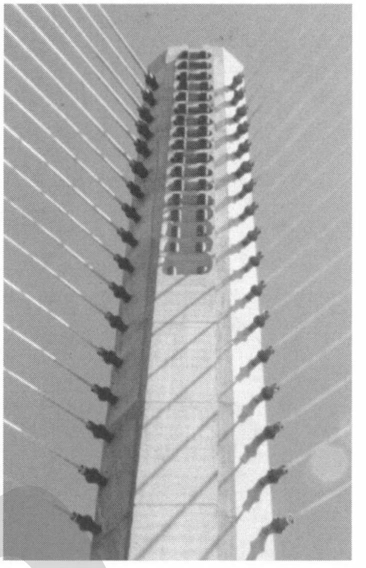

As an example of this determinism we can show the elastomeric guides and shock absorbers placed on the Lérez river bridge in Pontevedra. The metallic elements on the stay cables' exits can be solved with simpler forms than those imposed by the system. These simpler forms are not necessarily more difficult or more expensive to produce. Nevertheless we had no chance to change the system elements. Luckily the elements placed in the tower are little seen and those in the counterweights were covered with protective tubes against vandalism.

II.- FOUR MEDIUM SPAN CABLE-STAYED BRIDGES

We are going to present four cable-stayed bridges of quite different conceptions. In these bridges we are going to study the problems of design as well as special technical problems we came across:

II.a.- The bridge over the Lérez river in Pontevedra, Spain

The basic problems we faced in the design of this bridge were the following:

a) The riverbed and the streets situated along the riversides forced us to build a single span bridge, 125 m long, without the possibility of adding compensating spans at the ends.

b) The streets on either riverside made us fix the bridge at a minimum height above the water level. Moreover, this height is variable because it is affected by the tide of the Atlantic Ocean. At flood tide the deck height above the water can be as small as one meter.

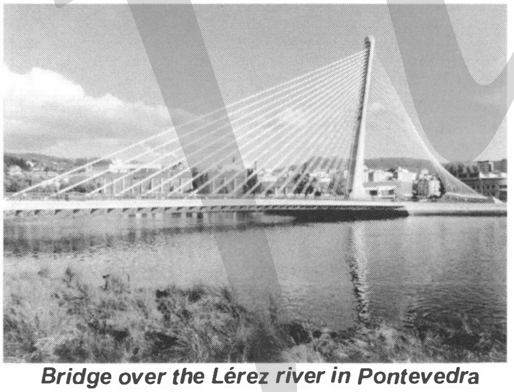

Bridge over the Lérez river in Pontevedra

These problems made us look for a minimum depth solution and therefore an upper structure. From among the different possibilities of bridges with an upper structure: upper arches, suspension bridges or cable-stayed bridges, we decided to use the last of these with a single pier on the left riverside with no compensation span, and therefore the rear stays were anchored in the counterweights. The general equilibrium of the structure is achieved by a polygon of forces formed by the deck, the pier, the stay cables, the counterweights and a tie beam between the pier foundations and the counterweights.

We used a similar structure with the same polygon of forces and a 140m long span in the Sancho el Mayor bridge over the Ebro river in Navarra. We had a similar problem as in Pontevedra: the main span could not incorporate a compensating span on the tower side.

The position of the counterweights on the side of the road gives a spatial configuration to the cable-stayed arrangement, because the three fans of cables, a front one along the bridge axis and two rear ones, mutually form angles of about 120°. Such spatial arrangement, one of the most expressive design elements of both bridges, was emphasised in the Pontevedra bridge by the hyperbolic paraboloid of the compensating fans. These hyperbolic paraboloids were the key elements in this project, as can be observed in the whole process from the very first drawing to the completed work.

In the physiognomy of both of these bridges the tower inclination, motivated by the composition of forces produced between the deck, piers and stays, is also essential.

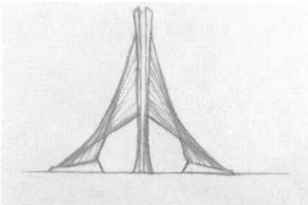

First sketch

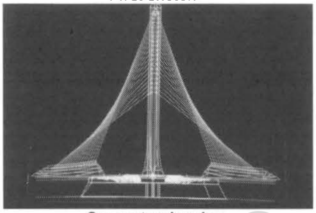

Computer drawing

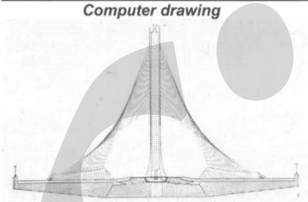

Project drawing

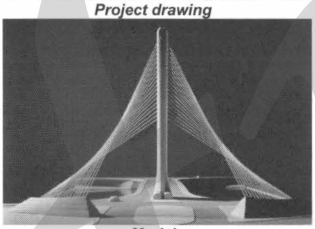

Model

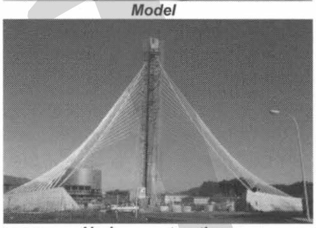

Under construction

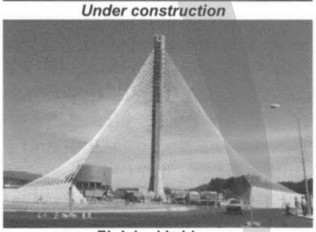

Finished bridge

We shall now compare some of the problems posed by the uniqueness of these bridges' structure:

1. Counterweights. The counterweights of the Ebro bridge were solved using gravity i.e. the concrete weight. In the Pontevedra bridge the compensation was carried out partly with concrete, and partly with anchorages in the ground; this allowed us to reduce their dimensions significantly and locate them on traffic islands on the left riverside.

2. Tie beams between the pier foundations and the counterweights. In the Ebro river bridge two problems were posed by these beams:

a) The pier foundations were made of slurry walls of great horizontal stiffness and the counterweights which, as we have said, were solved using the volume of concrete. Therefore the foundations admitted no horizontal movement in the base. The tie beams which connect these two elements were shortened due to the axial force introduced by the polygon of forces of the bridge balance. This shortening could not be absorbed in either of the extremes and it was therefore necessary to arrange flat jacks in an intermediate cross-section of the beam. These jacks were loaded in several stages during construction in order to compensate for the beam shortening.

b) An expert geotechnical study, performed to evaluate the settlements of the main foundation, show several centimetres of settlement that would occur during construction. These results surprised us all, and as a matter of fact it never occurred. However it had to be provided for and this made us introduce two provisional metal hinges in each tie beam, which were closed once the bridge was finished. The magnitude of the supposed settlements also required a retensioning programme organized in stages for the compensation stays, which was not carried out because, as we have said, the settlement that actually occurred did not require any special action.

In the Pontevedra bridge the pier foundation is deep, with 1.50 m diameter piles, and the counterweights also had profound foundations with 0.80 m diameter piles and anchorages in the rock. The flexibility of both foundations was sufficient to absorb the tie beam shortenings without requiring any special action to it.

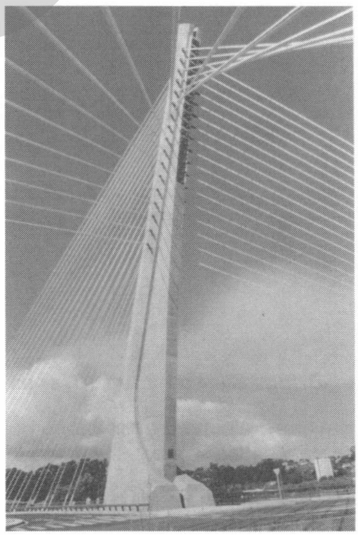

The construction of both bridges was carried out with cable-stayed free cantilevers. In the Sancho el Mayor bridge we used prefabricated segments assembled with the help of a crane from the deck which had been completed, and in the Lérez bridge the segments were cast in situ using a form traveller.

In the Sancho el Mayor bridge the distribution of bending moments was corrected by provisional piers situated near the definitive ones in front of the pier, and in the Lérez bridge it was corrected by lowering the support facing the pier.

I.b.-The Papaloapan river bridge in the state of Veracruz, Mexico

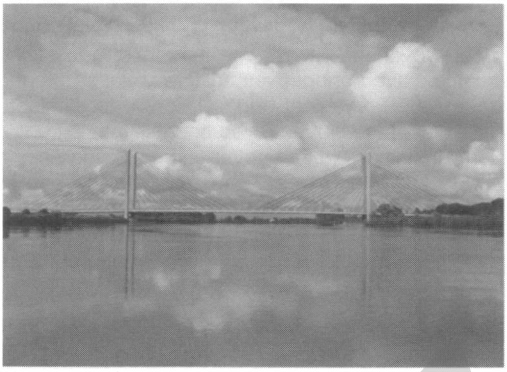

The Papaloapan river bridge

In the project of the bridge over the Papaloapan river we tried to simplify as much as possible all the elements that make up a cable-stayed bridge. We can say that we chose a minimalist solution although it has nothing to do with minimalism in architecture.

The bride crosses the riverbed with a 203 m long span and is continued on the riversides with 70 m long compensating spans. The deck continues over the abutments, which are made by 32 m long box girders. The deck is fixed on to abutments in order to resist horizontal forces produced by seismic activities.

The deck is made of two compact longitudinal 1.25 m deep girders connected by strut diaphragms and by an upper slab. This deck solution is classical in cable-stayed bridges with fan planes situated along deck edges.

The towers are made of two independent vertical piers situated on the deck edges. They are connected under the deck by a lattice which resists the transverse forces produced by earthquakes and wind, which can also be significant because the Paploapan river basin is situated in a hurricane area.

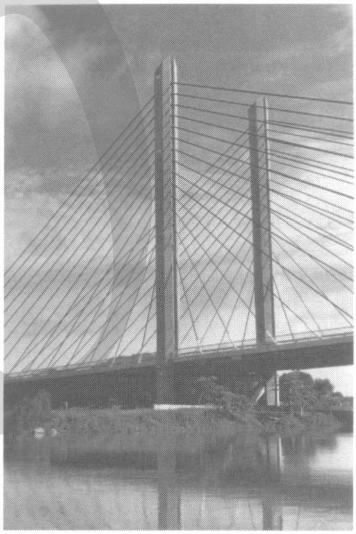

The anchorage of the stays in the towers is a difficult problem in cable-stayed concrete bridges of small or medium spans. This is due to the fact that the dimensions of the tower does not allow us to build an inner gallery to accommodate the anchors. The most frequent solution used in these cases is to cross the stays in the tower. The front and rear fans must therefore be arranged in different planes and we also must place tubes in the towers through which the stays are to pass. Some of these are too long which makes the construction complicated.

In order to avoid these problems in the Papaloapan bridge we designed metallic elements which were concreted on the towers. Onto each end of these elements, which protruded from the concrete, one front and one rear stay was anchored and they were balanced by means of this element. We thus avoided the tubes and managed to arrange the front and rear stay fans in the same plane. These elements were drilled into the concrete and such connection allowed us to tension separately the rear and the front cable. In order to avoid concrete cracking when the element was tensioned, we placed prestressed bars parallel to the element. The elements had two parts, one plated and other cast, which were welded together. This system produced problems in a few elements and for this reason we have modified the design of the element, avoiding the welding for future bridges.

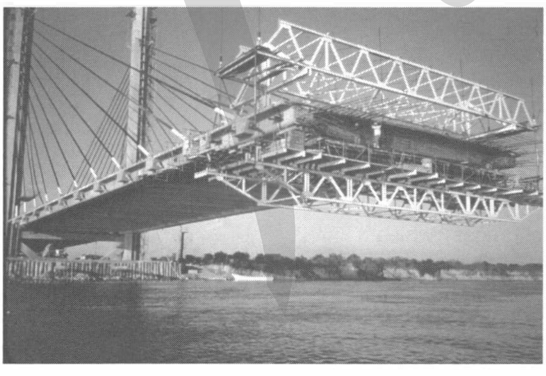

The bridge was built in cable-stayed free cantilevers, concreted on the form traveller, advancing symmetrically from the towers towards the centre of the main span and towards the abutments.

The following two bridges are new bridges alongside existing ones: the Grijalva river bridge in the town of Vllahermosa, the state of Tabasco, Mexico, is alongside an old movable bridge. The Juan Bosch bridge over the Ozama river in the city of Santo Domingo is the companion of the Juan Pablo Duarte bridge, a 180 m long suspension bridge built in the 1950s.

To make a bridge in parallel always poses a difficult problem in the bridge design because the two bridges hinder each other both physically and visually.

Physically there can be mutual disturbances, basically due to the wind effect. A clear example of this problem is the replacement of the Plougastel bridge over the Elorn river in France, one of the masterpieces of Eugène Freyssinet. To replace it, a cable-stayed bridge was built very close to it and this made it necessary to place “flaps” on the arches of the Freyssinet bridge in order to eliminate whirlwinds produced, which affected the aerolastic instability of the cable-stayed bridge.

The visual interference of both parallel bridges is obvious since we can never see one bridge alone, we will always see the whole, although from each side the bridge closer to us will be the one to dominate the view.

There are different solutions to this problem; we can repeat the original bridge, a solution often used in the past, or there are contrasting solutions, where we choose a bridge radically different from the initial one.

II.c.- The Grijalva river bridge in the town of Villahermosa, the state of Tabasco, Mexico

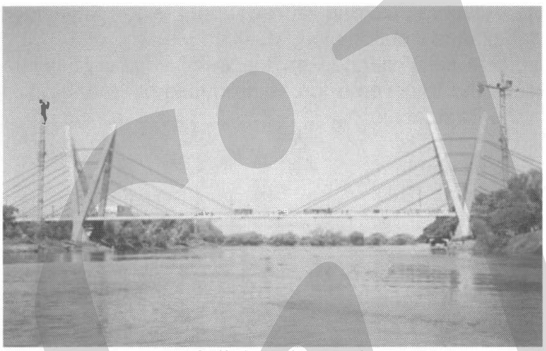

The Grijalva river bridge

This is a case of doubling of an existing bridge, an old movable bridge with large piers in the riverbed, which never opens any more and will probably be replaced in the future by a bridge like the one we built. This in the reason why we did not go for a solution that would give homogeneity to the two bridges. We rather looked for a contrasting solution.

A preliminary condition of the new bridge was to cross the river in a single span, and this made it necessary to build a 116-m long span. Since the bridge elevation is close to the river level it was necessary to adopt a solution of minimum depth, which is solved well with a cable-stayed bridge. The bridge has a narrow width, 10.80 m, and this makes it possible to give the deck a small depth, 0.80 m, because in bridges of these dimensions the deck depth is more conditioned by the bridge width than by its longitudinal span.

The deck is made of two longitudinal girders, as in Papaloapan bridge, connected with strut diaphragms and the upper slab, although given the total deck depth of this bridge, the whole looks more like a ribbed slab than a deck made of longitudinal girders and strut diaphragms.

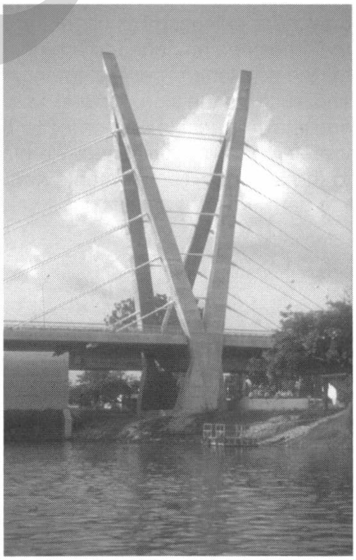

The relatively small span of this bridge among cable-stayed ones allowed us to chose a unique solution, putting the main emphasis on the towers with a spatial configuration, since they are V-shaped in the bridge elevation and A-shaped in the transverse plane.

The V-shaped tower makes it necessary for the stay cables to have three alignments, two inclined ones which connect the arms of the V and the deck and a horizontal one between the arms of the V. The stay fans are situated in the inclined planes defined by the arms of the V and each fan has five parallel stays.

The organization of the tower and stay cables makes it necessary to make the stay pass through tower shafts by means of saddles within, because to interrupt the stay cables would call for a large number of complex anchorages, which would render the solution unfeasible.

This made us study a system of saddles that would allow fixing of the stays to the towers to resist live loads, and to allow the replacement of the stays without disturbing the deck or the towers. This was achieved by making the saddles with a double tube, an external one connected

to the tower and an internal free one that holds the stay cables. At the saddles' ends away from the tower we placed passing anchorages in order to resist the load variations in the stays produced by the live loads. These anchors are fixed to the pier by screwing them to the fixed tube of the saddle.

To replace a stay cable it is necessary to first unload the deck anchors; after that the screws connecting the passing anchors to the tower are unscrewed, the cables are cut and then the saddles' interior tubes are removed.

The bridge was built in free cantilevers cast in situ using a form traveller, advancing symmetrically from each tower towards the centre of the span and towards the piers at the bridge ends. Due to the anchors of the cables in the deck, which are placed at every 10 m, and the 0.80 m depth of the deck, it was necessary to arrange a provisional cable-staying in all the 3.30 m long segments. Therefore, between each two definitive stays we arranged provisional stays that were removed once the next definitive stay was tensioned.

The bridge was continued at either end by approaches, each made of four 20-m long spans. In order to preserve the homogeneity with the main bridge, the same structure was maintained, made of two longitudinal girders placed along the edges. Nevertheless, the need to build piers with a single central column makes it necessary to take the loads from the slab first to the edge girders and then, over the pier, from the edge girders to the central column; this structure is not the most logical one but since the dimensions of the approaches are small we felt that the homogeneity of the whole bridge was a priority.

II.d.- The Ozama river bridge in the city of Santo Domingo

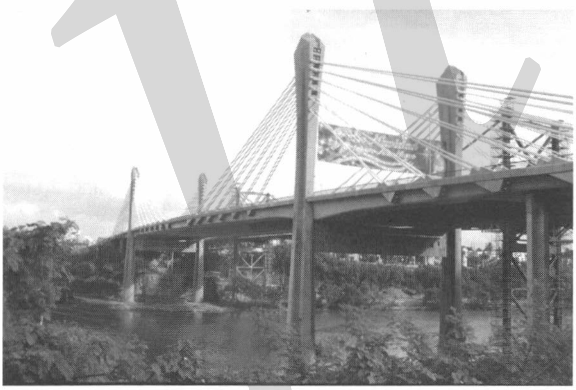

The Ozama river bridge

This is the doubling of a metallic suspension bridge built in the 1950s, with a 180-m long main span.

The project of the new bridge was based on two basic ideas: first of all we wanted to create a present-day bridge, which is to say with the technologies of the present moment, the beginnings of the 21st century, and secondly, we wanted to build a bridge that would live in harmony with the existing suspension bridge. This led us to reject the idea of duplicating the suspension bridge because in today's bridge technology a 180-m long span is far too small for a suspension bridge. Therefore, we designed a cable-stayed concrete bridge, the type we consider most suitable for spans of these dimensions.

The harmonisation of the new bridge with the suspension bridge made us build a unique cable-stayed bridge because the new bridge was designed with the same outline as the suspension bridge. Therefore, the towers of the cable-stayed bridge have been designed of the same height as those of the suspension bridge. In this way we manage to keep the area occupied by the cable system of both systems the same. The joint view of the two bridges is the superposition of the two cable systems: the parabolic cable with its hangers of the suspension bridge, and the cable stays of the cable stayed

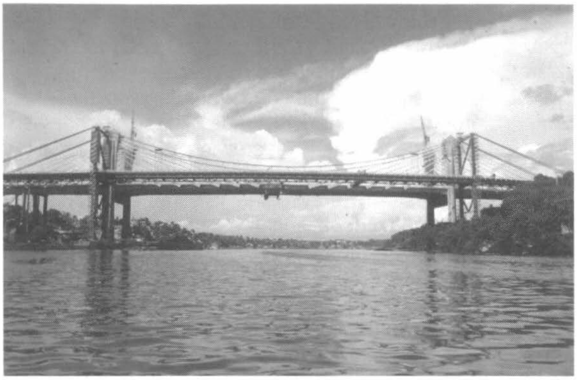

bridge. This view is similar to that of the New York City Brooklyn Bridge where both cable systems were used together: the parabolic cable and the hangers, plus the stay cables.

To build a cable stayed bridge of the same tower height as in a suspension bridge gives as a result a unique bridge, because usually for the same span, the towers of a suspension bridge are more of less half the height of a those in a cable-stayed bridge. Therefore, this bridge, among cable-stayed ones, belongs to a special group with reduced tower height, *called "bridges with extradorsal prestressing"*. Once we saw the completed bridge, we considered that the harmonie achieved by this coincidence of outlines of the two bridges is a real value of the whole and not only a theoretical idea.

The cable-staying system we adopted made us use a stiffer deck than that of a normal cable-stayed bridge; it has two box girders on the edges with a variable depth ranging from 4 meters in the supports, to 2.50 m in the most part of the main span. In lateral spans the depth becomes gradually smaller, reaching 1.50 m, the same depth that the approach viaducts, made of prefabricated girders have. The two lateral box girders are connected by strut diaphragms and the upper slab.

The towers are made of two vertical piers connected by a tie beam of a large depth, placed under the deck, used to give transverse stiffness to the whole when exposed to horizontal forces produced by seismic activities. The pier shape is due to the need for maximum stiffness in the base and the necessary dimension to hold the stays at the pier cap. The piers are independent above the deck, as is the case in the Papaloapan bridge.

The bridge width is 33.50 m, due to four carriageways, two possible lines of intercity railway and pedestrian sidewalks. The stay cables were anchored in the deck at every 10 m and this demanded cables of far too large a dimension. We were therefore forced to double the stays with two very close ones. The stays are situated in the same horizontal plane when passing through the pier and in the same vertical plane in the deck anchors. This produces a relative rotation between the cables and gives them a changeable vision although always unitary; each couple of cables forms a single stay cable.

The project was initially designed with saddles on the piers, of the same type as those used in the Villahermosa bridge, though larger. However, during construction, the providers of stay cables replaced the saddles by crossed stays, which forced us to widen significantly the pier caps that had been designed in the original project.

The lateral spans and the initial part of the main span were built on a centering. Once the centering was struck from these spans the main span was built in cable-stayed free cantilevers using form travellers until midspan.

III.- TWO ARCH BRIDGES OVER THE NERVIÓN RIVER IN BILBAO CONSTRUCTED BY MEANS OF PROVISIONAL STAY CABLES

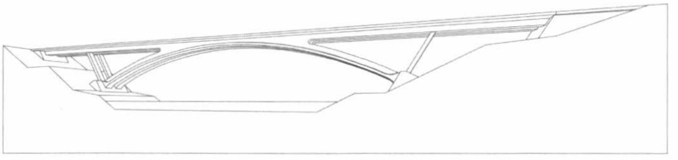

Leonardo Da Vinci defined the arch as *"a strength formed by two weaknesses... it is composed of two quarters of a circle, each one extremely weak by itself tending to fall. They oppose their own weakness in the other and thus two weaknesses become a single strength*". We think that that there is no better illustration of this dual definition of the arch than the construction system used in the two arches of the bridges over the Nervión river for the Metropolitan railway of the city of Bilbao.

The procedure consists of building the two semi-arches in a cuasi vertical position over abutments and then, by means of a back-stay, rotating the semi-arches until joining them at the keystone. In this construction system it is essential to study the semi-arches in their intermediate state because, as Leonardo said, they are very weak until they join at the keystone.

This construction procedure, like most of those which appeared one after the other in bridges, was first used in metallic arches. In concrete arches it was Ricardo Morando who first used it in the Torrente Lussia footbridge in Italy. The footbridge is 70 m long and it was completed in 1953. After that, in 1954 he used it in the Storms river bridge in South Africa. This bridge was 100 m long. In 1987 it was used again to build the arch of the Argentobel bridge in Germany, 145 m long.

The construction by the rotation of semi-arches is a method alternative to that of cable-stayed free cantilevers; either cast in situ or made of prefabricated segments, a system frequently used to build arches without centering and especially large-span ones. In this case we preferred the system of rotating the semi-arches instead of building them in cable-stayed free cantilevers for two reasons:

1. First of all because we think that for the span of these arches, around 60 m, the means necessary to carry out the rotation are not too powerful whereas if we were to assemble the whole system by cable-stayed free cantilevers it would be excessive for such short arches.

2. Secondly, because, although these two arch bridges are not exactly the same, all the means of assembling can be used for both of them, which makes the assembly process cheaper.

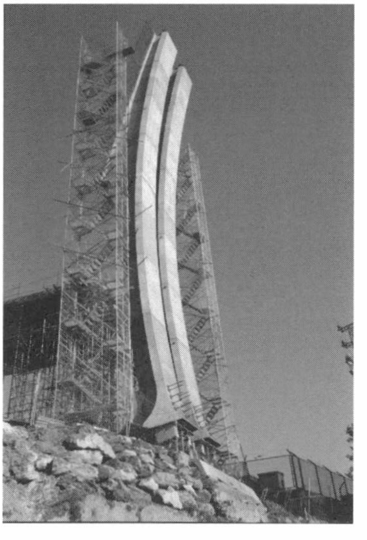

The two bridges cross the Nervión river, and are used for Bilbao' s underground railway whose track width is 1.00 m. Both bridges hold two tracks with a platform width of 8.50 m 1,00 meters.

The structure of both bridges is organised into two ribs, one under each track, connected by the upper slab. In the deck areas made of girders, the ribs are two box girders, while in the arch area they turn into two rings.

The crossing of the river is solved in both bridges by an arch. Viaduct 1 is 63 m long and Viaduct 2 is 56. 5 m long.

As we have said, we decided to construct semi-arches in cuasi vertical position over abutments using a climbing formwork, in the same way as we would build 30 m high piers of *a* bridge.

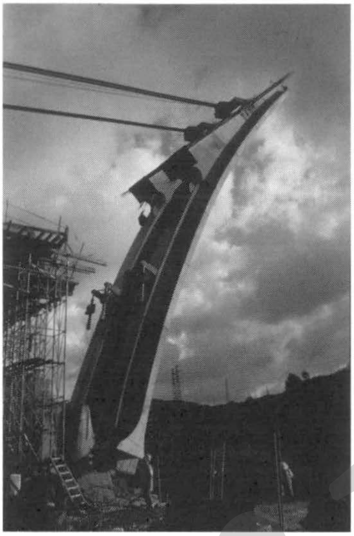

The semi-arches were built on hinges so they could be rotated. To ensure their stability during construction they were overturned outwards, which is to say with their gravity centres away from the vertical of the rotation point and they were fixed in the foundations by concrete wing walls. Once the semi-arches were completed, the concrete wing walls were desconected, and, given the initial position of the semi-arches, we needed to begin the rotation by thrusting with jacks until we reached a position in which the semi-arches rotated due to their own weight, and it was necessary to retain them by the stay cables. These stay cables were fixed at one end to bipeds situated out of the bridge except in the right riverbank of the Bridge 1, where the bipod was placed on the approach viaduct. At the other end the stay cables were fixed to intermediate points of the semi-arches. The stays were gradually released using double effect jacks, until the semi-arches reached their definitive position and were connected, at the keystone hinge.

The rotation of the semi-arches was carried out on hinges made of gusset plates joined with studs, which ensured their stability during the rotation process. These hinges were supported by horizontal jacks which allowed us to adjust the position of the arches once they were rotated, both in plan and in elevation.

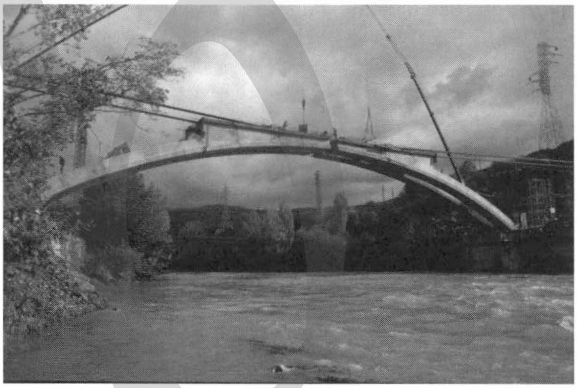

Once the keystone hinge is closed the arches become triarticulated. Both the abutments and the keystone were finished by a two-stage concreting, which allowed us to remove the hinges and reuse them again, once the first stage was completed.

Once the arches were embedded in the keystone and the abutments, the deck was completed over them until the whole bridge was finished.

CONCRETE FOR A NEW CENTURY

Joost C. Walraven
Delft University of Technology
The Netherlands

Keywords: Concrete, high performance, high strength, fibers, ductility, self-compacting

1 CONCRETE AS A CONVENTIONAL MATERIAL

"Concrete? Isn't that something the old Romans already made?" This statement was written down when it was argued over granting a research proposal in which concrete played a central role. And indeed, the old Romans already made concrete. And how! The existing structures from the Roman times lead to the conclusion that design for a life cycle of 2000 years or longer is possible. Remarkably, at present there is much discussion going on concerning many structures on how we can reach the 100 years! This discussion is based on advanced theoretical considerations.

Of course, this comparison is not honest. By far most Roman structures do not exist any more today. One has to realize this. Furthermore, the Romans made massive structures in which the concrete was purely loaded in compression. Reinforcement was not used, and therefore, it could not corrode. Such a method of building gives strong limitations. The concrete of this time had a low strength. This could not be different considering the inhomogeneity of the material, Fig. 1. The combination of a soft matrix with aggregates, which are irregular in shape and in size, leads to large inner stresses at loading. The strength of such a material must therefore be limited. The concrete shown in Fig. 1 was taken from the city wall in Cologne, which was built at about 50 a. C. The strength, which was measured on drilled cylinders, was about 10 MPa.

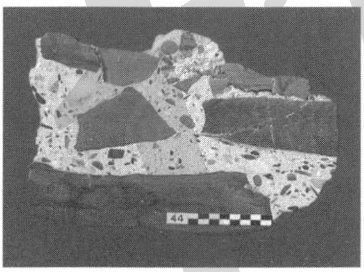

Fig. 1 Roman concrete

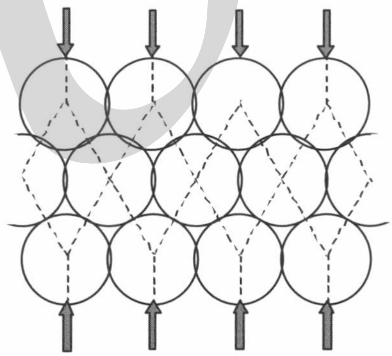

Fig. 2 Schematic distribution of forces in concrete subjected to compression

The way in which concrete transfers its forces can schematically be imagined as shown in Fig. 2. Fig. 2 shows what would happen if all aggregates had the same size. The forces in the concrete go from aggregate to aggregate. Furthermore, force components to the side appear. The binder material between the aggregates transmits these components. The concrete can be loaded centrically until the binder material fails. Therefore, the cracks in concrete loaded in compression develop into the direction of the compressive force. It is well known that realizing a dense packing of the aggregates can minimize the transversal forces inside the concrete. Therefore, grading curves are determined which give an orientation for the mix designer. A second well-known method in order to increase the strength is decreasing the water-cement ratio. The practical optimum was until quite recently a water cement ratio of about 0.4. Lower values lead to a loss of workability and thus automatically to a loss in strength. Up to about ten years ago, making a B45 at the building site was a big achievement. In the meantime, knowledge in concrete technology improved very much. This has lead to revolutionary developments.

2 CONCRETE WITH HIGH STRENGTH

At the beginning of the 90's, it was discovered that the addition of silica fume to concrete leads to a considerable increase in strength. This material, a waste product of the silicium production, has a significant effect on the force transmission in the concrete. The silica fume grains are a factor 100 smaller than the cement grains. This fact can be described as the filler effect. The small grains fit into the spaces between the cement grains and thus increase the density of the paste. Furthermore, they are reactive. The grains work as initiation point for the formation of crystals which grow through the coarser crystals of the cement paste. Furthermore the silica fume reacts puzzolanic. The amorphous silica fume converts the weaker CH crystals into the stronger C-S-H gel. Therefore the binder becomes much stronger. Furthermore, the transition zone between aggregate and paste is improved. Besides, the Young's modulus of the binder is much higher than before (roughly the same as for the aggregates). Thus, the concrete is more homogeneous. This also means that the side forces which pull the force transition system apart are much smaller. This double effect leads to a considerable increase in concrete strength. A nice example of engineering knowledge was the realization of the Second Stichtse Bridge, the first bridge with a large span (170 m) made of high strength concrete in Europe, Fig. 3.

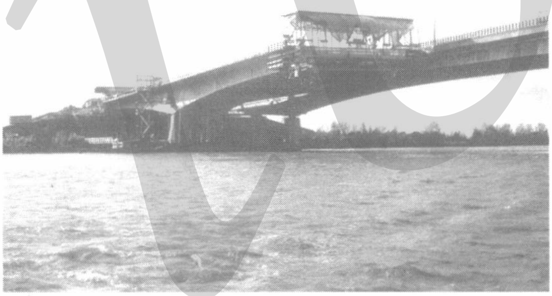

Fig. 3 Stichtse Bridge: first prestressed bridge made of high strength concrete in Europe

An analysis of the costs for building this bridge led to a result that surprised many people. The price for the high strength concrete used (474 kg/m^3 cement, 25 kg/m^3 silica fume, sand, broken gravel 4-16 mm and superplasticizer) was about twice as much as for a conventional B45. But considerable financial advantages were found in contrast to the price of the concrete itself. About 30% less concrete was necessary. Because of the smaller surface of the cross-section less prestressing steel was necessary (25%). Due to the decreased weight, the cantilever segments could be 5 m long instead of the formerly used length of 3.5m. Hereby, the construction period could be shortened by three months. Therefore, the costs for the bridge were not significantly higher than for building a traditional bridge. However, the quality of the bridge is much better. Because of the dense material structure of the high strength concrete, the durability is improved and the maintenance costs are expected to be lower. In addition, also an analysis of the environmental effects led to a surprising conclusion. As a lower volume of concrete with a higher cement content per m^3 is necessary the total amount of cement needed stays approximately the same. However, the saving in the amount of aggregate used is about 30%. Finally, the improved strength of the concrete was only one of the many advantages. The faster hardening and the improved durability might be even more important. Realizing this, the concrete used was more and more denoted as “high performance concrete” instead of “high strength concrete”.

3 SELF-COMPACTING CONCRETE

The labor conditions at the construction site and in factories are getting more and more attention. A large disadvantage of traditional concrete is that it has to be mechanically compacted. This compacting is an unpleasant job. Holding the vibrator can lead to disturbances in the blood circulation (“white fingers”). Furthermore, the noise emission during compaction is often tremendous. Also in this case, a small change in the mix composition appeared to lead to a significant improvement. The idea is rather simple. One adds a little more binder than is necessary for a good performance of the concrete in the hardened state. By this small amount of additional cement paste, small layers of lubricant develop around each grain. Thus, the grains start to “float”, Fig. 4.

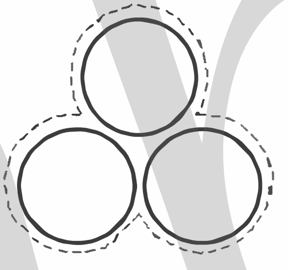

Fig. 4 “Floating grains” in self-compacting concrete

The inner friction during the flow of the concrete is further reduced by to the presence of fly ash or limestone powder as an extra component. These materials have a grain diameter, which roughly fits between the sand and the cement. A three-phase particle skeleton with high density is formed in this way, see Fig. 5. By well adjusting the grain sizes and by the presence of the thin lubricant the grains move and roll easily over and along each other, which makes the material very flowable. Because these layers are very thin they hardly have any influence on the properties of the hardened concrete. Due to the dense grain packing, the strength is further automatically relatively high. This explains that high strength and good workability go together.

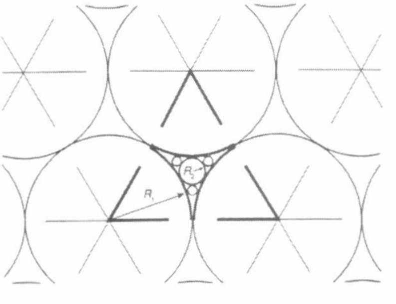

Fig. 5 Schematic concept of the three-component grain skeleton

The Japanese method, which solely aims at the realization of a good workability, results in a cube strength of about 60-70 MPa. The properties of the boundary layers are certainly important. The combination of superplasticizer and concrete plays an important role. If the boundary layers are a little too thick and the viscosity is a little too low then the larger aggregates will sink to the bottom and segregation will occur. If the layers are a little bit too thin and the viscosity a little too high then the mixture becomes sticky. The mixtures are therefore rather sensitive for small changes in the properties of the ingredients. Only providing the mixture composition for self-compacting concrete is insufficient information because upon arrival of new ingredients the workability needs to be tested again and the mixture has to be adjusted. It is therefore not surprising that the application of self-compacting concrete mainly develops in the prefab industry at the moment. The circumstances in a factory are relatively constant and actions are repeated. As the conditions hardly change and the workability control became routine work the sensitivity of the mixtures is not a problem any more. The advantages of self-compacting concrete for the prefab industry are clear. An interesting analysis of this was given by Dekkers [1]. He proved that significant improvements of the working conditions are achieved considering the noise emission, vibration, and dust. But not only the working conditions improved. The costs even decreased. It is true that the material self-compacting concrete is a little bit more expensive due to the extra costs for superplasticizers and filling agents. But considerable savings compensate for these costs due to decrease of energy consumption, decrease of absence due to illness, decrease in maintenance costs (vibration devices, moulds), more efficient moulds (lighter moulds, easier joints, faster building and demoulding), longer lifetime of the moulds and more efficient work (finishing is merely necessary, hardly any honeycombing or air entrapments are found). Furthermore considering the freedom in form, which increases by virtue of the use of self-compacting concrete through which innovative and beautiful products are possible it is clear that self-compacting concrete can mean an important breakthrough.

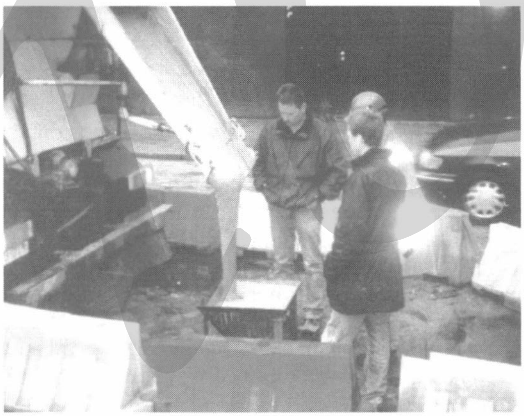

Fig. 6 Casting self-compacting concrete in a wall in the Koningstunnel in Den Haag

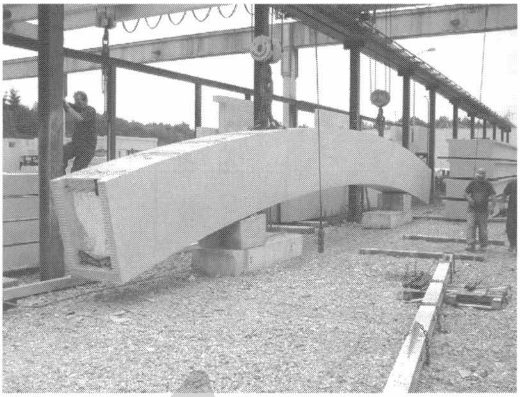

Fig. 7 Casting part of a concrete arch with self-compacting concrete

For the building site, self-compacting concrete is also an attractive material. The noise emission is lower for the environment. The neighbors are therefore more likely to accept the building site, especially in densely populated areas. Casting at night is a feasible alternative. As compaction is not necessary any more the work can be done more efficiently and with fewer personnel. On the other hand, on a construction site there are changing circumstances. Furthermore it is rather important for the choice of the optimum mixture composition whether one has to cast a high wall with dense reinforcement or a floor with a large surface and little reinforcement. This knowledge is being developed at the moment. Making the self-compacting mixtures more stable and less sensitive is one of the most important research objectives in this field.

4 CONCRETE WITH ULTRA HIGH STRENGTH

Looking at the theory of particle packing, Fig. 2, combined with the function of the binder, one can wonder what is the highest strength that can possibly be achieved. A number of important steps are the following:

- Improve the homogeneity of the material by reducing the grain/aggregate size. By leaving out the larger grains/aggregate the stress variation in the hardened material decreases through which the appeal done on the quality of the interface (usually the weakest link) decreases.
- Increase the packing density by using the three phase material principle as a basis (Fig. 5). Fig. 8 shows the corresponding grading curve, built up in steps, which is moved far to the left compared to traditional concrete (in the area of the smaller grains/aggregates).
- Add as little water as possible. This seems strange because this advice is contradictory to the classical way of thinking. In the past sufficient water was always added in order to let all the cement (the most expensive ingredient) hydrate. The remaining water was necessary in order to provide sufficient workability. A problem that was hardly recognized in this was that by the unavoidable drying of the concrete micro cracks are initiated, which undermine the performance of the binder. The new approach is therefore just the other way around: see to it that all the water is converted in the hardening cement paste. The remaining cement works as an additional filler in order to achieve an even higher packing density of the load-carrying skeleton. The workability is achieved by using suitable superplasticizers.
- Add steel fibers in order to make the material not only strong but also tough.

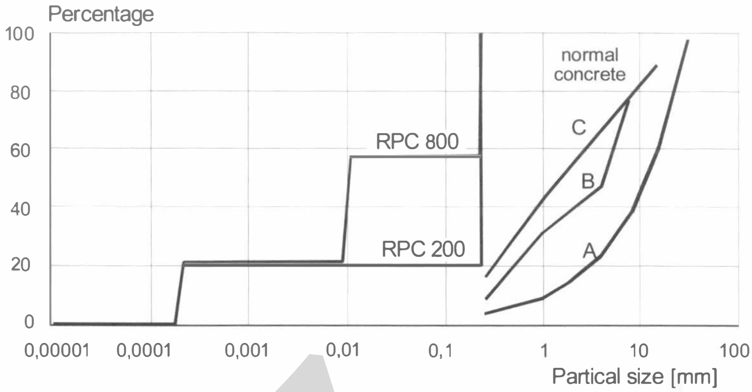

Fig. 8 Gap-graded particle distribution for concrete with a very high strength (> B200)

It is logical that these kinds of mixtures require a high cement content. One has to think about more than 800 kg/m^3 cement, more than 200 kg/m^3 silica fume, and at least 100 kg/m^3 steel fibers. When limiting the maximum aggregate size between 0.5 and 4 mm strengths of 200 - 250 MPa can be achieved with this. Using an extra heat treatment, these strengths can amount to 300 – 350 MPa. The material obtained has properties which lie somewhere between those of steel and classical concrete. The best-known field experiment performed up to now is the pedestrian/bicyclist bridge in Sherbrook, Canada. Other interesting applications include bridge girders, abrasion layers on bridges, or floodgates. Fig. 9 shows prefab girders, which only contain a few prestressing strands: other reinforcement is superfluous due to the presence of fibers.

Two Masters Theses carried out at TU Delft [2, 3] showed that the material offers interesting possibilities in spite of its relatively high costs. They investigated whether a B200 can be applied for the floodgates at the Oosterschelde, one of the big flood barriers in the Netherlands. The floodgate designed in very high strength concrete (Fig. 10) was hardly heavier than the existing steel floodgates, which require much maintenance. Considering the expected durability of a concrete B200, the maintenance costs for these floodgates would be much lower. Therefore, concrete floodgates would finally have been considerably more economic.

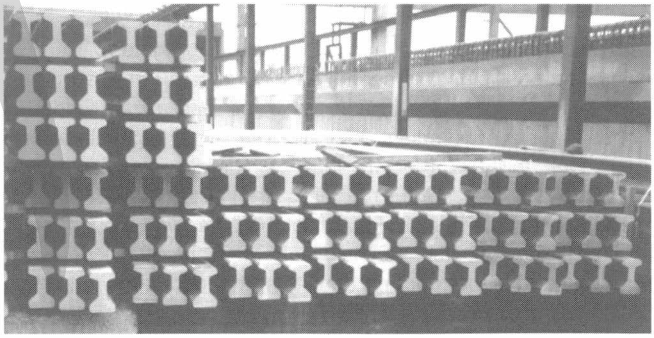

Fig. 9 Girders made of B200

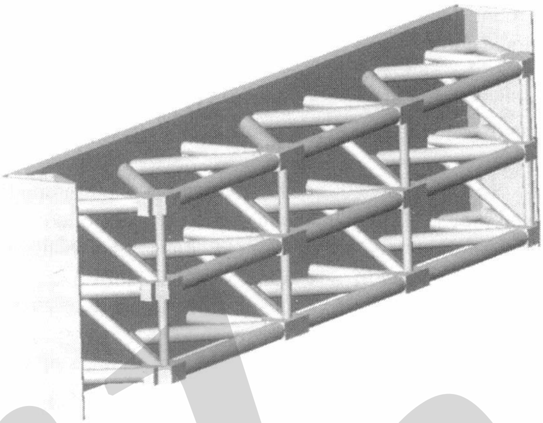

Fig. 10 Design of the concrete floodgate in B200 for the flood barrier Oosterschelde [2]

It is very natural to try to combine the positive properties, which were shown separately for different concrete mixtures in the preceding examples. Self-compacting fiber reinforced concrete is a very good example for this. Former experiences showed that the addition of fibers quickly decreases workability. However, with the knowledge of self-compacting concrete in mind there are new possibilities. Again, it is important to first think about the composition of the mixtures. Fibers disturb the coherence in the particle skeleton. The extent of this disturbance depends on the maximum aggregate size, the amount, shape, length, and aspect ratio of the fibers. Investigations into the packing of aggregates with steel fibers showed that it does not make much difference which kind of steel fibers (length varying from 30 to 60 mm) is applied when sand (0 – 4 mm) is used. If, however, the same experiment is repeated for coarse aggregates (4 – 16 mm), the packing density decreases with increasing fiber content. The higher the fiber aspect ratio (i.e. length/diameter) is the lower is the packing density. The fiber shape is also important. In order to achieve the maximum packing density for a certain kind and content of steel fibers, the sand content of the total aggregate has to be increased. Grünewald [4, 5] showed that even at a steel fiber content of 140 kg/m^3, self-compacting mixtures are still possible. Not only is this a surprising fact but also the fact that the mechanical properties of self-compacting concrete are excellent. Fig. 11 shows several load – deflection curves for beams made with fiber reinforced concrete subjected to three-point bending.

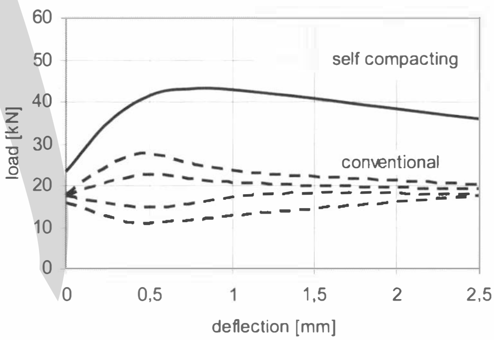

Fig. 11 Load – deflection relationships for conventional and self-compacting fiber reinforced concrete (B65 with 60 kg/m^3 steel fibers)

The dashed lines show the results of four tests on beams made of conventional concrete B65. The concrete contained 60 kg/m^3 steel fibers (Dramix 80/60 BP). These tests showed a considerable scatter of the results. The straight line shows the results of a self-compacting concrete made under the same conditions (B65), round river gravel with a maximum grain size of 16 mm, and the same kind and amount of steel fibers. The tests were performed in the same machine and in the same way. Not only the bearing capacity of the self-compacting concrete was higher. Also the scatter in results was much lower. This means that the basis for design (mostly a 5% confidence interval is used) for self-compacting fiber reinforced concrete is significantly better than for the conventional fiber reinforced concrete.

Also in the range of B100 and B200, self-compacting concrete can be an interesting material. Experiments were performed at TU Delft investigating the behavior of self-compacting fiber reinforced concrete with an average strength of 120 MPa at 28 days [6]. On this occasion, a mixture was developed containing 358 kg/m^3 CEM I 52.5 R, 555 kg/m^3 CEM III/A 52.5, 61 kg/m^3 silica fume en 125 kg/m^3 straight steel fibers 13/0.16. The strength after 12 hours was 75 MPa. This mixture is very interesting for the prefab industry because of its high early strength. Sheet piles were produced with this mixture in collaboration with a prefab company (Fig. 12). The price of this mixture was fixed at 444 Euro per m^3. Please note that half of the costs was caused by the specially made steel fibers. The price of this self-compacting fiber reinforced concrete is about four times as high as that of a conventional B65. As opposed to this, the cross-section of the walls was only 25% of that made of the alternative B65 [7]. Therefore, the price per element is the same. An added value lies in the cost savings for transportation and easier handling of the elements on the construction site. If it would be decided to manufacture the elements in series production the price (of the fibers) could decrease significantly. It is therefore an interesting new development.

Fig. 12 Prefab dam wall element made of self-compacting high strength concrete B120 [7]

5 SPECIAL EXAMPLES OF TAILOR MADE CONCRETE

Experimenting with particles and particle packing is always a major challenge in the development of new concrete mixtures. An interesting example is the development of an acid resistant concrete at the TU Berlin [8]. The target was to develop a concrete with a high chemical and physical resistance for the application in the highest cooling tower in the world, with a height of 200 m in Niederaussem, west from Cologne. A protective coating at the inside of the tower was not regarded as a feasible option, because the long-term quality was considered to be doubtful. The concrete was required to get the highest possible particle packing, even at the level of the binder. Further to that a high resistance of the binder matrix against the penetration of chlorides, water and gases was required. This should, however, not go along with a very high tensile strength, because then the high amount of reinforcement required for the control of the crack widths (imposed temperature effects) would cause significant additional costs. In this case both with regard to the aggregate and to the binder, the ideal particle distribution was aimed for. In order to close the gap between aggregate and binder, plastic micro hollow spheres were applied, Fig. 13. In this way two demands were satisfied at once. At the one hand a very high density concrete was obtained: at the other hand the tensile strength of the concrete was reduced with 40% due to the micro spheres (which act as a filler but hardly have any bonding capacity).

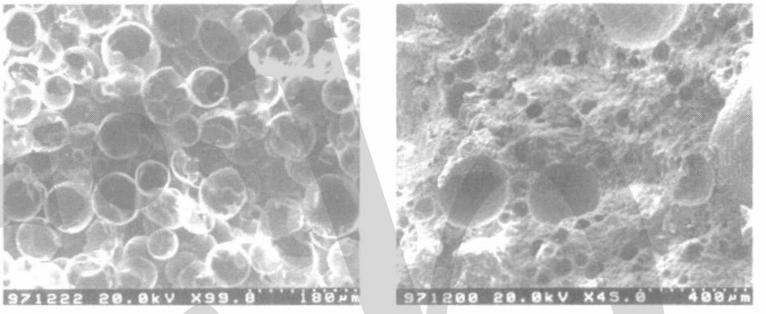

Mikrohohlkugeln/Micro hollow spheres

Matrix mit eingebetteten Mikrohohlkugeln
Matrix with embedded micro hollow spheres

Fig. 13 Application of plastic hollow micro spheres for obtaining a very dense concrete with simultaneously a limited tensile strength (Hüttl, Hillemeier [8]).

Another interesting idea was recently put forward by the Japanese researchers Noguchi and Tamura [9]. The idea was inspired by the observation that recycling of concrete intrinsically leads to lower performance applications. Already after a small number of cycles the material is only useful for applications like for instance road foundations. In order to keep after recycling a high quality aggregate it was proposed to coat the surface of the aggregates. There are principally two possibilities:

- a chemical treatment on the basis of mineral oil. Such a layer counteracts the formation of cement hydrates at the interface between particle and matrix. The bond between both components is therefore weakened, which enables easier recycling.
- a physical treatment with an emulsion, which is stable in fresh concrete. In this way the surface of the particles gets smoother, which reduces the bond between aggregate and binder. This enables more complete recycling.

Of course the strength of the concrete as a whole is reduced by the treatment of the particle surfaces (about 20%). However, by creating an optimum particle packing still a sufficient strength is obtained. During recycling the aggregate can be regained nearly in the virgin state, which enables new application on the same level.

The idea of treating the surface of aggregate particles in order to realize defined properties is also used in another respect: making self-compacting lightweight aggregate. As it was pointed out previously, self-compacting concrete is sensitive to small changes in its composition: slightly more or less water endangers the self-compacting. This would logically mean that the production of self-compaction lightweight concrete is a mission impossible, because the lightweight particles are porous, so that after mixing uncontrolled exchange of water between the particles and the surrounding paste would occur. Müller [10,1] showed how this could be solved. A special technique was developed in order to apply an isolating hull around the soaking lightweight aggregate. Fig. 14 shows a Liapor lightweight aggregate grain after being enveloped with cement past. The thickness of the paste layer is 0.25-0.35 mm on average. Tests showed that this layer causes a significant change of the moisture exchange. By virtue of this technique self-compacting lightweight concrete mixes behave in the same way as self-compacting normal weight mixes.

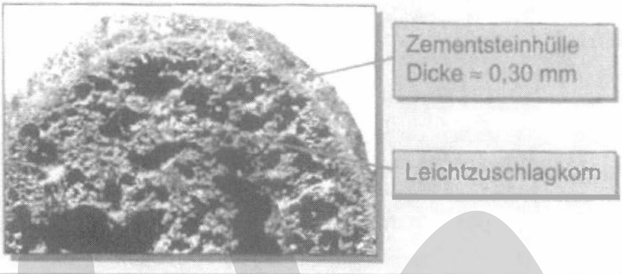

Fig. 14 Lightweight aggregate grain after enveloping with cement paste (Müller, [10])

6 GREEN CONCRETE

Environmental aspects are getting more and more interest. In Denmark the "Center for Green concrete" was founded. The expression "green concrete" has another meaning than in the past. The "green" stood for "just cast", now it has the meaning of "environmental friendly". The center was founded as a result of the wish to minimize the environmental effect of concrete. This means among other things to use as little as possible clinker in concrete, the use of "green" types of cement and binder and the responsible use of waste material. Up to now the knowledge of optimizing the packing density has inspired the development of concretes with higher and higher strengths. In the mean time an important challenge has been overseen: to make bulk concrete in an environmental friendly way with sufficient strength. This could give an important contribution to the reduction of the CO_2 emission. Table 1 gives a survey of five mixtures with a significantly reduced amount of binder. From the table it becomes clear that also with a low amount of cement an acceptable strength can be gained. There are many applications, especially in a non-aggressive environment, where this strength is sufficient. In the area of "green concrete" there are considerable possibilities for further research and development.

Table 1 Mix design characteristics for green concretes in passive environmental class [12]

	Reference concrete	50% FA + 10% KD	17% SSIA	Concrete slurry	100 % stone dust	30% FA from bio fuels
Cement kg/m^3	143	90	137	141	267	191
FA kg/m^3	51	128	15	52	-	-
SF kg/m^3	10	14	10	10	-	-
SPT, kg/m^3	-	1,1	3,2	-	1,8	1,9
Eq. wcf	0,75	0,66	0,78	0,77	0,72	0,69
Cube strength MPa		26	21	23	29	28

SSI Sewage sludge incineration ash
FA Fly ash
SF Silica fume
SPT Superplasticizer
KD Kiln dust

7 CONCLUSION

Concrete is a material that offers considerably more options than just design for minimum strength. During the last years a lot of new types of concrete have been developed. By combining the packing density and the binder in an optimum way, eventually in combination with the addition of fibers, an enormous variety of properties can be achieved. After the concepts of "high strength" and "high performance", the next challenge is "defined performance concrete". This means a major change with regard to the way that we look to materials. In the past all properties of concrete were linked to one basic property: the compressive strength. This relation is now not so self-evident anymore. Design of concrete for special properties without a direct relation to the strength is a new and challenging possibility. The work for a new Model Code for Concrete Structures is about to start. To comfort the application of defined performance properties is an important task.

REFERENCES

[1] Dekkers, J.: "Arboproblemen betonindustrie zijn verleden tijd", Belton Mei 2001, Nr. 2, pag. 24-27.
[2] Tol, H., "B-200 betonnen schuiven in zeer hoge sterkte beton voor de Stormvloedke-ring Oosterschelde", Master thesis TU Delft
[3] C.K. Cheung, "Detaillering B200-Hefschuiven Stormvloedkering Oosterschelde", Afstudeerwerk TU Delft, feb. 2002
[4] Grünewald, S., Walraven, J.C., "Maximum content of steel fibres in self-compacting concrete", Proceedings of the Second International Symposium on Self-Compacting Concrete, 2001, Ed. by Ozawa, K., and Ouchi, M., University of Tokyo.
[5] Grünewald, S., Walraven, J.C., "Rheological study on the workability of fibre-reinforced mortar", Proceedings of the Second International Symposium on Self-Compacting Concrete, 2001, ed. by Ozawa, K., and Ouchi, M., University of Tokyo.
[6] Grünewald, S., Bolo, T., van der Veen, C., Walraven, J.C., "Performance-based design of a high strength self-compacting fibre reinforced mortar", Report 25.5-01-30, Dec. 2001.
[7] Tol, R., "Spanwand van HSVVZVB", Afstudeerwerk Sectie Betonconstructies TU Delft, Jan. 2002
[8] Hüttl, R., Hillemeier, B., "Hochleistungsbeton – Beispiel Saureresistenz", Betonwerk und Fertigteiltechnik, Vol. 66, Jan. 2000, Nr. 1, pp. 52-60.
[9] Noguchi, T., Tamura, M., "Concrete design towards complete recycling", Structural Concrete, Journal of the fib, Vol. 2, Nr. 3, Sept. 2001, pp. 155-176.

[10] Guse, U., Müller, H., "Important research results and outlook in the new millennium", Betonwerk und Fertigteiltechnik, Vol. 66 nr. 1, Jan. 2000, pp. 32-44.
[11] Müller, H., Garrecht, H., Linsel, S., " Zementgebundene Umhüllung von Blähton-leichtzuschlägen zur Verbesserung der eigenschaften von frischem und erhärtetem Konstruktionsleichtbeton", Forschungsbericht des Instituts für Massivbau und Bau-stofftechnologie, Universität Karlsruhe, 2000.
[12] Damtoft, J.S., Glavind, M., Munch-Petersen, Ch., "Danish Centre for Green Concrete"

CAPACITY DESIGN AND ASSESSMENT OF REINFORCED CONCRETE STRUCTURES FOR EARTHQUAKE RESISTANCE

Robert Park
Department of Civil Engineering, University of Canterbury
NEW ZEALAND

Keywords: detailing, ductility, flexure, mechanisms of post-elastic deformation, moment resisting frames, reinforced concrete, seismic design, shear, structural walls

1. INTRODUCTION

Before about the mid 1970s it was customary in the seismic design of structures to use linear elastic structural analysis to determine the bending moments, axial forces and shear forces due to the design gravity loading and seismic forces and to design the members to be at least strong enough to resist those actions.

As a result, when the structure as designed and constructed was subjected to a severe earthquake, the manner of post-elastic behaviour was a matter of chance. Flexural yielding of structural members could occur at any of the regions of maximum bending moment, and shear failures could also occur, depending on where the flexural and shear strengths of members were first reached. Hence the behaviour of such structures in the post-elastic range was somewhat unpredictable.

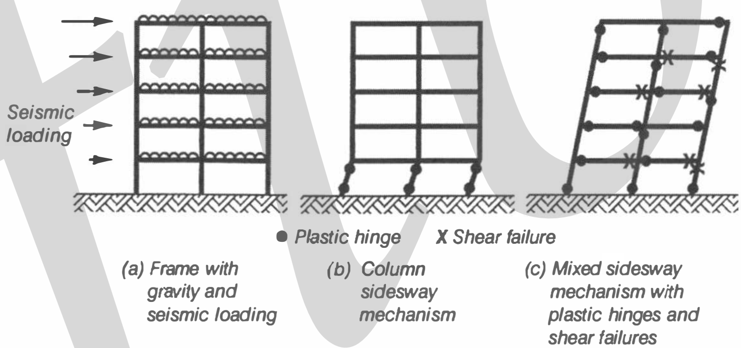

Fig. 1 Undesirable modes of behaviour for tall seismically loaded monolithic moment resisting frames in the post-elastic range [1,2]

For example, for monolithic moment resisting frames, overstrength of the beams in flexure or understrength of the columns in flexure could result in column sidesway mechanisms, in the bottom or upper storeys (see **Fig. 1b**). Also, flexural overstrength of members leads to increased shear forces when plastic hinges form which could result in shear failures (see **Fig. 1c**). These undesirable failure modes could cause catastrophic collapse of the frame.

In the case of cantilever structural walls there are a range of possible undesirable modes of behaviour. Overstrength of the wall in flexure could cause failure modes in either diagonal tension shear, sliding shear or hinge sliding (see **Fig. 2b, c** and **d**) which have limited ductility.

The reasons for overstrength in flexure in some regions of the structure, leading to flexural yielding or shear failure in other regions, are many and include:

- Variations in the actual steel and concrete strength from the specified characteristic strengths throughout the structure.
- Cross sectional sizes larger than assumed.
- Additional reinforcement placed in members for construction purposes or to satisfy minimum reinforcement requirements or to satisfy available bar sizes, and unaccounted for in the design calculations.
- Use of strength reduction factors φ or material factors γ in the design of cross sections.
- More critical loading cases for the design of some sections for gravity and wind loads.
- Participation of non-structural elements.

Some of these contributions to overstrength of regions of structures can be reasonably accurately predicted. For example, the fluctuations of the steel and concrete overstrength above the characteristic strengths can be estimated. Slab participation in the flexural behaviour of beams is important in the negative moment regions since the slab reinforcement can add significantly to the flexure strength. For example, the negative moment flexural strength of a T-beam when slab reinforcement is included in addition to those bars placed within the web width of the beam can be in the order of 1.3 times the flexural strength calculated including only those bars within the web width of the beam [3]. The effect of strength reduction factors (φ used in North American and New Zealand codes) or material factors (γ_c and γ_s used in Europe) can be calculated. For instance, if the strength reduction factor for flexure is φ = 0.85, the nominal flexural strength is equal to the design flexural strength multiplied by $1/\varphi = 1/0.85 = 1.18$.

The other contributions to overstrength listed above are more difficult to quantify. However, it is apparent that the actual flexural strength of regions of reinforced concrete structures could easily be 50 to 100% greater than the design flexural strengths of those regions.

In New Zealand in the late 1960s and the 1970s it was realized that the possible effects of overstrength in flexure of some regions of the structure need to be carefully considered in seismic design to ensure that undesirable failure modes do not occur during severe earthquakes. For this reason the design approach termed capacity design was developed and was first used in New Zealand in the 1970s.

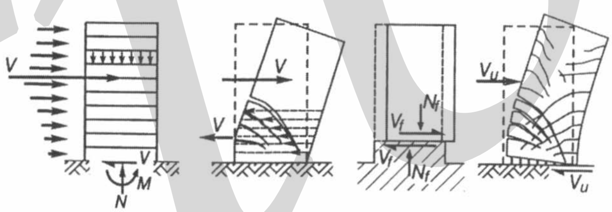

Fig. 2 Undesirable modes of behaviour for seismically loaded monolithic cantilever structural walls in the post-elastic range [1,2]

2. CAPACITY DESIGN

2.1 The capacity design approach

The intention of the capacity design approach is to protect non-ductile regions of the structure by restricting yielding to ductile regions as intended by the designer. There is no doubt that the confidence of New Zealand designers that adequate ductility may be achieved in concrete structures, either totally cast-in-place or incorporating precast concrete elements, has come about mainly as a result of the introduction of the capacity design approach.

The basis of the capacity design approach was first described in a paper by Hollings [4]. The method was developed by discussion groups of the New Zealand National Society for Earthquake Engineering and by Park and Paulay [1]. The capacity design approach was first recommended by the New Zealand loadings standard in 1976 and by the New Zealand concrete design standard in 1982. A recent account of the capacity design approach is given by Paulay and Priestley [5].

In force-based seismic design the horizontal equivalent static design seismic forces are obtained from the elastic response acceleration spectrum for the design earthquake factored down by a reduction factor which is a function of the period of vibration of the structure in the elastic range and the achievable displacement (structural) ductility factor, μ. The displacement (structural) ductility factor is defined as Δ_{max}/Δ_y, where Δ_{max} is the maximum horizontal displacement imposed on the structure during the design earthquake, generally at the point of action of the resultant horizontal seismic force, and Δ_y is the horizontal displacement at that point of the structure at first yield of the structure. According to the New Zealand design standards [6,7] structures resisting earthquakes may be designed either as ductile structures, or as structures of limited ductility, or as elastically responding structures. For ductile reinforced concrete structures μ = 5 or 6 is used, for structures of limited ductility μ = 2 or 3 is used, and for elastically responding structures μ = 1.25 is used.

The current New Zealand design standards [6,7] require for seismic design the use of the capacity design approach for ductile structures and for structures of limited ductility.

2.2 Steps in the capacity design approach and levels of strength

In the capacity design of ductile structures and structure of limited ductility the steps are:

(1) First, the appropriate plastic hinge regions of the primary lateral earthquake force resisting structural system are chosen and suitably designed and detailed for adequate *design strength* and ductility during a severe earthquake.

(2) Next, all other regions of the structural system, and other possible failure modes, are then provided with sufficient *nominal strength* to ensure that the chosen means for achieving ductility can be maintained throughout the post-elastic deformations that may occur when the flexural overstrength develops at the plastic hinges.

The intention of the above procedure is to ensure an appropriate hierarchy of member strength.

The above steps of the capacity design approach according to the New Zealand concrete design standard [6] require consideration of three levels of member strength; namely: design strength φS_n, nominal strength S_n and overstrength S_o as defined below.

Design strength is the nominal strength S_n multiplied by the appropriate strength reduction factor $\varphi \leq 1.0$, where φ is to allow for smaller actual material strengths than assumed in design and variations in workmanship, dimensions of members and reinforcement positions. Note that in Europe material factors γ_s and γ_c are used instead to reduce the characteristic steel and concrete strengths respectively, instead of φ factors.

Nominal strength S_n is the theoretical strength calculated using the lower characteristic strengths (5 percentile values) of the steel reinforcement and concrete and the member cross sections as designed.

Overstrength S_o is the maximum likely theoretical strength calculated using the maximum likely overstrength of the steel reinforcement and of the concrete including the effect of confinement, and any additional reinforcement placed for construction and otherwise unaccounted for in calculations.

3. FLEXURAL OVERSTRENGTH DUE TO THE STRESS-STRAIN CHARACTERISTICS OF THE MATERIALS

3.1 Reinforcing Steel

In practice the actual yield strength of the reinforcing steel will normally exceed the lower characteristic yield strength used in design. Also in the plastic hinge regions of ductile reinforced concrete structures during a major earthquake the longitudinal reinforcement may reach strains which are many times the strain at first yield and a further increase in steel stress due to strain hardening may occur. The maximum likely flexural strength at the plastic hinges is referred to as the flexural overstrength.

It is evident that the properties of the reinforcing steel to be used in seismic design should be based on thorough statistical analyses of the stress-strain properties, to determine the lower and upper bounds of the flexural strength of reinforced concrete elements. As an example, Andriono and Park [8] published in 1986 statistical studies of samples of 5 years of production of the grades of reinforcing steel manufactured in New Zealand to establish the 5 percentile value of the yield strength (below which not more than 5% of test results fall), the 95% percentile value of the yield strength (above which not more than 5% of test results fall), the ultimate strength, elastic modulus, strain hardening modulus, strain at commencement of strain hardening, and ultimate strain.

The 5 percentile value of the yield strength, referred to in New Zealand as the lower characteristic yield strength, is considered to be the appropriate value for use for determining the required areas of reinforcement in the strength design of members [6,8]. The lower characteristic yield strength is specified by the New Zealand standard for steel bars [9]. That standard also requires that the 95 percentile value of yield strength, referred to as the upper characteristic yield strength, does not exceed a specified value, in order to ensure that the overstrength of the steel is not too great. In addition, the absolute minimum and maximum values for the yield strength are also specified and the yield strengths are not permitted to lie outside the range of those specified absolute minimum and maximum values. The ratio of upper to lower characteristic yield strengths is 1.17 on average. The permitted range for the ratio of ultimate strength to yield strength is 1.15 to 1.5 depending on the steel [9].

The statistical results of the stress-strain properties of the steel reinforcement were used by Andriono and Park [8] in moment-curvature analyses of reinforced concrete beam sections, incorporating the Monte Carlo simulation technique, to assess the beam flexural overstrength factors for use in seismic design taking into account the likely variation in the steel and concrete properties. It was confirmed [8] that the flexural overstrength at plastic hinges in beams reinforced by New Zealand manufactured reinforcing steel should be taken as 1.25 M_n where M_n is the nominal flexural strength of the section recalculated using the lower characteristic yield strength of the steel reinforcement. This 25% increase takes into account the probability of the actual steel yield strength being greater than the lower characteristic value (approximately a 17% allowance) and the steel strength increase above the yield strength due to strain hardening at high strains (approximately an 8% allowance).

It should be noted that the steel strain at the ultimate strength of the steel (that is, at the peak stress of the stress-strain curve) should be at least about 10%, to ensure high available curvature ductility factors in beams. It is of concern that reinforcing steels with much lower strains at the ultimate strength of the steel have been used in some countries in seismic regions.

In beams the plastic elongation occurs mainly in the tension direction, since plastic strain in compression is reduced by the concrete in compression when cracks there close. The monotonic stress-strain curve gives a good envelop for the cyclic stress-strain curves in that case.

It is evident that it is very important for statistical information on the stress-strain relations of reinforcing steel used in seismic regions to be available. A proper capacity design cannot be undertaken without knowledge of the likely variations of the steel properties so as to permit the overstrength factor to be obtained. Also, adequate ductility of plastic hinges of members cannot be assured if the steel is brittle.

3.2 Concrete confinement

When detailing reinforced concrete members for ductility the compressed concrete can be confined by appropriate arrangements of transverse and vertical reinforcement in order to increase the available ultimate compressive concrete strain, and hence to improve the available ductility of the member. A consequence of the confinement is also an increase in the compressive strength of the concrete to above that for unconfined concrete, resulting in an increase in the flexural strength of columns.

The enhancement in flexural strength of reinforced concrete columns due to the increase in the concrete compressive strength as a result of confinement can be high. For example **Fig. 3** shows the theoretical enhancement in flexural strength found by Zahn et al [10] by cyclic moment-curvature analysis of a circular reinforced concrete column with $p_t m = 0.1$, $f_y = 275$ MPa, f'_c anywhere in the range 20 to 40 MPa, and various lateral confining pressures, where $p_t = A_{st}/A_g$, A_{st} = total area of longitudinal reinforcement, A_g = gross area of column section, $m = f_y/0.85f'_c$, f_y = yield strength of the longitudinal reinforcement and f'_c = compressive cylinder strength (unconfined) of the concrete. In **Fig. 3**, N^* = axial compressive load on the column, f_l = effective lateral confining stress acting on the concrete core due to the transverse reinforcement, M_{max} = maximum calculated flexural strength taking into account the increase in concrete strength and ductility due to confinement using the model of Mander et al [11, 12] but neglecting the effect of steel overstrength, and M_{code} = flexural strength calculated using the conventional approach of the New Zealand concrete design standard [6] which assumes a rectangular concrete compressive stress block with a mean stress of $0.85f'_c$, an extreme fibre concrete compressive strain of 0.003, the measured material strengths f'_c and f_y, and a strength reduction factor φ = 1. For the calculation of the maximum flexural strength M_{max} including the effect of both concrete confinement and steel overstrength an additional factor would need to be applied to the M_{max} in **Fig. 3** for steel overstrength. That additional factor for steel overstrength is more or less independent of the axial load ratio and can be taken as approximately 1.25. The enhancement of the flexural strength of confined columns has also been demonstrated experimentally. In fact laboratory tests have shown greater enhancements than in **Fig. 3** due to the additional confining effect of the beam or foundation adjacent to the critical section of the column (see Watson and Park [13]).

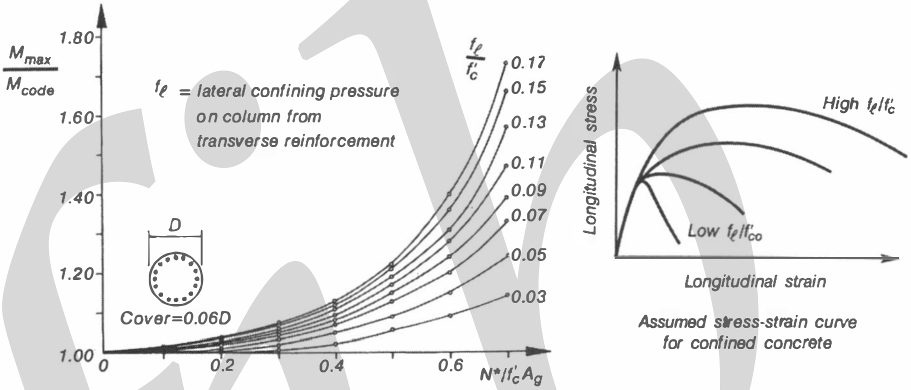

Fig. 3 Theoretical Enhancement in the Flexural Strength of a Circular Reinforced Concrete Column Due to Concrete Confinement [10]

4. CAPACITY DESIGN OF MOMENT RESISTING FRAMES

4.1 Desirable mechanisms of post-elastic behaviour for monolithic moment resisting frames

For moment resisting frames of buildings the best means of achieving ductile post-elastic deformations is by flexural yielding at selected plastic hinge position, since with proper design and detailing the plastic hinges can be made adequately ductile [1, 2, 14].

Significant post-elastic deformations due to shear or bond mechanisms are to be avoided since with cyclic loading they lead to severe degradation of strength and stiffness and to reduced energy dissipation due to pinched load-displacement hysteresis loops. Post-elastic deformations due to flexural yielding at well designed plastic hinge regions result in stable load-displacement hysteresis loops without significant degradation of strength, stiffness and energy dissipation.

The preferred mechanism for monolithic moment resisting frames is a beam sidesway mechanism (see **Fig. 4a**). A beam sidesway mechanism occurs as a result of strong column-weak beam design [1]. The ductility demand at the plastic hinges in the beams and at the column bases is moderate for this mechanism and can easily be provided in design. A column sidesway mechanism should not be permitted (except for the exceptions given below) since it can make very large demands on the ductility at the plastic hinges in the columns of the critical storey [1]. Column sidesway mechanisms (see **Fig. 1b**) (soft storeys) have often led to the collapse of buildings during earthquakes. The critical soft storey has generally been the bottom storey but maybe an intermediate storey up the height of the frame.

As a result of the above considerations, New Zealand design standards [6,7] require that the columns of multistorey ductile moment resisting frames should have adequate flexural strength so as to ensure, as far as possible, the formation of beam sidesway mechanisms (see **Fig. 4a**), with plastic hinges of adequate ductility during a severe earthquake. Thus a strong-column weak-beam design approach, with a displacement (structural) ductility factor $\mu = 6$, is advocated.

To ensure that failure in flexure cannot occur in parts of the structure not designed for ductility, or that failure in shear cannot occur anywhere in the structure, the maximum actions likely to be imposed on the structure are found taking into account the probable flexural overstrength at the plastic hinges in the beams, the effects of higher modes of vibration of the frame and the effects of seismic forces acting along both principal axes of the building simultaneously.

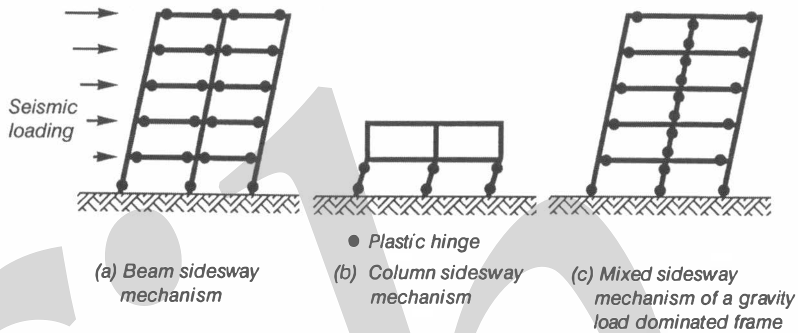

Fig. 4 Desirable mechanisms of post-elastic deformation of monolithic moment resisting frames during severe seismic loading according to the New Zealand concrete design standard [6]

The New Zealand concrete design standard [6] has only two exceptions to the requirement of the strong-column weak-beam design approach for ductile frames: (1) For one or two storey buildings (see **Fig. 4b**), or in the top storey of a multistorey building, column sidesway mechanisms are permitted (that is, a strong beam-weak column approach), since the curvature ductility demand at the plastic hinges in the columns in such cases is not high, and (2) If for tall frames strong-column weak beam design is impracticable (for example, in areas of low seismicity where gravity loading dominates the design, and/or if the beams have long spans) some columns may be permitted to form plastic hinges at the top and bottom simultaneously providing that the other columns (typically the exterior columns) remain in the elastic range and prevent a soft storey failure (see the mixed sidesway mechanism of **Fig. 4c**). In such case the permitted structure ductility factor used in design may need to be adjusted.

It should be appreciated that the mechanisms of **Fig. 4** are idealised in that they involve possible post-elastic behaviour obtained from static "push-over" analysis with the frame subjected to code type equivalent horizontal static seismic forces. The actual dynamic situation is different, due mainly to the effects of higher modes of vibration of the structure. For example, the curvature ductility demand at the plastic hinges in the beams in the lower region of the frame of a beam sidesway mechanism may be greater than in the upper region. However, considerations such as those shown in **Fig. 4** can be regarded as providing the designer with a reasonable feel for the situation. Non-linear dynamic analyses indicate that mechanisms such as those shown in **Fig. 4** do form.

4.2 Capacity design actions recommended in New Zealand for strong column-weak beam design of ductile moment resisting frames

4.2.1 Design shear forces in beams

The design shear forces in beams should be determined by a capacity design procedure for when the flexural overstrength is reached at the most probable plastic hinge locations within the span and the design gravity load is present. For example, for the beam in **Fig. 5** the design shear force at B will be:

$$V^*_B = \frac{M'_{oA} + M_{oB}}{L_{AB}} + \frac{wL_{AB}}{2}$$

where M^{*}_{oA} and M_{oB} are the flexural overstrength capacities of the sections for positive moment at A and negative moment at B, respectively, and w is the uniform dead and live load considered to be present at the ultimate limit state per un it length. The flexural overstrength capacities are calculated from 1.25 M_n where M_n is the nominal flexural strength of the section including an allowance for the slab reinforcement in negative moment regions. As a result of tests by Cheung et al [3] the New Zealand concrete design standard [6] recommends that the slab width, within which effectively anchored longitudinal slab reinforcement shall be considered to contribute to the negative moment flexural strength of the beam, in addition to those bars placed within the web width of the beam, for interior spans shall be defined as one quarter of the span of the beam extending each side of the beam from the centre of the beam section but not greater than the width to the centre of the slab panels each side.

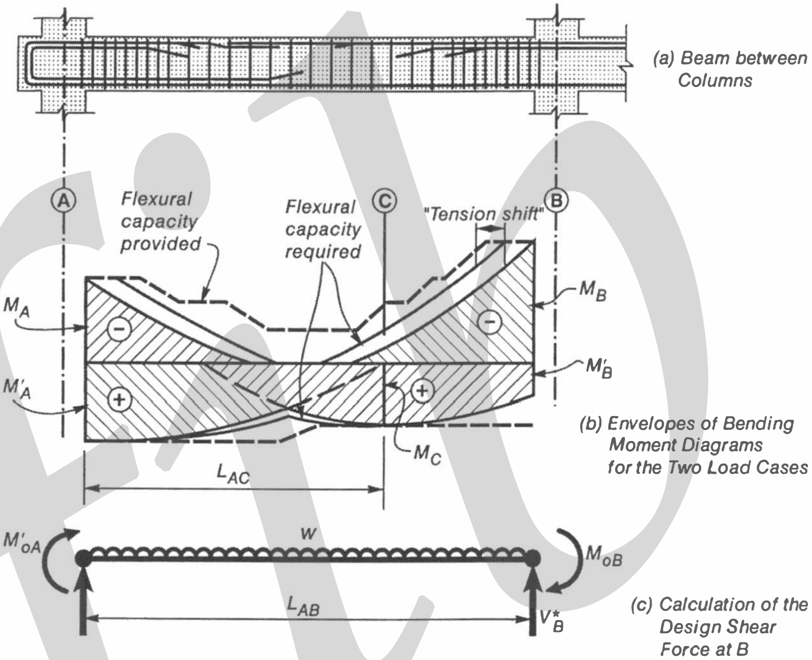

Fig. 5 Capacity design calculation of the design shear force of a beam in a moment resisting frame

4.2.2 Design bending moments in columns

The capacity design rules for protecting the columns of tall moment resisting frames, by ensuring that as far as possible strong-column-weak beam behaviour occurs, were first introduced in the New Zealand concrete design standard in 1982 and have remained practically the same in the 1995 standard [6].

The procedure for determining the design bending moments in the columns is illustrated in Fig. 6. The design bending moment for the column at the centre of the beam-column joint is:

$$M^{*}_{col} = \omega\ \varphi_o\ M_e$$

where M_e is the column bending moment at the centre of the beam-centre joint derived by elastic structural analysis for the equivalent static design forces; φ_o is the ratio of the sum of the flexural overstrength capacities of the beams at the joint as detailed to the sum of the bending moments of the beams at the joint resulting from the equivalent static design seismic forces ≥ 1.25/0.85 = 1.47, where 1.25 = overstrength factor applied to the nominal flexural strength and 0.85 = strength reduction factor; ω is a factor allowing for higher modes of vibration and bidirectional seismic load effects, given for one way frames as $\omega = 0.6T + 0.85$ but not less than 1.3 or more than 1.8, and for two-way frames as $\omega = 0.5T + 1.1$ but not less than 1.5 or more than 1.9, where T = fundamental period of vibration of the structure.

As shown in **Fig. 6**, the critical column section is assumed to be at the top and bottom of the beams and accordingly the centreline column bending moment $\omega\varphi_o M_e$ is reduced by 0.3 h_b V^*_{col}, which is based on an estimated gradient of the column bending moment diagram, where h_b = beam depth and V^*_e = column shear force.

The recommended amplification of column bending moments by this procedure can be significant, the combined factor ω**N**$_o$ being at least 1.91 for one-way frames and at least 2.21 for two-way frames.

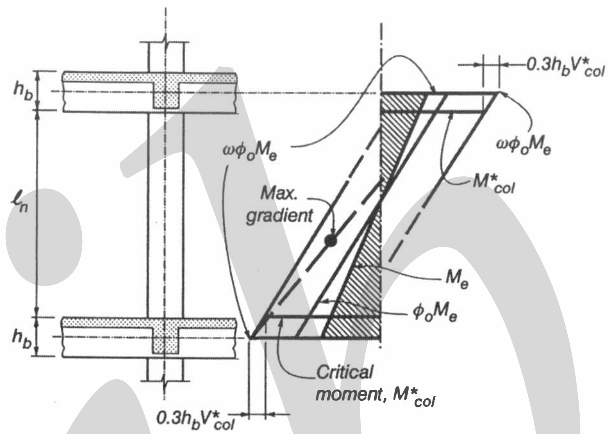

Fig. 6 Stages of amplification of column bending moments in capacity design [2]

Note that for two-way frames the columns are designed f or uniaxial bending only, since ω includes some moment amplification for the effect of biaxial bending. The above values of ω are based on dynamic analyses and judgement [15].

4.2.3 Design axial loads in columns

The design axial loads in the column N^*_{col} to be used with $\omega\varphi_o M_e$ - $0.3h_b V^*_e$ in the design of the column sections is found by summing all the shear forces applied at the column faces by the gravity loads on the beams and the moment induced shear forces from the beam plastic hinge moments acting in the two directions concurrently. An adjustment in the moment induced shears is allowed [6] to take into account the probability that not all beam plastic hinges re ach their flexural overstrength simultaneously up the height of the frame. A strength reduction factor φ = 1.0 is used for the section design when the column design actions are found using this capacity design procedure.

4.2.4 Design shear forces in columns

The design shear forces in the columns above the first storey of the building, ac ting separately in each of the two principal directions are taken for a one-way frame as $V^*_{col} = 1.3\ \varphi_o\ V_e$ and for a two-way frame as $V^*_{co} = 1.6\ \varphi_o V_e$ where No is the beam overstrength factor defined as in Section 4.2.2 and V_e is the column shear force derived f or the equivalent static design seismic forces at the ultimate limit state.

These forces were estimated from probable critical moment gradients along columns [15]. The larger value for two-way frames is to include the effect of concurrent seismic loading acting along both principal axes of the building simultaneously. For the column of the first storey the design shear forces are taken as $V^*_{col} = (M_{o,\,col,\,bottom} + M_{o,\,col,\,top})/l_n$, where $M_{o,\,col,\,bottom}$ and $M_{o,\,col,\,top}$ are the flexural overstrength capacities of the bottom and top critical plastic hinge sections of the columns, respectively, and l_n = clear length of column between beams. The flexural overstrength column capacities should include the effects o f both the steel and the concrete over strength s, obtained by multiplying the nominal flexural strength by a factor in the range 1.25 to 2.0 depending on the axial load ratio $N^*/f'_c\ A_g$ and the actual reinforcement contents [6].

4.2.5 Design shear forces in beam-column joints

The design shear forces in beam-column joints are calculated using the overstrength steel forces and the design shear forces for the members at overstrength. The calculation of the design horizontal joint shear force involves the determination of the net horizontal force above or below a horizontal plane passing through the centre of the joint core. Similarly, the design vertical joint shear force can be calculated from the net vertical force to one side or other of a vertical plane passing through the centre of the joint core.

4.3 Capacity design actions recommended in New Zealand for the strong column-weak beam design of moment resisting frames of limited ductility

For moment resisting frames of limited ductility in order to ensure a beam sidesway mechanism with plastic hinges takes in the columns permitted only at the base of the frame and in the top storey, the capacity design procedure to determine the column design actions takes account of possible beam overstrength, a general direction of seismic forces and magnification of column moments due to dynamic effects. However, the procedure is a relaxation of that used for ductile frames. The magnified column bending moments at the beam centre line (to be reduced for moment gradient to obtain the value at the critical sections) are taken as 1.1 $\varphi_o M_e$ for one-way frames and 1.3 $\varphi_o M_e$ for two-way frames. The shear forces in the upper columns are taken as 1.1 $\varphi_o V_e$ for one-way frames and 1.3 $\varphi_o V_e$ for two-way frames, where the notation is as in sections 4.2.2 and 4.2.4. The structural ductility factor of such frames should be taken as 3.

4.4 Comparison with design actions recommended for moment resisting frames by other seismic design codes of international standing

A comparison of major national seismic design codes and guidelines has been conducted by Booth et al [16]. The codes considered were Eurocode 8 [17], the guidelines of the Architectural Institute of Japan [18], United States codes (the building code of the American Concrete Institute [19] and the Uniform Building Code [20]), and the New Zealand standard [6]. It was found that all of those codes and guidelines recognise capacity design, although to varying degrees of clarity, and the degree to which capacity design is in corporate d in each cod e varies significantly.

Of particular note is the difference in opinion internationally with regard to the multiplier $\omega\varphi_o$ used to find the design bending moment M_{col} for a column from the column bending moment M_e found by elastic structural analysis for the equivalent static seismic forces (see Section 4.2.2). According to the New Zealand standard [6] for strong column-weak beam design ω varies between 1.3 and 1.9 for one-way and two-way frames and the combined factor $\omega\varphi_o$ is at least 1.9 for one-way frames and 2.2 for two-way frames. However, Pinto et al [21] as a result of the dynamic analysis of one-way four and eight storey symmetrical moment resisting frames have concluded that ω= 1.35 may be high enough. Also Panagiotakis et al [22] have concluded that somewhat smaller values for ω than specified in the New Zealand standard does not lead to soft storey formation. Also the 1999 edition of the building code of the American Concrete Institute [19] requires that the sum of the nominal flexural strengths of the columns at beam-column joint forces exceed the sum of the nominal flexural strength of the beams there by at least 20%.

However, recently Dooley and Braci [23] have studied three and six storey moment resisting plane frames subjected to seismic excitation using non-linear time-history dynamic analysis. Various column-to-beam flexural strength ratios were considered. For a column-to-beam flexural strength ratio of 1.2 it was found that the probability of the formation of a column sidesway mechanism was approximately 90%. Their results indicate that the minimum column-to-beam flexural strength ratio should be approximately 2.0 to have a significant probability of avoiding column sidesway mechanisms. This issue is still controversial, but this latest evidence [23] does indicate that the New Zealand recommended values may be in the right order. These differences incapacity design factors need to be resolved.

5. CAPACITY DESIGN OF STRUCTURAL WALLS

5.1 Desirable mechanisms of post-elastic behaviour of monolithic structural walls

5.1.1 Cantilever and coupled structural walls

In the capacity design o f ductile structural walls, plastic hinging at the bas e of the wall is sought. The design shear forces for the wall should be determined by a capacity design procedure for when the flexural overstrength is reached at the base of the wall. Note that the design flexural strength elsewhere up the height of the wall should be at least equal to that from the bending moment diagram for when the flexural overstrength is re ached at the base of the wall, displaced upwards by at least one half of a wall depth to allow for the tension shift effect due to yielding of vertical bars across 45° diagonal cracks.

According to the New Zealand concrete design standard [6] at the base of a cantilever wall the design shear force is given by $V^*_{wall} = \varphi_o \, \omega_w \, V_e$ where φ_o = ratio of overstrength moment of resistance to bending moment resulting from the equivalent static design seismic forces at the bas e of the w all, $T_w = 0.9 + n/10$ for buildings up to six storeys in height and $\omega_w = 1.3 + n/30 \leq 1.8$ for buildings over six storeys in height, where n = number of storeys, and V_e = wall shear force at the base derived from for the equivalent static design seismic forces.

According to the New Zealand concrete design standard [6] the displacement (structural) ductility factor to be used for ductile cantilever walls is $\mu \leq 6$, depending on the height to length ratio of the wall, and in the case of coupled w alls also depending on the ratio of the overturning moment resisted by the coupling walls to that resisted by the wall bases.

The preferred mechanism for a monolithic cantilever structural wall involves a plastic hinge at the base. **Fig. 7** shows desirable mechanisms of post-elastic deformation of monolithic structural walls during severe seismic loading with coupling beams between them. If the coupling is weak (for example, only from floor slabs) the walls will act as individual cantilever walls connected by pin-ended links (see **Fig. 7a**). If the coupling beams are stiffer and have significant flexural strength, but not sufficient to cause shear failure of the walls, plastic hinging will also develop in the coupling beams (see **Fig. 7b**).

Jointed precast concrete structural wall construction (with relatively weak joints between the precast elements) could develop other mechanisms of post-elastic deformation and nee d to be designed as structures of limited ductility or to respond in the elastic range.

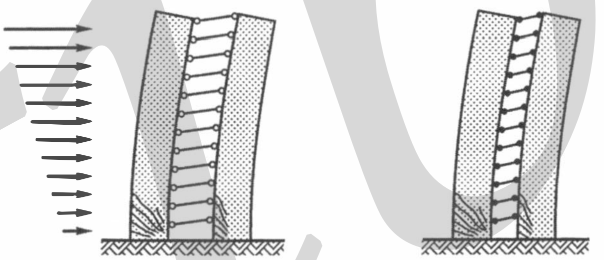

(a) Weak Coupling of Walls *(b) Stronger Coupling of Walls*

Fig. 7 Desirable mechanisms of post-elastic deformation of coupled structural walls [2]

5.1.2 Dual systems

For dual systems (combined moment resisting frames and structural walls) the deformations of the frames w ill be controlled and limited by the much stiffer walls. **Fig. 8a** shows the frame with weak beam-strong column behaviour with plastic hinging occurring in the beams and at the bases of the columns and walls. However, strong beam-weak column behaviour may be admitted in every storey of the frame (see **Fig. 8b**) because a structural wall, proportioned using capacity design principles, will remain in the elastic range above the plastic hinge at the bas e and its stiffness w ill prevent a "soft storey" failure from developing in the frame. Without a structural wall, such a frame system in New Zealand [6] designed for ductile response will normally have to be restricted to buildings of one or two storeys. Note that norm ally the frames are much more flexible than the walls and hence the plastic hinging in the frames w ill be very limited. In cases where the frames a re much m ore flexible than the walls the frames may remain in the elastic range and then can be de signed for nominal ductility.

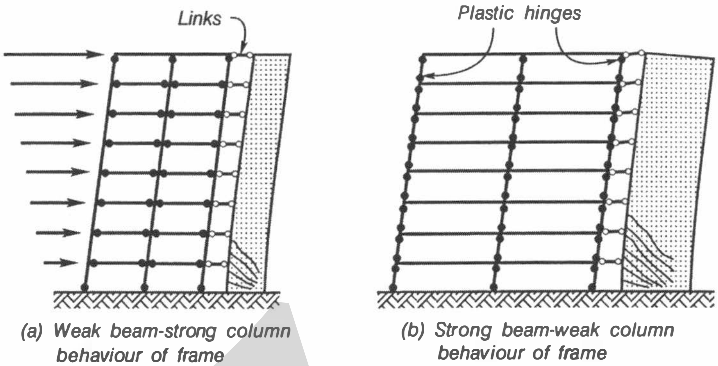

Fig. 8 Desirable mechanisms of post-elastic deformation of dual systems [2]

6. DETAILING FOR DUCTILITY

6.1 Transverse reinforcement for shear resistance, confinement of concrete and for preventing buckling of longitudinal reinforcement

The most important design con side ration for ensuring ductile plastic hinge regions of reinforced concrete members of moment resisting frames is the provision of adequate longitudinal compression reinforcement as well as tension reinforcement, and the provision of transverse reinforcement in the form or rectangular hoops with or without cross ties, or circular hoops or spirals (see **Fig. 9**). This transverse reinforcement is needed to act as shear reinforcement, to confine and hence to enhance the ductility of the compressed concrete, and to prevent premature buckling of the compressed longitudinal reinforcement. According to the New Zealand concrete design standard [6] in order to confine the compressed concrete of columns in potential plastic hinge regions the centre-to-centre spacing of transverse reinforcement along the member should not exceed one-quarter of the least lateral dimension of the cross section or 200 mm, whichever is greater. Also, the centre-to-centre spacing of transverse reinforcement along the member in potential plastic hinge regions of beams and columns should not exceed six longitudinal bar diameters in order to control bar buckling [6]. The amount of transverse reinforcement necessary in columns to en sure adequate available ductility to match the imposed ductility can be calculated by moment-curvature analysis incorporating the stress-strain relations for confined concrete [1, 10-12, 24].

The equation for the amount of transverse reinforcement required to confine the compressed concrete recommended by the New Zealand concrete design standard [6] was derived by Watson et al [24]. The amount is a function of the axial load level N^*/f'_c Ag, where N^* is the axial compressive load on the column, f'_c is the concrete compressive cylinder strength and Ag is the area of the column. According to the New Zealand equation the required amount of confining reinforcement increases with axial load level. Heavily loaded columns need more confining reinforcement since the greater neutral ax is depth c means that a greater extreme fibre concrete compressive strain ε_c, and hence a greater amount of confinement is needed, to achieve a given ultimate curvature $\varphi_u = \varepsilon_c/c$.

An example of the quantities of transverse reinforcement required by the New Zealand concrete design standard [6] for confinement of concrete in the potential plastic hinge regions of columns when a curvature ductility factor φ_u/φ_y of 20 is required is shown in **Fig. 10**, where φ_u is the ultimate curvature and φ_y is the curvature at first yield. Note that the requirement for concrete confinement in the New Zealand standard governs at higher axial loads and the requirement for preventing buckling of the longitudinal reinforcement governs at lower axial loads. Also in some cases transverse reinforcement required for shear resistance may govern. By comparison the ACI [19] amount, required for confinement, as shown in the example of **Fig. 10**, is a single constant value regardless of the axial load level. The EC8 [17] requirements are also dependent on the axial load level and generally lead to greater quantities of transverse reinforcement than the New Zealand requirements [16].

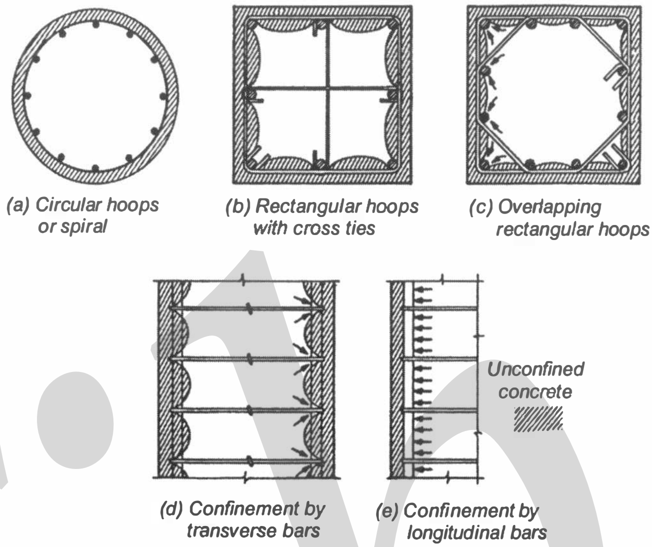

Fig. 9 Reinforcement in a column for shear resistance, concrete confinement and prevention of premature buckling of longitudinal bars

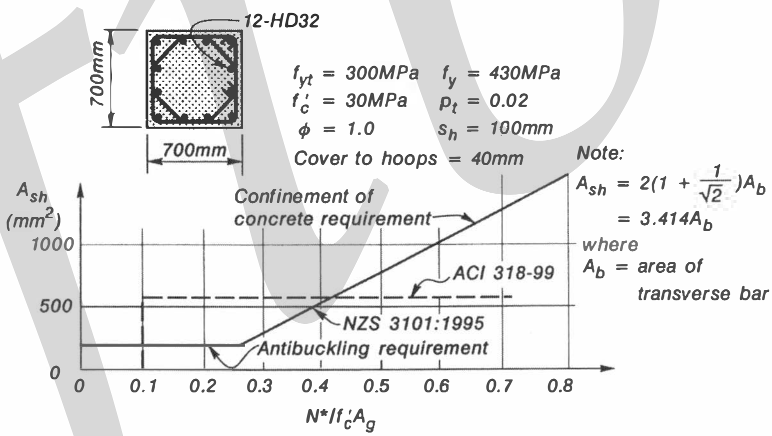

Fig. 10 Example of transverse reinforcement required in a ductile column

6.2 Length of end region of column to be confined

The confine d length of column adjacent to the section of maximum bending moment (see **Fig. 11**) needs to be sufficiently long to extend over the region of major plastic curvature and to ensure that the higher flexural strength of the column in the confined region does not lead to flexural failure of the column in the adjacent less confined region. The second requirement is particularly important for normal strength concrete columns with high axial compression, since for such columns the flexural strength is markedly increased by confinement of the concrete, Zahn et al [10], Watson et al [13, 24]. **Fig. 11** shows the distribution of bending moments for a cantilever column due to an imposed lateral load at the top, and the flexural strengths of the confined and nominally confined regions of the column. To compensate for the effects of the spread of yielding due to possible diagonal tension cracking, the moment diagram is spread by h/2 along the member, where h = column depth. The length of the region that needs to be confined L_c can be estimated knowing the enhanced flexural strength M_i in the confined region and the conventionally calculated flexural strength M_{code} outside the confined region.

An analysis by Watson et al [13] of the test results from the columns subjected to simulated seismic loading at the University of Canterbury since the late 1970s, resulted in the current requirements in the New Zealand concrete design standard [6], which are: (1) the confined length L_c for low axial load levels when $N^* < 0.25\ \varphi\ f'_c\ A_g$ is taken to be the greater of h or where the moment exceeds 0.8 of the adjacent end moment. L_c for high axial load levels with $N^* > 0.5\ f'_c\ A_g$ is taken to be the greater of 3h or where the moment exceeds 0.6 of the adjacent end moment. An intermediate value of L_c is taken for axial load levels in between. In the above N^* is the axial compressive load on the column, N is the strength reduction factor, f'_c N is the concrete compressive cylinder strength, A_g is the area of the column and h is the depth of the column. Hence typically the confined length L_c varies between h and 3h.

By comparison the other national standards recommend shorter confined lengths than the New Zealand standard [16].

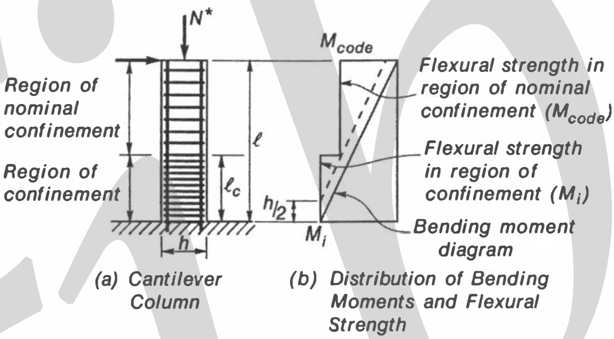

Fig. 11 Determination of the length of the confined end region of column

6.3 Shear reinforcement in beam-column joints

Probably the most controversial aspect of the seismic design of reinforced concrete moment resisting frames is the reinforcement of beam-column joints. **Fig. 12** shows the forces acting on and the crack pattern of an interior beam-column joint core during seismic loading. The horizontal shear forces acting on the joint core can be found by summing the horizontal forces from the column shear, the compressed concrete in the beams, and the reinforcing bars in tension and compression in the beams above or below the mid-plane of the joint core. The vertical shear forces acting on the joint core can also be found.

In the New Zealand concrete design standard [6] it is considered that the shear forces acting on the joint core are transferred across the joint core by two mechanisms, namely: (1) a corner-to-corner concrete diagonal compression strut mechanism, and (2) a truss mechanism consisting of a concrete diagonal compression field acting with horizontal and vertical joint shear reinforcement. The joint shear is apportioned between the two mechanisms and shear reinforcement provided. The horizontal shear loading reinforcement, in the form of hoops, must at least equal the transverse reinforcement placed for confinement in the adjacent ends of the columns. The vertical shear reinforcement is normally provided by the longitudinal column bars placed in the side faces of the column between the corner bars. The fundamental difference between the New Zealand and the United States approaches for the design of transverse reinforcement in beam-column joints is that whereas the New Zealand standard [6] regards that reinforcement is being placed mainly to resist shear, United States standards regards it more as confining reinforcement governed by the quantity placed in the adjacent ends of the columns. Also, the New Zealand standard insists on vertical shear reinforcement being present in the joint core, normally consisting of longitudinal column bars placed between the corner bars. This vertical reinforcement also has the function of improving the bond of the longitudinal beam bars by clamping action. This vertical shear reinforcement is not required by United States standards.

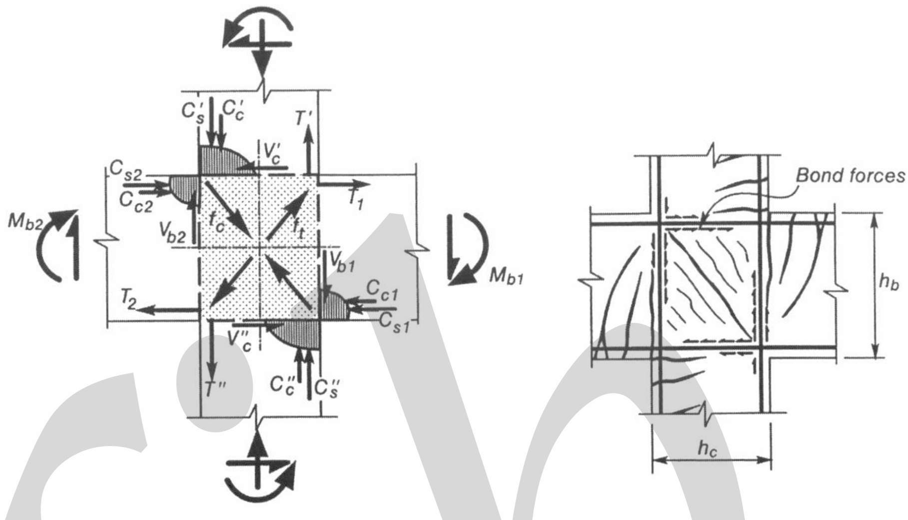

(a) Forces acting on joint core *(b) Crack pattern and bond forces*

Fig. 12 Interior beam-column joint during seismic

6.4 Anchorage of longitudinal reinforcement in interior joints

The plastic hinges in the beams normally occur near the beam ends and hence during seismic loading the top and bottom beam bars may yield in tension and compression alternatively at the column faces. The high bond stresses on the longitudinal bars in the joint core may lead to significant bond deterioration and some bar slip through the joint core. Design standards generally attempt to reduce bar slip by limiting the bond stresses by specifying maximum values for the d_b/h_c ratio for the joint where d_b is the diameter of the beam bar and h_c is the depth of the column. The maximum permitted values for d_b/h_c recommended by the New Zealand standard [6] and the A.I.J. guidelines [18] are in reasonable agreement, typically varying between 1/35 and 1/15, depending on the values of variables, for f'_c n the range 20-40 MPa and f_y in the range 300-430 MPa for top bars in one-way frames (see Hakuto et al [25]). However, United States codes recommend a single constant maxim um permitted value for d_b/h_c of 1/20 and hence place less emphasis is on limiting the bar slip. In New Zealand it is recognized that some bar slip is inevitable, but significant bar slip during a severe earthquake is considered to be undesirable for two main reasons: (1) It leads to considerable reduction in stiffness of the frame which is residual, (2) bond deterioration is difficult to repair by epoxy resin injection, and (3) It leads to a reduction in the available curvature ductility factor of the adjacent plastic hinges in the beams. If the bond deterioration is significant the bar tension will penetrate through the joint and the bar tensile force will be anchored in the beam on the other side of the joint. This means that the "compression" steel there will actually be in tension. The result is that, although the flexural strength of the beam may not be greatly reduced, the available ultimate curvature at a specified ultimate concrete compressive strain may be very greatly reduced, for example by 50% (Hakuto et al [25]). It is to be noted that small d_b/h_c ratios lead to small diameter bars and/or large columns. It is evident the maximum d_b/h_c values specified by codes is a matter of judgement.

7. EXAMPLES OF CAPACITY DESIGN

7.1 Moment resisting frames incorporating precast concrete elements

The use of precast concrete in moment resisting frames was shunned for many years in New Zealand, due mainly to the observation of poor performance of connection details between the precast concrete elements during major earthquakes in many overseas countries. However, since the 1980s in New Zealand there has been a significant increase in the use of precast concrete elements in moment resisting frames, due to the high quality control, the reduction in site labour and formwork, and the increased speed of construction.

Three arrangements of precast reinforced concrete members and cast-in-place concrete, forming ductile moment resisting multi-storey reinforced concrete frames, commonly used for strong column-weak beam designs in New Zealand, are shown in **Fig. 13** [26, 27]. The precast concrete beam elements of Systems 1, 2 and 3 are connected in the beam-column joint or at mid-span by longitudinal beam reinforcement protruding from the precast concrete into regions of cast-in-place concrete where they are anchored by splices using straight or hooked beam bars. For System 2 the vertical column bars of the column below the joint protrude up through vertical corrugated steel ducts in the precast beam unit, where they are grouted, and pass into the column above. They are connected to the bars in the column above by lap splices if the column is of cast-in-place concrete or by steel sleeves or ducts which are grouted if the column is of precast concrete. The precast concrete be am and column elements of System 3 are connected by longitudinal column bars which protrude into steel sleeves or ducts in the adjacent element and are grouted. A further commonly used system involves replacing the precast reinforced concrete beams of System 1 with precast prestressed pretensioned concrete U beams which are in filled with cast-in-place reinforced concrete when placed [28]. It is to be noted that the capacity design procedure will ensure that yielding of the column bars at the connections in Systems 2 and 3 is kept to a minim um. If the connections between the precast elements are placed in potential plastic hinge regions as in System 1 they are designed with sufficient stiffness, strength and ductility to behave as if of monolithic cast-in-place construction (monolithic emulation) [26, 27].

The trend in New Zealand for multi-storey moment resisting frames, without structural walls is to design the perimeter frames with sufficient stiffness and strength of resist most of the horizontal seismic loading. Then the more flexible interior frames will be called on to resist only a small proportion of the horizontal forces, the exact amount depending on the relative stiffnesses of the interior and perimeter frames. The interior frames then may carry mainly gravity loading. The use of one-way perimeter frames avoids the complexity of the design of beam-column joints of two-way moment resisting frames. The currently used connection details shown in **Fig. 13**, including System 1 with precast prestressed U beam s, have had experimental verification in New Zealand [28, 29]. The verification involved simulated seismic loading tests conducted on typical full-scale beam-column joint specimens, designed for strong-column weak-beam behaviour. It was found that behaviour equivalent to totally cast-in-place concrete construction could be achieved by properly designed connections. The results of the experimental studies led to design provisions which have been incorporated in the New Zealand concrete design standard [6]. The use of capacity design has given confidence that yielding can be restricted only to ductile regions as intended by the designer.

7.2 Other applications of capacity design

There are many other applications of capacity design. For example in the design of bridge piers the overstrength flexural capacities at the plastic hinge regions should be used to calculate the design shear forces at the plastic hinge regions and the design bending moments and shear forces elsewhere in the piers.

Another example is the de sign of steel embedments in concrete to anchor attachments. It is desirable that yielding be restricted to the steel attached to the embedment which should be capable of ductile behaviour and that brittle pull-out failure from the concrete be avoided. This can be achieved by ensuring statistically that the yield force of the steel attached to the embedment is less than the pull-out strength of the embedment from the concrete.

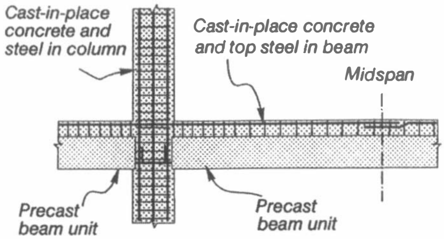

(a) System 1 - Precast Beam Units Between Columns

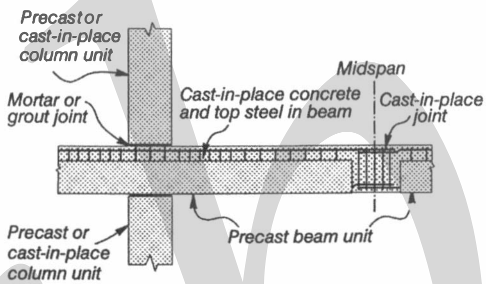

(b) System 2 - Precast Beam Units Through Columns

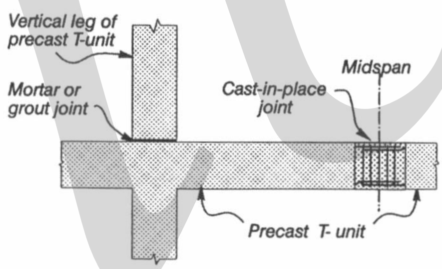

(c) System 3 - Precast T-Units

Notes: Precast Concrete Cast-in-place concrete

Reinforcement in precast concrete not shown

Fig. 13 Arrangements of precast reinforced concrete members and cast-in-place concrete for constructing strong column-weak beam moment resisting frames in New Zealand (monolithic emulation)

8. A CAPACITY DESIGN ASSESSMENT PROCEDURE FOR EXISTING STRUCTURES

8.1 Introduction

Developments in seismic design procedures have brought about the realization that many early reinforced concrete structures, particularly those designed before about the mid-1970s may be deficient according to the seismic design requirements of current codes. As a result there has been increasing emphasis in recent years on the assessment, and the retrofit of buildings if necessary, to improve their seismic performance.

The structural deficiencies of many existing reinforced concrete structures designed to early codes are generally not just a result of inadequate flexural strength. For example, longitudinal reinforcement in many existing structures results in a lateral load strength which approaches or exceeds that required by current standards for ductile structures. The poor structural response is normally due to a lack of a capacity design approach and/or to poor detailing of reinforcement, which means that the available ductility of the structure during the cycles of lateral loading in the post-elastic range imposed by a severe earthquake may be inadequate to withstand the earthquake without collapse. However, the evidence of tests and analysis is that not all early structures will respond poorly to severe earthquakes even when according to current codes the detailing of reinforcement in some regions is substandard. A detailed force-based capacity design assessment procedure for the seismic assessment of existing reinforced concrete frames has been suggested by Priestley and Calvi [30] and Park [31]. The suggested procedure is based on determining by static push-over analysis the horizontal load strength and ductility of the critical post-elastic mechanism of deformation of the structure. Once the available horizontal load strength and ductility of the structure has been established, reference to code seismic acceleration response spectra for earthquake loading then enables the designer to assess the seismic risk. The procedure uses recent analytical and experimental evidence of the behaviour of elements and joints subjected to simulated seismic loading [30, 31, 32]. The experimental information obtained includes the shear strength of beams, columns and beam-column joints with inadequate transverse reinforcement, the performance of lap splices and poorly anchored transverse and longitudinal reinforcement, and the interaction between the shear strength of members and beam-column joints and the imposed flexural ductility.

It is to be noted that time-history nonlinear dynamic analysis can also be used to estimate the ductility demand and the displacement response of an existing structure to major earthquake shaking. The force-deformation hysteresis loops used in the analysis need to realistically model any strength and stiffness degradation of the regions of the structure.

8.2 Steps of a force-based capacity design assessment procedure

The steps of a force-based seismic assessment procedure of an existing moment resisting frame are [31]:

Step 1: Establish the expected compressive strength of the concrete and yield strength of the reinforcing steel. Realistic mean measured values should be used. The nominal values specified in the original design are inappropriate since they will generally be exceeded.

Step 2: Estimate the expected flexural and shear strengths of the critical sections of the beams and columns and the expected shear strengths of the beam-column joints using the mean material strengths assuming that no degradation of strength occurs due to cyclic lateral loading in the post-elastic range.

Step 3: Determine by static push-over analysis the post-elastic mechanism of deformation of the frame that is likely to occur during horizontal seismic loading and the expected horizontal seismic force capacity of the frame, V. This will involve determining whether flexural plastic hinges occur in the beams or columns at the faces of each beam-column joint and/or whether shear failure occurs in the members or joints.

Step 4: Estimate the seismic coefficient $C_h(T,\mu)$ corresponding to the expected horizontal force capacity of the frame V found in Step 3 from:

$$C_h(T,u) = \frac{V}{W_t}$$

where W_t = seismic weight of the structure.

Step 5: Estimate the fundamental period of vibration of the structure, T. Then using the appropriate seismic acceleration response spectra of the seismic code determine the required displacement (structural) ductility factor: for the estimated $C_h(T,\mu)$ and T.

Step 6: Estimate whether the plastic hinges have the available rotational ductility to match the required displacement (structural) ductility factor μ. The frame will require retrofitting if the rotation capacity of the plastic hinges is found to be inadequate.

Step 7: Estimate the degradation in the shear and bond strength of members and joints during cyclic deformations to the imposed rotational ductility in the plastic hinge regions. Check whether any degradation in shear and bond strength will cause failure of the frame. If it does not, then the assessment a part from Step 8 is complete. If it does, the frame will require retrofitting.

Step 8: Estimate the interstorey drift and decide whether it is tolerable.

Each of the above steps is described in detail else where [31]. Although force-based design is the conventional approach it should be noted that a displacement based approach [33] which determines accurately the required maximum displacement for the design earthquake is a more realistic procedure and will become the way of the future. The expected displacement demand is based on the structural characteristics (effective stiffness and equivalent viscous damping) at maximum displacement capacity rather than the initial elastic characteristics. A set of displacement spectra for different levels of damping is used rather than the set of acceleration response spectra of force-based design.

9. CONCLUSIONS

1. The aim of the capacity design method of seismic design of structures is to ensure that the preferred mode of post-elastic deformation occurs during a severe earthquake. Brittle soft storey failures of buildings and shear failures are avoided by ensuring that in the event of a severe earthquake yielding occurs only at chosen ductile regions of the structure.
2. It is evident that the effects of overstrength in flexure of members are not always beneficial in seismic design. In the capacity design approach the effects of possible flexural overstrength of parts of the structure are taken into account when determining the design actions for shear.
3. The most common reasons for the flexural overstrength of reinforced concrete members are steel and concrete strengths higher than specified, member sizes and quantities of steel reinforcement larger than necessary, the use of strength reduction factors or material factors in design, other load combinations requiring greater strengths at some sections, and the participation of nonstructural elements.
4. The overstrength of steel reinforcement needs to be carefully assessed. It is evident that it is very important for statistical information on the stress-strain properties of reinforcing steel used in seismic regions to be available. A proper capacity design cannot be undertaken without knowledge of the likely variations of the steel properties to obtain overstrength factors, and adequate ductility of plastic hinges of members cannot be ensured if the steel is brittle. Analytical moment-curvature studies have shown that for New Zealand manufactured reinforcing steel the flexural overstrength of reinforced concrete beams due to fluctuation in steel properties can be taken as 1.25 M_n where M_n is the nominal flexural strength calculated using the 5 percentile value for the yield strength of the steel.
5. Confinement of compressed concrete can result in a significant increase in the compressive strength of the concrete and hence in the flexural strength of columns, particularly when the axial compressive load on the column is high.
6. Currently there are significant differences between national design standards and guidelines in important areas of the seismic design of reinforced concrete. These differences for moment resisting frames concern mainly: (1) the amplification factors used for design bending moments and shear forces used in capacity de sign to avoid soft storey failures of moment resisting frames and shear failures; (2) the rules used for the amounts of transverse reinforcement required to confine the concrete of members and to prevent buckling of longitudinal bars; and the extent of that reinforcement; (3) the design of beam-column joints with regard to shear strength, confinement of concrete and the anchorage of longitudinal bars passing through the joint core. These differences need to be resolved so as to obtain a more consistent seismic design approach.
7. The use of capacity design, appropriate connection details, and ductile detailing has given

designers in New Zealand confidence that moment resisting frames incorporating precast concrete elements can be designed to emulate monolithic cast-in-place construction for earthquake resistance.

8. A force-based step by step procedure based on capacity design for the seismic assessment of existing moment resisting reinforced concrete frames can be developed. The assessment procedure determines the expected horizontal load strength of the critical mechanism of post-elastic deformation of the frame. The required structural (displacement) ductility factor is then estimated from acceleration response spectra and the frame checked to determine whether that ductility is available.

10. ACKNOWLEDGEMENT

The author acknowledges the many discussions with his colleagues and graduate students at the University of Canterbury, and the contributions of the structural engineering profession in New Zealand, particularly the members of the study groups of the New Zealand National Society for Earthquake Engineering and the members of the concrete design committee of Standards New Zealand. Thanks are due to Miss Catherine Price for word processing and to Mrs. Val Grey for the graphics.

11. REFERENCES

[1] Park, R. and Paulay, T. : Reinforced concrete structures. John Wiley and Sons, New York, 1975, 769 pp.

[2] Park, R., Paulay, T. and Bull, D.K. : Seismic design of reinforced concrete structures. Technical Report No. 20, New Zealand Concrete Society, Wellington, September 1992.

[3] Cheung, P.C., Paulay, T. and Park, R. : Mechanisms of slab contributions in beam-column subassemblages. Design of Beam-Column Joints for Seismic Resistance, Special Publication, SP-123, American Concrete Institute, pp. 259-289, 1991.

[4] Hollings, J.P. : Reinforced concrete seismic design. Bulletin of New Zealand National Society for Earthquake Engineering, Vol. 2, No. 3, 1969, pp. 217-250.

[5] Paulay, T. and Priestley, M.J.N. : Seismic design of reinforced concrete and masonry buildings. John Wiley and Sons, New York, 1992, 744 pp.

[6] S.N.Z. : The design o f concrete structures (NZS 3101:1995). Standards New Zealand, Wellington 1995.

[7] S.N.Z. : Code of practice for general structural design and design loadings for buildings (NZS 4203:1992), Standards New Zealand, Wellington 1992.

[8] Andriono, T. and Park, R. : Seismic design considerations of properties of New Zealand manufactured steel reinforcing bars. Bulletin of the New Zealand National Society for Earthquake Engineering. Vol. 19, No. 3, September 1986, pp. 213-246.

[9] S.A.N.Z. : Steel bars for the reinforcement of concrete (NZS 3402:1989). Standards Association of New Zealand, Wellington, 1989.

[10] Zahn, F.A., Park, R. and Priestley, M.J.N., : Design of reinforced concrete bridge columns for strength and ductility. Research Report 86-7, Department of Civil Engineering, University of Canterbury, New Zealand, 1986.

[11] Mander, J.B., Priestle y, M.J .N. an d Park, R. : Theoretical stress-s train model for confined concrete. Journal of Structural Engineering of the American Society for Civil Engineers, Vol. 114, No. 8, August 1988, pp. 1804-1826.

[12] Mander, J.B., Priestley, M.J.N. and Park, R.: Observed stress-strain behaviour of confined concrete. Journal of Structural Engineering of the American Society for Civil Engineers, Vol. 114, No. 8, August 1988, pp. 1827-1849.

[13] Watson, S. and Park, R., : Simulated seismic load tests on reinforced concrete columns. Journal of Structural Engineering of American Society of Civil Engineers, Vol. 120, No. 6, June 1994, pp. 1825-1849.

[14] Park, R.: Ductile design approach for reinforced concrete frames. Earthquake Spectra, Professional Journal of the Earthquake Engineering Research Institute, Vo l. 2, No. 3, May 1986, pp. 565-619.

[15] Paulay, T.: Evaluation of actions, report of discussion group on seismic design of ductile moment resisting reinforced concrete frames. Bulletin of New Zealand National Society for Earthquake Engineering, Vol. 10, No. 2, June 1977, pp. 85-94.

[16] Booth, E.D., Kappos, A .J., Park,, R., Moehle, J.P., and Hikone, S. : Seismic design of concrete frame structures : A comparison of Eurocode 8 with other international practice, Proceedings of the 6th Conference of the Society for Earthquake and Civil Engineering Dynamics, Oxford, United Kingdom, March 1998, pp. 481-492.

[17] E.C.S. : Design provisions for earthquake resistance of structures. European Committee for Standardization, Brussels, various dates.

[18] A.I.J. : Design guidelines for earthquake resistant reinforced concrete buildings based on ductility concept. Architectural Institute of Japan, 1997 (in Japanese).

[19] A.C.I. : Building code requirements for reinforce d concrete (ACI 318-99). American Concrete Institute, Farmington Hills, 1999.

[20] I.C.B.O. : Uniform building code. International Conference of Building Officials, Whittier, California, USA, 1997.

[21] Pinto, P.E., Colangelo, F., and Giannini, R. : Stochastic linearization technique for the calibration of capacity design factors of RC frames, Institut für Baustatik und Konstruktion, ETH Zürich, IBK Publikation SP-004, 1995.

[22] Panagiotakos, T.B., and Fardis, M.N. : Effect of column capacity design on earthquake response of reinforced concrete buildings. Journal of Earthquake Engineering, Vol. 2, No. 1, 1998, pp. 113-145.

[23] Dooley, K.L. and B raci, J.M. : Seismic evaluation of column-to-beam strength ratios in reinforced concre te frames. Structural Journal of American Concrete Institute, Vol. 98, No. 4, November-December 2001, pp. 843-851.

[24] Watson, S., Zahn, F.A. and Park, R. : Confining reinforcement for concrete columns. Journal of Structural Engineering of American Society of Civil Engineers, Vol. 120, No. 6, June 1994, pp. 1798-1824.

[25] Hakuto, S., Park, R. and Tanaka, H. : Effect of deterioration of bond on beam bars passing through interior beam-column joints on flexural strength and ductility. Structural Journal of American Concrete Institute, Vol. 96, No. 5, September-October 1999, pp. 858-864.

[26] Park, R. : A perspective on the seismic design of precast concrete structures in New Zealand, Journal of the Prestressed /Precast Concrete Institute, Vol. 40, No. 3, May-June 1995, pp. 40-60.

[27] C.A.E. : Guidelines for the use of structural pre cast concrete in buildings. Centre for Advanced Engineering, University of Canterbury, New Zealand, 2nd edition, 1999, 144 pp.

[28] Park, R. and Bull, D.K. : Seismic resistance of frames incorporating precast prestressed concrete beam shells, Journal of the Prestressed Concrete Institute, Vol. 31, No. 4, July-August 1986, pp. 54-93.

[29] Restrepo, J.I., Park, R. and Buchanan, A.H. : Tests on connections of earthquake resisting precast reinforced concrete perimeter frames of buildings. Journal of the Prestressed / Precast Concrete Institute, Vol. 40, No. 4, July-August 1995, pp. 44-61.

[30] Priestley, M.J. N. and Calvi, G.M.: Towards a capacity design assessment procedure for reinforced concrete frame s, Earthquake Spectra, Professional Journal of the Earthquake Engineering, Research Institute, Vol. 7, No. 3, 1991, pp. 413-437.

[31] Park, R. : A static force-based procedure for the seismic assessment of existing reinforced concrete moment resisting frames, Bulletin of the New Zealand National Society for Earthquake Engineering, Vol. 30, No. 3, September 1997, pp. 213-226.

[32] Park, R. : A summary of results of simulated seismic load tests on reinforced concrete beam-column joints, beams and columns with sub standard reinforcing details, Journal of Earthquake Engineering, (to be published).

[33] Priestley, M.J.N., Displacement based seismic assessment of existing reinforced concrete buildings. Proceedings of Pacific Conference on Earthquake Engineering, Vol. 2, Melbourne, 1995, pp. 225-244.

PAST PRESENT, AND FUTURE OF CONCRETE

Hiroshi Naito
Assoc. Prof., Tokyo University
JAPAN

Keywords: Steel Era , New Concrete Era

1 INTRODUCTION

As an architect, I prepare architectural designs. I also started teaching at the Civil Engineering Department of Tokyo University last year. Today, based on my experience as an architect, I would like to talk about my long-held view on concrete. To start, I'll briefly show you my works to date as a kind of self-introduction.

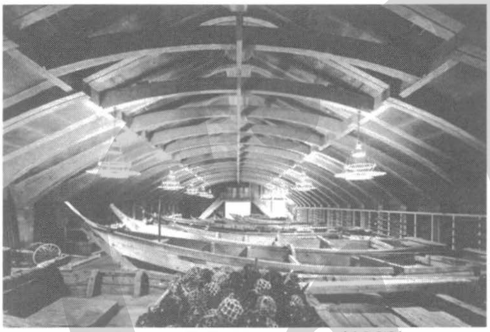

Fig.1 Sea- Folk Museum (1992)

Fig.2 Tenshin Memorial Museum of Art (1997)

Fig.3 Tohkamachi Public Library (1999)

Fig.4 Fuji Rinri Seminar House (2001)

I've been always thinking about how to evolve building materials into a new value of space by examining the nature of materials, from structure to design, and redefining them. Through such an approach, I now have my own concepts about concrete, which I'll talk about.

In order to talk about the role of concrete in architectural design of the 20th century within a limited time, I find it appropriate to focus on the works of architects who played a leading role in architecture. Those innovative architects always perceptively responded to various urban situations and cultural situations that surround them and developed their own works. Their work can be described as a mirror that reflects their days. So I will now discuss the relationship between the 20th century buildings and concrete through their work pieces.

2 CONCRETE ERA

One question has always been on my mind. Why were the great masters of modern architecture so committed to using concrete as exposed finish?

Exposed finish concrete is never an appropriate choice in terms of weather ability. I presume those architects had a message to tell us about concrete; they had a need to show that it is indeed concrete, beyond desired performance. It is, in other words, agreement between how it is shown and what it really is.

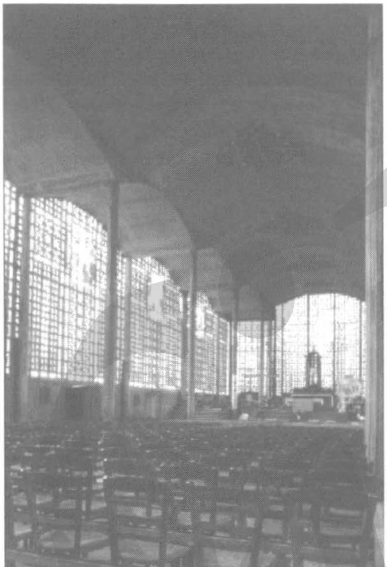

Fig.5 Notre Dome du Raincy

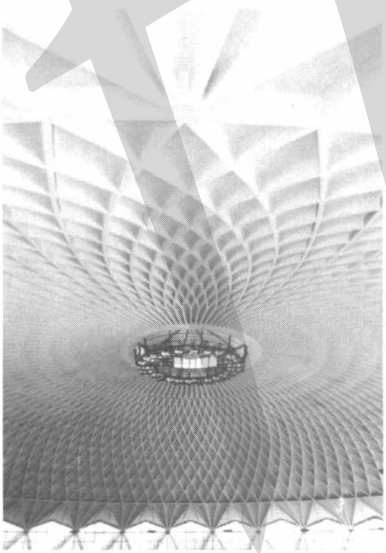

Fig.6 Palazetto dello Sport

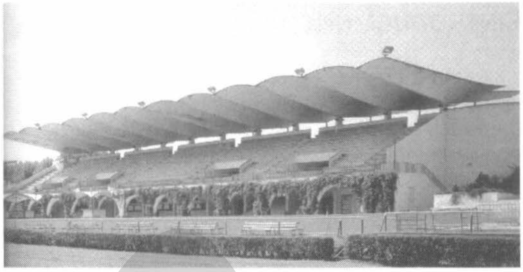

Fig.8 Zarzuela Racecourse

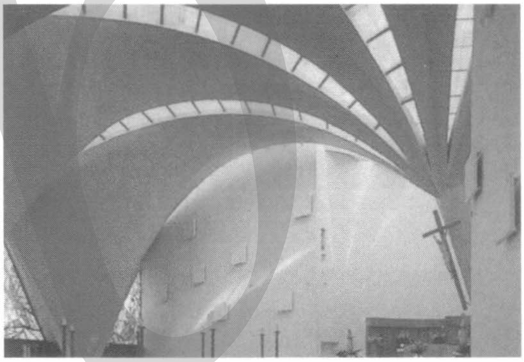

Fig.7 Church Santa Monica

Fig.9 Couveny de la Ste-Marie-de-la-Tourette

On reflection, the 19th century was an era of steel. As typified by the work of Eiffel, they achieved wonderful development in steel structures, such as bridges and station buildings. The era of concrete had to overcome its preceding era of steel. In the beginning of the 20th century, concrete successfully had the world know its value by being exposed.

3 PAST, PRESENT, AND FUTURE OF CONCRETE EXPRESSIONS IN JAPAN

In Japan, a large number of buildings were burned down during World War II and because of it, creating a city impervious to fires was set up as one of major national goals in building. Thus, any building, from small houses to mid-rise buildings, was made of concrete where possible. It resulted in creation of random, disorderly cityscape, which was contributed by inherently high degree of freedom of concrete structures.

Fig.10 Photos showing war damage

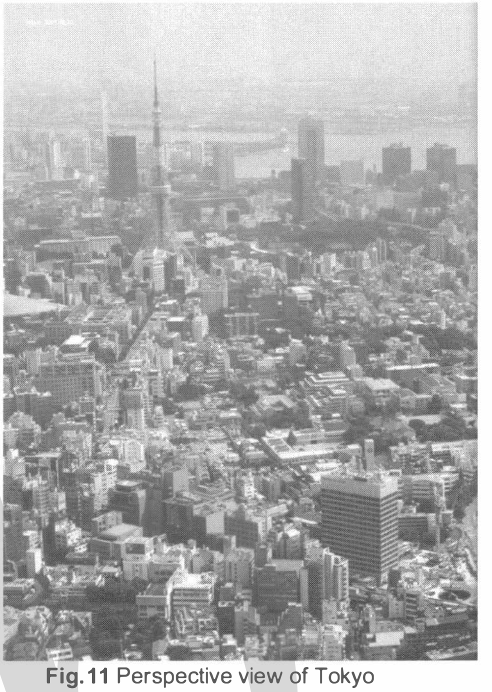

Fig.11 Perspective view of Tokyo

Concrete is a material of depth. It is changeable; it can take any form. No other building material is highly flexible and multi-purposeful as concrete. Concrete listens to every whim of the builder by changing its form as he wishes. I think of concrete as a maternal material that will warmly grant any selfish request.

Steel structures are characteristic of visual ease of understanding of how they are structured and constituted. But concrete, on the other hand, there are reinforcing bars that resist stress somewhere in concrete invisible from the outside. So it is difficult to see the constitution of a concrete structure. I have a feeling that Japanese architects have been constantly fighting this aspect of "potential and difficulty in understanding" of concrete structures.

The Peace Center designed by KENZO TANGE soars high in a desolate field of Hiroshima scorched by that atomic bomb. The "Atomic Dome" survived the atomic explosion because its roof was made of steel. A new era thus broke with concrete.

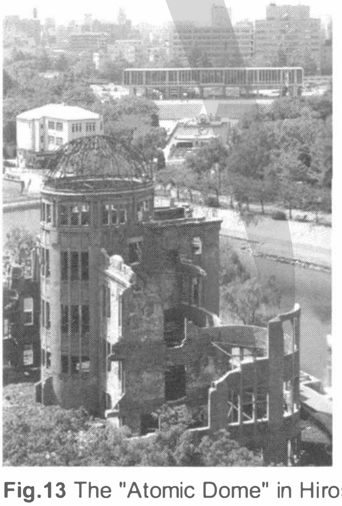

Fig.13 The "Atomic Dome" in Hiroshima

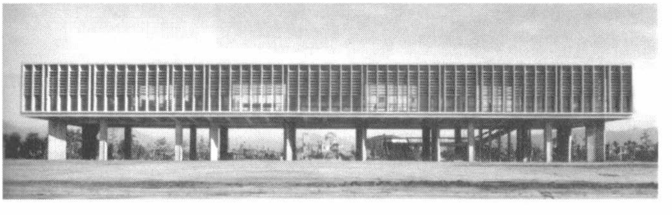

Fig12. Hiroshima Peace Center

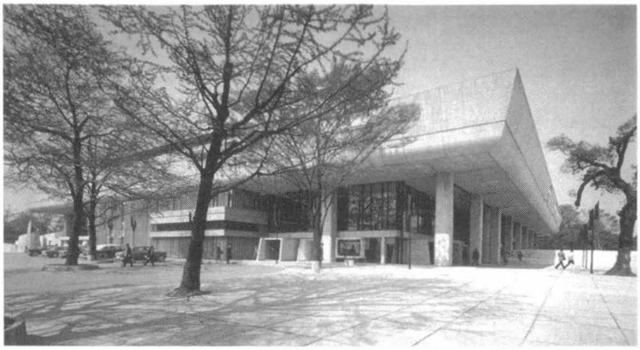

Fig.14 Tokyo Metropolitan Festival Hall

Tokyo Metropolitan Festival Hall designed by KUNIO MAEKAWA was constructed based on a theme of how to express the cultural foundation stone in the settling days following the rise of a once war-torn nation. The material chosen for the building was again concrete.

4 FROM CONCRETE TO STEEL

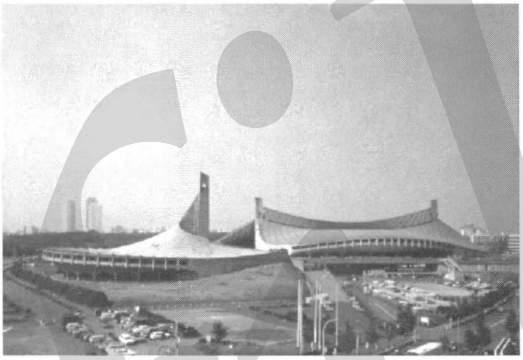

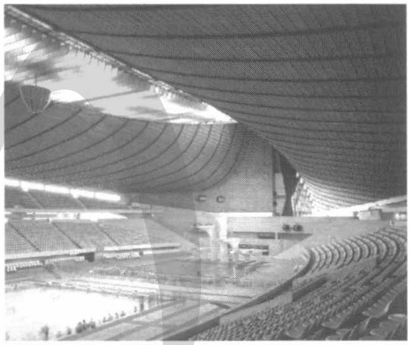

Fig.15, 16 National Gymnasium for the '64 Olympic Games

In 1964, the Tokyo Olympics was held in Tokyo. National Gymnasium for the Olympic Games is still the achievement of Architecture for Japan. It is a very outstanding building; two large concrete poles rise high like a mast and cables stretched from the poles are combined with steel girders to form a big roof. In it, there is a perfect harmony of shape by concrete and that by steel. Viewed from a different angle, it may be the building in the turning point when the essence of architectural expression in Japanese buildings changed from concrete to steel.

Fig.17 EXPO'70

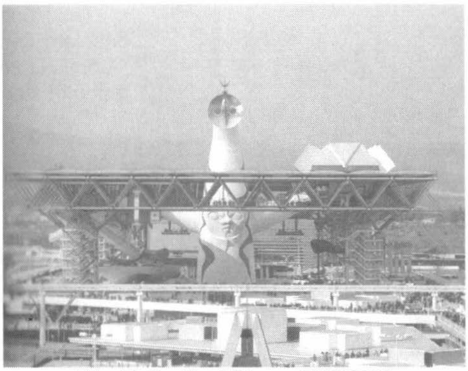

Fig.18 Festival Plaza, EXPO'70

Six years later, KENZO TANGE, KIYONORI KIKUTAKE, and KISHO KUROKAWA used steel space frames to design their own work, a big roof, tower, and pavilion, respectively, at the World Exposition held in Osaka. It was the dawn of the steel era.

5 STEEL ERA - AS A TOOL FOR STRUCTURAL EXPRESSIONISM

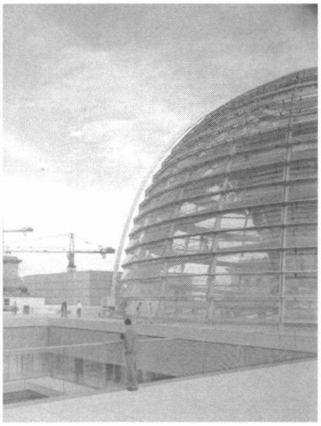

Fig.19 The New German Parliament, Reichsrag

It may sound rather exaggerated, but in the world of architectural expression, the mainstream of today's modern architecture is steel, both worldwide and in Japan. It seems everyone believes that modern architecture is heading towards lightweight, thin, and transparent. Partly thanks to the miraculous advancement of structural calculation technique using computers, the 1990s were a decade when structural expressionism came into spotlight. Steel structures always played the main role. It is difficult so show the flow of force with concrete and that is why, I suppose, concrete had always played a less prominent role.

Guggenheim Museum Bilbao designed by FRANK O GEHRY is a steel structure using computer technology. It has a plastic shape made up of curvature, but that is what concrete is originally good at. Luzern Cultural and Congress Center designed by JEAN NOUVEL surprises people by its 45 m long projected eaves. The eye-catching part of the roof is made of steel. There is nothing more to add about SANTIAGO CALATRAVA'S works.

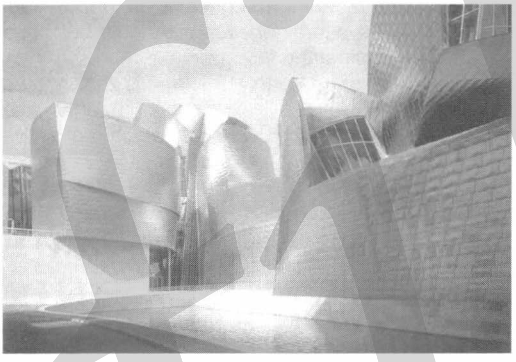

Fig.20 Guggenheim Museum Bilbao

Fig.21 Luzern Cultural and Congress Center

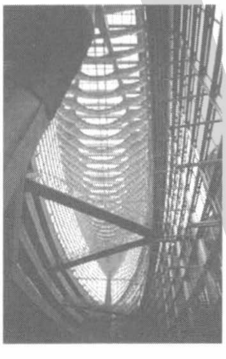

Fig.22 Tokyo International Forum

Fig.23 Sendai Mediatheque

Fig.24 Yokohama Internationa Passenger Terminal

Many of the major buildings that attract our attention in these days are made of steel. They are, for example, Tokyo International Forum designed by RAFAEL VINORY, Sendai Mediaaheque by TOYOO ITO, and Yokohama International Passenger Terminal by ALEJANDRO ZAERA POLO and FARSHID MOUSAAVI. Today, steel structures are enjoying their prime time.

6 TADAO ANDO'S CONCRETE WORK

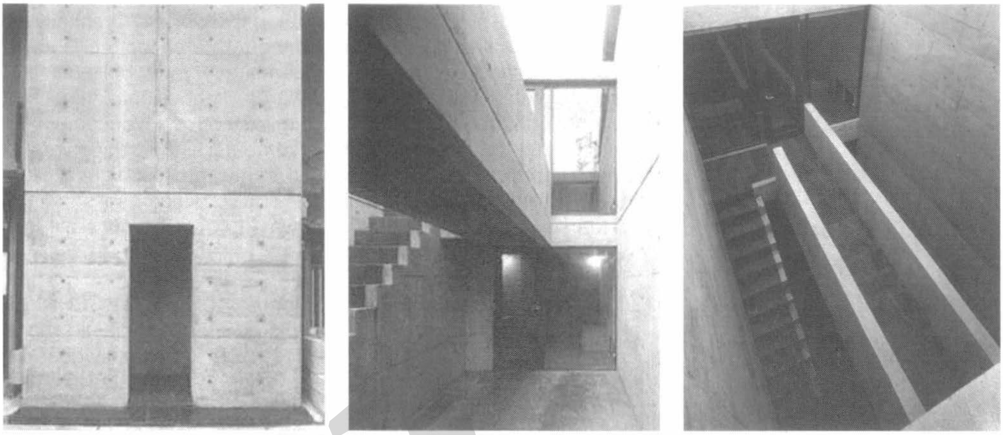

Fig.25 Row House,Suimyoshi – Azuma House

Despite the dominance of steel in modern architecture, there are architects who maintain the opposite. TADAO ANDO is one. He wants to give as powerful a meaning to concrete as that to steel by thoroughly toughening up the concrete surface. Avant-garde characteristics of Ando's buildings are wonderful in that they win the heart of people by swimming against the stream.

ANDO's concrete has a dual strategy. One is excellently finished concrete surfaces that makes them appear as if they were not concrete. It is Ando who gave a new type of beauty with "hand-touchable" texture to concrete. Forms he uses are made with 3 x 6 veneers, which means he intentionally incorporates the traditional Japanese module of *tatami* to concrete surface.
With these two features as his weapons, he established his own world.

7 TO NEW CONCRETE ERA

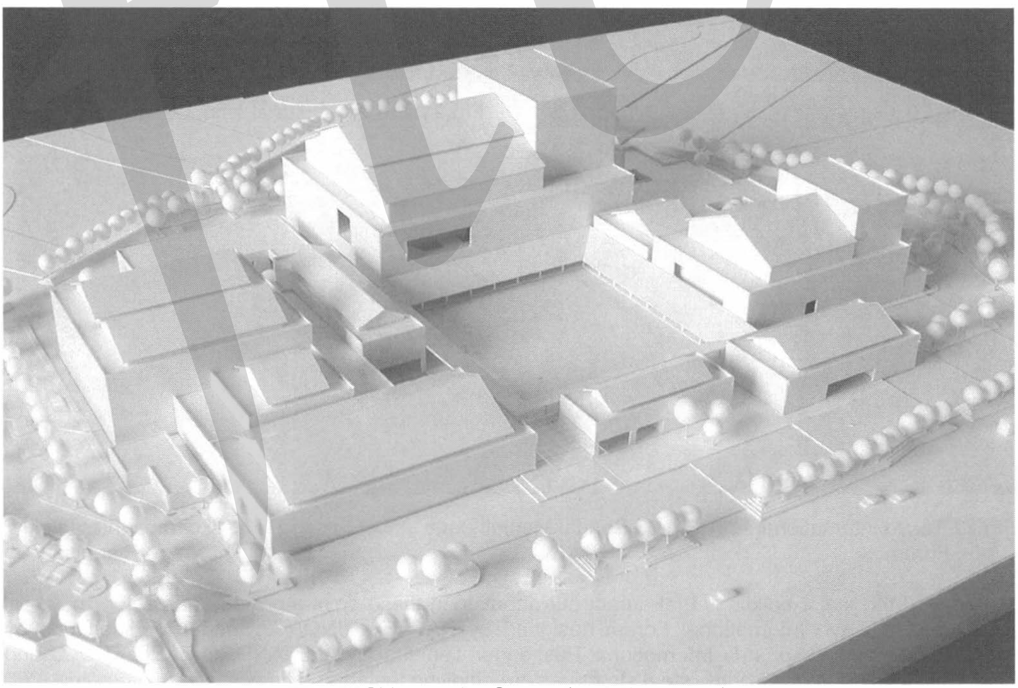

Fig.26 Shimane Art Center (tentative name)

Fig.27 Interior of a large theater (Shimane Art Center)

Let me introduce a project I am now working on. It is a big building that combines a museum and a theater in Masuda, a medium-size city in Shimane Prefecture. Its construction is planned to start this fall. The theme of the building is to provide the building with highest possible sustainability.

During the design development stage, I decided to turn to cast-in-situ concrete. The major reason for this decision is that concrete allows us to realize complex functions and seamless structure. The most conspicuous feature of the building is that the building is completely covered by tiles, of Japanese traditional building materials, in order to protect it against acid rain relatively common in that part of the country. Japanese traditional tiles fabricated by traditional manufacturing method promises long-lasting weather ability, over a few centuries. When I wanted very long-lasting sustainability, I decided to choose concrete. Unique building functions and architectural features are fused in this building, while traditional technology and modern technology go hand in hand.

8 TWO UNIGNORABLE TRENDS

As you already know, we are now in the middle of the first phenomenal change since the Industrial Revolution. Let me briefly talk about two major trends facing us.

The world population jumped from 1.4 billion at the dawn of the last century to 6.3 billion in only one century. This excessively rapid growth of population cannot be stopped and the world population is expected to reach 10 billion in 2050.

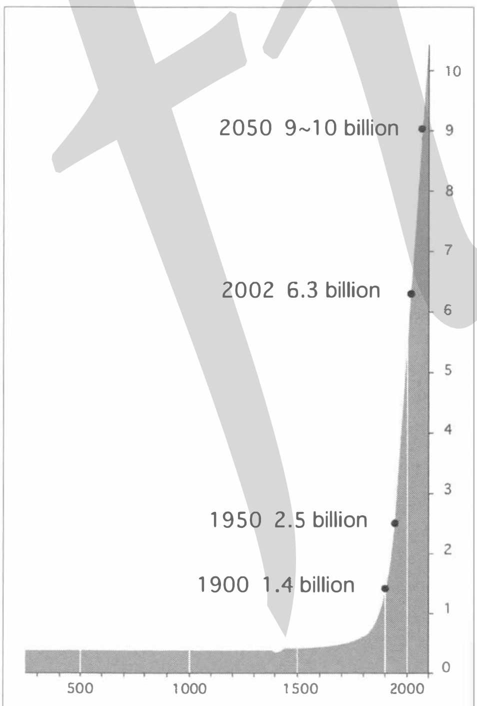

Fig.29 Crude steel production statistics

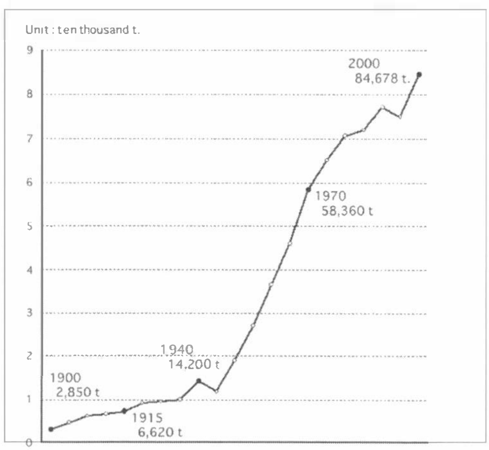

Fig.28 World population statistics

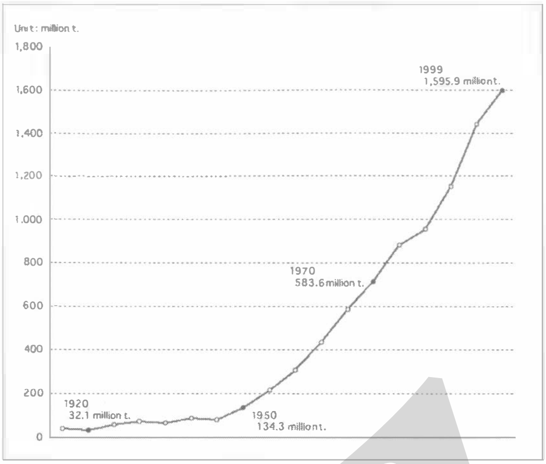

Fig.30 Cement production statistics

Here is a graph of crude steel production and concrete production. The curves show a tendency similar to the increase of the world population. This means the population growth in the 20th century was probably supported by the construction technology.

Recent computer technology has really made an awe-inspiring development. Computers are evolving at a doubling speed year after year. According to specialists, the current rate of development will continue for another decade. The doubling in speed the previous year means the level in 10 years will be that about 1000 times greater than it is today.

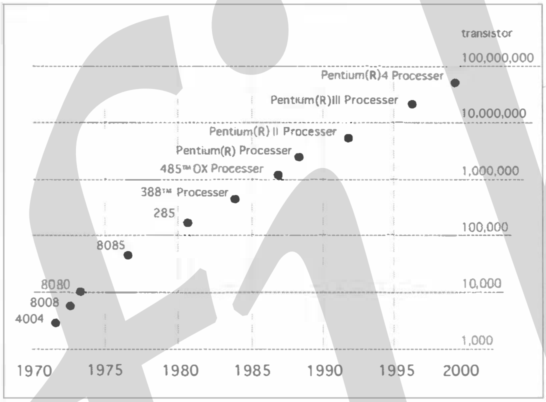

Fig.30 Moor's row

What would these two, world population growth and computer technology evolution, bring to us? I cannot spend a day without thinking about this, while living a day as a person and creating designs as an architect. What difficulties would they bring to us and what would they enable?

Whatever debate we do or whatever aspect of culture we discuss, we cannot get away from the current situation. How can the concrete field contribute to this situation? I feel it is the question now posed to us.

9 ISSUES AND PROPOSALS

I'd like to make proposals to end my speech.

- Megalopolitan city problems
  70% of the world population of 10 billion will live in cities. It is therefore an urgent task to set up a Strategy for building concrete structures in preparation for such situation.

- Advancement of simulation and network
  A strategy is necessary for concrete structures dealing with how to make an effective use of mate rials on earth and how to construct more sustainable cities. From the viewpoint of long-term advanced sustainability, concrete structure seems to be more advantageous than steel structure.

- Coordination between globalization (macro value) and locality (micro value)
  We should create a new city model and a new architectural value as an element that constitutes the model.

BRIDGE DESIGN AND MECHANICS:

STILL A DURABLE RELATIONSHIP IN THE XXI CENTURY?

Miguel A. Astiz
Carlos Fernández Casado S.L.
Grijalba 9, Madrid, Spain
maastiz@cfcsl.com, www.cfcsl.com

Keywords: bridge design, structural mechanics, aesthetics

1 INTRODUCTION

The proposed title of this paper is deliberately polemical. It is obvious that bridge engineering and structural mechanics are intimately related: they have been related in the past and they will be related in the future. Nevertheless we can see how bridge design is rapidly evolving, especially in the last decade, into a more open field in which architects, sculptors, landscape specialists, ecologists and politicians have become interested. Results are not always good from the standpoint of a traditional bridge engineer.

The starting point for these reflections may be the comparison of two paradigms. We have chosen two Spanish bridges: the Alcántara bridge (fig. 1), a roman bridge built 1900 years ago by Caius Julius Lacer (an engineer or an architect, the difference is not relevant), and the Petrer footbridge (fig. 2), built in 1999 and designed by Carme Pinós, a well known Spanish architect. The span lengths are very similar in both cases (about 30 m) and the working loads at the design time should also be similar. Results are radically different.

Figure 1 The Alcántara Bridge

Figure 2 The Petrer Footbridge

It is true that external constraints are not exactly the same in both cases. The roman bridge crosses an important river at 47 m height with respect to the riverbed and it has shown to be resistant to floods during almost 2000 years. The modern footbridge crosses a very small river, which is dry most of the time, and it has been conceived as the support for a new plaza, which will be integrated into the landscape. The function of communication, which is characteristic of any bridge, is somewhat diffuse and the structural solution follows the lines of the deconstruction movement.

These two extreme examples show that by no means can a bridge design be considered as the unique solution to cross a river or a valley. Nowadays the designer may consider a very large and diverse set of alternatives since the design and construction tools are very powerful; even the budget limitations are not as rigid as they used to be in the past. The result may be governed by more decisive criteria that the structural ones.

We will try in this paper to define the importance of structural concepts and structural analysis in the design of bridges as we see it now and in the near future. The paper is divided into three parts that will be devoted to analyse the importance of mechanics in three fields: design, definition of static schemes and structural concepts, development of specific construction details.

These ideas will be illustrated with some examples, most of them extracted from our recent experience in Carlos Fernández Casado S.L. which are the result of the close collaboration of a number of engineers.

2 THE ROLE OF MECHANICS IN BRIDGE DESIGN

When we refer to bridge design, as well as to the design of an object (a building, a car, a chair), many hidden aspects are governing the design process and not all of them are purely technical; history, culture and education play an important role through our knowledge of what has been done before and through the influence of all the elements which, in one way or another, constrain human activity in a society.

As a matter of fact, very few designs are really innovative or may be considered as a breakthrough. In the field of structural design we can recall the use of new materials such as steel, reinforced concrete and prestressed concrete and, more recently, the use of composite materials, the introduction of new structural concepts such as the three hinged arch, the cable-stayed bridge or the extradosed prestressing. In most of these cases there was an initial opposition to such innovations and after some time they were accepted since they were reasonable. Finally we may even qualify them as aesthetical.

Most of the designs are just a small evolution with respect to previous ones. This is especially clear when we analyse all the designs that were produced by a single designer along his life. Continuous work on the same topic makes us achieve a deeper knowledge of all the problems involved and we usually get small advances in each one of our designs. Sometimes a very different proposal rises but we generally may define somewhat as a personal style (not everybody may be as Picasso!). If we analyse the evolution of a certain field (as we are doing here with bridge design), the trends are not as continuous as for a single person but we can most of the time speak of an evolution and only very seldom of a revolutionary step.

These ideas lead us to a question: what are the very important constraints that make us work by such small steps? Many of them come from the relation between the designer and the client (which is in fact the society) but others are merely internal and we may even be unaware of them.

Coming back to classical authors we may remind the three conditions which were stated by Vitruvius: strength, utility and beauty, or, in our nomenclature, safety, functionality and aesthetics. Any engineer should add a fourth one: economy. Finally, others have been added more or less recently: durability, compatibility with landscape and even ecological compatibility. Such a broad spectrum of conditions has lead to a set of reliable solutions that are our first thought when we try to solve a design problem.

These solutions typically depend primarily on the total length of the bridge, on its height above ground and on the foundation conditions (the span length is in fact a consequence of them). Every experienced bridge engineer knows what is the range of application of a continuous girder, an arch, a cable-stayed bridge or a suspension bridge; this knowledge is based on experience and mainly on economical reasons. Then, among all the design conditions we have stated before it seems that one of them prevails. This is not exactly true since what we call experience also takes into account safety and functionality.

But an architect or an artist which is asked to design a bridge does not have this experience and he is not embarrassed with this knowledge which drives us naturally to well proven solutions. His proposals would be mainly based on aesthetics, functionality and landscape. Possibly they will be useless but they will incorporate a new insight into bridge design. Then a question arises: is the experience and knowledge of a bridge engineer an asset or an obstacle in the design of a bridge? The answer seems obvious: experience and knowledge are an asset provided there is still some room left for creativity. Here creativity not only means a capacity to develop new formal solutions looking for aesthetical aspects; it also means a capacity for innovation in all the aspects of the design of a bridge -conceptual design, development and construction procedures- to reach a solution which might fit as well as possible all the requirements which were set before. In this sense it is important to state that the kind of innovation that might come from ignorance is very rarely useful.

These comments are caused by the growing role of architects, artists and other professionals in the design of bridges. The design of bridges and other great structures used to be in the past the responsibility of a kind of professional whose knowledge was mainly based on experience and possibly artistic abilities but not on scientific knowledge. The XIX Century brought, along with the Industrial Revolution, a basic knowledge of the structural behaviour. Bridge design became an affair of engineers, of scientists, who made possible the development of new structural concepts, new shapes, new materials but who sometimes focused too much on the scientific aspects of their profession forgetting all the other aspects which are involved in the design of a bridge. As a consequence of this oblivion a certain separation between the engineering world and society may have happened.

The response to this problem in the different countries has been diverse. Some European countries tend to give the power of design to architects; in other countries the design responsibility is given to a committee including all the professions and even social groups that might be interested in the project. This organization does not guarantee by any means a good result. A more reasonable way of handling the problem consists in entrusting the design to a team or to a group which might incorporate all the necessary sources of information and knowledge and all the abilities which are needed to get a good solution; an example of this kind of cooperation is the team which was formed to compete for the Millennium footbridge in London incorporating the architect Frank O. Gehry, the artist Richard Serra and the engineer Jörg Schlaich. In any case, the design proposals have to overcome a lengthy process of approvals to be constructed and this is reasonable since any project will have a cost to be paid by society and society must have the last word.

Most of the innovations we can recall from the history of bridge design are based on structural mechanics. Their main qualities are generally a more efficient use of materials or a better adaptation to external actions. The arch, the suspension bridge or the cable-stayed bridge are obviously an invention of engineers in the sense that they are mainly based on a distribution of forces which is specially well suited to a certain material or to a certain construction procedure. Aesthetical aspects of such solutions came later. The same can be said about the use of new materials: in bridge engineering new materials have always been proposed to achieve a better efficiency and economy (durability might be included in both aspects).

Today, when the room for structural innovation is more reduced, we see that innovation is often coming from aesthetics and these innovations are also often contrary to structural mechanics principles and they do not produce benefits either in efficiency or in economy. The growing role of aesthetics in bridge design makes us wonder if the necessary equilibrium between all the design conditions is not broken in many of the projects that are being developed. What should be the role of aesthetics in bridge design?

Along history engineers have often focused their efforts in the goal of achieving the most economical solution. Even new mathematical tools have been developed to "optimise" a structural solution. But in bridge design economy is often related to girder depth and the most economical solution is often a deep girder, which is anything but aesthetic. Nowadays there is a growing concern about aesthetics, and engineers try to produce more elegant solutions; nevertheless results are not always positive. Reasons for such failures may be found in a lack of education and in the little time that is often spent in observation and in conceptual design. As a consequence we are presently faced with many proposals that pretend to achieve an aesthetical appearance either through an "original" design (contrary to structural mechanics principles and simultaneously awful) or through make-up arrangements (we could speak about decorated bridges). Many examples could be mentioned here but it is better not being specific on this topic.

Aesthetics in bridge design is usually related to such concepts as transparency, elegance, regularity, rhythm and relation with the surrounding landscape. Many of these concepts are related to mechanics although structural efficiency is not always synonym of transparency and elegance. A constant depth continuous girder is a very efficient structure and it may be very bulky in certain cases. A bridge should be very transparent in some cases to minimise its visual impact on a landscape while in other cases the bridge enhances the landscape (the Golden Gate Bridge may be the best example of the aesthetical synergy between a landscape and a bridge). Then aesthetics is not a quality which might be described by a mathematical variable and which might be included in a mathematical optimisation process. Fortunately enough, bridge engineering is still an art, although a skilful art, where there is not such a thing as a unique solution.

How skilful is this art? Is it a matter of engineers? Here a new concept becomes very important: scale. A small span bridge is not anymore a technical challenge. It might be a challenge if this bridge has to be repeated many times since any design decision might have important economical consequences (as, for instance, in overpasses in a long motorway). But if we refer to a single small bridge, the economical consequences of a design decision are not very important in absolute terms. In some respects, the small bridge may be considered as any industrial object (like a lamp) where the structural requirements loose their importance. In such objects, the stress distribution may be extremely complicated but all the structural problems may be solved by slightly increasing the material quantities. Other aspects of design such as functionality and aesthetics become the leading criteria (as it is the case for a lamp). To get such an object we can go to a department store (a prefabricated bridge) where we can even find beautiful examples or to an elegant design shop (an architect or a designer) where we can find extremely well adapted solutions.

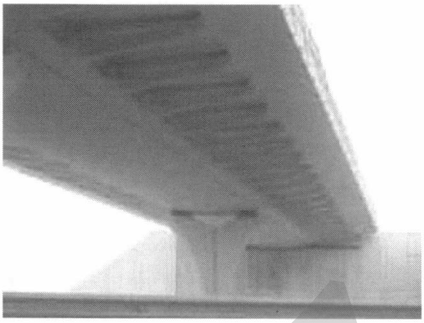

Figure 3 Prefabricated overpass in Zaragoza (Spain)

Figure 3 shows an example of a newly built prefabricated bridge in Zaragoza (Spain); it is a three span motorway overpass in which there has been a special care for the shaping of the deck. The above-mentioned Petrer footbridge (fig. 2) could be an example of the specially tailored bridges. We may say that technology has reduced the range of bridge spans that should be designed by bridge engineers.

Coming back to aesthetics, and provided we know what is an aesthetical solution an important question has to be asked: what is the cost of an aesthetical bridge and should we pay for it? The comparison with other industrial objects is also valid here. Scale is important since the price difference between two lamps may be important in relative terms but not in absolute terms; then we will possibly choose the best design even if it is also the most expensive. If we are trying to buy a car we will probably not choose the exclusive, stylish and extremely expensive sports car if we can buy a reliable, safe, functional, durable and reasonably aesthetic car for 20% of the price. Here the price difference is important in absolute terms.

In the case of a bridge many factors slightly modify the circumstances of this decision. The size of the bridge is important since it affects its absolute cost. Important relative cost increments may be admissible for a small footbridge while they should not be admissible for a long span bridge. The fact that the owner is a public organization is also very important: money should be spent with care since it comes from tax payers; the amount of money which is spent in one topic or in another is a political matter and a very important one since it defines the whole philosophy of a governing team.

In this respect ethics may collide with aesthetics since the excess of money that is spent in a public work will not be available for other social needs. Then, provided all the other conditions are the same, the optimum solution depends on the country for which it is being built: a rich country may pay a more expensive bridge than a poor country. But, in any case, there should be a limit to what can be designed in terms of cost. Aesthetics should always be limited by reasonable cost increases. Nevertheless this is a problem that has to be managed by politicians since it is a political issue. As bridge designers we do what we are asked to do although an ethic filter has to be applied to our capacity to propose so-called original solutions.

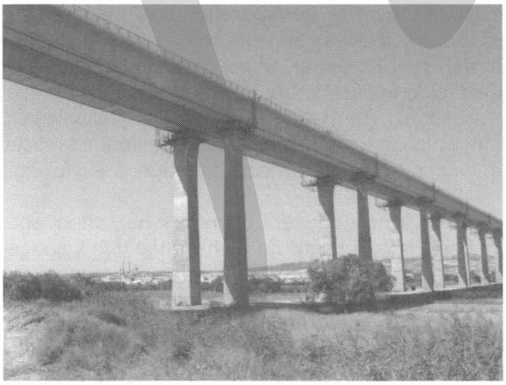

Figure 4 Bridge across the Huerva river (Spain)

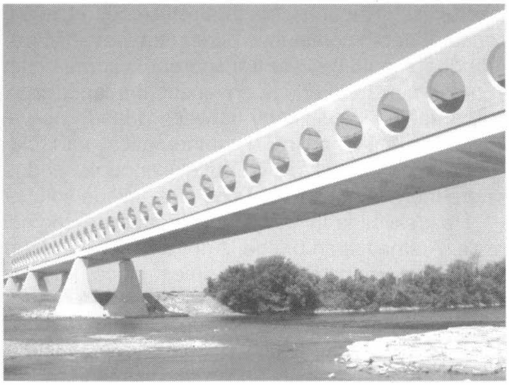

Figure 5 Bridge across the Ebro river (Spain)

An example of such decisions may be found in what is being done in Spain on the construction of railway lines for high-speed trains. The construction of the 850 km long line between Madrid and the French border will cost 9 billion euros of taxpayers' money. In this line the total length of bridges is 60 km (7%) with a cost of 1 billion euros (11% of total cost). Since the budget is limited and construction time is also very important, solutions which have been proposed are in most cases continuous, incrementally launched bridges (fig. 4), shaped to reduce as much as possible their impact on the landscape. Only in very singular cases a different solution has been permitted (fig. 5). This trend is the most reasonable, and structural mechanics is essential to achieve efficient continuous girder solutions, as it is to design a specially tailored bridge.

Structural mechanics may be used today to achieve two different goals: either to design an efficient solution or to make possible a non-efficient solution. That is to say synthesis and analysis, or conceptual design and finite element calculations. Both activities should be present in a good bridge design. The first one is essential while the second one, being more and more important, is not essential.

Conceptual design has to take always into account the structural mechanics aspects of all the alternatives and not necessarily to get the most efficient solution but to design a reliable, durable, functional and reasonably economical solution. Safety is obviously related to statics and to force distribution. Reliability and durability are related to materials behaviour, concrete cracking, corrosion resistance, materials aging, and all these aspects are ultimately related to mechanics. Functional design is related to stiffness, to limited vibrations as well as to an adequate shaping of the bridge (width, slope) and to an adequate election of materials (structural materials, pavement, painting, etc); structural mechanics is also essential here although a knowledge of other fields is important. Construction methods are always related to mechanics since the whole point consists in moving large masses and making the structure stable under conditions that are very different from its final state.

As a conclusion to this point one could state that the only design criterion that may be independent of structural mechanics principles is aesthetics. But designing a bridge on the basis of this single criterion is only possible for small spans; we would then speak about sculptures with a certain functional utility and not about bridges. Using aesthetics as the governing criterion would lead us to unbalanced solutions: possibly beautiful but unable to fulfil all the other conditions to be taken into account in any engineering or architectural work. The balance between these two apparently opposite criteria has to be found in controlling the extra cost that may be caused by a non-standard but aesthetical solution. This balance has to be achieved by the designer and by the owner as a cultural asset as well as an ethical demand.

3 THE ROLE OF MECHANICS IN THE DEFINITION OF STATIC SCHEMES

The title of this section may seem to describe an obvious relation. But this relation is not as obvious as one may think at first sight. Among the many differences we may find between a building and a bridge, an important one consists in the fact that the structure of a bridge is almost the whole bridge while the structure of a building is only a part of it and it is very often hidden. Then, when any constraint is imposed on a bridge it becomes externally apparent through its structure. A bridge located in a highly seismic region shows its strength against lateral forces (although the use of dampers has changed this relation a bit). Any new proposal mainly based on aesthetics will modify the structure and, consequently, the static scheme of the bridge.

The question we try to formulate is: as engineers, should we define the static scheme of a bridge solely on the basis of structural mechanics principles? Are the schemes based on mechanical principles those that last, which are considered valid by many generations? And, finally, can we reach beauty by only trying to follow structural mechanics? Or, asking it in a different way, is a structurally efficient solution necessarily aesthetic?

Structural efficiency of a static system is related to how directly are the forces transmitted through the structure towards the foundations. A smooth flow of forces is usually equivalent to less bending and less stress concentrations. But structural efficiency is not an absolute concept. It is related to the properties of the materials that are being used as well as to their cost. A suspension bridge needs a high-strength tension element to support the deck; the roman and medieval arch bridges were especially well suited to the use of stone blocks as primary resisting material. Then very different shapes are possible solutions and may be qualified as structurally efficient.

To develop such efficient schemes, it is not necessary to know the structural mechanics principles as a science. Prof. Kawaguchi [1] listed the sources of inspiration and the means to develop new ideas for different great engineers and architects and he found out that not only structural mechanics and computation were at the origin of these ideas; he mentioned also in many cases practice, experience and experiments. In any case we can state that either explicitly or implicitly mechanical principles are behind the very basic solutions: the suspension bridge, the cable-stayed bridge, the arch, the truss, the beam, etc. These schemes have their ups and downs depending on the fashion but they are still used since they are considered to be efficient and even, in most cases, aesthetic.

Nevertheless the aesthetic qualities of a bridge are defined by a number of personal sensations that are difficult to classify: order, regularity, elegance, transparency and imagination. Many of these sensations have no relation with the fact that the bridge is structurally efficient or not. As structural engineers we would like to think that a good scientific work in the definition of a static scheme will lead us to a beautiful bridge. This may be true for the reduced group of structural engineers. Structural mechanics may be considered as a language and those who know this language are able to understand the structure of a bridge and to enjoy it as a piece of engineering art. But to be considered as a piece of art, public has to qualify it as such; nobody would find artistic qualities in an engineering innovation in a car engine. The aim of any bridge designer should be to gain recognition from his peers as well as from general public.

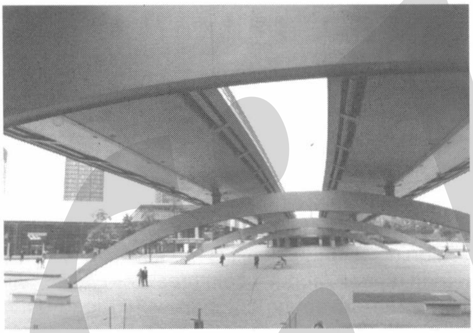

Figure 6 Le Corbusier Viaduct in Lille (France)

A significant example may be found in the Le Corbusier viaduct in Lille (France). This bridge (fig. 6) has two twin continuous decks being supported by transverse arches. This is not a structurally efficient solution since the arch is not the best shape to support two concentrated vertical loads; a portal frame or even two vertical columns would do a better job. But the succession of transverse arches does create a beneficial effect in the space below the bridge. There is regularity, order, transparency, elegance, imagination but no structural efficiency. The small cost increase is paying for a better urban environment.

Many engineers have claimed in the past, and still do it now, for the concept of structural veracity as guiding line in their designs (F.Arrabal, a contemporary Spanish drama author, also claims that beauty may be found in truth). But thanks in part to great advance in computational capacities this concept is losing importance. This concept is valid for an engineering elite and it is a very good goal to be achieved but times are changing in the sense that it is difficult to define in any field the absolute truth. Certain flexibility from the engineering profession, without falling into the excesses we begin to see in bridge designs, would ease the relations with society.

As it is difficult to determine what is the best way to proceed in defining our static schemes, we can refer to the most recent evolution in architecture, since bridge engineering and architecture have always been related. We still are living under the influence of the post-modern style, a movement with a weak theoretical background and a good acceptance record from public. Probably many of the bridges we reject as not structurally efficient could be classified as post-modern. There is little conceptual design in them, just a lot of analysis of a scheme supposedly aesthetic.

Contrary to the post-modern movement we find the deconstruction movement. The French philosopher J. Derrida laid its theoretical background, which is based on a translation into the architectural language of the analytical decomposition of our own language. A possible translation of these ideas into bridge engineering would consist in an analysis of all the resisting mechanisms of a structure (axial forces, shear, bending moments, torque) to assign them to different structural elements. This kind of analysis requires a very good understanding of the structural mechanics principles and it is reserved, at least at the beginning, to the engineering community. But, as well as some examples of the deconstruction movement are being generally appreciated, the most elaborate engineering pieces of art will also be generally appreciated in the future. The innovative work of some great engineers, like J. Schlaich, incorporates deep thinking about mechanics and it is an example to be followed by every bridge engineer.

Other contemporary architects, such as J. Nouvel, claim for a closer relation between the piece of architecture and the site: they give birth to the concept of thermodynamics of the site. This is what great engineers in the past have achieved with bridges like the Salginatobel and what every bridge engineer should work for.

Many examples could be given on how mechanics can be in the very centre of conceptual design of the static scheme of a bridge. The first two examples are the work of other engineers; all the other examples have been designed at Carlos Fernández Casado S.L.

The first one is the footbridge that was designed by J. Schlaich for the Deutsches Museum in Munich (fig. 7). This is a especially well suited example since it clearly shows its resisting mechanisms as it was the will of the bridge designer to enhance mechanics and to make it understandable for the visitor of a science museum. Vertical forces are supported by the suspension cable, which is self-anchored. A compression ring that also works as a girder for the deck resists unbalanced horizontal forces. Live loads on the deck are transmitted by transverse cantilevers and create a torque that is decomposed into a pair of forces. One of these forces is resisted by the compression ring and the other by a set of cables running parallel to the compression ring (fig. 8). This excellent exercise of mechanics is the origin of the whole structure and its beauty is purely intellectual, in a sense that would be supported by many philosophers, from Aristotle to Hegel.

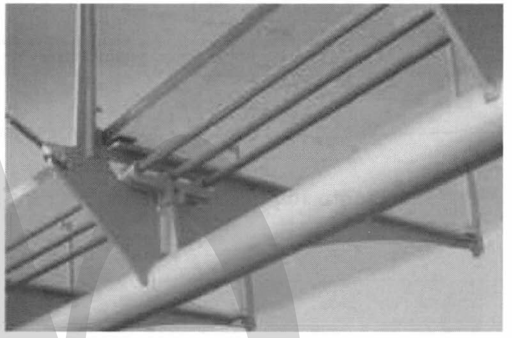

Figures 7 and **8** Deustche Museum footbridge in Munich (Germany). General view and detail.

Another example of a mechanically based design is the footbridge that has been designed by J. Strasky (fig. 9). A skilful combination of a stressed ribbon and an arch creates an elegant structure that is not necessarily an economical optimum since the arch is only loaded at its centre. Nevertheless, the combination of the tension and the compression elements obviates the main problem of the stressed ribbon, which is the anchorage of horizontal forces. This scheme is more or less self-anchored and foundations only transmit vertical forces and moments. Aesthetics is melted here with deep mechanical thinking.

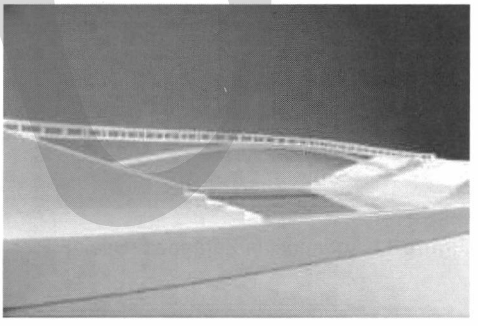

Figure 9 Stressed-ribbon overpass in Tcheck Republique

The next example is a bridge with the added function of being an aqueduct that has just been built in Zaragoza (Spain). Service loads correspond to two, 10 m wide, carriageways and to a 35.8 m^2 canal; as a consequence, vehicle and pedestrian loads are only 18% of total load. The solution that has been designed is a three-span continuous bridge (24+40+24m) with an open cross-section (fig. 10) where the canal is carried in the centre, between both carriageways. The structural concept is a variable thickness shell, which is stiffened at the supports by building the piers in the deck (fig. 11). The piers are simply supported at their base.

The bridge has a rather complicated behaviour, which was studied by means of the finite element method (fig. 12), but it has a very simple shape that reduces the apparent depth of the deck (4.45m) resulting in a rather light structure. The deck is prestressed with straight longitudinal tendons and with transverse tendons.

In this case the original concept was structural (a twin girder deck with external stiffening diaphragms) and this concept results in an elegant structure as well as in an interesting environmental alternative since the 12.2m wide canal located between both carriageways gives a bonus of quietness to surrounding traffic and increases the comfort in the pedestrians promenade (fig. 13-14).

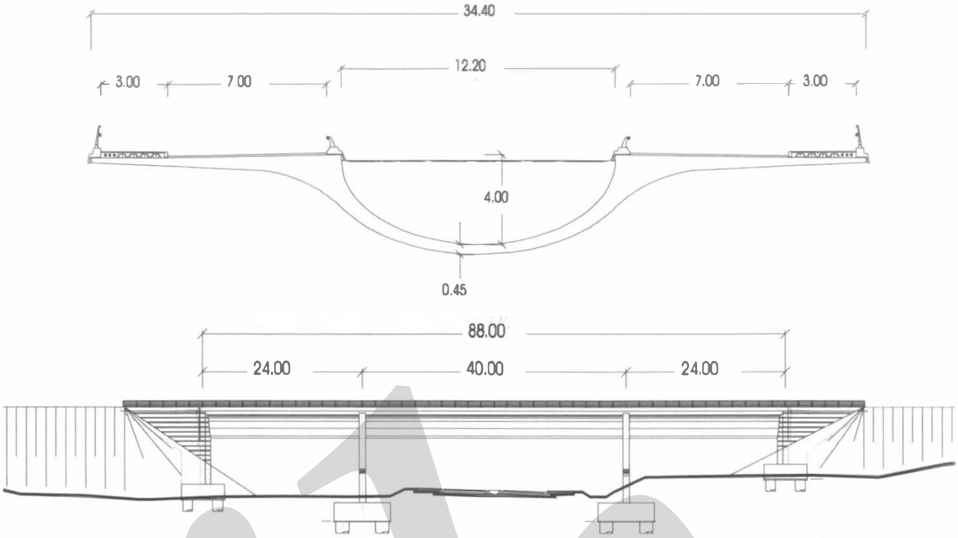

Figure 10 Aqueduct in Zaragoza (Spain). Cross-section and longitudinal view.

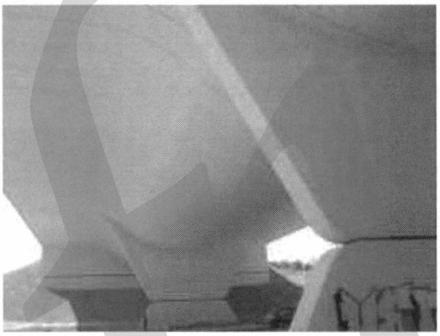

Figure 11 Aqueduct in Zaragoza (Spain). Pier.

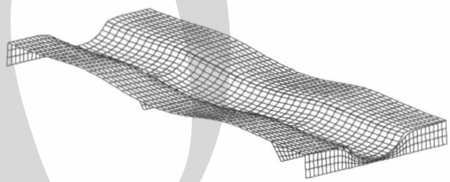

Figure 12 Aqueduct in Zaragoza (Spain). Deformed finite element mesh under hydrostatic load.

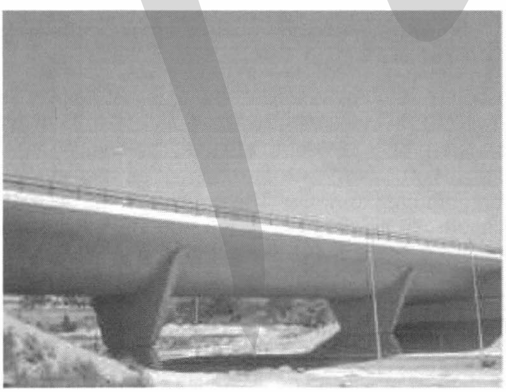

Figures 13 and **14**. Aqueduct in Zaragoza (Spain). Views from below and above the deck.

In the next example we had also the need of reducing the apparent depth of the bridge. This is the case of the already shown (fig.5) 546 m long bridge for high-speed trains (main span 120 m) crossing the river Ebro in Spain. To reduce the overall depth of the bridge plus the train as well as to reduce the impact of high-speed traffic on the river natural environment, the trains were enclosed inside the deck as it was done a long time ago with the Britannia bridge. Nevertheless we opened the deck as much as possible by opening circular windows in the webs and by closing the cross-section only with narrow beams at regular intervals (fig. 15). The ends of the closed box were also carefully designed to achieve a smooth transition between the main bridge and the approach spans (fig16).

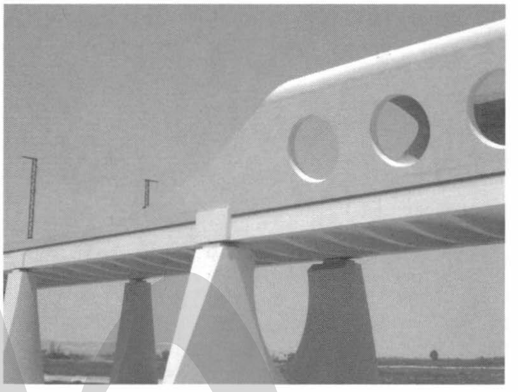

Figures 15and **16**. Bridge over the Ebro river for high-speed trains.

This is an example of a classical truss bridge updated to prestressed concrete and made as light as possible by using present day technology. A very important advantage of this solution is the fact that the level of the track is reduced as much as possible and the height of the approaches (earthworks and piers for the lateral spans) is also reduced while maintaining an adequate clearance over the river. Then, technology helps in reducing the environmental impact as well as in reducing costs of adjoining works.

The structural behaviour of this bridge is similar to a Vierendeel girder and it had to be very carefully studied by means of finite element models (fig. 17) to define its flexibility as well as to check the safety and serviceability states for the perforated webs, which had to be prestressed. The bridge has been incrementally launched from both sides and both halves have been connected at the centre of the main span.

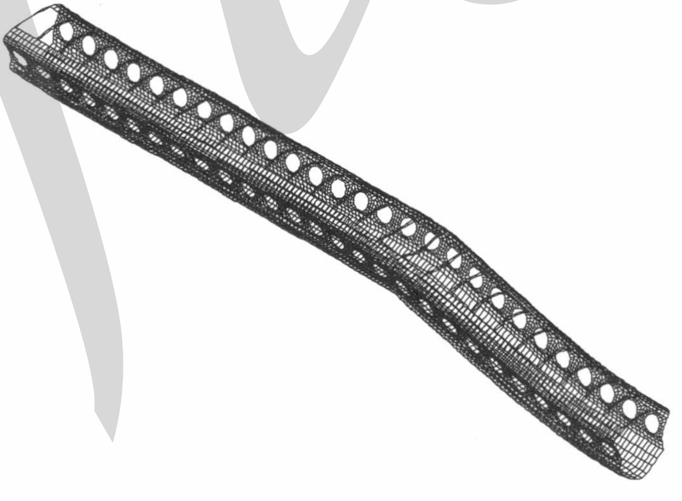

Figure 17. Bridge over the Ebro river for high-speed trains. Deformed finite element mesh.

Another shape that is very much related to structural mechanics constraints is the arch. We have recently designed a few of them and we tend to use the composite arch as a means of reducing the transverse dimensions of the arch and the inspection constraints of a steel arch. The bridge over the Escudo river in Spain (fig. 18) is a representative example since it may be appreciated that all the elements of the structure are extremely slender.

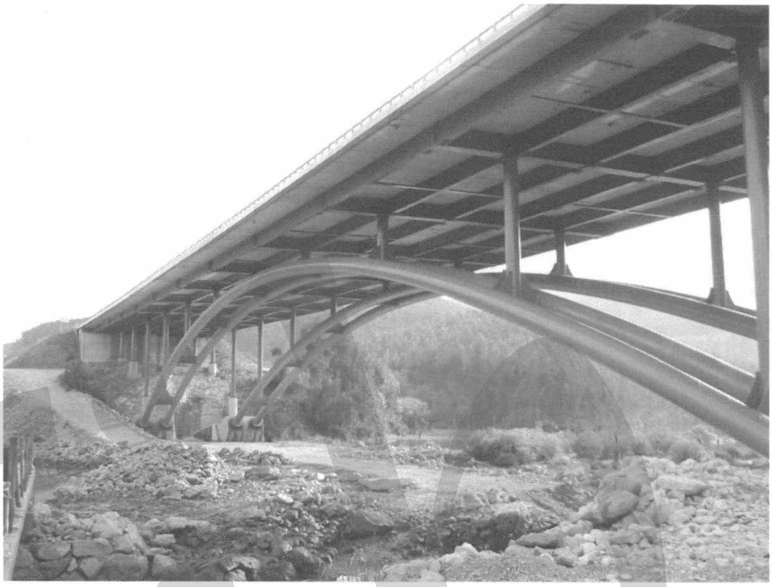

Figure 18 Bridge over the Escudo river (Spain).

The bridge across the river Ebro in Zaragoza (Spain) is a somewhat different example since in this case, the arch is a bow-string (fig. 19) and the prestressed concrete deck is hanging from the arch by means of vertical cables, which are anchored along the axis of the deck. The deck has a central box and lateral overhangs and it is prestressed both longitudinally, to support longitudinal bending and the horizontal thrust coming from the arch reaction, and transversally to collaborate in resisting transverse bending in the overhangs. High-strength concrete (70 MPa) was used in the supports of the arch where the arch load has to be transferred to the deck and to the underlying support.

A careful design of the details (the arch cross-section, which is triangular with chamfers at the corners, or the transition between the arch and the deck) has a very small cost and enhances the aesthetical qualities of the engineering work (fig. 20). A design of the details does not mean here a decoration or something that is added to a previous design. Detailed design should mean a structurally compatible modification that makes the bridge more elegant.

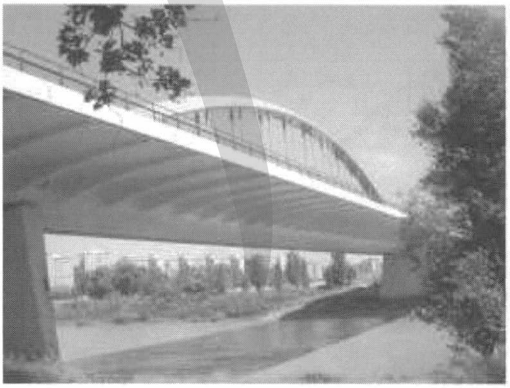

Figures 19 and **20**. Bridge over the Ebro river in Zaragoza (Spain)

A third composite arch is now under construction. The bridge over the Ebro river in Logroño (Spain) has a 140 m long main span suspended from an arch, which consists of two 1m diameter steel tubes filled with concrete (fig. 21). The distance between the tubes is 3m at the centre and null at the supports. Both tubes are connected by means a mesh of smaller steel tubes to provide stiffness against lateral forces. This stiffness is needed to support two parallel steel footbridges, curved in plan, which are also hanging from the arch.

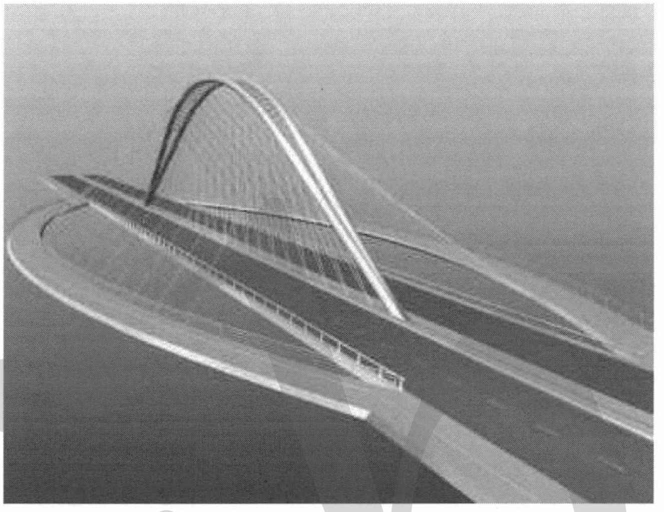

Figure 21. Bridge over the Ebro river in Logroño (Spain)

The shape of this arch has been optimised to minimise bending moments under dead and service loads. Here again, the structural concept was at the origin in the overall design concept of the bridge.

Another arch solution, although not filled with concrete in this case, is a footbridge just built in Zaragoza (Spain). The footbridge is supported by two arches that are located in symmetric inclined planes (fig. 22). The arches are 550mm diameter steel tubes and the deck girder consists of a central 550mm diameter steel tube a two lateral 300mm diameter tubes. This is obviously not the most efficient solution from the mechanical point of view since the arches will be supporting some transverse bending. However, since the span is small (54.80m), the economic consequences are not important.

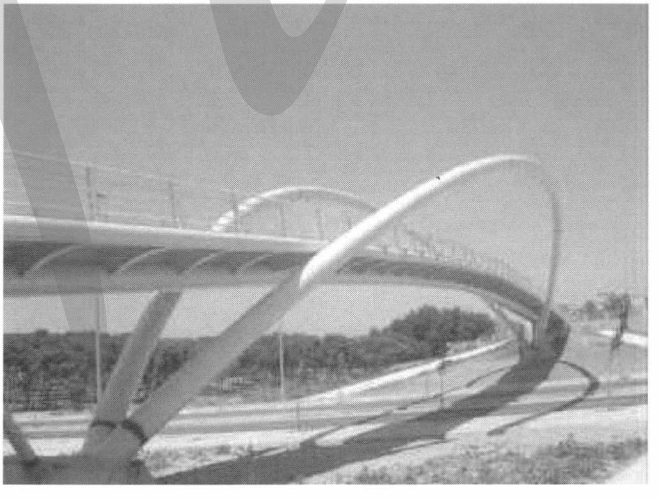

Figure 22 Footbridge in Zaragoza (Spain)

The static scheme is also not efficient against eccentric service loads. To resist such loads it relies on the deck's own torsional and transverse bending stiffness and on the support of the deck on the arches (fig. 23). This is something that can be done with a small span and narrow footbridge like this one since the defects of the static system are solvable at a small cost. The advantage of such design is its elegance, its openness, and its somewhat surprising shape.

Figure 23 Footbridge in Zaragoza (Spain). Connection between the deck and the arches

In this case, the structural mechanics concepts were present at the origin of the design although only for centred loads. A small transgression in the mechanical reasoning was made to allow a new esthetical solution. We should ask ourselves if, as engineers, we could do it; the answer for an engineer should be yes if the esthetical result is good, if the extra cost is marginal, and if all the conditions about safety, serviceability, and durability are fulfilled. The answer should be no if the cost is excessive or if safety, serviceability or durability are endangered. There is a third possibility, which becomes more frequent nowadays: the client is willing to pay the extra cost even if it is excessive. In this case, we come back to the ethical aspects of our profession but the answer could be affirmative if safety, serviceability, and durability are guaranteed (which is frequently not true if the basic mechanical scheme is wrong).

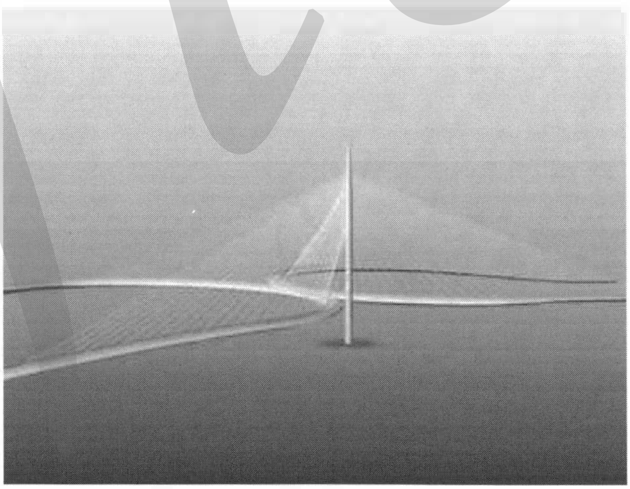

Figure 24 Cable-stayed footbridge in Madrid

The final example, a cable-stayed footbridge with four ramps and a central span of about 120m, which is being built in Madrid across the Manzanares river and a peripheral motorway (fig. 24), is the case of a static-based design that can be viewed as an aesthetically attractive solution. This is obviously not the cheapest way to solve the functional problem; nevertheless the construction of such a footbridge in a big city requires the fulfilment of certain esthetical conditions that lead us to such a bridge. The structural mechanics principles are in this case very important like in most cable-stayed bridges.

4 THE ROLE OF MECHANICS IN DETAILED DESIGN

The relation between detailed design and structural mechanics is obvious, although many of the esthetical qualities of a bridge depend on the design of small details. As a general principle, we tend to think that simple and rational details are aesthetic. In this case, structural efficiency may often be sacrificed in favour of ease of construction and inspection.

The finite element method is the perfect tool to analyse all the details both in the elastic range and in the non-elastic range. This tool has given to the designers the power to formulate new proposals, which may be numerically tested to check their safety as well as their durability. Geometrically non-linear effects, fracture, fatigue, plasticity, softening may be taken into account in these models. A better knowledge of engineering materials allows a more accurate modelling of new structures.

Nevertheless, details that have been proved by experience should not be forgotten. They should always be proposed as a first alternative. Only new constraints should require the definition of new details, which have to be very carefully analysed to check all their possible drawbacks. Not only stresses should be checked; ease of construction and durability are extremely important. The best detail is only the one that adequately fulfil all the conditions (not only safety or aesthetics, which are the first to be considered).

Many examples could be given about how structural mechanics may govern the design of a detail. Any bridge designer has had to design many of them. Just a few recent ones will be presented here.

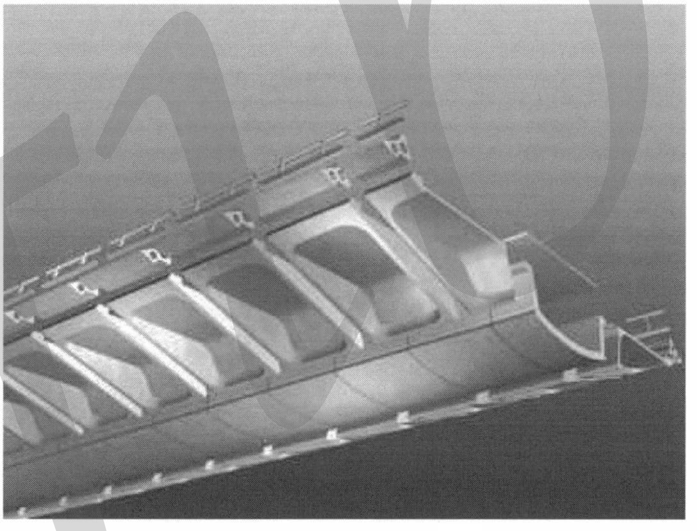

Figure 25 Acebosa bridge. Decomposition into pieces.

The connection between precast concrete segments in a bridge is an old problem and it is considered in the codes. The Acebosa Bridge is a 210 m long continuous curved girder with 45 m long spans. The deck consists of a central U-shaped girder, cantilever lateral segments, and an in-situ cast slab (fig. 25). The connection between the U-shaped girders was analysed by means of the finite element method considering the contact between both surfaces. Such models allow checking for the influence of the passing reinforcement bars (fig. 26) and for the stress distribution and corresponding reinforcement needs in the shear keys (fig. 27). Then again, structural mechanics careful analysis is at the origin of a prefabrication scheme, which results in a very high quality of the concrete surface (fig. 28).

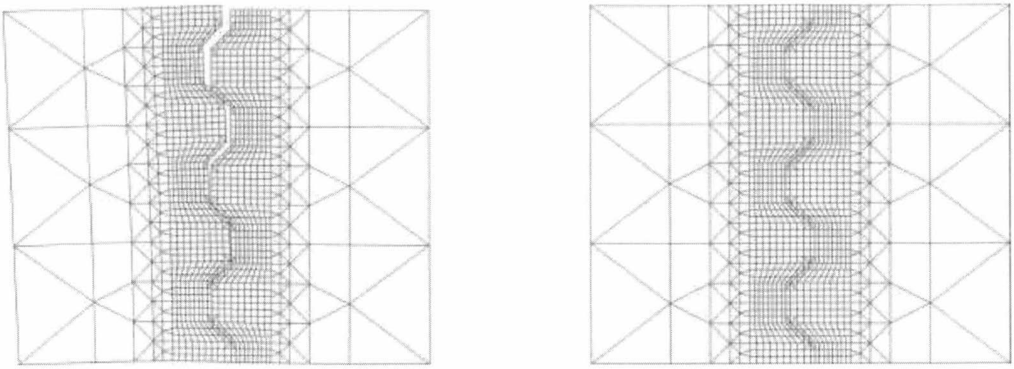

Figure 26 Finite element model of a shear key connection (without and with passing reinforcement)

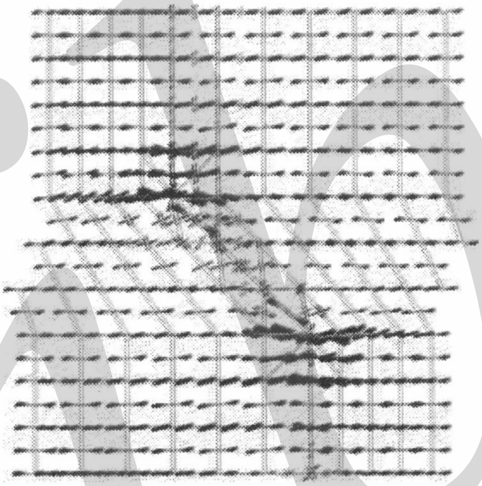

Figure 27. Stress distribution pattern in a shear key connection.

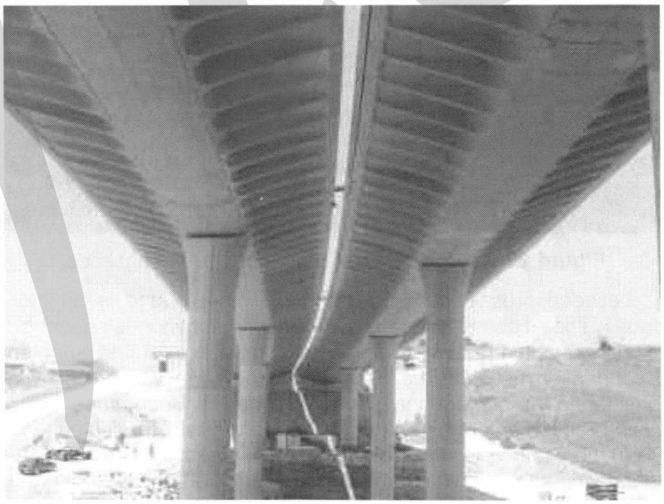

Figure 28 Acebosa bridge(Spain)

Another example of a new detail is the connection between a cable and a tubular structure since a concentrated force applied on the surface of a tube would produce high ovalization stresses. If the diameter of the tube is larger than about 0.80 m, it is possible to design an annular diaphragm as it was done for a preliminary solution of the Escudo Bridge (fig. 18). Figure 29 shows a magnified deformed finite element mesh, which helps in understanding the structural behaviour of this detail.

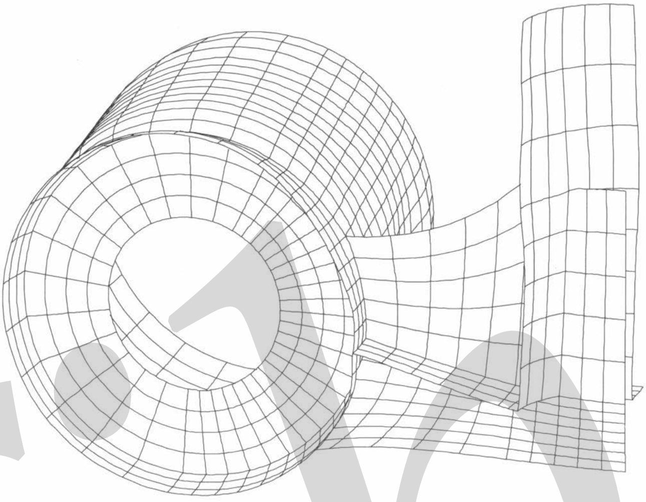

Figure 29 Finite element deformed mesh for an annular diaphragm connection

For smaller tubes, we have tried with an axial rectangular plate crossing the tube and welded along two opposite meridians. The safety of such connection depends mainly on the length of the plate and this kind of computation can only be performed by means of finite element models (fig. 30). This solution was applied in the above-mentioned Zaragoza footbridge (fig. 22) for the connection between the hangers and the arches (550mm diameter). To connect the same hangers to the deck tubes (300mm diameter), the same procedure was designed. This design had to be changed because of a construction problem to a different arrangement that shows very clearly the stress flow and the need of stiffening the cylindrical tube against ovalization (fig. 31).

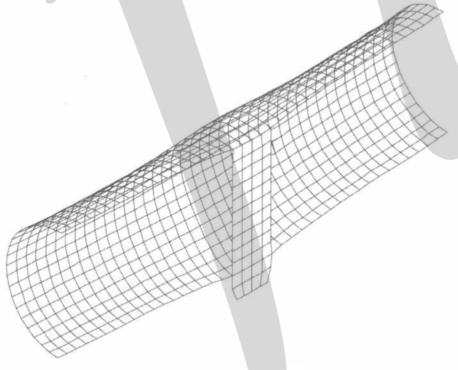

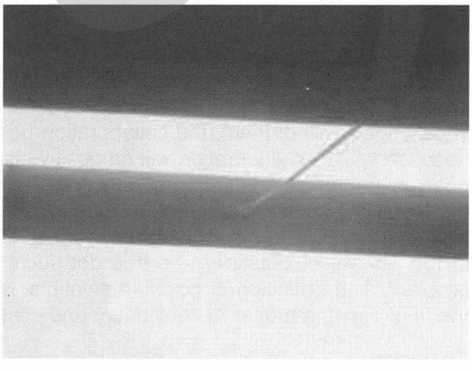

Figure 30 Anchorage in tube through meridian plate.

Figure 31 Alternative anchorage connection to a small tube.

5 CONCLUSIONS

Along this paper it has been shown that the role of structural mechanics in bridge engineering is somewhat changing because of a certain number of reasons. This change is especially important for small span bridges and for footbridges, where the shaping aspects of design may govern over the pure structural aspects.

Bridge engineers should consider esthetical constraints in their designs along with the classical constraints: safety, serviceability, economy, and, more recently, durability. Education programs in civil engineering should contain an important background on humanities since most of the civil works are very much related to mankind and they have very important social consequences. There is a growing concern on this issue as well as on considering structural engineering as an art [2].

Numerical methods, and among them the finite element method, are an extremely powerful tool which may help designers if their work to check for safety and serviceability of new designs. Nevertheless these methods should not be used as a tool to solve problems caused by a bad conceptual design.

Good bridge engineering means, among other things, good design by taking into account all the above-mentioned aspects. As these aspects are very diverse and it is impossible to have deep knowledge of all of them, the collaboration between different professionals becomes more and more necessary. This collaboration will be positive if all these people work jointly on getting the best design, possibly under the leadership of one of them. Only when all the design constraints will be respected, the result will have an adequate quality.

Structural mechanics should always guide the conceptual design but without forgetting that, unlike in the Theory of Elasticity, there is not such a thing as a unique solution for a bridge engineering problem. The definition of possible solutions is a matter of creativity and imagination; the election of the final one is a matter of equilibrium and consensus to fulfil all the design constraints.

REFERENCES

[1] Kawaguchi M., "Memorandum about Conceptual Design", IASS Journal, vol. 37, pp.27-29, 1996
[2] Billington D.P., "The New Art of Structural Engineering", Structural Engineering International, 3/94,pp.187-189, 1994

Session 1 | Big projects and innovative structures

ADVANCED STRUCTURE OF PRESTRESSED BRIDGES - NOVEL TECHNOLOGIES IN THE NEW TOMEI AND MEISHIN EXPRESSWAY -

Hiroyuki IKEDA Kazuyuki MIZUGUCHI
Japan Highway Public Corporation

Keywords: precast segmental method, curved bridge, Factory-fabricated precast segment, U-shaped core section, composite extradosed bridge

1. INTRODUCTION

The new Toumei and Meishin expressways, which are under construction, were planed to achieve the double network in the central part of Japan. The percentage of the bridges and viaducts in the expressways reaches approximately 40%, which is higher than any other existing expressways in Japan because of their conditions.

Especially the precast segmental bridges using short line match-casting and span-by-span erection have been widely adopted in an increasing number of projects, under a variety of bridging conditions. The precast segmental construction can achieve not only high quality products built at the casting yard under concentrated controlled conditions, but also time saving of construction.

For Furukawa Viaduct in the New Meishin Expressway, the factory-fabricated precast segments have been applied, in which the segments were fabricated at concrete factorie. The weight of a segment is held to be no more than 30 tons in order to be transported on the public roads with a trailer. The most distinguishing feature of this bridge is the shape of the girder section, designed to reduce the weight of the segments for the 16 m road width.The Kiso River Bridge and Ibi River Bridge in the New Meishin Expressway are composite extradosed bridges with center spans of 275.0 m and 271.5 m, respectively. Due to the environment and construction conditions at the bridge sites, the bridges were constructed using a precast segmental method with a maximum segment weight of 400 tons. On both bridges, steel girders were used for a 100-meter section in the center of the span.

2. KAWAGOE VIADUCT

Kawagoe Viaduct consists of 1298m long concrete box girder bridges for main ways (up-and-down) as well as 4 interchange ramps. The concrete segments are fabricated using short-line match casting method. Span-by-span and cantilever method is adopted for the construction of the continuous PC box girder. To arrange the prestressing tendons is planned to be installed in the box plates as inner cables, and also besides the webs as external cables. The plan view shows a very small curvature radius of R=85m and span length varies 30-78m.

The erection of segments is adopted span-by-span method and cantilever method using only one erection girder, which is developed for this project. At the end of the guided launching-girder, a hydraulic guide arm and hinged connecting element is installed to the main erection girder, so that the erection girder can be bent to the proportional line.

For the safety erection of curved ramp ways with the 168m long special erection girder, the moving of erection girder is controlled using GPS monitoring system to insure the levels of constructed segments and the geometry control of the guided launching-girder along the curved ways.

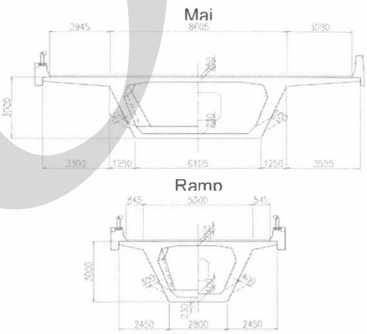

Fig.1 Standard cross section (Kawagoe Viaduct)

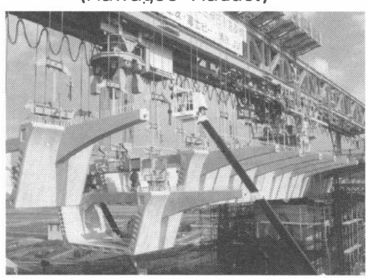

Photo 1 Erection of Furukawa Vladuct

3. FURUKAWA VIADUCT

The segments were fabricated in two precast concrete factories located approximately 60 km from the site of the bridge construction and the segments were transported from the factories to the site using a trailer with a 30 t load capacity.

The standard segments were erected after the construction of the pier segments with the erection girder and the span-by-span method. Epoxy joints are used for the connection of segment. After the segments were joined, eight 19ϕ15.2 mm external tendons were inserted and tensioned. A total of 12 external tendons were arranged consisting of eight single-span tendons and four double-span continuous tendons.

The upper slab consists of precast concrete panels and cast-in-place concrete. The precast concrete panels were first erected and placed between transversal ribs of the segments, one span behind the span-by-span erection. Approximately 200 panels were provided for each span, and each panel was erected with crane. After the erection of the panels, the slab reinforcements and transversal tendons were arranged and the slab concrete was placed. The precast concrete panels can serve as both formwork and work scaffolding. After the tensioning of the primary longitudinal tendons, after-bonded tendons (1ϕ21.8 mm) were used for the transversal prestressing and the secondary external tendons in the longitudinal direction were then conducted.

4. THE KISO AND IBI RIVER BRIDGES

All 357 segments were manufactured at the casting yard. Each pair of lines (the two lines for the Kiso River and the two lines for the Ibi River) was provided with a 400-ton gantry crane for transporting the segments, and there were mechanisms capable of transporting segments to the stockyard and shipping yard both longitudinally and transversely.

The concrete segments were erected by cantilever erection method. **(Photo 2)** Using an erection nose to lift the segments that had been shipped by barge, and then coating them with epoxy resin, rematching, and tensioning the internal and external cables and the extradosed cables performed cantilever erection. The erection cycle was generally four days.

When the erection of the concrete girders was complete, steel girders weighing 2,000 tons with a girder length of 100 m were lifted from the tip of the concrete girders and erected. **(Photo 3)** The steel girders on each span were temporarily connected, using hanger bars and pins, to joint segment placed at the ends of the concrete girders after lifting up. Furthermore, when the erection of all of the steel girders was complete, final connection of the concrete girders and steel girders was conducted using bolts.

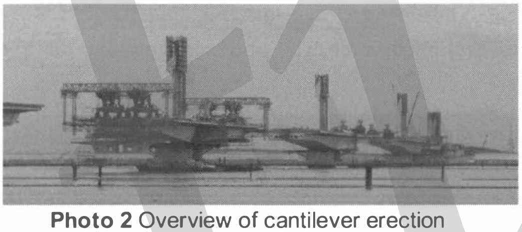

Photo 2 Overview of cantilever erection

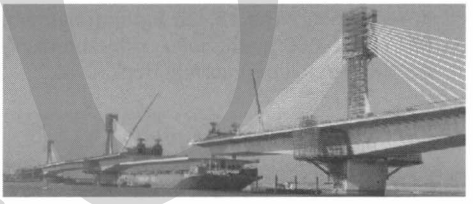

Photo 3 Erection of steel girder

5 CONCLUSIONS

This paper introduces the Advanced Structure of Prestressed Bridges in the New Tomei and Meishin expressways. These three types of bridges are adopted precast segmental construction. Kawagoe Viaduct is the first application of the precast segmental method for the curved bridge in Japan. The adopted IT technology could rise quality, speed and safety of the erection of precast segmental bridges. In the past, curved bridge structures were build with steel girder, however the Kawagoe viaduct shows the new technology of segmental concrete bridge for curved structures.

Furukawa Viaduct, which is designed as U-shaped segment, was confirmed through design and construction studies including full-scale span test. The factory-fabricated precast segment gives new solution for applying conventional precast segments against recent issues including land limitation in urban area, lack of experienced workers and cost reductions. The application of factory-fabricated precast segments has also the advantage of enabling the high quality products under stable conditions at concrete factories, without being affected by the various conditions at the erection site.

Kiso and Ibi River Bridges demonstrate that extradosed bridges can be applied to long spans. Based on the creation of standards and experience up to now, the extradosed bridge, streamlined in terms of both structural properties and economic considerations, will undoubtedly continue to develop in the future.

Although it is necessary to develop the new type of bridges and construction methods, it is more important to develop the new technologies, which reduce the maintenance cost and achieve the low maintenance under the consideration of increasing the old expressways required maintenance.

ANCHORING THE NEW SAN FRANCISCO – OAKLAND BAY BRIDGE MAIN SUSPENSION SPAN WITH PRESTRESSED CONCRETE

John Sun, Rafael Manzanarez, Marwan Nader, James P. Duxbury
T.Y. Lin International, San Francisco, California, USA

Keywords: prestressed concrete, self-anchored suspension bridge, seismic loads

1 INTRODUCTION

In May 1998, the Bay Area Metropolitan Transportation Commission selected the self-anchored, single tower suspension alternative as the signature span of the San Francisco-Oakland Bay Bridge East Span Seismic Safety Project (SFOBB). The rendering of the bridge is shown in Figure 1.

While the single tower asymmetric suspension bridge satisfies the aesthetic preference of the bridge type selection committee, the concept of "self-anchored" is dictated by the geotechnical condition, shown in Figure 2. At the East Anchorage pier, the combined depth of Young Bay Mud, Old Bay Mud, and sand layers reaches more than 100 meters above the Franciscan Rock formation. Such soil conditions make construction of the conventional earth anchorage undesirable in both technical and economic terms. The deck anchorage system becomes the natural choice for the East Anchorage, and consequently for the West Anchorage.

Among all the key structural components in this structural suspension system, the West Anchorage is one of the most critical elements for several considerations:

- The West Anchorage piers take up to 70% of total base shear in the critical longitudinal direction under critical seismic loads. This requirement results from the limited shear capacities of a very flexible tower and the East Anchorage pier being founded on a flexible pile foundation system in the Bay Mud.
- The post-yield behavior of the West Anchorage pier columns has a significant effect on the residual displacement, or "permanent set" of the main suspension span.
- It must anchor the 17,400 5.4-mm diameter wire cable which is capable of developing up to 700 MN (or 70,000 metric tons, cable-breaking capacity) cable force with approximately 280 MN (or 28,000 metric tons) uplift at deck level.

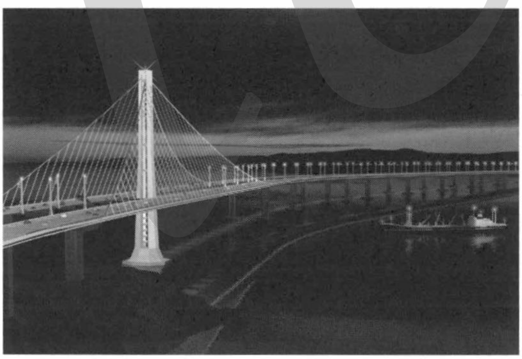

Figure 1 Rendering of the East Bay Suspension Span

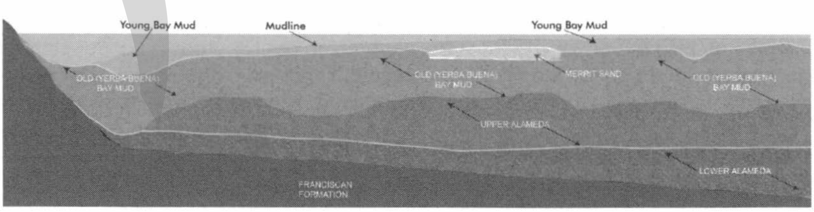

Figure 2 East Bay Bridge Soil Profile

- It must resist longitudinal compression thrusts from the orthotropic deck without significant local effects, such as bending or shear lag.
- It must satisfy all geometric requirements, such as roadway clearance, minimum saddle radius, the single plane requirement of the anchorage cable layout, and roadway elevation differential.
- It must also be compact and clean so that it becomes a natural part of the grace of the bridge.

2 LOOPING CABLE ANCHORAGE SYSTEM

A number of anchorage systems may be used to deliver these requirements. With extensive comparative studies on numerous alternatives, the new Looping Cable Anchorage system is recommended for the final design. The Looping Cable Anchorage system, as shown in Figure 3, essentially consists of a prestressed concrete portal frame, a looping anchorage cable, deviation saddles, a jacking saddle, independent tie-down systems, and piled RC foundations. It is chosen for its structural efficiency, reliability, and dimensional compactness.

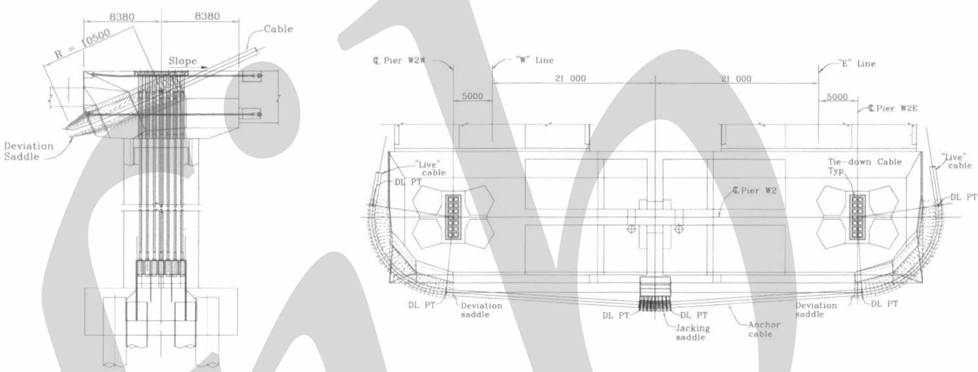

(3a) Side elevation (3b) Plan

Figure 3 Looping Cable Anchorage System Layout

3 CONCLUSIONS

The Looping Cable Anchorage System provides an efficient, reliable, and compact cable anchorage solution for the West Anchorage of the East Bay Bridge Suspension Span. It is developed to meet the challenges imposed by the unique bridge structural layout and aesthetic requirement.

ACKNOWLEDGEMENT

The Authors would like to acknowledge the invaluable discussions with Dr. Man-Chung Tang, Mr. Charles Seim of T.Y.Lin International, Mr. Paul Mueller of Mueller Industries, Inc., Mr. Herb Rothman of Weidlinger Associates, Mr. Jackson Durkee, Mr. Hajime Hosokawa of Nippon Steel, and Dr. Frieder Seible of UC San Diego. Our sincere thanks also go to Dr. Brian Maroney, Mr. Ade Akinsanya, Mr. Vong Toan, Mr. Wenyi Long of the California Department of Transportation for the comments made during the bridge final design phase.

PLANNING AND DESIGN OF RITTOH BRIDGE

Yoshiyuki Yasukawa :

Japan Highway Public Corporation, Kansai Regional Bureau, JAPAN

Hidetoshi Miyauchi :

Japan Highway Public Corporation, Kansai Regional Bureau, JAPAN

Hideki Kato :

Japan Highway Public Corporation, Kansai Regional Bureau, Head of Ohtsu Office, JAPAN

Akihiro Nakazono :

Japan Highway Public Corporation, Kansai Regional Bureau, Ohtsu Office, JAPAN

Keywords: corrugated steel web, extradosed bridge, steel diaphragm

1. INTRODUCTION

Rittoh Bridge is an extremely large scale bridge which is 495m and 555m in length, 16.5m in effective width, and 65m in pier height, is located east-southeast about 10km from the south end of Biwako-Lake, which will be constructed between Otsu JCT and Shigaraki IC on The 2nd Mei-Shin Expressway. Four and five span continuous prestressed concrete extradosed bridge with the maximum span length of 170m is adopted considering topographical and environmental condition, and constructivity and cost efficiency as well. The composite bridge with corrugated steel webs is adopted for the girder in consideration of constructivity and weight reduction and so on.

Although Japan Highway Public Corporation (JH) has already constructed Hontani Bridge, which is 10.5 m in effective width and 97m in main span, new problems as follows will be raised for Rittoh Bridge because of wider width and an extradosed structure.

- The transmission behavior of the force by stay cables (effective transmission length)

  Research of the stress distribution and the effective transmission length is necessary, because the force by stay cables is transmitted from the both ends of wide decks on this bridge.
- Torsional behavior and the distribution of shearing force for each web

  The cross section of the girder consists of three cells because of large width. And the girder with corrugated steel webs has less stiffness in the lateral direction than ordinary concrete web girders. The torsional behavior by the influence of the small lateral stiffness and the distribution of shearing for each web should be studied.
- Local stress at the near of stay cable anchorage

  For the design of the stay cable anchorage, the force by stay cable must be transmitted surely and smoothly. And also the local stress occurred on concrete deck and corrugated web is to be reduced.

This bridge is designed to the problems above mentioned, by using 3 dimensional Finite Elements Method (3D-FEM), and considered constructivity, durability and economic viewpoint.

The author will explain the study of the stay cable anchorage in detail as below.

2. ANALYSIS METHOD

The reinforcement by PC-tendons to the some cable stayed bridges has been adopted. Steel diaphragm is adopted from the viewpoint of weight reduction in the design of Rittoh Bridge.

The required performances of steel diaphragm are as follows.

- Steel diaphragm should be alone able to resist against the vertical component of stay cable force.
- No dangerous cracks of concrete deck composite to the steel diaphragm should be occurred.
- The distribution of shearing force to each web should be pretty even by the effect of the steel

diaphragms.
- The structure should have enough stiffness against torsional moment.

The procedure of the verification to them is as follows in concrete.
- The safety of diaphragm is confirmed by the 2 dimensional frame analysis.
- The local stress of concrete slab is checked and tensile stress of concrete is controlled less than 3 N/mm^2 by using 3-D FEM (local model).
- Distribution of shearing force to each web is analyzed by using 3-D FEM for the full-scale model. Both cases under and after construction are analyzed.
- Torsional behavior is examined against the torsional moment caused by own weight and live load onto full-scale model of 3-D FEM.

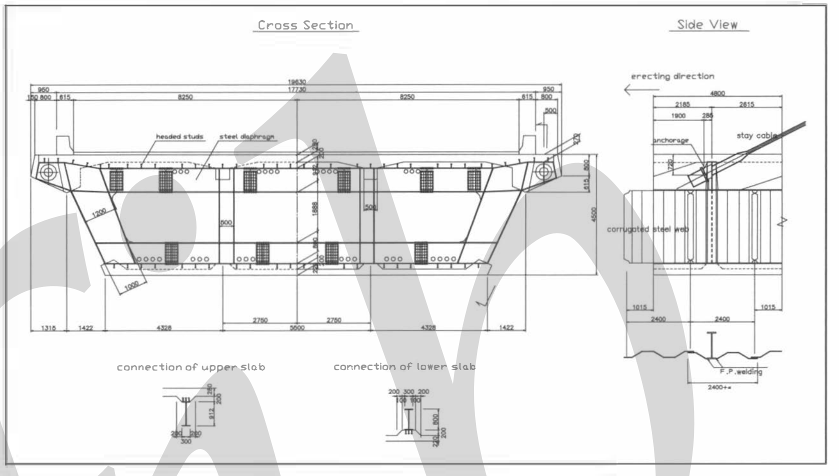

Fig.1 Steel diaphragm at anchorage of stay cable

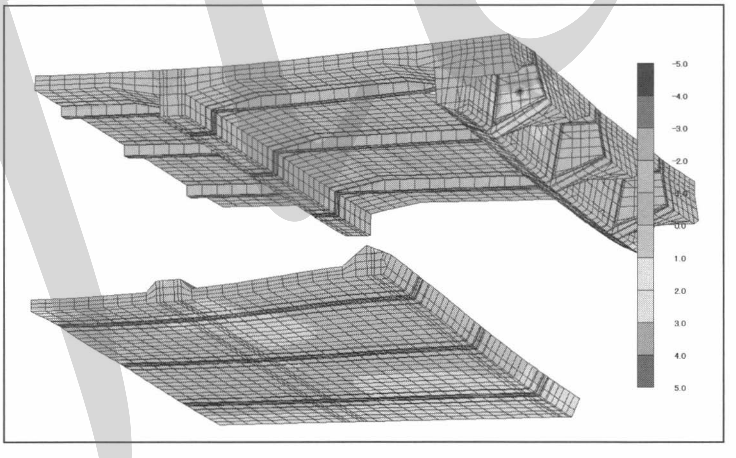

Fig.2 Result of FEM analysis

Although the structure is determined by these analyses above, the safety of it will be confirmed finally by the experiment with half-scale model.

DESIGNS FOR NEW BRIDGES ON THE CROATIAN COAST

JURE RADIĆ ZLATKO ŠAVOR VINKO ČANDRLIĆ GORAN PUŽ
University of Zagreb, Faculty of Civil Engineering
Kaciceva 26, 10 000 Zagreb, CROATIA

Keywords: arch bridge, cable-stayed bridge, bridge design

1 INTRODUCTION

Croatia is Middle European and Mediterranean Country, currently in the process of intensive development of its road network. In the country with many rivers and more than thousand islands many exceptional bridges are to be constructed. Some large bridges on new highways and fixed links to the islands that are currently under construction or in the design stage are highlighted. The review starts with experience gained from maintenance of existing bridges because it strongly influences new designs.

2 SERVICE PERFORMANCE OF SOME EXISTING BRIDGES

Four arch bridges, the Šibenik bridge, the Pag bridge and the Krk bridges (two arches) were built during the sixties and the seventies on the Adriatic coast in Croatia. The most famous is the Krk I bridge, which held the world record for twenty years with 390 m span. These bridges were designed and built in accordance with the regulations in force in late 1960's. Minimum statically admissible dimensions of all structural elements were utilised, in conjunction with a thin concrete cover.

The performance in service of the four older arch bridges cannot be deemed satisfactory. Structural defects were found at an early age and hence cannot be blamed primarily on the aggressive environment, but are attributed to conceptual design and errors and negligence on site.

All bridges have been investigated, and the Pag bridge was completely reconstructed. In 1991 complete repair of the arch was performed, consisting of removing the damaged concrete surface and placing an additional reinforcement mesh on all outer arch surfaces, covered by a fine mortar layer 4 cm thick. Both the superstructure and the piers were even in a worse state so that a radical solution had to be adopted by replacing the prestressed concrete superstructure with the new steel one [1].

The Maslenica highway bridge, completed in 1997, belongs to the second generation of bridge design, with the severity of the aggressive maritime environment taken into account. Dimensions of structural elements were increased in order to avoid reinforcement congestion and increase durability. Structural details and cross sections were simplified; in order to minimise execution problems [2].

3 BRIDGE ACROSS RIJEKA DUBROVAČKA

The Bridge across the Rijeka dubrovačka was opened for traffic in May 2002. [3]

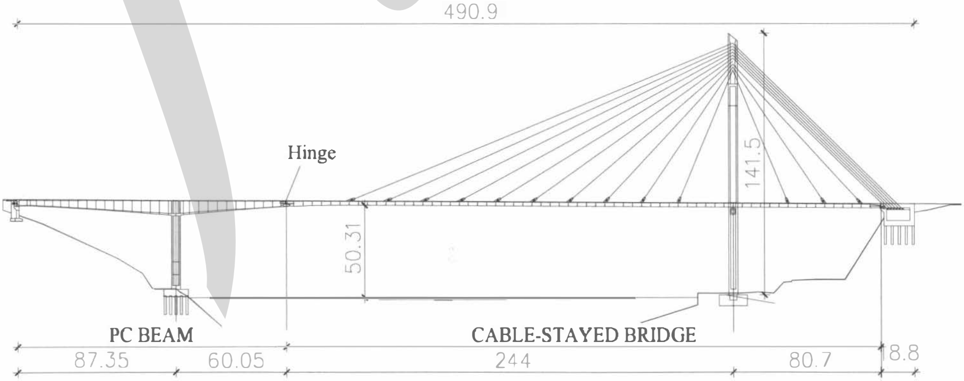

Figure 1. Layout of the Bridge across the Rijeka dubrovacka.

Asymmetrical layout with one pylon had to be chosen because the motorway from west enters the bridge in a sharp curve, so that the more economical three - span cable-stayed structure was not possible. The location of the bridge is in a highly active seismic zone and subject to very strong winds.

The adopted bridge lay-out comprises the 87,4 m span box type prestressed concrete approach viaduct with the 60 m cantilever and the 244 + 80,7 m cable-stayed bridge with composite superstructure. The longitudinal layout of the cables is of modified fan type with partial suspension.

The approach viaduct is partially curved in plan. The superstructure depth varies from 3,2 m at the west bank abutment and at the cantilever end to 8,2 m at the fixed connection to the pier. Two hydraulic dampers of 2000 tons capacity are installed at the connection of the viaduct to the west bank abutment. The pier base is designed to act as plastic hinge in case of a major earthquake.

Two different erection procedures were used for construction of the main bridge superstructure. The steel grillage of the 80,7 m side span and 33 m long adjoining part of the main span was erected by incremental launching from the left bank abutment. The remaining 211m long steel grillage of the main span was erected in 20 m long segments by free cantilevering. The construction of the approach viaduct was executed by free cantilevering procedure symmetrically from the pier.

4 NEW PROJECTS

4.1 Krka river canyon bridge

The new Adriatic highway crosses the Krka river canyon in very attractive environment, in the close proximity of the National Park Krka. Several preliminary designs were done for the crossing, revealing that the most suitable solution might be the concrete arch bridge with the 210 m span (Fig. 6). The bridge should be put in service by the year 2005. [6]

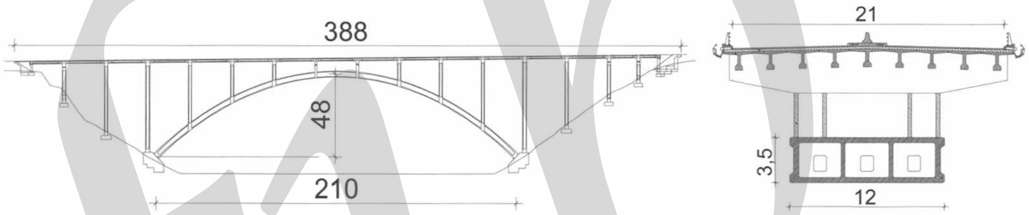

Figure 2. Preliminary design for new arch bridge over Krka river.

4.2 Preliminary design for Pašman island fixed link

Three alternative preliminary designs for the Pašman island bridge are made, all at the same most favourable location, resulting in the total bridge length of approximately 2,2 km.

Sea traffic requirements dictated the design. Port authorities asked for two separate sea-lanes of 140 m width and 40 m clear height. The first beam type bridge alternative has two 150 m central spans and the second cable-stayed alternative crosses both sea-lanes with one 500 m span. Designers thought that these requirements are much too stringent resulting in very expensive bridge structure and offered a third alternative with two 70 m spans over sea lanes which were reduced to the width of 60 m and clear height of 30 m.

5 CONCLUSION

All presented bridges are located in the maritime environment with concrete as dominant material. The choice of concrete over steel is based on economical evaluations. Presently in Croatia it is cheaper to build and maintain concrete bridges. Besides, concrete structures utilise more local resources.

6 REFERENCES

[1] Radić, J., Šavor, Z., Pičulin, S., Puž, G.: Large Concrete Arch Bridges in Croatia. Proc. ARCH'01, Third international arch bridges conference, Paris, pp. 49-58, (2001)

[2] Čandrlić, V., Radić, J., Šavor, Z.: Design and Construction of the Maslenica Highway Bridge. Proc. Fib Symposium; Structural Concrete, Vol. II, Prague, 551-555. (1999)

[3] Šavor, Z., Prpić, V., Hrelja, G.: Conceptual Design of Bridge across the Rijeka Dubrovačka. Proc. Proc. V General assembly of the Croatian society of Structural Engineers, Brijuni Islands, pp. 97-106., (2001.) (in Croatian)

CONSTRUCTION OF THE SUPERSTRUCTURES OF KISO AND IBI RIVER BRIDGES

Hiroyuki Ikeda, Kuniaki Nakamura, Makoto Nakasu
Japan Highway Public Corporation
JAPAN

Shoji Ikeda
Yokohama National University
JAPAN

Keywords : composite extradosed bridge, precast segmental method

1. INTRODUCTION

The Kiso River Bridge (Photo.1) and Ibi River Bridge (Photo.2) are composite extradosed bridges with center spans of 275.0 m and 271.5 m, respectively.[1)] (Fig.1) Due to the environment and construction conditions at the bridge sites, the bridges were constructed using a precast segmental method with a maximum segment weight of 400 tons. On both bridges, steel girders were used for a 100-meter section in the center of the span. The steel girders were assembled at the factory, then transported to the bridge site and joined to the concrete girders that had been erected through cantilever erection. Great progress has been made in the several years since the construction of the Odawara Blueway Bridge, the first extradosed bridge, and a variety of new technologies have been incorporated into the construction of the Kiso and Ibi River Bridges. Tests to verify the suitability of these technologies were pursued as the detailed design was being conducted. The Kiso River and Ibi River are two of Japan's major rivers, located next to one another. These bridges cross the mouths of the two rivers, separated by an expressway interchange. In terms of design they are composite extradosed bridges with the same form.

Photo.1 Kiso River Bridge

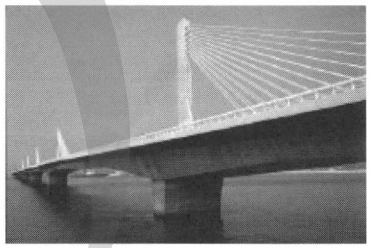

Photo.2 Ibi River Bridge

The extradosed bridge is a new concept in structures. Originally proposed by Mathivat in 1988[2)], it first came to flower in 1996 with the construction of the Odawara Blueway Bridge (span length 122 m). The appearance of this concept made it possible to integrate ideas from girder bridges to cable-stayed bridges in the design process. In Japan, following the construction of the Odawara Blueway Bridge, the 180-meter span Tsukuhara Bridge was completed in 1998, after which the Kiso and Ibi River Bridges were completed in 2001. The 5-span continuous girder Kiso River Bridge and 6-span continuous girder Ibi River Bridge, with a center span of almost 300 m, have a scale such that, in the past, cable-stayed bridges would have been constructed. However, in pursuit of economy and to satisfy the standards for a bridge form that would be in harmony with the river location, it was necessary to combine extradosed bridge and composite bridge technologies. Combining these technologies—both of which are keywords for bridge technology in the 21st century—has significantly increased the number of variations in bridge modes.

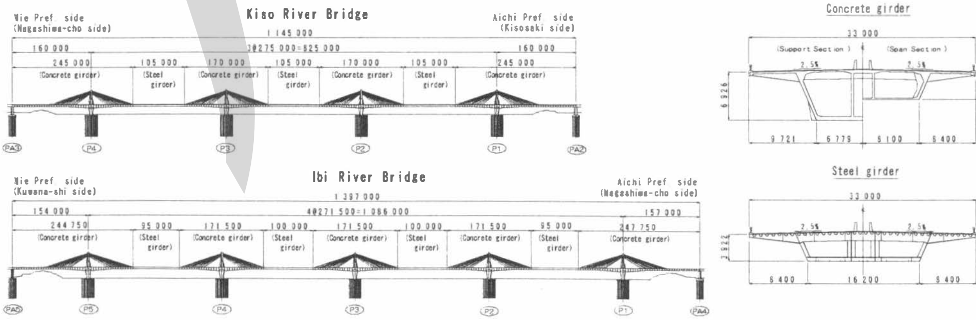

Fig.1 General view of Kiso and Ibi River Bridges

2. FABRICATION OF SEGMENTS

As shown in Photo.3 the 80,000 m^2 casting yard contained four fabrication lines and, in all, 357 segments were manufactured. Each pair of lines (the two lines for the Kiso River and the two lines for the Ibi River) was provided with a 400-ton gantry crane for transporting the segments, and there were mechanisms capable of transporting segments to the stockyard and shipping yard both longitudinally and transversely.

The process of fabricating segments was generally a four-day cycle. On the first day, the segments were removed from the casting form and separated, and then the bottom and side frames were set in place. On the second day, the reinforcing steel cage was hoisted in and the inner frame was set in place. On the third day, the inner frame was assembled and the prestressing tendons were secured in place. On the fourth day, the concrete was cast and cured.

Photo.4 shows overview of concrete segments.

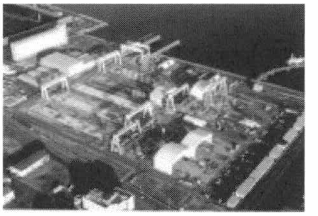

Photo.3 Segment casting yard

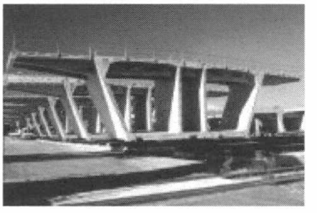

Photo.4 Overview of concrete segments

3. ERECTION OF CONCRETE SEGMENTS

The concrete segments were erected by cantilever erection method.(Photo.5) Cantilever erection was performed by using an erection nose to lift the segments that had been shipped by barge, and then coating them with epoxy resin , rematching, and tensioning the internal and external cables and the extradosed cables. The erection cycle was generally four days.

4. ERECTION OF STEEL GIRDERS

When the erection of the concrete girders was complete, steel girders weighing 2000 tons with a girder length of 100 m were lifted from the tip of the concrete girders and erected. (Photo.6) The steel girders on each span were temporarily connected, using hanger bars and pins, to joint segment placed at the ends of the concrete girders after lifting up. Furthermore, when the erection of all of the steel girders was complete, final connection of the concrete girders and steel girders was conducted using bolts.

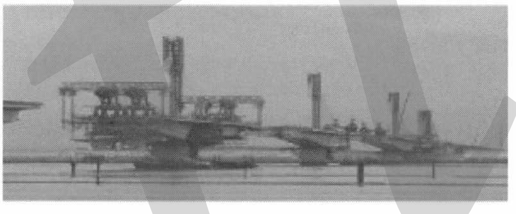

Photo.5 Overview of cantilever erection

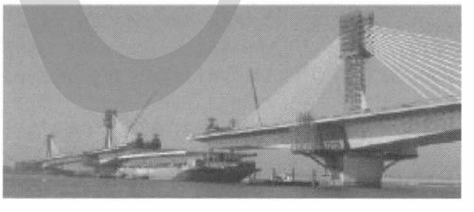

Photo.6 Erection of steel girder

5. CONCLUSIONS

In July 2001, the Kiso and Ibi River Bridges were completed. The differences between the extradosed bridges that first came to flower in Japan and cable-stayed bridges in terms of structural mechanics and design standards must be clarified to enable streamlined design. In order to solve this issue, design specification was made at the Japan Prestressed Concrete Engineering Association in 2000.

The Kiso and Ibi River Bridges demonstrate that extradosed bridges can be applied to long spans. Based on the creation of standards and experience up to now, the extradosed bridge, streamlined in terms of both structural properties and economic considerations, will undoubtedly continue to develop in the future.

REFERENCES

1) Minoru Hirano; Hiroyuki Ikeda; Akio Kasuga; Hideki Komatsu: "Composite Extradosed Bridge", Structural Concrete The Bridge Between People, fib Symposium 1999, Prague

2) Mathivat,J.: "Recent development in prestressed concrete bridges", FIP notes, 1988/2

RAMA VIII BRIDGE IN BANGKOK: STAY CABLE SYSTEM AND INSTALLATION

Roy LENGWEILER George CASSIMATIS
BBR Systems Ltd., SWITZERLAND

Keywords: stay cable system, full scale testing, installation and tensioning, damping devices

1. INTRODUCTION

Fig. 1: View of the completed bridge.

The Rama VIII cable stayed bridge is the most recent crossing over the Chao Praya River into Central Bangkok and was initiated by His Majesty the King. Despite the recent economic slowdown which Thailand experienced, the project was awarded in 1998 to the CSCEC-PPD-BBR Joint Venture. The project was constructed within 3 years and was opened to traffic at the end of March 2002. The key element of the project is the 475m long cable stayed bridge crossing the Chao Praya River with a 300m main span. The longitudinal arrangement is asymmetric and with only one single pylon. The bridge is one of the world's longest single pylon cable stayed structures.

2. STAY CABLES

2.1 Arrangement

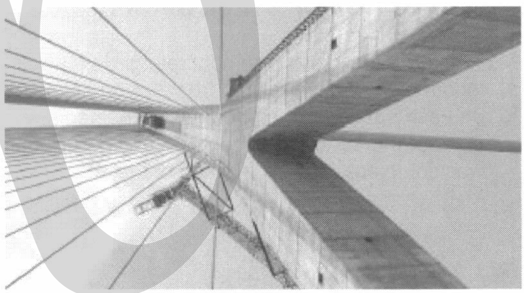

Fig. 2: Stay cable arrangement.

The 28 pairs of main span cable stays are in a semi harp configuration, with each stay consisting of between 15 to 29 nos. of 0.6''-diameter high strength steel strands. The lengths vary from 65m up to 325m. The 28 back stays are in a vertical center plane harp configuration, with a maximum size of 65 strands for the largest (235 m-long) stay.

2.2 System and Acceptance Test

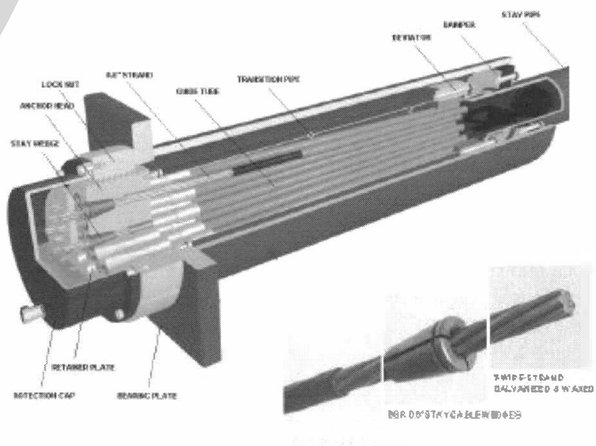

Fig. 3: Proprietary parallel-strand stay system.

A proprietary parallel-strand system, deemed to be most suited for site assembly and strand-by-strand installation, was selected for this project. Each of the high-strength 0.6"-diameter steel strands is individually secured in the anchor-head by high quality three-piece stay cable wedges. The anchor head is threaded and equipped with an adjustable lock-nut.

The stay cable external HDPE sheath has a yellow layer co-extruded with the inner black HDPE. The stay sheath will remain non-grouted thus allowing for replacement of individual strands. Compared to other projects, small sheath diameters were used which will reduce the risk of undesirable sheath vibrations under wind. The helical ribs on the outer surface of the sheath in combination with the specially designed elastomeric dampers address the wind-rain vibration problem and eliminate the need for secondary ropes. The stay cables are protected by four barriers against corrosion: Galvanization, wax and tightly extruded high density polyethylene coating of each individual strand plus the encapsulating HDPE stay sheath of the entire strand bundle. In the area of the anchorage zone, where the strand coating is locally removed to allow the gripping of wedges, special lithium grease is injected at each strand.

2.3 Dedicated Anchorage Test

The full-scale test on a 73-strand anchorage specimen was carried out in accordance with the relevant PTI Recommendations. The results were extremely satisfactory and exceeded the specified requirements for stay cable systems. The key parameters are the robust design and the high quality of the wedges.

Fatigue Test Result: no wire breakage recorded compared to the allowable number of 10 breakages.

Ultimate Tensile Test Result: 19'004kN (= 98% of UTS) peak static load was reached compared to the minimum required 18'412kN (=95% of UTS). No failure in any of the anchor parts was observed.

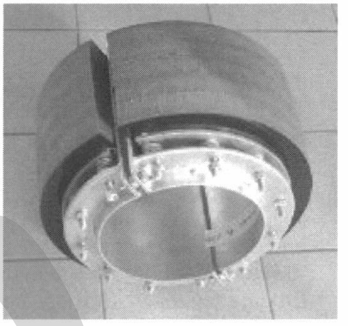

Fig. 4: Elastomeric damper assembly.

3. STAY CABLE DAMPING DEVICES

Specially developed dampers were installed on the longest main span stays. The dampers have to provide an equivalent viscous damping ratio which varies between 0.15% for M11 and 0.48% for M28 as stipulated by the designer. Extensive laboratory testing of the elastomer material for $2X10^6$ cycles proved its efficiency for the requested damping ratio. Actual measurements from site tests further confirmed the suitability of the dampers.

4. STAY CABLE INSTALLATION

The stay cables are site assembled without compromising the quality of the end product. By using a proprietary installation method, all the strands for a particular stay were cut to identical length. The cutting accuracy was 1/10'000 of the total length, whereby the difference between the individual strands was less than 4mm, resulting in a variation of 1/50'000 on a 200m long strand.

The strand installation into the pre-erected and rather snug HDPE pipes is carried out strand-by-strand, utilising custom made high speed pulling equipment.

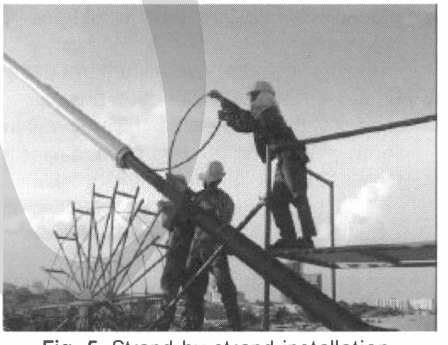

Fig. 5: Strand-by-strand installation.

The strands were tensioned to a predetermined stick-out length by single strand stressing jacks. Experience showed that stays could be tensioned to the exact predicted load, and it was further demonstrated that the strand forces are within a range of 1.5%, compared to the PTI standards which allow up to max. 2.5%. This confirmed that the stressing to length is accurate and superior to the commonly used method of stressing to equal force by means of a reference load cell on a master-strand.

5. CONCLUSION

The project is an excellent example that a carefully evaluated stay cable system in combination with the use of advanced installation methods are inseparable and essential for a rapid deck erection progress. The 300m long main span was constructed in free cantilever erection within only 5 months. This achievement proved the efficiency of the proprietary stay cable technology and applied installation methods, which were chosen for the realization of the prestigious Rama VIII bridge.

The experience gleaned from the very long stay cables (max. length 325m) encapsulated in a complete and small diameter HDPE pipe sheath, confirms that the described proprietary cable system is particularly suitable for long span bridges. The requirements on stay cables with regard to quality and erection speed for future record breaking bridges with 1000m main-spans and above can be realised with the technology presented herein.

THE DESIGN AND CONSTRUCTION OF THE MIYAKODAGAWA BRIDGE IN THE 2ND TOMEI EXPRESSWAY

Norio Terada Toshiaki Mochizuki
Japan Highway Public Corporation
JAPAN

Katsuaki Komai
OBAYASHI Corporation
JAPAN

Sadaaki Nakamura
PC Bridge Co., Ltd.
JAPAN

Keywords: Extradosed bridge, Composite steel pipe and concrete structure, Seismic Resistant Design, Control of Deflection

1 INTRODUCTION

The Miyakodagawa Bridge is a 268-meter, 2-span continuous, PC extradosed bridge. It was the first to be completed in the 147 kilometer Shizuoka area of the 2nd Tomei Expressway. Shizuoka Prefecture is included as an area requiring fortified measures for prevention of disaster due to earthquake under the "Extremely Large Earthquake Measures Special Emergency Law". Thus, seismic resistance was an important element of the structure. There is a campground upstream and a park downstream from the location of the bridge. In addition, emphasis was placed on design that would be perceived as a landmark.

Fig.1 shows the overall general design drawing of the bridge. The main girders are supported with three towers with consideration given to symmetric and simple form. With 96.5 meters of cantilever length, this is the largest extradosed bridge in Japan.

This paper mainly reports outline of the design and construction of the superstructure.

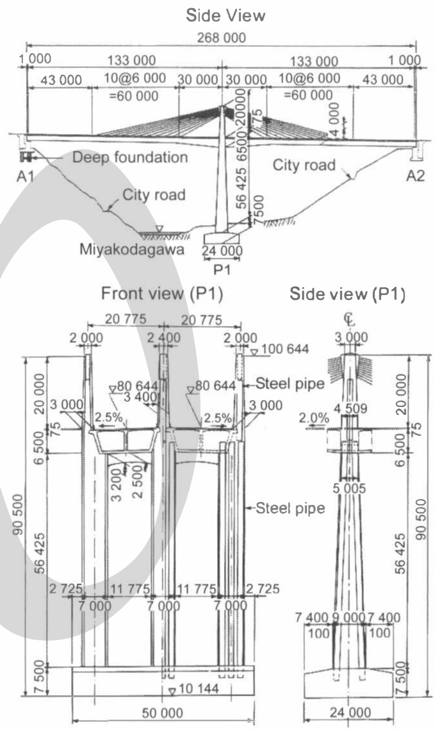

Fig.1 Overall General Design Drawing

2 DESIGN OF THE SUPERSTRUCTURE

A 3-cell type girder was planed as preliminary design according to the conventional method. In the detailed design, however, the main girders were changed to 2-cell type girder with the slab support span of 8 meters, as shown in Fig.2. The dimensions were adopted in order to achieve lighter weight, greater ease of construction and economy. The safety of the structure was verified by the design method based on 3-D FEM analysis (Fig.3).

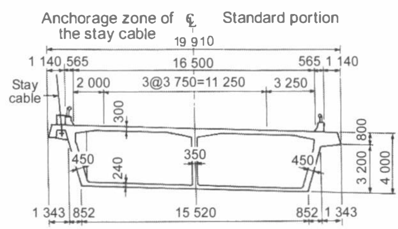

Fig.2 Cross Section

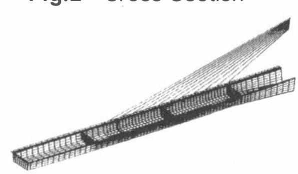

Fig.3 3-D FEM Analysis Model of the Superstructure

3 COMPOSITE STEEL PIPE AND CONCRETE STRUCTURE

As shown in Fig.4, a structure that utilizes steel pipes in place of the rebars was selected. The adoption of the steel pipe and the PC strand improves shear resistance and toughness, seismic properties and ease of construction significantly. In the case of this Bridge, the structure was not only used for the pier but also for the towers.

4 SEISMIC RESISTANT DESIGN

Since this bridge is a high level statically indeterminate structure with a high pier, dynamic analysis with respect to extremely large earthquakes formed the basis for the design.

Moreover, since the bridge has 3 piers forming rigid-frame structure, the axial force fluctuates in the event of an earthquake in the transverse direction and changes in resistance may be expected. For this reason, nonlinear dynamic analysis reflecting fluctuation in the axial force was performed in the design work.

High damping, multi-layered, rubber bearings were used as support. In order to confirm the effect of damping, the response values for the case in which damping is applied to the support was compared to for the case in which damping is not applied. The application of the damping reduced the response values for displacement, bending moment, and shear force in almost all locations. In particular, the maximum response value for shear force was kept below the resistance level in the main girder. The results of the review in the case of an extremely large earthquake in longitudinal direction are shown in Fig.5.

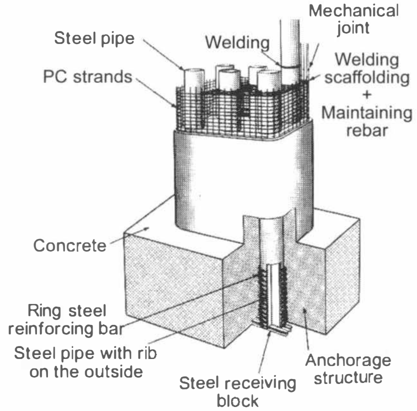

Fig.4 Composite Steel Pipe and Concrete Structure

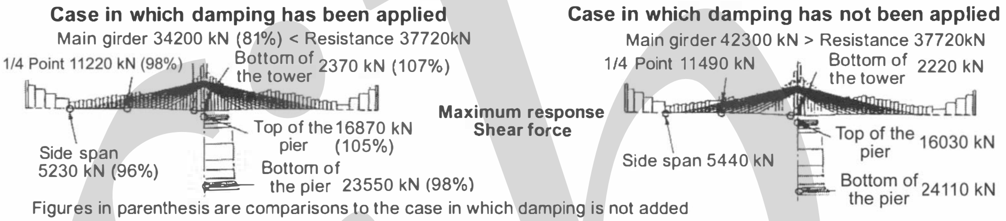

Fig.5 Effect of Seismic Mitigating Support

5 CONSTRUCTION OF THE SUPERSTRUCTURE

Election began at both sides simultaneously using travelers. The 22 stay cables for each bound were deployed to odd numbered segments with each spacing of 6 meters. The erection progressed by introducing the tensile force into the inner cables. The tensile force was applied to the two stay cables simultaneously to avoid causing unbalanced tensile force using four jacks with capacity of 5500 kN. The pump pressure was controlled at 4 locations to ensure uniform tension. To raise the precision of this operation, a digital measuring instrument was used to control the tension pressure centrally at one location.

6 CONTROL OF DEFLECTION

Control of deflection was undertaken after casting the concrete and prestressing to the stay cables by comparing the measured results with the design values. A control program utilizing a computer was produced in order to make calculations in a timely manner and accumulate data.

The factors that cause elevation error are: 1) deflection of the main girder as a result of the weight of the erection machinery, 2) deflection of the main girder as a result of temperature changes (Fig.6), and 3) displacement of the main girder in the vertical direction due to the incline of the piers. Through these 3 measures, it was possible to manage the elevation with adequate precision.

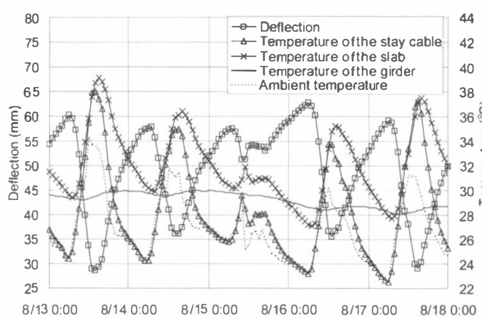

Fig.6 Results of Measurement

REFERENCE

[1] Kato: New Construction Method of Tall Bridge Piers with the Steel Pipe-Concrete Composite Structure; Bridge and Foundation Engineering, Vol. 33, No. 8, pp145 - 146, 1999

[2] Terada, Fukunaga, Mochizuki, Uehira, Komai: Design and Construction of Miyakodagawa Bridge in the 2nd Tomei Expressway; Journal of Prestressed Concrete, Japan, Vol. 43, No. 3, pp34 - 41, 2001

CONSTRUCTION OF THE LAO-NIPPON BRIDGE OVER THE MEKONG IN LAOS

Hiroshi Kikuchi
Shimizu Corporation
JAPAN

Monichiro Tsuchiya
Shimizu Corporation
JAPAN

Tomoki Nakamura
Shimizu Corporation
JAPAN

Keywords: precast segment, extradosed bridge

1 INTRODUCTION

The world's eighth longest Mekong River flows through six countries in Southeast Asia. Outside of China, prior to the present bridge construction at Pakse in southern Laos, there had been only two other bridges in operation across the Mekong. Now there is a third bridge, the Lao-Nippon Bridge, commonly known as the Pakse Bridge, constructed with Japanese grant aid. (**Fig. 1, 2**)

The Lao-Nippon Bridge is spanned by prestressed concrete box girder and composed of 384 precast segments. Its total length is 1380m and maximum span length is 143m.

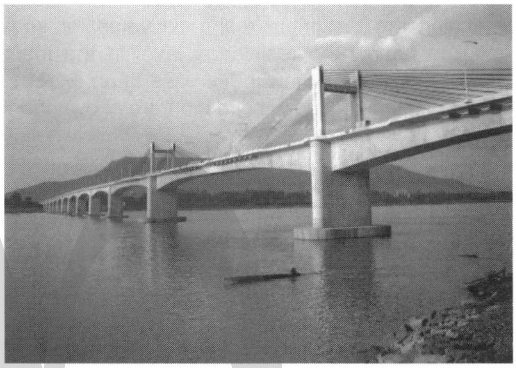

Fig. 1 Lao-Nippon Bridge

2 PAKSE BRIDGE PROJECT

Since Laos has no railway system, transportation greatly relies on its road networks. Until completion of the bridge, the only way for road traffic to cross the Mekong at Pakse had been by means of its limited number of ferries, and then only during the daytime.

The purpose behind the construction of the Lao-Nippon Bridge is firstly to further open this part of southern Laos to tourism, secondly to stimulate agricultural development in the nearby Bolovens Plateau, which is one of the country's most fertile areas, and thirdly to create an integrated road network within the region and with Lao's neighbouring countries.

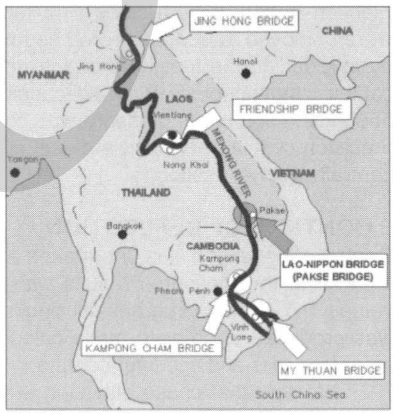

Fig. 2 Project Locations

3 STRUCTURAL OUTLINE OF BRIDGE

The Lao-Nippon Bridge is spanned by prestressed concrete box girder, 11.5 or 14.3m wide at the top deck and varying in depth between 3.0 and 6.5m. Spans are mainly composed of 384 precast segments of 2.5 or 3.5m in length. Structurally, there are four continuous rigid frame bridges including an extradosed (cable-stayed with small pylons) bridge separated by hinges at mid-span. (**Fig. 3**)

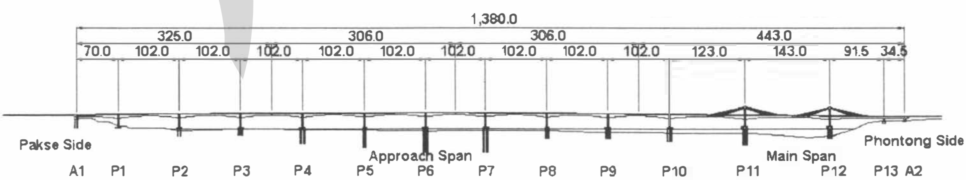

Fig. 3 General Arrangement

4 CONSTRUCTION OF BRIDGE

4.1 The Mekong and its Nature

Laos has a year of two seasons. Water level of the Mekong varies by up to 12m through the year in Pakse. (**Fig. 4**)

Construction of the bridge substructure was undertaken only in the dry season. The erection of the superstructure was executed using the method not affected by the water level.

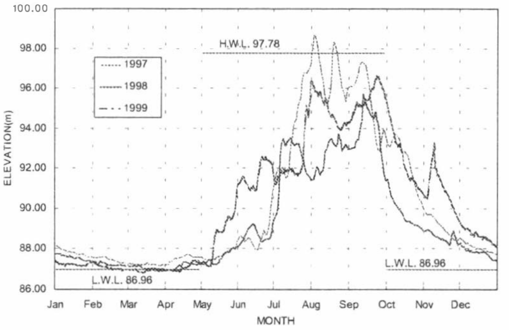

Fig. 4 Water Level of Mekong

4.2 Substructure Construction

The bridge is founded on 126 steel-cased bored piles with a diameter of 1.5m. Application of an appropriate drilling rig to the different soil conditions was a way to the early completion of piling work.

In total, 426 precast panels, forming the soffit and the sides of the pile caps, allowed for rapid construction of the pile caps. All of the piles, pile caps and lower 10m of piers were completed in the first dry season of the construction period.

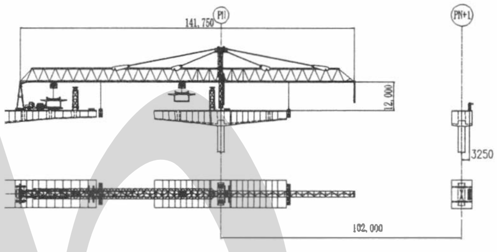

Fig. 5 Launching Girder

4.3 Superstructure Construction

Space is not at a premium in Laos. Precast segments were produced on a long line bed. The bridge has curved spans at both ends with straight spans in between. A total of 48 segments of curved spans and 336 segments of straight spans were made by the short line and long line methods, respectively. In the conventional long line method, the formwork is moved and the old segment remains stationary on the long line bed. For the curved span segments, a short line application to the long line bed was adopted, whereby the formwork is moved and the old segment is rotated in place on a transfer cart. (**Fig. 6**)

After the construction of cast-in-situ pier heads, precast segments were placed by the balanced-cantilever method using a launching girder. (**Fig. 5**) The shortest completion time for a single approach span was 14 days.

Main span pier has 21 pairs of segments including 9 pairs of stayed segments. For the main span erection, the launching girder was extended from 141.75m to 156.75m and its structure was changed from a two- to three-point supported one. A temporary pier was constructed midway between P11 and P12. (**Fig. 7**)

Stay cables run through saddles in the tower. Saddle frame unit was prefabricated at a factory for the rapid installation on site. Strand bundles were assembled on the previously erected spans. These were then transferred to the tower bottom by the cableway and erected using winch.

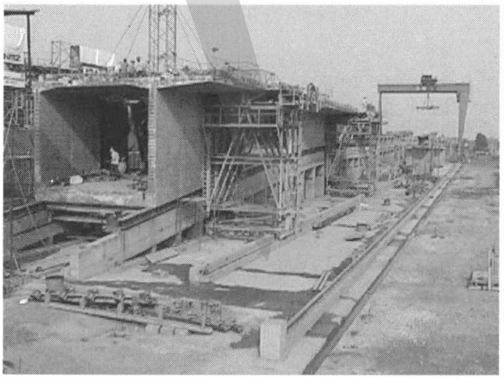

Fig. 6 Segment Production Yard

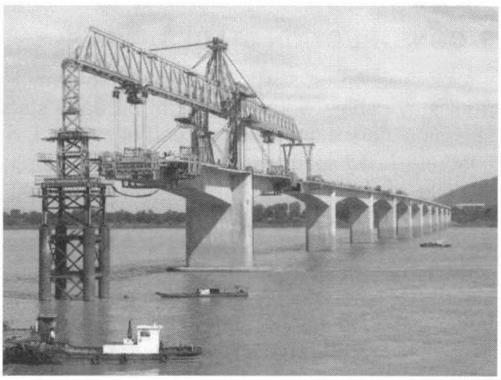

Fig. 7 Segment Erection of Main Span

CABLE STAYED ARCH BRIDGE
SERVICE STATE DEFINITION BY STAY CABLE AND HANGER TUNING

Pascal Klein, Klein Engineering – BBR Systems, Zurich, Switzerland
Michael Yamout, PJSI Consultant, Kuala Lumpur, Malaysia
Dr. Pietro Brenni, BBR Systems, Zurich, Switzerland

1 INTRODUCTION

Putrajaya is the new Administrative Centre of the Federal Government of Malaysia. It is the new 'Intelligent Garden City' erected on green grass and is designed to host more than 300'000 people. The 'Core Area' will be surrounded by a huge artificial lake which is bridged by distinctive structures. The government explicitly wanted to erect important landmarks to emphasize the leading spirit of this location. The subject of this paper is Bridge 8 – Jambatan Seri Saujana – the world's first cable stayed arch bridge handed over in June 2002 just after inundation of the main part of the lake.

2 DESCRIPTION OF THE STRUCTURE

Bridge 8 is a combination of an overhead inclined arch structure and a 'classical' twin-pylon cable stayed bridge. The main span is 300 m and the sword shaped pylons are 73.00 m high. The centre spine of the 32.00 m wide deck is suspended to a uni-planar stay cable arrangement, whereas its wings are supported by the arch hangers (Fig. 1).

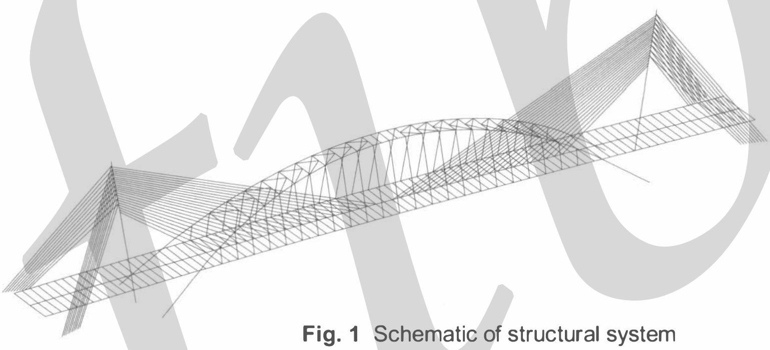

Fig. 1 Schematic of structural system

The structure is therefore highly statically indeterminate in the longitudinal and lateral directions. This provides a unique opportunity for engineers to actively impose a particular service state condition being able to manipulate the main structural members – stays and hangers – on site.

3 CONSTRUCTION STAGES

Deck erection on scaffolding and climb-forming of the pylons took place simultaneously. Two initial front stay cables were installed in an early stage to stabilize the pylons. Stay cable installation and stressing started once a major part of the deck was cast. The initial cable tensioning compensated the concrete dead load. Therefore, the supporting towers were released to a small stabilizing force. Casting of the deck box girder was completed with the exception of the closing pour. The centre portion was only closed after completion of the arch to allow for creep and shrinking of the concrete under prestressing.

For logistic reasons the assembly and welding of the arch sections was pushed ahead on the north side, whereas the cable installation and stressing took place on the southern part of the bridge. Once both operations reached the centre, teams were switched to complete the opposite part of the work.

In October 2001 arch assembly and cable erection were finished. Stay cables were stressed to compensate the concrete dead weight. The arch was locked but still resting on the temporary supports. The hangers were installed but not yet tensioned.

A few hangers could be stressed to an initial force after partial release of the arch supports. They acted as temporary arch stabilizations during complete release and dismantling of the arch supporting towers. After removal of all temporary arch supports and completion of hanger tensioning the deck support forces were expected to be almost zero.

By end of the year 2001 all temporary supports were dismantled and the inundation of the lake began. An initial intensive monitoring period lead to the conclusion, that the deck alignment could be improved by fine tuning of the front stay cables.

4 STAY CABLE AND HANGER STRESSING SEQUENCE

The stay cable installation and stressing took place under the following circumstances:
- The pylon was completely erected and kept in the 'zero position' by one initial front stay,
- the deck partly cast, supported on temporary towers,
- the arches were under construction, whereas their self weight and the temporary towers were supported by the deck. The statical system according to Fig. 2 was adopted.

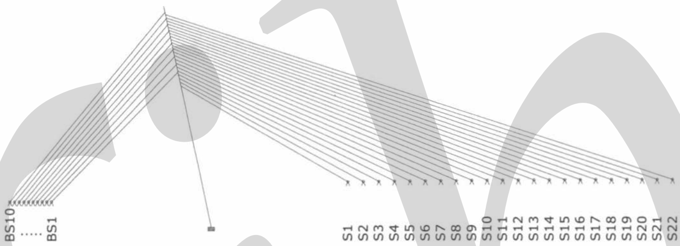

Fig. 2 Cable designations

The tensioning of the hangers was executed with the below premises:
- The deck and both pylons were completed, the arch was erected and welded,
- the closing pour of the deck was cast,
- all temporary arch supports were released and a few hangers (H4/H8/H12/H16/H20) were stressed to a low level to prevent arch instability. The statical system according to Fig. 3 was adopted.

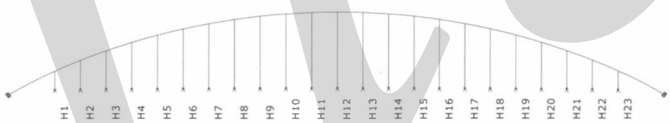

Fig. 3 Hanger designations

Due to the stay and hanger stressing operations the following situation was expected:
- 92% of the deck dead load supported by the stay cables,
- 8% of the deck dead load supported by the hangers,
- temporary supporting towers completely released,
- deck in position to receive premix, parapet and other superimposed loads before reaching the final design alignment.

5 DEFINITION OF SERVICE STATE

The core question to this structure is 'what is the contribution of the arch versus the cable stayed bridge?'. The load distribution given by a simple elastic analysis by the computer program is definitely not what we were looking for. The active tensioning of all cables and hangers gave us the chance to define the load participation as well as the alignment of the various structural members.

Several scenarios were investigated before the preferred distribution was found. The alignment, all cable and hanger forces as well as the stress situation in the deck (longitudinally and laterally), arch and pylons had to be verified.

DESIGN AND CONSTRUCTION OF THE HIMI BRIDGE – EXTRADOSED BRIDGE WITH CORRUGATED STEEL WEB –

Yoshifumi Maeda, Yasuo Imaizumi
Japan Highway Public Corporation

Akio Kasuga, Koji Tazoe
Sumitomo Construction Co.,Ltd

Keywords : extradosed bridge, corrugated steel web

1 INTRODUTION

The major distinguishing feature of the Himi Bridge (tentative name) is its composite configuration, using a corrugated steel web in the main girder. This is the first bridge in the world to use this mode for suspension structure. (Photo. 1)

This paper will give an overview of the design and construction of this bridge, with particular focus on the use of a new extradosed cable anchorage structure for extradosed bridge with corrugated steel web.

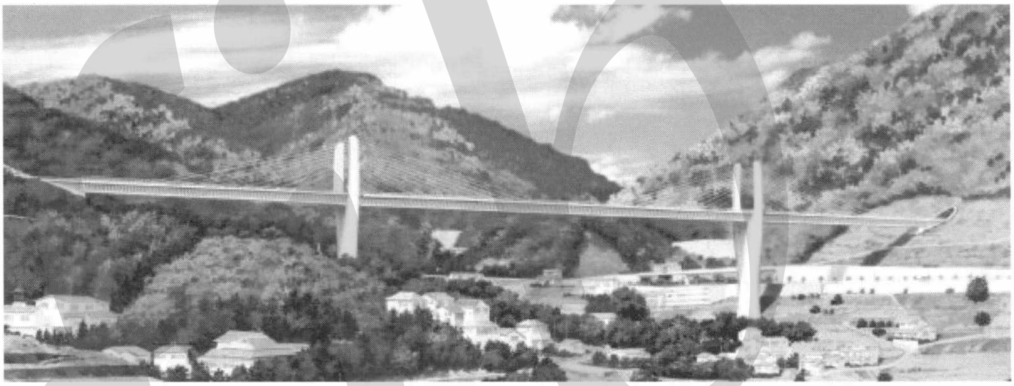

Photo. 1 Himi bridge

2 DESIGN

2.1 Design concept

From the initial planning stages, priority has been given to structural form, aesthetic appearance and harmony with the environment in the design of this bridge, and "durability" and "lightweight" were used as watchwords. The result is the world's first extradosed bridge with corrugated steel web.

Accordingly, in the design of this bridge, the focus for selection of the height and section shape of the main girders has been on economy, ease of construction and streamlined configuration, and it was necessary to achieve a configuration that was as slender as possible with the objective of reducing the weight of the girders, and based on aesthetic appearance as well. For this reason, the following were established as preconditions for the design.

2.2 Detailed extradosed cable anchorage

The precondition for determination of the extradosed cable anchorages for the main girders is that the vertical component of the extradosed cables must be transmitted efficiently to the main girders and that little additional stress should be applied to the corrugated steel web, and that the weight of the main girders themselves should be reduced. The steel diaphragm, a configuration in which both vertical and horizontal ribs were reinforced with steel members, was intended to be both more rational and more lightweight.

Figure 1 show a view of the main girder section for this bridge and the detailed structure of the interface near the cable anchorage.The corrugated steel webs were joined using single plane lap splice fillet welding. Furthermore, the method used to join the concrete slab and corrugated steel webs was an angle dowel structure using flange plates. Accordingly, the corrugated steel webs and diaphragm were fused into a single unit through complete joint penetration welding on the same web surface, so the vertical component of the extradosed cables and the shear force of the main girders could be transmitted smoothly.

As the mechanism by which extradosed cable force is transmitted, the structure is one in which vertical force is transmitted from the stay cable anchorages through the concrete to the diaphragm. When this occurs, it is predicted that localized stress will be produced at the joints between the corrugated steel web and the concrete short web and near the corners of the corrugated steel plates and the diaphragm. Accordingly, a vertical FEM analysis will be conducted to determine local stress, and after the detailed structure of the joints has been finalized, safety will be confirmed through experimentation and then the results will be reflected in the actual bridge.

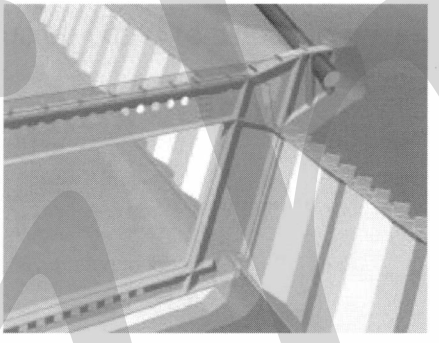

Fig.1 Bird's-eye view of extradosed cable anchorage

3 CONSTRUCTION

A major feature of this bridge is the fact that the use of an ultra-large form traveler (10000kN·m capacity) made it possible to use a standard segment length of 6.4 m, enabling the number of cantilever blocks to be reduced and shortening the work time. This form traveler was twice as large as ordinary ones, and it enabled the number of segment to be reduced by half, greatly contributing to shortening the amount of time required for the work and constituting a very economical method of construction as well.

4 CONCLUSION

The Himi Bridge is the world's first bridge to combine the use of corrugated steel web structure with the extradosed mode whose use has developed rapidly in Japan in recent years. A variety of new trials are being implemented in the design and construction of this bridge. In February 2002, a 1/2 scale model test are planned in order to verify and confirm the safety of the structure .

Construction of the bridge superstructure is expected to begin in earnest in April 2002. In the midst of these new efforts, issues linked to the expanded application of extradosed bridges will be resolved, and technical innovation efforts aimed at further development will be conducted, in preparation for the completion of the bridge at the end of 2003.

THE PRIMARY DESIGN OF HYBRID SYSTEM OF CABLE-STAYED PRESTRESSED CONCRETE BRIDGE

T.Ohura, K.Morohashi & S.Nakai
P.S.Corporation, Japan

T.Tanabe
Nagoya University, Japan

Keywords: cable-stayed suspension PC

SUMMARY: The span of cable-stayed prestressed concrete bridges combined with steel girder has been longer than 800m such as Tatara Ohashi and Normandy Bridge. But it is not expected that it will be longer than 2000m because of structural and economical problems. On the other hand, there are many steel suspension bridges with long span more than 1000m, and furthermore, there are some projects to construct bridges with very long span at straits in Japan. In such projects, it is said that their spans are more than 2000m. In this paper, the authors propose a hybrid system of cable-stayed prestressed concrete bridge and steel suspension bridge, which enables us to construct bridges with longer span and is expected to have an economical advantage compared with ordinary steel suspension bridge.

1.CONCEPT OF HYBRID SYSTEM OF CABLE-STAYED AND SUSPENSION BRIDGE

The figure of concept of hybrid system bridge is shown in Figure 1. The girder near pylons is supported by stayed cables, and another girder is supported by hanger cables.

The bridge shown in Figure 2 is now under construction in Japan.

Hybrid system of cable-stayed bridge and suspension bridge has many structural features compared with ordinary cable-stayed bridge and suspension bridge. The typical features are shown below.

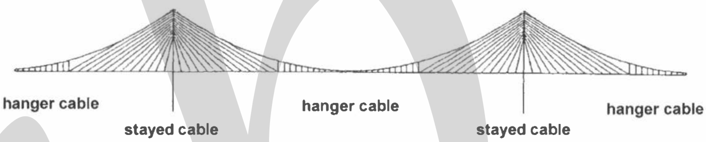

Fig.1 Concept of hybrid system bridge

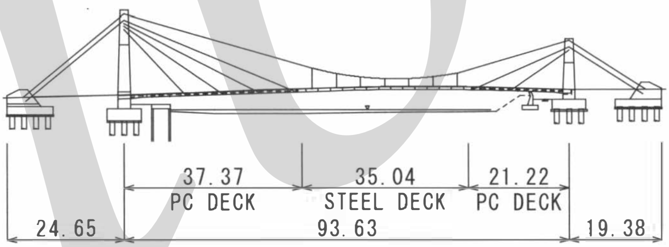

Fig.2 Under construction bridge in Japan

- compared with cable-stayed bridge
(1) Buckling stability improves because the axial force in the girder decreases by reducing the number of stayed cable.
(2) It leads having long span because of the above-mentioned reason.
(3) It has advantages for cable erection and vibration problems because the length of stayed cables are short.
(4) The height of pylons can be short by reducing the number of stayed cables.

- compared with suspension bridge
(1) Aerodynamic stability improves because the rigidity for deformation of the girder increases by having the stayed cables.
(2) It enables to lessen the tension force occurring in the main cables because its share for loads decreases by having the stayed cables.
(3) It enables to lessen the diameter of main cables because of the above-mentioned reason.
(4) It has an advantage for its anchorage because of the same reason.

2.TRIAL DESIGN

2.1.models

The trial design for a hybrid system bridge was performed to confirm the structural characteristics and to compare with ordinary cable-stayed prestressed concrete bridge and steel suspension bridge. In this trial design, the authors remodeled from actual steel suspension bridge named Hakucho Ohashi into hybrid system bridge. Hakucho Ohashi has a 720m length of center span, a 2.5m height of girder, and a 72m height of pylon.

In case of remodeling into hybrid system bridge, the rate of stayed cable section and hanger cable section is one of the important issues. In this design, the authors set up the rate to 60:40 in center span. How to set up it properly is a subject which should study later. How to set up the height of pylon adopted 0.2L (L: span length) which is general height for cable-stayed bridge. Therefore, the height of pylon is 86m (L=432m). The material of pylon was changed from steel for Hakutyo Ohashi to reinforced concrete.

Cable-stayed prestressed concrete bridge was also designed to compare with steel suspension bridge and hybrid system bridge. It is not realistic to set up so that girder is composed of prestressed concrete entirely. Therefore, the rate of prestressed concrete and steel is the same as that of hybrid system bridge. It is a cable-stayed prestressed concrete and steel composite bridge. The height of pylon is 145m which is equal to 0.2L (L=720m).

2.2.estimated material amount and cost

The material amount of hybrid system bridge and cable-stayed prestressed concrete bridge are estimated based on the results of the trial design. They are compared with the actual amount of steel suspension bridge, Hakutyo Ohashi, in Table 2.

Table.2 Comparison of estimated amount of materials and costs

		unit	steel suspension bridge	cable-stayed PC bridge	hybrid system bridge
girder	concrete	m^3	---	17200	17200
	steel	kN	111300	37400	37400
cable	main cable	kN	35600	---	16100
	hanger cable	kN	2400	---	100
	stayed cable	kN	---	20700	15800
pylon	concrete	m^3	---	14360	8860
	steel	kN	53100	---	---
cost		%	100	92	93

3.CONCLUSIONS

The authors proposed a new type of bridge which can have long spans. It is a hybrid system of cable-stayed prestressed concrete bridge and steel suspension bridge. The conclusions for this study are describes below.

(1) This bridge does not have complex structural characteristics, even if the different type of bridges, cable-stayed bridge and suspension bridge, are combined.

(2) In hybrid system bridge, the amount of main cables and hanger cables reduced largely compared with steel suspension bridge. The total amount of cables was 84% for steel suspension.

(3) The cost of hybrid system bridge was 7% lower than that of steel suspension bridge. That was almost the same as that of cable-stayed prestressed concrete bridge.

(4) Hybrid system of cable-stayed prestressed concrete bridge and steel suspension bridge is very attractive, because it can have very long spans compared with cable-stayed prestressed concrete bridge, and have an economical advantage for steel suspension bridge.

REFERENCES

- R.Walther & D.Amsler, Hybrid Suspension Systems for Very Long Span Bridges, A.I.P.C.-F.I.P., 1994
- K.Nomura et al, Feasibility Study of the Dishinger Type Bridge, Journal of Structural Engineering, 1994 (in Japanese)
- N.J.Gimsing, Cable Supported Bridge Concept and Design, 1994 (in Japanese)
- N.Narita et al. Applicability of Dishinger-Type to Ultra-Long Span Bridge,
- H.Takemura et al. A study on a hybrid system of cable stayed prestressed concrete bridge and steel suspension bridge, Proceedings of The 11th Symposium on Developments in Prestressed Concrete 2000 (in Japanese)

RESEARCH AND DEVELOPMENT OF AN INNOVATIVE PC BRIDGE WITH LARGE ECCENTRIC EXTERNAL TENDONS

Thiru Aravinthan
University of Southern Queensland, Australia

Hiroshi Mutsuyoshi
Saitama University
Saitama, Japan

Yuzuru Hamada
DPS Bridge Works Co., Ltd.
Tokyo, Japan

Muneki Watanabe
Mitsui Construction Co., Ltd.
Tokyo, Japan

Keywords: external prestressing, flexure, continuous girders, linear transformation, precast segments

1 INTRODUCTION

External tendons are widely being used in prestressed concrete (PC) bridges recently. A further extension on the use of external tendons is to place them at large eccentricities. In this concept, the compressive forces are borne by concrete and tensile forces by external tendons, thus taking advantages of both materials effectively [1]. In addition, by extending this concept for continuous girders, the structural performance can be further improved. Considering the above concept, an innovative continuous girder bridge with large eccentric external tendons was developed. In this structure, the external tendons are placed below the girder in the midspan region by means of steel struts, the function of which is similar to a truss. At the intermediate support region, it is placed above the bridge deck. The tendon in the support region could be arranged in a fin-shaped web member or a short tower similar to an extradosed bridge.

To study the fundamental behavior of such bridge structures, series of tests were conducted using two span continuous model girders by changing the tendon layouts and loading arrangements. Further, the behavior of precast segmental girders was verified by model tests, in view of enhancing the methods of constructions. The behavior of such girders under shear loading was also investigated using model girders. Based on this research and development, a two span continuous PC bridge was designed and constructed for a pedestrian bridge, first of its kind in the world. The combination of subtended cables in the span regions and fin-back type concrete web at the intermediate support makes this bridge a unique one with aesthetically pleasing appearance. The fatigue characteristics of the unbonded external tendons and the steel strut members were verified using scaled model tests. A vibration test on the completed bridge was carried out to verify the serviceability of this bridge under live loads. This paper describes the research and development of this innovative bridge, highlighting the main findings of the above tests.

2 EXPERIMENTAL INVESTIGATION USING MODEL GIRDERS

A series of test was carried out on two span continuous monolithically cast girders consisting of different tendon layouts to obtain the fundamental mechanical behavior of such structures (Fig. 1). The main objective of this investigation was to verify the flexural behavior of continuous girders with external tendons provided according to the law of linear transformation. It was found that the beams with linearly transformed tendon profile show the same flexural behavior [2]. This enables the designer to take advantage of arranging the external tendon layout freely, depending on the site conditions. The concept of large eccentric external tendons can be also extended to precast segmental construction.

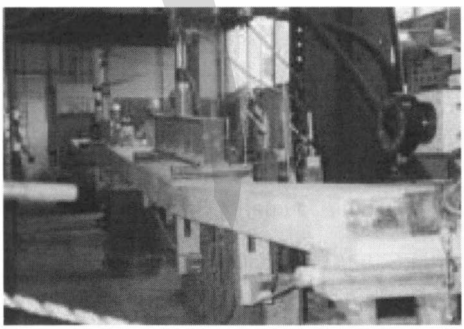

Fig. 1 Flexural test setup

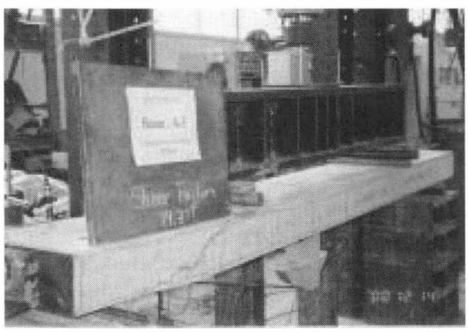

Fig. 2 Shear test setup

Fig. 3 Vibration test on bridge

Fig. 4 Completed view of the bridge

Experimental investigation was carried out on precast segmental beams with large eccentric external tendons showed that precast segmental specimens behave nearly the same as the monolithically cast ones. One of the concerns raised was the shear capacity of this structure, since the girder height is considerably reduced. As such, the shear characteristics of this structure were investigated by carrying out model tests (Fig. 2). It was found that the shear capacity of the girder with large eccentric external tendons is much higher than that of the conventional girders.

3 APPLICATION IN AN ACTUAL BRIDGE

The research and development discussed in the previous sections led to the design and construction of a prototype bridge in Mori Town of Hokkaido. This is a pedestrian bridge constructed as a monument structure, crossing the Torisaki River, as part of the town improvement plan. Considering the site conditions, the bridge was designed as a two span continuous girder with unsymmetrical span lengths. Due to the nature of this structure, several challenges were encountered during the design and construction stages. The structural analysis was carried out considering the bridge as a 2D framed structure, incorporating the cross-sectional variation along the bridge axis. However, considering the complexity of the structure, it was necessary to verify the validity of the assumptions made in the frame analysis. A 3D FEM model was developed to check stresses in the fin-shaped web and the effect of skew in the bridge. Reasonably good agreement was found between the results of the 2D-frame analysis and 3D-FEM analyses, indicating that a simplified 2D frame analysis could be used with good accuracy for practical design, with appropriate sectional properties incorporating the varying cross-section. In view of obtaining the fatigue durability of the external tendons and the strut member, a fatigue test was conducted. This test was done on a system consisting of 7S15.2 mm (SWPR7B) multi-unbonded tendon. The result of this fatigue test confirmed that the multi-unbonded external tendon used in this bridge had sufficient fatigue durability. After completion of construction, a vibration test and simulations under live loads were conducted on the actual bridge in order to check the vibration characteristics of this bridge (Fig. 3). It was found that even under the worst case of simulation, the amplitude of vibrations was within the accepted limits.

4 CONCLUDING REMARKS

An innovative prestressed concrete bridge with large eccentric external tendons was developed. Based on this research and development, a two span prototype was constructed for a pedestrian bridge. Due to the nature of this structure, several challenges were encountered in the design and construction, which were solved successfully by the use of appropriate technology. Finally, the authors believe that the proposed bridge would pave way to a wider use of external prestressing in the construction industry, leading to improved structural performance as well as cost effective structures.

REFERENCES

[1] Mutsuyoshi, H.: State-of-the-Art Report on External Prestressed Concrete Bridge with Large Eccentricity, Concrete Journal, Vol 38., No12., pp. 10-16, 2000. (in Japanese)

[2] Aravinthan, T., Mutsuyoshi, H., Hamada, Y. and Watanabe, M. : Experimental Investigation on the Flexural Behavior of Two Span Continuous Beams with Large Eccentricities, Transaction of Japan Concrete Institute, Vol.21, pp. 321-326, 1999.

DESIGN AND CONSTRUCTION OF THE OIDAIRA VIADUCT –THE LARGEST BRIDGE PROJECT IN JAPAN USING THE INCREMENTAL LAUNCHING METHOD AND ENTIRE EXTERNAL POST-TENSIONING TENDONS–

Yoshinobu Ishikawa Toshio Yokoyama
Oriental Construction, Kawada Construction and Zenitaka Joint Venture

Masatoshi Takeda Norio Terada
Japan Highway Public Corporation
Shizuoka Construction Bureau

Keywords: Incremental Launching method, external tendons, concrete rib, high strength concrete

1. INTRODUCTION

The OIDAIRA viaduct in the New TOMEI Expressway is 833 m long, and consists of thirteen continuous prestressed concrete box girders. An incremental launching method was employed. The girders were launched from the bridge abutments at both left and right ends of the bridge. The total launching length of 490m from the one side and the each launching length of 64m without temporary bents is the greatest in the application of incremental launching method in Japan.

All tendons are externally placed except for temporary tendons necessary during construction in order to reduce the dead load and make inspection and repair of tendons easier from the durable point of view.

The followings are characteristics of this bridge.

① incremental launching method
② whole external tendons of 27S15.2
③ high-strength concrete(σ ck=50N/mm^2)
④ long cantilever slab with ribs
⑤ isolated bridge with isolation bearing
⑥ shortening the construction cycle stroke by applying prefabricated reinforcement

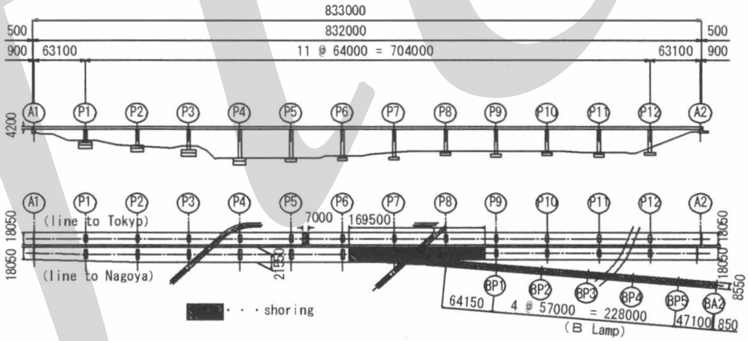

Fig.1 General view

2. OUTLINE OF EXTERNAL TENDONS 2. OUTLINE OF EXTERNAL TENDONS

In order to decrease the dead weight, make construction easier and reduce the burden of maintenance, all tendons are externally placed and tensioned. This is the first application of the incremental launching method with all external tendons.

In the OIDAIRA viaduct the girder is first launched in the prefabrication yard and temporary supports without being prestressed. Just before the girder leaves the temporary supports, the tendons are tensioned between diaphragms which are located at the supports. The followings are conditions which make the application of the incremental launching method possible in this bridge with whole external tendons.

①The tendons are anchored at every two spans. As shown in Fig.3 tendons are placed almost symmetrically to the centroid to induce axial prestress which counteracts tensile stresses set up during construction. Temporary tendons during construction are de-tensioned and removed after completion.

② The span consists of three standard segments and a diaphragm segment. Three standard segments are launched one by one without being post-tensioned on temporary supports placed at every 16m. After launching the diaphragm segment tendons are placed and tensioned between diaphragms.

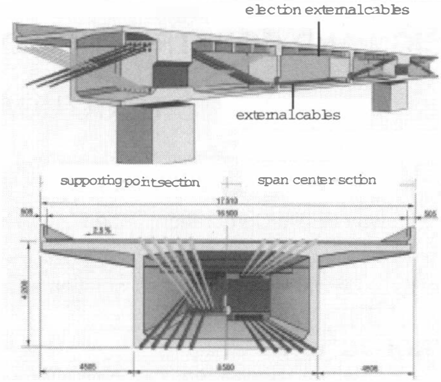

Fig.2 Layout of external cable arrangement

③Since launching and post-tensioning is conducted in the manner mentioned above, the prefabrication yard is located at a distance corresponding to seven segments from the abutment.

④Large tendon (27s15.2) is used in order to decrease the number of tendons.

3.DESIGN OF CANTILEVER RIBBED SLAB

A span of 64 m is divided into four blocks of 16 m and launched in four times. The spacing of the ribs is 4.0 m so that each block has four ribs. The number of tendons required in the center slab should be the same as the number of tendons which are needed at the root of the cantilever slab. To satisfy the condition mentioned above, the rib section of 30x80cm is employed.

Strengthening the cantilever slab with rib disturbs stress distribution at the inside surface of the web. Fig.6 describes schematically the mechanism of stress concentration at the web. In order to counteract this tensile stress there could be two ways,
1) Decreasing the bending moment induced at the web through increasing the rigidity of the upper slab or
2) Strengthening the web with rib.

A rib with the appropriate rigidity is attached at the center of the slab. Increasing the rigidity of the rib therefore reducing the deformation of the upper slab, also decreases the bending moment induced at the web.

The ribbed slabs make a single-cell-box section possible. This leads to reduction in the width of the box section, and decrease the width of the piers. Finally it can be said that this makes it possible to cut the initial construction cost of both super and sub structures.

4. INCREMENTALLY LAUNCHING METHOD

The launching equipment consists of a vertical jack, horizontal platform, sliding platform, horizontal jack, hydraulic pump and interlocking device. The New TOMEI Expressway has three lanes and the lines to Tokyo and Nagoya are separated. Consequently a large cross section of the main girder is inevitable, increasing reaction due to dead load. The dead load reaction of the line to Tokyo is 120,000kN for launching from A1 abutment and 170,000kN from A2 abutment, which requires very large launching equipment. Four vertical jacks with the capacity of 8,000kN are placed to bear the maximum reaction of 25,000kN.

5. CONCLUSION

In the construction of the OIDAIRA viaduct of the New TOMEI Expressway the safety, durability and easy construction are the aims, employing updated technologies. Much effort is also made to cut construction costs. The launching of the line to Tokyo from A1 abutment is completed and launching of both the line to Tokyo from A2 abutment and the line to Nagoya from A1 abutment is under operation. The whole bridge will be completed by 2005. The line to Nagoya has two-cell-box section because of the connection to a ramp bridge. This could make the control of the launching more difficult. To solve unknown problems higher quality control will be required.

DESIGN AND CONSTRUCTION OF THE NEW TOMEI EXPRESSWAY TENRYUGAWA BRIDGE

Yasuo Fukunaga, Masayuki Watanabe
Japan Highway Public Corporation, Japan

Masatoshi Saiki, Yuji Ishii
Sumitomo Construction Co., Ltd., Japan

Keywords: external tendon, seismic isolation design, thermal stress

1. INTRODUCTION

The Tenryugawa Bridge on the New Tomei Expressway is a 23-spans continuous prestressed concrete box girder bridge. It crosses the Tenryu River from Hamakita city to Toyooka village in Shizuoka prefecture, Japan. The overall length is 1585.5m with typical spans of 85.5m. It represents the longest continuous concrete girder bridge in Japan. And furthermore, the external cantilever prestressing system with tendons of 19 strands of 15mm diameter was adopted without precedent in Japan. In order to confirm the design for the external cantilever prestressing system, full-scale cantilever model test and other tests were carried out.

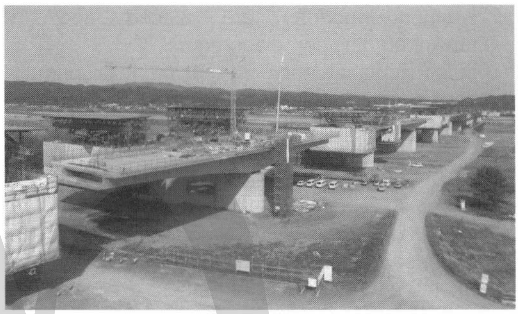

Phot.1

2. DESCRIPTION OF THE BRIDGE

Fig.1 shows a general layout of the Tenryugawa Bridge. For center spans, the span length is 85.5m and the deck height varies from 5.3m at the pier head to 2.4m at the midspan with the ordinal effective width of 16.5m, and the overall deck width of 17.14m (Fig.2).

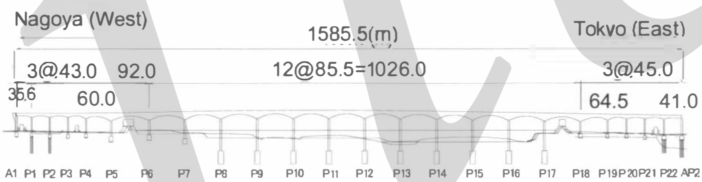

Fig.1 General layout

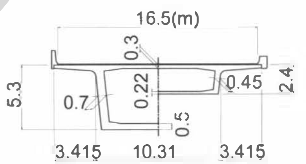

Fig.2 Half cross-sections

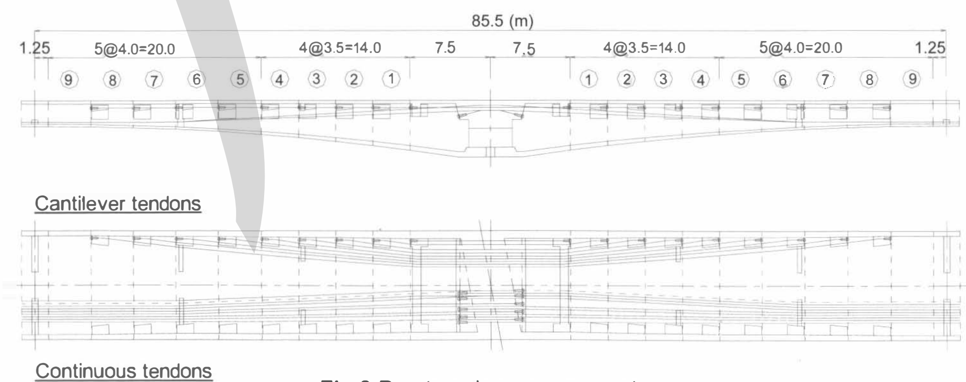

Fig.3 Prestressing arrangement

3. DESIGN AND CONFIRMATION TEST FOR THE EXTERNAL CANTILEVER PRESTRESSING

Fig.3 shows the longitudinal prestressing arrangement for center spans.

- Cantilever tendons : 2 x 9 tendons composed of 19 strands of 15 mm diameter
- Span tendons : 2 x 1 tendons composed of 27 strands of 15mm diameter
- Continuity tendons : 2 x 7 tendons composed of 27 strands of 15 mm diameter

All the above tendons are external. The strands of them are epoxy coated and belong to the 1,860MPa class. Continuity tendons are extended over two spans. As is shown in Fig. 4, the prestressing and the deviation force introduce local bending and vertical tensile stress at the anchorage and web panel. The configuration of the concrete anchorage for cantilever tendon was determined with the FEM analysis so that the local tensile stress should not exceed 3N/mm^2. The confirmation test was carried out with the full-scale cantilever model. At the prestressing of 3,470kN as the design load, no cracking was observed and measured concrete tensile stresses were under 3N/mm^2 around the anchorages. At the prestressing of 4,210kN as the ultimate load, cracks of 0.04mm and under in width were observed at the side and lower boundary of the anchorages. But the anchorage system fulfilled its function.

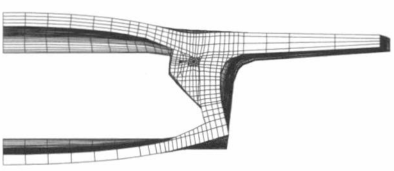

Fig.4 Deck deformation by external prestressing

4. COUNTERMEASURES FOR THE LONG CONCRETE BRIDGE

In order to improve seismic performance of the bridge, the seismic isolation system was adopted using laminated rubber bearings with lead plugs. The temperature change of 10°C cause restraint axial stress at the center spans of approximately 0.8N/mm^2. We have to take the thermal stress into consideration as design load. But, by introducing the shear deformation adjustments to the rubber bearings, the restraint axial force caused by differential creep and drying shrinkage is able to be eliminated.

5. ERECTION

The construction of the bridge is consisted of four stages as follows:(1)Cantilever erection for the center spans from Pier 5 to Pier 18, and closure to the pier head of Pier 4 and Pier 19, (2)Span by span erection from Pier Abutment 2 to Pier 19, (3)Span by span erection from Abutment 1 to Pier 4, (4) Shear deformation adjustments of the rubber bearings to eliminate the restraint axial force of the girder. On the cantilever erection, longitudinal tensile stress at the end of the cantilever slab is caused by the heat of hydration of the newly cast segments and the progress of drying shrinkage (Fig.5). The deck width and segment length have effect on the value of the local stress. Against this tensile stress, longitudinal prestressing strands of 28.6 mm diameter and reinforcing bar were installed in the cantilever slab.

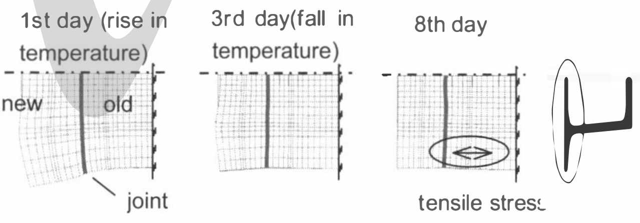

Fig.5 Thermal stress of the deck

6. CONCLUSION

(1)The external cantilever prestressing system was adopted. (2)The design for external prestressing system was confirmed by full-scale cantilever model test. (3)The seismic isolation system using laminated rubber bearings with lead plugs was adopted in order to improve seismic performance of the bridge. (4)Shear deformation adjustments to the rubber bearings are installed to eliminate the restraint axial force of the girder caused by creep and drying shrinkage.

REFERENCES

1) Roberts-Wollmann,C.L., Breen,J.E., and Kreger,M.E.: "Temperature Induced Deformation in Match Cast Segments," PCI JOURNAL, Vol.40,No.4,July-August,pp62-71,1995

CONSTRUCTION OF THE JAPAN-EGYPT FRIENDSHIP BRIDGE PYLONS

Ahamed Fouad, Chairman of board
Sanyout Shaker, Project Manager
General Authority for Roads, Bridges and Land Transport, Ministry of Transport, EGYPT

Noriaki Ishitate, General Manager, International Division
Kazuto Kamisakoda, Chief Engineer, Civil Engineering Design Div.
Kajima Corporation, JAPAN

Keywords: cable-stayed bridge, reinforced concrete pylon, slip-form method, heavy lifting

1 INTRODUCTION

With a total length of about 162 km, the Suez Canal runs between Suez, a city located at the northern end of the Red Sea, and Port Said, a city facing the Mediterranean Sea. At present, there are only a few means for crossing the canal: the road tunnel located near the southern end of the canal, and shuttle ferry services provided at several locations. Because of the rapid economic growth in Egypt in recent years, the importance of developing the Sinai Peninsula is increasing and there has been a growing demand for improving access roads. Recognizing this trend and in response to the request from the Egyptian Government, the Japanese Government agreed in 1995 to construct the Egypt-Japan Friendship Bridge as an grant aid project.

The construction of the central portion by the Japanese Government's grant aid was undertaken by a joint venture consortium comprising Kajima Corporation, NKK, and Nippon Steel. As shown in Fig. 1, the central portion is composed of the main bridge (cable-stayed bridge) with a total length of 730 m, and 560-m approach viaducts with elevations exceeding 49.5 m on both sides of the canal. This report covers the construction of the reinforced concrete pylons for the bridge.

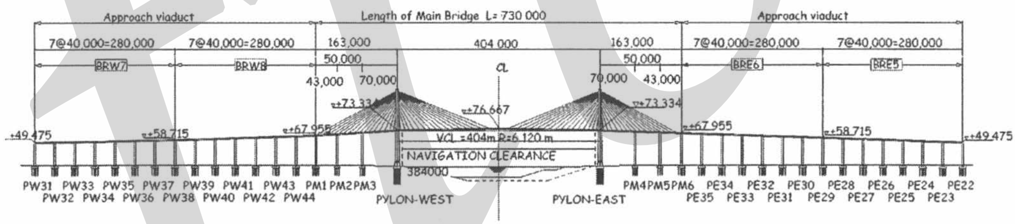

Fig. 1 Elevation view of the Japan-Egypt Friendship Bridge (unit:mm)

2 CONSTRUCTION OF PYLONS

The general view of the pylon is shown in Fig.2. The footing and pedestals were constructed by a conventional method, and the pylons were built using the slip-form method and heavy lifting system up to EL + 153.0 m. The top 3 m sections were constructed by piling up precast concrete blocks.

Construction sequence of the reinforced concrete pylons is as follows. (The elevations are given in values including a camber. For example, EL + 153.0 m includes a camber of 13 cm.)

After casting concrete for the pedestals, a tower crane, an elevator, and, a working platform on which the slip form system was assembled, were installed. The hollow pylons up to EL + 65.457 m were continuously constructed using the slip forms (Phase 1).

After installing wooden bottom forms and removing inner forms at EL + 65.457 m, the slip form system was raised up to EL + 73.970 m (Phase 2).

After lifting and fixing the support truss (assembled on the working platform during Phase 2) in position using the heavy lifting system, the lower cross beam was constructed in the order of bottom slab, side walls, and top slab (Phase 3).

Following Phase 3, inner forms were installed in position, and the construction of the pylons by slip forms was resumed. After reaching EL + 115.0 m, the inner forms were modified. The pylon construction using slip forms was then continued up to EL + 120.899 m (Phase 4).

The lifting of the slip forms was continued up to EL + 131.50 m, while removing the inner forms at EL + 120.899 m and installing them again at EL + 126.816 m (Phase 5).

After lifting and fixing the arched support truss (assembled on the lower cross beam during Phase 5) in position using the heavy lifting system, the upper cross beam was constructed in the order of bottom slab, side walls, and then top slab (Phase 6).

The slip form system was then lifted up to EL + 153.130 m (Phase 7) while constructing the pylons.

Table 1 shows the actual duration for each phase of pylon construction. Minimizing the duration for cross beam construction was most important to shorten the entire project period. This requirement was achieved by 24-hour operation with day and night shifts, which took advantage of lower labor costs in Egypt. Furthermore, the improvement of the skills of workers allowed the duration for constructing the cross beams for the western pylon to be shortened compared to that for the eastern pylon.

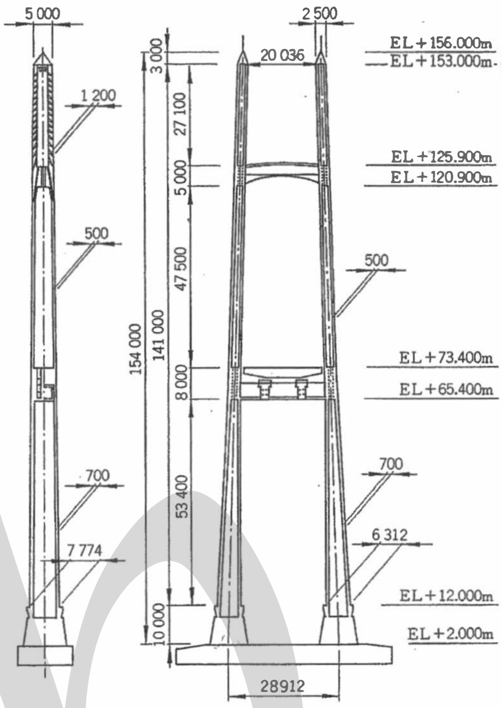

Fig. 2 Dimensions of pylons (unit: mm)

Table 1 Actual duration of pylon construction

Activity	1999 (eastern pylon)							
	5	6	7	8	9	10	11	12
Assembling slip forms								
Phase1								
Phase2								
Phase3								
Phase4								
Phase5								
Phase6								
Phase7								
Dismantling slip forms								
...... Eastern pylon	1	2	3	4	5	6	7	8
▬▬ Western pylon	2000 (western pylon)							

REFERENCES

[1] Sharaf, M., Ishitate, N., and Ishii, T. : Construction of Suez Canal Bridge (Central Portion). Bridge Engineering Conference 2000, IABSE

[2] Fouad, A., Taha, N., Shaker, S., Bakhoum, M.M., Onuma, N., Yamane, T., Ishitate, N. and Ishii,T. : Design and Construction Aspect of The Suez Canal Cable Stayed Bridge. IABSE Conference Seoul 2001

[3] Ishitate, N., Ishii, T., Okumomo, T., Saito, K., Kamisakoda, K., and Okada, K. : Construction of Suez Canal Bridge. Bridge and Foundation, Vol.35, No.11, Nov. 2001 (in Japanese)

DESIGN AND CONSTRUCTION OF THE KASHIRAJIMA BRIDGE

Kouhei Sugita
Okayama Prefecture Development Corporation
JAPAN

Masashi Yamawaki
Osaka Branch, Chodai Co.,Ltd , JAPAN

Takefumi Aramaki
Sumitomo/Aisawa Construction Joint Venture
JAPAN

Atsushi Nakamura
Sumitomo Construction Co.,Ltd , JAPAN

Keywords: composite arch, Melan arch method, main girders with few steel components

1 INTRODUCTION

The Kashirajima Bridge linking the islands of Kashirajima and Kakuijima, located in the Seto Inland Sea in Okayama Prefecture, will be Japan's largest composite arch bridge. It will have main girders with few steel components and an arch span of 218.0 m.

This bridge is distinguished by the use of an arch configuration that is extremely flat for a large arch bridge (arch rise ratio 1/8), due to the conditions at the bridge site, as well as a complex configuration with a superstructure consisting of main girders with few steel components in order to reduce weight, and high strength concrete (σ_{ck} = 50 N/mm^2) for the arch ribs.

The cast-in-place arches will be constructed using a forestay supported cantilever method from both ends. Then the 60% of the arch span was formed using a temporary steel arch,Melan. The strongest point of this Melan arch method is to close the arch quickly and to decrease the anchorage tension caused by overturning moment. Due to the site conditions in which this is an ocean bridge, plans call for the Melan arch members to be erected in a single lift using a floating crane.

Photo. 1 Kashirajima Bridge (artist's conception)

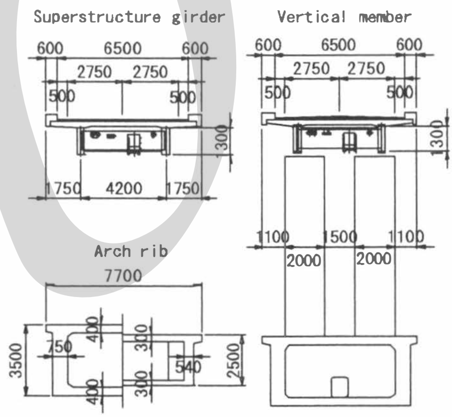

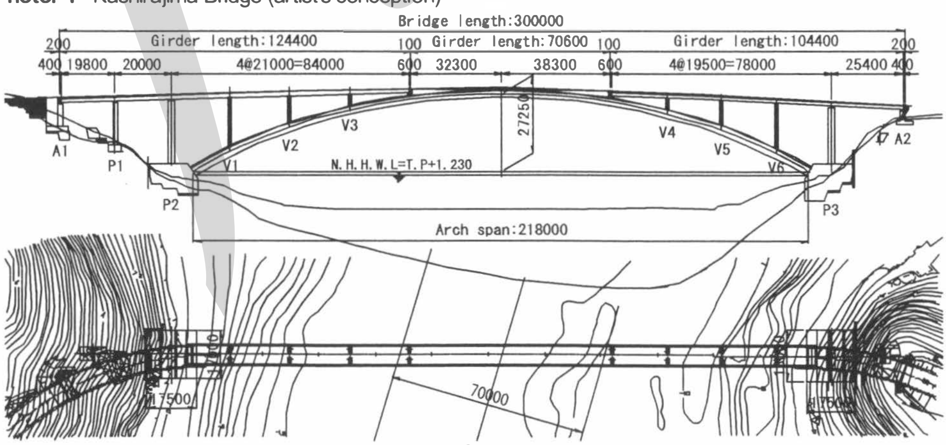

Fig.1 General view

2 CONSTRUCTION PROCEDURE

After the springing section is constructed on the supports, the form traveler for erecting the arch will be assembled.

Nine blocks will be erected from the arch ribs with the combined forestay cables and cantilever erection method, using end posts from both shores.

The remaining center section of the arch will be closed through election of Melan arch members using floating crane, and then the arch ribs will be completed through concrete jacketing construction. Subsequently the vertical members will be constructed and then the superstructure girders will be erected.

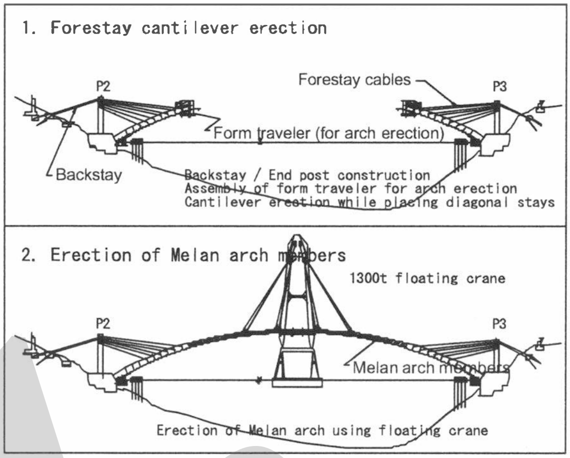

Fig.2 Construction Procedure

3 STUDY OF STATUS DURING ERECTION

3.1 Forestay cantilever erection

On this bridge, to establish a streamlined method for constructing the arch bridge, the form traveler has been modified so it would not interfere with the stay cables, and a distributed layout system will be used in which the forestay cables for all of the blocks will be erected and tensioned during the cantilever erection process.

Table 1 Comparison of arrangement of forestay cables with the forestay cantilever erection method

	Concentrated placement method	Distributed placement method
Conceptual diagram	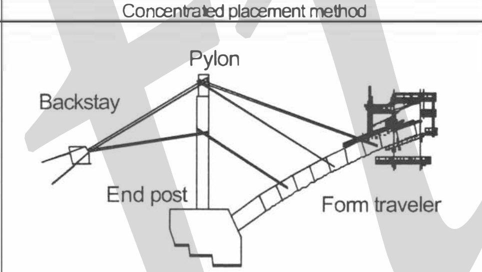	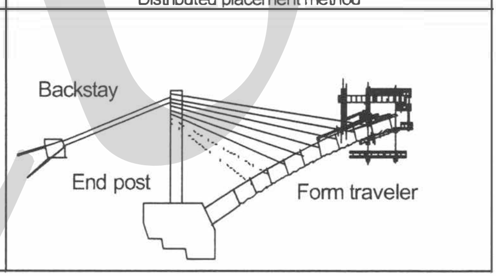

3.2 Melan arch method

Table 2 Comparison of Melan arch member placement positions

	Conventional method	New method
Conceptual diagram	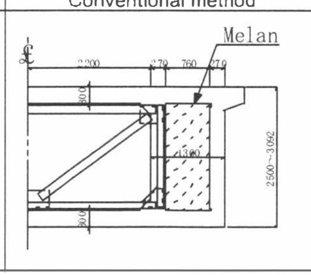	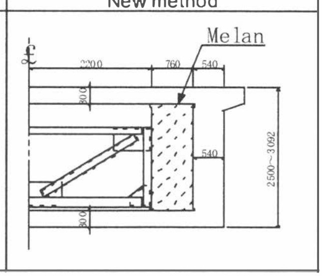

In order to close the arch quickly, the 60% of the arch span is formed using a temporary steel arch,Melan. This Melan has a length of 130.4 m with a two -rectangular box cross section. With this Melan arch method, after the arch configuration is completed, concrete jacketing is conducted. However, a study was made of ways to streamline the construction considering the configuration of the Melan arch members. On this bridge, however, as shown by the comparison in Table 2, they will be placed on the outside of the web so they can double as inner formwork.

PLANNING AND DESIGN OF THE NEW TOMEI EXPRESSWAY FUJIKAWA BRIDGE

Yasuo Fukunaga   Kouji Osada   Makoto Sadamitsu   Toshio Ichihashi
Japan Highway Public Corporation, JAPAN   Taisei Corporation, JAPAN

Keywords: steel-concrete composite arch bridge, pylon method, prestressed concrete slab with twin steel beams, jacking-up, seismic design

1 INTRODUCTION

The New Tomei FUJIKAWA Bridge, which spans over Fujikawa River, is the first steel-concrete composite arch bridge in Japan, which consists of a composite girder, RC arch rib and RC columns. The span length 265m will be the longest among all Japanese concrete bridges after completion.

The basic principles of this bridge are;

- Pursuit of rationality not only for completed structure, but also throughout the whole construction process.
- High ductility against enormous earthquake.
- Improvement of durability.

Through design and construction process of this bridge, many kinds of study, model tests, and trial and error have been carried out. Some of them are based on new structural ideas, some are design concepts, and some are advanced analysis methods. As a result, rationalization has been successfully realized under very severe condition of earthquake. Moreover, combination of advantageous characteristics of concrete and steel led to eliminate the conventional wall between two fields of arch bridge, that ae concrete arch and steel arch.

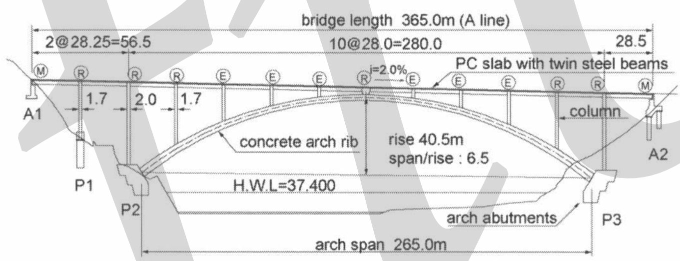

Fig.1 General view of the bridge (A line)

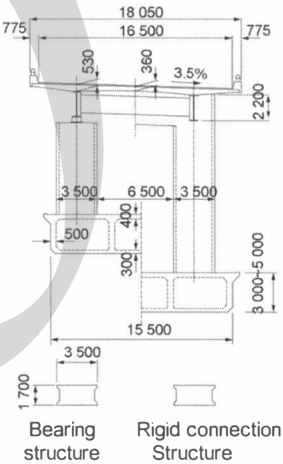

Fig.2 Standard cross-section

2 CONSTRUCTION METHOD

Basic construction method is shown in Fig. 3. Temporary pylons are located in the river, instead of on the top of end-posts, which is the conventional "pylon method". By this idea, amount of stay cables and ground anchors, that are both temporary materials, are considerably reduced. Moreover, comparing to "truss method", which is often adopted for a long span arch bridge, great amount of concrete was saved.

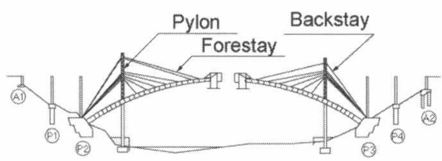

Fig.3 Pylon method

3 NEW IDEAS AND NEW TRIALS

3.1. Design of arch abutments

Concerning the stability of the arch abutment, a virtual plane perpendicular to the resultant force of "axial force from the arch rib" and "self weight of the abutment" was assumed. In order to minimize the turnover moment, the shape of the abutment was determined as such that the resultant force acts at the center of the virtual plane. As a result, total concrete volume of four abutments was about 50% reduced comparing to the conventional calculation method.

Against thermal effects due to temperature increase of mass concrete, parametric analyses were carried out by means of quasi 3 dimensional finite element method in order to determine the type of cement, thickness of each concrete layer, and amount of reinforcing bars. As a result, adoption of "Low Heat Portland Cement" led to extreme reduction of re-bar arrangements and cost savings.

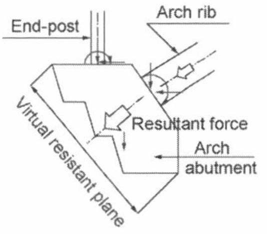

Fig.4 Check on stability on completion (virtual resisting plane)

3.2. Design of arch rib

For the construction stage, arch rib was designed as a PRC member, allowing crack width up to 0.25mm. A model test was carried out in order to make sure that the cracks close after the bridge is completed. Adding to this, when the cantilever length of the arch rib reached to the pylon position, jacking-up operation has been carried out. Vertical force of 16MN with movement of 7.5cm in upper direction was acted at the pylon position. As the result, tensile stress in the upper side of the arch rib was reduced for 5MPa at springing. By these two ideas, the amount of temporary stay cables was considerably

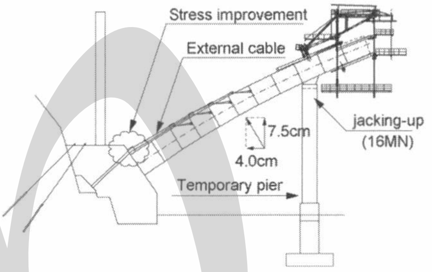

Fig.5 Conceptual view of jacking-up

3.3. Stay cables

As stay cables are limited in temporary use, we decided to allow the tensile strength up to 70% of characteristic strength of the strand. In order to assure the safety under such a high stress usage, and also for correct selection of type of strand coatings, tests were performed. Temperature changes of 11 types of specimens were measured for 2 weeks in summer under condition of exposed to weather.

3.4. Seismic design

Because FUJIKAWA Bridge is a part of most important expressway in Japan, even in case of an large earthquake, this bridge is not allowed being seriously damaged. However, it is not practical to restrict bridge behavior in elastic range under condition of a large earthquake. Therefore, elasto-plastic studies were carefully carried out in order to assure damages in the following limitations.
Not to allow yielding of the steel beams and reinforcing bar in the slab.
Only limited damages can be accepted for the arch rib and columns. (place, length and number of plastic hinges are limited)
Time history dynamic analyses adopting 6 types of waves, maximum ground acceleration of over 812 gal, were executed. Two kinds of non-linearity, that are material non-linearity and large deformation non-linearity (geometrical non-linearity), were taken into account simultaneously. These analyses were accurately done by means of "fiber model method" which has been recently developed.

Photo 1 Plan view

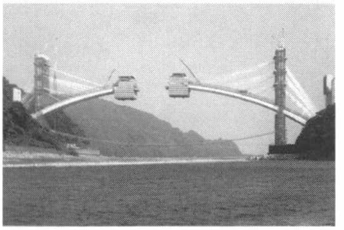

Photo 2 View of under construction

TALBRÜCKE REICHENBACH, GERMANY DESIGN AND CONSTRUCTION

Dipl.-Ing. Robert Schedler Dipl.-Ing. Dr. Dieter Pichler
FCP-Fritsch-Chiari & Partner ZT GmbH
AUSTRIA

Prok. Ing. Herwig Handler
STRABAG Österreich AG
AUSTRIA

Keywords: composite bridge, dual carriageway, rehabilitation concept, construction concept

SUMMARY

Presentation of a large roadway composite bridge from the viewpoint of the designer and contractor. Introduction of a very wide one cell composite bridge deck containing dual carriageways including a rehabilitation concept of the roadway slab.

The Talbrücke Reichenbach is a 1,000 m long composite bridge erected for the new BAB 71 from Erfurt to Schweinfurt in Thüringen, Germany. The client is DEGES (Deutsche Einheit Fernstraßenplanungs und -bau GmbH, Berlin) and tendered the bridge as design and built structure on the basis of a preliminary design. The construction period is between Sept. 1999 and Nov. 2002.

The total width of the roadway between the railings is 28.5 m and contains 2 + 1 lanes in both directions at max. 60 m over natural ground level. The 14 spans of the bridge vary between min. 40 m and max. 105 m. The constant sections are 3.70 m high and for the longest span of 105 m the deck height varies between 6.50 m at the piers and 3.70 m at midspan.

A one cell composite cross section with a constant 8.50 m wide bottom slab and a constant distance of the upper flanges of 10.50 m leads to variable inclined webs. To provide sufficient support conditions for the reinforced (no prestressing) concrete slab outer diagonal struts in combination with transverse steel tension elements perform a grid type load carrying system in a 5 m interval.

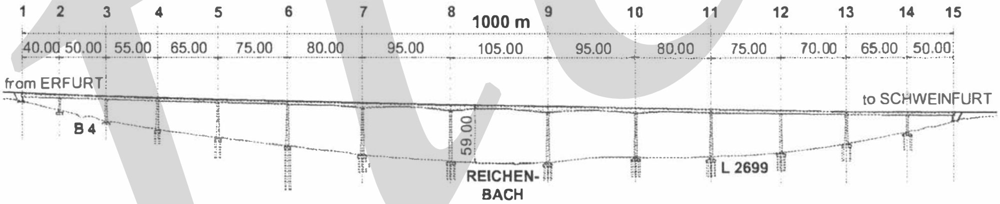

Fig. 1 Longitudinal section

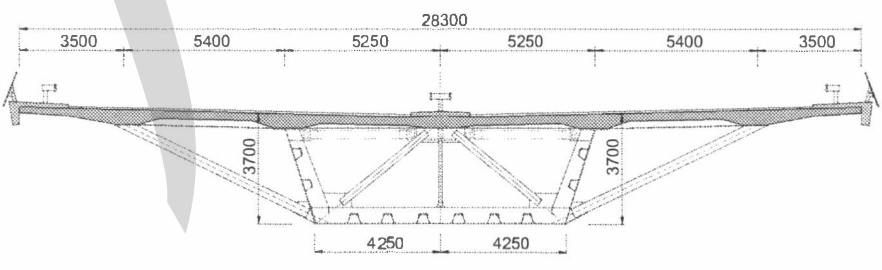

Fig. 2 Typical cross section, constant height

The method of construction of the steel girder is launching of the sections with constant height from both sides of the abutments and lifting from the ground of the five haunched center spans. The casting of the concrete slab takes place in segments with 15 m regular length beginning in the center of every span (Pilgerschrittverfahren).

Due to the fact that both carriageways are resting on one bridge structure a rehabilitation concept for the concrete slab with 4 lanes under traffic was developed and considered in the current design and construction phase already.

The large total length of bridge in combination with the height of piers and the bearing layout requires limited longitudinal deformations at the abutments of ±365 mm by use of appropriate tension and compression carrying elements to minimise the necessary deformation capacity of bearings and expansion joints.

CONCLUSION AND FUTURE WORK

The current knowledge on composite bridge design and construction is able to provide very economic structures in combination with life cycle and rehabilitation concepts. For future investigations special attention should paid on highly flexible and sustainable structures considering the economic evaluation within a full life cycle of the bridges.

Fig. 3 After launching of west part and launching of first pier segment

REFERENCES

[1] Fritsch, Chiari & Partner: Statisch konstruktive Ausführungsplanung für die Talbrücke Reichenbach.

[2] Richtlinien für die Bemessung und Ausführung von Stahlverbundträgern, Ausgabe März 1981. Ergänzende Bestimmungen zu den Richtlinien für die Bemessung und Ausführung von Stahlverbundträgern, Ausgabe März 1984 und Juni 1991.

[3] ENV 1994-2, Eurocode 4: Bemessung und Konstruktion von Verbundtragwerken aus Stahl und Beton – Teil 2: Verbundbrücken, Dezember 1997.

[4] ARS 4/1997: Ergänzende Bestimmungen für die Bemessung und Konstruktion schlaff bewehrter Fahrbahnplatten und der Hänger von Stabbogenbrücken.

[5] ARS 12/1994: Ergänzende Bestimmungen (BMVBW) zu den Richtlinien für die Bemessung und Ausführung von Stahlverbundträgern. Fassung Juni 1994

[6] EDIN 1045-1, Tragwerke aus Beton, Stahlbeton und Spannbeton, Teil 1: Bemessung und Konstruktion. Dezember 1998

TSUBAKIHARA BRIDGE —— DESIGN AND CONSTRUCTION OF A THREE-SPAN COMPOSITE TRUSS BRIDGE

Yukihiro Kutsuna, Japan Highway Public Corporation, Japan
Hiroyoshi Noto, Miyaji Iron Works, Tokyo, Japan
Shinichi Kondoh, Sumitomo Construction, Tokyo, Japan
Teruhiko Yoda, Waseda University, Tokyo, Japan

Keywords : composite truss bridge, cantilever erection, prestressed concrete deck, model test

1 INTRODUCTION

Tsubakihara Bridge is a three-span warren-type composite truss bridge (Fig.1). The superstructure consists of a prestressed concrete deck, upper chords, lower chords, diagonal members, sway bracings and shear connectors (Fig. 2). Each pier has base-isolating bearings at its top. The composite truss bridge proved economical to construct and produced the right proportions for the setting.

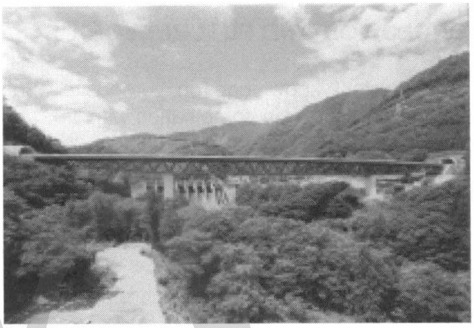

Fig. 1 Tsubakihara Bridge

2 DESIGN

The bridge is 322m long and has spans of 82 m, 155 m and 82 m. The width is 10.49m. The depth of the main structure is 9.5m (Fig.3). This bridge is based on the concept that, even when the bridge has its maximum limit load and thus has large cracks in its concrete deck, the steel truss as a whole must retain the strength to withstand the load. The deck is a cast-in-place prestressed concrete structure.

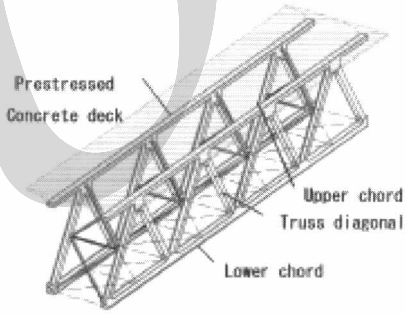

Fig. 2 Truss members

Shear studs are welded to upper chords to achieve composite action. Shear studs are in the box-shaped opening of the deck, and rubber pads are installed on the upper chords so that the chords do not restrain the prestress. The opening are filled with concrete after prestressing to achieve a composite.

Pre-grout type, 28.6 mm diameter prestressing strands are used for the deck to resist the tension force caused by the dead load, live loads, creep, shrinkage, and other forces of the bridge. The deck is transversely prestressed by 21.8 mm diameter strands.

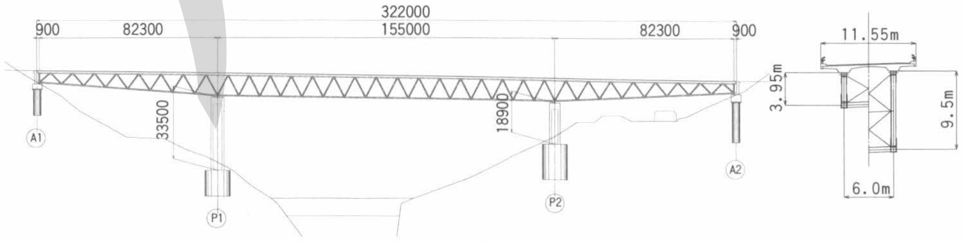

Fig. 3 Elevation and transverse section of the bridge

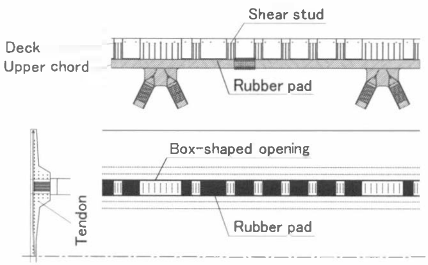

Fig. 4 Arrangement of Shear Studs

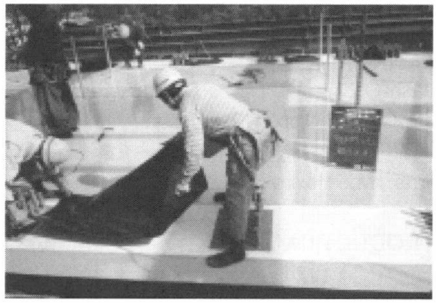

Fig. 5 Rubber pad on the upper chord

Shear studs in the box-shaped opening of the deck are welded to achieve composite action; They are arranged as shown in Fig.4. When the concrete deck is prestressed in the longitudinal direction, the box-shaped opening enables effective prestressing. The rubber pads installed on the steel members also facilitate prestressing. The openings are filled with expanding concrete after prestressing, and the concrete deck and the steel upper chords are connected by shear studs.

3 CONSTRUCTION

The bridge was erected by the cantilever method of construction; the steel truss was allowed to overhang, and the deck was formed by the cast-in-place method. The construction procedure is shown in Fig.6.

Phase 1 Prestressing the concrete deck after erecting the steel truss by a crane.

Phase 2 The deck is connected to the upper chords only after the part has been prestressed.

The box-shaped opening is shown in Fig.7.

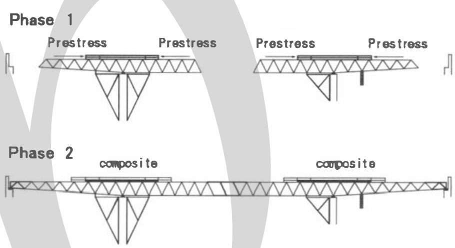

Fig. 6 Construction procedure

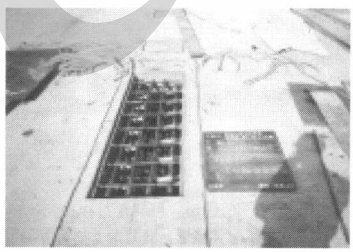

Fig. 7 Box-shaped opening

4 MODEL TESTS

Fatigue tests and static load tests of three types of the bridge model were carried out in order to study the load bearing behavior and the force transfer mechanism at truss joints (Fig.8).

In type A, rubber pads are installed between the upper chords and the concrete deck, and box-shaped openings for studs are filled with concrete after longitudinal and transverse prestressing. In Type B, the opening is filled with concrete after longitudinal prestressing but before transverse prestressing. Type C has no rubber pads.

Though cracks occurred in types A and B at lower-level loads than for type C, the cracks in types A and B were small enough and were not considered to cause problems in structural members. Based on the static load tests and fatigue tests, type B was chosen for the Tsubakihara Bridge.

Fig. 8 Test set-up

DESIGN AND CONSTRUCTION OF JAPAN PALAU FRIENDSHIP BRIDGE

Hisashi Oshima, Nobuyuki Suzuki
Nippon Koei, Japan

Tomohiko Kashiwamura, Ichiro Oda
Kajima Corporation, Japan

Keywords: hybrid, extra-dosed bridge, cantilever erection, erection nose

1 INTRODUCTION

The Republic of Palau, which is well known all over the world as a mecca for diving, is a beautiful archipelago county at the South Pacific (**Fig.1**). On September 26,1996, the old K-B Bridge, which was the most important life-line to connect Koror island and Babeldaob island, built in 1977, suddenly collapsed and socio-economic activities in Palau were suffering from various adverse effects (**Fig.2**). Construction of the Japan Palau Friendship Bridge began in November 1999, and was completed in December 2001 to restore the important life-line by a grant aid from the Government of Japan (**Fig.3**).

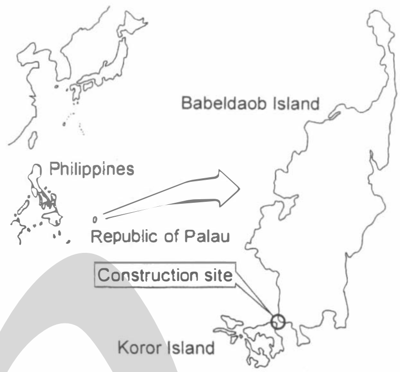

Fig .1 Location map

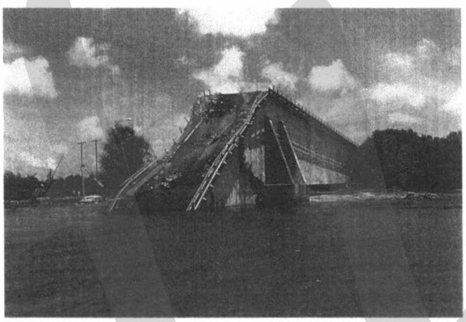

Fig .2 Collapse of old K-B Bridge

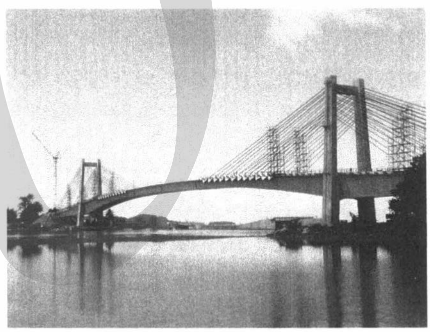

Fig .3 Japan Palau Friendship Bridge

2 DESIGN AND CONSTRUCTION

The Japan Palau Friendship Bridge is a 3 span hybrid extra-dosed bridge (**Fig.4**). The purpose of this project was to build a durable structure taking into consideration of environmental and economical aspects, under the difficulties caused by geographically factor of Palau. Therefore the bridge has several special features in its design and construction methodologies, which are summarized as follows;

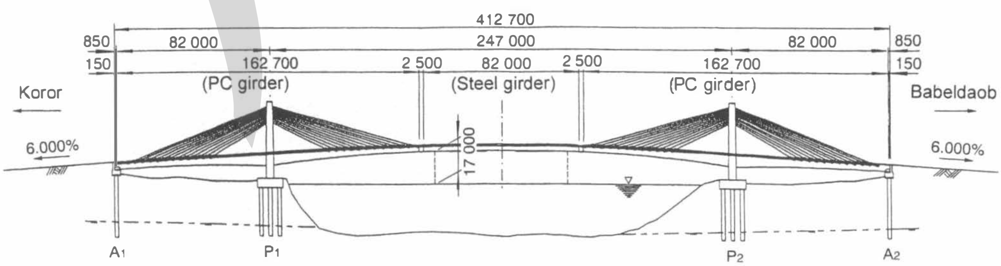

Fig .4 Bridge elevation (unit; mm)

1) The bridge was designed to minimize the unbalance between the center span and the side span by adoption of the steel girder at the center span, the counter weight concrete at the side span and others (**Fig.5**). And the construction procedure was also planned out carefully from above-mentioned viewpoint.
2) The bridge was constructed at the same location as the old bridge. Therefore the rotary casing pile-driving machine was adopted for the cast-in-place reinforced concrete piles in order to penetrate the existing piles for the old bridge.
3) The prestressed concrete (PC) girder was constructed by means of balanced cantilever erection (**Fig.6**), and the side span was closed at the girder end in such a manner that the bending moment at the pylon leg could be reduced.
4) To reduce the repainting cost the zinc-aluminum alloy metal spray with fluoride resin paint coat was adopted at outside of the steel girder rather than the ordinary painting system.

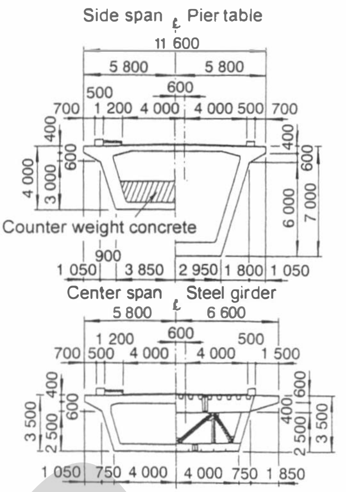

Fig .5 Girder cross-section (unit; mm)

5) The steel girder, which consists of main block (77m long, 470t) and two steel shells (4m long, 37t), were transported form China to Palau by the barge (**Fig.7**).
6) The connection segments, which consist of the steel shell and the cast-in-place concrete, were constructed using the form traveller and the self-compacted concrete.
7) The steel shells and the main block were lifted up from the barge, which was moored under the bridge, by means of hydraulic jack sets on erection noses (**Fig.8**, **Fig.9**).
8) The connection segment and main block was jointed using high strength friction grip bolts and splice plate in such a manner that the variable joint gap could be adapted for.

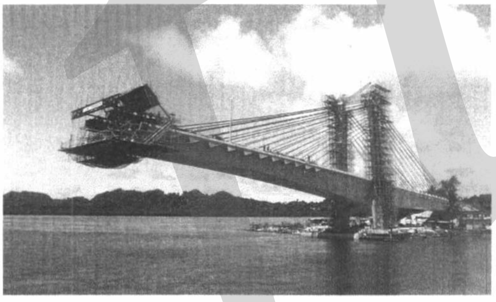

Fig.6 Balanced cantilever erection of PC girder

Fig.7 Transportation of the steel girder

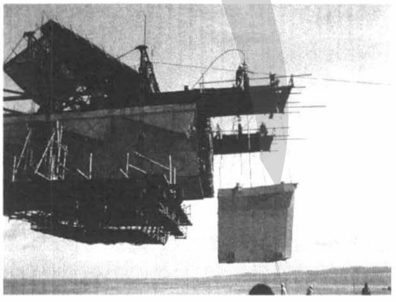

Fig.8 Lift-up of the steel shell

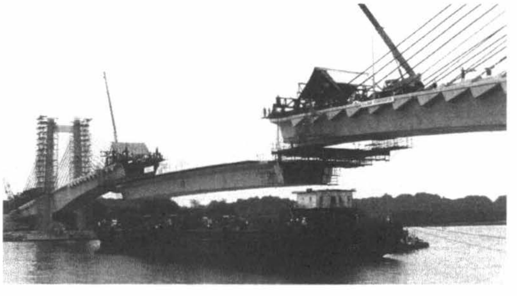

Fig.9 Lift-up of the main block

DESIGN AND EXECUTION OF THE PC BRIDGE WITH CORRUGATED STEEL WEBS ADOPTED TO THE RAILWAY BRIDGE

Koji Saito, Chikao Hiraoka, Makoto Kanamori
Japan Railway Construction Public Corporation

Masaru Ochiai
Oriental Construction

Keywords: railway bridge, corrugated steel web, high quality weather plate, embedded connection system, flat plate

1. INTRODUCTION

The Kurobegawa Bridge is located in Toyama Prefecture, and it is constructed between Itoigawa-Uozu of the Hokuriku Shinkansen, that is a railway bridge with a length of 761m and with 14 spans. Among those, sections that adopts PC Bridge with corrugated steel webs is between P4 – P10, with a length of 344m and with 6-spans. This paper reports mainly on the design of corrugated steel webs and a connection part about sections of the PC Bridge with corrugated steel webs. Moreover, an outline is given on the construction that began in November 2001.

2. OUTLINE OF THE BRIDGE

The Kurobegawa Bridge is a PC box girder bridge with corrugated steel webs. This structure is adapted to 6-spans, continuous rigid frame, fixed at middle three piers, and has a 344m length. The height change from 4.8m at pier, to 3.3m at midspan in the central spans (P6-P8), and it is 3.3m in the side spans (P4-P6, P8-P10). A general view of the Kurobegawa Bridge is shown in **Fig. 1**

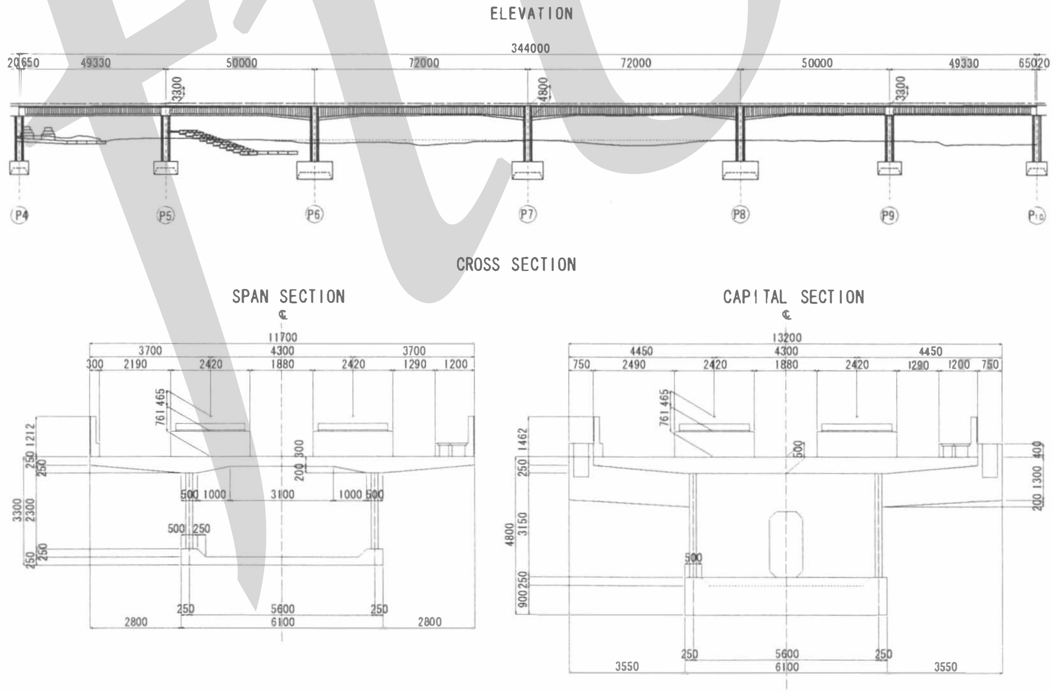

Fig1 General view

3. OUTLINE OF CONNECTION PART

Generally, there are two types of connection systems between corrugated steel web and concrete slab. One is embedment type where corrugated steel web is embedded in concrete slab directly, and the other is non-embedment type. In the case of the embedment connection system, the penetrating steel through the steel plate hole was used, and a connection steel bar which was welded on the top of a steel plate was embedded in a concrete slab. In this bridge, as shown in **Fig.2**, a flat plate was adopted instead of a connection steel bar, and connected with a corrugated steel plate. This flat plate plays the same role as the connection steel bar. In addition, the diagonal panel of corrugated steel plate acts effectively as a shear connector, and resists to the horizontal shear force by the jointed flat plate.

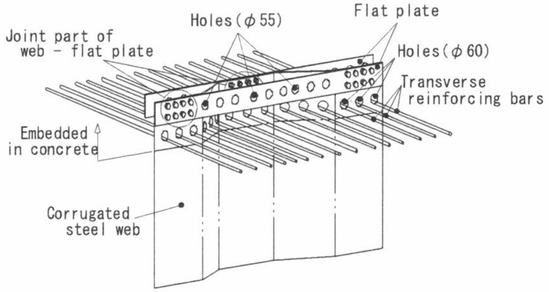

Fig.2 Outline view of connection part

The horizontal shear force on each section changes the material and the scale of the plate joined to the corrugated steel web. In addition, in order to try to attain of concrete to a flat plate, it is prepared by making holes(φ55mm) separated by 125mm.

4. OUTLINE OF THE EXECUTION

It is constructed on the staging follows as ①P6-P8, ②P5-P6 and P8-P9, ③P4-P5 and P9-P10, construction with a three division part. After construction of the lower slab, the inner timbering is assembled, and then the upper slab is constructed, while internal and external tendons are prestressed following the construction sequence. Scenes of the construction site in February 2002 are shown in **Photo.1-2**.

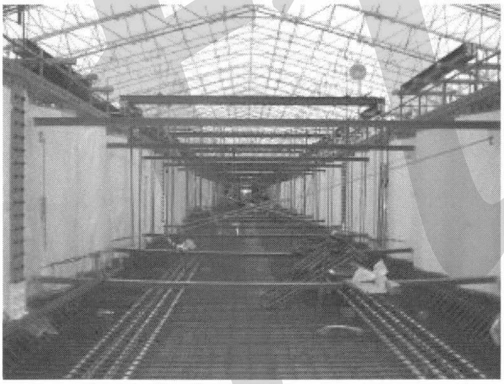

Photo.1 Inside the box girder (Execution of lower slab)

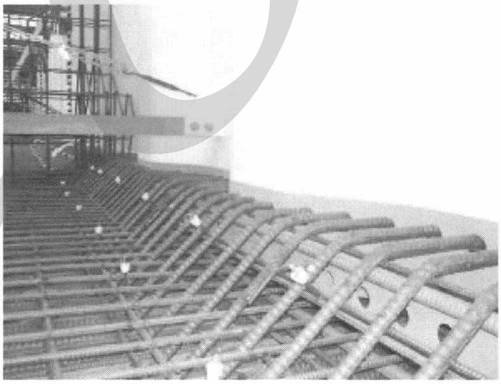

Photo.2 The arrangement of the reinforcing bars

5. POST SCRIPT

Since it is the first railway bridge with corrugated steel webs, the 'Committee of Design Method for Railway Bridges with Corrugated Steel Webs' had been established and examined. Following its purpose, an original method was adopted for its design in the connecting part between corrugated steel webs and concrete slabs. This paper will hopefully become a reference for the connection method described above.

Finally, the authors would like to thank the members of the examination committee.

DESIGN AND CONSTRUCTION OF KOINUMARUKAWA CORRUGATED STEEL WEB BRIDGE

Fujio Sogo Takeshi Abe
Japan Highway Public Corporation.
JAPAN

Akio Kasuga Naoki Nagamoto
Sumitomo Construction Co., Ltd.
JAPAN

Keywords: corrugated steel web, external tendon, shear apportionment ratio, shear experiment

1. INTRODUCTION

The Koinumarukawa Bridge is a 6-span continuous rigid-frame bridge. The maximum span is 81.0 m and the overall length is about 430 m. A corrugated steel web was used to reduce the weight of the main girder and provide rational shear reinforcement for this bridge. Also, an all-external cable system was used for the main cables.

Several points had to be considered in the detail design of a bridge with these characteristics. Firstly, the concrete web near the upper decking was left in place and external cable anchor projections were installed at these points. Using a configuration such as this means that the shear forces are shared by the parts of the concrete web that were left and the corrugated steel plates. In order to examine shear, it was necessary to clarify the proportion of the shear forces borne by each side.

This paper draws attention to the above points and presents an outline of the design and the results of investigations.

Fig. 1 and 2 show a general view and cross section diagram.

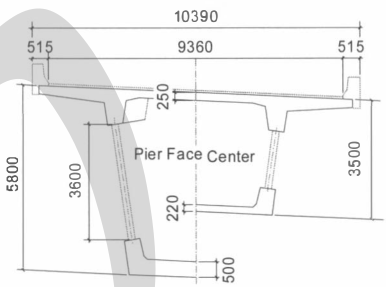

Fig.2 Cross Section

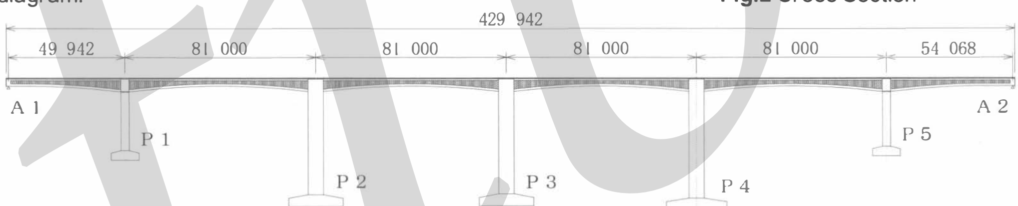

Fig.1 Shape of Koinumarukawa Bridge

2. EXAMINATION OF AREAS AROUND EXTERNAL CABLE ANCHOR PROJECTIONS

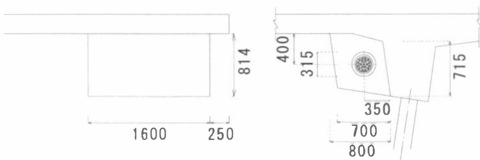

Fig.3 Shape of the External Fixed Projection

As previously mentioned, this bridge is an all-external cable structure and the external cables have to be anchored to support the cantilever in order to proceed with the cantilever construction. High capacity 19S15.2 external cables are used. Therefore the anchor projections need to be strong. Consequently, the concrete web, which is more rigid than corrugated steel plates, was left in place in the vicinity of the upper decking and the external cable anchor projections were installed in the corners of the web and the upper deck system to ensure adequate strength. Fig. 3 shows the shape of the anchor projections.

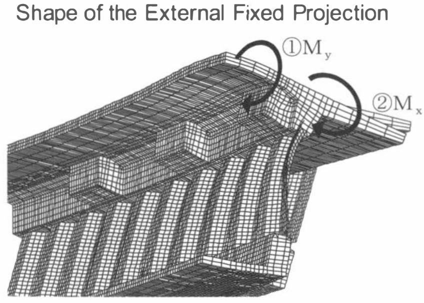

Fig.4 Disp. by the External Tendon

Deformations such as are shown in Fig. 4 occur in the corrugated steel plates due to the tensioning of the external cables. These deformations caused localized deformation to occur in the nearby corrugated steel plates, resulting in localized stresses in the corrugated steel plates. Stresses due to the localized stress had a limited range but the stress levels were high, up to 80 (N/mm^2) (See Fig. 6). For this reason, it was considered necessary to take these stresses into account in the design of the welds in the joints between the corrugated steel plates and upper flanges.

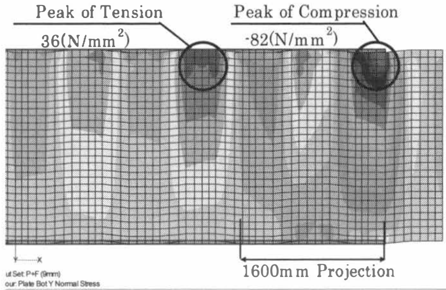

Fig.5 Stress of the Cor. Steel near Projection

3. FULL SIZE SHEAR EXPERIMENTS

To ensure the behavior of a corrugated steel web bridge, full size shear experiment was executed (Fig. 6).

Fig. 7 shows the relation between displacement of span center and vertical load. At about 15,000 (kN), bend cracking occurred in the lower deck system in the center of the span, after which the elasticity of the entire girder appeared to fall. The ultimate design of the actual bridge is being checked for all active shear forces to be accepted by the corrugated steel plates but based on this assumption the ultimate load on the test model in this experiment is about 10,000 (kN) and it is clear that adequate safety with respect to the ultimate calculated load can be assured. Moreover, taking the apportionment of shear forces between the corrugated steel plates and the concrete sections to be in accordance with the FEM analysis (in which the proportion of shear borne by the corrugated steel plates is about 37%), the corrugated steel plates were loaded up to 22,000 (kN), which is the yield point, but no shear buckling, etc. of the corrugated steel plates could be confirmed.

Furthermore, the curve indicated in the diagram by a dotted line is a simulation of this experiment by non-linear analysis using fiber elements. Since shear deformation of the girder cannot be considered in fiber analysis, the shear deformation of the test piece for this experiment was calculated by three-dimensional FEM analysis this, and total deformation of these two is shown in the diagram by a dashed line. Thus, it is possible to make an assessment to some extent by taking into account the amount of shear deformation calculated according to the non-linear analysis and three-dimensional FEM analysis, and by analyzing the behavior of the corrugated steel web bridge.

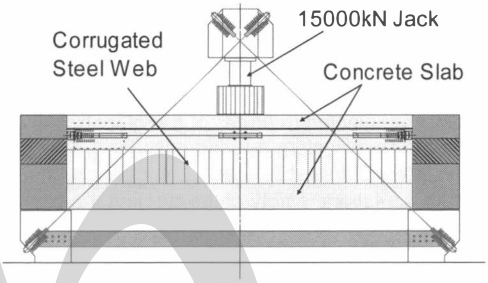

Fig.6 Outview of Shear Experiment

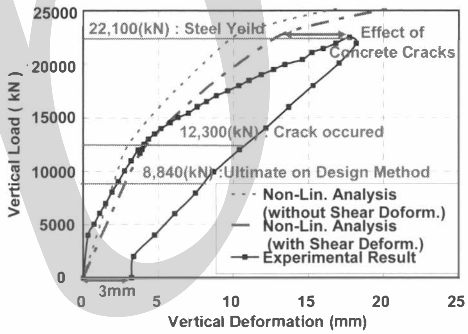

Fig.7 Experimantal Result (Deformation)

Fig. 8 shows the ratio of apportionment of shear in the corrugated steel plates at various vertical load stages. It is clear that the apportionment of shear in the corrugated steel plates is increasing gradually from the time when cracking occurred in the concrete of the lower deck system. This is thought to be caused by the apparent decline in shear strength due to the outbreak and development of cracking in the concrete associated with loading.

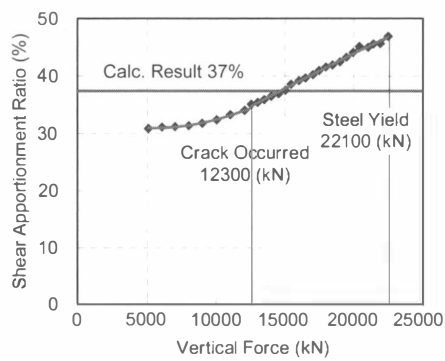

Fig.8 Change of Shear Apportionment Ratio

FATIGUE TESTS OF CONNECTION BETWEEN PRESTRESSED CONCRETE AND STEEL ORTHOTROPIC DECK

Yukihiro Kutsuna*, Makoto Nakasu*, Katsuyoshi Akehashi**, Yasuyuki Koga***

*Japan Highway Public Corp., **Yokogawa Maintech Corp., ***Yokogawa Bridge Corp.

Keywords: hybrid bridge, connection girder, fatigue test, traveling wheel load

1. INTRODUCTION

Kiso River Bridge and Ibi River Bridge are hybrid extradosed bridges, each of which consists of prestressed concrete (PC) box girders in the side spans and on the piers and an orthotropic steel box girder in the center span, the PC girder and the steel girder are connected with each other through a composite section. Abrupt change in rigidity is naturally unavoidable in the connection between a member of a PC girder and that of a steel girder on a hybrid bridge, which causes concerns over a stress concentration and even the reliability of the connection between different materials. Particularly a deck is subjected to forces of the global main girder response, as well as the local behavior of the deck and the floor system due to trucks load. This paper reports in detail the process to select the connection girder form on said bridges. It also reports the results from the travelling wheel load tests conducted to verify the fatigue safety of the deck in the connection girder.

2. TEST METHODS

Full-scaled specimens were used in the tests. The specimens were of deck span of 5.4 m and an overall width of 5.8 m, taking into consideration maximum specimen width mountable on the test machine (7 m), the width of a cell on the real bridge (0.9 m), and about 70 percent of interval between interior and exterior web (70% of continuous slab was assumed since the specimen was of a simple slab). This allowed duplicating the real bridge behavior at the focused points that were positioned at the front and the rear of the composite section. The composite girder section was structured to have high-fluidity concrete filled in the sealed steel box (900 wide×600 high×1000 long). Prior to the traveling load fatigue test, static load tests were conducted using rubber tires. Influence plane load was conducted to identify the critical traveling load position, and to measure the stress amplitude induced by the traveling loads. Cyclic load tests were conducted at the most critical load position as determined by the static load tests. Traveling loads were applied with iron wheels.

It is common in the verification of fatigue strength to assure that no damage is sustained after two million cycles of stress amplitude caused by the application of traveling load of a set of trucks loads (100 kN per wheel and 200 kN per axle). Table-1 shows the applied load and cycles used in the traveling load tests.

Table-1 Test cycles and T-load equivalent cycles

Load(kN)	Cycles	T-load equivalent cycles (sccumulated)
1.26×200=252	500,000	1,000,000(1,000,000)
1.50×200=300	300,000	1,000,000(2,000,000)
2.00×200=400	200,000	1,600,000(3,600,000)

3.TEST RESULTS

3.1 Results from Static Load Tests

As the result of the influence surface loading with rubber tires, it was found that a stress concentration occurred at the toe of the groove weld between the steel deck plate and the rear surface plate, and that the stress highest when the wheel load was applied directly on this part. This was considered to be a local stress caused by an abrupt change in rigidity, i.e. a relative flexibility of steel deck plate was in the direct neighborhood of rigid composite deck. Only low stresses (0.5 N/mm2 or less) were observed with the composite deck and the PC deck, both in longitudinal and transversal directions, irrespective of the point of loading. Also, since the load around the boundary section caused no steep gradient of stresses, it was confirmed that a good transfer of the load was performed between the composite and the PC deck sections.

3.2 Travelling Load Test Results

No crack was visually detected on the steel members and PC deck after the completion of the scheduled cycles of the traveling load test.

In the course of the traveling load test, the static loadings in the similar manner to the previous section were conducted before the beginning of the tests, after 300,000 cycles, 500,000 cycles, 800,000 cycles and 100,000 cycles (or the completion of the test). Figure-1 shows the influence lines of the longitudinal stress on the deck plate (C1) and the cold-bend corner of the trough rib (C2) as well as of the stress in the main reinforcement direction of the composite and the PC decks. The stresses on the composite and PC decks remained virtually unchanged between any static loading steps and their absolute values were small. Since there was no damage observed on outside, it can be said that the vicinity of the connecting surface is sufficiently safe against repetitive wheel loads.

4. EVALUTION OF FATIGUE DURABILITY OF CONNECTION

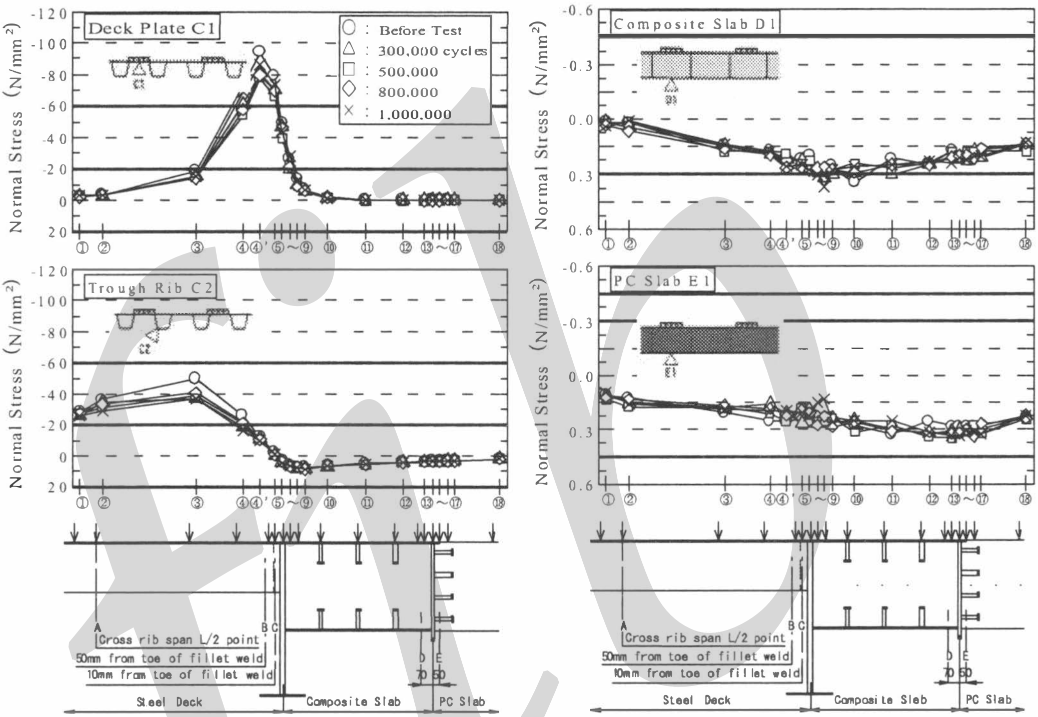

Figure- 1 Stress influence lines at various points under travelling load

There was a significant stress concentration on the orthotropic steel deck. Judging from the influence lines shown in Figure-1, the number of stress cycles in each section was:

Deck plate: Go-return stroke counted as two cycles

Corner of trough rib: Go-return stroke counted as a single cycle

Shown in Figure-2 is a S-N diagram obtained by plotting the stress amplitudes and cycles together with the fatigue design standard values by JSSC.

The joint on the orthotropic steel deck under the stress concentration is a load-transferring cross joint or of category E. It is inferred that the stress at that joint on or below the category E design curve resulted in no fatigue crack.

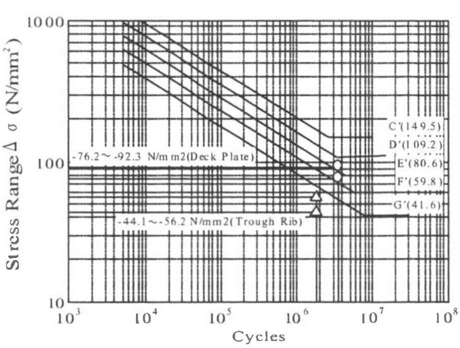

Figure- ,Q S-N diagram

References

Japanese Society of Steel Construction: Guidelines on Fatigue Design of Steel Construction / interpretation thereof, Gihodo Shuppan Co., Ltd., April 1993

GENEVA EXHIBITION CENTER

BRIDGING 44'000 m^2 IN 14 MONTHS

Jean-François Klein

Dr ès sc. Tech, civil engineer
Tremblet SA – Geneva Switzerland

Keywords : platform, bridge, innovative precast element, construction technique

1 INTRODUCTION

The exhibition center is located across the Geneva bypass freeway from the international airport. Due to space and general layout contingencies, extension of the exhibition halls was only feasible over the freeway and side roads, making it necessary to build a platform to support the future constructions.

This 230 by 180-m platform offers a total of 44'000 m2 of deck area in continuation with the existing exhibition halls to accommodate the new hall, a future congress center, the lobby, the necessary circulation areas for supply by trucks of all materials and equipment required for exhibitions set up as well as terraces for visitors.

2 OBSTACLES TO OVERPASS

The project requirements are numerous and very restrictive. Starting from existing hall, the platform overpasses successively a parking access with a visitors drop zone for buses, two main roads (access to Geneva airport), the freeway platform, a local road and an elevated roadway that allows a direct off customs access from nearby France to Geneva airport

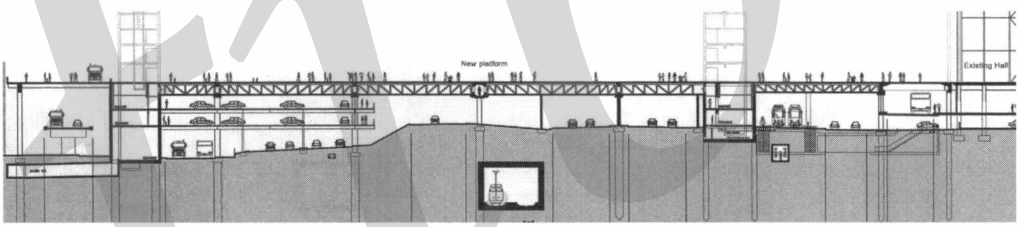

Fig 1 : Cross section of the platform, obstacles to overpass

3 GENERAL CONCEPT OF THE PLATFORM DECK

A hollow double deck system including a technical space between the lower and upper concrete slabs was the perfect answer to very demanding specifications. This technical space allows a two-way distribution of all the energies and fluids under the exhibition slab to floor channels and connection boxes built in the concrete deck (figure 2). This guarantees maximum flexibility for the various events taking place in the hall and, at the same time, ensures thermal and acoustical insulation of the exhibition hall from road traffic below.

This structure has to support live loads (20 kN/m2) about 4 times heavier than for a normal bridge and its construction has to comply with the tight schedule and traffic requirements.

The platform double deck is made of prefabricated, composite truss beams at 2.40 m on centers whose bottom chords are prestressed concrete slabs (figure 4). They have the shape of inverted T-beams. They span a maximum of 25.60 m between their support girders. A concrete slab cast on steel decking spanning between these beams makes the exhibition deck slab. The composite beams rest on main pretensioned girders supported on a grid of columns. These main girders have a standard span of 9.60 m. Each girder carries an average slab field of 240 m^2, i.e. a total service load of 820 kN/m.

The use of prefabricated beams makes it possible to reduce to a minimum traffic disturbances on existing roads and risks connected with construction activities above open roads. It is also essential to the planning since prefabrication can begin at the same time as construction of the infrastructure.

The prefabricated beams span the roads and freeway lanes between cast-in-place girders with lengths ranging from 10 to 25 m (figure 5). Because the bottom chord of these inverted T-shaped truss beams is a 2.40-m wide and 15-cm thick prestressed slab, a continuous deck is formed once the beams are erected side by side, allowing works to proceed without interruption above open roads that are fully protected.

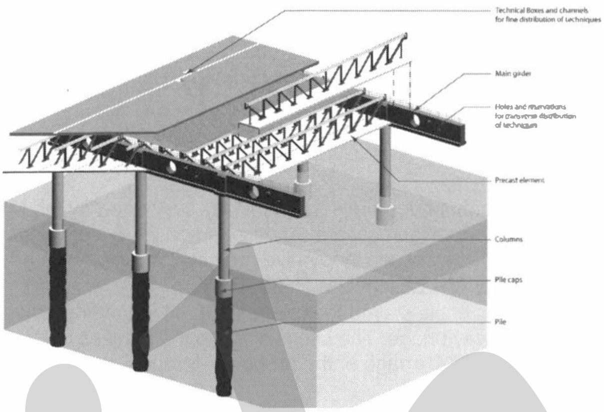

Fig 2: Structural principle of the platform construction

The choice of steel trusses as beam webs was dictated on one hand by operation requirements as already mentionned (ease of installation of the various technical equipment in both directions), and on the other hand by weight limitations for the erection process: the jobsite was too crowded to allow the erection of each beam with two mobile cranes. By limiting the maximum beam weight to 30 tons erection could be done with a single mobile crane of intermediate capacity. Such parameters are essential to planning control and traffic restriction limitations during nightly erection.

In addition, the truss system easily allows an evolution of the statical system perfectly suited to the construction process of the platform.

4 CONCLUSIONS AND COSTS

Construction of the platform for the new exhibition hall is the success story of a complex operation in a very difficult and restrictive environment. Only the tight collaboration of all the actors - Owner, Engineers, Contractors, Operators, airport, police, highway maintenance, public transports, etc. - could make it possible to deliver within 14 months a 44'000-m2 platform, an underground gallery for a high voltage power line in operation, a 250-m access bridge and all the required road works. The political commitments of the Owner could thus be met. The innovative technical design proved its outstanding efficiency as far as performance, speed and costs are concerned. The actual total unit cost of US$ 920/m2 is within budget

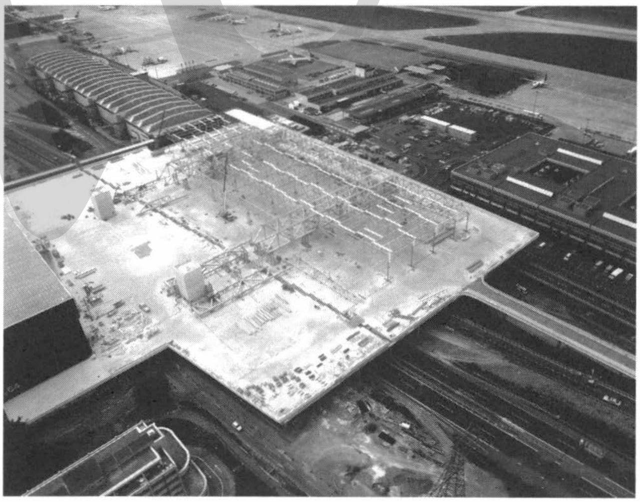

Fig 3: General view of the 44'000 m^2 completed platform

TWO MILLENNIUM BRIDGES

Gordon Clark – Director, Gifford and Partners, UNITED KINGDOM

Keywords: footbridge; cable stays; architects

1. BACKGROUND

The UK has some significant bridge projects financially supported by the Millennium Commission, the result of collaboration between Architects and Engineers and involve significant innovation. This paper describes two such innovative projects.

2. HUNGERFORD BRIDGE MILLENNIUM PROJECT

This is a pair of multi-span cable stayed footbridges 350m long over the river Thames in London, alongside the Hungerford railway bridge. The site is close to the Houses of Parliament and the London Eye. A computer generated image of the proposed bridges is shown in Fig 1 and described fully in Reference 1.

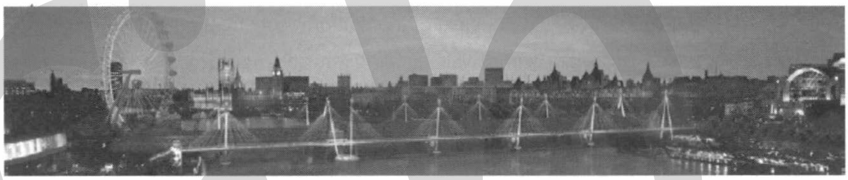

Fig 1 Proposed new Hungerford Thames Footbridges

The two light, symmetrical footbridges are suspended a short distance either side of the existing railway bridge (fig 2). The reinforced concrete bridge decks are suspended from inclined steel pylons with arrays of stay bars. Lifts and stairs at each end provide access to ground level.

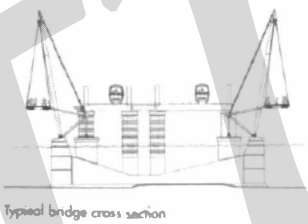

Fig 2 Cross Section

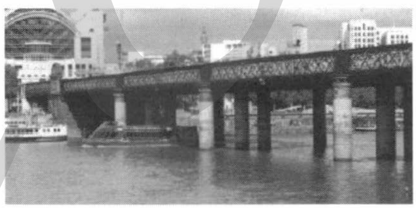

Fig 3 Existing Railway Bridge

Precast concrete beams were lowered to the riverbed to link the footbridge foundations either side of each pier bent. These were designed to resist 30MN impact from errant ships and to share the loads across the foundations. The bridge decks were incrementally launched (Fig 4), suspended over the entire 350m length from a temporary steel truss and supported on temporary piers. The pylons and deck stay bars were then installed (Fig 5) and the deck suspended in position. The

Fig 4 Incremental Launch

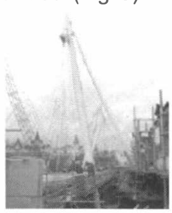

Fig 5 Pylon Installation

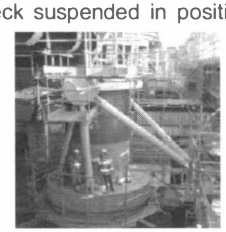

Fig 6 Steelwork Arrangement

requirement was that no additional loads should be imposed on the adjacent historic railway bridge so separate foundations were positioned alongside each of the existing piers. Tie-back stay bars and steel collars were designed for restraint of the new bridges, to impose no change in load to the old bridge (Fig 6).

3. THE GATESHEAD MILLENNIUM BRIDGE

This bridge spans just over 100m, and the design provides an innovative and adventurous solution in the form of a tilting bridge formed of a pair of arches, pivoting from a common springing point within concrete pile caps. It can be compared in the way it operates, with the raising visor of a motorcyclist's helmet or the blinking of an eye. The design is described in reference 2.

The whole 800 tonne bridge rotates and opens to allow 30m headroom for passage of ships underneath. In this respect it is unique but simple. The operating system has hydraulic jacks, which push on a paddle from under a pivot point and rotate the bridge.(Fig 7,8) The steel superstructure is prestressed down to the 8000m3 concrete substructures which are large hollow caissons housing the plant and machinery.

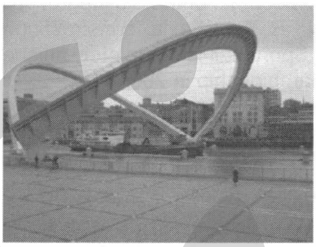

Fig 7 Opening of the Gateshead Bridge

Fig 8 Lighting of the bridge

Construction of 28 bored piles 1.5m diameter for the foundations in the river started in 1999 from floating plant. Temporary steel cofferdams were then built and an underwater concrete plug enabled them to be dewatered. The reinforced concrete caissons were constructed insitu, with their base some 14 metres below the water level and designed to support the bridge in any position. To open the bridge, two groups of 3 hydraulic cylinders (Fig 9) exert a force of about 1000 tonnes to start the structure rotating. After about 25 degrees of rotation the load reduces to zero because the centre of mass moves directly over the rotation point. The rams then have to act in tension, as the bridge wants to lean backwards. The fully open position is at a rotation of 40 degrees, by when the stay cables are horizontal.

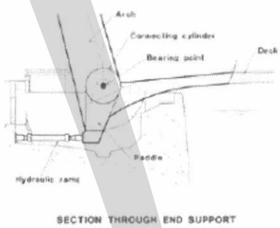

Fig 9 Opening Mechanics

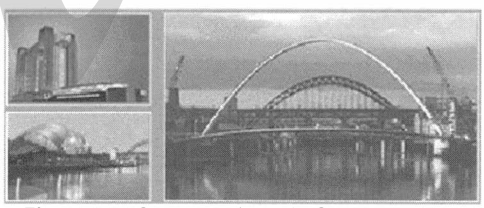

Fig 10 Arts Centre and Music Centre

The bridge is the catalyst and focal point of regeneration on the south bank of the river Tyne where a new Arts Centre and a new Music Centre are under construction (Fig 10). The bridge has received huge international publicity and has certainly achieved for the client, Gateshead Council, the aim of being the focus for regeneration of the area.

REFERENCES

[1] Andy Pearson. Bridge on the River Thames. *Building* 19 April 2002.
[2] G M Clark and J Eyre. The Gateshead Millennium Bridge. The Institution of Structural Engineers *The Structural Engineer* Vol 79 No 3 February 2001 pp30-35

EXTERNALLY PRESTRESSED ROOF STRUCTURE OF THE NEW SPORT HALL IN BELGRADE

Milorad Ivković, Života Perišić, Mirko Aćić, Aleksandar Pakvor, Vanja Alendar, Snežana Marinković
Faculty of Civil Engineering of the University of Belgrade, Belgrade, YUGOSLAVIA

Keywords: prestressed concrete, external prestressing, two-chord grillwork, roof structure

1 INTRODUCTION

A new universal Sport Hall, the "Belgrade Arena", for all indoor sports including ice sports and athletics, as well as cultural and social gatherings for more than 20,000 visitors, has been built in Belgrade. The Authors of the paper are the main designers of the Hall structural system. The main contractor is the Consortium of construction companies Energoprojekt and Napred from Belgrade.

The construction of the Arena began in 1992 and it was planned to be the venue of the 1994 World Basketball Championship in Belgrade. Unfortunately, because of the disintegration of the former Yugoslavia and the sanctions imposed by UN to the new FR Yugoslavia, construction of the Arena was interrupted for several years. Now the structure of the Sport Hall is completely finished and tested and it will be the venue of the next European Basketball Championship in 2004.

2 DESIGN AND CONSTRUCTION CONCEPT OF THE ROOF STRUCTURE

The Hall has a rectangular base with rounded corners. The spans between the axes of the 14 main columns which support the roof structure only in facade walls are 132.70×102.70 m. The surface of the roof is somewhat larger than 15,000 m^2. The height of the structure is slightly over 36 m.

The Hall roof structure has a shape of a prestressed shallow lens made by a double-chord orthogonal grillwork of 7 externally prestressed reinforced concrete girders – 3 in the longitudinal direction of the Hall, with the span of 132.7 m, and 4 in the lateral direction, with the span of 102.7 m. The upper, compression chords are made of reinforced concrete. They polygonally follow the convex paraboloidal surface with the elevation in the middle of the roof of +8.0 m over the supporting plane. The lower, tension chords are formed of prestressing tendons which are free in space, outside of concrete section, and polygonally follow the concave paraboloidal surface with the sag of - 4.0 m under the supporting plane.

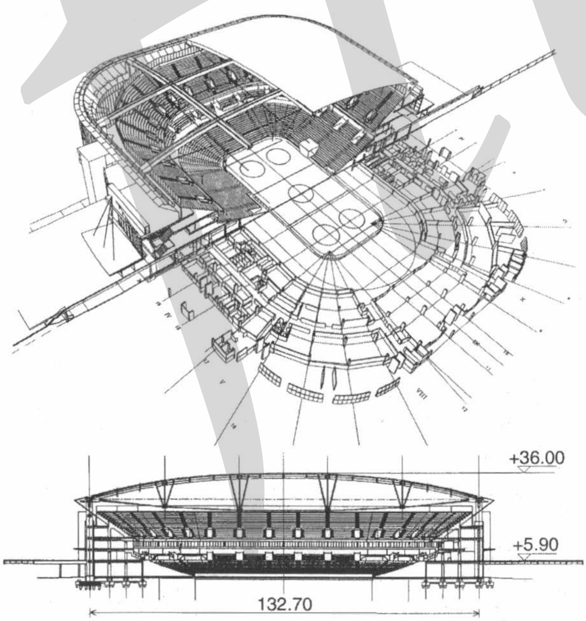

Fig. 1 Axonometric view and longitudinal section of the new Sport Hall in Belgrade

The reinforced concrete chords of all 7 main girders have the same cross-section, constant along the entire span, composed of twin girders 2x140/40 cm at the clear spacing of 80 cm.

The lower chords of all girders are composed of 9 prestressing tendons each. The tendons are formed of 11 Neptun grade low relaxation S strands ∅15.80 mm, with the area of 150 mm^2, tensile strength of 1,860 N/mm^2, protected by grease in hard polyethylene sheaths.

All 14 main columns consist of two separate reinforced concrete C 40 wall-flanges, with cross-section 2x50/220 cm at the clear spacing of 2.0 m, that were

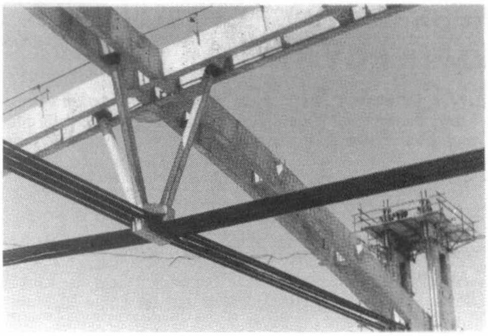

Fig. 2 Reinforced concrete "chair" between the two chords and the deviator block

designed to provide the free space for the supporting parts of girders and for the lifting of the roof girders grillwork to the top of columns in the construction stage.

The adopted construction solution for the roof structure was the prefabrication and "low level mounting" on the temporary mounting level of + 5.90 m above the floor of the Hall. The main girders were divided into the total of 43 elements, with the weight ranging between 50 and 100 t.

High sensitivity of the system as a whole to tensioning of individual tendons is characteristic for such structural systems. That is why the grill-work prestressing had to be carried out simultaneously with 16 hydraulic jacks so that in each prestressing step all tendons of two symmetric girders were tensioned at the same time.

The lifting of the roof girders grillwork from the mounting level + 5.90 m to the top of main columns on the level of 26.0 m was carried out with 96 hydraulic jacks by pulling the whole grillwork from the tops of columns.

The sensitivity to relatively small changes of forces in prestressing tendons, and especially constant reconstitution of the structural system during prestressing, while the whole structure was gradually self-lifting from temporary supports on scaffolds, required detailed control of the system during construction. The results of detailed measuring and monitoring confirmed with great accuracy the preliminary structural analyses and enabled the implementation of the planned building procedure of the structure with full reliability, in spite of the unforeseen very long interruption in construction.

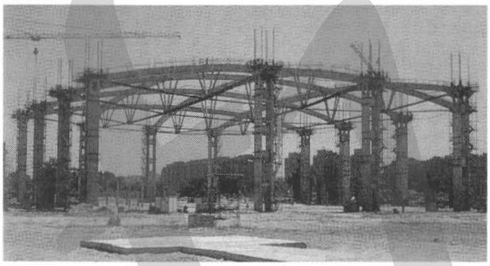

Fig. 3 Roof structure on the top of columns

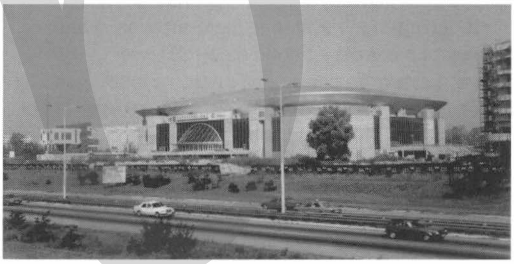

Fig. 4 Belgrade Arena

3 CONCLUSIONS

The applied spatial system of the roof structure of the Belgrade Arena - a new universal Sport Hall in Belgrade, in spite of its very large dimensions is a very lightweight, rational and economical structure. By external prestressing, with high eccentricity of prestressing tendons, both the dead and live loads were resisted by relatively small forces in tendons.

The roof structure was completely prefabricated and it was relatively quickly and easily mounted and constructed. It covers the area of more than 15,000 m^2 with the equivalent thickness of concrete in the main roof girders of only some 8 cm/m^2, the weight of prestressing tendons of about 6.5 kg/m^2 and the weight of the reinforcement lower than 12 kg/m^2.

REFERENCES

[1] Ivković, M., Aćić, M., Perišić, Ž. and Pakvor, A.: Concrete Structures with Steel Elements outside the Concrete Section. 12th IABSE Congress, Vancouver BC., Canada, September 3-7, 1984

[2] Ivković, M., Perišić, Ž., Pakvor A. and Aćić M.: New Prestressed Concrete Hangar at the Belgrade International Airport. X FIP Congress, New Delhi, February 16-20, 1986, also: FIP notes, 1986/4

[3] Ivković, M., Perišić, Ž., Aćić, M., et all: Design and Construction of the "Belgrade Arena" - the New Sport Hall Roof Structure in Belgrade. XII FIP Congress, Washington, USA, National Report of Yugoslavia. Proceedings IMS, Vol. XXI, No 2 (1994), pp. 7-26

DEVELOPMENT OF THE PRESTRESSED CONCRETE TOWER FORLARGE-SCALE WIND ENERGY SYSTEM USING PRECAST SEGMENT METHOD.

Kiyokazu Shinagawa Kotaro Ikegami Kiyoroku Fukayama
PC Bridge Company Limited
JAPAN

Keywords: wind energy system, prestressed concrete tower, precast segment, durability, life-cycle cost,

1 INTRODUCTION

In recent years, renewable energy resources, such as wind power, have been gaining worldwide attention due to the reduction in the impact on earth's natural environment. In Germany, Denmark, the U.S.A., and other countries where wind power generation has been employed extensively, large-scaled land/ sea based wind farms have been developed. Progress of wind energy system in each country is shown in **Fig.1**. In Japan as well, the interest in the introduction of wind power generation is increasing. Small-scale and medium-scale wind power plants have been constructed in various areas.

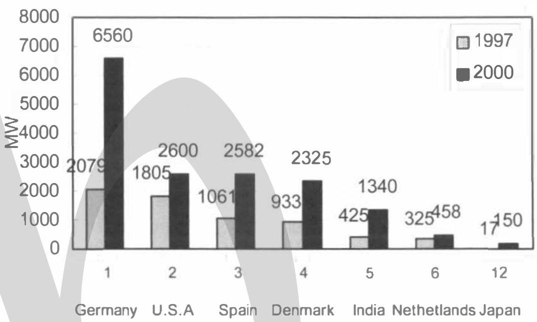

Fig. 1 Progress of wind energy system

At present, all towers in Japan constructed for large-scale wind energy systems are made of steel. Even foreign countries where introducing many systems, there are only a few cases of prestressed concrete (PC) tower. A PC tower for a large-scale wind energy system has recently been developed. This system was developed using the knowledge gained from the actual bridge construction using the precast segment method. The towers constructed using PC technology are both highly durable and economical.

This paper describes the overview of concept, design, and construction of PC towers, and the future applicability of PC towers to the wind farms on the ocean.

2 CONCEPT OF PC TOWERS

In addition to the safety, constructability, and economics required of wind energy systems, PC towers have high durability so that they can be constructed even in the coastal areas and on the sea.

This tower consists of precast segments. Each segment is tightly interconnected and integrated via a prestressing steel to resist wind load and seismic load.

PC towers have four major features.

-1- Durability; Use of high performance concrete
-2- Safety; Excellent in wind and earthquake resistance
-3- Constructability; Rapid installation with the precast segment method
-4- Construction Cost; Comparable to steel towers

3 OUTLINE OF DESIGN

The basic Design of a concrete tower is divided into two stages, such as structural analysis and durability analysis.

The height and outside diameter of a concrete tower are determined by the scale of wind energy system and the specifications of the turbine to be used. The scale of each segment is restricted by both capacity of manufacturing plant and road regulation. PC towers fall into two major types: a standard type,

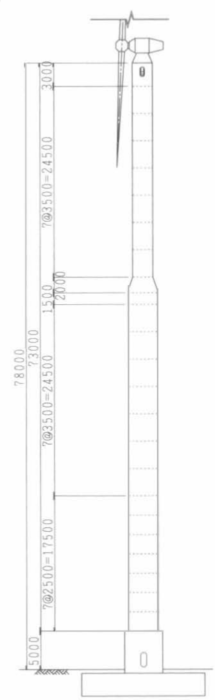

Fig.2 PC tower structural diagrams(Standard type)

which is shown in **Fig.2**, and a tapered type. The standard tower can be reduced in cost by converting formworks.

4 DURABILITY ANALYSIS

Wind power is usually generated in mountainous regions and coastal areas. Power generation near the ocean raises concern over the likely corrosion of the steel material due to chloride ions; salt damage. However, since concrete towers, make use of high performance concrete, they are durable under the severe environmental conditions accompanying construction at sea. In order to verify the durability of PC towers against salt damage, the diffusion of chloride ions was analyzed. The degree of penetration of the chloride ions over a 40 year service life has been calculated with the height above the sea level and the concrete cover over the reinforcing bars as parameters, subject to Fick's equation.

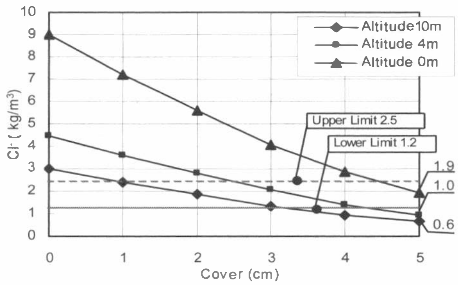

Fig.3 Analytical results on chlorine ion penetration

Results are shown in **Fig.3**. The analysis showed that the chloride ion content in concrete at an altitude of 4.5 m near the shoreline, at which concrete towers are likely to be exposed to very severe conditions, is 1.0 kg/m^3. It is generally accepted that the chloride ion content limit at which the reinforcing bars inside concrete can withstand corrosion under 1.2 kg/m^3. It is concluded that the PC towers have an acceptable level of durability because the chloride content of the concrete at the steel reinforcing at 40 years of age is lower than allowable level.

5 OUTLINE OF FABRICATION AND CONSTRUCTION

PC towers are constructed using the precast segment method. Fabricated segments are transported to the construction site and stacked up by crane. Each segment is tightly interconnected and integrated using PC bars. A conceptual CG of PC tower construction is shown as **Fig.4**

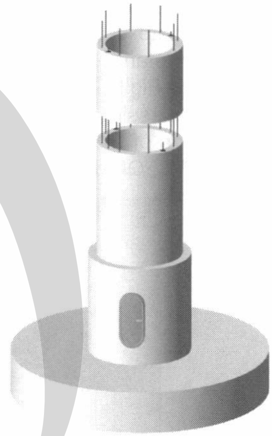

Fig.4 Conceptual CG of PC tower construction

6 CLOSING REMARKS

A perspective view of an example ocean wind farm is shown as **Fig.5**. Because of their excellent durability, PC towers are structures suitable for construction even in the coastal areas, on the sea, and at the other locations exposed to severe environmental conditions. In Japan, a nation completely surrounded by ocean, construction of large-scale wind energy systems along the coast is expected to increase.

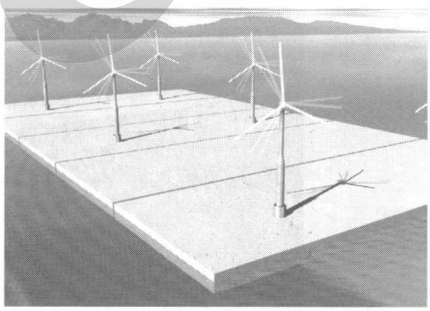

Fig. 5 Ocean wind farm planning

The construction of an extremely large tower with the huge turbine has already started to seek higher efficiency of wind energy generation. Even in this case, PC tower still be able to adapt for this change that is to cast concrete in place at the site. If a combination with site precast method can be applied, a construction period would become much shorter. In this way, we believe that the PC towers will contribute to the progress in the wind power generating business through the development of PC technology.

REFERENCES

[1] Shinagawa, K., Wu, T., Tanaka, Y., Study on a New Preventive Device from Chloride Attack for Prestressed Concrete Precast Segmental Bridge, The 10th Symposium on Developments in Prestressed Concrete, pp. 563-568, Oct., 2000

[2] Hiromatsu, A., Nishikawa, K., Uchida, K., Ito, K., Investigation of Method to Estimate Life-cycle-Cost of Prestressed Concrete Bridges, The 10th Symposium on Developments in Prestressed Concrete, pp. 725-730, Oct., 2000

DEVELOPMENT AND APPLICATIONS OF PRESTRESSING TECHNIQUES IN HUANGLONG STADIUM

Yu Bin & Nie Yongming
China Building Technique Development Corporation

Feng Dabin
China Academy Of Building Research

KEYWORDS: stadium, presstressing, coupler, stay cable.

1 INTRODUCTION

Huanglong Sports Center is situated in Hangzhou City, Zhejiang province, P. R. China. It is composed of the main stadium, training stadium and gymnasium, the auxiliary service facilities. The main stadium, one of the super large-scale stadium throughout China, occupies an area of 48,000 square meters, and its building area is about 80,000 square meters. The main stadium can accommodate 60,000 persons. The structure of the main stadium consist of the concrete towers, frames of stand, outer concrete box girder, inner steel box girder, the latticed shells and stay cables(See Fig I).

The prestrssing Company of China Building Technique Development Corporation undertakes the construction of the separate prestressing project. The prestressing anchorage system adopts the sets of QM, QML, QMU and QMS system developed by China Academy of Building Research.

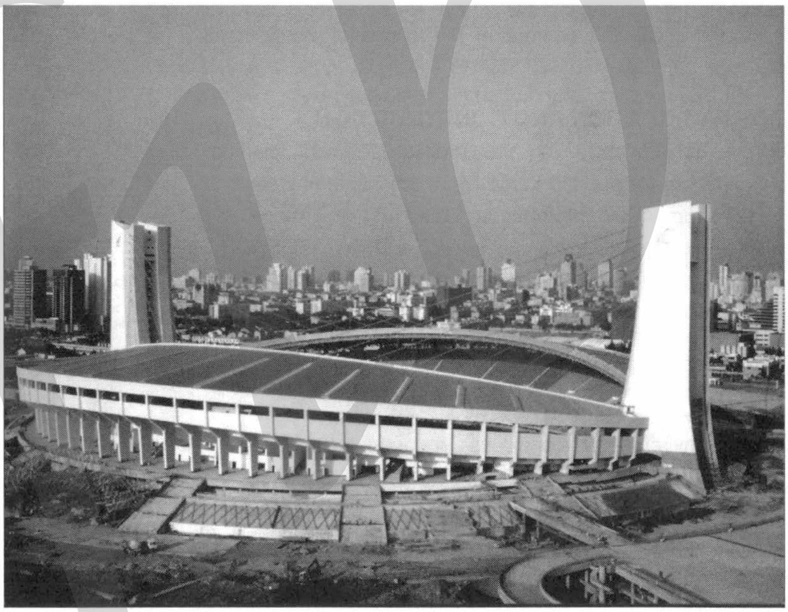

Figure 1

2 PRESTRESSING CONSTRUCTION OF CONCRETE TOWERS

The concrete towers with heights of 85m include the southern and northern ones. The double towers with four legs are prestressed reinforcement tube structures. The towers mainly undertake the huge horizontal action forces made by the stay cables. The basements of the towers are two-story ones and the structures above the ground are 24-story ones. C40 concrete is applied in the towers. The post-tensioning bonded technique is used to guarantee the strengths and rigidities of the cantilevers of the towers.

3 PRESTRESSING CONSTRUCTION OF OUTER GIRDER

The outer girder is a super long, curved box girder. Its spatial continuous length is about 781 m, the girder is 2.2m high, 2.8～3.0m wide. The thickness of webs at both sides of the girder are 550～750m. The thickness of the top and bottom plates are 250～450mm.The C40 concrete is used for the outer girder, and the total concrete consumption is about 3100 m^3. The post-tensioned PC Technique was adopted in order to resist the actions of all kinds of loads. The 1860N/mm^2, ϕ^j15.24mm steel strand is used as the tendons. The specification of duct is ϕ65×0.35mm.

4 INSTALLATION OF STABLE CABLE

In order to resist the upward loading of the roof caused by the negative wind pressure, there are 9 stabilizing cables equipped on the main truss purlins of the eastern and western zones. This cable is made of ϕ^j 15.24mm steel strands, and its length is 200m. The ϕ 75.5x3.75mm galvanized steel tubes are adopted as the outer protection sleeves of the cables. The QMS 15-5 anchorage for stayed cable is applied. The installation of the cables is carried out by using the method of hoist pulling. The tensioning and cable adjusting is done by using the YCQS 150 Type jack. The final anti-corrosion measure of the cable is realized by grouting.

5 CONSTRUCTION CONCLUSION

So far, the main stadium project of Huanglong Sports Center, is the one with the most types of prestressed reinforcement, complicated construction technologies and difficulties among the same kinds of projects in China. This project includes the plans such as the installation of stayed cables and stabilizing cables, vertical bonded construction for the towers, super long spatial circular bonded and unbonded construction. This project also uses many advanced construction methods such as the construction technologies of steel strand stayed cables, steel strand connecting and changing angle stressing technique.

The excellent designs, reasonable construction plans and adoption of advanced construction technologies overcome very well the technical difficulties during the construction. The whole course monitoring to all the data during construction indicates that the testing data coincide with the designs and satisfy the requirements of the designs.

The specialized prestressed construction, excellent management group, strict quality control and high level construction teams ensure the construction of this project to be carried out smoothly and receive the good evaluations from the clients supervision party, Design departments and construction companies.

THE NEW TERMINAL AT NAHA AIRPORT, OKINAWA, JAPAN

Hideo Moritaka Nobuhiro Yamaura Hideichi Tsuji
YASUI Architects & Engineers
JAPAN

Kazunori Osako
P.S.Corporation
JAPAN

Keywords; salt damage, durability, precast construction, post-tensioning, speed of construction

1 INTRODUCTION

The new terminal building at Naha Airport (Fig.1) was opened in May 1999 as a gateway of Okinawa's economic regions, including East Asian countries, in the 21st century. A nearly ¥30 billion investment was provided for the facility, with a capacity of more than 10 million passengers per year, which consists of a main passenger terminal, two finger terminals and 13 passenger boarding bridges.

Okinawa Islands, located in the south end of Japanese Archipelago, is one of the most distinguished aveas of salt damage (Chloride-induced corrosion), because it is surrounded by the sea and is located in the subtropical zones with high temperature and high humidity. The Naha airport is situated near the seashore.

The buildings completely adopted precast construction method with post-tensioning technology in order to secure the durability against salt pollution. In addition, this structural system provides flexibility in use to create a large free internal space, realization of large-scale structure without expansion joints, speed of construction, qualities and environmental issues.

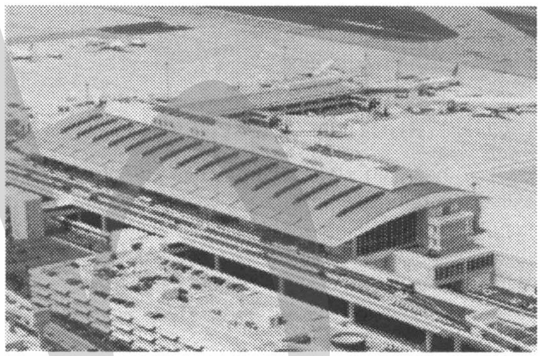

Fig.1 Perspective view of new Naha Terminal

2 NEW TERMINAL FEATURES AND STRUCTURAL SYSTEMS DESCRIPTION

The new Naha Air Terminal adopts a "Finger system" layout, which functionally connects the main terminal with two finger terminals. For the main terminal, the multi-layer system has been applied to separate Departure (the 3rd floor), Arrival (the 1st floor) and other concessions as shown in Fig.2.

The main terminal is a 5-story concrete structure with a length of 348m (beam span 12m), a width of 57.6m (beam span 14.4m) and a height of 33.9m. The finger terminals are 2-story concrete structure with a length of 144m, a width of 33.6m and a grid of 12m×12m. Their total area is 77,000 m².

The structural system of the main terminal is a moment-ductile seismic frame with precast post-tensioning (Fig.3). The roof structures are designed like the form of a wing-shape of airplane. They are composed of three structural components.

- Precast post-tensioned double girders with a length of 39.6m (28.8m +10.8m cantilever canopy) which have a slender shape
- Pre-tensioned double-tee slabs with a length of 10m
- Cast in situ double columns to support the girders

Skylights installed between the double girders have introduced natural light inside the airline ticket counters and the lobby, thereby providing a widely comfortable space (Fig.4).

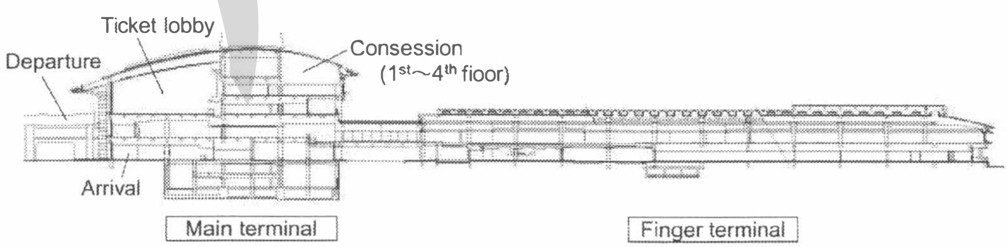

Fig.2 Vertical Section

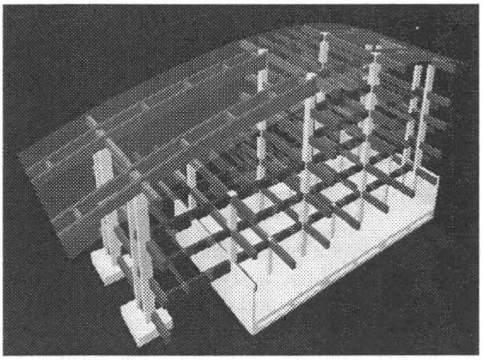

Fig.3 Skeletal frame system (Main terminal)

Fig.4 Inside of the ticket lobby

3 PRECAST CONSTRUCTION WITH POST-TENSIONING

There was no factory in Okinawa Islands that manufactures large-sized precast reinforced concrete components and precast post-tensioned segments exceeding a weight of 20 ton. Therefore, an open-air factory with a total area of 40,000m² was temporarily constructed at an industrial complex area 10km away from the construction site.

The 5-story main terminal was constructed with a speed of one floor per one month using the precast construction procedure as shown in Fig.5. As a result, it totally took eight months to complete the structure from the 1st floor to the 5th floor, including the period for manufacturing the precast elements at the temporary factory.

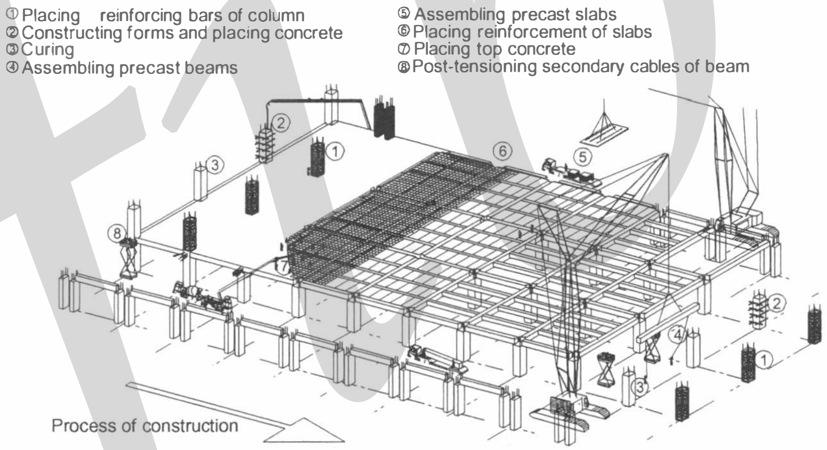

Fig.5 Cyclic process of construction (the 1se～5th floor)

4 CONCLUSION

The precast construction with post-tensioning mentioned above is expected to be applied increasingly in Japan from now on, because it has the following features.

1. Creating an aesthetic structure
2. Providing a comfortable large free space with flexibility in use
3. Improving efficiency and productivity
4. Shortening construction period
5. Contributing to environmental issues

REFERENCE

1. Moritaka H. et al., Development of prestressed concrete beams with web openings and their application, FIP Congress, Amsterdam, May 1998, pp911-915

STRUCTURAL DESIGN OF HUGE PRESTRESSED CONCRETE FRAME OF DA ZHONGHUA TRADE PLAZA IN SHENZHEN

Li Dongbin Weilian Dai Weiming Qu Jinghui Sun Renfan
(China Academy of Building Research, Beijing 100013, China)

Keywords: Huge Frame, Arch, Torsion, Large Partial Pressure, Hinged Waffle Beam

The Da Zhonghua International Plaza in Shenzhen in China has a total building area of 310,000 sq.m. The plan of the Building is rectangular and consists of a central hall and 4 towers with elevator shafts on the corner sides of the building. The central hall is 34m x 42.5m and in three floors at levels 17m, 27 m and 39 m. respectively above the ground and supported by four columns at the four corners of the hall which is 34m x 42.5 m. in dimension. The full configuration of the whole building is somewhat unusual (see accompanying figure 1) and its structural design solution which should be in compliance with the aseismic requirements of the locality has recourse to the certain special structural design solutions as well as the application of prestressed concrete. Otherwise, if the structure were designed in the ordinary way, the torsion effects of the side beams of the central hall and the moments of the four columns of the central hall would be quite prohibitive.

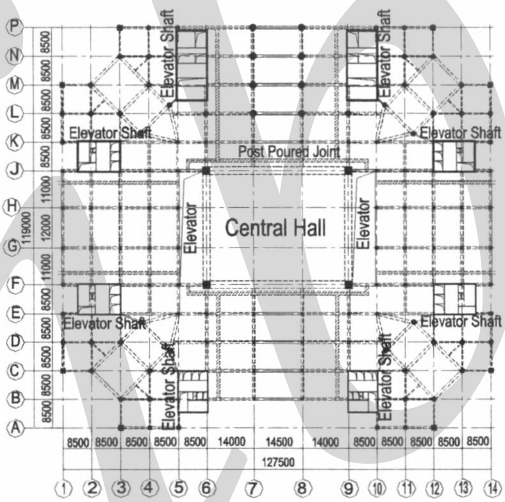

Fig.1 Structural Plan Layout

Thus, some structural artifices in the design must be devised to overcome the difficulties which may summarized as follows:

1. Measures must taken to reduce the very large torsional moments as well as the large eccentricities In the two directions of the main columns of the central hall and effective devices must be figured out to reduce the difficulties thereto pertaining through the method of the post poured joint and further appropriate prestressing of the structure;
2. The floor slab is designed as the one way waffle beam hinged to the main frame so that it cannot transfer the moments thereby reducing the torsional effects in the side beams and the bending moments of the columns;
3. An arch is used to each side of the 34 m. span direction of the central hall on both sides of the hall, the depth of the upper chord and the lower chord being only 0.8 m.;
4. The floor slab, the main beams, the upper and lower chord of the arch as well as the columns are all designed through the use of prestressed concrete to increase the stiffness and the ability against cracking.

With the above measures are taken in the structural design, the Project becomes feasible and quite easy and efficient in design and construction.

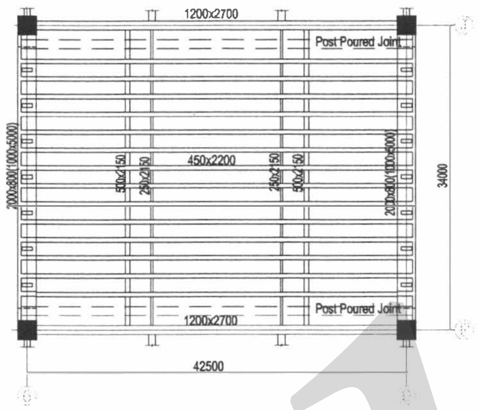

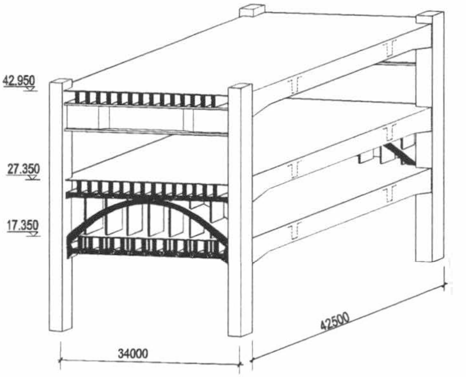

Fig.2 Structural Plan of Simply Supported Ribbed Floor Slab

Fig.3 Perspective of the Huge Frame

REFRENCES

[1] Tao Xuekang: Design Handbook of Post-Tensioned Concrete, China Publishing House of Building Industry, 1996.

DESIGN AND CONSTRUCTION OF UNBONDED POST-TENSIONED PRESTRESSED STRUCTURE IN QINGDAO BROADCASTING AND TV CENTER

Wang Ni Meng Luxiang Chen Gang Wang Liyun
China Academy of Building Research
People's Republic of China

Keywords: Unbonded prestressed structure, ribbed beams, crossed beams, tall building

1. INTRODUCTION

The main building in area A of Qingdao Broadcasting and TV Center is a 33 storied tube-inside frame-outside structure, the concrete strength grade is C50, and inner tube size of 17.5m x 21m. In the original design of the inner tube, it is slab column system with column spacing of 3.5m and main/secondary beam structure, which is not good for use. To improve the usage function, reduce the floor height and increase the number of floors, the inner tube floor slab of some floors in the main building is changed into the unbonded post-tensioned prestressed structure. This project was completed in 1998 (see photo 1).

In this structure four types of unbonded prestressed structure are adopted: prestressed ribbed beams to undertake common office load, prestressed main beams to undertake the load of upper stories, prestressed crossed beams to undertake inequality amass loads, and 3 span continuous beams with cantilever beams.

The crack resistance requirement of this project is: under short-term load combination, the concrete tensile stress control coefficient is α_{ct}<0.6; under long-term load combination, α_{ct}<0.30 and live load quasi-permanent coefficient is 0.5; under construction load combination, α_{ct}<0.8.

The concrete design strength of this project is C50. During tension, when the concrete strength reached the 75% of the design strength, tendons can be tensioned.

Photo 1 The building in construction

2. UNBONDED PRESTRESSED RIBBED BEAM STRUCTURE

Unbonded prestressed concrete ribbed beam structure is adopted for the inner tube of the 4th, 18th, 19th and 20th floor slabs of area A of main building of Qingdao Broadcasting and TV Center. Slab thickness is 80mm. The spacing of prestressed ribbed beam is 1.5m on the fourth floor and 1.75m on other floors, the ribbed beam cross section dimension is B x H = 400mm x 600mm~680mm. The span/height ratio of the ribbed beam is 29~26, and each ribbed beam is placed with 6~8 unbonded strands. The calculation result is shown in Table 1.

Table 1 Ribbed beam calculation result

α_{ct} under long-term load	α_{ct} under short-term load	α_{ct} under construction situation I	α_{ct} under construction situation II
0.15	0.30	0.77	-0.02
Deflection under short term load	Prestressed deflection	Long-term deflection	Counter-arch under construction situation II
11.8	-9.8mm	11.8x2-9.8=13.8mm	-4mm

The photo 2 shows construction situation of prestressed ribbed beams.

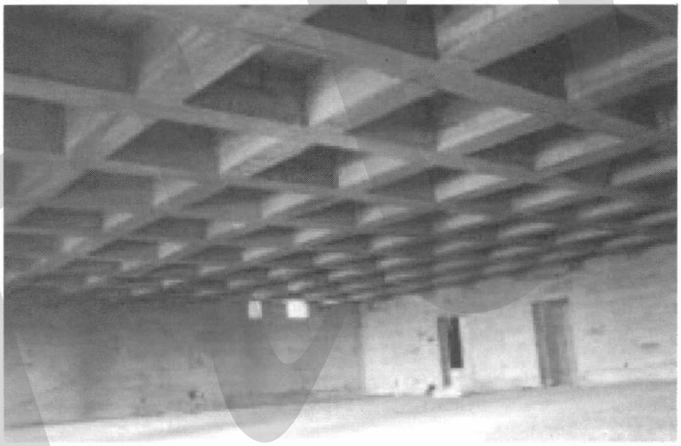

Photo 2 Prestressed ribbed beams

3. CONCLUSION

The results of application of unbonded prestressed technique in main beams, crossed beams and ribbed beams are good. So long as to apply high quality anchors and effective corruption resistant measures in construction, the unbonded prestressed technique has advantages of good operational functions, easy construction and economy as well as results in obvious reduction of materials and energies.

REFERENCE

(1) Tao Xuekang, Unbonded prestressed concrete design and construction, Beijing, Seismic Publishing House, 1993

RESEARCH AND DESIGN OF INVERSE BEAM-SLAB FLOOR OF COMPOUND PRESTRESSED CONCRETE FRAME STRUCTURE

Xue Lihong Xu Jinsheng
China Academy of Building Research
P. R. CHINA

Keywords: Compound, Prestressed, Inverse Beam-Slab, Floor

The No.9 High-rise of Jingdu, which has 21 floors, is located in Beijing. Its floor adopts a new structure form: Compound Prestressed Concrete frame Inverse Beam-Slab Floor (a patent of China). Post-tensioned beams are hidden in the floor. The beams are inverse T in shape, wide and flat. There may be secondary beams between frame beams. The plate between beams likes sandwich, which consists of three layers. The bottom and the top layer are cold-rolled ribbed steel wire welded fabric concrete plate. The middle layer is light and hydrophobic pre-cast blocks. Pipelines of the building can be embedded in the middle layer. Concrete of beams and plates is cast at one time in construction. Normal floor structure is illustrated in fig. 1. The largest column-grid of the project is 8.7m×7.5m; the structural thickness of the floor is 250mm for common rooms, 200mm for lavatory. The size of beam is 1600×250mm.

Application of the Prestressed Concrete frame Inverse Beam-Slab Floor in this building is successful. The main advantages of the floor structure are: 1) the rigidity of the floor is large due to the beam with I shape. 2) The function of building is improved by using hydrophobic expanded perlite precast block that is sound insulating and heat insulating material. 3) The weight of the floor can be reduced efficiently. 4) It is convenient to set partition wall. 5) It can reduce the height of structural floor while satisfying the headroom of the building. 6) Pipelines of the building can be embedded in the middle layer of the floor. 7) The formwork is simple and the construction efficiency is high.

REFERENCES

[1] Xu Jinsheng, Xue Lihong: Modern Prestressed Concrete floor Structure, China architecture & building press , 1998(in Chinese)

[2] Xu Jinsheng, Xue Lihong: Inverse Beam-Slab Floor of Compound Prestressed Concrete Frame Structure，a patent of Peoples Republic of China, PN:ZL95224061.0, 1996

Fig 1 Normal floor structure

THE BANGNA – TRAD EXPRESSWAY REVISITED

Prof. Dipl.-Ing. Dipl.-Kfm. Christian Brockmann
University of Applied Sciences, Bremen

Keywords: Expressway, construction contract, fast-track approach, world's longest bridge, segmental construction

1 INTRODUCTION

The Expressway and Rapid Transit Authority of Thailand (ETA) plans to alleviate the traffic congestion in the Bangkok metropolitan area by an extended and interconnected system of expressways. With the BangNa-Trad Expressway ETA wanted to facilitate the industrial development of the South-East of Bangkok and to connect the planned Second International Airport as well as the deep water harbor with the city. This expressway forms therefore an important part of the overall traffic plan for the metropolitan area.

The expressway is 55 kilometers long and, together with 40 additional kilometers of ramps and intersections, covers a deck surface of 1.820.000 square meters. At its completion it became the longest bridge in the world. The client chose a lump-sum design-build contract on payment basis in order to implement the overall project in the shortest time possible. In 1993 the terms of reference were drafted; the contract was signed in June 1995 and in the year 2000 the entire expressway was completed. The contract called for turnkey construction, and financing by Joint Venture BBCD until completion of the project.

2 THE CONTRACT, ITS ANTECEDENTS AND RESULTS

The owner ETA chose for the project a fast-track approach, spending little time on preliminary planning. The bidders were able to influence the project from the conceptual design to construction, all within a clear contract and AASHTO specifications. Details are given in Fig. 1.

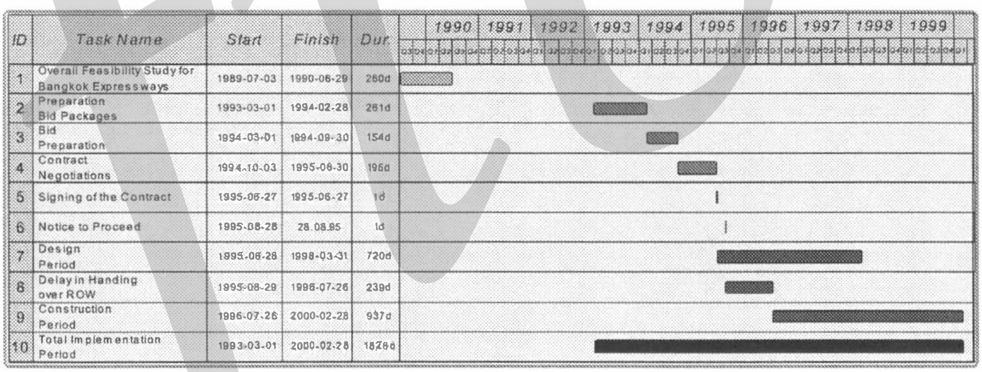

Figure 1: Gantt-chart for the Bang Na –Trad expressway

The low bidder – JV BBCD – quoted a price including interest during construction of 1 billion US dollars based on a deck area of 1.9 million square meter. This is equivalent to a price of not even 530 US$ / m². To the author's knowledge it is the lowest price ever quoted for an expressway worldwide. It became possible, because the contractor had almost complete freedom to design the least expensive overall solution, optimizing the product and the process. The total design and construction time was 53 months including 11 months for a time delay caused by the unavailability of the right of way. In 2001 an arbitration committee accorded JV BBCD a compensation of 250 US$ (in exchange rates of 1995 and therefore comparable with the contract price) because of the delay. As a result, the square meter price increased to 690 US$, based on the final deck area of 1,82 million m². Compared with the other expressway projects in Bangkok, this is still by far the lowest price achieved by ETA.

The overall picture?

- The Bang Na – Trad Expressway is the longest bridge in the world, surpassing the old record by almost 50%
- It took the owner (ETA) seven years from conception to completion, less time than would be necessary in most countries to even finalize the intra-governmental conception phase.
- Taking into account all problems encountered, the final price to be paid by the owner is less than 690 US$ /m², definitely very competitive in any part of the world.
- The quality of the expressway is according to the owner's engineer among (if not the) highest achieved in Southeast Asia.
- The aesthetics of the structure is highly appreciated by the Thais and visitors.

3 CONSTRUCTION

The BangNa – Trad Expressway was constructed throughout its entire length of 55 kilometers in the center and outside medians of the existing at-grade Highway 34, where by contract the traffic had to flow without interruptions at a speed of 80 kilometers/h (Fig. 2). The Department of Highways was at the same time improving Highway 34, and the two projects had to be carried out concurrently over the same route. JV BBCD facilitated the coordination between the projects in parallel to the construction operations.

It was decided at the tender stage that the only way to complete the expressway during the very short construction period was to use prefabricated elements for the largest part of the works. JV BBCD compared segmental construction with cast in place deck slabs on I-beams and we found segmental construction to be more advantageous with regard to speed and overall cost. A box girder solution allows at the same time for an aesthetically pleasing structure.

The precast yard, which covered an area of 650.000 square meters, had the greatest output capacity for box girder segments ever installed. There, a total of 40.000 segments was produced. Roughly 60% of the total concrete requirements of the project were fabricated at this location. The repetitive construction sequences were carefully planned to increase the speed of production and the quality of the prefabricated segments.

4 CONSTRUCTION SPEED

The biggest advantage of segmental construction with external post-tensioning and dry joints is the speed with which the superstructure can be erected. Since in bridge construction the critical path after a starting period always moves to the superstructure, this is equivalent with an acceleration of the construction period. For the BangNa – Trad Expressway six overhead trusses (D2/D3), five underslung girders (D6) and three portal trusses were used. When all girders were in operation 2.600 meters of ramps and 2.600 meters of main line deck were erected per month. With each D2/D3 girder one span every two and a half days was erected, with the D6 girder one span in two days and one portal every three days per truss. The erection speed for D6 girders was per square meter deck area twice as high as for D2/D3 trusses. At the same time all the logistics (i. e. production, transport) were simplified.

5 CONCLUSION

The described construction method is especially apt for serial production when a limited number of structural elements has to be reproduced many times. The possible construction speed is unsurpassed. At the same time a very high product quality can be assured. The planning of an industrialized serial production must encompass all steps of the process: Planning of the production output, delivery of materials, production itself, storage, transport and erection of the segments. The required means of production form a fixed ratio. Increase of output means increase of all parts at the same rate. Therefore, the complete planning process and its adaptation to a changed environment requires special attention.

These circumstances and working in the context of Thai society, culture and under its geographical conditions made the BangNa - Trad Expressway one of the most interesting and challenging bridge structures of our times.

DESIGN AND CONSTRUCTION OF PRESTRESSED CONCRETE GIRDER BRIDGES BY THE SEGMENTAL METHOD ON THE NEW MEISHIN EXPRESSWAY

Hiroyuki IKEDA Japan Highway Public Corporation
Masami FUJITA Japan Highway Public Corporation
Naohiko KAWAMURA P.S.Corporation
Toyoshige NAKAJIMA Oriental Construction Co.,Ltd.

Keywords: precast segmental method, New Meishin Expressway, large scale application

1 INTRODUCTION

The Construction of New Tomei and Meishin Expressway, as the total cost should be extreme, aims reducing the cost, labor and construction period. The almost 50-km length's section between Toyota-JCT, where it is connected to the Tomei Expressway, and Yokkaichi-JCT, where it is connected to the Meihan Expressway, is constituted by almost Bridges and Viaducts continuously.

Along almost 9-km in that section, viaducts between Yatomi-IC and Kawagoe-IC adopts the precast segmental method with large casting yard neighboring on the expressway. The Japan Highway Public Corporation (JH) has already adopted this method in some cases like the Shigenobu viaduct of Matsuyama Expressway.

To the construction of New Meishin Expressway, JH adopted more advanced technologies like as distributed deviators for external tendons, groutless protected PC tendons, wet joint without rebars, proportional segment production and erection to the formation, fully-external prestressing and transverse prestressing with pre-tention by thick 21.8 tendons. And JH is now progressing the construction by larger order unit.

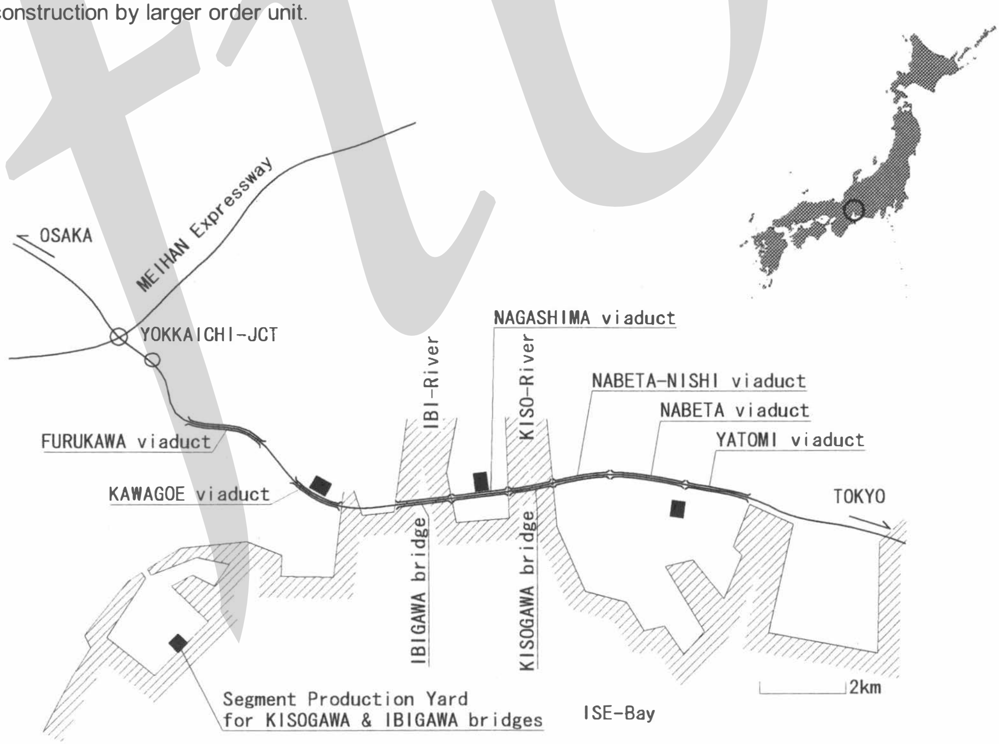

Fig 1 location of viaducts of New Meishin Expressway

2 DESIGN AND EXECUTION

Characteristics of design and execution of these projects are as follows:

1) To improve the durability and workability, the ratio of external tendons are tried to be raised in the design for longitudinal direction. Deviators' placing is adopted the distributed arrangement. It enables to simplify the forming works and to shorten production period.

2) To produce segments, short-line match-casting method is adopted. Except Kisogawa bridge and Ibigawa bridge, segment length is up-to 3.0m and weight is up-to 80ton for on-land delivery.

3) The typical span length of the viaducts is about 50m. For the typical-length spans, span-by- span erection method is adopted.

4) Some spans above the existing road or other crossing obstacles, have longer span length than the typical ones. For such spans, cantilever erection method is adopted. New type of erection-nose is developed for this erection.

Photo 1 Segment production (Yatomi viaduct)

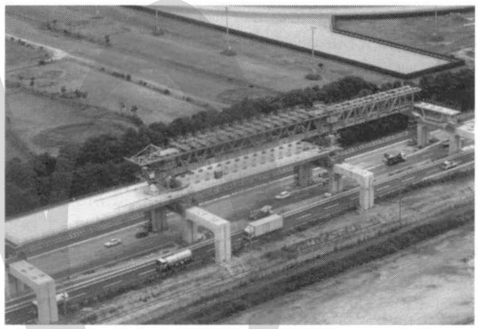

Photo 2 Span-by-span erection (Yatomi viaduct)

Photo 3 Cantilever erection (Yatomi viaduct)

3 EXPERIMENTAL STUDIES

Among these projects, some experimental studies are held. These are as follows:

1) To confirm the accuracy of analysis for deviators and the safety to lateral force of external tendon, a full-scale deviator loading test was held. Through this experiment, the accuracy of analysis and the safety to the failure is confirmed.

2) Wet-joint, whose width is 15-20cm, has no reinforcing bars. To confirm the resistance against the fatigue failure, full-scale load-moving experiment was held. Through this experiment, it is recognized that normal wet-joint has enough failure resistance.

3) Furthermore, to confirm that wet-joint had enough failure resistance to shear forces, shear failure test was held. It is recognized that wet-joint has enough strength against shear failure.

4 CONCLUSION

For New Meishin Expressway, large-scale execution of segmental method could reduce labor and cost, raise quality. In last spring, this section of New Meishin Expressway was opened successfully.

Continuously, JH is trying for full opening of New Tomei and New Meishin Expressways with more rational constructions for not only concrete bridges but also steel bridges or composite bridges.

DESIGN & CONSTRUCTION OF PRECAST CONCRETE SEGMENTAL VIADUCTS KCRC WEST RAIL PROJECT,HONG KONG.

Ir. N.D. THORBURN
Manager Special Projects, VSL Intrafor Asia

Ir. N. J. SOUTHWARD
Director, Benaim (China) Ltd.

Keywords: Alternative Design, Precast Segmental Construction, Railway Viaducts

1.INTRODUCTION

This paper is for The West Rail Viaducts, which were built to an Alternative Design prepared by Benaim (China) Ltd. The design saved several hundred million HK$ in reduced material costs, programme savings and future life cycle costs, achieved through innovative design and detailed acoustic analysis. The approximately 10 km Viaducts comprise two construction contracts, CC-201, Viaduct - Kam Tin to Tin Shui Wai Viaducts and CC-211 Viaduct - Tin Shui Wai to Tuen Mun North. Maeda Chun Wo Joint Venture (Viaducts) submitted a successful alternative tender bid of HK$2.1 billion. Viaduct construction started in July 1999 and was substantially completed in December 2001.

Both the conforming design by Arup and Maunsell, and Benaim's alternative, resulted from onerous constraints imposed by the HK Noise Control Ordinance ("NCO"), the Environmental Permit granted by the Environmental Protection Department and KCRC's own performance criteria. The NCO sets stringent statutory limits on operational noise from trains, and the viaduct and trackform designs were developed to meet these requirements by reducing structure-borne noise re-radiated from the viaducts.

2.NOISE ANDVIBRATION STUDIES

Benaim, with specialist advisers Institute of Sound and Vibration Research in the UK, established that not only the mass of the viaduct deck was important in controlling noise, but also the disposition of that mass within the cross-section and in relation to the sources of vibration. Studies showed the more closely the viaduct web panels were placed beneath the floating track slab bearings, the greater the impedance of the deck opposing input vibrations, and the less the noise radiated from the deck. This is because the narrower box resists input vibration via the greater in-plane stiffness of the girder webs, rather than via the smaller transverse stiffness of the top flange. The benefit of the narrower box girder was maintained, even when panel thicknesses were significantly reduced.

The alternative deck section has a box width of only 2000mm, compared with 3600mm for the conforming design. If the alternative boxes were supported conventionally on bearings, the bearing spacing would have been only 1000mm, and unstable in typhoon winds. Various stability options were considered, but the adopted solution was to make the bridge deck and piers monolithic.

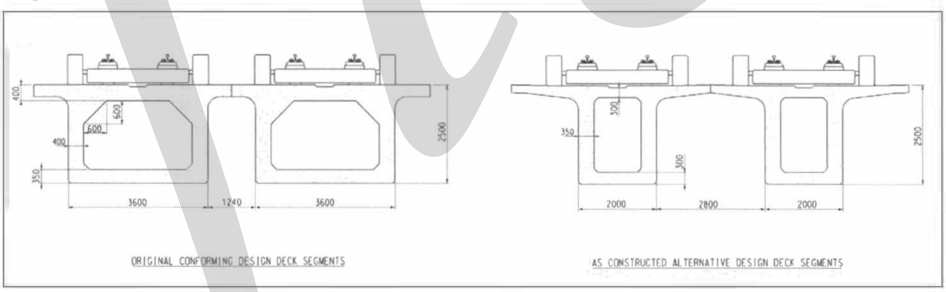

3.DETAILS OF DESIGN

Benaim's alternative retains individually articulated spans, as the conforming design, but makes each end of each span monolithic with an individual column. Each span forms a portal frame with the piers at either end, and each pier comprises two independent columns framing into the spans on either side. Thus, at typical pier locations there are four leaf columns, each supporting a deck span, resulting in a viaduct consisting of a series of back-to-back portals, with no bearings. As bridge bearings have a life considerably shorter than the structure, the monolithic piers of the alternative avoid significant maintenance costs, benefiting KCRC.

Dimensions of the RC leaf columns are carefully proportioned to allow piers to flex due to flexural rotation of the deck and thermal, creep and shrinkage movements, while still providing sufficient rigidity and strength to sustain applied loadings. The four columns at each pier rest on a common RC pilecap, typically founded on two 1.8m diameter bored piles.

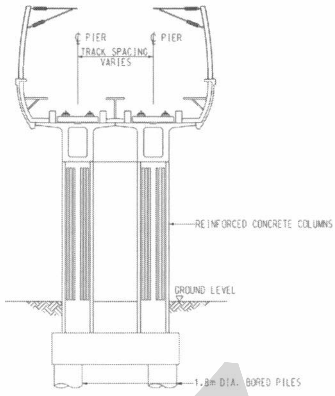

TYPICAL TWIN TRACK VIADUCT

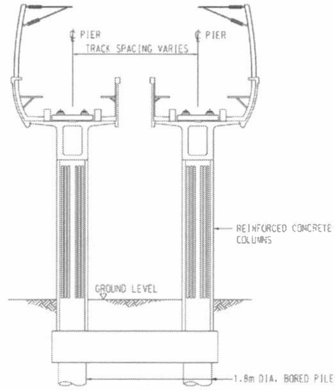

TYPICAL SINGLE TRACK VIADUCT

4.PRECAST SEGMENTAL VIADUCT SUPERSTRUCTURE CONSTRUCTION

Late in 1999 Maeda Chun Wo JV awarded subcontracts for the precasting of the segments to Redland Precast Concrete Products Ltd, and for the Erection of the Segments to VSL HK Ltd.

Precasting was carried out in yards in the Pearl River Delta Region of the Peoples Republic of China, with the first segment cast in December 1999 and the final segment cast in October 2001. In all a total of 28 moulds were used for the operation.

Initial erection studies had been focused on the use of sophisticated Overhead Launching Girders however with the advent of the Alternative Design it was decided to utilize a greater number of simple lightweight girders which could be easily moved around the site thus providing greater flexibility. Three different types of Erection system were utilised Type 1(1 Number) for areas where there were multiple parallel spans, Type 2 (8 Number) for areas where there were long runs of parallel twin spans and Type 3 (1 Number) for Long Span Balanced Cantilevers. (See pictures below.)

Segment erection started on CC201 in May 2000, on CC211 in June 2000 and on CC213 in January 2001. Erection was completed on CC201 in December 2001, on CC211 in August 2001 and on CC213 in December 2001. In all a total of 9287 segments were erected in less than 20 months; i.e. an average rate of 464 segments per month or approximately 19 per day (24 w/d per month)

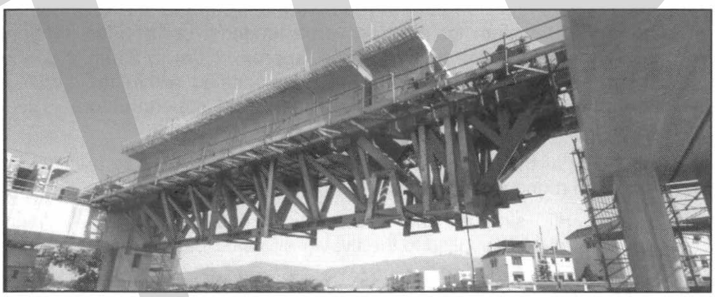

Type 1 Erection Girder

Type 2 Launching Girder

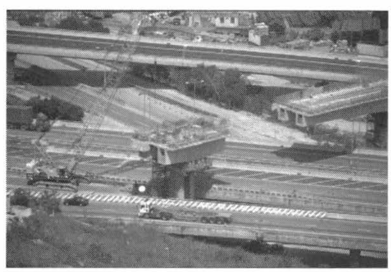

Type 3 Erection System

SIRSI CIRCLE FLYOVER, BANGALORE - POST TENSIONING ASPECTS

S. Sengupta
Span Consultants Pvt. Ltd., INDIA

Keywords : launching girder, epoxy glue, couplers

1 INTRODUCTION

This 2.65 Km long flyover from Sirsi circle to Townhall in Bangalore has been opened to traffic in 1999. The project incorporates a number of innovative features. The superstructure consists of aerodynamically shaped PSC box girder, 16m wide. Each bridge unit is continuous over 8 to 9 spans with span varying from 36m to 45m. Superstructure comprises of large number of 2.9m long precast segments epoxy glued and held together by bonded post-tensioning using tendon couplers for each span. The pier segments are transversely post-tensioned. This is presently the longest flyover completed in India. Erection is done with a launching girder from top allowing busy vehicular traffic underneath to flow uninterrupted. The paper highlights the post-tensioning aspects of the superstructure and general particulars of the flyover with illustrations.

2 GENERAL ARRANGEMENT OF SUPERSTRUCTURE

The elevated portion of the flyover is 2.65 Km long with an overall deck width equivalent to four lane carriageway. The alignment follows the existing geometrics of road at ground level with modifications in the horizontally curved portion. Four numbers entry / exit ramps are connected to the main deck to provide smooth traffic flow on the flyover in both directions.

The flyover is designed with precast segmental construction with spans varying between 36m to 45m. The entire length of superstructure comprises of a number of bridge units. Each bridge unit consists of 8 or 9 spans in a continuous module. Overall deck width of the main flyover is 16m while that of the ramp portions is 5.5m. Each span is composed of 13 to 17 nos precast segments, each segment has a length of 2.9m and width of 16m. All permanent post tensioning has been provided with bonded tendons with couplers and conventional cement grouting.

Widthwise, a central single pier with 2 nos Pot/PTFE bearings support the bridge deck. Both the box girder and the piers are aerodynamically shaped with curvilinear profiles, aesthetically pleasing.

3 ARRANGEMENT OF POST TENSIONING (PT)

3.1 Permanent PT

All permanent PT tendons are of 19 nos 0.5" dia HT (1905) strand system for the longitudinal ones and 7 nos 0.5" dia HT strand (705) system for the transverse tendons. Longitudinal tendons are continuous throughout the entire length of one bridge unit i.e. approx. 280m to 330m. Continuity of longitudinal tendons has been established by K - type couplers located within the girder webs. Accordingly, no blister has been required anywhere in the box girder superstructure. BBR post-tensioning system has been used in this project.

Transverse PT is provided only at the diaphragm locations above piers. These are 705 system passing through the deck slab with round metallic ducts.

All prestressing hardwares, HT strands and prestressing equipments are indigenously manufactured to strict Quality Control and supplied to the flyover site after passing through QC tests.

3.2 Temporary Post - Tensioni ng (PT)

Temporary PT is required at the erection stage during assembly of the epoxy glued matchcast segments at site (refer construction scheme discussed later). Macalloy bars have been used for this purpose. Temporary PT has been used for the following site activities :

i) Connecting the glued matchcast segments by horizontal post tensioning
ii) Vertical hangers from the overhead launching girder to carry the weight of segments in one span.
iii) Connecting the structural steel temporary frames (required for horizontal PT and vertical hangers) to the segments during erection or handling from the casting yard.

4 CONSTRUCTION SCHEME

The precast segments have been manufactured in a large casting yard located close to the flyover site. Average weight of each segment is about 65 MT and these are transported from the casting yard to their respective location in the flyover by means of flat bed multiaxle trailers. One segment is transported on one trailer and this activity is performed during the night when traffic intensity is low.

The construction follows span by span method, whereby all the segments of one span are temporarily suspended from an overhead launching girder until about 2/3 of the permanent PT tendons are stressed. Thereafter the assembled span is gradually lowered onto the Pot bearings and balance stressing work is completed.

5 QUALITY CONTROL (QC) OF POST - TENSIONING WORK

QC on post tensioning work are split up into various activities as follows :

5.1 QC on prestressing hardware

5.2 QC on prestressing strands

5.3 Checks during stressing of tendons

5.4 Grout injection check : based on guidelines of Indian Roads Congress IRC : 18 and report of PCI committee on post tensioning

5.5 In addition to above, unscheduled internal checks are carried out both at manufacturing works and at site in presence of BBR Swiss prestressing specialists covering following PT items :

6 PRECASTING YARD (PRESTRESSING ACTIVITIES)

Installation of anchorage cones, sheathing ducts and their precision profiling are carried out in the casting yard. Utmost care is taken in this activities in checks and counter checks conducted at all stages in order to ensure that minimum or no problems should arise during threading of the strands through the sheathing ducts with draped profiles after assembly of the segments at site by launching girder.

Elaborate infrastructure is mobilised at the precasting yard for manufacture of the segments as per the construction schedule. Matchcasting is carried out by long line method.

7 INNOVATIVEASPECTS

The project incorporates a number of innovative aspects in design and construction, many of them adopted for the first time in India, although the method of construction has been used abroad. Special mention is to be made on the following innovative construction features :

- large scale use of tendon couplers for establishing continuity of spans. Each 1905 coupler is capable to transmit a force of about 3420 kN
- no blisters anywhere in the box girder, smooth internal surface of girder
- aerodynamic profile of box girder and central pier
- large scale use of matchcast glued segments, no concreting activity at site (for superstructure)
- use of temporary prestressing during erection
- very low cycle time for erection, 5 days per span
- absolute minimum traffic interruption during erection

8 CONCLUSIONS

a) This type of construction technology is useful for flyovers in congested traffic situations.

b) Knowledge of such complex prestressing procedure should be available to the prestressing agency. The site team for post-tensioning work must be trained in all aspects of such construction for smooth co-ordination.

c) Meticulous planning of each activity at site (micro & macro) should be made well ahead of execution.

d) Substantial infrastructure (viz. over head launching gantry, cranes, batching plant, casting yard etc.) is required to ensure a low cycle time of erection.

CONSTRUCTION OF BANG NA EXPRESSWAY, BANGKOK, THAILAND

Chris Petrov
Senior Bridge Engineer
Earth Tech / JMI, USA

Keywords: Pre-cast, Segmental, Erection

The Bang Na-Bang Pli-Bang Pakong (BBBE) is the world's largest elevated expressway. The 54-km-long, 6-lane-wide viaduct stretches from the eastern edge of Bangkok toward Chon Buri, a rapidly growing city to the east.

This gigantic project provided an important link in the transportation system around the highly congested Bangkok.

The time frame for building this expressway was very aggressive and challenging for the JV-Bilfinger+Berger, Germany, with the local partner, Ch. Karnchang. The total deck area of the viaduct, 1.9 million m^2, was planned to be completed within 42 months–-with the inclusion of all the ramps and intersections. The expressway superstructure alone is about 1.4 million m^2.

To achieve this extraordinary rate of construction, the design solution utilized pre-cast segmental, span-by-span construction.

A total of 21,320 D6-segments were cast and temporarily stored at the giant casting yard near Bangkok. From the casting yard, the segments were transported to the construction site on specially designed trucks. During construction, each segment was lifted and placed on the under slung erection girder. Upon the completion of the span, the girder was launched forward and positioned into the next span.

The erection technology and erection equipment specially designed for this project comprise the focus of this paper.

1 SPECIFICATIONS – SPECIAL REQUIREMENTS FOR THE ERECTION EQUIPMENT

1.1 In order to meet the tight schedule and to build the expressway over a constantly busy highway, the requirements on the erection equipment were very strict:

- The erection cycle consisted of a maximum of two days.
- Alternative ways of segment delivery had to be developed.
- The equipment had to be self-launched, and operations from the ground had to be avoided.
- During construction, safety was a major concern regarding the construction workers and for the traffic on the highway below.

1.2 Structure characteristics

- There were three typical span lengths – 44.4m, 41.85m, and 39.3m.
- The minimum radius at the tightest curvature was R=960m.
- The maximum segment cross slope was 4.6%.
- Each segment had the width of 27m, with a maximum weight of 100t.
- The erection girder had to fit within the H-shaped columns.

Figure 1

2 ERECTION PROCEDURE

2.1 Span erection

Two schemes for the location of the swivel crane were developed: The swivel crane was either placed at the nose of the girder (Fig. 1) or on a previously erected span. Each segment was placed on a chassis by a swivel crane and then transported to its final position. The chassis was one essential component of the system, whose function was to receive the pre-cast segment. With the segment, the chassis was pulled along the top flange of the girder to the final segment position. This chassis allowed for three-dimensional adjustments-— i.e., with vertical, horizontal, and rotational movements.

Once all segments were positioned on the girder and the post-tensioning was completed, the span became a self-supported unit. In this way, the erection cycle was completed.

2.2 Launching

A rack and pinion technique was selected as the most efficient and safe launching system.
All the temporary devices, as well as the main supports, were moved from pier to pier by the erection girder; so there were no construction operations from the ground. This was a very important advantage of the system, since the construction of this 54km expressway took place above the always-busy Bangkok streets.

The front part of the girder was a plate girder with a trapezoidal cross section capable of carrying the span weight. To make the launching of the girder possible in curves, the tail was designed with a triangular-shaped cross section. The tail could be offset 800mm from the centerline pier.

The entire system was modular, so it could be assembled, disassembled, and relocated as necessary to meet the demanding construction schedule.

Five sets of this innovative erection system were fabricated and used for safe and fast construction of the six-lane expressway over the constantly heavy traffic in Bangkok.

REFERENCES

[1] Brockmann, C., Rogenhofer, H.: Bang Na Expressway, Bangkok, Thailand — World's Longest Bridge and Largest Precasting Operation, PCI Journal, pp. 26-38, Jan.-Feb., 2000

[2] Shafer, G.: Bangkok Blockbuster. Civil Engineering, pp. 32-35, Jan., 1999

CONSTRUCTION TECHNOLOGY IN KAWAGOE VIADUCT

Hiroyuki IKEDA Kazuyuki Mizuguchi
Japan Highway Public Corporation
JAPAN

Kaname ABE Eisuke YAMAMOTO
Obayashi Corporation
JAPAN

Keywords: precast segmental method, New Meishin Expressway, curved bridge, pre-tension

1 INTRODUCTION

Kawagoe Viaduct is located at the Mie-Kawagoe Interchange of New Meishin Expressway, between Nagoya and Yokkaichi. The Viaduct consists of 1298m long concrete box girder bridges for main ways(up-and-down) as well as 4 interchange ramps. The concrete segments are fabricated using short-line match casting method. Span-by-span and cantilever method is adopted for the the construction of the continuous PC box girder. To arrange the prestressing tendons is planned to be installed in the box plates as inner cables, and also besides the webs as external cables. The plan view shows a very small curvature radius of R=85m and span length varies 30-78m(**Fig.1**).

Fig.1 Virtual view at completion

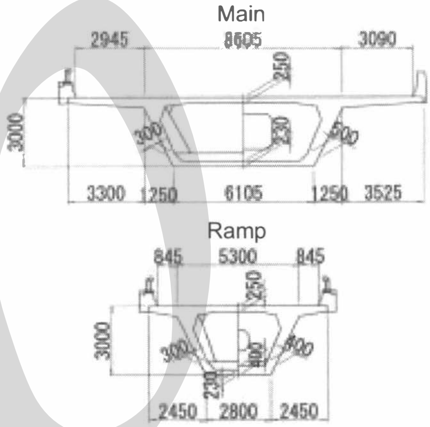

Fig.2 Standard cross section

2 STRUCTURAL DESIGN

The standard cross section of main bridges and ramps consist of one box girder and have girder height of H=3.0m as shown in **Fig.2**. The characteristics of Kawagoe viaduct are;

1) The slender span/height ratio L/H=12-22(main bridge), L/H=10-28(ramp).
2) Ramp bridge has a small curvature radius R=85m,therefore it is sensitive for twisting moment.

The curved bridges need the transverse and longitudinal displacement control system. So that a new type bearing technique with high damping rubber and displacement control system is applied to the middle support piers(**Photo.1**).

For quality control of grout mortar fulfillment of external prestressing cables, transparent plastic ducts are utilized.

3 SEGMENT PRODUCTION

To produce segments, short-line match casting method is adopted. Although existing of the widening ramps of Mie-Kawagoe interchange, only standard main and ramp box sections are provided, and different width of widening parts is adjusted in overhang slab pouring.

To accurate of match casting in the short-line produced segments is controlled by new developed Geometry Control System, using the survey instrument online with personal computer.

For achieving high durability of concrete slab, better workability, and better reliability of prestressing, pretensioned transverse tendons are placed as indent-formed wire strands of ϕ21.8mm for main bridges(**Photo.2**).

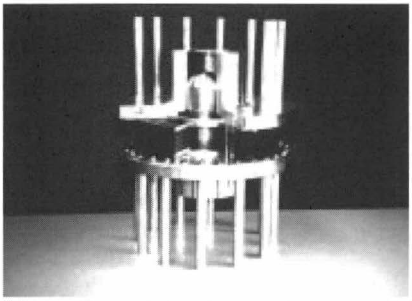

Photo.1 Bearing at pier

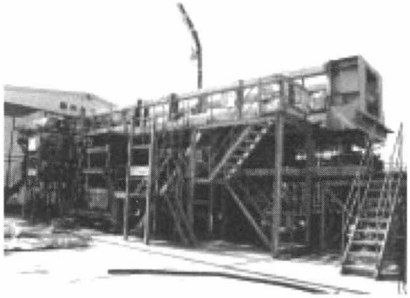

Photo.2 Casting cell

4 ERECTION OF SEGMENT

The erection of segments is adopted span-by-span method and cantilever method using only one erection girder, which is developed for this project. At the end of the guided launching-girder, a hydraulic guide arm and hinged connecting element is installed to the main erection girder, so that the erection girder can be bent to the proportional line(**Photo.3,4**).

For the safety erection of curved ramp ways with the 168m long special erection girder, the moving of erection girder is controlled using GPS monitoring system to insure the levels of constructed segments and the geometry control of the guided launching-girder along the curved ways(**Fig.3**).

Photo.3 Cantilever erection

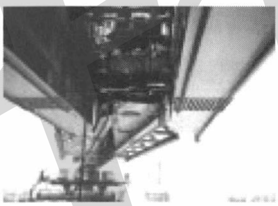

Photo.4 Hinged connecting

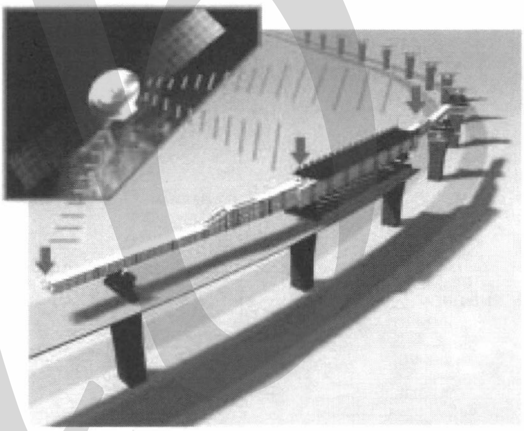

Fig.3 GPS system for erection

5 MANAGEMENT CONTROL OF ERECTION

At the Kawagoe erection site, there are total 120 spans and 1 829 pieces of segments. Each segment form should be adjusted 3-dimensional to the different formation of bridges. For such large number of segments, the segment control system is developed. In this system, not only 3-dimensional geometry control of segments and the control of the planned timetable at site, and also the management control at town office is possible to use IT technology.

6 CONCLUSION

This is the first application of the precast segmental method for the curved bridge in Japan. The adopted IT technology could rise quality, speed and safety of the erection of precast segmental bridges. The Kawagoe viaduct shows the new technology of segmental concrete bridge for curved structures.

REFERENCES

(1) Ikeda, Mizuguchi, Abe, Kawahigashi, Yamamoto, Ymaguchi ; Construction of the Superstructure of Kawagoe Viaduct (In Japanese),pp.2-9 Bridge and Foundation Vol.35,No.6,June,2001
(2) Moreton;Three Dimensional Geometry Control of Segmental Bridge,Person Brinckerhoff,Mar,1993

DECK RECONSTRUCTION OF JACQUES CARTIER BRIDGE USING PREFABRICATED HIGH PERFORMANCE CONCRETE PANELS

Adel R. Zaki, P.E.
Bridges & structures, SNC-Lavalin
Montreal, CANADA

Guy Mailhot, P.E., M. Eng.
Jacques Cartier & Champlain Bridges
Montreal, CANADA

Jean Paul Payet, Eng.
Demathieu et Bard
Metz, FRANCE

Keywords: bridge, integral deck system, prestressed, post-tensioned, high performance concrete

1 INTRODUCTION

Opened to traffic in 1930, the Jacques Cartier Bridge spans the St. Lawrence River between Longueuil and Montreal, Canada. Composed primarily of steel truss approach spans and a cantilever type main span, the bridge was originally built with a reinforced concrete deck (Fig. 1).

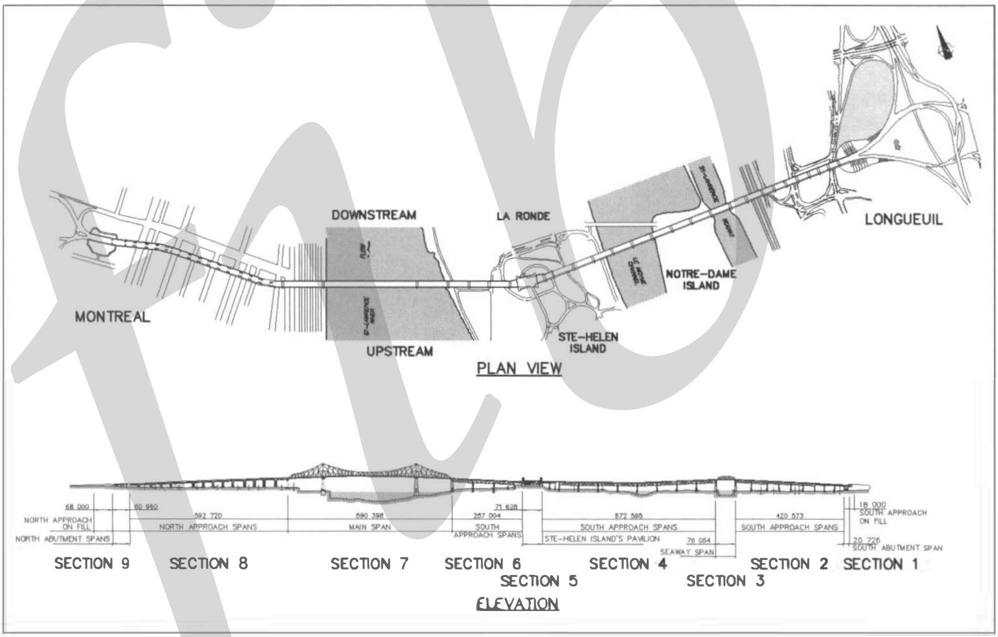

Fig.1 General Layout of Bridge

With five lanes and a traffic signaling system for reversing the direction of traffic flow in the centre lane, this bridge carries more than 43 million vehicles every year making it one of the busiest bridges in North America on a per lane basis.

The combined effects of age, heavy vehicles and the extensive use of deicing chemicals since the 1960's has led to undertake the replacement of the existing reinforced deck by a new deck system made of precast, prestressed, high performance concrete panels (60 MPa) forming an integral deck system, which is subjected to transverse and longitudinal post-tensioning after being installed on the bridge.

This major deck replacement project which extends over a distance of more than 2.7 km and over a width of 23.5 m., including a sidewalk and bicycle path, represents a deck area of more than 60 000 square metres to be replaced.

With a total project cost of approximately 110 million dollars Canadian, this two-year project (2000-2002) represents one of the biggest bridge deck rehabilitation project ever carried out in Canada.

The main parameters describing both the technical project constraints and technical solutions developed to successfully carry out the project are as follows:

- use of state-of-the-art materials including high performance concrete to meet both strength and weight requirements and to provide a design life of more than 50 years
- use of prefabricated, prestressed deck panels to replace the existing deck during night closures while eliminating disruptions to users during rush hour traffic
- use of longitudinal and transverse post-tensioning to ensure a durable performance of the deck system, particularly at the joints between the panels.

2 CONCEPT FOR APPROACH SPANS

The new deck for the north and south approach spans consist of a series of deck spans, typically 7.67 m long. Each deck span is composed of four precast, prestressed concrete panels installed side-by-side (Fig. 2). Each panel has a 180 mm thick slab and possesses three integral stems with variable moment of inertia which are reinforced with four 15 mmΦ draped prestressing strands (Fig. 3). The concrete barriers are also integrated with the panels. Following the installation of a number of panels which are supported by existing floor beams, transverse and longitudinal post-tensioning is applied. This is followed by the grouting of ducts, and the installation of a waterproofing membrane and an asphalt wearing surface.

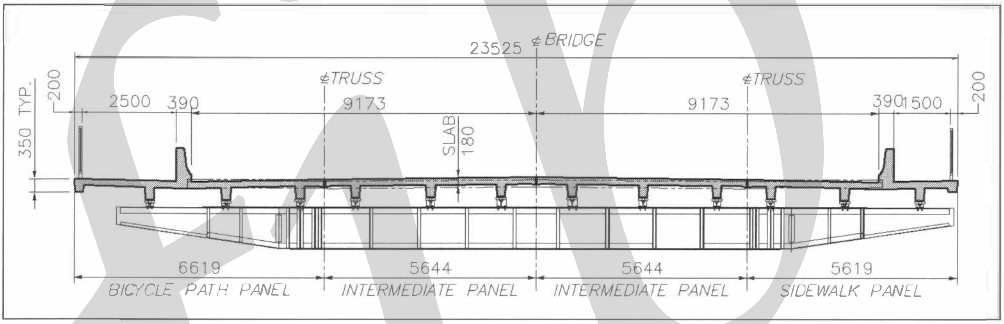

Fig.2 Approach Span – Typical Deck Cross-Section

The live load used for design is a QS-660 kN Truck Load (Fig. 4) and a uniform load of 5.0 kPa for sidewalks. The new deck system was designed to carry the full live load for all stages of construction while a section of deck is open to traffic.

The deck panels for the approach spans represent 70% of the entire surface which is to be reconstructed.

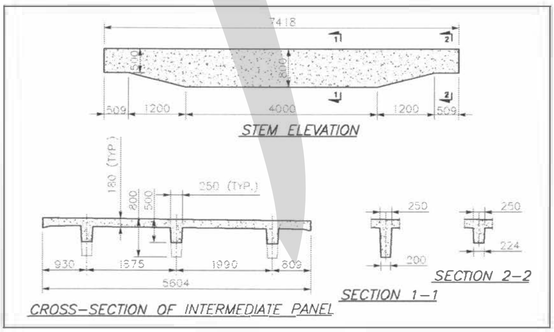

Fig.3 Typical Deck Panel

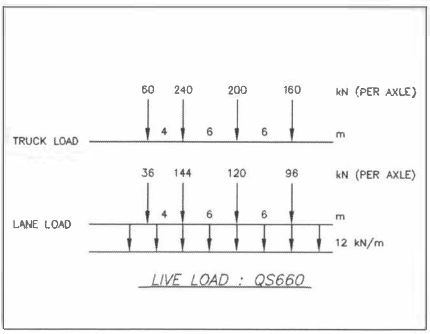

Fig.4 QS-660 Truck load configuration

BHAGALPUR BRIDGE ACROSS THE RIVER GANGES, INDIA

C.R. Alimchandani
Chairman & Managing Director,
STUP Consultants Ltd..
Mumbai, India

Vijay Kumar
Managing Director,
U.P. State Bridge Corporation
Lucknow, India

V. K. Kanitkar
Chief Consultant,
STUP Consultants Ltd..
Mumbai, India

The Bhagalpur Bridge across the River Ganges (Fig 1) has a length of 4.37 km – the second longest in India. The bridge has four types of structures (Fig 2, 3) corresponding to the 4 regimes of the river :

The approach viaduct Zone D, 162 m long, (Fig 2) has 5 simply supported box girder spans of 32.4 m, (at center to center (c/c) of piers), constructed on staging. The piers are founded on shallow cylindrical RCC well foundations sunk 18m deep below the highest riverbed in this Zone.

The next Zone 'A' (Fig 2) across the deepest part of the river, consists of 120 m spans (at c/c of piers), with a total length of 1104 m constructed over standing water, which at Low Water Level has a maximum depth of 7 m. The superstructure is supported on hollow RCC piers constructed on 9 cylindrical RCC well foundations which were to be sunk from sand islands upto 7 m deep, by excavating soil from within the wells by grabs. The superstructure consists of prestressed concrete cantilevers of 48 m fixed to the pier and a 24 m reinforced concrete suspended span across the cantilever tips, to give effectively 8 spans of 120 m, (at c/c of piers), and approach spans of 72 m, (at c/c of piers), on either side.

Zone 'B' (Fig 2) which is 1139.4 m long, is dry in the fair season, and is covered with water only during floods. This Zone has well foundations which are sunk upto a depth up of 70 m. In this Zone the superstructure is made of simply supported prestessesd concrete box girders having a length of 63.3 m supported on hollow RCC piers.

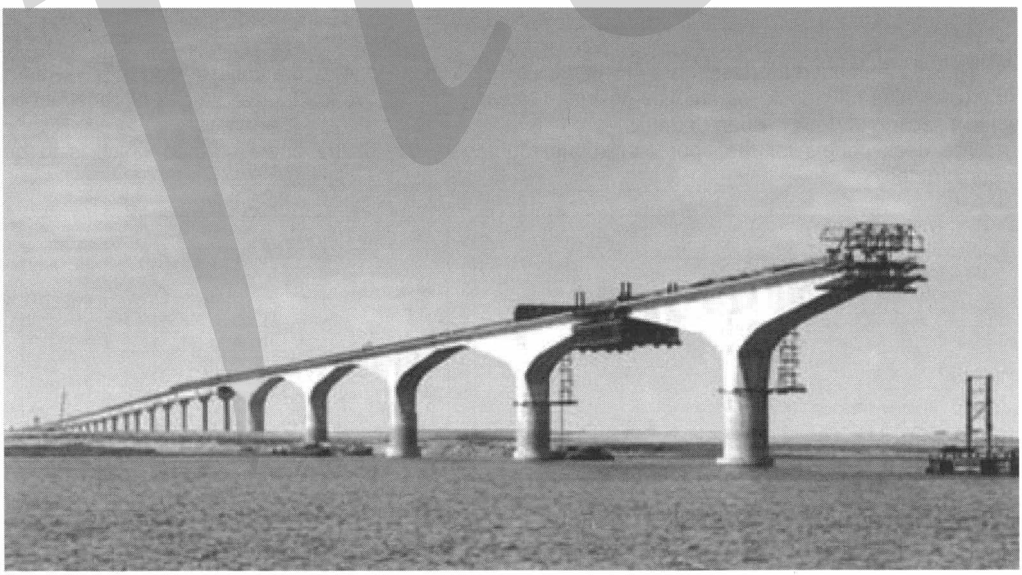

Fig. 1

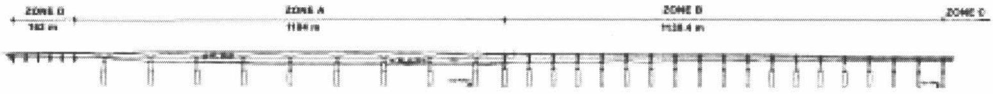

Fig. 2

Fig. 3

Zone 'C' which has an aggregate length of 1961.8 m is constructed in a zone beyond the left bank (at the end of Zone B) to cross the backwaters which occur during high floods. It consists of wells sunk upto 60 m below the highest ground level in this area.

During high floods the river reaches a maximum velocity of 4.5 m/s and is therefore expected to scour below High Flood Level to a depth of: 47 m in Zone A and B, and 40 m in Zone C. Therefore the wells go down by an additional depth of 22 m in Zones A and B, and 16 m in Zone C in order to provide sufficient grip length, to resist the horizontal forces due to high floods, earthquake and wind effects.

One would be exceptionally lucky if a bridge of this size, across a great Indian river is executed without any mishap. The alluvium in the Indo-Gangetic plain has a depth of 700 m, the scourable zone at the top is usually sandy and below that one can come across highly compressed sand, sandy silts, stiff sandy clays, etc, which are difficult strata for well sinking. At this site, the maximum shift recorded at the top of a well was 186 cm.

Sometimes there can be unseasonal floods due to the early melting of Himalayan snows and the wells can also tilt and shift during such an event if they have not been sunk adequately. In the case of those wells which tilted excessively, smaller additional wells were cast and connected to the tilted wells at well cap level so as to act as counterweights.

During such an unexpected flood, wells that were not yet sunk adequately toppled over. Also a part of the bed which had been scoured did not get re-filled. The minimum depth of standing water became 22 m instead of the normal maximum depth of 7 m at Low Water Level. The wells in this portion had to be cast by sinking hollow steel caissons. The space between the inner and outer walls of the caissons had a thickness equal to the lower part of the RCC well steining. It was constructed using catamaran barges and the sinking technique involved bolting together segments of the hollow caissons with foam rubber gaskets to obtain water tightness. Concrete was then poured into the hollow caisson wall to facilitate the lowering of the same, till it touched the river bed – verticality was maintained by equally stressed prestressing cables (on a common hydraulic circuit) which were used for lowering the caisson. The same vertical cables supported the hollow steel caissons at the beginning, till enough segments were bolted together to permit the caisson to float on its own. Thereafter the construction was completed by the tradtional sinking process utilised for all the other well foundations.

The only regret while working on this major bridge was that the Terms of Reference of the turnkey bid did not permit either segmental precast cantilever construction or a cable stayed solution, the pier locations were already fixed and therefore the span arrangement could not be optimised. However, building a great bridge is always satisfying to all concerned - Uttar Pradesh State Bridge Corporation constructed the bridge, STUP carried out the design and construction engineering and provided construction assistance where required by this very capable contractor. The owners were the Bihar Public Works Department and the proof consultants were Cowi, Denmark and CES, India.

DESIGN AND EXECUTION OF CAPPING WORKS ON OUTER FLOODWAY SHAFT IN METROPOLITAN REGION

Makoto Kanai and Naruhiko Eto
Obayashi Corporation
Japan

Shinji Taura and Osamu Takeshita
Fuji P.S. Corporation
Japan

Keywords: Use of precast members, Prestressing, high altitude work, shorter construction time

1. INTRODUCTION

This Metropolitan Region Outer Floodway referred to herein is an underground floodway of approximately 6.3 km under construction about 50 m below the ground level of National Highway Route 16 to reduce flood hazards during torrential rain.
This paper relates to the construction of a cap of prestressed concrete girders at the crest of the shaft provided in the underground floodway to serve as an operation base.
The shaft is one of the largest of its kind in Japan with an inside diameter of 31.6 m and a depth of 72.1 m below the ground level.

To facilitate safe and speedy installation of top slabs at the crest of the shaft, precast main girders, cross girders, and floor slabs were used and the prestressed concrete type of structure incorporating a partial reinforced concrete structure was selected for the shaft cap.

2. OUTLINE OF DESIGN

One of the major purposes of this project was how to simplify the difficult high altitude works. The shaft cap lay 72 m above the ground level of the shaft and this made it difficult to provide supports for the purposes of capping work. It was thus decided to use precast structural members and to dispense with supports. Prestressed concrete members were selected instead of reinforced concrete members to reduce weight of the shaft cap and to facilitate the handling of the structural members.
The design calculations assumed simple support (frame) in the case of dead load and used the grid theory (FEM) in the case of live load.
The values obtained from both design calculations were added to find the proper solution.

Main Girder

The design assumed the main girder as a post-tensioned rectangular cross section and structural stability calculations were made assuming simple support in the case of dead load and employing the grid theory (FEM) in the case of live load.

Cross Girder

The design also assumed the cross girder as a post-tensioned rectangular cross section and structural stability calculations were made employing the grid theory (FEM) in the case of both dead and live loads.

Floor Slab

The floor slab was designed as a prestressed concrete composite slab.

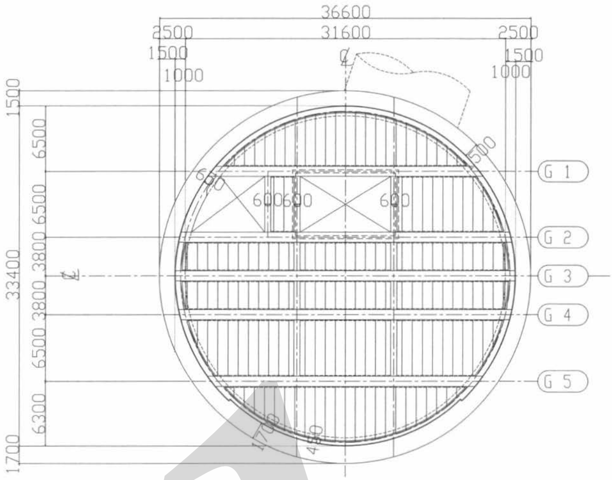

Figure-1 General plan

3. OUTLINE OF CONSTRUCTION SEQUENCE

The main girders, intermediate cross girders, and structural members having simple shapes were fabricated at the job site, while peripheral cross girders of complex shapes were produced at the factory. The factory production of the peripheral cross girders led to improved quality and reduced construction time. Each main girder weighed 147 tons and was lifted and erected by two 400-ton capacity cranes. Shorter construction time achieved represented a major advantage for the project. The construction sequence was as illustrated below.

1. Fabrication of Girders
↓
2. Erection of main girder
↓
3. Erection of intermediate cross girder
↓
4. Erection of end cross girder
↓
5. Joint filling
↓
6. Lateral bracing
↓
7. Erection of floor slab
↓
8.Bar arrangement and placement of in-site concrete

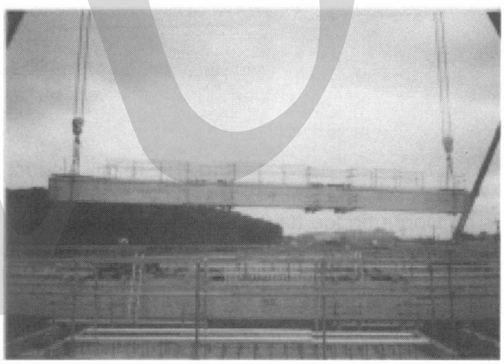

Photo-1 Erection of Girders

REFERENCES

[1]Specifications for Highway Bridges with Explanatory Notes·Parts I and III, Dec. 1996, Japan Road Association
[2]Guidelines for Prestressed Concrete Composite Floor Slab Design and Construction (Draft), Mar. 1987, Japan Society of Civil Engineers.

CONSTRUCTION OF PRESTRESSED STRUCTURE ABOVE KUPA AND DOBRA RIVERS ON THE ZAGREB – RIJEKA MOTORWAY

Petar Sesar, MSc.CE Darinko Velan, BSc.CE, Jadranka Ivkovic, BSc.CE, Damir Tkalcic, BSc.CE
Civil Engineering Institute of Croatia,
Janka Rakuše 1, HR-10000 Zagreb, Croatia
tel. +385-1-6144-725, fax: +385-1-6146-200, e-mail: psesar@zg.igh.hr

Keywords: precast girders, 70 m span, river crossing, full continuity, construction sequence

1 INTRODUCTION

On the Zagreb – Rijeka Motorway it was necessary to construct several bigger bridges two of which across rivers. The Viaduct Drežnik (2485 m long) across the Kupa river and the Dobra bridge (550 m long) are made mostly of spans that are 35 m long. At rivers crossings it was necessary to insert spans of double length (70 m), and that imposed partialy modified construction method. Bridges have similar deck structures, consisting of precast prestressed concrete girders with deck slab cast-in-situ.

2 BRIDGES BEARING STRUCTURE

2.1 Superstructure

The superstructure consists of precast prestressed concrete I-shaped girders, cross girders and deck slab cast-in-situ. Longitudinal girders are 1.82 m high, with exception of part over the river. Distance between girders axis is 2.57 m. On Drežnik viaduct flanges are 1.46 m wide and slab part between them was supported by movable formwork during concreting (Fig. 1).

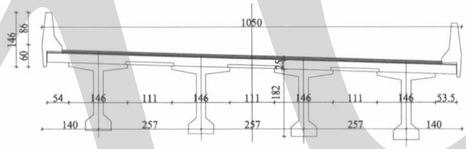

Fig. 1: Drežnik viaduct cross-section

Girders on Dobra bridge have flanges which are intentionally wide (2.53 m) to simplify the deck slab formwork (Fig. 2). Cross beams are of rectangular section, 1.5 m wide. To enable faultless concreting of longitudinal girders and cross girders conection, cross girders bottom edge is 30 cm below longitudinal girders.

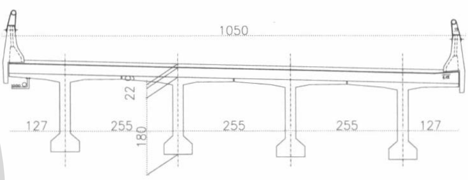

Fig. 2: Dobra bridge cross-section

2.2 Substructure

Single hammer shaped piers were constructed. Cross-section of piers was determined on the basis of statical and aesthetical considerations. Hammer shaped pier caps serve not only as permanent supports to longitudinal girders but also as temporary support for longitudinal girder mounting.

The abutments of both bridges are horse-shoe shaped. They have a massive bearing wall, with slightly corbelled breast wall. The wing walls are fixed in connection with bearing wall and partly supported with step like footings.

2.3 River crossing construction sequences

Dreznik viaduct and Dobra bridge structures differ only at crossing of rivers because Dobra bridge has shifted display of piers due to skew crossing over river Dobra. Therefore only Dreznik viaduct (Fig. 3) construction will be shown here.

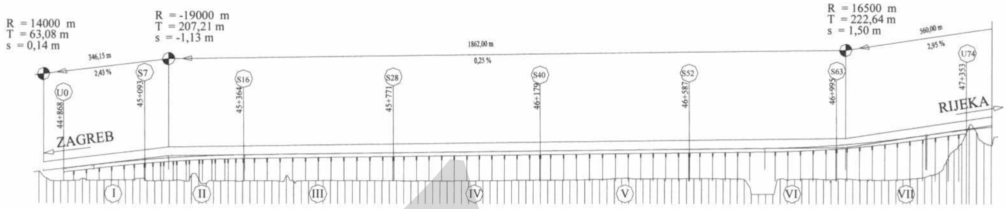

Fig. 3: Longitudinal profile of Dreznik Viaduct

Part of the structure at river crossing differs a lot from the other parts. Piers at river banks and pile cap dimensions are bigger. Number of piles is increased (from 4 to 6). Pile cap was elevated above water level so complicated construction pit protection could be avioded. For protecting the piers most sensitive part, its bottom was filled with fill concrete up to the level of 6 m. Pier cap at the top of the pier was constructed in two phases due to construction of main span over the river. Girders at main span have alternating hight. They are concreted at ground level and then mounted to the pier. There they were connected by two Dywidag bars to the pier cap. After all four girders were mounted, cross girder, deck slab and compression slab at the bottom of girders parabolic haunches were constructed (Fig. 4).

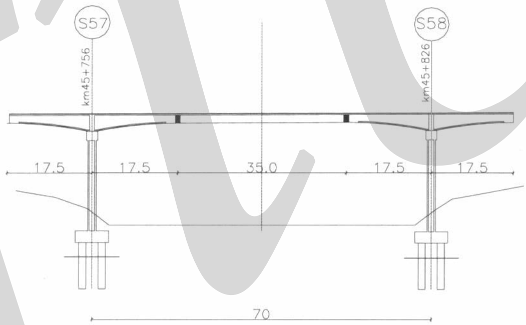

Fig. 4: Longitudinal section of the river crossing

After all four riverbank pier positions were completed, regular girders 35 m long were implanted from river between existing supports. Girders were temporarily fixed to riverbank supports. At that point wet connections were constructed and it was possible to drag continuous tendons through all 140 m long structure.

SOIL STRUCTURE INTERACTION ANALYSIS OF THE SETTLEMENT FREE SLAB OF THE HIGH SPEED RAIL LINK IN THE NETHERLANDS

R.S. Beurze
Design Manager for the HSL-Combinatie Zuid-Holland Midden
and Deputy Managing Director of Delta Marine Consultants bv, the Netherlands

Keywords: soil-structure interaction, pile-slab connection detail

1 INTRODUCTION

In the western part of the Netherlands, the design and construction of the supporting structures of the new high speed rail link has been started in the year 2000. It is expected that the high speed rail link will be in operation in the year 2006. Due to the soft soil conditions, the track is mainly supported by a piled foundation. One of the supporting structures along the line, exists of a concrete slab founded on piles on an approximately 4.5 metres high constructed embankment (the so-called Settlement Free Slab, SFS), see figure below.

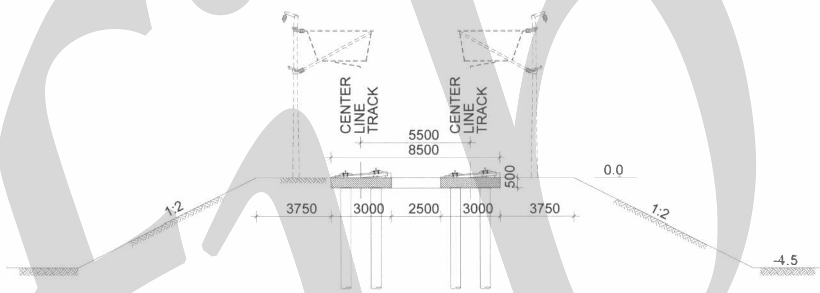

SECTION A-A

For the analysis of the lateral resistance of this structure under horizontal loads and deformations, the non-linear behaviour of the embankment and subsoil, including the pile group effects, play an important role. This condensed paper only describes the soil-structure interaction analysis. The full-size paper also presents a review of the pile-slab connection detail.

2 SOIL-STRUCTURE INTERACTION ANALYSIS

The applied design method is based on a split of the soil-structure interaction analysis into the following main analyses:

- Foundation Analysis
- Structural Analysis with dummy piles

2.1 Foundation Analysis

One section of the Settlement Free Slab with a length of 35 metres between the expansion joints, has been considered as a pile group. The pile forces and displacements under various loads and load levels have been determined with a suitable pile group programme. The stiffness of the concrete structure is modelled with the help of a stiffness matrix. As the pile group programme assumes a horizontal ground level, the effects of the slopes of the embankment on the lateral resistance of the foundation have been determined by a separate analysis and taken into account as a reduction of the P-Y curves. The reduction is shown in Figure 2.1.

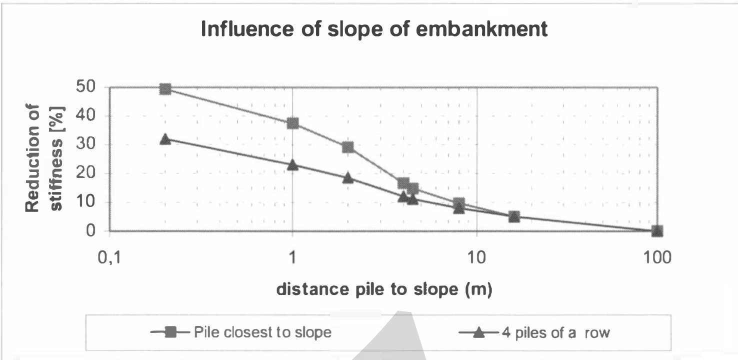

Figure 2.1

The stiffness of the pile group including the pile group and the slope effects is approximately 66% of the stiffness of the pile group excluding these effects.

2.2 Structural Analysis with dummy piles

The pile top forces $M_{xx}, M_{yy}, F_{xx}, F_{yy}$ and the pile top displacement δ_x, δ_y following from the foundation analysis are used to determine the equivalent length of the dummy piles l_{eq}, and the associated equivalent pile stiffness $EI_{eq,x}$ and $EI_{eq,y}$. These dummy piles are used in the linear structural model.
The equivalent length is calculated using the following formula (for the x-direction)

$$[l_{eq}]_x = \frac{3(M_{yy}\varphi_y - F_x\delta_x) + \sqrt{9(F_x\delta_x - M_{yy}\varphi_y)^2 + 48M_{yy}\varphi_y F_x\delta_x}}{4F_x\varphi_y}$$

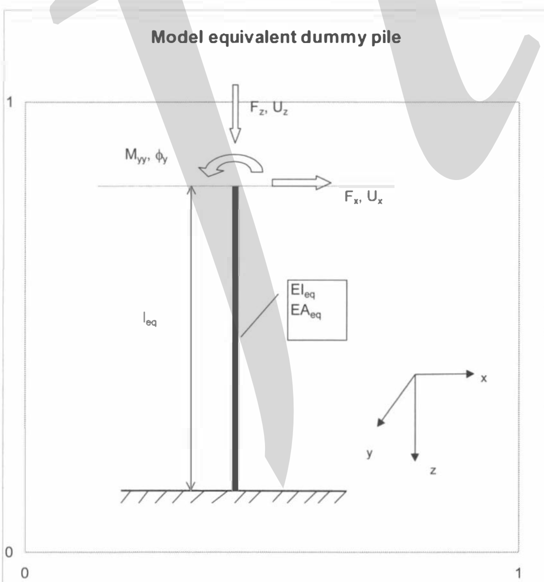

If φ_x and φ_y are very small, which is true for the Settlement Free Slab, the equations become. For the x-direction:

$$[l_{eq}]_x = \frac{2M_{yy}}{F_x} \text{ and } [EI_{eq}]_x = \frac{2M_{yy}^3}{3\delta_x F_x^2};$$

and for y-direction: $[l_{eq}]_y = \dfrac{2M_{xx}}{F_y}$ and

$$[EI_{eq}]_y = \frac{2M_{xx}^3}{3\delta_y F_y^2}$$

In the structural model an average l_{eq} and the $[EI_{eq}]_x$ and $[EI_{eq}]_y$ are used. As the equivalent dummy pile is a linear representation of the non-linear pile behaviour, it is important that the correct load level is used in the foundation analysis. Hence, it is necessary to use different equivalent piles for the ULS and SLS.

HUGE EXPRESSWAY PROJECTS BEING UNDERWAY IN OSAKA METROPOLITAN AREA

Isao Sugie — Chief Engineer
Yasuyuki Sakasita — Senior Engineer
Hirohisa Imagi — Senior Engineer
Hanshin Expressway Public Corporation, JAPAN

Keywords: urban expressway, tunnel, culvert, shield, super levee

1 EXPRESSWAY NETWORKS IN OSAKA AND IT'S IMPROVEMENT PLAN

Since it's founding in 1962, Hanshin Expressway Public Corporation (HEPC) has been involved in an urban expressway development for the second biggest metropolitan area in Japan. Currently, Hanshin Expressway's total length is 221.2 km with an average traffic volume of 0.92 million vehicles and 1.4 million users per day.

Yamato River Route and Yodo River Route, these new big projects that will constitute the nucleus of Hanshin Expressway Network, are started in the end of 20's century and now under construction by HEPC to improve serious congestion around Loop Route (Rt.1). (See Figure 1)

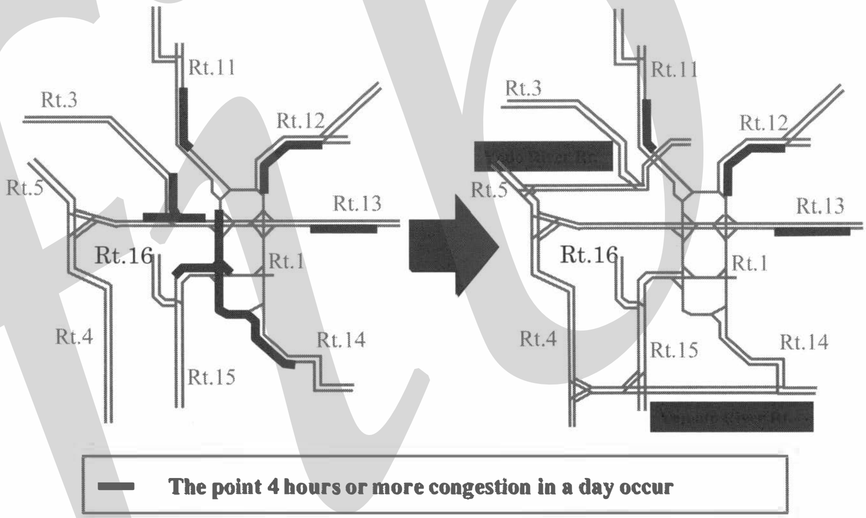

(a) Before improvement **(b)** After improvement

Figure 1 Effect of completion of two big projects

2 THE PLAN OF THE PROJECTS

The routes, approximately 10 km length and 4 lanes in each, were planned as the part of the Second Ring Road in Osaka, while the previous inner one (Loop Route) was completed in 1960's. They are planned to complete by 2010 and total cost is expected more than 8 billion dollars.

Most of the routes are planned as tunnel structures taking into consideration environmental aspect and the use of their roofs. Tunnels will be constructed just aside embankments and the safety has to be checked as composite structures of them using seismic analysis, saturation analysis etc. Picture 1 shows the present view of Yodo River Route site, and Figure 2 shows its image.

Picture 1 Present view of Yodo River Route site

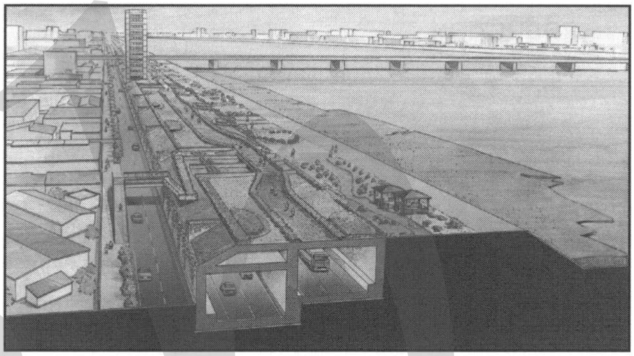

Figure 2 Image of Yodo River Route

Yodo and Yamato River are registered as the ones Super Levee has to be constructed by Japanese government. As shown in Figure 3, the Super Levees are much wider and stronger than conventional levees (embankment). Figure 3 shows the image of Yamato River Route constructed by cut and cover tunnel method in the area of Yamato River Super Levee.

Cost reduction effort is one of the main issues to accomplish the projects, and some of them are shown in the paper. For example, about 13 metre diameter shield tunnel, use of high performance materials, improved earth retention wall etc. are now studied.

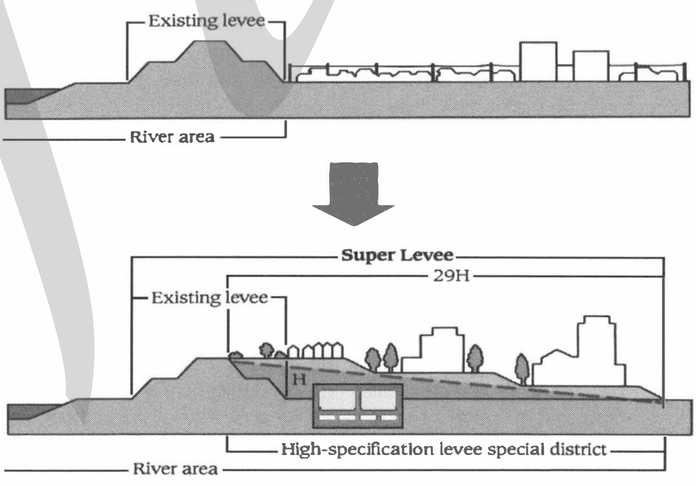

Figure 3 General view of super levee and Yamato River Route

EXECUTION OF PC WORKS FOR SUPERLARGE COAL SILO AT TACHIBANA BAY THERMAL POWER STATION OF ELECTRIC POWER DEVELOPMENT CO.,LTD.

Tokio Ishikawa
Electric Power Development Co., Ltd.
JAPAN

Akira Hirayama Yoji Kawata
SE Corporation
JAPAN

Keywords : thermal power station, silo, Slipform, prestressed concrete, grout

1 INTRODUCTION

At this coal thermal power station, which is the largest in Japan with a total combined output of 2.8 million kilowatts for Electric Power Development Co., Ltd. and Shikoku Electric Power Co., Ltd., a total number of 12 units of 70,000 tons class indoor storage facilities are constructed; 8 units by Electric Power Development Co., Ltd. and 4 units by Shikoku Electric Power Co., Ltd., and they are of the largest scale in Japan among the existing coal silos. The construction works of this superlarge coal silo were executed with Slipform method for disposing tendons simultaneously (patented method) of Ring Beam system.

2 OUTLINE

The superlarge coal silo structure is a vessel structure with a maximum height of 74.5 m and a barrel height of 52.0 m, an inside diameter of silo of 46.0 m, a wall thickness at the top of barrel of 50.0 cm and a wall thickness at the bottom of barrel of 130.0 cm. The post-tensioned tendons, including both SEEE/F100 (7×ϕ11) and SEEE/F200 (19×ϕ9.5) [together screwed type anchorage (SEEE method)], are disposed in 93 stages on the external wall side. The barrel, for which prestress is introduced in the circumferential direction, has a full-prestress structure against static pressure and a partial prestress structure against dynamic pressure at delivery.

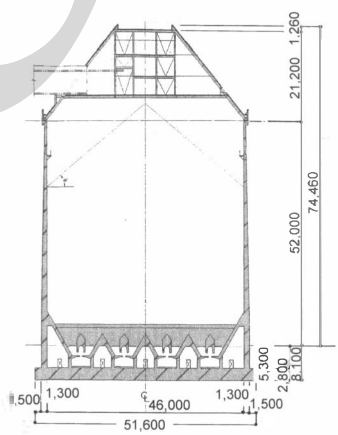

The following points were studied in particular, as matters to be examined at the time of construction by Slipform method for disposing tendon simultaneously : (1)Possibility of disposing tendons through the yoke, frame and the reinforcing bars. (Clearance), (2)To complete the disposition within an extremely limited time in line with the lifting time by sliding. (Time limit), (3)Not to put any obstacle to other works such as laying of reinforcing bars, concrete casting, etc. (Safety management), (4)The equipment for disposing tendons to be kept in moderate scale. (Weight limit), (5)Flexible adaptation to the change of wall thickness. (Length and position of tendons), (6)Possibility of execution without any collapse or damage of sheath having influences on the prestressing or grouting. (Verification of quality)

The following method of disposition of tendons was adopted, considering the problems mentioned above: (1)A stage for delivering tendons was provided on the horizontal yoke near the pilasters. (2)A tendon wound with a sheath at a diameter of 1.2 m was loaded on a vertical material called bobbin on the ground, lifted onto the bobbin base on the stage by using a crane, and disposed. (3)To

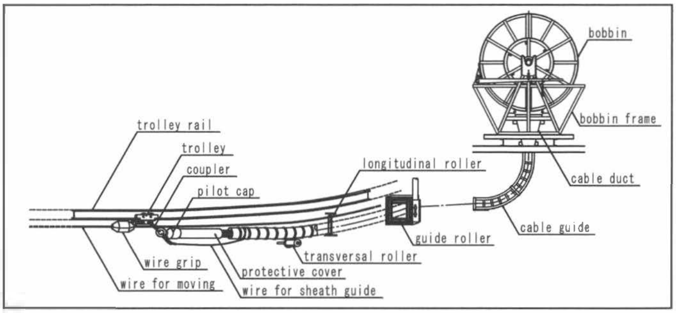

dispose the sheathed tendon smoothly, the tendon was made to travel on rollers. A longitudinal roller was installed to prevent the tendon from drawing to the inner side. (4)The transversal roller is of a structure enabling to slide the tendon in a way to remove it, after moving it to the prescribed position. (5)A trolley traveling on the rail under the horizontal yoke was drawn out by means of a winch , the tip of the tendon was connected with an endless wire, and the tendons were disposed one by one. (6)The transversal roller, to be mounted on the mobile yoke normally because of a changing wall thickness, was attached to the solid fixed yoke on the inner side because there was a fear of inst ability such as the change of rail, etc. The tendon was let drop in a sliding jig for temporary laying, after moving to the prescribed position, and then moved to outside the prescribed position. (7)It is very difficult to keep the accurate disposition of tendons, on a stage where such operations as laying of reinforcing bars, concrete casting, etc. are executed side by side. For that reason, we disposed Marking Posts of joint type, marked the position of the transversal tendon in advance, installed a bracket in that position, and bound the tendon for inc reasing the disposing accuracy. (8)The tendon changes in length at each stage because of the changing wall thickness. Here, different colors were used for each stage to avoid error. In the same way, different colors were used at the respective pilasters also for the Marking Posts. The disposing of tendons was executed by a total number of 15 to 17 workers including those at the top and those on the ground, and this made it possible to perform disposing of 10 to 15 tendons a day with no particular problem.

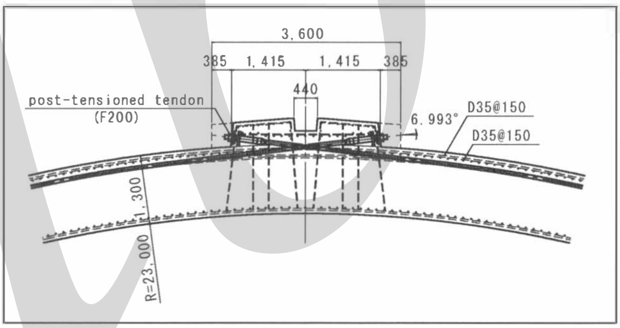

To avoid any sudden stress on the barrel, the tensioning procedure was divided into 3 phases considering elastic deformation of concrete and separately for group 1 and group 2. The tensioning was made on 3 tendons of a single turn by tensioning simultaneously them by using 6 units of jack.

At the grouting work, GF1700 of non-bleeding type was selected. This selection was made considering the following points: (1) To be of non-bleeding type. (2) Horizontal grouting. (3) A comparatively long distance of 50 m and a moderate porosity.

We adopted and executed a mixing judged as most suitable to the weather and atmospheric temperature of the day between 42% and 45%, according to the results confirmed by means of flowability test made by mixing at 42%, which is considered to be the best quality, before execution every morning. For the grouting, 2 teams were organized who washed the inside of the sheath with water before the grouting, and made sure that the poured grout becomes about equal in concentration to the grout at the discharge port, before stopping the grouting. Setting time was advantageous, especially for execution in elevated places, and it also contributed to the improvement of quality.

3 CONCLUSION

For the construction by Slipform method for disposing tendon simultaneously, we thought of disposing integrated tendon-sheath type quickly in limited time, and could deploy the working processes smoothly by completing operations, which can be made in a place other than the working stage either on the ground or in the product-manufacturing factory as much as possible. This became possible through careful planning and study made in advance. Moreover, the works could be executed with higher quality speedily and in safety, thanks to efficient combination of the characteristics of various processes and methods as symbolized by this Ring Beam Type Slipform method.

Design and Construction of Shimotabaru Bridge

Authors Yukihide Yamamoto-Nishi-Usuki County Branch Office,Miyazaki Prefecture,Japan
Mituhiko Nakashima -Kyushu branch,P.S.Co.,Ltd.,Fukuoka,Japan
(Presenting) Yuichiro Nakamura-Kyushu branch,P.S.Co.,Ltd.,Fukuoka,Japan

Keywords: composite arch, lowering method, π form section

1 INTRODUCTION

Shimotabaru bridge is an RC fixed arch bridge. This bridge is characterized by that the composite arch wrapping method is adopted for the construction of the arch rib, and by that the lowering method is adopted for the erection of a square-section steel pipes used for the bridge, of which arch span erected by this method is the longest in Japan. This paper reports mainly on the construction of the steel arch by the lowering method and on the composite arch wrapping method, for Shimotabaru bridge.

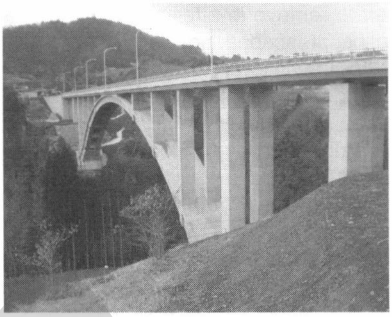

Photo-1 View at Completion

2 OUTLINE OF CONSTRUCTION

After construction of the arch abutment and side spans, the square-section steel pipes are erected vertically, and the square-section steel pipe arch is formed by lowering. Then springing part is constructed and then its base part is fixed, and concrete is filled into the square-section steel pipe in order to form a composite arch. Different from a form traveller for the ordinary cantilever method, the front part ahead of a form traveller is also supported by the composite arch (the part behind is of concrete already placed), and wrapping work is carried out sequentially to complete the RC fixed arch. Characteristics of this construction method are as follows;

1. As concrete is filled into the steel pipe, the arch becomes a rigid composite the square-section steel pipe structure at an early stage, which leads to enhance the stability and safety during the construction, and to reduce the number of temporary structural members.
2. The arch rib becomes an SRC structure after the wrapping work, but the square-section steel pipe members are not accounted for the design section at the completion, and actually it becomes a structure having high toughness.
3. There are not so many changes in structural system compared to the truss method or pylon method(cable-stayed erection methood), thus quality control in construction can be simplified.
4. A form traveller can also be supported by the front part, which enable to reduce some weight.

(1) Erection of Steel Pipe

As a rotation bearing being embedded in front of the arch abutment, and square-section steel pipes being supported by temporary fixing metal, it is erected vertically. In case of this bridge, the steel pipe in a half side of the bridge is divided into 10 sections, and two main girders connected each other with cross frames are erected from the first to eighth section by using 120 ton crane, and the ninth and tenth sections are erected by one main girder considering the capacity of the crane . Construction cycle is such that the delivery to the site and frame assembly on the ground takes one day, and erection and connection takes another day, and these two days make one cycle. This steel erection, including temporary metal fixing, was completed within about one month.

(2) Lowering Erection, Closure at Mid-span

Lowering work was executed in two days; one day for shifting the center of gravity, and another day for the lowering erection. It took about 2 weeks from the end of the steel pipe assembly to the completion of the lowering, including placement of the lowering cables and construction of the ground anchors.

1) Placement of the lowering cable

The lowering cables consisted of 6 numbers of SWPR 19 1S21.8 as main cables for one main girder, and total 12 cables were placed. The final design tensioning force was 1620 kN (A1 side), and was 1720 kN (A2 side). In addition, four reserve steel bars for each main girder, total eight steel bars were placed in case of emergency such as troubles on the lowering jack, or sliding out of the main cable.

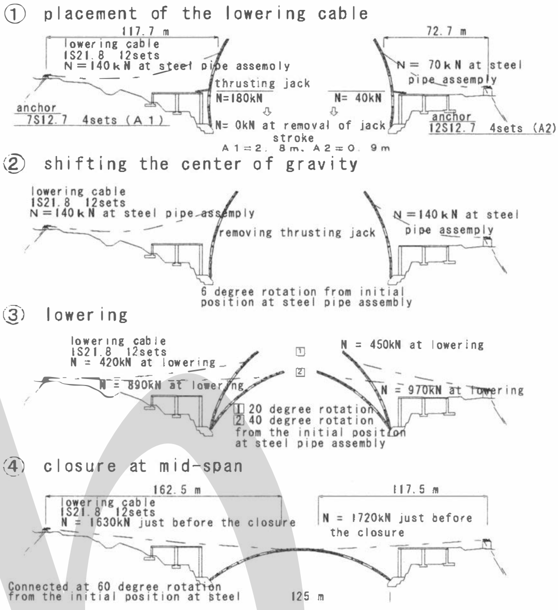

Figure-1 Sequence of Lowering Erection

2) Shifting Center of Gravity

When the steel pipe is assembled vertically, its center of gravity is located in front of the rotation bearing. However, when the lowering cables are set, as tensions are applied into the cables, the center of gravity shall be shifted forward. After pushing the steel pipes by the thrusting jack attached at the front end of the stiffening girder, the jack was removed and the cables were pushed out subsequently, and it was rotated to the designated position.

3) Lowering and closure at mid-span

Remaining cable length to be sent during the lowering is about 36 m. One stroke of the jack is 450 mm, and closure at mid-span was achieved by about 80 strokes. For the height just before the closure, the staff pre-set on the steel pipe was monitored by a level, and it was lowered down to the designated height. It took about 8 hours from the start of the work to the closure, including the time taken for adjustment of the lowering jack. For the closure, it was first temporarily fixed by closure metal fittings at the mid-span, and then the splice plate was treated by drilling, and it was connected by torshear type high strength bolts. Errors in the lateral direction for the steel pipe was monitored by a transit time to time during the lowering, and difference in the length pushed by two lowering jacks at both side, was checked during the lowering by the length of the cable pushed, and by the errors of the steel pipes.

(3) Construction of the springing part, and concrete filling into the steel pipe

After the closure of the steel pipe, the springing part was constructed and a fixed arch was formed. Mix proportion of the concrete used was 40-20-8(H). Subsequently, concrete was filled into the steel pipe in order to form composite arch.

(4) Wrapping of concrete by form traveller

After filling concrete into the steel pipe, a form traveller was assembled. The weight of a form traveller is about 50 ton per one stage, and two cables, 1s21.8, were placed for transporting. For the section of the arch rib this time, not a box girder type which has ordinary been used for the arch section, but a open cross section (π form section)type is adopted. Advantages of this open cross section are a) no works on the lower slab, and b) that the upper slab can be easily supported from the bottom plate of a form traveller by column members, as supporting member for the upper slab. The cross section of the arch rib and rebar arrangement might be affected by the stress generated during the construction period, from the start to the end of the arch rib wrapping, (of which situations applicable to this bridge). That is, for construction of composite arch, negative bending moment is generated at the springing part similar to the case of the cantilever method, thus the open cross section in which rebar can be placed on the upper edge side, the tension side, is not a problem.

Reference

1) Sato, Watanabe, Harima, "Design and Construction of Arch Bridge by CLCA Method (Kawahari Bridge), Prestressed Concrete Vol.40, No.6, 1998

CONSTRUCTION OF THE SHINTAKACHIHO BRIDGE WHICH IS BUILT UP OF THE INVERTED LANGER CONCRETE ARCH BRIDGE

Matujirou Baba Sigeyoshi Turuda
Ministry of Land, Infrastructure and Transport,
Nobeoka Construction Office,JAPAN

Yoshiharu Funakawa Masashi Ikeda
P.S. Corp. / Koatsu Kogyo Co., Ltd. Joint Venture
JAPAN

Keywords: Inverted Langer bridge, Meran members, truss overhanging

1. INTRODUCTION

Centrally located midway along the Takachiho Bypass of Route 218, the area surrounding the Shintakachiho Bridge forms a deep V-shaped ravine called the *Takachihokyo*, which is a Designated Natural Monument. The bridge has a 300 meter-long RC inverted Langer arch of 143.0 meter span and PC stiffening girders that takes the steep topography and landscape into consideration. This is the largest span in the country for bridges with one continuous inverted Langer arch action. The bridge boasts an arch rise of 46.8 meters, the largest in the country for concrete arch bridges, and a gradient of the arch rib at the springing points reaches approximately 60 degrees (see table 1). The truss supported overhang method, combined with the first Meran members used in a inverted Langer bridge, was used to erect the arch span section. Using a specially designed transfer vehicle, stiffening girders, arch ribs and perpendicular members are extended one at a time while forming the truss structure of diagonal suspension members. While construction is half-complete, this paper reports primarily on the method of constructing the arch.

Photo1: Construction in Air with Truss Supports

Table 1: Inverted Langer bridges built in Japan

Name of bridge	Location	Year completed	Arch span	Span rise rate
Shintakachiho Bridge	**Miyazaki Pref.**	**Not yet complete**	**143.0m**	**3.1**
Higashimine Bridge	Ehime Pref.	2000	132.0m	6.2
Matanogawa Bridge	Tottori Pref.	1992	119.0m	4.7
Akatanigawa Bridge	Gunma Pref.	1979	116.0m	4.3
Amako Bridge	Ehime Pref.	1993	116.0m	5.0
Nakatanikawa Bridge	Kumamoto Pref.	1996	106.0m	5.3

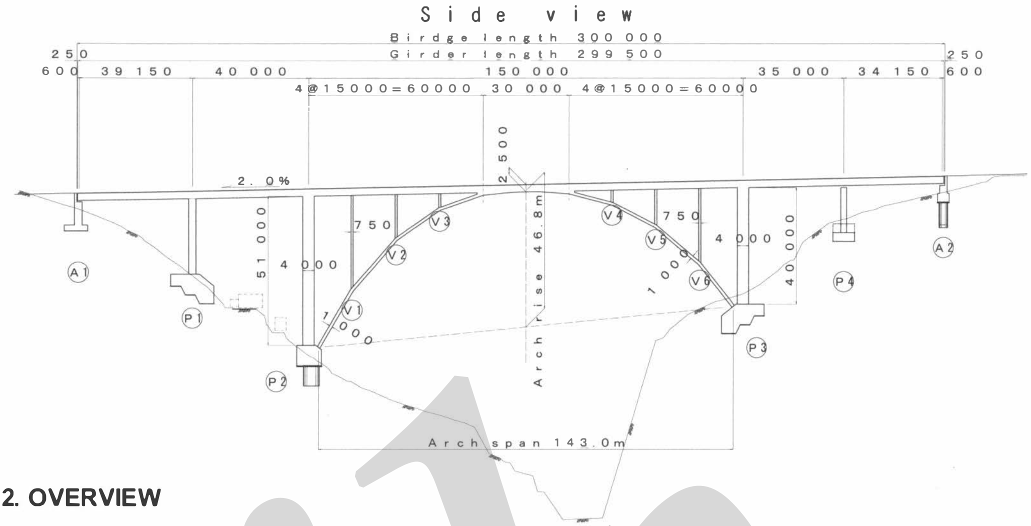

2. OVERVIEW

2.1 Bridge specifications

Road name: Route 218
Location: Miyazaki Prefecture, Nishiusuki,
Takachiho-cho
Road standard: Type 3, Class 3
Velocity of cars over bridge: V = 50 km/h
Bridge rating: B live load
Structure type: RC inverted Langer arch bridge
with PC continuous box girders
Bridge length: 300.0 m
Arch span: 143.0 m
Arch rise: 46.80 m (left: 53.80 m, right: 39.80 m)
Stiffening girder span: 39.15m+40.00m+150.00m
+35.00m+34.15m
Effective width: 4.00m+2@3.75m+4.00m=15.50m
Longitudinal slope: 2.00%

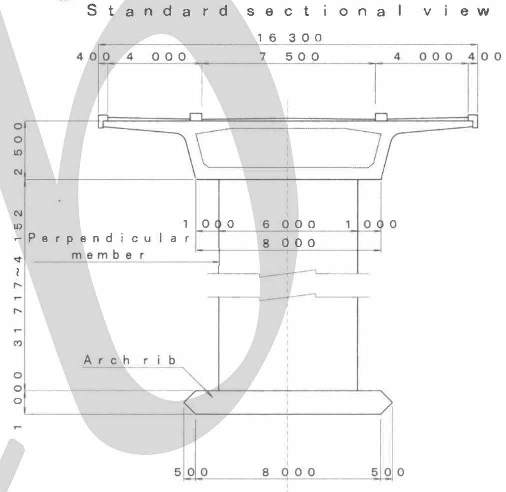

Fig.1:Overall drawing

2.2 Construction outline

Construction of superstructure was started at the end post furthest from the center, to one side of the arch. Span A1-P1, span P3-P4 and span P4-A2 are built by timbering. Bridge piers P2 and P3 (end posts) were constructed in the same period. Span P1-P2, which straddles the present road, was constructed by building out from both end piers. The anchors behind both piers were constructed at the same time the side spans were built.
The foundations of the springing points of the arch ribs were constructed, after which the Meran members was erected and an arch traveller specially designed for moving arch ribs was put together. For the stiffening girders a stiffening girder traveller specially designed for moving stiffening girders also was assembled, and building out toward the middle was carried out. After the middle was joined, diagonal suspension members and anchors were released and removed. Work was completed by surfacing the bridge.

THE KISO-GAWA RIVER BRIDGE－ANCHORAGE BLOCK OF BRIDGE SURFACE CABLE FOR INVERTED-CANTILEVER ERECTION EXPERIMENT

Koji Saito
Oriental Construction Corporation
JAPAN

Tsukasa Sato
Japan Highway Public Corporation
JAPAN

Masamichi Tezuka
Oriental Construction Corporation
JAPAN

Hidehiko Terunuma
Nihonkoatsu Corporation
JAPAN

Keywords: inverted-cantilever , anchorage block, reinforcing steel bracket.

1 INTRODUCTION

For the side span of the Kiso-gawa River bridge, temporary anchorage block was arranged on the surface and, by applying some kind of reaction to the girder on the neighboring span, the inverted-cantilever erection was established to have prestressing force. This anchorage block of the bridge surface cable was applied (post-constructed concrete block) and used a reinforcing steel bracket to hold it firm on to the bridge floor slab using prestressing bar. It was designed so that the prestress force would be transmitted to the floor slab. We implemented this real-scale experiment on the anchorage block of the bridge surface cable, to conclude the configuration (size) of the anchorage block and steel bracket and to verify the overall safety.

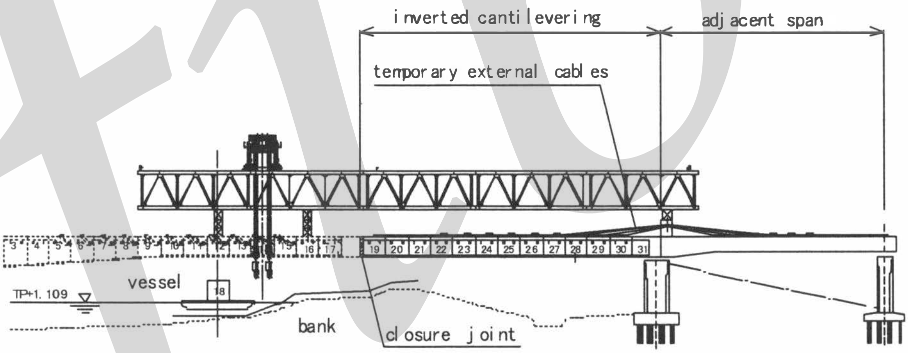

Fig.1 Application of Inverted Cantilever

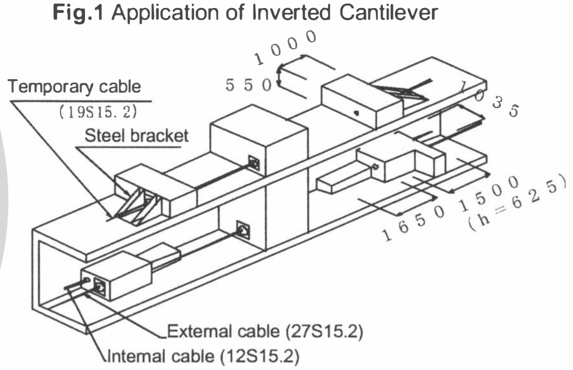

Fig.2 Schematic Drawing of Block of External Cable of Bridge Surface

2 OUTLINE OF EXPERIMENT

The lists of experimental parameters are indicated in table-1.

Table 1 Experimental Parameter

Symbol	Bracket	Horizontal fastening	Bracket reinforcement	Construction joint processing method
N	No	----	---	Expand metal processing
OB1	Yes	No	No	Treatment using a broom
B1h	Yes	Yes	No	Expand metal processing
B1h'	Yes	Yes	No	Expand metal processing
B2h	Yes	Yes	Yes	Integral construction processing
B2	Yes	No	Yes	Integral construction processing

(Note. In case of B1h', the tensile force of PC bar for vertical tightening of the block was arranged as half of the planned loading (30 tf / piece)).

3 CONCLUSION

According to the above result, we can confirm the following:

(1) The configuration of the anchorage block of the bridge cable and reinforcing bar arrangement that have been planned through this design have no problems.

(2) When reinforcing the member of the anchoring side or horizontal fastening, the steel bracket performed effectively, reducing the stress of the reinforcing bar on the floor slab, and preventing the occurrence of cracks.

(3) As a fastening method of anchorage block, the frictional connection method applying the prestress force has sufficient safety.

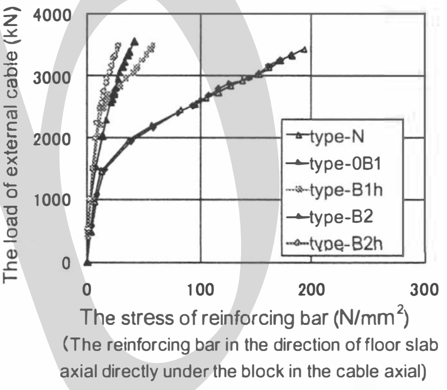

Fig.3 The Stress of Reinforcing Bar for Each Bracket Type (Measured Value)

We found that some types tested this time were satisfactory with the design conditions, non-horizontal PC steel type is easier to set securely, therefore we can choose: Reinforcing bracket + Non-horizontal fastening type (B2).

Considering both the experimental results and the characteristics of execution, we selected the type of reinforcing bracket and non-horizontal fastening as the best one, and actual execution was conducted without cracks to complete the erection.

REFERENCES

[1] Kazuyuki Mizuguchi, et al.,"*General Outline of Bridges for the New Tomei and Meishin Expressway, JHPC, Nagoya Construction Bureau*", Journal of Prestressed Concrete, Japan, Vol.41, No.2, pp. 27-33, Mar.-Apr., 1999.

[2] Hideki Komatsu, et al., "*Design and Construction of the Kiso River and Ibi River Extradosed Bridges*", Journal of Prestressed Concrete, Japan, Vol.41, No.2, pp. 63-70, Mar.-Apr., 1999.

[3] Hideki Komatsu, et al., "*Study on Cantilever Construction of Kiso River Bridge and Ibi River Bridge*", Proceedings of the 9th Symposium on Development in Prestressed Concrete, pp. 603-608. Oct., 1999.

[4] Hiroyuki Ikeda, et al., "*Design of Superstructure of Kiso and Ibi River Bridges*", Bridge and Foundation Engineering, Vol.33, No.11, pp. 19-28, Nov., 1999.

DESIGN AND CONSTRUCTION OF THE OBORO CONCRETE ARCH BRIDGE

Shoji Motomura
Fukuoka Prefectural
JAPAN

Hironobu Takematu
Civil Engineering Technology
Center Co.,Ltd, JAPAN

M.Terayama, M.Shibata, K.Tamaki
Joint venture of Sumitomo·Fuji P.S
Construction Co.,Ltd , JAPAN

Keywords: Computerized construction, camber control, change temperature

1. ABSTRACT

The Oboro Bridge has been constructed at the northern entrance to Joyo-town, Yabe-county, a region in southern Fukuoka Prefecture that is known for fireflies and stone bridges. It is be a reinforced concrete fixed arch bridge that spans the Hirokawa Gorge, a V-shaped valley located in the Chikugo River Prefectural Natural Park.

Consideration was given to harmonization with the surrounding environment in the design of this bridge. Its major features are the bifurcated arch rib shape, upside-down V-shaped vertical members and other aesthetic design that gives the bridge an uplifting appearance. The construction plan incorporates computerized construction, done with the aim of reducing the number of erected members, as well as the diversion of erection members and so on. These actions were conducted in an effort to prevent the generation of industrial wastes and shorten the work time, thereby saving costs.

This paper will present an overview of the design and construction of the Oboro Bridge, as well as the computerized construction being used in its construction.

2. OVERVIEW OF CONSTRUCTION

Photo 1and 2 shows the completed bridge. The distinguishing characteristic of the structural form is that the arch ribs curve and widen from the crown to the springing section, and that they are bifurcated in the 45-meter interval leading to the springing section. The construction site is a V-shaped valley called the Hirokawa Gorge, and there is a height of approximately 72 meters from the river bottom to the surface of the bridge.

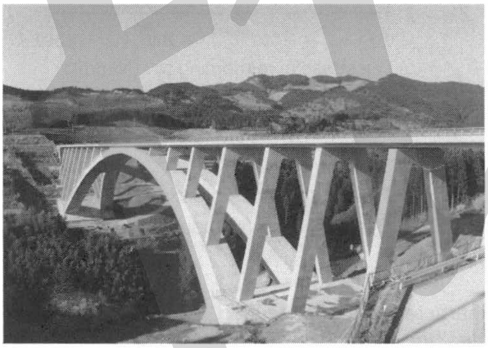

Photo1 Oboro bridge

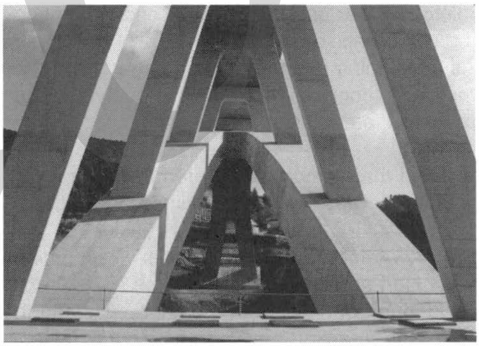

Photo2 Bifurcated arch ribs

3. COMPUTERIZED CONSTRUCTION

All displacement and stress (strain) data items were stored in the PC in the measurement control room set up on the site and transferred via a wireless network to the site office located approximately 100 m away. All PCs in this office were connected using a LAN, enabling the measurement data to be monitored from any PC. In addition, intercoms were used to enable continuous communication between the measurement control office and the pylons used to adjust the tension of the stays. When the tension of the stays and backstays was adjusted, the measurement data could be analyzed in real time and instructions given regarding the amount of tension adjustment.

4. INFLUENCE OF TEMPERATURE CHANGES ON ARCH RIB CAMBER CONTROL

The influence of temperature changes on shape control for arch bridges is complex and varied, as noted below, and it is extremely difficult to accurately determine and control these values. Their behavior can be roughly divided into the pre-closure Melan arches that are free in the lateral direction, and the post-closure Melan arches that are constrained in the lateral direction. In addition, the different thermal transfer properties of steel and concrete and other factors also result in different behavior during the erection process, when many steel members are used, and in the completed system, which consists only of concrete members.

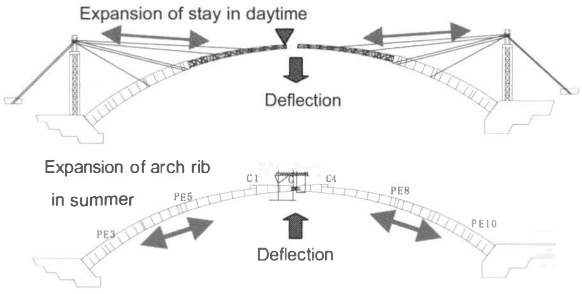

Fig.1 Arch rib deflection by temperature changes

(1) During Melan arch erection

During the Melan arch erection, the deflection in the arch ribs caused by temperature expansion and contraction of the stays became comparatively great. Just before closure of the Melan arches, the difference in deflection between day and night was about 40 - 50 mm.

Starting immediately after the closure of the Melan arches, the temperature expansion and contraction of the stays had no effect on deflection but appeared as fluctuations in tension. In return, deflection was produced in the arch ribs due to temperature expansion and contraction of the steel members in the Melan arch. Along with this, starting in the wee hours, when the Melan arches were closed, the deflection caused by changes in arch rib temperature during the day and during the night was reversed. Fig.2 shows the history of deflection at the ends of the Melan arches before and after Melan closure.

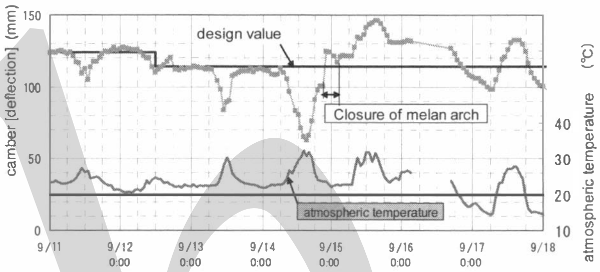

Fig.2 Melan arch deflection before and after closure

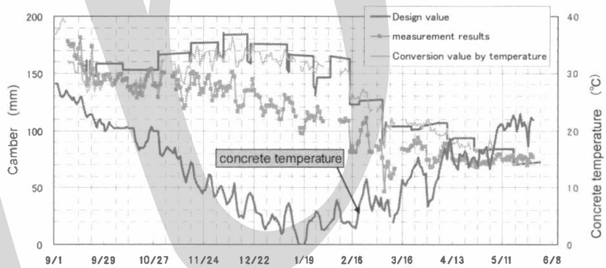

Fig.3 Arch rib camber during concrete jacketing

(2)Completion of concrete jacketing and post-completion

The steel members exhibited considerable change in temperature between daytime and nighttime. In contrast, the concrete showed almost no change in temperature between day and night. Accordingly, as concrete jacketing progressed, the difference in deflection between day and night disappeared almost completely. However, it is a well-known fact, that in this type of structure, seasonal temperature changes will cause considerable up-and-down fluctuation to continue even after the arch bridge has been completed. Fig.3 shows the measurements for deflection at the apex of the Melan arches during the concrete jacketing process. In winter, the measurements were about 40 - 50 mm, which was lower than the design values, but it can be seen that the measurements approached the design values as the average daily temperature rose.

Table1 shows the temperature conversions for arch rib deflection used during this work process. Table was used to convert the temperature for control of arch rib camber so the value was always 20℃, the height of the arch ribs was almost exactly in line with the design values.

Table1 Conversion of arch rib camber by rising temperature 10℃

		PE3	PE5	C1	C	C	C4	PE8	PE10
Immediately before Melan closure									
change in year	concrete temperature	0.9	4.5	8.4	10.6	9.5	7.8	4.0	0.8
change in daily	atmospheric temperature	−0.5	−6.5	−16.3	−22.2	−22.8	−17.6	−6.3	−0.5
Immediately after Melan closure									
change in year	concrete temperature	1.4	12.7	31.1	33.3		28.2	12.1	1.3
change in daily	atmospheric temperature	0.3	4.6	19.1	20.8		17.1	4.4	0.3
Completion of concrete jacketing									
change in year	concrete temperature	1.5	13.5	27.0	28.5		26.3	13.3	1.4

THE VIADUCTS IN LENGTH OF 1400 M AND 200 M ON THE SECTION IN HUNGARY OF THE RAILWAY LINE LINKING SLOVENIA

András Zsigmondi
Executive Vice President
Hidépitő Ltd, **HUNGARY**

Keywords: viaduct made of stressed reinforced concrete, incremental launching, stressing cable, pile, pier, technology, pushing nose, hydraulic pushing press

1. INTRODUCTION

The viaducts made of stressed reinforced concrete in length of 1400 m and 200 m on the 23 km long section in Hungary of the railway line connecting Slovenia were carried out within an all-time short duration of 13 months by Hidépitő Ltd, the oldest construction company of Hungary with its past of 137 years. The two bridges were implemented by use of incremental launching technology, applying in many cases technological and structural innovations.

The 1400 m long viaduct is the fourth in length among the bridges in Europe made of stressed reinforced concrete.

The bridge for leading through the single track railway line was prepared with one-cell box-girder structure made of stressed reinforced concrete.
The method of placing the fix bearings by means of steel pins built in the pier of the bridge was of new type. The preparatory works of the construction started in year 1997. The planned date for putting into operation was, according to the Interstate Agreement, the 31st December, 2000. The cost demand of the entire investment approached 23 thousand Hungarian forint (equivalent of 80 million USD)
The international tender for the realisation of the investment was invited sliced into more sections.
The two viaducts, owing to the incremental launching technology, gives back to the time of completion almost to its original state the natural landscape in the vicinity of the bridge.

2. IN GENERAL ABOUT THE TWO VIADUCTS

Studies were prepared previous to the preparation of the Tender Documents and these found as most favourable the construction of bridge structures with opening of 40 to 50 m and led through on them the crushed stone bedding of the railway's permanent way.
During the preparation of the designs for permission, which were later even the Tender Designs, two variants were elaborated for

- compound bridge made of steel girder and interworking reinforced concrete deck, and
- incremental launched bridge made of stressed reinforced concrete.

In answer to the Tender Documents for the two viaducts 17 offers, prepared by five international (Italian, Austrian, Swedish, Portuguese and Hungarian) tenderers, were submitted.

Successful Tenderer was awarded the "Zalahidak" Consortium, leaded by the Company Hidépitő Ltd and composed of the following Companies, as members: DUMEZ-GTM (France) and Betonútépitő Nemzetközi Épitőipari Ltd.

The designs of the Successful Tender were prepared by the Technical Department of Hidépitő Ltd, as an alternative proposal to the structure of incremental launched bridge made of stressed, reinforced concrete and pile foundation, for both bridges.

By construction of the so-called Viaduct I the bridge fourth in length among the railway bridges of Europe was completed, having the length of 1400 metre. The superstructure with box cross-section made of stressed, reinforced concrete has been divided into three parts: Two bridge sections constructed with incremental launching technology and a monolithic bridge structure with two spans located between the two former ones. The distribution of the spans of the bridges:

Bridge "A": 37.0 + 14 * 45.0 + 37.0 = 704.0 m, Bridge "B": 2 * 38.5 = 77.0 m,

Bridge "C": 37.0 + 12 * 45.0 + 37.0 = 614.0 m

The entire bridge structure is supported by 33 piers, at both ends can be found an abutment, and at each join of the three bridges has been created a common pier. The fix supports bearing also horizontal forces are at the middles of the bridges. The measure (6000 kN, as a maximum) of the braking or starting forces and caused by the train charges, respectively, reasoned that on each of the two long bridges 2 fix bearings should be placed (on piers 8 and 9 as well as 24 and 26).

This size of horizontal force cannot be borne by the usual bearings, therefore special "pins" with steel structure had to be applied which transmit the braking force from the superstructure to the fix piers. Cross-section of the bridges: One-cell box-girder with vertical side-walls. The width of the box-girder's bottom is 4.50 m, its height is 3.75 m at the axis.

Single track railway line is led through the bridge on a railway substructure with bedding of crushed stone ballast. On both sides of the railway track has been prepared an inspection sidewalk with handrail. The cross-section of Viaduct II with a length of 200 m is identical with that of Viaduct I, while it has the following distribution of the spans: 32.50 + 3 * 45.00 + 32.50 m.

3. THE STRUCTURE OF VIADUCT I

There are more reasons which made expedient to construct the 1400 m long bridge structure cut into 3 independent bridges. The *bridge foundation* was made by bored piles of great diameter.

The bridge piers were prepared with hollows and there were made four types and dimensions of structural beams for the piers:

- normal structural beams where the bearings moving in one or two directions were situated on top,
- structural beams at the fix bearings where the moving bearings and the steel structures (pins) taking the braking force find their position on top,
- structural beams at the launching supports,
- structural beam on the common pier for location of 4 bearings.

The *superstructure of the bridge*: built for leading through a single track railway line, has a cross-section with one-cell box-girder made of stressed reinforced concrete. The superstructure has been made of concrete strength C35-24 with slightly plastic consistence, meeting the requirements of frost-resisting at a degree of 50 and waterproofness at a degree of 4.

Three cable families were applied for stressing the superstructure.

The *first group of cables* with straight alignment were placed in the bottom and upper flanges. They are provided that during launching forces with alternating senses were stood but, as a matter of course, they participate also in bearing the structure's final power activity.

The *second group of cables* were stressed after placing the bridge on the permanent bearings and aimed to bear the forces originating from the structure's final power activity.

The *third group of cables* for bearing the useful railway load are so-called free cables placed inside the box, led through the upper and lower direction changing ribs. The direction changing ribs are above the support and in one third part of the spans.

The *medial, two-spans bridge "B"* differs both in manufacture and in its static system from the launched bridge structures joining it from two sides (bridge "A" and bridge "C") since this one has been constructed on scaffold, as monolithic cast concrete bridge structure.

4. SUMMARY

It was a serious challenge for Hidépitő Ltd to construct within one year the two viaducts in the lengths of 1400 m and 200 m on the railway line connecting Slovenia to Hungary. In this case the community of the Company's staff members prepared the bridge designs (structure, technology, auxiliary structures) over the bridge execution. Only superlatives can be told about the bridge construction, of the rhythm of designing & building and in the domain of the applied solutions of latest type:

- the cycle of one week was kept during the whole project implementation - independently of season and weather,
- there was a period in the course of the construction when the bulks having each a length of 22.50 m were manufactured simultaneously at three sites (at the same time week by week the bridge augmented by 67.5 m),
- complete prefabrication was used at mounting the reinforcement of the box-girder,
- the bridge parts of 700 m in length and of 14,000 tons in weight were launched by means of synchronous operating hoisting-pushing presses 4 pieces in each case,
- that was the first time in Hungary when free cables were applied for stressing in order to bear the forces originating from the useful load of the railway traffic,
- central stressing cables were used for standing the braking forces resulting from the design speed of 160 km per hour,
- the method of placing the fix bearings by means of steel pins built in the pier of the bridge was of new type.

BRIDGE OVER THE RIVER RHINE

Dr.-Ing. Michael Blaschko, Bilfinger Berger AG, Munich, Germany

Keywords: high strength concrete, prestressing, free cantilever

1 INTRODUCTION

A new road communication has been built between France and Germany south of Strasbourg. The main part is a new crossing of the river Rhine, which also constitutes the border between the two countries.

2 DESCRIPTION OF THE CONSTRUCTION WORK

The new Rhine crossing consists of three bridges, which are all prestressed concrete bridges: two ramps on the respective sides and the main bridge over the river (Fig. 1). The superstructure, which is 14.75 m in width, carries a two-lane road and a cycle track. With the cycle track being given up this roadway can be transformed into four lanes later.

The 295 m ramp on the German side comprises five spans. According to the agreement between the two countries this bridge was built by the Germans. So German rules and codes were used. The bridge consists of a concrete box girder with internal prestressing steel. It was constructed on supporting framework.

The ramp on the French side and the main bridge were built by the French government. Therefore these structures follow French rules and codes. The ramp consists of four spans totalling 215 m. The length of the inner spans is 53.75 m. The superstructure was built using the method of incremental launching.

The 461.7 m main bridge consists of a 205 m mid span above the fairway and two side spans of 123.4 m and 133.3 m. In the following the main bridge will be described in more detail.

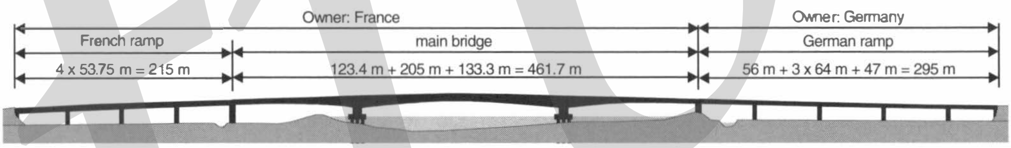

Fig. 1 Overall construction work of the Rhine crossing (longitudinal section)

3 SUPERSTRUCTURE OF THE MAIN BRIDGE

The superstructure consists of a haunched box girder. The total height ranges from 8.60 m at the diaphragm over the supports to 4.50 m in the middle of the centre span and 3.20 m at the end of the side spans. The box girder is prestressed in longitudinal and transverse direction.

The transverse prestressing in the top slab is composed of unbonded mono-strands. The longitudinal prestressing elements are internal bonded tendons and external unbonded tendons. 15.7 mm strands and steel grade 1860 are used for all cables. The initial stress is up to 0.9 of the yield stress or 0.8 of the ultimate stress of the prestressing steel. So the internal cables with 25 strands each have an initial prestressing force of 5580 kN. 32 cables of this kind are used at each web to cover the moment at the support and 7 cables are used at each web in the bottom slab (Fig. 2).

After the completion of the superstructure the unbonded cables were installed to carry the traffic loads. They consist of 31 strands each, so an initial prestressing force of 6919 kN results for each cable. The strands are placed in a PE-tube, which is filled with anti-corrosion wax. The drape points are formed by bent steel tubes which are trumpet-shaped on both ends.

Altogether 480 tons of internal and 180 tons of external steel were used for the longitudinal prestressing. That means about 83.5 kg of steel per m³ of superstructure concrete or 100 kg of steel per m² of bridge deck.

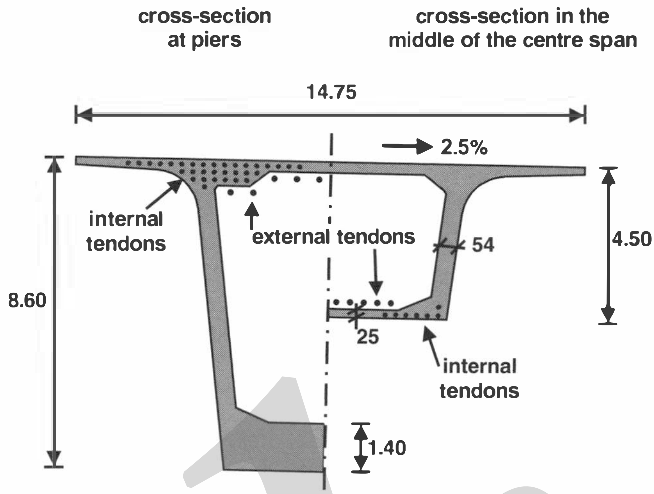

Fig. 2 Cross-sections

High performance concrete is used for the superstructure. The characteristic compression strength which is demanded for design reasons is 65 MPa (cylinder compression strength after 28 days). A strength of 43 MPa is required at the time of prestressing. This strength must be obtained within 2.5 days so that the superstructure can be realized in cyclic work of one week. On the other hand the maximum temperature in the concrete during the hardening process has to be limited. This data led to the concrete formulation given in Table 1.

Table 1 Concrete formulation C65

	Concrete C65
aggregate 0-4 mm	670 kg/m³
aggregate 4-8 mm	280 kg/m³
aggregate 8-16 mm	900 kg/m³
cement CEM I 52.5	410 kg/m³
silica fume	30 kg/m³
water	150 kg/m³
superplasticizer	1.6 % = 6.6 kg/m³
w/c-ratio	0.37

The superstructure was constructed using the free cantilever method with travelling falsework. First a starter section was built above the water piers on supporting framework. Then the travellers were erected on the starter section. The box girder was built in segments 3.50 to 5.0 m long using two pairs of travellers. The concrete was cast in-place in a single stage at a rate of one segment per week and cantilever. For the safety against overturning the starter section was temporarily fixed to the pier. An auxiliary column was erected to construct the overlength of the side spans.

4 CONCLUSION

The bridge over the river Rhine is an example of how high performance materials can be used to construct a long-span and slender bridge in an efficient way. A strict quality assurance system is necessary to handle high strength concrete and high strength prestressing elements on site.

DESIGN AND CONSTRUCTION OF SAKATA-MIRAI FOOTBRIDGE USING REACTIVE POWDER CONCRETE

Yoshihiro Tanaka Hiroyuki Musya Akio Ootake Yoshihide Shimoyama Osamu Kaneko
Taisei Corporation, JAPAN
Taiheiyo Cement Corp., JAPAN
Maeta Concrete Ind., JAPAN

Keywords: fiber reinforced ultra strength concrete, heat treatment, wet joint, outer cable

1. INTRODUCTION

Fiber reinforced reactive powder concrete under the brand name Ductal® has not only out of range unique mechanical properties but also strong durability. Because of the ultra high compressive, bending and tensile strength, the concrete bridge made of Ductal can enormously reduce the dead weight and this results in that the dimension of the foundation becomes very small. In this paper, the design and construction process of Sakata-Mirai Footbridge, which is the first application of Ductal in Japan, are discussed to establish the future guideline for design and construction. The span of Sakata-Mirai Footbridge is 50m and the width is 2.4m. Taking account of the efficient application of mechanical advantages of the material, Sakata-Mirai Footbridge was designed as a boxed type cross section with perforated webs, therefore the self-weight super-structure resulted in about 1/4 of the ordinary pre-stressed concrete bridge.

2. MATERIAL PROPERTIES OF DUCTAL

Ductal is improved from RPC200 (Reactive Powder Concrete 200MPa) [1] and its mixing principle design is based on RPC200. The self-leveling performance is achieved that a flow value is around 240 mm for the material temperature of 20~25°C even for including the steel fiber (0.2 mm diameter x 15 mm) by 157 kg/m^3 (2% in vol.) in the matrix. Therefore it is possible to cast it into the very thin shell mold or into the complicated shaped mold. The mean compressive strength value is 238MPa with 90°C heat treatment for 48 hours. The flexure property exhibits linear behavior up to its first crack stress (25~30MPa), a post-first-crack strain hardening phase up to its ultimate flexural stress (40~45MPa), and a post-ultimate-load strain softening phase. The incorporation of small-size steel fibers results in ultra-high energy absorption capabilities. The bending fracture energy is 36,000Nm/m^2, on the other hand one for ordinary concrete with 30~50MPa in compression strength is at least a range of 50~200Nm/m^2.

Because of the densest packing mixing design of the grain particles and the minimum mixing water to hydrate with cementitious material, Ductal includes extremely low porosity and it results in ultra high performance durability. The input permeability method injecting 200~300MPa pressurized water into the specimen provided the permeability coefficient will be smaller than 10^{-13}~10^{-12}cm/sec. The chloride irons diffusion coefficient 0.0019cm/sec was obtained by the 6 months penetration test soaking the specimens into the artificial salt water.

3. FUNDAMENTAL DESIGN CONCEPT

New Maeta Footbridge is planed to replace the old pre-stressed concrete pedestrian bridge that was built about 40 years ago crossing over the first class Niita River located in Sakata city, Yamagata prefecture. Therefore, the following restrictions are requested to design and construct the new bridge.

1) The level and slope to the connecting road can not be changed.
2) The bridge bottom line should have 0.6m clearance from the high water level.
3) The longitudinal slope of the bridge should be less than 5%.

Photo 1 Schematic view of Sakata-Mirai Footbridge

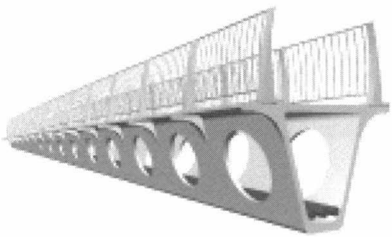

Fig. 1 Middle cross section

The limit state design method was basically employed for this project, and material constitutive laws and checking method for each limit state condition were followed by "Design rules for DUCTAL pre-stressed beams" published by Bouygues [2] in France. The tensile members due to SLS are not allowed to generate any cracks, on the other hand the tensile members due to ULS are allowed to generate cracks but they have to sustain the ultimate limit state load by bridging steel fibers. The schematic completion view of final Sakata-Mirai Footbridge is shown in Photo 1. The schematic middle cross section is drawn in Fig. 1. In order to take full advantage of the characteristics of the material and especially to use it without any passive reinforcement, the structural concept and unique points of Sakata-Mirai Footbridge are as follows.

1) All pre-stressing cables are set outside of the cross section with deviators.
2) The deviators also play an important role in the diaphragm.
3) The perforated webs are employed for the sake of design view and reduction of dead weight.
4) Eight pre-cast blocks are transversely and longitudinally by wet joint and post-tension cables.
5) No passive reinforcement by rebars even for the pre-stressing anchorage.
6) The cross-sections with variable web height are employed to effectively resist for the load.

For the detailed design step, 3-D FEM analyses for 1/2 modeling whole structure taking into account of the circular holes on the web have been conducted. Elastic FEM analysis is employed for SLS and non-linear finite displacement 3-D FEM analysis for ULS. The results of those analyses make it clear that the circular hole effects on the stress field in the web. The results are also used for the check of wet joint stress, the deflection in the middle span of the bridge due to the live load and the effects of the deviators on the final maximum load resistant capacity.

4. CONSTRUCTION EXPERIMENTS FOR VERIFICATION

Various kinds of mixing and casting experiments using the molds for beams, plates and shells have been carried out considering the control of the fiber orientation. Before producing the prototype pre-cast segment blocks, the verification experiments of mixing, casting and curing have been conducted to make the prototype scale specimens for the verification loading experiments. The wet joint in comparison with the dry joint does not need the match cast process in producing pre-cast segment blocks. The past records of wet joint are not so many, so it is necessary to verify the construction process and the structural performance.

5. STRUCTURAL LOADING EXPERIMENT

The anchorage for longitudinal pre-stressing is about 0.55m in depth, 1.2m in width and 1.0m in length. It is surprising that there are no passive reinforcement by steel rebars and furthermore the size of the anchor plate for 31S15.2 tendon is reduced about 21% in length from the standard plate. Three-dimensional FEM analysis and the loading experiment also have been conducted to verify the anchorage can withstand for the pre-stressing forces without any cracks. The bending and shearing loading experiment for the prototype pre-cast block, has been carried out to verify the crack behavior for SLS and the ultimate load carrying capacity for ULS. There are no observations of cracks for SLS. The ultimate strength was 2,500kN (ultimate shear force=1,250kN) that was about 1.8 times for the load by ULS. The final failure mode was shear destruction.

6. CONCLUDING REMARKS

Through the various kinds of material and structural experiments, the fundamental design method has been clarified and the design result has been verified. Maeta Footbridge is now under construction and it will be completed in September 2002. It should be noted that the design and construction management rules for Ductal should be further developed through the actual construction process in the future. From the point of view of the life cycle cost, the long term monitoring of this bridge is also necessary to accumulate the field data of durability. This project has been proceeded under the judge and the recommendation by "Technical Committee of Bridge Construction Applying New Material" (chairman: Prof. Ikeda, Yokohama National University) organized by Yamagata prefecture. We deeply express our gratitude to the people involved in this project.

REFERENCE

[1] Cheyrezy, M. : Structural applications of RPC, Proc. of the International Conf. New Technologies in Structural Engr., Lisbon, Vol.1 pp.5-14, July 1997.

[2] Behloul, M. : Design rules for DUCTAL pre-stressed beam. Technical Information from Bouygues, pp. 1-15, Feb. 2000.

DESIGN AND CONSTRUCTION OF THE MAETANI BRIDGE WITH CORRUGATED STEEL WEBS AND ENTIRELY EXTERNAL TENDONS

Yoshifumi Maeda Kiyotaka Agawa Yosihiro Fujiki Yasuhiro Miura
Japan Highway Public Corporation Oriental Construction Co., Ltd.
JAPAN

Keywords: Corrugated Steel Webs, Entirely External Tendons

1. INTRODUCTION

Since the first Prestressed Concrete (Hereinafter called "PC".) bridge was constructed in 1951 in Japan, the Cantilever erection method and a lot of research and technical development enabled us to construct a bridge with a longer span. In this trend, the weight saving of the main girder should be given priority from the point of view of earthquake proofing, the profitability, and the workability. As a solution to such matters, lots of studies have been conducted and this entirely external tendon method that uses the corrugated steel webs are included in it as a countermeasure.

Based on these conditions, Japan Highway Public Corporation (JH) aims to establish a structure which can easily perform rust prevention and the inspection of the PC steel, and therefore they basically decided;①All the longitudinal tendons are taken as an external cable system which can be checked visually.②The tendons arranged in the webs for shear reinforcement would be abolished, and webs are taken as corrugated steel , which does not restrain introduction of the longitudinal prestressing.③The transversal tendons arranged in the upper slab are taken as pre-grouted tendons, which do not need cement grout.

This bridge, Maetani Bridge in Higashi Kyusyu National Expressway, has been designed and constructed according to the ideas mentioned above.

2. THE OUTLINE OF DESIGN AND CONSTRUCTION

The Maetani Bridge is a T-shaped rigid Frame Bridge with a maximum span length of 83.4m.

Additional to the full-external tendons and the structure of corrugated steel webs, this bridge has adopted new ideas concerning the work method,and the anchoring structure of external tendon to:

1) To adopt the cantilever erection method with temporary PC bars and large capacity external tendons.
2) To adopt the transparent poly vinyl chloride sheath and cement grout for rust prevention of the external tendons.
3) The anchorage part of external tendons adopts a composite structure for weight saving.
4) The part near the pier head where corrugated steel is more than 5.0m high adopts the concrete composite webs for the prevention of buckling.
5) As a shear connector between the concrete slab and the corrugated steel webs, we have adopted angle dowel that is used in many Dole bridges.

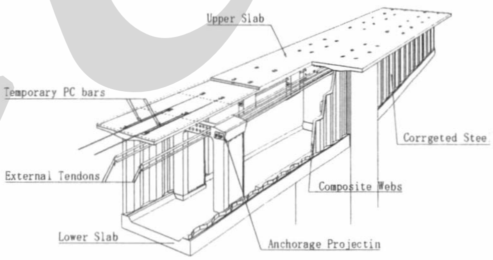

Fig. 1 Structure of Maetani Bridge

Fig. 1 shows the structure of this bridge.

Noteworthy is that this bridge, has applied the cantilever erection method with the external tendons, and ①As the procedure 1-3 in **Fig. 2** show, this construction method arranges the temporary PC bars in the upper slab and it is similar to the cantilever erection method using PC bars that have given a satisfactory results so far. ②The large capacity external tendons are tensioned and anchored every 2-3 segments in procedure 4 and the prestress force is removed from the temporary PC bars to the external tendons.

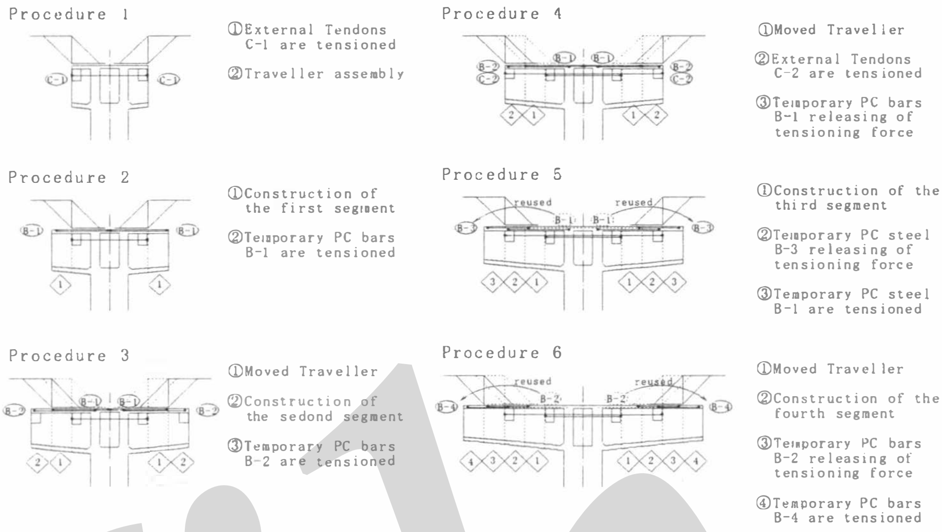

Fig. 2 The process of the cantilever erection method

③After releasing the tensioning force of the temporary PC bars that become useless in the procedure 5-6, it is moved to the next cantilever erection segments and reused to repeat a series of construction cycles.
Furthermore, the above-mentioned structure can save deadweight by 15% over the Maetani Bridge, compared with that of PC Bridge with concrete webs and internal tendons.

3. THE FULL-SIZE TEST

3.1 The Outline of Test

This was the first PC box-girder type bridge with the corrugated steel webs to apply the entirely external tendons. Therefore we implemented the full-size test (Photo 1) to confirm the workability and to measure the member stress so that we could make full use of problem discovery and make the appropriate improvements to the design.

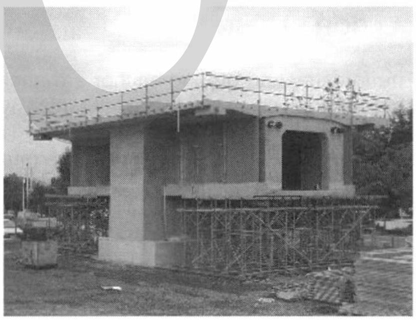

Photo.1 The full-size test

3.2 Measuring Test of the Stress for the Member

To confirm the stress at the pier head of the cantilever slab using entirely external tendons, we measured the concrete stress at the segments joint. The measured value of stress when the external tendons were tensioned showed near 90% of the value of the FEM analysis. However, the measured value at the pier head of the cantilever slab on the composite webs side was only 75% of the value of FEM analysis because the stress on that side occurred at a lower level.

REFERENCE

[1] Kadotani, Aoki, Shoji, and Maruyama."A study of ultimate bearing power for the PC bridge with corrugated steel webs through a entirely external tendons" from the 10th Symposium on the evolution of Prestressed concrete, 2000.10 in Japanese.
[2] The society for the study of the composite structure of corrugated steel webs. Planning Manual of PC bridge with corrugated steel webs. (Draft) 1998.12 in Japanese.

LABOR SAVING METHOD OF CANTILEVER ARCH RIB ERECTION ON THE SUDOGAWA OHASHI BRIDGE

Shoji Tajima
Shizuoka Pref, JAPAN

Hirofumi Takayama
Central Consultant Inc. JAPAN

Kazuhiko Terashima, Kenichi Kata
Sumitomo Construction Company, JAPAN

Keywords: Ground anchor backstay, Forestay cable, Rebar cage prefabrication

1 INTRODUCTION

The Sudogawa Ohashi Bridge (provisional name) is a newly constructed concrete arch bridge with an arch span of 105 meters on the forest road Ashitaka line across Sudogawa Valley in Fuji City in Shizuoka Prefecture. The arch rib has an arch span–rise ratio of 7.8 and an arch span-girder height ratio of 75. (Its height varies from 2.2 meters to 1.4 meters.)

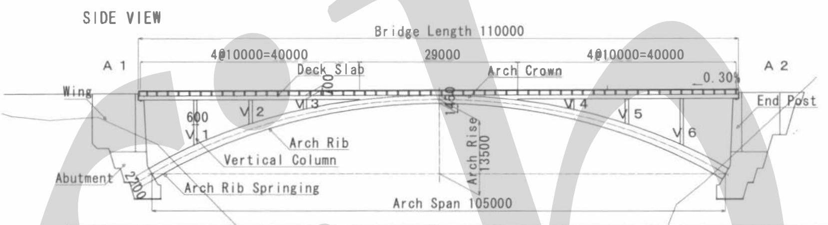

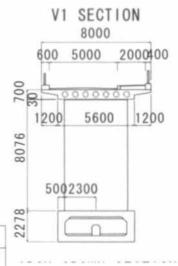

Construction name	Bridge construction on Ashitaka *Fureai* Forest Road
Location	Hinachinai, Fuji city, Shizuoka Pref. JAPAN
Construction period	2000.7.12～2003.1.15

Fig.1 Overall drawing

2 LABOR SAVING METHOD

The forestay and ground anchor are anchored directly at the wing.(**Table.1**). This method makes it possible to do without a backstay which would otherwise require setting up scaffolding, tensioning prestressing steels, and concreting cover. This saving helps to decrease industrial wastes and shorten construction time. And we anchored the forestay at the tip of every block after concreting of new block and moved the form traveler forward and were able to decrease the quantity of prestressing steel (**Fig.2**).

Table.1 Comparison of prestressing steel arrangement

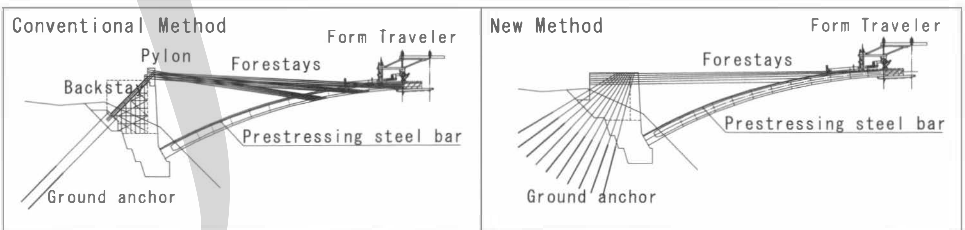

Conventional Method			New Method		
Forestays	SWPR930/1180 φ32	35t	Forestays	SWPR7BL 9～12S15.2	25t
Ground anchor	SWPR7BL 19S10.8	14t	Ground anchor	SWPR7BL 19S11.1	14t
Backstay Concrete		87m³			
Backstay	SWPR930/1180 φ32	10t			
Prestressing steel	SWPR930/1180 φ32	22t	Prestressing steel	SWPR930/1180 φ32	8t

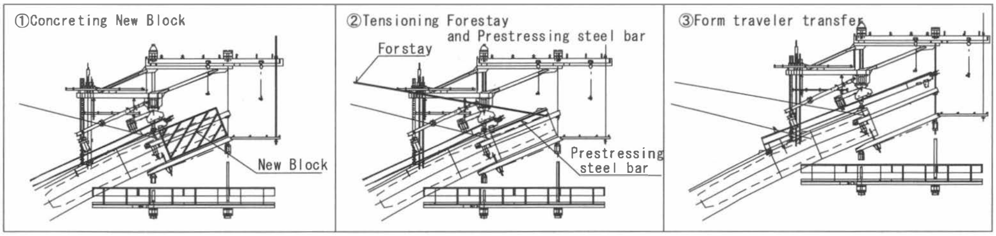

Fig.2 Block erection order

In construction of arch ribs, labor typically takes place on a slope, which is more difficult than working on flat ground, leading to deterioration in working efficiency. So, we use the rebar cage. It consists of reinforcement, prestressing-steels, and a section form. All components are pre-fabricated on the ground and then the rebar cage is lifted and moved by cable crane and drawn into the form traveler by chain hoist. Furthermore, in order to raise the ratio of prefabrication of the rebar cages and shorten their lengths, loop lap splices are used for the longitudinal rebar joints. As a result, a prefabrication ratio of 97% by weight was achieved.

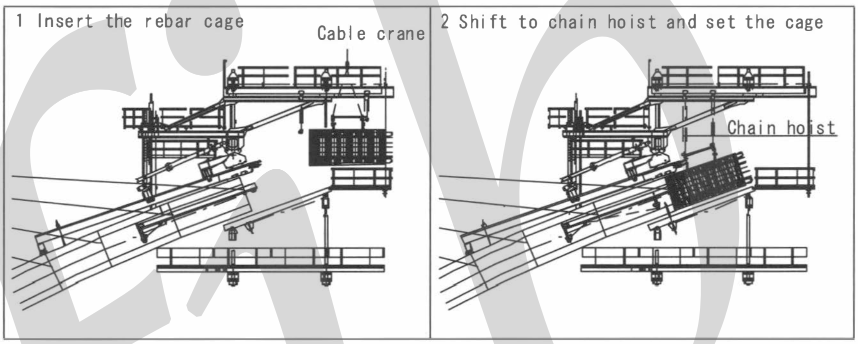

Fig.3 Placing rebar cage inside the form traveler

By these methods in cantilever erection, we could reduce required days in a block erection operation by 5days compared with conventional method (**Table.2**) and it amounts to 1 month.

Table.2 Block erection work programs

Original Plan	1	2	3	4	5	6	7	8	9	10	11	12	13	14
Form traveler transfer	■													■
Rebar erection		■	■	■	■	■	■	■	■					
Prestressing steel bar erection							■							
Form construction		■	■	■	■	■	■	■	■					
Concrete placement										■				
Concrete Curing											■	■	■	
Tensioning prestressing steel bar													■	■
Tensioning forestay													■	■

New Method	1	2	3	4	5	6	7	8	9
Form traveler transfer	■								■
Drawing rebar cage		■							
Prestressing steel bar erection		■							
Form construction		■	■	■					
Concrete placement					■				
Concrete Curing						■	■	■	
Tensioning prestressing steel bar								■	
Tensioning forestay								■	
Rebar cage erection				■	■	■	■	■	

REFERENCES

[1] Hara, K., Kishigami, I., Saitou, K., Ukena, M.: Construction of the extradosed Hozu Bridge. Proceedings of the 10th Symposium on Developments in PC.pp.167-172, Oct., 2000(in Japanese)

[2] Tajima, S., Takayama, H., Kuroawa, J. and Saitou, K.: Design and construction of Sudo Bridge. Proceedings of the 11th Symposium on Developments in PC. pp.281-284, Oct., 2001(in Japanese)

THE RION-ANTIRION BRIDGE STAY CABLES: A SEISMIC APPROACH

Benoît Lecinq Jean-Pierre Messein Sébastien Petit
Freyssinet International

Jean-Marc Tourtois
Vinci Construction

Keywords: Stay cable, seismic protection, dampers, wind vibration.

1 INTRODUCTION

The Rion-Antirion bridge in Greece is on course for completion by the end of 2004. The bridge will cross the Straight of Corinthe, and link the ferry port of Rion, on the Peloponnese, with Antirion on the mainland (**ref.** [1]). It is a multispan cable-stayed bridge, 2 250 m long with three main spans, 560 m long each. The Freyssinet stay cable system will be used on this project, as it fully meets the requirements of such an ambitious project, notably ease of installation, durability and stability against wind induced vibrations.

As the Rion-Antirion bridge is located in a very seismic area, the stay cable technology had to be specially adapted to meet the seismic requirements of this area. This paper presents the major features of the Rion-Antirion stay cable system. It focuses on the wind vibration and seismic analyses carried out for the stays and describes the mitigation measures adopted.

2 STAY CABLE SYSTEM

The stay cables selected for the Rion-Antirion bridge are bundles of parallel seven-wire strands, as on most major bridges built since the late 1980's in the world. In addition, the Freyssinet HD system is based upon the total independence of each strand and offers the following features :

- individual anchoring ;
- individual corrosion protection ;
- possibility of individual erection, stressing, dismantling and replacement of each strand.

The free length of the cable is formed of a bundle of parallel seven-wire strands placed inside a high density polyethylene (HDPE) duct. For the Rion-Antirion bridge, the stay cables consist of 43, 55, 61 or 75 strands, 15.7 mm nominal diameter and class 1770 MPa. The minimum thickness of the HDPE coating is 1.5 mm.

Two special anchorages transfer the tension of the stay cables to the structure (deck and pylon). Each strand is individually anchored in a high-grade steel anchor block, with high fatigue performance wedges resisting over 200 MPa fatigue stress amplitude combined with angular deflection during 2 million cycles.

3 VIBRATION MITIGATION

The Rion-Antirion stay cables lengths range from 77 to 293 meters. As high fatigue resistant stay cables have a low internal damping factor, the longer cables are more sensitive to wind vibrations. Therefore, a comprehensive analysis of stay cable vibration was carried out by CSTB (Scientific and Technical Centre for Construction).

The following mitigation measures were proposed :

- use profiled stay pipes to prevent rain and wind induced vibration. Indeed this is known to prevent the formation of organised water rivulets along the stays ;
- increase stay cable intrinsic logarithmic decrement above 3.0 %, using dampers ;
- the need for cross-tie cables was investigated.

In order to increase the damping of the stays, viscous dampers will be installed near the bottom end of every cable. Two types of Freyssinet dampers will be used :

- internal hydraulic dampers (IHD) located inside a tube rigidly connected to the steel gusset of the bottom anchorage ;
- external hydraulic dampers (EHD) placed a few meters away from the bottom anchorage and connected directly on the deck.

IHD are used on the shorter stays, numbered #1 through #10 and EHD on the longer stays, numbered #11 through #23.

4 SEISMIC PROTECTION

The stay cables could not be set aside in seismic design. A time-history analysis of several cables was carried out by Vinci Construction Design Office on ANSYS to determine the extreme forces and displacements of the stay cables during seism.

In case of seism, anchorage displacement and dynamic response of the stays result in axial tension variations as well as angular deflections of the cable close to the anchorage. Therefore, a design criterion combining axial tension and bending forces was necessary. The following criterion was adopted :

$$\sigma_T + \sigma_B < f_y$$

where
. σ_T is the normal stress resulting from axial tension ;
. σ_B is the normal stress resulting from bending ;
. f_y is the 0.1% yield stress of the cable (1593 MPa for class 1770 strands).

This criteria was defined to prevent the reduction of fatigue resistance that could occur in case of plastic yielding of the strand during a seism. The highest seismic deviation angle is in the order of 170 milliradians. Without any mitigation, this angle results in a high bending stress $\sigma_{B\ free}$ and the criterion is exceeded. Therefore, a device, called paraseismic deviator, will be used to guide the deflection of the cable over a sufficient angle so that the remaining bending stresses meet the criterion.

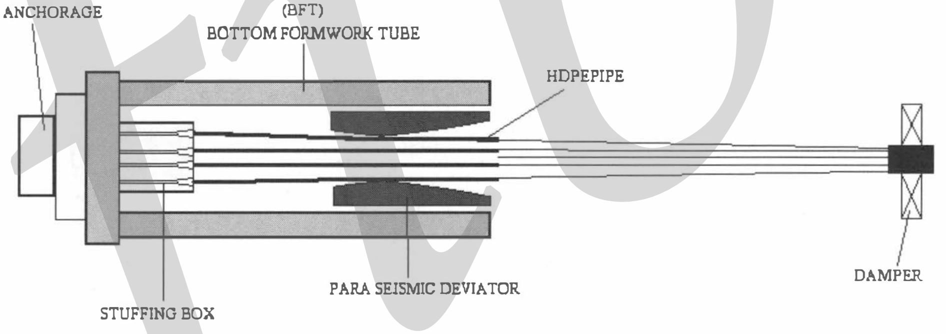

Fig. 1: view of paraseismic deviator

5 REFERENCES

[1] *The Rion-Antirion Bridge, an Exceptional Structure with a European Calling*, J.P. Teyssandier, J. Combault, Travaux n°748, December 1998 (in French).

[2] *Construction of the Piers of the Rion-Antirion Bridge in Greece: Labours of Hercules*, P. Morand, S. Safiratos, Ph. Tavernier, L. Boutillon, Travaux n°782, January 2002 (in French).

[3] *CIP Recommendations on Stay Cables Design and Testing*, SETRA, France, November 2001.

DESIGN AND CONSTRUCTION OF TENSHO CONCRETE ARCH BRIDGE

Kazuhisa Kamimura
Miyazaki Prefecture
JAPAN

Motoharu Kouno Koki Okada Toshihiko Tsuka
Taisei Corporation
JAPAN

Keywords: concrete arch, truss cantilever, temporary steel girders

1 OVERVIEW OF THE PROJECT

TENSHO BRIDGE, a concrete arch bridge, is located in Kyushu Island, which is in southern Japan. The arch span length of 260 meters is the longest in Japan among completed concrete bridges including cable-stayed bridges. The arch-rib was cast in place using the cantilever method from both sides with temporary members and the mid span portion of 78.5 meters in length was cast after span closure with the steel trussed girders. The construction of this bridge was completed in July 2000.

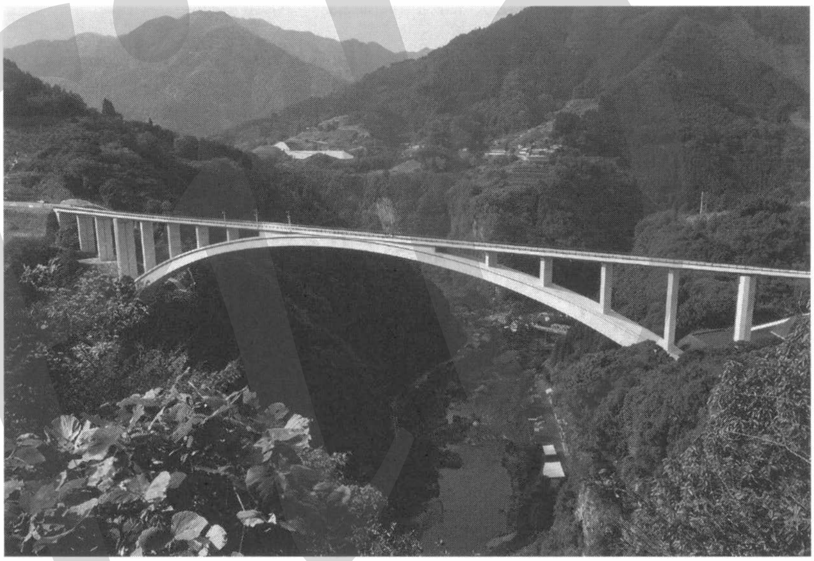

Photo 1 Panoramic view

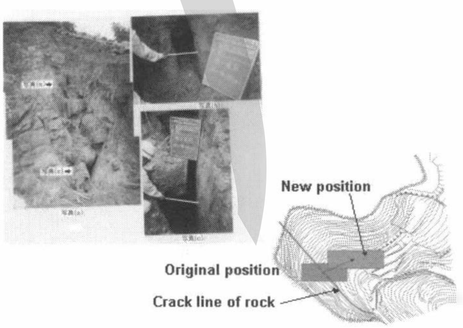

Photo 2 Bedrock crack

The construction site is in a volcanic area covered by a lava field. At first, a reinforced concrete fixed arch bridge with an arch span of 240m was designed. However, at the moment of construction of the right bank arch abutment, cracks in the rock of up to about 40cm wide, crossing the center part of the abutment, were found. So the construction position of the arch abutment was moved 20m backwards, resulting in an increase of the arch span from 240m to 260m.

2 CHARACTERISTICS OF THE TENSHO BRIDGE

1) Aesthetic design

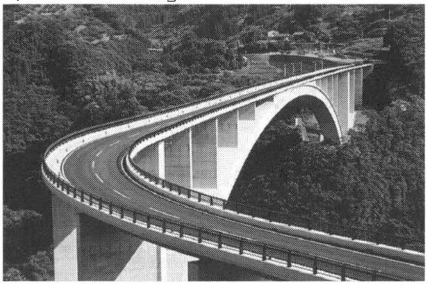

Photo 3 Overall view

Structural aesthetic considerations made the arch-rib look slender due to use of the shadow effect. These considerations also gave a continuous and rhythmical impression to the whole bridge though the elimination of abrupt change in the piers at the side spans and in the thickness of the vertical members and through the employment of the convex sections for the end piers.

When we selected the color of the handrails, we chose natural colors to blend into the color of the environment.

2) Simplification for end post top

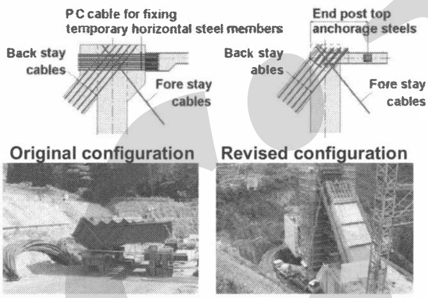

Photo 4 Comparison of end post top structures

The end post tops were designed as concrete structures into which the back stay, the fore stay, and the temporary horizontal steel member from three different directions, were anchored with PC bars and cables. Using the anchorage steel block, the structure and construction for the end post top could be simplified.

3) Development of new measuring system

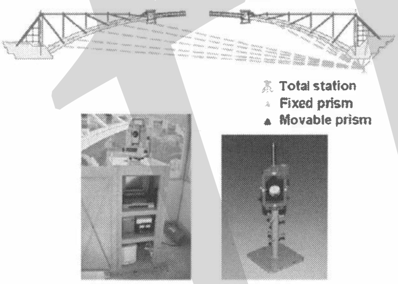

Photo 5 Total station

When a large span arch bridge is constructed by cantilever erection, the geometry control is quite difficult, because of its large and changeable displacement. In this project, to cope with the difficulty, a new construction management system using a total station of automatic object capturing/focalizing type was developed. This was the first time in Japan for a construction company, to adopt the system usually used for land-slide observation, for bridge construction management.

4) Environmentally friendly issues

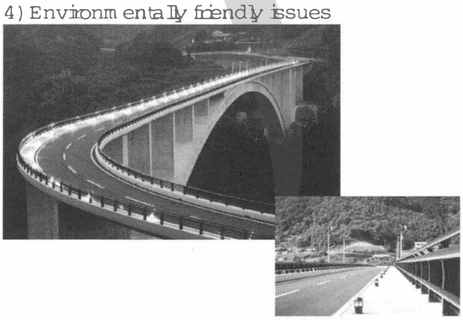

Photo 6 Deck lightings and small wind force generators

Concerning the deck lightings, the small wind force generators have been adopted for 2 reasons. One of the reasons was that the force of the wind was very strong around the erection site. The other was that there was no need to provide a big power supply that would harm the farm's agricultural growth and habitat by too much brightness. Therefore it was possible to supply a big portion of the power via the small wind force generators.

ERECTION OF THE WEST SIDE SPAN OF IBI RIVER BRIDGE

Hiroshi SHIRATANI, Taisei Corporation, JAPAN
Masato ITO, Japan Highways, JAPAN
Takuya INADA, PS Corporation, JAPAN
Masaru TADA, Hidehiko INAHARA, TAISEI Corporation, JAPAN

Keywords: extradosed bridge, precast segment, erection truss, hanging erection

1 INTRODUCTION

The Ibi River Bridge of the New Meishin Expressway, in Mie Prefecture, Japan, is a composite extradosed bridge with total length of 1397 m and standard deck width of 33 m. This bridge has four main spans of 271.5 m long, of which mid portions of 95 m to 100 m are steel girders. Its west side span lengths is 154 m. This side span was planned to be made of precast segments.

The side span cross over the river embankment. However, land transportation of the side span segments was impossible because of their size (33m in width) and weight (290 to 450 tons). Furthermore, there arose many problems such that the clearance between the built girder and the embankment was small, and no bottom-founded temporary piers were permitted on the embankment. The problem of the clearance resulted in the restriction of the girder height up to about 4.0 m. This paper describes the erection of the west side span employed under this circumstance and its design.

2 OUTLINE OF ERECTION EQUIPMENT

Figure 1 shows the outline of erection equipment for the west side span. 30th segment at the girder end on the pier PA5 was cast-in-situ prior to the erection of the side span segments. The segments up to the 17th were elected as a cantilever. Twelve side span segments, 18th through 29th, were all hanged individually from a couple of erection trusses. After adjustments of the level, direction, and gradient of each segment, they were tied together one by one in order. Then the stitches between 18th and 19th segments and 29th and 30th segments were casted in situ to make closure of the span. After that, releasing of the temporary stay cables and installation of prestressing tendons along the bottom slab were carried out step by step alternately.

Main advantage of the present method is its capacity of coping with geometrical error in the built deck. There were many possible reasons considered for the geometrical error, such as the size of the segments, the length of the P5 cantilever as long as 85 m, unpredictable tilt of the pier P5 because of small lateral resistance of the soft silt, and the asymmetrical cross section of the girder due to the road alignment. In this method, however, the adjustment of the position and gradient of the hanged segments is easy because the adjustment is done for each segment individually while hanged.

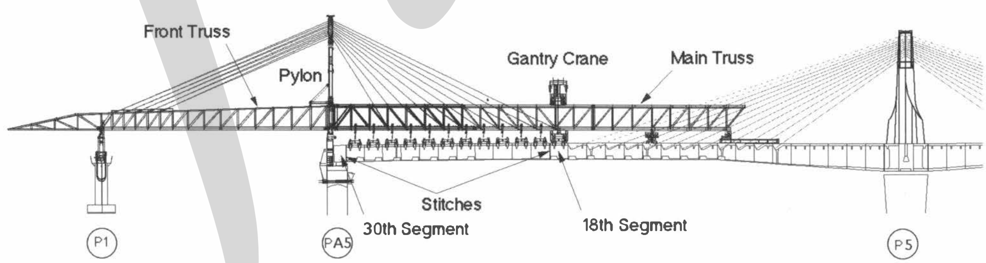

Fig. 1 Outline of erection equipment for side span

3 DESIGN

A two-dimensional frame analysis was conducted modelling the P5 cantilever, the side span, and principal erection equipments. In this analysis the erection sequence was traced up to the removal of the erection equipment. With the progress of the phased release of the temporary stay cables, the dead load of the main girder is gradually transferred from the trusses to the girder itself; consequently its deflection increases. The deflection induces elongation in the already installed prestressing tendons and resulting negative bending moment in the girder. This effect is significant for this side span because of large deflection of the girder and large amount of prestressing tendons, thus could contribute to reduce the positive bending moment of the girder. Therefore it was determined that as many prestressing tendons as possible be tensioned at early stages after closure, to obtain larger negative bending moment. The tendons tensioned at early stages were also helpful to resist the stress in the hanged main girder caused by the thermal effect on the main girder and erection equipment. The detailed stress field of the segments was also examined on the basis of the three-dimensional finite element analyses tracing general sequence.

The design of the erection equipments was based on a three-dimensional frame analysis. In addition, the dynamic behavior of the erection equipments with all the side span segments hanged was studied using a three-dimensional dynamic analysis. It has been found from the analysis that the natural period of the hanged segment was much longer than the period of expected earthquakes, and the hanged segments would oscillate out-of phase with the trusses, thus the section forces in the trusses and the reaction forces on PA5 were much smaller during earthquakes than concerned at the beginning. Consequently the safety of the whole structures against earthquakes has been confirmed.

5 CONSTRUCTION OF SIDE SPAN

The erection trusses had a total length of approximately 200 m, and the incremental launching span was more than 100 m. It was the biggest scale of launching construction in Japan. Furthermore, there was a series of construction with no precedent, such as hanging of twelve large precast segments with the weights of approximately 400 tons at one time and tensioning of large amount of external prestressing tendons (27s 15.2), toward the completion of the side span erection and the large steel girder erection at the central spans.

The Ibi River Bridge was completed successfully July 2001. The erection sequence of the side span is as follows:

* Dec. 1999 – Mar. 2000 : Erection of the P5 cantilever segments up to the 9th by erection noses.
Cast-in-situ erection of 30th segment on PA5.
* Apr. - May 2000 : Incremental launching of erection trusses.
* Jun. – Jul. 2000 : Erection of the P5 cantilever segments up to the 17th by erection trusses.
* Aug. – Sep. 2000 : Temporary hanging of side span segments with truss stays.

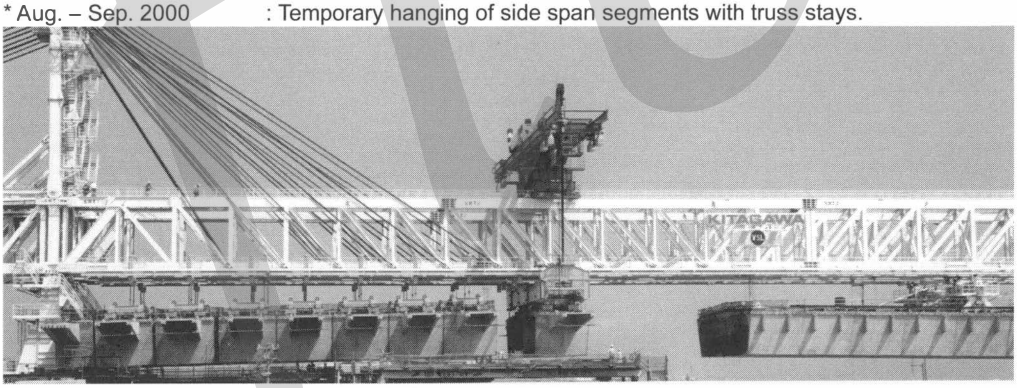

* Sep. 2000 : Jointing of 29th to 19th segments.
Lifting and jointing of 18th segment (to 17th).
Adjustment for the position of the tied segments (29th-19th).
Closure (concretiong of the two stitches).
* Oct. 2000 : Tensioning of prestressing tendons and release of temporary stay cables.
* Nov. – Dec. 2000 : Launching back and removal of the erection trusses.
Tensioning of remaining prestressing tendons.
* Dec. 2000 : Erection of the steel girder between P4 and P5.

Session 2 | Advanced design and construction of prestressed concrete structures

PROBLEMS, SOLUTIONS, DEVELOPMENTS AND APPLICATIONS AT DIFFERENT KINDS OF POST-TENSIONING TENDONS FROM THE EUROPEAN POINT OF VIEW

Professor Dr.-Ing. D. Jungwirth,
München

Dipl.-Ing. Balthasar Gehlen, Head of R&D,
DSI, München

Keywords: Durability, recommendations, high-tensile members, prestressed concrete construction

1 INTRODUCTION

Since the beginning of this year the Euro is introduced in Europe as official currency. It is supposed to open new ways between the EU-countries – as symbolically shown with bridges of 7 epochs on the backside of the EURO-banknotes. Globalisation and elimination of trade restrictions require European Recommendations. This procedure goes on sluggishly due to the society with different cultures, the states with different politics and laws as well as the non-uniform economical structures.

Therefore many of the European Standards for construction material, loading, design, testing and execution are still in the stage of pre-standards. However, a satisfactory fact is the European communication and the national conformities of Standards regarding design models and requirements to material qualities. This gives suggestions to further developments, overlapping special fields, for example tension and pressure members in geotechnics or in case of hybrid structures. Similar is happening in other markets as well.

Beside Standard Committees also national and international associations with their guidelines and recommendations are very active as for example fib, PTI, ASBI a.s.o. For structural design the most important part -beside aesthetics- is still playing the equilibrium and the compatibility. Dimensioning of durability is gaining an increasing importance, same as total cost considerations before start of construction, furthermore operation (with maintenance) until demolition. Under the conception of "sustainability" it is tried to leave a viable environment to the following generation.

Considering the aforementioned aspects it is intended to report on problems, solutions, developments and applications of external and internal tendons at the corresponding structures, specially from the European point of view, extensively treated at different highlights. The results may be transferred to tension members in geotechnics and to stay cables.

2 PROBLEMS

Every year about 1 million tons of stressing steel are installed, a 2/3 portion that means 66 % of all bridges is executed in prestressed concrete construction; a spectacular case of damage lies by far below the failure probability as indicated in the 10E-6 of the recommendations for dimensioning.

The experience of this comparatively young construction type is consequently compiled and then executed in an increased durability of modern prestressed concrete structures (also see [1]).

3 SOLUTIONS

Modern European Standards, such as prEN1992 and guidelines for approval for post-tensioning systems (ETAG No. 013, 2002) require a high level to the applied materials and to the execution.

The lecture deals with the advantages and disadvantages of the construction system with internal post-tensioning with/without bond and with external post-tensioning as well as with their combination.

The economy during erection and maintenance of prestressed concrete structures depends on the chosen type of post-tensioning and on the level of post-tensioning as well as on the characteristics, such as destruction-free monitoring, restressability and exchangeability. Of special importance is the choice and the execution of corrosion protection with cement grout or corrosion protection compounds which is critically investigated.

The lecture also gives attention to construction details and execution, like requirements to deviators, admissible prestress in regard of friction-problems during post-tensioning, Fig. 1, destressing of cement-grouted external tendons and a specially smooth cutting (Fig. 2).

4 DEVELOPMENTS AND NEW CONSTRUCTIONS

The experience gained from testing and application of the external prestressing is used for the improvement of internal post-tensioning. Developments such as a new bundle tendon without bond installed in cross-section or the electrical isolation of internal tendons are presented as solutions.

Extradosed bridge constructions or arches with beam ties represent an enlarged application of the external post-tensioning.

5 OUTLOOK

Regardless whether internal or external tendons, whether prefabricated corrosion protection with corrosion compound or active corrosion protection with cement-mortar will be applied, the technical level of the products and of the performance has got a high "niveau". Robustness and durability are continuously under elaboration. The market for prestressed concrete products is still capable to grow. The so created structures may not only be successful in their industrial respect but may also contribute to the wellness of the society by their aestetics and environmental awareness

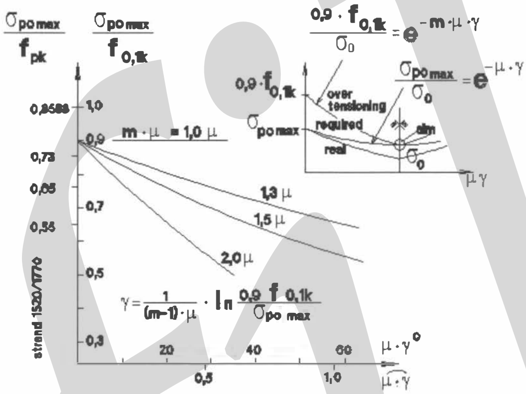

Fig. 1 Admissible prestress in regard of riction-problems, [2]

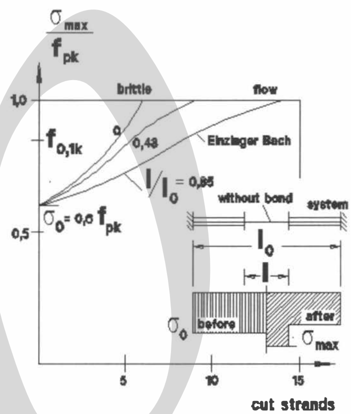

Fig. 2 Stressing condition at smooth cutting of a 140 m long, cement grouted external PT-tendon

REFERENCES

1] fib bulletin 15, Technical report: Durability of post-tensioning tendons, Workshop 15-16 November 2001, Ghent (Belgium)

[2] FIP State of the Art Report: Tensioning of tendons: force-elongation relationship, 1986

DESIGN AND CONSTRUCTION OF FURUKAWA VIADUCT

Shoji Ikeda — Yokohama National Univ., JAPAN
Hiroyuki Ikeda, Kazuyuki Mizuguchi — Japan Highway Public Corporation, JAPAN
Kei Muroda, Yoshihiko Taira — Sumitomo Construction Co., LTD., JAPAN

Keywords: Factory-fabricated precast segment, U-shaped core section, external prestressing

1. INTRODUCTION

The precast segmental bridges using short line match-casting and span-by-span erection have been widely adopted in all over the world, under a variety of bridging conditions. However, this type of bridge generally requires large casting and stock yard near the construction site and it could be difficult to apply this bridge type such as in the urban or in the mountain area due to the site limitations in which few yard for fabricating segments can be used near the site. In such cases, the segments should be fabricated at a separate location and transported on ordinary public roads, therefore, the weight and the size of the segment is imposed to be limited against traffic regulations.

For Furukawa Viaduct on the New Meishin Expressway in Japan, the factory-fabricated precast segments have been applied. The weight of a segment is held to be no more than 30 tons in order to be transported on the public roads with a trailer. The most distinguishing feature of this bridge is the shape of the girder section, designed to reduce the weight of the segments for the 16 m road width. The girder comprises U-shaped core segment with transversal horizontal ribs and cast-in-place upper slab including precast concrete panels on the ribs. This enables the erection weight to be reduced and also makes the erection girder more lightweight.

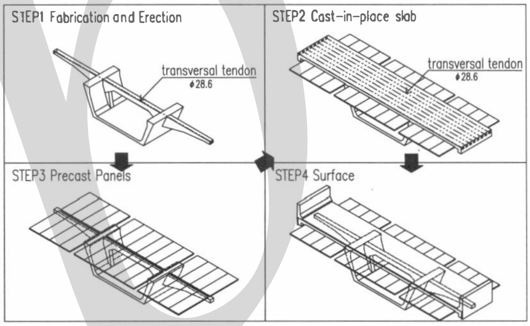

Fig. 1 Construction processes

2. DESIGN

2-1 Selection of section shape

Prior to the detailed design, several section shapes were compared in order to reduce the weight of segments focused on economy, ease of construction and structural adequacy.

Regarding the configuration of segment length and slab structure, there is no major difference between the rib structure and the strut structure in terms of economy, but the strut configuration is more adequate in terms of the force transfer. Nevertheless, with regard to the struts, some are still considered to be relatively inadequate for this viaduct, including the connection of the struts and the handling during construction. As a result, the U-shaped core section with transversal horizontal rib, is adopted for the segment shape.

2-2 Design of girder

(1) Design at construction state

Compared to the conventional box section, the U-shaped core section with rib configuration had narrow compression flange width on the upper edge as well as low torsional stiffness until casting slab.

During the casting of slab concrete, an uneven load induces torsional moment and longitudinal additional stress. Furthermore, a horizontal alignment of R = 700 m also creates torsional moment. The study was conducted under the assumption that the uneven load would be applied to one-fourth of the span, measuring 9.5 m long in each. When torsional moment acts on the U-shaped open section, the warping torsion produced stress in the axial direction as well as shear stress.

(2) Design at service limit state

At design load state, the secondary internal stress between the precast girders and the cast-in-place slabs was calculated based on time dependent strain analysis with respect to creep and shrinkage. For the upper and lower edge of girders at service limit state, tensile stress less than nominal tensile strength of concrete was allowed for girder that includes cast-in-place slab, and no tensile stress was allowed for the joints on the bottom edge of the segments.

(3) Design at ultimate limit state

The cast-in-place slab concrete gives continuity of the reinforcements although precast segments are used, but all the prestressing tendons are arranged externally. Non-linear analysis was implemented in order to confirm the ultimate capacity. Load application was studied by adding load constant γ_i sequentially for γ_i*(D+L) until the maximum concrete strain reached 2500 μ. Two cases of live load were performed: Case 1, which focused on the section at center of span, and Case 2, which focused on the section at pier. For Case 1 and Case 2, the load coefficient γ_i when the concrete reached the maximum strain of 2500 μ was 2.963 and 2.702, respectively, which exceeded the load coefficient γ_i = 1.7 for the ultimate limit state. The tensile stress increase on the external tendons was 338 N/mm^2 for Case 1 and 330 N/mm^2 for Case 2.

(4) Design of Shear Keys

The shear keys were designed both at the construction state and at the ultimate limit state. The allowable shear stress for shear keys was set at 1.5N/mm^2 during construction and 2.0 N/mm^2 at ultimate limit state, in accordance with the Japan Road Association's Specifications for Highway Bridges. The shear keys comprised the placement of trapezoidal keys at the four corners of the section and multi- trapezoidal keys at webs.

The design at ultimate limit state was conducted for two cases: one in which the torsional moment was at the maximum, and another in which the shear force was at the maximum. Even though the slab was cast-in-place with continuous reinforcements, it was also confirmed that the shear key at each location could be kept to within τ_a = 2 N/mm^2.

Since it was the first time to build a U-shaped precast segmental bridge with span-by-span erection, a full-scale span test was also conducted and the adequacy of design was confirmed prior to the construction.

3. CONSTRUCTION

The segments were fabricated in two precast concrete factories located approximately 60 km from the site of the bridge construction and the segments were transported from the factories to the site using a trailer with a 30 t load capacity.

The standard segments were erected after the construction of the pier segments with the erection girder and the span-by-span method. Epoxy joints are used for the connection of segment. After the segments were joined, eight 19-ϕ15.2 mm external tendons were inserted and tensioned. A total of 12 external tendons were arranged consisting of eight single-span tendons and four double-span continuous tendons.

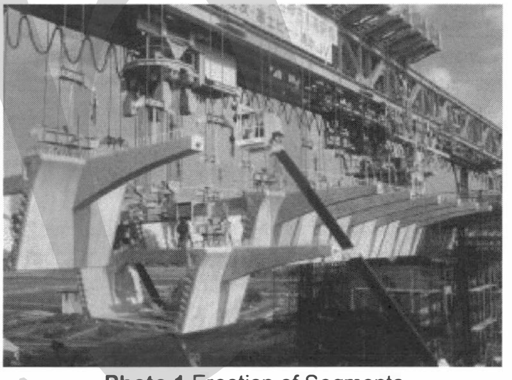

Photo 1 Erection of Segments

The upper slab consists of precast concrete panels and cast-in-place concrete. The precast concrete panels were first erected and placed between transversal ribs of the segments, one span behind the span-by-span erection. Approximately 200 panels were provided for each span, and each panel was erected with crane. After the erection of the panels, the slab reinforcements and transversal tendons were arranged and the slab concrete was placed. The precast concrete panels can serve as both formwork and work scaffolding. After the tensioning of the primary longitudinal tendons, after-bonded tendons (ϕ21.8 mm) were used for the transversal prestressing and the secondary external tendons in the longitudinal direction were then conducted.

REFERENCES

[1] H. Ikeda, K. Mizuguchi, A. Kasuga, K. Muroda: Design and Construction of Furukawa Viaduct –Design-, Bridge and Foundation Engineering, Vol. 35, No.2, pp.2-9, Feb., 2001 (in Japanese)

[2] H. Ikeda, K. Mizuguchi, S. Yamanaka, K. Nakatsumi: Design and Construction of Furukawa Viaduct –Construction-, Bridge and Foundation Engineering, Vol. 35, No.3, pp.11-16, Mar., 2001 (in Japanese)

[3] J. Strasky: Segmental Structure with Replaceable CIP Deck Slab, International Bridge Conference, 2000

DESIGN AND CONSTRUCTION OF OKITSU-GAWA BRIDGE —CANTILEVER METHOD WITH ALL EXTERNAL CABLES AND PARTIAL CORRUGATED STEEL WEB—

Norio Terada,Japan Highway Public Corporation
Yasuo Fukunaga, Japan Highway Public Corporation
Kazumi Nakamura, Japan Highway Public Corporation
Hitoshi Sato,Oriental Construction,Kawada Construction Joint Venture

Keywords: All external cables,Corrugated steel webs,Full-scale experiments

1 INTRODUCTION

The Okitsu-gawa Bridge on the Daini Tomei Expressway is being constructed 3.5 km northwest of the Yoshiwara Junction, which is between the Shimizu and Shizuoka Interchanges, to cross Okitsu-gawa River (Class B river classified by the Japanese River Act). The bridge is characterized by all cables being external and large-capacity prestressing steels (19S15.2, 27S15.2) and the use of corrugated steel webs at the side spans to improve the unbalanced moments during construction. Since no cantilever structures of this scale have been built using all external large-capacity cables, full-scale model experiments were conducted to examine the safety of the anchorage.This paper describes the results of the full-scale experiments of the anchorage to member projection, reasons for adopting corrugated steel webs, and the design and construction of the bridge.

2. OUTLINE OF THE PROJECT

The bridge is 4 span and 3 span prestressed reinforced concrete continuous rigid box girder structures. The bridge has a maximum span of 148.0 m, a maximum pier height of 68.5 m, and the forth longest span length in Japan. Fig.1 shows a prognostic image of the completed bridge. Fig. 2 shows a cross section of the inbound of the Okitsu-gawa Bridge.

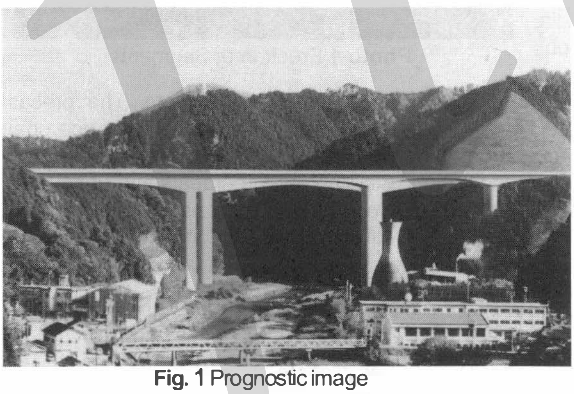

Fig. 1 Prognostic image

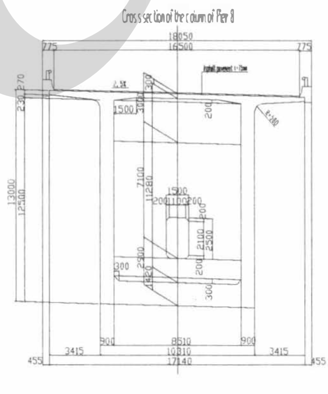

Fig. 2 Cross section

3. OUTLINE OF THE EXPERIMENTS

Since the local stress at the anchorage was to be examined, the specimens were prepared so as to reproduce the full size of the anchorage and the minimum web depth to which the anchorage to member projection was to be fixed (t = 400 mm). One of the sides reproduced the corrugated steel webs, which were to be used for parts of the bridge. The difference in strength that was attributable to the cross sectional asymmetry to the right and left direction was adjusted by applying tensile force based on preliminary FEM analyses. The girder height of the specimens was the height of the block to which the corrugated steel webs were to be fixed.

The experimental results showed the necessity to control the tensile stress of concrete to not exceed 3 N/mm^2 at the element center of FEM analysis (10 cm meshes) and the tensile stress of reinforcement bars to not exceed 120 N/mm^2 to ensure durability.

4. EMPLOYMENT AND DESIGN OF PARTIAL CORRUGATED STEEL WEBS

1) Reasons of employment

The inbound side span A2 is 130.60 m long and has a central span of 142.0 m. It was noticed since the initial planning stage that such a long span requires improvement of unbalanced moments during construction. Two general mitigation methods were investigated, namely the retrograding cantilever erection and the one-directional cantilever erection. The retrograding cantilever erection included the use of pylons, temporary supports, counter weights, and incremental launching method. As the one-directional cantilever erection methods, the use of hybrid structures, such as steel truss webs and corrugated steel webs, were investigated to reduce the weight of the structure. The former temporary support method was judged not appropriate due to the difficulty of using the slope in front of Pier A2. The counter weight method and the incremental launching method were not available due to insufficient seismic strength of the ground at the back of Pier A2. Of the latter method, the more widely used corrugated steel webs were precisely analyzed.

Our investigation showed that the one-directional cantilever erection that uses the corrugated steel web cross section was economical and not restricted by the ground. The method is shown in the lower diagram of Fig.3.

The outside of the corrugated steel web was decided to be lined with concrete after closing the spans to enable easy maintenance and have beautiful extemal appearance.

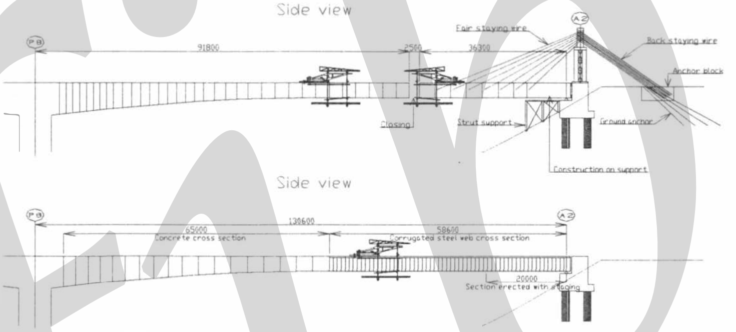

Fig.3 Investigation of methods for constructing Side Span A2

2) Designing corrugated steel webs

The shear stress of corrugated steel webs is usually verified for both the design and ultimate loads. For this bridge, the effects during cantilever erection were also examined. The thickness of some steel webs was determined based on the shearing force during cantilever erection. As described above, this bridge was decided to be finished by lining the exterior surfaces of the corrugated steel webs with concrete after completing the bridge body. Casting of surface concrete enabled the rigid cross sections of both the corrugated steel webs and concrete webs to resist the residual load (deck and live loads). Therefore, the surface concrete web section was validated by dividing the shearing forces according to the strength ratio of the cross sections to arrange reinforcements.

5. CONCLUSION

The Okitsu-gawa Bridge has its cantilever erection completed on one of its pier columns and is working on the cantilever erection for the other pier columns. Such a large scale cantilever structure has not been constructed using all cable being extemal and large. Analytical methods and construction methods were examined by conducting full-size experiments. The works of partial corrugated steel webs will soon begin, for which safety, durability, and working performance will be thoroughly investigated.

Finally, we would like to thank all persons involved in designing and constructing this bridge for their precious instruction and advice.

DESIGN AND CONSTRUCTION OF SANTNIGAWA BRIDGE

-- PC EXTRADOSED-TYPE BRIDGE --

Masaru Nishimura※2 Hidetugu Mochizuki※1 Yoshio IIZUKA※1 Teruyoshi Akiyama※2
※1 Japan Highway Public Corporation ※2 Kawada Construction Co.,Ltd.
JAPAN JAPAN

Key words: extra-dosed prestressed concrete bridge, external prestressing cables

1. INTRODUCTION

Santanigawa Bridge, located on Tokushima Expressway, Tokushima, Japan was extra-dosed type bridge. The bridge, erected by the cantilever erection method, had some restricting features including: large width (20.4m), curved geometry (1000 radius) and unequal span (1:1.6). These features lead to the adoption of a rather flat single tower located at median (1.0m x 5.5m) and one plane suspension. The general view of Santanigawa Bridge is shown on Fig. 1.

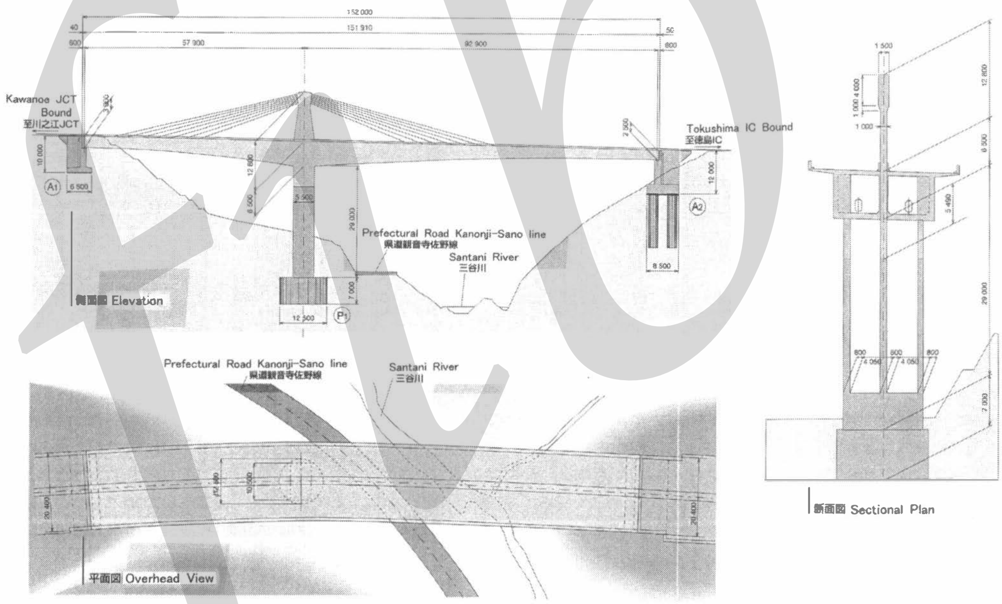

Fig.1 General view

2. DETAILED DESIGN

Major design considerations included: designing the tower as a PRC structure taking into consideration the significant out-of-plane force from stayed cable tension and the design of a special type of saddle to anchor the cables at the tower. In addition to full scale testing on the saddle, a series of FEM analysis were done for stress transfer from stayed cables to girders, shear distribution in web plates and tower base stress. Fem Analysis items and the models is shown on Table 1.

Table 1 Analysis items and the models

Analysis items	Applied models
①Effective conduction length of diagonal cable tension	Total model (erection)
②Shearing allotment rate of the web	Total model (completed/erection)
③Stress of tower base part and pier head part	Partial model (tower base part)
④Stress of girder side diagonal cable fixation part	Partial model (fixation part)
⑤Stress of main tower saddle part	Partial model (saddle part)

3. OUTLINE OF THE CONSTRUCTION

Major construction considerations were: the use of prefabricated re-bars(Photo 1), the use of a new type of traveler , and the monitoring of real time tower stress through the use of a satellite circuit(Fig.2).

Photo 1 prefabricated reinforcements assembly

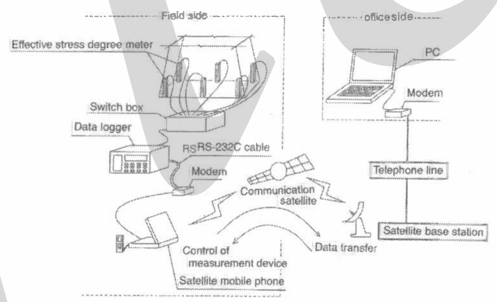

Fig.2 Measurement system

REFERENCES

[1] "Planning and Design of Santanigawa 2nd Bridge (Part 1)"
"Symposium Papers on the Development of Prestressed Concrete (Vol. 8, P551-556, Oct. 1998)"
Iizuka, Hanada, Nishimura, and Oishi

[2] "Planning and Design of Santanigawa 2nd Bridge (Part 2)"
"Symposium Papers on the Development of Prestressed Concrete (Vol. 8, P557-561, Oct. 1998)"
Mochizuki, Ando, Kitano, and Ryu

[3] Design of Santanigawa 2nd Bridge (Extradozed Bridge), the Full-scale Examination for Saddle Structure, and Prestressed Concrete (Vol. 41, No.1, P51-57, Jan-Feb 1999)"
Iizuka, Akiyama, and Nishimura .

THE DESIGN AND CONSTRUCTION OF YAMANAKAGAWA VIADUCT (PC OPEN-BOX GIRDER BRIDGE)

Yoshio Taira
The Ministry of Land, Infrastructure and Transport
Japan

Shin Suzuki, Hiroshi Nishi, Hideki Manabe
Fuji P.S.Corporation
Osaka, Japan

Keywords : PC Open-Box girder Bridge, External Prestressing System, FEM Analysis, Saving Cost

1 INTRODUCTION

Yamanakagawa viaduct that was constructed on order by Ministry of Land, Infrastructure and Transport had been planned to be a continuous PC box girder bridge adopting conventional structure type. But we proposed to change the plan of the structure into the open section structure which using both internal and external cables in terms of cost-reduction, and we were going to design and construct that bridge. PC open-box girder bridge has the structure that eliminates the lower slab from conventional PC box girder bridge. By adopting this style, the load for substructure can be reduced, therefore construction time and cost can be reduced comparing to a box girder bridge. This is the first attempt to adopt such the open section structure and external cable systems in Japan.

2 OUTLINE OF THE BRIDGE

The outline and specification of this bridge are shown below. Fig.1 shows a section view, and Fig.2 shows the structure general view.

Project name: 2nd Hanwa national road Yamanakagawa viaduct superstructure construction work
Owner: Ministry of Land, Infrastructure and Transport, Kinki Regional Development Bureau, Naniwa Road Work Office
Structure type: PC 4-spans continuous open-box girder bridge
Bridge length: L = 209.500m
Width: Whole width 10.600m, Effective Width 9.500m
Used Steel Material Outer Cable 19S15mm., Inner Cable 12S15.2mm

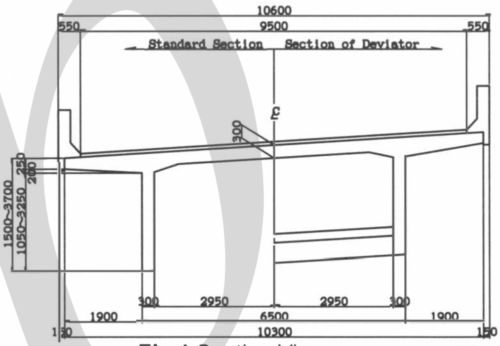

Fig.1 Section View

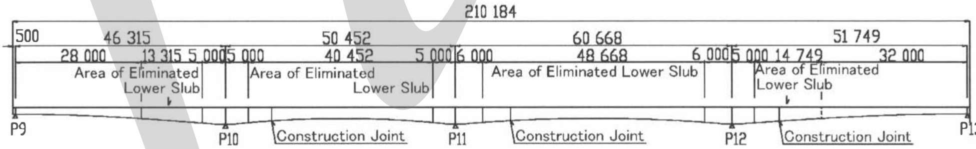

Fig.2 General Structure View

3 OPEN-BOX GIRDER BRIDGE

Open-box bridge can: (1) reduce the thickness of materials in the superstructure and the load for the substructure by reducing the own weight by eliminating the lower slab, and it improves cost efficiency; (2) shorten the construction time by laborsaving in building of the upper slab; and (3) be constructed without separating the construction of the box part and lower slab, in contrast with the conventional box girder bridge in which those parts constructed separately. And by eliminating the lower slab,

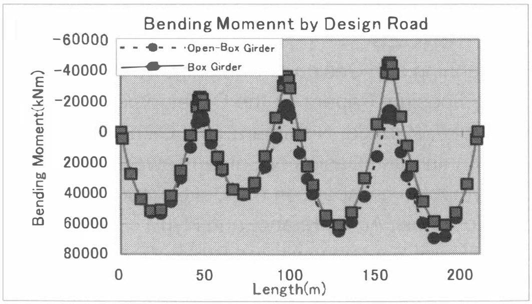

Fig.3 Comparison of Section Force

the times of pouring can be reduced because the amount of concrete for a pouring can be reduced and the pouring section length can be extended. Fig.4 shows the graph, which compares the analytic section force of the conventional box girder and the open-box girder of the 4-span continuous bridge (P9 - P13) in this bridge. Particularly, the negative bending moment is reduced by 40% on the middle supporting point.

4 INVESTIGATIONS

This bridge has a specific section shape that does not have a lower slab. With this structure, the following problems were conceivable.

① Consideration for the part of eliminated lower slab It is considered to occur the local concentrated stress in the part of eliminated lower slab in the section where the box section sharply changes into the open section (see Photo. 1). We allocate the transverse PC steel in the part of eliminated lower slab of this bridge to introduce the presteree against such that concentrate stress

②Consideration for the upper slab

When a load is charged on the open section part, the bottom of the web tend to spread outward (this phenomenon is called "web splitting"). As a consequence of this phenomenon, the positive bending moment is added to the middle of the span. The influence of this "web splitting" cannot be taken into account in the frame (box rigid frame) analysis which ordinarily done for the cross direction analysis of a box girder, therefore a FEM analysis should be performed.

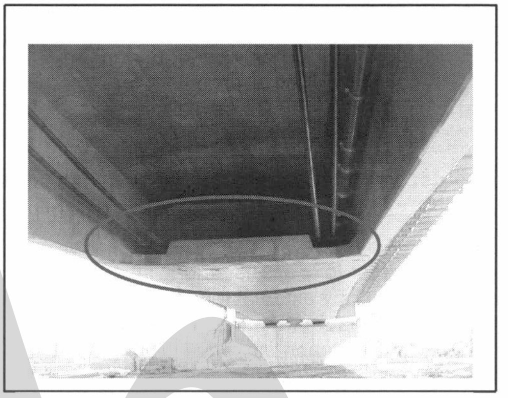

Photo.1 Part of eliminated lower slab

5 COMPARISON OF QUANTITY

From the detailed design of this bridge, the reduction in quantity can be accomplished in a 4-span continuous bridge (P9 - P13) by changing from box girder (closed section) to open section structure, as shown in Table 1.

Table 1 Comparison of Quantity

work		class		unit	Box	Open-Box	difference	note
Concrete		$\sigma ck=40N/mm^2$		m^3	1712.10	1545.27	-166.83	
Formwork				m^2	206669.00	4978.73	-201690.27	
Reinforcement		SD295		t	206669	196108	-10561	
PC steel	Internal Cables	PC steel Strand	12S15.2(SWPR7B)	kg	69670.10	35534.80	-34135.31	no extra length
	External Cables	PC steel Strand	19S15.2(SWPR7B)	kg	0.00	25838.81	25838.81	no extra length
	Transvers Cables	PC steel Strand	1S28.6(SWPR19)	kg	15157.00	17377.77	2220.77	Pre-grout

6 CONCLUSION

So far we have outlined the investigations of the PC open-girder bridge with external prestressing system concerning YAMANAKAGAWA Viaduct project. As the results, adopting this style, the self-deadweight, the load for the substructure, and the quantity can be reduced, therefore the construction period and cost can be diminished comparing to the conventional box girder bridge. No problems occurred in on-site work and this project was completed in March 2002 safely.

REFERENCES

[1] Specifications for Highway Bridges・PART I Common, PARTIII Concrete Bridges, The Japan Society of Roads,1996

[2] Suga,K. , Ikeda,K. , Abe,K. , and Hashimoto,M. :Design and Construction of Double T-Girder Bridge,The 9th Symposium on Developments in Prestressed Concrete, pp635-640,Oct.,1999(in Japanese)

DESIGN OF JOINTS IN SEGMENTAL HOLLOW BOX GIRDER BRIDGES

G. Rombach , A. Specker

Department of Concrete Structures

Technical University Hamburg-Harburg, D 20171 Hamburg, Germany

e-mail: rombach@tu-harburg.de

Keywords: segmental bridges, joints, external prestressing

Segmental bridge construction is one of the major new developments in civil engineering in the last years. In contrast to 'classical' monolithic constructions a segmental bridge consists of „small" pieces stressed together by external tendons (Fig. 1). Although many segmental bridges had been built in the last years, especially in South East Asia, the design of the unreinforced joints between the segments, which is of critical importance regarding the safety of the structure, is still under discussion (Fig.4). The known models are either too conservative and thus too uneconomic (German Specification) or not valid for high compressive stresses (AASHTO). Numerical calculations verified by full-scale tests will be presented in this paper, which lead to a better understanding of the behaviour of segmental constructions and a more realistic design of the joints.

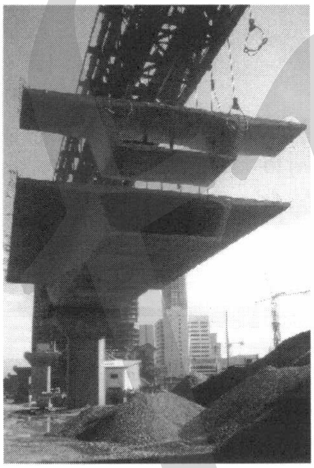

Fig. 1 Method of construction of a segmental bridge

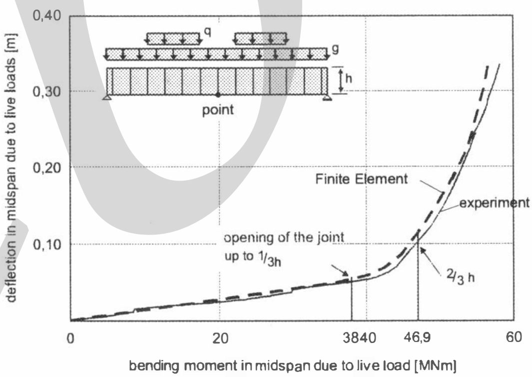

Fig. 2 Comparison between full-scale test and numerical results

To investigate the bearing capacity of a segmental bridge and the forces in the joints finite element calculations had been conducted taking into account the nonlinear behaviour due to the opening of the joints under tension. In contrast to known investigations, the fine indentation had been modelled [Fig. 3] which is of great importance regarding torsion effects. In Fig. 2 a typical moment-deflection curve of a segmental bridge is shown. The calculations are verified by a full-scale test carried out in Bangkok. A good agreement between the numerical results and the test data can be seen. This demonstrates that the finite element model is capable to model the real behaviour of a segmental bridge.

Several load combinations corresponding to bending, shear and torsion are examined to determine the stresses resp. the forces in the joint. The results emphazise that the shear keys have a significant influence on the behaviour of a segmental bridge under torsion loads. Calculations with plain joints are insufficient when torsion effects become significant.

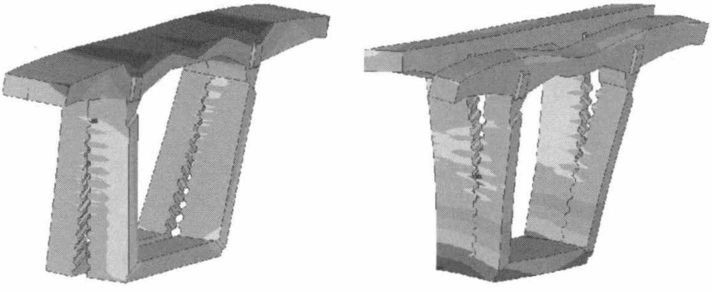

Fig. 3 Joint opening due to positive resp. negative bending moments

To develop a design concept for the joints tests with specimens having one or multiple shear keys (Fig. 4) are conducted to calibrate the finite element model. Parameter studies lead to a design model that differs from the existing concepts (eq. 1, Fig. 4). The shear capacity of a keyed dry joint $V_{d,j}$ is a combination of a frictional and a shear part. For the first one the total area of the joint A_{joint} is used and not only the smooth parts (A_{Sm}) like in AASHTO recommendations. The load bearing capacity of the keys depends on the concrete tensile resp. compressive strength and the area of the failure plane A_{key}.

for dry joints: $$V_{d,j} = \frac{1}{\gamma_F}\left(\mu \cdot \sigma_n \cdot A_{joint} + f \cdot f_{ck} \cdot A_{key}\right) \qquad (1)$$

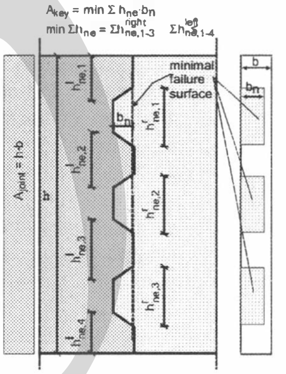

where:
- $\mu = 0{,}65$ coefficient of friction
- $\gamma_F = 2{,}0$ safety coefficient
- σ_n average compressive stress across the joint
- A_{joint} area of the compression zone
- f_{ck} characteristic concrete compressive strength
- b width of the web
- $f = 0{,}14$ factor for the indentation of the joint
- A_{key} min. area of the base of all keys in the failure plane
- h_{ne} height of keys, with $h_{ne} \leq 6b_n$
- b_n width of the keys

The failure plane A_{key} will have the least area of key breakage. A relatively high safety coefficient of $\gamma_F = 2{,}0$ should be used as the failure of the joint is brittle. For glued joints only the frictional part can be used.

Fig. 4 shows the load bearing capacity of a keyed joint according to various design models. The great differences between AASHTO and the German recommendations can be seen. The first model can not be used for high compressive stresses. Furthermore it seems to overestimate the load bearing capacity of a joint.

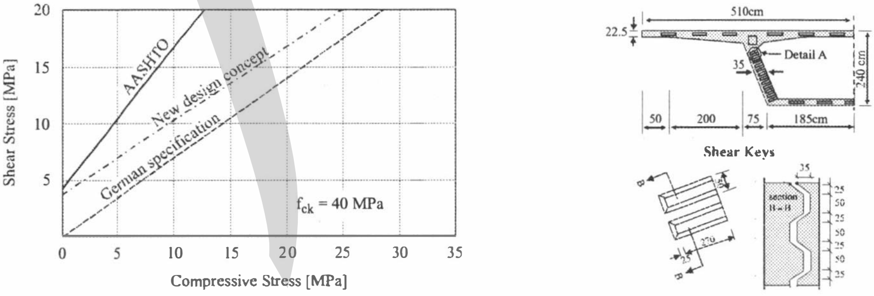

AASHTO [4]: $\tau = 4{,}17 + 1{,}06 \cdot \sigma_n$ DBV [3]: $\tau = 0{,}7 \cdot \sigma_n$ [MPa]

Fig. 4 Comparison between different design models (standard segment SES)

PLANNING AND DESIGN FOR FABRICATION IN THE SHOP OF PRECAST SEGMENTAL PC BOX GIRDER BRIDGE FOR THE KAMIKAZUE AND ANJO VIADUCTS ON THE NEW TOMEI EXPRESSWAY

Yuji Suzuki Hideaki Sakai Yukihiro Kutsuna
Chubu Branch, Japan Highway Public Corporation
JAPAN

Kenji Uehira
DPS Bridge Works Co., Ltd.
JAPAN

Keywords: precast segment, double-loop joint, pretensioned transverse girder, EM sensor, CCD camera

1 INTRODUCTION

The Kamikazue and Anjo viaducts are parts of the New Tomei Expressway, which is currently under construction. The Innovative feature of these viaducts is that two single box-girder segments are connected by means of RC slab, where lapped reinforcement in the form of double loop is used in the transverse direction. This forms a double-box girder cross-section, first of its kind in the world. The Kamikazue consists of two viaducts (17 span continuous) of 630m length while the Anjo has four viaducts (12 span continuous) of 450 m, both having an overall width of 16 m. The girder is prestressed in the longitudinal direction using epoxy coated external tendons. The slabs of the individual segments are prestressed by pretensioning method. The RC slab reinforced in the form of double loop at the connection, is cast-in-place, using fiber concrete and expansive admixtures, to prevent shrinkage cracks and spalling of concrete. Static and fatigue wheel load tests were carried out to investigate the mechanical behavior and fatigue durability of these kinds of slabs.

The construction site is surrounded by residential area, which has limited land for the precast yard. This was overcome by designing the overall cross-section to effective sub-sections that were precast in a factory and then transported to the site to make the monolithic section using the looped connection. The development of this new technology paved way to the construction of this structure, even with the weight limits on the national routes and restricted land in Japan, which would have been impossible with the conventional techniques.

This paper describes the structural characteristics of the connection consisting of lapped reinforcement in the form of double loops and method of prestressing. Furthermore, the use of EM Sensor for measuring the external tendon force to verify the coefficient of friction at deviators, the use of CCD cameras to control the dimensions and non-destructive technique to control the quality of the precast segments are also discussed.

2 FEATURES OF THE STRUCTURE

The major feature of these viaducts is that two separately cast precast box girders are connected in the transverse direction by means of cast-in-place slab, as shown in Fig. 1.

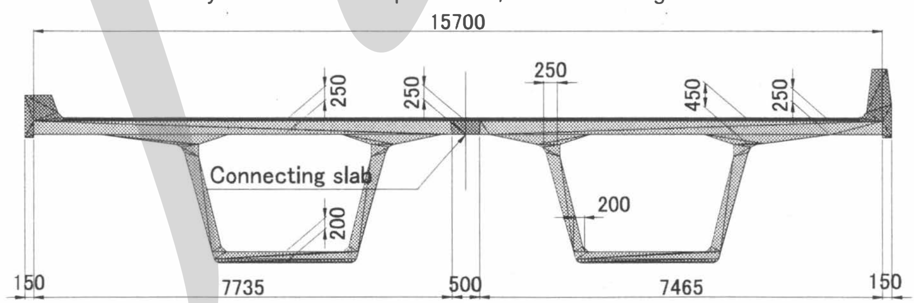

Fig.1 Cross-sectional diagram of the main girder

The construction of the main girder was carried out by span-by-span method using a supported type construction girder. The precast segments were cast in the factory and transported to the site for assembling. Double-loop joint is adopted at the cast-in-place connection part as shown in Fig. 2. The arrangement of rebars was in such a way, that a closed loop rebar (so-called center-loop rebar) was placed to overlap the two looped rebars (so-called side-loop rebar) that projected from the precast segments, as shown in figure. The center-loop rebar is of an annular shape, with a lap that is welded adopting enclosed welding method, considering the ease of construction.

The safety of this type of double-looped joint slab (RC slab) was verified by carrying out full-scale model tests simulating the actual slab, under flexural loading. It was found that the mechanical characteristics of the proposed joint were similar to that of the conventional joint. Moreover, since wheel loads directly affect this slab, full-scale tests were carried out on slabs cast for this purpose, which was subjected to an equivalent moving load with repeated loading. It was confirmed that the fatigue durability of the slab was sufficient.

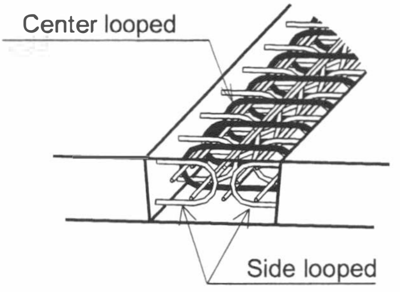

Fig. 2 Layout of double-loop

3 METHOD OF PRESTRESSING

This structure is of fully external prestressing with six numbers of 19S15.2 mm prestressing tendons arranged in each of the box section. Moreover, the intermediate deviation within the span has been established at two places where concentrated deviation system has been adopted. Epoxy-coated tendons were used for the external prestressing system adopted in this structure. At the deviator section, these tendons are placed inside polyethylene duct, which is arranged inside a steel deviator duct. It was necessary to verify the friction coefficient at the deviator, since its value has a great influence in the design. The friction coefficient was verified for this type of deviator in the full-scale model test. In verifying the friction coefficient, the tendon force on both sides of the deviators was measured and from the force difference, the friction coefficient was calculated. To measure the prestressing force of the 19S15.2 mm tendon as a whole, an Elasto-Magnetic (EM) sensor was used as shown in Photo 1, which also improved the accuracy of measurements. The EM sensor technology is a non-destructive method that makes the measurements easier, while it is possible to measure the residual stress present in the tendon, thus being a suitable method of monitoring of the tendon stress. From these measurements, the friction coefficient including a factor of safety for external tendon was set to 0.15 per radiant.

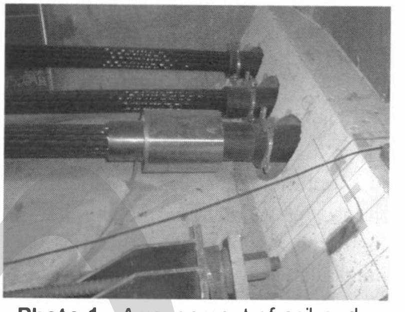

Photo 1 Arrangement of coil and layout of EM sensor

4 QUALITY CONTROL METHODS FOR PRECAST SEGMENTS

It is necessary to control the shape of segments very precisely as any errors would propagate further, especially in a short-line match cast technique, where the previously cast segment is used as part of the formwork. Due to the demand of higher precision for the control of the shape of segments, measurements were made using CCD cameras with three-dimensional automated measurements. It was possible to control the error within 1.5 mm (standard deviation) by using high-precision CCD cameras. Targets were placed on segments as shown in Fig. 3 and measurements were made from two CCD cameras located at established locations. Precisely measuring the cover using cover-meter controlled cover of the rebars. It was found that the cover of rebars was within plus or minus 1.0 to 2.0 mm of the allowable limits.

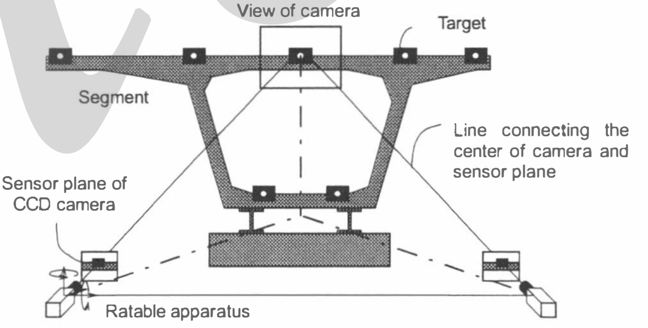

Fig. 3 Three dimensional measurement using CCD cameras

REFERENCES

1. Sakai, H. and Uesugi, T., "The Quality Control for Fabrication in the Shop of Precast Segmental PC Box Girder Bridge", *J. of Prestressed Concrete, Japan*, Vol.43, No.3, pp. 62-67, 2001. (*In Japanese*)

DESIGN OF NISHI HIRAO VIADUCT

Yosuke Yagi Shin Suzuki Noritaka Sugano Hirotaka Shiota Takumi Kinoshita

Fuji PS Nihonkogen Concrete Joint Venture
JAPAN

Keywords : precast segment, pretension system, all-external-tendon, span by span method, banana deformation, transport by road.

1. INTRODUCTION

The Nishi Hirao Viaduct is a 10-span continuous PC box girder bridge that will be built in a mountain-ringed region by the precast segment method. Various methods have been introduced for this bridge: the short line match cast method for manufacture of segments at an existing factory, the span by span method for installation of segments, the all-external-tendon method for pre-stress, and the pre-tension method for transverse tendon of slabs. Manufacturing segments at an existing PC factory and transporting them by road to the worksite can eliminate the need for a large segment manufacturing area near the worksite.

To make optimum use of the above features, restriction of segment weight, distribution of segments, and shape and arrangement of deviators have been taken into account in designing the Nishi Hirao Viaduct.

This paper gives an outline of the design of the Nishi Hirao Viaduct.

Fig. 1 Location of the Bridge

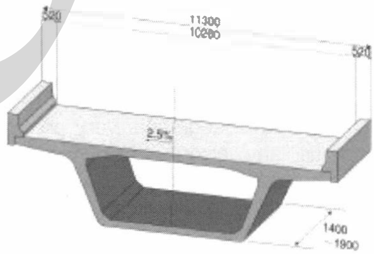

Fig. 2 Segment

2. STRUCTURE

Bridge type	Pre-stressed concrete highway bridge
Structure	10-span continuous PC box girder
Construction method	Precast segment method
Erection method	Span by span method
Bridge length	426.000 m
Girder length	425.600 m
Overall width	Single cross section: 22.800 m Partition cross section: 11.300 m
Effective width	10.850 m
Span	Up line 42.800+43.500+2@43.000+3@45.000+2@40.000+37.300 (m)
	Down line 37.300+40.000+6@45.000+40.000+37.300 (m)

3. DETAILED DESIGN

3.1 Segment Distribution

The segment size was determined based on restriction of transport on ordinary roads so that the weight of a single segment does not exceed 300 KN. The length of a single segment was set between 1.45 and 1.9 m, and distribution of segments for each span was decided.

3.2 All-External-Tendon

3.2.1 Anchoring Partition Wall and Deviators

As a result of the introduction of the all-external-tendon method, a large number of external cables (maximum 14 cables in the case of Nishi Hirao Viaduct) need to be anchored on a partition wall that also acts as a cross girder. With the Nishi Hirao Viaduct, to maintain safety of partition walls and deploy fixtures that convey pre-stress effectively, arrangements of fixtures proposed by ASBI (American Segmental Bridge Institute) were studied.(Fig.3,4)
FEM analysis was conducted to analyze local stress around tendons. The maximum local principal stress targeted at approximately 2.0 N/mm^2.

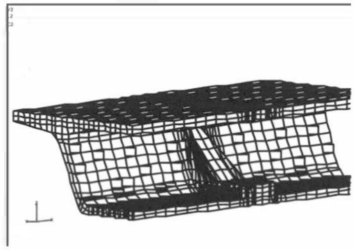

Fig. 3 Analysis Model (ASBI)

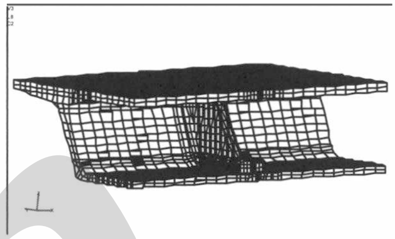

Fig. 4 Analysis Model (Conventional)

3.3 Pretension Traverse Tendon

For slab transverse tendon, prestress by the pretension method was introduced.
1S21.8 type steel (19-strand, 3-layered) was used, and lateral pre-stressing was performed on the surface. (Fig.5)

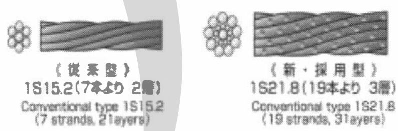

Fig. 5 Pre stressing steel strand

4. BANANA DEFORMATION

For calculation of banana deformation, the proposed formula that appeared in the PCI Journal Magazine was used, and measurement was conducted at the worksite.

5. CONSTRUCTION

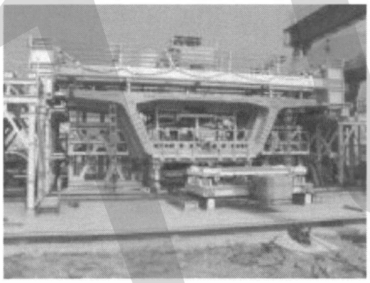

Fig. 6 Produce segment

Fig. 7 Under erection

REFERENCES:

[1] Moriyama, Tsuji, Takahashi and Yagi : Design of Nabeda Viaduct, Prestressed Concrete VOL11, No.2, P48 to 55, 1999

[2] Carin Roberts· John Breen and Michael Kreger : Temperature Induced Deformations in Match Cast-Segments, PCI JOURNAL July-August 1995 P62-71

[3] AMERICAN SEGMENTAL BRIDGE INSTITUTE : Recommended Practice for Design and Construction of Segmental Concrete Bridges April 2000

[4] AMERICAN SEGMENTAL BRIDGE INSTITUTE : Segmental Box Girder Standards

[5] Yagi, Ikeda, Goto, and Shiota : Design of Nishihirao viaduct , The 11th Symposium on Developments in Prestressed Concrete , P625 to 628

BRIDGE CONSTRUCTION BY INCREMENTAL LAUNCHING METHOD WITH HIGH STRENGTH CONCRETE AND EXTERNAL TENDONS

Masayoshi Moroda Agricultural Project Office of the Western Gunma Prefecture, Japan
Kenji Ayabe Gunma Prefectural Government, Japan
Naoki Arakawa Tomoki Kurita P.S. Corporation, Japan

Keywords: incremental launching method, high-strength concrete, external tendons

1 INTRODUCTION

This paper describes the incremental launching method adopted for the construction of a 180.9-m long four-span continuous prestressed concrete box girder bridge (Haruna Bridge No. 10), which is located 1 km upstream the Narusawa Lake in Gunma Prefecture and crosses a 45 m deep valley. In order to minimize the thickness of members and reduce loads transferred to substructures, high-strength concrete(design compressive strength: 60 N/mm^2) and external tendons was used for the main girder. The box girder segments were launched in one direction from abutment A 2 where all incremental launching jacks were installed. Since the web thickness was only 25 cm because of the use of external tendons, the stresses in the box girder during the incremental launching operation were monitored using strains measured by gauges placed on its surfaces, to ensure safety. Shoes, which were designed to distribute the reaction forces and move in the transverse direction as well during girder segment erection, were provided on the top of each pier.

2 PROJECT OUTLINE

The project outline is as follows:

- Project owner: Agricultural Project Office of the Western Gunma Prefecture
- Length: 180.9 m
- Span arrangement: 41.6m+ 48.0m+48.0m+ 41.60m
- Width : 10.0 m (carriageway: 6.5 m, sidewalk: 2.5 m)

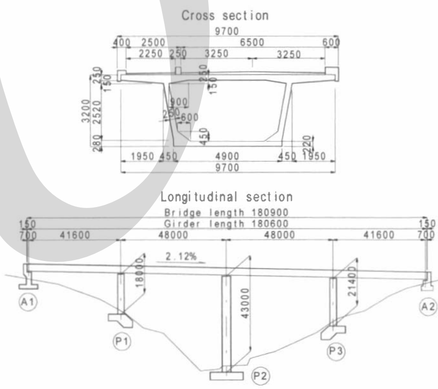

Fig.1 General View

3 CONCRETE PRODUCTION

Prior to the bridge construction, trial mixing was performed to check the following three items of high-strength concrete with a design strength of 60 N/mm2: (1) compressive strength, (2) fluidity, and (3) whether concrete of this type could be supplied to the construction site without problems. Based on the trial mixing results, the mix proportion was determined at the on-site batching plant considering (1) transportation time, (2) measures to control quality, and (3) admixtures to ensure a slump of 20 cm. For the mix design for hot weather, the admixture was changed to lengthen the setting time and prevent cold joints, and unit cement content was modified to minimize drying shrinkage cracks.

4 CONCRETE PLACEMENT

Table 1 Specification of truck-mounted concrete pump

Maximum pumping pressure	11.9 MPa
Maximum output	51 m3/h
Maximum boom length	17.5 m
Maximum boom height	20.7 m

The concrete volume for each segment, measuring about 12 m in length, varied from 70 to 110 m3. Truck-mounted concrete pumps with placing boom were used for concreting, considering the concrete volume for each segment and construction easiness. Since the necessary pressure for concrete conveyance was assumed to bebetween 4 and 10 MPa because of the high viscosity of the concrete, concrete pumps with a large pumping pressure were employed. The specification of the concrete pumps used in the project is shown in Table 1.

Prior to the commencement of the bridge construction, high-strength concrete was experimentally placed near the bridge site in order to check (1) changes in slump with time, (2) placeability, and (3) surface regularity after placement, and its specimens taking into consideration the construction conditions were prepared. As a result, it was found that the mix design used in the experimental placement would be applicable to the bridge construction.

Concrete for the webs with a very small thickness of 25 cm was supplied through tremies produced from 100 mm by 100 mm rectangular pipes, to minimize the free fall height and segregation and maintain a constant pouring rate.

The average pouring rate was 15 m3/hr for the bottom slab and webs, and 25 m3/hr for the top slab, and concrete placement for each segment (average volume: 80 m3) took about five hours on average.

Semi-transparent plates were used as form materials for the webs to monitor whether concrete was properly poured and compacted to form a uniform and void-free mass. To facilitate the compaction of the high-viscosity concrete, high-frequency vibrators with a 60 mm diameter rod were employed in combination with form vibrators.

5 INCREMENTAL LAUNCHING METHOD USING EXTERNAL TENDONS

The advantages of using external tendons in the incremental launching method are as follows: the external tendons for temporary use can be removed after girder completion; thickness of webs can be minimized; and maintenance of the tendons are easy. The weights of main tendons used in the project are shown in Table 2.

Table 2 Total weight of main tendons

Classification	Permanent tendon			Temporary tendon
	Internal tendon		External tendon	External tendon
Tendon diameter	19S11.1	12S12.7	19S15.2	19S15.2
Weight (kg)	8482	10511	15983	22269

The girder was constructed by extending segments in one direction using the segment launcher installed on abutment A 2. Sliding shoes were provided at the top of each pier.

6 REACTION FORCE DISTRIBUTING SHOES

The rubber bearings were designed to move in the transverse direction as well during the incremental launching of segments (Fig. 2).

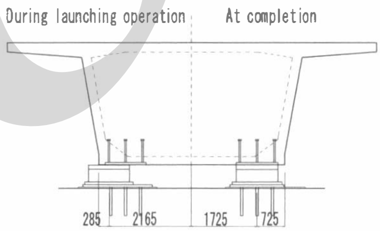

Fig.2 Reaction force distributing shoes

7 MEASUREMENT DURING INCREMENTAL LAUNCHING

Since the thickness of the webs consisting of high-strength concrete (design compressive strength: 60 N/mm2) and external tendons was only 25 cm, the stresses working in the box girder during the incremental launching were monitored in real time using tri-axial gauges placed on the webs and uni-axial gauges placed on the upper and bottom surfaces of the girder. Fig. 3 shows the stresses (due to the dead load of the girder) at the bottom surface of segments Nos. 8 to 15, with tensile stresses as positive. These eight segments formed the spans on the both sides of pier P1. As shown in the figure, the curves for bending stresses obtained from calculation and measurement are almost the same. The changes in stresses calculated using measurement data are gentle. This indicates that the incremental launching for the box girder was successfully completed without causing excessive stresses.

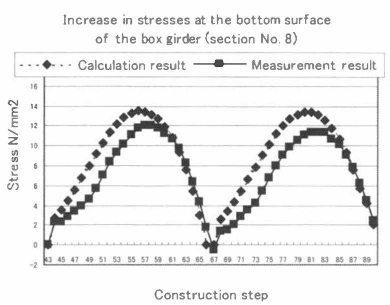

Fig. 3 Comparison of stresses obtained from calculation and measurement

DESIGN OF THE 10TH HARUNA BRIDGE

- a prestressed concrete box girder launched with temporary external tendons -

Kenji TAKEMOTO and Tadao WAKASA
New Structural Engineering, Ltd.
Japan

Masayuki MORODA
Gunma Prefecture
Japan

Keywords: launching erection method, concordant tendons, temporary tendons, high strength concrete

1 INTRODUCTION

The 10th HARUNA Bridge is a four spans bridge (41.6m – 48.0m – 48.0m – 41.6m) which crosses the deep valley of the Narusawa swamp 1km upstream the Narusawa lake in Misato (Gunma prefecture).

With piers of height 45m, a continuous concrete box girder placed using the incremental launching method was chosen between many other steel or concrete altematives and an additional temporary extemal prestressing system was designed for the launching stage instead of the intemal ones usually designed in Japan.

The additional temporary external tendons were placed before launching in such a way to counteract the permanent ones which were placed before launching and so allowed the box girder sections to support the altemation of positive and negative bending moment during the launching stage.

Added to a compressive strength of concrete of 60N/mm^2, the use of extemal prestressing for this temporary system allowed a reduction of 20% of the concrete cress-section area, a reduction of 50% of the tendons and so reduce the cost of bridge.

This report describes the design and method of erection of this 4 spans continuous PC bridge.

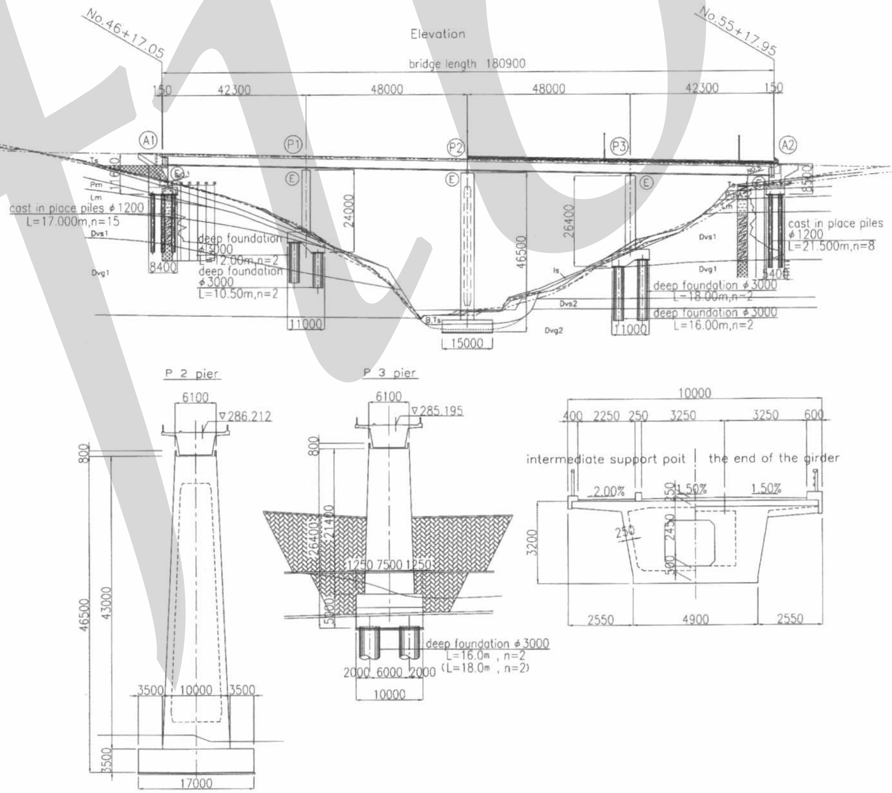

Fig. 1 General View of the 10th HARUNA Bridge

2 CHARACTERISTICS OF THE LAUNCHING ERECTION METHOD USING CONCORDANT EXTERNAL TENDONS

The conventional launching erection method was adopted at locations where ground constraints, as crossing railways or roads, did not allow the use of scaffoldings. One example of the launching erection method using concordant external tendon is the Iwanamezawa bridge which was constructed among Waga - Yuda of the JH Akita express highway in Japan[1]. But the launching erection method is basically used in France, U.S.A., etc. with use of concordant external tendons.

This erection method becomes very economic by use of concordant external tendons and high strength concrete. The main characteristics of the launching erection method using external tendons are given in the following paragraphs.

2. 1 Characteristics of the Design

① **Weight of the main girder:** The use of a high strength concrete allows a reduction of the girder height to L/15 - L/18. Arrangement of tendons becomes a more effective one by adoption of concordant tendons removed after construction. The web thickness can be so reduced and the area of the cross-section is smaller. The weight of the girder is so smaller and a smaller prestressing force obtains the same prestressing stress.

② **Decrease of the prestressing steel and the anchor:** The friction losses in prestressing occur only in the deviators and anchors and they are smaller than for usual internal tendons. With the external concordant tendons arrangement, the total quantity of prestressing steel it decreases and the construction is more economic.

2. 2 Characteristics of the Construction

① **Laborsaving:** The girder is produced in a yard provided behind the abutment and produced girder blocks are launched gradually. So laborsaving can be obtained by doing work repeatedly and with a small number of persons, without using scaffoldings, etc..

② **Speeder construction:** As all the production works are carried out in a yard with shelter, the work processes are not influenced by the weather condition and are done speedily. Also, doing repeated tasks carries out the girder and the work cycle becomes shorter: 10 to 14 days.

③ **High quality of the production:** The workability of the concrete can be improved and a high quality can be obtained by placing the PC tendons outside the webs.

④ **Environmental improvement:** As many works are done on the yard, an environmental improvement of the works can be obtained.

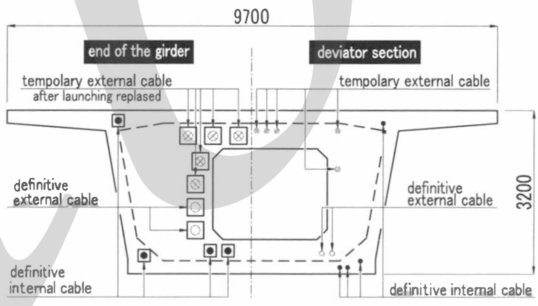

Fig. 2 Arrangement of Tendons in the Cross-section

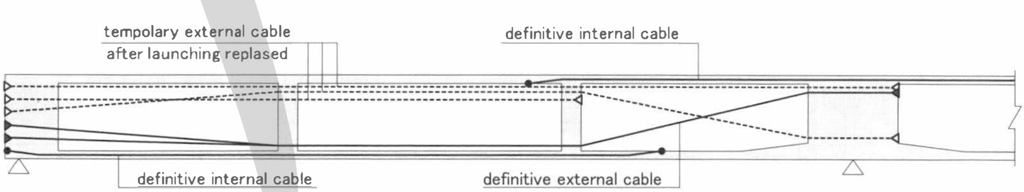

Fig. 3 Arrangement of Tendons in the Longitudinal Direction

REFERENCES

[1] Sakuma, S et al., Design of Launched Prestressed Concrete Box Girder with External and Inner Cables, Bridge and Foundation Engineering, Vol. 29, No. 5, pp. 26-35, 1995

[2] Takemoto, K et al., Design of 10th Haruna Nanroku Bridge, Bridge and Foundation Engineering, Vol. 35, No. 4, pp.9-14, 2001

STRENGTHENING OF CONTINUOUS BEAMS USING VARIOUS EXTERNAL TENDON PROFILES

TAN Kiang Hwee Robert A TJANDRA
Department of Civil Engineering
National University of Singapore, SINGAPORE

Keywords: strengthening, continuous beams, external prestressing.

1 INTRODUCTION

In recent years, there has been an increasing demand for the structural strengthening of reinforced concrete bridges, fueled not only by the global phenomena of heavier traffic loads but also by the progressive structural aging and corrosion of reinforcement in existing bridge structures. A popular and efficient strengthening method is external prestressing, whereby tendons are installed on the outside of concrete member and the prestressing forces are transferred to the concrete via anchorages and deviators.

External prestressing of beams and girders has several favorable aspects such as installation speed, and it adds little weight to the structure, with the possibility of monitoring, replacing and re-tensioning the tendons in the future.

This research is conducted to investigate experimentally and analytically the flexural behavior of continuous span beams strengthened using different external tendon profiles (straight, draped and parabolic), tendon materials (steel and carbon fiber-reinforced polymer/CFRP), and subjected to different types of loading (symmetrical and unsymmetrical third-point loading). The ultimate loads, failure modes, internal steel and external tendon stress development, deflections and crack widths were compared among the beams and with theoretical predictions.

2 TEST PROGRAMME

A total of seven two-span continuous T-beams, each measuring six meters in total length, 300 mm in overall depth and designated C0, C1, C1P, C2, C2L, C3 and C3F, were fabricated and tested. The beams had the same cross-section dimensions and internal reinforcement but differed in external tendon type, profile and type of loading (Table 1).

Table 1 Parameters of test beams

Beam	Tendon profile	Tendon type	Loading type
C0	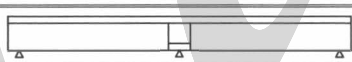	No tendons	Symmetrical
C1		Steel	Symmetrical
C1P	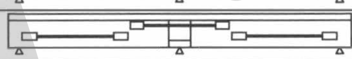	Steel	Symmetrical
C2	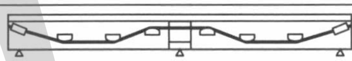	Steel	Symmetrical
C2L	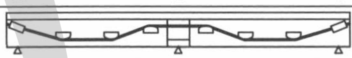	Steel	Unsymmetrical*
C3	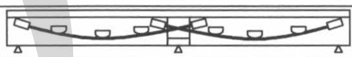	Steel	Symmetrical
C3F	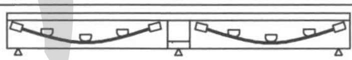	CFRP (left span), steel (right span)	Symmetrical

*Total load on the left span was thrice that on the right span

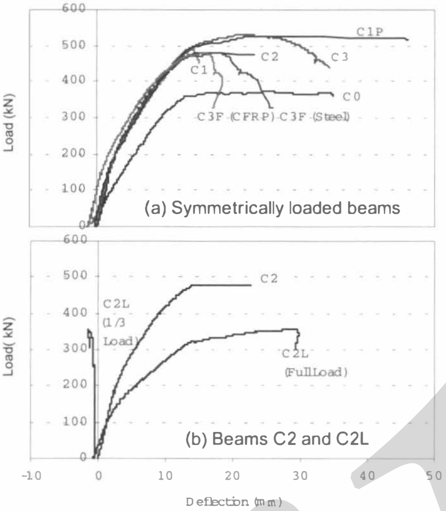

Figure 1 Load-deflection response

3 TEST RESULTS

The load-deflection response of beams under symmetrical and unsymmetrical loading is shown in Figure 1.

All strengthened beams under symmetrical loading exhibited very similar response before the formation of "plastic" hinges, which were assumed to develop when the internal steel yielded.

Test results of beams C1 and C1P indicated that anchoring positive moment tendons within spans as adopted in beam C1P led to higher ultimate load and much ductile response before failure. Beams C2 and C3 showed better failure characteristics compared to C1. Comparing beams C3 and C3F, both of which were strengthened using parabolic tendon profile, it can be seen that anchoring the tendons beyond the interior support is beneficial, as the overlapped tendons at the interior support provide compression forces that not only increase the ultimate load but also result in better failure characteristics, as vindicated by a more ductile response. Beam C3F, due to the absence of tendons over the negative moment region, suffered from shear distress at the ultimate, after the formation of "plastic" hinges in both spans. All the strengthened beams subjected to symmetrical loading showed higher ultimate load and stiffer response compared to the control beam. The strength gain was more than 30%.

Beam C2L, subjected to unsymmetrical loading, exhibited reduced stiffness for the span subjected to the full load when compared to beam C2 whereas the span subjected to one third of the full load experienced minimal deflection. At ultimate, unsymmetrical loading on beam C2L resulted in larger deformation in the fully loaded span, lower ultimate strength but comparable ductility as C2.

Table 2 Predicted and observed ultimate loads

Beam	Ultimate load, P_u (kN)		Test / Predicted
	Predicted	Test	
C0	355	368	1.03
C1	505	490	0.97
C1P	511	526	1.03
C2	540	478	0.89
C2L	363	357	0.98
C3	506	531	1.05
C3F	495	479	0.97

4 THEORETICAL PREDICTIONS

The analysis for the behavior of continuous beams strengthened using external tendons is member-dependent due to the unbonded nature of the tendons. As proposed by Naaman and Alkhairi [1], a section analysis could be used to obtain the response of such beams, provided that the stress increase in the external tendons due to the applied load is multiplied by a strain reduction factor.

In this study, the strain reduction factors for continuous beams strengthened using various external tendon profiles have been derived for different stages of loading [2]. The ultimate load was calculated by assuming three hinges to have formed at the interior support as well as at the sections of maximum positive moment, thus forming a collapse mechanism.

Table 2 summarizes the observed and predicted ultimate load of the beams. In general, a good agreement was obtained.

REFERENCES

[1] Naaman, A.E. and Alkhairi, F.M., 'Stress at Ultimate in Unbonded Post-Tensioning Tendons: Part 2 – Proposed Methodology', ACI Structural Journal, Vol. 88, No. 6, Nov-Dec, 1991, pp. 641-651.

[2] Tan, K.H. and Tjandra, R.A., 'Strengthening of RC Continuous Beams by External Prestressing – Part 1 : Analysis for Piece-wise Linear Flexural Response', paper submitted for review, ASCE, Journal of Structural Engineering.

NON-LINEAR BEHAVIOR OF THE IBI RIVER BRIDGE UNDER ULTIMATE LOADS

Yukihiro Kutsuna
Japan Highway Public Corporation
JAPAN

Akio Kasuga, Akira Morohashi
Sumitomo Construction Co., Ltd.
JAPAN

Keywords： composite extradosed bridge, behavior under ultimate loads

1. INTRODUTION

The Ibi River Bridge[1)] is the world's first composite extradosed bridge, constructed to take the New Meishin Expressway across the Ibi River in Mie Prefecture. This bridge has six spans and a 271.5m maximum span. Two-thirds of the concrete girder is supported by extradosed cables. In fatigue design for the serviceability limit state, 60% of tensile strength is used as the stress limit of the extradosed cables. However, the behavior of girders and extradosed cable forces under ultimate loads depends on the type of structure. In order to simulate the behavior of the whole structure in the ultimate limit state, non-linear analysis, including analysis of the extradosed and external cables, is performed. This analysis incorporates consideration of material and geometrical non-linearity. The results show that all extradosed cables reach yield stress, and that the stress increase for external cables is approximately 100 N/mm^2 under ultimate loads. This paper offers very important design data for the extradosed bridges.[2)]

Fig.1 shows a general view of the Ibi River bridge.

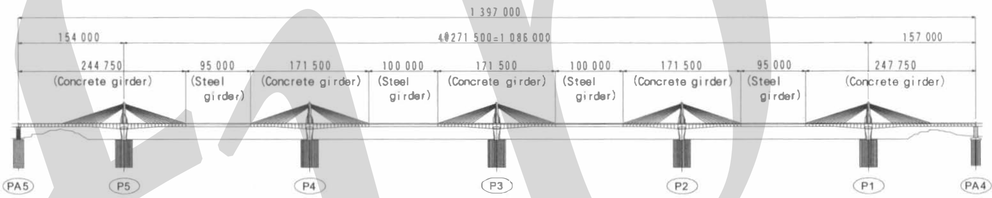

Fig.1 General view

2. STUDY OF ULTIMATE LIMIT STATE USING NON-LINER ANALYSIS

2.1 Overview of analysis

The study focused on the support section (P2) and a side span section (P1 – PA4). A non-linear analysis was conducted for a model of the overall system and the behavior of the main girder, internal and external cables and extradosed cables at the ultimate limit state was verified. The analysis method and conditions were as follows.

(1) Sections studied： P2 support section (on P3 side) and P1 – PA4 side span section

(2) Target load: Dead load(D) + Live load(L) (for the case of the combination of 1.7×(D + L) that would be critical)

(3) Loading method: (D + L) increased gradually until concrete reached ultimate strain (ε cu = 2500μ)

(4) Prestressing tendons layout: Shown in Fig.2

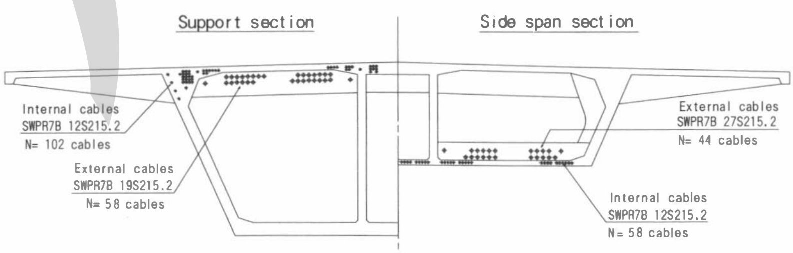

Fig.2 Prestressing tendons layout

2.2 Results of Analysis

Results at the P2 support section are as follows.

(1) Concrete stress at the support section

The concrete stress at the lower extreme fiber of the support section increased together with load, and the ultimate strain of 2500μ was reached at (D + L) x 1.8 – 1.9 (Fig.3). At the upper extreme fiber of the support section, the compression stress decreased as the load increased, and the initial compression was canceled out at the (D + L) x 1.5 step. After this point, the increase in tensile force generated at the upper extreme fiber of the main girder was borne by the internal and external cables.

(2) External cable stress at the support section

For the external cables of the P2 support section, there was almost no increase in tension up to (D + L) x 1.5. After (D + L) x 1.5, the external cable tension increased gradually. Ultimately, just before the ultimate state for the entire structure, at (D + L) x 1.7, the increase in external cable tension became approximately 100 N/mm^2. (Fig.4)

(3) Extradosed cable tension

For the P3 side extradosed cables for the P2 pylon, the extradosed cable tension increased as the load was increased. The speed of the increase was greatest for the uppermost extradosed cable, and the yield point (0.79 fpu) was reached at (D + L) x 1.5. For the lowermost extradosed cable, for which the speed of the increase was the lowest, the speed of the increase became greater after (D + L) x 1.5 at which the uppermost extradosed cable yielded. At (D + L) x 1.7, all extradosed cables down to the lowermost extradosed cable exceeded the yield point. (Fig.5)

In the extradosed bridge, a limit of 0.6 fpu was provided for the tension of the extradosed cables that constitute the resisting tendons for the outermost extreme when the bridge is in service, so it is thought that they will reach the yield point at the ultimate state. This is because the extradosed bridge effectively utilizes the capabilities of the extradosed cables not only when the bridge is in service but at the ultimate state as well.

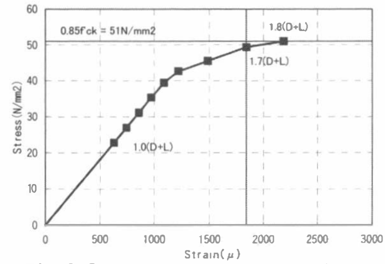

Fig.3 Concrete stress at the lower extreme fiber of the support section

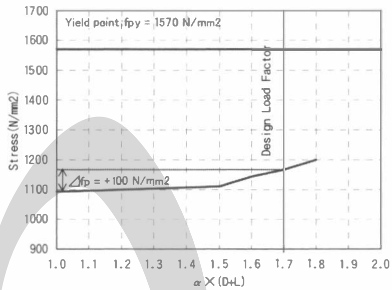

Fig.4 External cable stress at the support section

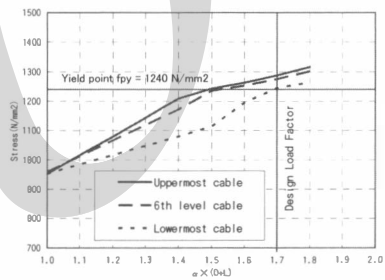

Fig.5 Extradosed cable stress at the P2 pylon

3. CONCLUSION

In the Ibi River Bridge, which is one of the world's first composite extradosed bridges, a non-linear analysis at the ultimate limit state was performed, and the behavior of main girders, internal and external cables and extradosed cables was verified and safety was confirmed. As a result of the analysis, it was determined that the extradosed cable tension reaches the yield point at the ultimate state, and so the configuration of the extradosed bridge was such that the capabilities of the extradosed cables could be effectively used not only when the bridge was in service but at the ultimate state as well.

REFERENCES

1) Minoru Hirano; Hiroyuki Ikeda; Akio Ksuga; Hideki Komatsu: "Composite Extradosed Bridge", Structural Concrete The Bridge Between People, fib Symposium 1999, Prague

2) Hiroyuki Ikeda; Haruto Maeda; Akira Morohashi; Akio Oooka: "Non-linear Behavior of the Ibi River Bridge under Ultimate Limit State", Proceedings of the 9th Symposium on Developments in prestressed concrete, The Japan Prestressed Concrete Engineering Association, October 1999

DESIGN AND REPORT OF FULL SCALE MODEL TEST ON CONCRETE ANCHORAGE BLOCK OF EXTERNAL TENDONS IN SETOGAWA BRIDGE

Mitsuhide Yoshida, Joint Venture of fuji p.s. Co., Ltd Abe Kogyosho Co., Ltd
Tadashi Kuroiwa, Japan Highway Public corporation
Dai Wakabayashi, Japan Highway Public corporation
Hiroshi Fukaya, Joint Venture of fuji p.s. Co., Ltd Abe Kogyosho Co., Ltd
Noritaka Sugano, Joint Venture of fuji p.s. Co., Ltd Abe Kogyosho Co., Ltd

Keywords : external tendon, local stress for concrete anchorage

1 INTRODUCTION

This report deals with loading tests conducted using a full scale model in connection with the construction of the Setogawa Bridge on the Second Tomei Expressway. The Setogawa Bridge, which is planned to be built at Fujieda City, Shizuoka Prefecture Japan, is a prestressed concrete continuous box girder bridge incorporating the all-external tendon design and consisting of 11 spans northward and 7 spans southward.

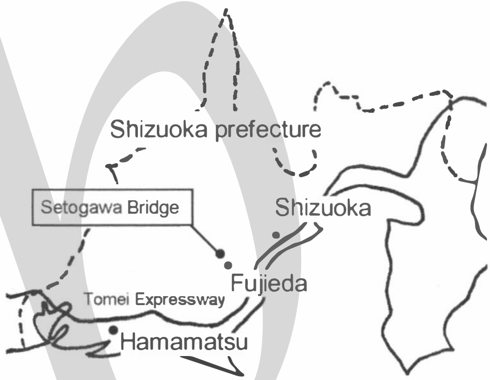

Fig. 1 Location of Setogawa Bridge

The bridge was designed to be a single-chamber box girder structure with a main girder width of 17.14 m with the aim of reducing the weight of the main girder and the shape of the substructure. The adoption of the single-chamber box girder design resulted in a one-side floor slab width of approximately 4.0 m. Consequently, the underside of the overhanging floor slab system is ribbed to balance the moments at the slab system and those at the intermediate floor slab system. However, bending stresses are produced at the ribs in the underside of the floor slab by dead and live loads and has an influence on the web. Therefore, the main girder needs to be reinforced. The Setogawa Bridge was designed for construction by cantilever erection and thus an anchorage block is needed to anchor external tendons to the main girder webs.

Photo 1 Main girder shape of Setogawa Bridge

The main girder webs would have a complex stress distribution with bending stresses acting on the webs through the ribs and prestress introduced into the external tendons. Therefore, loading tests were conducted on a full scale model of the box girder bridge to verify the

adequacy of the bridge design and safety of the bridge structure through comparison between the loading test results and those of FEM analysis.
Fig. 1 gives the location of the Setogawa Bridge and Photo 1 shows the main girder shape.

2 METHODS OF LOADING TEST ON FULL SCALE MODEL OF BRIDGE

2.1 Purpose of Test

(1) Stresses generated at the anchorage block for external tendons and at the main girder webs were compared with FEM analysis results to verify the safety of the bridge structure against load transmitted through prestress in the large capacity external tendons (19S15.2B) and through the ribs. Photo 2 shows the Full Scale Model of Bridge .

Photo 2 Full Scale Model of Bridge

(2) Verify the appropriateness of the bridge design.
(a) Prevent cracking in key structural members
(b) Prevent harmful cracking at the anchorage block

3 SUMMARY

3.1 Measurement of Stresses during Prestressing

(1) For the stress distribution in the anchorage block, though it showed some variations, the values obtained from the FEM analysis were considered to be in substantial agreement with the measurement values. The measured value of stress at the target positions were lower than those derived from the FEM analysis, indicating no problem with structural safety of the anchorage block.

(2) The cracks produced in the side of the anchorage during the prestressing of Block No. 1 were superficial and microscopic and considered not to be of such harmful nature as to damage the load carrying capacity of the anchorage structure. No major change was measured in the reinforcing bar stress 20 days after the prestressing of the anchorage block. The amount of reinforcing bars arranged was considered to be adequate.

3.2 Loading tests

(1) In the area where there was a sudden change in the cross section, the stress values measured were smaller than those obtained from the FEM analysis, indicating the structural safety of the anchorage block.

(2) Loading tests were conducted on a full-scale model of the bridge structure with external tendons anchored. However, any growth of the cracks produced during the prestressing of the external tendons was not observed. Nor was a sharp stress gain discernible in the reinforcing bars.

REFERENCE

[1] Proceedings of The 10th Symposium on Developments in Prestressed Concrete,2000,pp69-74

DESIGN AND CONSTRUCTION OF THE NARUSEGAWA RIVER FIN-BACK BRIDGE

Hideyuki KOBAYASHI
East Japan Railway Company, JAPAN

Yoshio TAKAKI
East Japan Railway Company, JAPAN

Hideto KOBAYASHI
Simizu Corporation, JAPAN

Keywords: Fin-back girder; cantilever erection system; seismic design; aesthetic design; camber

1. INTRODUCTION

The Narusegawa River and the Yoshidagawa River flow across Miyagi Prefecture (**Fig.1**). The old Narusegawa and Yoshidagawa River railway bridges of the Senseki-Line were built in 1928. These rivers were sometimes flooded therefore safe-river-management and the reconstructions of these bridges were planned. The new bridge which crosses both rivers is called the Narusegawa River Bridge. PPC Fin-back girder which consists of six continuous spans was adopted as the structure of the new bridge. It is the first PPC Fin-back railway bridge in the world (**Fig.2**).

This paper, first of all, describes the selection of bridge type, design features of Fin-back girder, and especially the seismic design and aesthetic design. As for the execution, this paper describes the execution of superstructure by P&Z cantilever erection system, and management of camber under the specific conditions of railway construction.

Fig.1 The Site of the Narusegawa River Bridge

2. SELECTION OF BRIDGE TYPE

There are several conditions to decide the bridge type; geographical condition, planned river condition, crossing conditions of roads, and gradient condition of the railroad. But these restrictions are not strict enough to adopt a through girder, so a box girder whose webs protrude over the bridge deck to make up for the lacking strength is adopted. This type of bridge is called "Fin-back girder", which has advantages in construction period, efficiency and aesthetic design.

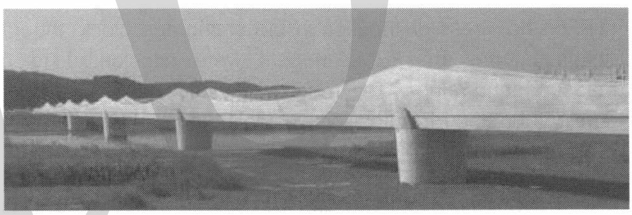

Fig.2 View of the Narusegawa River Bridge

3. DESIGN FEATURES

The distinctive features of this PC Fin-back Bridge are as follows. (1)By the protrusions of girder to the upper level, just like the "Fin-back", the structure of this bridge is against moment and shearing force. (2)Though prestressing tendons are placed inside girders like an ordinary girder bridge, this structure enables prestressing tendons to be more biased against the bridge axis than an ordinary girder structure. Furthermore, the height of the girder just on the piers can be reduced. (3)The structure of the PC Fin-back Bridge has an advantage in the limitation of girder height.

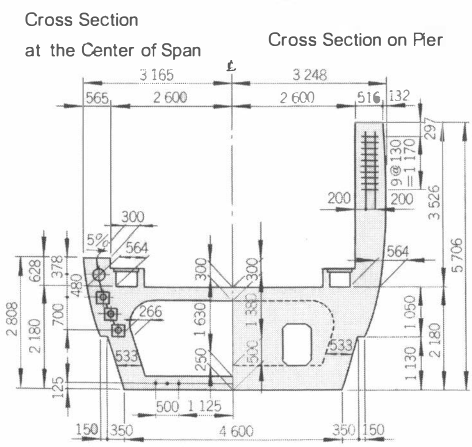

Fig.3 Cross-section of the Fin-back Bridge

Cross sections of this Fin-back bridge are shown in **Fig.3**. The Narusegawa River Bridge consists of a six-span continuous girder, the length of this bridge is 488.92 meters, and the longest span is 85 meters in length. This girder is designed as a PPC structure in the main direction, and as a RC structure in the cross direction. This bridge was executed by the P&Z cantilever erection system, and was analyzed under the consideration of temporary load and condition of bearing shoe in accordance with structural mode at each step of the execution.

In the seismic design, this bridge is designed against influences in the case that an earthquake like The Hanshin-Awaji Great Earthquake in Japan (1990) happens near this bridge. Design ductility factor is assumed as 10, this bridge is designed to endure about 1500gal of acceleration of elastic response due to earthquake.

In the aesthetic design, the total design concept of this bridge is the harmony with the landscape. The bridge is designed with a 15 cm gap on its outside for shadow contrast effect. This shadow contrast effect emphasizes the undulate shape of the Fin-back shape and to give sharpness to the whole image of this bridge. And the outside of the Fin-back girder is rounded in order not to give pressed impression and to harmony with the countryside landscape (**Fig.2**).

4. EXECUTION FEATURES

The P&Z cantilever Erection System was adopted as the execution method of the superstructure (**Fig.4**). This method doesn't require any ground work, so it is especially effective for multi-span continuous bridges, bridges with high piers, and bridges built over oceans, rivers and valleys.

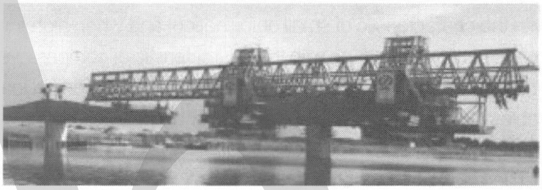

Fig.4 Execution by P&Z cantilever Erection System

On the Narusegawa River Bridge, temporary piers and all staging supports could not be set up. Therefore, this method was adopted without using all staging supports except the segments of girder on the pier, and the superstructure could be executed throughout the year.

The direct fastened track structure, which was invented by East Japan Railway Company, is adopted as a track structure of the Narusegawa River Bridge. Since this track structure requires accuracy in the formation level, the girder was required to minimize the margin of error on execution. Creep and dry shrinkage of concrete were considered with respect to the camber of girder, and the slack of the erection truss by the weight of concrete and the amount of stretch of the hanging steel bars were also considered.

The results of the planned value and gauged value on segments on the front side of pier 5P showed that the girder leaned more against the front side than we had expected. To solve this problem, it was necessary that the temporary loads on the erection truss to the basis are the same on each basis during execution of concrete work. So, the way that steel bars support a lower slab form was changed, from the way that they are jointed to the lower slab of the already executed segment to the way that they are jointed to the erection truss directly. The whole management and gauged values of camber are shown in **Fig.5**. At the side spans of the girder near abutment 2A, some gauged values exceed upper management values. Planned values are calculated on the assumption that the bearing shoes on the piers are pin structures, but the rotation of the girder is restricted by elasticity of rubber bearing shoes. Therefore, the amount of slack is less than we had expected. So planned values were revised with calculation of the modulus of elasticity of rubber bearing shoes.

5. CONCLUSION

In this paper, the outline of design and construction on the Narusegawa River bridge is reported. PPC Fin-back girder was adopted as the structure of railway bridge for the first time in the world. It was designed to endure a big earthquake considering the geographical features of Japan and to harmony with the countryside landscape. This bridge was completed successfully in about two years under the specific conditions of the railway. We hope this report will be of some use in the design and the construction of similar bridges.

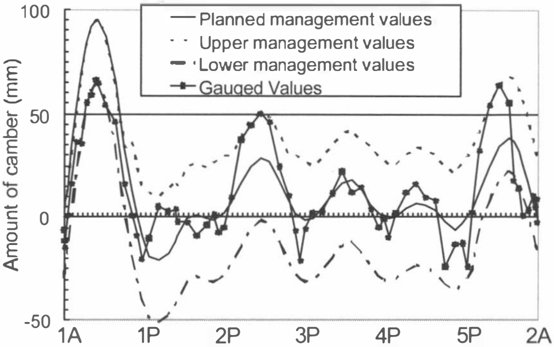

Fig.5 Management and Gauged Values of Camber

STRUCTURAL AND ECONOMICAL CHARACTERISTICS OF EXTRADOSED BRIDGE WITH MULTIPLE SPAN AND HIGH TOWER

Hiromichi Matsushita
Faculty of Engineering
Kyushu University
JAPAN

Hideaki Kawasaki
National Institute for Land
and Infrastructure Management
JAPAN

Ryoichi Shiota
Design Section 2
Japan Bridge & Structure Institute,
Inc.,JAPAN

Keywords:PC extradosed bridge, PC cable-stayed bridge, PC extradosed bridge with multiple span & high tower

SUMMARY

The purpose of this report is to develop further the studies [1], [2] for 2 spans high tower type extradosed bridge with the characteristic of small deformation, and when high tower type extradosed bridge is applied to 3 (or more) spans continuous bridge with the characteristic of comparatively large deformation, this paper proposes the most optimal design method of extradosed bridge, using vertical load ratio of stay cable β (β : vertical loads of stay cables / total vertical loads of main girder and stay cables) as an index, by examining structural and economical characteristics of members of extradosed bridge.

The analytical model of the examination is the 3 spans continuous bridge with maximum 205m central span length for PC superstructure as shown in Figure 1. The case of examination is shown in Table 1, including 7 types of bridges such as Girder Bridge, ordinary type extradosed bridge, and high tower type extradosed bridge with 12 cases of single suspension at center and double suspension.

As the result of the study, it is found that fluctuating stress of stay cable Δf_p (Δf_p: maximum fluctuating stress of stay cable caused by distribution traffic loads) is in proportional relation with vertical load ratio of stay cable β, as shown in Figure 2. Based on Figure 2, the costs of these structures were estimated by using the allowable stress of cable f_{pa} and type of stay cable referring to "The Draft of the Design and Construction Standard of PC Cable-Stayed Bridge and Extradosed Bridge" [3].

As a result, it is found that any extradosed bridge with single suspension at center is more economical than that with double suspension because of large occupation of tower out of total concrete volume of superstructure.

Even though high tower type extradosed bridge (case2') has best economical feasibility (construction cost ratio "C" = 0.88 for girder bridge (=1.0)), but difficult workability during construction because of varying girder depth, it was analytically confirmed that high tower type extradosed bridge (case4'-2) has best structural characteristics, second economical feasibility (C = 0.90), and easy workability because of constant girder depth except for the column capital part varying depth.

Consequently, there are 2 answers to the most optimal design method of extradosed bridge for reasons of similar construction cost ratio c of each case.

As the most optimal design method of extradosed bridge under the design condition such as deck arrangement, bridge length (span), loading etc., it is proposed to determine the tower height, main girder stiffness, and stay cable arrangement, to be suitable vertical load ratio of stay cable β, considering with fluctuating stress of stay cable Δf_p and the allowable stress of stay cable f_{pa} between 0.4 and 0.6 f_{pu} prescribed in Japan (f_{pu}: characteristic strength of prestressing tendon) consulting to the reference [3], as shown in Figure 2.

REFERENCES

[1] Hideaki Kawasaki and Akio Yamauchi: New design consideration construction technique in Matakina Bridge, Prestressed Concrete VOL.42 NO.3 2000

[2] Hideaki Kawasaki and Hiromichi Matsushita: Structural character of two spanned extradosed bridge with high tower, Civil Engineering Association Thesis Collection, No.669 / V- 50, pp. 233-242, Feb. 2001

[3] "The Draft of the Design and Construction Standard of PC Cable-Stayed Bridge and Extradosed Bridge", Prestressed Concrete Technological Society, Nov. 2000

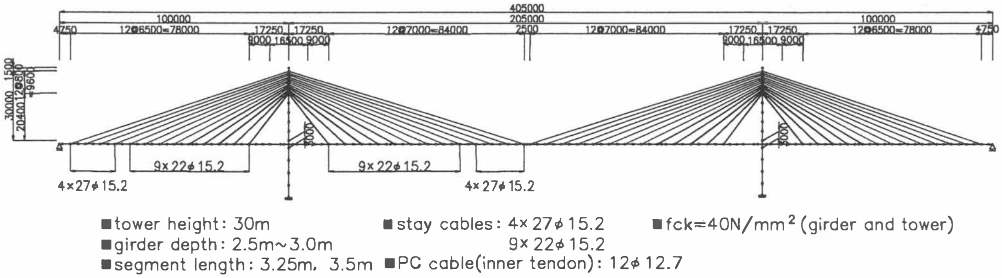

Fig.1 Analysis model of the examination (in case4')

Table 1 Case of analytical examination

Structure type	Number of suspension	Tower height Ht(m)	Girder depth H(m)	Stay cable arrangement: Total number	Stay cable arrangement: Details	Remarks	Varying girder depth	Constant girder depth ※3	Case No.
Girder bridge	—	—	5.0～12.0	—		—	○	—	case0
Extra-dosed bridge	Double suspension	20.5※1	5.0～7.5	11	11×19φ 15.2	Ordinary type	○	—	case1
		30※2	3.0～5.0	12	6×15φ 15.2 6×12φ 15.2	High tower type	○	—	case2
			3.0～3.5	13	6×15φ 15.2 6×12φ 15.2	High tower type	—	○	case3
			2.5～3.0	13	7×15φ 15.2 6×12φ 15.2	High tower type	—	○	case4
				25	25×7φ 15.2	High tower type	—	○	case5
			2.0～3.0	13	7×15φ 15.2 6×12φ 15.2	High tower type	—	○	case6
	Single suspension at center	20.5※1	5.0～7.5	11	5×37φ 15.2 6×37φ 15.2	Ordinary type	○	—	case1'
		30※2	3.0～5.0	12	4×27φ 15.2 8×19φ 15.2	High tower type	○	—	case2'
			3.0～3.5	13	4×27φ 15.2 9×19φ 15.2	High tower type	—	○	case3'
			2.5～3.0	13	4×27φ 15.2 9×22φ 15.2	High tower type	—	○	case4'
				25	25×15φ 15.2	High tower type	—	○	case5'

※1 Tower height of the ordinary type is assumed to be Ht/L=1/10(L=205m).

※2 Tower height of the high tower type is assumed to be maximum height (=30m) of which the rifting cage of maintenance car can be reached.

※3 It is assumed that the girder depth of this case is constant except for the column capital part of 16.5m long, varying depth.

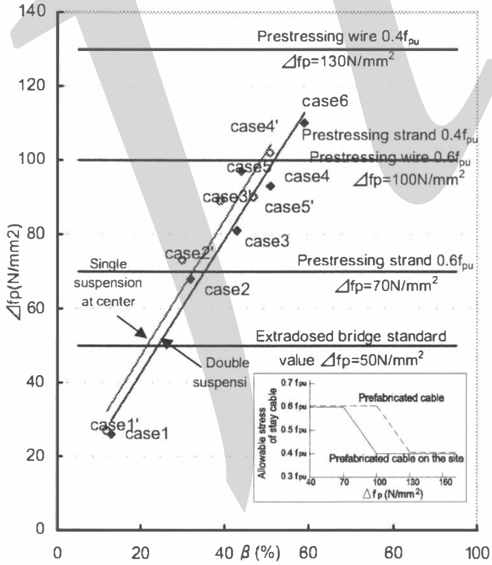

Fig.2 Fluctuating stress of stay cable ⊿f_p of vertical load ratio of stay cable β

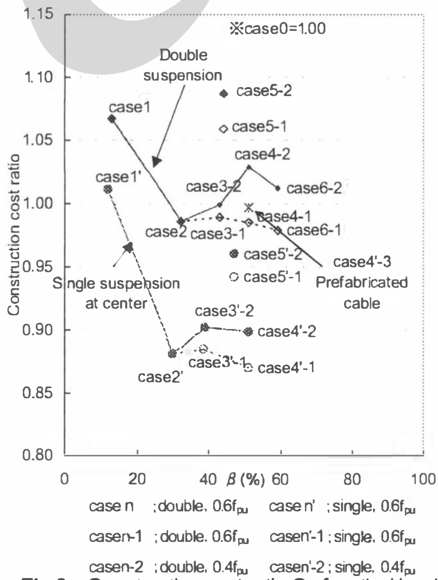

Fig.3 Construction cost ratio C of vertical load ratio of stay cable β in this examination

DESIGN OF THE YUKISAWA-OHASHI BRIDGE AND EXPERIMENTAL FUNCTION TEST OF ITS SADDIE SYSTEMS

H.Nunoshita
The Zenitaka Corp.,Japan

T.Kawabe
Akita Pref.,Japan

M.Hasegawa
Asia Consulting Engineers Corp,Japan

H.Kibe
Se Corp,Japan

Keywords: Extradosed PC bridge, performance test of the saddle system, Epoxy Anchor fitting

1. INTRODUCTION

Odate Towadako line that the Yukisawa-Ohashi bridge was constructed is a main arterial road of about 42km overall length which makes Akita-ken Odate City to be an origin.

This bridge is 3 spans connected Extradosed PC bridge of 177.1m overall length, and 2 main towers have been separated. The Stay Cable fixation structure of the main tower part was made the saddle form that a Stay Cable went through the main tower part. In the extra dosed PC bridge, the screw fixing system using the steel sleeve of the field assembly was adopted for the first time in this fixation structure, and labor saving of the construction and improvement countermeasure of saddle division fatigue performance were attempted.

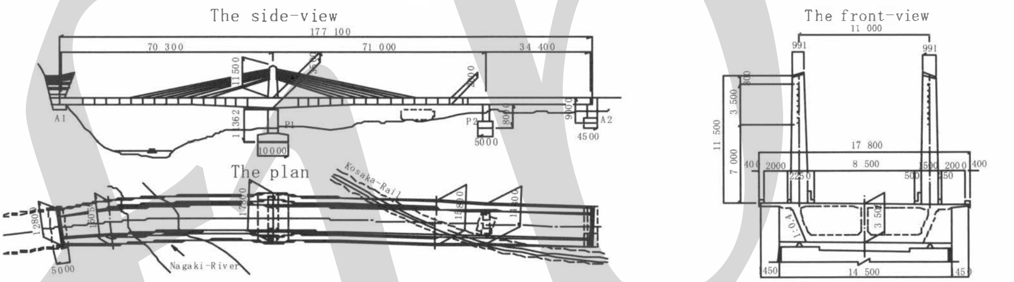

Fig. -1. Structural drawing

2. THE STRUCTURE OUTLINE.

At screw division of this structure, the steel sleeve which conducted the screw processing to the circumference as a PC anchoring method with many use results is used. The steel sleeve as a half division is assembled after the Stay Cable tension in Stay Cable, and the epoxy resin injected in the sleeve unites cable and sleeve.

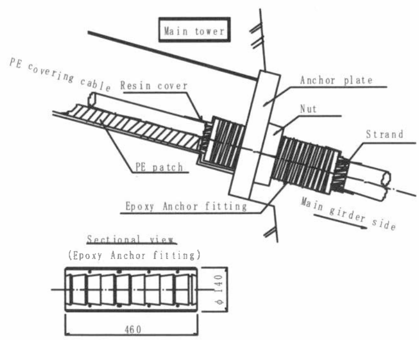

Fig. - 2. saddle division construction plan

This time tensile force remains behind Stay Cable during screw fixing of the saddle inside in order to fix saddle double end right after the Stay Cable tension in the screw. Since the tension in introducing by progress and creep of the construction step decreases, in the Stay Cable free length division, it becomes a condition that the Stay Cable tension in which the completion of the saddle inside is higher than that of the free length division is kept. Therefore, the saddle inside the stress variation in Stay Cable is absorbed in the Epoxy Anchor fitting part, and it becomes the structure which does not receive the effect of the stress variation. Features of this structure are shown in the following.

① The saddle inside does not receive the effect of the stress variation.

② The stress concentration of stationary portion is eased Stay Cable in order to fix in epoxy resin with the comparatively small modulus of direct elasticity.

③ Since it is the single cylinder structure, there are no grout and necessity for the double tubular structure.
④ Exchange and re-tension of Stay Cable are easy, because it is the screw fixing.The performance test of the saddle structure.

3. THE PERFOMANCE TEST OF THE SADDLE STRUCTURE

3.1 The covering polyethylene compression creep test

Since polyethylene covering has been conducted, configuration and grout of the protected tube become unnecessary for the Stay Cable cable, after the rust prevention material is applied. However, in the saddle division, large abdominal muscle pressure force affects the cable, and the high compressive force will work in the polyethylene covering. There is the fear which can not ensure the long-term rust prevention, when the damage is generated by this abdominal muscle pressure force for the polyethylene covering. Therefore, the compression creep test was carried out on compressive strength test of polyethylene and compression proof stress in the long term.

Based on the result of the test, in this system, the Stay Cable receiving seat made of polyethylene should be placed in the saddle inside in order to reduce compressive stress which affects the polyethylene covering of Stay Cable. By this, it became possible that degree of design bearing stress in the polyethylene covering was held at about σ PE=10N/mm2 under the yield compressive stress.

Test outline of the compression creep test is shown at table -4. From the result of this test, The result that over of 400 years was required was obtained in order to generate 1/4 strain of the covering thickness, because the compressive strain after 100 years becomes 21.3%. From these results, it was possible that the durability of covering polyethylene of the cable at the design stress level judged that it is sufficient.

3.2 The saddle structure break test.

It is known that the fatigue strength of diagonal member lowers, because saddle division of Extradosed PC bridge is generally accompanied by fretting fatigue. Then, in adopting the new saddle system, fatigue break test for real model was carried out in this bridge.

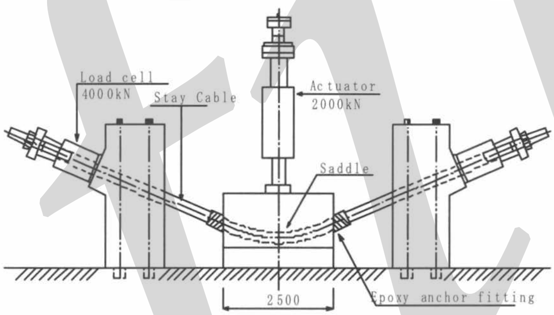

Fig.-3. fatigue test equipment

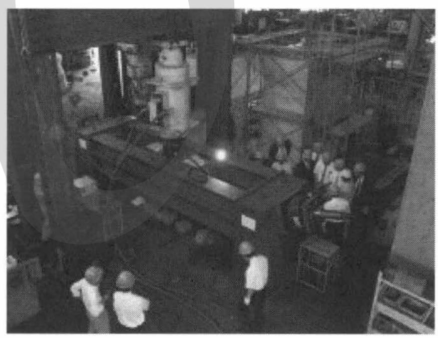

Phot.-1. fatigue test situation

The result of the test was approximately good. From the result of the test, next fact was proven.
① It not confirmed after 2 million time repeated-load, rupture of the strand and generation of the fretting corrosion.
② As the result that it took out the Epoxy Anchor fitting part after the fatigue test end and carried out the cable pull-out test,This becomes the about 1.5 times the safety factor for the design action load.
③ As a result of crack checking of the saddle division polyethylene covering and wall thickness measurement, there was no, and the sufficient proof stress was able to confirm the abnormality.
④ The injection volume of epoxy resin was insufficient, and crack and adhesion peeling with the strand were detected in the Epoxy Anchor fitting inside.

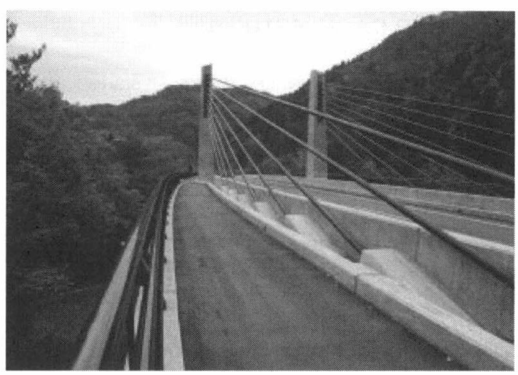

Phot.-2. completion photograph

REBAR CAGE APPLICATION TO CAST-IN-PLACE CANTILEVER BOX GIRDER, HOZU BRIDGE

Toshiaki Sumida, Kyoto Prefecture, Japan
Junji Makita, Sogo Engineering Inc.
Hideo Arai, Kenichi Saito, Sumitomo/Kawada/Kaneshita Construction Joint Venture

Keywords: rebar cage, prefabrication, labor saving, rapid erection, loop lap splice

1 INTRODUCTION

Hozu Bridge (Fig.1) is a newly constructed prestressed concrete extradosed bridge spanning the Katsuragawa River upstream from Kyoto in Kameoka city. Its total length is 368 meters (Fig.2) including a 100-meter center span.

To save labor and accelerate construction, we used rebar cages for cast-in-place cantilever box girder construction, developed special loop lap splices for rebars, and improved the form travelers. This enabled the time required for erection to be reduced by 30% [1,2]. The equipment required by this approach cost a certain amount, but it was much smaller than what would have been required with a pre-cast segmental method. The hatching in Fig.2 marks the areas where rebar cages were used.

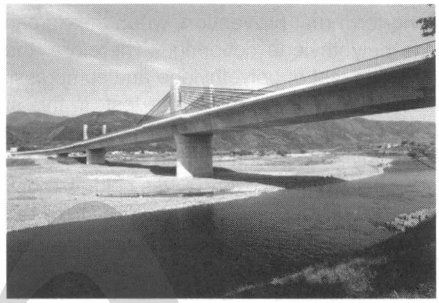

Fig.1 Hozu Bridge

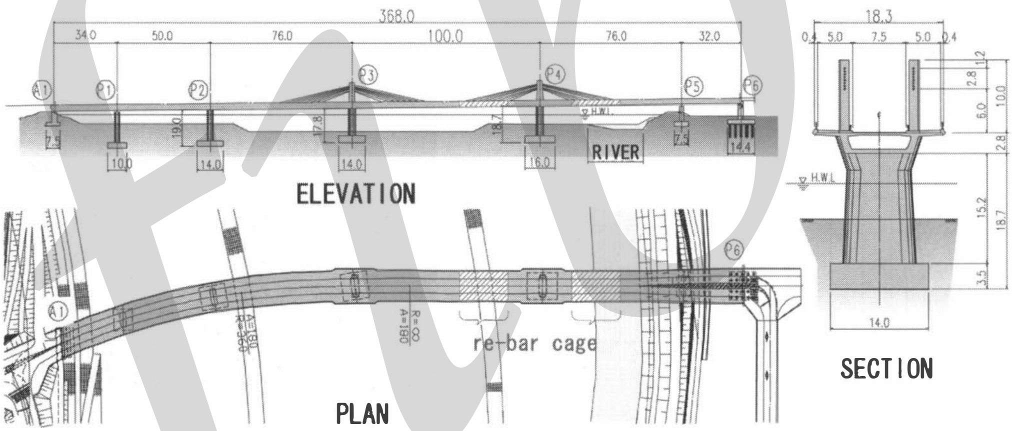

Fig.2 Elevation

2 REBAR CAGE METHOD

The erection sequence (Fig.3) started with prefabrication of the rebar cage on the ground.

The truck trailer carried the cage (1) to Pier 4. Then, the truck cranes loaded the cage to the transporter (2). The sliding bottom was already moved forward (3).

Next, the transporter carried the cage to the tip (4) of the girder. When a transporter arrived at the form traveler, the 4 chain blocks hoisted the cage (5) into the traveler (Fig.4). Finally, the sliding bottom was pulled back (6) to support the cage weight.

This sequence took just two hours for a cage.

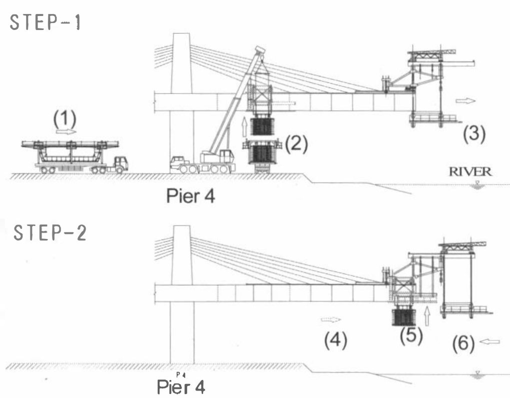

Fig.3 Rebar Cage Erection over the river

Table 1 Comparison of days required by 2 methods

	days	1	2	3	4	5	6	7	8	9	10
Cast-in-place method	pouring concrete	■									
	curing concrete		■	■							
	post-tensioning			■	■						
	moving a travele				■						
	setting forms					■	■	■	■		
	fabricating rebars and prestressing steel					■	■	■	■	■	■
Rebar Cage method	pouring concrete	■									
	curing concrete		■	■							
	post-tensioning			■	■						
	moving a travele				■						
	setting forms					■	■				
	installing Cage					■	■				
	jointing						■	■			
	REDUCED 3 days								■	■	■

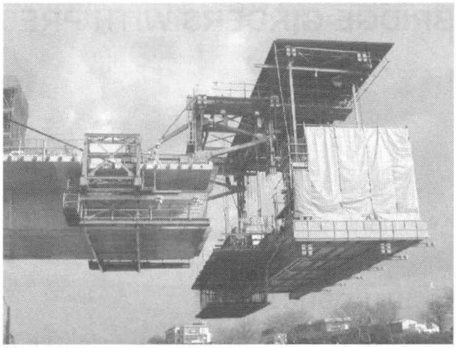

Fig.4 Hoisting a Rebar Cage over the river

Table-1 is the comparison of days required by the two cantilever launching methods. The top chart shows the days required by the conventional cast-in-place method for pier-3, and the bottom chart shows days required with the rebar cage method for pier-4. The conventional method took 10 days, but the rebar cage method took only 7 days.

The cost of equipment was about 5% of what would be required for the pre-cast segmental method.

We believe this result shows that the rebar cage method is applicable for medium and small-sized bridge construction.

3 PROBLEMS RESOLVED BEFORE APPLICATION

This method presented 2 problems — how to install the cage in the form traveler, and how to raise the ratio of pre-fabrication work.

3.1 Form traveler improvement

We added large upper beams, and sliding bottom to the traveler, which provides the rebar cage with enough installation space from below. And 4 electric chain blocks were added to the beams for rapid hoisting. (Fig.5)

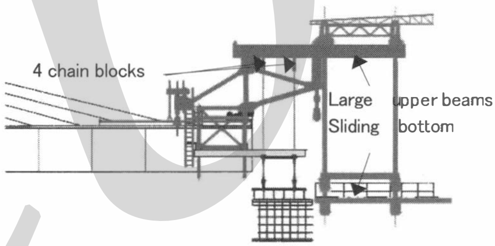

Fig.5 Improved Form Traveler for Rebar Cage Method

3.2 Loop lap splice all in one plane

Longitudinal rebars were loop lap spliced in order to shorten their joints. A short rebar joint was indispensable to obtain a high ratio of prefabrication with the rebar cages.

To confirm structural characteristics for seismic performance, an experiment was made on a life-size slab model using pushing and pulling cyclic loads with intensities equivalent to those measured in the Kobe Earthquake. We found that the spiral reinforcement (hatching in Fig.6) prevented the loop from opening, and stopped the cover concrete from spalling off.

Eventually, the rebar cage weighed 95% of all components.

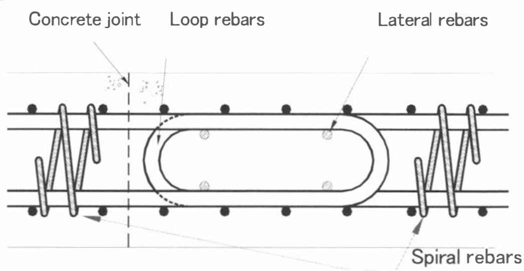

Fig.6 Spiral Reinforcement of Loop Lap Splice

REFERENCES

[1] Tsunoyama,I., Sumida,T., Shiomi,H., Makita,J., Arai,H. and Yoshioka,K.: Design and Construction of Hozu Bridge. BRIDGE AND FOUNDATION ENGINEERING, pp.13-18, Sep., 2000 (in Japanese)
[2] Site-Close-up / Hozu Bridge, Kyoto: NIKKEI CONSTRUCTION, pp.36-40, Feb. 11, 2000 (in Japanese)

BRIDGE GIRDERS WITH PRESTRESSED CONCRETE TENSION TIES

Peter Marti
ETH
Zurich, SWITZERLAND

Keywords: bridges, conceptual design, girders, prestressed concrete, segmental construction.

1 INTRODUCTION

In the late 1980's, Menn proposed a new concept for prestressed concrete bridges with spans in the order of 30 to 40 m [1, 2]. A continuous deck slab with or without shallow longitudinal ribs is connected at the supports with a steel tension tie that is trapezoidally deviated under the deck. Because of the tie's low stiffness Menn suggested to use cross bracings between the deviators or similar arrangements to increase the overall stiffness of the system.

Nine years ago, a bridge concept for an elevated lightweight railway line was worked out by the author in collaboration with VSL International Ltd. [3]. The concept was based on Menn's proposal but instead of using steel ties and cast-in-place concrete it was suggested to use prestressed concrete tension ties assembled from precast concrete segments along with precast deck slab and deviator segments. Combining the stiffness of the concrete with the high strength of the prestressing steel the prestressed concrete tension ties resulted in a very efficient behaviour of the overall system. Despite its advantages, however, the proposed concept was dropped in favour of a more conventional externally prestressed segmental box girder construction. The uncertainties associated with the new concept were deemed to be too big considering the substantial size of the project.

In the meantime a number of similar but smaller bridges were designed and built by Muttoni [4]. Fürst performed tests to failure on four model girders with spans of 12 m [5] and examined the response of bridge systems involving prestressed concrete tension ties [6].

After a review of the response of prestressed concrete tension ties and a comparison with alternative solutions the present paper addresses the conceptual design of inverted bowstring bridge girders with prestressed concrete tension ties and webs minimised to their static requirements. Some remarks on the related development potential conclude the paper.

2 DESIGN RECOMMENDATIONS

It is generally recommended to dimension inverted bowstring girders such that the tension tie remains compressed and the extreme fibre stresses in the deck remain below f_{ct} under service loads. Typical values of κ, l/a, l/f and $l\sqrt{A/I}$ (see Fig. 1) are in the order of 0.1 (0.2 for railway bridges), 3, 12 and 140 (100 for railway bridges), respectively. Apart from selecting the geometrical proportions combining the tie and deck prestressing with suitable amounts of non-prestressed reinforcement allows to adjust the tie and deck stiffnesses and strengths to the specific requirements of the design on hand.

3 DEVELOPMENT POTENTIAL

In order to (i) simplify the connection details between deck, tie and web members; (ii) allow for construction tolerances; and, hence (iii) facilitate erection it is suggested to normally use prefabricated concrete segments only for the deck. Steel tubes are recommended for the tie and the web members. The tie tube is to be filled with concrete to gain the necessary stiffness (κ) for post-tensioning which is applied by means of a prestressing tendon with its duct held in place at appropriate spacings inside the tie tube.

If a scaffolding is used to assemble and prestress the deck segments the steel construction can be attached to the underside of the deck followed by filling the tie tube and, after sufficient hardening of the concrete infill, post-tensioning and grouting of the duct. If no scaffolding is used (e.g. if full span deck segments are placed by a crane) it is recommended to compensate an appropriate portion of the dead load deflections by a first stage of post-tensioning prior to connecting the steel construction with the deck; after this the same construction procedure as with scaffolding can be applied.

Deck dimensions and deck weight can be minimised by using high-performance concrete. Two developments can be envisaged. The first uses externally post-tensioned deck segments whereas the second aims at full span pre-tensioned deck segments. In either case, sizing, shaping and detailing of the concrete segments have to carefully address prefabrication, transport, erection and service requirements. Material efficiency and stiffness demands will result in a trend towards thin-walled ribbed constructions. The feasibility and durability of such constructions have yet to be explored.

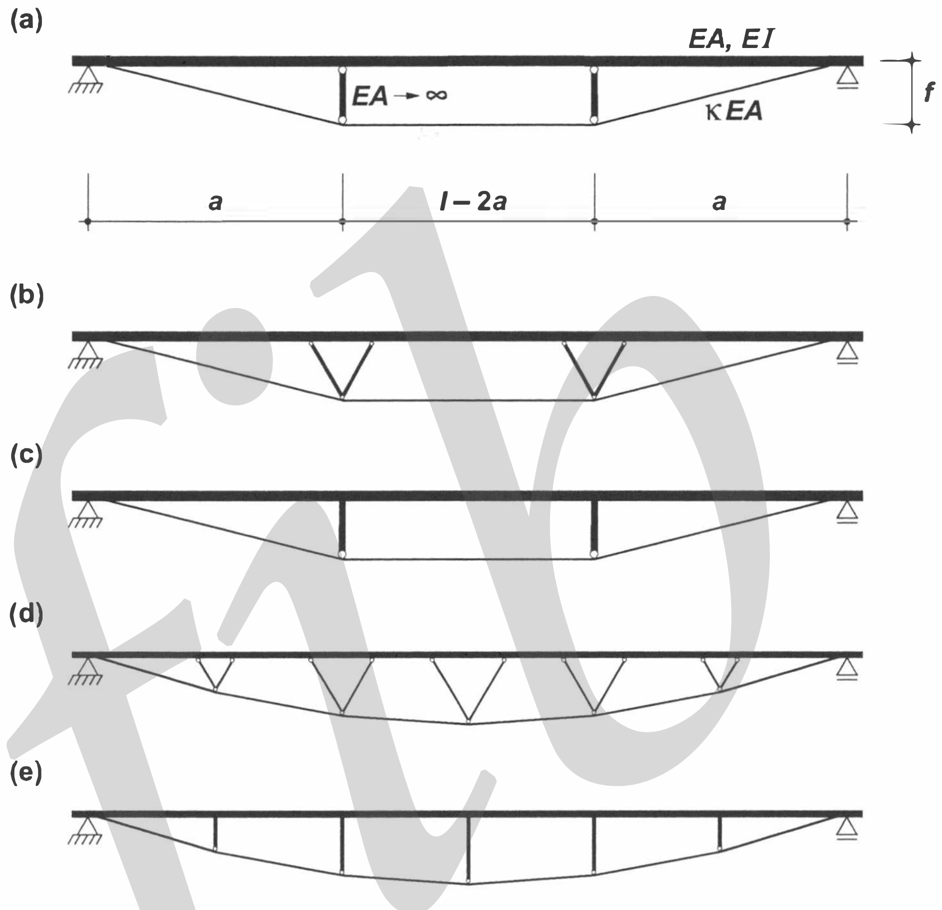

Fig. 1 Inverted bowstring girder systems.

REFERENCES

[1] Menn, C., “Brückenträger mit Unterspannung”, *Schweizer Ingenieur und Architekt*, V. 107, Nr. 9, Zürich, 1989, pp. 200-203.

[2] Menn, C., “Unterspannung von Brückenträgern mit gedrungenem Querschnitt – Eine sinnvolle Anwendung der externen Vorspannung”, *Bauingenieur*, V. 65, Berlin, 1990, pp. 209-219.

[3] Ganz, H.R., und Meyer, M., “Segmentbauweise”, *Schweizer Ingenieur und Architekt*, V. 115, Nr. 26, Zürich, 1997, pp. 528-533.

[4] Muttoni, A., “Brücken mit einem innovativen statischen System”, *Schweizer Ingenieur und Architekt*, V. 115, Nr. 26, Zürich, 1997, pp. 548-551.

[5] Fürst, A., und Marti, P., “Versuche an Trägern mit Unterspannung aus vorfabrizierten, vorgespannten Betonzuggliedern”, Institut für Baustatik und Konstruktion, ETH Zürich, IBK *Bericht* Nr. 243, Juni 1999, 118 pp.

[6] Fürst, A., “Vorgespannte Betonzugglieder im Brückenbau”, Institut für Baustatik und Konstruktion, ETH Zürich, IBK *Bericht* Nr. 267, Juli 2001, 124 pp.

DESIGN AND CONSTRUCTION OF TORIZAKI RIVER PARK BRIDGE – AN INNOVATIVE TWO SPAN CONTINUOUS PC BRIDGE WITH LARGE ECCENTRIC EXTERNAL TENDONS

Toshiji Matsui Hitoshi Kaneko
DPS Bridge Works Co., Ltd.
Japan

Hiroo Shinozaki
Mitsui Construction
Co., Ltd. Japan

Michifumi Hojo
Civil Engineering Service
Co., Ltd. Japan

Hiroshi Kamazawa
Mori Town Office
Japan

Keywords: external prestressing, large eccentricity, continuous girder, pedestrian bridge, construction

1 INTRODUCTION

The Torizaki River Park Bridge, shown in Photo 1, is a two span continuous pedestrian bridge which was built to connect the right and left bank squares of the riverside park as a part of an improvement plan of Mori Town in Hokkaido, Japan. It was the first application of an externally prestressed concrete truss structure with large eccentricities to a continuous span bridge, where the eccentricities of the external tendons were larger than the girder height.

This paper describes the design and construction of this bridge, focusing on the factors, which required special considerations, such as, evaluation of the ultimate strength, construction of falsework and formwork, and installation of the external tendons.

Photo 1 View of Torizaki River Park Bridge

2 STRUCTURAL FEATURES AND SPECIFICATIONS

The external tendons were laid out with remarkably large eccentricities into a shape resembling the bending moment diagram of the main girder, thereby allowing prestress to be introduced. The structure was also designed to form a pseudo truss, with the main girder made of concrete as compression chords, the external tendons as tension chords, and the deviators as diagonal members. This allowed the girder height to be reduced significantly, which makes the bridge lightweight. By determining the amount of eccentricities in the external tendon layout based on the law of linear transformation, various kinds of site requirements such as unsymmetrical span lengths and clearance were met successfully. The external tendons above the center support were covered with a fin-shaped concrete web member. This was a landscaping consideration to provide the bridge with a symbolic feature of the park since it was constructed as a landmark structure. Figure 1 shows a general structural view of the bridge.

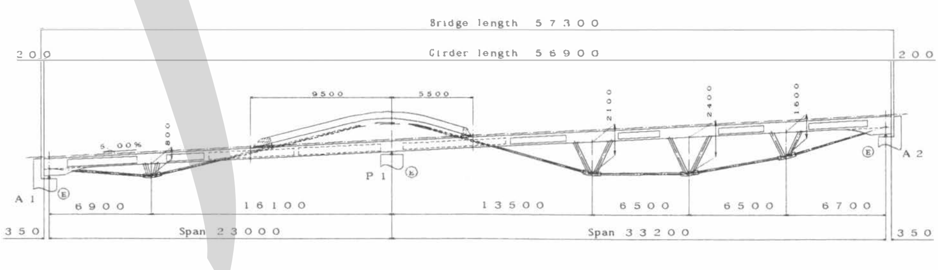

Fig. 1 General structural view

3 DESIGN

The bridge has a continuous girder structure with external tendons laid with eccentricities larger than the girder height, conventional design methods cannot be applied. Therefore, elastic frame analysis considering equivalent member properties was used in the design. To calculate the ultimate flexural strength, it was necessary to properly evaluate changes in effective depth of the external tendons and stress increase in the external tendons caused by deformation in main girder. Taking this into account, the authors adopted a general-purpose nonlinear frame analysis program (DIANA) to verify the ultimate flexural behavior.

Stress in this structure is transferred from the external tendons laid with large eccentricities to the main girder through the struts and the fin, and all of the highly prestressed tendons are anchored to the ends of the girder. Since these make the stress distribution of the main girder complex, design stress needs to be verified. The authors carried out 3D FEM analysis to confirm the validity of the design.

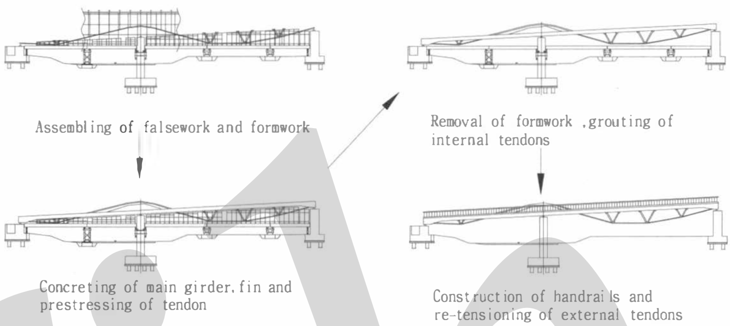

Fig. 2 Outline of the construction

4 CONSTRUCTION

Since the main girder, struts and large eccentric external tendons form a truss in this bridge, construction precision of individual members has a significant influence on the structure. For this, it was necessary to give special consideration to techniques and procedures to be used for constructing the falsework, formwork and external tendons. Figure 2 shows the outline of construction. Photos 2-4 show the construction at different stages.

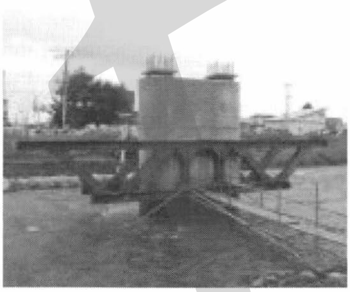

Photo 2 Erection of falsework

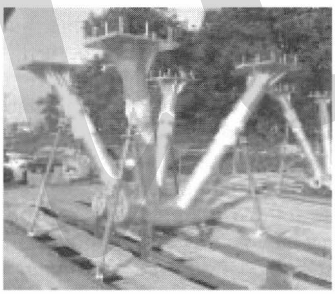

Photo 3 Erection of struts

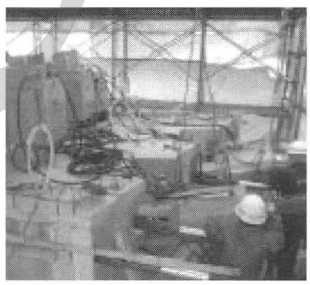

Photo 4 Prestressing

4 CONCLUDING REMARKS

The Torizaki River Park Bridge, a pedestrian bridge completed in March 2001 was the first application of an externally prestressed concrete truss structure with large eccentricities. The research and development of this structure was jointly investigated by DPS Bridge Works Co., Ltd., Mitsui Construction and Prof. H. Mutsuyoshi of Saitama University. Further research is in progress, to extend such applications to road bridges.

The authors wish to express their sincere gratitude to all concerned for their valuable guidance and cooperation offered for design and construction of this bridge.

REFERENCE

[1] Japan Highway Association: Specification for highway bridges with commentary, Vol. III: Concrete. Dec., 1996 (in Japanese)

CONSTRUCTION OF CURVED CORD TRUSS BRIDGE USING STRESS RIBBON ERECTION METHOD

Shinichi Kondoh
Sumitomo Construction
Tokyo, JAPAN

Shoji Ikeda
Yokohama National University, JAPAN

Takayuki Komatsubara
Ishikawa Prefectural Office, JAPAN

Shinichiro Kumagai
Sumitomo Construction
Tokyo, JAPAN

Keywords : prestressed concrete, truss bridge, self-anchored, stress ribbon bridge, vibration test

1 INTRODUCTION

The Ganmon Bridge is the world's first prestressed concrete curved cord truss bridge erected by the stress ribbon erection method (Fig.1).

A prestressed concrete curved cord truss bridge is economical for longer span highway bridges in the 60m to 90m range in remote areas where falsework cannot be used or requires the use of expensive equipment.

The curved cord truss bridge can be erected in the same method used for stress ribbon bridges and can achieve stability without depending on ground anchors in the service stage.

Fig. 1 Ganmon Bridge

2 SUPERSTRUCTURE

The bridge consists of a roadway slab deck, steel struts that support the roadway slab deck, and a bottom curved cord slab (Fig.2, Fig.3).

During erection, the precast bottom slab segments are hung on the bearing cables and the segments are assembled. The bearing cable acts as a perfectly flexible unit and is anchored at the abutment. The horizontal force is transmitted from the abutments into the foundation. When the tension of the bearing cables is released after the roadway slab is completed, the structural system changes to a self-anchored system from an externally-anchored system.

The bearing cables are anchored to the end segments in the service stage (Fig.4a) and further connected to prestressing rods and bear on the abutment backwall in the erection stage (Fig.4b).

The inverted V-shape struts are formed from steel pipes. The struts are placed at intervals of 2.0 m. The structure stiffness is mainly provided by the inverted V-shape struts.

The roadway slab deck is assembled from precast segments supported at struts. The precast segments have a trough cross-section. Once erected, the trough is filled with concrete, and combined with the precast segment to form the complete roadway slab deck.

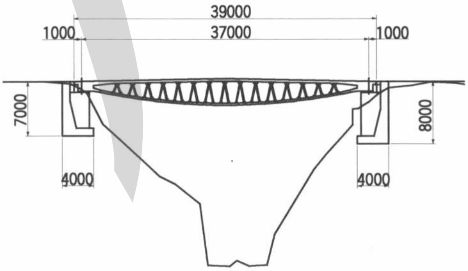

Fig. 2 Elevation of the bridge

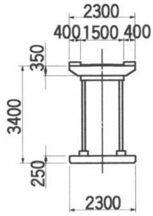

Fig. 3 Transverse section

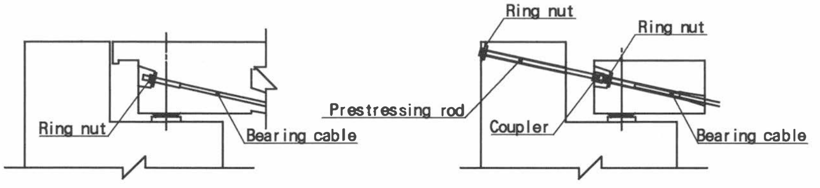

(a) Service stage (b) Erection stage

Fig. 4 End Segment and Bearing Cable

Fig. 5 Erection of bottom slab segments

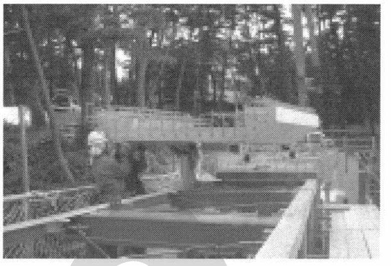

Fig. 6 Erection of roadway slab segments

3 ERECTION

The segments were assembled in a way similar to that described for the stress ribbon bridges. The construction of the superstructure was started in August 2001 and finished in October.

After the abutment was completed, the end segment was placed on elastomeric bearings on the abutment. The end segment was temporarily fixed into the abutment.

The bearing cables spanning the creek were drawn by a winch. After drawing, the cable was temporarily anchored into the abutment backwall using the coupler and the prestressing rod.

The bottom slab was assembled segment-by-segment. The segment with a strut was suspended on the bearing cables and moved alomg them to the final design position by a winch (Fig.5). The tops of the steel struts were connected to each other with rails. The roadway slab segment was lifted by a crane and moved on the rails to the determined position (Fig.6).

After the segments had been placed and connected, the bearing cable was detensioned by the hydraulic jack. After this operation, the anchor of the bearing cable was transferred to the end segment. At the same time, the ground anchor was also detensioned.

4 MODEL TESTS AND FIELD OBSERVATIONS

Model tests were performed in order to determine whether the bridge erected by the new method could in fact be a self-anchored structure. The design assumptions were checked by vibration tests carried out on the completed Ganmon Bridge in October 2001.

5 CONCLUSION

The major feature of a prestressed concrete curved cord truss bridge using the stress ribbon erection method is that it is more economical than other types when bridging over a deep gorge with no intermediate piers. The successful completion of the Ganmon Bridge shows that new structural concepts of concrete truss bridges are possible and that the best structural solution can be both architecturally pleasing and cost-effective.

REFERENCES

[1] Noritake,K., Ikeda,S., Kumagai,S. and Mizutani,J., Study on a New Construction Method for Concrete Structures Using Suspended Concrete Slabs, Proc. of FIP Symposium '93, pp.425-431, Kyoto, 1993

DESIGN AND CONSTRUCTION OF THE STRESS-RIBBON BRIDGE WITH EXTERNAL TENDONS

Tsutomu Machi Hiromitsu Yanai Teruyuki Nikaidou
Oriental Construction Co.,Ltd.

Takashi Kumagai
Iwaki Construction Office
in Fukushima Prefecture

Keywords: stress-ribbon bridge, external tendon, nonlinear analysis, static load test, natural vibration

1 INTRODUCTION

"Morino-Wakuwaku" bridge is a pedestrian bridge that has been constructed in the prefectural Iwaki park of Fukushima prefecture of Japan. This bridge was constructed as the first Stress-ribbon Bridge with External Tendons in the world. This new structural type was adopted for the following reasons; (1) The bridge is located on the hilly land where the long span length of 128.5m is required. (2) Structural type of superstructure was desirable to go well with the landscape. (3) The load bearing layer is the mudstone, so that it is necessary to decrease the horizontal force generating from the superstructure.

In this new type of stress-ribbon bridge, prestressing cables are placed outside the deck as external cables using supporting members, instead of inside the concrete deck as conventional stressed-ribbon bridge [1]. Characteristics of this structural type compared with the conventional stress ribbon bridge are following:

1) The horizontal force acting on substructures decreases to about 70% by setting sag of external cables larger than that of the concrete deck. Therefore it is possible to be applied at various geological conditions.
2) The torsion oscillation characteristic is amended. As a result, the wind velocity during generating the flutter vibration increases and the aerodynamic stability is improved.
3) Because prestressing cables are arranged outside the deck, there is no restriction of the number of cables to be arranged.
4) Because the prestressing cables are prefabricated, the grouting is not required which might become a weak point for the durability of prestressing cables. Moreover, replacing and retensioning of cables are also possible.
5) For the erection method of pre-cast concrete decks, it is possible to apply the same method as the sliding erection method applied for the conventional stress-ribbon bridges, and there is no restriction with conditions below the bridge.

This paper reports the outline of designing and construction method, and the result of static loading test and vibration test on actual bridge.

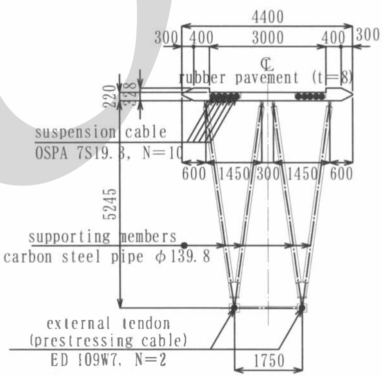

Fig.1 Section of the center of span

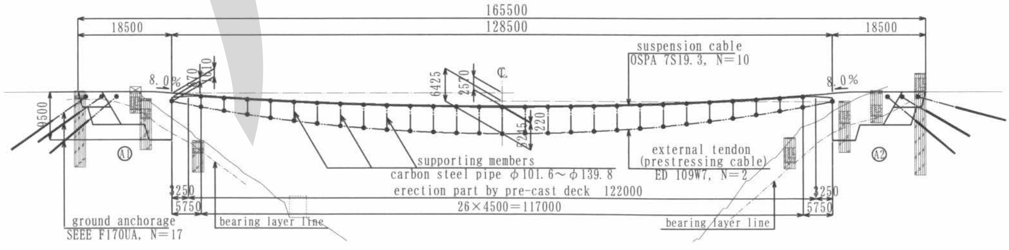

Fig.2 Morino-Wakuwaku Bridge (Side view)

Table 1 The design condition and used material

Suspended span	128.500 m		
Basic designed sag	Concrete deck : 2.570 m (L／50), External tendon : 6.425 m (L／20)		
Live load	Footway track live load : 2.0 kN/m^2		
Temperature variation	Concrete deck : ±15℃, External tendon・Sporting member : +25℃, −15℃		
Concrete	Concrete deck	Anchoring part on abutment	General part on abut Abutment
	σ_{ck}=50N/mm^2	σ_{ck}=40N/mm^2	σ_{ck}=21N/mm^2
PC steel	Suspension cable	Prestressing cable	Ground anchor cable
	SWPR19L, 7S19.3	SPWC, 109W7	SWPR7AL, 7S15.2
Steel pipe	STK400, ϕ101.6, t=5.7～ϕ139.8, t=4.5		

2 THE OUTLINE OF DESIGN

Fig.1 and 2 show the general view and **Table 1** shows the design condition and material used. Because the bridge is a type of suspended structure and local stress caused by bending moment in fixing portion of concrete deck has to be verified, the bridge was designed using FEM analysis considering geometric and material nonlinearity.

The main portion of deck was designed by criterion in which the occurrence of tensile stress was not allowed because the joint of pre-cast deck was constructed with mortar. While, the fixing portion of deck was designed by criterion of crack width limit because that portion was constructed by cast-in-place concrete.

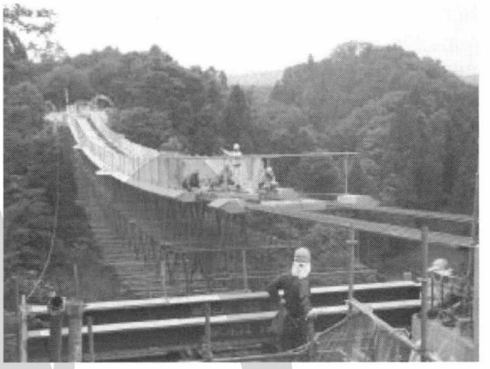

Photo 1 Sliding erection of the pre-cast deck

3 THE OUTLINE OF CONSTRUCTION

Photo 1 shows the sliding erection of the pre-cast deck. The hanging scaffolding and supporting members were installed before the sliding erection of pre-cast deck.

The weight of the external tendons was rather large; 350N/m/piece and it was erected by the extension on the hanging scaffolding which had been completed. After the attachment of the external tendons to the cable saddle was completed, residual tensile force for the designed sag was provided. **Photo 2** shows the arrangement of external tendons after the superstructure was completed.

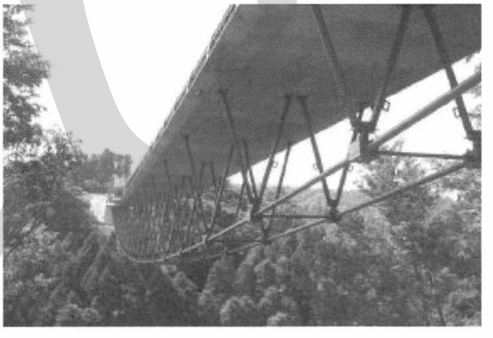

Photo 2 Arrangement of the external tendons

4 STATIC LOADING TEST AND VIBRATION TEST

Static loading test using a truck (46kN) and vibration test were performed to grasp the structural characteristics and the vibration characteristics of the stress-ribbon bridge with external tendons [2].

REFERENCES

[1] Tsunomoto, M., Shigenobu, T, and Suda, T., "Structural Characteristics of the Suspended Stress Ribbon Bridges," Proceedings of The 7th Symposium on Developments in Prestressed Concrete, Japan, October 1997, pp.627-632.

[2] Kajikawa, Y., Fukada, S., Ooki, F., Tsunomoto, M., Machi, T., and Kumagai, T. "Structural and Vibration Characteristics of Stress Ribbon Bridge with External Tendon," Journal of Structural Engineering, JSCE, Vol.48A, March 2002.

PLANNING AND CONSTRUCTION OF SHIBUKI BRIDGE

Norihito Matsumoto
Construction Division
Kawada Construction Co., Ltd.
Tokyo ,JAPAN

Keywords: Stress-ribbon bridge , precast segment , Suspending conveyer

1 INTRODUCTION

Shibuki Bridge is a stress-ribbon bridge constructed just in front of Nagashima Dam under construction at the upstream of Ohi River in Shizuoka prefecture. Stress-ribbon bridge is a type of hanging bridge structure where Prestressing tendons in the concrete slabs are prestressed to support the load by the axis rigidity of the slabs. Recently, the structural rationality, slender view, and operability are highly evaluated and such type of pedestrian bridges are increasing.

The construction of the bridge was planned as follows. First, scaffolding is prepared between the abutments, and bearing cables are placed. The precast deck are suspended on bearing cables and shifted along them to their final position by winch, and fixed. Prestressing is applied after casting the joints between the segments to ensure sufficient rigidity of structure. The paper is a report mainly on the planning and construction of the bridge.

Table 1 Outline of design

Bridge length	: L=114.000m
Span length	: l=97.000m
Width	: w=2.0m
Sag	: 2.8m
Live load	: 200kg/m2
Concrete	: σ ck=40N/mm2
Ground anchor	:SEEE F230
Bearing cable	:SEEE F200
Prestressing cable	: 7S12.7

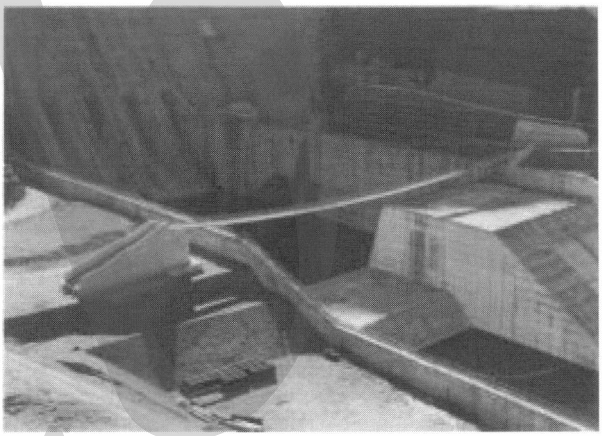

Photo 1 Completed view

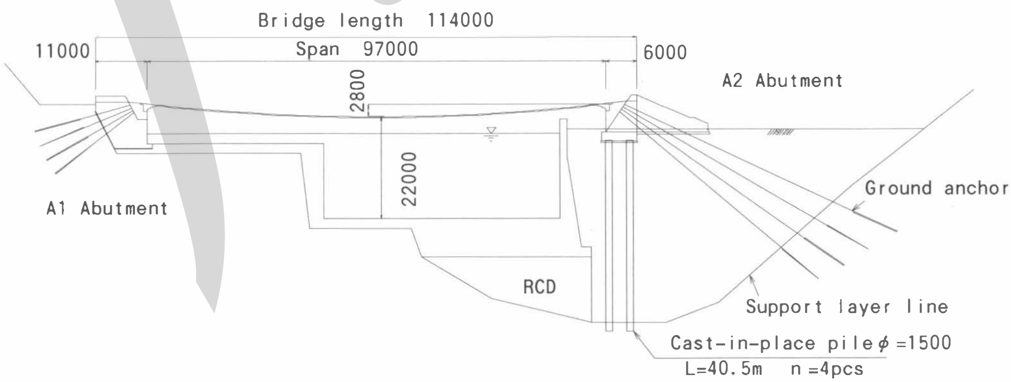

Fig. 1 General side view

2 GROUND ANCHOR

A2 abutment is pile foundation, and all the horizontal reaction force of superstructure is loaded on the ground anchors. On the design calculation, the tension of anchor was designed to stabilize the abutment after completion. However, when such tension is applied at a time before construction of superstructure, horizontal force is applied to the abutment, the abutment loses stability and is turned over. To stabilize the abutment in any condition, ground anchors are planned to be tensed step-by-step according to the progress of constructing superstructure.

3 INSTALLATION of PRECAST SEGMENTS

Installation procedure of a precast segment is as below.

① Horizontally move a precast segment by truck crane and place on the rail.

② Horizontally move the panel just below the bearing cables.

③ ift it again with truck crane, and suspend on the bearing cables by the suspending conveyer.

④Move it by winch to the appointed position and fix the panel.

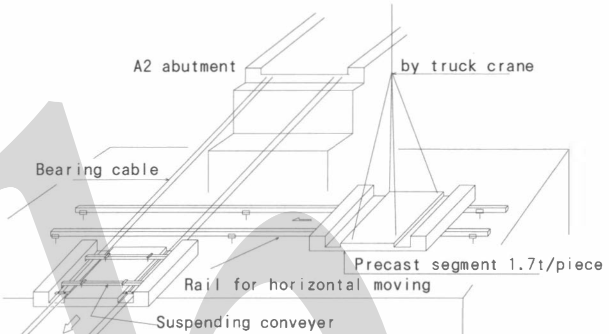

Fig. 2 Method of installing precast segment

Suspending conveyer for precast segments was designed as shown in Fig.3. The method suspend precast segments on the bearing cables by the suspending conveyer that consists of bearing unit, round bar and H-steel, slide to the appointed position by winch, fasten the steel plate with nut to be fixed. Installation was considered to be possible with only steel plate, but the method was planned and executed considering the installation efficiency and safety when moving. As a result, precast segments were installed safely without damaging the bearing cables.

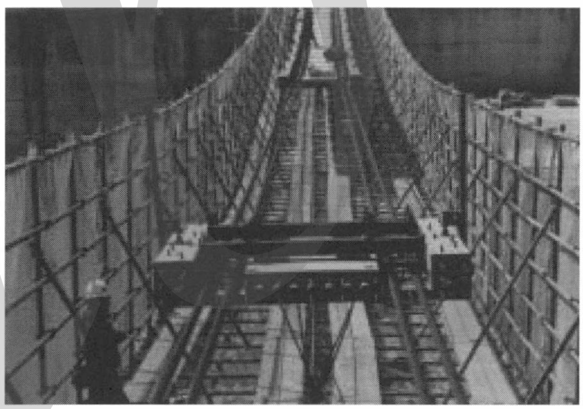

Photo 2 Precast segment installation

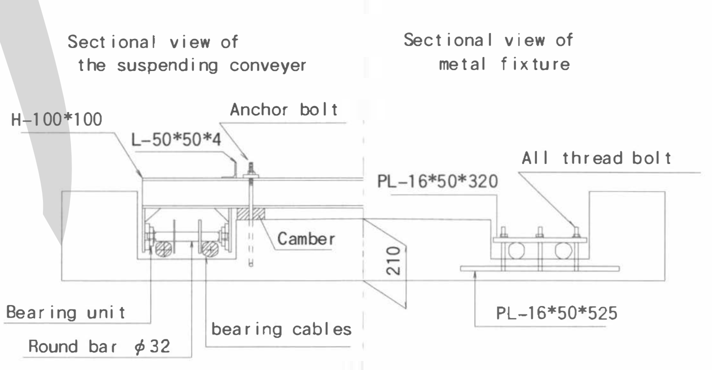

Fig.3 Suspending conveyer and metal

HISTORY OF PRESTRESSED CONCRETE BRIDGES CONSTRUCTED OVERSEAS BY JAPANESE CONTRACTORS AND FUTURE PROSPECTS

Yoshishige Ito
Taisei Corporation
JAPAN

Keywords: Official Development Assistance (ODA), Overseas market share, lump sum contract, alternative proposal, design-build contract

1 INTRODUCTION

Prestressed concrete (PC) was introduced to Japan from Europe in the 1950s and greatly contributed to the subsequent tremendous growth of highway construction. Since then, the domestic construction market for PC bridges has grown dramatically, reaching as high as US$4 billion a year in construction volume in the last 10 years. During that time, Japanese contractors built a large number of bridges, accumulated considerable experience, and raised the levels of bridge design and construction technology. Overseas, Japanese companies also constructed PC bridges in various Asian countries under foreign aid programs sponsored by the Japanese government. However, their track records in the overseas market has not reflected their capabilities in terms of technical level and market scale.

2 REVIEW OF PC BRIDGES CONSTRUCTED OVERSEAS BY JAPANESE CONTRACTORS

The PC bridges constructed overseas by Japanese contractors during the past ten years or are currently under construction are surveyed. Then some features are found by comparing bridges constructed in Japan in recent years. They have the following technological features. These technologies have rarely been applied to bridges overseas.

- Composite bridge girder such as PC box girder with corrugated steel at web to reduce the weight of the girder.
- Transparent sheath and pre-grout tendon for better grouting capability and enhanced durability
- Use of fiber concrete to prevent scaling; high-flowing concrete to improve pouring; and light-aggregate concrete to reduce the dead weight of the main girders
- Construction of structures with a higher-order of statical indeterminancy through the use of information-based methods, personal computers, and a variety of sensors

In summary, the bridges constructed overseas by Japanese contractors have the following characteristics.

- Advanced technologies developed in Japan were not used overseas.
- Conventional design and construction method were adopted.

3 FEATURES OF OVERSEAS MARKET FOR JAPANESE CONTRACTORS

(1) Proportion of overseas sales to gross sales

The proportion of overseas sales by Japanese contractors is lower than that of the contractors in advanced countries in Europe and Asia.

(2) Main market and Funds of projects

- According to the Overseas Construction Association of Japan, Inc., sales by Japanese contractors in the overseas market totaled US$6,218 million in fiscal 2001. Sales in Asia reached US$4,489 million, more than 70% of the total. This means Asia was the dominant market.
- Of the sales in Asia related to Japanese ODA projects, US$195 million were from grant aid projects and US$1,022 million were from yen loans projects , total US$1,217 million, or 27.1%. Taking into account that orders from asian public institutions which include bridge construction projects amounted to US$2,391 million, sales from ODA projects made up 50.9% of the sales from public institutions in Asia.

4 FEATURES OF JAPAN'S DOMESTIC MARKET

(1) Ample domestic market

Fig. 1 shows changes over time in the construction investment per capita in Japan, Asia, USA and Europe. Construction investment per capita in Japan has been high, approximately five times that of Europe, indicating that the market in Japan is quite large. However, construction investments have been decreasing for the last several years, particularly in public works that relate close to bridge construction projects, as shown in Fig. 2.

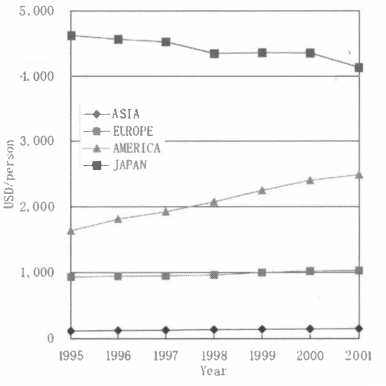

Fig. 1 Change with time in construction investment per capita in Japan, Asia, USA and Europe

(2) Fair-share construction market

In the Japanese public works construction market, there is a belief that opportunities to receive orders should be fairly shared among companies. Lots ordered in Japan have been smaller than in the Western countries, which gives many more companies opportunities to receive orders.

(3) Conventional forms of contracts

Under Japan's construction contract system for public works, the works are subject to strict regulations, a design is usually prepared in-house, and contractors must implement the design using the construction method specified by the owner. This system has long been used for public works in Japan. Other forms of contract systems, such as design-and-build contracts, Private Finance Initiative (PFI), and contract with an alternative proposal clause, have never been applied.

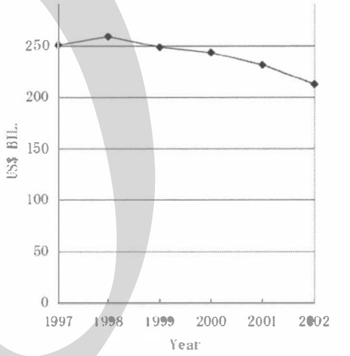

Fig. 2 Changes over time in Japan's domestic construction investments

5 FURURE PROSPECTS OF OVERSEAS PROJECTS

As shown in Fig. 1, domestic construction investments will continue to decrease. For Japan's excellent bridge contractors to survive, they need to actively pursue overseas construction projects and outperform their competitors. Fig. 3 shows the total bridge spans constructed for ODA and non-ODA projects over the past ten years. The bridge span total for non-ODA projects has been steadily increasing.

Japanese contractors are shifting to projects having a lump sum contract with an alternative proposal clause, projects with a high degree of technological difficulty and a limited number of competing companies ,and PFI projects with a design-build contract so that they can propose a novel idea or an alternative proposal and make an adequate profit.

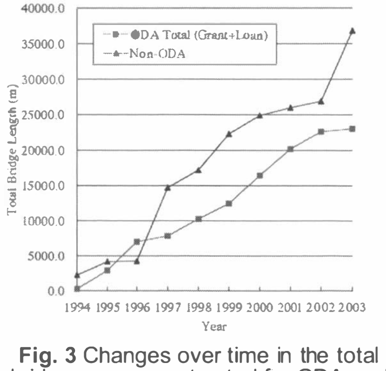

Fig. 3 Changes over time in the total bridge spans constructed for ODA and non-ODA projects

REFERENCES

[1]Bridge and Foundation Engieering/August 2000
[2]Journal of Prestressed Concrete/Sep.-Oct.2000
[3]Engineering News-Record/August 20,2001
[4]Construction Economy Report No.38 "The Japanese Economy and Public Investment"/Research Institute of Construction and Economy

THE CONSTRUCTION OF AYUNOSE BRIGDE

Masaki Uryu, Sumitomo Construction Co., Ltd. Japan
Yoji Mizuta, Kyushu Sangyo University
Takami Nagaki, Kumamoto Prefectural office
Takefumi Aramaki, Sumitomo Construction Co., Ltd. Japan

Keywords: Y-shape rigid frame bridge、cable-stayed bridge、large diameter deep foundation viscous shear damper

1 INTRODUCTION

The Ayunose Bridge has a unique construction that combines a Y-shape rigid frame bridge and a prestressed concrete cable-stayed bridge. The topography at the site is extremely severe: a V-shaped valley 140 m deep and 300 m wide. Construction began in December 1993 and was completed approximately five and a half years later, in July 1999. This paper will report on the result of the construction implemented under these conditions of precipitous terrain and unique design. Fig.1 shows a general view of the bridge.

2 OVERVIEW OF CONSTRUCTION

Fig.2 shows the procedure used for the construction.For the foundation for the bridge piers, the large-diameter deep foundation construction method was adopted.The Y-shaped P1 bridge pier in particular was constructed using a "self-lifting stage" .The main girders for both the P1 rigid frame girder bridge section and the P2 cable-stayed bridge section were constructed by a balanced cantilever method using form travelers. The P2 cable-stayed bridge was made up of 12 stay cable blocks each on the center span and side span sides, and these were constructed on both sides simultaneously.

3 CONSTRUCTION OF LARGE DIAMETER DEEP FOUNDATION

The construction of the large diameter deep foundation involved the use of the New Austrian Tunneling Method (NATM), used for tunnel boring, to drill vertical shafts and then using concrete, ring beams, rock bolts and other support materials to conduct the excavation. The foundations measured 14.0 m in diameter and 36.0 m in depth for the P1 bridge pier and 18.0 m in diameter and 31.0 m in depth for the P2 bridge pier. For the excavation and construction of the deep foundation, a new system called the "large diameter deep foundation construction management system" was developed.

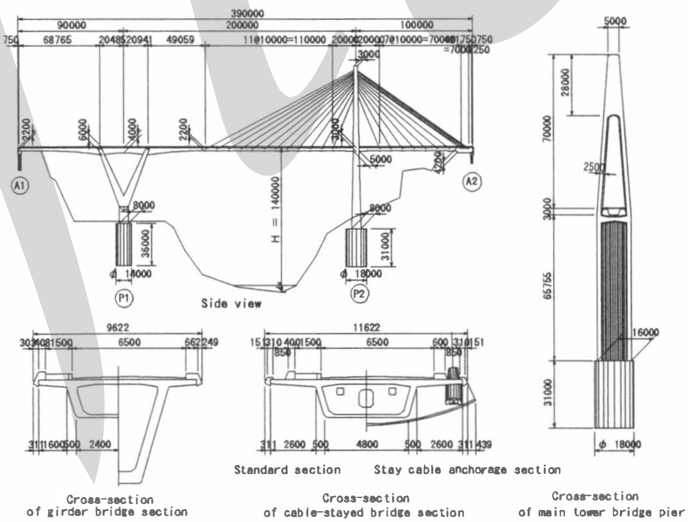

Fig. General View

4 CONSTRUCTION OF Y-SHAPED RIGID FRAME BRIDGE PIER

The Y-shaped bridge pier was made up of a vertical member and diagonal members that constituted a configuration with significant changes in section. After the pier table was complete, the diagonal member opening would form a stable inverted triangle structure. During the construction, however, the weight of the body and the hoist stage made it an extremely unstable structure. Accordingly, struts were placed in three levels (bottom, middle and top), to ensure that no excessive stress would be produced in the concrete. The hoist stage was made up of a hoist unit that provided overall support, a girder section, a stage floor and scaffolding section capable of moving horizontally, and a formwork panel. Hydraulic jacks were used for horizontal and vertical movement. When movement was complete, the setup of the formwork was also complete, resulting in labor-saving construction as well.

5 CONSTRUCTION OF PRESTRESSED CONCRETE CABLED-STAYED BRIDGE

The A-shaped main tower is made up of two pillars and a connecting piece. As the two pillars are placed at an angle, three levels of struts are provided to prevent member toppling. The stay cables are concentrated on the connecting piece, so before each block was constructed, the anchorage for each stay cable was installed on an assembly base constructed in advance with a predetermined height and direction. The main girder has arc-shaped crossbeams 2.2 meters in height that anchor the stay cable anchorages at 10 m intervals. The construction work was performed by form travelers, using a large metal form that can be used for both the standard section and the stay cable anchorage section.

6 DEMONSTRATION VIBRATION TEST

In the demonstration vibration test, the natural frequency and attenuation constant were determined, using a 10 tf truck and a large exciter as vibration sources. In addition, in the test for the cables, an actuator was used to apply vibrations, and the damping effectiveness of the cable dampers (viscous shear dampers) was examined.

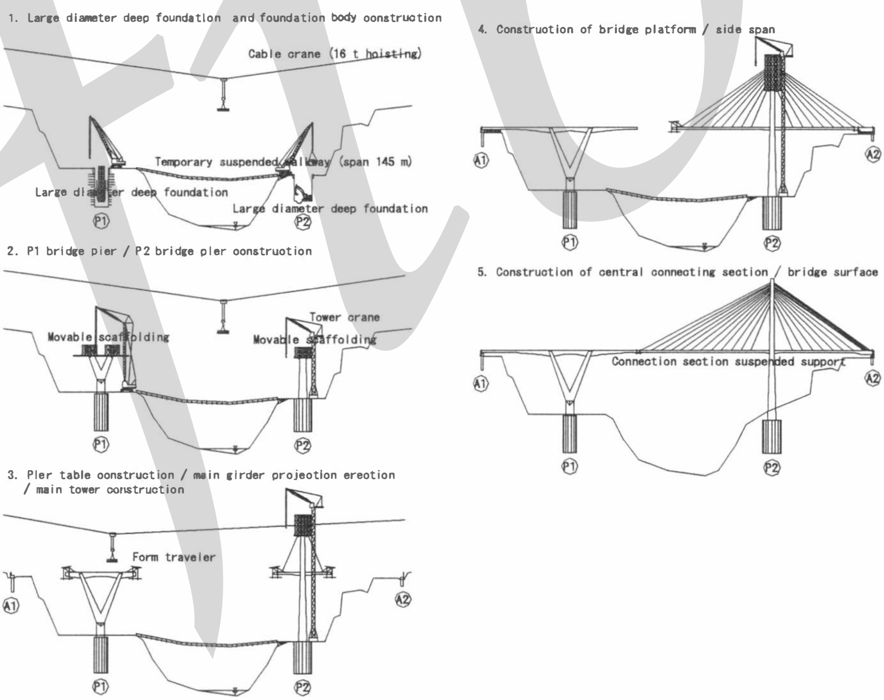

Fig. 2 Construction Procedure

SOME THOUGHTS ABOUT LONG SPAN CONCRETE CABLE-STAYED BRIDGES

By
Man-Chung Tang
T.Y. Lin International, San Francisco, USA

Keywords: bridges, cable-stayed bridges, long span bridges, concrete bridges, bridge design

1 INTRODUCTION

The first bridge that fully utilized the features of a modern concrete cable-stayed bridge is the Main Bridge in Germany, which was built in 1972. Although it's span of 148 meters was not exceptionally long at the time, it has incorporated all the main features of a modern long span concrete cable-stayed bridge: It has a relatively slender tower and closely spaced cables; It also depend more on the intermediate piers and the cables in the end span to stiffen up the tower to reduce live load deflection in the main span. The bridge was designed for extremely heavy live loads: highway, railway and pipelines.

Then came Brotonne (320m, 1977) in France, Barrios de Luna (440m, 1984) in Spain and finally the longest span today, the Skarnsunde (530m, 1991) in Norway.

Two bridge designs deserve mention as we talk about long span cable-stayed bridges: the Ruck-A-Chucky Bridge and the Dames Point Bridge, both in USA. Both bridges were fully designed in late 1970s with the same span length of 1,300 feet (396m). The Dames Point Bridge, was delayed due to financial problems but was finally built in 1989. The Ruck-A-Chucky, a very special design crossing over a planned water dam. Because the dam is delayed, the bridge is still not built.

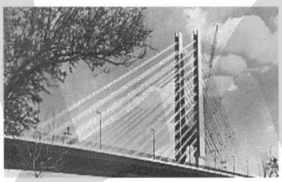
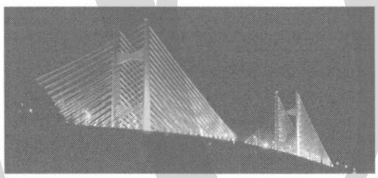
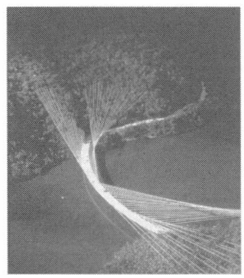

Fig. 1 Main Bridge (left). Dames Point Bridge (center), Ruck-A-Chuck Bridge (right)

2 THE TREND

Will longer span concrete cable-stayed bridges be built in the future? Obviously it will. The question is then: how long, and when?

If history can provide clues for the future, it may be reasonable to extrapolate from historic data to see what the trend may lead us. Plotting up the milestone record spans for concrete cable-stayed bridges, it appears that by the year 2020, we will have a concrete cable-stayed bridge of 1,200 meters span.

3 DESIGN ISSUES

In the lateral stability direction, the girder is a bridge carrying wind and other loads. The width to span ratio is an important indicator.

The required width of a bridge girder results from the number of traffic lanes the structure is designed for. It is independent of the span length. For a typical 6 lane bridge, the required deck width is about 34 meters. If the span is 1000m, the width to span ratio is 1:30, which is acceptable. When the span gets longer, this ratio decreases and may not provide the required stability for a cable-stayed bridge.

The most straight forward method is to directly increase the width by separating the girder into two or three boxes and connecting them with cross beams and bracing.

A second method is to brace the deck transversely by cables. This approach is popular in pipe bridges where the girder is very flexible. It can be either a suspension bridge system or a cable-stayed bridge system in the lateral direction.

Another often-discussed method is the use of three dimensional cable arrangements. If sufficient inclination is provided to the main cables in the lateral direction, the lateral stiffness of the girder is automatically increased. To do this, the tower top must be spread wide apart.

Aerodynamic is usually less of a problem for concrete cable-stayed bridges than for steel cable-stayed bridges. The methods of increasing the lateral stability described above also improve the aerodynamic stability of a cable-stayed bridge. A wider bridge is less susceptible to wind induced vibrations. Adding wind fairing is another way to increase the aerodynamic stability. Concrete is relatively easy to mold, so it can achieve the best aerodynamic shape without major cost penalty.

Concrete inherently provides higher damping to the bridge than steel. The damping increases significantly when the concrete starts to crack. Cable-stayed bridges are extremely redundant structures. Provided that the bridge girder is reinforced properly, some local cracking is not detrimental to the safety of the structure.

Sag Problem of Long Cable is the actual effectiveness of a very long, inclined cable can be drastically reduced by the sag caused by the dead weight of the cable itself. There are several ways to deal with this problem. But the basic idea is to divide the length of the cable into smaller sections so that the change in the sag is small.

Nonlinear behavior of cable-stayed bridges becomes more pronounced as the span length increases. Concrete cable-stayed bridges are inherently stiffer than comparable steel cable-stayed bridges. It does not appear that, in a practical sense, this should be in any way a limitation of the span length.

4 WHAT IS THE LIMIT

The one factor that limits the span length of a concrete cable-stayed bridge is the allowable stress in the girder.

If we assume that the flexural stress is 10% of the total stress at the critical section, the maximum span length will then be: L(max) = 1,500 meters based on 10% flexural stress.

5 A NEW STRUCTURAL SYSTEM

A straddle cable system; by anchoring some back span cables to an external anchor block and make them continuous over the main span, we create a different cable supporting system that does not cause compression force in the girder. The center portion of the cable will work like a straddle offering vertical supports to the bridge girder.

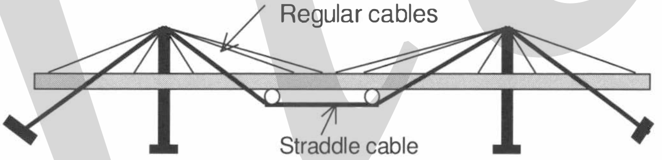

Fig. 2 Straddle Cable-Stayed Bridge

The maximum span of such a bridge system is limited by the capacity, or the allowable stress of the straddle cables. The longest cable may end up just carrying its own weight. It is very similar to a suspension bridge except that, based on tradition, the towers will be twice as high.

6 CONCLUSION

Based on the materials we have today, we are capable of building true cable-stayed bridges with very long spans. The limitation comes from the allowable concrete stress. Moreover, if we add straddle cables, we can significantly increase the possible span length of a cable-stayed bridge.

Today's longest concrete cable-stayed span is 530m. We are still far from approaching the limit, even just with the materials we are using today. In reality, the cost is the deciding factor of the maximum span length of a cable-stayed bridge, not the technology. As engineers, we can proudly pronounce that we can build a cable-stayed bridge of any span length the society can afford!

DESIGN AND CONSTRUCTION OF KAZURA BRIDGE, TOKAI-HOKURIKU EXPRESSWAY

Hiroyuki IKEDA , Masahiro AZETA
Chubu Branch, Japan Highway Public Corporation, Nagoya, Japan

Hiroshi AKIYAMA, Manabu KATO, Yasuaki MATSUO
The Zenitaka Corporation, Tokyo, Japan

Keywords: Incremental Launching Erection, Cantilever Erection, External Prestressing, Unbalanced Spans

1. INTRODUCTION

Kazura Bridge is a 131m long prestressed concrete 3 span continuous box girder bridge of Tokai-Hokuriku Expressway, located in Shirakawa Village, Gifu Prefecture, Japan where is famous for Gassho Style Historical Houses registered as World's Cultural Heritage of UNESCO.

It bridges the adjacent tunnels across the steep narrows of Kazura River and the side spans are cased in the portals of the tunnels because of the geometric condition (Fig.-1).

The combination of incremental launching method and balanced cantilever method are employed for short construction period and safety improvement to overcome the severe climatic conditions and tight construction period, which were applied to the side spans and main span respectively.

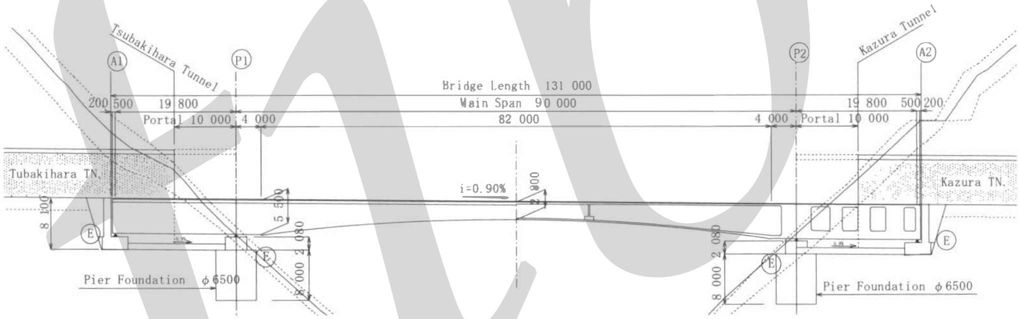

2. GENERAL FEATURES

The general features of the bridge and its quantity of materials are shown as follows.

General Features

Type of Structure	: 3 Span Continuous Prestressed Concrete Box Girder Bridge
Bridge Length	: 131.0m
Span Arrangement	: 19.8 90.0 19.8m
Width	: 10.900 12.300m
Vertical Slope	: 0.900%
Horizontal Alignment	: R=5000m
Erection Method	: Balanced Cantilever Erection (main span)
	Incremental Launching Erection (side spans)

3. GENERAL OF SUPERSTRUCTURE

3.1 OPTIMUM DIMENSIONING

The geometric condition of the bridge required the unbalanced span alignment (19.8+90.0+19.8m) and side span location - in the portals of the tunnels. The dimensioning of the cross section was optimized taking into account the completed performance and construction requirements such as allowable reaction of the bearings, stability of the girder under construction and crack control for the hydration heat stress.

Because of the variable reaction for the bearings, it was decided that the side span should have comprised two components - structural member and non-structural counterweight fill concrete that would be filled in proper state with the cantilever erection procedure to control the weight balance.

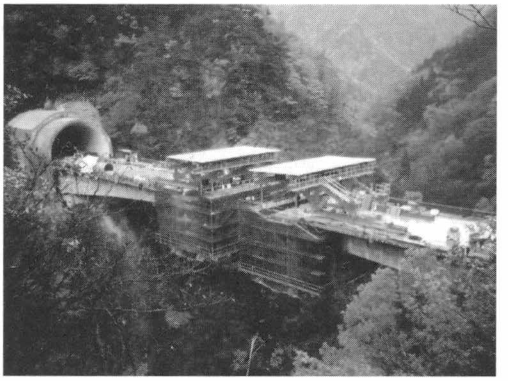

3.2 EXTERNAL PRESTRESSING

The longitudinal prestressing is given only by epoxy coated external tendons that would provide good protection layer against corrosion. The external tendons (19S15.2) were anchored at the cross beams in the side spans and the blisters in the main span.

4. CONSTRUCTION METHOD

The snowy climatic condition prevents the construction outside the tunnels in winter seasons – from the beginning of the December through the middle of April.

The hybrid construction solution of incremental launching erection for side spans in the portals and cantilever erection for the main span was employed to overcome the climatic and tight period.

The sophisticated erection sequence made it possible to cast the side spans even in winter season, earlier beginning of cantilever erection and improvement of the safety for assembling the travelers outside of the portals.

In the incremental launching construction, though it was only for 2 cast in situ segments of side spans and pier tops, was performed by 3 deformed prestressing bars (D32) and jacks (500kN/jack).

In the cantilever construction, the permanent vertical tendons for negative reaction (up-lift) were set in the neighborhood of the end bearings (not tensioned at first) so that they could work as passive fail safe device in case unexpected forces acted on the girder. After the 7th cantilever segment cast, the vertical tendons were tensioned, since the reaction on the bearing exceeded the allowable value until the 7th segment casting.

Besides above, the lining of the portals were cast when cantilever erection was being performed. This measure enabled not only the earlier start of side span assembly, but also more economical execution to make it unnecessary to build the false-work stage for it than the lining in advance to the side span assembly.

5. CONCLUSION

The special features the design and construction of Kazura Bridge are as follows.

1. The dimensioning was optimized considering the difference of the reaction forces between construction state and completed state.
2. The anchorage zones were designed to restrict the tensile stress and reinforced with prestressing steel in need.
3. The sophisticated construction sequence enabled the construction in snowy season with improvement of the safety and economical portal lining construction.
4. Thermal influence for the transverse tendon in the deck was verified by maturity based evaluation. The measurement in actual tensioning proved it appropriate.
5. Honeycomb plastic damper was employed as fail-tolerance device for extreme event.
6. The up-lift prevention tendon was designed considering seismic influence.

REFERENCE

1 Japan National Railway: Guide for the Design and Construction of Prestressed Concrete Bridge by Incremental Launching Erection ,1980.3

2 H. IKEDA, M. AZETA, H. AKIYAMA, K.SHOJI, Y.MATSUO: Design of Kazura Bridge, Proceedings of the 11th Symposium on Developments in Prestressed Concrete, Japan Prestressed Concrete Engineering Association, pp. 55-60, Nov., 2001

DESIGN AND CONSTRUCTION OF ISHIBASHI KAMINOKAWA VIADUCT (OVERBRIDGE PART)

Norifumi Wada Shin-ichiro Kamino
Japan Highway Public Corpration
JAPAN

Noriyuki Monma Hirayoshi Imai
Kawada Constrauction Co.,Ltd
JAPAN

Keywords: 3-night consecutive incremental launching,cantilever,launching girder,temporary pillar

1 INTRODUCTION

This report is on the design and construction of 3-span continuous rigid-frame box-girder bridge, the overbridge part of JR Tohoku Shinkansen, Tohoku Honsen, and Cargo Line (total 17 lines) in the Kitakanto Expressway Ishibashikaminokawa viaduct superstructure construction.

The upper air of Tohoku Honsen down line and Tohoku Shinkansen is constructed by incremental launching method, the upper air of Tohoku Honsen up line and Cargo Line is by cantilever method, and the central joint part is by cast-in-place. Specially, the incremental launching part is launched at a time within the stop time of feeding electricity for Shinkansen and Tohoku Honsen after constructing the launching girder that is a special case. (Fig. 1)

First, 122.0m girder is constructed with cantilever method with the center of P26, and the span of P27 side is constructed by hanging support. Next, 96.0m girder of P24 side is by incremental launching method, and the center span is by hanging support to complete the structure system.

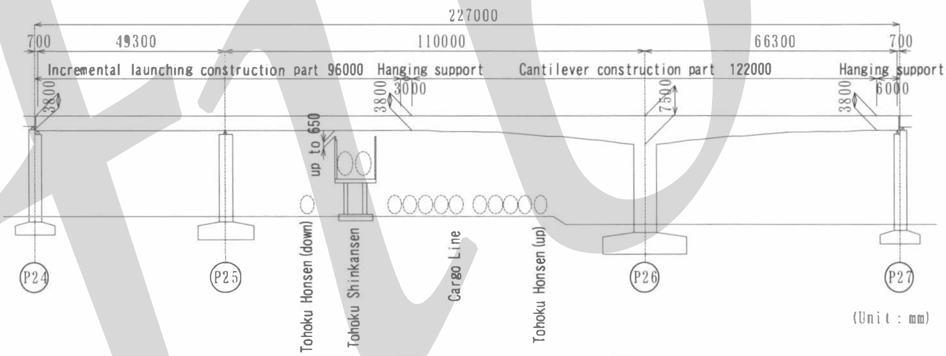

Fig. 1 Ishibashi Kaminokawa Viaduc General View

2 POLICY OF INCREMENTAL LAUNCHING CONSTRUCTION

1) Incremental Launching Part's Separation into Blocks

①Supporting on more than two points

②Three-night consecutive launching for the upper air of JR during power supply is stopped.

To meet the above conditions, large block of 96m shall be manufactured at a time.

2) Incremental Launching Method

Incremental launching method shall be concentrated method, and launch with the support point of P25 so that turning of support point will be unnecessary. Max stroke 30cm and 3700kN center-hole jack was used for incremental launching unit considering the launching weight (approx. 3000t), longitudinal slope (Max 3%) and friction factor (5%). Launching speed is approx. 1 min for 1 stroke of 25cm push back, and transfer speed was decided with 1.5 safety rate.

Considering not making temporary structure in JR site and launching speed, launching girder length was decided as below.

Launching girder length 33m = (Launching side margin 5m + Upper air of Shinkansen 23m + Center closing part 3m + Cantilever side margin 2m)

3) Span of Temporary Pillars

Main girder of incremental launching part is the portion with negative bending moment at most of the part on the completion system. To minimize the changes of bending moment on completion and construction, also to repress the positive bending moment and to be able to construct without placing installation prestressing steels, further to make the maximum reaction force at the temporary pillar shall be below 10000kN and temporary support size shall be approx. 40cm x 100cm, the span of temporary pillars were decided to be 12m.

4) Incremental Launching Step

Incremental launching step (Fig. 2) is as below. 3-night consecutive incremental launching is made at STEP 3-6.

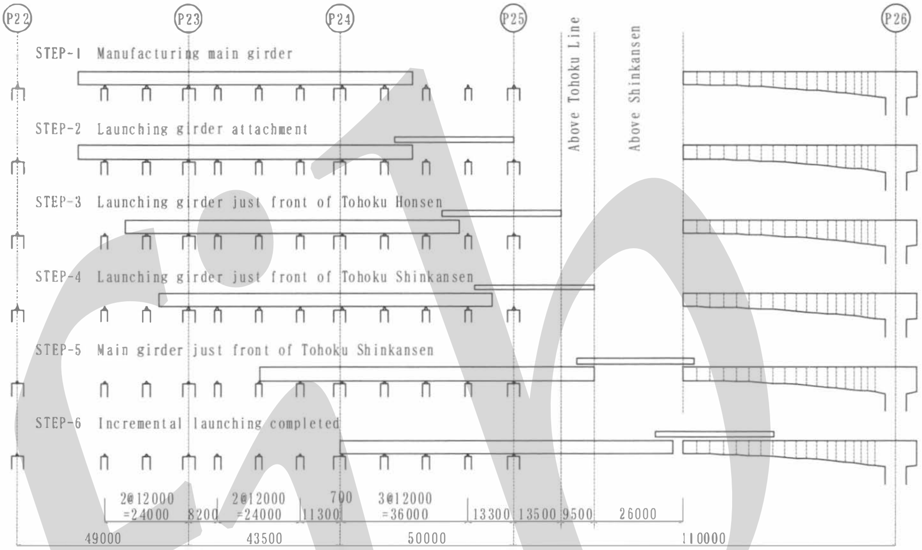

Fig. 2 Incremental launching steps

3 CONCLUSION

Incremental launching construction of down line overbridge part was carried out three times from February 26 to 28, 1999 at night. During the incremental launching works at night, reaction force of sliding bearing, strain, incremental launching force, and transfer distance were automatically measured to continuously check the sinking of temporary pillar, and cracks of the bridge. Incremental launching construction of up-line overbridge part was carried out three times at night from October 9 to 11, 1999. The incremental launching construction was completed smoothly same as the result of down line.Ishibasikaminokawa viaduct were completed at June 28,2000. Presently, Kitakanto Expressway is partially opened to traffic.

The characteristic point of the construction is to carry out construction securing normal operation of JR line utilizing the combination of incremental launching construction and cantilever construction. We would be glad if our method will be a reference for the planning of construction methods for railway, road, and city center with limitation of space below the girder.

REFERENCE

[1] Fuse, Kamino, Tanaka, Imai: Planning and Design of 3-span Consecutive Rigid-frame Bridge with Combination Method of Incremental Launching and Cantilever. The 8th Symposium Papers for Prestressed Concrete Engineering Association, pp.447-480, 1998

[2] Koga, Kobayashi, Hosokawa, Onishi: Batch Incremental Launching Method of PC Girder Bridge (Ishibashi Overbridge) above Shinkansen. The 9th Symposium Papers for Prestressed Concrete Engineering Association, pp.227-282, 1999

[3] Wada, Fuse, Kamino, Imai: Design and Construction of Ishibashi Kaminokawa Viaduct (Overbridge Part). Journal of Prestressed Concrete, Japan, pp54-58,Vol42 No1, 2000

DESIGN AND CONSTRUCTION OF THE NEW HAMANA LAKE BRIDGE

Tadao WAKASA, Mitsuo OKADO, **Masato TADOKORO*** and Kenichi SATO
New Structural Engineering, Ltd.
Japan

Michio MATSUI
Shizuoka Prefecture
Japan

Keywords: 9 spans continuous PC box girder, rigid frame structure after erection, indeterminate force

1 INTRODUCTION

The new HAMANA Lake Bridge is a 9 spans continuous prestressed concrete box girder bridge that will be constructed on the east coast of the HAMANA Lake in SHIZUOKA Prefecture (refer Fig. 1). This bridge will constitute the entrance road for the "SHIZUOKA International Gardening Exhibition" meeting place that will be held on the Shounai peninsula in 2004.

The sand and gravel foundation layer is found at a depth of 35 to 40 m, under a fragile alluvium silt layer, and the bridge shall be founded on depth foundations. Due to that bad ground quality, a rigid frame structural system has been selected. The result of this structural choice, which improve the stiffness of the whole structure, gives smaller displacements under earthquake and an efficient distribution of reaction that improve the seismic resistance of the bridge.

To reduce the effects of creep and shrinkage, the connection between deck and piers is movable during construction and the final embedded connection is made with vertical tendons placed between deck and piers after completion of the whole structure. With this method, the standard continuous rigid frame bridge length can be exceeded.

This report presents the design and construction of this bridge.

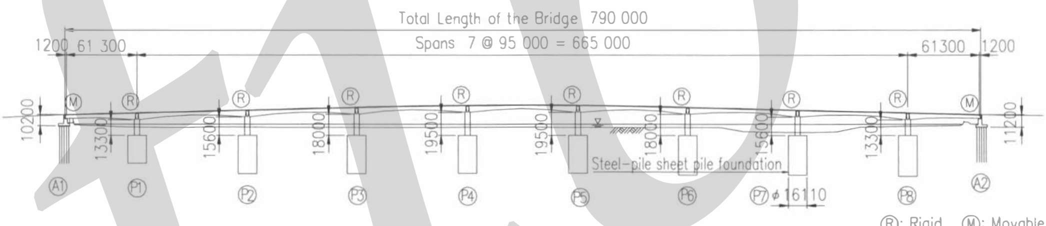

Fig. 1 Vertical alignment of the bridge

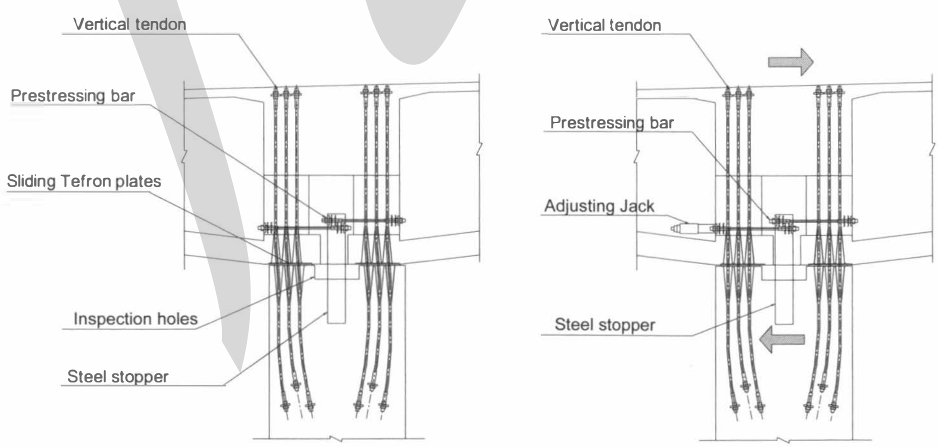

Fig. 2 Lateral view of the rigid frame connection during and after construction

2 CONTINUOUS RIGID FRAME STRUCTURE AFTER ERECTION

The method used for this bridge consists in the adoption of movable bearings during erection. After completion of the girder, the forces due to creep and shrinkage of the girder were released and the rigid frame structure is obtained by a vertical prestressing arranged between the girder and the top of the pier connecting the superstructure and the substructures.

By delaying the rigid connection in this way, the indeterminate forces due to creep, shrinkage and longitudinal prestressing can be strongly reduced. The main points of the design of the rigid connection are the followings:

① The creep and shrinkage effect was reduced by use of sliding Teflon plates.
② Trumpet shaped sheaths able to absorb the longitudinal displacement between the girder and the piers have been designed for the vertical tendons.
③ Steel stoppers, connected to the girder crossbeam with prestressing bars, have been designed on the top of the pier, allowing an adjustment of the displacement under creep and shrinkage.
④ Inspection holes designed in the crossbeams allow check and measurement of the longitudinal displacement.

The rigid frame structure after erection and details of the pier top are shown in Fig. 2.

The adoption of a rigid frame structure only after erection allows a longer fixed span length for multi-spans continuous rigid frame structure, even in the case of small pier height.

3 LONGITUDINAL PRESTRESSING OF THE GIRDER

The longitudinal prestressing of the girder comprises internal tendons designed for the loads during erection and external tendons placed after erection for the in service loads.

The int. tendons are located in the upper slab allowing a reduction of the webs thickness to 300 mm.

4 CONSTRUCTION METHOD SELECTION

The main construction conditions for this bridge are the following:

① Marine equipments are required for transport and supply of materials by a cantilever erection method with traveling formwork as the bridge is erected over the lake.
② The construction location is the famous fishing zone of the HAMANA Lake.
③ The duration of the construction shall be short.

Considering these conditions for the construction of the main girder, a cantilever erection method with movable erection girder was adopted. The Polensky & Zollner AG Company from Frankfurt in Germany has developed this method.

5 CONCLUSION

If the fixed span length of multi-spans continuous rigid frame structure is long in comparison with the pier height like for this bridge, it sometimes becomes difficult to deal with the resistance in the end piers. There was a conventional limit for this relation.

We expected that the development of multi-spans continuous rigid frame structure, which is economic and excellent for seismic resistance, could be increase by the adoption of a rigid frame structure only after completion like this bridge.

We hope that the rigid frame structure construction method exposed in this paper will be able to contribute to this development.

REFERENCES

[1] Survey and research regarding to the new structure case of PC bridges: (an incorporated foundation) highway investigation committee 1996.3
[2] P & Z construction method "the guidance of design and construction": P & Z organization 1999.10
[3] Kubota, Shimokawa, Takena: the development of the new technology for long bridge construction of highway together with railway concomitant: Committee of Civil Engineering 1983

PLANNING AND CONSTRUCTION OF SHIN-ITAJIMA BRIDGE

Akinori Oeki
Kawada Construction Co., Ltd
JAPAN

Takao Takashima
Ministry of Land, Infrastructure
and Transport Sikoku Bureau

Masayosi Higuchi
Kawada Construction Co., Ltd
JAPAN

Keywords: prebeam girder, girder height reduction, maintenance, life cycle cost, environmental loading

1. INTRODUCTION

The 21st century is a major turning point for planning Japan's social capital with the background of regional differences including less children and aging society, advanced information technology, environmental problems, decreases in population, etc. Under these circumstances and to structure rich and prosperous society, wide regional network necessary for communication zone including wide-area municipalities independent in terms of life and economy is required.

On the other hand, effective planning of social capital is also necessary under the recent bleak economy. Especially, considering the increasing concrete structures being degraded recently and also maintenance for the social capital structured in the high economic growth period, reduction of total costs such as improved durability is strongly requested for maintaining the social capital after this.

This report includes the effects obtained as a result of adopting a composite structure named Prebeam for the superstructure of the bridge (hereafter "Shin-itajima Bridge") at Route 56 Uwajima Road, one of the wide-band networks currently under maintenance.

2. FEATURES OF SHIN-ITAJIMA BRIDGE

2.1 Outline of the Construction

Structure type: Compound beam with sequential prebeams on 5 spans
Bridgelength:130m(Span:21.4m+3@28.5m+22.2m)
Effective width: Driveway 7.5m+footway 3.5m
Bridge class: B live load

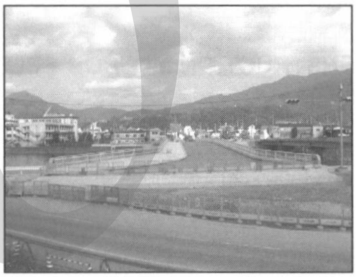

Photo-1 Shin-itajima Bridge

2.2 Features of the Construction

Shin-itajima Bridge was built at the river mouth area in a river flowing in Uwajima city, and there were following restriction. **Photo-1**

①Reducing the height of the structure to minimize the influences to the surrounding houses.
②Taking counterplans for salt damages and decrease maintenance costs.
③Securing the working yard at the town area.
●Mutual-hanging construction method by crawler crane using temporary pier when constructing the substructure. The temporary pier had to be removed in early period to start common use with Itajima Bridge. **Fig-2 Photo-2**

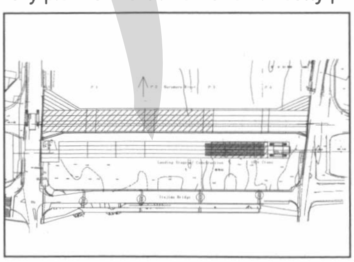

Fig.1 Top view of the construction

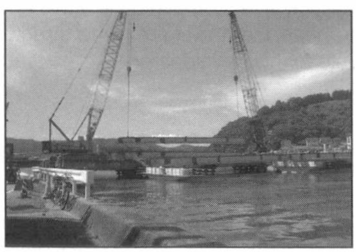

Photo 2 Constructing condition

3 ADOPTION OF PREBEAM METHOD

3.1 Features of Prebeam Method

Prebeam method utilizes the flexural rigidity of steel beam and prestress is applied to the lower flange concrete. **Fig. 2**.

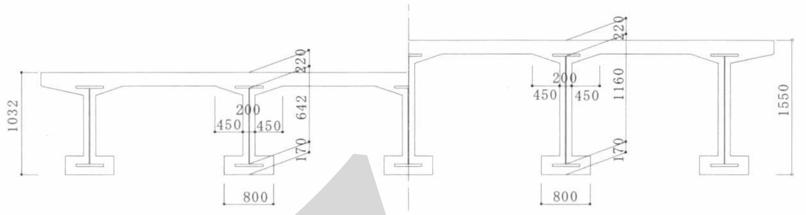

Fig. 2. Cross section of prebeam girder

①The steel girder is I-girder assembled and welded with specified arch.
②High-strength (σck=45 N/mm2) for lower flange concrete. High-quality water reducing is used for mixing 33% water-cement ratio and 18cm slump
●Recently, after applying the stress of prebeam, the segment method to split into segments, transport, and connect at the constructing point is often adopted.
④ Dead load is relatively small and small influence to the substructure.

⑤Large girder rigidity reduces bending and vibration during transportation.

Photo 3 Manufacturing segments

4. APPLICATION AND EFFECTS OF PREBEAM METHOD

Prebeam method was applied for the bridge as described below.
①Girder height of the bridge edge part is 103.2cm (H/L=0.046)
②The segments were manufactured in the factory during construction of substructure, and the works to web concrete was carried out at the factory as shown in **Photo 3.**

The effects obtained from the above method are described below.
①Repressing the girder height enabled to lower the height of landfill at the access road, and minimized the influence to the surrounding houses and intersections.
②In the area influenced by salt damage, steel girder was coated with concrete to reduce the maintenance cost.
③Segment method shortened the field construction period for approx. 4 months and reduced the load to the local habitation and transportation environment.
④Shortening the field work process restrained the amount of construction wasted from making and removing the manufacturing yard.
⑤Started manufacturing of girder simultaneously with the construction of substructure, and just after completing the substructure construction, we started main construction of the bridge.
Accordingly, we completed removing the temporary bridge approx. one month after finishing the substructure and it realized lower costs than the initial design.

REFERENCE:

(1) Uwajima Road: Ministry of Land, Infrastructure and Transport, May 2001
(2) PREBEAM: Prebeam Association, No.12, 1999

CONSTRUCTION OF AGANOGAWA BRIDGE OF THE NIHONKAI COASTAL TOHOKU EXPRESSWAY

Kaoru Sakamoto Nobuyuki Yamada
Hokuriku Branch of the Japan Highway
Public Corporation,JAPAN

Shuichi Takefusa Hiroaki Okamoto
Kajima-Kawada-Tobishima Joint Venture
JAPAN

Keywords: Precast segment method,Long-line match cast method,Balanced cantilever method
Span-by-span method

1.INTRODUCTION

The Nihonkai Coastal Tohoku Expressway("Nichi-en Express way") is 440 km in total length and extends from Niigata to Aomori cities along the coast of the Sea of Japan. Aganogawa Bridge is located at one end of expressway and is a 951 m - long 12-span continuous prestressed concrete box girder bridge across Agano River,which flows from southeast to northwest through the center of Niigata Prefecture.The bridge was constructed using the precast segment method,and the segments were produced long line match casting.The bridge was erected mostly by balanced cantilever using by erection girders and partly by span-by-span construction.

2.PRODUCTION OF PRECAST SEGMENTS

We used the long line method for constructing Aganogawa Bridge due to the following three reasons : i) the configuration of the yard for producing segments was appropriate for the long line method, ii) the structure of the main girder has a varying cross section, and iii) it had been decided to erect the bridge by balanced cantilever.

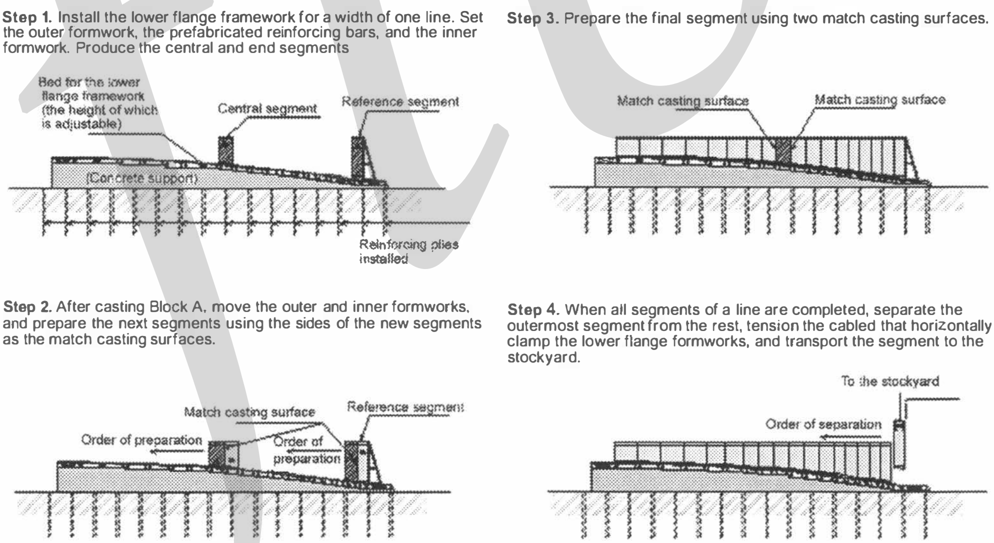

Fig.1 Process of segment production

3.ERECTION OF PRECAST SEGMENTS

Precast segments are usually erected by span-by-span construction when the span is relatively short and by balaced cantilever for relatively long spans. This bridge was erected by span-by-span construction for side span section,where the clearance under the girder was limited,by lifting segments. The other spans were relatively long (83.5 m on average) and were erected by balanced centilever. Figure 2 shows the process of segment erection by the span-by-span and balanced centilever methods.

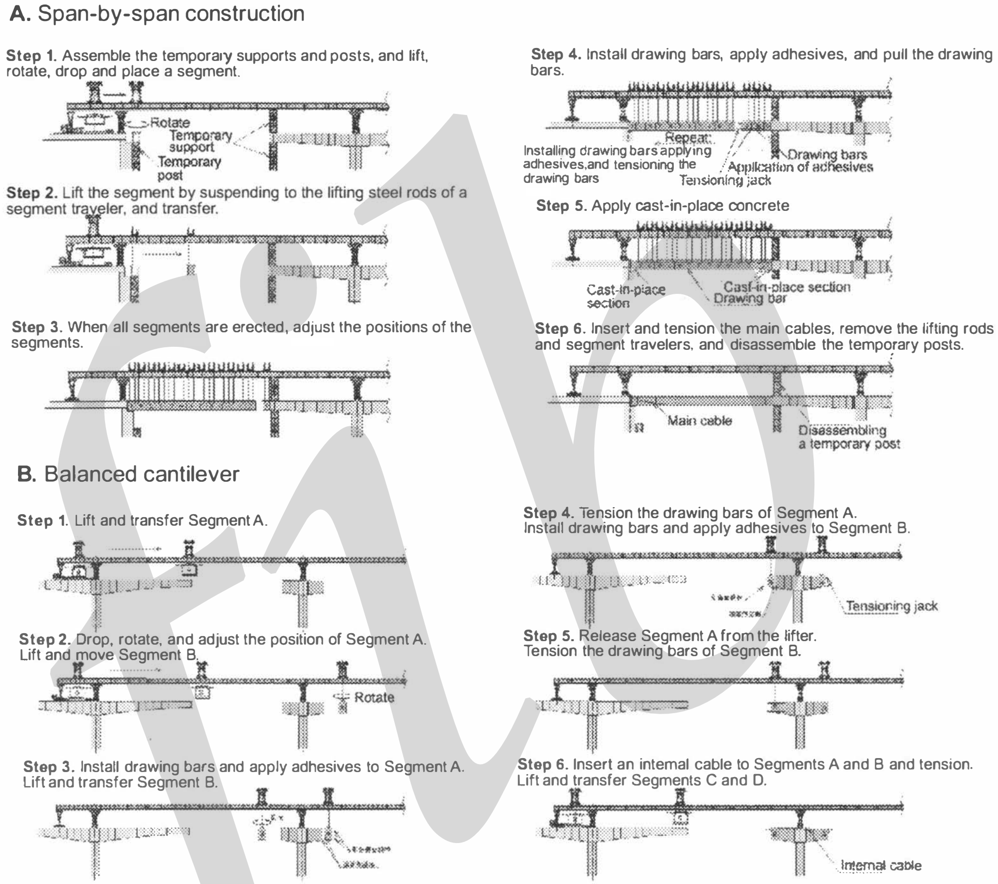

Fig.2 Process of segment erection

REFERANCES

1)Chikuni, Yamada, Ito, and Asano: Nihonkai Coastal Tohoku Expressway, Construction of Aganogawa Bridge -- Preparation of precast segments by long line match casting -- (in Japanese), Proceedings of the 10th Symposium on the Development of Precast Concrete,October 2000.

2)Sakamoto, Morooka, Okamoto, and Asano: Nihonkai Coastal Tohoku Expressway Constructon of Aganogawa Bridge -- Erection of precast segment -- (in Japanese), Proceedings of the 11th Symposium on the Development of Precast Concrete,November 2001

3)Sakamoto, Morooka, Takefusa, and Okamoto: Designing and constructing precast segment bridges of varying cross section --Nihonkai Coastal Touhoku Expressway, Construction of Abeno-gawa Bridge (prestressed superstructure) --(in Japanese), Prestressed Concrete, Vol.43,No.3,May 2001/

ADVANCES IN THE EXTERNAL POST-TENSIONING OF SEGMENTAL BRIDGES

Prof. Dipl.-Ing. Dipl.-Kfm. Christian Brockmann Dipl.-Ing. Steffen Springer
University of Applied Sciences, Bremen, Germany

Keywords: External post-tensioning, segmental bridges, elongations, camber, temporary post-tensioning

1 INTRODUCTION

The significant advantages of segmental bridge construction in combination with external post-tensioning promoted in recent years the erection of numerous bridges of this type throughout the world. The greatest benefit in comparison to conventional bridge building methods is the shorter construction period and therefore a considerable reduction in cost. A very high quality can be assured due to the industrialized prefabrication of segments. Segmental bridges with external post-tensioning have been built in various climatic conditions and perform to the full satisfaction of the owners.

This paper is based on experience gained by Bilfinger Berger AG during the construction of numerous segmental bridges in Africa, Asia and Australia. A total amount of 3.000.000 m² bridge deck area erected in recent years led to a sound knowledge of the construction method and the highly developed post-tensioning systems. Conditions that favor this method as well as the problems of external post-tensioning (bowing effect, deflections, camber, elongations, and temporary post-tensioning are discussed by the example of the BangNa-Trad Expressway (Thailand), where segments of 27.20 m width were used.

2 DEFORMATIONS

2.1 Segmental construction and match-casting

The principal of segmental construction is to assemble a bridge span from transversal segments which are placed by erection girders and then connected by external longitudinal post-tensioning. The match of adjacent segments is one of the key problems of this method. By the external post-tensioning a force up to 7.800 t must be transferred through the joints. If these do not fit perfectly together, they will crack under such loads. Dry joints without any filler, such as epoxy, exacerbate this problem.

The fit of the segments can only be insured by the so-called match-cast method. As a principle, the former segment is used as bulkhead for the successive one. From match-casting, joints will result which initially (at t_0 = 0 hrs.) fit perfectly together. Since a new segment "N" will be cast against its predecessor, the old segment "N-1" will experience a temperature increase due to the developing hydration heat of segment "N". This temperature increase will be transferred through the match-cast joint. Due to differential temperature between the hardened and the fresh concrete, segment "N-1" will bulge into segment "N". Since the concrete of segment "N" is still fresh when this happens, there will remain a permanent curvature after setting of the concrete. This phenomenon is called "bowing effect". The elastic deformation of segment "N-1" due to differential temperature will leave a gap between the segments (at t_1 = 10 hrs.). Right at the wing tips the joint will be thoroughly closed and it will gradually open towards the center of the segment. The critical aspects of this problem are that bowing effect deformations will add up over the length of the span.

Empirical evidence of the bowing effect for a single 27.20 m wide segment could not be measured. For a whole span, however, the gaps added up to approx. 10mm after applying the initial post-tensioning. They were distributed over 17 joints and it did not pose any problems when erecting the segments on site. After the full post-tensioning force was applied the joints were closed tightly.

Because of the great slenderness of the segments, time dependent deformations such as creep and shrinkage can pose problems and must be controlled tightly. Mostly, the different transversal stiffness between the pier segments and the typical segment is of importance. In addition to the different stiffnesses , different layouts for the transverse post-tensioning can complicate the matter. Evaluation of a test span showed differences in deflections of up to 4.0 cm right at the wing tips, which was not acceptable for site production. After a careful assessment of this phenomenon it became necessary to adjust the initial p/t in transverse direction.

3 EXTERNAL POST-TENSIONING

3.1 General requirements

In general the requirements on external p/t systems can be summarized as follows:

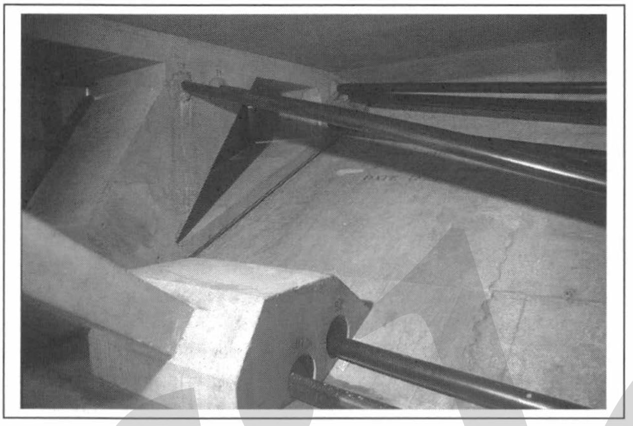

- Durable corrosion protection of the p/t steel
- Straightforward replacement of tendons
- Easy re-stressing of tendons

In consideration of the non-severe corrosion environment in Bangkok and the applicable specifications, a grouted external p/t system was chosen with tendons of up to 22 strands (0.6" diameter and 260 kN ultimate load/strand). The corrosion protection is ensured by a HDPE duct with a diameter of 110 mm and a wall thickness of 5.2 mm..

Figure 1: External tendons, deviator block, typical and pier segment

3.2 Longitudinal deformations due to post-tensioning

An important part of the design is both the computation of longitudinal deformations due to the application of the p/t forces and the determination of anticipated deformations during the lifetime of the structure. The aim was to guarantee leveled spans after 4.000 days. During and after erection a constant survey was conveyed which showed that the actual displacements of the spans were smaller than the computed ones. In the end, the spans were cast without any camber for the 27.20 m segments.

3.3 Elongations – a question of Quality Assurance

During the design stage it is the normal approach to use conservative stressing coefficients according to applicable codes, such as AASHTO, for the computation of p/t losses. This is justified, since specific p/t system parameters are not yet available. For the production of shop drawings and stressing protocols the specific values are, however, required. Big projects often justify a field test in order to determine specific parameters. This was done on the BangNa-Trad project with a one-to-one test span of 44.40 m length and 27.20 m width. The differences of the p/t parameters between design assumptions and field values proved to be of importance.

3.4 The application of temporary prestressing

While an initial p/t force of 100 bars is more than sufficient in conventional applications and segmental construction with temporary stressing measures, this initial stress has proved not to be sufficient to control the joint closure without temporary stressing. An initial force of 100 bars would be sufficient to take the slag out of the tendons but resistant joints can withstand this pressure. These joints will then influence the calculated elongations in a negative way, since they are only closing while recording the elongations. In order to overcome this problem, tests were performed and finally a new initial p/t sequence was designed. According to this new method up to 10 out of a maximum of 20 tendons were stressed up to 250 bars without registering elongations. Then the first tendon in row was stressed up the to final force with recorded elongations. With this method, obviously it is not possible to control the affected tendons during the first 250 bar but the relatively small force and the small likelihood of serious blockage along the tendon justify this approach. Once this method was introduced the theoretical elongations could be matched correctly.

DESIGN OF PRECAST SEGMENTAL BOX GIRDER BRIDGE WITH STRUTTED WING SLAB

Norio Terada Atsushi Homma Tadashi Kuroiwa Kimio Saito
Nihon Doro Kodan, Shizuoka Construction Breau Kajima Corporation
JAPAN JAPAN

Keywords: precast segment, strutted wing slab, progressive erection

1. INTRODUCTION

The Uchimaki Viaduct is a multiple span continuous box girder bridge that will be constructed as part of the New Tomei Expressway. Diagonal struts support the wing slab of the superstructure. Application of the diagonal struts reduces the self-weight and bottom slab width, and therefore allows the scale of substructure including pier columns and foundations to be reduced.

Since 36 of 42 spans are standardized into approximately 50m, span-by-span erection with precast segments is applied. The central rectangular part of the box girder section is fabricated as a precast member (hereafter referred to as the 'core segment'), which does not include most of the wing slabs in order to obviate the need for large-scale erection facilities or casting and storage yards. Cast-in-place construction with form travelers is applied to the wing slab (Fig. 1). For the Uchimaki Viaduct, precast concrete struts are adopted. After struts are installed to the core segments, concrete of the wing slab is placed.

Reporting on the design of the superstructure of the Uchimaki Viaduct, this paper focuses on the transverse design considering the effect of the diagonal struts and the longitudinal design considering the time-dependent effects for both the precast core segments and the cast-in-place wing slabs.

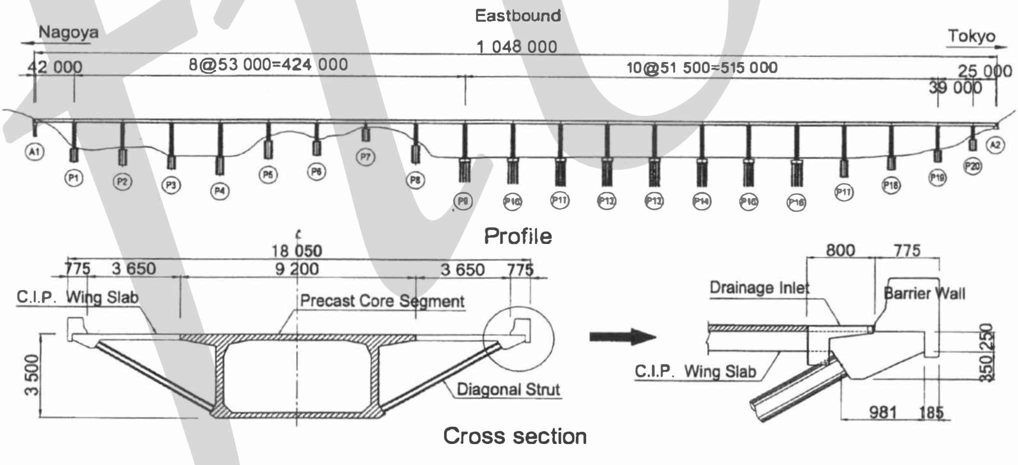

Fig. 1 General view

2. DECK SLAB AND STRUT DESIGN

For the purpose of designing the deck slab, a cross section in which a strut is located and a cross section between strutted cross sections were defined as design sections. Sectional forces were calculated through a 3D FEM analysis using solid elements.

3D FEM showed similar bending moment distributions at both design sections excluding the portion around the strut connecting point. As a result, there was no difference between the required PT tendons for both design sections.

The 3D FEM indicated that sectional forces in struts under the load combination excluding the wind effect are dominated by the axial compression, and that the bending moment and shearing force are very small. Tensile stress, therefore, will not be induced in the cross section of the struts.

Meanwhile, the axial compression will be drastically decreased by the wind effect, because a 9m-high noise-cutting wall will be installed at both side ends.

3. LONGITUDINAL DESIGN

In the longitudinal design, the core segments and wing slabs are treated as individual members even though they are integrated. Tensile stress is not allowed for the core segments, while for the wing slabs, tensile stress of less than the tensile strength of the concrete is allowed.

All post tensioning tendons were externally assembled. The longitudinal tendons can be divided into two types: primary tendons to be tensioned after core segment erection and secondary tendons to be tensioned after wing slab construction. To introduce as large prestress as possible into the wing slabs, the number of primary tendons is minimized and secondary tendons are used as much as possible. In a typical span, fourteen 27-15.2mm-strand tendons, consisting of eight primary tendons and six secondary tendons, are installed.

In the construction method utilized for the Uchimaki Viaduct, there occur differences in creep and shrinkage between core segment and wing slab. In the longitudinal design of the Uchimaki Viaduct, the effects of these phenomena were evaluated by Mattock's method, which is often used when designing a composite girder bridge.

The magnitude of internal stresses is related to the difference in age between subsections. Focusing on the stresses in a wing slab, as the difference in concrete age between subsections increases, the internal stress varies from compression to tension.

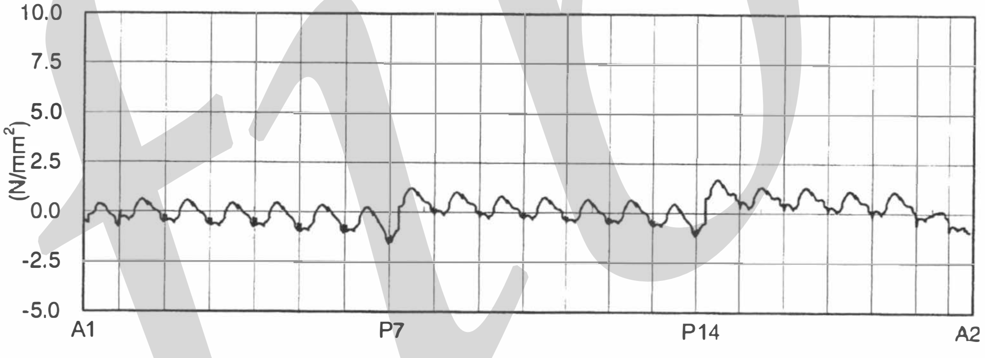

Fig. 2 Internal stress distribution in the wing slab

4. CONCLUSION

This paper has reported on the superstructure design of the Uchimaki Viaduct, a box girder bridge with strutted wing slab that will be constructed by the combination of precast core segments and cast-in-place wing slabs. The deck slabs, struts and edge beams are strongly interrelated. In the design of the Uchimaki Viaduct, those interactions were analyzed through 3D FEM. In the longitudinal design, the influence of internal stresses due to differences in creep and shrinkage of the core segments and wing slabs was taken into consideration (Fig. 2).

REFERENCES

1) Yasuo INOKUMA, Atsushi HONMA: Study of a PC Box-Girder Using Corrugated Steel Webs and Cantilever Deck Slab Supported by Inclined Struts, Journal of Prestressed Concrete, Japan, Vol. 40, No. 5, Sep.-Oct., 1998

2) Kimio SAITO, Atsushi HOMMA, et al.: The Superstructure Design of the Uchimaki Viaduct, The 11th Symposium on Developments in Prestressed Concrete, Japan, Nov., 2001

DESIGN AND FABRICATION OF PRECAST SEGMENTS PRESTRESSED TRANSVERSELY IN THE SLAB BY MEANS OF LARGE CAPACITY PRETENSIONING METHOD – PRETENSIONING METHOD USING EXTRA FAT STRANDS –

Hiroyuki Ikeda,Terumi Kato, Masami Fujita
Japan Highway Public Corporation

Mikio Hara, Hiroyuki Aburano
Nippon P.S CO.,Ltd

Keywords : Large Capacity Pretensioning Method , The constant used in design , Precast Segments , Match casting system using a short line

1 INTRODUCTION

Nagashima Viaduct on the Second Tomei Expressway is a bridge constructed at the delta sandwiched by the Kiso River, which comprises the border between Aichi and Mie Prefecture, and the Ibi River. This viaduct is a large-scale bridge and is basically a prestressed concrete (PC) continuous box girder structure consisting of precast segments. A match casting system using a short line was adopted as the segment fabrication method with transverse prestressing of slabs done by a large capacity pretensioning method employing ϕ21.8 prestressing strands. As for erection, it was done by the span-by-span system employing erection girders for the main roadway and temporarily supports for ramp portions.

In adopting the pretensioning system for transverse prestressing of slabs, the characteristics of large capacity pretensioning method were grasped through experiments, following which application to segments was examined. As a result, it was found the problem of elastic deformation due to prestressing was an obstacle to precasting, so a precast segment fabrication system using a reaction beam type prestress transferring device differing from conventional apparatus was adopted to deal with the problem.

This report describes the transverse prestressing system adopted for Nagashima Viaduct and the segment fabrication system using this device.

2 STUDY FOR USING LARGE CAPACITY PRETENSIONING METHOD

1.1 Study of Large Capacity Pretensioning tendons

The ϕ21.8 prestressing tendons were composed of three layers of element wires,differing from the conventional strand composition of ϕ15.2 prestressing tendons (double-layer stranded wires))(**Fig.1**).

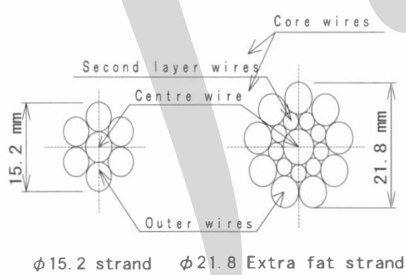

Fig.1 Difference of prestressing tendons cross section

As results of mechanical property confirmation tests, special features such as slipping phenomena of core wires and increase of bonded anchoring length were found and, at the same time, that these features were influenced by the quality of concrete was ascertained[1].

Hence, based on the results, bond transfer length of 90ϕ as the constant used in design and 0.7 σ_{pu} as stress intensity of steel at failure used for checking at ultimate load were decided upon. As for slipping in of core wires, indentation of element wires of prestressing strands was done a measure to eliminate slipping.

1.2 Study for Precast Slab Application

At Nagashima Viaduct, the situation was that a large fixed abutment system was difficult to provide form the standpoint of the segment fabrication yard layout so that a prestressing device with compact reaction beam was developed, and the problems of deformation and movement by prestress transferring were dealt with using the system of the following concept:

1) A reaction beam type prestressing device with a traveling apparatus
2) A prestressing device what can traverse to previously cast segment (herein to be called "OLD segment") position for match casting.
3) De-stressing of OLD segment 2 days after a NEW segment is cast

3 REACTION BEAM TYPE PRETENSIONING DEVICE[2]

The reaction beam type-pretensioning device is as shown in **Fig.2**, with compression beam, reaction prestresing tendon rod, anchoring post, and all-direction rubber hinge as principal members. The construction is such that when pretensioning tendon is tensioned, the tensioning force on the anchoring post will be transmitted to the reaction-prestressing rod by means of the rubber hinge. After tensioning, reaction force will act on the compression beam with both ends hinged, and the reaction steel rod and pretensioning tendon located above will be in a balanced state. As a consequence, tensioning force is maintained inside the device and does not act outside so that the device can be moved while only being supported.Releasing the pretensioning tendon fixed to the anchoring post does transfer of prestress, and at the time of operating the jack for releasing, the device is displaced by the elongation-contraction effect and the hinge effect of the rubber hinge, so that the segment will be in an immovable state.

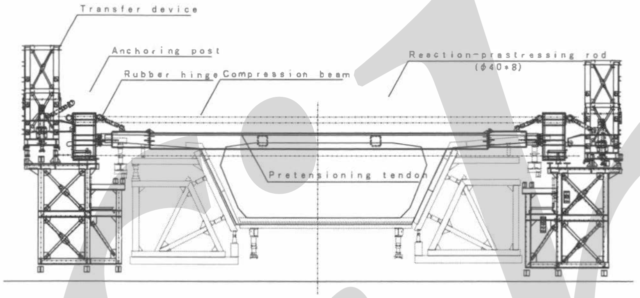

Fig.2 The reaction beam type-pretensioning device

4 SEGMENT FABRICATION SYSTEM

The segment fabricating system employed at Nagashima Viaduct were two reaction beam type pretensioning device units, the time of transferring prestress being controlled by moving the devices and fabricated segments integrally. The devices move transversely atop the platform for movement, while movement up and down is by an oil hydraulic jack for vertical movement. The segment placed moves integrally with the pretensioning device toward the OLD segment. After movement, without prestress yet transferred, the next NEW segment is made. Transfer of prestress is done after completed match casting and separating the OLD segment. The OLD segment is hauling out after cutting the prestressing tendons, lifting up the device.

5 CONCLUSION

At Nagashima Viaduct, it was succeeded in utilizing the advantages of pretensioning systems without hindering the fabrication cycle by a moving prestress transferring device using a large capacity pretensioning system. With this system, even though it is a pretensioning system, there is the feature that it is possible to control the time of transferring prestress and sufficient curing period can be secured, concrete strength at the time of transferring prestress could be stabilized, and increase in bonded anchoring length of prestressing tendon , which is the problematic point in large capacity pretensioning method, prevent.

REFERENCES

[1]Ikeda, Katou, Hara and Aburano : Pre-tension System Evaluation Experiment with ϕ 21.8 Steel Strand Wire, pp.97-102 Proceedings of the 9 th Symposium on Developments in Prestressed Concrete, Oct. 1999

[2]Komatsu, Ikeda, Katou and Hara : Transverse Prestress of Slabs by Large Capacity Pretension Steel, pp.361-366 Proceedings of the 10 th Symposium on Developments in Prestressed Concrete, Oct. 2000

STUDY OF LONG TERM BEHAVIOUR OF ESPIÑEIRO, FERREIRAS, ACEBO AND SELLA VIADUCTS

Leonardo Fernández Troyano
Carlos Fernández Casado S.L.
Ph. D. Civil Eng.
Grijalba, 9. 28006 Madrid
Spain
cfcsl@cfcsl.com

José Ignacio González Esteban
Fomento de Cons. y Contratas
Ph. D. Civil Eng.
Acanto, 22. 28045 Madrid
Spain
jigonzalez@fcc.es

Celso Iglesias Pérez
Carlos Fernández Casado S.L
Ph. D. Civil Eng/MSOA(ENPC)
Grijalba, 9. 28006 Madrid
Spain
cfcsl@cfcsl.com

ABSTRACT

The object of this paper is both presenting the step-by-step erection of two segmental precast bridges and some results of the service analysis of these bridges, accounting for long term effects of creep, self-induced and superimposed deformations. Fig. 1

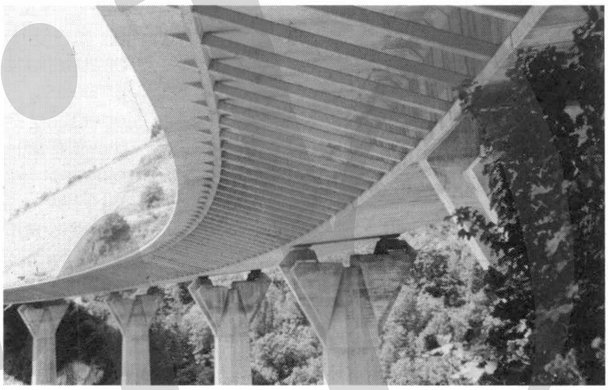

Fig. 1

The deck of these bridges is made in two steps. The core is precast and then the flanges of the box girder are cast in situ. They are supported by means of two precast struts placed at 4 m distance. Fig. 2

Both bridges are erected using the free cantilever method. The precast segments are put in place by means of a metallic traveller. Figs. 3 and 4

The analysis is based on the multilayer model, which has been developed assuming the Navier Law which relates the analysis at a "cross-section level" with the global analysis at a "structure level" and is the consequence of a Ph.D. Thesis developed by one the authors.

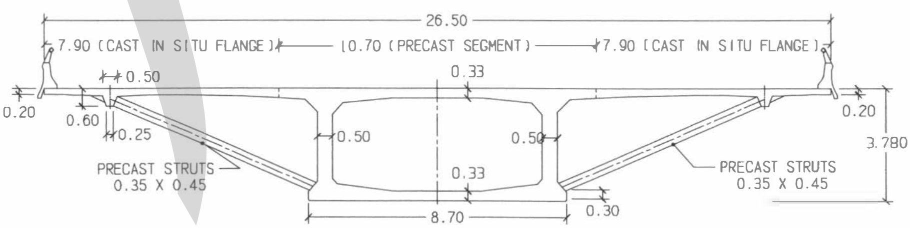

Fig. 2

Fig. 3

As all the prestressing forces are applied only on the core it is important to evaluate how much of the prestressing force is transferred to the flanges. Another important fact is the lack of reinforcement passing through the core which makes very important the correct stress service analysis.

This paper is an attempt to provide a practical treatment of the serviceability analyses of concrete members:
1º. A simplified approach for the inclusion of the time-dependent effects of creep and shrinkage is presented.
2º. An "exact" approach, using the classical incremental time step-by-step procedure, is also presented.
3º. Comparison of both approaches is made showing their advantages and disadvantages.
In both approaches the cross-section may be formed by concrete of different ages, prestressed and non-prestressed reinforcement and even by a section of steel. Any sequence of construction may be taken into account.

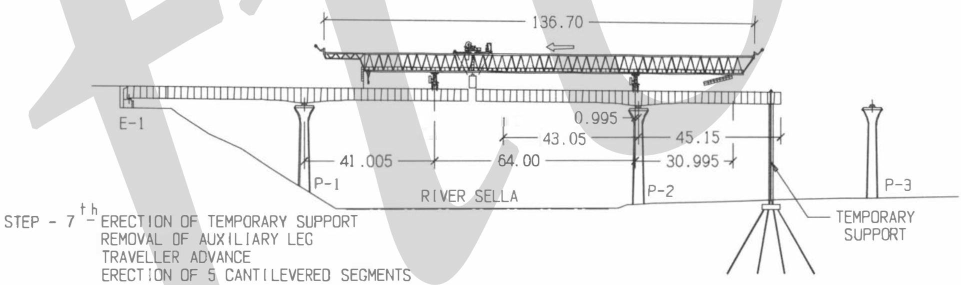

Fig. 4

PRECAST CONSTRUCTION METHOD OF RAILWAY RIGID-FRAME VIADUCT

Toshiaki Oh : Construction Sec., Construction Management Div., Kawada Construction Co., Ltd.
Tetsushi Konishi: Design Sec., Engineering Div., Kawada Construction Co., Ltd.
Hisamichi Hattori: Civil Engineering Technology and Design Div., Production Technology Div., Tokyu Construction

Keywords: HPCa(Half-precast), Railway, Rigid-frame Viaduct

1. INTRODUCTION

To improve the condition of traffic network in urban space being concentrated, railway viaducts according to multiple line and multi-level crossing improvements are being planned and constructed in various fields. Generally, such constructions need to be carried out within temporal and spatial restrictions to give priority to the traffic of operating lines. For this reason, overhead construction just above the operating lines has been done using large-scale falsework in same cases.

Accordingly, we developed "Precast Construction Method of Railway Rigid-frame Viaduct" that factory-manufactured precast columns, beams, and slabs are assembled on site. The method has the characteristic points of ①labor saving on the construction by using precast members combined with function of the form and falsework, ②reduced period of construction and costs according to improvement of working efficiency, and ③stable quality by manufacturing precast members at the factory not affected by weather. The precast members of this method are composed of half-precast (hereafter "HPCa") element and cast-in-place concrete to reduce the weight. It has the function as the form and falsework when building, also functions as a part of structure members after completion, and is combined with cast-in-place concrete to resist against the load.

This report refers to the characteristic points of the method, various test results to confirm the applicability for actual structures executed for developing this method, and the results on construction costs and period, etc. compared with conventional methods. For details of the method, these examination results were summarized and published from Railway Technical Research Institute in March 1999 with a title "Design and Construction Index for Railway Rigid-frame Viaduct by Half-precast Method."

2. OUTLINE OF THE CONSTRUCTION METHOD

2.1 procedures of the method

Fig. 1 shows the construction procedures of the method.

(1) Step 1

After installing HPCa column elements on the foundation, place and connect the reinforcement of axis direction. Arrange the hoops of column base part, carry out root winding and place filling concrete.

(2) Step 2

After installing HPCa beam elements, fix them on the column using beam fixing fixture.

(3) Step 3

After installing and fixing HPCa slab elements, arrange the reinforcement of column and beam connection part, place beam filling concrete to structure the rigid frame.

Arrange the reinforcement on the upper side of slab, and place slab concrete.

(4) Step 4

Construct the surface structures and the viaduct is completed.

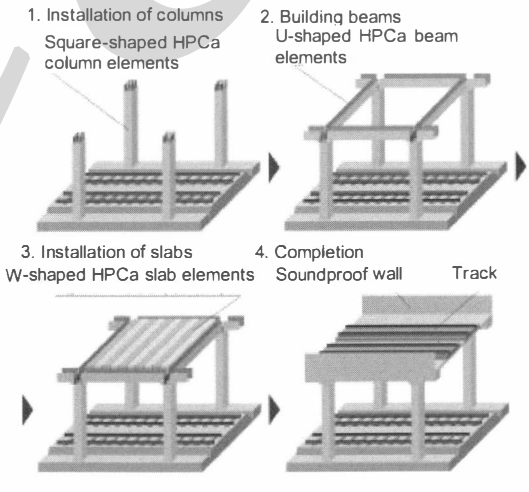

Fig. 1 Concept of construction procedures

2.2 Outline of each member

Fig. 2 shows the shape of HPCa element

(1) Column Member

HPCa column element has hollow cross section, the axis-direction reinforcement is inserted and fixed with grout in the sheath molded in the element's wall.

Hoops are placed surrounding the sheath.

(2) Beam Member

HPCa beam element has U-shaped cross section. Prestressing steel, lower-side axis-direction reinforcement, side reinforcement, and stirrup are placed on the axis direction of the element. During construction, it is simply supported and prestress is applied to resist against the load of self-weight and the weight of cast-in-place concrete. It becomes PPC structure to allow cracks for the load after completion.

(3) Slab Member

HPCa slab element has a convex cross section on the upper side, and prestressing steel are arranged on the element-axis direction, and lower-side reinforcement on the lower-side axis-direction reinforcement and to the element-axis right-angle direction. Lower-side reinforcement at the element connection part of element-axis right-angle direction uses loop joint with excellent workability. During construction, element axis direction is simply supported as one-way slab, and prestress is applied to resist against the load of self-weight and the weight of cast-in-place concrete. After completion, element-axis direction becomes PPC structure, and element-axis right-angle direction to be RC structure.

In addition, on each HPCa element of column, beam, and slab, round-shaped convex (4-5mm height, 40-50mm diameter) is made on the joint surface to secure the integrity with cast-in-place concrete.

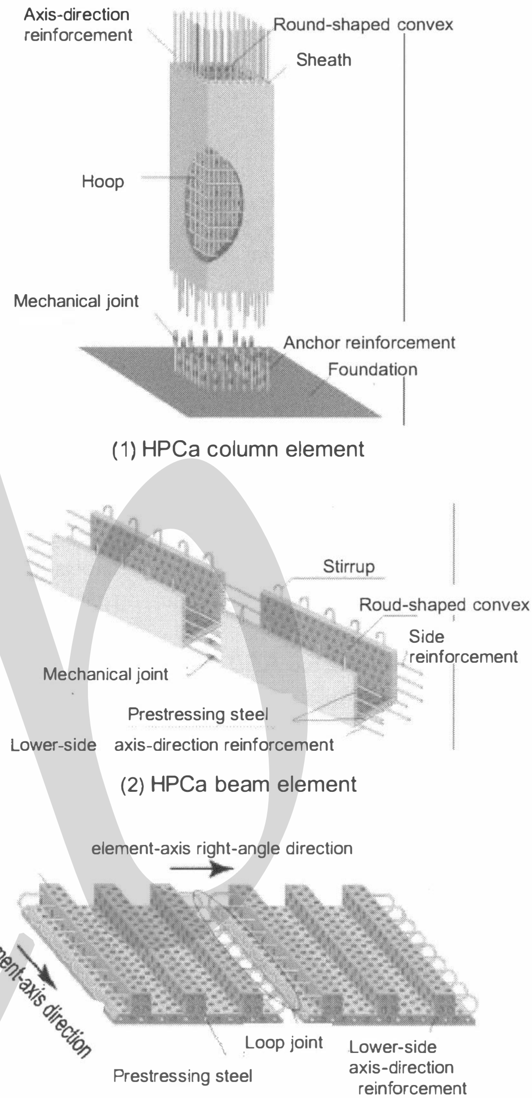

(1) HPCa column element

(2) HPCa beam element

(3) HPCa slab element

Fig. 2 Shape of HPCa element

3. COMPARISON BETWEEN CONVENTIONAL METHOD AND THIS METHOD

The method is most effective in rigid-frame viaduct construction just above operating line in urban area. Approx. 10% of construction costs and approx. 20% of construction period can be reduced with this method compared with conventional methods.

4. CONCLUSION

This method satisfies the performance required for each member, reduces the construction period by using factory-manufactured HPCa element combined with function of the form and falsework, and improves quality and durability. The method is expected to contribute to the railway viaduct in the concentrated urban area, reduction of construction costs for elevated structures and also life-cycle costs.

LONGITUDINAL STRESS DISTRIBUTION AROUND CONSTRUCTION JOINTS MADE CONTINUOUS BY TENDON COUPLERS IN PSC BRIDGEs

Byung Hwan Oh
Professor, Department of Civil Eng.
Seoul National University, Korea

Sung Tae Chae
Chief Engineer, Structural Section
Highcon Engineering Co., Korea

Keywords : construction joint, coupled joint, tendon coupler, prestressed concrete bridges

1. INTRODUCTION

In segmentally constructed bridges, there are many construction joints which require continuity of adjacent segments to introduce continuous prestress through superstructure of bridges. These construction joints usually require coupling of tendons to introduce continuous prestress. The stress states around the coupled joints are very complex and that uniform compression due to prestressing may not be achieved at the joints, which may provide some possible causes of cracking around the joints under live loads and shrinkage effects. It is, therefore, necessary to explore accurate stress distributions around the tendon coupling joints due to sequential prestressing at coupled joints.

2. TEST MEMBERS AND INSTRUMENTATION

The concentrically post-tensioned test members were designed to represent segmentally erected prestressed concrete bridge girders under a uniform state of compression. The cross section of test members is 40 cm wide and 200 cm high. The longitudinal length of each segment is 500 cm and is designed to satisfy the uniform compression in the middle part of a segment.

Tendon arrangements of test series are shown in Fig. 1. The series 1(SP1) has no tendon couplers at the construction joint, i.e, continuous prestressing, which represents uniform compression as a reference case. The series 2(SP2) has one tendon coupler among two tendons at the construction joint and the other tendon is continuous at the joint. The two tendons are all coupled at the joint in test series 3(SP3) to see the effects of tendon coupling.

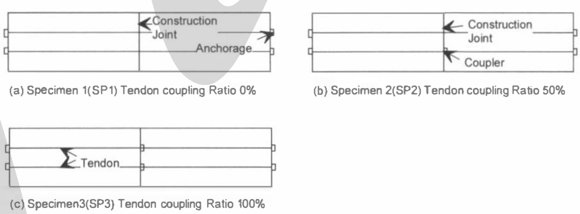

Fig. 1 Arrangements of test members

The nominal concrete compressive strength for the test members was designed to be 45 MPa at 28 days. The seven wire strand with the diameter of 15.2 mm has been used and each tendon consists of 12 strands. The tensile strength of strand is 1890 MPa.

To explore the longitudinal stress and strain distributions around the coupled construction joints due to sequential prestressing at tendon couplers, the strain gages in concrete and steel reinforcements, which are of particular importance are installed and measured along the edge line of test members,

3. TEST RESULTS AND FINITE ELEMENT ANALYSIS

The test members which simulate the segmental construction of prestressed concrete girder bridges have been modeled for the finite element(FE) analysis.

The strain distribution obtained from finite element analysis has been compared with measured test data. Fig. 2 shows the comparison of analysis results with measured data on the longitudinal strain distributions along the edge of test members. It is seen that the analytic results correlates fairly well with test data. Fig. 2(a) gives the longitudinal strain values for the test member SP1 without any tendon couplers. It is seen that uniform compression is achieved in the middle part(construction joint region) due to prestressing, because it has no tendon couplers in the joint. Fig. 2(b) shows the strain distribution along the edge of test member SP2 with tendon coupler at the joint. It can be seen that the uniform compression is not achieved. The compressive strains are reduced at the middle joint up to about 70 % for full-coupled case.

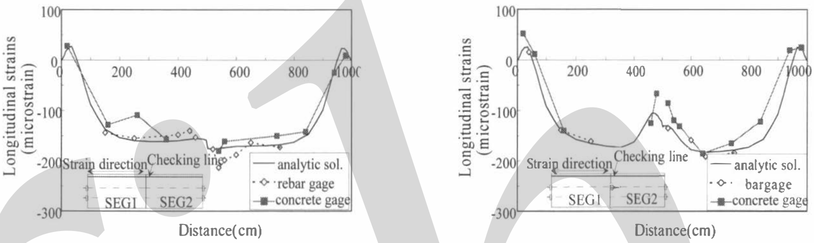

(a) Longitudinal strain state (SP1) (b) Longitudinal strain state (SP2)

Fig. 2 Comparison of analysis with test results on the longitudinal strain distributions along the edge of test members

4. CONCLUSIONS

The stress states around coupled joints are very complicated and the uniform compression may not be achieved at these joints due to tendon coupling, which may cause serious cracking problems when live loads, shrinkage and temperature effects are superimposed. The purpose of the present study is therefore to explore thoroughly the complex stress behavior around the coupling joints in prestressed concrete bridge structures.

The present study indicates that the compressive stresses in concrete introduced by prestressing are reduced by about 35 % around the coupling joints for the coupling ratio of 50 percent. This reduction of compressive stresses at the tendon coupling joints reaches up to 70 percent in the case of fully coupled joints(i.e., coupling ratio 100 %). Large reduction of compressive stresses around the coupling joints may cause serious cracking problems in PSC girder bridges due to tensile stresses when live loads, shrinkage, and temperature effects are superimposed. This result indicates that appropriate amount of reinforcements are required in the vicinity of coupling joints to avoid deleterious cracking.

ACKNOWLEDGEMENT

The support from National Research Laboratory Program of Korea is greatly appreciated.

REFERENCES

[1] Ruhberg, R., and Schuman H., " Schaden an Brucken und Anderen Ingenieurbauwerken", Verkehrsblatt-Verlag, 1982

[2] "Risse in Spannbetonbrucken, insbesondere in Koppelfugenbereichen, Ergebnisse der Risserfassung", Bundesanstalt fuer Strassenwesen, West Germany, 1994

PARTITIONING SEGMENT METHOD USING PRECAST SLABS AND U-SHAPED SEGMENTS FOR PC BOX GIRDER BRIDGES

Shin Suzuki, Yosuke Yagi and Hideki Manabe
Fuji P.S. Corporation, JAPAN

Keiichiro Sonoda
Professor
Osaka Institute of Technology, JAPAN

Keywords: Segment methods, U-shaped segments, PC precast slabs, Shear-connector

1 INTRODUCTION

In conventional segment methods precast segments are manufactured at the factory and transported to the construction site. However, there are problems in applying this full segment method to large bridges in Japan because the domestic road traffic law limits the maximum carrying weight that are restricted weight and size of a segment.

This paper describes the partitioning segment method which was proposed to meet the traffic conditions in Japan. In developing this method, a special consideration was given to the analysis of the connection between the U-shaped segments and upper slab segments during erection. The authors proposed a method to lay shear connector bars grouping on the top face of the webs, which are projecting into a small square hole of slab in advance and afterwards filled with fresh concrete. They verified the safety of this method through punch-out tests using models with full-scale slab depth, and discussed the optimum connection method based on the test results that we obtained.

2 PARTITIONING SEGMENT METHOD

2.1 Concept

In this method the upper slab segments (PC precast slabs) are manufactured independently from the web-lower slab blocks (U-shaped segments) at the factory, and they are connected and unified into a single structure at the site of construction.

2.2 Advantages

The code of transport in Japan specifies a weight limit of W_{max} = 30 t, which restricts the size of segments in designing bridges by conventional full segment methods. With the new method in which the upper slab segments and the web-lower slab blocks are manufactured independently, the size of each segment can be determined more freely since they can be brought in the site one by one. This improvement also leads to the following advantages: (1) segments can be designed longer (maximum length L_{max} = 3.0 m); (2) equipment rents and machinery remodeling expenses for erection can be reduced; (3) erection is possible under any site conditions including busy cities and mountainous places; and (4) all members are factory-made precast products with more secured quality and durability.

3 PUNCH-OUT TEST

Punching shear test was carried out to check the applicability of collectively laid shear connector bars to the connection between the U-shaped segments and PC precast slabs.

Four types of specimens having dimensions shown in Fig. 1 were prepared. The shear connector bars consisted of 16 bars of D19 laid in four rows in four columns or nine bars of D29 laid in three rows in three columns. Unbonded specimens were treated to prevent the concrete blocks from bonding with non-shrinkage mortar to be injected into the shear connector bars holes and the gaps between the concrete blocks. Data described below are those for the specimens with 16 bars of D19.

None of the concrete blocks exhibited cracks or other damage, irrespective of presence or absence of bonding by the sealant. A fracture was found only in the non-shrinkage mortar filling a gap between the concrete blocks. These results suggest that the proposed method can provide adequate capacity against horizontal shear force to the joints. Fig. 2 shows the relative displacements between the concrete blocks due to shear, indicating that it is necessary to add bonding capacity to the non-shrinkage mortar (sealant) when applying this method to a real bridge.

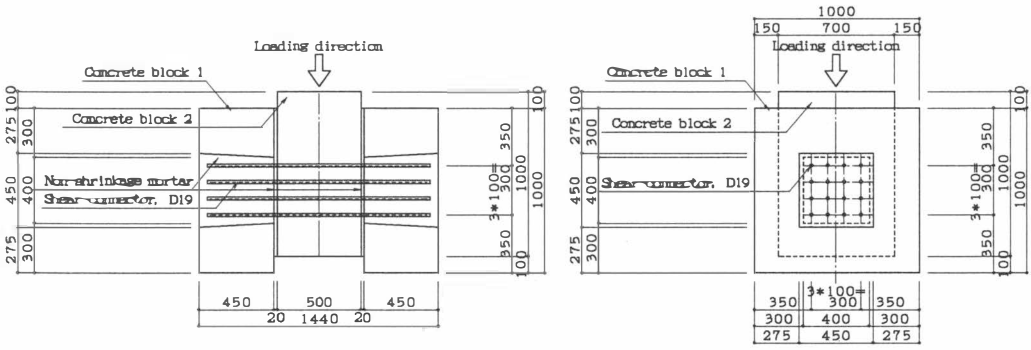

Fig. 1 Example of a specimen structure

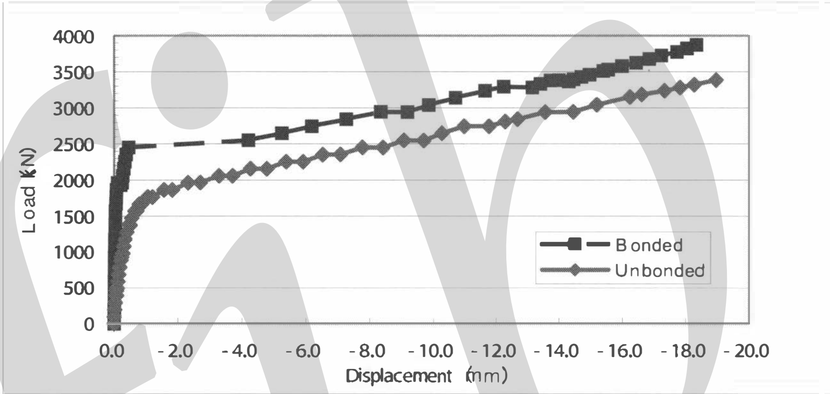

Fig. 2 Shear-displacement relationship

4 CONCLUSION

The punch-out test results allow the conclusion that the proposed method is applicable to real structures. The authors will continue to study extensively, including full-scale experiments, to follow up the current theoretical analysis and verification experiment where they focused primarily on the shear force acting on the joints.

REFERENCES

[1] The Japan Society of Roads, 1996. Specifications for Highway Bridges, Part II, Steel Bridges.

[2] The Japan Society of Roads, 1996. Specifications for Highway Bridges, Part III, Concrete Bridges.

[3] Japan Society of Civil Engineers, 1997. Design Code for Steel Structure PartB ; Composite Structure.

[4] H.Nakai, 1988. Design and Fablication of Composite Girder Bridges by Prestressed Concrete Slabs. Morikita pub.

[5] Y.Yagi, H.Ikeda, M.Goto, H.Shiota, 2001. Desigh of Nishihirao Viaduct., The 11th Symposium on Developments in Prestressed Concrete.

EXTERNALLY PRESTRESSED SLABS WITHOUT INTERNAL STEEL

Ammar Hassan Makoto Kawakami
Akita University
JAPAN

Tamio Yoshioka Kyoji Niitani
Research Laboratories of Oriental Construction Co. Ltd.
JAPAN

Key words: arch-action, corrosion, deck slabs, prestressing, reinforcement-free concrete.

1 INTRODUCTION

Lifecycle cost of bridges is becoming increasingly a very important issue in the field of civil engineering today. The corrosion of the embedded steel reinforcement bars in bridges burdens huge costs of repair and replacement which affect in turn the lifecycle cost of bridge structures. In slab-on-girder bridges the corroded steel causes an early deterioration of concrete because of spalling, especially the concrete of the deck slab where cover concrete thickness is minimum due to the small thickness of the slab structure.

A new approach of getting around the problem of the presence of reinforcement steel inside the concrete is simply by removing the steel from the concrete and confining the concrete externally using steel as well. This would allow the steel to be accessible for monitoring and maintenance at any time. In addition, corrosion of steel will not impose a danger on the concrete.

Based on this approach, a new system called steel free deck slab has been developed and experimented in Canada during the past ten years. This system is based on the concept of using the arch action that develops inside restrained slabs. Restrained deck slabs have high ultimate resistance and are much stronger than slabs in pure bending because of an internal compressive membrane action (arch action) caused by the restraining action in the lateral direction [1].

The deck slabs tested and constructed in Canada were totally devoid of all internal steel reinforcement and restrained by external steel straps. These straps were either welded to the top flanges of the adjacent girders, or studded straps that lay above the girder flanges and are integrated with the concrete slab by means of shear connectors [2]. Figure 1 shows a three dimensional view of the steel free slab and the tow types of steel strap confinements.

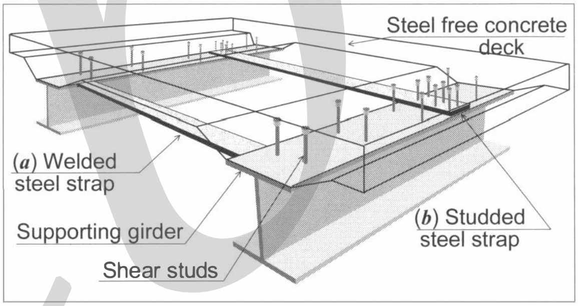

Fig. 1 Original strap confined steel free deck slab

2 PRESTRESSED STEEL FREE SLAB RESEARCH

The main aim of the research is to develop a system that allows the replacement of all internal steel embedded inside the concrete with an external prestressing. The research is thought to lead to a bridge with a maximum durability and minimum maintenance requirements and thus with a lower lifecycle coast than the conventional designs.

The research consisted of several stages of consequent experiments aimed at establishing the possibility and applicability of the idea of an externally prestressed concrete member without internal reinforcement.

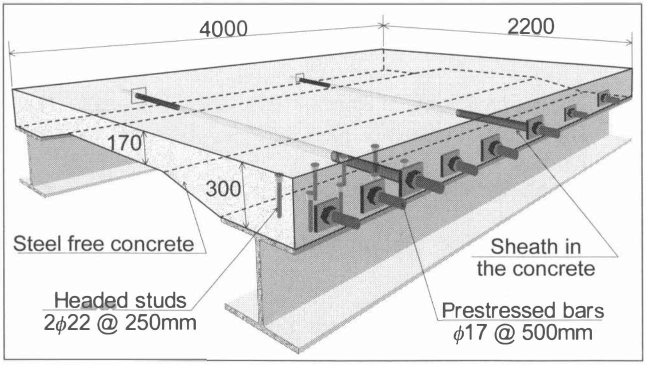

Fig. 2 Large scale Prestressed steel free deck slab specimens

To investigate the concept from its

basics thirteen non-reinforced beams restrained externally with steel straps, four one-meter-long slab segments restrained by prestressed and non-prestressed bars, and seven full-scale slab specimens restrained by prestressed bars were built and tested under static loading. The main stage of this research was investigating the behavior of the new slab design in large scale models.

The prestressed steel free concrete deck slabs were cast without any internal reinforcement and were confined using steel bars that pass, unbonded, through sheaths left in the concrete as illustrated in Figure 2. New parameters, which their effects on the steel free slabs haven't been tested before, were investigated: Firstly, the bars were prestressed to different levels of prestressing force for each different slab in order to study the effect of prestressing stresses. Secondly, one set of the slabs was cast using normal concrete and the other set using high strength concrete with the aim of studying the effect of concrete strength. Lastly, one slab was prestressed with bars that had a bigger cross-section in order to study the effect of steel ratio [3]. Table 1 gives details of the tested parameters and the test results.

Table 1 Details of the tested prestressed steel free slabs and test results

Slab	Steel ratio %	Concrete strength N/mm^2	Prestressing stress in concrete N/mm^2	Cracking load kN	Punching failure load kN	Cracking load / Punching load %
DS1	0.27	37.8	0	99	554.6	18
DS2	0.27	37.4	0.38	124	746.2	17
DS3	0.27	38.4	0.49	147	730.9	20
DS3'	0.49	36.1	0.48	132	696.1	19
DS4	0.27	90.7	0	157	862.9	18
DS5	0.27	94.0	0.59	225	853.2	26
DS6	0.27	88.4	0.85	231	980.5	24

3 RESEARCH CONCLUSIONS

1- The preliminary series of experimental investigations done within the scope of this research aimed at establishing the possibility and applicability of the idea of an externally prestressed concrete member without internal reinforcement. The outcome of the research was in favor with the new proposed prestressed steel free slab design providing strength under dynamic loading is verified. The system has an ample capacity under static loading and its bending strength is high so that the failure mode of the slabs was always a punching shear failure.

2- The system needs to incorporate nominal amounts of FRP reinforcement in the mid-depth of the deck with the concrete to improve the cracking strength of the slab. Particularly to prevent a longitudinal crack that develops along the full length of the underside of the deck at mid span between the supporting girders. This crack always appears in the laboratory tests as the deck are loaded to failure, but it has also occurred in all built field steel free slabs under service loads.

3- Prestressing proved to have a positive effect on increasing the punching capacity of the slabs without internal reinforcement. Prestressing also changed the cracks development after the first crack and therefore affected positively the serviceability limit of the slabs. It proved to significantly delays the occurrence of the above-mentioned longitudinal crack. Nevertheless prestressing could not avoid the occurrence of this crack, which was a problem in the original design of strap-confined steel free slab as well.

4- High strength concrete increased both the cracking and ultimate punching shear of the slabs. Nevertheless the effect wasn't considerably high comparing the increase in concrete strength. Steel ratio of the prestressing bars was an important factor in giving the slab more stiffness, therefore less deflection.

REFERENCES

[1] Bakht, B., and Mufti, A.A., "FRC deck slabs without tensile reinforcement", Concrete International, V. 18, No. 2, pp. 50-55, 1996.

[2] Newhook, J.P., and Mufti, A.A., "Fiber reinforced concrete deck slabs without steel reinforcement, half-scale testing and mathematical formulation", Nova Scotia CAD/CAM Center - Research Report, No. 1, 1995.

[3] Hassan, A., "Cracking and ultimate punching shear strength of externally prestressed concrete deck slabs without internal reinforcement", M. Eng. thesis, Grad. Schl. of Mining and Eng., Akita Univ., Japan, 2001.

CHARACTERISTICS OF PC SUSPENSION BRIDGE AND APPROACH TO LONGER SPAN

Hirofumi Watanabe
Civil Engineering Division
Kawada Construction Co., Ltd.
Tokyo,JAPAN

Keywords: suspension bridge, precast, wind resistance

1 INTRODUCTION

Suspension bridge has the most advantageous structure to realize longest span, but rope has almost no resistance against flexing, and suspension bridges with rope as main structure quickly responses to external force, and the live load bending or the vibration due to wind may become a problem. On medium or small scale suspension bridge, the mass of girder is enlarged to increase the cable tension and apparent rigidity that is specially effective for small-scale bridges with large ratio of live load. Reinforced concrete slabs are usually used to increase the girder mass. By applying prestress to the bridge axis direction on the slabs, both mass effect and stiffening girder effect can be simultaneously obtained (PC suspension bridge). Further, by precasting the slabs and building the manufactured parts at the factory, shorter construction period is realized. The thesis describes the outline of three PC suspension bridges constructed in Japan, and the result of examining the design for longer span.

2 CONSTRUCTION EXAMPLE

Outline of PC suspension bridge constructed in Japan is described below.

Photo 1 Shinonome Sakura Bridge

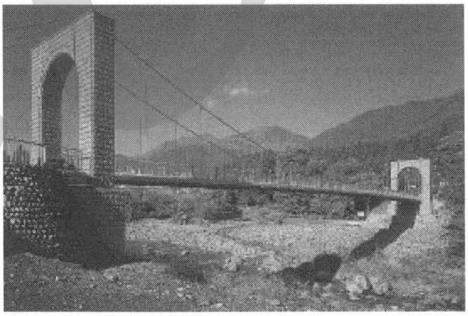

Photo 2 Dainichi Bridge

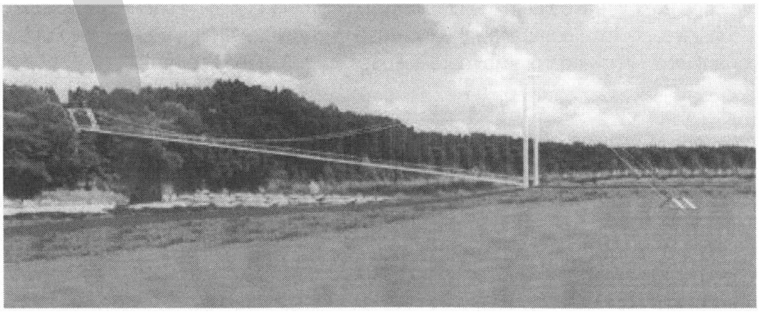

Photo 3 Minaminasu Suspension Bridge (conceptional drawing)

3 EXAMINATION OF LONGER SPAN

Geometry parameter
Span : A100m; B150m, C200m
Effective width : n3.0m, w5.0m
Sag ratio : H1/8, M1/10, L1/12

Table 1 Cable sag

	Unit	A	B	C
Span	m	100	150	200
Sag ratio H1/8	m	12.5	18.75	25.0
M1/10	m	10.0	15.0	20.0
L1/12	m	8.3	12.5	16.7

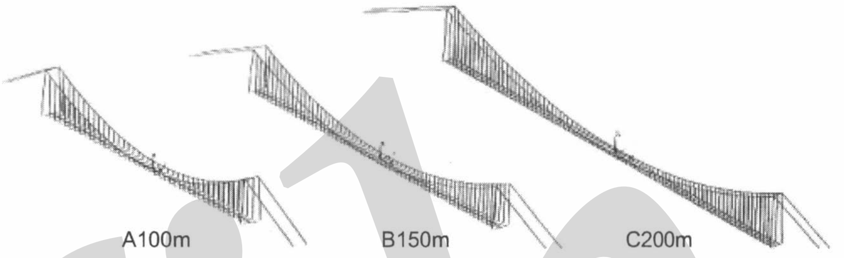

Fig. 1 Examination model

4 EXAMINATION RESULTS

4.1 Live Load Stress by Stiffening Effect of Slabs

Slab stress is analyzed by Peery's influence line method [1]. When using precast slabs for PC suspension bridge, full-prestress is required for live load on designing the joint. But the model of 100m span, 5.0m effective width, and 1/8 sag ratio has large slab stress, and the structure does not meet the allowance. It is requiered to change the area of cable, or cable sag ratio.

4.2 Divergent Vibration by Characteristic Value

Spatial analysis program (ANSYS) was used for calculating the characteristic value (frequency) of each model. The result was assigned in the wind velocity estimated formula of bending torsion coupled flatter incidence by Selberg[2], to calculate the incidence wind velocity of divergent vibration. Estimated wind velocity exceeds the design wind velocity(55m/s) within the range up to 200m span, and is safe for divergent vibration.

5 CONCLUSION

The report introduced PC suspension bridges that have not been constructed in many cases in Japan, and examined the possibilities for longer span. After this, we are planning to continue examinations regarding earthquake.

REFERENCES

[1] Kawada, T.: Theory and Calculation of Long-span Suspension Bridge, Mar. 1969 (in Japanese)
[2] Japan Road Association: Handbook for Windproof Designing of Road Bridge, Mar. 1991 (in Japanese)
[3] Strasky, J.: Design-Construction of Vranov Lake Pedestrian Bridge, PCI Journal, NO.6, 1997
[4] Watanabe, H., Gunji, K., Murakami, T., Kishi, Y.: Design , Construction and Performance Test for Shinonome Sakura Bridge (Precast PC Suspension Bridge), Proceedings of The 8th Symposium on Developments in Prestressed Concrete, pp625-628, Oct. 1998 (in Japanese)
[5] Watanabe, H., Fukuda, E., Suzuki, H., Kishi, Y.: Design and Construction of Dainichi Bridge (PC Suspension Bridge), Proceedings of The 10th Symposium on Developments in Prestressed Concrete, pp675-678, Oct. 2000 (in Japanese)
[6] Japan Road Association: Small-scale Suspension Bridge Index and the Description, Apr. 1984 (in Japanese)

NUMERICAL PREDICTION MODEL OF TIME-DEPENDENT DEFORMATION OF CONCRETE UNDER VARIABLE ENVIRONMENTAL CONDITIONS

Tatsuya Tsubaki
Yokohama National University
JAPAN

Helly Sulistyawan Putro
Graduate Program, Yokohama National University
JAPAN

Keywords: environmental conditions, shrinkage, creep, concrete, modeling

1 INTRODUCTION

The time-dependent deformation of concrete such as shrinkage and creep is influenced by various factors, for example, environmental conditions and material properties. The non-uniform distribution of the moisture inside concrete under variable environmental conditions produces a non-uniform stress distribution which eventually causes micro-cracking in concrete. This process makes the phenomenon of time-dependent deformation of concrete nonlinear. Thus, it is necessary to consider this nonlinearity to evaluate the time-dependent deformation of prestressed concrete structures with sufficient accuracy. In this study, therefore, a numerical model to predict the time-dependent deformation of concrete is developed instead of a conventional closed form prediction model.

2 MODEL OF TIME-DEPENDENT DEFORMATION UNDER DRYING CONDITION

2.1 Moisture movement due to drying

In this model, the humidity-dependent diffusivity D is represented by a tri-linear model as shown in **Fig.1** where it is assumed for simplicity that $h_2 = 0.98$ and $D_1 = 0.15D_2$.

In this model it is also considered that there is a thin fictitious layer with thickness T connecting the surface of a specimen to the ambient air as shown in **Fig.2** [1]. It is assumed that moisture diffuses linearly in this layer so that a linear diffusion equation with diffusivity D_{fl} is used. In order to model the difference between the drying and wetting phases, D_{fl} is also considered to be proportionally dependent on the ambient humidity, as given in Eq. 1.

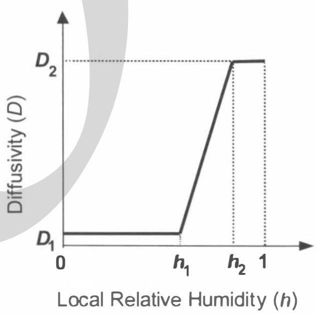

Fig.1 Model of Diffusivity

$$D_{fl} = Ch_a \tag{1}$$

where h_a is the ambient relative humidity and C is a proportional constant. At the interface between the fictitious layer and the ambient air, a fixed boundary condition is applied. This layer is conceived to regulate the rate of moisture inflow and outflow which is assumed to be dependent on the ambient relative humidity. It has been confirmed by preliminary simulation that almost the same simulation results can be obtained using a proper value of film coefficient and a convective boundary condition.

2.2 Strain due to drying shrinkage

For strain calculation, a linear relationship between an incremental local relative humidity Δh and the corresponding incremental change of shrinkage strain $\Delta\varepsilon$ is assumed, as given in Eq. 2.

$$\Delta\varepsilon_i = \alpha_{sh}\Delta h \tag{2}$$

where index i is used to stand for r, θ, z components and α_{sh} is a proportional constant.

2.3 Mechanical properties

For stress calculation which takes into account the effect of creep, the effective modulus E_{eff} is used. For simplicity the creep Poisson's ratio ν_{cr} is considered the same as the elastic Poisson's ratio ν.

3 NUMERICAL SIMULATION

3.1 Finite element modeling

The model of shrinkage in the previous section is implemented into finite element modeling for numerical simulation. A four-node isoparametric axisymmetric linear element is used. The same element is used to model the fictitious layer. The thickness of the fictitious layer T is set constant throughout the drying surface of the specimen. The incremental change in local relative humidity Δh is introduced to the finite element equation as equivalent incremental nodal forces.

The schematic finite element modeling of a cylindrical specimen and the fictitious layer is shown in **Fig.2**. The fictitious layer is represented by two layers of elements. A fixed boundary condition is applied on the external surface of the fictitious layer.

The Euler backward scheme is used for time integration. The integration of the element diffusivity and stiffness matrices employs 2-point Gaussian numerical integration scheme.

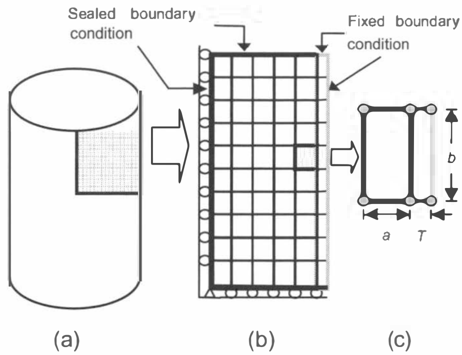

Fig.2 Discretization and boundary conditions

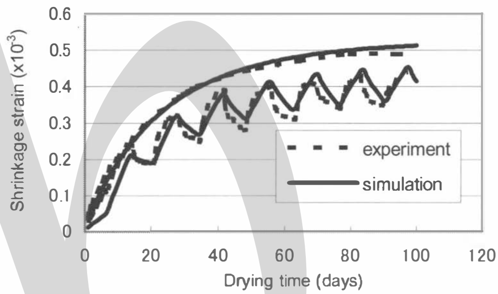

Fig.3 Drying shrinkage under variable humidity

3.2 Simulation of drying shrinkage of cylinders under cyclic humidity

The experimental data to be simulated are those by Muller *et al.*[2]. Cylindrical specimens with the diameter (d) to height (h) ratio d/h = 50 mm/200 mm are allowed to dry after curing in water at 20°C for 8 days after demolding. The specimens were then exposed to either a constant ambient humidity of 65% RH or a cyclic ambient humidity. For the cyclic humidity experiment, the cycle started with 90% RH for 7 days then was followed by 40% RH for 7 days. The temperature was constant at 20°C and strain was measured at the drying surface. The elastic modulus at the beginning of drying was 29840 N/mm^2. A 2.5 mm x 2.5 mm element size is used to discretize specimens. The size of the fictitious layer element is 0.5 mm x 2.5 mm. Since there is no sealed surface in this experiment, the fictitious layer is applied to the entire surface of the specimen. The time step Δt is 0.5 day. The values of parameters used are: D_2=0.6cm^2/day, h_1=0.5, C=0.015cm^2/day, T=1mm, α_{sh}=1.5x10^{-3}, ϕ=2.5, ν=0.2. The simulation result is shown in **Fig.3** indicating a good agreement with test data.

4 CONCLUSIONS

Through numerical simulations, it is confirmed that the time-dependent deformation of concrete under constant and cyclic environmental humidity conditions can be predicted by the present numerical model with the tri-linear diffusivity model and the fictitious surface layer concept.

REFERENCES

[1] Putro, H.S. and Tsubaki, T.: Simulation of Drying Shrinkage under Cyclic Ambient Humidity Condition, Proc. of the Japan Concrete Institute, Vol.23, No.2, pp.757-762, 2001.

[2] Muller, H.S. and Pristl, M.: Creep and Shrinkage of Concrete at Variable Ambient Conditions, Creep and Shrinkage of Concrete, Proc. of the Fifth Int. RILEM Symposium, pp.15-26, 1993.

THE DEFLECTION CALCULATIONS OF REINFORCED CONCRETE AND PARTIALLY PRESTRESSED CONCRETE MEMBERS

Katsuya OKADA, Haruhiko OKAMOTO, Yoshihiro OHTA
Takenaka Research & Development Institute , JAPAN

Keywords: long-term deflection , slippage of tension steel , cracking , creep , shrinkage

1 INTRODUCTION

The purpose of this study is to present procedures for calculating long-term deflections, including additional deflections due to cracking and subsequent creep, shrinkage and, in the case of a member with edge fixity, slippage of tension steel at span ends, that can be easily applied, mainly, to the design of reinforced concrete and partially prestressed concrete beams and larger-span one-way slabs. In the study, validity of the proposed procedures is verified through full-scale long-term deflection testing.

2. LONG-TERM DEFLECTION CALCULATION PROCEDURES

This study focuses mainly on continuous-span beams or one-way slabs whose two ends are restrained by columns or crossing girders. In the case of reinforced concrete members, cracking is permitted, and in long-term deflection calculations, the stiffness of members is evaluated basically in terms of the cracked section stiffness that also takes into consideration the contribution of the concrete in tension. In this study, the cross section shown in **Fig. 1(b)** is assumed in order to consider the concrete in tension at the cracked section. The contribution of effective tension area surrounding reinforcing bars ,A_{ce}, for rigidity of the members is converted into a cross-sectional area of reinforcing steel, and the rigidity of the cracked section is evaluated by using of the value of the effective reinforcement coefficient.

In the proposed calculation procedures, long-term deflection δ_ℓ is calculated by multiplying the elastic deflection δ_{ef} based on the effective depth d of the section by the deflection multiplier K_{ef} as following.

$$\delta_\ell = K_{ef}\delta_{ef} \qquad K_{ef} = K_{cr} + K_{cp} + K_{sh} + K_{bc}$$

where ,K_{ef} is the long-term deflection multiplier based on effective depth of the section

In the above equation, K_{cr}, K_{cp}, K_{sh} and K_{bc} are long-term deflection multipliers based on the effective depth of the section for cracking, creep, shrinkage and slippage of tension steel, respectively.

The proposed calculation method is an application of the "load balanced design method" to long-term deflection calculation. Basically, in the proposed method, the suspending force due to the prestress introduced by prestressing tendons arranged parabolically is subtracted from the load acting on the member. Then, long-term deflection is calculated assuming that the remaining load (residual load) acts in a sustained manner on a reinforced concrete member .K_{ef} used to long-term deflections of a partially prestressed concrete member, the value of the effective reinforcement coefficient is determined according to the evaluation of the effects of prestress assuming that the tensile stress F_t of the concrete increases by the amount equal to the mean prestress σ_g acting as an axial force.

3. LONG-TERM DEFLECTION TESTING

For the purpose of verifying the validity of the proposed calculation procedures, a series of long-term deflection tests was carried out. **Fig. 2** shows the test apparatus. Test specimens are 0.36-meter-thick, 0.67-meter-wide, fixed one-way slabs having an effective span length of 1.3 m. As shown in **Table 1**, three types of test specimens were used: one reinforced concrete specimen and two partially prestressed concrete specimens. At an early stage of loading, a loading test was carried out, and loads roughly equal to construction loads were applied. As shown in **Fig. 3**, the deflection rate was low for about 150 days after the loading test. Deflections of the test specimen with an overall load cancel ratio due to prestress of 70% (No. PC-70) were about 20% of those of the reinforced concrete specimen (No. RC-1).Long-term mid-span deflections of members were calculated by the simplified method based on the residual load deflection and an rigtous method (referred to as the "dividing method"). **Table 2** compares the results thus obtained with the test results. In simplified method, F_t=0.07F_c was assumed for Method 2; and F_t=0.07F_c+σ_g was assumed for Method 3. The reinforced concrete specimen, showed greater differences between calculated and measured values.

4. CONCLUSION

The residual load deflection method is proposed for calculating long-term deflections by applying the simplified procedures for reinforced concrete members. In view of the full-scale test results, it can be said that long-term deflections of partially prestressed concrete members can be calculated with the required level of accuracy by the proposed method.

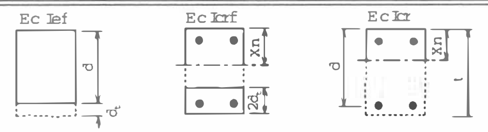

a)Section of effective depth (without reinforcement) b)Cracked section (with effective tension area) c) Cracked section (without contribution of concrete in tension)

Fig.1 Assumed section for deflection calculation

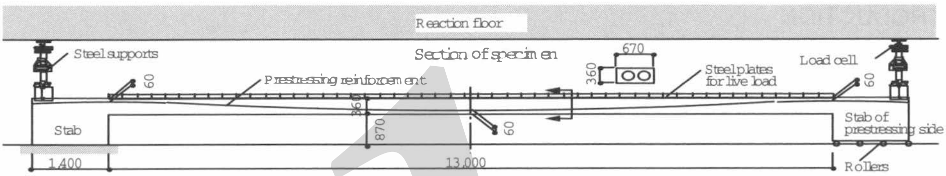

Fig.2 Test apparatus and dimensions of specimen

Table1 Prestresssing stresses and reinforcing bars of specimens

Specime No.	Prestressing reinforc.	Canceled load ratio (%)	ave. prestressing stress P/A(M_{pa})	Reinforcing bars / Reinforcement ratio: end-span upper side p_t(%)	end-span lower side p_t(%)	mid-span upper side p_t(%)	mid-span lower side p_t(%)
PC-1	—	0	0	6-D19 0.83	5-D13 0.31	5-D13 0.31	6-D16 0.57
PC-40	2-ϕ12.7	41	1.19	6-D16 0.57	5-D13 0.31	5-D13 0.31	5-D16 0.48
PC-70	3-ϕ12.7	68	1.98	6-D13 0.37	5-D10 0.17	5-D10 0.17	5-D13 0.31

Table2 Calculated and measured deflections at mid-span

Duration of load t=663

Specimen No.	Measured (mm) ①	Simplified method: calculated ②(mm)	Simplified method: ①/②	Dividing method: calculated ③(mm)	Dividing method: ①/③
RC-1	52.20	31.26 1)	1.67	18.02 1)	2.90
PC-40	22.03	15.72 2)	1.40	20.37 2)	1.08
PC-70	11.49	10.02 2)	1.15	16.15 2)	0.71

1) Calculation Method 1 (F_t=0.07F_c) , 2) Calculation Method 2 (F_t=0.07F_c+σ_g),

REFERENCES

[1] Recommendations for Design and Construction of Partially Prestressed Concrete (Class Ⅲ of Prestressed Concrete) Structures2000,1986

[2] Okada,K.,Okamoto,H. and Ohota,Y. : Simplified Method of Predicting the Long-term Deflections of Reinforced Concrete Members. J.Struct.Eng.,AIJ,No.532,pp.145-152,Jun.,2000(in Japanese)

[3] Okamoto,H. , Ohota,Y., Okada,K. and Sugata,M. : Unified Calculation of Long-term Deflection of Prestressed and Reinforced Concrete Floor Slabs.J.Struct.Eng.,AIJ,No.525, pp.93-100,Jun.,1999(in Japanese)

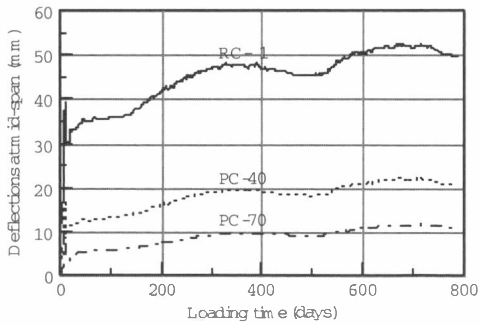

Fig. 3 Measured deflections at mid-span versus time under load

FLEXURAL STRENGTH AND DEFORMATION CHARACTERISTICS OF PRECAST PRESTRESSED CONCRETE BEAM-COLUMN CONNECTION WITH UNBONDED TENDONS

Masahiro Sugata Haruhiko Okamoto Yoshihiro Ohta Akira Sumi Hiroyuki Ueda
TAKENAKA CORPORATION, JAPAN

Keywords: Precast concrete, Unbonded Tendons、Post tensioning steel

1 INTRODUCTION

Recently, it tends to be very popular to use precast concrete members for moment frames in Japan. Because precast concrete member is much more reliable compared to cast in place concrete member in terms of structural quality and period of construction. Those members are usually made in a well-organized factory where quality control is easier than on the construction site. But it is sometimes difficult to design and construct precast concrete systems in regions of severe seismic activity especially for moment connections such as column and beam joint. A moment connection system for precast concrete commonly used in Japan is shown in Figure-1. A beam that is cast as a one bay long is post-tensioned against a column by tendons (PT Steel) that run in the beam and column. This system was developed several decades ago and has been applied for many buildings. However, because of Japanese Building Standard Law, all post-tensioned steel that is used for seismic resisting frame have to be grouted in case of fracture of the PT steel. Post-tensioned precast moment frame system with unbonded tendon has been developed and applied to a 39-story apartment tower in California, USA [1]. Mild steel bars are used in parallel with unbonded PT steel as continuity bars at a bean-column joint, those mild steel bars are set in the ducts that runs through the beam-column joint and then grouted as illustrated in Figure-2 [2]. In the paper, they said that the system, which is 'Precast Hybrid Moment Resistant Joint', has distinct advantages compared to the ordinary cast in place reinforced concrete structures or beam-column joints.

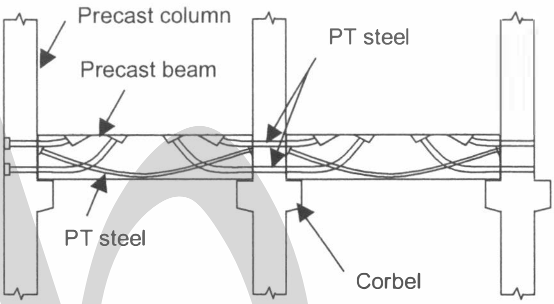

Fig.-1 Precast post-tensioned frame Commonly used in Japan

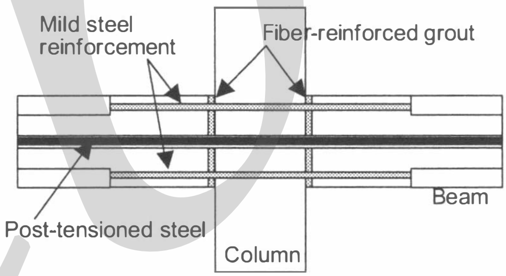

Fig.-2 Precast Hybrid Moment Resistant Joint [2]

Also in Japan, the law is going to be revised and the use of unbonded PT steel for seismic frame will be accepted. In this paper a post-tensioned precast seismic resistant frame system with unbonded tendon is studied experimentally and a method to estimate the strength and deformation, in considering for compressive deformation of the concrete, is also studied. One of the features of this system is a beam continuity bar that is placed only in the upper side of the topping concrete. No continuity bars are placed on to the lower side of the beam, so that the construction process is made much easier. In addition to this, slab that is attached to the frame is also examined experimentally. This is because behavior of the slab when the connection's interface is lifted off has not been studied well before.

2 PROTOTYPE BUILDING

Two types of moment frame systems are proposed here. Both are planned to use in apartment building and planned to use precast concrete beams, columns and unbonded PT steel, illustrated in Figure-3.

3 ESTIMATION OF STRENGTH

The compatibility condition and force equilibrium condition of the beam-column interface model proposed in this paper is shown in Figure-4. In order to estimate the concrete force, C_c, a function β need to be introduced. The function can convert the average concrete strain into the strain that is suitable to calculate the concrete force.

$$\delta_c = \alpha \cdot X_n \beta \cdot \varepsilon_c \qquad \text{Eq.-1}$$
$$C_c + T_p + T_s = 0 \qquad \text{Eq.-2}$$

The relation of Moment-rotation angle of the interface can be calculated by the equations-1 and 2 with material models. Figure-5 shows the result of the step by step analysis with Fiber-method concerning B-11, in the figure the test result for the envelope of 1st cycle is also shown.

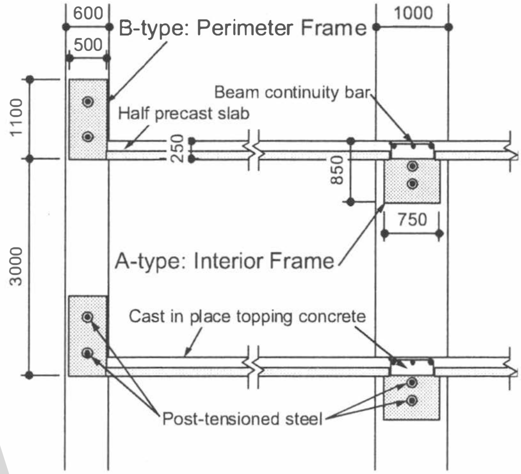

Fig.-3 Proposed tow systems

5 CONCLUSIONS

Two types of seismic moment frames with precast concrete and unbonded PT steels are proposed. The 40% scaled models are examined under cyclic seismic force. The test result shows that these two frames including attached slabs behave well under seismic force.

The force-displacement behavior for the joint interface can be estimated with the theory of compressive concrete's deformation. To estimate the deformation, the function β, that is an adjustment of concrete strain around the interface region must be considered.

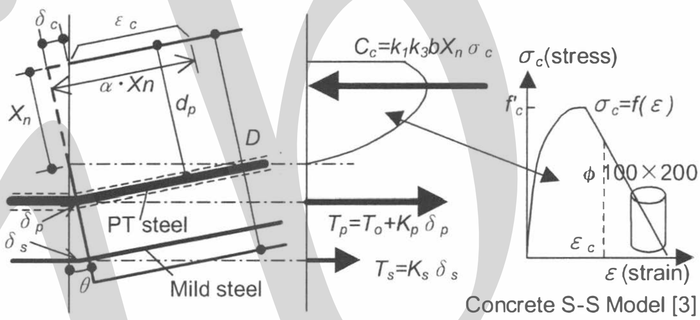

Fig.-4 Compatibility condition and Equilibrium condition of the interface

AKNOWLEDGMENTS

Prof. Tadashi Nakatsuka, Osaka University and Prof. John F. Stanton, Prof. Gregory A. MacRae, University of Washington led this research consistently and are gratefully appreciated.

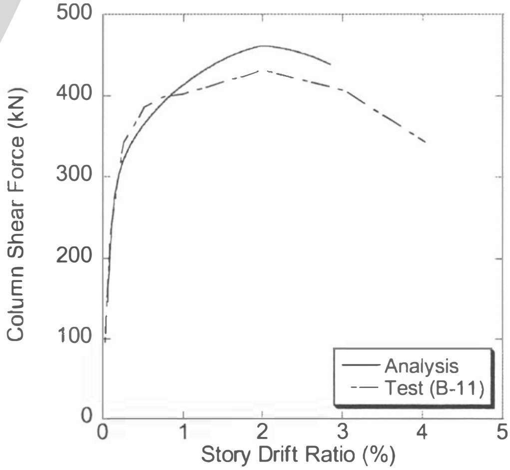

Figure-5 Result of the analysis

REFERENCES

[1] 'New heights for concrete seismic framing', BUILDING DESIGN & CONSTRUCTION, September 1999, pp.16

[2] Suzanne Dow Nakaki, John F. Stanton, S. Sritharan : 'An Overview of the PRESSS Five-Story Precast Test Building', PCI JOURNAL, March-April 1999, pp. 26-39

[3] Masahiro Sugata, et al. : 'Study for A Moment-Deformation Relationship of Precast Prestressed Concrete Beam with Unbonded Tendon -Analytical Study for Deformation of A Compressive zone -, Summaries of Technical Papers of Annual Meeting Architectural Institute of Japan, 2001, C-2, pp.947-948

PRECAST PRESTRESSED CONCRETE OFFICE BUILDING WITH BASE ISOLATION DEVICES

Katunori Kaneda
Structure Enginieer, Structural Design Plusone Inc.

Kiyoshi Ogawa
Construction Engineer, Takenaka Corporation

Hiroshi Sakata
Prestressed Concrete Engineer
Fudo Building Research Co.Ltd

Hiroyuki Tanaka
Prestressed Concrete Engineer
Fudo Building Research Co.Ltd

Keywords: precast prestressed concrete structure, base isolation, seismic response analysis.

1 INTRODUCTION

Due to the Hyogoken-Nanbu earthquake, a lot of buildings were destroyed or damaged, and thousands of people suffered from it.

As it is urgent to maintain seismic safety of buildings, structural reinforcements are enforced on old existing buildings, and also base isolation or energy dissipation system is installed to provide enhanced protection in new building constructions.

On the other hand, many buildings having large spans are designed to improve the environment of the office space. Generally, when designing a building with base isolation devices, magnifying the differences of the stiffness between the main-structure and isolated story with connecting stiffer main-frame and softer isolated story in series is effective to get energy dissipation due to the large drift at the isolated story.

Therefore, precast prestressed concrete frames that are stiffer than conventional steel frames are valid in designing the large span office building with base isolation devices.

This report is written about one project of precast prestressed concrete office building with base isolation devices.

2 BUILDING OUTLINE

Name of building ;	Shimano head office building (west wing)			
Address of construction ;	12-1 Kita-Machi, Ishizu, Sakai-Shi, Osaka, Japan			
Use ;	Office			
Design ;	Structure	Structural Design Plusone Inc.		
	Architect	Ashiwara Taro Architectural Office		
Construction ;	Building	Takenaka and Kounan Joint Venture		
	Precast prestressed	Fudo building research		
Scale ;	Building area	1487.13m^2		
	Total floor area	5086.91m^2		
	Height	15.19m(from G.L.)		
	Story	1 basement and 3 stories from ground		
Construction period ;	From September, 2000 to the end of June, 2001			
Structure ;	Foundation	Mat foundation		
	Mainframe	Under ground	Precast prestressed assembling	
			Partially site reinforced concrete	
		Above ground	Precast prestressed assembling	

3 GENERAL OF BUILDING

This is Shimano head office building.

A basement floor with base isolation devises is designed as a warehouse and 1st to 3rd floors are occupied as offices. The 1st floor plan, north elevation, and section of the building are shown in Figure 1, 2, and 3 respectively. The plan of this building is 29.35m (3 spans) X 44.0m (8 spans) rectangular shape. 8 spans are located by 5.5m pitches equally, but 3 spans are composed of short and long spans 5.1m-19.5m-5.1m. A central large span is occupied by the office section, and it is successfully realized to make wide area without columns for 19.5m by using precast prestressed concrete beam.

Each side span of 5.1m is occupied by meeting section, stairs, restrooms, and so on. East side of the plan has 3 stories well entrance.

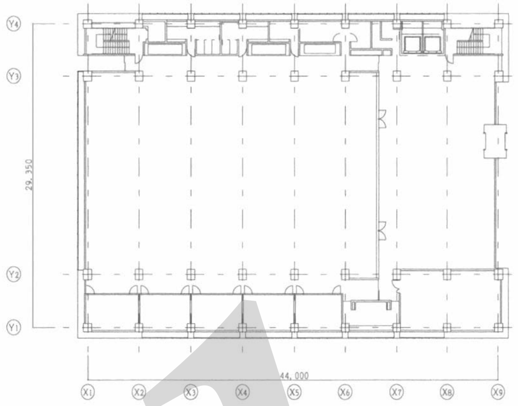

Fig.-1 Top view of the first floor

4 WHY PRECAST PRESTRESSED CONCRETE STRUCTURE?

The reasons why precast prestressed concrete structure is adopted for this building are the followings.

1. Shorter construction period and lower cost than a conventional reinforced method can be expected because the office section has very large span.
2. In spite of the long span, large stiffness can be expected. That is, it is possible to magnify the differences of the stiffness between the building and devices. As a result, great energy dissipations can be expected.
3. Big bearing pressure concentrates at one column due to the large span, and then the base isolation devices become effective and economical.
4. Precast prestressed concrete structure is excellent in the restoration, and the cracks are completely closed after the earthquake. Not only the damage under the earthquake is decreased, but also the building can be reused after the earthquake and is excellent in the resistance against the aftershock.
5. Exterior walls are composed of Glasses and supported by C-shaped precast prestressed concrete beams that have letterings to set them directly without sash. Combination of precast prestressed concrete structure and base isolation system makes it possible to adopt such details because it increases the stiffness and decreases the vibration.

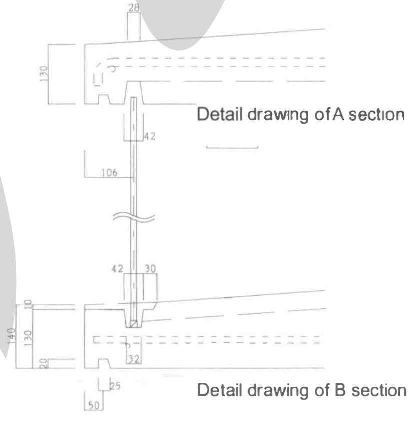

Fig.-2 Detail drawing of glass mounting

DEVELOPMENT OF LONGER AND ECONOMICAL INCREMENTALLY PRESTRESSED CONCRETE(IPC) GIRDER

Man Yop Han
Ajou University
Suwon, KOREA

Eui Seung Hwang
Kyunghee University
Suwon, KOREA

Keywords: incremental presressing, prestressed concrete, girder, long span, full scale test

ABSTRACT

In this study, the concept of incrementally prestressed concrete (IPC) girder has been introduced and the ultimate loading test of the IPC girder was performed to prove the validity of design concept and to find out structural behavior of IPC girder. Two full scale specimens (bracket type and coupler type), with span length of 30m, are designed, manufactured and tested up to failure load. During the test, strains of reinforcing steel and concrete and deflections are measured. Cracks are also marked at each load step during the test. Test results show good agreement with the theoretical values in terms of stresses, deflections, cracking moment and ultimate strength. The ultimate strength of IPC girder is higher than the traditional prestressed concrete I-type girder of twice higher beam depth. Deflections are observed within the design limit. It can be concluded that the IPC girder has full safety and ductility and can be used as longer span bridge girders than conventional girder bridge.

1 INTRODUCTION

New prestressing technique overcoming the above-mentioned shortcomings of traditionally prestressed concrete girder is introduced in this paper. By applying prestressing forces at different loading stages, the stress in the girder is redistributed by applying prestressing force additionally to keep the stress within the allowable stress range of concrete. The IPC girder needs only small sectional area because the stress change due to additional load is always adjusted by additional prestress. In this study, bending test of IPC girder is performed to prove the validity of design concept and to find out structural behavior of IPC girder. Two specimens (one with bracket type and the other with coupler type), with span length of 30m, are designed according to bridge design code of Korea [2] and fabricated using the concept of incremental prestressing. During the test, strains of reinforcing steel and concrete and deflections are measured. Cracks are also marked during the test.

2. CONCEPT OF IPC GIRDER

Fig. 1 shows the exposed anchors for additional prestressing, which makes the multi step prestressing possible. The construction procedure of IPC girder bridge is almost same except for the 2nd prestressing after the hardening of concrete slab. The 3rd prestressing can be applied when additional prestressing is necessary. And also one of the most important features is the self strengthening function of the IPC girder.

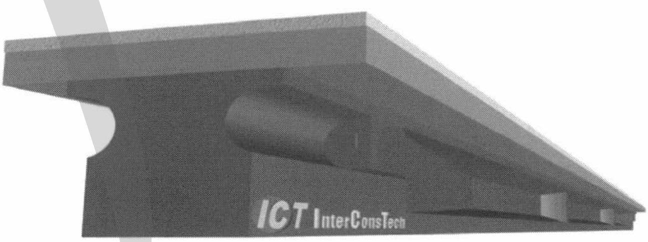

Fig. 1 Exposed anchor for additional prestressing at the end of IPC girder

Comparisons on maximum possible span are made between developed IPC girder and existing girders such as NEBT, PCI BT and ASHTOⅡ. The NEBT, PCI BT and AASHTOⅡ are prestressed concrete I-type girders developed by New England Highway Department, Prestressed Concrete Institute and AASHTO, respectively. The comparison shows that IPC girder is longer than any other girder used previously, by 20-30%.

3 FULL-SCALE TEST OF THE IPC GIRDER

The design conditions of IPC girder are simple span, 30m long girder, spaced by 200cm, and slab thickness is 22cm. The height of the girder is only 100cm, which is 30% shallower than the lowest girder ever developed. The concrete compressive strength of girder and slab are 500kg/cm^2 and 300kg/cm^2 each. Steam curing is used for 12 hours after casting to avoid the effect of the shrinkage.

4 TEST RESULTS

The load-deflection diagrams at mid-span are shown in Fig. 2. In case of IPC-C girder, there is a change of the slope at about 50ton possible due to cracking. The first crack by naked eye was actually found at 44ton, which is close to theoretical cracking load of 39.8ton. Since design live load including the impact load is 28.1ton, it can be considered that the girder has enough safety margin. Deflection at mid-span was measured as 18.1mm at the design load level (28.1ton) comparing the theoretical value of 26.2mm. The difference may be due to reinforcement not included in the calculation and actual strength of concrete. At cracking load, measured deflection was 30mm, which is 19.1% less than theoretical value of 37.1mm. Yield strength of the specimen is measured as 135.8ton, which is very close to theoretical value of 132.9ton. It was measured that the prestressing tendon yields at about 140ton. Deflection at mid span was measured as 29.6cm. The specimen was unloaded after yielding and deflection of 5.7cm remains. The specimen is loaded again up to its failure. Measured ultimate strength is almost the same as theoretical value of 165ton, which is almost 30% larger than that of the traditional prestressed concrete I-type girder.

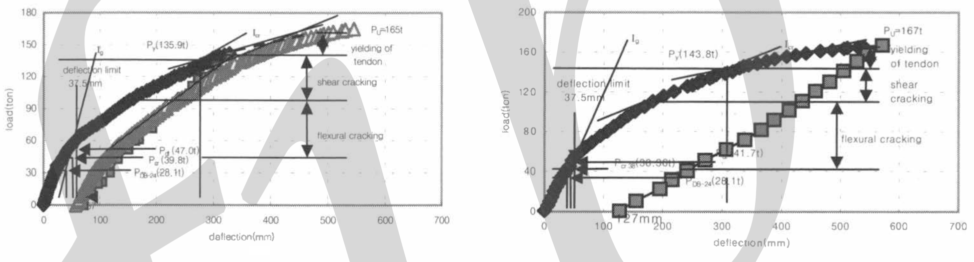

Fig. 2 Load-deflection diagram at mid-span

5 CONCLUSIONS

In this paper a new concept of prestressed concrete I-type girder - IPC girder - has been proposed and its structural behavior has been tested

1) The IPC girder can be achieved the longest span for the same height or the shallowest height for the same length among the prestressed concrete I-type girders. (Economy)
2) The maximum strength of the IPC girder bridge is very close to the theoretical value, which is 5.5 times larger than designed load. (Safety)
3) Both the measured and theoretical deflections at the design live load satisfy the deflection limits s specified by the code. (Stiffness)
4) The first crack occurred at 44ton and 45ton, which is approximately 1.6 times higher than the design load. (Crack resistance - Anti-corrosion durability)
5) Both deflection and deflection recovery are large (Ductility & Restoration capability).

The IPC girder has enough safety, stiffness, durability, ductility and economy, and it is good for constructing continuous bridges and it has self strengthening function.

REFERENCES

[1] Alexander, K. B., et. al. Design, Fabrication and Construction of the New England Bulb-Tee Girder, PCI Journal, Nov.-Dec. 1997.
[2] PCI Committee, State-of-the-Art of Precast/Prestressed Concrete Spliced I-Girder Bridges, 1995
[3] Francis, J., "Study of Long Span Prestressed Concrete Bridge Girder," PCI Journal, Mar-Apr 1991.

FUNDAMENTAL STUDY ON BOND PROPERTY BETWEEN GROUT AND PRESTRESSING STEELS

Takashi Ichiki
Sumitomo Electric Industries Co., LTD JAPAN

Kiyotaka Hosoi
Shinko Wire Co., LTD
JAPAN

Tadashi Nakatsuka
Osaka University
JAPAN

Keywords: Grout, Prestressing Strand, Bond Property, Test Method

1. INTRODUCTION

An accurate understanding concrete member deformation is essential to the optimal design of prestressed concrete structures. However, our current understanding of concrete member deformation remains incomplete, and actual maximum bearing loads at guaranteed limit states have not been thoroughly investigated. One major reason for this state of affairs is our incomplete understanding of the bonding properties between grout and prestressing steel, which represent a design consideration with important consequences for the behavior of prestressed members. This report discusses a unique test method devised to measure bonding properties required for the structural design of actual prestressed concrete members. The study described herein also evaluated the effects of tensioning load and grout strength on the bonding properties of prestressing strands.

2. CONVENTIONAL PULLOUT TEST

In a conventional pullout test, the strand is pulled out the specimen by twisting it within the groove formed inside the grout. However, the strand does not rotate evenly, because the tensioning end is tightly secured and is not allowed to rotate. In this condition, each component wires of the strand tends to open (de-strand) as the strand is pulled out. The de-stranding phenomenon generates expansion forces within the grout and may affect the pullout load.

On the other hand, the de-strand force is distributed along the "free length", the portion of the strand exposed between the concrete specimen and gripping device. It may be that the longer free length reduces the expansion load inside the grout and affects the pullout load.

The two pullout tests were conducted with free length of 45mm and 735mm. Fig-1 shows the relationship between pullout stress and slip length, while Fig-2 shows the relationship between the strand's rotation angle and slip length. Fig-1 indicates that the first peak load appears at the beginning of the slip, then increases gradually after dropping from the peak load.

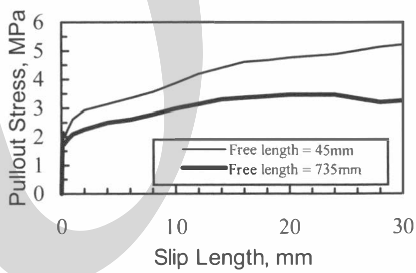

Fig-1 Slip Length and Pullout Stress

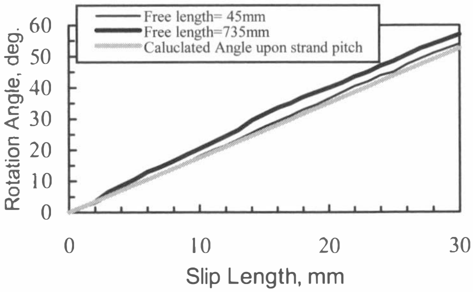

Fig-2 Slip Length and Rotation Angle

In this test, both the peak load and maximum pullout load with a free length of 45mm were greater than with 735mm. A permanent deformation having a "flared" shape was also observed on the strand sample following testing with free length of 45mm. This result indicates that when the strand sample is given 45mm of free length, the twisting load of the strand is poorly absorbed due to the short free length, resulting in the application of greater expansion loads upon the interior surface of the grout. As shown in Fig-2, both samples rotate in proportion to strand pitch during the pullout test. These test results confirm that free length affects on the pullout load.

3. PROPOSAL FOR A NEW TEST METHOD

3.1 Test method

As explained above, various free lengths can result in differing pullout loads with the conventional test method. Since the strands may not twist when it moves at an actual structure, conventional test methods may not be appropriate for evaluating real pullout loads involving actual concrete structures.

A new test is proposed here. The test procedure is as follows,

1) Insert a prestressing strand into a concrete specimen in which a metal sheath has been embedded.
2) Provide a tension load upon the strand installed in the steel frame.
3) Inject grout into the sheath.
4) After the gout cures, move the concrete specimen itself using a tensioning jack.
5) Measure a slip length of the strand by extensometer and a pullout load by a load cell.

This purpose of this testing method is to recreate the environment of strands in real-world concrete structures. The strand is subject to a tensioning load, and both ends are constrained from twisting.

3.2 Test results and considerations

(1) Effect of the tensioning load upon the strand

Fig-3 shows the relationship between the bond strength and slip length of the strand at various tensioning loads applied to the strand. The bond strength increases in the sequence ① (0.0Py), ③ (0.7Py),②(0.2Py).

In the case of ①, due to the freedom of rotation at one end, no squeezing force was applied to the strand, and the pullout load was lower than for strands constrained from twisting at both anchor points. Since this condition is similar to a conventional pullout test, measurement of pullout loads by conventional method may return values lower than actual loads.

The reason pullout load at ③ was lower than at ② may be that the longitudinal force generated by the tensioning load absorbs the expansion force created by the "flaring phenomenon" of the strand by constrained rotation.

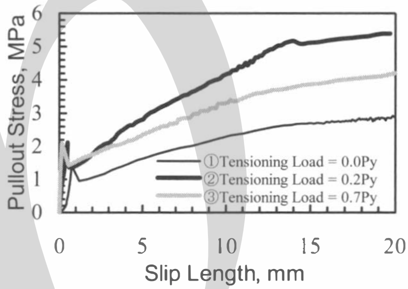

Fig-3 Pullout Stress by Tensioning Load

(2) Effect of grout strength

Fig-4 shows the relationship between the pullout load and slip length depending on various degrees of grout strength. The results appear to indicate that pullout load is nearly proportional to grout strength. As shown in Fig-12, the initial pullout load, the other significant factor in the bonding properties was also proportional to grout strength.

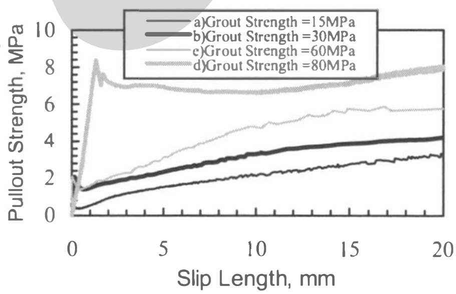

Fig-4 Pullout Stress by Grout Strength

4. CONCLUSION

The results of this study indicate the following:

(1) The conventional test method used to evaluate strand bonds may provide misleading results, because it disregards strand twisting.

(2) The new test method suggested by this study provides the following information:

(a) Different tensioning stresses on strands result in different pullout loads.

(b) Pullout loads increase in proportion to grout strength.

PC AS A CULTURAL MANIFESTO OF OUR AGE

Akihiko Higuchi, D.Des.
Kyushu University
JAPAN

Keywords: aesthetic design, urban design, culture, heritage, monument

1 INTRODUCTION

As the PC technology advances, various cutting-edge PC structures have been made possible, and their futuristic forms impress not only engineers but also ordinary citizens. However, the share of these great structures in the PC market is small and the majority of the PC structures in our society is ordinary one that can be built without applying any new technology. Among those ordinary PC structures, we have been seeing increasing numbers of unwelcome products from the urban design's point of view. They are harmful in making better urban environment. While many of the PC engineers may not recognize it yet, PC, as the leading technology of our age, already have a great deal of responsibility in preserving and strengthening the quality of urban environment both functionally and aesthetically.

Last year the Japanese Society of Civil Engineers (JSCE) published an inventory of monumental civil engineering structures remaining in Japan. [(1)]The book contains about 2000 structures located nationwide, and about 400 of them are regarded as class A monuments. These structures are appraised as great monuments of the period of modernization of Japan (1865-1945). The inventory is meaningful in many aspects. It provides us the opportunity to trace the pioneers' works. It also shows us a concise history of technology advancement in Japan. But there is another thing. From the inventory we can learn that civil engineering structures can demonstrate not only technology but also the atmosphere of the age. Time makes any cutting-edge technology out of date. But, if the structure is well placed and welcomed by the local society as an important element of the local life and culture, it will eventually acquire cultural value, and time might even strengthen it.

2 LESSONS FROM THE PIONEERS' WORKS

In Western Europe a firm social consensus exists over the value of old civil engineering structures as important elements of the history and culture. In European cities, where huge amount of culturally valued stock of structures exist, engineers have no choice but pay particular concern to the impact of the structure they are designing to the existing landscape and atmosphere of the area. The stock of the past does not allow the emergence of poor design. By respecting and criticizing the past, engineers can find their position from which they can generate original designs. But in Japan, where the past has not been well valued and sometimes ignored, engineers cannot rely on the past stock in finding ways of connecting their works with both the past and the future. The inventory will provide Japanese PC engineers an opportunity to start paying reasonable respect and interest to their pioneers' works and learn that they have to add "something" to their structures besides cost efficiency and structural rationality if they wish their structures survive for a long time and be valued by the people in the future.

3 THINGS TO DO

If the PC argues that it is the leading technology of today's civil engineering, PC must also share the role of contributing in enriching of the contemporary culture through producing quality PC structures. Constant improvement of technology and occasional breakthrough make cutting-edge structures possible, and those structures are often beautiful enough without adding anything. But, as the PC technology becomes popular, if we don't work hard to add beauty and grace on those numerous ordinary PC structures, the urban landscape will be eroded and devastated by the flood of faceless concrete cubes and boards. The life span of concrete structures is very long. Once some structure is built it will be very difficult to get rid of it. In the worst case, a mass of rubbish shamelessly keep standing on a major corner of the city center and pollute the cityscape for ever. It is often said that infrastructures have to be designed modestly so that they would not pop out in the landscape. But this does not mean that the design can be poor. We know that the era of PC will last for a while. It means that we will see more PC structures emerging in our built environment. What we have to do is to advance PC from a mere concrete structure to a major element of contemporary urban life. By maximizing the structural advantage of the PC system, PC engineers can contribute our society not only in realizing reasonable design to fulfill the functional requirement but also in realizing a beautiful form to enhance the surrounding urban landscape.

Once upon a time, when it was built, Nihonbashi bridge was designed to play a role of normative structure which would encourage the emergence of desired cityscape around it in Tokyo. We need to see the emergence of such PC structures that could perform as the norms of the contemporary cityscape and manifesto our age. Well, the road might be a tough one, but it will be a very creative and meaningful job to do for us all. The arch, which was applied in building aqueducts and many other structures by the ancient Romans, is a major symbol of the Roman era. The same is the role of the steel technology during the period of modernization. And it might be reasonable to predict that PC will be regarded as one of the major icons of our age in human history. But in order to expect that, first we have to establish an original PC culture which is rich enough to manifesto our age.

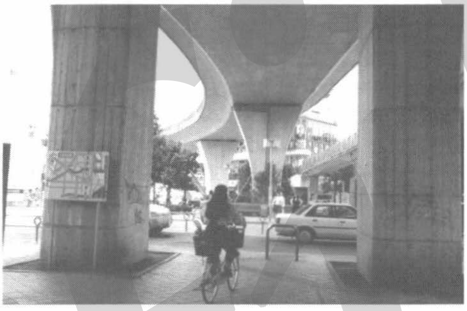

Photo-1 Mismatch of scales between PC structure and existing urban environment

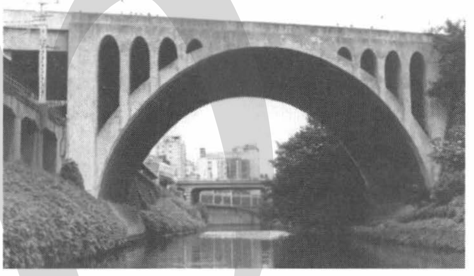

Photo-2 Hijiribashi Bridge:
Many of the monumental structures symbolize good old days.

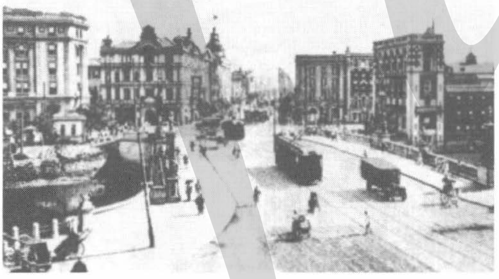

Photo-3 Nihonbashi Bridge and its surroundings in 1910s

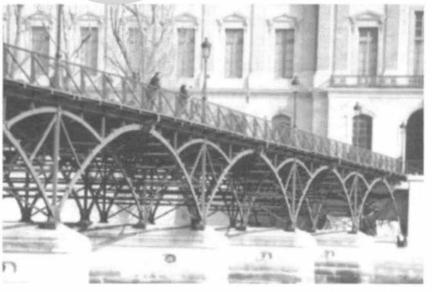

Photo-4 Pont des Arts:
PC needs to manifesto our age.

REFERENCE:

(1) *Civil Engineering Heritage in Japan: Important 2000 Structures as Monument of the Modernized Japan 1865-1945*, Japan Society of Civil Engineers, 2001.
(2) *Design Selection 2001: The Landscape & Design Prize*, Japan Society of Civil Engineers, 2001.

"TOKIMEKI BRIDGE" (PROVISIONAL NAME) FLAT ARCH BRIDGE WITH SUSPENDED DECK (SELF-ANCHORED STRUCTURE)

Tatsuru Tanaka , Masateru Kawakami
Mie Prefecture.

Yoshihiko Teramoto
Japan Engineering Consultants Co., Ltd.

Takehiro Kuribayashi , Koichiro Shimizu
Sumitomo Construction Co., Ltd.

Keywords: composite structure, self-anchored structure, landscape design

1 INTRODUCTION

The Tokimeki Bridge (provisional name) is a 68.0 m pedestrian bridge located in the center of Kameyama Sunshine Park. It has a composite structure of a suspended deck and an arch.

This bridge is to be the most important and symbolic of the landscape structure elements in the entire park, so from the planning stage it has not simply been provided with the function of a pedestrian bridge but has been designed to be "nature-friendly" and "people-friendly," taking into account the perspectives of both the natural environment and park users and consideration for the needs of pedestrians. The soft slender curve created by the arch and the suspended deck harmonizes with the surrounding natural landscape, and opening up the piers creates a feeling of openness and lightness.

A suitable combination of suspended deck, arch and inclined concrete struts forms a self-anchored structure and is designed to reduce the foundation structure. The result is a new concept in prestressed concrete bridges with a streamlined, composite structure. Figure 1 shows a perspective view of the completed bridge.

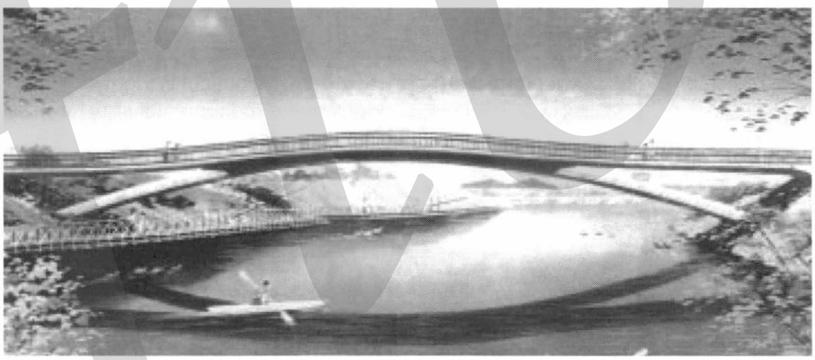

Fig. 1 Perspective view of the completed bridge

2 BRIDGE SPECIFICATIONS

- Project name: Kameyama Sunshine Park (multi-purpose park) Park facility construction
- Client: Mie Prefecture
- Road standard: Pedestrian path
- Location of bridge: Within Kameyama Sunshine Park, Takatsuka, Fuke-cho, Kameyama City, Mie Prefecture
- Structural form: Prestressed concrete suspended deck bridge + reinforced concrete fixed flat arch bridge (self-anchored structure)
- Length of bridge: 68.0 m (suspended deck span 23.0 m)
- Arch span: L = 50.0 m (arch rise ratio: 1/12.2)
- Basic sag: f = 475 mm (sag / span ratio: 1/48)
- Effective width: 2.5 m (total width 3.0 m)

3 STRUCTURE

Normally, the horizontal force produced by suspended deck bridges is anchored to the foundation through the use of ground anchors. However, it was determined that many anchors would be needed due to the soil conditions at the site. For this reason, in order to reduce costs and from a maintenance perspective, it was decided to use a self-anchored structure that eliminated the need for ground anchors and used struts to integrate all of the concrete members.

The major structural feature of this bridge is that the horizontal force produced by the suspended deck is transferred to the arch foundation through the inclined concrete struts. This makes it unnecessary to use the permanent anchors that are used for normal suspended decks. Moreover, canceling out the compressive axial force applied from the arch reduces the force acting on the foundation.

A suitable combination of suspended deck, arch and struts forms a self-anchored structure and is designed to reduce the foundation structure. The result is a new concept in prestressed concrete bridges with a streamlined, composite structure. Figure 2 shows a conceptual view of the flow of force in the self-anchored structure.

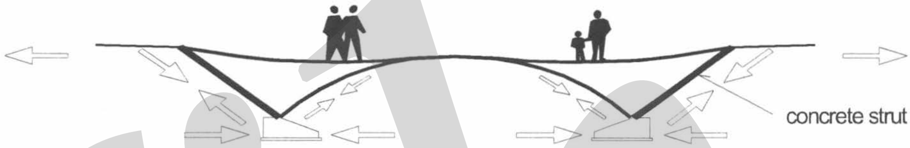

Fig.2 Conceptual view of the flow of force in the self-anchored structure

4 DESIGN

As this bridge has a self-anchored structure that combines a suspended deck with a flat arch, in the design process, attention focused on verification of the structural model mixing suspension members with flexural members and the stability of the entire structure is paid. For the behavior of the suspended deck in particular, at each stage of the construction, it was necessary to consider the fact that the amount of sag on the part of the suspended deck would change continuously. In addition, for the safety of the entire structure, attention focused on the deformation of the top of struts was paid and control values were established to confirm safety both during construction and after completion.

5 CONSTRUCTION

The arch was constructed using the pipe support erection method. The suspended deck was erected using the precast deck erection method (hung on bearing cables).

6 CONCLUSION

A bridge with a new structural form called "flat arch bridge with suspended deck" debuted in the center of Kameyama Sunshine Park on December 2001. This represented a step ahead from the concept up to now, that a pedestrian bridge was simply designed to allow people to cross in safety. It shows that it was possible to create a bridge of structural beauty while at the same time harmonizing with the surrounding environment. What made it possible to build a bridge with this new form was, more than anything else, the courage to enter a new domain and the technical ability that made this possible, and the fact that the project was favored by good people of understanding who were united in their will to turn the idea into reality.

Finally, the authors would like to thank all relevant parties who helped with various types of study and construction in various fields, from basic design through detailed design of this bridge.

REFERENCE

[1] Strasky, J., Kulhavy, T. :Self-Anchored Stress-Ribbon Structure Stiffened by Arch. fib SYMPOSIUM 1999, Vol.2, pp.781-782, Oct., 1999

DESIGN AND CONSTRUCTION OF THE ANCHORAGE BRACKET FOR EXTERNAL CABLE USING THE ARAMID FRP TENDON. – FUJIMI BRIDGE REINFORCEMENT WORK –

Harumitsu Takayama
Civil Engineering Division,
Sumitomo Construction Co., Ltd.

Masato Kameyama, Satoru Sugimura
Civil Engineering Department,
Shizuoka Branch, Sumitomo Construction Co., Ltd.

Keywords: Aramid FRP Tendon, reinforcement work, anchorage bracket for external cable

1 INTRODUCTION

The Fujimi Bridge is a post-tension 28 spans T girder bridge completed in 1961 at a location where national Route 150 crosses the Oi River. This project was conducted to reinforce the bridge to enable it to handle B live loads, and a method of introducing prestressing through the use of external cables was adopted for this purpose. Anchorage brackets made of concrete were attached to both sides of the main girder in order to fasten the anchorages for the external cables. The main girder and anchorage brackets were integrated by prestressing using tendons. For this project, Aramid fiber reinforced plastic (FRP) rods were used as the anchorage bracket tendons. These tendons exhibit great elastic expansion and little stress fluctuation due to displacement. In addition, they have excellent chemical stability and neither corrodes nor deteriorates.

Photo 1 Fujimi Bridge

This paper will report on design and construction with the external cable anchorage bracket fastening method utilizing Aramid FRP tendons.

Fig.1 shows the outer cable arrangement and the locations of the anchorages and intermediate supports. Photo 1 shows an overview of the Fujimi Bridge.

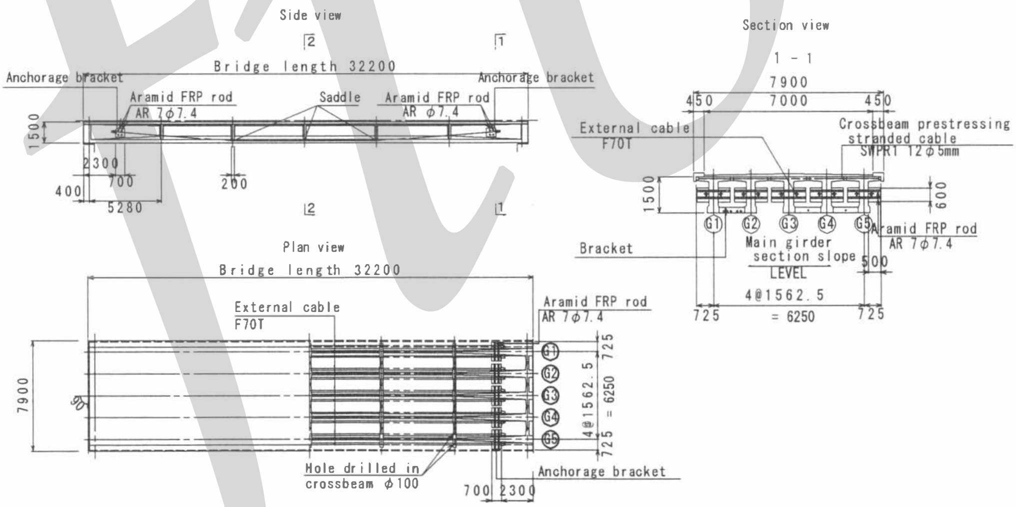

Fig 1 Overview

2 OUTLINE OF ARAMID BRACKET CONSTRUCTION METHOD

2.1 Overview

The Aramid bracket construction method is implemented in the following manner. Anchorage brackets are manufactured, and sheaths or the like protects the sections in which Aramid FRP tendons will be arranged. Next, the Aramid FRP tendons are inserted and tensioned, after which the interior of the sheath is filled with non-shrink mortar to form an integrated whole. For this project, a method in which five main girders were tensioned all at once was used. The main girders were tensioned together at right angles to the bridge axis, through the intermediate supports and the tensile reaction force stands. Then the Aramid FRP tendons between the main girders and on the tension side and fixed side were severed and prestressing was introduced.

2.2 Features

The special feature of this method in structural terms is that Aramid FRP rods, due to their excellent bonding properties, are used to pretension anchorage the anchorage brackets. The major features are as follows.

(1) Aramid FRP rods are lightweight and are easy to use in cramped spaces.

(2) The use of Aramid FRP rods, which have a low modulus of elasticity, as tendons enables the anchorage brackets to be securely fastened with no great loss of the applied prestressing due to member shrinkage or the like.

(3) External cable anchorage brackets fastened to multiple main girders can be fastened with a single Aramid FRP rod using the pretensioning method. Thus no tensioning space is needed between anchoring brackets, so a smaller installation space is needed than with the conventional technique.

(4) Aramid FRP rods pose no danger of rust and are extremely durable. Moreover, as the pretensioning method is used for bond anchoring, the anchorage brackets do not remain, so this method is advantageous in terms of maintenance and repair.

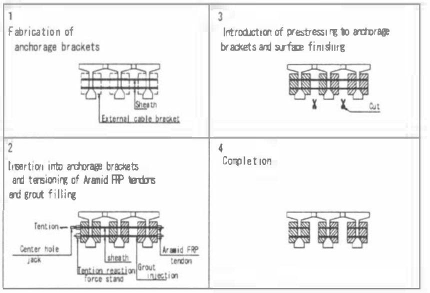

Fig 2 Overview of construction

Photo 2 Tensioning the Aramid FRP tendons

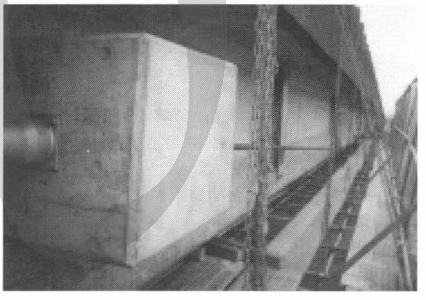

Photo 3 Construction completed

2.3 Procedure used for construction

(1) Main girder and crossbeam steel member sensing
(2) Drilling of holes in main girders and crossbeams
(3) Fabrication of anchorage brackets
(4)Fabrication of Aramid tendons and insertion into anchorage brackets
(5) Tensioning of Aramid FRP tendons and grout filling
(6) Introduction of prestressing to anchorage brackets and surface finishing
(7) External cable arrangement and tensioning

3 CONCLUSIONS

In this project, the tensioning work for the steel members used to fasten the anchorage brackets was done all at once for five main girders, reducing the labor required for the tensioning process as compared to the conventional method. In addition, Aramid FRP rods with excellent durability with respect to corrosion and the like were used as the tendons, and the method used for anchoring was binding, so no anchorage components were needed and the anchorages were maintenance-free. This method increased construction efficiency in the external cable reinforcement work for girder bridges with a narrow main girder interval, which was difficult with the conventional method, and helped to reduce construction costs.

It is hoped that this paper will prove helpful as a reference for construction under similar construction conditions in the future.

REFERENCES

1) "Standard Specification for Concrete Structures" (established 1996), DESIGN manual (Japan Society of Civil Engineers, March 1996).
2) "Recommendation for Design and Construction of Concrete Structures using Continuous Fiber Reinforcing Materials (draft)" (Concrete Library 88, Japan Society of Civil Engineers, September 1996).
3) Matsumoto, etc., "Application of the External Cable Bracketing Method Using Aramid Reinforcements in Confined Construction Environments" (Proceedings of the 8th Symposium of the Japan Prestressed Concrete Engineering Association, October 1998).

CARBON BASED POST TENSIONING TENDONS IN THE DINTELHAVEN BRIDGE IN THE NETHERLANDS

Authors: A.H.J.M. Vervuurt (TNO Building and Construction Research, the Netherlands)
N. Kaptijn (Dutch Ministry of Transport and Public Works, the Netherlands)
W.B. Grundlehner (Spanstaal B.V., the Netherlands)

Keywords: CFRP, experiments, post tensioning

1. INTRODUCTION

Whereas in the early 1990's activities in the field of Fibre Reinforced Plastics (FRP) continued, interest in the Netherlands seemed to decrease. For studying whether resuming the application of FRP in the Netherlands was desirable, in 1994 a research project was started under the auspices of CUR (Dutch Centre for Civil Engineering Research and Codes). The recommendations given by CUR research committee PC97 [1] have contributed to the initiative of the Civil Engineering Division of the Dutch Ministry of Transport and Public Works for a pilot project concerning the application CFRP tendons in the Dintelhaven Bridge.

The Dintelhaven Bridge, which has been put into use in 2001, is a concrete box girder bridge with a main span of almost 185 m and was build by the balanced cantilever method. In the bridge four conventional steel tendons have been replaced by an equal number of CFRP tendons, each consisting of 91 wires (5 mm diameter). The tendons have a length of about 75 m and have been manufactured by Spanstaal BV, the Netherlands. The CFRP wires in the tendons are anchored by means of an resin wedge anchorage system. For avoiding stress concentrations a variable stiffness of the resin was adopted. As a result the shear stress along the wire axis is distributed more evenly, and the high tensile strength of the fibres is utilised maximally.

In order to guide the project and advise the principal with respect to the various questions related to the application of the CFRP tendons, CUR committee C97A was installed. In the committee various independent specialists in the field of pre-stressed concrete and FRP participated [2].

2. EXPERIMENTS

As a part of the activities of CUR committee C97A an experimental study, focussing upon the long and short term behaviour of the CFRP tendons in the Dintelhaven Bridge has been carried out at TNO Building and Construction Research in the Netherlands. Moreover, several tests on single wires have been performed. Among test results obtained by EMPA [3], the results of the latter tests are summarized in Table 1. A full description of the tests is given in [4].

From the tests performed at TNO it was noticed that in 57% of all tests, failure occurred due to slipping of the wire from the resin wedge. In these tests generally a lower failure load was reached, yielding a lower calculated efficiency of the anchorage (see Table 1). When the tests where slipping of the wire was noticed, are omitted from the results (final row in Table 1) it is observed that the average failure load increases (61.3 kN) and the variation of the results (σ/μ) decreases substantially.

Table 1 Summary of results with respect to the wire tests performed at TNO and EMPA. The numbers between brackets indicate the standard deviation.

	number of tests	failure load (kN) μ	(σ)	σ/μ	failure stress (MPa)	anchorage efficiency (%)	Young's modulus (GPa)
overall results	42	56.3	(9.5)	*17%*	2827	81.1	178
overall results (slipping excl.)	23	61.3	(7.6)	*12%*	3086	87.9	177

*) the efficiency of the anchorage is defined as the ratio of the wire strength based on the experiments and on the strength of the fibres.

Next to tests on single wires, also two tendons similar to the tendons applied in the Dintelhaven Bridge were tested at EMPA. The short term tensile strength as obtained from these tests (4085 kN) was taken as a starting point for the long term tensile tests carried out at TNO. In these tests three different load levels were adopted, namely 2650 kN, 3000 kN and 3500 kN. During the tests the load was measured, as well as the strains in several wires and the settlement of the resin wedge anchorage.

From the test results (Fig. 1a) it was found that the largest decrease of the load is found in the first day after tensioning to 2650 kN (1.2%). In the period of three months thereafter an additional decrease of the load of again 1.2% was found. From the results with respect to tendon B it was found that the additional decrease of the load in 3 to 6 months at 2650 kN was only 0.17%. Because the loss of load (relaxation) is mainly attributed to settlements in the anchorage, it is expected that tendons longer than the tested tendons will show less relaxation than observed in the tests.

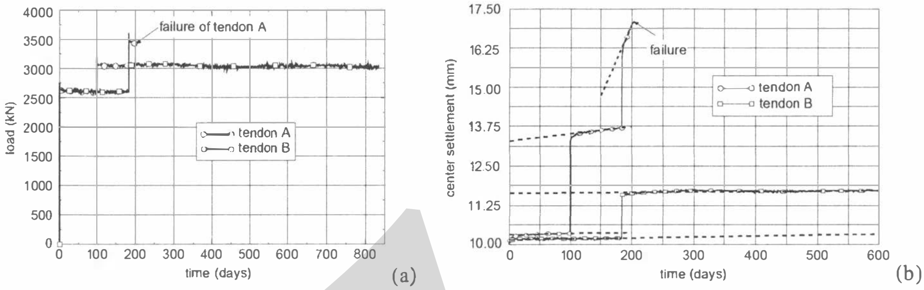

Fig. 1 Development of the tendon loads in time (a) and the settlement of the centre of the anchorages of tendon A and B.

From the behaviour of tendon A it was found that the decrease of the load after tensioning to 3500 kN was more pronounced than during the previous load levels (Fig. 1a). In Fig. 1b it is shown that the excessive decrease of the load in this period is attributed to ongoing settlements of the anchorage, finally resulting in failure of the tendon. It is believed that failure of tendon A was caused by a combination of radial compressive and tensile stress in the wires. Due to creep in the resin wedge, stresses in the anchorage redistribute and the stresses perpendicular to the wires increase. Due to this combination the shear stress may have exceeded the strength, resulting in cracking of the resin and, eventually, failure of the wires.

Another effect that may have attributed to failure of tendon A is that the epoxy resin has been squeezed out of the anchor sleeve. Due to a relative displacement of the wires inside the resin wedge of about 14 mm, additional shear stresses in the wire/resin interface cause an increase of the tensile force in the outer wires.

3. PRODUCTION AND INSTALLATION OF THE TENDONS IN THE BRIDGE

The procedure for manufacturing the CFRP tendons for the Dintelhaven Bridge was as follows. The preparation of the anchor sleeve consisted of degreasing the inner side of the sleeve first and thereafter applying an anti-adhesive coating in the sleeve. Next, a prepreg sheet was applied firmly to the inner side of the sleeve. In order to form the anchorage at each end of the bundle, the wires were sandpapered lightly, spread out parallel and fanned out towards the end of the anchorage. Thereafter the wires were glued to a GFRP end plate and the anchor was lifted vertically in order to prepare the resin wedge. After adding granular beads for controlling the stiffness of the wedge, a two component epoxy resin was added. After completion of both anchorages, the tendon was rolled on a reel with a diameter of 2.5 m and transported on a low-loader to the construction site. For bringing the tendons in the box of the bridge, a small opening was left in the concrete closing section.

For monitoring the behaviour of the CFRP tendons, a number of measurements have been carried out during and after tensioning in the bridge. From these measurements it was found that the anchorage settlements, as well as the load development in time was in accordance with the behaviour expected from the long-term laboratory tests at TNO.

REFERENCES

[1] Centre for Civil Engineering Research and Codes (CUR). *Kunststofwapeningselementen in beton: Preadvies*, report number 96-9, Gouda, 1996 (in Dutch).

[2] Vervuurt, A.H.J.M. and Hordijk, D.A. *Carbon Fibre Based Tendons: Experience with the Pilot Project "Dintelhaven Bridge".* TNO report 2000-CON-BM-R3008, July 2001.

[3] Swiss Federal Laboratory for Materials, Testing and Research. *Zugversuche an Einzeldrähten aus CFK*, **EMPA bericht nr. 145'464/11**, November 1997 (in German).

[4] Vervuurt, A.H.J.M., Kaptijn, N. and Bruggeling, A.S.G. Koolstof voorspankabels in de Dintelhavenbrug (II): voorgeschiedenis en experimenten, *Cement*, **2**, 2000, pp 58-62 (in Dutch).

A DESIGN EQUATION OF PRESTRESS IN PRESTRESSED REINFORCED HIGH STRENGTH CONCRETE

Ryoichi SATO*, Yang YANG*, Nour-Allah HUSSEIN* and Yoshio KAKUTA**
*Hiroshima University, Japan **Hokkaido University, Japan

Keywords: design equation, prestress loss, shrinkage, prestressed reinforced high strength concrete

1 INTRODUCTION

High strength concrete has been increasingly applied to prestressed concrete superstructures in order to enhance durability and to decrease self-weight of structural members. High strength concrete shrinks significantly due to self deccication at very early ages which results in the production of tensile stress or cracking when restrained by steel bars and so on. If this tensile stress is neglected in prestressed concrete reinforced with non-stressed steel bars made of high strength concrete, design prestress should be overestimated. Therefore, the design equation for prestress should be also established.

Having the above mentioned situation, a new design equation is proposed for prestress in prestressed reinforced high strength concrete members, into which the autogenous shrinkage stress induced by the restraint of non-stressed reinforcing bars before prestressing is incorporated as a component of the loss of prestress. The design equation is verified by comparing its results with those obtained by a numerical analysis based on the principle of superposition, in which creep coefficients loaded at different ages were applied. The former was 0.82-0.95 of the latter excluding one case.

2 FORMULATION

The proposed equation is derived based on Bernoulli-Euler's assumption as well as strain compatibility condition that strains in steel reinforcemens at different two depth are equal to those in concrete at the same depths as steel reinforcements. Design prestress is obtained by superposing the stress induced by shrinkage before prestressing to those due to prestressing and shrinkage after prestressing. Applying the concrete stresses $\sigma_{css,j}$ at bottommost reinforcement and $\sigma_{css',j}$ at uppermost reinforcement produced instantaneously by autogenous shrinkage at the middle age between setting and prestressing, the stress losses due to creep in bottommost, uppermost non-stressed reinforcements and prestressing steel $\sigma_{scs,j}, \sigma_{s'cs,j}$ and $\sigma_{pcs,j}$ can be obtained as follows;

$$\begin{Bmatrix} \{\Delta\sigma_{scs,j}\}_{sh} \\ \{\Delta\sigma_{s'cs,j}\}_{sh} \end{Bmatrix} = \begin{bmatrix} 1+\alpha_{ssj}+\alpha_{psj}n_{ps}\beta_{13} & \alpha_{s'sj}+\alpha_{psj}n_{ps}\beta_{23} \\ \alpha_{ss'j}+\alpha_{ps'j}n_{ps}\beta_{13} & 1+\alpha_{s's'j}+\alpha_{ps'j}n_{ps}\beta_{23} \end{bmatrix}^{-1} \begin{Bmatrix} n_{s,j}\phi_j\sigma_{css,j} \\ n_{s,j}\phi_j\sigma_{css',j} \end{Bmatrix} \tag{1}$$

$$\{\Delta\sigma_{pcs,j}\}_{sh} = n_{ps}\left(\beta_{13}\{\Delta\sigma_{scs,j}\}_{sh} + \beta_{23}\{\Delta\sigma_{s'cs,j}\}_{sh}\right) \tag{2}$$

where, $\alpha_{ssj} = n_{s,j}A_s\alpha_{11}J_j \quad \alpha_{s'sj} = n_{s,j}A_{s'}\alpha_{21}J_j \quad \alpha_{psj} = n_{s,j}A_p\alpha_{31}J_j \quad n_{s,j} = E_s/E_{c,j}$

$$\alpha_{ss'j} = n_{s,j}A_s\alpha_{12}J_j \quad \alpha_{s's'j} = n_{s,j}A_{s'}\alpha_{22}J_j \quad \alpha_{ps'j} = n_{s,j}A_p\alpha_{32}J_j \quad J_j = 1/\chi_{e,j} + \chi_{cr,j}\phi_j$$

$$\alpha_{11} = (1/A_c + e_s^2/I_c) \quad \alpha_{21} = (1/A_c - e_{s'}e_s/I_c) \quad \alpha_{31} = (1/A_c + e_pe_s/I_c) \quad e_s = d - c$$

$$\alpha_{12} = (1/A_c - e_se_{s'}/I_c) \quad \alpha_{22} = (1/A_c + e_{s'}^2/I_c) \quad \alpha_{32} = (1/A_c - e_pe_{s'}/I_c) \quad e_{s'} = c - d'$$

$$\alpha_{13} = (1/A_c + e_se_p/I_c) \quad \alpha_{23} = (1/A_c - e_{s'}e_p/I_c) \quad \alpha_{33} = (1/A_c + e_p^2/I_c) \quad e_p = d_p - c$$

d, d', d_p, c: distance from upper surface to bottommost and uppermost reinforcements, prestressing steel, distance from upper surface to centroid of cross section

A_c, I_c: cross sectional area and second moment of area of concrete

A_s, $A_{s'}$, A_p: cross sectional areas of bottommost and uppermost reinforcements, prestressing steel

$\chi_{e,j}$, $\chi_{cr,j}$: aging coefficients for development of Young's modulus with time and creep in concrete

$\chi_{e,j}$=1.0, $\chi_{cr,j}$=0.8 are recommended in the design equation of prestress in view of convenience and safety. Stress losses in reinforcements give those in concrete.

3 VERIFICATION

The validity of the proposed equation is verified by comparing concrete stress obtained by the proposed design equation with that by numerical creep analysis based on the principle of superposition.

All specimens used for verification are listed in **Table.1**, which is 200mm wide, 250mm deep and

2400mm long. And d, d' and d_p are 210mm, 40mm and 160mm, respectively.

Water binder ratio of concrete used to make specimens is 0.25 and its compressive strength and Young's modulus at 28 days cured in water of 20℃ were 105N/mm^2 and 41.0kN/mm^2. Shrinkage strains developed before and after prestressing supposed to be done at the age of 3 days are 430$\times 10^{-6}$ and 75$\times 10^{-6}$ at 360 days. Creep coefficient loaded at 1 and 7 days were 1.4 and 0.8 at 360 days, respectively.

Table.1 Properties of Beam Specimens

No.	Tension RB		PC tendon		Compression RB		σ_c***
	A_{ts}** (mm^2)	ρ_{ts}* (%)	A_{ps}** (mm^2)	ρ_{ps}* (%)	A_{cs}** (mm^2)	ρ_{cs}* (%)	(N/mm^2)
CASE1	317.5	0.64	80	0.16	397.2	0.79	-2.5
CASE2	184.9	0.37	128	0.26	397.2	0.79	-3.9
CASE3	184.9	0.37	180	0.36	397.2	0.79	-5.9
CASE4	397.2	0.79	80	0.16	---	---	-2.4
CASE5	253.4	0.51	128	0.26	---	---	-3.7
CASE6	146.7	0.29	180	0.36	---	---	-6.0

* ρ_{ts}, ρ_{cs}, ρ_{ps} : Ratio of tension RB, compression RB and PC tendon;
**A_{ts}, A_{cs}, A_{ps} : Cross section area of tension RB, compression RB and PC tendon
*** σ_c : Concrete stress on the bottom just after prestressing

Fig.1 shows elastic stresses on the bottom due to autogenous shrinkage as well as the stresses lost due to creep up to 360 days calculated by the proposed method compared with those by the creep analysis. The positive and negative stresses denote those in tension and compression. The significant tensile stress is predicted by both methods, if tension reinforcement ratio exceeds 0.5% and no compression reinforcement is arranged. The maximum stress at 360 days obtained by the proposed equation reaches 1.0 N/mm^2 in CASE4, which is 16 % larger than that by creep analysis.

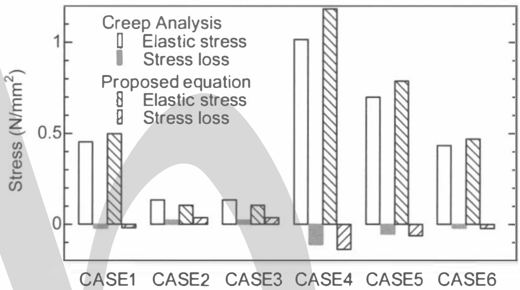

Fig.1 Elastic Stress and Stress Loss

The comparison between the proposed design equation and the creep analysis for stress on bottom at 360 days is shown in **Fig.2**, which is performed by the ratio of the stress obtained by the former to that by the latter. The ratios for the stresses due to autogenous shrinkage are in the range of 1.1-1.16 when the specimen is reinforced with steel bars in tension more than at least 80% of those in compression. The ratios for the stresses created by the combined action of shrinkage and prestressing at 360 days of all cases excluding CASE4 subjected to the effect of autogenous shrinkage varies 0.82-0.95. This result should mean that the present design equation coupled with aging coefficient of 0.8 for autogenous shrinkage gives the reasonable values of prestress from design point of view.

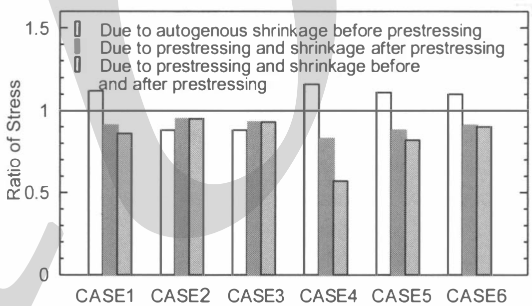

Fig.2 Ratio of Stress Obtained by Proposed Design Equation to That by Creep Analysis

4 CONCLUSION

The following conclusions are drawn from the present study.

1) A new design equation for evaluating prestress in prestressed reinforced high strength concrete was proposed, considering the effect of shrinkage before prestressing.
2) The maximum stress due to shrinkage before prestressing obtained by the proposed equation reaches 1.0 N/mm^2, which is 16 % larger than that by creep analysis based on the principle of superposition.
3) The ratios of prestress obtained by the proposed method to that by creep analysis method based on the principle of superposition of all cases excluding one case considered the effect of autogenous shrinkage varies 0.82-0.95. This result should mean that the present design equation coupled with aging coefficient of 0.8 for autogenous shrinkage gives the reasonable values of prestress from design point of view.

DESIGN AND EXPERIMENTAL RESEARCH OF PRESTRESSED CONCRETE BOX GIRDER BRIDGE SUPPORTED CANTILEVERING DECK SLAB WITH INCLINED STRUTS

Yasuo FUKUNAGA,Japan Highway Public Corporation
Koji OSADA,Japan Highway Public Corporation
Toyoshige NAKAJIMA,Oriental Construction,Joban Kosan Joint Venture
Minoru NISISU,Oriental Construction,Joban Kosan Joint Venture

Keywords: a box girder bridge with inclined struts, steel pipes of struts, full-scale model specimen

1 INTRODUCTION

The Shibakawa Viaduct is a bridge that will be constructed under the New Tomei Expressway project at a point about 160 km west of Tokyo. Since mountains extend to the coastline in this region, all major traffic routes currently in service,i.e., the Tomei Expressway, National Highway Route 1, Shinkansen (high-speed railway) and the JR Tokaido Line (railway) are located within one kilometer from the coast. Consequently, all traffic could be cut off at large earthquake. The New Tomei Expressway was planned, therefore, to run about 10 km inland to risk distribution although that meant constructing the road in a steep mountain region. In order to reduce tunnel firerisk, the tunnels in this area were designed to be short and were planned at high elevations.

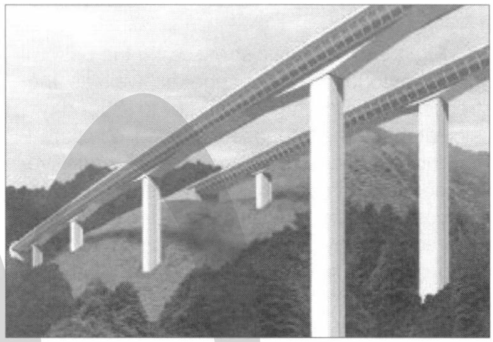

Fig.1 Photomontage of the Sibakawa Viaduct

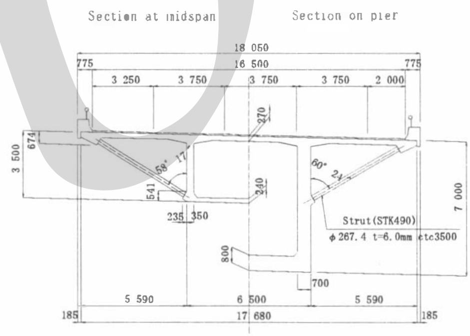

Fig.2 Typical cross section

As a result, the Shibakawa Viaduct was planned as a bridge spanning over an area with an average slope of more than 45 degrees and a maximum elevation difference of more than 80 m. Only using long distance of temporary tunnel and bridge available to approach piers. No contractor gets enough areas for build up steel girder or some other purpose without big money. In consideration construction of the superstructure, prestressed concrete box girder structure, which permits the use of the cantilever construction method, was adopted. Under the Japanese design standards, the bridge piers and foundations must be designed to achieve the sufficient seismic performance. Reduction of the self-weight of the superstructure, therefore, enables economical design of the piers and foundations. In the case of a bridge with high piers, this tendency is particularly pronounced because the percentage of the cost of pier and foundation is high. In the case of the Shibakawa Viaduct, the volume of the piers and foundations was reduced to half thanks to the narrow box girder with inclined strut, which enable to reduce not only width of top of the pier but self-weight 20%. Figure 1 is a photomontage of the Shibakawa Viaduct and figure 2 is shows the typical cross-section.

2. INVESTIGATING THE STRUCTURES OF BOX GIRDER BRIDGES WITH STRUTS

2.1 Design concepts

The design concepts of the Shibakawa Viaduct are shown in Table 1.

Table 1 Design concepts of the Sibakawa Viaduct

Part to be designed		Design concept	Steels used
Deck slab	Along the bridge axis	Controlled crack width (reinforced concrete structure)	Deformed reinforcing bar
	Across the bridge axis	No cracks allowed (partial prestressed concrete structure to control fiber stress of concrete)	Deformed reinforcing bar prestressing cable
Strut joint	Along the bridge axis	No cracks allowed (partial prestressed concrete structure to control fiber stress of concrete)	Deformed reinforcing bar prestressing cable
Strut		Safe against buckling and fatigue	Steels pipeson market

2.2 Struts

Since it is difficult to manufacture struts by reinforced cast-in-place concrete, struts had to be either precast concrete or steel. To minimize the crane facilities since the bridges were to be constructed in deep valleys by the cantilever method, the struts were decided to be steel, which weigh 1/4 of concrete struts. Struts are compressed members in principle, and the steel pipes shown in Figure 3 were selected from steel pipes on market by examining the safety against possible buckling loads.

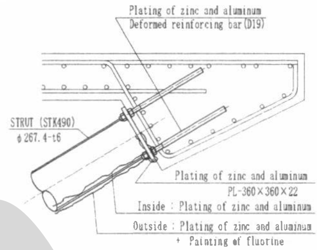

Fig.3 Strut (the steel pipes)

3. EXPERIMENTAL RESEARCH USING FULL-SCALE MODEL SPECIMEN

3.1 Outline of the experiments

To validate our elastic FEM analyses used to check the design of the bridges, full-scale model experiments were conducted (Fig.4).

The specimen was a 10.250 m-long full-scale model that consisted of the pier head and the first segment. The actual girder depth shows cross sectional changes of 7.0 to 3.5 m, but the depth of the model was uniformly 5.5 m due to manufacture limits.

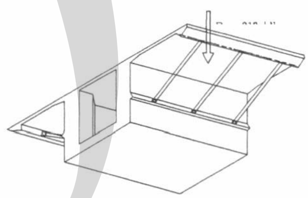

Fig.4 Full-scale model experiments

3.2 Results of the experiment

Figure 5 shows the experimental and analytical results of the relationship between the load and the displacement of the loading points. As the figure shows, the load and the displacement were in a linear relationship even when a load of 350 kN, which corresponds to overloading, was applied. The experimental and FEM analytical results well agreed with each other for the relationship between load and displacement.

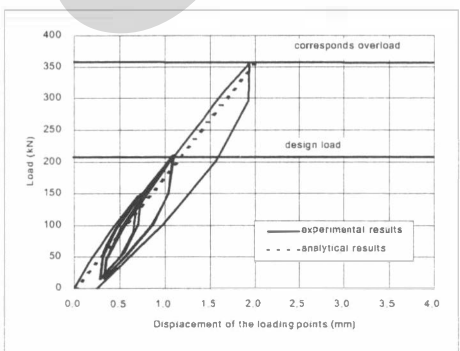

Fig.5 The relationship between load and displacement

4. CONCLUSION

In Japan, which is prone to earthquakes, reduction in the dead load of superstructures is effective to reduce the sizes of bridge piers and the foundations. Such an economic effect is especially notable in bridges that have high piers. The dead load of the superstructure of a prestressed concrete box girder bridge was reduced to approximately 80% by implementing struts to support the cantilever slabs, which requires slightly difficult to formworks. The structure was experimentally verified and was adopted to design bridges that have high piers of over 80m. The designed bridges proved the economical advantages of the structure. The bridges will be completed in March 2004.

DESIGN AND CONSTRUCTION OF THE PRESTRESSED CONCRETE GIRDER BRIDGE WITH CORRUGATED STEEL PLATE WEB

Kensaku HATA — Hanshin Expressway Public Corporation
Kazuo KOBAYASHI — Osaka Institute of Technology
Hiroshi KOBAYASHI — Hanshin Expressway Public Corporation
Mitsuya NAGASAWA — Hanshin Expressway Public Corporation

Keywords: corrugated steel web, prestressed concrete, bridge

1 FEATURES OF NAKANO BRIDGE

Nakano Bridge is one of the viaducts on the Kita Kobe Line of the Hanshin Expressway, and this bridge is a prestressed concrete bridge with corrugated steel plate webs.

Comparing with the existing corrugated web bridges, the technical characteristics of the Nakano Bridge is as following.

1) Nakano Bridge is the first curved corrugated web bridge. The radius of the horizontal alignment is 440m for main line bridges, and 250m in the minimum for ramp way bridges.
2) A new type of connector between steel webs and concrete slab is developed for the Nakano Bridge. CT rolled shapes is used for the upper flange, and the hole is punched in the web and the web is embedded into concrete slab as the perfobond strip. The studs are also used with the perfobond strip as the shear connector. Figure 1 shows this connector.
3) The field fillet welding joints are used for the splice of the corrugated steel web plate, because only the shear force is transmitted at the connector of the web plate and adjustment at the site was considered to be easier with this type of joint. Since this type of joint is used for the first time in Japan, the large-scale loading tests were conducted to examine the distribution of the stress and to confirm the strength of the joint.
4) Partial prestressing (PPC) design, in which the tensile stress in concrete is allowed but is controlled within an allowable range where no crack occurs, is used for the design of the concrete slab deck.

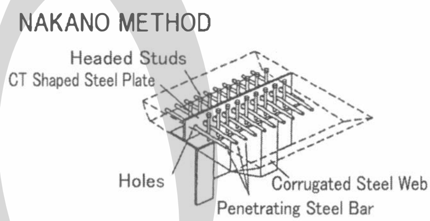

Figure 1 Nakano Method Connection

2 LOADING TESTS

Since some of these technical features were adopted for the first time in Japan, three series of large-scale tests were conducted to confirm the safety and the structural characteristics.

2.1 Push-out Test for Shear Connector

To confirm the slip-resisting strength of the shear connector with the perfobond strip and/or the studs, push-out tests for shear connector was conducted.

Figure 2 shows this test.

The safety of the joints was confirmed with this test because the measured maximum strength of the joint is much larger than the ultimate strength based on the strength of the perfobond strip (Leonhardt et. al. 1987) and the strength of the headed stud.

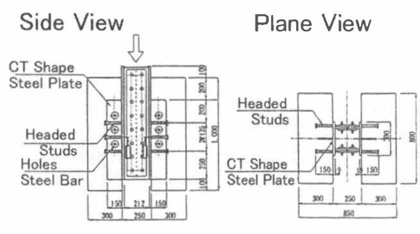

Figure 2 Push-out Test

The strength of combined connector was just the addition of those of perfobond strip and headed stud.

2.2 Test on the Mechanical Property of the Fillet Welding Joint

To confirm the strength of fillet welding joints, and, to obtain the stress distribution in the corrugated steel plate web near the joint, loading test on the fillet welding joint was conducted.

Figure 3 shows the test.

The results of the test show that the strength of fillet welding joints is sufficient, and there would no failure occur under design load even the welding parts are damaged. The distribution of shear strain in the steel web shows that the fillet welding joint behaves same as the plate without joint under the load smaller than the design load.

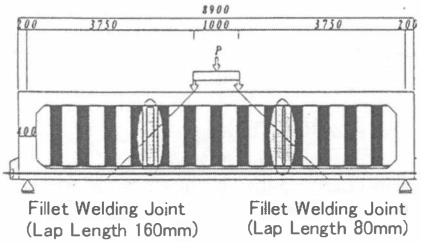

Figure 3 Test on Joint

2.3 Loading Test on Concrete slab in Transverse Direction

To examine the behavior of the partial prestressed concrete slab, loading test on concrete slab was conducted.

Figure 4 shows the test.

The result shows that the PPC slab has enough strength and the Nakano method connector is effective connector.

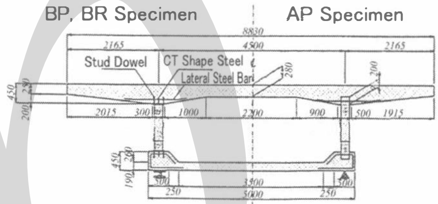

Figure 4 Test on Concrete Slab

3 CONCLUSION

Based on the test results, it was confirmed that the design method developed for the Nakano Bridge is adequate. The detail of the test results are as following,

1) The shear strength of the connector with perfobond strip and headed studs can be estimated by adding strength of each connector,
2) The field fillet-welding joint between corrugated steel webs can transfer shear force efficiently,
3) The stress concentration occurs near the scallops of corrugated webs at the joint, and further studies on fatigue behavior are needed, and,
4) The Nakano method connector with partial prestressed concrete slab is efficient and has the same strength as the embedded connector.

REFERENCES

(1) Ebina, T., Takahashi, K., Uehira K., Yagishita, F., "Basic study for shear capacity of perfobond rib", Proceedings of the 8th Symposium on Developments in Prestressed Concrete, 1998. pp. 31 –36

(2) Leonhardt, F., Andra, W., Andra, H.P., Wharre, W., "New improved shear connector with high fatigue strength for composite structures", Beton-Und Stahlbetonbau, 1987, pp.325-331.

(3) Yoda, T., Oura, T., "Torsional behavior of composite PC box girders with corrugated steel webs", Structures Engineering Joumal Vol.39A, 1993, pp.1251 -1258.

(4) Nanjo, A., Mori, Y., Iguchi, H., Kobayashi, H., "Design and Experimental Study of Nakano Viaduct in Hanshin Expressway", 10th REAAA Conference, 2000.

DESIGN AND CONSTRUCTION OF THE USUYUKI BRIDGE

Motoshi Goto, Department of Public Works, Morioka Regional Development Bureau, Iwate Prefecture
Norimoto Abe, Civil Engineering Division, Tohoku Branch, P.S. Corporation
Tomoaki Matsushima, Technology of Civil Engineering Division, Tohoku Branch, P.S. Corporation
Yoshiharu Hatakeyama, Civil Engineering Division Tohoku Branch, Sumitomo Construction Co., Ltd.

Keywords: prestressed concrete strutted rigid frame bridge, prestressed reinforced concrete structure, large temporary column, upward lifting

1. INTRODUCTION

The Usuyuki Bridge was constructed in 1999 across the reservoir of the Hayachine Dam, which is a multipurpose dam at the foot of Mt. Hayachine. The Usuyuki Bridge is the largest continuous three-span prestressed concrete strutted rigid frame structure in Japan, which has a total length of 207.0 m, a central span of 95.0 m, and a span of 125.0 m between the piers.

The bridge has the following design and construction characteristics:

1) The lower parts of the diagonal piers are to be submerged in water during flood control periods. The conventional steel framed concrete structures that use melan materials were likely prone to durability loss after the generation of cracks. The piers were decided to be built by prestressed reinforced concrete, which is durable and easy to control cracks.

2) Temporary columns were decided to be used to support the diagonal piers, which do not stand by themselves while building the cantilevered section of the main girder. Since the columns must support enormous forces of up to approximately 24,300 kN and are important for the safety during the construction of the bridge, the safety of the columns was examined by performing three-dimensional FEM analyses.

3) The stresses of the diagonal piers were adjusted by lifting the main girder upward so that we could adjust stress, correct deflection, and take control measures during accidents.

4) To ensure the safety during construction, we embedded strain gauges and reinforcing bar stress transducers in the concrete of the diagonal piers, and monitored changes in stress to examine the effectiveness of the jacks.

2. OUTLINE OF THE BRIDGE

A general drawing of the bridge is shown in Figure 1.

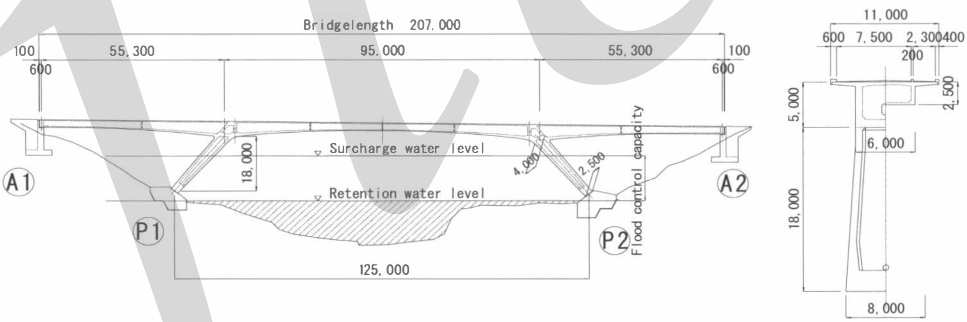

Fig. 1 General drawing of the Usuyuki Bridge

3. DESIGNING THE DIAGONAL PIERS

In most strutted rigid frame bridges, the diagonal piers are constructed using steel framed concrete and melan materials. The Usuyuki bridge used the prestressed reinforced concrete structure by considering durability when submerged in water.

A design calculation of reinforced concrete showed possibilities of cracks on the diagonal piers. The piers were therefore designed by setting limits of tensile stress of concrete for each construction process. The stresses on the diagonal piers were adjusted and cracks during construction were controlled by lifting the piers using hydraulic jacks and installing supplementary pre-stressing steels at the foot of the piers to keep the bending stress, which is determined as an effective stress for the total cross section of concrete, below the bending strength of the concrete, the act of which was likely to prevent cracks after the completion.

4. DESIGNING TEMPORARY COLUMNS

Temporary columns were to receive a large reaction force of approximately 24,300 kN. The columns were therefore designed by considering an effect of 20% by the eccentric loading of the vertical force and a horizontal force of 5% of the vertical load to the directions along and across the bridge axis. The design was then examined by performing a three-dimensional frame analysis that modeled the steel pipe posts and sway braces. The local stress and buckling safety were examined by three-dimensional FEM analyses. The analyses showed a safety factor of approximately 6 times.

5. LIFTING THE DIAGONAL PIERS

The diagonal piers were lifted upward to adjust the stresses at the foot of the diagonal piers of the completed bridge and to compensate for the elastic contraction of the temporary columns, which was caused by the reaction force of the main girder, for 10 mm when the heads of the piers were completed and for 7 mm when two blocks were completed. The extent of lifting consists of 7 mm to adjust the settlement of the temporary columns and 10 mm to adjust the stresses at the foot of the piers.Two hydraulic jacks with lock nuts, which were 100 mm in maximum stroke and 15,000 kN in maximum capacity, were mounted on each temporary column since the reaction force was as large as 24,300 kN, and the piers were to be lifted for units of millimeters for approximately six months.

6. MONITORING

Monitoring was conducted to understand the stress intensity of the piers and examine the effectiveness of lifting. Monitoring was conducted by setting the design and upper limit values for each monitoring item and comparing with the monitored data. Stress intensity values were corrected using thermocouples and non-stress meters to eliminate the effects of temperature changes and creep drying shrinkage. Figure 2 shows a plot of stress intensity at the upper surface of the foot of Diagonal Pier P1. The stress of the reinforcement were closer to the designed effective stress on the total cross section than to the design calculations for reinforced concrete, suggesting that there were no cracks on the pier. The stress of concrete was slightly different from the design values since the values were small, but was almost similar. The results show the effectiveness of the lifting to adjust the stresses on the diagonal piers and to ensure the safety of the structure.

We also confirmed that the initially aimed forced displacement of 10 mm was maintained when the center span section was closed. The results as well as the stress measurements show that the stresses on the diagonal piers were adjusted as planned.

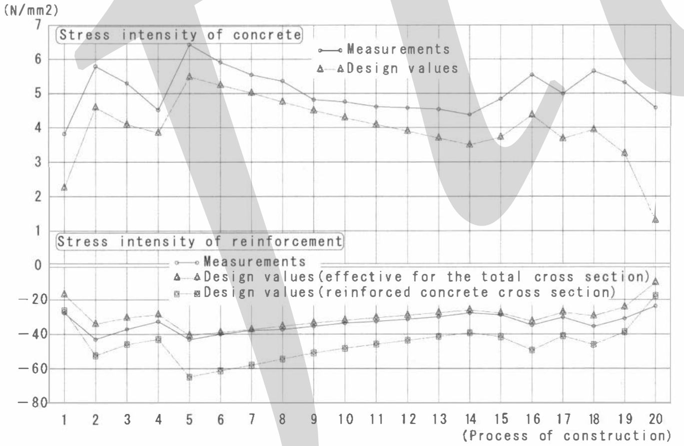

1) When the head of the pier was completed
2) When the pier was lifted for the first time
3,4) After placing Block 1,2
5) When the pier was lifter for the second time
6～14) After placing Block 3～11
15) When the form traveler was removed
16) When loading on the hanging support
17) When the center section was closed
18) When the temporary column was removed
19) When the span was closed
20) When the structure was completed

Fig. 2 Stress intensity at the foot of a diagonal pier

REFERENCES

[1] Goto Motoshi, Abe Norimoto, Matsushima Tomoaki, and Yoshiharu Hatakeyama: Design and construction of the Usuyuki Bridge (in Japanese), Proceedings of the 9th PC Symposium, No. 126, p. 665, October 1999.

[2] Goto Motoshi, Matsushima Tomoaki, and Akira Noguchi: Design and construction of the Usuyuki Bridge, Proceedings of the 23rd Japan Road Congress (B), No. 6072, p. 390, October 1999.

EXPERIMENT TO DETERMINE ULTIMATE SECTION STRENGTH OF GERBER (NOTCHED) PORTIONS OF CONCRETE GIRDER ENDS

Okada Masasumi Kojima Hiroshi Osada Mitsumasa
Design and Research Division
Maintenance and Facilities Department
Metropolitan Expressway Public Corporation
JAPAN

Keywords: Gerber cantilever bridge, ultimate section strength, failure mode, reinforcement, post-tensioning method

1. INTRODUCTION

With a total length of approximately 270km, the Tokyo Metropolitan Expressway handles an average traffic volume of around 1.16 million vehicles (about 10% of which are heavy-duty cargo vehicles) and about 2 million people daily. Over 80% of the structures are elevated constructions, which, when tunnels and subsurface structures are included, account for 95% of the expressway's total length. Approximately 15% of these elevated structures are made of concrete, and have a total length of 38km. Sections opened to the public in 1962 are expected to have a life span of nearly 40 years. Routes in use for over 30 years account for about a third (36%) of the entire expressway, while routes opened over 20 years ago amount to roughly half (52%).

Some of the concrete structures consist of Gerber cantilever bridges whose main girder ends have lower web heights than other bridge sections in order to secure a clearance with roads under the bridges and with the structures over the expressway. Crack formation has been observed in corner areas in some of these prestressed concrete girders.

To determine the ultimate section strength and failure mode of this type of prestressed concrete girder and establish the effect of reinforcement work using the post-tensioning method, we conducted a series of load-carrying capacity tests on full-size specimens with the actual bridges. This paper gives an overview of the test results.

2. METHODS AND RESULTS

The scope of the experiments covered the prestressed concrete girders with Gerber (notched) portions at the girder ends. The tests were conducted on the simple PC T- and I-girders, which account for 38% of all girders of the expressway. The simple PC T-girders account for 71% of these and were taken as the specimen model. Prior to the experiments on specimens with a T-shaped cross section, pre-experiments were carried out on rectangular cross section specimens to (1) assess the validity of the existing reinforcement bars and steel tendons in the longitudinal direction and (2) ascertain the reinforcing effect of the prestressing bars.

The effects of three types of post-tensioning method for the oblique cracks at the Gerber (notched) portions were confirmed in the experiment: ①post-tensioning method (oblique prestressing bar technique), ②post-tensioning method (horizontal and perpendicular prestressing bar technique), ③ Non-Abutment Pretensioning and Precompressing (NAPP) method.

The specimens were turned upside down and a simple increasing static load was applied from the top of the support position of the girder end by using a 300tf(3MN) jack. A support was positioned at a distance equal to or more than the girder height (1750mm) from the load point in order not to affect the stress flow (Fig. 1).

In order to establish load-carrying capacity, load-carrying mechanism and failure mode of the Gerber (notched) portions in the girder ends, and to determine the effectiveness of reinforcements using the post-tensioning methods, we conducted load application tests using full-size specimens. For the PC girder specimens it was found that the stresses in the Gerber (notched) portions were relieved by tensioning the steel tendons in the longitudinal direction and that, as a result, the formation of oblique cracks tended to be diminished. Further, in the case of the specimens that had been reinforced by the prestressing methods, it was found that the stresses in the oblique reinforcements were substantially relieved and that, as a result, the crack propagation tended to be suppressed, and that the specimen's yield strength substantially increased (Table 1).

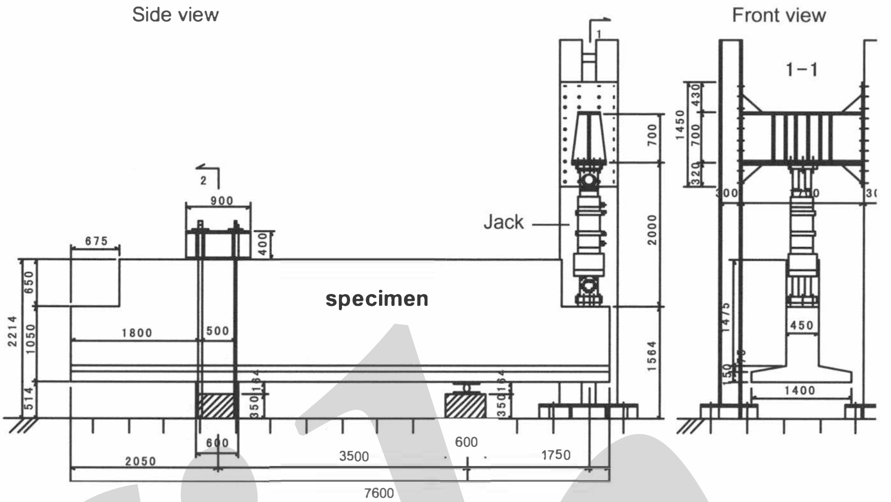

Fig.1 Schematic of Load Application Test Unit

Table 1 Failure Load

Specimen No.	Failure Load(tf)	%	Failure mode
1−PC−1	210	94	Compressive failure
1−PC−2	222.5	100	Compressive failure
3−RC−3	190	85	Shear failure
2−HS−4	300	135	No failure
2−HV−5	285	128	Compressive failure
3−TO−6	245	110	Compressive failure
4−TH−7	300	135<	No failure
4−TH−8	320	144<	No failure

REFERENCES

1. Road Maintenance and Management on the Most Heavily Used Expressway in the World - The Tokyo Metropolitan Expressway, H. Mitani, K. Izumi. Dec. 2000
2. Road Bridge Manual, Concrete Bridges, Dec. 1996, The Japan Road Society (Japanese)
3. Investigation and Research on Metropolitan Expressway Inspection, Repair and Reinforcement (FY 2000). Concrete Structures Committee Report, Feb. 2001 Metropolitan Expressway Public Corporation, Metropolitan Expressway Engineering Center (Japanese)
4. Investigation and Research on Metropolitan Expressway Inspection, Repair and Reinforcement (FY 1998). Concrete Structures Committee Report, Feb. 1999 Metropolitan Expressway Public Corporation, Metropolitan Expressway Engineering Center (Japanese)
5. Investigation and Research on Metropolitan Expressway Inspection, Repair and Reinforcement (FY 1998). Report, Feb. 1999. Metropolitan Expressway Public Corporation, Metropolitan Expressway Engineering Center (Japanese)

THE CONCEPT OF SPLICED BRIDGE AND THE MECHANICAL BEHAVIOR

Dr. Yasuhiko SATO and Prof. Yoshio KAKUTA
Division of Structural & Geotechnical Engineering Hokkaido University
JAPAN

Dr. Akihisa IMAMURA and Tadahiro MOHRI
Design Division DPS Bridge Works Co.,ltd.
JAPAN

Keywords: spliced PC bridge, cost performance, construction joint, crack width, capacity

1 INTRODUCTION

With the aim of reduction in construction cost, a new type of bridge called spliced PC bridge has been developed. The spliced PC bridge (see Fig.1) is a hybrid structure consisting of pre-tensioned precast member made in an existing factory under the high quality control and reinforced concrete member of cast-in-site with flexibility at construction. The precast and cast-in-site members are spliced by post-tensioning cable.

In this paper, aspects of the spliced PC bridge are introduced. Furthermore, flexural and shear behavior of spliced PC beam and applicability of the ordinary design method to the proposed structure are discussed.

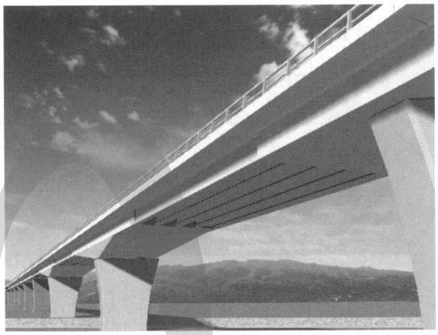

Fig.1 The view of spliced PC bridge

2 ASPECTS OF SPLICED PC BRIDGE

Major aspects of the spliced PC bridges are follows:

(1) Construction period and cost can be reduced because, preparation of precast girder and construction of cast-in-site girder can be synchronized, formwork and falsework are not required in the region using precast girders, simple wet joint i.e., joint using reinforcing steel bars is adapted for coupling of precast girder and cast-in-site girder, the number of bearing can be reduced because box girder structure is adapted above the support, and lateral bracings are not used.

(2) It is possible to reduce height of girder by using both post-tensioning and pre-tensioning systems in precast girder with high strength concrete. The girder height at the center of span is about 1.8m and the span-depth ratio of girder is about 0.03.

(3) Varying cross section of cast-in-place girder can allow the sufficient eccentricity of prestressing steel bar on the support.

3 EXPERIMENTAL INVESTIGATION ON FLEXURAL AND SHEAR CHARACTERISTICS OF SPLICED PC BEAMS

3.1 Specimens

Twelve beam specimens are prepared in this study (see Table 1). All the specimens consist of a precast pre-tensioned segment and a reinforced concrete of cast-in-site except specimens M-1 and S-1. In all the specimens except specimens M-1 and S-1, post-tensioning bar with the length of 3m is passed through the segments and two segments are coupled with the prestress of 940 kN.

The specimens are categorized into two series. The series 1 containing seven specimens is prepared to evaluate the flexural characteristics and the series 2 containing another five specimens is prepared to evaluate the shear characteristics.

In series 1, type of joint, shape of cross section and confinement at joint are chosen as a parameter. In series 2, type of joint and shape of cross section are chosen as a parameter.

3.2 Flexural characteristics

Typical flexural failure was observed in all specimens. Crushing of concrete after yielding of tension reinforcing and prestressing bars took place around the construction joint except specimen MC-1. In specimen MC-1, crushing of concrete was observed around the loading point.

Ultimate load are shown in Table 2. The ultimate load of specimens with the joint was identical to that without the joint and could be predicted by the ordinary beam theory except for specimens M-5 and M-C1. It can be considered that the bond deterioration brought the reduction of the capacity in specimen M-5 and M-C1.

It was also confirmed in this study that the crack width at the construction joint in the spliced PC beam could be predicted by JSCE equation[1].

Table 1 Details of specimens

Test Beams		Joint	Section Shape *)		Concrete Strength (N/mm^2)		Prestress (N/mm^2)		Type Splice of reinforcing bar
Series	Name		Pre-Cast	Cast-in-situ	Pre-Cast	Cast-in-situ	Pre-tension	Post-tension	
1	M-1	No	I	-	60	-	940	-	-
	M-2	Yes	I	I	60	40	940	940	Lap
	M-3	Yes	I	I	60	40	940	940	Loop
	M-4	Yes	I	R	60	40	940	940	Lap
	M-5	Yes	I	R	60	40	940	940	Loop
	M-C1	Yes	I	R	60	40	940	940	Lap
	M-C2	Yes	I	R	60	40	940	940	Loop
2	S-1	No	I	-	60	-	940	-	-
	S-2	Yes	I	I	60	40	940	940	Lap
	S-3	Yes	I	I	60	40	940	940	Loop
	S-4	Yes	I	R	60	40	940	940	Lap
	S-5	Yes	I	R	60	40	940	940	Loop

*) I : I-shape cross section, R : Rectangure cross section

Table 2 Experimental results (series 1)

Test Beam		Failure section	Experiment		Analysis	
NO.	Name		Crack P_{cr}(kN)	Max. Load P_u(kN)	Crack P_{cr}(kN)	Max. Load P_u(kN)
1	M-1	Center	80	220	83	157
2	M-2	Joint	29	202	39	186
3	M-3	〃	30	197	39	186
4	M-4	〃	30	200	39	186
5	M-5	〃	32	179	39	185
6	M-C1	Cast-in-situ	42	156	39	186
7	M-C2	Joint	40	202	39	186

3.3 Shear characteristics

In specimens with the joint, shear crack appeared at the precast beam (left side) but the crack stop at the joint. The shear crack propagated into the beam of cast-in-site across the joint just before the maximum load.

In all specimens, diagonal tension failure took place. Ultimate force and shear capacity are shown in Table 3. Shear capacity in the experiment is the shear force at the stirrup started to yield. It was clarified that the shear capacity of the spliced PC beam can be predicted by JSEC equation[1].

Table 3 Shear capacity

Specimen	Ultimate force(kN)	Shear capacity(kN)		Exp./Cal.
		Exp.	Cal.	
S-1	451.1	256.8	217.4	1.181
S-2	329.9	239.0	199.9	1.196
S-3	355.0	239.3	199.9	1.197
S-4	385.4	259.9	199.9	1.300
S-5	424.4	274.4	199.9	1.373

CONCLUSIONS

(1) Crack width at the joint can be predicted by JSCE equation regardless of the type of splice and the shape of cross section.

(2) The flexural and shear capacities of the spliced beams can be predicted by the ordinary design method.

REFERENCES

[1] JSCE, "Standard Specification for Design and Construction of Concrete Structures", 1986.

STRENGTH-MAXIMIZED PRESTRESSED CONCRETE STRUCTURES

Mechyslav Chekanovych
Kherson Agrarian University,
UKRAINE

Keywords: strength-maximized, regulating, utilization

1 INTRODUCTION

Modern reinforced concrete structures do not fully use strength properties and energy failure resistance of concrete and steel under loads. It is especially important for beams and columns compressed with significant eccentricity, where a considerable and sometimes the greater part of the cross section is excluded from performance even before the carrying capacity is exhausted. Prestressing application raises stiffness and crack resistance, but tells little on strength of structures. When loads are high, prestressing is here exhausted, cracks appear, that also exclude part of the structure's cross section from work. Close to neutral layer, concrete does not realize its strength properties in flexural members compressed with significant eccentricity.

Concrete's strength properties are utilized more effectively in columns compressed centrally and with insignificant eccentricity. But here we also have considerable strength reserves. In traditional columns it is difficult to fully realize high strength of best steels, as concrete fails at stresses and strains much lower than high strength steels do.

A somewhat lesser but still considerable property difference is preserved when using high strength concrete (HSC). In this case, high strength of concrete is gained by maximum utilization of strength properties of its components and their compounds, taking into account modern technologies and design methods [1].

Maximizing strength and providing for high failure resistance energy of reinforced concrete as a whole makes it possible to achieve a more efficient utilization of prestressed concrete structures in modern construction.

2 ANALYTICAL METHODS

2.1 Maximization of strength of materials

Application of high strength steel contributes to reaching maximum strength of a structure with optimal metal (steel) consumption. Maximization of concrete strength is possible by maximum utilization of strength properties of components. It is achieved by means of a thorough selection of materials, their rational granulometric and chemical combination, binder quality, activizing additives, temperature and moisture hardening regime, packing conditions, hardening under pressure [2] and other factors.

2.2 Structures strength maximization

Original prestressed concrete structures with maximum utilization of strength properties of concrete and steel have been developed. It is due to the structure's simultaneous acquiring maximum concrete and steel strength. As concrete and steel strains are hundreds of times different when reaching their maximum strength, to compensate this difference the tensile bars are provided with a force regulating system. Thanks to this self - regulation, when changing structure loading strain amplitude is several times higher than that of the concrete, thus ensuring a positive effect and a chance for concrete's crackless performance.

At the moment of reaching maximum strength of concrete and steel compressive strains are also different, but to a smaller extent. To see concrete and steel revealing their maximum strength synchronically when under stress, non-contact steel - concrete interaction proposed by the author proved sufficient. More intensive steel strains in the structures are ensured by creating a special contact zone at the reinforcing bar surface.

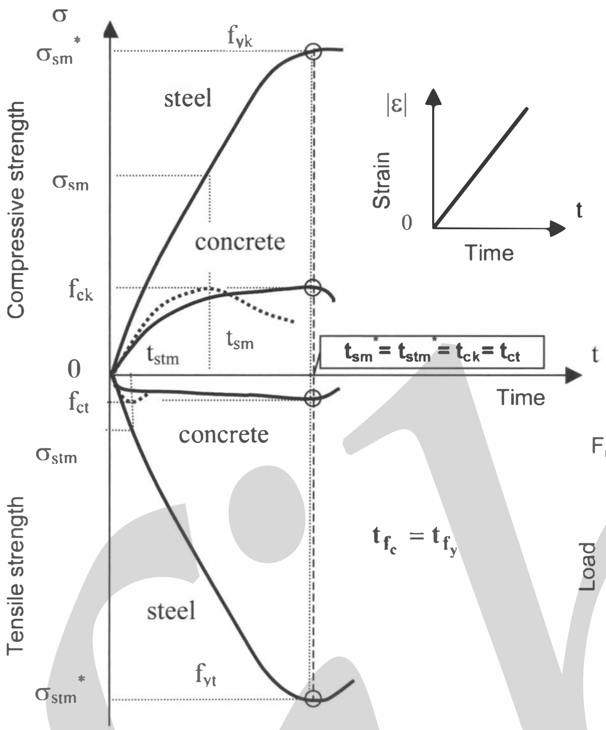

$$W = F\delta - \int_0^\delta \delta dF$$

$$W_{max} = W_{full} - W_q$$

$$W_q \to 0; \quad W \to W_{full};$$

$$W = W_{max}$$

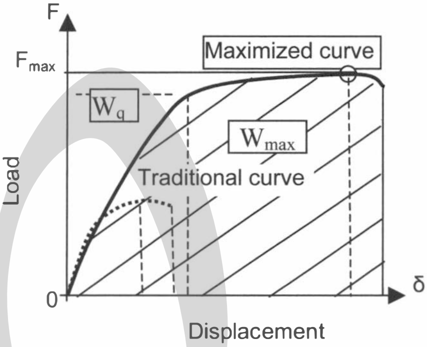

Fig.1 Synchronized diagrams

Fig.2 Maximized curve

A synchronized display of maximum resistance of concrete and steel (Fig.1) is ensured by additional work of the mediator (or regulation device) W_m

$$W_{max} = W_{cmax} + W_{smax} + W_m \tag{1}$$

that leads to achieving maximally possible strength of a structure (Fig.2):

$$F_{max} = \gamma\left(\sum_{i=1}^{n} f_{ci} A_{ci} + \sum_{j=1}^{k} f_{sj} A_{sj}\right) \tag{2}$$

On Fig.1 a stress – strain diagram of concrete also includes influence of the mediator. The maximized curve on Fig.2 takes into account limitation of the stress value by the top line of microcracking that allows preventing self-failure of concrete within time. The above mentioned agrees with the law of energy conservation.

The structures developed are used in construction in Ukraine. Strength maximization of prestressed concrete structures has led to an increase in their carrying capacity from forty per cent to four times, to concrete's crackless performance, and a considerable deflection decrease of the structures.

REFERENCES

[1] Walraven J. : Challenges for new materials in concrete structures. Proceedings of the XIII-th FIP Congress on Challenges for concrete in the Next Millennium, 23-29 May 1998, Amsterdam, vol. 1, pp.3-8

[2] Chekanovych M. : New Building Technology for Prestressed concrete Structures, Long- Span and High-Rise Structures, IABSE Symposium, 2-4 September 1998, Kobe, vol. 79, pp. 507-512

SELF ANCHORED PRESTRESSED CONCRETE SUSPENSION BRIDGE

Narushige MATSUNAGA
SE Corporation,
Tokyo,Japan

Jean-Pierre RAGARU
SE Corporation
Tokyo,Japan

Keywords: suspension bridge, self-anchored, concrete, design method

1. INTRODUCTION

When we design a suspension bridge, we usually use computer software taking into account large displacements. For self-anchored suspension bridges, thermal variations induce a bending moment in the girder that shall be taken in account in the design. This problem increases when the suspended girder is a prestressed concrete one, under the effect of creep and shrinkage.

Doing that, we have to manage between two opposite considerations: The girder must be strong enough to resist internal forces and flexible enough to keep these forces in acceptable limits. Finding a fine equilibrium between these two opposite problems is not easy and, due to the many parameters involved, many computer calculations can be done without right results.

We have carried out an analytical study of the behavior of this type of bridge under various load cases in order to facilitate the design and better apprehend the effect of a modification of each parameter and this paper summarize some simple rules we established to evaluate these effects and their evolutions according to the value of the main parameters of the bridge. These rules have been correlated with the multiple calculations we have done with a second order, finite elements, program and we hope they will help designer to choose between many alternatives the best one to develop.

2. ANALYTICAL STUDY

2.1 General

The aim of the study is the longitudinal flexure of the suspension bridge and we will conduct the analysis on a 2D basis. As shown on Fig.1, the study was done for a 2 spans and for a symmetrical 3 spans suspended bridge.

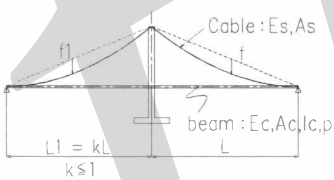

Fig.1 2 Spans Bridge

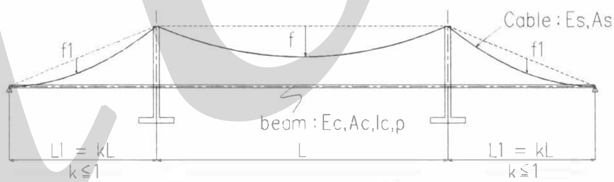

Fig.2 3 Spans Bridge

The following dimensionless parameters will be used: $\zeta = f/L$; $\varphi = H/L$; $n = E_s/E_c$; $\gamma = fL^3/I_c$; $\mu = L^2/A_c$; $\nu = L^2/A_s$ $\rho = p_1 b_1/pL \, or \, P_1/pL$; $\chi = pL^2/8ff_e A_s$ and standard additional hypothesis have been done like neglecting the variations of length of the hanger, the horizontal reactions of the towers.

2.2 Permanent state

The study of the permanent state of the bridge is well known and doesn't require computer software. If we know the vertical alignment of the bridge and the initial state required, we are able to calculate easily, for a given tension of the cable, the parabolic geometry of the cable.

2.3 Behavior under loads applied after erection

The behavior of the bridge depends on the additional horizontal component Q_a of the cable thrust. The calculation shows that one of the particularities of self-anchored suspension bridges is their linear behavior under a load applied after erection.

2.3.1 Behavior under live load applied on the deck

The analytical calculations show that the additional thrust can be expressed as

$Q_a = \frac{m\gamma\zeta\chi f_e}{\upsilon C_1} L^2 .f(k,\rho) = C_4 f_e L^2 .f(k,\rho)$ where f(k,ρ) is a function depending only on the distribution of the loads on the girder and of the ratio between side and main span. We can write C_1=A1+A2+A3 with:

Table 1 Formulae for coefficients A1 and A2

Type of Bridge	2 spans	3 spans
A1	$\upsilon \sum_{\alpha=k.1} \sqrt{\alpha^2+\varphi^2} (1+16\alpha^2\zeta^2 + \frac{\varphi^2}{\alpha^2} - \frac{8\alpha^4\zeta^2}{\alpha^2+\varphi^2} + \frac{96\alpha^{10}\zeta^4}{5(\alpha^2+\varphi^2)^3}$	$\upsilon\left(1+2\frac{(k^2+\varphi^2)^{3/2}}{k^2} + 8\zeta^2\left\{1+2k^2\frac{2\varphi^2+k^2}{(k^2+\varphi^2)^{1/2}}\right\} + \frac{96\zeta^4}{5}\left\{1+\frac{2k^{10}}{(k^2+\varphi^2)^{5/2}}\right\}\right)$
A2	$n\mu(1+k)$	$n\mu(1+2k)$

Table 2 Formulae for coefficient A3

Type of connection	Simply supported spans	Continuous girder Simply supported	Embedded girder
2 spans	$\frac{8}{15} m\gamma\zeta(1+k^5) \quad = ①$	$① - \frac{1}{3} m\gamma\zeta \frac{(1+k^3)^2}{(1+k)}$	$\frac{1}{5} m\gamma\zeta(1+k^5)$
3 spans	$\frac{8}{15} m\gamma\zeta(1+2k^5) \quad = ①$	$① - \frac{4}{3} m\gamma\zeta \frac{(1+k^3)^2}{(3+2k)}$	$\frac{2}{45} m\gamma\zeta(2+9k^5)$

2.3.2 Behavior under thermal variation

The analytical calculations show that the additional thrust for a strain ε in the cable can be expressed as $Q_a = -\frac{C_2}{C_1} E_s L^2 .\boldsymbol{\varepsilon} = -C_6 E_s L^2 .\boldsymbol{\varepsilon}$ and

the additional thrust for the strain ε in the deck can be expressed as $Q_a = \frac{C_3}{C_1} E_s L^2 .\boldsymbol{\varepsilon}$ where C_1 is the coefficient previously mentioned and C_2 and C_3 are coefficient given in table 3.

Table 3 Formulae for coefficient C_2 and C_3

	C_2	C_3
2 spans	$1+k+\frac{(1+k)}{k}\varphi^2 + \frac{16}{3}(1+k^3)\zeta^2$	$1+k$
3 spans	$1+2k+\frac{2}{k}\varphi^2 + \frac{16}{3}(1+2k^3)\zeta^2$	$1+2k$

2.4 Creep and shrinkage effect

The creep and shrinkage effect can be studied using the linear behavior of the self-anchored suspension bridge. The variation of horizontal thrust and of bending moment on support due to strain ε and to free supported span bending moments μ_i can be generally expressed as:

$$\Delta Q = \alpha_1 \varepsilon + \alpha_2 \sum_{k=1}^{N} \int_0^{Lk} \mu_k y_k dx + \sum_{k=1}^{N} \alpha_3^k \int_0^{Lk} \mu_k x dx + \sum_{k=1}^{N} \alpha_4^k \int_0^{Lk} \mu_k dx$$

$$\Delta M_s^j = \beta_{1j} \varepsilon + \beta_{2j} \sum_{k=1}^{N} \int_0^{Lk} \mu_k y_k dx + \sum_{k=1}^{N} \beta_{3j}^k \int_0^{Lk} \mu_k x dx + \sum_{k=1}^{N} \beta_{4j}^k \int_0^{Lk} \mu_k dx$$

k is the span (1 to N), j the support (0 to N) and the coefficients α_i and β_i depend on the type of bridge (2 or 3 spans) and type of connection between girder and tower. The creep and shrinkage effect can be evaluated easily step by step without integration of the moments

This calculation requires the evaluation of some integrals like $I_j = \sum_{k=1}^{N} \int_0^{Lk} \Delta M^j(x) y_k(x) dx$

$K_j^k = \int_0^{Lk} \Delta M^j(x) x dx$; $L_j^k = \int_0^{Lk} \Delta M^j(x) dx$, but we can calculate these integrals step by step as they are only sum and products of previously calculated values.

INVESTIGATION ON LINER TEARS OF A 1:4-SCALE PRESTRESSED CONCRETE CONTAINMENT VESSEL MODEL SUBJECTED TO INTERNAL OVERPRESSURE

Satoru Shibata[1], Michael F. Hessheimer[2], Tomoyuki Kitani[3], Makoto Kondo[3], James F. Costello[4]
1) Nuclear Power Engineering Corporation, Japan、 2) Sandia National Laboratories, USA
3) Mitsubishi Heavy Industries, LTD., Japan、 4) U. S. Nuclear Regulatory Commission , USA

Keywords: PCCV, mock-up test, liner tear analysis, inelastic FEM structural analysis,

1. INTRODUCTION

The Nuclear Power Engineering Corporation (NUPEC) and the US Nuclear Regulatory Commission (NRC) had co-sponsored and jointly funded a Cooperative Containment Research Program at Sandia National Laboratories (SNL). The purpose of the program is to investigate the response of representative models of nuclear containment structures under overpressurized loading beyond the design basis accident and to compare analytical predictions with measured behavior. This is accomplished by conducting static, pneumatic, overpressurization tests of scale models at ambient temperature. A 1:4-scale prestressed concrete containment vessel (PCCV) model based on the containment structure of Unit 3 of the Ohi Nuclear Power Station in Japan was conducted by SNL in September 2000. This PCCV model had an equipment hatch, several penetrations, and liner with T-anchors and is shown in Fig 1. When the test was conducted under pressurizing with nitrogen gas, a small leak 1.5% mass/day (allowance was less than 1% mass / day) was detected at the pressure 2.5Pd[*1] (0.98MPa). The acoustic system could also catch the small sound on a leak at same time. After this first leak, the amount of leak grew to 800% mass/day at the maximum 3.3Pd and the test was terminated prior to structural failure since the leak late exceeded the capacity of pressurizing system.

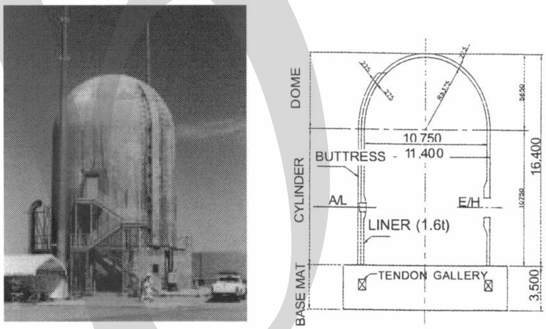

Fig 1 Outlook and Section Structure of the PCCV 1:4 Scale model

2. POSTTEST INSPECTION AND METALLURGICAL ANALYSIS

Posttest inspection revealed that there were 18 groups containing 26 tears assumed to occur at from 2.5Pd to 3.3Pd. It shows that tears were distributed in the region of the largest global strain on the middle height of cylindrical liner. And moreover all the tears located at the heat affected zones (HAZ) adjacent to the vertical welded lines. We never found a deficiency in the liner material and welds contributed to tearing.

First tearing was assumed to occur near the equipment hatch (E/H) between at 2.4 and at 2.5 Pd through the acoustic data. 38 acoustic sensors were mounted on outer concrete surface and 16 acoustic sensors were set on the cylindrical liner. 4 sensors near E/H could catch the sound of escaping gas clearly at 2.5Pd and locate the region of the first tearing with computing analysis. We measured the thickness near the every tear and analyzed the sample pieces cut out.

3. SIMULATION ON FIRST LINER TEAR AT 2.5PD (0.98MPA)

From a point of view on a structural design, we have not made use of the reasonable evaluation method with causing a tear on a steel liner. We tried to establish how to evaluate the local strain at the point caused a tear through the analysis and inspection after the PCCV model test and have gotten some good findings. The estimation flow for simulating on the first liner tearing at 2.5Pd is shown in Fig 2.

---

*1) (Pd) denotes a design pressure. In this plant case, 1Pd corresponds to 0.392MPa.

As shown in Fig 2, at first we calculated the global strain ε_0 near the inspected points with an axisymmetric FEM model. We confirmed that this analytical model had its behavior to meet with the limited state test data.

And next we calculated a concentration coefficient α of local strain at the inspected point based on some typical detail structures of the liner under each pressure loaded. And at third, we calculated a concentration coefficient β of local strain at the vertical weld line with the typical weld bead section patterns under each pressure load. Finally we estimate each local strain caused a tear with $\alpha \times \beta \times \varepsilon_0$ and apply the criterion of causing a tear to its local strain.

For establishing this criterion of local failure strain, we conducted 6 mock-up tensile tests and their FEM simulations. We chose larger than 15% on local failure strain as the criterion for occurring a tear on the model liner. The local strain behavior at the first tear is shown in Fig3. This figure shows that the first tearing occurred at 2.4 Pd. Considering the pressure 2.5Pd at which the small leak began in the test, this result means that our evaluation method on occurring a tear is reasonable.

4. CONCLUSION

Through our test of PCCV 1:4 scale model, the followings are summarized.

(1) In post-test inspection of PCCV model test pressured to maximum 3.3Pd, 26 tears (18 groups) in the severest global strain region of the middle height of PCCV cylinder were founded and all the tears occurred at vertical weld lines

(2) Through macro examination of liner, metallurgical analysis and metallographic examination of cross-section at tear, the reduced thickness of liner by grinding in small extent was found adjacent to each tear although there is no defect of material and no miss welding.

(3) As the criterion of the local strain to cause a tear on 1:4-sacle PCCV model liner (1.6t), we chose the failure strain 15% which based on tensile tests with thin liner welding specimens and its FEM analyses.

(4) Applying this criterion, it was confirmed that our evaluation method could infer the pressure to cause a tear.

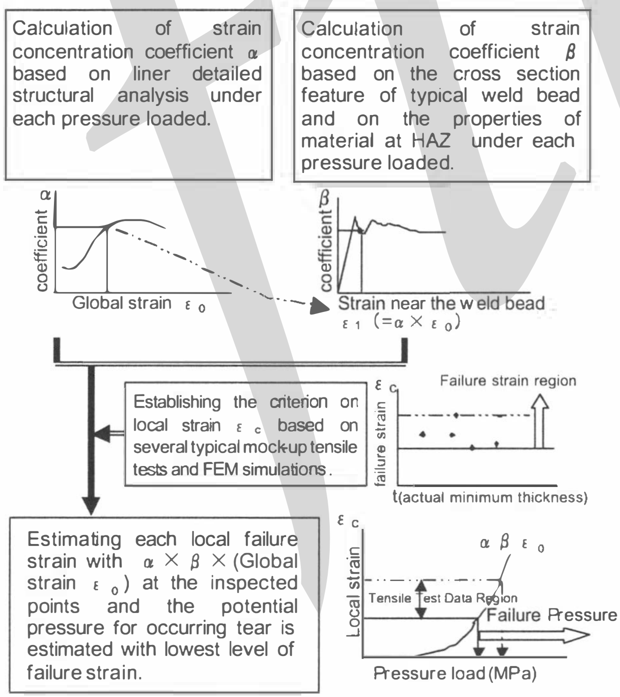

Fig 2 Estimation flow for the first liner tearing at 2.5 Pd

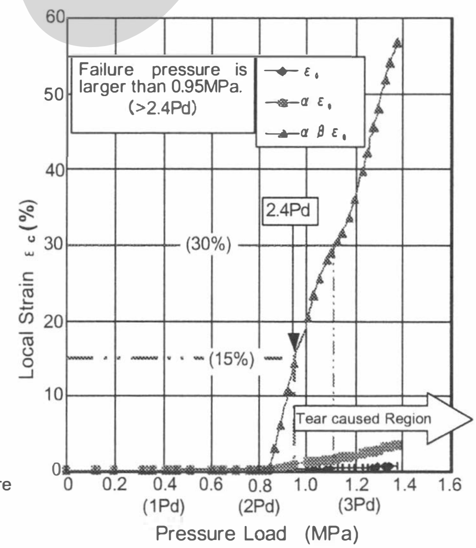

Fig 3 Failure Pressure evaluation with Local strain near the first tearing

BEHAVIOR OF TENDONS IN A PRESTRESSED CONCRETE CONTAINMENT VESSEL MODEL FROM INITIAL TENSIONING THROUGH OVERPRESSURE LOADING[a]

M. F. Hessheimer[1], S. Shibata[2], and J. F. Costello[3]

1) Sandia National Laboratories, Albuquerque, NM, USA
2) Nuclear Power Engineering Corporation, Tokyo, Japan
3) United States Nuclear Regulatory Commission, Washington, D.C., USA

Keywords: nuclear containment, prestressed concrete, pressure testing

1. INTRODUCTION

Sandia National Laboratories (SNL) is conducting a Cooperative Containment Research Program that is co-sponsored and jointly funded by the Nuclear Power Engineering Corporation (NUPEC) of Japan and the U.S. Nuclear Regulatory Commission (NRC), Office of Nuclear Regulatory Research. The purpose of the program is to investigate the response of representative scale models of nuclear containments to pressure loading beyond the design basis accident and to compare analytical predictions to measured behavior. This objective is accomplished by conducting static, pneumatic overpressurization tests of scale models at ambient temperature. This research program consists of testing two scale models: a steel containment vessel (SCV) model (tested in 1996) and a prestressed concrete containment vessel (PCCV) model, which is the subject of this paper.

2. DESIGN, CONSTRUCTION AND INSTRUMENTATION OF THE PCCV MODEL

The prestressed concrete containment vessel (PCCV) model is a uniform,1:4-scale model of the containment structure of Unit 3 of the Ohi Nuclear Power Station in Japan. Ohi Unit 3 is a 1180 MWe pressurized-water reactor (PWR) plant designed, constructed and operated by Kansai Electric Power Company. The Ohi-3 containment vessel is a steel-lined, prestressed concrete cylinder with a hemispherical dome and two vertical buttresses. Model construction occurred at the Containment Technology Test Facility at Sandia National Laboratories between January 3, 1997 and June 25, 2000. The overall geometry of the model is shown in Figure 1(a). The design pressure (P_d) is 0.39 MPa. Details of the design, including the design drawings, and construction are reported in the PCCV test report.[b]

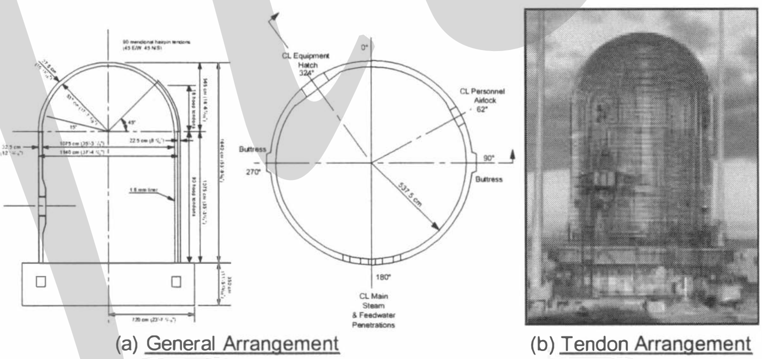

(a) General Arrangement (b) Tendon Arrangement

Figure 1 Prestressed Concrete Containment Vessel (PCCV) Model

---

[a] This work is jointly sponsored by the Nuclear Power Engineering Corporation and the U.S. Nuclear Regulatory Commission. The work of the Nuclear Power Engineering Corporation is performed under the auspices of the Ministry of Economy, Trade and Industry, Japan. Sandia is a multi program laboratory operated by Sandia Corporation, a Lockheed Martin Company, for the U.S. Department of Energy under Contract Number DE-AC04-94AL85000.

[b] Hessheimer, M. F. "Overpressurization Test of a1:4-Scale Prestressed Concrete Containment Vessel Model." (To be published.)

TENDON INSTRUMENTATION

Each tendon in the prototype was represented by a tendon in the PCCV model. There are 108 hoop tendons, each spanning 360°, alternately anchored in opposing buttresses at 90° and 270°. There are also 90 'hairpin' vertical tendons, arranged in two orthogonal sets anchored in the tendon gallery in the basemat. The general arrangement of the tendons is shown in Figure 1(b). In the prototype, each tendon consists of fifty-five 12.5mm diameter seven-wire prestressing strands[3]. Keeping the 1:4-scale, each tendon in the PCCV model consisted of three, 13.7mm seven wire strands. The tendons were inserted in 40mm diameter galvanized steel ducts which were not grouted after tensioning, i.e. the tendons are unbonded.

The tendon instrumentation consisted of a combination of foil-type strain gages mounted on individual tendon strand wires and Tensmeg® strain gages mounted at discrete locations along selected tendons coupled with load cells at both tendon anchors. Figure 2 shows the locations of the instrumented tendons and the arrangements of the strain gages on the tendons.

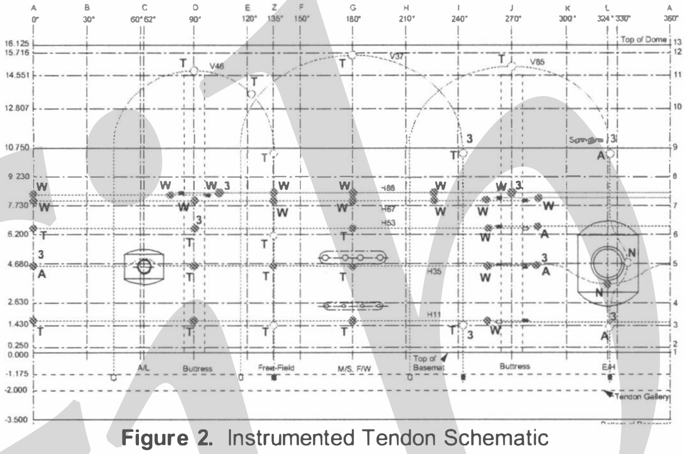

Figure 2. Instrumented Tendon Schematic

3. PRESSURE TESTING

The Limit State Test (LST), conducted on September 26 & 27, 2000. At 2.5 P_d a calculated leak rate of 1.6% mass/day gave the first evidence that the pressure boundary. At 3.3P_d the leak rate exceeded the capacity to pressurize the model and the test was terminated. Figures 3 compares the measured responses during prestressing, before and after seating to the design force distributions for tendon H67. The figure also shows the tendon force profiles during the LST at multiples of the design pressure (0x, 1x, 2x, 2.5x, 3x) up to the maximum pressure of 3.3 P_d

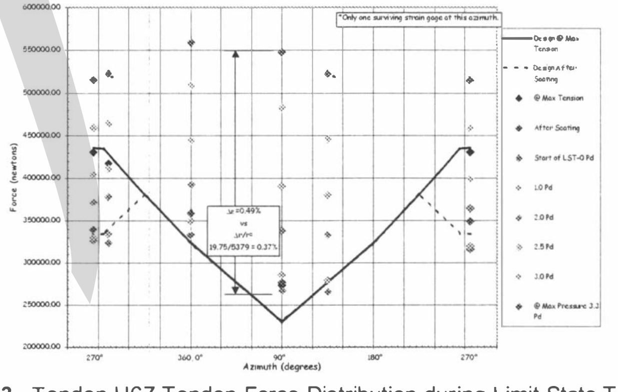

Figure 3. Tendon H67 Tendon Force Distribution during Limit State Test

TOPICS OF CONSTRUCTION OF PRESTRESSED CONCRETE TANK FOR WATER SUPPLY

Hiroyuki INOUE, Katsuji IMAO, Kazuo WATABE,
Shosuke HARAGUCHI and Shigemasa KATADA
Abe Kogyosho Co., ltd. 3-13-3 Rokujyo Omizo, Gifu, Gifu 500-8638, JAPAN

Keywords: prestressed concrete tank, large, scenic design, short construction period

1 INTRODUCTION

Since the construction of the first prestressed concrete tank in 1957[1)], prestressed concrete tanks are widely used in Japan to store domestic water, agricultural water, sewage, and liquefied gases.

Recently, owners of such tanks demand for diverse performances from prestressed concrete water tanks, such as tanks that (1) are larger, (2) have designs that more match the environment, and (3) require shorter construction periods.

This paper describes our studies on (1) control measures against cracks on a large prestressed concrete tank that was built under very hot temperatures, (2) precast panels (PCa panels) that were covered by porcelain tiles and were used for the exterior of an elevated water tank to improve the appearance, and (3) the air-inflated membrane formwork method (air dome method) that was used to construct the bottom slabs of a composite prestressed concrete tank to reduce the construction period.

2 CONSTRUCTION OF A LARGE PRESTRESSED CONCRETE TANK IN HOT WEATHER

The Yamazato Dai-ichi Regulating Reservoir, which was constructed in Okinawa Prefecture, is one of the largest prestressed concrete tanks in Japan, and has an inner diameter of D = 60.10 m, a total water depth of H = 19.92 m, and a total capacity of V = 56,000 m^3.

Figure 1 shows a general drawing of the tank.

The bottom slab of the tank is 50 cm in depth at the inner circle section of uniform depth and 150 cm at the thickened outer circle section. The side walls are 120 cm-thick at the lower section and 65 cm-thick at the section of uniform depth. The tank was likely to be a mass concrete and needed measures against thermal cracks that are attributable to cement hydration heat. Since the bottom slab and the side wall had to be built in the hot summer of Okinawa Prefecture, various measures were adopted to control cracks on these sections. The methods effectively controlled detrimental cracks.

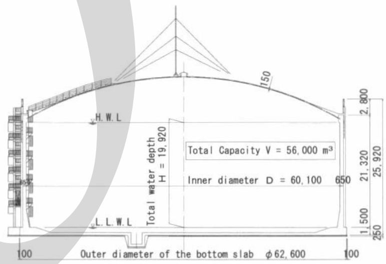

Fig. 1 General structure

3 CONSTRUCTION OF AN ELEVATED PRESTRESSED CONCRETE TANK OF A SCENIC DESIGN

The Yoshikita Distributing Reservoir in Fukuoka Prefecture is an elevated prestressed concrete structure of 26.70 m in total height with a water tank at its top. The water tank has an inner diameter of D = 15.60 m, effective water depth of He = 4.50 m, and effective capacity of Ve = 800 m^3.

Figure 2 shows a general drawing of the structure.

Since the structure was to be located in a park, the owner of the tank requested a design that is pleasant and reflects the lives of people in the a rea. After a comparative investigation, a design was adopted that consists of external walls forming a regular dodecagon and the inclined roof, and imitated a silo. The external walls and the roof were decided to be built by precast concrete panels (PCa panels) to which porcelain tiles were previously laid.

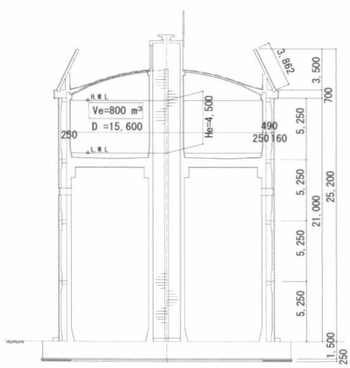

Fig. 2 General structure

Various preliminary investigations were performed concerning the production, transportation, and installation of the PCa panels covered by porcelain tiles, whose use was rare. We successfully produced highly precise PCa panels, with which the tank was built.

4 CONSTRUCTION OF A COMPOSITE PRESTRESSED CONCRETE IN A SHORT CONSTRUCTION PERIOD

The Azuma-mura Composite Distributing Reservoir in Gunma Prefecture is a composite prestressed concrete structure with two vertically piling up water tanks of 36.80 m in total height. The sizes of the water tanks are: an inner diameter of D = 19.00 m, effective water depth of He = 10.00 m, and effective capacity of Ve = 2,830 m^3 for the upper tank, and an inner diameter of D = 18.00 m, effective water depth of He = 16.70 m, and effective capacity of Ve = 4,260 m^3 for the lower tank.

A general drawing of the structure is shown in Figure 3.

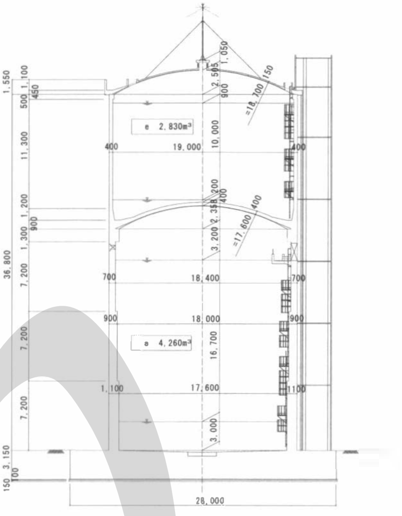

Fig. 3 General structure

Since the owner requested to reduce the project construction period, the air dome method was employed to construct the upper tank bottom slab, which uses a membrane that is supported by air pressure and a mortar shell that is placed on the membrane as the support, instead of the conventional method that uses curved plywood formwork, single pipes, and pipe supports.

The air dome method is widely used to build the dome roofs ordinary prestressed concrete tanks, but is seldom used to construct the bottom slabs of composite prestressed concrete water tanks. Since the bottom slab of a water tank receives not only its weight but water pressure, the cross sectional area is larger than that of a dome roof. Therefore, various studies were conducted concerning the construction of the bottom slabs, including the process of placing concrete. The bottom slabs of the water tanks were successfully built, and the tanks were constructed in a short period of time, which was our initial objective.

5 CONCLUSION

Since 1957, a number of prestressed concrete water tanks have been constructed.

Since the performances will increasingly be important in designing and constructing structures, it is necessary to understand the properties of structures and develop new technologies based on accumulated knowledge and technologies. Recently, good external appearance, reduced labor, and mechanization are demanded. These needs should be met by maintaining the qualities of the structures. Especially, prestressed concrete water tanks for water supply, which are built in large numbers, should be constructed by considering these points and developing maintenance methods.

REFERENCES

[1] Nishio, H. : The Ijira-mura PC TANK, Journal of Prestressed Concrete, Vol.35, No.6, p.55, 1993

[2] Nishio, H. : Recent Prestressed Concrete Tanks and Future Prospects for Their Technology, Journal of Prestressed Concrete, Vol.41, No.1, pp.15-20, 1999

[3] Yokoyama, H., Nishio, H. : History of Prestressed Concrete Tanks in Japan, Journal of Prestressed Concrete, Vol.42, No.6, pp.66-71, 2000

[4] Inoue, H., Shimokawa, H., Haraguchi, S. and Miyagi, Y. : Construction of Large-sized Prestressed Concrete Tank Under Intensely Hot Condition, Proceedings of The 9th Symposium on Developments in Prestressed Concrete, pp.355-358, October 2000

DESIGN AND CONSTRUCTION OF CLOVER-SHAPED SILO

Shunetsu Miura, Erectric Power Development Co.,Ltd
Yoshizou Tsuchida, Sato Kogyo Co.,Ltd
Fumimaro Nagasaki, P.S.Corporation

Keywords: coal storage silo, four-leaf clover shaped, prestressed concrete

1. INTRODUCTION

Isogo Thermal Power Plant (265 MW X 2 units) of Electric Power Development Co., Ltd., which is located in Yokohama city, is being rebuilt to a new plant (600MW X2 units). As one of the work projects, the coal storage silo, which is uniquely shaped, was constructed with the prestressed concrete structure.

The prevention of pollution and effective coal piling are the reasons why silo-type is selected for coal storage facility.

Coal fired power plants usually burn a mixture of 2 or 3 kinds of coal for calorie adjustment and SOx control etc. To fully utilize the extremely small land space, it was planned to build only one silo of world's largest capacity of 100,000 tons with the 4-partition structure; this uniquely designed silo can store four kinds of coal at a time.

Major characteristics of this silo are as follows.

1) Four-leaf clover planar shape
2) Prestressing system and procedures
3) Seismic design
4) Landscape

The clover-shaped silo, which was realized from functional demand, is matching its surroundings beautifully. (see Photo 1)

Photo 1 Bird's-eye view

2. DESIGN

2.1 Planning

This clover-shaped silo, which is called a crowd silo, is composed of four bins. The coal storage capacity of each bin is 25,000 tons. The wall is composed of outer cylindrical wall and cross-shaped wall which is bulkhead of each bin. Because four bins are gathered together, the floor area of the silo can be reduced by 30% compared with total floor area of four separate 25,000 ton silos.

The shape of the roof is conspicuous. The conical shape is determined by the requirement for coal piling; the coal shoot is fixed at the center top of each bin.

Prestressing was applied to the upper ground part of the outer and the cross-shaped wall to cancel the membrane tensile stress caused by internal piled coal pressure.

Tendon layout is shown in Fig. 1.

In-plane shearing of the outer and the cross-shaped wall act as main resistance force to seismic load.

As for the foundation design, resistance to overturning moment got outstandingly larger owing to bearing slab which combines the foundations of 4 parts. Therefore, we could use prefabricated reinforced piles, which are economical, instead of continuous

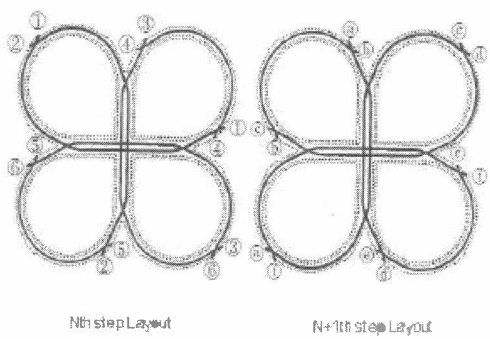

Fig.1 Tendon layout

underground wall.

2.2 Design Criteria

In structural design, allowable stress design is applied to stress calculation due to sustained loading and temporary loading. And ultimate strength design is applied to ultimate load in order to confirm safety.

2.3 Load combination

Dead load, live load, prestress force, coal pressure and earthquake force are taken into consideration for design loads.

Since the silo is a 4 bin-crowd silo, all of the possible cases, for instance only one or two divisions out of four are stored with coals, are taken into consideration in seismic designing.

2.4 Design Prestress

Prestressing shall be carried out so that the tensile force would not be induced in the cylinder wall from the horizontal pressure that is given by multiplying the coal horizontal pressure by dynamic pressure coefficient: Cd(=1.0)at the full load of coal.

Also, it shall be designed to prevent any excessive cracks when unloading coals.

3. Construction

3.1 Work flow

The linkage between the whole execution flow and the prestressing works is shown in Fig. 2.

The slipform system was applied for construction of the cylindrical wall. The structure is 4 bin-in-one type and the whole structure was slid at one time. To cast concrete, the bent support was erected at the center of each bin. On the top of each bent support, a distributor was equipped.

The construction period was 31 months.

3.2 prestressing

Test stressing was done from one end at a time for both end of one cable.

Using the results, stressing control charts with load and elongation was completed.

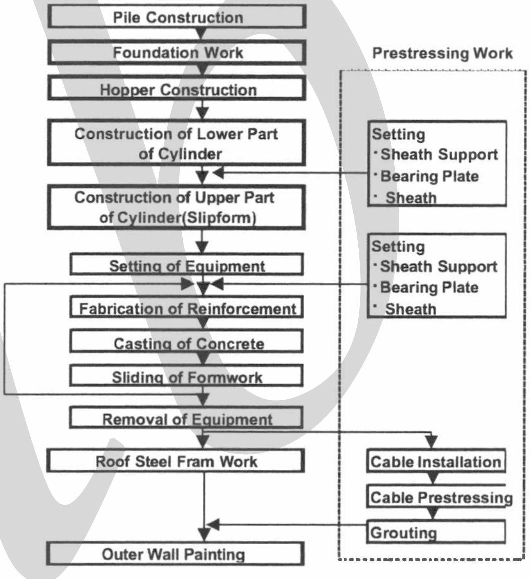

Fig. 2 Work flow

4. Conclusions

An ordinary cylindrical silo with a crisscross wall inside was initially proposed. This idea was not realized because calculations showed that the walls should be very thick . After investigating various shapes of cluster silos, the four-leaf-clover shape was finally hit upon.

Because of the complicated shape of the cylindrical structure, building frame works, roof steel frame works, safety management and other works sometimes required sophisticated technologies.

References

1) Architectural Institute of Japan:Standard for Structural Design and Construction of Prestressed Concrete Structures,1987
2) VSL Association:VSL Method ,Design and construction Standard,1995.5
3) Architectural Institute of Japan:Design Recommendation for Storage tanks and their Supports,1996
4) Architectural Institute of Japan:Standard for Structural Calculation of Steel Reinforced Concrete Structures,1991

THE LATEST TECHNOLOGY UTILIZED IN DESIGN AND CONSTRUCTION OF PRESTRESSED CONCRETE LNG STORAGE TANK

Takeyoshi Nishizaki Tomoki Ushida
Osaka Gas Co., Ltd., JAPAN

Fumio Kamada Minoru Okudate
Obayashi Corporation, JAPAN

Keywords : Prestressed concrete LNG storage tank Self-compacting concrete Quality control Self-lifting scaffolding Information technology

1. INTRODUCTION

Osaka Gas has constructed three prestressed concrete LNG tank. Two of these are 140,000m^3 tanks and another one is 180,000m^3. The 180,000m^3 tank is the world's largest above ground LNG storage tank. We have been constructing a tank of the same capacity at Himeji Terminal and will complete the tank in 2003. (LNG Tank No.2-4)

In this construction, we employ various latest technologies in order to increase efficiency of design and construction with a view to reduce construction workers, construction cost and period.

2. OUTLINE OF HIMEJI TERMINAL LNG TANK NO.2-4

A prestressed concrete LNG tank integrates the conventional double-shell metal tank and the prestressed concrete outer tank. Fig.1 shows the schematic diagram of the 180,000-m^3 prestressed concrete LNG tank.

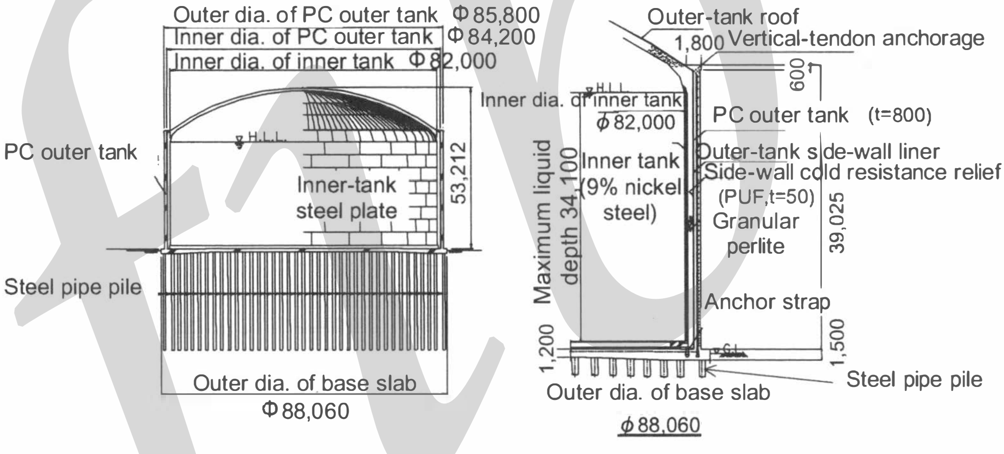

Fig.1 Schematic Diagram of the Construction of Himeji Terminal LNG Tank No. 2-4

3. HIGH-STRENGTH , SELF-COMPACTING CONCRETE

Table1 shows the materials and proportion of the high-strength, self-compacting concrete used to build the outer tank. It has enabled to reduce a thickness of the outer tank wall and also to realize high durability as well as cost and labor saving.

Table 1 Specified Mix Formula of High-strength, Self-compacting Concrete

Maximum size of coarse aggregates (mm)	Rank of self-com -paction performance	Water binder ratio (%)	Water powder ratio in volume (%)	Air content (%)	Quantity of coarse aggregates per unit Volume (m^3/m^3)	Unit content (kg/m^3)							SPA
						W	P			S	G	BP	(P × %)
							C	EX	LS				
20	2*	32.1	29.3	4.5	0.300	170	515	15	50	770	786	0.5	1.2

C : Low-heat Portland cement, EX : Expansive additive(calcium-sulfoaluminate base), LS : Fine limestone powder
S : Sea sand, G : Crushed stone 2005, BP : Thickener(β -glucan base), SPA : Superplastizer (polycarboxylic-acid base)
*) Rank 2 concrete is self-compacting when the minimum opening between steel tendons is 60 mm to 200 mm (as per the "Highly Flowable Concrete Construction Guidelines, "Japan Society of Civil Engineers).

4. CONSTRUCTION WORK AND QUALITY CONTROL

4.1 Outer-tank construction work using the self-lifting scaffolding

To speed up outer-tank construction work, we used the method in which the self-lifting scaffolding were used. Fig. 2 presents the schematic diagrams of this method.

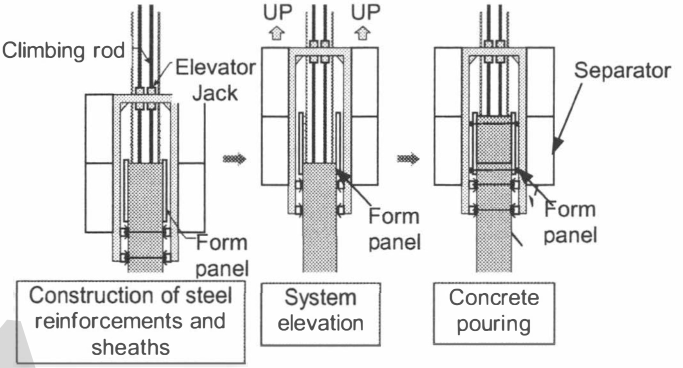

Fig.2 Outer-tank Construction Procedure Using Self-lifting Scaffolding

4.2 Quality control of self-compacting concrete using information technology

We adopt information sharing system by Internet into both design and construction phases. In the system, all project members can access all documents and drawings and measured data such as generated stress and temperature. And also members can monitor load of mixer during concrete mixing and measured value of each component of concrete in real time, through this system we can grasp variation of quality and self-compactability of concrete during mixing, therefore we can take prompt response and control quality everywhere.

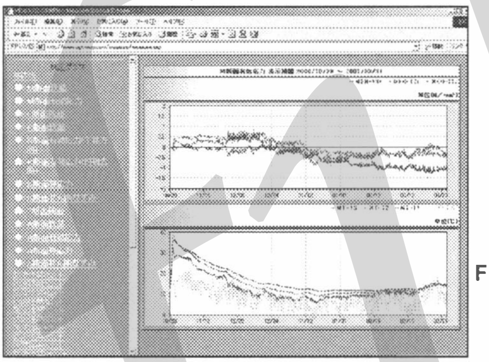

Fig.2 Prestressed Concrete Tank Measurement Data Shown on the Display (Example of stress measurement)

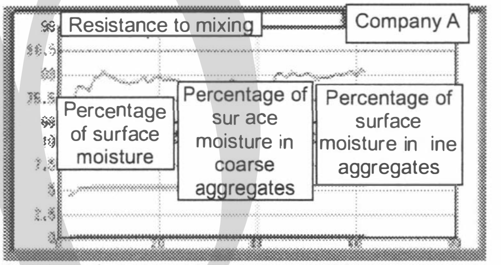

Fig.3 Diagram of Variation in Mixer-load Measurements and Setting of Percentage of Surface Moisture shown on the display in real time

5. CONCLUSION

(1) Depending on using self-compacting concrete and rapid construction method using self-lifting scaffolding, cost was cut by 20% and civil work period was shortened by 4 months compared to last same capacity LNG tank.

(2) By using monitoring system by internet for quality control, we built an outer tank that is superior in durability and reliability.

REFERENCES

1) Kitamura, H., Nishizaki, T., Sono, A. and Kamada,F.: Construction of Japan's First 140,000-kiloliter Prestressed Concrete LNG Tank,Concrete Journal, Vol. 31, No. 4, pp. 42–56, Apr.,1993(In Japanese)

2) Nishizaki, T., Okudate, M, Chikamatsu, R. and Kawashima, H.:Construction of Prestressed Concrete Outer Tank for LNG Storage Using High-Strength Self-Compacting Concrete, Concrete Journal , Vol. 37, No. 10,pp. 40--44,Oct.,1999(In Japanese)

3) Takahashi, H., Miyagawa, K., Chikamatsu, R. and Kawashima, H.:Development of Information Technology–based Quality Control System for Highly Flowable Concrete, Transactions of the Japan Concrete Institute , Vol. 23, No. 2, pp. 1153–1158,Jun.,2001(In Japanese)

APPLICATION OF UNBONDED PRESTRESSED EXTRAWIDE FLAT BEAM-PLATE FLOOR SYSTEM IN A TALL INDUSTRIAL BUILDING

Gu Lei Fu Xueyi Liu Chang
Architectural Design & Research Institute of Shenzhen University
Shenzhen 518060, P.R.China

Keywords: unbonded prestress, extrawide flat beam, flat beam-plate, industrial building

1 INTRODUCTION

Unbonded tension technology is widely used in prestressed concrete floor slabs. Unbonded prestressed wide flat beam-plate floor system is developed upon flat plate floor without beam. Flat beam is conceived as thickening of a slab along the line of columns, banded tendons are placed in flat beams, two-way inner plate can choose normal RC slab, thus, prestressed flat beam-plate floor system is formed, and then, flat beams with columns constitute the prestressed two direction flat beam frame.(Fig.1)

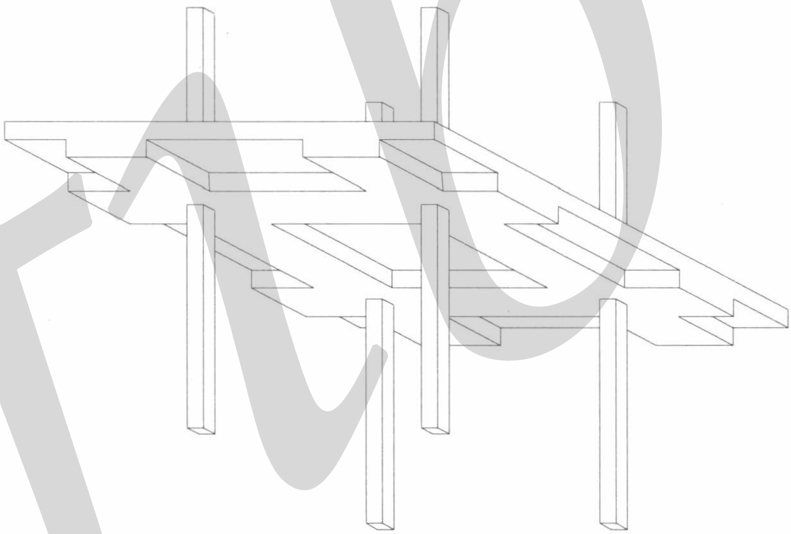

Fig.1 Flat Beam-Plate Floor

2 ADVANTAGES OF UNBONDED PRESTRESSED EXTRAWIDE FLAT BEAM-PLATE FLOOR SYSTEM

The characteristic and advantage of this new floor system can be briefly stated as follows:

(1) On the one hand, it can enlarge column grid, on the other hand, it can reduce structure height efficiently, so that the story number is added and useable floor area is increased.

(2) Flat beam is very suitable to use unbonded prestress technology. Tendons can enhance the rigidity of flat beam, and the drape of tendons is doubled in flat beam comparing with tendons being placed in two-way plate, more significant upward force is provided. Hence, post-tension steel can be economized.

(3) The width of two direction extrawide flat beam exceeds column section. Spot test during construction shows, if $b_b \approx b_c + 2h_b$ (b_b, h_b is the width and height of flat beam respectively,

b_c is the width of column), two perpendicular flat beams crossing at column forms an extend rigid region, this rigid region works as flat beam's support which can reduce positive and negative moment.

(4) Because the height of flat beam is 2 times as plate, Punching shear is no longer a problem.

(5) The clear span of inner plate is reduced with a great range when the width of beam increasing, so that the thickness of inner plate can be decreased. In this project, column grid is 7.2m× 7.2m, width of flat beam is 1.5m, the clear span of inner plate is 5.7m, normal RC two-way plate is adopted, the thickness is 160mm, span thickness ratio is 36.

(6) Unbonded tendons are banded placed in flat beam, simplify the process of tendons layout, construction speed is faster.

(7) Extrawide flat beam-plate structure has good architecture performance, inner space is roomy, the caisson ceiling formed by flat beam and inner plate is the natural decoration of public building.

3 FLOOR STRUCTURE DESIGN

Because the beam width exceeds column section, the structural behavior of extrawide flat beam frame differs from normal frame which beam width is not wider than column section. On the other hand, prestressed flat beams form the spring supports for inner plate, so flat beam-plate structure can no longer be treated as flat plate.

Finite element method was used to analyze floor structure, main conclusions are follows:

(1) The width of flat beam can be determined by $b_b \approx b_c + 2h_b$, if the column section is larger, the width of flat beam can be bigger, width height ratio can reach 5, that is extrawide flat beam.

(2) Analysis shows, flat beam formed spring supports for the two-way inner plate, h/t (*h* is the height of flat beam, *t* is the thickness of inner plate) is the main influence factor to the moment of inner plate, the relation between moment and h/t is as follows:

$$\text{negative moment:}\quad M' = \left(0.126\frac{h}{t} + 0.396\right)M_0'$$

$$\text{positive moment:}\quad M = \left(-0.0795\frac{h}{t} + 0.92\right)M_0$$

where, M_0', M_0 is the negative moment of fixed boundary two-way plate and the positive moment of simple boundary two-way plate respectively, calculation span is clear span.

(3) Considering the benefit of extend rigid region, the calculation of flat beam moment can be simplified as normal beam, but the positive moment can multiply a modifying coefficient of 0.7.

(4) When computing average precompression of flat beam, effective flange width shall be taken as:

$$b_f' = b + \frac{2}{3}l_0 \quad (l_0 \text{ is the clear span of inner plate})$$

REFERENCES

[1] ACI-ASCE Committee 432: Recommendation for Concrete Members Prestressed with Unbonded Tendons. ACI Structure Journal, May-June 1989, pp.301-318.

[2] Bijian O.Aalami: Design of Post-Tensioned Floor Slabs. Concrete International, June 1989, pp59-67.

[3] Technical Specification for Concrete Structures Prestreesed with Unbonded Tendons(JGJ/T 92-93). China Code.

CALCULATION FOR STRETCHING VALUE OF SPACE-CURVED TENDONS

Yao Shiwei
The Science Research Institute, SHCC, Ministry of Communications
The People's Republic of China

Keywords: stretching value, arc-length, subtended space angles, linear integral

1.INTRODUCTION

To calculate the stretching value of tendons, we first must to calculate the arc-length and subtended space angles of space-curves. Most of the vertical bending curves and horizontal bending curves are the composite curves by the straight lines, circle arcs and parabolic curves, the stretching value is calculated by these composite curves.

2. ALGORITHM

The arc length S of space curve is calculated by the linear integrals in calculus as follows:

$$S = \int \sqrt{1 + y_x^2 + z_x^2}\, dx \qquad (1)$$

where S is arc length of space curve; y_x is the derivative for x in the horizontal bending curve; z_x is the derivative for x in the vertical bending curve.

Case 1 Vertical and horizontal curves are all circle arcs, as follows:

$$(x - A_1)^2 + (y - B_1)^2 = R_1^{\,2} \quad ; \qquad (x - A_2)^2 + (y - B_2)^2 = R_2^2 \qquad (2)$$

then $S = \int_a^b \sqrt{1 + y_x^2 + z_x^2}\, dx$

$$= \frac{1}{4}\left[R_1 \ln\left| \frac{(b - A_1) + R_1}{(b - A_1) - R_1} \cdot \frac{(a - A_1) - R_1}{(a - A_1) + R_1} \right| + R_2 \ln\left| \frac{(b - A_2) + R_2}{(b - A_2) - R_2} \cdot \frac{(a - A_2) - R_2}{(a - A_2) + R_2} \right| \right] \qquad (3)$$

A_i, B_i, i=1,2 are the circle center coordinates respectively; R_i, i=1,2 are the radius; b, a is the upper and lower limit of integral respectively.

Case 2 Assume that the vertical curve is the line $z = kx + b$, horizontal curve is the circle $(x - A)^2 + (y - B)^2 = R^2$, then:

$$S = \int_a^b \sqrt{1 + y_x^2 + z_x^2}\, dx$$

$$= \sqrt{1 + k^2}\left[\left(1 - \frac{1}{2(1 + k^2)} \right)(b - a) + \frac{R}{4(1 + k^2)} \ln\left| \frac{(b - A) + R}{(b - A) - R} \cdot \frac{(a - A) - R}{(a - A) + R} \right| \right] \qquad (4)$$

Case 3 The vertical curve and horizontal curve are all straight lines, i.e. the space curve is a straight line, then $S = \left[(a_1 - a_2)^2 + (b_1 - b_2)^2 + (c_1 - c_2)^2 \right]^{1/2}$, where S is the length of the space curve; (a_1, b_1, c_1), (a_2, b_2, c_2) are the coordinates of two points on the space curve.

The calculation of subtended space angles θ: θ is calculated separately the vertical subtended angle θ_{iV} and the horizontal subtended angle θ_{iH} at each curve section, then the subtended space angle θ_i is calculated as follows:

$$\theta_i = \left(\theta_{iH}^2 + \theta_{iV}^2\right)^{1/2} \quad (5)$$

θ_{iH} or θ_{iV} may be equal to zero. When θ_{iH} =0 or θ_{iV} =0, it represents the projection of the curve section in the horizontal plane or vertical plane as a straight line. The total subtended space angle θ is calculated as follows:

$$\theta = \sum_i \theta_i = \sum_i \left(\theta_{iH}^2 + \theta_{iV}^2\right)^{1/2} \quad (6)$$

θ_{iH} or θ_{iV} can be calculated by trigonometric functions. Sum up these arc-lengths S_i and subtended space angles θ_i in each segment, i.e. $S = \sum_i S_i$ and $\theta = \sum_i \theta_i$. S is total arc-length of space-curved tendon, and θ is total subtended space angle. Finally, theoretical stretching value of tensioned tendons can be calculated as follows:

$$\Delta L = \sigma_k \cdot \frac{\left[1 - e^{-ks-\mu\theta}\right]}{ks + \mu\theta} \cdot \frac{S}{E_g} \quad (7)$$

where σ_k is the control tensile stress of tendons; E_g is the elastic modulus of tendon; k is the duct profile coefficient; μ is the friction coefficient between tendons and duct.

3. CASE HISTROY

Length of Yong Village Interchange Bridge No.II belong to the Second Yangtze River Bridge is 485.88~486.65m, its superstructure is the prestressed concrete continuous box girder, this girder is divided into 16 segments, and tension segment by segment. The calculation parameters are as follows:

$\sigma_k = 0.75 R_y^b = 1395 MPa$; $E_g = 1.98\times 10^5 MPa$; $k = 0.0015$; $\mu = 0.25$.

There are less difference between the space calculation value of arc length S and its vertical bending value alone, but there are large difference between the subtended space angle θ and its vertical subtended angle. In order to reduce the computed quantity, the value of arc length S uses its vertical bending value, but θ value still uses its subtended space angle. Alternatively, when $\theta_{iH} << \theta_{iV}$, let $\theta_i = \theta_{iV}$, and when $\theta_{iV} << \theta_{iH}$, let $\theta_i = \theta_{iH}$; and let $\theta = \sum_i \theta_i$.

Where calculation for stretching value of space-curved tendons in two direction tension, first calculate each segment arc length S_i and subtended space angle θ_i, then search the point of $\sigma_{left} = \sigma_{right}$ by the iterative method at the left and right ends, calculate the stretching values ΔL_{left} and ΔL_{right}, and let $\Delta L = \Delta L_{left} + \Delta L_{right}$.

4. CONCLUSION

The deviations between the measured stretching value of tendons and its theoretical calculation value are less than 6%. This shows that the comparison of calculated results with measured values is in close agreement, so that the calculation method is effective and practical.

FURURE TRENDS IN FE-MODELLING OF PRESTRESSED CONCRETE STRUCTURES

Ane de Boer
Civil Engineering Division
Ministry of Transport, Public Works and Water Management
Utrecht, The Netherlands

Cornelis van der Veen
Faculty of Civil Engineering
Delft University of Technology
Delft, The Netherlands

Keywords: design, FE-modelling, post-tensioned prestressed reinforced concrete

ABSTRACT

In Civil Engineering practice it is quite common to set-up FE-models in 1D en 2D. By speeding up the CPU of the computer and the easier way of transferring 3D geometric data from CAD systems to FE code, 3D FE-models are becoming closer to the design practice.
By this approach the time consuming pre-processing process of the FE model will be reduced. Today it is also possible to transfer the results of a common 3D FE-model to the accepted distributed bending moments and membrane forces, projected on 2D reference surfaces.
This approach and the advantages of it can be shown for a simple beam and a skew post-tensioned concrete bridge deck, for the well-known loads and the envelope of the road traffic loads.

1. INTRODUCTION

Presently there are a lot of tools used in the design process of civil structures to convince the authorities of the best solution in civil engineering. By using very quick visualisation packages the designer can make a lot of alternative solutions. Computers are rapid; media tools are available so drawings and movies can be made. The connection between those media tools and the engineering tools are coming in the future. The 1D and 2D approach of designing civil structures will become a 3D approach. Today the 3D approach is already possible in engineering.
Advantages like total geometric description and the availability of all six stress components including a direct view to B- and D-regions is automatically incorporated into 3D models. Indirect the total elapse time of modelling will decrease while the quality of the model and its results are increasing.
The disadvantage of no direct results of membrane forces and bending moments from the 3D model can be solved by integrating the stress results over a certain height. By projecting these integrated results to a reference line or surface the necessary membrane forces and bending moments can be given to calculate the reinforcement quantities. So by using the 3D modelling approach, there is no change in calculating the reinforcement quantities.

2. EXAMPLE OF A SIMPLE BEAM

It's a typical example of B- and D-regions, where B stands for Beam or Bernoulli and D stands for Discontinuity, Disturbance or Detail. Commonly, the total beam can be seen as a B-region. The regions near the support and the nodal force in this example are such a D-region. The length of this D-regions is not known exactly. In 1D FE-modelling the stress σ_{xx} along the half-length of the girder on the neutral axis has a value of zero, if the girder isn't prestressed. In 3D modelling all the stress components are available.

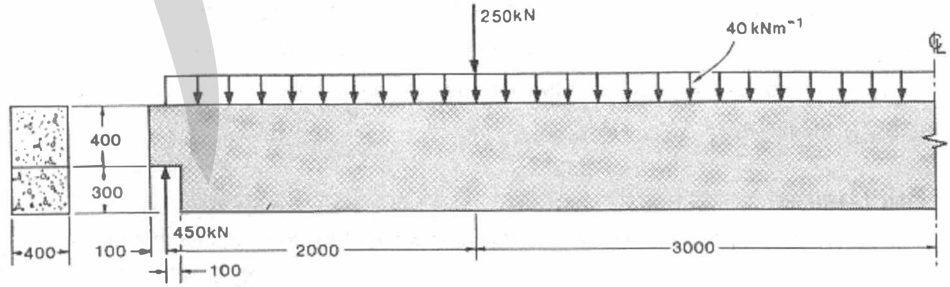

Fig. 1 Geometry and loading of a simple beam

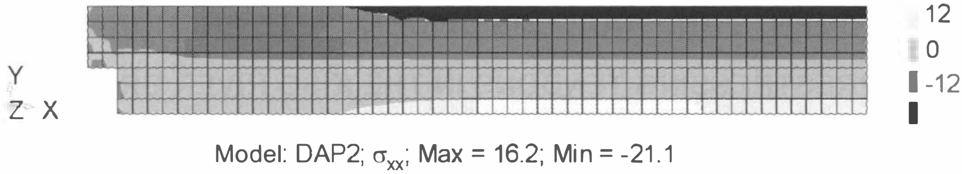

Fig. 2 Contour plot stress σ_{xx} of the beamgirder loaded by nodal and distributed force

In the contour plot of the last figure the σ_{xx} stress lines are laying horizontal until the nodal force region. From the nodal force region till the support region only the positive and negative areas are separated. With a plot of the stress σ_{xx} on the middle of the height of the beamgirder, we get a very good impression of the length of the different B- and D-regions.

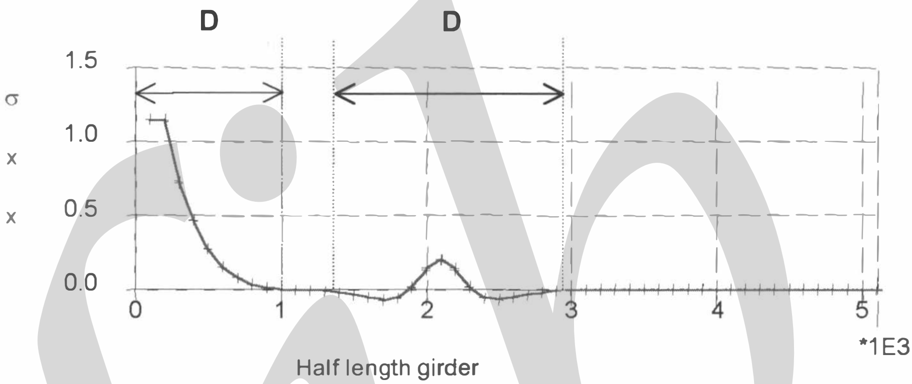

Fig. 3 Stress σ_{xx} on the middle of the height of the beamgirder (neutral axis) along the half-length of the girder of a nodal point force

Extending this 3D-modelling approach to realistic civil structures is no problem and can been seen in the example of the fly-over bridgedeck, which is part of the full paper.

3. CONCLUSIONS

In the simple example of the beam, the so-called D-regions are not only restricted to the support region, but also to the nodal force region. The lengths of the so-called D-region as ratio over the length of the beam can be pointed out very easy.
By integrating the 3D stress results to the belonging 2D reference surface or line, the traditional bending moments and membrane forces can be calculated. Therefor the 3D approach doesn't change the workprocess of the design engineer.

REFERENCES

[1] Marti, P., Basic Tools of Reinforced Concrete Beam Design, Title no. 82-4, ACI Journal, January-February 1985, pg. 46-56.
[2] Schlaich, J., Schäfer, K. and Jennewein, M., Toward a consistent design of structural concrete, PCI Journal, May-June 1987, pg. 74-149.

EXPERIMENTS AND ANALYSIS OF CONCRETE ANCHORAGE FOR PRESTRESSING TENDONS IN THE KISO RIVER BRIDGE

Hiroyuki Abe   Shinzo Eguchi   Tamio Yoshioka   Komine keizou   Jan Cervenka
Research Laboratory   Fukuoka Branch
Oriental Construction Co., Ltd   Cervenka Construction
Japan   Czech Republic

Keywords: concrete anchorage, linear 3-D F.E.Analysis, nonlinear 3-D F.E.Analysis

1 INTRODUCTION

The KISO-River bridge is a bridge which is located at the mouth of the KISO river where the second MEISHIN Highway crosses the KISO river. The bridge is 1,145m in length, 275m is the maximum span. This bridge is an extradosed prestressed concrete five span continuous box girder bridge composed of steel girders. In the side span very large prestress is required to counteract the dead load. In order to withstand the large prestressing force an anchor block shown in Fig.1 is employed. Employed prestressing tendons are 27S15.2 for external tendons and 12S15.2 for internal tendons. In the same anchor block both external and internal tendons are anchored and the anchor block is planned to be as small as possible considering dead weight of the block.

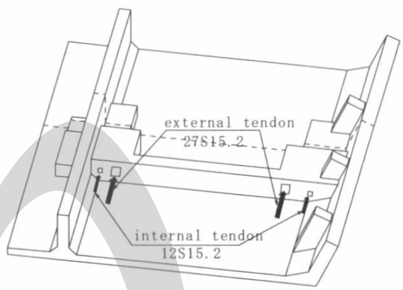

Fig.1 Overview of anchor block

The shape and reinforcing of the anchor blocks are determined using 3-D elastic Finite Element Analysis. In the procedure there could be following problems: 1) if stress re-distribution takes place after cracking, there could be a difference between the design calculation and elastic analysis, and 2) the shape and re-bar arrangement are decided under the serviceability limit state without taking the ultimate limit state into account. In order to solve these two problems an experiment was conducted using a full-scale specimen. This paper reports results of this experiment and they are checked by 3-D nonlinear Finite Element Analysis.

2 OUTLINE OF THE EXPERIMENT

Fig.2 (a) and (b) show the section of the specimen and re-bar arrangement in the anchor block. The depth of the lower deck is the same as the real deck of 230mm and the thickness of the web is the same as the real center web of 300mm.

The specimen was first loaded up to the design load of the serviceability limit state. Next the specimen was loaded up to the maximum load of the ultimate limit state.

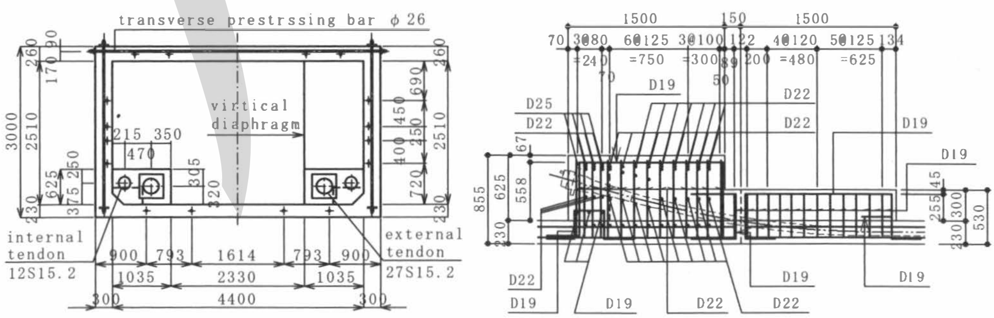

(a) Section   (b) re-bar placement in the anchor block

Fig.2 Specimen (unit:mm)

The elastic F.E. analysis shows stress concentrations at the places shown by narrow hatching in Fig.3. In the experiment cracks (transfer crack) were observed there but the crack width was not outstanding. On the other hand large cracks were detected at the place shown by wide hatching in Fig.3 where the elastic F.E. analysis does not predict cracks (diffusion crack). The cracks penetrated through the lower deck. Fig.4 shows diffusion crack patterns of the lower surface of the lower deck. The maximum crack width was less than 0.1mm, which is less than the allowable crack width of 0.141mm. The same cracks were detected also on the upper surface of the lower deck, but the extension was limited. During the design load was kept for 24 hours and the load was increased up to the ultimate load, cracks did not extend and their width did not wide.

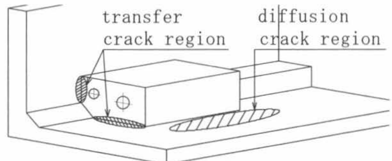

Fig.3 Cracked regions

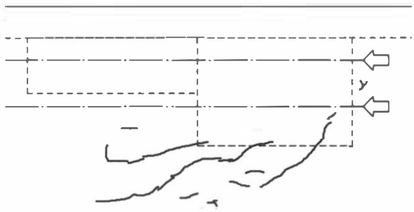

Fig.4 Diffusion crack pattern

3 NON-LINEAR FINITE ELEMENT ANALYSIS

Non-linear F.E. Analysis is performed to predict real cracks which can not be predicted using the elastic analysis. 3-D non-linear F.E. Analysis (ATENA). In the non-linear analysis cracking is taken into account when the tensile stress exceeds the tensile strength of the concrete, causing a decrease in rigidity transverse to the crack. Fig.5 shows a comparison between observed and predicted cracks. In the analysis the initial cracks develop at the boundaries both between the front surface of the anchor block and the lower deck and between the front surface of the anchor block and the web. Afterward the next cracks develop in the lower deck at the side surface of the anchor block. However, cracks in the analysis extend more than the experiment but almost similar to the experiment.

Fig.6 shows the relationship between external prestressing forces and transverse re-bar stresses, which are measured just below the anchor block in the lower deck. In the non-linear analysis the compression sets up first and tensile stress of re-bar increases from external prestressing force of 3,500kN. Although there is a small difference between the load intensities of the experiment and analysis when increase of re-bar stress starts, the non-linear analysis describes well the tendency that re-bar stress changes from compression to tension. On the other hand the linear analysis cannot describe the phenomenon showing almost zero still at 5,000kN. The difference between linear and non-linear analysis explains that a change of stress transfer mechanism happens when increase of prestressing force is increased.

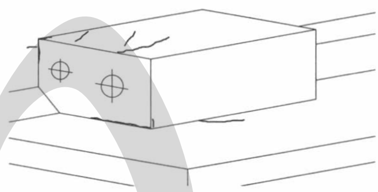

(a) Observed crack

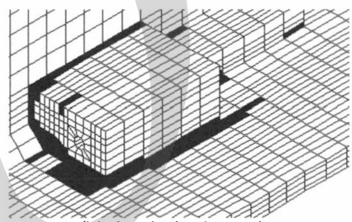

(b) Analytical results

Fig.5 Comparison of crack

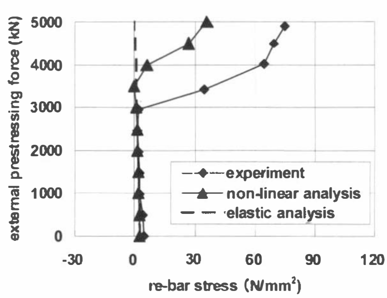

Fig.6 Relationship between external prestressing force and re-bar stress

4 CONCLUSION

Following conclusions are drawn from both the experiment and analysis;

(1) the performance of the anchor block is guaranteed under the serviceability limit state,

(2) the anchor block is structurally safe under the ultimate limit state,

(3) cracks (diffusion cracks) which develop in the lower deck along the side surface of the anchor block are caused by stress re-distribution due to initial cracks (transfer cracks)

(4) the non-linear Finite Element Analysis describes very well the phenomenon of stresses and cracks around the anchor block and is very practical.

PARTIAL PRESTRESSED CONCRETE USED IN TALL BUILDINGS

Zuhua Wang Kemei Liao
South China University of Technology,
P.R.China

Hui Wang
Pierce Goodwin Alexander & Linville,
USA

Keywords: tall buildings, partial prestressed concrete, unbonded prestressed concrete

1 INTRODUCTION

In modern tall buildings, it is an expectancy to increase useful areas, extend a width of a room and a span of a structure, meet the manifold needs of functions, do not limit for arranging a room arbitrarily. In China, because post-tensioned partial prestressed concrete, including unbonded and bonded, had been used in a series tall buildings, above expectations have been achieved. In those tall buildings, partial prestressed concrete had been used in the floors and roofs of them.

In addition, there are many other advantages for use of partial prestressed concrete. We can use materials and cost sparingly, increase the sum total of a story or net height of a story, decrease deflections and cracks of structures, shorten construction time, lighten weight of structures and use foundations sparingly and so on.

It is the purpose of this paper to approach the aspects of partial prestressed concrete used in tall buildings and to introduce some practical projects used partial prestressed concrete structure systems in tall buildings. The main content is as follows.

2 PARTIAL PRESTRESSED CONCRETE USED IN TALL BUILDINGS

Partial prestressed concrete has been used in tall buildings growing with each passing day in China. The main aspects of them are as follows:

a) Unbonded prestressed concrete flat-beam-slab floors and beam-and-girder floors in frame-tube and tube-in-tube structures.
b) Unbonded prestressed concrete flat-slab floors in a tube-in-tube structure.
c) Unbonded prestressed concrete flat-slab-column structure systems.
d) Unbonded prestressed concrete slab-wall structural systems in tall buildings.
e) Frame structural systems with bond and unbonded partial prestressed concrete.
f) Bond and unbonded prestressed concrete used in the extra-long building for reducing shrinkage and temperature cracks and so on.

3 PRACTICAL PROJECTS USED PARTIAL PRESTRESSED CONCRETE

Here are some practical projects to use partial prestressed concrete structure systems.

In Guangdong International Large Building at Guangzhou , a structure of tube-in-tube with 63 stories and square plan of $37.0\times35.1m^2$, flat-beam-slab floors of unbonded prestressed concrete, including flat beams and one-way slabs, had been used at all 7^{th}~63^{rd} between inside and outer tubes[1]. The span and depth of a slab are respectively 7.35~9.05m and 220mm in a type story and prestressing steels are tendons consisting of seven wires of 5mm diameter with usage volume of 2 bundles per meter. This is a large building of the tallest and the using first unbonded prestressed concrete at Guangzhou.

In Beijing International Trade Large Building with 34 stories, a frame-tube, unbonded prestressed concrete beams and floors with one-way slabs had been used also.

Guangdong Archives is a tall building, a flat-slab-column structure, with 24 stories [2]. The spacing of columns is $7.2m\times7.2m$. Unbonded prestressed concrete beamless flat-slab floors had been used in the large building .The depths of two-way slabs are 160mm、180mm and 200mm.The prestressing steel is ϕ15.0 cable with strength of 1570 N/mm^2 and 4 cables per meter for slabs with 180mm depth. The concrete strength grade is C25~C60 (25~60 N/mm^2). SAP84, a finite element analysis software, has been used for structural analysis in which the floor was as a elastic slab consisting of non-coordinate slab-shell elements of four joints with 6 freedoms. The maximum deflections are 4.3~4.8 mm which are about 50% lower than non-prestessesd concrete beamless flat-slab floors.

In Guangzhou South Airline Large building [3], frame-tube structure with 61 stories and 204.2 meters high, partial bond prestessed concrete floors are used. The span and depth of two-way slab system are respectively 8m and 200mm.The prestressing steel is cable with Φ15.2 and Φ12.7 and strength of 1860 N/mm^2. The spacing is 3Φ15.2@600(column slab-band) and 3Φ12.7@1000(space slab-band between columns).

Yuecai Large Building to have been completed last year at Guangzhou is a frame-tube structure with 50 stories and 210.9 meters high. In the transfer girders with section of 3.8m×4.5m, bearing 41 stories and located at 9th story ,and girders of 32m span, partial bond prestressed concrete had been used all to control deflections and cracks of them. In addition, unbonded prestressed concrete has been used in the girders of 16m span of 80m long building below 7th story for reducing shrinkage and temperature cracks. In this case, the section height of the girder had been reduced also to 900 mm.

In table 1, the main conditions of partial prestressed concrete projects of 8 large buildings at Guangzhou of China, designed by authors and constructed by Guangdong Fu-Yin Prestressing Engineering Company, are given.

Table 1. The main condition of tall buildings
Using partial PC in Guangzhou of China

Project	Height (m)	Total Story	The condition using PC
Guangzhou Tianwang Large Building	168	48	Partial PC transfer girders with 3.0m highs of a section
Guangzhou Jianyin Large Building	150	46	Partial PC girders
Guangzhou Junhui Large Building	90	26	Unbonded PC beamless flat-slab floors
Zhong Lu Qiao Garden	54	18	Unbonded P C flat-slab-column structure system
Guangzhou Longjin Commerce and Trade Large Building	90	28	Unbonded PC beamless flat-slab floors
Tian Yu Large Building	98	30	Unbonded PC beamless flat-slab floors
Guangzhou Yidelu Commerce-Residence Large Building	75	24	Unbonded PC beamless flat-slab floors
Hai Ying south Garden	81	27	Partial PC beamless flat-slab basement floor

REFERENCES

[1] Bosheng Rong et al., Construction practice of Guangdong International Large Building with 63 stories. In "Design and Construction of Unbonded PC structure" by Xuekang Tao, or "Practical Design and Construction Examples about High-effective Prestressed Concrete Structures (in Chinese)", by Huiling Chen, China Building Industrial Publishing House, 1997.

[2] Zuhua Wang, Maoqing Zhou, Analysis and design of prestressed concrete flat-slab-column structure system used in Guangdong Archives with 24 stories (in Chinese), The Congress Proceedings of 10th National Conference of Prestressed Concrete Structures (China), 1999.

[3] Zhenzhang Li, Xuzhao Liao, Structural design of bond prestressed concrete flat-slab in Guangzhou South Airline Large Building with 61 stories (in Chinese). In "The Congress Proceedings of 16th National Conference of Tall Building Structures" (China), 2000.

THREE-SPAN CONTINUOUS BOX GIRDE R PRESTRESSED C ONCRETE BRIDGE CONSTRUCTED BY C ANTILEVER METHOD HEIGEN BRIDGE

Yuji Kanazawa
Sumitomo Construction Co.,Ltd
JAPAN

Ryuichi Takagi Hiroaki Iwasaki
P.S Corporation
JAPAN

Keywords: mantled traveller,curing machine,temperature management

1 INTORODUCTION

Otofuke Town located in the north side of Obihiro City; Hokkaido attracts attention as a bed town of Obihiro City in recent years. Therefore, in each route, which connects these two areas, the traffic congestion during morning and evening rush hours poses a serious problem with the increase in population.

The Heigen Bridge is on the Tokachi River, dividing Otofuke Town from Obihiro City, and is a part of Obihiro north bypass (common name : frontier passage) which connects a national highway No.241 and a national highway No.38. Although the Heigen Bridge was opened for traffic with two lanes in 1990, it is under construction to expand into four-lane road from1999.

The Heigen Bridge is 755m in length, and 13.75m in width, and which is composed of Three-Span Continuous Box Girder Prestressed Concrete Bridge, which is 382m in length. The maximum girder depth of this bridge is 10m, and the length of center span is 170m, and this bridge is the longest one in this type of bridge in Japan.

This study is mainly focused on the construction of long span bridge in cold districts through the year.

Photo. 1 Over view

2 CONSTRUCTION OUTLINE

Structure : Three-Span Continuous Box Girder Prestressed Concrete Bridge
Bridge length : 382.000m
Span : 105.0m+170.0m+105.0m
Width : 13.750m
Owner : Hokkaido Development Bureau (Obihiro Development and Construction Department)
Contractor : Joint Venture of Sumitomo Construction Co.,Ltd and P.S Corporation
Construction Period : Aug. 25, 2000 – Mar. 20, 2003

3 CONSTRUCTION

3.1 Outline

Although this bridge was ordered at the end of August 2000, in order to construct by the end of March 2003, therefore every year, it is necessary to construct also during winter. As for the Obihiro district where the construction is to take place, the lowest temperature will be less than 0 degree from the middle of November. Moreover, the mean air temperature is below the freezing point from the beginning of December till the end of March, which is severe condition. The quality control of concrete is very difficult in such environment. Therefore, the bridge construction plan during winter is centered on placing and a quality control of concrete is mainly considered, and all possible efforts is exerted to keep the same quality in concrete as good as in summer.

3.2 A measure to Winter Concreting

Temperature management and curing management of the placed concrete are the most important in winter concreting.

The measure of Winter Concreting adopted to construct this bridge is summarized as follows.

3.2.1 The measure in a concrete plant

As for winter concreting, it is desirable to keep the water content per unit volume of concrete as small as possible. Then, the water cement ratio was taken as 34% for this bridge. Moreover, air content was set up to 5% in an effort not to have the effect of freezing and thawing.

3.2.2 Measure on construction management

The following measures were taken in construction management.

① curing machine was put into operation from the previous night where concrete placing is to take place, to keep the mold and steel cage (re-bar assembly) warm enough.

② after concrete placing, curing solution was sprinkled on the concrete surface to prevent rapid moisture evaporation.

③ the traveller has been instrumented with IC thermometer internally and externally to monitor the curing temperature and control the curing temperature with computer all day long.

3.2.3 Measure in equipment

In order to construct the long span bridge all the year round in cold districts, where the temperature drops below -20 C˚, the completely mantled traveller is used constructing by cantilever method.

In order to fill up the gaps the ceiling portion is made up of the roof deck, and the floor portion is composed of the scaffold board and the heat insulting sheet, in addition, the wall portion (so-called Sun-panel), is using the mold made of the polycarbonate. Insulation was improved since the heat loss coefficient decrease compared to the case when a sheet is used. (The heat loss coefficient; sheet is 6.0, Sun-panel is 5.5) Moreover, there is also an additional merit of having no influence on the adjacent bridge by breakage of a sheet etc., at the time of a strong wind.

Heat insulation was improved by using a mantled traveller closed completely, enabling construction in the severe cold.

Concrete temperature after placing was maintained around 5 C˚ during the first 3 days and kept 0 C˚ or more for the next 2 days with a warm air circulator sending worm air to the traveller. In addition, temperature management is performed by automatically with Concrete Furness thermostat.

4 CONCLUSION

This study described the measure for the bridge whose length of center span are 170m and which is the longest bridge in Japan constructed all the year around in the severe cold in Obihiro City; Hokkaido.

This bridge is finished up to P2 bridge pier by the cantilever method and P3 pier by the same method and side span of P1 is under construction by scaffolding method, scheduled to finish by March, 2003.

Authors would be pleased if this report serves as reference of the construction in the winter of a huge bridge.

DESIGN AND CONSTRUCTION OF SHIN-MEISEI BRIDGE

Jiro Iida, Hiroaki Nakayama
Nagoya Expressway Public Corporation
JAPAN

Tadao Wakasa
New Structural Engineering.Ltd
JAPAN

Akio Kasuga, Katsuhiko Mizuno
Sumitomo Construction Co.,Ltd.
JAPAN

Keywords : extradosed, precast segment, composite structure, reduction of erection

1 INTRODUTION

The Shin-Meisei bridge on Nagoya Expressway No. 3 crosses the class-1 Shonai River in western Nagoya. From both the aesthetic and economic viewpoints, continuous three-span prestressed concrete extradosed bridge construction was used for this bridge. To reduce the weight of the main girder cross-section due to constraints on the substructure, and to avoid giving a sense of oppression to vehicles traveling the road below the bridge, diagonal webs were used to form an inverse trapezoidal three-chamber box girder cross-section that has reduced the width of the bottom plate.

Since the location for this bridge in the river and directly over the road imposed severe constraints on the construction, the following construction methods were employed.

- As methods used for constructing side spans, some precast cross-sections were erected by crane and the sections remaining after linking the main girders were cast-in-place using a form traveler.
- Use of composite steel and concrete construction for the main tower anchor points for cable stays is reducing the use of erection equipment and improving workability.
- High tensile SD490 steel reinforcement is used because of the limitation on pier width derived from existing piers.

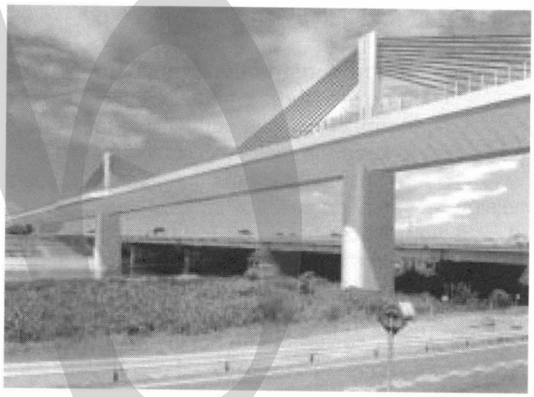

Fig.1 Prospective view of the Shin-Meisei Bridge when completed

This paper is a report on the design and construction of the Shin-Meisei Bridge.

2 FEATURES OF THIS BRIDGE

2.1 Shape of main girder cross-section

This bridge is a prestressed concrete extradosed bridge with single plane suspension type cable stays, having a wide cross-section. For this reason, the shape of the main girder cross-section is required to effectively transfer the cable stay tension acting in the center of the cross-section as well as reducing the weight of the main girder due to the conditions restricting work on the lower section. Therefore, choosing an inverse trapezoid three-chamber box girder cross-section to maintain a constant width for the lower decking (4.0 m) has achieved a main girder cross-section shape that reduces the weight of the main girder and is excellent in

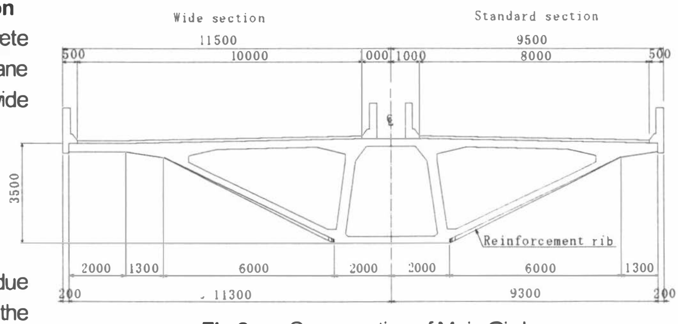

Fig.2 Cross section of Main Girder

transferring the cable stay tension. Also, with respect to the change in width, as shown in Fig. 2, this involves only the cantilever section without changing the box shape. Reinforcement ribs provided on the outside of the diagonal web were considered not only structurally but also from the aesthetics of the existing bridge.

2.2 Main tower structure

In the main tower structure, having a composite steel and concrete structure for attaching cable stays to the main tower results in the horizontal components of the tensile forces in the cable stays being borne only by the steel shell while the vertical components of the tensile forces in the cable stays are borne by the composite steel and concrete cross-section. This enables the weight of the steel shell to be reduced by comparison with the conventional arrangement in which the steel shell carries all of the cable stay tension. As a result, there is no need for the steel shell to be welded on-site in order for it to be compounded with the concrete section.

Also, for the installation of the steel shell section, several separately formed steel shell units (of about 50 kN per unit) overlap in each anchor structure. This method of construction enables the work to be done easily, even in places like this bridge where there are weight restrictions on erection and transportation.

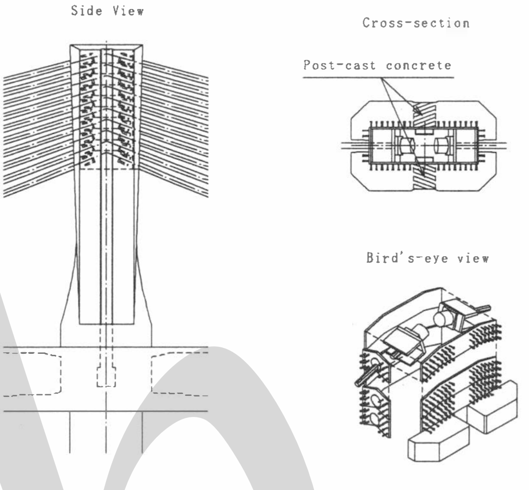

Fig.3 Main tower details

2.3 Side span erection method

For this bridge, the following construction methods were used, which involved separating the main girder cross-section in the side spans into a core part and side parts.

Step 1: Pre-cast core parts are erected by slinging from a truck crane and core parts only are connected first.

Step 2: Side parts are constructed by the cantilever method and cast in place using a form traveler.

To keep the total weight of a core cross-section block below 250 kN, the width perpendicular to the bridge axis was set at 6.0 m and the block length at 1.8 m, with a weight of about one-fifth that of a standard block constructed by the form traveler.

Figure 4 shows the main aspects of the side span construction work.

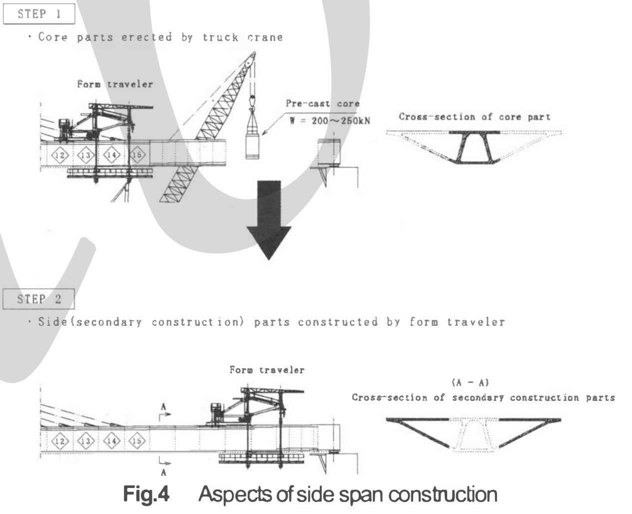

Fig.4 Aspects of side span construction

REFERENCES

[1] Ito, Imaizumi, Ooka and Kasuga: Design and construction of side spans for the erection of a partitioned cross-section for Ibi River Bridge, 10th Symposium papers, Prestressed Concrete Technical Association, pp.October 2000.

[2] Ikeda, Mizuguchi, Komatsu, Nakasu and Maeda: Design of superstructure for No. 2 Meishin Expressway Kiso River Bridge and Ibi River Bridge, Bridge Girders and Foundations, Vol. 33, No. 11, pp.November 1999.

DESIGN OF NISHINOYAIKE BRIDGE
SECOND TOUMEI EXPRESSWAY
CANTILEVER METHOD WITH ALL EXTERNAL TENDON SYSTEM

Masatosi takeda
Japan highway
Public corporation

Yasuhiro katsuyama
Japan highway
Public corporation

Hideyuki nakajima
fuji p.s.co.,ltd
kawada construction
co.,ltd JV

Mitsuru inokawa
fuji p.s.co.,ltd
kawada construction
co.,ltd JV

Keywords: all external tendon system, local stress for anchoring tendon, thermal influence

1 INTRODUCTION

Nisinoyaike Bridge is located between Hamakita I.C. and Inasa I.C., in the second Toumei expressway, and crossing over Nisinoyaike pond, and has 4-spans continuous box girder, with a length of 295.0 meters. This bridge has two characteristics, that this has one box girder regardless of wide girder (16.50 meters), and that all external tendon system is chosen as a longitudinal tendon system. But the problems that we did not understand as problem appear. For example, member with anchoring tendon has excelling local stress, the stress is not expected appear in the girder for the lock of stiffness. In the design of this bridge, we examined for solving this problems in detail with FEM analysis because the influence of this problems against total structure could not be neglected. This report is mentioned about the examinations and that results in the design of Nisinoyaike Bridge.

2 GENERAL FEATURES

Bridge Name: Nisinoyaike Bridge
Owner: Japan Highway Public Corporation
Type of Structure: 4 span Continuous Prestressed Concrete Box Girder Bridge
Bridge Length: 295.000m
Span arrangement
: 52.300m+70.000m+90.000m+80.250m
Width: 16.500m
Construction Method: Cantilever Method

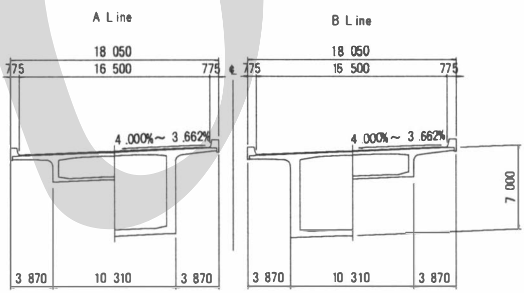

Fig.1 Cross Section (mm)

3 ALL EXTERNAL TENDON STRUCTURE

The all longitudinal tendon of this bridge was adopted the external tendon.These tendon's arrangement pattern was adopted, all of these were bended at the first cantilever block, and were bended moreover at the rib was positioned beside the anchorage block anchored the tendon.

4 DESIGN OF ANCHORAGE BLOCK FOR EXTERNAL TENDON

The cantilever external tendons were anchored at the anchorage block positioned at the web inside on each block. We expected, the local stress around the anchorage block was more larger than the stress, that appeared in case the inner tendons were anchored into the member. Therefore anchorage block was designed with FEM analysis.

The memorable characteristic of this anchorage block and arrange of the cantilever external tendon, that tendon anchored at (n)block was bended at (n-1)block, this force for bending tendon tended to alleviate the local stress around the anchorage block. In result, the maximum principal stress of concerned block for anchoring the external tendon was registered –2.84N/mm^2, however, in case the tendons were anchored at the next block, that stress was registered –1.47N/mm^2.

5 THERMAL INFLUENCE OF THE PIER TOP

The pier top (P3) has a large cross section (7.0m as a high of girder, 4.5m as a wide of cross beam), and was planed to construct during spring to summer. This member was needed to take measure of mass concrete. Therefore, the type of cement was changed high-strength portland cement was planed from the beginning to ordinary portland cement, and the time of casting was divided 4 times, because of lowering the heat of hydration.

6 TENSILE STRESS AT THE GIRDER FOR THERMAL INFLUENCE AND DRYING SHRINKAGE

The cantilever method is that the girder is constructed step by step. The longitudinal tensile stress at the top of the wing slab in the block have been cast appeared for the heat hydration and drying shrinkage at the block positioned the top of girder, and is accumulated as the construction of the girder progress. Therefore, we calculated this stress by FEM analysis in consideration of heat hydration and drying shrinkage, and took measure to solve this problem.

According to the result of analysis, this constant stress was registered –2.8N/mm^2 at the girder constructed by cantilever method, and –6.7N/mm^2 at the pier top. Against this stress, we took measure that the single strand prestressing tendons were arranged at the top of the wing slab. In result, the stress appeared at the top of the wing slab was controlled –1.21N/mm^2 at the girder was constructed by cantilever method, -3.15N/mm^2 at the pier top.

7 DESIGN OF LOWER SLUB RIB

Lower slab is popularly designed by using two-dimensional structural analysis by box rigid frame model. But, in case we compare the stress of width direction (σ_y) calculated by this method with that stress calculated by FEM analysis modeled a span, it tends that the result of FEM analysis is larger than the result of conventional method[2)].

In this bridge we took measure that lower slab was reinforced by rib positioned at center of span, because of lowering the stress of width direction. As a result of this examination, In case the rib shaped 500×500mm was positioned, the stress of width direction was controlled –2.20N/mm^2 (σ_y=-3.15N/mm^2 by no rib model) , this was approximately lowered until the stress calculated by box rigid frame model.

8 CONCLUSION

The memorable characteristics of this bridge was that the girder had total wide of 18.050m was adapted one box girder type, and that all external tendon system was chosen. In design of this bridge, we examined by FEM analysis, took some measure against some problems. However, we hope to establish more easy design method.

REFERENCES

1) Kuroiwa,T, Goto,A, Tada,I and Umeda,H : Design and Construction of Setogawa Bridge, Proceedings of The 10th Symposium on Developments in Prestressed Concrete, Oct, pp431, 2000 (in Japanese)

2) Fukunaga,Y and Homma,A The examinations of local stresses by FEM analysis, Prestressed concrete VOL43, No.2, Mar-Apr, pp.84, 2001

CONSTRUCTION OF AN EXTRADOSED PC BRIDGE BY INCREMENTAL LAUNCHING METHOD

Atsuyuki Tsukamoto Hideyuki Okagawa Shinichi Yoshino Yasuto Konishi
Taisei Coporation Hokkaido Railway Company
JAPAN JAPAN

Keywords : extradosed bridge, incremental launching method, stay cable, through girder

1. INTRODUCTION

A bridge with length of 111.0 meters was constructed over the cross point of existing National route 5 and Sasson Motorway which run in parallel. This bridge was to be constructed as a part of a double tracking and viaducting project of the Sasshyou Line of Japan Railway Hokkaido.

At some phases during the launching erection for crossing point, the section force was adjusted by tensioning, unloading, and releasing of the temporary extemal cables, temporary stay cables, and permanent stay so as to reduce section force in the main girder. Photo1 shows the launching erection for crossing point. This paper describes the unprecedented construction sequence and the management techniques.

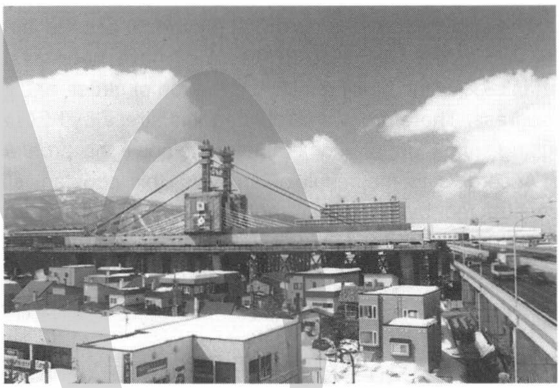

Photo 1 Erection by incremental launching for crossing point

2. CONSTRUCTION PROCEDURE

Figure 1 shows the construction procedure of this bridge. Main girder divided into 10 blocks was casted at the casting yard located at 130 meters behind of the erection site at crossing point. The main tower was erected at the time of casting of 7th block of the main girder and the pylon was erected at the time of casting of 8th block. After erection of the main girder and the main tower, permanent stay cables, temporary stay cables, and temporary extemal cables were installed, then the launching erection of the crossing point was carried out. After that, tension adjustment for permanent stay cables, installation of permanent bearings, and removal of other temporary equipment were carried out, and finally all constructions were completed.

3. INCREMENTAL LAUNCHING AT CROSSING POINT

Temporary extemal cables, temporary stay cables, and permanent stay cables were tensioned, unloaded, and released at the designated phases by the design, in order to reduce the section forces of the structure to the designed values. Figure 2 shows the erection equipment.

Temporary extemal cables were installed for the purpose of reducing the negative bending moment that occurred at the supporting point during cantilevering at the initial stage of launching. Due to the small fluctuation of tensile force, the introduced tensile force was set to 0.7Pu. 2 numbers of 19 ϕ15.2mm strands were arranged on the upper side of each webs. One by one tensioning by single jack was adopted due to the arrangement of permanent stay cables and the handrail of wall, and then releasing was carried out when launching nose arrived at the final position.

Temporary stay cables were installed for the purpose of reducing large bending moment in the girder at the

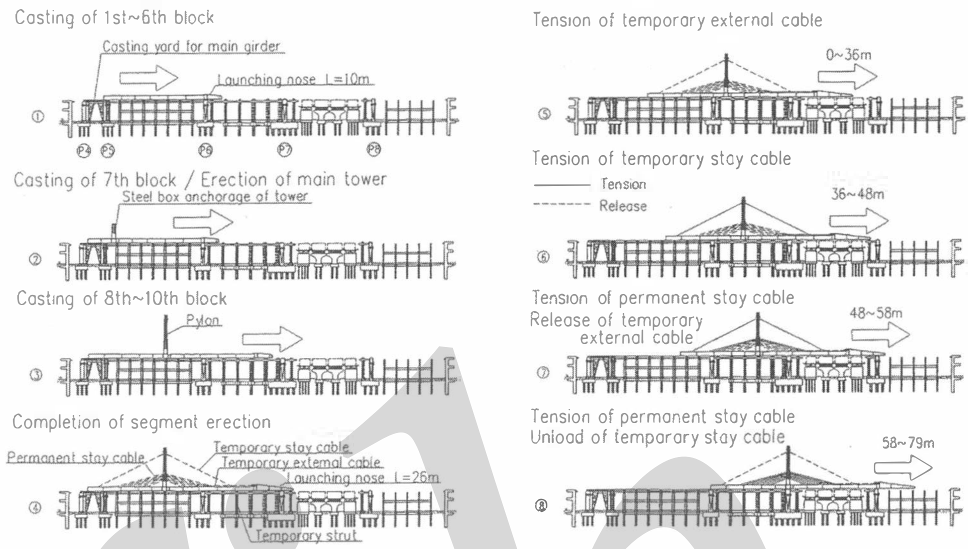

Figure 1 Construction procedure

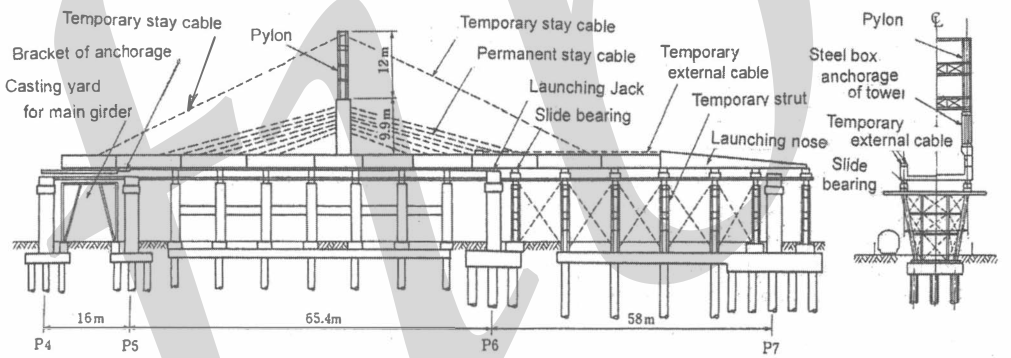

Figure 2 Erection equipment

span of crossing point. The introduced tensile force was set to 0.6Pu to take account of influence of wind load even though the fluctuation of the tensile force was small. 2 numbers of 36 ϕ 15.2mm strands were arranged through the saddle on top of the pylon. For tension of stay cables, the saddle was raised to approximately 70cm. The saddle was to be hoisted through lifting steel member by lifting jack. Tensioning management was carried out by the monitoring of the saddle displacement and the pressure gauge of the lifting jack with capacity of 5000 kN. To check the fluctuation of tensile force during launching, the load cell was installed to a PC strand of the anchorage zone of main girder and tensile force was measured.

4. CONCLUSION

Due to various measures for safety and detailed construction plan and procedure, all staff could be fully understood what to do for this construction and carried out reliable construction management. As a result, the launching erection was successfully completed without any control to traffic of national roads and expressways.

THE DESIGN OF LONG CANTILEVER BEAM USING POST-TENSIONED TENDONS IN KUMJUNG STADIUM

Dong-Sub Choi Jong-Soo Kim Dong-Hwan Kim
C.S Structural Engineers Inc., #413-4, Tokok2 dong, Kangnam-Gu, Seoul, KOREA 135-272,
cs@cs.co.kr

Keywords: post-tension, cantilever beam, prestress loss, serviceability

1 INTRODUCTION

The 2002 Asian Olympic Stadium(mainly intended for cycle racing) that will open in Pusan, Korea, is a structure with one story below and four above the ground. It has a seating capacity of about 20,000 spectators. The structure has seats for general spectators from the 1st floor to 3rd floor. The VIP seatings is on the fourth floor. At first, this stadium was designed as structure with one story below and two above the ground. After this game(Asian Olympic Game), there will be a change in the bicycle race track. This is designed as a reinforced concrete and steel system from one story below to two above the ground. A precast/prestressed concrete system from the column of the 2nd story above of it was built because of design modifications.

2 SELECTION OF SYSTEM

The key point of this project under design modification was construction in a short amount of time. Additionally, there is a comparison between reinforced concrete, steel and precast/prestressed concrete systems taking into consideration the cost of construction and serviceability by vibration and displacement. As a result of comparing each system, reinforced concrete and precast/prestressed concrete have a cost advantage in construction, while steel and precast/prestressed concrete can be built in a short time. Especially the serviceability of 8m cantilever beam was a careful consideration. In cases using post-tensioning in such aspects, a prestressed one had advantage in serviceability. Therefore, it was designed as prestressed one that is the best in regards to time and cost of construction and serviceability.

3 DESIGN OF LONG CANTILEVER BEAM

The aspect that was the most difficult in the design of this structure was the 8m long cantilever beam. The reason of using Post-tension for its design was described above. I was taken account of the stability of building about the load of every step under construction as well as dead load and live load of the fourth floor. Especially, if it is produced as a monolithic member in a horizontal direction because the section is 800mm wide and 1500mm deep, there is a problem in lifting it. For that reason, it was divided in the top of columns.

The construction sequence is divided in Self-load step, Superimposed-load step and Live-load step. The load condition and values of every step are described as Table 1. Accroding to such step, there is a need to check the 8m long cantilever beam by the service load design as well as the ultimate strength design.

Table 1 Load condition and value at every step

Construction sequence	Load condition	Load value (tonf/m)
Self load	A condition that install PC cantilever beam	3.30
Superimposed load	A condition that construct of topping concrete after the installation of DTS	5.64
Live load	A condition of final live load	4.00

4 CONCLUSION

The key point of design in this structure is the 8m long cantilever beam. Key considerations are time and cost of construction and serviceability. The condition of construction now is after DTS and topping concrete installation. There is a need to check additional stress by live load and serviceability by vibration continuously.

Consequently, a cantilever beam is designed with an effective section that could control vibration and displacement by post-tensioning.

REFERENCES

[1] Michael P. Collins and Denis Mitchell : Prestressed concrete structures, Prentice Hall, pp.25-54,1991

[2] Edward G. Nawy : Prestressed Concrete - A Fundamental Approach, 2nd ed., Prentice Hall, pp. 72-92, pp.325-333,1996

[3] The Ministry of Construction and Transportation : Concrete Design Code(in Korea), pp.181-192, 1999

[4] Prestressed Concrete Institute : PCI Design Handbook – Precast and Prestressed Concrete, 4th ed., pp.(4)41-45, pp.(9)61-63, 1991

THE NEW PRESTRESSED CONCRETE BRIDGE OVER THE VISTULA RIVER IN KRAKÓW

Kazimierz Flaga
Kraków University of Technology
POLAND

Teresa Matuszkiewicz
Silesian University of Technology
POLAND

Piotr Wanecki
BBR Polska Sp. z o.o.Gliwice
POLAND

Keywords: prestressed bridge, free cantilevering method

1 INTRODUCTION

In recent years, Kraków has been blocked as a result of there being too few bridges and a huge traffic. In 1998, a competition was announced for an architectural – town-planning conception of two bridges: Kotlarski and Zwierzyniecki. For the Zwierzyniecki bridge, the winning solution suggested one span steel girder [1], [2]. The designer of the bridge stuck to the suggested shape, but changed the material, using prestressed concrete instead of steel.

2 BRIDGE CONSTRUCTION

The bridge has a two-cell box girder with vertical webs. It is 11.6 m wide. In the cross-section, the bottom slab of the girder is curved. The deck slab, 23.7 m wide, is supported at its edges by steel struts, fixed in the webs. The struts also support elements of the elevation, which smoothly continues the curve of the bottom slab. The bridge girder has no diaphragms between support axes.

It is post-tensioned in the longitudinal direction by means of 162 BBR CC1906 tendons (140 in the deck slab and 22 in the bottom slab). Structural depth of the girder varies from 7.0 m at the support section to 3.5 m at the ¼ of span. The bottom chord of the girder up to ¼ of the span is parabolic in shape.

Abutments of the bridge are founded on bored piles 1.5 m in diameter. The pile tips are driven 1.0 - 1.5 m into Jurassic limestone layer. There are 30 piles, arranged in five rows, below each abutment (Fig. 1). Piles of external rows can be tensioned. The length of the left abutment piles varies from 11.08 to 13.37 m, and of the right abutment piles - from 20.34 to 26.20 m. Maximum compression pile load at u.l.s. is 11'488 kN, while the compressed pile capacity is 24'155 kN; maximum tension pile load at u.l.s. is 903 kN, while the tensioned pile capacity is 928 kN, a little more than the load. An additional safety reserve for tensioned piles is guaranteed by neglecting in calculations the dead load of the pile (c.a. 460 kN) and possible friction in the limestone. Tension pile load at s.l.s. is 300 kN. For the sake of control a test load of one pile was made. Compression force during the test reached 16'190 kN and the corresponding settlement of the pile amounted to 31 mm.

The pile caps have dimensions of 28 x 30 m in plan. Their thickness is 1.5 m. There are post-tensioned with 28 BBR CC1906 tendons in longitudinal direction and with 12 BBR CC1906 tendons in transversal direction. On each pile cap there are two main transversal ribs, which transmit forces from girder to foundation. In the east abutment the ribs are monolithically connected with girder diaphragms and in the west one there are pot bearings between ribs and diaphragms. The pile caps also have longitudinal ribs, 5.5 m high.

Abutments are filled with soil, which is a counterweight necessary to keep the girder in balance. Over ground level the retaining walls rise from the abutments, forming a part of river dams. The retaining walls surround side spans of the bridge. The spans are massive frames, consisting of two vertical diaphragms, located over the main ribs of abutments, a fragment of deck slab and inclined rigid strut.

Closing diaphragms of the girder are stressed with 36 vertical BBR CC1906 tendons. The tendons built in the west abutment have additional steel sheets made of pipes 300 mm in diameter and are grounded with soft resin. Such a solution makes thermal displacements between abutment and girder possible. The tendons installed in the east abutment, where diaphragms are monolithically jointed with ribs, have standard sheets with cement ground. The works were carried out on both sides of the river simultaneously, according to the same time schedule.

The piles were made up to ground level and then excavations were made between steel cofferdams for pile caps. The caps were cast and stressed in three stages. After completing caps the ribs were made. The side spans of the girder were constructed after the abutments had been filled with soil. They were poured on the scaffolds in two stages, together with 3.5 m long cantilevers of the main span.

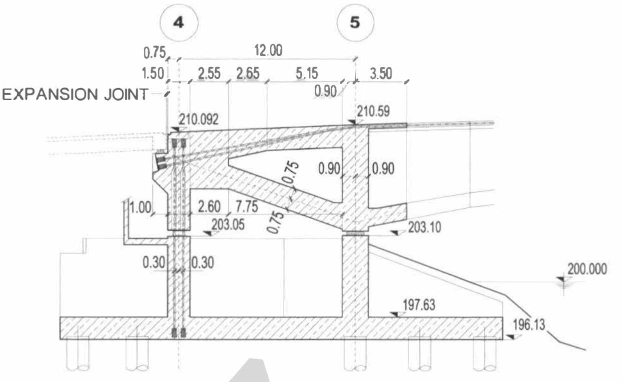

Fig. 1 Longitudinal section of the abutment

The main span was constructed by means of free cantilevering. Each of the formwork travelers weighed 140 t. There were 13 cantilevered elements, each 4.8 m long, made from each abutment. Closing pour made after dismantling the travelers. During the cantilevering process, due to the necessity of installing the steel struts, the deck slab was narrower than in the final stage. Its side parts were cast after closing the girder and installing the struts.

3 MATERIALS

The bridge was built of concrete grade B-50, reinforcing steel grade BSt-500 and 34GS and the prestressing steel of strength of 1860 Mpa. The consumption of those materials is shown in the table below.

Table 1 Consumption of materials

Material	Consumption (actualization 08-10-2001)	Consumption factor
Pile concrete	1'883 m^3	0.51 m^3 / m^2
Pile reinforcement	212'600 kg	57.5 kg / m^2
Abutments concrete	6'181 m^3	1.67 m^3 / m^2
Abutments reinforcement	927'150 kg	250.8 kg / m^2
Superstructure concrete	2'105 m^3	0.57 m^3 / m^2
Superstructure reinforcement	266'200 kg	72.0 kg / m^2
Prestressing steel	267'900 kg	72.5 kg / m^2

The main contractor of the bridge was KPRM Skanska S.A. The bridge was opened on 30th October, 2001. It has two carriageways, each 7.0 m wide, two pedestrian paths 1.5 m wide and two cycle ways 1.5 m wide, located symmetrically to the center line of the bridge. The carriageways are separated with a safety line,1.6 m wide. They also have safety lines, 0.5 m wide, outwards.

4 RESULTS

The erection of the bridge was completed 11 months after the starting day. This shows that the chosen construction method is effective, even with respect to the relatively complex shape of the girder. It has also been noted that the architectural concept of the bridge causes sharp increase in consumption of structural materials.

REFERENCES

[1] Barycz R.: Most Zwierzyniecki. „Architektura & Biznes", Mar. 1998
[2] Długosz A.: O jeden most... dalej, czyli krótka historia mostu Zwierzynieckiego. „Polski Cement",Oct. 2001

DESIGN AND CONSTRUCTION OF THE KOBARU VALLEY BRIDGE BY LOWERING METHOD

Kazuo Teshima, Oriental Construction
Hiromichi Matsushita, Kyushu University
Mitsunari Shinwashi, Oriental Construction
Keiji Fukada, Oita Prefecture
JAPAN

Keywords: concrete arch bridge, Lowering Method, vertical construction of arch ring

1 INTRODUCTION

The Kobaru Valley Bridge crossing over the Kobaru River of Japan is a concrete arch bridge with a span length of 135m. The bridge has the largest arch span among the bridges constructed by Lowering Method in Japan [1], just following the Argentobel Bridge [2] in Germany whose arch span is 145m, the world record of the arch bridge constructed by the Lowering Method. This paper describes the outline of design and construction of this bridge and the results measured during the erection of the arch ring.

2 OUTLINE OF DESIGN AND CONSTRUCTION

The Kobaru Valley Bridge has the following characteristics:
(1) To restrict the sectional forces of the arch springing, the Lohse type arch bridge was adopted.
(2) Considering various conditions of the construction site, the Lowering Method, which is not influenced by the clearance of the arch and enables the weight of arch ring to be reduced, was adopted.
(3) Due to the topographical feature, the arch is unsymmetrical with different arch rises on each side.

In the Lowering Method, the two halves of arch ring are constructed vertically on each abutment, and are then incrementally lowered using Lowering cable, rotating around the shoes installed at the bottom ends of the two halves of arch ring. Although the arch rises of this bridge were different on each side of P1 and P2 according to the topographical features, the position of the arch crown was determined on the condition that the final tension forces of the Lowering cables were almost equal. The weights of the two halves of the arch ring were 9.56MN and 12.11MN on the P1 and P2 side respectively, but the final tension forces of the Lowering cables were 10.2MN and 10.16MN on both sides respectively.

During the Lowering erection process, the pulling cables were used together when the rotating angle was less than 20 degrees for stabilization of the arch ring against earthquake motion and wind. After the rotating angle was greater than 20 degrees, the arch ring was lowered by its own weight only. The upper and lower limits for the tension of the Pulling cable were determined using the crack width constraint to 0.005C=0.27mm (C: cover).

The relative error of both arch ring tips in the transverse direction after Lowering erection, the most important item in the construction management in the Lowering Method, was 17mm.

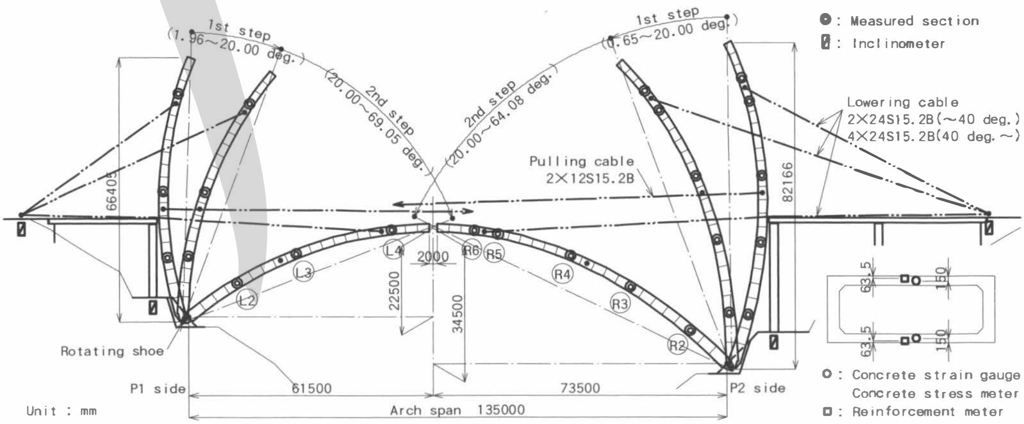

Fig. 1 Outline of Lowering Method and measurment

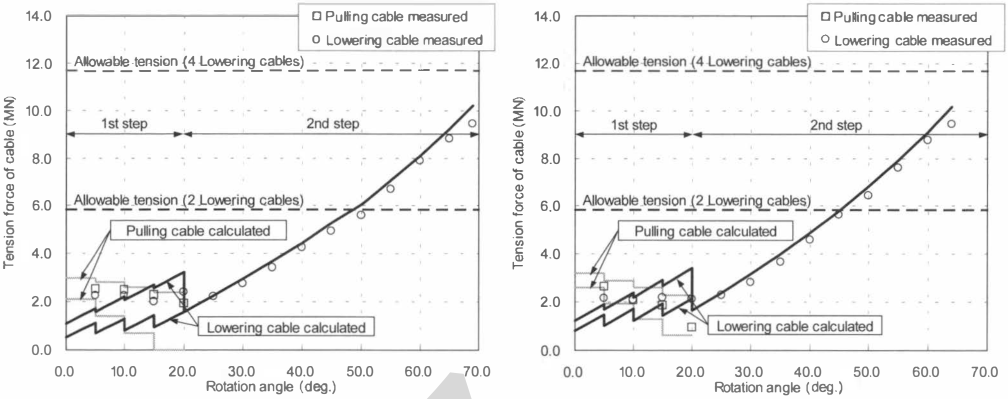

(a) Arch ring of P1 side (b) Arch ring of P2 side

Fig. 2 Tension force of cable during Lowering condition

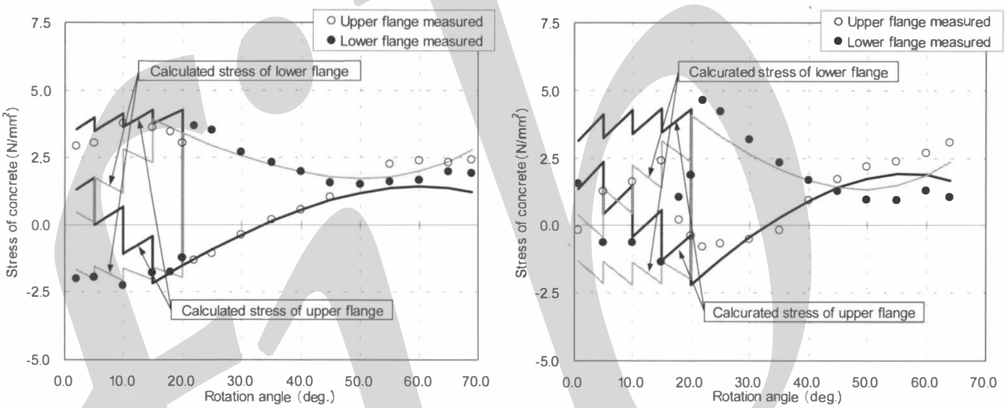

(a) Arch ring of P1 side [Measured point L3] (b) Arch ring of P2 side [Measured point R4]

Fig. 3 Concrete stress of arch ring during Lowering condition

3 ERECTION OF ARCH RING BY LOWERING METHOD AND MEASURING

Since the arch span of this bridge is close to the upper limit of the application of the Lowering Method, various measurements shown in **Fig. 1** during the erection were applied to investigate the validity of the design method of this bridge.

The relation of the Lowering rotating angle and the tension force of Lowering and Pulling cables is shown in **Fig. 2**. The measured value of the tension force in the Lowering cable was 5 to 10 percent less than the calculated one at the Lowering of 2nd step in which the Pulling cables were not used. However, in the Lowering of 1st step, especially in the case when the rotated angle was smaller, the difference of the measured and the calculated value became bigger. It was attributed to a measurement error because the manometer pressure was small.

Stresses of the concrete in the arch ring closed to the anchor zones of the Pulling cables (measured points L3 and R4) are shown in **Fig. 3**. The calculated results were calculated by the assumption that the entire concrete section was effective, and the measured stress of the concrete was calibrated by the calculated one at the rotating angle of 40 degrees, where the entire measured section was compressed. The measured results agreed with the calculated ones on both sides of P1 and P2.

REFERENCE

[1] Abe, K., Shigenobu, T., Nakamura, K. and Maeda, A. : Erection of Tainokawa Bridge by Lowering Method, FIP symposium '93, pp.441-447, 1993.

[2] W. Hünleine, M. und P. Ruse, H. : Ein neues Verfahren für den Bau von Bogenbrücken, dargestellt am Bau der Argentobelbrücke, Bauingenieur, 60, pp.478-493, 1985.

ULTIMATE LOAD BEHAVIOR IN ACTUAL PRESTRESSED CONCRETE GIRDER BRIDGES

Byung Hwan Oh
Professor, Department of Civil Eng.
Seoul National University, Korea

Kwang Soo Kim
Senior Engineer, Hyundai Institute
of Construction Technology, Korea

Young Lew
Senior Engineer, SK Engineering &
Construction, Korea

Keywords: In-situ failure test, prestressed concrete girder bridge, ultimate load behavior

1. INTRODUCTION

Structural capacity is one of the most important aspects in the design of bridges. The purpose of the present study is to investigate the behavior of an actual prestressed concrete girder bridge at ultimate load stage. For this purpose, a 30-year-old prestressed concrete girder bridge was tested up to failure at site. Two different loading systems were designed to capture not only service load behavior, but also the ultimate load behavior. Four-wheel loads which simulate actual standard truck were applied on the slab of two lane bridge. The deflections, strains and crack widths are automatically measured and stored in the computer at every loading step.

2. DIMENSION OF THE BRIDGE

Test bridge is simply-supported with the span length of 30m. The thickness of cast-in-place RC deck slab is 180mm. The height and web thickness of PSC girders are 1890 mm and 200 mm, respectively. The bridge has six equally-spaced intermediate diaphragms in a span.

To simulate wheel loads of a design truck, four-point loading plates are installed on the slab above the girder 1 and 2. This loading system can avoid premature punching failure of RC deck slab. Besides, this loading system may allow investigation of load distribution in transverse direction.

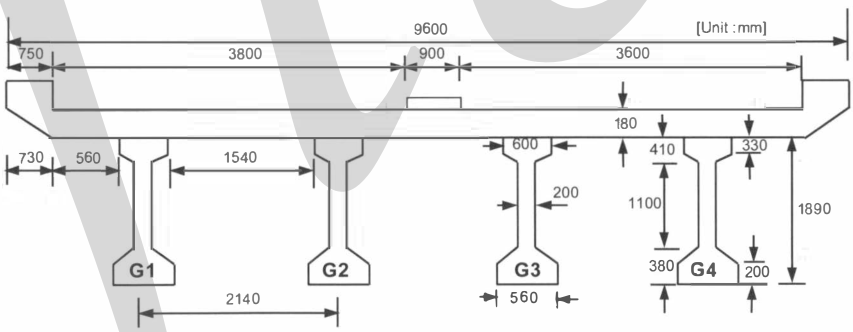

Fig. 1 Cross section of the actual bridge in service

3. TEST PROCEDURE AND RESULTS

The load was applied cyclically in a step-by-step manner until the first crack occurs at the main girder. The first crack appeared at the bottom surface of girder 1 at the load of 313.6 kN. After the first crack occurred, the load was reduced to zero to close the flexural cracks and the crack gages were installed to measure the crack widths automatically.

As load increases, cracks are developed from the central region of the girders. It is seen that major shear cracks occur mainly at the quarter point region of the girders. Fig. 2(a) represents deflection behavior under initial cyclic loading of Girder 1 and Fig. 2(b) shows different deflection behavior up to ultimate load for all four girders. The present test results indicate that the deflections at the ultimate load stage of the bridge are about 240 mm for girder 1, 170 mm for girder 2, 80mm for girder 3, and 25 mm for girder 4, respectively.

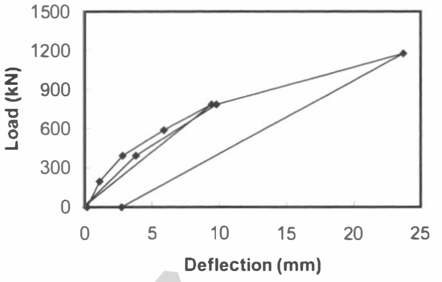

(a) Cyclic Loading of Girder 1

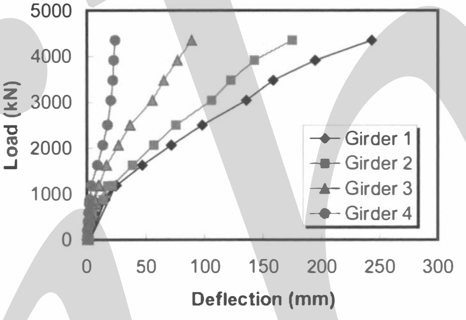

(b) Ultimate Loading

Fig. 2 Applied loads versus vertical displacements of bridge girders

The failure of the bridge was initiated from the compression crushing of the curb in the loaded side. This indicates that the curb plays some important role in resisting the longitudinal flexure, i.e., like an edge beam. The failure load of the bridge was found to be 4,312 kN at which the crushing of compression side in the curb and slab has occurred. This failure load capacity is much larger (i.e. about ten times larger) than the design load of the bridge (about 318 kN).

4. CONCLUSION

In-situ failure load test is performed for the PSC girder bridge in service. At ultimate state, the deflection of girder 1 reached almost 240mm. The tested PSC girder bridge showed large ductility and the deformation of girders was recovered considerably after removing applied loads. The tested slab-girder system reached the ultimate state at the load of 4,312 kN. This ultimate load is much larger than the design load of this bridge. This large conservativeness must be considered for more economic design of PSC girder bridges.

REFERENCES

[1] Shenoy, C. V., and Frantz, G. C., “Structural Tests of 27-Year-Old Prestressed Concrete Bridge Beams.” *PCI Journal*, Sep.-Oct. 1991, pp. 80-90.

[2] Tabatabai, H., and Dickson, T. J., “Structural Evaluation of a 34-Year-Old Precast Post-Tensioned Concrete Girder.” *PCI Journal*, Sep.-Oct. 1993, pp. 50-63.

Session 3 | Recent contribution of concrete to tunnel and underground structures

SHOTCRETE USE IN JAPAN IN TUNNEL AND UNDERGROUND WORKS

Koichi Ono
Kyoto University
JAPAN

Various advantages of underground space use have been realized by human beings for the long history. Natural caverns and underground spaces have been used efficiently by human beings. Creation of tunnel and underground space has been tried by human beings at their every stage of development although these works have always been difficult. In every age, considerable use of underground structures has been made for mining and defensive purposes.
The most rapid increase in the use of tunnel and underground space appeared in the 19th and particularly in the 20th century. During these periods, tunnel and underground space use has been extended to various facilities such as roads, waterways, railways. subways, underground infrastructures, car park, shopping mall, powerhouse, warehouse, sewage station, storage for oil, gas and radioactive waste, museum, concert hall, sport center, etc.

Underground space has various fundamental characteristics, such as easier creation of new space, mechanical, thermal, acoustic and opaque isolation and less disturbance to the ground surface. Various advantages of tunnel and underground use have strongly encouraged human beings to go underground even with difficult conditions. Strong demand to conquer such difficult conditions has yielded various excavation and support technology in tunnel and underground works. Untiring efforts for construction of tunnel and underground space will continue.
Use of shotcrete in tunnel and underground excavation has been realized to be very efficient for rock support although the support mechanism by shotcrete lining is not fully understood yet.

Tunnels and underground spaces have been constructed aggressively and utilized very efficiently in Japan as well. Tunnels are constructed by NATM, shield method, TBM or cut and cover method, in general. Immersed tube tunnel is adopted in the case of strait crossing or bay area. Underground spaces are created by the combination of these methods. Concrete is used in these constructions in the form of shotcrete, placed concrete, shield segment or immersed tunnel element.
Tunnels are used for railway, subway, road, waterway, pipelines, underground river and various lifelines. Underground space is used for power station, oil or gas storage, sewage station, disposal of radioactive wastes, parking lots, shopping malls, etc.
About 1/3 of Shinkansen lines in service is tunnel and more than one half of Shinkansen lines under construction is tunnel.
No.2 Tomei-Meishi Highway now under construction includes 224 km of tunnels in the total length. This highway has 6 lanes and each tunnel in this highway has about 200 m2 of the cross section area for the 3 truck lanes.

The use of shotcrete for rock support began in 1970th in Japan. Since then, various experiments and testing for shotcrete and rock bolt were performed in laboratories and construction sites. In 1980th, the tunneling method with shotcrete and rock bolt became a standard tunneling method in Japan. This tunneling method was named as NATM, New Austrian Tunneling Method. The use of NATM made the tunnel construction cost to one half and the human accidents during construction to one tenth.
During these periods, shotcreting method altered from dry mix process to wet mix process. Various types of accelerator for shotcrete and shotcreting robot have been developed. The use of alkali free slurry accelerator is proved to be less harmful to workers and yet to produce less rebound and less dust during shotcreting. On the other hand, various types of dust control agent and shotcrete machine have also been developed. Owing to the increase of tunnel and underground construction, Japanese annual use of shotcrete reaches 2 million m3 every year.

The idea of single shell lining and the strong demand to go deep underground have been forcing to

improve shotcrete strength and quality as well as shotcreting system.
The role of shotcrete is to stabilize a newly excavated tunnel or underground space by covering the newly cut surface immediately. Local scaling off of rock is also protected by shotcreting. Although the mechanism of rock support by shotcrete has not been fully understood, following effects of shotcreting are pointed out. That is bond effect, ring effect, force redistribution, strengthening of weak area and covering of cut surface.
The wet method is extremely dominant in Japan and shotcreting is done by machine in these days. Use of silica fume and steel fiber is increasing. Both alkali free liquid and slurry type of accelerator have been paid attention recently to the role of dust reduction. Power up of shotcrete spraying machine is continuing along with enlargement of tunnel diameter. Airless type of spraying machine is introduced for a strong demand to reduce dust emission during shotcreting.

Rebound and dust emission are the major problems during shotcreting. Particularly, workers exposed to dust with the grain size smaller than 5μm are in danger of falling in pneumoconiosis
The Ministry of Land, Infrastructure and Transport enacted "Guideline for health control to dust emission during tunneling" in 2001.
Dust emission during shotcreting can be reduced by the use of accelerator of alkali free or slurry type. Alkali free accelerator is health friendly type. The use of dust control agent or high viscous concrete is also effective to reduce the dust emission. Dust emission can also be reduced by the use of new type of shotcrete machine such as rotary type or airless type. Pre-lining and concrete placing method have been developed as an alternative tunnel lining method.
Airless shotcrete machine has the spraying capacity of 20 m3/hour and produces much less rebound and dust during shotcreting compared to the conventional machines. In the shotcreting test using a model tunnel with 6m high, 10m wide and 6m long, this machine achieved less than 10% of rebound and less than 2mmg/m^3 of dust for steel fiber concrete.

CONCLUDING REMARKS

The use of tunnel and underground space has been contributing to human life for the long history. The more and more efficient use will continue to improve environment of the earth and to develop the quality of life. Technology for planning, construction and maintenance for tunnel and underground space has also been developed up to the very high level. Contribution of concrete in creation of tunnel and underground space should also be paid attention together with its remarkable technical progress. However, the technology should be developed more and more for better use of tunnel and underground space. More organized planning will be needed for better use of underground space. Technology to maintain safety of tunnel and underground space particularly against fire should be developed more. Durability of tunnel lining should also be improved particularly in the case of shingle shell lining by shotcrete. Construction techniques should also be developed particularly in the field of robotics for dangerous and unbearable works. Shotcrete technology should also be developed to reduce rebound and dust and increase its efficiency.
Tunnel and underground space use has tremendous future.

FULL SCALE TESTS ON A SEGMENTED TUNNEL LINING

Authors: A.H.J.M. Vervuurt (TNO Building and Construction Research, the Netherlands)
J.A. den Uijl (Delft University of Technology)
F.B.J. Gijsbers (TNO Building and Construction Research)
C. van der Veen (Delft University of Technology)

Keywords: shield driven tunnels, full scale experiments

1. INTRODUCTION

In order to gain a better understanding of the complex structural behaviour in shield driven segmented tunnel linings for the specific Dutch soil conditions, a set up has been realised in the Stevin Laboratory of Delft University of Technology (the Netherlands). In the test set up three segmented rings of a tunnel lining can be tested at full scale size.

From practical observations as well as from earlier studies it was concluded that a significant part of the stress distribution in the lining is dominated by concentrated axial loads in the construction phase. In the tests which are currently carried out in the full scale test set-up, the behaviour of the lining during construction is emphasised (series B). In these tests initial gaps between the segments are prescribed in order to study the effect of inaccurate positioning of the segments. The data of these tests will serve for validating the results of three dimensional FEM analyses. At the moment this paper is written, it is studied at which positions gaps will be introduced and which load scheme will be used. The results of the tests will be presented at the conference. Preceding to the tests in series B, recently tests have been carried out in which the construction behaviour under service load conditions was studied (series A). The results of the latter tests are presented in this paper.

The behaviour of the tunnel lining under service loads is dominated by the radial ovalisation load and is significantly influenced by the magnitude of the uniform axial and radial loads. These loads determine the behaviour of the ring and segment joints respectively. In test series A the behaviour of the lining due to an ovalisation load is studied for three different combinations. The combinations which refer to a high (A3), medium (A2) and low (A1) uniform load are given in Table 1.

Table 1 Summary of tests in series A

test-number	axial uniform (kN/m^2)	radial uniform (kN/m^2)	amplitude (kN/m^2)
A1	985	148	13.1
A2	1970	295	13.1
A3	2955	443	19.7

2. EXPERIMENTAL TEST SET-UP

The full scale test facility used for the experiments is shown in Fig. 1. In the set up a tunnel lining consisting of three rings with an external diameter of 9.45 m and a wall thickness of 0.4 m is positioned.

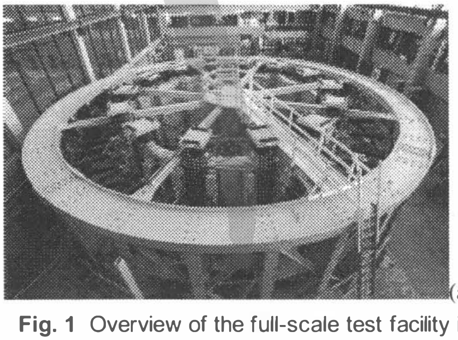
(a)

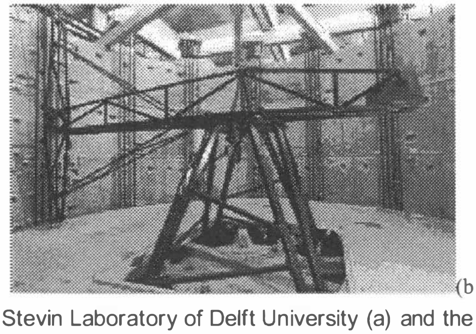
(b)

Fig. 1 Overview of the full-scale test facility in the Stevin Laboratory of Delft University (a) and the rotating frame with lasers for measuring the radial lining displacements (b)

The lining in the set-up is surrounded by a steel reaction frame for balancing the radial loads which are applied by the 84 hydraulic actuators (28 per ring). The axial forces representing the loads from the tunnel boring machine are applied by 14 actuators placed at the top and connected by a closed frame to the bottom of the lining. In order to avoid friction at the bottom supports the first ring is mounted on Teflon layers. Moreover, the bottom ring (ring 1) is supported by four tangential active supports, whereas the reaction frame is prevented from rotating by four tangential pendulums.

During testing the loads are applied in steps. After each load step measurements are performed with respect to the forces, the joint deformations as well as the axial and tangential strains on both sides of the segments. Moreover, laser measurements are performed for obtaining the radial deformations of the lining (Fig. 1b).

3. RESULTS

The measurements obtained from the experiments have been analysed and compared to the results of finite element calculations of the test. Some of the most important results of test A3 are shown in Fig. 2. With respect to Fig. 2b it is mentioned that the calculated results are given by the solid lines, whereas the measurements are indicated by the dashed lines with the same (yet filled) markers. The applied radial load in test A3 was $443\text{-}19.7 \cdot \cos(2\theta)$ (see also Table 1).

From Fig. 2a it can be seen that the axial strains are strongly influenced by the concentrated load transfer at the joints. Close to the working lines of the axial loads (at the segment joints) large compressive strains are observed, whereas in between the segment joints (at each quarter of a segment) a rather low compressive strain is found. From the finite element analyses it was found that the stress in the elements is strongly influenced by lateral contraction effects due to the axial loads. The maximum and minimum calculated stress was about –1 N/mm^2 and –5 N/mm^2 respectively. This yields the conclusion that the stress distribution cannot be derived directly from the strain measurements in the tests. It is mentioned that the calculated average axial stress (–3 N/mm^2) corresponds to the expected stress for experiment A3 (i.e. 2955 kN/m^2, see Table 1).

The tangential bending moments linearly depend on the tangential curvature in the segments. When the curvature is defined as $\Delta\varepsilon_{tan}/t$ (Fig. 2b) it can be seen that there are quite some differences found in the curvature between neighbouring rings. In the experiments the same tendency is found as in the finite element calculation, however, less pronounced. The differences are caused by the (locally) low bending stiffness of the segment (and ring) joints. For infinite stiffness a uniform behaviour may be expected, for zero stiffness $\Delta\varepsilon_{tan}$ yields to zero. Consequently, large differences between the subsequent rings in the calculations indicate that the bending stiffness of the segment joints is too low. These findings are supported by the measurements of the axial strains and the radial deformations.

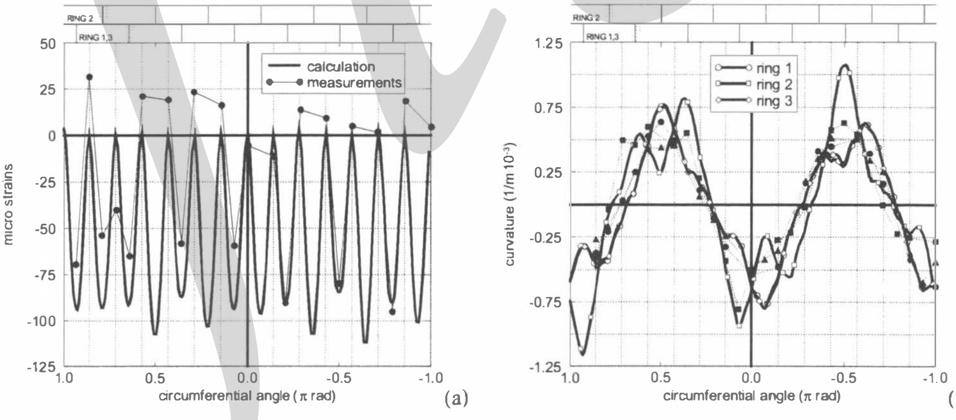

Fig. 2 Calculated and measured average axial strain in ring 2 (a) and the tangential curvature $\Delta\varepsilon_{tan}/t$ in ring 1, 2 and 3 (b) for test A3

REFERENCES

[1] Vervuurt, A.H.J.M., Den Uijl, J.A. Gijsbers, F.B.J. and Van Der Veen, C. Aanvullende Proeven in de Tunnelproefopstelling: Constructiegedrag Onder Gebruiksbelastingen en het Effect van Plaatsingsonnauwkeurigheden. Deel 1: Opzet en Resultaten van Serie A, **Delft Cluster Report DC 01.06.02-01**, in preperation (in Dutch)

EXPERIMENTAL STUDY OF A PROPOSED CUT AND COVER TUNNEL STRUCTURE APPLYING STEEL-R/C COMPOSITE WALL

Tetsuo Hirose, Fumio Hakamada
Hanshin Expressway Public Corporation
JAPAN

Koichi Ono
Kyoto University
JAPAN

Kosuke Furuichi
Kajima Corporation
JAPAN

Keywords: composite structure, reduction of cost

1 INTRODUCTION

A conventional cut and cover tunnel is usually constructed by casting reinforced concrete after constructing the temporary sheathing with H-section steels in soil cement and excavating inside soil. The proposed tunnel structure will be composed of temporary H-section steels and R/C for the sidewall in order to reduce the construction cost by utilizing temporary members effectively.

2 STRUCTURAL CONCEPT

The conventional tunnel structure is constructed with temporary sheathing by using H-section steels consisted of the watertight joint and R/C walls as the tunnel sidewalls. This soil sheathing is only a temporary wall, which is set up outside the structure in order to excavate soil and allow the construction of the tunnel. After completing the construction work, this wall becomes unnecessary. However, this temporary sheathing is a very large-scale structure and plays an important role in supporting the earth pressure in a comparatively loose ground and controlling the displacement caused by adjacent structures in the overcrowded cities [1]. During the design process, the size of H-section steel is usually determined not by stress but the required restrict the deformation of adjacent structures under construction. Therefore, it should be able to be effectively applied as the tunnel sidewalls in composition with R/C structure. Outlines of this structure are shown in **Fig.1**.

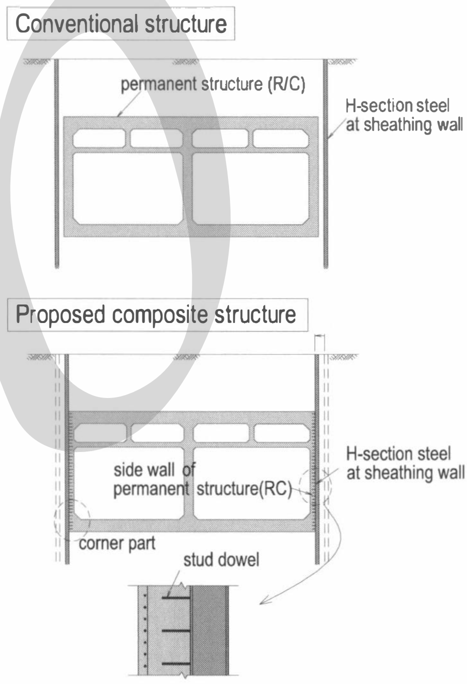

Fig. 1 Outline of composite tunnel structure

3 FULL-SCALE TESTS OF SIDEWALL

Bending and shear tests were carried out on three full-scale steel-R/C composite beams, which simulate a part of the tunnel sidewall, to examine the

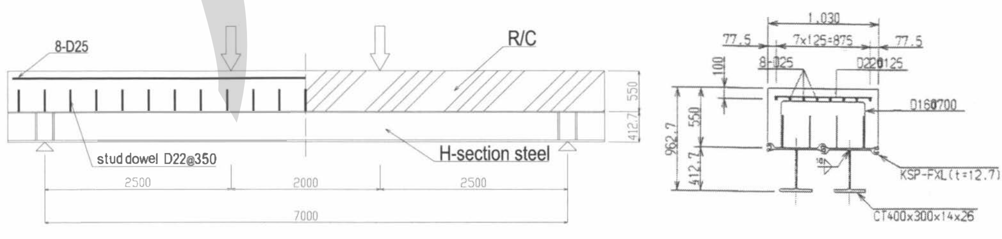

Fig.2 Profile of specimen

(mm)

deformations and the load-carrying capacities of this composite structure. Profile of a specimen is shown in **Fig.2**.

A sample of strain distributions at a section of a specimen (specimen 3; Shear Test) is given in **Fig.3**. It was recognized that the distribution was linear and was corresponding with the Bernoulli-Euler theory within the allowable load. The result indicates that the structure can be designed as a composite structure with steel and concrete in the body.

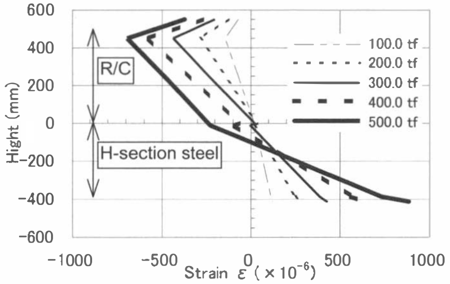

Fig.3 Strain distribution of specimen 3 (Shear Test)

4 HALF-SCALE TEST OF CORNER PART

In order to investigate the seismic performance of the corner part in this composite tunnel structure, a reversed cyclic loading test was carried out using a half scale L-shaped model specimen. Profile of specimen is shown in **Fig.4**.

The load-displacement relationship is shown in **Fig.5**. The investigation shows that the corner part possesses the sufficient seismic performance, integration during an earthquake and also the sufficient deformational capacity and a high ductility up to the ultimate state.

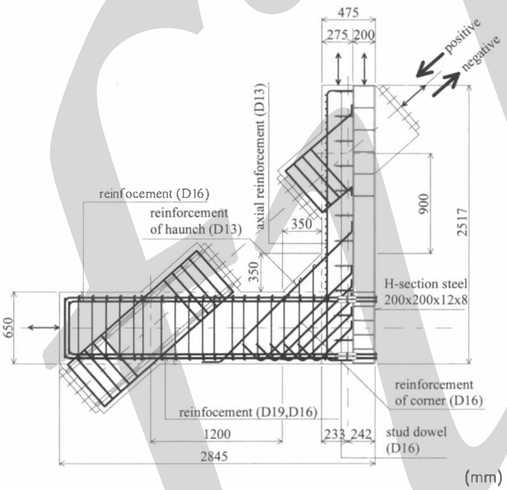

Fig.4 Profile of specimen

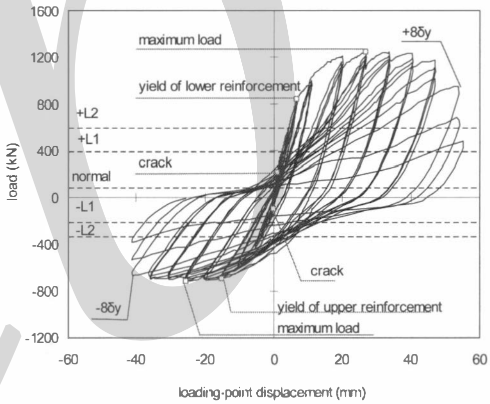

Fig.5 Load - displacement relation

5 ANALYSIS OF CORNER PART TEST

Numerical analyses were carried out using the fiber model and FEM, aimed at establishing a method for analyzing this composite structure. As a result, both numerical methods can simulate this structure with high accuracy.

6 CONCLUDING REMARKS

The proposed composite structure can shorten the width of tunnel, consume less space for construction and reduce the total construction cost. The results of this study indicate that this composite structure has sufficient performance to be applied as a cut and cover tunnel.

REFERENCE

[1] Hanshin Expressway Public Corporation, Design and Construction Guideline Considering Adjacent Structures, May 1996.

CONSTRUCTION AND EXPLOITATION PROBLEMS AT SVETI ROK TUNNEL IN CROATIA

Damir Tkalcic, BSc.CE, Marko Hranilovic, PhD.CE, Ana Krecak, BSc.CE
Civil Engineering Institute of Croatia,
Janka Rakuše 1, HR-10000 Zagreb, Croatia
e-mail: dtkalcic@zg.igh.hr

Keywords: tunnel, cracks, phased construction, applied materials, on site testing, design recommendations

1 INTRODUCTION

At present the construction of several tunnels is underway in Croatia. The biggest is Sveti Rok tunnel through the Velebit mountain. Its length is 5680 m. The tunnel consists of two separate tubes and because of its lenght it is being drilled in two phases. First phase is drilling of right tube and 2500 m of left tube which acts as service tunnel. The right tube will be completed when the left tube will be drilled to completion. At the time of drilling of the left tube right tube linning will be completed. Minning of the left tube will represent special loading on the right tube linning. When the design of Sveti Rok tunnel was done the soil surrounding the linning was modeled in finite elements (Figure 1.).

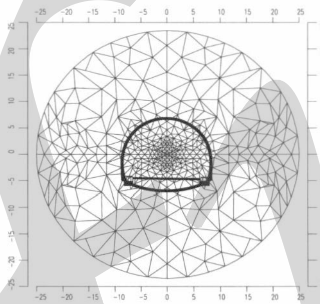

Fig.1: Linning model with surrounding soil

Simmilar method was used when analysis of blasting impact on existing linning was done. It was difficult to define the velocity of impact without onsite examination. Therefore while blasting the left tube, we measured movement in the rock mass in the right tube where the linning was not yet constructed. The scheme of measuring instruments is shown on Figure 2. The results of measuring was later gathered and diagram relating rock movement speed and time was made. The conclusion after this experiment was that void occurrence is inavitable and that linning of right tube on sections where left tube was not already drilled has to be reinforced.

2 ANALYTICAL CALCULATIONS

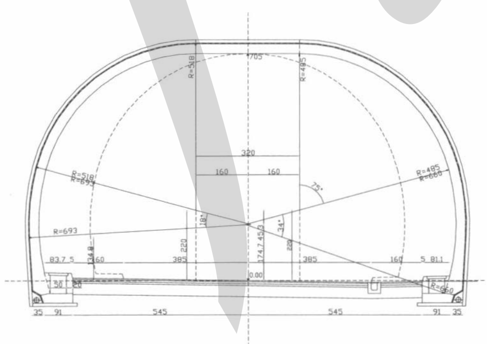

Fig. 2: Linning model on the place of thewidenings

Sveti Rok tunnel in its length passes through several types of soil, ranging from mud to solid rock. Tunnel linning shape is made so it can bear loadings without beeing reinforced. For the reason that the soil type differs linning on the mud type soil has support arch which is not needed on the other parts of the tunnel. Analytical calculations for all types of linning were made. On xyz places in tunnel there are the linning is widened (Figure 2). It is obvious that the straight part on the linning in the top of the arch is a week point that has to be reinforced. The bending moments diagram on that part of the linning has its peeks.

The other problem in tunnel construction is void occurrence due to creep and shrinkage. This time dependent impact was taken in consideration during linning design. Void occurrence will cause problems during tunnels exploitation. Curing of voids that will occur will have to be done under heavy traffic which is expected to be going through Sveti Rok Tunnel. Therefore during design some recommendations for construction were made with purpose to limit void occurrence. Such as: concreting sequence maximaly 12 m, changes of linnig thickness should be continuous, high concrete initial strenght (3N/mm^2), concrete temperature at casting relatively high 10-30°C, prevent draft occurrence in tunnel, usage of measures to prevent shrinkage of young concrete (concrete curing), keeping constant temperature in tunnel (8°C) and nests in concrete that can occur are to be cured properly. If the contractor during construction is applying this recommendation it can be expected that void occurrence will be reduced to minimum. Even though on the tunnel parts where soil is weaker minimal reinforcement according to Croatian Norms was designed with intention of reducing void occurrence. Some sections of tunnel linning were made with addition of polypropilen fibers to reduce void occurrence caused by creep and shrinkage. This was the first time this kind of fibers was used in construction of tunnel linning in Croatia.

3 CONCLUSIONS

Design of complex structures such as tunnels is a long process. Design of tunnel linning and problems that occur during tunnel exploitation is only a part of tunnel design process. Our aim in linning design was to insure that its maintenance cost were cut to the minimmum and that linning forfills its purpose regarding durability and stability. It was the reason recommendations for construction were given to contractor. We are collecting data submitted by contractor and Engineers office concerning construction course, problems that occur during construction and material and works quality. It is our intention to monitor linning behaviour during tunnel exploitation and with data obtained from contractor and Engineers office we will be able to compare theoretical conclusions made during design with real time data. Unfortunately, it is time that will show whether recommendations given in this report were correct.

REFERENCES:

[1] Tomicic, I.: Concrete structures, Croatian Structural Engineers Society, Zagreb 1996 (in Croatian)

[2] Main design of Sveti Rok tunel, Civil Engineering Institute of Croatia, Zagreb, Croatia, 2000

[3] Implementation design of Sveti Rok tunel, Civil Engineering Institute of Croatia, Zagreb, Croatia, 2000

RECENT APPLICATION OF STEEL-CONCRETE COMPOSITE STRUCTURE TO IMMERSED TUNNEL TUBES IN JAPAN

Kiyoshi Ikeda Kiyomi Kusachi Masafumi Miyata
Kinki Regional Development Bureau
Ministry of Land, Infrastructure and Transport
JAPAN

Keywords: composite structure, sandwich structure, immersed tunnel, high fluidity concrete

1 INTRODUCTION

This paper will describe the latest technology being applied to immersed tunnel tubes in Japan, such as steel-concrete composite structures, together with some examples of actual applications.

2 STRUCTURES AND FEATURES OF IMMERSED TUNNEL TUBES

For a steel-concrete composite structure, its main structural member is a composite structure made by integrating steel products into concrete. Steel-concrete composite structures are variations of an RC structure where the deformed bars are replaced by a combination of shear connectors and steel plates. General configurations of the RC structure and steel-concrete composite structure (full sandwich structure) are illustrated in **Figs. 1** and **2**, respectively.

The full sandwich structure is a composite structure in which concrete is sandwiched integrally by two steel plates. In addition to two steel plates fitted on both sides, this structure consists of shear connectors, shear reinforcing steel plates, stiffeners, and other members. The shear connectors are welded to the steel plates provided on both sides so that they cooperate with the concrete to bear the stress. The shear reinforcing steel plates are welded to the main steel plate to bear the shear stress on the structure. The stiffeners are arranged to secure the strength and work safety during high fluidity concrete filling and dock shifting in the structure production process.

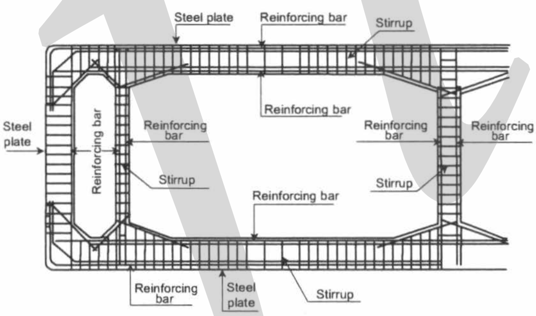

Fig.1 RC structure

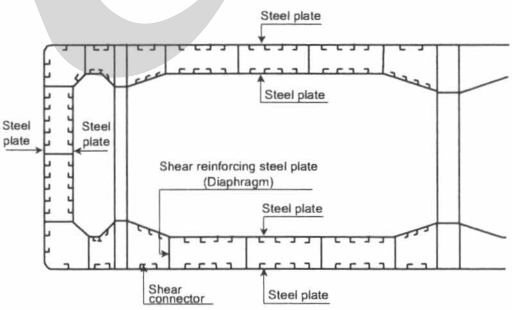

Fig.2 Steel-concrete composite structure (full sandwich structure)

3 EXAMPLES OF PRACTICAL APPLICATIONS

For the Osaka Port Sakishima Tunnel, tunnel tubes of steel-concrete composite structure were adopted for the first time in Japan. This tunnel is providing a link connecting Chikuko district in Minato-ku, Osaka City and Sakishima, a man-made island. The floor slab and sidewall were constructed of open sandwich design and roof slab is of reinforced concrete. Compared with an RC design, the open sandwich structure enabled us to reduce the total weight of the reinforcing rods, showing that this structure is advantageous in terms of construction costs and construction workability.

For Kobe Port Minatojima Tunnel, the floor slab and sidewall were constructed of full sandwich design with the exception of one tube element. This road tunnel is connecting the central urban area of Kobe City and the Port Island, an offshore urban area. The roof slab and sidewall were constructed of full sandwich design and floor slab is of open sandwich design with the exception of one tube element. In comparison with the open sandwich structure, the full sandwich structure enabled to cut construction costs and reduce the construction period.

For the Naha Port Submerged Tunnel, all members including the floor slab are of full sandwich design. This tunnel is a road tunnel presently under construction. It crosses the port entrance of the Naha Wharf to provide a link connecting the Naminoue district and Naha Airport. Since there is no suitable concrete casting yard near this tunnel, concrete was forced to cast by floating the steel shells on the sea. To secure the strength and work-safety during the tunnel tube production, all members including the floor slab are of full sandwich design.

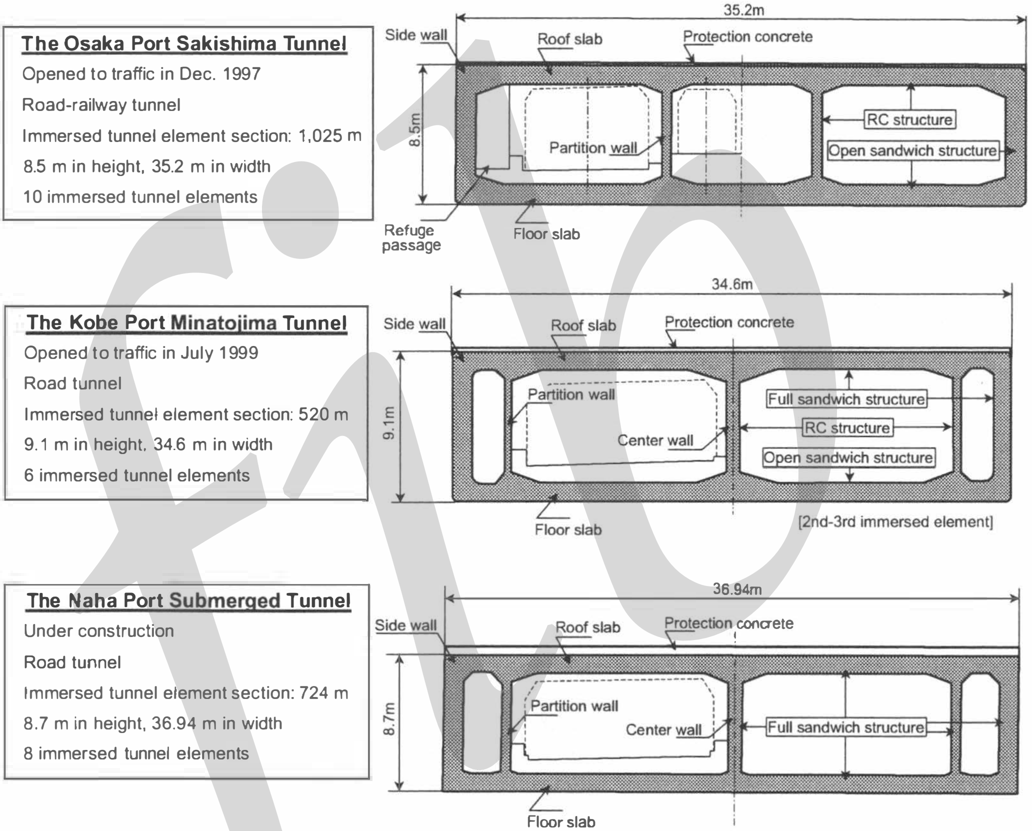

Fig.3 Standard Section of immersed tunnel element

ACKNOWLEDGEMENTS

We would like to express our sincere appreciation to the guidance and instructions given by Port and Airport Research Institute (PARI), Osaka Ports and Airport Construction Office (Kinki Regional Development Bureau), Kobe Ports Construction Office (Kinki Regional Development Bureau), and Naha Ports and Airport Construction office, Okinawa General Bureau, Okinawa Development Agency.

SOTTO MAYOR PALACE - DESIGN AND PERFORMANCE OF RETAINING AND UNDERPINNED STRUCTURES

Alexandre Pinto Sandra Ferreira Vasco Barros Rita Costa Pedro Lopes João Dias
Tecnasol FGE – Fundações e Geotecnia S.A.
Rua das Fontainhas, nº 58, 2700-391 Amadora, PORTUGAL
apinto@tecnasol-fge.pt

Keywords: excavation, retaining structures, underpinning

1. INTRODUCTION

In the last years the progressive valuation and occupation of Lisbon central areas, combined with the social pressure to preserve historic constructions, has stimulated the development of retaining and underpinning solutions, adapted to the uniqueness and restraints of each scenario [1]. The Sotto Mayor Palace underpinning and deep excavation is presented in this paper as an example of this situation. The main purpose of this 150,000m^3 excavation, mainly in the Lisbon Miocene soils, was the construction of 8 floors below ground level on a 7,600m^2 area, keeping in the middle of the site area the centenary building of Sotto Mayor Palace, with masonry structure and three floors, resting on a 900m^2 area. On this paper the main restraints and the adopted solutions are pointed out, as well as the Palace performance during the underpinning and excavation works

2. ADOPTED SOLUTIONS

In order to face the new project, which demanded a 25m average depth excavation around the Palace, as well as the construction of one central gallery under its structure, the Palace was underpinned internally with micropiles, capped by a grillage of prestressed concrete beams, and externally with reinforced concrete bored piles (figures 1, 2 and 3).

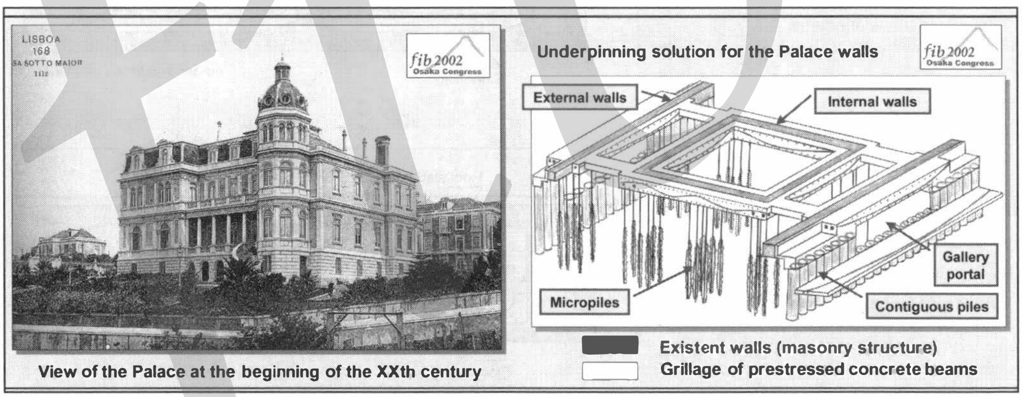

Fig. 1 View of the Palace and grillage of prestressed concrete cap beams

For the internal load transference scheme, N80 ∅127x9mm micropiles (f_y=560MPa), carrying a maximum service load of 600kN, were used. The micropiles were capped by prestressed concrete beams, which were connected to the masonry walls with pairs of ∅32mm Gewi bars spaced 0,5m (figure 1). The cap beams prestress cables were designed to balance the vertical permanent loads. Half of the prestress load was applied before the beginning of the external excavation.

The underpinning of external walls was done with contiguous bored piles ∅800mm spaced 1,0m, connected to the masonry walls trough the concrete cap beam. The piles wall was lined with 6cm of sprayed concrete, reinforced with one steel mesh layer. Due to the building geometry and the existence of the internal micropiles, the external piles were braced by 6 levels of 3m high prestressed concrete ring beams. Those beams were cast against the ground and its levels were defined in order to coincide with the underground slabs levels and thickness of 0,425m (figures 1, 2 and 3).

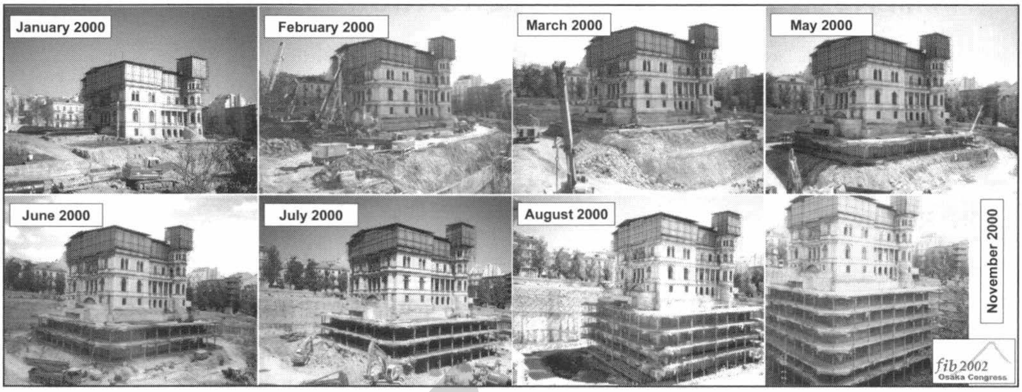

Fig. 2 General views of the excavation sequence around the Palace

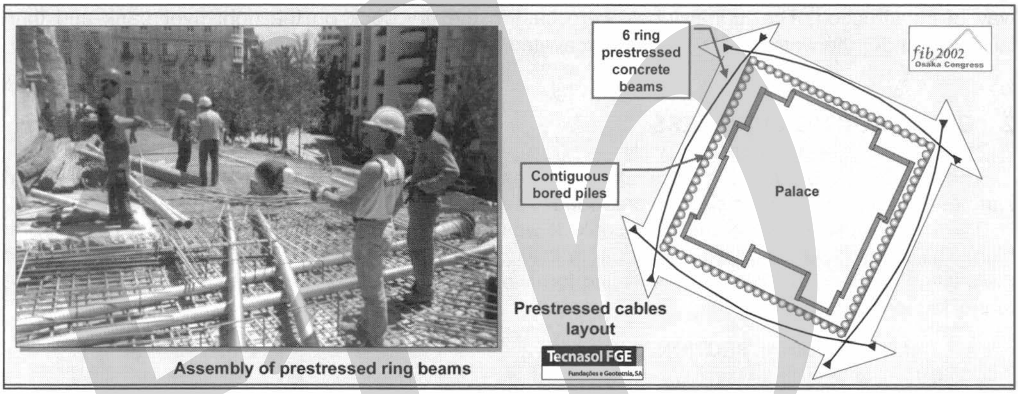

Fig. 3 Ring prestressed beams bracing the contiguous bored piles

For the external walls the adopted solutions were: 1.0m and 0.6m thickness reinforced concrete diaphragm wall (h^{max}=27m), ∅0.8mm spaced 1.0m contiguous reinforced concrete bored piles, lined with 6cm of sprayed concrete reinforced with one steel mesh layer (h^{max}=23m), and 0.35m thickness Berlin reinforced concrete wall, supported by N80 ∅127x9mm micropiles (h^{max}=18m).

3. CONCLUSIONS

The Sotto Mayor Palace underpinning and excavation works proved how the range and versatility of several retaining and underpinning solutions can fit the uniqueness and restraints of a complex scenario. It was also proved how important is the rule of the Monitoring and Survey Plan in this kind of works, allowing to survey the performance of the underpinned, retaining and surrounding structures.

REFERENCES

[1] PINTO, A., FERREIRA, S. and BARROS, V.: Underpinning solutions of historical constructions. Historical Constructions 2001 - 3rd International Seminar, November 2001, University of Minho – Guimarães, Consolidation and Strengthening Techniques, pp. 1003 – 1012

ACKNOWLEDGEMENTS

The authors acknowledge the Owner of the Palace for his permission to the presentation of this paper, as well as the supervision team leaded by Mr. Frederico Almeida and Mr. António Pinelo from ÁREA CHAVE. The authors must also point out that the presented work was performed by a Tecnasol FGE multitask team, involving more than 40 experts from different areas.

IMMERSED TUNNELS OF UNDERGROUND LINE IN PRAGUE

Jan L. Vítek
Metrostav, a.s., Czech Republic

Keywords: concrete, dry dock, excavation, buoyancy, hydraulic equipment

1 INTRODUCTION

The new underground line consisting of the two separate tunnel tubes continues from the existing station downwards under the river bed, where the lowest point is reached and then follows upwards to to the north. This arrangement required the line to be close under the river bed (1-2 m), which made the usual driving technology impossible. The tunnels are also curved in the horizontal direction. The original construction designed in the tender documentation assumed to cast each of the tube in three segments in cofferdams built in the river. The construction time would be long and the costs high.

Metrostav, a.s., main contractor of the almost 4 km long underground line, proposed an alternative way of construction. The tunnel tubes were cast in the dry dock on the right river bank and then launched under the water into the trench excavated in the river bed.

2 CONSTRUCTION PROCESS

The trench in the river was excavated from the ships. The river bed is composed of gravel and sand (~ 4 m) underneath the slates were found. The trench is about 2 - 4 m deep in slates.

The dry dock was built in the right bank. It was separated from the river by a sheet pilling 13 m high. The longitudinal concrete strips cast in the dry dock formed a foundation for the tunnel tube in the casting position, the track for the sliding formwork and finally they served as a sliding track for the tunnel launching.

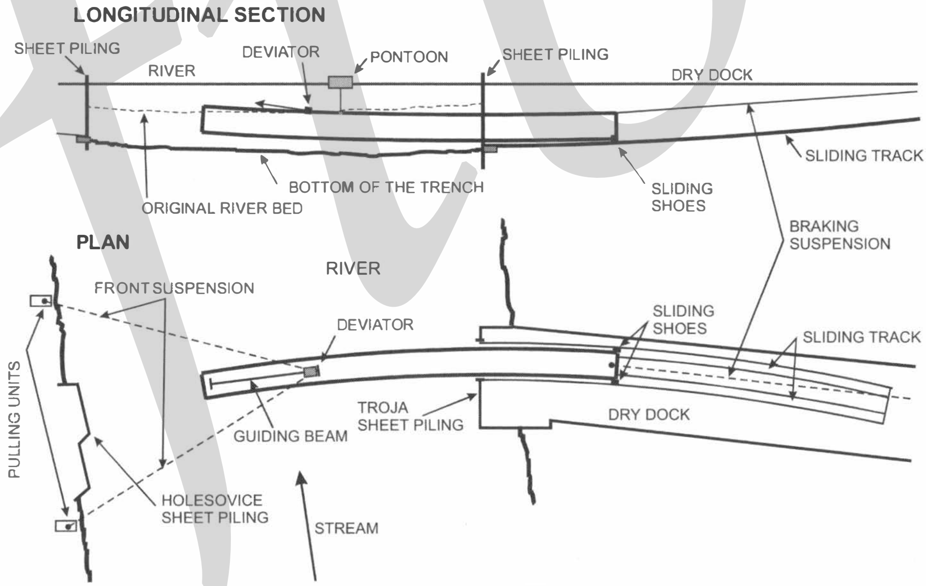

Fig. 1 Scheme of the launching operation

The tunnel tube was cast in the sliding formwork. The curved tube 168 m long with rectangular cross section was cast in segments 12 m long. Each segment was cast in one pour. The watertight concrete was developed for the tunnel. The reinforcement was designed using the results of finite element analysis taking the hydration heat and early shrinkage into account. In order to eliminate cracking in areas adjacent to the working joint due to heating of the fresh concrete, electric resistant wires embedded inside the concrete heated the old segment.

After casting, the water tanks were installed into the tunnel. The tube was closed at the ends by steel covers. The back cover was equipped with a steel access chimney. The sliding telescopic shoes with hydraulic cylinders were welded to the tunnel at the back end. The dry dock was flooded. Hydraulic jacks lifted the tunnel and the weight of the tunnel was measured. The water level in the tanks inside the tunnel was adjusted so that the designed weight of the tunnel was achieved, the stability in the lateral direction was guaranteed and the bending of the tunnel was minimised.

The tunnel was suspended on the pontoon in the front part and the sliding shoes in the back were lifted about 100 mm. The dry dock was opened to the river and the two pulling units located on the opposite (left) side of the river pulled the tunnel along the circular trajectory. The back of the tunnel moved along the concrete track using the sliding shoes. The contact of the tunnel with the track guaranteed the stability, while the buoyancy reduced the horizontal and vertical forces necessary for the launching and lifting of the front of the tunnel (Fig.1).

The pulling and braking hydraulic units were designed and delivered by VSL Heavy Lifting. The point, where the pulling cables were connected to the tunnel, moved back during the launching (using deviator) so that the tunnel could reach the final position.

Then the definitive supports of the tunnel were cast. Into the space between the trench bed and the bottom of the tunnel, the bags were placed by divers and then filled with concrete. Finally the tunnel was anchored to the river bed using micro piles.

The dry dock was used for casting and launching of the second tunnel tube and then for the definitive cut and cover tunnels.

3 PARTICULARITIES OF THE CONSTRUCTION

- Watertight structure (concrete design, cracking elimination)
- Precise construction of the tube aiming to reach the required loading of the tunnel.
- Weighing verified the structural analysis and guaranteed the safe launching of the tunnel.
- Launching – design of the pulling and braking equipment and execution of the launching in a limited space of the trench and sheet wall opening.
- Measuring system checking the position of the tunnel during launching.
- Definitive supports (concrete bags and micro piles)

Table 1: Technical data of the 1st tunnel tube

Weight	6 700 t
Weight in the water after balancing	70 t
Cross-section width x height (outside)	6.48 x 6.48 m
Top and bottom slab thickness	0.7 m
Wall thickness	0.73 m
Length	168 m
Radius in plan	750 m
Speed of casting (typically)	1 segment in 4 days
Time required for pulling (length 168.3 m)	9 hours
Maximum speed of launching	40 m/hour
Deviation from the designed trajectory during launching (typically)	< 0.1 m

4 CONCLUSIONS

- The required quality of concrete and watertightness was achieved.
- The excavation works were limited to the minimum necessary extent, which made the construction environmental friendly.
- The shipping disturbance was limited. The launching operation, including all preparation works, was done comfortably in 1 week.
- Risk of problems in the case of flooding was reduced.
- No costs for waterproofing.
- The manipulation forces were significantly reduced, since the weight in the water was small.
- The stability of the curved tube was guaranteed due to the combination of launching and floating.
- The time of construction was significantly reduced.
- The total costs were reduced.

ACKNOWLEDGEMENT

Some results obtained from the research of the projects supported by the Grant Agency of the Czech Republic No. 103/00/0615, 103/00/604 and from the research project of the CTU in Prague No.210000003 were applied. This support is gratefully acknowledged.

HUGE UNDERGROUND TUNNEL CONSTRUCTED BY MULTI-MICRO SHIELD TUNNELING

Mitsuo Tanaka, Kentaro Mori
Metropolitan Expressway Public Corporation, KANAGAWA Construction Bureau, JAPAN
Yoshio Abe, Weijian Zhao, Koichi Kano, Osamu Mochizuki
Taisei Corp., JAPAN

keywords: MMST Method, large cross-section tunnel, the Trans-Kawasaki Expressway Route

1 OUTLINE OF TRANS-KAWASAKI EXPRESSWAY ROUTE AND APPLICATION OF MMST METHOD

The Trans-Kawasaki Expressway Route is now under construction by the Metropolitan Expressway Public Corporation, and it is a part of plan route connected to the Tokyo Nagoya Expressway Route from the coastal area in Kawasaki City. It constitutes the arterial road network of the metropolitan area, and is integrated with arterial roads.

The Trans-Kawasaki Expressway Route goes from Route 15 of the Kawasaki station east, and it is a total length of 7.9km which connects for the Bay-Shore Route and the Tokyo Bay Aqua-Line in Ukishima reclaimed land (Fig.1). The interval of about 2km, which holds the Daishi junction, has been planned to construct with the tunnel structure. Approximately 500 meters long near this junction, the large cross-section tunnel construction must be carried out within the width of the existing Route 409, under the condition of ensuring the necessary traffic volume. Based on these restrictions, the MMST Method was developed as the technology, which constructs the large cross-section tunnels, by the non-cut-and-cover method.

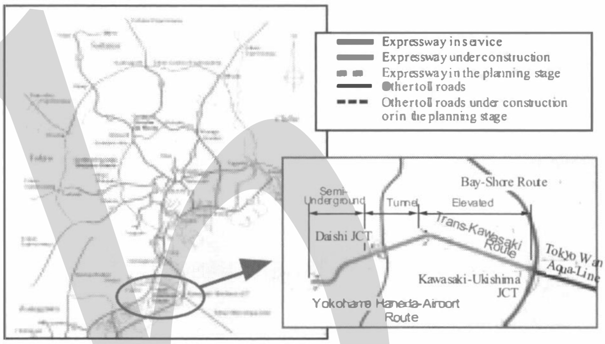

Fig.1 Metropolitan Expressway and Trans-Kawasaki Expressway Route

As it is shown in Fig.2, the planned tunnel is about 28m wide, and about 24m high in the largest cross-sectional shape. With the aim of the completion in 2007, execution design and construction planning are advancing at present.

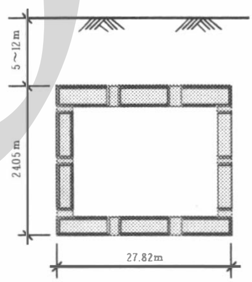

Fig.2 MMST tunnel cross section

2 OUTLINE OF MMST METHOD

The MMST (Multi-Micro Shield Tunneling) Method is a non-cut-and-cover tunneling method which constructs large cross-section tunnel based on a new idea developed by the Metropolitan Expressway Public Corporation. The sequence of construction is shown in Fig.3.

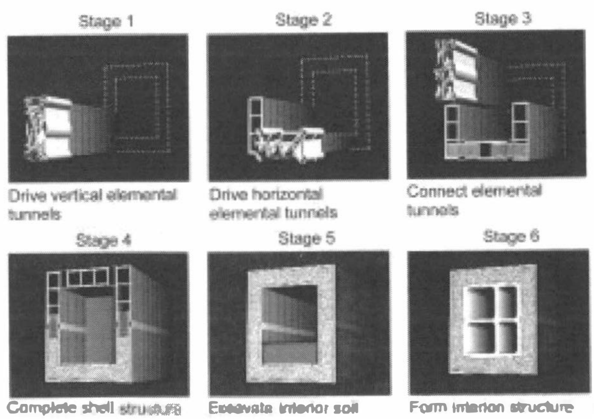

Fig.3 MMST construction sequence

Generally, a road tunnel needs a rect-

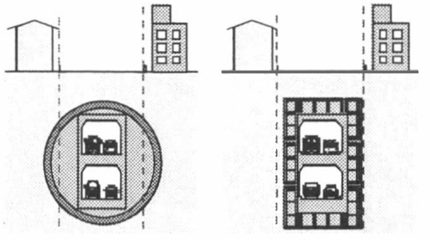

Fig.4 Comparison of MMST Method and conventional shield tunneling methods

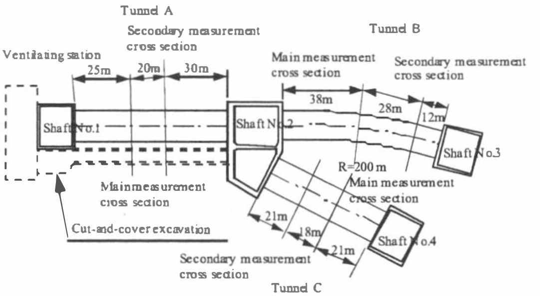

Fig.5 Plan of test construction structures

angular cross section. In a conventional shield tunneling method using a large-diameter single-face shield machine, extra excavation space inevitably occurs. As shown in Fig.4, because the cross section by MMST Method is more rational, a tunnel can be constructed within a minimum width.

3 FOR THE PRACTICAL APPLICATION OF THE MMST METHOD

The Metropolitan Expressway Public Corporation has organized the investigation research council in 1995. Various investigation researches have been carried out for the practical application of the MMST Method, while the intellectual opinion has been taking in. And construction of the ventilation ducts in the Daishi junction was carried out as a field trial of the MMST Method.

3.1 Outline of test construction

With a view to practical application of the MMST Method, a test implementation was carried out to confirm methods of design and construction for the elemental tunnels, the linking of elemental tunnels, and the overall structure of the MMST tunnel. In total, there are three tunnels, A, B, and C, with a combined length of approximately 210 m. There are also four shafts. Photo.1 shows the complete situation of test construction for Tunnel B.

3.2 Challenge to route line tunnel

The design flow of the route line MMST structure is shown in Fig.6. After the experience of the Hanshin Earthquake's disaster, seismic design was also examined for the great earthquake (Level 2), which rarely arose during in-service period. It was judged that improvement of joint and connective structure and further cost reduction had to be attempted. The birth of the enormous shield tunnel in rectangular cross-section, which is unigue in the world, has been scheduled for this summer.

Photo.1 Completion situation of test construction(Tunnel B)

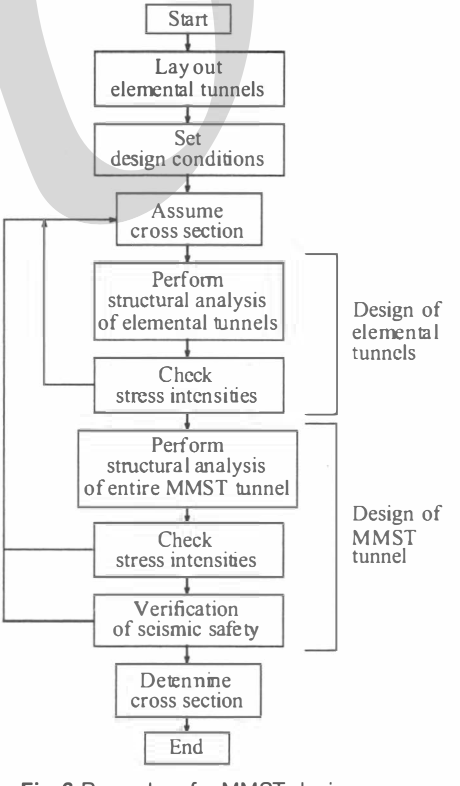

Fig.6 Procedure for MMST design

ADVANCES IN STRUCTURAL UNDERWATER CONCRETE TECHNOLOGIES

Sam X. Yao
Project Manager, Ben C. Gerwick, Inc.

Ben C. Gerwick
Chairman, Ben C. Gerwick, Inc.

20 Califomia Street, San Francisco, CA, USA

Keywords: underwater concrete, structural applications, tremie method, mix design

1 STRUCTURE APPLICATOINS IN UNDERWATER CONCRETE

The marine civil construction has witnessed a significant trend towards structural uses of underwater concrete in the last several decades. One of the earliest applications of underwater concrete as a structural material was for the U.S. Navy drydocks between 1941 and 1945. These drydocks were constructed with pre-installed precast concrete shell segments as in-situ forms into which large amounts of tremie concrete were placed. The tremie concrete worked in composite action with the reinforced concrete shells and constituted an integral part of the drydock structures.

In 1955, the contractor of the Richmond-San Rafael Bridge in the San Francisco Bay developed an altemative design for the bridge foundation and pier utilizing in-the-wet construction techniques, which was approved for construction by California Department of Transportation. The design consisted of using precast concrete shells filled with tremie concrete in lieu of the conventional steel-formed cofferdam system [1,2]. The patented concept was later used in construction of many major bridges with substantial cost saving and schedule reduction.

In recent years, the U.S. Army Corps of Engineers has launched major developments in underwater construction of locks and dams utilizing the in-the-wet technology. This innovative method employs offsite prefabricated concrete modules as the in-situ form into which tremie concrete is placed directly. Thus, the locks and dams are constructed almost entirely under water without use of cofferdams. The method provides substantial benefits in cost, construction time, risk reduction, facility utilization, river traffic alleviation, and environmental impact.

2 CONCRETE MIX DESIGN

The structural underwater concrete refers to highly flowable, cohesive and high performance concrete that can fully encase reinforcing steel or embedments, and bond well to in-situ forms as part of composite structural members. A common range of mix proportion variables for both the standard tremie mixture and the high-performance structural mix are provided. Based upon past experience and research, the authors single out four goveming variables that have the most significant effects on workability of underwater concrete: (1) a water-to-fines ratio of concrete, (2) particle packing characteristics, (3) composition and content of cementitious materials, and (4) dispersion characteristics of solid particles in concrete.

Development and widespread acceptance of the high range water reducing admixtures and anti-washout admixtures have had significant impact on advanced applications of structural underwater concrete. However, there are constructibility problems with use of these chemical admixtures. For example, high range water reducers are prone to react with certain cements to cause rapid or erratic slump loss. Using set retarders can effectively offset slump loss, but also lead to a prolonged delay of the set. Such a situation may not be acceptable when the construction schedule is very tight or site conditions change drastically over time. Thus, chemical admixtures cannot be used to compensate for poor mixture proportions and poor materials quality. Only when the basic concrete mixture is optimized can chemical admixtures be effectively used to enhance the performance.

3 CONCRETE PLACEMENT

In structural applications of underwater concrete, laitance developed during concrete placement is detrimental to structural strength and integrity. Laitance is a direct result of cement washout, bleeding and segregation of concrete. A low water-to-cement ratio and proper use of the anti-washout admixture in concrete mixes are the most effective means to minimize laitance formation. In addition, laitance are also caused by improper construction operations. In principle, concrete placement should cause as little disturbance to the concrete as possible.

In practice, the common underwater concrete placement methods are the tremie method and the pump method. The pump method, although often preferred by contractors, has led to numerous incidents and poor quality concrete. It is a technically risky procedure for placing concrete underwater due to several reasons: (1) when the concrete was directly pumped down into deep water, the weight of concrete plus pumping pressure surges are at times much greater than the hydrostatic head from the water outside the pipe. Thus, concrete exits the pipe at an uncontrollably high speed, causing significant disturbance and wash out of the concrete; (2) a pump system is closed to the atmosphere. When concrete is pumped downward, it at times falls through the pump line at a rate much faster than the pump output, creating a vacuum in the line. The vacuum pressure so created tends to suck away the cement paste from aggregates, causing segregation of the concrete and plugging of the pump line; (3) pumping into a confined space can potentially result in excessive discharge pressures; (4) if the end of the pump line is not adequately submerged in concrete, excessive pump pressure surges can kick the pump line out of the in-place concrete, causing mixing of the concrete with water.

For placement of high quality structural underwater concrete, the tremie method has proven to be the most sound and reliable method. The tremie method can be defined as a way of placing underwater concrete through a rigid pipe by means of gravity flow. There is always a hydraulic balance point at which the gravity of the concrete inside the tremie pipe is in equilibrium with the resistance to flow. Any concrete added above the hydrostatic balance point will cause concrete to flow. Thus, the tremie system is a self-adjusting system that balances the concrete outflow with the concrete inflow fed into the tremie. The main advantage of the tremie method over pumping is that the tremie concrete flow will be continuous and slow enough without causing turbulence.

Substantial research has shown that the quality of in-place underwater concrete is correlated with the concrete flow pattern during placement. During the construction of Philadelphia Navy dry dock in 1943, large-scale mock-up tremie pours with several different dyes were made to determine the flow pattern [3]. In the 1980's, large-scale laboratory tests were conducted to further verify the tremie concrete flow patterns and their effects [4]. These tests conclusively show that the concrete flows out of tremie in two distinctive patterns: (1) the bulged pattern and (2) the layered pattern. The bulged flow pattern tends to develop smooth, flat surface and is associated with uniformly distributed, good quality concrete. The layered pattern often develops very steep and rugged surface with large quantities of laitance. The concrete flow pattern is dependent upon consistency of the concrete mixture and the concrete placement rate. The tests show that highly flowable and cohesive concrete mixtures usually flow in the bulged pattern, while less flowable concrete mixtures flow in the layered pattern.

The tremie concrete placed into the reinforced form is required to pass through reinforcing cage without jamming or entrapping water. Attention should be given to the layout and detailing of the reinforcement as well as the concrete mixture proportions. The arrangement of reinforcing bars should be simple with adequate space between them. The space between steel bars should be at least 8 times the maximum aggregate size. This requirement generally exceeds the requirements for spacing of bars in many codes for concrete placement in the dry conditions. But it is necessary, because the driving force to produce concrete flow is reduced approximately by half due to buoyancy of water.

Recent experience with several major bridge foundations shows that there is a serious danger of erosion of exposed fresh concrete by river current and waves before the tremie concrete gains adequate strength. This problem is especially pronounced with high performance structural underwater concrete, because these concrete mixes typically contain high amounts of chemical admixtures which tend to delay the set time or early strength gain. Several effective preventive measures are recommended to protect the underwater concretefrom detrimental exposure to current.

4 FORM PRESSURE

Mass tremie concrete tends to exert significant hydrostatic pressure on formwork due to increasing uses of chemical admixtures and pozzolans, and delay of concrete set time. Structural underwater concrete typically needs to be placed in a continuous manner in order to eliminate cold joints and entrapment of laitance in the concrete. The continuous concrete placement may leave inadequate time for concrete to stiffen so that the form pressure increases proportionally with the depth of fresh concrete. Thus, accurate evaluation of the form pressure becomes critical for structural design of the precast in-situ forms. Based upon experimental tests, the paper provides a time-dependent form pressure design formulas that accounts for the rate of concrete placement and the rate of concrete slump loss.

REFERENCES

[1] Gerwick, B.C., “Bell-Pier Construction, Recent Development and Trends”, Journal of American Concrete Institute, Vol.62, 1965

[2] Yao, S.X. Berner, D.E. and Gerwick, B.C., “Assessment of Underwater Concrete Technologies for In-the-Wet Construction of Navigation Structures”, U.S. Army Corps of Engineers ERDC Technical Report INP-SL-1, 1999

[3] Halloran, P.J. and Talbot, K. H., “The Properties and Behavior of Underwater Plastic Concrete”, Journal of American Concrete Institute, Vol, 39, 1943

[4] Gerwick, B.C., Holland, T.C. and Komendant, G.J., “Tremie Concrete for Bridge Piers and Other Massive Underwaer Placements”, Federal Highway Administration, Report No. RD-81/153, 1983

PRESTRESSED CONCRETE SHIELD SEGMENTS

Koji Ishii Yoshiyuki Shakiyama
P.S.Corporation, Japan

Hirohide Hashimoto
Ishikawajima Conctruciton Materials Co.,Ltd, Japan

Kenji Okubo
Daiho Construction Co.,Ltd, Japan

"Keywords:" shield-tunnel, pc-structure, full-size segments

1 INTRODUCTION

PC structures are counted on to provide the following benefits.
1) Integration of the assembled structure improves dynamic strength and water tightness.
2) The gains in structural dynamic strength are accompanied by the reduction of segment thickness, the amount of steel reinforcement, and reduced construction costs.
3) It provides the unique and superior deformation restoration properties of a PC structure.

It can also permit more efficient section shapes and the lining. The PCNet segment, which is a PC structure, provides even greater value by further improving the efficiency in the execution of PC steel materials. However, since only a few shield tunnels making use of PC structures have been constructed, it is necessary to perform tests to accumulate data, so that the optimal design and execution methods may be established.

This test was undertaken to verify the assembly performance of PCNet segments by assembling full-size segments under conditions that approximate actual work-site conditions.

2 ASSEMBLY VERIFICATION TESTING

2.1 Outline of the test

A simulated erector (able to hold, rotate, perform rough positioning, and make fine adjustments of the manufactured segments) was constructed and used to perform the assembly testing. The insertion and tensioning of the PC steel was performed in the tunnel; the insertion was performed by the automatic insertion apparatus. The assembly performance was evaluated and the quantity of prestress checked by measuring the strain of the concrete. **Figure 1** and **photo 1** show the assembly diagram and assembly in progress.

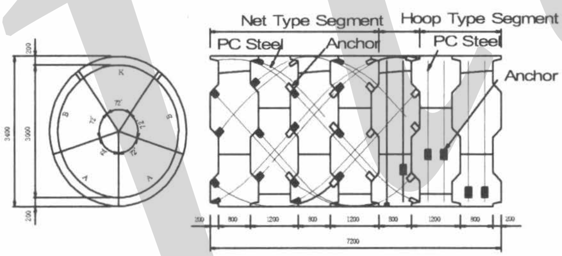

Figure 1. Assembly diagram

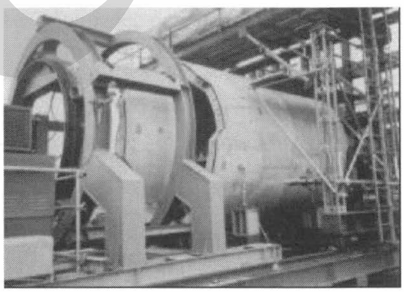

Photo 1. Assembly in progress

2.2 Shape and dimensions of the segments

The shape and dimensions of the segments using the hoop pattern were selected based on the following design considerations, using common design methods. The shape and dimensions of the segments using the net pattern were identical to the hoop segments. The same kind of PC material was used in both segment types in order to compare the amount of prestress applied.
1) Internal diameter of the tunnel: 3 m
2) Segment width: 1 m
3) Soil: clay
4) Earth cover: 2D (D: external diameter of the segments)
5) Coefficient of lateral earth pressure: 0.6

6) Coefficient of subgrade reaction: 5 MN/m^3

2.3 Inserting and tensioning the PC Steel

The PC steel used for the hoop arrangement was tensioned using the system shown in **Figure 2** after each ring was assembled. **Photo 2** shows the tensioning of the PC steel. **Photo 3** shows the tensioning being performed in the net arrangement case. In both cases, it was clear that the prestress levels by measurement were the same as by calculation.

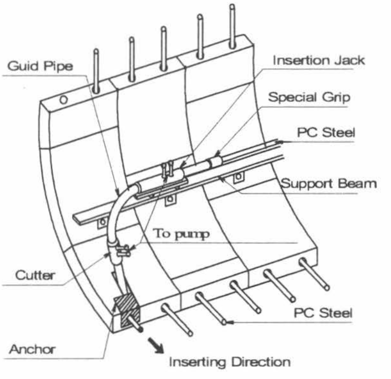

Figure 2. Assembly diagram

2.4 Assembly performance

The assembly is evaluated by measuring the circularity of the rings and the gaps between the joints. In all PC steel arrangements, tensioning improved the circularity and reduced the gap widths on the joints between the segments.

Photo 2. Tensioning of the pc steel in the hoop arrangement

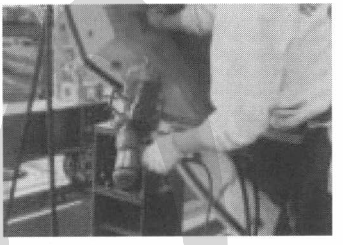

Photo 3. Tensioning of the pc steel in the net arrangement

3. CONCLUSIONS

Full-size assembly verification testing of PCNet segments that are of the post-tension type was performed. The testing provided the following information:

1) The automatic insertion of PC steel can reduce labor requirements.
2) The measured prestress in both the hoop arrangement and net arrangement closely approximate the calculated values.
3) Prestress improved circularity and narrowed the gaps between joints.

Future development and improvement projects to establish PCNet design and execution methods are scheduled.

CONSTRUCTION OF A 200,000KL CAPACITY UNDERGROUND LNG STORAGE TANK

Atsuhiro Fukada Yoshiaki Shamoto Masafumi Nakano Hiroyuki Aoki
Kajima Corporation Tokyo Gas Corporation
JAPAN JAPAN

Keywords: LNG underground storage tank, concrete dome roof, air-raising, air-support

1 INTRODUCTION

TL21, the biggest LNG underground storage tank in the world, was constructed at Tokyo Gas Ohgishima Terminal (Tsurumi-ku, Yokohama). It is an underground cavity of 72 m in inner diameter and 49.2 m in depth, which stores 200,000 kl of LNG.

The major characteristics of this tank are that it has a 9.8 m thick reinforced concrete slab so as to make it resistant against the uplift pressure, and a low-rise reinforced concrete dome so as to support the earth cover since the entire structure of the tank is built below ground level.

The bottom slab is provided with six layers of reinforcement D51 placed 190 mm apart in the upper part. For placing reinforcement, a re-bar assembly machine was used for efficiency.

Concrete for the roof was placed by the air-raising method and air-support method using a temporary steel roof, which eliminates the need for scaffolding and platforms, so that costs can be reduced and construction period can be shortened.

2. OUTLINE OF STRUCTURE

From the viewpoint of effective use of land and harmony with the surrounding environment, the LNG underground storage tank is of a totally buried type with the entire structure including the roof built below ground level. In order to resist the weight of earth cover atop the roof, a conventional steel roof was replaced by a reinforced concrete roof.

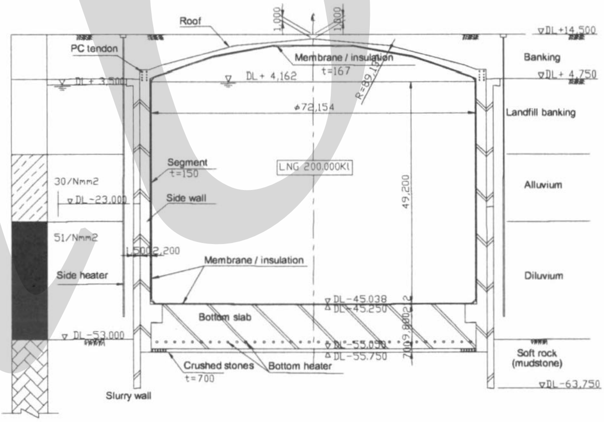

Fig. 1 Structural drawing

3. BOTTOM SLAB WORK

The bottom slab is an extra large disc of 72 m in diameter and 9.8 m in thickness.

The quantity of reinforcing bars is determined in consideration of the combination of these loads when designing the bottom slab, and the moment of upper tension due to the uplift pressure and temperature loading are conspicuous in this member. Therefore, large-diameter re-bars (D51) are arranged in 6 stages at 190 mm pitches on the upper side of the bottom slab.

Therefore, a re-bar assembly machine was used for this work to efficiently assemble re-bars.

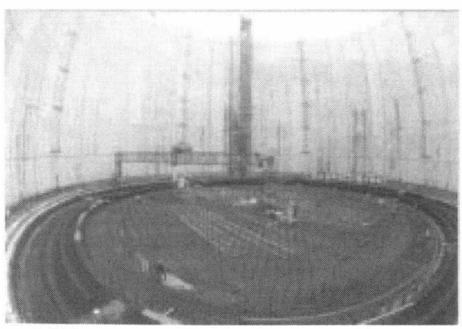

Photo 1 Panoramic view of assembly machine

4. ROOF CONSTRUCTION

This storage tank is of a totally buried type, and in order to support approx. 40,000 tons of earth cover, a dome roof structure made of RC was adopted.

For construction of the RC dome roof, the air-raising method for the temporary steel roof, which would function as a framework, and the air-support method for supporting the weight by pneumatic pressure during re-bar assembly and concrete placing were adopted.

After examining a rational, economical construction method to make the roof including the roof of the temporary steel roof, the roof was made by placing two layers of concrete. The weight of the first layer (50 cm in thickness) was supported by pneumatic pressure, while the weight of the second layer (50-150 cm in thickness) was supported by the hardened first concrete layer.

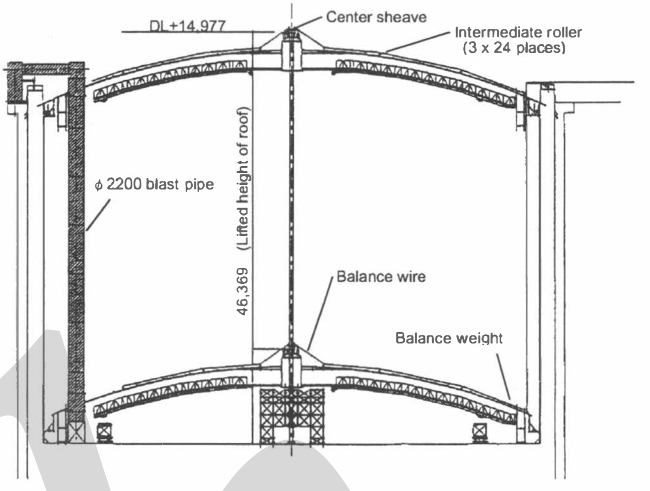

Fig.8 Outline of air-raising method

The steel roof raised by the air-raising method weights about 700 tons, and has a surface area of about 4,100 m^2. The required pneumatic pressure was assumed to be 196 mmH_2O. The required supply air volume was assumed to be 1,400 m^3/hr. The final lift of the roof was undertaken successfully in about 3.5 hours, up to the prescribed position 46 m above the bottom slab. Axial displacement after the lift was 9 mm.

After air-raising, the tank interior was pressurized to 1,700 or 1,950 mm H_2O, so that re-bar work and concrete work for the first lift could be performed. Since the rigidity of the temporary roof was low, it could undergo buckling if pneumatic pressure was not continuously applied during construction. Hence, air-support was provided continuously until sufficient strength had developed in the first-lift concrete to support itself. Pneumatic pressure applied during the reinforcing bar work of the first lift was 1,700 mm H_2O, and that during concrete placement was 1,950 mm H_2O.

After the first lift concrete developed the prescribed strength, the structure was prestressed at the side wall crest, and the pneumatic pressure was removed. The prestress was intended to resist the horizontal thrust induced by the weight of the RC roof structure.

The second lift concrete was placed on top of the first lift concrete, for which the re-bars were assembled and concrete was placed sequentially. The main dome structure was completed when the dome crown was prestressed so that it could resist the earth cover weight.

REFERENCE

[1] Yanagiya, K., Ogawa, T.: Construction of an Underground Storage Tank, LNG Journal, Nov/Dec 1999

[2] Nakano, M., Ogawa, T., Tsunakawa, H.: Construction of the Largest 200,000 KL Buried Type LNG underground Tank in the World, Mechanization of Construction, April 1998, (in Japanese)

[3] Nakano, M., Seto, S., Shamoto, Y.: Construction of Reinforced Concrete Dome Roof for Buried Type LNG Tank - Construction of Temporary Steel Roof by Air-Raising Method, Civil Engineering Works, Vol.39, No.11 (in Japanese)

[4] Nakano, M., Miyazaki, S., Seto, S., Shamoto, Y.: Construction of Reinforced Concrete Dome Roof for Buried Type LNG Tank - Construction of Reinforced Concrete Roof by Air-Support Method, Civil Engineering Works, Vol.40, No.4 (in Japanese)

THE LOAD CAPACITY OF SPUN CONCRETE CULVERTS BURIED DEEP UNDERGROUND

Kimio FUKUZAWA Masakazu MITSUI Kazuya YASUHARA
Dept. of Urban and Civil Engineering
Ibaraki Univ., JAPAN

Toshimitsu HATTORI
Technical department, Nakagawa
Hume Pipe Ind. Co., JAPAN

Keywords: concrete culvert, non-linear FEM, earth pressure

1 INTRODUCTION

The progress of the human activity has expanded our life zone to a weak ground region, and as a result of this, the depth of the embedded conduits for the under ground drains have increased. Cylinder-shaped, spun concrete culverts (circular culverts) are widely used for the conduit of under ground drains in Japan. However, the circular culverts can not be used as a conduit for deep under ground drains, since the culvert cannot bear the large earth pressure which is proportional to the buried depth. In order to increase the limit in depth, many kinds of culverts have been developed. Square, arched or pentagonal shaped spun concrete culvert with a hole through the center, have been developed. Moreover a method to set the square shaped culvert to an incline of 45 degrees has been developed. Experiments on the structural behavior of spun concrete culverts subjected to the earth pressure were carried out in order to evaluate the effect of the shape and the setting method on the load capacity. Pressure was applied to concrete culvert by pressing the top surface of the sands, which were filled around the concrete culvert set in the center of a steel tank. A numerical analysis using a non-linear finite element method was applied to simulate the structural behavior of the culverts under loading.

2 EXPERIMENT

2.1 Test culverts

The culverts used in the experiments have the cross-sectional shape shown in Fig. 1. The inner diameter of all culverts is 300mm, and the smallest thickness of all culverts except circular culverts is 60mm. The thickness of a circular culvert is 57mm due to the restriction in the manufacturing.

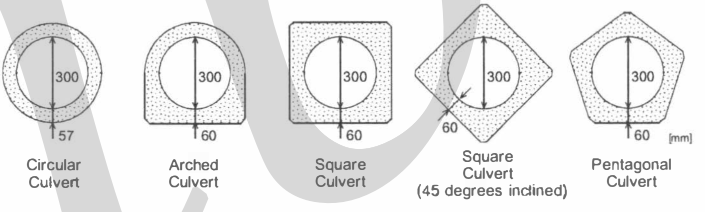

Fig. 1 Cross-sectional shape of test culverts

2.2 Testing arrangement

The steel tank used in the experiments is shown in Fig. 2. The inner space of the tank is 1800mm in height, 1200mm in width and 500mm in depth. After the test culvert had been set up, the steel tank was filled uniformly with a silica sand using a hopper. Rubber tubes filled with water were arranged at the top and the bottom of the tank in order to transmit the added pressure to the sand uniformly. The load was added to the sand using a 1MN hydraulic testing machine through a steel plate.

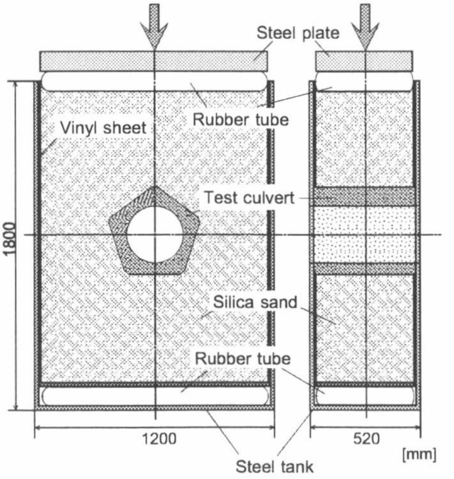

Fig. 2 Testing arrangement

3 ANALYSIS

To study the structural behavior of the culvert under the load, a non-linear finite element method (FEM) was used. The meshing for the experiment on the pentagonal culvert is shown in Fig 3. Two dimensional plane-stress elements, consisting of 4 nodes quadrilateral elements, were used to model the concrete and sand. The steel wire was modeled as a two dimensional embedded reinforcement element which increased the stiffness of the concrete element in the direction of the reinforcement. The uniformly distributed load was applied to the upper surface of the sand. DIANA Ver.7.2 (TNO (1993)) was used in the analysis.

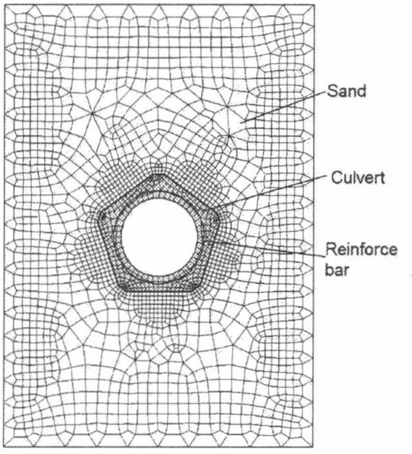

Fig. 3 FEM analytical model

4 STRUCTURAL BEHAVIOR OF CULVERTS

The measurements of the maximum strain at the inner surface of the culverts are compared to that of the FEM in Fig. 4, which represents the relation between the loading stress p and the maximum tensile strain of each culvert. The maximum tensile strain point of each culvert is also shown in Fig. 4. The maximum tensile strain of each culvert is generated at the bottom of the inside surface, except for the square culvert. The maximum strain was generated at the top of the inside surface, in the case of the square culvert. It is observed from the figure that the increase in the strain and the increase in the load is very significant when the largest strain exceeds about 150×10^{-6}. It is observed from Fig. 4 that the gradient of the stress-strain curves changes at the strain of 150×10^{-6}. We observe that the crack was produced in the concrete at that strain, without being recognized by the naked eye. We also observe from Fig. 4 that the load capacity of the square culvert set at an incline of 45 degrees is the maximum and that of the circular culvert is the minimum among all culverts. From the comparison between experimental and analyzed behavior, it is proven that the nonlinear FEM analysis proposed in this study can accurately simulate the structural behavior of various culverts buried in the sand.

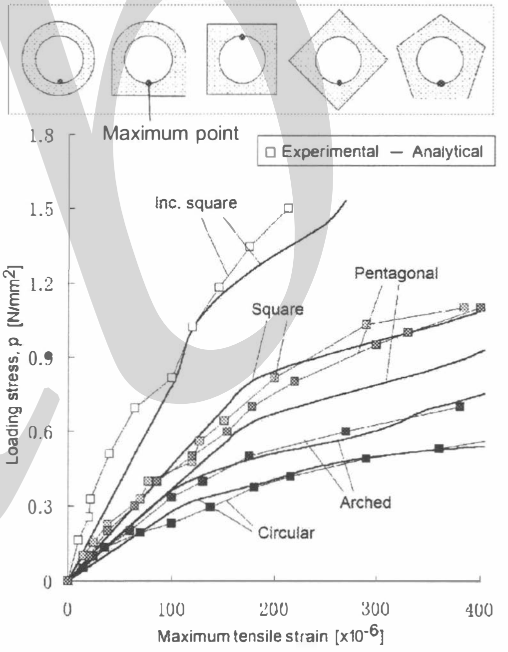

Fig. 4 Relation between loading stress and the maximum tensile strain

5. CONCLUSIONS

The findings obtained from this paper can be concluded as follows:

(1) It is confirmed that the earth pressure distribution on the surface of culverts buried in the sand is influenced by the shape of the culvert and the proposed non linear FEM can accurately simulate the earth pressure distribution caused by the load stress.

(2) The proposed FEM analysis can accurately simulate the structural behavior of culverts buried in the sand.

(3) The square culvert set at an incline of 45 degrees has the maximum bearing capacity from both experiments and analysis.

CONSTRUCTION OF THE SAGAMIKO- UNDER-BOX BY THE PRESTRESSED CONCRETE ROOF METHOD

Torimoto Yasuhiro, Japan Highway Public Corporation
Mizutani Yoshinobu, Takenaka Doboku Corporation
Ito Keisuke, Oriental Construction Co.,Ltd.
Hou Hei, Oriental Construction Co.,Ltd.

Keyword: Box type tunnel form, Underpass, Non-excavating method , PCR girder, Small sectional element propulsion

1 INTRODUCTION

Recently several projects have been promoted to construct an under-pass crossing a main road or a railway in service.

For the Sagamiko-Under-Box, a box tunnel type was adapted for which of no excavation is needed, which is the first achievement of such method in Japan.

This construction realizes the road for local residents who cross the Chuo Expressway with a road-width extension construction, which extends the vertical 4 present lanes into 6 lanes as a solution against traffic congestion between Uenohara IC where confusion is the most intense - Otsuki JCT, and a cure against traffic by alignment improvement.

As a construction method, the PCR(Prestressed Concrete Roof) method was adopted as a method for construction, with which the safety of the construction is secured, and the construction is possible at a minimum space, and can be realized in a short period of time.

This is a method of construction on the basis of the propulsion technique producing a small section element made of steel and precast concrete without excavating, which was unified by prestressing.

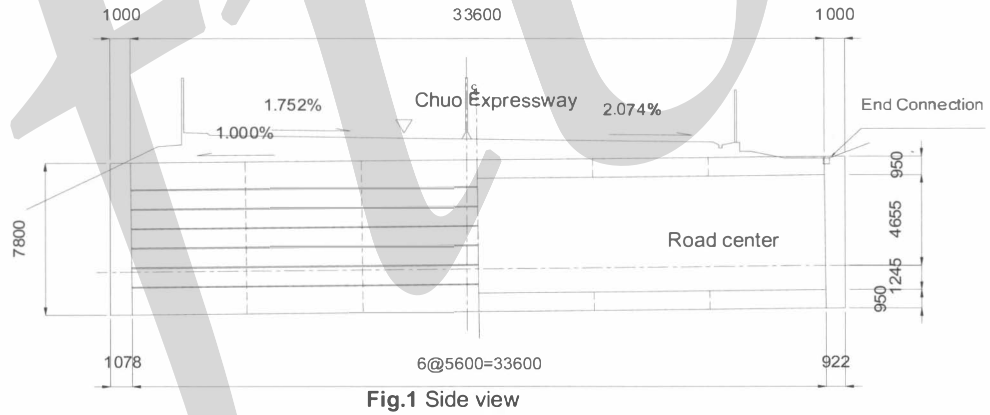

Fig.1 Side view

2 OVERVIEW OF THE CONSTRUCTION METHOD

The PCR method is a construction method developed for the purpose to build crossing structures, such as an underground passage and a river, safely, certainly and economically below an existing railroad or a road in service.

A cross-sectional view of the box type tunnel is shown in Fig.2.

In this type of box tunnel , the sidewall portions are prestressed vertically, and the adjoining PCR girders are prestressed horizontally to apply the top floor slab and the bottom floor slab, and subsequently, the corners are rigidly joined with the sidewalls and the floor slabs .

Square-shaped steel elements providing a working space for prestressing are arranged to the corners, and PC cables are inserted and tensioned in them.

They are filled up with a non-shrinkage mortar. And the after-bond-type post-tensioned cables to have excellent resistance to corrosion are used .

In the bottom floor slab, cast-in-place of highly flowable concrete is arranged to adjust the deformation caused by the earth pressure and the elements-propulsion accuracy.

In the case of a single box type, whose scale is comparatively small, there is also no concern for sinking of the structure while the weight of the soil and sand becomes small after removal from the stabilized foundation before excavation. Moreover, it is thought that a single box type will adapt to the deformation of the circumferential foundation in the case of an earthquake.

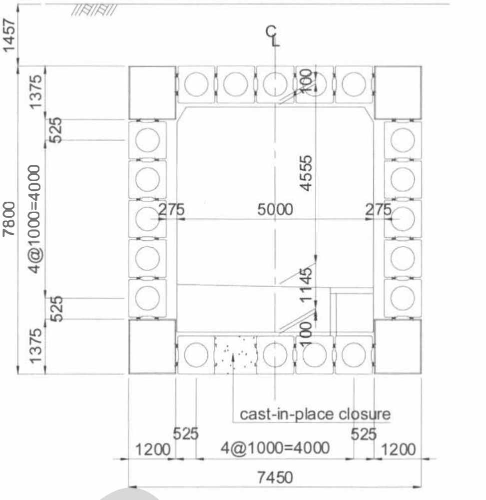

Fig.2 Cross-sectional view

3 THE FEATURE OF CONSTRUCTION

The main features of the construction are as follows.

(1)Improvement in construction accuracy was aimed at by adopting the parallel replacement method of construction which transposes a central square shape steel pipe to a PCR girder, after carrying out the pre-propulsion of three square shape steel pipes in parallel,

(2) The ground was hardly disturbed, by adopting the one by one propulsion method of PCR girders and by using the friction-cut-plate for dissolution between the upper layer.

(3) With adopting the replacement method, safety was aimed at propulsion of the square shape steel pipe taking precautions to subterranean objects, such as big and small stones.

(4) Since the main material was high strength concrete, there was no concern for corrosion.

(5) Under the restriction to make the vertical shaft small, the segments were fabricated and unified one by one, connecting by PC bars after the propulsion works, which were divided into 6 pieces of all elements longitudinally.

(6) In order to use the unified structure consisting of the propulsive elements as a main part of the final structure, quick and safe machine- digging for the whole section was adopted after structure completion, using no work such as temporary works or temporary support.

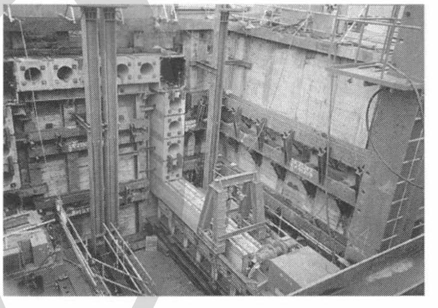

Fig.3 Propulsion of side wall

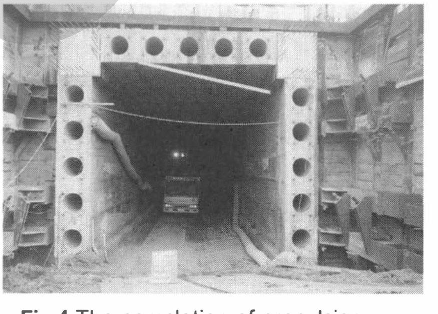

Fig.4 The completion of propulsion

APPLICATION OF SELF-COMPACTION CONCRETE CONTAINING AN EXPANSIVE ADDITIVE TO A SECONDARY TUNNEL LINING

Toshihiro Hattori Satoshi Akai Shigeru Aoki Masayoshi Ookubo
Obayashi Corp.,JAPAN

Keywords: self-compaction concrete, expansive admixture, secondary tunnel lining

1 INTRODUCTION

Tunnels in Japan are usually designed to have a secondary concrete lining thickness of 30 cm, so that the concrete can be properly placed and sufficient strength can be obtained. In the tunnel project described in this paper, new materials were employed to minimize the supports and shorten the construction period. For the secondary lining, high-strength concrete was required, since it was designed to be 20 cm in thickness. However, normal concrete would be difficult to compact and could cause defects such as honeycombs. Self-compacting concrete was therefore adopted for the project. It allowed a void-free secondary lining to be constructed without segregation.

Therefore, self-compaction concrete containing an expansion additive was planned to be used to solve these problems. The self-compaction concrete was filled perfectly in the form of the secondary lining concrete without any segregation.

The chemical prestress by the expansion additive can not be introduced easily to plain concrete because there is no restraint of steel reinforcement. The concrete expands 3-7days after placing and the chemical prestress is introduced in the same time. In case that the form is removed early,the concrete expands freely and the chemical prestress is hardly introduced because of lack of restraint. The secondly lining concrete is plain concrete and the form is removed 15 hours after placing. The chemical prestress seemed to scarcely be introduced. However, in fact, the chemical prestress was introduced as the effect of arch action and the secondary lining concrete in this tunnel was constructed without any drying shrinkage crack.

2 CONCRETE MIX

2.1 Requirements for self-compacting concrete

As shown in Table 1, the characteristics of fresh concrete for self-compacting concrete for the secondary lining are designed to be equivalent to Rank 2 specified in the Recommendation of Self-Compacting Concrete(JSCE)[1]. The design compressive strength at 28 days (f'28) was 35 N/mm^2. The compressive strength sufficient for the removal of forms was found to be 1 N/mm^2, based on the results of an analysis performed prior to the project. (The forms were removed 15 hours after concreting)

Table 1 Mix design specification

Maximum size of coarse aggregate (mm)	Filling height of U-type compaction test (mm)	Slumpflow (mm)	Air content (%)	V-funnel Time (sec)	Specified design strength (N/mm^2)	
					15hours	28days
20	≧300	650±50	4.5±1.5	7～13	1.0	35

2.2 Specified mix proportion

The possibility was examined to use a shrinkage reducing agent and an expansion admixture, in order to improve the shrinkage resistance.

The specified mix proportion determined,based on the test results ,is shown in Table 2.

Table 2 Mix proportion

W/(C+EX) (%)	s/a (%)	Unit quantity (kg/m^3)						SP (P×%)
		W	C	EX	LF	S	G	
50.4	49.2	175	317	30	216	745	822	1.5

C: Normal portland cement
EX: Expansive admixture
LF: Limestone powder
SP: Air entraining and superplasticizer
P=C+EX+LF

3 TEST PLACEMENT

3.1 General

The void-filling efficiency of self-compacting concrete and the effectiveness of the expansion admixture were tested in the trial construction span.

3.2 Evaluation of the workability and void-filling efficiency of self-compacting concrete

The conditions of the poured concrete were finally checked from another opening provided at the crown of the side form panel. Because of the large flow length, concrete at this location tends to cause a little segregation. The concrete sampled from this opening, however, contained sufficient coarse aggregates, indicating that the concrete was poured without segregation. A concrete core sampled after hardening also showed that the concrete had been uniformly poured.

Concreting imperfections such as honeycombs were not observed during the visual inspection at the time of removal of the forms, and the surface was in good condition.

3.3 Measurement

The temperature, strain, and effective stress in the secondary concrete lining were measured to evaluate the effectiveness of the expansion admixture.

3.3.1 Thermal expansion coefficient

The thermal expansion coefficient was calculated from the measured strains and temperature variation(Fig. 1). The coefficient during temperature decrease was calculated to be 7.0 $\times 10^{-6}$ (/°C), smaller than the common value of 10.0 $\times 10^{-6}$ (/°C) which is given in the Guideline for Crack Control for Mass Concrete Structures (JCI)[2]. This indicated that the shrinkage of the self-compacting concrete used in the tunnel was small due to expansion admixture which compensated the shrinkage.

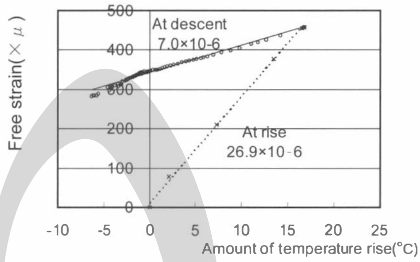

Fig.1 Thermal expansion coefficient

3.3.2 Effective stress

Fig.2 shows the changes in the effective stress. A compressive stress of about 1 N/mm2 occurred in both longitudinal and circumferential directions immediately after concreting. This compressive stress is considered to be chemical prestress by expansion admixture,and caused by the arch action of the lining. Although tensile stresses occurred with the temperature decrease, the circumferential and longitudinal stresses one month after concreting were both in compression and -1.0 N/mm^2 and -0.3 N/mm^2, respectively. This is probably because the compressive stresses caused by the expansion admixture were larger than the tensile stresses due to the temperature decrease and other reasons.

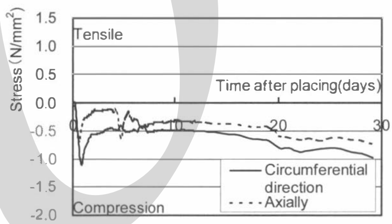

Fig.2 Stress measurement result

3.3.3 Cracks

At present, there are no visible cracks in the concrete lining of the test placement section.

4 CONCLUSION

This report explained the application of self-compacting concrete using an expansion admixture to the secondary lining of a tunnel. The test placement during the tunnel project proved that concrete of this type has an excellent shrinkage resistance and can form a solid void-free mass. This feature allowed the secondary lining of a 2 km-section to be constructed with a thickness of 20 cm as designed.

Although more than one year has passed since the first concrete placement, all spans are free from such defects as cracks, and the surface irregularities are small.

REFERENCES

[1] Recommendation of Self-Compacting Concrete,JSCE,1998.7(in Japanese)
[2] Guideline for Crack Control for Mass Concrete Structures,JCI,1986.3(in Japanese)

APPLICATIONS OF HIGH QUALITY UNDERGROUND DIAPHRAGM WALL USING SELF-COMPACTING CONCRETE TO VARIOUS UNDERGROUND CONSTRUCTIONS

Takeshi OHTOMO Jun SAKAMOTO Takefumi SHINDOH
TAISEI CORPORATION Technology Center, JAPAN

Keywords: self-compacting concrete, underground diaphragm wall, high strength concrete, cut-off wall, foundation

1 INTRODUCTION

Self-compacting concrete has high deformability and resistance to segregation with which it can be placed into every corner of formwork and narrow space around reinforcement without vibration while maintaining uniformity of members, thereby increasing the reliability of structures.

These properties of self-compacting concrete provide high quality and various additional functions to fulfill the purpose and requirements for underground diaphragm walls constructed using tremies in artesian slurry in very deep ground where placing cannot be visually checked.

This paper describes the applications of self-compacting concrete to various underground diaphragm walls including the techniques to overcome difficulties resulting from actual large-scale underground construction works. Techniques to adjust the specifications, mix-proportions, and composition of cementitious materials and admixtures are described as well to adapt to various requirements, such as high strength, low heat, watertightness, and adaptability to complex shapes and reinforcement.

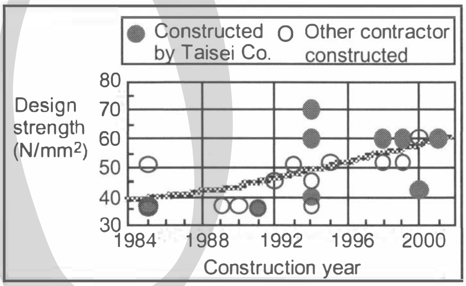

Fig.1 Past projects of diaphragm walls

2 DEVELOPMENT OF HIGH STRENGTH DIAPHRAGM WALL CONCRETE

Figures 1 and 2 show the number of diaphragm wall projects with design strengths exceeding 36 N/mm^2 and the consistency related to the design strength in these projects, respectively. A design strength of the order of 60 N/mm^2 has become common practice for diaphragm walls since 1994. The consistency of high strength concrete with a strength exceeding 52 N/mm^2 has been entirely controlled by slump flow.

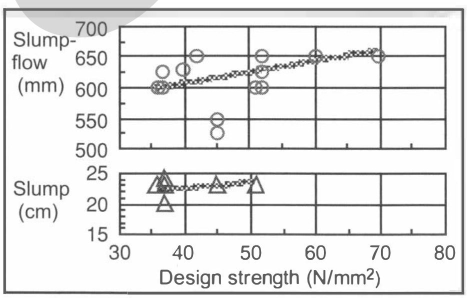

Fig.2 Relation among strength and consistency

High strength self-compacting diaphragm wall concrete with a design strength of the order of 60 N/mm^2 was put into practical use for the first time in a large-scale underground tank project in 1994 (Fig.3) [1]. In this project, the thickness of the diaphragm walls as temporary retaining walls was reduced by the use of high strength concrete. Moreover, the diaphragm walls were made to serve as cut-off walls after completion of the underground tanks, while adopting a depressurized flexible bottom slab on which no lift-up pressure is allowed to act. This substantially reduced the quantities of the wall, bottom slab concrete, and excavated soil, resulting in a much higher cost efficiency owing to the reliability of the high strength and high water-stopping performances and quality stability of high strength self-compacting diaphragm wall concrete.

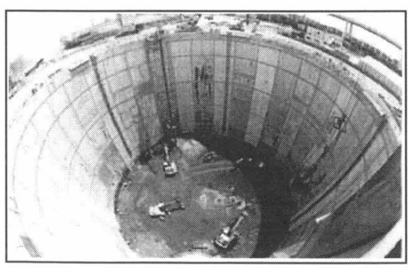

Fig.3 Tokyo Gas' Ohgishima LPG tank

Table 1 Projects of diaphragm walls using self-compacting concrete

Owner	Structure	Purpose of apprication	Quantity (m^3)	Type (Design strength)	Width(m) Depth(m)	Rebar (kg/m^3) (Steel menber)
Kawasaki City	Shibukawa shield shaft	performance Investigation	500	High strength (70)	1.5 93	68 (102)
Tokyo Gas Co.,Ltd.	Ohgishima LPG inground tank	Reduce wall thickness by high strength concrete	12,000	High strength (60)	1.0 69	95 (130)
Tokai Railway	Central Towers foundations	Ensure filling around congested rebars	8,000	Standard (24)	1.5 20	125
Hokkaido Devel-opment Agcy	Fill dam of Chubetsu Dam	Ensure cut-off (reliability as permanent cut-off)	4,400	Low heat (24)	1.2 22	64
Met. Expressway Public Corp.	Nishi-Shinjuku Tunnel	Ensure filling in irregular section	1,300	Low heat (24)	1.2 68	[illegible] (130)
Tokyo Bureau of Sewerage	Konan mains shield shaft	Reduce wall thickness by high strength concrete	2,200	High strength (60)	0.8 74	72
Tokyo Bureau of Sewerage	Kamiya mains shield shaft	Reduce wall thickness by high strength concrete	2,500	High strength (60)	0.8 63	81
East Japan Railway	Rifu Bridge	Ensure filling around congested rebars	7,400	Standard (24)	1.5 44	263 (340)
East Japan Railway	Akihabara Station foundations	Increase strength with hightension steel strands	1,900	Medium strength (42)	Pile dia.1.8 27	119 ~197
Met. Expressway Public Corp.	Daishi shaft	Inhibit deformation of re-taining wall by high rigidity	1,830	High strength (60)	1.5 55	139 (165)
Met. Expressway Public Corp.	Daishi shaft	Ensure filling in irregular section	3,020	Low heat (24)	1.5 55	119 (156)

3 APPLICATION OF HIGH QUALITY DIAPHRAGM WALL CONCRETE TO VARIOUS STRUCTURES

Owing to its excellent fluidity, self-compactibility, and uniformity, self-compacting high quality diaphragm wall concrete has been applied to a wide range of uses other than underground tanks in recent years. By adjusting the proportions of powders (binder and mineral admixture), it can adapt to changes in the design strength and lower heat requirements while maintaining the excellent self-compactibility and quality stability.

Table 1 gives the experience of Taisei Corporation with high quality diaphragm walls using self-compacting concrete, including a cut-off wall of a fill dam, irregular-section underground walls excavated by the SATT method, underground walls for shield shafts, underground diaphragm rigid foundations for a bridge, and a pile system reinforced with high strength steel strands.

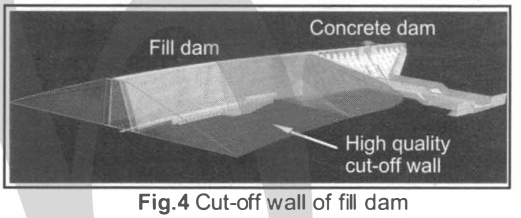

Fig.4 Cut-off wall of fill dam

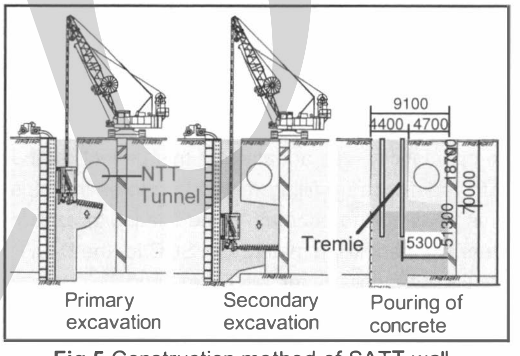

Fig.5 Construction method of SATT wall

4 SUMMARY

The technology for constructing high quality deep diaphragm walls is supported by not only technical innovation of high strength self-compacting concrete but also comprehensive technologies including design technology, such as structural design techniques for high strength, advanced analysis techniques for earthquake-proofing and ground seepage flow, and mechanical / construction technology, such as high precision excavation and information-intensive execution.

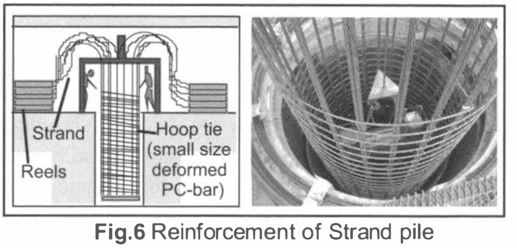

Fig.6 Reinforcement of Strand pile

REFERENCE

[1] Takagi,S.,et.al: Construction of super water tight underwater diaphragm wall used high strength and self-compacting concrete, Concrete Journal, Vol.34, No.12, pp26-29, 1996.12

APPLICATION OF SELF-COMPACTING CONCRETE TO STEEL SEGMENTS OF A MULTI-MICRO SHIELD TUNNEL

Mitsuo TANAKA Kentaro MORI
Metropolitan Expressway
Public Corporation, Japan

Takefumi SHINDOH
TAISEI Corporation
Technology Center, Japan

Keywords: shield tunnel, steel-concrete composite structure, self-compacting concrete

1 INTRODUCTION

The Multi-Micro-Shield Tunneling (MMST) method [1] was devised as a new non-open cut method applicable to large-section tunnels for urban tunnel construction under various restrictions, such as site conditions, construction conditions and environmental conditions in recent years. This is a method in which multiple unit tunnels are constructed by small-section shields and connected with one another. And then the internal space is excavated to eventually form a large-section tunnel body (Fig. 1).

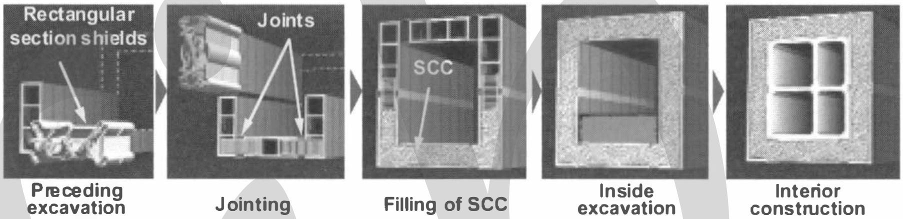

Fig. 1 Outline of MMST method

At the Daishi-Junction in which ventilation facilities for the tunnel zone of Trans Kawasaki Route, the MMST method was adopted for three ventilation tunnels (A, B, C-line) connecting the ventilation facility with the expressway tunnel, marking the world's first application of this method.

Especially, Self-compacting concrete (SCC) of a combination type with the highest self-compactability was adopted for this project, and detailed verification tests were conducted beforehand with regard to the filling method and venting pipe layout to formulate an elaborate construction plan. This enabled the concrete to be filled with extreme accuracy. This paper reports on the outline of the steel segment filling mainly with SCC for the B-line ventilation tunnel by the MMST method.

2 OUTLINE OF THE PROJECT

The B-Line tunnel is a horizontally curved tunnel (R=200meter) composed of 66 rings with a construction length and standard width of 77.7 meter and 1.2 meter, respectively. The cross section of a ring measures 13.6 meter in width and 15.5 meter in height, which are made of six units steel segments 7 meter or 7.5 meter in width and 2.5 meter in depth. These units are combined via reinforced concrete joints (Fig. 2).

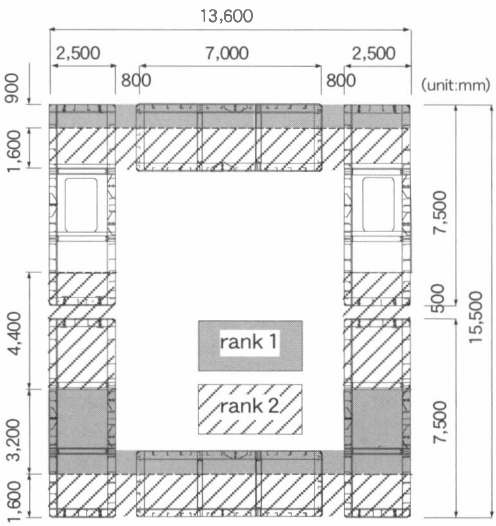

Fig.2 Cross section of Line-B tunnel

Two types of SCC with different self-compactability ranks were used for each of the top and bottom slabs. Specifically, the depth of the slab segment was divided into two layers. The lower layer was filled with SCC with Rank 2 self-compactability (general rank in recommendation of JSCE [2], the mixture R-2) with a slump flow of 650mm, whereas the upper layer was filled with a SCC with rank 1 self-compactability (the mixture R-1) having a slump flow of 700mm to ensure filling behind steel segments and around the main girders and shear connectors.

3 FIELD EXPERIENCE

In the filling of the upper layer, for which it is particularly necessary to ensure filling behind steel segments and around main girders and share ribs, care was exercised to optimize the method of filling and venting pipe layout. Air confined in closed spaces, which results in absence of concrete, may surely be let out by placing a venting pipe leading to the outside in each of such closed areas. Accordingly, communicating pipes were minimized, while U-pipes were arranged across main girders and longitudinal share ribs (Photo 1).

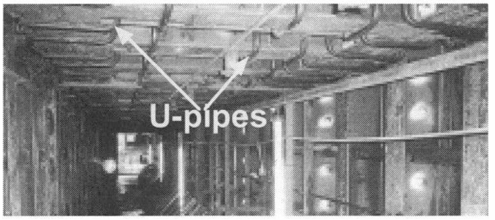

Photo 1 Arrangements of U-pipes for venting

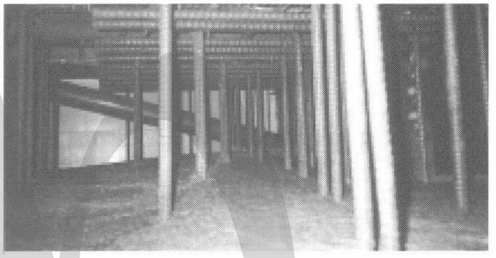

Photo 2 Flowing condition of the SCC beneath the upper layer

The state of flow and filling of the first and second lots for the bottom slab was carefully measured and investigated to determine the placing procedure to ensure filling of all corners of steel segments, in terms of the positions of discharge ports, pumping rate, and adequate venting pipe layout. And when placing the upper layer of the bottom slab, optical sensors for filling control were laid out over the entire area of the back of the steel segments at 60 cm intervals to examine the horizontal progress of concrete.

The condition of concrete flow of the upper layer of Lot 1 slab is shown in Photo 2. The SCC was placed uniformly, maintaining a flow gradient of approximately 1/20 over the entire area.

The third and later lots were placed in full scale, each lot filling 10 to 12.5 rings. In the placement of the upper layer for such a wide area, particular care was exercised so that filling to the back of steel segments could be completed within the time limit for quality retention (90 minutes). And then one placing area was subdivided into sections of 4 or 4.5 rings with an expanded metal with 5 $\times$ 35 mm mesh, which was used to divide the blocks.

4 SUMMARY

The unprecedented application of the MMST method led to placement of 8,000 m^3 of SCC with high accuracy (Photo 3).

The success of this project enhanced the rational design/execution method, paving the way for the application of this method to the main highway tunnel with a larger cross section.

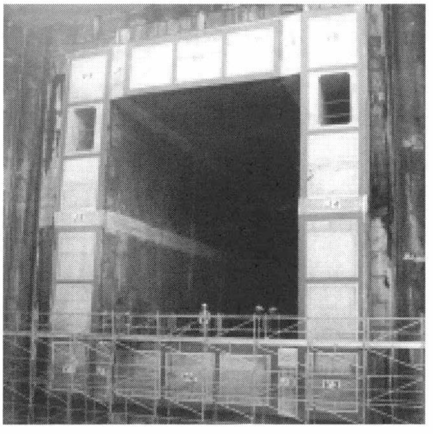

Photo 3 Completed view of B-Line tunnel

REFERENCE

[1] Egawa et al.: Investigation for practical application of MMST method, Tunnels and Underground, Vol. 28, No. 1, pp. 47-53, 1997 (in Japanese)

[2] Research Subcommittee of Japan Society of Civil Engineers: Recommendation of Self-Compacting Concrete, Concrete Engineering Series 31, August 1999 (in Japanese)

CHARACTERISTICS OF SELF-COMPACTING CONCRETE USING GROUND GRANULATED BLAST-FURNACE SLAG - APPLICATION AS CONCRETE IN A DEEP DIAPHRAGM WALL-

Tateki Kanno
Civil Engineering Design Dept.
Bureau of Sewerage
Tokyo Metropolitan Government
JAPAN

Kiichiro Kimishima
Civil Engineering Dept
Tokyo Office

Hideaki Taniguchi
Institute of Technology
and Development

Kotaro Mimura
Civil Engineering
Design Dept

Sumitomo Construction Co., Ltd
JAPAN

Key words: Diaphragm wall, self-compacting concrete, ground granulated blast furnace slag thermal stress analysis, cage subsidence measurement

1. INTRODUCTION

The Second Asakusa Pump Room Construction Project for the enhancement and renovation of the old facility of Mikawashima Sewer Treatment Plant is one of the biggest projects of the Tokyo Metropolitan Government Bureau of Sewerage. The scale of excavation is 57 m wide, 45 m long and digging soft silty ground for 45 m deep. In order to minimize the effect by excavation on the dense residential neighborhood and resist strong lateral pressures, a highly rigid diaphragm wall, with a thickness of 1.5 m and 70.8 m deep is adopted. Additionally, this diaphragm wall had to be extremely watertight, since it would also serve as a wall of the pumping station. The concrete under consideration was slump-controlled ordinary concrete, with a nominal strength of 40 N/mm^2.
However, due to concerns about imperfect filling in the dense reinforcement, blocking in tremie pipe, slime mixture with the concrete caused by incomplete rising of the slime, and thermal cracking in the concrete, it was concluded that the initially planned concrete for the diaphragm wall would be incapable of filling its intended role as a high water pressure resistant, watertight wall.

This paper reports on the characteristics, strength, and thermal stress analysis of self-compacting concrete made of ground granulated blast furnace slag, which was considered to be the most useful concrete for this diaphragm wall project due to its excellent capacity in self-filling densely reinforced forms. Also measurements of subsidence stress on the cage are described.

2. OVERVIEW OF THE DIAPHRAGM WALL

2.1 Structural specifications

- Wall thickness t = 1,500 mm, wall length L = 70.8 m, wall surface area = 14,200 m^2
- Materials used: Concrete with nominal strength of 40 N/mm^2; Reinforcing steel SD345

3.STUDY OF THE REPLACEMENT RATIO OF THE GROUND GRANULATED BLAST FURNACE SLAG

After a series of mixing tests (Fig.1) in which the ground granulated blast furnace slag (Blain value: 4,000) replacement ratio was set to 50, 60, and 70% of the powder content per unit of volume (450 kg/m^3) necessary for self-compaction, a replacement ratio of 60% was selected. (Table.1)

Table 1. Mix Proportion Table

Replacement Ratio	W/C (%)	s/a (%)	Unit Weight (kgn/m^3) Water	Cement	Blast Furnace Slag	Coarse Sand	Sand	Gravel	HRWR AE	Remark
50%	39	52	175	225	225	548	354	856	4.73	
60%	39	52	175	180	270	548	351	856	4.50	Adopted
70%	39	52	175	135	315	548	348	856	4.28	

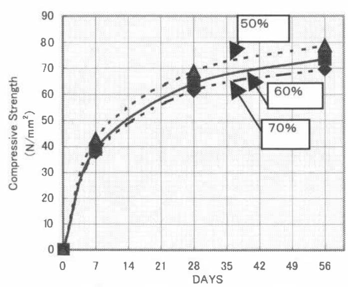

Fig.1 Compressive Strength

3.1 Properties of fresh concrete

The slump flow test results for all mix proportions satisfied 60 cm, ±5 cm (Fig.2)

The air content was 2.0%, ± 1.0%, and the u-shaped filling height was within 35 cm, ±5 cm. (The testing method used was a standard method proposed by The Japan Society of Civil Engineers.)

Fig.2 Slump Flow Measurement

4. THERMAL STRESS ANALYSIS

4.1 Thermal stress analysis results

Figure 3 shows the change of the thermal stress – tensile strength relationship over time. The tensile strength was computed by two equations: [1] "Standard Specification for concrete: Execution" (Japan Society of Civil Engineers)[3], and [2] "Design and Execution Guideline for Concrete of Ground granulated blast furnace slag (Draft)" (Japan Society of Civil Engineers)[4]. The diagonal lines in the figure represent the strength in Case 3 as the criterion for comparing tensile strength and stress. In every case, as illustrated in this figure, our tests confirmed that the stress on the 360th day of aging, when the stress was at its maximum value, was 5.2 N/mm^2 in Case 1, 4.7 N/mm^2 in Case 2, and 4.1 N/mm^2 in Case 3. In Case 3, the stress was about 20% lower than in Case 1. The stress was lower than the tensile strength only in Case 3.

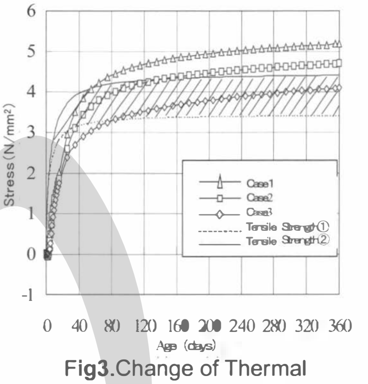

Fig3. Change of Thermal

5. MEASURING THE SUBSIDENCE STRESS OF THE CAGE

(1) Measurement results show that no uplift behavior occurred. Two reasons for these results are given below. (Fig 4)

- A reinforced frame, extending to the bottom edge of the diaphragm wall, acted as an anchor and resisted uplift.

- The low viscosity of self-compacting concrete containing a high percentage of ground granulated blast furnace slag inhibited the lifting of the cage.

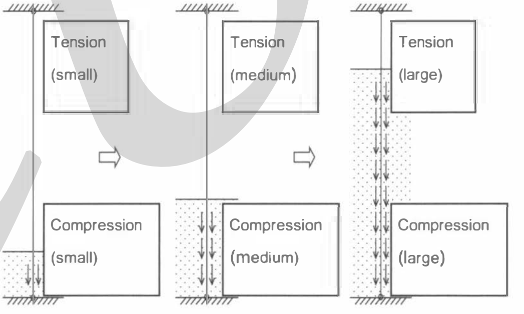

Fig.4 Subsidence stress of the cage

6. CONCLUSIONS

This method posed risks such as excessive strength manifestation and rising temperatures caused by hydration, which could result in thermal cracking. Such potential problems were considered unavoidable. But as this study shows, self-compacting concrete can also be made by separately adding ground granulated blast furnace slag at a ready mix concrete plant. This makes it possible to manufacture more cost-effective, self-compacting concrete for diaphragm walls, which not only achieves the required strength, but by adjusting the replacement rate, also resists the thermal cracking caused by the heat of hydration.

The use of ground granulated blast furnace slag can cut the quantity of carbon dioxide gas produced during sintering of the cement clinkers while lowering the production of carbon dioxide gas during the combustion of fuel necessary for sintering. Thus, this method sharply lowers the environmental impact in proportion to the replacement rate. (In this case, the production of carbon dioxide gas was cut by 45%.)

Session 4 | Practical application of concrete to marine structures

STANDARDIZATION OF THE PRESTRESSED-CONCRETE SHEET-PILE METHOD FOR PORTS

Shuichi Ohyanagi
ex) CDIT,Japan
pr) P.S.Co.Japan

Yusuke Sato
CDIT,Japan

Tsutomu Fukute
Ministry of Land,Infrastructure and transport ,Japan

Yosiaki Suzuki
PC Marine Structures ,Japan

Keywords : prestressed-concrete sheet pile, durability, calculation method, standard section

1 INTRODUCTION

Since prestressed-concrete sheet piles (PC sheet piles) were standardized in Japan under the Japan Industrial Standards (hereinafter referred to as "JIS") in 1965, the method has been improved in various ways, and has been used extensively in river revetment projects and the construction of earth retaining walls. However, the PC sheet-pile method has rarely been used (18 instances) in harbors in Japan, primarily because steel piles are stipulated by Japanese port work standards and there are no design and execution standards for the use of PC sheet piles in port structures.

Sheet piles used under the severe conditions that exist in port environments must provide high durability if exposed to seawater. The durability of PC sheet piles against seawater and their maintenance properties are superior to those of steel sheet piles, and it is believed that they can provide performance adequate for the severe conditions found in port environments.

The Coastal Development Institute of Technology has published the "Port-Use PC Sheet-Pile Technology Manual" to provide design and execution methods and to standardize PC sheet piles for use in port and harbor environments. This report introduces the Port-Use PC Sheet-Pile Technology Manual.

Fig.1 PC Sheet-pile

2 PRIMARY ISSUES IN STANDARDIZATION

The following is a list of challenges that must be overcome if PC sheet piles are to be used in ports:

- Application of the tensile-stress limit state
  The tensile-stress limit state is studied as the serviceability limit state because the standardized port-use PC sheet piles introduced in this report are intended primarily for use under the harsh conditions of port environments.
- Appropriate concrete covering thickness
  The standard concrete covering thickness for the port-use PC sheet piles was set at 5 cm.
- Stress resultant calculation method
  It describes a design method of counterfort-type and self-supporting PC Sheet Pile.
  In counterfort-type PC Sheet Pile, verification by Rowe's method to account for the effects of the sheet-pile section stiffness
- Section verification method
  The study of the stability of port-use PC sheet-pile material is conducted based on the limit-state design method. The serviceability limit state and ultimate limit state are also studied.
- Repair
  We describe methods of dealing with cracking and partial loss of the section area.

3 STANDARD SECTION

Based on the above results, a standard section shape for PC sheet piles to be used in ports and harbors was proposed. Fig.2 shows the standard port-use PC sheet-pile section form. The sheet-pile section is determined by calculating the bending moment generated in the sheet-pile wall, and the section and steel arrangement at which the acting maximum bending moment does not exceed the section strength may be selected from Table 1.

Table 1 Port-Use PC Sheet-Pile Standard Section Performance

	Symbol	Characteristic	Unit
compressive strengh	f'ck	70.0	MPa
compressive strengh:prestressing	f'ctk	35.0	MPa
compressive strengh:the serviceability limit state	σ'ca	31.5	MPa
modulus of elasticity	Ec	35000	MPa
creeping coefficient	ψ	3.0	
shrinkage strain	ε'cs	0.00025	

Prestressing steel

	Symbol	Characteristic				Unit
Grade		7wire strand				
Symbol		SWPR7B				
		T9.5	T11.1	T12.7	T15.2	
Sectional Area	Ap	54.84	74.19	98.71	138.7	mm^2
Ultimate Load	fpuk	1860				MPa
Yield point Load	fpyk	1570				MPa

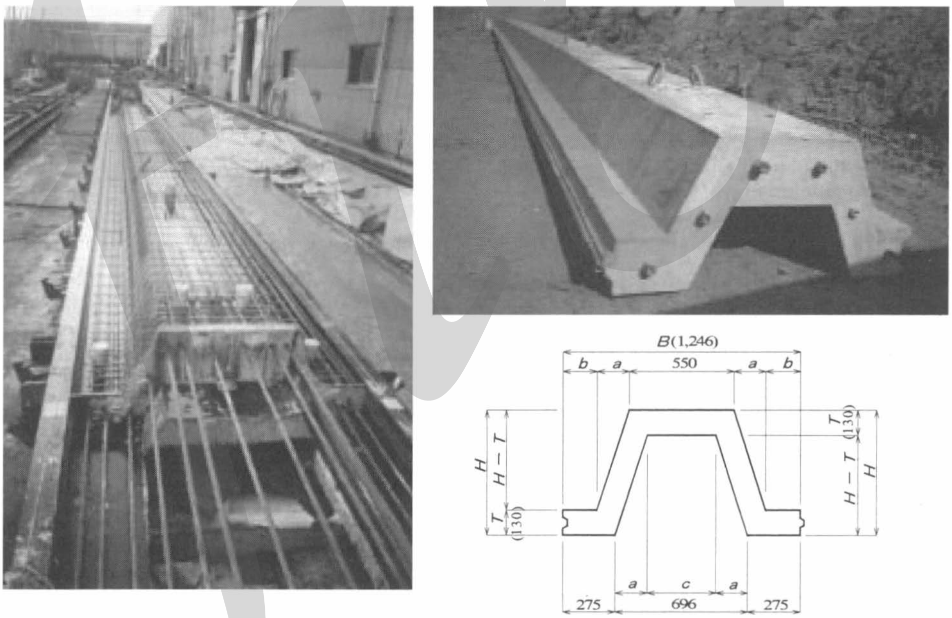

H:350～1200

Fig.2 Poat-Use PC Sheet-pile Section Form

REFERENCE

1) Coastal Development Institute of Technology, Port-Use PC Sheet-Pile Technology Manual/2000

PRESTRESSING OF THE MONACO DOCK LOT # 2

José Manuel Illescas Villa Juan José Santos Ureta
FCC CONSTRUCCION, S.A.
Spain

George Cassimatis
BBR Systems Ltd.
Switzerland

Keywords: Prestressing, durability, vacuum grouting.

1. SUMMARY

The principal requirements of the Condamine Port expansion project in Monaco are those pertaining to coastal morphology and environmental protection. An innovative construction technique has been applied to meet these unique requirements. One of the structural elements consists of a pre-constructed semi-floating dike, which will be attached at one of its extremities to a coastal abutment whilst the other will be cast anchor on the sea bottom.
For the enlargement project, a one-hundred-year lifetime requirement is specified for every structural element. Therefore, the most stringent regulations for offshore structures are being applied.
FCC CONSTRUCCION takes part in the consortium awarded for the semi-floating dike that is under construction at Campamento San Roque (Cádiz, Spain), and is working within a joint-venture company with BBR Systems for the prestressing operations on this project.

2. THE MONACO PORT EXTENSION PROJECT

In the preparatory design stage, special emphasis was placed not only on morphologic features, but also the lifetime of the structure in addition to providing a sheltered environment for the construction.
In order to ensure the best environmental protection, it was decided that the pre-construction of the main parts would be carried out at yards located in La Ciotat, Marsella and Campamento San Roque. The completed structure would then be abutted onto the pre-constructed in-situ foundation work at the Port of Monaco.
The civil works that comprise this construction project have been divided into two lots; one for the mobile caisson and the other for the fixed parts.

2.1 Lot # 1

This lot was executed by an international consortium which built the fixed parts of the work, which included an embankment, the abutment of the semi-floating dike and a counter dike.

2.2 Lot # 2

The semi-floating dike is being constructed by an Spanish, French and Monegasque consortium in which FCC CONSTRUCCION is a partner.

3. THE SEMIFLOATING DIKE:

The dike is 352m long, 44m wide at its base, 28m at the main body, and a 19m high (not including the superstructure) prestressed concrete structure.
It is basically made up of 3 horizontal slabs, 4 longitudinal walls and 45 cross-sectional walls, 10 of which extend through the section and the reminder keeps the central space clear.

4. BBR PRESTRESSING SYSTEM

A joint-venture of FCC CONSTRUCCION and BBR Systems is in charge of the prestressing of the semi-floating dike, using BBR CONA Compact M1 Type anchorages for cables with 7, 12, 19, 22 and 31 strands 0.6".
More than 3,000t of prestressing steel for tendons and 150t for prestressing bars Ø 50mm have been used.

4.1 Cable installation

In order to achieve maximum durability, 2mm thick steel pipe instead of corrugated sheath of steel are being used.
Plug-in connections using thermo-shrinking sleeves to ensure watertightness are being used in the different joints between pipe or between a pipe and the anchorage polyethylene trumpet.
The lengths of the cables range between 274m and 8m. The vertical prestressing is carried out by 17m high, 44m stretch out loops.

The threading of the cables is being carried out strand by strand.
For special cases, pneumatic winches have been provided for threading complete pre-cut cables.

4.2 Stressing

Before stressing each group of tendons, a friction test is conducted in order to accurately determine the theoretical elongation. This enables to monitor with great accuracy the forces applied on the inner sections of the structure by means of the actual elongation achieved by the stressing process.
Owing to the difficult approach conditions to the internal anchorages of the watertight cells, formed in the dike perimeter, some special tools and equipment for handling the stressing jacks have been designed and adapted to the special work conditions.

4.3 Grouting

To ensure the specified lifetime, grouting is considered to be the most significant work of the prestressing. Therefore, it has been opted to grout tendons and bars with the vacuum grouting technique. This ensures that the pipes are completely grouted and allows the vertical loops to be injected from the upper end without the risk of causing air locks in the anchorage sections.
In spite of the fact that the chosen formula does not show any water or air remount on the vertical pipes, some grout inlets have been allowed for to allow regrouting as the need arises. The cement grout, which the cross tendons and vertical loops are injected with, is produced by compact equipment consisting of a 400 litre-capacity high turbulence mixer, a 800 litre grout agitator and a grouting pump assembled on a portable chassis. Alternatively, special equipment made up of two high-turbulence mixers, like the one built in the compact equipment, a 1200 litre cement grouting agitator tank and a peristaltic pump that makes the grouting is also available.
This equipment allows grouting of the biggest tendon of the work (274m long, 135mm diameter) in nearly one hour from the time the cement pumping process commences.

4.4 Prestressing work completion schedule

The completion of the prestressing work is scheduled for 15 months since the beginning of the supply, while the threading, stressing and grouting of 80% of the PT steel takes three months.

5. WORK FILE OF THE MONACO DOCK LOT # 2

Owner...............PRINCIPAUTE DE MONACO, SERVICE DES TRAVAUX PUBLICS.
Contractor ....BEC – FCC CONSTRUCCION – DRAGADOS – HT – SMMT consortium
Engineering......DORIS ENGINEERING
Prestressing .....Joint venture FCC CONSTRUCCION – BBR Systems

MECHANICAL BEHAVIOR OF RC MEMBERS SUBJECTED TO REPEATED IMPULSIVE FORCES DUE TO WAVES

Hiroshi Yokota   Shigeo Takahashi
Port and Airport Research Institute, JAPAN

Masao Yamada
Kyushu Regional Development Bureau, MLIT, JAPAN

Muneo Tsuda
Toa Corporation, JAPAN

Keywords: repeated impulsive force, reinforced concrete, fatigue, dynamic strength magnification

1 INTRODUCTION

Repeated impulsive forces due to waves often apply to marine structural members during storms, which may bring catastrophic effects. The wave breaking impulsive force is characterized that it applies to structures many times and each impulse lasts for only about 60ms.

Two experimental tests were undertaken in this study. At first, hydraulic experiments were carried out in an experimental wave flume where waves were repeatedly applied to reinforced concrete beams. During the test, the dynamic response of the beams was examined subjected to one impulse. Moreover, the mechanical behaviors of reinforced concrete beams subjected to repeated impulsive forces were discussed and the process to the ultimate stage was made clear. Then, as a subsequent test, loading tests were carried out on small sized reinforced concrete beams subjected to repeated impulsive loads simulated by actuator with controlled frequency and amplitude that obtained by the precedent experiments. The dynamic strength magnification was investigated and the effect of loading frequency was discussed. Also the mechanism of low cycle fatigue failure was examined.

2 RESPONSE OF RC BEAMS UNDER WAVE BREAKING IMPULSIVE FORCES

2.1 Descriptions of hydraulic experiment

The tested beam for the hydraulic experiment was horizontally supported just in front of a reflection wall with the clearance of 0 or 300mm from the still water surface. Regular standing waves were generated with varied heights and periods. The view of the test is shown in Fig.1. At first, reinforced concrete beams with 100mm, 200mm or 300mm thick, 400mm wide, and 2400mm in span length were tested for measuring the wave force resultant and dynamic response under wave breaking impulsive forces. Then, reinforced concrete beams with 50 or 80mm thick, 1000mm wide, and 2400mm in span length were tested to entire collapse to understand the process of failure.

2.2 Experimental test results

The duration of impulsive force applied was about 34ms. Wave pressure measured ranged from 19 to 26kPa when the Bagnold type [1] impulsive force was observed. The response acceleration was more than 10m/s^2 with the period of about 25ms. In case that the Wagner type [1] impulsive force was recognized, the peak of the wave pressure reached 97kPa and its duration was only 3ms.

The process of failure of tested beams was examined by applying repeated waves with increasing height from 100 to 600mm; the total number of waves was about 2000. At first, a crack was initiated at the fixed end of the beam, and then three cracks occurred at the other end and the midspan. Under further application of waves, concrete was crushed at the both ends of the beam to reach the ultimate state. Action by waves formed plastic hinges at the both ends and plenty of cracks and falling of concrete were observed. Finally, concrete was totally removed at some parts, as shown in Fig. 2, and rebars were broken. Before initiating a first crack, induced strains in concrete were rather small even if large impulsive forces were applied. However, once cracks formed, local failure was rapidly spreading, resulting in entire collapse by repeated waves as roughly equivalent to those during only one storm. Rebars were broken in the repeated impulsive loading test, but not broken in the static loading test. It

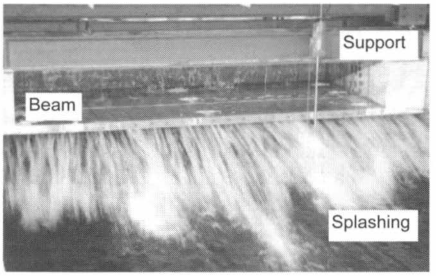

Fig.1 Impulsive force application

Fig.2 Appearance of a beam after the test

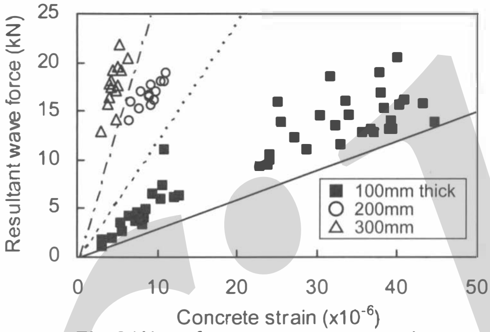

Fig.3 Wave force vs concrete strain

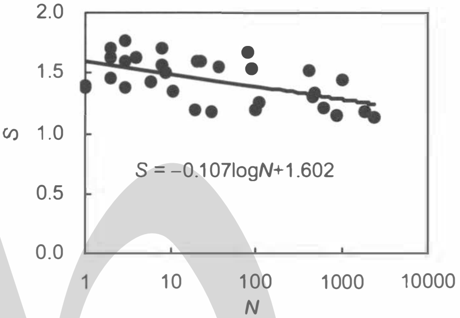

Fig.4 *S-N* relationship

seemed that the test beam has high ductility after rebar yields but can easily be broken due to repeated impulsive forces. Figure 3 shows the relationship between resultant wave forces and concrete strain of the tested beams of 100, 200, or 300mm thick. The lines drawn in this figure are the results of static loading tests, which were almost 30% larger than the dynamic loading tests.

3 FAILURE OF RC BEAMS DUE TO REPEATED IMPULSIVE FORCES

3.1 Test description

Reinforced concrete beams having a 100mm by 100mm square cross section and 400mm in length were tested. The beam was reinforced by a deformed rebar with the nominal diameters of 10mm or 13mm. A repeated impulsive bending load was applied by using a servo-controlled testing machine. Four-point load was applied with each loading span of 100mm. The frequency of loading was parametrically changed as 1Hz, 5Hz, 10Hz, and 20Hz. The time interval of each repetition of impulse was 15 seconds, which is almost the same period of natural waves.

3.2 Results of dynamic cyclic loading test

It was found that dynamic strength magnification [2] slightly increased or kept almost constant with increase in the loading frequency. The average value of dynamic strength magnification ranged from 1.28 to 2.14. Figure 4 shows the *S-N* relationship, where *S* and *N* refer to the ratio of the average load obtained from dynamic cyclic loading test to the maximum load during static test and the ultimate cycle, respectively. It was found that *S-N* relationship for this dynamic test was almost linear. The equation to express the *S-N* relationship was proposed in the figure.

REFERENCES

[1] Takahashi, S., Tsuda, M., Shimosako, K., Yokota, H. and Kiyomiya, O.: Numerical Calculations on Dynamic Response of Caisson Wall due to Impulsive Breaking Wave. Proc. Coastal Engineering, JSCE, Vol.45, pp.751-755, 1998 (in Japanese)

[2] Takahashi, S., Tsuda, M., Yokota, H., Takano, T. and Kiyomiya, O.: Experimental Study on RC-Plate Failure due to Impulsive Wave Pressure. Proc. Coastal Engineering, JSCE, Vol.46, pp.811-815, 1999 (in Japanese)

CONSTRUCTION OF NEW-TYPE PIER USING JACKET THAT COMPOSED OF SUPERSTRUCTURE AND SUBSTRUCTURE

Shozo Kawasaki Hiroshi Maruyama Hirofumi Yokoyama Akinori Nishisako Takashi Habuchi
Electric Power Development Company Toa / Nippon Steel JV Toa Corporation
Japan Japan Japan

Keywords: jacket type pier, self-compacting concrete, middle fluidity concrete, anti-washout concrete

1 INTRODUCTION

On the Pacific coast of Japan, an unloading pier of 385m in length has been constructed for a coal-fired thermal power plant. A new type of structure, its foundation-type with belonging to the spread foundations, was adopted for this pier in which steel jackets with a superstructure and substructure were attached the steel works, and were then installed at the construction site. This new-type structure is intended to reduce the cost and time required for construction by reducing the amount of fieldwork required, provided that the site is on the ocean and the foundation is firm.

In this paper, the following three characteristic types of concrete, which have made it possible to adopt this new type of structure, are described.

2 OUTLINE OF JACKET-TYPE PIER

The pier is a coal-unloading pier for a coal-fired thermal power plant currently under construction on the Pacific coast of Japan. It is an open type pier with a total length of 385m. In the construction of this pier, a jacket structure was adopted in which the principal structural members are prefabricated at the steelwork and then installed at the construction site, to ensure high quality, low cost, and a reduced construction period. Moreover, the spread foundation type was adopted in which the jacket legs are installed directly on the foundation (seabed surface), as it had been confirmed at the construction site that the bearing ground was existed along the entire length of the planned pier. The pier is composed of twelve jackets, each measuring approximately 32m in length and 25-33m in width. **Fig.1** indicates the flowchart of construction, and a typical section of this pier is shown in **Fig.2**.

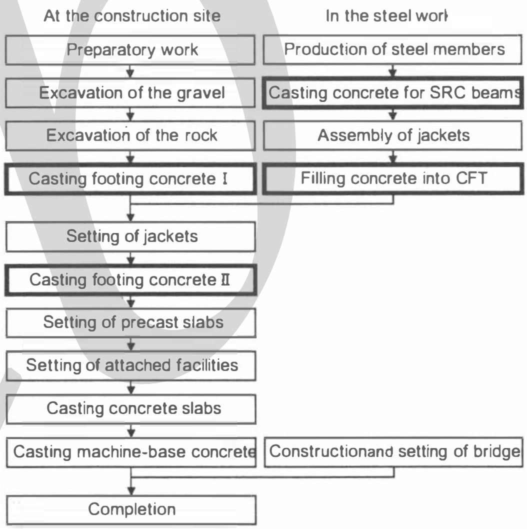

Fig.1 Flowchart of construction

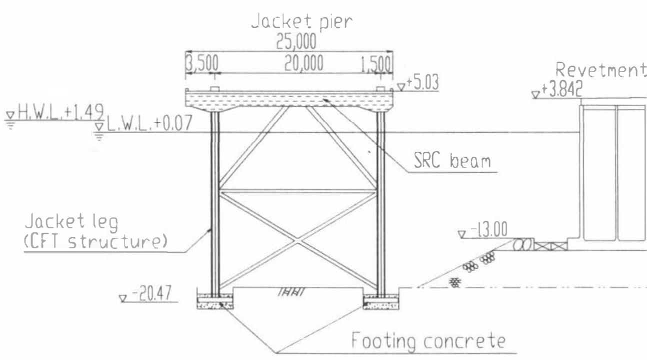

Fig.2 Typical cross section of pier

To take full advantage of the superior characteristics of this structural type, the jacket leg was designed with a concrete-filled steel-tubular composite structure (CFT structure) for the purpose of stabilizing against the external force by increasing jacket's weight and heightening the strength, the rigidity and the toughness of legs. The beam of superstructure was built into an SRC structure, the

Table 1 Mix proportions of three types of concrete

Type of Concrete	Specified strength	G_{max}	Slump flow	Air content	W/C (%)	S/a (%)	Unit weight (kg/m^3)					
							W	C	S	G	SP*	Ad.
Middle Fluidity Concrete	30N/mm^2	25mm	35-50 cm	3-6%	40.0	52.5	160	400	905	832	3.80	----
Self-Compacting Concrete	40N/mm^2	25mm	50-60 cm	3-6%	35.9	50.6	163	453	853	832	5.71	6.8** (g/m^3)
Anti-Washout Concrete	30N/mm^2	25mm	52-58 cm	0-5%	40.0	47.2	233	494	588	913	2.80	2.5***

* Superplasticizer, ** AE water reducing agent, *** Viscous agent

span length of this pier could be made longer than that of an ordinary RC pier. In addition, the footing concrete placed at water depth of over 20m in the ocean was necessitated in order to achieve the required height accuracy for installation of the jacket legs and the enough strength as foundations.

3 SPECIAL CONCRETE APPLIED TO THE JACKET-TYPE PIER

The following three types of special concrete are applied to this new-type jacket pier. The mix proportions of these three types of concrete used in the execution are shown in **Table 1**.

The first type is middle fluidity concrete, which has a slump flow of 35-50cm for long-span SRC beams with a large cross section, densely arranged rebars and little space to compact when the concrete is placed. This concrete can be compacted well through the application of slight vibration and enables the reliable and high-quality construction of large-section SRC beams with densely arranged rebars. These were ascertained through the experiment on full-scale model.

The second is self-compacting concrete, with a slump flow of 50-60cm. This concrete can be filled securely into steel-pipe jacket legs designed with CFT structure, with good workability, excellent resultant quality, and reliable filling free from the production of excessive residual stress. These were measured through the execution.

The third type is anti-washout concrete, which has a slump flow of 52-58cm in water over 20m in depth. This concrete is used as the footing for the jacket leg's setting foundation. The concrete used exhibits enough strength, and enables a sufficient height accuracy and flatness for the structure foundation to be secured. These were confirmed through the execution.

The jacket pier when installed and completed construction is shown in **Photo 1** and **Photo 2**.

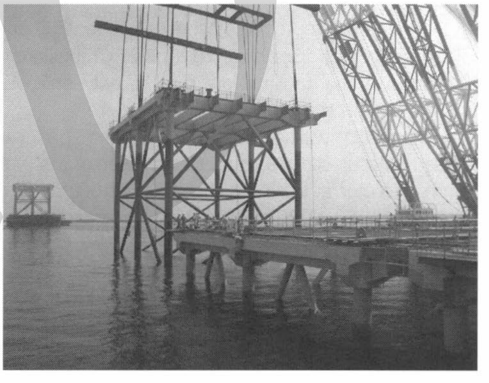

Photo 1 Installation of a jacket

Photo 2 Completion of construction

4 CONCLUSIONS

The authors describe three types of special concrete used in the construction of an unparalleled spread-foundation-type jacket pier. The conclusions are as follows:

The special concrete reported above are used, it is possible to adopt a new structural method that consists of fabricating jackets with an integrated superstructure and substructure at a steel work and installing them at the construction site, provided that the site conditions include a firm foundation of seabed. Moreover, they have been clarified that these characteristic types of concrete can contribute to the development of new types of marine structures.

EFFECT OF SHEAR REINFORCEMENT IN FOOTINGS OF CAISSONS FOR MARINE STRUCTURES

Masao Yamada Hiroshi Yokota
Port and Airport Research Institute, JAPAN

Keywords: deep beam, cantilever, shear capacity, distributed load

1 INTRODUCTION

Concrete caissons are widely used for marine structures such as breakwaters or wharves. Caissons are settled on a rubble mound and filled inside with sand. They resist external forces by their weight. In some design conditions, overturning of caissons or failure of mound is critical. In such cases caissons with footings as shown in Fig.1 are advantageous. The thickness of the footing is about 1m and the extension length of the footing used to be about 1.5m, but recently 5 to 6m long footings of steel-concrete hybrid structures are utilized.

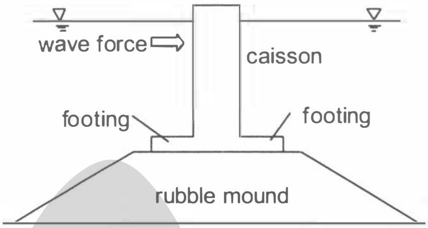

Fig.1 Breakwater caisson with footings

The footings are cantilever panels subjected to distributed load. There is not sufficient data on shear capacities of cantilevers subjected to distributed loads. Thus in this study distributed loading tests of cantilevers were carried out. Effective depth, amount and type of shear reinforcement, and structural type of cantilevers were varied as test parameters.

2 EXPERIMENTS

Six HB, which represents hybrid, eighteen RC and four PC cantilevers were tested. All the cantilevers were 0.25m wide and 1.5m long. The basic dimensions of the cantilevers were given to be about a half of 3m long footings. Actual footings are panels, but cantilever beams were used in this study neglecting the effect of secondary moment.

One of each series of cantilever had no shear reinforcement. Another one of each series of cantilever had closed vertical stirrups of 6mm diameter at the interval of 125mm. Other RC cantilevers had the stirrups of 6mm diameter at the interval of 150 or 100mm, or bent-up bars of 10mm diameter, which were bent up at the interval of 450 or 300mm at 45 degrees to the beam axis to join top bars.

HB cantilevers had 8mm thick steel plates at the bottom as main steel. RC and PC cantilevers had four steel bars of 25mm diameter as main steel. Target effective prestress at the bottom surface of PC cantilevers was 3.92N/mm^2.

Fig.2 shows the overview of the loading test. The loads by two hydraulic jacks were distributed with steel blocks and joints uniformly on the bottom surface of the cantilever. Loads were applied statically and monotonically up to the maximum loads of the cantilevers.

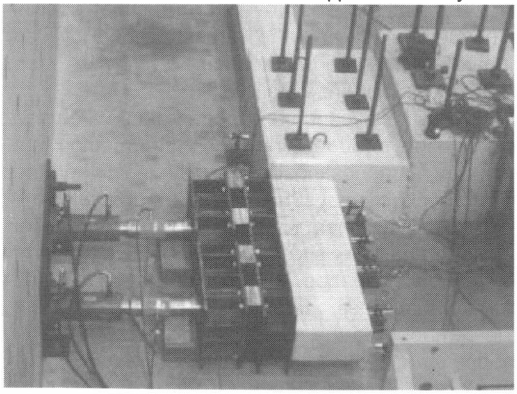

Fig.2 Overview of loading set-up

3 ANALYSIS

3.1 Calculation of flexural and shear capacities

According to ordinary beam theory, ultimate flexural moments of the root cross sections were calculated. Shear capacities were calculated according to JSCE code [1].

3.2 FEM analysis

WCOMD (ver.1.00.06), which is two dimensional nonlinear FEM program for RC structures developed by Okamura et al. [2], was used for FEM analysis .

4 RESULTS AND DISCUSSION

Cracks extended to the top surface of cantilevers at the fixed end and concrete crushed in compression at the ultimate stage of loading test. The test and analysis results of crack pattern were similar as to the region where crack occurred. The measured strain of shear reinforcement was almost zero outside the cracking region. Thus only shear reinforcement crossing cracks was considered to be effective. Such simulation of crack pattern is useful to arrange shear reinforcement effectively.

The average and the standard deviation of the ratios of the measured capacities to the calculated capacities by theory were 1.63 and 0.30 respectively, while those to the calculated capacities by FEM were 1.18 and 0.23 respectively. Thus FEM predicted capacities better.

Effect of shear reinforcement was defined as the ratio of the difference between the capacities of a cantilever with and without shear reinforcement to the capacity without shear reinforcement. As shown in Fig.3 the tests results of HB and RC cantilevers show the peak of the effect at around 3.7 of L/d, where L : length of cantilever and d : effective depth. In the test results of L/d=3, the effect was smaller than expected by analyses, especially for RC almost no effect was obtained, because arch action was dominant load bearing mechanism in the ultimate state of cantilevers of L/d=3.

In the test results of L/d=5, the effect was the same as or smaller than expected by analyses. The effect in L/d=5 was smaller than in L/d=3.7, because the effect of flexure to the capacity became large as a cantilever became slender.

As to PC cantilevers, the tendency was different from as to HB and RC. In the test results of L/d=3.9 there was no effect, but in the test results of L/d=5.2 shear reinforcement seemed effective.

Besides the bent-up bars had the effect as well as stirrups, which implies it is not essential to close stirrups to restrain concrete in order to make effective shear reinforcement.

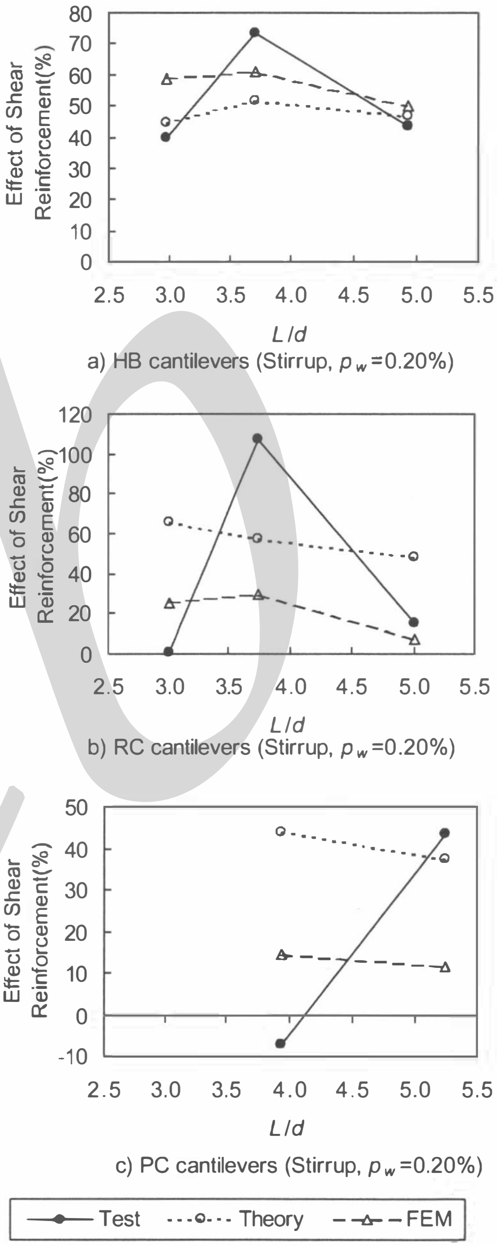

Fig.3 Effect of shear reinforcement

5 CONCLUSIONS

FEM analysis could predict the capacities of the tested cantilevers better than the calculation by beam theory and equations. The simulation of crack pattern is expected to be useful to arrange shear reinforcement effectively. As to HB and RC cantilevers, tests results show the peak of the effect of shear reinforcement at around 3.7 of L/d. In the test results of L/d=3, the effect was smaller than expected by analyses. In the test results of L/d=5, the effect was the same as or smaller than expected by analyses. As to PC cantilevers, the tendency was different from as to HB and RC.

REFERENCES

[1] JSCE : Standard specifications for concrete structures, 1996 (in Japanese)

[2] Okamura H. and Maekawa K. : Nonlinear analysis and constitutive models of reinforced concrete, Gihodo-Shuppan Co. Tokyo, 1991

DESIGN OF DURABLE PRESTRESSED REINFORCED CONCRETE BEAMS FOR AN EXTENDED UNLOADING PIER IN INDIA

Luc Maertens
Engineering Manager
BESIX
Brussels, Belgium

Manfred Zinserling
Engineering Review Consultant
BERGER/ABAM Engineers Inc.
Federal Way, WA, USA

Dominic Izzo
Manager of Projects
Dabhol LNG Terminal
Houston, TX, USA

Keywords: precast concrete, slag cement, durability, quality control

1 INTRODUCTION

The Dabhol Power Company (DPC) is constructing India's first Liquefied Natural Gas (LNG) terminal on a remote strip of India's western coast along the Arabian Sea about 160 kilometers south of Mumbai (Bombay). Designed to handle the world's largest LNG carriers, the terminal's marine facilities include a pile-supported trestle that extends 1,620 meters into the open sea to reach adequate depth and an LNG unloading dock. The project site is not only fully exposed to incoming waves from the open sea, but also subject to earthquake loads from a peak ground acceleration of 0.16 g. Driven by a short schedule, the difficulty of mobilizing major equipment to this region, and the hostile marine environment, DPC determined to use a reinforced concrete superstructure supported by steel piles. The 29.1-meter-long prestressed concrete beams had to be manufactured primarily from local materials, on site, yet meet stringent quality standards and a 40-year design life. During the early phases of the project, a significant design discussion ensued as to whether the beams would be more suitable designed with 75 mm of cover over mild reinforcing steel or with 50 mm of cover and a "no crack" criteria. The solution finally selected included use of ground granulated blast-furnace slag (ggbs) cement, pretensioning, and elevated temperature curing. This paper discusses the various alternatives considered during the design process, as well as the final selection. It concludes with recommendations for future code development, as well as for design and project planning in difficult environments.

2 DURABILITY AND CONCRETE COVER

The contract specifications called for 75-mm cover for all concrete structures and made no distinction was made between plain reinforced and prestressed elements. The prestressed beams consisted of 250-mm-thick webs. From a structural point of view, excessive cover to the mild steel stirrups would reduce the sections resistance to torsional loads. As a result, the Contractor recommended using 50-mm cover for the precast, prestressed beams only with the following factors as further justification.

- The beams are located well above the maximum seawater level, in the less critical conditions of the zone exposed to sea spray. The beams would not be subjected to the more severe environmental conditions of the splash zone, even under the wave conditions of the 100-year design storm.

- The beams will be fabricated in a casting yard under controlled conditions and with special curing measures in place.

- Both the Contractor and DPC would employ additional, experienced quality control personnel to ensure that standards were met.

The approach way design life was 40 years and it was essential to demonstrate that the reduction in cover from 75 to 50 mm would in no way result in a structure with reduced durability. Following extensive discussions with DPC, the Contractor commissioned the services of the University of Leuven (Belgium) to perform computational analyses to establish the anticipated rate of penetration of chlorides into concrete for various design mixes. It was assumed that the initial chloride concentration in the concrete after casting was C_O = 0.1% Cl^- /cement (by mass). The chloride concentration at the concrete surface, from environmental conditions, was assumed to be 3.0% Cl^- /H_2O (by mass). A minimum cementitious content 500-kg per cubic meter and a maximum w/cm ratio of 0.50 were assumed for the concrete. The various mixes were then compared to the allowable chloride threshold limit; C_T = 0.2% Cl^- /cement (by mass) for prestressed tendons, and C_T = 0.4% Cl^- /cement (by mass) for the mild reinforcing steel as specified in European Standard ENV 206 (1992)[1]. Two types of cements were investigated; ordinary Portland cement (OPC) and granulated blast furnace slag (ggbs) cement which were both acceptable according to the contract specifications. The chloride ingress (during the design life) depends on the Diffusion Coefficient μ(D) of the concrete. For OPC-cement concrete, μ(D) = 29.6 x 10^{-9} cm²/sec and for ggbs-cement concrete, μ(D) = 1.2 x 10^{-9} cm²/sec were used. The main difference between the two cement types is the permeability of the resulting concrete matrix.

The probability that corrosion will occur at the level of the reinforcing steel or the level of the prestressing steel (tendon) as a function of the concrete cover was investigated. The reinforcing steel has a cover of 50 mm, and the prestressing steel a cover of 64 mm. Table 1 gives the resultant probabilities of failure for both 50/64-mm cover and for 75/89-mm cover, as originally specified.

Table 1 Corrosion Probabilities (P_f) for ggbs and OPC Cement Concretes

Cover	Reinforcing Steel		Prestressing Steel	
	ggbs	OPC	ggbs	OPC
50 mm/64 mm	10^{-18}	$>10^{-2}$	10^{-7}	$>10^{-1}$
75 mm/89 mm	$<10^{-22}$	10^{-3}	10^{-9}	$>10^{-1}$

According to Eurocode 1 (EC1, 10/1994), the probability for failure shall be $<10^{-4}$ when ultimate limit state (ULS) is considered, and $<10^{-2}$ when serviceability limit state (SLS) is considered. Mostly, corrosion is considered as SLS. DPC and the Contractor concluded that the corrosion risk was too high with OPC cement but in the case of ggbs cement, a cover of 50 mm over the mild reinforcing steel is sufficient.

3 PROPOSED SOLUTION

After the above investigation revealed the much higher risk of corrosion damage to prestressing tendons compared to mild steel reinforcement, DPC and the Contractor decided to use ggbs cement with the proposed 50-mm cover. They took this decision although ggbs is not commonly used to fabricate precast, prestressed beams mainly because ggbs cement reduces the heat of hydration, which results in a lower rate of increase in concrete strength versus time. The rate of precast fabrication typically relies on early concrete strength so that the prestressing force can be transferred into the concrete beams. The Contractor used heated formwork to speed up the development of early concrete strength and offset the lower rate of strength gain in ggbs cement concrete.

4 CONCLUSIONS

The use of ggbs cement in a highly controlled manufacturing process on site led to improved durability and strength for the prestressed beams. Excellent quality control and supervision ensured that the beams met the high design standards required for a minimum 40-year design life. With a state-of-the-art batch plant and precast yard, the beams were produced in time to support the construction schedule. In retrospect, the decision to change to ggbs (slag) cement could have been made earlier to facilitate the development of the production infrastructure.

Design codes for marine structures should encourage the use of ggbs (slag) cement and incorporate a requirement to evaluate all concrete mix designs for chloride penetration. Research and testing in this project has demonstrated that increased concrete cover is not the best solution to increase durability and design life. Plant cast, prestressed concrete elements should be considered for all marine structures.

REPAIR WORK FOR CONCRETE SUPERSTRUCTURE OF PIER CARRIED OUT ON LARGE-SCALE CONTAINER TERMINAL REDEVELOPMENT PROJECT

Yukio Okudaira Hideo Kawada Akira Hagino Yoshitaka Matsumuro Takashi Habuchi
Tokyo Port Terminal Public Corporation DRAM Engineering Toa Corporation
JAPAN JAPAN JAPAN

Keywords: repair work, salt attack, life cycle cost, superstructure of pier

1 INTRODUCTION

At a large-scale container terminal named Ohi Wharf with a total length of 2,300m in the Port of Tokyo, a redevelopment project was initiated in 1996 that would refurbish the terminal constructed in the 1970s. The goal of this project is to transform existing terminal facilities into a large-scale, efficient, and high-quality international container terminal that can meet the needs of the 21st century, while utilizing existing facilities. Because of these plans, it is very important to continue careful maintenance of the functions of the existing pier. However, the existing superstructure has exposed in severe marine environments for many years, so it has sustained some deterioration due to salt attack. Therefore, this project required large-scale repairs in order to ensure that this terminal will be able to be used long.

This container terminal is composed of open-type piers supported by pile and consists of eight berths. The current redevelopment project plans to construct a new pier in front of the one built in 1970s, thus increasing the depth of the front of berths to 15m. The project will also provide seven berths with larger lengths than the existing ones. **Fig.1** shows a typical section view of this pier.

In the following study, we outline this redevelopment project, describe the repair strategy for the superstructure of the existing pier, and explain the repair work practically applied. This strategy has the aim of increasing the effect of repair work and minimizing the life-cycle cost.

2 REPAIR DESIGN AND REPAIR WORK FOR EXISTING PIER

In laying out the repair plan, it was decided to select measures that would meet the following two performance requirements [1]: (1) Members not presently deteriorated must remain free from deterioration in the future, regardless of whether or not the members are repaired under the plan. (2) When members already deteriorated are repaired, they must not deteriorate again after repair.

To achieve the performance requirements, repair methods were chosen according the flow chart shown in **Fig.2** and selection way represented in **Table 1**. The examination and quantitative evaluation of chloride in concrete are applied for each group divided by the careful consideration of the present state of deterioration and location, because the chloride supply for concrete is largely dependent on the height above the sea surface, distance from the berthing side, and other environmental conditions [2]. And, the surface chloride concentration C_0 and apparent diffusion coefficient D for the repair design are arranged for safety evaluation by probability. The deterioration survey was carried out in 1991, and the

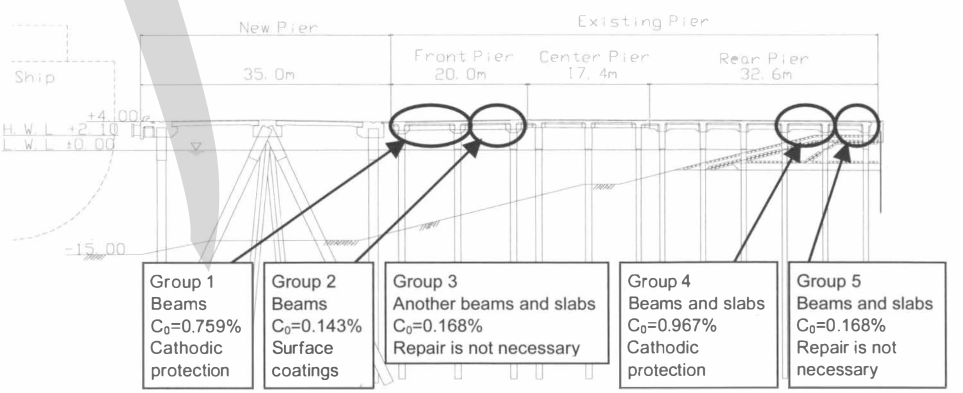

Fig.1 Typical section of the pier, divided environmental Group and selected repair methods in one berth

repair plan for all eight berths was drafted based on the survey's results [3]. Also, when the repair design for each berth was in the planning stage, a deterioration survey was again conducted on each. The section recovery using permanent forms and cathodic protection with embedded anode system are newly developed repair systems that have been adopted with the aim of reducing life-cycle cost.

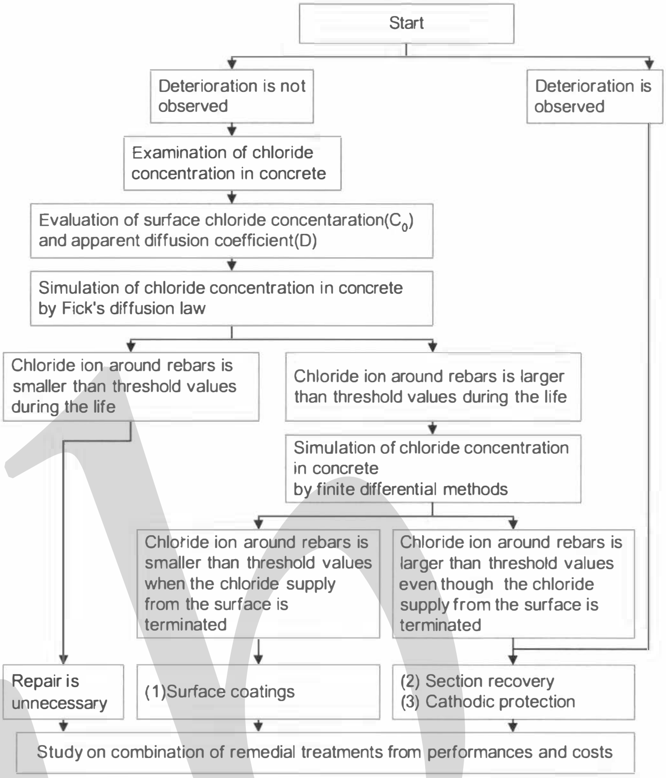

Fig.2 Flow chart of the selection of repair methods

Table 1 Selection of section recovery and cathodic protection

Loose cover and/or spooling area (Versus total area of member)	Location of members	Section Recovery: Normal type	Section Recovery: Permanent -form type	Cathodic protection: Normal type	Cathodic protection: Embedded*
Less than about 80%	Receive direct actions of waves	●	▲	▲	■
	In dry conditions	▲	▲	■	▲
More than about 80%	Receive direct actions of waves	▲	■	●	▲
	In dry conditions	■	▲	▲	▲

* Embedded anode system, ■ Recommended, ▲ Possible, ● Applicable with care

3 CONCLUSIONS

The conclusions are follows:

1) We should choose repair methods that will be highly effective in minimization of the life cycle cost, for a large-scale superstructure of pier. These can be chosen by dividing the members into appropriate groups, and then evaluating durability based on chloride diffusion in concrete.
2) The saline environment of pier varies depending on the plane metric positions and height above the sea surface, and can be evaluated using surface chloride concentrations.
3) By the simulation of chloride diffusion, it is possible to evaluate the necessity of repairs and the effect of surface coatings.
4) It is important to take safe values for the typical values of each group in performing durability evaluations, to ensure that large-scale deterioration will not occur again after repairs.
5) When section recovery and/or cathodic protection are applied, adoption of permanent forms and/or the embedded anode system has possibilities of increasing durability and reducing life-cycle cost.

REFERENCES

[1] Manual for the Survey and the Repair of Deteriorated Jetties in Ohi Wharf, Tokyo Port Terminal Public Corporation, 2000.3 (in Japanese)

[2] Habuchi, T., Muramatsu, M. and Moriwake, A.: Evaluation on Saline Environment of Concrete Jetty using Surface Chloride Concentration, Third International Conference on Concrete Under Severe Conditions, volume one, pp.214-221, 2001.6

[3] Fukute, T., Moriwake, A., Seki, H. and Kawada, H.: Repair Work Strategy for Concrete Jetties Deteriorated by Salt Attack, Second International RIREM Conference, pp.279-290, 1998.9

APPLICATION OF CATHODIC PROTECTION AGAINST CHLORIDE INDUCED DETERIORATION TO A JETTY DAMAGED BY THE GREAT HANSHIN EARTHQUAKE

Hideto Yasui
Konan Futo Co., LTD, JAPAN

Atsuro Moriwake Kazuo Shimokawa
Toa Corporation, JAPAN

Keywords: cathodic protection, steel plate bonding, chloride, earthquake, jetty.

1. INTRODUCTION

Various concrete structures in the Hanshin districts suffered serious damage after the Great Hanshin earthquake in 1995. The jetty investigated here was seriously damaged as it carried heavy facilities above the structure. After the earthquake, an investigation revealed damage such as large bending and shear cracks on beams as well as vertical and horizontal cracks on pile caps. Also the jetty suffered from chloride-induced deterioration even where a surface coating had been applied. The retrofitting was undertaken immediately after the earthquake to allow the facility to resume functioning.

Retrofitting and/or remedial measures were performed in two stages. In the first stage, members damaged by the earthquake were restored to enable mechanical functioning with a focus on urgently resuming full utilization of the facility. Remedial measures against chloride-induced deterioration were taken in the second stage, which was performed several years after the earthquake. This paper introduces the combination of remedial measures against serious mechanical damage and deterioration induced by chloride.

2. DAMAGE DUE TO THE EARTHQUAKE AND RETROFITTING

2.1 Outline of damage due to the earthquake

When the earthquake hit the Hanshin district the jetty was 25 years old, constructed in1970. The damages by the earthquake were observed in the pile caps in the form of wide cracks in the horizontal and vertical direction as shown in Fig.1. On the beams, wide bending cracks were observed at the center and serious shear cracks were observed at both ends.

2.2 Retrofitting

Immediately after the earthquake, retrofitting work commenced to resume the utilization of the jetty.

As for the wide shear cracks observed on the beams, the steel plates of 6 mm in thickness coated with anticorrosive paint were bonded to the concrete surface with epoxy resin paste. Bending cracks were restored with CFRP bonding at the bottom of the beams. These measures were finished as shown in Fig. 2.

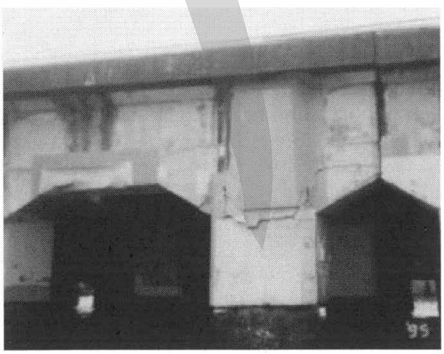

Fig. 1 Cracks observed on pile caps

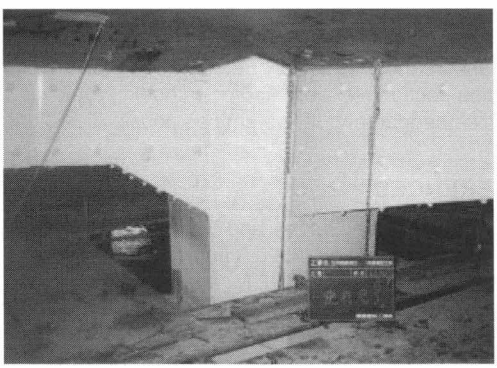

Fig.2 Completion of retrofitting at pile cap and beams

3. COMBINATION OF CATHODIC PROTECTION AND REINFOCING MEASURES

For the beams, which were damaged by the earthquake and reinforced by steel plate or CFRP bonding, the cathodic protection using insert type anode was applied. Out-line of the anode installation can be seen in Fig. 3.

In this case, a ribbon type active titan mesh, 13 mm in width and 0.6 mm in thickness, was used after being doubled to 600 mm in length and welded to a titan plate, which had enough length to insert and adjust the anode to the intended position. Before the installation, a minimum amount of surface steel plates was removed so as not to diminish its reinforcing function, and the hole was made 35 mm in diameter until the correct depth was reached.

From the simulation using the Finite Element Method, intervals of 250 mm were recommended. These anodes were inserted between the two-layers of main steel.

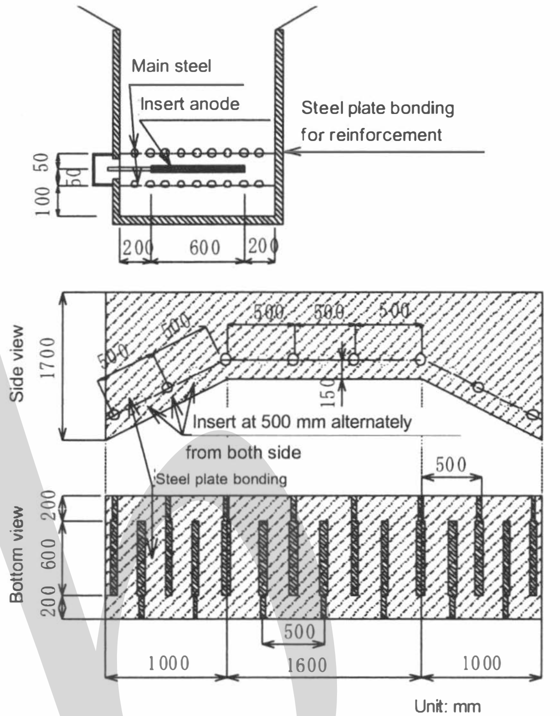

Fig.3 Arrangement of insert type anode for the beams with reinforcing plate

4. CURRENT SUPPLY AND EFFECTS

The protection current was supplied using the constant potential method. Depolarization during a 24-hour period measured at two weeks, three months, and six months from the start of cathodic protection is shown in Fig. 4.

The current density to get sufficient depolarization decreased during the first six months of cathodic protection.

For example in Fig. 4, a current density of 31.3mA/m^2 (per concrete surface) at two weeks decreased to 17.7 mA/m^2 at six months when the potential was increased from 5.4V to 5.7V. During the current supply over six months the steel bars shows sufficient depolarization, i.e., more than 100mV. Even in the stirrups, which was insufficient in depolarization due to low conductivity, the depolarization appeared to increase along with the duration of the current supply.

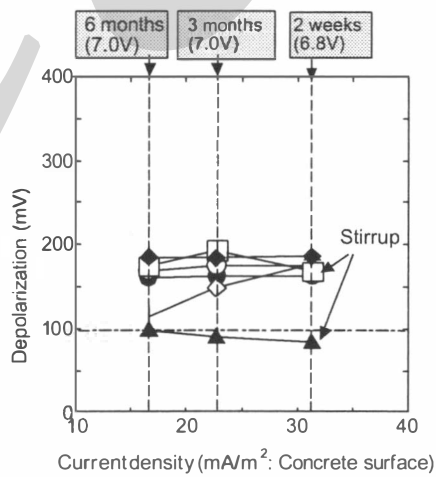

Fig. 4 Depolarization of reinforcing steel in block 10

5. CONCLUDING REMARKS

The combination of the cathodic protection with steel plate of CFRP bonding was understood to make the jetty to survive the devastating earthquake and the severe chloride environment.

LIFECYCLE DESIGN FOR DURABILITY OF OFFSHORE CONCRETE STRUCTURES

Nobuaki Otsuki
Professor, Department of International Development Eng., Tokyo Institute of Technology, Japan

Hiroshi Yokota Hidenori Hamada Tarek Uddin Mohammed
Port and Airport Research Institute, Japan

Keywords: durability, lifecycle design, offshore concrete structures

1 INTRODUCTION

In the middle of the last century, the concrete engineers were so optimistic to believe that the lifecycle of a concrete structure would be forever. The situation was changed dramatically over the previous fifty years. Recently, engineers are so pessimistic even for a very limited lifecycle of a structure. Especially, for offshore concrete structures, the lifecycle is considered to be around 50 years or less. What a big change! Design strategy for the achievement of a long lifecycle is necessary to be developed, and also the constraints against this achievement are necessary to be pointed out and solved based on laboratory as well as long-term exposure tests in the natural environment.

In this paper, the authors summarize the present situation of lifecycle design strategy of the offshore concrete structures in Japan mainly from the durability viewpoint. The paper will be very useful to the engineers concerning about the lifecycle design strategy for offshore concrete structures mainly from the durability viewpoint.

2 PERFORMANCE-BASED DESIGN CONCEPT OF OFFSHORE CONCRETE STRUCTURES

In this section, the performance based design concept of offshore concrete structures used in Japan is explained from the planning stage of a structure to it's demolition. The principle performances related to offshore concrete structures are: (1) maintaining safety and serviceability during service loads in normal use, (2) safety and serviceability are not lost even after possible deterioration of materials, particularly due to the corrosion of steel bars, and (3) local failure within the range of restorability is allowed to occur but not entire collapse during and after earthquake.

3 LONG-TERM PERFORAMNCE OF PC PILES AND BEAMS IN SEAWATER

In this section, long-term performance of PC piles and beams exposed in Kobe, Sakata and Kagoshima Ports in Japan for 20 to 37 years is summarized. No reduction in compressive strength of concrete was found after a long-term of exposure. Young's modulus of concrete was also increased compared to the 28 days modulus. Chloride over the steel bars was estimated at more than 10 kg/m^3, however only thin rusts were observed over the bars. Load carrying capacity of the beams was satisfied the initially designed capacity. It was understood that mechanical properties of concrete and structural performance is remained as initial level. The results indicate that seawater is not harmful for the reduction in mechanical properties of concrete, such as compressive strength and Young's modulus. Also, thin rust over the steel bars may not cause to reduce overall load carrying capacity and serviceability of the structures.

4 CORROSION OF STEEL BARS DUE TO THE VOIDS AT THE STEEL-CONCRETE INTERFACE

Corrosion of steel bars due to the voids at the steel-concrete interface is summarized in this section. It is important to note that this matter is generally omitted in the durability design of reinforced offshore concrete structures. However, based on the long-term exposure tests on offshore concrete specimens, it was clearly understood that this matter should be taken into account to enhance long-term durability of concrete structures. The summary of an accelerated laboratory investigation to clarify the formation of corrosion cells over the steel bars in concrete with the presence of voids at the steel-concrete is presented in this section. The results clearly indicated that with the presence of voids over the steel-concrete interface an anodic area is formed very easily under marine environment. Also, the area subjected to a high level of micro-cell corrosion. Corrosion pits occur from the combined effect of macro- and micro-cell corrosion. The results of the accelerated laboratory investigation are confirmed with the several long-term exposure tests. To enhance long-term durability, steel-concrete interface should be free from voids.

5 ELECTRO-CHEMICAL REHABILIATION

The electro-chemical rehabilitation methods, such as cathodic protection, desalination, and electro deposition are summarized in this section. Long-term performance of different anode systems, such as titanium mesh system, titanium wire system, and zinc sheet system was compared and found that the effectiveness of the cathodic protection is significantly influenced by the anode system used in the protection. Careful selection of anode system is essential to prevent the corrosion of steel bars in concrete. Titanium wire system showed the worst performance to prevent corrosion of steel bars in concrete. On the other hand, titanium mesh system and zinc sheet system were found to be very effective to prevent corrosion of steel bars in concrete. A case history of desalination used in a 30 years old road pier is explained in this section. An application of a current of 1.0 A/m^2 for eight weeks caused to significant reduction of chloride concentration over the steel bars. It improved the passivity grade of the steel bars in concrete also. A case history of application of electro-deposition applied to a sea wall made in 1998 at Matsuyama Port in Japan is described. A current of 0.5 A/m^2 was applied for 5 months. It was found that the surface of concrete was covered with 0.5 to 2.0 mm thick $CaCO_3$ and $Mg(OH)_2$ deposits. The ratio of $CaCO_3$ to $Mg(OH)_2$ deposits was about 1.7. In addition to the concrete surfaces, the minute cracks were also healed. The alkaline deposits reduce the corrosion over the steel bars.

6 LIFECYCLE DESIGN

In this section, lifecycle design is briefly addressed including design life, lifecycle story and strategy, lifecycle management considering lifecycle cost and prediction of deterioration grades. For a design life of 30 years, the ultimate limit state will be critical. For a design life of more than 50 years, in addition to the ultimate limit state, the durability limit state related to the serviceability of the structure should be considered. To keep the structure serviceable throughout it's design life, three different repair strategies are proposed, such as do nothing repair strategy, regular holding repair strategy and once-off full repair strategy. Based on the service life of the structure, the suitable repair strategy can be selected. Lifecycle cost is also an important factor in this process. An example of total cost estimation is provided for different repair processes. It is also necessary to predict the deterioration progress of the structure to predict the lifecycle cost. Here, the deterioration progress is predicted based on the estimated chloride concentration using the Fick's second law of diffusion. For grade 0, the chloride content is expected to be less than 1.2 kg/m^3, for Grade 1~2 as 1.2 ~ 2.0 kg/m^3. On the basis of the laboratory tests and long-term exposure tests, the limit value of each grade from Grade 3 to 5 is proposed based on the cross-sectional loss of the steel bars, up to 1% for Grade 3, and 5% for Grade 4, and up to 20% for Grade 5.

7 NECESSARY RESEARCH

In this section, the necessary research area related to the chloride threshold value with perfect steel-concrete interface was mentioned. Also, further studies on the effective application of electro-deposition, and desalination in cracked and uncracked concrete are proposed.

8 CONCLUDING REMARKS

The concluding remarks on this report are summarized in this section. The information summarized in this report will be very useful to the design engineers concerning the lifecycle design of concrete structures. The authors believe that young researchers will come ahead to deal with and solve the unresolved issues related to the lifecycle design of offshore concrete structures.

ULTIMATE SHEAR CAPACITIES OF BUTTRESSES FOR BREAKWATER CAISSONS

Masao Yamada
Port and Airport Research Institute, JAPAN

Osamu Kiyomiya
Professor, Waseda University, JAPAN

Keywords: buttress, footing, shear capacity, deep beam, distributed load

1 INTRODUCTION

Caisson-mound composite breakwaters are designed to be safe against sliding, overturning of the caissons and collapsing of rubble mound foundation. The overturning or the collapsing of foundation should be critical rather than the sliding, if the breakwater is constructed in relatively calm and deep sea. In such cases it should be economical to reduce the width of the caisson by extending footings as shown in Fig.1.

Since widely extended footings are subjected to large bending moment and shear force at the joint of footings as cantilever beams, installing buttresses between footings and side walls is considered to be effective to reinforce the footings. The structural form of a buttress is similar to that of a corbel, which JSCE code [1] prescribes to design as a deep beam, except for that a corbel is expected to bear a concentrated load. Thus in this study, the applicability of the equation of JSCE code for a deep beam to buttresses was investigated.

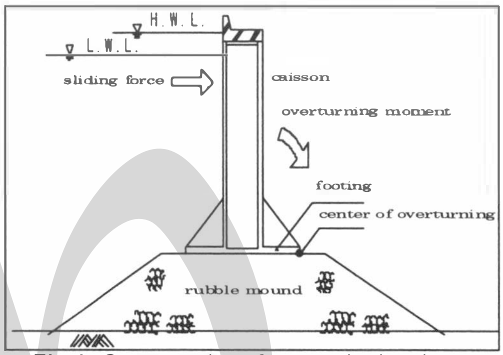

Fig.1 Cross section of composite breakwater

2 EXPERIMENTS

RC buttresses of 1.0, 1.5, and 2.0m high and open-sandwich (OS) composite buttresses of 1.5m high were tested. All the buttress were 0.1m thick and 1.5m long extended. In RC buttresses steel bars with the diameter of 6mm were arranged at the spacing of 100mm parallel to the footing and to the side wall. This mesh was arranged in two layers with cover of 20mm thick.

OS buttresses were unsymmetrically reinforced, by steel plate of 3mm thickness on one side and by steel bars mesh with the cover of 20mm in the other side. Headed studs were welded on the steel plate as shear connectors. The footings were over-reinforced to prevent from yielding of steel in the footings prior to the rupture of the buttresses.

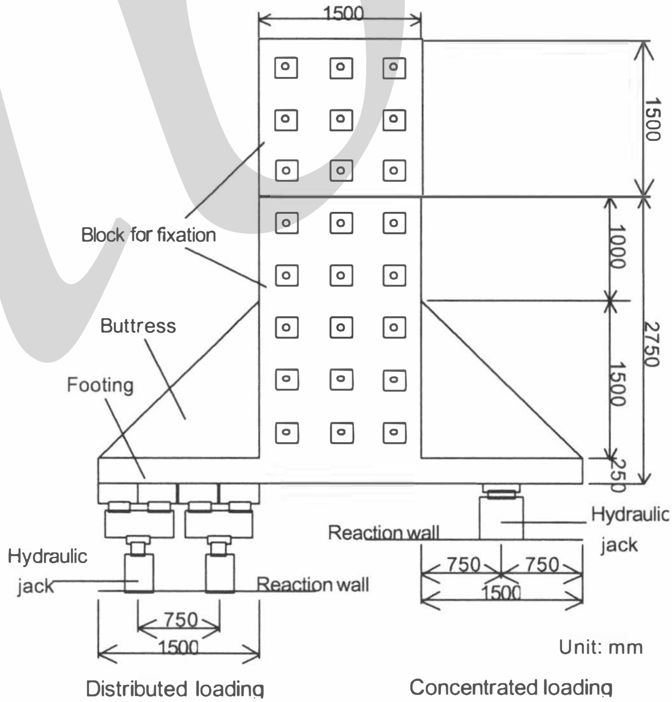

Fig.2 Plan view of loading set-up

Fig.2 shows a plan view of loading set-up. Loads were applied statically and monotonically .

3 RESULTS

More cracks appeared on concentrated loaded specimens than distributed loaded ones, when comparing at same load. Finally shear failure followed crushing at compressive edge in RC specimens, and buckling of steel plates occurred in OS specimens.

Fig.3 shows the principal compressive strains on some buttresses at the loads of 90% of their peak loads. Compressive strain flow from loaded part to the fixed edge was observed. The widths of the flow in the concentrated loaded buttresses were narrower than those in the distributed loaded ones.

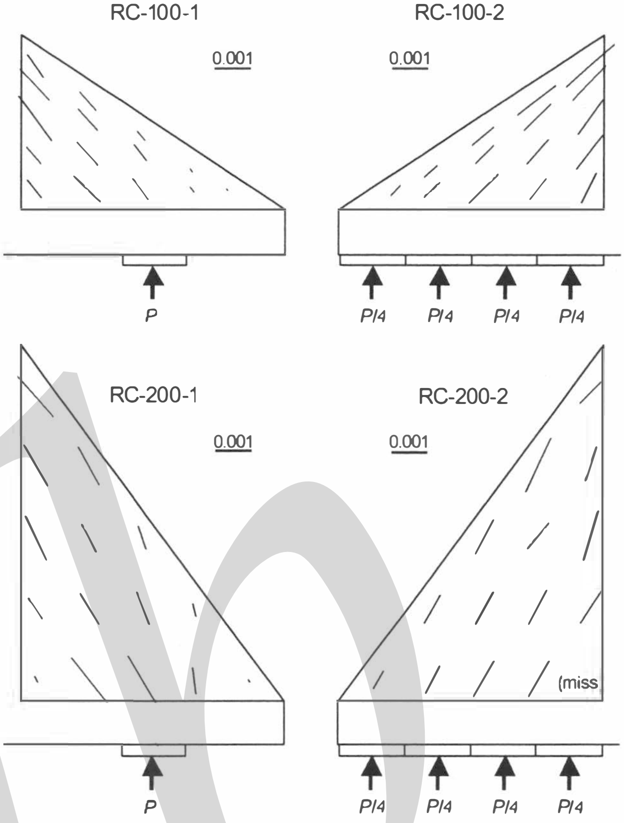

Fig.3 Principal compressive strains at 90% of the peak loads

Table 1 shows the calculation results by the JSCE equation and test results. The measured capacities of RC specimens were approximately in proportion to the heights of the buttresses. The ratios of the measured capacities to the calculated ones were from 1.27 to 1.64 for concentrated loaded specimens. On the other hand, the ratios of the test results to the calculations for distributed loaded specimens were from 1.65 to 2.06, so that the calculations were too conservative. This is considered to be caused by the difference of the width of the compressive strain flow, which was not evaluated in the calculation, since the effects of the length of supporting plates were omitted in the JSCE equation. Thus the authors propose to multiply the equation by a factor β_r (=1.3 for a uniformly distributed loaded buttress) .

Table 1 Calculations and test results of shear capacity

Specimen	A_s (cm^2)	b_w (m)	d (m)	β_d	β_p	β_a	V_{dd} (MN)	Test results (MN) (Ratio to V_{dd}) Concentrated loading	Distributed loading
RC-100	79.42	0.10	1.125	0.971	1.5	3.46	0.712	0.98 (1.38)	1.47 (2.06)
RC-150	79.42	0.10	1.625	0.886	1.5	4.12	1.118	1.42 (1.27)	1.84 (1.65)
RC-200	79.42	0.10	2.125	0.828	1.5	4.45	1.474	2.04 (1.38)	2.76 (1.87)
OS-150	70.00	0.1218	1.757	0.869	1.49	4.23	1.466	2.41 (1.64)	2.56 (1.75)

Notes) a_v =75cm, f'_{cd} =43.7N/mm^2, γ_b =1.0 for all the specimens

4 CONCLUSIONS

In this study, ultimate capacities of buttresses for a new type of composite breakwater caissons with long footings were investigated by loading tests. Capacity, which is the measured peak load, of each specimen was approximately in proportion to the height of buttress. The capacities of distributed loaded specimens were greater than those of their concentrated loaded counterparts by from 30 to 50% for RC and by 6% for OS. The capacities of OS specimens were greater than those of RC specimens of the same height of buttress by from 39 to 70%, so that the composition of steel plate and concrete was effective as to capacity.

Compressive strain flow in concentrated loaded buttresses was narrower than that in distributed loaded ones. The existing equation for deep beams was too conservative for the distributed loaded buttresses. Thus the authors proposed to multiply the equation by a factor considering distribution of load.

REFERENCE [1]JSCE : Standard specifications for concrete structures, 1996 (in Japanese)

SURVEY OF PIERS REPAIRED WITH A HIGH CHLORIDE-RESISTANT COVER REPLACEMENT MORTAR

Toshio Azuma Nobufumi Yamagata
Ministry of Land, Infrastructure and Transport
Kyushu Regional Development Bureau, Japan

Hiroshi Jitosono
Ube-Mitsubishi Cement
Research Institute
Japan

Kiminori Kuno
P.S.Corporation
Japan

Keywords: harbors concrete structures, repair, chloride attack, corrosion of reinforcement

1 INTRODUCTION

Harbors concrete structures, which are located in the marine environment, are influenced by the chloride ion in the sea or the spray. The maintenance of these structures, which are deteriorated by chloride attack, is one of the important problems for operating harbors. However, reports concerning the repair and reinforcement method for the harbors concrete structure by which the damage is received is few in Japan.

The Investigation on the piers of Kitakyushu harbor Kuzuha area was executed in 1987. As a result, it has been understood that the repair is necessary for about 85% of the bridge girders and about 75% of the floor slabs. Therefore, extensive 5-year works were executed there from 1989 to 1993. We assumed the durability after it had repaired to be 30 years. In the bridge girders, we substituted all stirrup reinforcements after chipping the deterioration part of the concrete, and did the rust-proofing of main reinforcement. And the bridge girders were treated with cover replacement method by using high chloride-resistant mortar. Moreover, a floor slab was newly constructed of precast concrete with the thickness of the slab changed from 25cm of existing to 35cm.

In this paper, we present the result that specimens exposed for 10 years were taken place.

2 REPAIR AND REINFORCEMENT OF THE BRIDGE GIRDERS AND THE FLOOR SLABS

2.1 Bridge girder

In the bridge girders, we substituted all stirrup reinforcements after chipping the deterioration part of the concrete, and did the rustproofing of main reinforcement. And the bridge girders were treated with cover replacement method by using high chloride-resistant mortar. Because the covering depth of the stirrup reinforcement became 3cm when the section was returned to the previous section, we used the epoxy coated reinforcement for the stirrup reinforcement according to concrete standard specifications [1]. And the dry mortar (hereafter, abbreviated to DM) with high chloride-resistance for the material which restored the section was used. The shrinkage of DM is small and its bond strength is high. The physical properties of DM are shown in Table 1.

2.2 Floor slab

Because the loading condition was changed, the thickness of the floor slab has been increased from 25cm to 35cm. Then, A precast floor slab was newly constructed a made of reinforced concrete.

3 EXTERNAL INVESTIGATION FOR 10 YEARS

The external investigation was executed in 3, 7 or 10 years after having repaired. The investigation position was executed in No.2 block, No.4 block, and No.6 block in the 8th quay. We took the photograph in the deterioration part.

The rust fluid from the separator mark was confirmed at the bridge girder 3 years later. However, even if 10 years pass, no changes were observed in the cover replacement parts repaired with DM.

The crack and efflorescence to the floor slab were confirmed 3 years later. And, a similar deterioration was confirmed 10 years later.

4 PREDICTION OF DISTRIBUTION OF CHLORIDE ION

In general, the diffusion of the chloride ion in concrete and in mortar is approximated by the Fick's law [2]. The chloride ion on the surface (C_0) and appearance diffusion coefficient (Dc) of the chloride ion were calculated by using (1). The diffusion coefficient of the appearance of DM is about $0.38\times10^{-8}cm^2/sec$ for 3 years. There is no difference in Dc of 7 years and Dc of 10 years, and they are about $0.14\times10^{-8}cm^2$ /sec on the average.

It is a value about 10 times DM. There is no difference in C_0 of DM and NM for 3-10 years, and they are about 1.3% and 0.8% on the average.

The diffusion coefficient of DM which used the diffusion cell was $0.09\times10^{-8}cm^2/sec$, however, the diffusion coefficient of the specimen which had been exposed for 10 years became about $0.16\times10^{-8}cm^2/sec$. We think that this difference is the influence of the temperature changing and the repetition of dry and wet under the marine environment.

Table1 Physical properties of DM

Item		Physical properties
Flow		250
Bleeding ratio (%)		0
Compressive strength (N/mm^2)	1 day	10.6-28.1
	3 day	36.1-52.6
	7 day	51.5-64.6
Flexual strength (N/mm^2)	28 day	72.0-85.8
	7 day	10.4-11.7
Bond strength (N/mm^2)	28 day	11.3-12.3
Shrinkage (%)	28 day	0.009-0.023
Diffusion coefficeint (cm^2/sec)		$0.08\text{-}0.10 \times 10^{-8}$

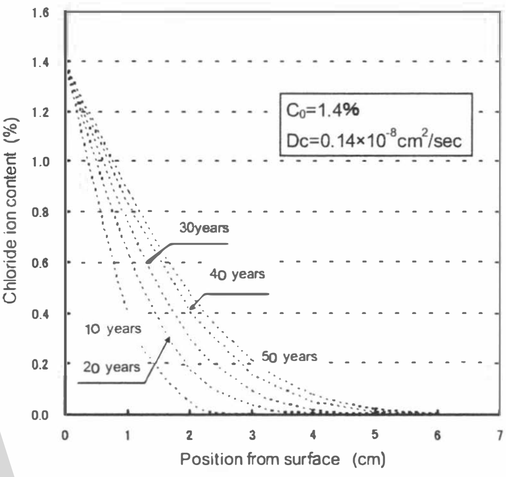

Fig.1 The result of forecasting the infiltration situation of the chloride ion of DM in the future

$$C=C_0(1-\mathrm{erf}(x/2(Dc\cdot t)^{1/2})) \quad \cdots\cdots \quad (1)$$

C : Chloride ion content (%)
C_0 : Chloride ion on the surface (%)
Dc : Virtual diffusion coefficient of the chloride ion (cm^2/sec)
x : Position from surface (cm)
t : Time (sec)
erf : Error function

The result of forecasting the infiltration capacity of the chloride ion of DM in the future is shown in Fig.1. The average of Dc ($0.14 \times 10^{-8} cm^2/sec$) and C_0 (1.4%) was used for the calculation. The amount of chloride ion position from surface by 3cm is 0.03% ($0.8kg/m^3$) after 20 years, and it is 0.09% ($2.1kg/m^3$) after 30 years, and it is 0.15% ($3.5kg/m^3$) after 40 years, and it is 0.21% ($4.9kg/m^3$) after 50 years. Moreover, the amount of the chloride ion position from surface by 6.6cm is about 0.002% ($0.06kg/m^3$) after 50 years.

That is, at the position of the stirrup reinforcement, the period to reaching to the corrosion generation limit concentration has been about 23 years since the repair, and it has been about 110 years since the repair at the position of the main reinforcement.

5 CONCLUSIONS

At the position of the stirrup reinforcement, the period to reaching to the corrosion generation limit concentration has been about 23 years since the repair, and it has been about 110 years since the repair at the position of the main reinforcement.

REFERENCE

[1] Japan Society of Engineers: Design of concrete standard specifications, pp.99, 1986
[2] Takeda, N.: Study of durability and evaluation of reinforced concrete under marine environment. Thesis of Kyushu Institute of Technology, 1999

THE SEISMIC REINFORCEMENT BY USING PRECAST PANELS TO PIERS IN WATER

Itaru Yamaguchi
Ministry of Land, Infrastructure and Transport
Kyusyu Regional Development Bureau, Japan

Noritomo Ebihara Tomonori Kato Hisashi Iwai
P.S.Corporation
Kyusyu Branch Office, Japan

Keywords: PC confined method, underwater construction

1 INTRODUCTION

This construction work is to provide seismic reinforcement to 6 underwater piers that have been in service for about 20 years.

For the seismic reinforcement of underwater piers, in general, temporary cofferdam closure with sheet piles or else is provided, and then the work is carried out in a dry condition after water being drained. However, in this way, the temporary work becomes of too large scale, and accordingly the portion of the temporary work cost increases. Therefore, in order to reduce the scale of the temporary work, to minimize the cost and to shorten the schedule, the seismic reinforcement with prestressed concrete by using precast panels (called as PC confined method, hereinafter) was adopted for this bridge.

PC confined method is to install the precast panels made in the factory, around the existing bridge pier, and by tensioning and confining with prestressing steel, to improve seismic-resistance capacity of the pier. By tensioning the prestressing steel placed spirally around the pier, the integration effect with the existing pier is achieved, and thus the toughness of the pier is enhanced. In addition, by using the precast panels manufactured in the factory, the work at site can be reduced and the construction schedule can be shortened.

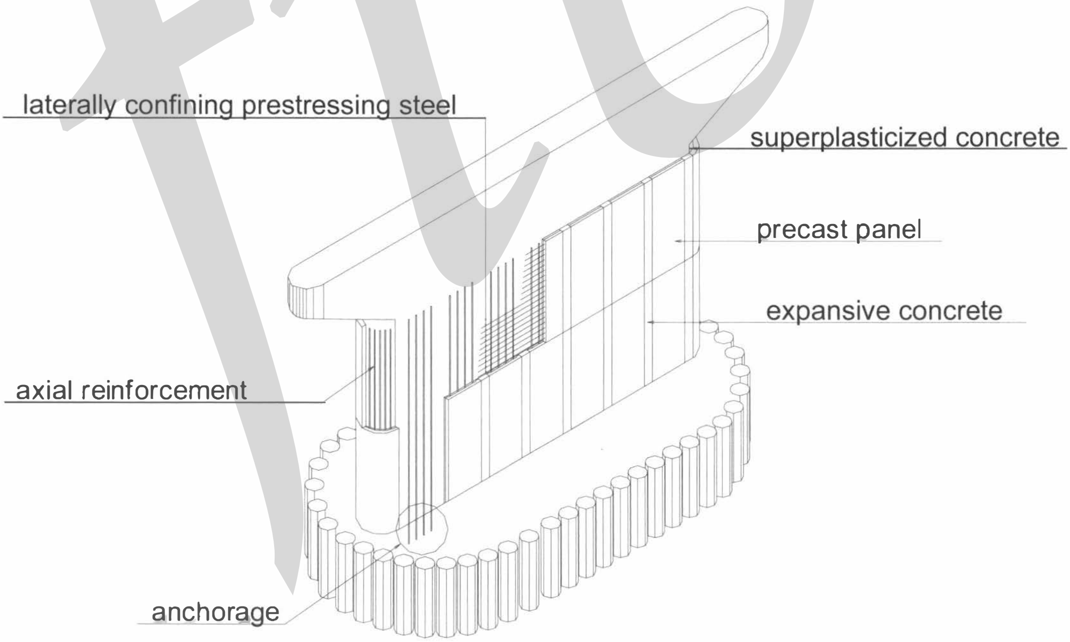

Figure-1 Schematic Drawing of PC Confined Method

2 CHARACTERISTICS OF THE CONSTRUCTION WORK

The feature of this construction work was to carry out the PC confined method underwater. For execution of the underwater construction, the following trial works were executed.

① As the site was on the sea, epoxy coated reinforcements and polyethylene covered prestressing steel were adopted as the countermeasure against the steel corrosion due to sea salts.

② The precast panels to be installed underwater were assembled temporarily on the sea, and were sunk as a whole, in order to reduce the work underwater.

③ For the important locations where tensioning of prestressing steel to be done, a semi-circular metal shaft was installed, and water was drained from the shaft so as to carry out the work in a dry condition, in order to achieve good construction management.

3 CONSTRUCTION METHOD

3.1 Placement of Pollution Protection Fence and Construction of Temporary Cofferdam

As it is a pier reinforcement work on the sea, maximum care was taken for prevention of seawater pollution.

In addition to the pollution protection fence, steel sheet piles were placed around the steel pipe wall open caisson type foundation in order to prevent the polluted water from diffusing outward.

3.2 Dredging

In order to remove the soil in the temporary cofferdam, dredging by pumps was carried out.

3.3 Staging, Assembling Transverse Moving Installation, Drilling and Anchoring Axial Rebar

A precast stage framed by H-beam was placed on the footing after completion of the dredging, and a temporary work stage was assembled on it, and a transverse moving installation to be used for erecting the precast panel was placed. For drilling for the axial rebar placement, the SDI method, which was considered not to damage the rebar in the existing pier without executing rebar sensing, was adopted. The SDI method is high pressure jet drilling by using slurry of sand and water.

3.4 Temporary Erection for Precast Panel, Submerging of Whole Set

A precast panel support was placed, temporary erection of the precast panel was executed by using a barge with a crane and the transverse moving installation. Jointing of the panels was done with high tension bolts and epoxy adhesive and prestressing steels were inserted.Submerging was executed in a menner that whole set of panels temporarily assembled in a ring shape was lowered, the VSL heavy lifting method, which was able to centrally control the state of lifting for heavy equipment, was adopted.

3.5 Fixing Precast Panel, Placement of Primary Concrete

After the submerging of the precast panel, primary concrete was placed into the gap between the existing pier and the precast panel. Then metal pits (semi-circular preset corrugated pipe) were attached. This was devised in order to carry out important work in a dry condition, such as tensioning.

3.6 Work in metal shaft

After the water in the metal shaft was drained out by pump, tensioning work for the prestressing steel was carried out by using double-cylinder type jack. Then grouting and drilling for the interim perforation cable and its assembly work, and secondary concrete placing work to fill up the holes used for tensioning work and for the interim perforation cable, were carried out in a dry condition

4 CONCLUSIVE REMARKS

There are many places where seismic reinforcement for the pier located underwater has not been provided, and the seismic reinforcement by using precast panels is considered to be increasing.

Session 5 | Composite structures

CONCRETE-FILLED STEEL TUBE COLUMN SYSTEM - RECENT RESEARCH AND CONSTRUCTION IN JAPAN -

Shosuke Morino, Mie University, Japan

Keywords: concrete-filled steel tube, column, beam-column, design formula, construction data

1 INTRODUCTION

CFT column system has the following advantages compared with ordinary reinforced concrete and steel systems. i) Interaction between steel tube and concrete: delayed local buckling of steel tube, moderate strength deterioration after local buckling, confining effect on concrete strength, no concrete spalding, and smaller drying shrinkage and creep of concrete. ii) Cross-sectional properties: larger steel ratio, and effective use of steel tube. iii) Construction efficiency: no works for forms and reinforcing bars, saving of manpower and constructional cost and time, and clean construction site. iv) Fire resistance: high fire resistance, and saving of fireproof material. v) Cost performance: better cost performance than ordinary steel system. vi) Ecology: no form works, and reuse of steel tubes and high-quality concrete.

2 RESEARCH ON CFT COLUMN SYSTEM

The results of recent research works in the category of structural mechanics, construction efficiency, fire resistance, and structural planning have provided the following knowledge on the CFT column system. i) Compression members: Confining effect appears in a circular short column, but not in a square short column. Buckling strength of a long column can be evaluated by the sum of the tangent modulus strengths of each component. Constitutive laws for concrete and steel in a CFT column have been established that take into account confining effect and scale effect on concrete strength, strain softening in concrete, effect of ring tension stress on steel tube strength, and local buckling and strain hardening of steel tube. ii) Beam-columns: Bending strength of a circular beam-column exceeds superposed strength due to the confinement effect, but not in the case of a square beam-column. Circular beam-columns show larger ductility than square ones. Empirical formulas to estimate the limit rotation angle of CFT beam-columns are available. Fiber analysis based on the constitutive laws mentioned above well traces the flexural behavior and well estimated the ultimate strength of an eccentrically loaded column. An effective mathematical model is available to trace the cyclic behavior of a beam-column. iii) Beam-to-column connections: Design formulas have been established for outer and through diaphragms, and ring stiffener. Several new types have been proposed, such as the connections using vertical stiffeners, long tension bolts, and thicker tube at the shear panel without diaphragm. Stress transfer mechanism has been proposed to trace the load-deformation behavior of a connection. iv) Frames: Tests of subassemblages with weak shear panel show very ductile behavior. Energy dissipation capacity of a column-failing CFT frame is equivalent to that of a steel frame. v) Quality of concrete and casting: Gap between concrete and steel may be produced by the bleeding of concrete underneath the diaphragm. It is necessary to mix concrete with small water cement ratio, small water content, and large cement content to reduce the bleeding. Pumping-up method is recommended to cast compact concrete without void area underneath diaphragms. vi) Design characteristics: Lateral story stiffness of the CFT column system is larger than that of a steel system, but story weight of the former is larger than that of the latter. This leads to no major differences in the vibration characteristics of both systems. Total steel amount of the CFT column system is about 10% less than that of the steel system. vii) Fire resistance: CFT column can sustain axial load by filled concrete after the capacity of steel tube is lost by heating, and thus fireproof material can be reduced or even omitted. Fire tests of beam-columns forced to sway by the thermal elongation of adjacent beams have shown that the column carries only the axial load at final stage.

3. DESIGN OF CFT COLUMN SYSTEM

CFT Recommendations[1] was published by Architectural Institute of Japan (AIJ) in 1997, based on the recent research developments, which is characterized by covering following topics: i) special type of CFT members such as braces and truss members, in addition to compression members, beam-columns and connections, ii) formulas to evaluate deformation capacity of CFT columns and frames, iii) structural characteristics under fire, iv) manufacturing of steel tube and mixture of concrete, v) analysis of the behavior of CFT columns and frames, and vi) strength formulas used in the world. The newest edition of SRC Standard of AIJ[2] published in 2001 contains the design provisions for the CFT column system, according to the contents of CFT Recommendations[1]. The full paper shows the design formulas for CFT compression members, beam-columns, and diaphragm and shear panel of beam-to-column connections.

4. CONSTRUCTION OF CFT COLUMN SYSTEM

Structural designs of 156 CFT buildings provided by the Association of New Urban Housing Technology show the following characteristics of the CFT system:
i) Among 156 buildings, 43(27%) are shops and warehouses, and their total floor area shares 42%. Application of CFT to those buildings indicates building designer's recognition to the spannability of the CFT system. ii) The CFT system is not very often applied to braced frame buildings. It may not be necessary to use the braces, since the tube section has identical strength and stiffness in both x- and y-directions. iii) Floor area carried by one column is much larger than that in the ordinary reinforced concrete or pure steel buildings. The floor area exceeds 90 m2 in 37% of all buildings, and in 43% of office buildings. iv) Variety of the aspect ratio of span grid indicates the CFT system's possibility for free planning about the span grid. In the case of office buildings, rectangular span grid of 8 m × 18 m is fairly often used, and the aspect ratio exceeds 2.2, while the span grid of shop buildings is fairly close to square.
v) Both square and circular column sections are mixedly used in a number of buildings. Size of tube section often used is between 500 and 700 mm in the case of square CFT columns, and 600 and 711 mm in the case of circular CFT columns. vi) Inner or through diaphragms are used in most cases of beam-to-column connections. vii) Embedded type column bases are most popularly used, which is the best in view of the structural reliability. viii) Ratio of the buckling length of the CFT column is much larger than that in the ordinary reinforced concrete or pure steel buildings. ix) Design standard strength of steel often used is 325 MPa, and that of concrete is 36 and 42 MPa.

5. CONCLUDING REMARKS

Rational design method for the CFT column system has been established through extensive research done by Architectural Institute of Japan, New Urban Housing Project and U.S.-Japan Cooperative Earthquake Research Program, and several design standards, recommendations and guidelines are available. More than 40 buildings have been constructed every year in the last 5 years in Japan. Trial designs of unbraced frames have shown that the structural characteristics of the CFT and steel systems are almost the same, but the total steel consumption of the CFT system for entire building is about 10 % less than that of the steel system.

It must be noticed that the CFT system is not very stiff against lateral load, and thus the investigation on other structural system rather than the moment frame is now needed to utilize the large axial load carrying capacity of the CFT column more effectively, such as braced frame or the combination of reinforced concrete shear wall and CFT columns in which CFT columns mainly carry the vertical load.

Weak point of the CFT system is the beam-to-column connections. To fabricate a beam-to-column connection with through diaphragms, the column is cut into three pieces, and welded together with diaphragms. Therefore, the fabrication requires large amount of welding and increase the possibility to make defects in cast concrete. It is needed to develop a new type of connection without cutting the column body and without using welding, such as the connection using long bolts or steel tube whose wall thickness is partly increased at the connection. A few research work has been done on these new types, but design formulas are not yet well prepared.

Most of design engineers have treated the CFT system as an alternative to the steel system, trying to cut the cost by reducing the steel consumption. However, isn't it possible to look at the CFT system as an alternative to the reinforced concrete system? The investigation by trial design is needed to clarify advantages and disadvantages of the CFT system against the R/C system.

References

[1] Recommendations for Design and Construction of Concrete Filled Steel Tubular Structures, Architectural Institute of Japan (AIJ), 1997.10. (in Japanese)
[2] Standard for Structural Calculation of Steel Reinforced Concrete Structures, 5th Ed., AIJ, 2001.1. (in Japanese)

DEVELOPMENT OF NEW-TYPE CONNECTIONS BETWEEN CFT COLUMNS AND RC BEAMS

Toshiyuki Shioya, Katsuyuki Dewa, and Hideyo Shiokawa
Shimizu Corporation
JAPAN

Masaaki Takagishi
Dai-ichi High Frequency Co., Ltd.
JAPAN

Key words: connection, cyclic loading, CFT column, T-headed bar

1. INTRODUCTION

CFT (Concrete Filled steel Tube) has high loading capacity and high ductility. CFT construction has been used for columns of high-rise buildings quite often, and also for the columns of the elevated railroad of the Akita Shinkansen for the first time in Japan. In the case of the Akita Shinkansen, the upper beams and underground beams were SRC (Steel Reinforced Concrete) construction. However, the connections of CFT columns and SRC beams were very expensive. Therefore, this paper describes the development of new-type connections between CFT columns and RC beams, which are much cheaper compared with the former type.

2. EXPERIMENTAL PROGRAM

2.1 Test models

Figure 1 shows the dimensions and basic configuration of specimens. To evaluate the strength of the connection, three specimens were tested.

(1) TH1 specimen: TH1-specimen connection was made using T-headed bars[1]. The header of T-headed bars is processed firstly by heating the end of rebar up to 1300℃ using the high frequency induction method and then processed by pushing the end of the rebar into a holder. To break at the base of the column, there are 10mm spaces between the steel tube and RC beam. Normal strength concrete (f_{ck}=27N/mm^2) was used.

(2) PC1 specimen: In order to transfer the maximum capacity of CFT to the RC beam, PC bars were used. High strength concrete (f_{ck}=60N/mm^2) was used.

(3) TH2 specimen: TH2-specimen connection was made using double steel pipes and T-headed bars. High strength concrete (f_{ck}=60N/mm^2) was used.

2.2 Materials

Steel pipes: STK400, Rebars: SD345, PC bars: SBPR100/12.5

2.3 Loading test method

Figure 2 shows the loading apparatus. The axial force was 569kN for the TH1 specimen, and 2140kN for the PC1 and TH2 specimens.

3. TEST RESULTS

Table 1 shows the loading test results.

Table 1 Test results

	Axial force (kN)	Maximum horizontal force (kN)	Failure mode
TH-1	569	107	flexure
PC-1	2140	121	flexure
TH-2	2140	198	flexure

3.1 Displacement behavior

The relationship between horizontal force and displacement, and also that between axial force and flexural moment are shown in Figs. 3 to 5. The symbol ● in the figures means flexural maximum moment considering P-δ effect due to horizontal displacement at the column top. As noted previously, TH1 showed the RC capacity, PC1 and TH2 showed the CFT capacity. The experimental results showed that the maximum bending capacities were almost the same as the calculated values. Therefore, these three types of connection may be used for connections between CFT columns and RC beams according to various purposes. Figures 6 to 8 show the relationships between the section moment considering P-δ effect and displacement. The section moment did not decrease at the maximum displacement. Therefore, these three connections have enough ductility.

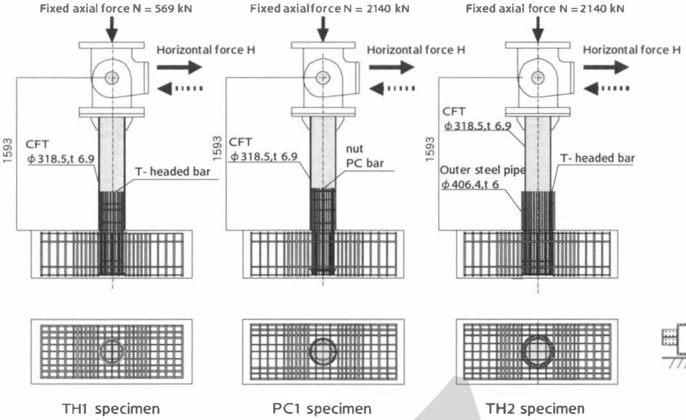

Fig. 1 Test models

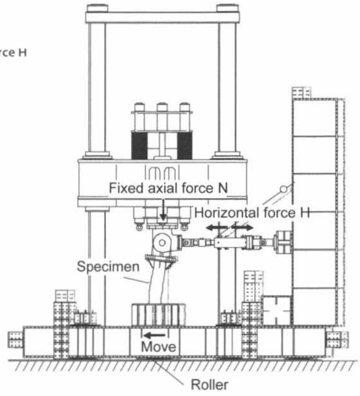

Fig. 2 Loading aparatus

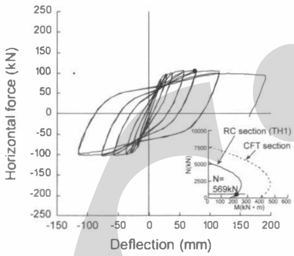

Fig. 3 Horizontal force vs. deflection-TH1 specimen

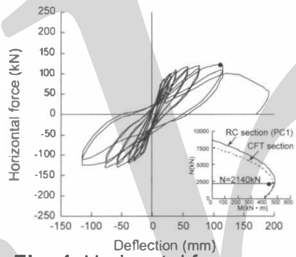

Fig. 4 Horizontal force vs. deflection-PC1 specimen

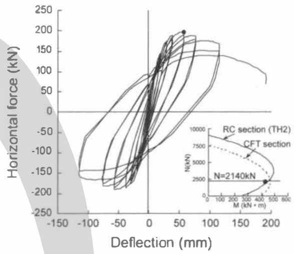

Fig. 5 Horizontal force vs. deflection-TH2 specimen

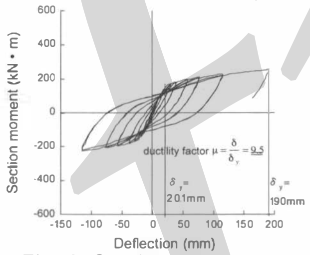

Fig. 6 Section moment vs. deflection-TH1 specimen

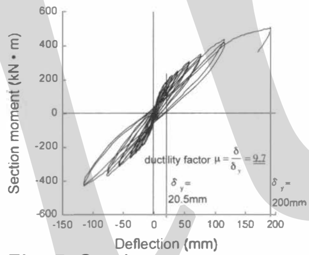

Fig. 7 Section moment vs. deflection-PC1 specimen

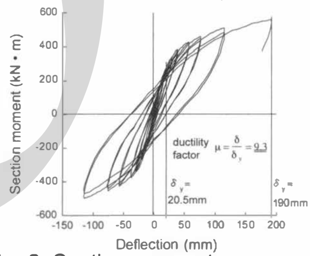

Fig. 8 Section moment vs. deflection-TH2 specimen

3.3 Ductility factor

In order to calculate the ductility factor, it is necessary to define displacement at yield of the CFT column. However, there are few definitions of the displacement at yield of CFT columns, and no definition has been decided. In this paper, the displacement at yield of the CFT column is defined as the displacement when the fiber of the steel pipe reached the yield point. The displacements at yield of the CFT column are shown in Figs. 6 to 8. As shown, the ductility factor is bigger than 9 in all cases. Therefore, in the design of CFT columns, the ductility factor of 9 can be used.

4. CONCLUSION

(1) Experimental results showed that the maximum bending capacities were almost the same as the calculated values. Therefore, these three types of connection can be used for connections between CFT columns and RC beams according to various purposes.
(2) The ductility factor is bigger than 9. Therefore, in the design of CFT columns, the ductility factor of 9 can be used.

REFERENCE

[1] Shioya, T., Nakazawa, H., Nagasawa, Y. and Takagishi, M.: Development of T-Headed bars, Proc. of JCI, Vol.22, No.3, pp.1291 - 1296, 2000.6 (in Japanese)

AN EXPERIMENTAL STUDY ON TOUGHNESS OF COMPOSITE BRIDGE PIERS USING STEEL PIPES WITH OUTER RIBS

Hiroshi Mikami
Mitsui Construction,
T.R.I, JAPAN

Norimitsu Kishi
Muroran Inst. of Tech,
JAPAN

Kenji Ikeda Masaki Minagawa
Civil Engineering Research Inst.
of Hokkaido, JAPAN

Keywords: composite bridge pier, steel pipe with outer rib, toughness, dilatancy

1. INTRODUCTION

Recently, a reduction in costs for providing of infrastructures has been strongly assigned. For a example, regarding the improvement of highway net work, even though the piers of bridges constructed in mountainous road intend to be higher, saving the construction costs and shortening the construction period are demanded. From these points of view, the authors propose a composite bridge pier using steel pipes with outer ribs for reduction in construction costs of bridge piers. However, the influences of thickness of steel pipe, material property and volume of stirrup and tie-bar on load-carrying capacity have not been clarified yet. In this study, in order to investigate the influences of thickness of steel pipes on load-carrying capacity under varying thickness of steel pipe and volume of axial rebar to keep a sectional bending capacity constant, lateral cyclic loading tests were conducted using three composite pier models with various thickness of steel pipe and one RC pier models as Test Series I. And then, the other cyclic loading tests (Test Series II) for four composite pier models were conducted taking the material property and volume of stirrup and tie-bar as variables.

2. EXPERIMENTAL OVERVIEW

Table 1 shows a list of the test specimens. The steel pipes used in Test Series I are of the same inner diameter = 68.6 mm among three specimens and thickness = 4.5, 3.5 and 2.5mm in each. The axial rebar volume is controlled for bending capacity to be similar among the specimens corresponding to magnitude of the sectional area of steel pipe. In Test Series I, D6 stirrups and tie-bars were arranged with the intervals of 120mm for all specimens. All the steel pipes used in Test Series II are of inner diameter = 68.6mm and thickness = 3.5mm. 12 D10 axial rebars were arranged. In case of II-1 Specimen, an interval of stirrups was enlarged to 1.25 times that of standard specimen (I-2) and no tie-bar was arranged. The dimensions of II-2 Specimen are the same with those of I-2 Specimen. In II-3 Specimen, D6 stirrups and tie-bars are arranged with intervals of 60 mm long which is a half that of II-2 Specimen. In II-4 Specimen, ϕ2 mm PC wire is spirally wounded with intervals of 30 mm in height, but tie-bar is not arranged. The dimensions and rebar/stirrup arrangement for each specimen are shown in Fig. 1. In case of composite pier models, two steel pipes with outer ribs are arranged in the long-side direction. The steel pipes were installed in the footing at 200 mm below the basement, which is about three times the inner diameter of the pipe.

Table1 List of specimens

Spec -imen	Steel pipe Outer diameter (Thickness) (mm)	Axial rebar Nominal Name (Numbers)	Stirrup Nominal name (Interval) (mm)	Tie-bar
I-1	ϕ77.6 (4.5)	D6 (16)	D6 (120)	Used
I-2	ϕ75.6 (3.5)	D10 (12)		
I-3	ϕ73.6 (2.5)	D10 (16)		
I-4	-	D13 (16)		
II-1	ϕ75.6 (3.5)	D10 (12)	D6 (150)	Not-used
II-2*			D6 (120)	Used
II-3			D6 (60)	Used
II-4			PC wire** (30)	Not-used

*Specimen II-2 and I-2 is the same.

** ϕ2 mm PC wire was spirally winded.

3. EXPERIMENTAL RESULTS

Experimental and analytical results are listed in Table 2. From this table, it is observed that the experimental ultimate loading capacity ratio P_u/P_y for I-4 Specimen which is of RC type, is smallest and is about 1.1. These for composite type (I-1~3) are

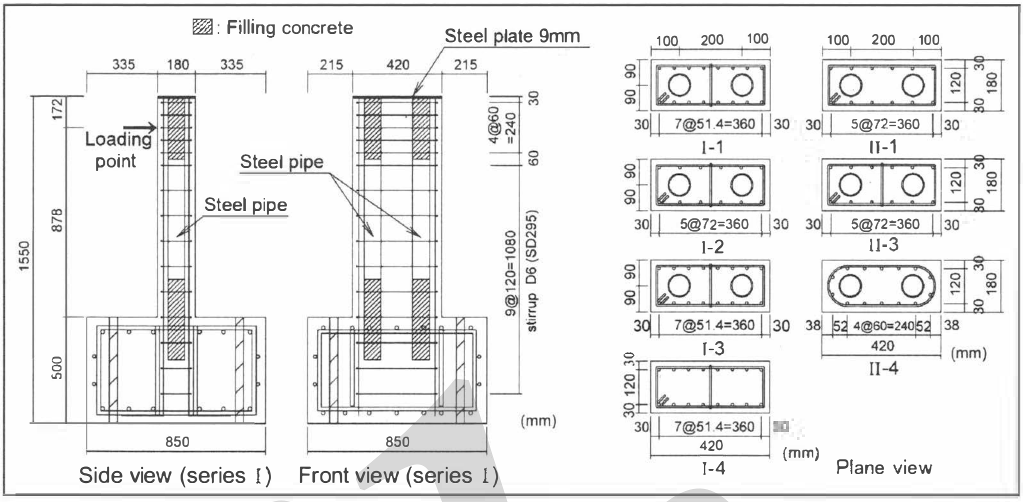

Fig. 1 Outline of specimens

bigger than that for RC type (I-4) and are distributed in the region from 1.3 through 1.5. The ratio for I-1 Specimen with the biggest thickness of steel pipe among all specimens is the biggest and for II-3 Specimen with stirrup and tie-bar being most closely arranged is the second biggest.

The ultimate plasticity ratio of I-1 Specimen is the biggest among all specimens and of II-3 Specimen is the second one. But the difference is very small. Then, it is seen that the increment of thickness of steel pipe by 1 mm and the volume of stirrups and tie-bars by twice with reference to that for I-2 standard Specimen have a similar influence on the ultimate plasticity ratio. Comparing between experimental and analytical results on yield and ultimate loading capacities, it is seen that the experimental results for I-4 Specimen which is of RC type, are about 20 % below the analytical results. However, these for composite type are in a good agreement with these analytical ones. On the other hand, experimental displacements at reaching yield point are a little larger than those of analytical ones because slipping out of steel pipe or rebar from footing was not considered in the analysis.

Table 2 List of results both experiment and calculation

Specimen	Ultimate stage: Capacity P_u (kN)		Ultimate stage: Displacement δ_u (mm)		Loading capacity ratio P_u / P_y		Ultimate plasticity ratio δ_u/δ_y	
	Exp.	Cal.	Exp.	Cal.	Exp.	Cal.	Exp.	Cal.
I-1	52.7 (62.4)	59.1	69.7	70.1	1.39 (1.64)	1.65	12.4	14.9
I-2	60.5	61.7	62.0	67.2	1.34	1.39	8.9	12.7
I-3	65.0	60.5	55.7	62.5	1.33	1.31	8.1	11.6
I-4	48.3	59.1	37.5	65.8	1.08	1.07	5.6	12.7
II-1	60.2	61.0	57.3	64.4	1.31	1.37	7.7	11.7
II-3	64.0	64.0	80.3	82.1	1.45	1.44	12.3	14.9
II-4	68.9 (54.5)	61.7	64.0	67.3	1.47 (1.17)	1.39	8.9	12.2

In case of specimen I-1 and II-4, results obtained from both loading direction are shown by adding ( ).

4. CONCLUDING REMARKS

1) Toughness of proposed bridge pier model is superior to RC type pier model, the ultimate load-carrying capacity is also 20 through 30% higher than that of RC type, and also, the loading capacity ratio defined as P_u/P_y and toughness (plasticity ratio) indicate a good correlation each other.
2) The ductility/toughness of composite type pier model can be improved by increasing in volume of stirrup and tie-bar. And also, toughness of composite type is more influenced by tie-bar than stirrup.

HYSTERESIS CHARACTERISTICS OF BARE TYPE COLUMN BASE CONNECTION IN STEEL REINFORCED CONCRETE STRUCTURES UNDER HIGH AXIAL TENTION AND CYCLIC HORIZONTAL LOADS

Kazushi Sadasue
Graduate School of Engineering,
Koichi Minami
Professor, Dept. of Architecture, Faculty of Eng.,
Fukuyama Univ., Sanzo 1 Gakuen-cho Fukuyama Hiroshima 729-0292 JAPAN

Keywords: Hyogoken-Nanbu earthquake, Ultimate strength, Deformation capacity, Elasto-plastic analysis

1 INTRODUCTION

Steel reinforced concrete (SRC) structures possesses the properties of both reinforced concrete (RC) and steel (S) structure, and by appropriate design it is possible to provide good earthquake resistance in such structures. Though it is necessary to think about many to design the SRC building reasonably, the seismic performance is most strongly influenced from the steel web types of member and the types of column base.

Fig. 1 shows that SRC building adopting bare type column base. In the case of bare type column base of which steel portion is set on the surface of the RC foundation beam. Accordingly bare type column base is the connection in which the structural form changes SRC to RC, the stresses at the base are transferred to the foundation through the steel column base consisting of base plate, anchor bolts and the RC portion surrounding the base plate.

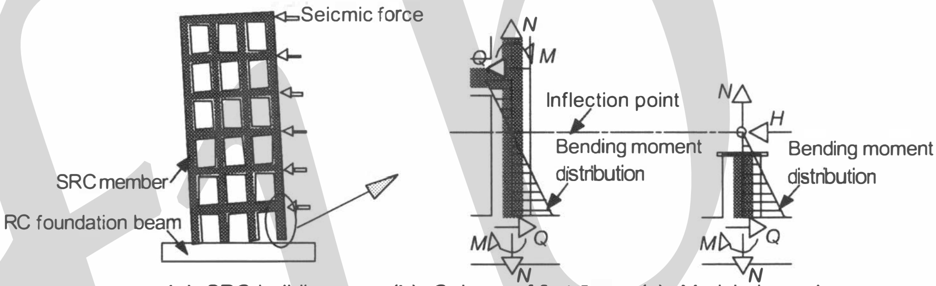

(a) SRC building **(b)** Column of first floor **(c)** Modeled specimen

Fig.1 SRC column adopting bare type column base

Bare type column base have the advantage of constructing and economically compared with embedded type column base. Consequently, bare type column base is often adopted. However, bare type column base connection in SRC buildings were damaged sinuously owing to 1995 Hyogoken-Nanbu earthquake in Japan. According to the report on the damage [1], it is thought that the tension forced due to overturning moment is the reason why these damages. This paper presents the results of the experiment carried out in order to study elasto-plastic behavior of the bare type SRC column base connection under a constant high tension load and cyclic horizontal load. Main discussion is concentrated on the maximum strength, the behavior after the attainment of the maximum strength and hysteretic characteristics involved in the large deformation range under alternate repeated loading. In addition, elasto-plastic analysis on some specimens was carried out, and the structure characteristic was examined.

2 EXPERIMENTAL WORK

The specimen is a cantilever which assumes below inflection point of the column of first floor in building. The following experimental parameters were selected, tension load level, shear span and composition of column base section. Fig. 2 shows the specimen.

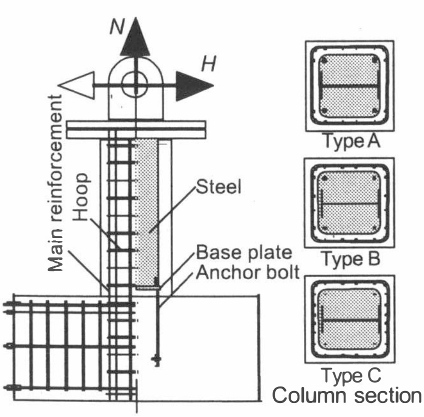

Fig.2 Test specimens

Relationships of axial load N and the ultimate strength Q_{fu} (flexural strength) and Q_{su} (shear strength) of the column bases by the design in AIJ [2] are shown in fig. 3. Dotted points show the experimental maximum strength. Relationships of the experimental parameters and limit deflection angle R_{tu} of column are shown in fig. 4. The following results were obtained from the experiment:

1. Ultimate strength of the bare type column base connection under the axial tension can be evaluated by the design code in AIJ.
2. The limit deformation capability can be improved by increasing the anchor bolt at the column base.

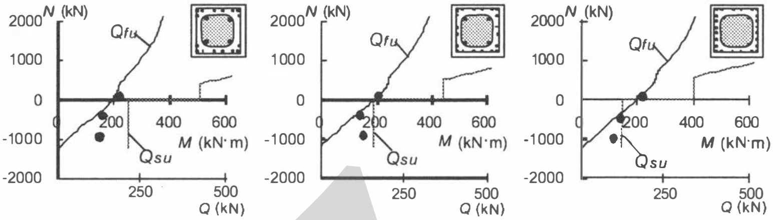

Fig.3 Axial force-ultimate strength curves and maximum values (Shear span 1200mm)

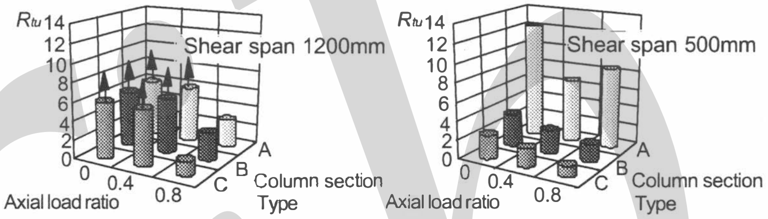

Fig.4 Limit deflection angle of column

3 ELASTO-PLASTIC ANALYSIS

A strain-compatibility is assumed, and the relation between moment- rotation angle is calculated according to the fiber model. Fig.5 shows the relationships between moment M and rotation angle of column base θ_B. The following became clear by the comparison between the experiment and the analysis. For the amount of the anchor bolt is large, the Analysis well predicts the experimental results. But, for the amount of the main reinforcement is large, Hysteresis loops are spindle shaped too much with an analytical result. This is because the analysis dose not take into consideration the deterioration in bond strength of main reinforcement. However, in other words if deterioration in bond strength of main reinforcement can be prevented, it is thought that to increase the amount of main reinforcement can improve the energy dissipation capacity of column more than the amount of the anchor bolt is increased.

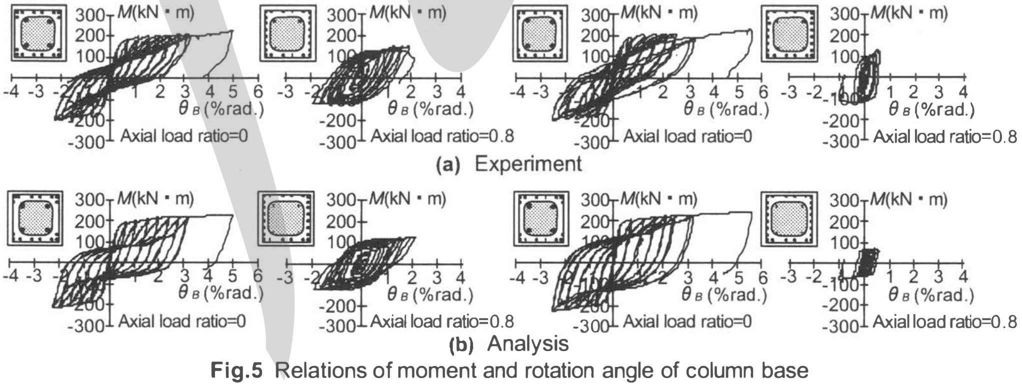

Fig.5 Relations of moment and rotation angle of column base

REFERENCES

[1] AIJ, Editorial committee for the report on the Hanshin-Awaji earthquake disaster:report on the Hanshin-awaji earthquake disaster, Building series volume 2, structural damage to steel reinforced concrete buildings, august, 1998, pp.93-502

[2] AIJ: Standard for structural calculation of steel reinforced concrete structures, January 2001

FLEXURAL STRENGTH OF FRP-CONFINED RC COLUMNS

Roberto Realfonzo Andrea Prota Gaetano Manfredi
Department of Structural Analysis and Design
School of Engineering, University of Naples "Federico II"
Naples, ITALY

Marisa Pecce
Department of Engineering, School of Engineering, University of Sannio
Benevento, ITALY

Keywords: confinement, flexural strength, FRP, modeling, RC columns.

1 INTRODUCTION

Experimental tests on cylindrical specimens have underlined the effectiveness of FRP-based confinement systems; tests conducted on cubic samples have also pointed out the reduction of the confinement effectiveness due to the high stress concentration in the corners; it has been observed that such effect becomes lower as the corner radius increases (i.e., cubic tends to cylindrical). Along with experimental work, some researchers have attempted to develop numerical models able to predict the behavior of FRP confined concrete. The present paper focuses on the behavior of RC members subjected to axial load plus bending and confined by composite materials. It presents a model that allows computing the flexural capacity of such elements and evaluating the moment curvature curve for a given square or rectangular cross section under a fixed axial load. The analytical results are compared to experimental data obtained by tests on RC columns confined with steel hoops and FRP.

2 MODELLING OF THE CROSS-SECTION

The procedure herein presented is capable of providing the moment-curvature relationship for any square or rectangular cross-section confined with steel hoops and FRP laminates, and subjected to axial load (even zero) and bending. An equivalent cross-section is considered and parabolic areas are substituted by equivalent rectangular areas. Such approach allows simplifying the problem from a numerical standpoint and provides important advantages for the discretization of the cross-section, which is divided into rectangular strips having height equal to $\delta = H/n$ (n equal to the number of strips). Depending on its position, the strip is related to different constitutive relationships for concrete. In the general case of FRP-confined member, three regions are defined with concrete unconfined in the exterior portion, confined with FRP in the intermediate region (Spoelstra and Monti model [2]) or confined with both steel hoops and FRP in the core (superposition of effects modeled by Mander et al. [1] and Spoelstra and Monti [2]) (Figure 1). When only steel hoops are present, an exterior portion of unconfined concrete and an interior steel-confined core (Mander et al. [1]) are considered.

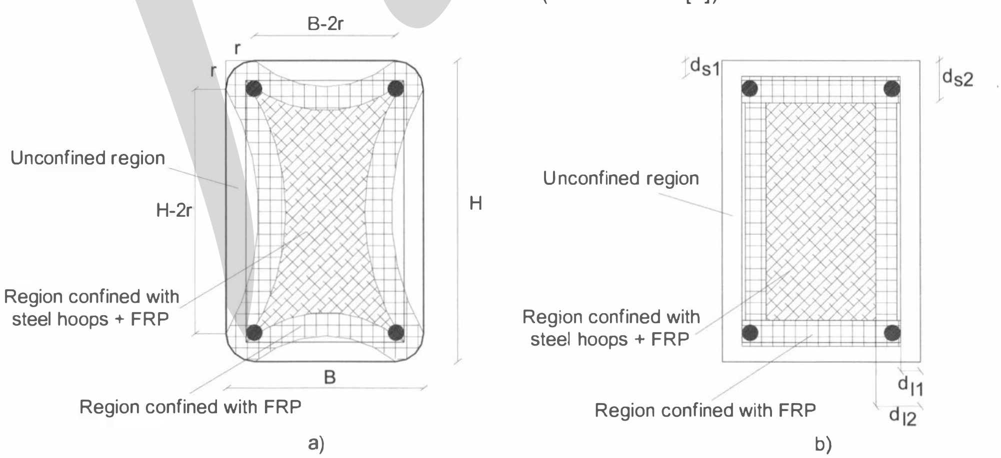

Figure 1. Confinement with Steel Hoops plus FRP Laminates: Actual (a) vs. Modeled (b) Areas

3 EXPERIMENTAL-THEORETICAL COMPARISON

The reliability of the proposed model was assessed by comparing its theoretical predictions with experimental outcomes from tests on 37 square columns subjected to axial load plus bending. Theoretical-experimental comparisons are depicted in Figure 2 in terms of theoretical versus experimental ultimate moment. On both axis, the moment has been divided by the product of the section basis, b, times the square of the effective depth, h. A parametric analysis was also performed by applying the model for the same rectangular cross-section under different axial load ratios. The outcomes of the simulation are depicted in Figure 3 for two values of the axial load ratio.

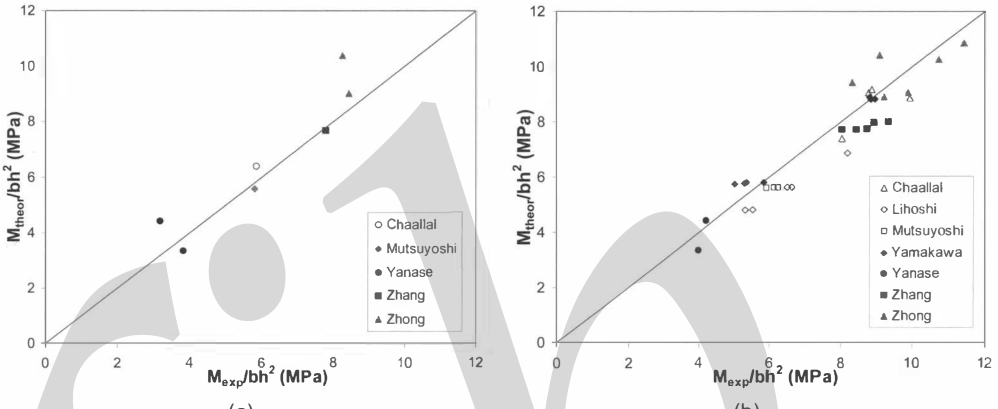

Figure 2. Theoretical vs. Experimental Flexural Capacity: Confinement with Steel Hoops (a) and with Steel Hoops plus FRP Laminates (b)

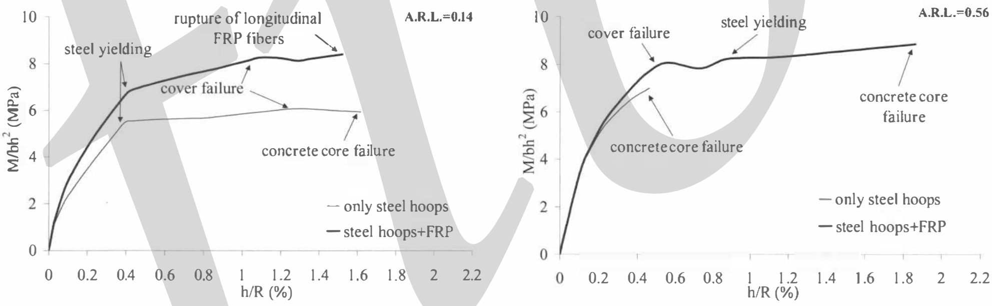

Figure 3. Normalized Moment-Curvature Relationships at Different Axial Load Ratios

4 CONCLUSIVE REMARKS

A numerical procedure based on the strip model has been proposed for the capacity assessment of RC columns externally confined with FRP laminates. Such procedure transforms the actual into an equivalent cross-section characterized by differently confined concrete regions (unconfined, confined only with FRP or confined with both steel hoops and FRP). This approach allows for a lighter discretization and then reduces computational efforts. The experimental-theoretical comparison showed that the proposed model provides strength predictions that are more reliable for FRP-confined columns than for simply tied elements. Numerical simulations confirmed the effectiveness of FRP confining systems for boosting both strength and sectional ductility (i.e., curvature) of RC columns.

REFERENCES

[1] Mander J.B., Priestley M.J.N. and Park R. : Theoretical stress-strain model for confined concrete. ASCE Journal of Structural Engineering, Vol.114, No. 8, pp. 1824-1826, 1988
[2] Spoelstra M.R. and Monti G. : FRP-confined concrete model. Journal of Composites for Construction, ASCE, Vol. 3, No. 3, pp. 143-150, 1999

EXTERNALLY REINFORCED CONCRETE BEAMS -- AN INNOVATIVE FORM OF COMPOSITE CONSTRUCTION

Prof. Franz A. Zahn, Ph.D. Prof. Dr.-Ing. Wolfgang Francke
Fachhochschule Konstanz, GERMANY

Key words: composite construction, experimental investigation, ductile behaviour

1 INTRODUCTION

Externally reinforced concrete beams consist of a folded steel sheet casing filled with concrete. The steel casing acts as form work during construction, and after hardening of the concrete it resists tension forces transferred by bond stresses. Neither reinforcing bars nor stirrups are required in principle, except that a small amount may be provided for fire rating. Fig. 1 shows a typical cross section of an externally reinforced concrete T-beam. The steel sheet is shaped to provide a ledge to support prefabricated concrete slab elements or profiled steel sheets for composite slab types. Holes punched into the top edges of the steel sheet, act as concrete dowel shear connectors (`Perfobond´ principle), so that the concrete slab acts as compression flange. The steel section is folded from a single sheet.

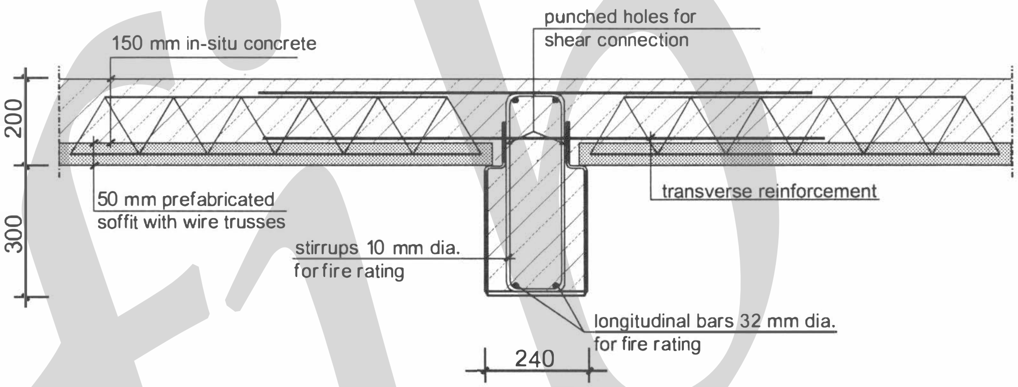

Fig. 1: Typical cross-section of externally reinforced concrete T-beam

Both simply supported and continuous beams and frames can be constructed in externally reinforced concrete, the columns being constructed from concrete filled structural steel hollow sections (RHS). The folded steel sheet of the beam is placed into a pocket cut into the face of the RHS. For continuous beams, negative moment capacity is provided by reinforcing bars placed in the concrete slab. Fire rating can be provided by additional reinforcing bars (longitudinal and stirrups) placed inside the steel casing. The design of externally reinforced concrete beams is as for conventional composite construction, applying the well known principles including the assumption of rigid bond between concrete and steel casing.

2 EXPERIMENTAL INVESTIGATIONS AND COMPARISON WITH ANALYTICAL RESULTS

In order to investigate the performance of externally reinforced concrete beams and their connections to concrete filled RHS columns a series of tests was carried out on half scale models representing the construction state and the final (composite) state. These tests are reported in [1] and [2]. First, a simply supported beam was tested in the construction state, i.e. when the steel sheet casing acts alone carrying the weight of the fresh concrete. Since the steel casing is an open profile it possesses very little torsional stiffness which is expected to result in rather large deformations of edge beams during the construction state. In order to investigate this problem, a half scale steel casing was supported at its ends in pockets cut into RHS column stubs and loaded excentrically along the ledge of the steel casing. The clear span was 2.70 m and no intermediate support was provided. The measured deformations were compared with the corresponding values obtained from a finite element analysis of the test beam [3]. The measured and calculated values agreed well and showed that the deformations were surprisingly low. The mid span twisting angle was only 0.7° under the maximum applied load of 3.2 kN/m. However, a finite element analysis of a 6.0 m span edge beam indicated that then one central prop would be required to prevent lateral torsional buckling of the steel casing.

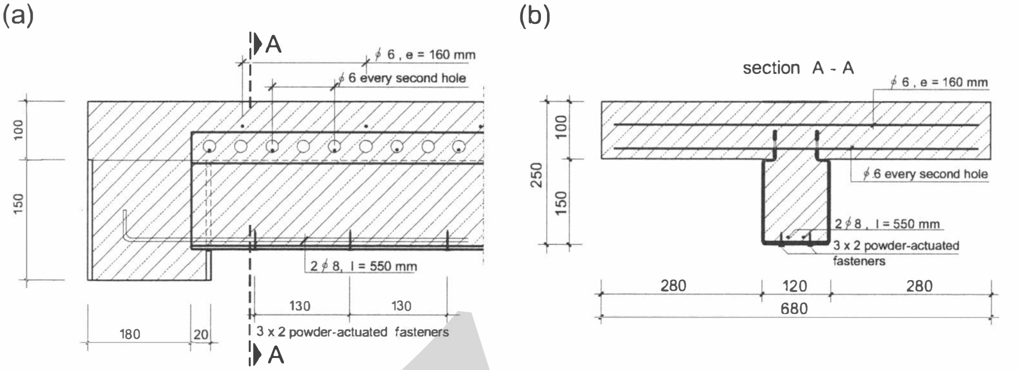

Fig. 2: Simply supported T-beam for ultimate load test: (a) longitudinal section with support details, (b) cross section

The steel casing from the torsion test was then used to construct a simply supported composite T-beam with a clear span of 2.70 m. The cross section and the detail of the end support are shown in Fig. 2. The end supports consisted of RHS column stubs that were filled with concrete together with the beam and flange. Longitudinal reinforcement bars were only placed at the ends of the beam. Two point loads spaced at 420 mm were applied at the centre of the span. The load was applied in several steps of increasing level, up to imminent failure of the beam in concrete compression at the top of the flange near mid span. Fig. 3 shows the load – deflection curves recorded during the test. The extremely ductile behaviour of the test beam is evident from the long post-yield load bearing capacity. The distribution of the steel strains in the bottom flange indicated that there was full bond between steel casing and concrete. From the shear strains measured using electrical resistance strain gauges placed on the webs near the supports the shear force carried by the steel casing could be back-calculated. It was found that the steel casing carried only about 40 % of the total shear force, indicating that concrete mechanisms represent a considerable reserve in shear strength of externally reinforced beams.

The third test specimen was a balanced cantilever beam to simulate the behaviour of continuous externally reinforced concrete T-beams in the negative moment region. The negative moment capacity is provided by reinforcing bars placed in the top flange. Two identical point loads were applied near the cantilever ends. The load was increased stepwise up to failure of the beam by the breaking of two longitudinal reinforcing bars. The post-yield load carrying capacity of the balanced cantilever test beam was excellent, and a considerable part of the total shear force was resisted by concrete mechanisms.

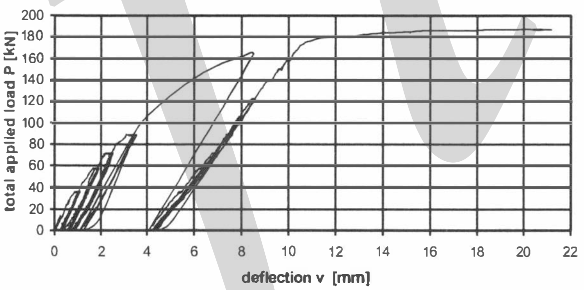

Fig. 3: Load-deflection-diagram for the simply supported T-beam

REFERENCES

[1] Stefan Wachter: Experimentelle Untersuchungen an Extern Bewehrten Betonunterzügen – Teil Biegebalken; Diploma Thesis at Fachhochschule Konstanz, 04.09.2000 (not published)

[2] Stefan Wauer: Experimentelle Untersuchungen an Extern Bewehrten Betonunterzügen – Teil Waagbalken; Diploma Thesis at Fachhochschule Konstanz, 12.09.2000 (not published)

[3] Jürgen Heiss: Rechnerische Traglastuntersuchungen von extern bewehrten Betonunterzügen mit dem FEM-Programm ANSYS; Diploma Thesis at Fachhochschule Konstanz, 20.09.2000 (not published)

EXPERIMENTAL STUDY ON A COMPOSITE GIRDER WITH A CONCRETE FILLED STEEL TUBE

Yoshihiro Hishiki
Supervisory Research Engineer
Kajima Corporation
Tokyo, Japan

Tomonori Tominaga
Senior Research Engineer
Nippon Steel Corporation
Chiba, Japan

Shinichi Yamanobe
Chief Research Engineer
Kajima Corporation
Tokyo, Japan

Kentaro Yoshida
Research Engineer
Kajima Corporation
Tokyo, Japan

Keywords: composite deck; cable-stayed bridge; concrete filled steel tubular; static bending test, fiber model analysis

1. INTRODUCTION AND PURPOSE OF THE TEST

In recent years, interest has grown in composite structures or mixed structures (hereafter called "hybrid structures ") from the viewpoint of improvement and rationalization of structural performance and cost reduction that can be achieved through the improvement of construction efficiency. The field of bridge engineering is no exception. New types of composite bridge structures, such as hybrid cable-stayed bridges and hybrid extradosed bridges for long-span applications and hybrid truss bridges and corrugated steel web bridges for medium-span applications, have been designed and constructed, and active research and development is being carried out in the field of hybrid bridge design .

The authors paid attention to the structural characteristics, particularly high axial compressive strength, of concrete-filled steel tubes (CFT), which have conventionally been used mainly as columns. To use CFTs as cable-stayed bridge girders, in which axial force is dominant, the a uthors have been working on the development of concrete-filled steel tube girders (CFT composite girders). [1] Figure 1 shows CFTs-cable-stayed bridge girders.

CFT composite girders are already in use in railway viaduct bridges, and have been subjected t o member bending tests in connection with that application. [2] Since, however, research in this area aims to apply CFTs to girder bridges in which axial forces do not occur, existing CFT composite girders cannot be applied to structures in which axial for ce is dominant, such as cable-stayed bridge girders. With a view to determining the ultimate strength and deformation properties of CFT composite girders used in cable-stayed bridges, therefore, a bending test on axially loaded CFT composite girders was conducted and a simulation of the deformation properties of test specimens was executed by use of a fiber model, and proposed ultimate strength equations. Figure 2 shows cross section of test specimen.

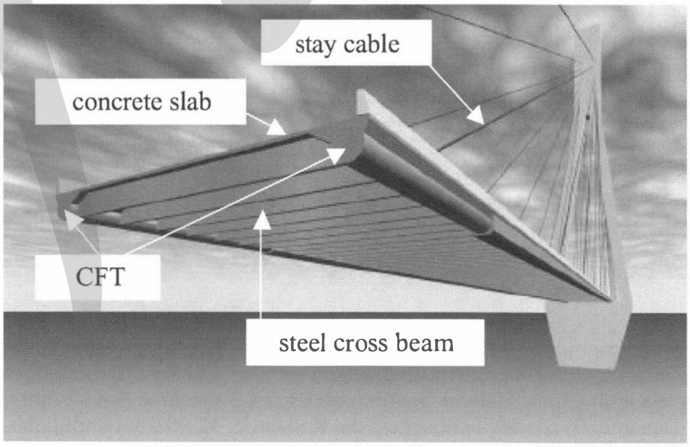

Fig.1 CFT composite girders

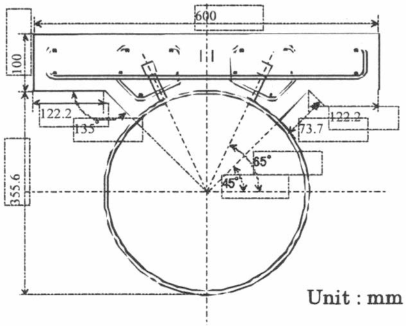

Fig.2 Cross section of test specimen

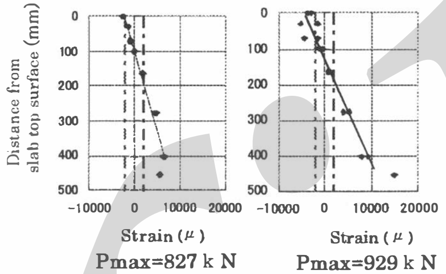

(a) No.1 specimen (b) No.2 specimen

Fig.3 Strain distribution within cross section

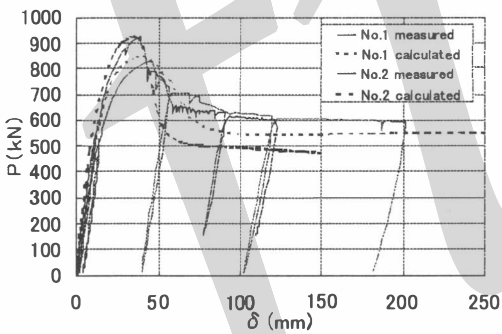

Fig.4 Load-displacement curve

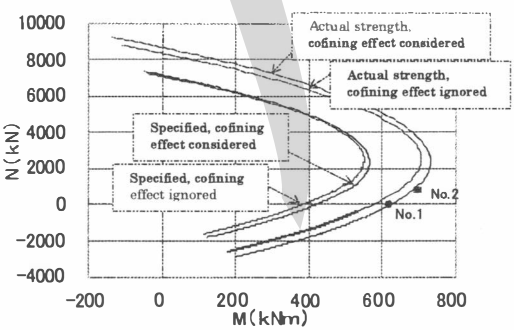

Fig.5 Nu-Mu curves for test specimens

2. CONCLUSION

Findings of this study can be summarized as follows:

(1) The CFT composite girder specimens retained stiffness and ultimate load levels that were higher than those of CFT girders, regardless of the presence or absence of axial force. The test specimens showed that they retained large deformation capacity, even after the ultimate strength was reached, by changing to CFT girder structures.

(2) By the time the ultimate load was reached, the CFT composite girder, except the neutral axis zone, had mostly yielded, indicating that the girder was in a perfectly plastic state. Figure 2 shows cross section of test specimen. Figure 3 shows strain distribution within cross section.

(3) The deformation properties of a CFT composite girder can be expressed fairly accurately with a fiber model by introducing a σ- ε model that takes into consideration the confining effect of the steel tube and the filling concrete. Figure 4 shows load -displacement curve.

(4) CFT composite girder ultimate strength equations based on the perfect plasticity theory and a stress model that takes the confining effect of the steel tube into consideration have been proposed. Comparison of ultimate strengths calculated from the proposed equations and measured ultimate strengths confirmed accuracy of the proposed equations. Application to cases involving axial forces greater than the force range covered in the test, however, requires further study. Figure 5 shows Nu -Mu curves for test specimens.

REFERRENCES

[1] Okimoto, M., Tominaga T., Hishiki, Y. and Furuichi, K.: "Long -span composite cable-stayed bridge with new hybrid girder," IABSE SYMPOSIUM, pp. 149-154, 1998.

[2] Hosaka, T., Nakamura, S. and Nishiumi, K.: "An experimental study on flexural strength of steel tube girder and shear connection with reinforced concrete slab" (in Japanese), JSCE Journal of Structural Engineering, Vol. 43A, pp. 1301-1312, 1997.

INNOVATIVE COMPOSITE BRIDGE SYSTEM

Kazunori Minotani
PC Bridge Company
Limited, Japan

Aaron Yakel
Research Associate
Civil Engineering Department
University of Nebraska
Lincoln, Nebraska, U.S.A.

Atorod Azizinamini
Professor of Civil Engineering
Civil Engineering Department
University of Nebraska
Lincoln, Nebraska, U.S.A.

Keywords: Composite bridge system, Concrete filled steel tube, Flexural loading test

1 INTRODUCTION

Locating concrete or steel within a section to efficiently utilize positive attributes of each material allows composite members to structurally dominate those constructed solely of either material. Coupling steel advantages of high tensile strength and ductility with the low cost compressive strength of concrete results in highly efficient structures and allows for innovative shapes limited only by the imagination.

Therefore, a research project entitled "Development of Innovative Bridge System" has been undertaken. Of particular interest is the replacement of currently deficient structures. The primary criteria for bridges in this investigation include a demand for high durability, simplified construction, and reduction of cost. In order to develop a new bridge system, several motivations were given. The target span was selected in the short to intermediate range to satisfy the demand of the construction market.

This paper describes a concept of innovative bridge construction with the results based on the analysis, design and experimental work.

2 CONCEPT OF DESIGNED SECTION

Closed steel sections were chosen as the main flexural members of the new bridge system. In particular, the shape experimentally investigated was a round tube. A closed steel section provides high torsional stiffness and lateral stiffness compared with conventional steel I sections. The level of lateral stiffness could permit elimination of cross frames. Although local buckling is a particular problem of thin steel members, filling the section with concrete will prevent local buckling of the tube wall, eliminating the interior stiffeners and diaphragms commonly found in box girders. The concrete filling would be pumped into the tube once the tube was set in place, thus requiring smaller equipment. Reinforcement is set in the bottom area of the section so that the internal concrete will behave as a reinforced concrete beam. Additionally, the use of a hollow void can be used to reduce weight. Therefore, a concrete filled closed steel section was adapted to this challenge research project.

One of the keys of the system is that the concrete filling inside the tube will act as a reinforced concrete beam to carry the dead load of the deck pour, while the steel wall of the tube and deck carry additional live load as composite beam.

3 TEST SPECIMEN

A flexural loading test was carried out to confirm the capacity of the designed section as structural member and observe the actual behavior under loading. The comparison to the analysis prediction of load-deflection was a main objective of this experimental test. The test specimen was simply supported with a span of 7800 mm (26 feet). Steel tube was 355.6 mm (14 inches) outer diameter and 9.5 mm (3/8 inches) thickness. Contained inside the tube were concrete, deformed bars, and a void. The void was made from Sched-40 PVC. Three longitudinal reinforcement bars were arranged with 25.4 mm (1 inch) clear cover from the surface of the steel. The section details are shown in figure 1.

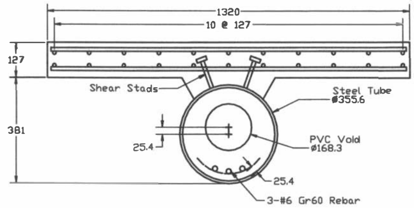

Fig. 1 Cross Section of Test Specimen

4 EXPERIMENTAL TESTING

The specimen tested as a simply supported beam and subjected to a concentrate load at the center of the span. Figure 2 shows the set-up of test specimen and the loading system. Linear variable potentiometers were used to measure displacements. Spring pots were attached to the end of the specimen to monitor the deflection of the concrete filling relative to the steel tube. Bondable strain gauges and embedment strain gauges were also utilized and placed at various locations on the surfaces of steel tube, on the reinforcement bars and within the concrete both inside the tube and within the deck to monitor to the distribution of strain throughout the test. The load was applied in stages with a short pause during each stage for data collection. Once the specimen began yielding the increment of arc length along the load deflection curve was held approximately constant. The specimen was loaded until collapse to obtain the ultimate capacity.

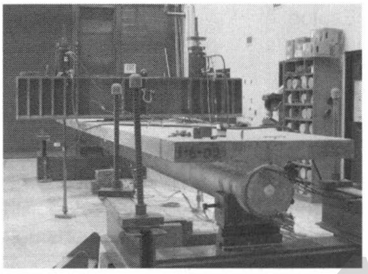

Fig. 2 Flexural Loading Test

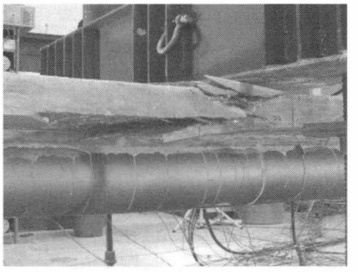

Fig. 3 Crushed Concrete at the lab

5 TEST RESULT

The specimen behaved quite well under load. Although a slight deviation is observable, the load deflection curve was relatively linear until around 622.7 kN (140 kips). From the analysis, it was observed that the bottom of the steel tube was expected to yield when the load was approximately equal to this load. This was confirmed by the strain gauges attached to the bottom of the tube. The ultimate failure mode was a localized crushing at the top of the concrete slab near midspan. Figure 3 shows the crushed concrete slab after failure. It was observed from the test data in figure 4 that the ultimate flexural strength of the test specimen had reached about 783 kN (176 kips) and the deflection at that time was about 96 mm (3.8 in). Also shown in the figure is the predicted load deflection curve. It can be seen that the analysis did a decent job predicting the actual behavior

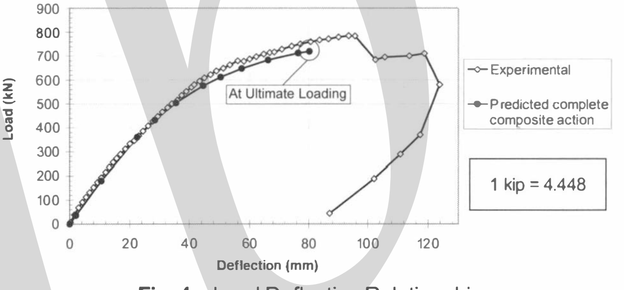

Fig. 4 Load-Deflection Relationship

6 CONCLUSIONS

The following conclusions were obtained from the results of the analysis and the experimental test of the bridge system being considered.

(1) The test specimen exceeded the most ambitious estimation of strength available. Despite the absence of internal shear connectors, it appears as though all elements of the system, deck, tube, concrete core, and reinforcement behaved nearly compositely. This has been confirmation utilizing the strain data and the fact there was no displacement of the concrete core relative to the steel tube at the ends.

(2) The system displayed good ductility with an ultimate deflection to span ratio of 1/85. No unexpected behavior was observed and the mode of failure was similar to the failure mode of composite slab on I-girder systems.

(3) Although the fabrication of the core consisting of the PVC and reinforcement was awkward, this was attributed to the fact that it was a first time experience using limited resources. Already from this one experience, a number of simplifying procedures have been devised. Assuredly, if the system were to be used on a larger scale the assembly of the core would become trivial.

(4) Proper pumping technique and selection of concrete slump provided a good filling inside the steel tube. It was expected that the concrete was almost definitely filled inside of the steel tube without gap from the result of the comparison study between test result and the analysis. This has been tentatively confirmed using ultrasound techniques looking for any variances in the return which could indicate a void. Further dissection of the specimen will provide confirmation.

The testing conducted indicates that the proposed bridge system has the structural capability, both capacity and mode of failure to be applied to an actual structure.

A NEW KIND OF PRESTRESSED COMPOSITE RAILWAY BRIDGE DECK

[1]Stéphanie Staquet
[1]Department of Civil Engineering
University of Brussels, BELGIUM

[1]Bernard Espion

[1,2]Henri Detandt
[2]Bridge Department
Tucrail s.a., BELGIUM

1 INTRODUCTION

A new kind of bridge deck has been developed recently in Belgium for the replacement of old steel railway bridges with moderate spans and for the construction of multi-spans viaducts for the new high speed lines. Up to now, these bridge decks have been used for simply supported spans up to 26 m.

The bridge decks are prefabricated in workshops and transported by train to the construction site where they are placed on their supports by cranes. These composite steel-concrete structures belong to the trough type with U shaped cross section (Figure 1). The two steel (hot-rolled or welded) I-girders are curved in plant to produce an initial camber. Then, the construction begins in the workshop by applying two local loads on each steel girder at ¼ and ¾ of the span in order to straighten the girders and to obtain at this stage a camber equal to zero. The stress level in the steel girders during this preflexion phase is limited to 80% of the yield strength. These two girders will be parts of the webs of the bridge. Then, the bottom slab of the deck is constructed: reinforcing bars (transversally) and naked tendons (longitudinally) are disposed in the space which will be filled by the concrete bottom slab (slab depth:0.25m). The bottom slab is then concreted. The bridge decks are sometimes heated at 45°C during the first day after casting. At two (for the decks with heat treatment) or three (for the non heated ones) days of age, the bottom slab is prestressed by releasing the preflexion of the steel girders and by transferring the prestressing force from the tendons. The remaining naked (upper) parts of the steel girders are enclosed in a 2nd phase concrete to complete the webs of the deck. This kind of deck has been designed, among other reasons, to minimize construction depth.

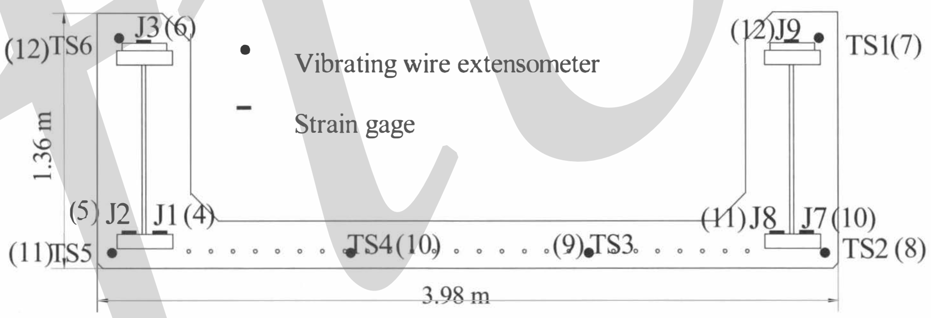

Fig.1 Trough shaped cross section of the bridge with location of the extensometers at mid-span (TSi and Ji) and at the third of the span (between ()).

Prestressing is transferred at an early age (2 or 3 days) and at high stress levels (around 0.5 $f_{c,cube}$) on high strength concrete ($f_{c,cube}$ = 45MPa at the age of transfer). The composite character of the construction, with the association of the steel of the girders (S355), the steel of the prestressing tendons (grade 1840 MPa) and the two-phases concreting should also be noted. All this induces theoretically a significant time-dependent redistribution of internal stresses between steel and concrete, thereby reducing the prestressing of the slab. Since the behaviour in service of the bridge is a prime consideration, design should ensure that no cracking occurs in the bottom slab.

Up to 300 of these bridge decks have now been constructed since ten years and seem to perform according to expectations. It is now considered to apply this construction method for the erection of continuous bridges (with larger spans) by connecting simply supported decks on their supports. It is known that this kind of construction will induce an additional and strong time-dependent redistribution of internal forces within the structure. The method used until now to design these bridge decks is a simple classical computation method with a variable modulus. But it is known that this method yields the exact solution of the time-dependent problem in the case of pure creep only with no stress redistribution. Its application to this problem gives only approximate results and it was felt that an in-depth understanding of the influence of the concrete time-dependent effects in this kind of composite structures is needed before proceeding with the design of statically indeterminate bridges. This research is intended to provide experimental data to calibrate more advanced computational models.

2 LABORATORY AND IN SITU INVESTIGATIONS

In our laboratory, an extensive experimental program is conducted in order to evaluate finely the properties of the concrete and provide data for an enhanced modelling of the time-dependent behaviour of the bridge deck. In particular, creep and shrinkage tests on cylinders (with diameter 15 cm and height 60 cm) are performed according to the recommendations proposed by RILEM TC 107 under drying (20°C, 53 % relative humidity) and sealed (20°C) conditions [1].

A simply supported bridge deck with 26 m span and the cross section illustrated on figure 1 (belonging to a viaduct constructed at the entrance of Brussels South Station [2]) has been instrumented at the third of the span and at mid span with resistive strain gages on the steel girders and vibrating wire extensometers embedded in the concrete (figure 1). For each instrumented section, we have placed two vibrating wire extensometers at 8 cm below the top section fiber and four others at 5 cm above the bottom section fiber. Concerning the strain gages, we have bonded four of them on the bottom flanges of the girders and two others on the upper flange of the girders. Strains have been recorded since the construction of the deck in June 2000. The reference (t=0) of the strain measurements is taken just before the preflexion of both steel girders.

3 CONCLUSIONS

Creep and shrinkage tests carried out in our laboratory show that after 1½ year, strains in the concrete C60 of the bridge deck are well reproduced by the CEB-MC90 model code (1999) for the autogeneous shrinkage and the fundamental creep and by both versions of it (1993 and 1999) for the total creep and shrinkage [1].

For the bridge deck, the measured strain values and the strain values computed within the framework of a rough pseudo-elastic analysis with a variable elastic modulus are quite different from measured strains, in particular 1½ year after construction. The values computed with the step-by-step method show a better agreement with the measured strains than the values computed with the age adjusted effective modulus method. The step-by-step method evaluates more finely the time-dependent redistribution between steel and concrete than the age adjusted effective modulus method. However, these methods have some limitations. Besides the usual assumptions of the age adjusted effective modulus method concerning the numerical evaluation of the hereditary integral of the principle of superposition, we would like to underline : 1) the average section behaviour hypothesis in relation with the desiccation which implies that the relative humidity remains constant whereas the bridge deck goes through a variable history from the point of view of its waterproofing;2) the linearity hypothesis towards the applied stresses level which does not agree with the applied prestressing level. The prestressing is applied at a very early age (2 days) and at a high stresses level (50% of concrete strength at this age).

This justifies our initial intention to evaluate more finely the time-dependent effects of concrete in such composite (and rather complex) structures with variable loading history. The next numerical simulation will have to take into account the evolution of the bridge deck desiccation with time.

4 REFERENCES

[1] Staquet S., Detandt H., Espion B., Time-dependent behaviour of a railway prestressed composite bridge deck, Proceedings of the international conference Concreep-6@MIT, F.-J. Ulm, Z.P. Bažant & F.H. Wittmann editors, Elsevier, pp.373-378, 2001

[2] Couchard I., Detandt H., Entrance of the high speed line in the Brussels South Station, Proceedings of the 16th IABSE Congress, Lucerne, Switzerland, 2000

THE APPLICATION OF A SEMI CIRCULAR CELL SHAPED STEEL-CONCRETE SANDWICH STRUCTURE TO A COFFERDAM IN GREAT DEPTH UNDERWATER

Syunsuke Sugimoto
International Division,
Toyo Construction Co., Ltd., JAPAN

Osayuki Hashimoto
Deputy Director Okutadami-Otori,Hydro Project Construction Office,Electric Power Development Co., Ltd., JAPAN

Takashige Taji
Fukushima Office, Tohoku Branchi,
Toyo Construction Co., Ltd., JAPAN

Eiji Sueoka
Technical Research Institute,
Toyo Construction Co., Ltd., JAPAN

Kazuya Gouda
Civil Design Division
Toyo Construction Co., Ltd., JAPAN

Noboru Sakata
Kajima Technical Research Institute Corporation
JAPAN

Keywords : cofferdam, lateral pressure, antiwashout underwater concrete, steel-concrete sandwich structure

1 OUTLINE

In an extension project for Okutadami Power Plant , it was nessesary to construct a cofferdam under water for the intake construction. Accordingly, a semicircular temporary cofferdam of steel-concrete sandwich construction was planned and constructed. Such a structure was selected to permit construction and demolition in short periods while withstanding high water pressure at a depth of 50 m. The general drawings of the cofferdam are shown in Fig. 1.This paper reports on the proportioning of antiwashout underwater concrete to be filled in the cellular sheet piles, lateral pressure testing to derive detailed lateral pressure equations necessary for structural design and construction control, and results of lateral pressure measurement during construction.

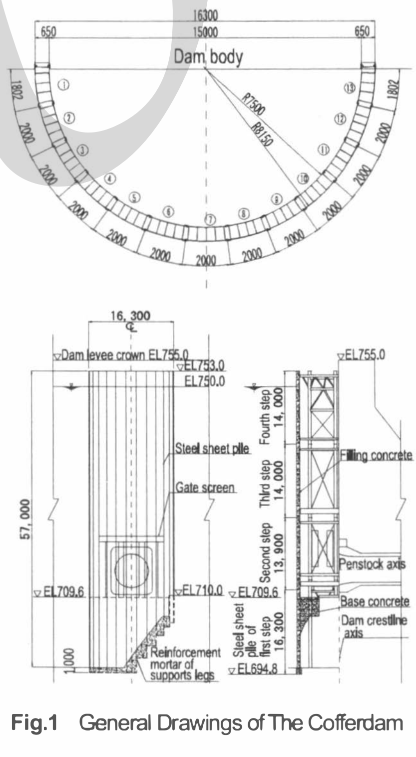

Fig.1 General Drawings of The Cofferdam

2 MIXTURE PROPORTIONS OF ANTIWASHOUT UNDERWATER CONCRETE

Antiwashout underwater concrete was adopted for concrete to be filled in the box sheet piles, the body of the cofferdam, to ensure underwater concreting. Superplasticizer and nonfreezing admixture were added to retain the slump flow and shorten the initial setting time. Mixture proportions of this concrete are given in Table 1.

3 LATERAL PRESSURE TESTING

Lateral pressure tests were conducted to determine precise lateral pressure equations for the mixture proportions determined from the performance requirements of concrete (Table 1). The test method is as follows: Place a steel column formwork measuring 0.4 by 0.4 by 3 m in a water tank. While measuring the lateral pressure, place concrete up to a height of 3 m using a tremie at specified intervals of 1 m and 2 m. Then place 16 weights, each weighing 170 kg, one after another at intervals to assume a total placing height of 19 m. Ts and a in lateral pressure estimation equations (1) and (2) were determined from measurement data.

Table 1 Mixture Proportions of Concrete

W/P (%)	s/a (%)	Unit Weight (kg/m^3) W	C	F	S	G	UW	P×wt% SP	PS
44	40	220	425	75	629	924	2.53	2.0	1.0

P=C+F F : Flyash UW : AntiwashoutAdmixture
SP : Superplasticizer PS : Nonfreezer

When t≤Ts, $P = (\gamma c - \gamma w) \cdot V \cdot (t - t')$ (1)

When t>Ts, $= \{1 - a \cdot (t - Ts)\} \cdot \gamma c \cdot V \cdot (t - t') - \gamma w \cdot V \cdot (t - t')$ (2)

where P = lateral pressure (kN/m^2) t = time after mixing (hr) V = placing rate (m/hr)
γc = density of concrete(kN/m^3) γw = density of water (kN/m^3)
Ts = time to the beginning of reduction in lateral pressure coefficient (hr)
a = lateral pressure coefficient (1/hr) t' = time from mixing to placing (hr)

4 CONSTRUCTION

4.1 Construction method

The construction flow of the cofferdam is shown in Fig. 2. After completing the erection of cellular sheet piles, antiwashout underwater concrete (filling concrete) was filled in the sheet piles. A placing rate of 1 m/hr or less was adopted based on the investigation of the sheet pile stress under lateral pressure using the experimentally obtained lateral pressure equations. Concrete was placed with the height of a single concreting layer being limited to 1 m. Since concrete had to be filled into narrow spaces with a clearance of 65 cm through web openings in the circumferential directions, a placing hopper that can be inserted in the spaces was fabricated to achieve this from the aspect of preventing segregation. The slump flow of filling concrete are shown in Fig. 3.

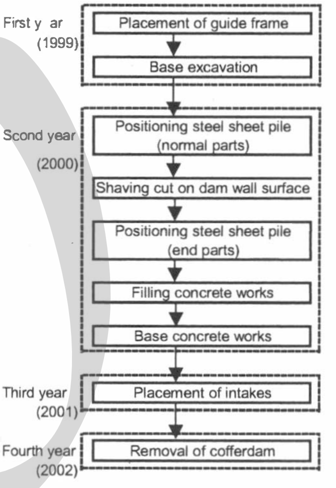

Fig.2 Construction Flow

4.2 Lateral pressure measurement

The placement control of concrete was carried out while logging the real-time lateral pressure. Figure 4 shows the relationship between the placing rate and the peak lateral pressure in the field in comparison with the peak lateral pressure determined by the lateral pressure equations. The equations obtained from lateral pressure testing are found to express the time-related characteristics of converted lateral pressure.

5 CONCLUSION

By examination of properties of antiwashout underwater concrete including lateral pressure properties and by conducting measurement-monitoring construction control using the lateral pressure estimation equations, concrete was filled safely and efficiently in cellular steel sheet piles of a semicircular steel-concrete sandwich structure.

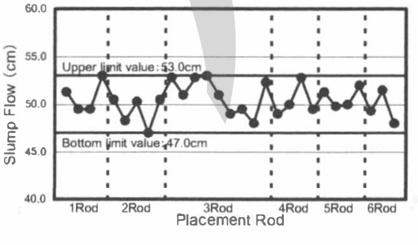

Fig.3 Test Results of Slump Flow

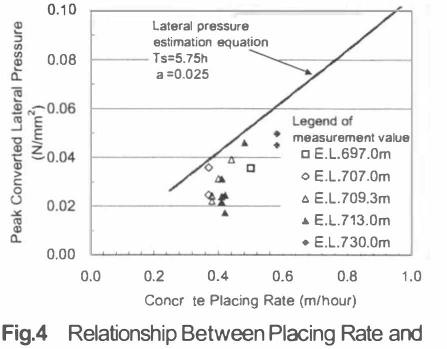

Fig.4 Relationship Between Placing Rate and Peak Lateral Pressure

DESIGN OF THE NEW TYPE BREAKWATER USING STEEL-CONCRETE COMPOSITE CYLINDRICAL SHELL PANEL

Yoshiki Sukeyasu*, Susumu Matsuno*, Setsuo Iwata*, Hiroshi Tanaka* and Hiroshi Yokota**

* Hitachi Zosen Corporation
** Independent Administrative Institution Port and Airport Research Institute

Keywords: breakwater, cylindrically curved steel-concrete composite panel, perfobond rib, rigidity, ultimate strength

1 INTRODUCTION

Breakwater caissons using steel-concrete composite panels are widely used instead of conventional reinforced concrete breakwaters, because of their higher structural performances, lightweight, and rapid fabrication [1]. For rationalization of structural configuration of composite caissons, cylindrically curved panels are applied to the caissons as shown in Fig.1. Their applicability is ranging from shallow to deep sea [2]. The cylindrically curved shape is effective to increase the rigidity and ultimate strength. The application of the cylindrically curved panel realizes the easy design and cheap construction.

This paper proposes three new design concepts for the breakwaters with cylindrically curved steel-concrete composite panels as shown in Fig.2. The first concept is utilization of perfobond rib plates as shear connectors between reinforced concrete and a steel plate. The second one is the inventive application of composite cylindrically curved panels to walls of breakwater caissons including footings. The third one is the a new idea in designing bottom slabs made of steel reinforced concrete panels. These concepts were verified theoretically and experimentally. The finite element method was mainly applied to estimate stress resultants and strength properties. The prototype model test established the construction method and its experimental load tests guaranteed mechanical strength. The comprehensive studies by experiments incorporating with analyses certified the proposed design concepts.

The idea of the new breakwater showed good performances in both strength and construction. This type of caisson is useful to reduce construction cost of port and harbor facilities.

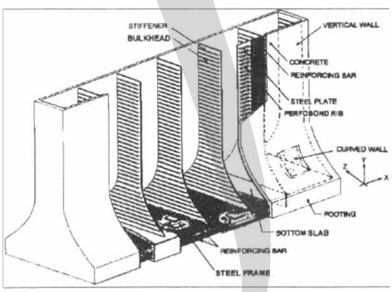

Fig.1 New type breakwater with curved composite walls

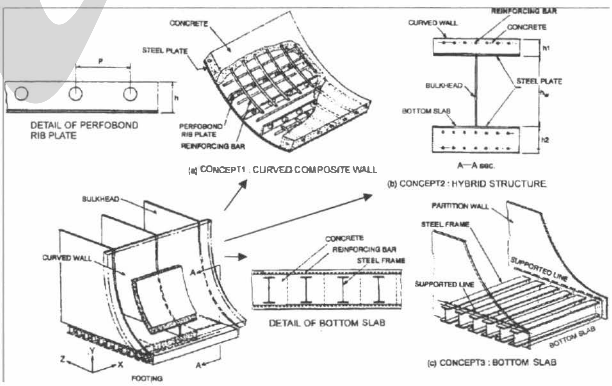

Fig.2 Design concepts for new type breakwater

2 THEORETICAL INVESTIGATIONS FOR STRUCTURAL DESIGN

2.1 Theoretical investigations for structural design of the wall

Three investigations were conducted through FEM analysis. The first investigation found that the stress due to the application of loading fluctuates smaller when the radius of curvature is larger as shown in Fig.3. The second one gave the evaluation method of the effective width featured by the following equation (1):

$$b_e = 170(rt)^{0.17} \qquad (1)$$

where r: the radius of curvature (mm) ; t: the thickness of the curved wall (mm).

The third one clarified the quantified superiorities of the curved composite panel to the conventional one: 1.3 times in ultimate strength and 5.5 times in toughness.

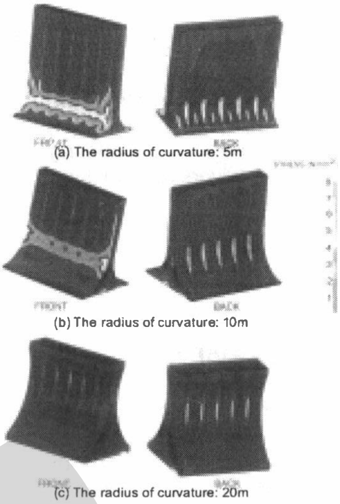

Fig.3 Distributions of maximum principal stress

2.2 Theoretical investigation for structural design of the footing

The rigidity was investigated through FEM analysis. The new type footing was generally judged to be rigid under the 10m of the footing length, although the rigidity varies with the ground reaction coefficient in the vertical direction. The judgment was based on the established method [3].

3 EXPERIMENTAL INVESTIGATIONS FOR STRUCTURAL DESIGN

Four investigations were conducted through the construction of prototype model as shown in Fig.4. The first investigation developed effective methods for cheap construction, which are featured by the perfobond rib plate and elimination of expensive press-operating process. The second one invented optimal mix proportion of concrete, which enables full compaction within the curved wall mold. The third one carefully observed shrinking strain on the curved wall concrete after the casting and no crack was detected. The approximation for shrinking strain was also formulated by the following equation (2):

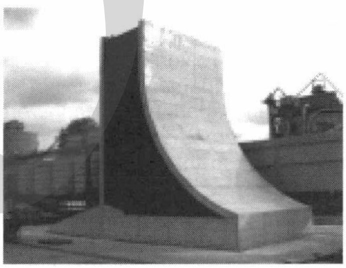

Fig.4 Complection of prototype model

$$\varepsilon'_{cs}(t,t_o) = [1-\exp\{-0.168(t-t_0)^{0.32}\}]\varepsilon'_{sh} \qquad (2)$$

where t: passing time after the concrete casting; t_0 : time when drying shrinkage starts; ε'_{sh} :convergence of shrinking strain value [4]. The fourth one verified the mechanical superiority of the curved wall to the flat one through the loading tests on prototype model.

REFERENCES

[1] Coastal Development Institute of Technology: Design Code for Composite Caisson, 1999. (In Japanese)

[2] H.Tanaka et al.: Development of a New Breakwater with the Steel-concrete Composite Cylindrical Shell Wall, The HITACHI ZOSEN TECHNICAL REVIEW, Vol.60, No.4, 2000. (In Japanese)

[3] Japan Road Association: Specifications for Highway Bridges PartVI Substructure, pp180-181, 1994. (In Japanese)

[4] Japan Society of Civil Engineers: Concrete Standard Specifications for Design, pp26-29, 1996. (In Japanese)

REINFORCED ECC - AN EVOLUTION FROM MATERIALS TO STRUCTURES

Victor C. Li
Department of Civil and Environmental Engineering
University of Michigan, U.S.A.

Gregor Fischer
Department of Civil and Environmental Engineering
University of Hawaii, U.S.A.

Keywords: ECC, composite materials, composite structures, damage tolerance, response control

1 OVERVIEW

While significant advances have been made in concrete materials and in concrete structures over the last decade, research in materials and in structural engineering are often carried out separately. As a result, opportunities in major leaps in structural performance may be missed, or research emphasis in materials development may be misguided. This paper introduces the concept of integrated structures and materials design (ISMD), which links structural design and materials design via material mechanical properties (Fig.1).

Specifically, an example of composite evolution from materials to structural systems illustrating the ISMD concept is presented, bridging the length scales associated with microstructures, composite materials and composite structures. The linking of these length scales suggests integrating composite materials design into design considerations for structures to improve their performance in terms of load-deformation response, energy absorption, deformability, structural stability, damage tolerance, construction efficiency (reinforcement detailing requirements), and rehabilitation needs. This approach is expected to benefit the safety and life-cycle cost of modern structures and enables innovative design solutions for demanding applications with severe environmental and loading conditions such as seismic resistant structures.

The fundamental cause of structural damage in reinforced concrete (R/C) structures is the brittle deformation behavior of concrete in tension. The design of Engineered Cementitious Composites (ECC) is targeted at creating a fiber reinforced cementitious material with a deformation behavior analogous to that of metals, specifically at achieving pseudo strain-hardening and multiple cracking behavior.

The presented research activities on ECC, the interaction of ECC with structural reinforcement, and on the deformation behavior of reinforced ECC flexural members under reversed cyclic loading conditions have shown that the combination of ECC with structural reinforcement leads to significant improvements of their structural performance as compared to conventional reinforced concrete members.

Particularly, the combination of reinforcement and matrix material with elastic/plastic stress-strain behavior results in a composite where both materials are deforming compatibly in the inelastic deformation regime. Consequently, damage induced by local slip and excessive interfacial bond stress between reinforcement and matrix is prevented. The ECC matrix stiffens the specimen at uncracked sections and also strengthens it at cracked sections. Hence, the composite load-deformation response is significantly improved in terms of axial load-carrying capacity as well as ductility. In order to maintain this composite action at relatively large inelastic deformations, strain hardening and multiple cracking of the ECC matrix are essential. It should be emphasized that the resulting composite behavior is not primarily achieved by enhanced material resistance in terms of matrix tensile strength, confinement effect or interfacial bond strength but rather by reducing internal stresses which would necessitate such resistance. Compatible deformation between ECC and steel reinforcement implies that bond strength in R/ECC is not as significant as in R/C for enhanced structural performance.

Steel reinforced ECC flexural members are found to provide significantly improved ductility and energy dissipation capacity compared to steel reinforced concrete. Similarly, FRP reinforced ECC flexural members show larger elastic deformation capacity compared to FRP reinforced concrete, however, the sensitivity of the FRP reinforcement to damage from induced compressive strain demands must be considered.

In general, transverse steel reinforcement requirements in reinforced ECC flexural members are found significantly reduced compared to current design requirements in conventional reinforced concrete. Reinforced ECC flexural members are also found to experience controlled composite damage by flexural crack formation without showing performance degradation at increasing flexural deformations resulting from composite disintegration and damage. Premature failure modes caused in reinforced concrete by crushing of the concrete core and buckling of longitudinal reinforcement, are not observed in reinforced ECC members, which maintain stable composite interaction mechanisms between structural reinforcement and ECC matrix.

Significant differences in the deformation behavior of reinforced ECC and reinforced concrete members have been established in this study. These differences are systematically derived and substantiated by contrasting the significant mechanisms in both composite systems at increasing dimensional and functional scale. This approach has lead to a thorough understanding of the reasons for improved structural performance of reinforced ECC flexural members and has provided a basis for the design of reinforced ECC members for seismic resistant structures.

The application study of R/ECC flexural members in a collapse resistant model frame structure has successfully demonstrated the potential of R/ECC structural composites to modify and improve the behavior of seismic resistant structures. The suggested concept offers an alternative approach to current practice and enables engineers to design a structure for a specific response to seismic events. This response is built into the structure and is expected to reduce the structural demand by adapting the frame stiffness as a function of the level of induced excitation.

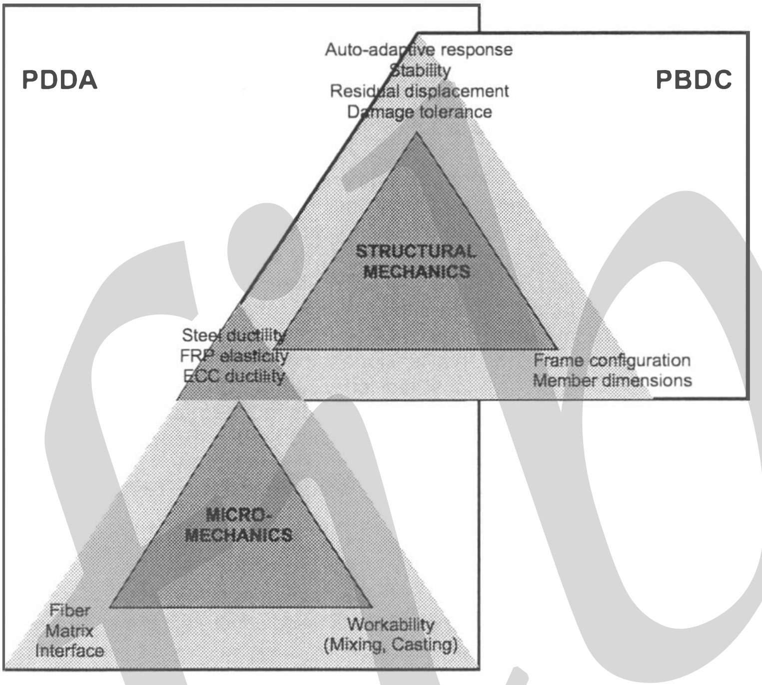

Fig.1 Specific components of the ISMD concept outlined in described research activities

In the context of ISMD, the auto-adaptive performance of the portal frame described above depends on the judicious choice of steel reinforcement in the beam member and FRP reinforcement in the column member. In turn the performance of these members depend critically on the tensile strain-hardening behavior of the ECC. Hence materials design of the ECC focuses on optimal combination of fiber, matrix and interface tailored to meet the strain-hardening property requirement. Integration of the performance need of the portal frame structure and the design of the ECC, using the tensile strain-hardening property as a bridge, is central to the successful development of the auto-adaptive portal frame.

The interrelationships between the various components of the integrated structures and materials design (ISMD) concept illustrated in this paper by a specific example are shown in Fig.1. ISMD aids in elevating the materials performance of ECC to the structural level, while directing the focus of materials engineering to enhancing concrete material ductility via judicious choice of fiber, matrix and interface of the ECC composite material. It is expected that ISMD provides a rich platform for collaborations between structural engineers and materials engineers.

GLASS – FRP PRESTRESSING UNITS IN CONCRETE BEAMS

Ľudovit Naď, Assoc. Prof., MSc., PhD.
Anton Bajzecer, PhD Student
Branislav Spernoga, PhD Student
Faculty of Civil Engineering, Technical University in Košice, Slovak Republic

Keywords: GFRP, prestressing, concrete, beams, creep

1 INTRODUCTION

One of main advantages of FRP reinforcement – absolute resistance against corrosion, is a principle reason for long time research in many countries all over the world. In opposite, the general disadvantage - relatively high price comparing to steel reinforcement restrains the large utilization of FRP reinforcement in concrete structures. From this point of view, CFRP and GFRP are the most convenient.

The paper presents the main results of relatively large experimental program done at the Technical University in Kosice, Slovak Republic. A few years ago, glass fiber reinforced plastic (GFRP) - bars were produced in the laboratory of the Department of Concrete Structures and Bridges. First, the tests of mechanical properties (strength of 600 MPa, modulus of elasticity of 40 GPa, bond strength) were carried out. Then, 12 concrete beams ordinary reinforced with GFRP bars were prepared and tested. 12 concrete beams prestressed by GFRP bars completed third part of research. These beams were divided into four groups containing three beams each :
- pre-tensioned, short time loaded (VK)
- pre-tensioned, long time loaded (VD)
- post-tensioned, short time loaded (DK)
- post-tensioned, long time loaded (DD)

One of most important part of the research project is the investigation of the rheological properties of GFRP bars (with fiber content of 60 %). The creep tests at different stress level are in progress (actually more than one and half year). The GFRP – bar samples were stressed to : 19 %, 21%, 34 %, and 60 % of their nominal strength.

2 EXPERIMENTAL PROGRAM

One GFRP bar as prestressing unit was used in each of 12 prestressed concrete beams. All beams were identical in cross-section (I cross section), 2,5 m long, as it is shown at Fig.1.

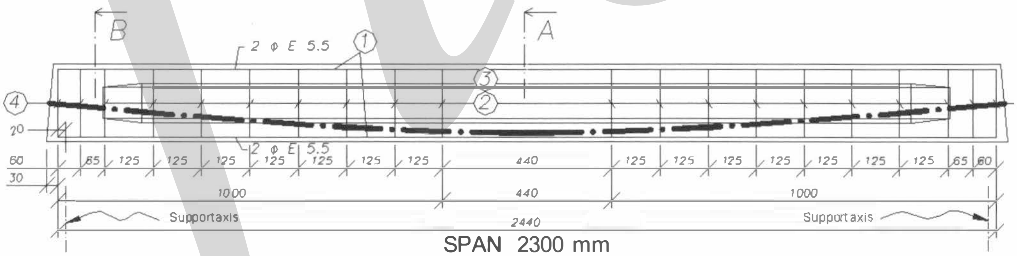

Fig.1 Shape and dimensions of prestressed beams (both – pre-tensioned and post-tensioned).

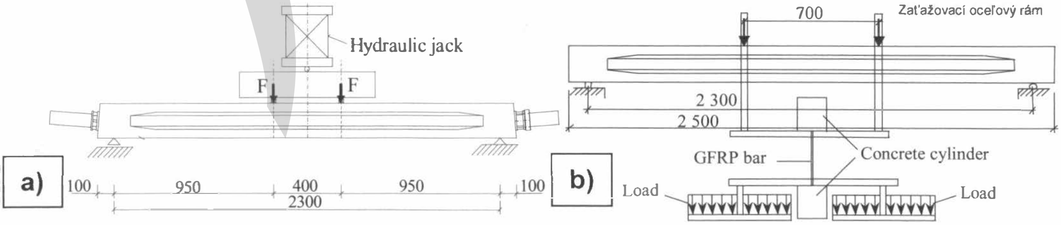

Fig. 2 Loading set-up. a) short-time (VK, DK in the laboratory), b) long-time loading (VD, DD in exterior) with GFRP bar hinge

All beams were loaded in the laboratory, progressively up to "service load" – M/M_d = 1,0, then deloaded to the "dead load" level (M/M_d = 0,5) and submitted to repeated – cyclic load (10 cycles). Then 6 beams were loaded up to collapse (series VK and DK); the rest 6 beams (series VD and DD) were installed in the exterior and exposed to the sustained load (M/M_d = 1,0) (Fig. 2)

3 RESULTS

Short time loading gave satisfying results. The observed short-time load bearing capacity do not exceed 1,75 multiple of design moment. Beam deflection under service-load does not exceed 1/600 of the span. The cracking started at approx. 0,8 x M/M_u (80% of service load). Average maximum crack width under service load is 0,2 mm (Fig. 3).

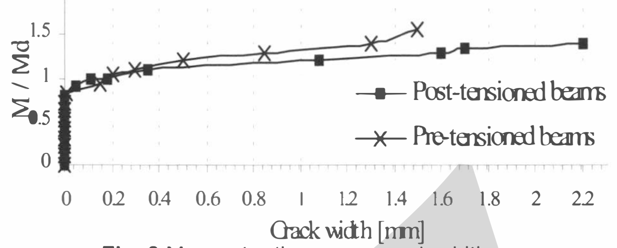

Fig. 3 Moment ratio versus crack width

Long-time loading was oriented to creep effect of GFRP bars on the deformation of beams, to the crack width increasing and to the lifetime of beams prestressed by GFRP bars. The time dependent deflection curve of the beam DD2 (post-tensioned) allows to well distinguish typical three part of creep curve of GFRP (Fig. 4) – primary creep ~30 days, secondary creep ~ 30 to 100 days and tertiary creep over 100 days. The creep diagram for GFRP bars exposed to free air (as a hinge for beam loading) shows to small deformation increasing. These bars are slightly stressed – to 19 %, 21 % and 34 % of nominal short-term strength.

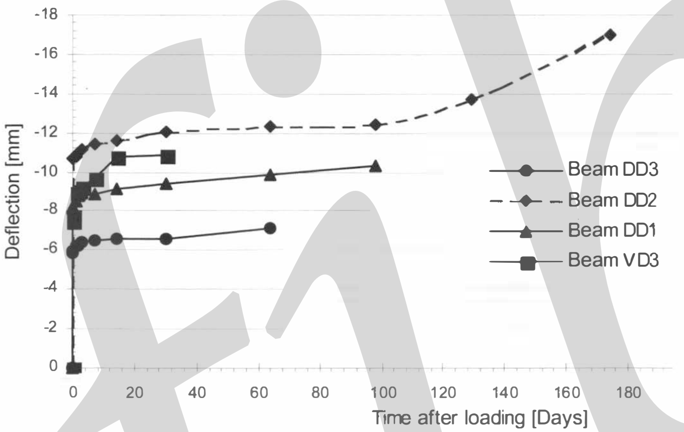

Fig. 4 Beam deflection vs. time

The short term GFRP prestressed concrete beams showed to a small safety ratio where this phenomenon asserted during the long term loading experiments. It is essential to reduce the stress in GFRP bar to less than 60% of its tensile strength. More research is needed for reliable knowledge of GFRP long-term behavior and design model development.

4 CONCLUSIONS

The sand pasted rough surface of the GFRP bar assures bond continuity and high bond strength in concrete. The short term GFRP prestressed concrete beams showed to a small safety ratio where this phenomenon asserted during the long term loading experiments. It is essential to reduce the stress in GFRP bar to less than 60% of its tensile strength. More research is needed for reliable knowledge of GFRP long-term behavior and design model development.

REFERENCES

[1] Naď, Ľ., Muruts, M., Špernoga, B., Bajzecer, A. and Šváb, R. : *Nové technológie pre výstavbu a opravy dialničných a cestných mostov, interakcia podložia s mostným telesom*", reports of the R&D project No. 0402840506, Ministry of Construction and regional Development of Slovak Republic, Košice 1998 - 2001 (in Slovak)

[2] Budelmann, H., Rostasy, F.S. : Creep rupture behavior of FRP elements for prestressed concrete – phenomenon, results and forecast models. ACI International symposium on FRP reinforcement for concrete structures. Vancouver, Canada 1993

[3] Scheibe, M., Rostasy, F.S. : Engineering model of stress-rupture of AFRP in concrete. Non-metallic reinforcement for concrete structures. Edited by L. Taerwe, London 1995

[4] Naď, Ľ., Muruts, M., Bajzecer, A. and Špernoga, B. : Non-metallic composites as reinforcement in concrete structures. ELFA Publisher, Košice 2001. Book, in Slovak

BOND BEHAVIOR OF FRP BARS EMBEDDED IN FIBER REINFORCED CONCRETE

Kenneth Campbell, Graduate Research Assistant
Abdeldjelil Belarbi, Associate Professor

Department of Civil Engineering,
University of Missouri-Rolla, Missouri, USA

Keywords: Bond; Concrete; Fiber Reinforced Concrete(FRC); Glass Fiber-Reinforced Polymer(GFRP); Reinforcing Bars.

1 INTRODUCTION

Currently many bridges in the United States of America are experiencing accelerated deterioration due to various environmental stimuli such as long-term exposure to deicing salts and saltwater which serves to render them structurally deficient. In many cases, the deterioration reaches a level that requires the complete replacement of the bridge and that a totally new design approach be implemented so as to assure this problem does not become worse. New bridges will have to be built with a focus on longer design lives and greater durability so as to alleviate the existing infrastructure problem. Current design practices will have to be studied to determine how well they account for the issue of environmentally induced deterioration of structures. New technologies and design approaches will then have to be developed so as to provide for economical and safe structures. The use of FRP and FRC in the civil infrastructure is one possible way to assure that bridges of the future are long lasting and cost-effective.

This research is part of a larger on-going project that focuses on the development of a non-ferrous reinforcement system for concrete bridge decks that involves the use of randomly distributed, discrete fibers and GFRP reinforcing bars. It is believed that this steel-free hybrid reinforcement system for bridge decks would be stronger, more durable and have a longer design life than traditionally designed bridge decks. The primary objective of this study was to determine the bond behavior of the GFRP rebar embedded in a FRC matrix. The bond between concrete and its reinforcement is one crucial issue that has to be investigated to assure the stability of a steel-free bridge deck system.

2 EXPERIMENTAL PROGRAM

Two factors that were considered to have an influence on the bond behavior of GFRP rebar embedded in a FRC matrix included the 1) rebar diameter and 2) the volume fraction of fibers. These two factors were varied in the experimental matrix such that a full factorial program could be developed and any interactions present might be fully accounted for. Two rebar diameters were chosen, which included 9.5 mm and 19.0 mm. Two volume fractions of fiber were used, which included Vf = 0.5 and 1.0%.

The GFRP rebar used in this investigation was characterized by E-glass filaments embedded in a vinylester resin. The surface treatment of the rebar was created by a tensioned tow of E-glass fiber wound helically around the longitudinal axis of the bar, forming symmetric indentations in the bar. The surface was then covered with a sanded finish. The discrete fibers used in this project were 54 mm in total length with an aspect ratio that ranged from 100 - 150. The fibers consisted of a fibrillated network and monofilament blend, which were comprised of a virgin copolymer and polypropylene, respectively.

The test used to determine the bond characteristics of GFRP rebar embedded in concrete was the flexural bond test developed by RILEM [1]. The free end slip of the rebar was measured using linear variable differential transformers (LVDTs). The testing apparatus used to load the specimens was a 500-kN MTS 880 Universal Testing Machine. The applied load rate was controlled by the MTS through an external feedback loop. The deflection of the beam was measured using a ± 250 mm LVDT and the load to the specimen was applied such that a constant rate of deflection in the beam was achieved. This method of testing was used view the post-peak bond behavior of the specimens.

3 RESULTS AND CONCLUSIONS

The addition of discrete fibers to concrete reinforced with GFRP rebar had no statistically significant effect on the observed bond behavior. The main exception to this was the specimens containing 9.5 mm diameter rebar and discrete fibers at a dosage of V_f = 1.0%, which exhibited a significant decrease in bond capacity. This was thought to have occurred due to poor consolidation of the specimens during the placement of the FRC. The fibers at this dosage caused a significant decrease in the workability of the concrete, which made it difficult to place and consolidate. Figure 1 illustrates the typical bond stress-slip response obtained for each specimen.

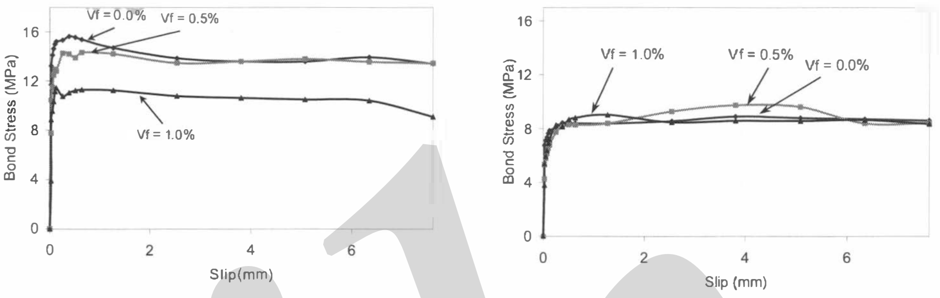

(a) **(b)**

Figure 1 Typical Bond Stress-Slip Response for: a) 9.5 mm Specimens b) 19.0 mm Specimens

There was however, a noticeable trend for the ultimate bond stress values of the19.0 mm specimens, which exhibited marginal increases after the addition of the fibers. Furthermore, slight increases in the energy absorption characteristics were noticed. This was thought to have occurred due to the crack limiting behavior of fibers and the fact that these specimens were prone to fail in a bond splitting mode.

For both the specimens reinforced with the 9.5 mm and to a limited extent the 19.0 mm rebar, the failure of bond was controlled by the failure of the outer layer of resin of the bar. For the 9.5 mm specimens the failure of the resin layer was more catastrophic, whereas the 19.0 mm bars saw only localized failures.

Two models were fit to the observed data, which included the CMR Model and the Malvar model [2]. Parameters were fit for each treatment combination in the experimental program to see how the fibers affected the behavior of the specimens. After fitting the CMR model to the data, it became apparent that as the dosage of fibers increase, mobilization of bond failure occurred at lower stress levels and slightly larger slippages. This behavior arose from the issue of consolidation of the members due to the lower workability of the FRC mix. The empirical constants, F and G, were fit for the Malvar model further illustrated this trend. One noticeable feature of the fitted Malvar model, however, was that to model the post peak bond stress increase observed for the 19.0 mm specimens, the form fitting constant G became negative. The negative value of G forced the formation of an asymptote in the function, which gave it the ability to describe the post-peak stress increase that was observed in the test data.

REFERENCES

[1] RILEM 7-II-28 D, "RC5: Bond Test for Reinforcing Steel. 1. Beam Test." RILEM technical recommendations for the testing and use of construction materials, U.K.: E & FN Spon, 1994. 96-101.

[2] Cosenza, E., G. Manfredi, and R. Realfonzo. "Behavior and Modeling of Bond of FRP Rebars to Concrete." Journal of Composites for Construction. 1.2(1997): 40-51.

COMPOSITE FLAT-PLATE STRUCTURES WITH FRC PRECAST MEMBERS

Andrzej Ajdukiewicz Jacek Hulimka Alina Kliszczewicz
Department of Structural Engineering, Silesian University of Technology, Gliwice, Poland

Keywords: concrete structures, composite structures, flat plate systems, high performance FRC

1 INTRODUCTION

The proper structural solutions for slab-column joints in flat plate structures have been considered since the beginning of applications of these very effective building systems. On the basis of experimental tests, followed by theoretical models for analysis, it was stated that the most stressed zone of concrete in triaxially compressed part of slab adjacent to the column is particularly important for the load carrying capacity as regards punching shear of slabs. This was the reason of many investigations how to strengthen the crucial part of joints and many constructional methods have been used in practice.

The idea of composite structures combined from head-and-column prefabricated elements with small flexural reinforcement only and cast-in-situ slabs was proposed in 1993 [1] to avoid steel heads or labour consumable traditional shear reinforcement. The first step on this way was introduction of high-performance concrete in precast members to obtain relatively small column cross-sections and strong zone of compressed concrete in the part of slab adjacent to the column.

To clarify the effectiveness of such composite slab-column joints the series of full-scale models were tested up to failure. The initial results of tests were presented in [2]. On the basis of tests the models for numerical analysis were proposed [3]. In general, the benefits of HPC used in heads were significant. Despite of the high level of load capacity recorded at axisymmetrical and eccentric punching the rapid failure in the final phase was not quite satisfactory. This enhanced the authors to introduce fibre reinforced HPC to improve the behaviour of joints.

2 MODELS FOR EXPERIMENTAL TESTS

The series of four models with precast elements from FRHPC were assumed in connection with similar models with HPC prefabricates tested before [2]. Particularly, the constant values were hold in models for overall thickness of slabs, thickness of precast heads and diameters of columns, properties of flexural reinforcement and fractions of aggregate in concrete of both parts. There were three sizes of heads introduced in four models and the model with intermediate size of head was doubled because this size had been chosen for the first application in practice.

Such a way enabled direct comparisons of results obtained for models with HPC and FRHPC precast members. Also the effectiveness of reinforcement with fibres could be controlled during the whole course of tests.

3 BASIC RESULTS FROM EXPERIMENTS

The ultimate loads recorded in the tests of joints with FRHPC elements are presented in Table 1 and compared with results obtained earlier in the corresponding series of models with HSC elements. Additionally, there are given also in Table 1 the mean values of compressive strength of concrete in precast members, f_{cm}, as a crucial data in further analysis. In general, very similar concrete mixtures were provided in corresponding elements, with the only difference in fibres amount addition.

The behaviour at failure of composite slab-column joints with FRC precast head-and-column elements is significantly different from that known from homogeneous joints but similar to the behaviour observed in composite joints with HPC precast members of the same shape [2]. In all composite joints after failure the different inclinations of cone-like surfaces were measured in heads and in slabs outside heads (Fig. 1).

The main difference between series of joints with FRC and HSC elements was observed in the course of failure. In comparable HSC series with small and medium heads the two-phase failure was

Table 1 The ultimate loads recorded in tests of joints

Type of the head	Models with FRHPC elements			Comparable models with HSC elements		
	Model No.	f_{cm} [MPa]	V_u [kN]	Model No.	f_{cm} [MPa]	V_u [kN]
small	M-FRC-1	85.6	1150	M-HSC-I	89.1	950
medium	M-FRC-2	82.6	900	M-HSC-II	65.5	780
medium	M-FRC-3	84.9	1000	M-HSC-III	66.2	820
large	M-FRC-4	101.5	1500/1800	M-HSC-IV	90.3	1150/1330

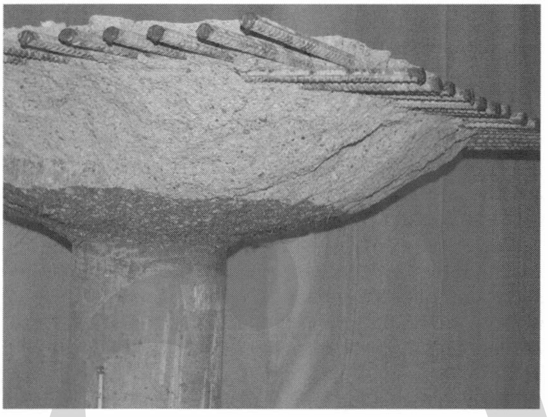

Fig. 1 Example of the element extracted from the punched joint with medium size of FRC head

observed with tangible increment of displacement. After few further steps of load the rapid final failure happened when crack passed the head and reached the bottom surface at the column face. But in joints with FPC heads the second phase of failure was elongated in time in form of cracking development inside the head.

In joints with large heads from HPC and FRC, the first phase of failure was connected with simultaneous punching shear of slab outside the head and flexural destruction of head, while the second phase was punching of the head itself.

4 CONCLUSIONS

Introduction of FRHPC in precast members, with reasonable contribution of fibres (50 kg/m^3) added to approximately the same concrete mixture, improved the behaviour of joints at least in two aspects:

- significantly increased load-bearing capacity under axisymmetrical load (18.8% to 30.4 %) in comparison with similar joints but without fibres in high-strength concrete;
- changed the rapid final phase of punching shear into more yield process, observed rather as multi-phase failure, typical for ductile joints.

Both these differences are on the safe side of behaviour of joints, therefore, the solution may be undoubtedly recommended in all cases of dominating axisymmetrical loading of joints. Such cases are typical for interior joints in flat plate structures.

Introduction of data from experiments into verification of analytical model formerly proposed in [3] has confirmed the proper assumptions in model for the limited size of heads. These kinds of head are particularly useful in practice, because the load-bearing capacity of the joints with such members highly exceeds the requirements of real structures.

REFERENCES

[1] Ajdukiewicz A. and Kliszczewicz A.: Application of high-strength concrete in composite skeletal structures. 3rd International FIP/CEB/ACI Symposium on "Utilization of High Strength Concrete", Lillehammer, Norway, vol. I, pp.449-456, 20-24 June 1993

[2] Ajdukiewicz A., Kliszczewicz A. and Hulimka J.: Tests of Joints in Composite Slab-Column Structures with HSC/HPS Head-and-Column Precast Members. 4th. International Symposium on Utilization of High-Strength/High-Performance Concrete, Paris, pp.1009-1014, 29-31 May 1996

[3] Ajdukiewicz A., Hulimka J. and Kliszczewicz A.: Models for flat plate joints combined from precast and cast-in-place concrete. *fib*-Symposium on "Structural Concrete - The Bridge between People", Prague, Czech Republic, 12-15 October 1999, Vol.1, pp.265-270.

ADVANCED COMPOSITE MATERIALS IN FLEXURAL MEMBERS FOR AUTO-ADAPTIVE STRUCTURAL RESPONSE MODIFCATION

Gregor Fischer
Department of Civil and Environmental Engineering
University of Hawaii

Victor C. Li
Department of Civil and Environmental Engineering
University of Michigan

Keywords: ECC, moment resisting frame, composite, collapse mechanism, passive response control

1 INTRODUCTION

The response of moment resisting frame structures to seismic excitation is strongly dependent on the ability of particular structural members to sustain relatively large inelastic deformations without significant degradation of lateral and axial load-carrying capacity. Conventional reinforced concrete frame structures are typically designed according to the strong column/weak beam concept, which prescribes inelastic deformations to occur exclusively in the beam members to dissipate energy while the columns remain elastic in order to maintain stability and prevent possible collapse. This ideal frame deformation mechanism is enforced by a strength differential between beams and column intersecting at joint locations, however, usually requires the formation of plastic hinges at the base of the first story columns in order to initiate frame sway and utilize the energy dissipation capacity of the beam members. The formation of plastic hinges at the column base is anticipated and not necessarily critical for the stability of the moment resisting frame, assuming that further inelastic deformations occur exclusively in the beam members. However, the possibility of formation of additional plastic hinges in the columns above or within the first story in conjunction with plastic hinges at the columns base may lead to a kinematic mechanism and collapse of the structure.

The frame configuration investigated in this paper does not require the formation of plastic hinges at the column base in order to initiate frame sway and subsequent utilization of inelastic rotations in the beam plastic hinges. In this suggested configuration, the formation of plastic hinges at the column base is prevented by employing advanced composite materials, in particular Fiber Reinforced Polymer (FRP) reinforcement combined with a ductile engineered cementitious composite (ECC) to substitute brittle concrete. These FRP reinforced ECC column elements have a relatively large elastic deformation capacity and sufficient flexural strength to enforce inelastic deformations in the beam members in accordance to the strong column/ weak beam concept.

Utilizing the particular load-deformation characteristics of steel and FRP reinforced structural members in the suggested moment resisting frame system, a bi-linear load-deformation behavior can be obtained with considerable energy dissipation capacity and reduced residual displacements at unloading. The auto-adaptive stiffness modification is expected to reduce base shear forces during a seismic event by increasing the period of the structural system at exceeding a particular lateral displacement.

2 CONCEPT AND VERIFICATION

In a portal frame assembled from a steel reinforced beam and FRP reinforced column members, the load-deformation response can be schematically described with an idealized graph of the individual beam and column response characteristics (Fig.1) at sequential frame deformation stages.

In the first stage at small, elastic frame displacements and prior to the formation of plastic hinges, the steel reinforced beam has a larger flexural stiffness relative the FRP reinforced columns and experiences relatively small deflections, while the relatively soft columns largely accommodate the imposed lateral frame deformations. At this frame deformation stage, the frame responds at an initial, relatively large stiffness and resumes its undeformed shape at unloading.

At increasing frame deformations the system modifies its deformation mode and adapts to the increased level of loading by converting into a strong column/ weak beam mechanism, effectively responding at a lower, secondary system stiffness. At this stage, plastic hinges in the beam are formed due to the flexural strength differential between beam and columns, thus dissipating energy by inelastic rotations in the beam plastic hinges. At further increasing lateral frame displacements, the columns remain elastic due to the elastic nature of the FRP reinforcement and prevent the formation of plastic hinges at their base, i.e. formation of a kinematic mechanism.

Depending on structural performance requirements such as the expected level of excitation and acceptable temporary and residual displacements, the details of the frame response, i.e. initial and secondary stiffness as well as transition load and transition displacement can be defined in the design procedure. In contrast to conventional moment resisting frame systems, this suggested configuration shows an intrinsic bi-linear load-deformation response with auto-adaptive stiffness modification capabilities.

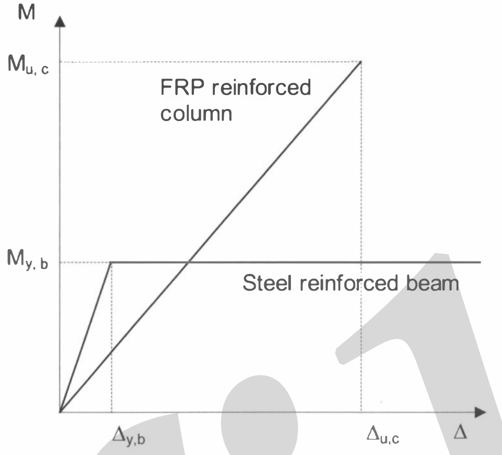

Figure 1 Schematic load-deformation behavior of steel reinforced beam and FRP reinforced column

This concept was experimentally verified using small-scale portal frame specimens under reversed cyclic loading conditions. Four specimens were tested, specifically a control specimen exclusively reinforced with steel reinforcement in beam and columns (S-1), and three specimens of the suggested configuration with steel reinforced beam and different types and amount of FRP reinforcement in the column members (S-2, S-3, S-4).

The analytically derived monotonic response of the tested specimens (Fig.2) illustrates the qualitative difference of the conventional configuration with elastic/plastic load-deformation behavior compared to the suggested configuration with a bi-linear load-deformation response, which is defined by its initial and secondary frame stiffness. The transition between these response stages is triggered by the formation of plastic hinges in the beam member. Tests of different configurations of the suggested system presented in this paper indicate the potential of this concept to design a moment resisting frame with a specified response in terms of initial and secondary stiffness as well as transition load and displacement upon which the frame auto-adaptively modifies its response characteristics. The transition between initial and secondary frame stiffness is intended to increase the period of this structure in order to decrease the shear forces acting on the system in case of seismic excitation.

In the suggested response mechanism, inelastic deformations and energy dissipation are exclusively assigned to the beam members of the frame while the columns remain elastic particularly at the column base and do not form plastic hinges at this location. The relatively large elastic deformation capacity of the columns is achieved in this particular case by combining elastic FRP reinforcement with a ductile, engineered cementitious composite (ECC). The interaction of ductile ECC matrix and elastic FRP reinforcement results in a relatively large deflection capacity of the FRP reinforced ECC column members.

Besides the reduction of shear forces due to an elongation of the period of the suggested frame system, the reduction of residual displacements and self-centering capabilities of the structure are expected to reduce permanent damage and the need for rehabilitation efforts after experiencing a seismic event.

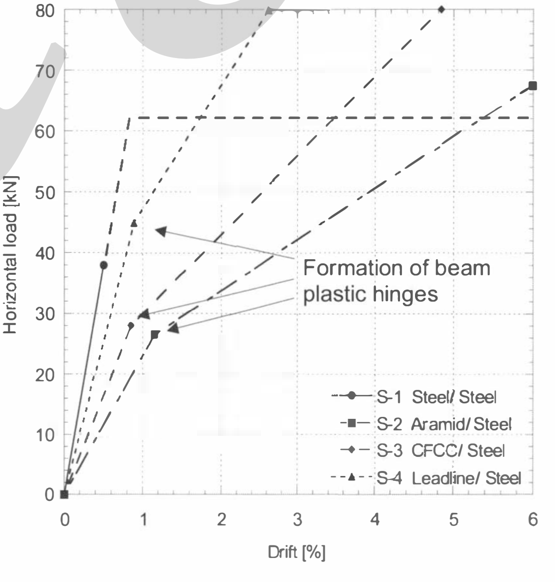

Figure 2 Analytically derived response of tested frame configurations

A PROPOSAL OF DESIGN PROCEDURE FOR FLEXURAL STRENGTHENING RC BEAMS WITH FRP SHEET

Yusuke Kurihashi, Civil Engrg. Research Inst. of Hokkaido, JAPAN
Norimitsu Kishi, Muroran Inst. of Tech. JAPAN
Hiroshi Mikami, Mitsui Construction T.R.I, JAPAN
Sumiyuki Sawada, Muroran Inst. of Tech JAPAN

Keywords: RC beams, FRP sheet, flexural strengthening, sheet debonding

1. INTRODUCTION

In this study, to establish a rational flexural strengthening design procedure of RC beams in case using FRP sheet (FRPS), load-carrying behavior for T-shape RC beams strengthened with FRPS was experimentally discussed. Furthermore, prediction method for failure mode of RC beam strengthened with FRPS was also discussed.

2. EXPERIMENTAL OVERVIEW

Total six T-shape RC beams used in this study are listed in Table1. Nominal name of these RC beams are designated in order of main-rebar ratio p_t (T1~T4 (0.80~2.46 %)), shear span ratio r_s (R5 or R7, rounded to the nearest integer), and sheet volume ratio p_f (1 or 2 ‰). An example for dimensions of RC beam is shown in Fig. 1. A distance of two loading points was fixed as 500 mm long, so that the clear span was 2.6 m or 3.4 m long corresponding to the value of r_s. The 130 mm wide Aramid sheet (AFRPS) was bonded onto the central portion of the lower surface of beam 100 mm inside supporting points. AFRPS with 0.415 kg/m^2 was used for all RC beams considered here. In design of these RC beams, it has been analytically confirmed that the bending capacity was less than the shear capacity even after strengthening.

Table 1 List of RC beams

Specimen	Rebar ratio p_t (%)	Shear span ratio r_s	Sheet volume ratio p_f (‰)
T1-R5-2	0.80	5.0	2.0
T2-R5-2	1.26		
T3-R5-2	1.82		
T4-R5-2	2.46		
T2-R5-1	1.26	5.0	1.0
T2-R7-2		6.9	2.0

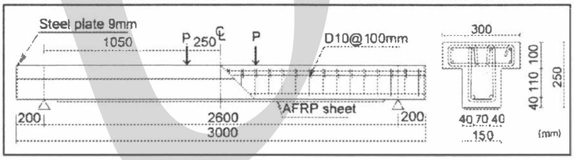

Fig. 1 An example for the dimensions for RC beams (r_s = 5.0)

3. EXPERIMENTAL RESULTS

3.1 Relationship between load and displacement

Figure 2 compares the load (P) and the mid-span displacement (δ) relations from experimental results with those of analytical results for T1~T4-R5-2 (p_t = 0.80~ 2.46). Analytical results are estimated by means of multi-section method. From these figures, it is seen that experimental ultimate load and displacement on T4-R5-2 beam are as large as analytical ones. This suggests that T4-R5-2 beam is referred as FCF type, which is defined as strengthened RC beams reaching the ultimate state with flexural compression failure mode before FRP sheet being debonded. On the other hand, in case of T1~T3-R5-2 beams in which the value of p_t for these beams is smaller than that for T4-R5-2 beam, the $P-\delta$ curves are lower than the analytical ones. This suggests that these beams are referred as DF type, which is defined as RC beams reaching the ultimate state with sheet being debonded before the cover concrete in the compression side reaching the ultimate state. Moreover observing these results in detail, it can be seen that the smaller the p_t value, the more remarkably the RC beams are failed with DF type.

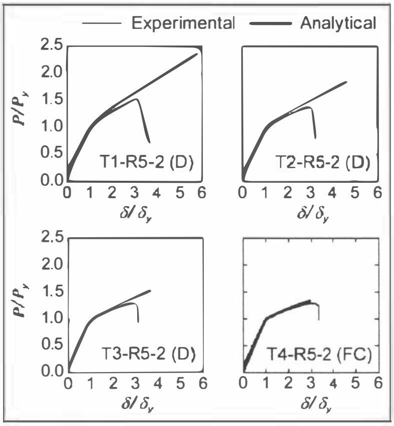

Fig. 2 Normalized $P-\delta$ relation referring to T1~T4-R5-2 beams ("D": DF type, "FC" : FCF type)

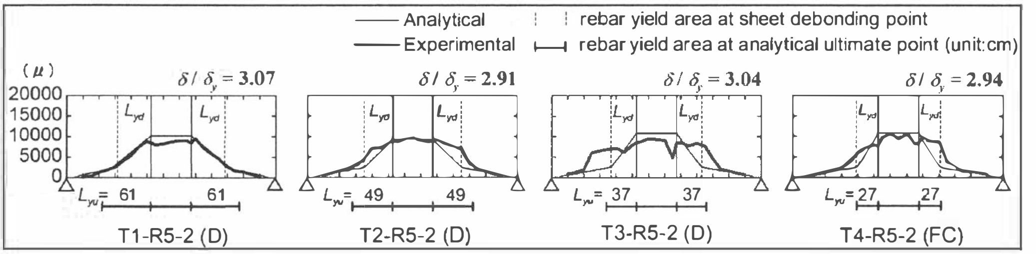

Fig. 3 AFRPS strain distribution at the sheet debonding point ("D": DF type, "FC": FCF type)

3.2 Strain distribution of AFRPS

Figure 3 shows the strain distributions of AFRPS comparing with the analytical results at the beginning of sheet debonding (hereinafter, sheet debonding point). In case of T4-R5-2 with FCF type, the distribution at analytical ultimate point is drawn, since AFRPS is debonded after the cover concrete in compression side reaching analytical ultimate state. In these figures, L_{yu} and L_{yd} are rebar yield area in equi-shear span at analytical ultimate point and that at sheet debonding point, respectively, and they are estimated by numerical analysis.

These figures show that all DF type beams are failed due to AFRPS being debonded before the length L_{yd} extends that of L_{yu}. In contrast, FCF type beam (T4-R5-2) is not failed at the analytical ultimate point, so that the length of L_{yd} is similar to that of L_{yu}. Observing these AFRPS distributions in detail, it is recognized that the experimental results in equi-bending area are in comparably good agreement with analytical ones. On the other hand, the experimental results in the region of rebar yield area L_{yd} are larger than the analytical ones. This implies that AFRPS may be debonded due to peeling action of concrete blocks pushing out in the downward direction in the region of rebar yield area of equi-shear span. This suggests that sheet debonding is closely related to the expansion of rebar yield area.

4. PREDICTION OF FAILURE MODE

The prediction method of failure mode has been proposed by the authors, considering the relationship between rebar yield area L_{yu} and characteristics of sheet-debonding. Referring to this prediction method, the experimental results on failure type are plotted on $L_{yu}/d - r_s$ diagram (Fig. 4), in which d is the effective depth in cross section. In this figure, the lower and upper bound equations for DF type and/or FCF type, respectively, are drawn in addition. From this figure, it is seen that both bound equations can be applied to the case of T-shape RC beam strengthened with AFRPS. Here, replacing r_s with a/d (a: shear span length), and using $L_{yu}/a - M_y/M_u$ relation (M_y: rebar yield moment, M_u: ultimate moment), these bound equations are converted as follows:

Equation for the upper bound of DF type:

$$M_y/M_u = 0.65 \quad (1)$$

Equation for the lower bound of FCF type:

$$M_y/M_u = 0.70 \quad (2)$$

If both failure types are estimated considering some safety margin, prediction equations of failure types are obtained as: $M_y/M_u < 0.70$ for DF type; $M_y/M_u > 0.70$ for FCF type. Thus, it is made clear that failure mode of RC beam strengthened with AFRPS can be expected using M_u and M_y estimated using multi-section method irrespective of cross sectional shape of RC beams.

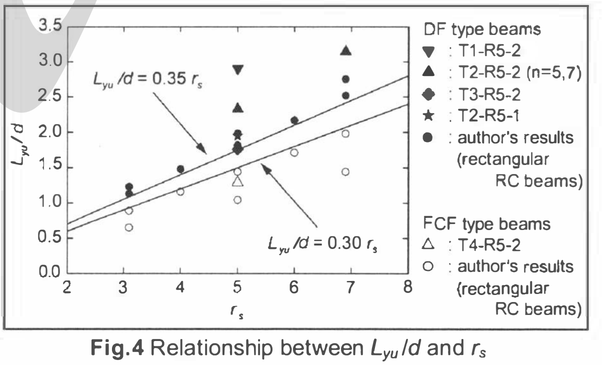

Fig.4 Relationship between L_{yu}/d and r_s

5. CONCLUDING REMARKS

The results obtained from this study are summarized as: 1) failure mode of T-shaped RC beams strengthened with AFRPS is divided two types apart; Sheet Debonding Failure (DF) and Flexural Compressive Failure (FCF); 2) sheet debonding is developed due to peeling action of concrete blocks pushing out in the downward direction; 3) failure mode of T-shaped RC beam strengthened with AFRPS can be expected using M_u and M_y estimated by means of multi-section method.

ABOUT RC BEAMS STRENGTHENED IN SHEAR WITH FRP SHEETS

Carlo Pellegrino Davide Tinazzi Claudio Modena
Department of Construction and Transportation Engineering, University of Padova, ITALY

Keywords: shear strengthening, bond, steel reinforcement, FRP.

The theme of shear is actually a very complex problem. The current codes (ACI 318-95, Eurocode 2) quantify the nominal shear strength by means of a simple sum of the contributions of the concrete (V_c) and the steel (V_s). For RC beams with externally bonded FRP sheets the further contribution of the sheets (V_f) is added.

An experimental approach is actually used for the quantification of the contribution of externally bonded FRP sheets. If the current formulations of the shear capacity of simple RC beams were validated with great quantity of experimental tests, it does not exist a comparable quantity of tests for the validation of the expression of the FRP contribution to the shear capacity. The aim of the paper is to define a field of applicability of the current formulations which lead to safe predictions.

A number of important contributions about the design of RC beams with externally bonded FRP laminates are actually present in literature. Nevertheless, the debate on the contribution of externally bonded FRP sheets to the shear capacity of RC beams is still open. The bond mechanism and the influence of the amount of existing transverse steel reinforcement on the shear capacity of the beam strengthened in shear with FRP sheets does not seem totally understood. Many papers discussed the shear behaviour of RC members strengthened by FRP [1, 2] laminates and bond behaviour between FRP sheets and concrete [3, 4] and produced valuable findings.

The contribution of externally bonded FRP laminates to the shear capacity of RC beams depends on several parameters (such as the stiffness of the sheets, the type of resins, the compressive strength of the concrete, the strengthening pattern and the sloping of the fibers) and is the subject of a research program carried out by the authors [5].

In particular, in the authors' opinion, 1) the bond behaviour and 2) the influence of the ratio $\rho_{s,f}$ between the stiffness of transverse steel reinforcement and the stiffness of transverse FRP sheets on the ultimate behaviour of beams failing under shear are worth clarifying. This ratio is correlated to the cracking pattern in the web failing under shear which modifies the anchorage conditions of the sheets and their effective contribution to the ultimate shear strength of the beam.

An empirical reduction factor of the shear capacity, called R*, has been proposed (Fig. 1) to take into account the mentioned phenomenon [5], but a more precise analytical model is still in need and should presumably be developed on the basis of a deep understanding of the parameters influencing FRP-concrete adhesion and debonding mechanisms.

On that particular topic, available research works and codes (cfr. ACI 440, FIB TG 9.3 guidelines), are not in agreement on the prediction of the strength of bond and of the extent of the minimum required area to achieve it (Fig. 2). Nevertheless, a precise formulation of the minimum development length, named "effective bond length" and indicated with L_e, is a fundamental issue for development of both anchorage specifications and flexural/shear models.

Given the relatively small number of test results, the quantification of a new empirical reduction (Fig. 1), though it was demonstrated that it is necessary, must be interpreted only as a proposal which should be improved with other tests on beams with different values of the ratio $\rho_{s,f}$ with different strengthening configurations.

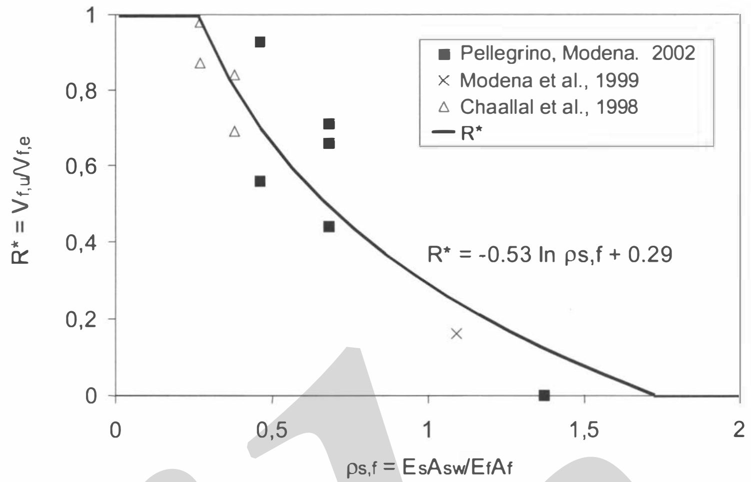

Fig. 1: Reduction factor of the shear capacity R* function of $\rho_{s,f}$

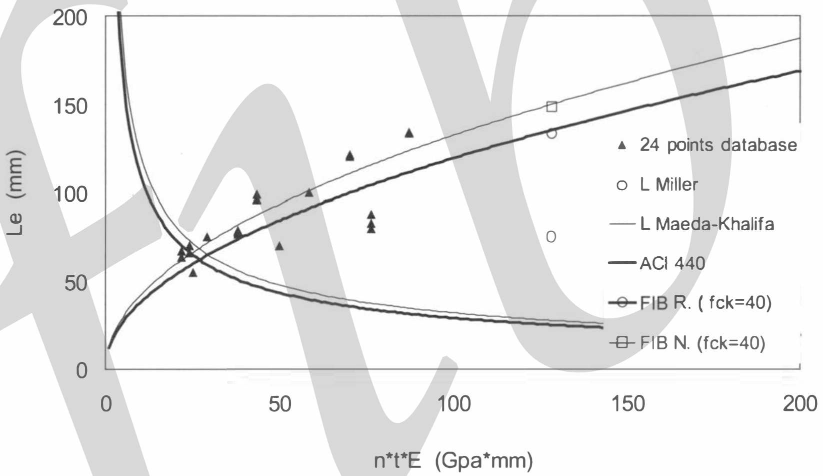

Fig. 2: Effective bond length vs. stiffness curves provided by early research works

REFERENCES

[1] Khalifa A., Gold W. J., Nanni A., Abdel Aziz M. I. (1998) "Contribution of externally bonded FRP to shear capacity of RC flexural members", *Journal of Composites for Construction*, ASCE, 2(4), 195-202.

[2] Chaallal, O., Nollet, M.-J., Perraton, D. (1998) "Shear strengthening of RC beams by externally bonded side CFRP strips", *Journal of Composites for Construction*, ASCE, 2(2), 111-113.

[3] Maeda, T., Asano, Y., Sato., Ueda, T., Kakuta, Y. (1997) "A study on bond mechanism of carbon fiber sheet", *Non-Metallic (FRP) Reinforcement for Concrete Struct., Proc., 3rd Int. Symp.*, Vol. 1, Japan Concrete Institute, Tokyo, Japan, 279-286.

[4] Miller B. (1999) "Bond between carbon fiber reinforced polymer sheets and concrete" MSc Thesis, Dept. of Civil Engineering, University of Missouri, Rolla, MO.

[5] Pellegrino C., Modena C., (2002) "FRP shear strengthening of RC beams with transverse steel reinforcement" *Journal of Composites for Construction*, ASCE, in print (May, 2002).

EXPERIMENTAL STUDY ON THE REINFORCED CONCRETE BEAMS STRENGTHENED BY USING CARBON FIBER SHEETS

XU Fu-quan, TAO Xue-kang, GUAN Jian-guang, CHEN Yu
China Academy of Building Research, Beijing 100013, China

1 INTRODUCTION

Recently, an advanced composite material named Carbon Fiber Reinforced Plastic (CFRP) has emerged as an alternative to traditional strengthening materials. The existing reinforced concrete structures can be strengthened by externally bonded CFRP to improve their mechanical performances. Many advantages such as lightweight, non-corrosive, simple construction, and high tensile strength have made it find more applications in strengthening of concrete structures in China. The paper introduces some experimental study in the field in China Academy of Building Research (CABR)[1].

2 EXPERIMENTAL PROGRAM

A total of twelve simply supported beams of 200mm×300mm×3000mm, strengthened by Carbon Fiber Sheets (CFS), were tested in the laboratory of CABR. The influence factors of concrete strength, reinforcement ratio and the number of plies of CFS etc. were taken into consideration. Additionally, the beams strengthened with prestressed CFS, and the use of CFS for strengthening the initially loaded beams, were also investigated. In order to avoid sudden debonding failure, anchorage system was used in this test.

3 RESULTS AND DISCUSSION

3.1 Ultimate load

The details of test beams were shown in Table 1. All the beams strengthened by externally bonded CFRP performed significantly better than the control beams, in terms of strength and stiffness.

Table 1 Details of test beams

Specimen	f_{cu} (MPa)	Reinforcement	Area of CFS(mm^2)	Ultimate load (kN)	Type of failure	Annotation
La-2-U	48.5	2Φ14	None	71.4	Steel yielding	Control beam
La-2-1			25.05	103.2	CFS rupturing	None
La-2-2	38.4		55.78	142.7	CFS rupturing, Concrete crushing	
La-2-3			83.67	171.1	Concrete crushing	
Lb-2-U	60.3		None	75.0	Steel yielding	Control beam
Lb-2-1			25.05	106.6	CFS rupturing	None
La-4-U	31.2	4Φ14	None	135.0	Steel yielding, Concrete crushing	Control beam
La-4-1			25.05	156.7	CFS rupturing	None
La-2-1-0.1	44.1	2Φ14		100.4		Initially loaded with crack width of 0.1mm
La-2-1-0.2	33.1			95.1		Initially loaded with crack width of 0.2mm
La-2-1- 3000	38.4		16.65	91.2		Prestressed with 3000 $\mu\varepsilon$
La-2-1- 4000	44.1			89.7		Prestressed with 4000 $\mu\varepsilon$

The experimental results were reached as follows:

1. The ultimate loads of the beams strengthened by externally bonded CFRP were substantially increased.
2. When the type of failure was the CFS rupturing, the ultimate load of the strengthened beam, which was increased by the CFS, was affected slightly by the concrete strength and the interior reinforcement because of the larger ultimate strain for the CFS.
3. The yield loads and the ultimate loads of the initially loaded beams were decreased as the

initial load was increased.

3.2 Analysis on the crack and deflection

From the test results, the following phenomena were observed:

1. The crack appeared late for the beams strengthened by externally bonded CFRP, and the crack developed slowly. The crack width was less than the control beam at the same load.
2. When the interior reinforcement was in a large quantity, the effect of CFS on cracks development was less obvious.
3. Before the steel yielded, the deflections of the strengthened beams were a little less than that of the control beam.
4. The beams strengthened by externally bonded CFRP could provide enough ductility.
5. The cracking and yield loads of the beams strengthened with prestressed CFS were obviously greater than the strengthened beam, and the ultimate deflections of the beams strengthened with prestressed CFS were less than that of the control beam.

4 FLEXURAL LOAD-BEARING CAPACITY OF NORMAL SECTION

The normal section flexural load-bearing capacity of an beam strengthened by externally bonded CFRP can be determined based on strain compatibility, internal force equilibrium, and the controlling mode of failure.

When the type of failure is concrete crushing, the normal section flexural load-bearing capacity can be calculated in the following equation:

$$M = \alpha_1 f_c bx\left(h - \frac{x}{2}\right) + f_s' A_s'\left(h - a'\right) - f_y A_s a \quad (1)$$

$$\alpha_1 f_c bx = f_y A_s - f_s' A_s' + \gamma f_{cf} A_{cf} \quad (2)$$

When the type of failure is CFS rupturing, the normal section flexural load-bearing capacity can be calculated in the following equation:

$$M = \gamma f_{cf,u} A_{cf}\left(h - \frac{x}{2}\right) + f_y A_s\left(h_0 - \frac{x}{2}\right) \quad (3)$$

Using the calculating method above, the results for the test beams and other beams[2][3] are estimated. From the results, it is known that the calculated results are in good agreement with the test ones.

5 CONCLUSIONS

Based on the experimental and analysis investigation above, the following conclusions can be made:

1. The ultimate loads of the beams strengthened by externally bonded CFRP were substantially increased;
2. The beams strengthened by externally bonded CFRP could provide enough ductility;
3. The cracking loads of the beams strengthened with prestressed CFS were obviously greater than that of the strengthened beam, but the ultimate deflections were less than that of the control beam;
4. The method for calculating the normal section flexural load-bearing capacity is proposed, which can meet the Chinese engineering requirements.

REFERENCES

[1] Xu Fu-quan, Experimental and analytical study on the behavior of concrete beams strengthened by carbon fiber sheets under static loading, doctoral thesis, China Academy of Building Research, 2001.

[2] Yan Zhi-han, Experimental study and analysis on the reinforced concrete flexural member strengthened by using carbon fiber sheets, magisterial thesis, General Research Institute of Building and Construction of Ministry of Metallurgical Industry. (in Chinese)

[3] Qu Wen-jun, Zhang Yu, Chao Yu-ming and Zhang Peng-fei, Calculating method for the flexural load-bearing capacity and constructing suggestions of concrete beams strengthened by carbon fiber sheets, The proceedings of the first symposium for applications of CFRP in concrete, June, 2000. (in Chinese)

FLEXURAL STRENGTHENING OF RC BEAMS BY USING THE TENSIONED CFRP PLATE

Takayuki Kojima, Nobuaki Takagi
Ritsumeikan University
JAPAN

Yuzuru Hamada
DPS Bridge Works
Co., Ltd, JAPAN

Masumi Inoue
Ritsumeikan University
JAPAN

Akira Kobayashi
Nippon Steel Composite
Co., Ltd, JAPAN

Keywords : CFRP plate, prestress, flexural strengthening, peeling, fatigue test

SUMMARY

In order to investigate the flexural strengthening effects of the existing bridges by using carbon fiber reinforced polymer (CFRP) plate, the static and fatigue tests of RC beams(Fig.1) strengthened with non-tensioned and tensioned CFRP were carried out. Tensile test results of CFRP plate [1] are shown in Table 1. CFRP plate was fabricated by the Pultrusion method.

RC beams strengthened by the tensioned CFRP plate failed in flexure immediately after the peeling of CFRP plate. The flexural deformability and load bearing capacity of beam were improved largely, in the beams strengthened by using the tensioned CFRP plate and the intermediate anchoring device, no matter how the beam was deteriorated. It is also evident that CRRP plates can increase the fatigue strength of RC beams. It is necessary to evaluate the fatigue strength of RC beams strengthened by the plate based on both the fatigue strength of reinforcing bar and the peeling fatigue strength of plate. Fatigue strength at 2 million cycles of the RC beams strengthened by the tensioned CFRP plate was confirmed with about 50% of the static flexural load bearing capacity.

Table 1 Mechanical properties of CFRP plate

Designed size (width x depth)	Tensile strength*	Modulus of elasticity	Maximum strain
50 x 2 (mm)	234 (kN)	150(kN/mm^2)	15600 (μ)

*:Tensile strength calculated by 3σ method

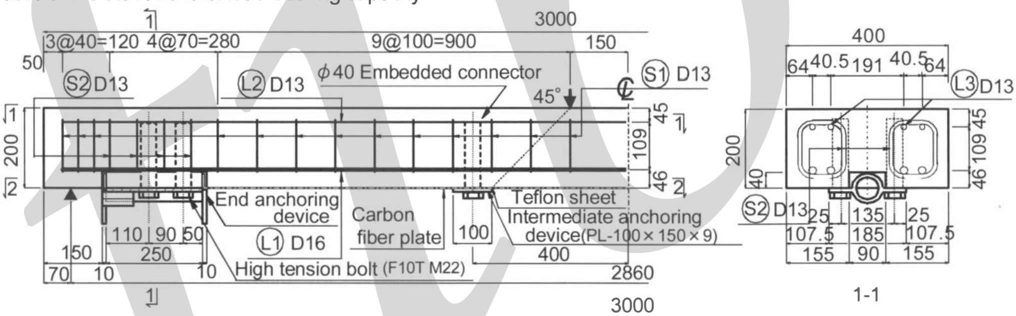

Fig.1 RC beam specimens and strengthening condition

OUTLINE OF TEST RESULTS OF STATIC LOADING TEST

Sound RC beams(Type N) , and deteriorated RC beams(Type D) to which the load was applied until the yielding of the longitudinal reinforcements before strengthening were used. The tension forces of plate were 0, 25 and 50% of the tensile strength of the plate. In some beams, intermediate anchoring devices (P) were installed in the shear span to improve the bond, and to delay the peeling failure of the plate.

Results of static loading test are shown in Table 2.The ultimate load of the beam strengthened by the tensioned CFRP plate increased, when compared with that of the reference beam without strengthening, no matter how the beam was deteriorated. The flexural failure of the beams strengthened by using the tensioned CFRP plate occurred immediately after the peeling of CFRP plate. The peeling of CFRP plate was influenced largely by the intermediate anchoring device. Relation between load and deflection at mid

Table 2 Results of static loading test

Name of specimens	P_{cr}	P_y	P_{stp}	P_{ult}	P_{cal}	P_{ult}/P_{cal}
N	11	58	—	67	61	1.10
N-00(1)	18	72	86	86	83	1.04
N-25(10)P	10	81	109	110	99	1.11
N-50(38)	39	100	110	113	106	1.07
N-50(34)P	34	106	126	126	114	1.10
D-25(26)P	{10}	86	110	110	109	1.01
D-50(31)	{7}	89	104	104	101	1.03
D-50(48)P	{5}	106	126	126	123	1.03

P_{cr} : Flexural cracking load, P_y : Yielding load
P_{stp} : Peeling load of plate , P_{ult} : Ultimate load
P_{cal} : Calculated value of ultimate load
( ): Measured tension force/tensile strength of plate
{ }: Initial flexural cracking load before strengthening

span is shown in Fig.2. The flexural deformability and load bearing capacity of beam were improved largely, in the beams strengthened by using the tensioned CFRP plate and the intermediate anchoring device, no matter how the beam was deteriorated.

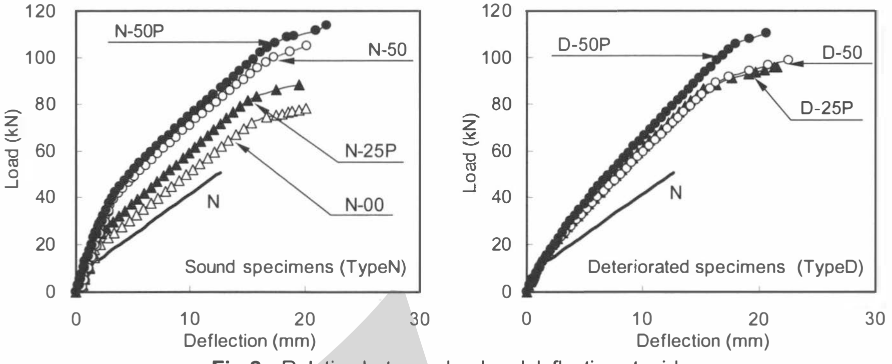

Fig.2 Relation between load and deflection at mid span

OUTLINE OF TEST RESULTS OF FATIGUE LOADING TESTS

Sound RC beams and deteriorated RC beams were used. The tension forces of plate were 0 and 50% of the tensile strength of the plate. In all beams, intermediate anchoring devices were installed, except for the beam strengthened by non- tension plate(I -N-00 specimen). In Series I , the effects of tension force of CFRP plate on the fatigue characteristics were examined under the action of B live load(245kN) in the bride designed for the TL-20 load(196kN). The upper and lower loads were 26.0kN(B live load) and 11.0kN(dead load) respectively until 2 million cycles of loading, and then after each 20×10^4 cycles of loading the upper load was increased until the failure of beam. Each increase of upper load was 9.8kN. In Series II, the flexural fatigue behaviors of the beams strengthened by the plate were examined. The upper load ratios were 70,60 and 50% as the percentage of the ultimate load. The lower load was 11.0kN.

Table 3 Results of fatigue loading test

Name of specimens	Upper load (kN)	Number of cycles to failure N	Type of failure
I -N-00	75.0*1(82.1)	92,461[2,892,461]	B
I -D-50P	85.1*1(68.9)	67,024[3,067,024]	P→B
II-N-50P-70	88.2 (70.3)	192,581	P→B
II-N-50P-60	75.6 (60.9)	647,417	P→B
II-N-50P-50	63.0 (51.2)	2,000,000	——

*1: Final upper load, *2: Upper load/ultimate load
[ ]: Total number of cycles to failure,
P: Peeling of plate, B: Breaking of longitudinal reinforcement

Results of fatigue loading test are shown in Table 3. It was confirmed that the sufficient fatigue load bearing capacity of the beam strengthened by the CFRP plate was obtained until 2 million cycles of loading. And it is also evident that CFRP plates can increase the fatigue strength of RC beams.

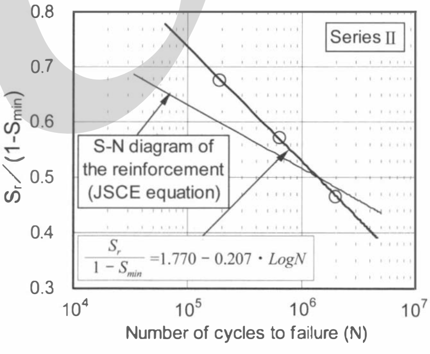

Fig.3 S-N diagram

S-N diagram and regression equation in Series II are shown in Fig.3. In case $S_r/(1-S_{min})$ was more than 0.5, fatigue life of longitudinal reinforcement decreased in comparison with RC beams strengthened by the plate. It is because that JSCE equation[2] gives safely the fatigue life of the reinforcement [3]. It is necessary to evaluate the fatigue strength of RC beams strengthened by the plate based on both the fatigue strength of reinforcing bar and the peeling fatigue strength of plate. Fatigue strength at 2 million cycles of the RC beams strengthened by the tensioned CFRP plate was confirmed with about 50% of the static flexural load bearing capacity.

REFERENCES

[1] Kojima,T., Takagi,N., Hamada,Y., Sakagami,N. and Imamiti,H. : Tensile strength and bond properties of continuous fiber plate. JSCE Kansai Chapter Proc. of Annual Conference of Civil Engineers, V-1-1～2, 1999
[2] Japan Society of Civil Engineers. : Standard specification for design and construction of concrete structures (design). pp.35-36, 1996
[3] Okamura,H. and Niwa,J. : Fatigue of reinforced concrete members. Concrete Joumal, Vol.21, No.1, pp.22-30, Jan., 1983

GFRP SHEAR STRENGTHENING OF RC BEAMS

Ugo Ianniruberto
Department of Civil Engineering
University of Roma "Tor Vergata", ITALY

Maura Imbimbo
Department of Mechanics, Structures and Environment
University of Cassino, ITALY

Keywords: shear capacity, fibre reinforced plastic sheets, experimental behaviour

1 INTRODUCTION

The shear behaviour of reinforced concrete beams strengthened by FRP sheets still needs a better understanding especially for what concerns the prediction of the sheets contribution to the shear strength of RC beams. In this paper we discuss the results of an experimental investigation carried out on beams reinforced by GFRP composite sheets with a span to shear ratio equal to three and finalised to evaluate the ultimate shear capacity of these elements. The experimental results expressed in terms of ultimate shear capacity, composite contributions and strain fields are compared to the results predicted by means of some theoretical models found in literature. The main conclusion of the work is the necessity of examining carefully the field of applicability of the theoretical models in terms of the values of the shear span to depth ratio.

2 EXPERIMENTAL PROGRAM

Six reinforced concrete beams of dimensions 150mm x 350mm x 3200mm, strengthened in shear by GFRP sheets, were tested. The beams were collected in tree couples of beams strengthened in shear by applying, respectively, one (ST1a and ST1b), two (ST2a and ST2b) and three (ST3a and ST3b) GFRP sheets entirely wrapped around the lateral surface in the shear span (Fig. 1).

Fig. 1 The wrapped zone of the beams and the positions of the strain gauges

3 COMPARISON BETWEEN ANALYTICAL MODELS AND TEST RESULTS

Some analytical models [1], [2], [3], [4] are applied to the beams tested in the experimental program. The theoretical and experimental results are reported in Tables 1 to 3. In the first two columns of the tables are reported the shear capacity V_u and the strength increase ΔV_u. In the third columns are reported the maximum experimental value of the strain in the fibre at collapse and the analytical predictions. The fourth columns report the values of the measured and predicted composite contribution to the shear strength. The values shown in the fifth column are the ratios in per cent between the composite contributions and the average of the strength increases. The last columns shows the ratios between predicted and measured composite contributions.

Table 1 Comparison between analytical models and test results for the beams ST1a and b

	V_u (KN)	ΔV_u (KN)		$\varepsilon_{u,frp}$ (‰)	V_{frp} (KN)	$V_{frp}/\Delta V_{uex}$ (%)	$V_{frp}/V_{frp,meas}$
Experimental	240	88	54	1.81	9	12	1
Chajes et al. [1]	152	24		5,0	24	34	2,76
Triantafillou [2]	174	46		9,6	46	65	5,28
Khalifa and Nanni [3]	166	32		6,0	32	45	3,66
Ianniruberto and Imbimbo [4]	161	21		3,1	15	21	1,74

Table 2 Comparison between analytical models and test results for the beams ST2a and b

	V_u (KN)	ΔV_u (KN)		$\varepsilon_{u,frp}$ (‰)	V_{frp} (KN)	$V_{frp}/\Delta V_{uex}$ (%)	$V_{frp}/V_{frp,meas}$
Experimental	274	122	88	-	-	-	-
Chajes et al. [1]	176	48		5,0	48	46	-
Triantafillou [2]	201	73		7,5	73	69	-
Khalifa and Nanni [3]	205	65		6,0	65	61	-
Ianniruberto and Imbimbo [4]	185	44		4,1	40	38	-

Table 3 Comparison between analytical models and test results for the beams ST3a

	V_u (KN)	ΔV_u (KN)		$\varepsilon_{u,frp}$ (‰)	V_{frp} (KN)	$V_{frp}/\Delta V_{uex}$ (%)	$V_{frp}/V_{frp,meas}$
Experimental	318	166	132	1.77	26	18	1,00
Chajes et al. [1]	201	73		5,0	73	50	2,82
Triantafillou [2]	212	84		5,8	84	58	3,28
Khalifa and Nanni [3]	225	97		6,0	97	67	3,78
Ianniruberto and Imbimbo [4]	215	74		4,8	69	48	2,70

5 CONCLUSIVE REMARKS

The comparison shows that all the models predict values of the ultimate load lower than the experimental one. On the contrary the theoretical composite contribution is highly overestimated because the maximum experimental values of strain level in the composite fibres were much lower than those provided by the models. The fact that the ultimate shear capacity of experimental beams was greater than that predicted by the analytical models, in particular the model proposed in [4], which takes into account the variation of the concrete contribution with respect to unstrengthened beams, suggests the consideration that, with reference to the geometry of beams characterised by a shear span to depth ratio equal to three and reinforced by composite sheets, as that analysed in this work, the ultimate shear capacity is provided by an arch mechanism in addition to the beam action, aggregate interlocking, dowel effect, composite and steel reinforcement contributions. Another point in support of the above hypothesis is that the experimental stress level in the fibres are lower than both the analytically predicted values and the stress value corresponding to the experimental ultimate shear capacity increase. It should be noted that the experimental results could have been affected by the anchorage steel plates whose role has not been adequately investigated.

The principal conclusion of the study is the necessity of examining carefully the field of applicability of the theoretical models in terms of the values of the shear span to depth ratio. Indeed clearly, even if the number of the experimental tests performed in this work was quite limited, it is highly probable that shear span to depth ratio was not enough large to clear the arch mechanism contribution.

SELECTED REFERENCES

[1] Chajes, M. J., Januszka T. F., Mertz D. R., Thomson Jr., T. A. and Finch, Jr., W.W. "Shear strengthening of reinforced concrete beams using externally applied composite fabrics", *ACI Struct. J.*, 92(3), 95-303, 1995.

[2] Triantafillou T. C. "Shear strengthening of reinforced concrete beams using epoxy-bonded FRP composites", *ACI Struc. J.*, 95(2), 107-115, 1998.

[3] Kalifa, A. and Nanni, A. "Improving shear capacity of existing RC T-section beams using CFRP composites", *Cement & Concrete Composites,* 22,165-174, 2000.

[4] Ianniruberto U. and Imbimbo, M. "Shear resisting contribution of composite for RC beams strengthened with FRP sheets", *Proceedings of the International Conference Advancing with Composite 2000*, Milan, May 2000, pp. 233-241, 2000.

FIRE DESIGN OF CONCRETE ELEMENTS STRENGTHENED WITH FIBRE COMPOSITE LAMINATES

Hendrik Blontrock, Luc Taerwe, Dep. of Strucural Engineering of Ghent University, Belgium
Paul Vandevelde, Dep. of Fuel Technology and Heat Transfer of Ghent University, Belgium

Keywords : fire, fire resistance, FRP, strengthening

1. INTRODUCTION

Beams and columns are successfuly repaired and/or rehabilitated by external strengthening with glued composite laminates, consisting of carbon fibres. The structural behaviour of these elements under normal environmental conditions is satisfactory. A particular problem arises when the behaviour of these elements is considered in fire. Indeed, reinforced and prestressed concrete elements have a good fire resistance due to the thermal insulation of the internal steel reinforcement by the concrete cover. The absence of an insulating concrete cover on the external composite laminate, will cause very quickly loss of interaction between the composite laminate and the concrete due to weakening of the adhesive (glass transition temperature of the epoxies is normally between 50°C and 100°C) [1].
In order to investigate the problem in more detail, a test programme was performed at Ghent University, comprising a total of ten beams [2]. Test results on five of these beams are summarized in this paper.

2. EXPERIMENTAL PROGRAMME

2.1. Test specimens

The dimensions of the tested beams are: height of 300 mm, width of 200 mm and a length of 3150 mm. The tensile reinforcement consists of 2 bars ϕ 16 mm, the shear reinforcement of closed stirrups ϕ 8 mm (fig. 1). A concrete mix with siliceous aggregate is used with a mean compressive strength of 57.5 N/mm². Sika Carbodur S1012 is used for strengthening these elements.
Beam 1 (unstrengthened reference beam) and beam 2 (strengthened reference beam) are statically loaded to failure at room conditions. Beam 3 (unstrengthened and unprotected beam) and beams 7 and 9 (strengthened and protected beams) are submitted to a fire test.
The composite laminate for beams 7 and 9 is thermally protected with calcium silicate plates. For Beam 9 only the bottom face of the beam is protected with an insulating plate (thickness of 25mm). The bottom face of Beam 7 is protected as well as the side faces of the beam over a height of 80 mm with insulating plates. The protection is mechanically fixed in the concrete. (Fig. 2)

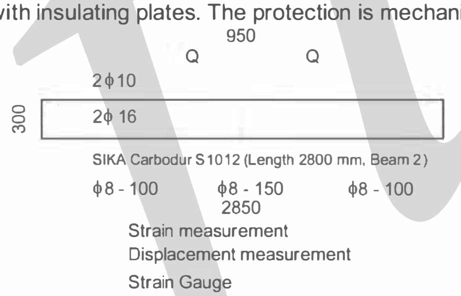

Fig. 1 Test set-up beams 1 and 2

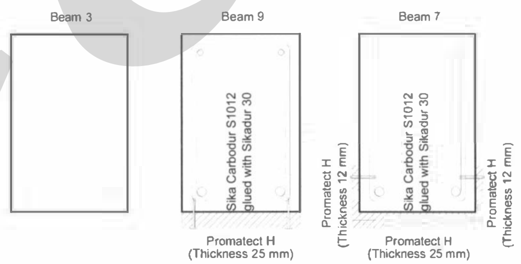

Fig. 2 Beams 3, 7 and 9 in fire test

2.2. Test procedure static loading of reference elements

A calculation is made for the maximum service load of beam 1 in accordance with Eurocode 2. Steel stresses for beams 1 and 2 are assumed to be equal for full service loading. The strengthened beam 2 has a 33% increase in maximum service load.
Beams 1 and 2 are first loaded in four-point bending to its maximum service load, then unloaded and reloaded up to failure. (fig. 1).

2.3. Test procedure fire tests

Beam 3 is placed above the horizontal furnace with a clear span of 2.85 m, beams 7 and 9 are placed above the furnace with a clear span of 3.00 m. The beams are loaded in four-point bending, similar to the test set-up for the static loading tests. During fire testing beam 3 is loaded to the maximum service load of an unstrengthened beam during fire testing. Beams 7 and 9 are loaded to the maximum service load of a strengthened beam.

The fire test is executed according to ISO 834. This standard prescribes the heating by the combustion gases in function of time.

3. TEST RESULTS AND VERIFICATION

3.1. Results of static loading tests

The load-deflection curves for beams 1 and 2 are given in figure 3. The failure load increases from 2 x 68.3 kN for the unstrengthened beam to 2 x 105.5 kN for the strengthened beam. The failure for the strengthened beam is characterized by yielding of the internal steel reinforcement followed by sudden delamination of the externally glued laminate. The composite laminate and a thin concrete layer is ripped off the concrete surface.

3.2. Results of fire tests

A time-deflection curve for beams 3, 7 and 9 is shown in figure 4. The time-deflection curves for beams 7 and 9 show a similar behaviour up to a point where a quite sudden increase in deflection occurs. At that time, it may be assumed that the interaction between the composite and the concrete is lost totally. For beam 9, the increase in deflection happens after 18 minutes when the temperature increase of the adhesive is 55°C. For beam 7, interaction between the concrete and the laminate is lost after 26 minutes when the temperature increase of the adhesive reaches 70°C.

3.3. Verification

A verification was made for the deflection behaviour of the strengthened and unstrengthened beam that were tested at room temperature. The unstrengthened reference beam failed due to concrete crusching, the strengthened beam failed due to debonding of the laminate. The calculated load-deflection curve can be found in figure 3 as well.

Also a calculation was made for the beams in the fire test. The calculation comprises two parts: a thermal calculation in order to obtain the temperature distribution in the cross-section, followed by a mechanical calculation of the time and temperature dependent moment curvature. The mechanical calculation takes into account thermal expansion and temperature dependent material properties. The increase of deflection for the tested beams is obtained through integration of the moment-curvature relationship.

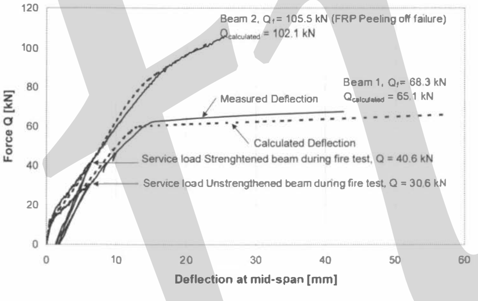

Fig. 3 Force-deflection for beams 1 and 2

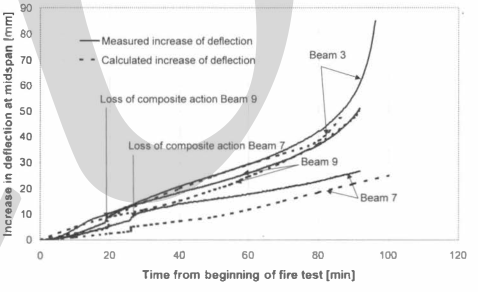

Fig. 4 Time-deflection for beams 3, 7 and 9

4. CONCLUSIONS

Based on the fire tests on the externally strengthened concrete beams, the following conclusions can be drawn:

- A thermal protection for the external strengthening system is needed in order to maintain interaction between the externally strengthening system and the concrete. Without a thermal protection, it is impossible to reach the same fire resistance as for the unprotected and unstrengthened beam.
- For the particular conditions of this test programme, interaction between the externally glued composite laminates and the concrete is lost when the temperature of the adhesive is about 70°C to 86°C.
- The fire resistance of the strengthened and protected beams is at least the same as for the unstrengthened and unprotected beams.

REFERENCES

[1] M. Deuring, *Brandversuche an nachträglich verstärkten Trägern aus Beton*, Empa nr. 148'795; Dübendorf, Switzerland, 1994

[2] H. Blontrock et al., *Fire tests on concrete beams strengthened with fibre composite laminates*, 3rd PhD Symposium, Vienna, 2000

TORSIONAL BEHAVIOR OF REINFORCED CONCRETE BEAMS STRENGTHENED WITH FRP COMPOSITES

Saravanan Panchacharam, Graduate Research Assistant
Abdeldjelil Belarbi, Associate Professor

Department of Civil Engineering, University of Missouri – Rolla, Missouri, USA

Keywords: Composites, Fiber Reinforced Polymer, Reinforced Concrete Beam, Strengthening, Torsional Moments, Twist Deformation.

1 INTRODUCTION

The method of strengthening structures with externally bonded Fiber Reinforced Polymer (FRP) composite materials gained significant attention in the last two decades. The addition of externally bonded FRP sheets to improve the flexural and shear performance of reinforced concrete (RC) beams has been actively pursued during the recent years. Research reveals that strengthening using FRP provides a substantial increase in post-cracking stiffness and ultimate load carrying capacity of the members subjected to flexure and shear. Research related to the strengthening of torsional members with FRP composites is very limited and meager data or design guidelines are available in the literature. The lack of experimental and analytical studies along with the increasing interest in the use of FRP materials in the repair and rehabilitation of concrete structures led to this study on torsional behavior of reinforced concrete beams strengthened with FRP sheets. This paper presents the results and behavior of RC members strengthened with externally bonded Glass FRP sheets and subjected to pure torsion.

2 EXPERIMENTAL RESEARCH PROGRAM

The main objectives of this study were to investigate the torsional behavior of RC beams strengthened with externally bonded GFRP sheets and to identify the influence of the design variables considered in the effectiveness of strengthening. The variables considered were (1) fiber orientation (parallel or perpendicular to the beam axis), (2) three vs. four faces of the beam being strengthened, (3) one ply vs. two plies orthogonally placed, (4) continuous wrap vs. strips and (5) influence of anchors in U-wrap strengthening schemes. Based on the variables considered in the study, totally eight beams were tested. Out of the eight beams tested in this program, seven were strengthened with MBrace EGlass FRP laminates and one beam was kept un-strengthened and tested as reference beam. Schematic representations of the strengthening schemes and test beams designations are shown in Fig. 1.

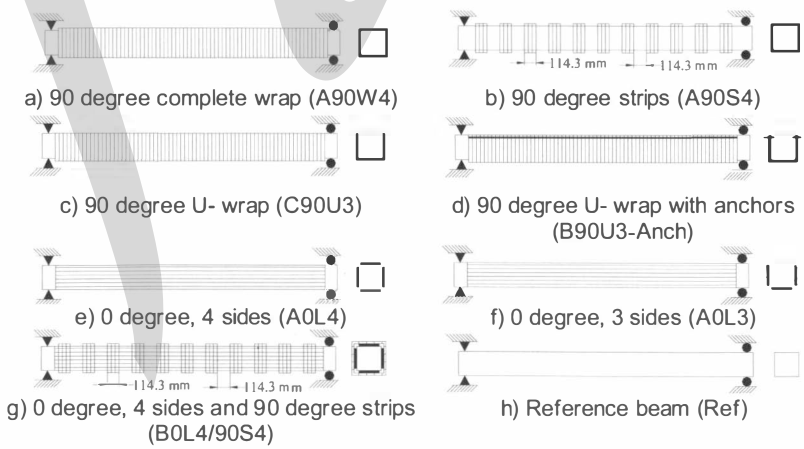

Fig. 1 Schematic representation of strengthening schemes

3 TEST RESULTS AND CONCLUSIONS

Test beams are grouped according to the investigated variables considered in the study. Effects of different variables on the torsional behavior of RC beams are illustrated in Figs. 2, 3 and 4. The analytical predictions along with the experimental results are summarized in Table 1. While the followings are some of the pertinent concluding remarks, further details are given in the full-length companion paper.

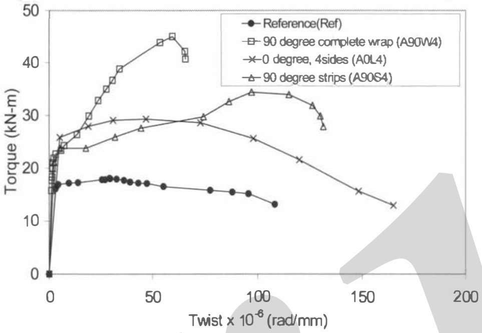

Fig. 2 Effect of fiber orientation and continuous wrap versus strips

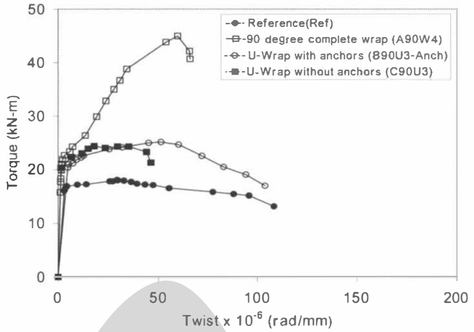

Fig. 3 Effect of complete wrap and U-wrap (with and without anchors)

(1) Torsional reinforced concrete beams strengthened with GFRP sheets exhibited a significant increase in their cracking and ultimate strength as well as ultimate twist deformations.

(2) Strengthening schemes with complete wraps in 90-degree fiber orientation with respect to beam axis provided an effective confinement and, therefore resulted in a significant increase (about 150%) in the ultimate torsional strength.

(3) Substantial increase in cracking strength was observed when RC beams were strengthened with FRP sheets oriented in the longitudinal direction of the beam, where the FRP provided passive prestress forces.

(4) Strengthening with FRP sheets in the longitudinal direction of the beam on three faces or four faces of the cross-section provided similar behavior.

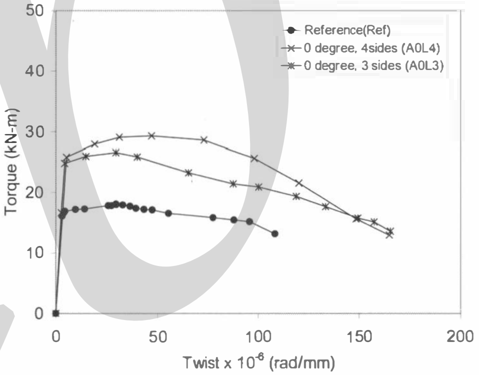

Fig. 4 Effect of number of sides strengthened longitudinally

(5) The proposed design equations seemed to predict both cracking and ultimate torsional moments very closely as shown in Table 1.

Table 1 Comparison of experimental and analytical cracking and ultimate torsional moments

Test-beams	Cracking Torque (kN-m)			Ultimate Torque (kN-m)		
	Experimental (Ex)	Analytical (An)	Ex/An	Experimental (Ex)	Analytical (An)	Ex/An
Reference	17.1	15.7	1.09	18.2	16.9	1.07
A90W4	22.9	20.8	1.10	47.1	45.4	1.04
A90S4	22.1	17.7	1.25	36.0	36.4	0.99
A0L4	27.0	29.9	0.90	30.7	29.9	1.03
A0L3	26.3	28.8	0.91	27.8	28.8	0.97
B0L4/90S4	20.1	24.4	0.82	32.6	35.9	0.91
B90U3-Anch	22.0	18.2	1.20	26.3	28.1	0.94
C90U3	20.6	19.1	1.08	24.6	26.4	0.93

RECENT DEVELOPMENT OF STEEL-CONCRETE HYBRID BRIDGES IN JAPAN

Akimitsu Kurita
Osaka Institute of Technology
JAPAN

Osamu Ohyama
Katayama Stratech Corp.
JAPAN

Keywords: composite bridge, mixed bridge, corrugated steel web plate, composite column

1 INTRODUCTION

The steel-concrete hybrid bridges have been remarkably developed during the last decade in Japan due to the technological and economical advantages throughout the design and construction process and service life [1]. There are two ways to realize the hybrid bridges. First one is from the steel bridge and the other one is the approach from concrete bridge.

The steel-concrete hybrid bridge consists of composite- and mixed bridge. Therefore, not only latest composite bridge examples, but also mixed ones are reported in this paper. In addition to those superstructures, one example of the substructures by using the idea of the composite columns and other new technologies concerning the composite constructions are also presented in this paper.

2 COMPOSITE BRIDGES

2.1 Approach from Steel Bridge

One of the examples, Inabe River Bridge, girder bridge, is a 4-span continuous bridge (86.2+91.5+97.5+96.7m) with 2-main box girders (overall length 373.5m), where the precast prestressed concrete (PPC) deck and the headed stud, 25mm in diameter and 250mm long, were applied (see Fig.1). Furthermore, PPC decks were prestressed longitudinally to prevent the cracks of concrete in the region of intermediate supports. This bridge was completed at the end of 2000.

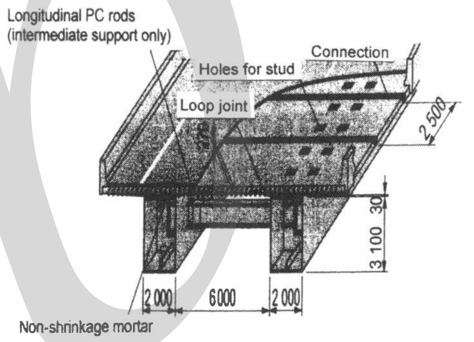

Fig.1 Outline of the Inabe River Bridge

2.2 Approach from Concrete Bridge

As the typical composite girder bridge has been developed from concrete bridge, the prestressed concrete box girder bridge with corrugated steel webs is introduced firstly. Fig.2 shows the outline of the prestressed concrete box girder bridge with corrugated steel plates. Some of the characteristics of this type of the bridge are as follows:

a) The corrugated web bridge makes the girder lighter than a conventional concrete web bridge. This leads to a reduction of foundation sizes and horizontal seismic forces.
b) Prestress can be effectively introduced to the top and bottom concrete slabs due to the accordion effect of the corrugated steel plates

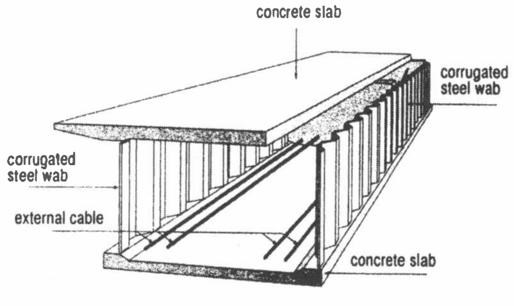

Fig.2 Outline of the concrete box girder bridge with corrugated steel web plate

3 MIXED BRIDGES

3.1 Connection of Steel and PC Girder

For example, the Shinkawa Bridge with overall length of 278m is located in Takamatsu, Shikoku. The bridge extends over a river, intersecting roads, box culverts and so on, therefore it is necessary to have the center span of 118m. Thus, steel girders, relatively light and easy for erection work, were used for the center span portions, and concrete girders were used for the side span portions in order to balance weight that the entire bridge receives. There is a 5-span continuous mixed bridge, working in harmony with landscape, economy and structural performance. This bridge was completed in 2000.

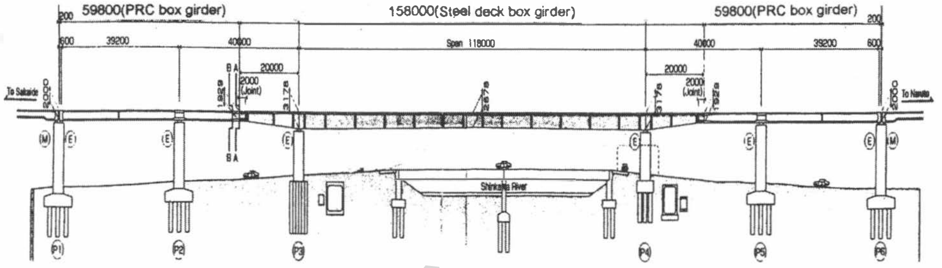

Fig.3 Side elevation of the Shinkawa Bridge

3.2 Connection of Steel Girder and RC Pier

In order to increase an earthquake resistance of whole bridge structure, the rigid connection system between steel girder and reinforced concrete pier is adopted. One of the examples, the Imabepugawa Bridge is a 3-span (48.2+81.5+57.2m) continuous twin I girder bridge where two intermediate RC piers were connected with steel girders rigidly. At two connecting parts, a special structural detail was used. Four web plates of main and cross girders form the closed box section on the top of pier and cast in-situ concrete was filled into the box. Diaphragms and vertical stiffeners attached inside the box act as the shear connectors, because they have many holes. The idea of perforbond rib was applied in this connecting part. By adopting the rigid connecting structural system, the cantilever erection of main steel girder could be done easily and speedily by using gantry crane.

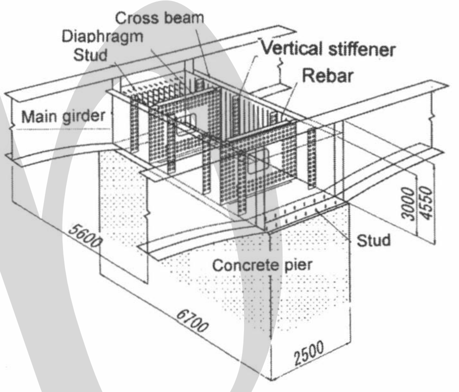

Fig.4 Connection of the Steel Girder and RC

4 CONCRETE ENCASED STEEL PIPE COLUMN FOR HIGH PIER

The conventional RC hollow high pier needs a large amount of reinforcement, because of the standard of earthquake resistant design. Therefore, the construction cost as well as the construction period is serious subjects. The high bridge piers with steel pipe-concrete composite structure exhibit not only high seismic resistance in effect of ductile steel pipe and spiral high strength strand, but also an advanced construction method.

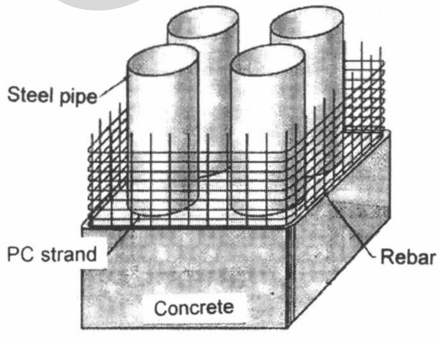

Fig.5 Outline of the Concrete Encased Steel Pipe Column for High Pier

5 CONCLUSION

The share of hybrid bridges in Japan is increasing within the last five years, because they have a high competitiveness. In the future, therefore, various new types of the hybrid bridges will be developed in the world.

REFERENCES

[1] Subcommittee on Steel-Concrete Hybrid Bridges: Recent Development of Steel Concrete Hybrid Bridges, JSCE, Nov., 2001(in Japanese).

STUDY ON TRANSVERSE BEHAVIOR OF CONNECTION BETWEEN CONCRETE SLAB AND CORRUGATED STEEL WEB

K. Shito, Y. Kamihigashi, N. Suzuki
Japan Highway Public Corporation
JAPAN

T. Tsujimura, M. Sakurada
Japan Prestressed Concrete-Contractors Association, JAPAN

F. Machida
Kawada Industries, Inc.
JAPAN

Keywords: corrugated steel web, concrete slab, connection, transverse behavior, static test, fatigue test

1 INTROCUCTION

In recent years, composite prestressed concrete bridge with corrugated steel webs (hereinafter called Corrugated steel web bridge) have been actively planned, designed and constructed in Japan in an effort to reduce the dead load of prestressed concrete bridges, improve the seismic performance, streamline the construction, and minimize the cost as a result of these effects (Fig.1). On ordinary I-section steel plate girder bridges, the out of plane stiffness of the web is small, therefore, even if T-load acts on the slab, the out-of-plane bending moment hardly arises at the connections between the concrete slab and the steel I-girder, with the exception of the position near the crossbeam with the vertical stiffener. However, as for a corrugated steel web bridge, the out-of-plane stiffness of the web is large, therefore the transverse bending moment arises at the connections between the upper concrete slab and the corrugated steel web (hereafter simply "connections"), as shown in Fig.2. This transverse bending moment may cause the extraction stress of dowels, therefore, it is believed that study on this stress is needed. For this reason, static load tests and fatigue tests were conducted by the use of real-size test specimens modeled on the transverse direction of connections with stud dowel connection, angle dowel connection and embedded connection, respectively, and these connections had been adopted in actual corrugated steel web bridges (Fig.3). This paper will report on the results of these tests.

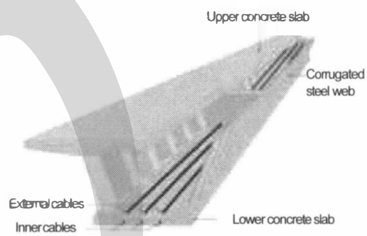

Fig.1 Corrugated steel web bridge

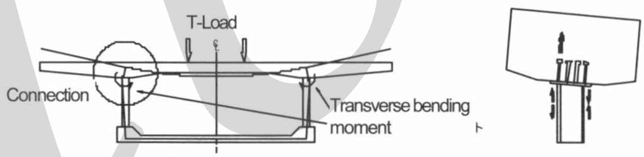

a) Transverse bending moment by T-load b) Extraction of dowel

Fig.2 Transverse bending moment in the connection

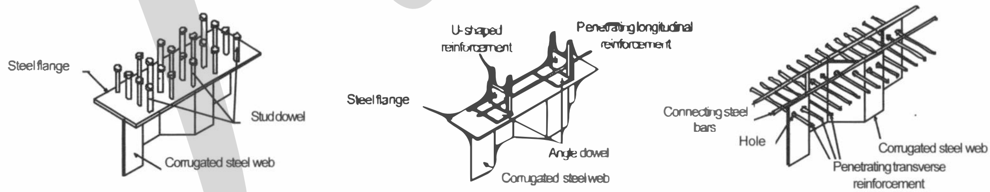

a) Stud dowel connection b) Angle dowel connection c) Embedded connection

Fig.3 Connections between concrete slab and corrugated steel web

2 EXPERIMENTAL PROGRAM

The test specimens were full scale that modeled the transverse direction of stud dowel connections, angle dowel connections and embedded connections (hereinafter, called stud dowel specimen, angle dowel specimen and embedded connection specimen, respectively) as shown in Fig.4.

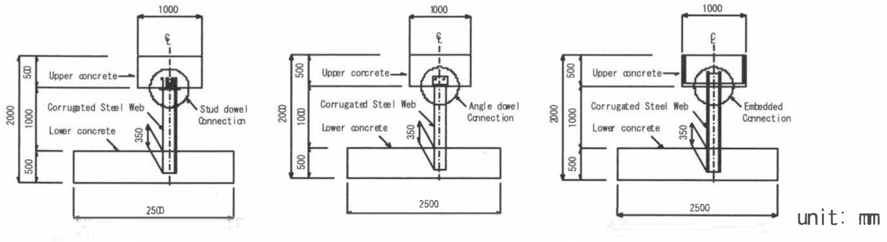

a) Specimens with Stud dowel b) Specimens with Angle Dowel c) Specimen with Embedded connection

Fig. 4 General view test specimens

Fig. 5 shows the test set-ups. The concentrated load was applied at a position of 1 meter from the center of the connection, and transverse bending moment was applied to the connection. In static test, the load was applied in a static manner and continued until the specimen was broken. In the fatigue test, the load was applied repeatedly with a load amplitude of 34kN (maximum load P_{max}=52kN, minimum load P_{min}=18kN).

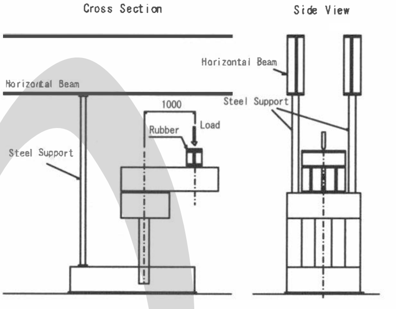

Fig. 5 Test set-ups

3 RESULTS AND CONSIDERATION

Table 1 show the results of the static load tests. The transverse ultimate strength of the stud dowel specimens did not reach the calculated value. On the other hand, the ultimate strength the angle specimen and embedded connection specimens almost matched the calculated values. As for stud dowel specimens, the experimental ultimate strength was smaller than calculated values because the studs which could not resist the transverse bending moment exist in the connection due to the positional relationship of the stud dowels and the corrugated steel web as shown in Fig.6

. In this study, the authors conducted static loading tests and fatigue tests for angle dowel connections and embedded connections as well. The following knowledge was gained as a result.

Table 1 Results of Static load test

Specimen	Ultimate Strength Experimental Value (kN)	Ultimate Strength Calculated Value (kN)	Ratio
S-1	90	210	0.43
S-2	139	262	0.53
S-3	162	425	0.38
A-1	253	211	1.20
A-2	267	235	1.14
E-1	251	231	1.09

1) Static load tests

- As for angle dowel connection, the ultimate strength almost matches the calculated value. The design method of transverse ultimate strength for the angle connections can be said to be almost completely valid.
- As for embedded connection, the concrete slab tends to suffer damage from embedded steel, therefore, it would be better that the concrete slab is reinforced by the transverse prestressing as in the case of the Hondani Bridge to prevent the damage of concrete slab from embedded steel.

2) Fatigue tests

- The fatigue strength with respect to stud pull-out force is JSSC- H.
- The angle dowel connection with not-welded U-shaped reinforcements has higher resistance to fatigue as compared with the connection with welded U-shaped reinforcement. Besides, since the crack from the weld toe of flare welding of U-shaped reinforcement is confirmed as for the angle dowel connection with welded U-shaped reinforcements, it is thought that it would be better not to weld U-shaped reinforcements to the angles.
- The fatigue strength of the embedded connection was superior to that of the stud dowel connection and angle dowel connections with flanges.

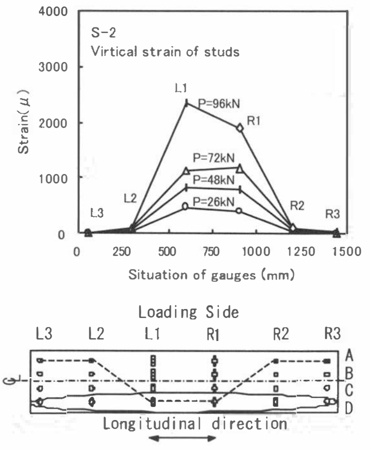

Fig.6 Distribution of stress in studs

FATIGUE CHARACTERISTICS OF CONNECTION BETWEEN STEEL PLATES IN A PC COMPOSITE GIRDER WITH CORRUGATED STEEL WEBS UNDER TRANSVERSE LOADING

K. Shito, Y. Kamihigashi, N. Suzuki
Bridge division,
Expressway Research Institute,
Japan High Public Corporation,
Japan

T. Ooura, H. Tategami
Japan Prestressed Concrete
Contractors Association,
Japan

T.Yanaka
Yokogawa Bridge Corp.,
Japan

Keywords: corrugated steel web, scallop, transverse bending moment, fatigue test

1 INTRODUCTION

Iln recent years, the composite prestressed concrete (PC) bridges with corrugated steel webs have been actively planned, designed and constructed in Japan, In order to decrease the weight, improve seismic performance, streamline construction, and to reduce costs, A typical layout of this bridge is shown in Fig. 1 [1], [2], [3].

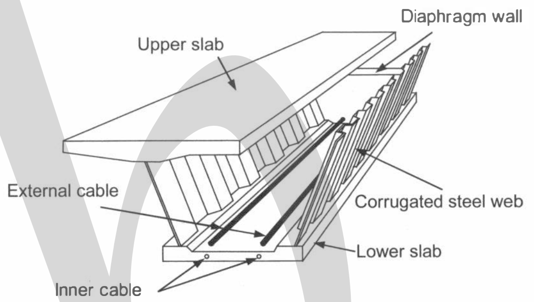

Fig. 1 Layout of PC Bridge with corrugated steel webs

On ordinary steel I-girder bridges, the stiffness of the web is low, so when type T-load imposed loads (as specified by [4]) acts on the slab, almost no out-of-plane bending moment is produced at the connections between the upper slab and the steel I-girders. However, on a corrugated web bridge, the out-of-plane stiffness of the web is large, so transverse bending moment is produced at the connections between the upper slab and the corrugated steel web. This transverse bending moment may cause the dowels to pull-out of the connections in the corrugated web bridge or produce localized stresses at the welds between the steel flanges and the corrugated steel web (hereafter "welds for neck portion") or scallops. Such problems do not occur on ordinary steel I-girder bridges but occur only in corrugated steel web bridge. As such, it was necessary to investigate the behavior of such connections under transverse loading.

Until now, bolt joints (H.T.B. (single), tensile bolted) and welded joints (butt weld and lap weld) have been used for the connections between the corrugated steel members on PC box girder bridges with corrugated steel webs in Japan

Full-scale model tests were carried out on connections having overlap fillet welding together with scallop as shown in Fig.2, to confirm the fatigue performance of such connections under transverse loading. The results of this investigation are presented in this paper, with emphasis on the stresses around the scallop region of the connections.

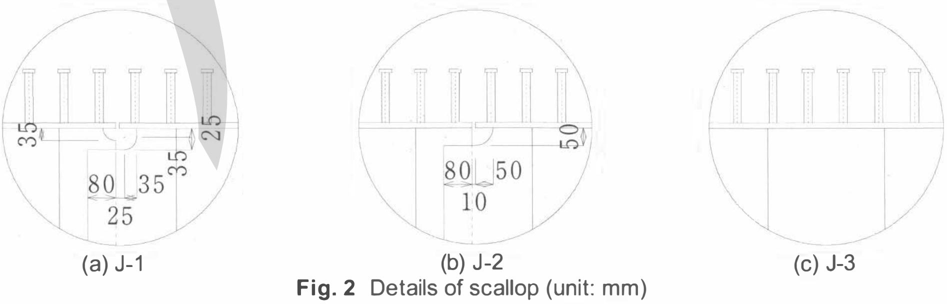

Fig. 2 Details of scallop (unit: mm)

2 LOADING METHOD

The fatigue test was conducted by using the loading unit shown in Fig. 3 to apply fixed-point loading.

The maximum load for the fatigue test was 52 kN and the minimum load was 18 kN. These loads were determined from the results of tests with basic static loading test specimens and the minimum load that could be controlled by the fatigue loading tester. The maximum load of 52 kN was determined so the stress amplitude of the studs on the basic static loading test specimen would be 100 MPa. Cyclic loading was performed at 3 Hz. After 3 million loading cycles, the maximum load was increased to 1.5 times from 52 kN, to 78 kN, and the minimum load was maintained at 18 kN.

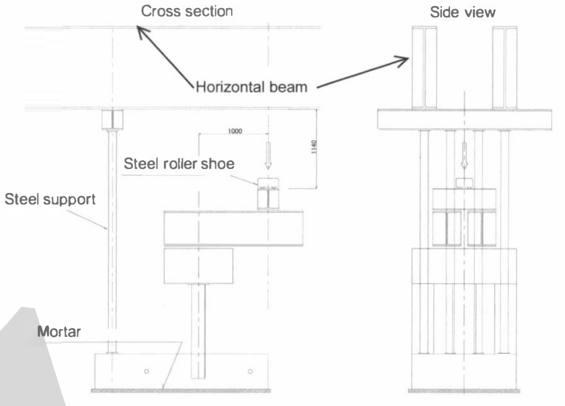

Fig. 3 Overall loading diagram (unit: mm)

3 CONCLUSION

The following is a summary of the FEM analysis and the results of fatigue tests with the full-size test specimen.

- The FEM analysis for the design live load of the actual bridge model show that transverse bending moment at the connections between the steel flange and the corrugated steel web produced great tensile force at the outer web and great compressive force at the inner web. This is greater than that produced by shear force.
- This transverse out-of-plane bending moment caused about twice as much stress to be concentrated at the field joints between the corrugated steel web members as in the ordinary sections. This is due to the presence of the scallops. The degree of stress can be reduced by modifying the shape of the scallops.
- A fatigue test was implemented with load applied for 3×10^6 cycles with a stress amplitude equivalent to the JSSC-C class [5](albeit under compressive stress). No fatigue cracking occurred at the welds in any of the test specimens. The fatigue test was continued with the load amplitude increased by 1.5 times. Failure occurred in the stud dowel at the connection between the upper slab concrete and the corrugated steel web, but no failure occurred around the welds.
- A simple fatigue check using the results of the FEM analysis and loading test found that modifying the scallop shape would enable the fatigue life to be extended by 1.5 times or more.
- For both test specimen J-1 and test specimen J-2, no damage to the scallop section due to fatigue was noted. However, when compared in terms of ease of construction, construction of the boxing welds for J-1 type scallop is thought to be easier than J-2 type.

REFERENCES:

[1] Mizuguchi K., Terada N., Ashizuka K, Ohura T., Kato T. :Design and Construction of Hondani Bridge, PC Bridge with Corrugated Wteel Webs, fib Symposium 1999 Proceedings, Vol.2, pp.725-730,Oct., 1999

[2] Mizuguchi K., Ashizuka K., Yoda T., Sato K., Sakurada M., Hidaka S. :Loading Tests of Hondani Bridge -PC Bridge with Corrugated Steel Webs by Cantilevering Construction Method-, Bridges and Foundations, Vol. 32, No. 10, pp.25-34, Oct., 1998 (in Japanese)

[3] Mizuguchi K., Ashizuka K., Furuta F., Oura T., Taki K., Kato T.: Design and Construction of Hondani Bridge, Bridges and Foundations, Vol. 32, No. 9, pp.2-10, Sept., 1998 (in Japanese)

[4] Japan Road Association: Specifications for highway bridges Part I, 1996 (in Japanese)

[5] Japanese Society of Steel Construction: Specifications for fatigue design of Steel structures, 1993 (in Japanese)

DEFORMATION CAPACITY OF PRESTRESSED CONCRETE BRIDGES WITH CORRUGATED STEEL PLATE-WEB CONNECTION

Kenji Kosa (Assoc. Prof., Kyushu Institute of Technology, Japan)
Hiroshi Kobayashi (Senior Engineer, Hanshin Expressway Public Corporation, Japan)
Zang Jiandong (Senior Engineer, PS Corporation, Japan)
Kenji Fujibayashi (Graduate Student, Kyushu Institute of Technology, Japan)

Keywords: corrugated steel web, connection, FEM

INTRODUCTION

The Hanshin Expressway providing a major highway network in the Kansai region has decided to construct a PC box girder bridge with corrugated steel plate webs for an elevated bridge section on the Kita-Kobe Route. This type of bridge enables to reduce construction costs and increase construction efficiency. However, the connection of the concrete slab and the corrugated steel plate web is a major problem with this type of bridge, a composite structure incorporating the material characteristics of both concrete and reinforcement. Embedding the corrugated steel plate in the concrete slab is one of the methods commonly used, but for the planned Nakano Bridge, a combination of the stud dowel and the perforated rib made of CT shape steel is selected to further improve constructivity. For cost reduction, the bridge is designed as a partially prestressed concrete (PRC) structure that allows the tensile stress up to –1.5 N/mm^2 but does not allow cracking. As there has been no application example of such structure, static loading tests were conducted to investigate the behavior of the bridge in the direction perpendicular to the bridge axis. Parameters were the connection method and the amount of prestress introduced. Then, 2D elasto-plastic analysis by the FEM is conducted on the obtained results. The deformation capacity of the bridge and the performance of the connection are evaluated analytically in terms of the maximum strength, the damage observed, and the distribution of strain on the reinforcement and the concrete.

EXPERIMENTAL PROGRAM

Three specimens, AP, BP, and BR, were constructed. Specimen BP constructed under the same design conditions with the Nakano Bridge was selected as the control specimen. Their size and length are shown in Fig. 1. Vertical loads were applied to the loading point A on both ends of the specimen until the connection area reached the ultimate state. During loading, vertical displacement at the span center (loading point B) was kept constant by the load control

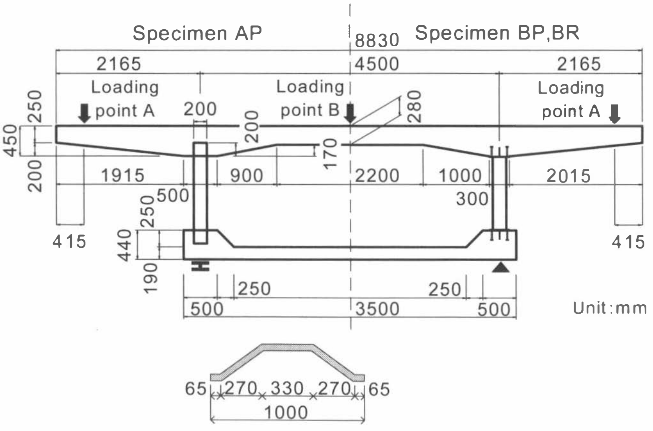

Fig.1 Structure of specimens

method. According to the experimental results, the capacity of specimens AP, BP, and BR, was 310, 325, and 291 KN, respectively. As to Specimen AP, cracks propagated toward the embedment position of the corrugated steel plate, and a level difference was caused on the left and right sides of cracks when the specimen reached to fracture. In contrast, cracks of Specimen BP were better dispersed than those of Specimen AP in terms of their number and width. All the specimens showed a gentle drop curve after reaching the maximum load, without causing a brittle fracture.

ANALYSIS

For the present analysis, a 2D analysis model is used instead of a 3D model because the analysis time of the latter model is enormous and its evaluation method complex. As the specimens are right and left symmetrical, only the half portion of each specimen is modeled. The model for the connection is shown in Fig. 2.

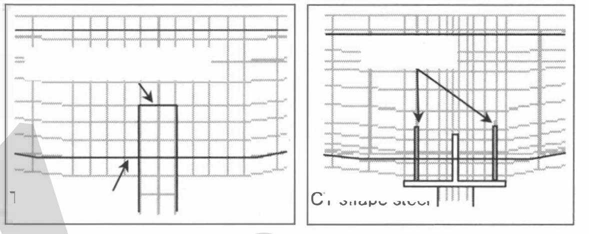

Fig.2 Connection models (left: embedment type; right: Nakano Bridge type)

According to the analysis, deformation of all specimens is concentrated only on the upper slab, and no conspicuous deformation observed on the corrugated steel plate and the lower slab. This indicates that fracturing depends on the type of connection on the upper slab and the amount of prestress introduced.

With regard to the effect of prestress, specimen BR of the PRC structure was analyzed by changing the prestress amount to 0.5, 0.75, 1.25, 1.5 times of the specimen's original prestress (392.0 kN/mm^2). It was found that deformation behavior of the specimen after the yielding of the upper reinforcement in the upper slab differs by the difference of the prestress amount. However, in view of about 20% probable deviation at introduction, it can be said that the effect of the prestress amount on the strength of the specimen is not so significant.

CONCLUSIONS

As a result of the 2D elasto-plastic analysis conducted on the results of static loading tests, the following conclusions can be drawn:

① Analysis is capable of evaluating the behavior of the specimens in the direction perpendicular to the bridge axis, though reproduction was slightly difficult around the maximum load.

② In the embedment type connection, damage tended to concentrate around the embedment position of the corrugated steel plate. But, in the case of the Nakano Bridge type connection, damage tended to disperse because of the existence of the flange.

③ The amount of prestress does have effect on the deformation capacity of the specimen, but the effect is not so significant in view of possible deviation of prestress amount at the time of application.

From the above finding, it can be said that the both embedment type and the Nakano Bridge type connections exhibit roughly similar deformation behavior with regard to the direction perpendicular to the bridge axis, though their damage mechanism differs because of the difference of the support structure for the upper slab.

REFERENCES

Suzuki, M., Iguchi, A., Kuramoto, O., and Kobayashi, K.: Full-scale loading tests on a PC bridge with corrugated steel plate webs., The Proc. of the 10th symposium on the development of PC concrete.

BEHAVIOR OF CORRUGATED STEEL WEB GIRDER AROUND MIDDLE SUPPORT

Hiroshi SHIRATANI, Katsuyuki SAKASHITA, Hirotoshi OBI, Shuichi FUJIKURA
Taisei Corporation
JAPAN

Keywords: composite girder, corrugated steel web, shear resistance, buckling, flexural resistance

1 INTRODUCTION

Composite bridge girder, consisting of top and bottom slabs of prestressed concrete and webs of corrugated steel, is a prospective form because of such advantages as the lightness of the girder, short construction period, and resulting cost-saving. This type of composite girder has been originally developed in France [1]. Recently, as an increase of projects for this type of bridges in Japan, several authors such as [2] have thoroughly investigated the performance of corrugated steel web girders.

However, with respect to this type of composite girder around middle support, where severe and complicated stress field may be formed in many cases of continuous girders, its performance has not been fully investigated, except for the suggestion of Combault [1] that the local bending moment in the slabs may be remarkable because of the small stiffness of the steel web. Although the moment occurs when the slabs restrain the shear deformation of the web with its flexural rigidity according to his suggestion, the behavior of the girder after cracking of the slab has not been made clear.

In this context, the authors have investigated the fundamental characteristics of the composite girder of this type around middle support up to the ultimate flexural and shear state.

2 EXAMINATION OF SHEAR BEHAVIOR

Figure 1 shows the cantilever model for the experimental and analytical study of the shear behavior of the corrugated steel web girder. The model has been designed so that the shear failure of the web should precede the flexural failure, although the amount of longitudinal reinforcing bars in the concrete slab was set out to have yielded before the shear failure of the web.

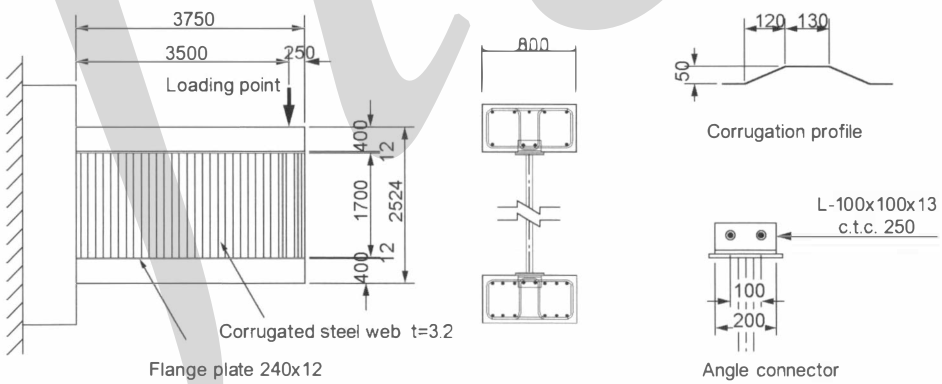

Fig. 1 Model for shear behavior

In the experiment the girder failed with sudden shear buckling of the web. Figure 2 shows the ratio of the shear carried by the web to the total shear force, R_w, at the time instants before cracking of the slab (applied load: 200kN) and shortly before buckling of the web (1200kN). R_w becomes smaller near the footing, while both shear force and cross section are uniform longitudinally. This is because concrete slabs restrain the shear deformation of web near the footing as Combault has suggested. Although the shear carried by the slab decreases after cracking, this characteristic of the slabs is still effective even with remarkable cracks. This behavior of the slab could provide larger shear strength of the girder at middle support than conventionally expected, if the slab is appropriately designed. The general behavior is predicted suitably by the finite element analysis with nonlinear elasticity and geometrical nonlinearity into account. The measured load-defection relationship was also in good agreement with the calculated one with an error of less than 5%.

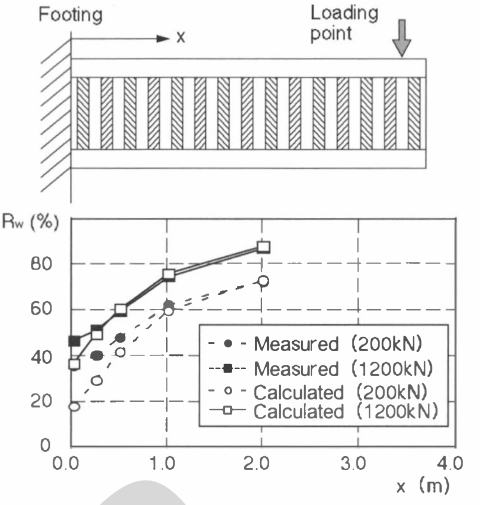

Fig. 2 Distribution of ratio of shear carried by web to total shear force

3 EXAMINATION OF FLEXURAL BEHAVIOR

In the designs of bridges with corrugated steel webs, the flexural strength of the girder is generally estimated on the assumption that the longitudinal stiffness of the corrugated steel web is so small (generally said to be 1/300 to 1/500 of flat plate) that the stiffness of the web could be neglected.

However, in an experiment previously conducted by the authors with a full-scale cantilever box girder model, the measured flexural strength was over 25% larger than the predicted strength by a fiber element analysis with web stiffness neglected. On the other hand, the fiber element analysis could predict the load-displacement relationship of the full-scale model accurately when the web stiffness was taken into account, although the stiffness was reduced to 1/30 of the real stiffness of the flat plate. This fact has implied that the corrugated steel web contributed somehow to the flexural strength. The authors subsequently investigated the ultimate flexural behavior of the girder with corrugated steel web around middle support, based on three-dimensional finite element analyses.

The scaled model for this analytical study is a cantilever of I-shaped cross section, with cantilever length of 10.5 m and girder height of 2.024 m. The girder has been designed so that the flexural failure should precede the shear failure. The wave profile of the corrugated steel web and the material properties are identical with those of the model in Fig. 1.

For comparison, the following analyses were carried out for this girder:

- Three-dimensional finite element analyses (Two cases changing web thickness)
- Two-dimensional fiber element analysis (Longitudinal stiffness of corrugated steel web neglected)

From this study the following results were obtained:

(1) The flexural strengths obtained by the finite element analyses was 12 to 24% larger than that by the fiber element analysis with web stiffness neglected. In addition, the girder with larger web thickness had higher strength and ductility.

(2) It was confirmed that the axial stiffness of corrugated steel web fixed to top and bottom slabs is about 10 times larger than conventionally expected, thus the web can function as reinforcing steel.

4 CONCLUSIONS

This study has demonstrated that composite girder with concrete slabs and corrugated steel webs could have larger ultimate flexural and shear strengths than conventionally expected, with the help of mutual aids of concrete slabs and steel webs. However, since the present study has only identified fundamental characteristics, further investigation may be necessary toward the establishment of a reasonable design method with the identified performances appropriately into account.

REFERENCES

[1] Combault, J. : The Maupré Viaduct near Charolles, AISC National Steel Construction Conference, February, 1988

[2] Yamaguchi, K., Yamaguchi, T. and Ikeda, S. : The mechanical Behavior of Composite Pestressed Concrete Girder with Corrugated Steel Webs, Concrete Research and Technology, Vol. 8, No. 1, January, 1997 (in Japanese)

SHEAR BUCKLING BEHAVIOR OF PRESTRESSED CONCRETE GIRDERS WITH CORRUGATED STEEL WEBS

Tsutomu Kadotani Keiichi Aoki Kenichiro Ashizuka
Japan Highway Public Corporation, Tokyo, JAPAN

Takuya Mori
P. S. Corporation,
Tokyo, JAPAN

Makoto Tomimoto
Haltec Corporation,
Tokyo, JAPAN

Masato Kano
Bridge & Computer Engineering Co., Ltd.,
Osaka, JAPAN

Keywords: corrugated steel web, shear strength, shear buckling

1 INTRODUCTION

Recently, hybrid structures making use of different structural material components are gaining popularity in Japan. One example of such structures may be prestressed concrete box girders with corrugated steel webs. It has several advantages such as: 1) reduction of the girder weight, 2) efficiency of introducing prestress forces due to what is called accordion effect of corrugated plate, 3) no need for additional stiffeners of webs because of its high shear strength and 4) easiness for the long-term repair and maintenance.

The shear buckling behavior of corrugated steel webs, however, has not been fully investigated in the world. In the present Japanese design codes, the ultimate strength of the corrugated steel web is only evaluated based on the elastic shear buckling strength and then reduced according to the yield stress in the inelastic buckling region. Furthermore, the local and global bucklings have been taken into account only separately and their interaction has remained unsolved.

In this study, to begin with, parametric studies of the elasto-plastic and finite displacement analyses are carried out for the shear buckling strength of simply supported beams composed of a corrugated steel web without concrete flanges. Next, experimental tests of simply supported beams composed of a corrugated steel web without and with concrete flanges are carried out. The inelastic global buckling strength of the corrugated steel web subjected to the shearing force and bending moment is presented and compared with the present design code. Furthermore, the following problems are discussed: 1) the distribution of the normal strains in the longitudinal direction at a cross section of a corrugated steel web with concrete slabs (Bernoulli-Euler's hypothesis) and 2) share of shearing force between a corrugated steel web and concrete slabs.

2 PARAMETRIC STUDY

Fig.1 shows the shear buckling strength curve proposed in ref. [1]. The elastic global shear buckling strength of corrugated steel web is based on ref. [2]. A shear buckling parameter λ_s is introduced and then the global shear buckling strength is evaluated according to the value of λ_s.

Fig.3(a) shows the analytical model, which is a simply supported beam composed of a corrugated steel web with steel flanges. The wavelength of corrugation of the web is 400mm. Thickness of web plate t and depth of corrugation d are variable. The results are plotted in Fig.2 with the shear strength curve as designated by [1]. From this figure it may be seen that the shear strength curve of Fig.1 is appropriate in the inelastic buckling region.

3 EXPERIMENTAL STUDY

3.1 Experimental tests of corrugated steel web without concrete flanges

To investigate the validity of the modeling and the accuracy of the program used for the elasto-plastic and finite displacement analyses, the experimental tests are carried out. Three types of specimens such as B-3 (d=20mm), B-4 (d=30mm) and B-5 (d=60mm) are provided for the tests. Although the shape of the specimens remains the same but their material property is slightly different from the analytical models of the parametric studies. Fig.4 shows the experimental and the analytical results of the shear strength of B-3, B-4 and B-5 compared with the shear strength curve of Fig.1. The shear strength of the test specimens is smaller than the one from the shear strength curve of Fig.1. It may be due to the effect of the initial imperfections.

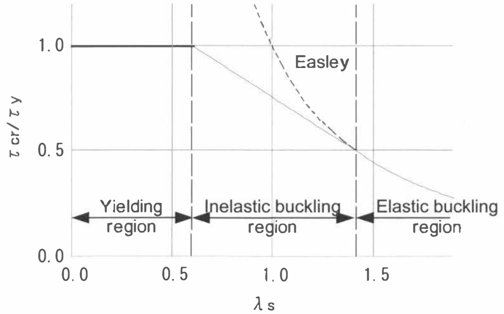

Fig.1 Shear buckling strength curve

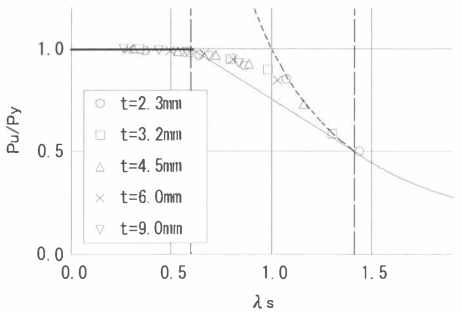

Fig.2 Results of parametric analyses

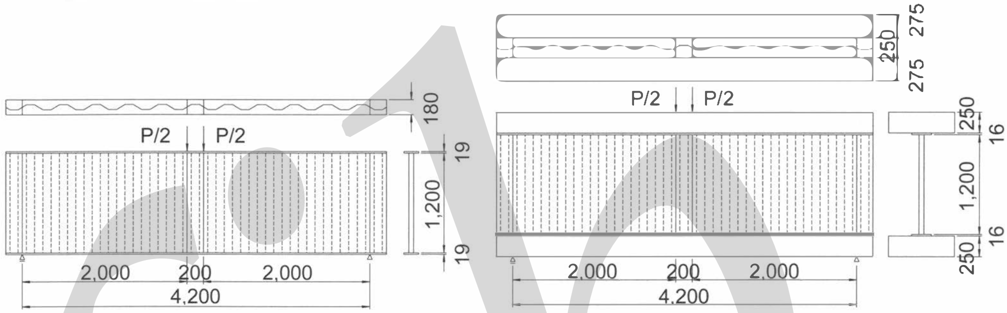

(a) without concrete slabs (b) with concrete slabs

Fig.3 Specimen (unit : mm)

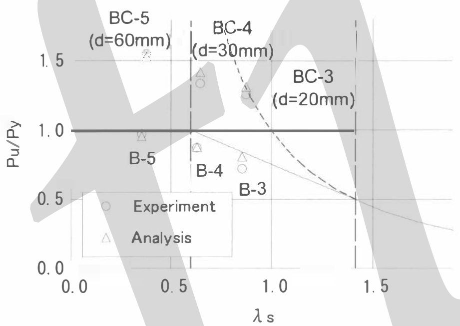

Fig.4 Results of experimental tests

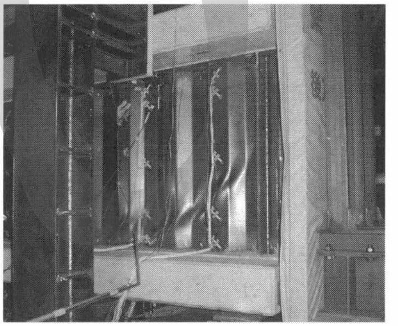

Fig.5 Shear buckling mode (BC-5)

3.2 Experimental tests of corrugated steel web with concrete flanges

The experimental tests of a simply supported beam composed of a corrugated steel web with concrete slabs are carried out. Three types of specimens such as BC-3 (d=20mm), BC-4 (d=30mm) and BC-5 (d=60mm) are provided for the tests as shown in Fig.3(b). Fig.4 shows the experimental and the analytical results of the shear strength of BC-3, BC-4 and BC-5 compared with those of B-3, B-4 and B-5 and with the shear strength curve of Fig.1. This figure shows that the shear strength of the corrugated steel web with concrete slabs is about one and half as high as the one of the corrugated steel web without concrete slabs. Fig.5 shows the shear buckling mode of the corrugated steel web of BC-5 after the loading.

REFERENCES

[1] Research Group of Composite Structure with Corrugated Steel Web : Design Manual of PC Box girders with corrugated steel webs (Draft), 1998.

[2] Easley, J.T. : Buckling Formulas for Corrugated Metal Shear Diaphragms, Journal of the Structural Division, ASCE, ST7, pp.1403–1417, 1975.

EXPERIMENTAL RESEARCH RELATING TO FATIGUE OF CORRUGATED STEEL WEB BRIDGES

Itsuro Sakai Akio Kasuga Kenji Umezu Naoki Nagamoto
Sumitomo Construction Co., Ltd. JAPAN

Keywords: Corrugated Steel Web, Scallop, fatigue, welding, experiment

1. INTRODUCTION

When a corrugated steel web bridge is built by the cantilever construction method, the method that has recently become more frequently used as the structure for joining the corrugated steel plates to make the bridge girders is lap and fillet welding. When joins such as this are used, to facilitate welding workability, it is necessary to make scallops in the steel plates near the upper and lower deck system.

High shear forces are acting in the corrugated steel plates as well as moments of bending around the bridge axis due to the traffic load (hereafter referred to as the oscillating moments) in the vicinity of the joins with upper decking. When scallops are made under stresses such as these, the local stresses are concentrated around them and variable stresses are generated due to the live loading. Then the fillet welding could not be expected to perform with respect to fatigue to the extent as the parent material so it is considered necessary to make a detailed investigation of the fatigue characteristics of these sections.

Accordingly, in this research a scallop shape is proposed for which it is thought that the concentration of local stresses will be small and its characteristics with respect to stress concentration, as well as its fatigue characteristics, have been investigated by analysis and experiment. The results are reported below.

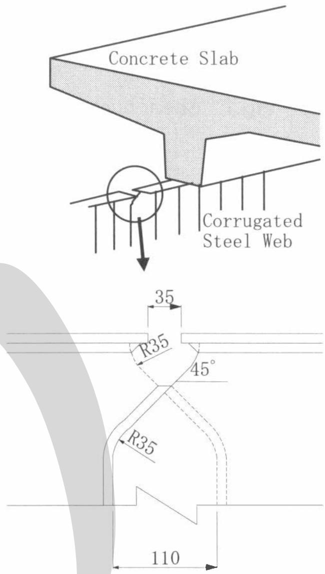

Fig.1 Shape of Proposal Scallop

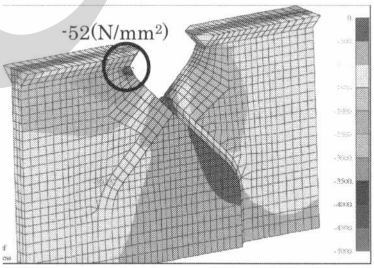

Fig.2 Min. Principal Stress by Vertical Force

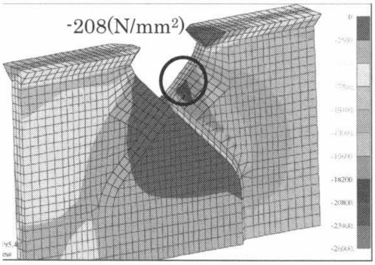

Fig.3 Min. Prin. Stress by Horizontal Shear Force

2. PROPOSED SCALLOP SHAPE

Fig. 1 shows the shape for scallops that we'll propose at this time. The concepts for this scallop are as follows:

(1) To transfer stress smoothly by having as few corners as possible and a horizontal yawing angle of 45 degrees for the notched shape of the scallop.
(2) To improve workability for welding the edges.
(3) To ensure that welding workability will not be affected if the length of overlap is varied to adjust for errors in execution.

3. EXPERIMENTS WITH THE BOX GIRDER MODEL

3.1 Overview of Experiment

When we consider the case of an actual corrugated steel web bridge, since the corrugated steel plates are the main members that resist shear forces, we can regard them as being constantly acted upon by shear forces. Under these conditions, the action is a variable vertical load due to traffic. In other words, we can consider oscillating moments caused by traffic to be acting under conditions in which high horizontal shear forces are constantly acting on the scalloped parts of the corrugated steel plates that are involved in joins with the upper decking. Even in analyses that concentrate on local stresses near the scallops, the local stresses generated by horizontal shear forces are about 200 (N/mm^2) and the local stresses due to traffic are about 50 (N/mm^2), so we can see that the constantly acting horizontal shear forces have an extremely large effect on stress (see Fig. 2 and 3).

Therefore, in addition to examining the fatigue characteristics of these parts, since it can be considered important to temper the effect of these horizontal shear forces, it was decided that the repeated vertical loadings in this research would be imposed under the conditions by which horizontal shear forces were imposed.

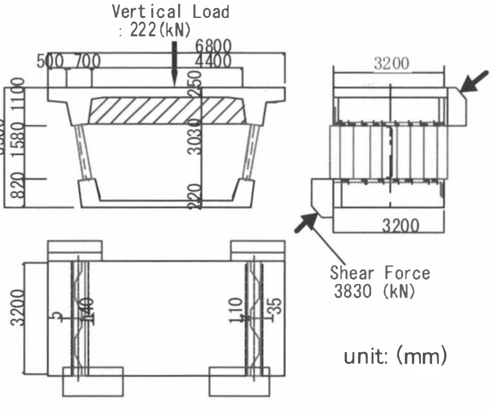

Fig.4 Outview of The Box Girder Test Model

The shape of the box girder, corrugated steel plates and loadings were to be the same as the standard cross-sections of the Koinumarukawa Bridge on the Sanyo Expressway and they were made full size in order to avoid the influence of size effects. Fig. 4 shows the shape of the experimental test piece.

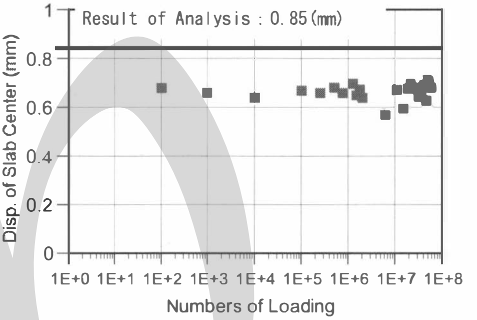

Fig.5 Change of Disp. of the Slab Center

3.2 Result of fatigue experiment

While the conditions for imposing horizontal shear forces mentioned above were maintained, additional vertical loads were imposed repetitively. From the capacity of the test equipment, the loading cycle was set at 0.4 s (2.5 Hz).

As a result, up to two million loading cycles were imposed without any sign of change in the stress conditions or increased displacement around the scallops. At this point, liquid penetrant testing and magnetic particle testing were conducted in order to investigate cracking around the scallops in more detail. These results also produced no sign of cracking and it is considered that soundness is ensured up to two million loadings.

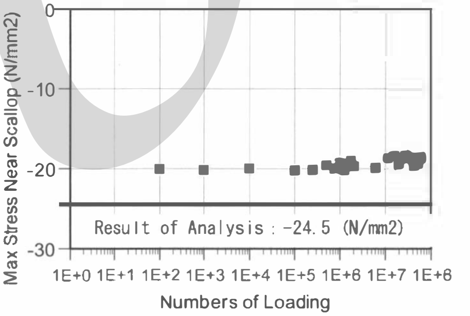

Fig.6 Change of Stress near the Scallop

After that, fatigue testing was continued with the imposed vertical loading doubled to 444 (kN). This load was then imposed repeatedly 500,000 times, without any cracking being confirmed or any increased displacement or variation in the amount of stress being observed.

At that point, in order to determine the fatigue capacity of this scallop, the imposed load was increased to 666 (kN), or three times the wheel loading of an ordinary truck, and the repetitive imposition was continued. Two million loading cycles were imposed with the triple load but in that period, there was no confirmation of any increase in stress or displacement and no sign of cracking (see Fig. 5 and 6). In accordance with the minor's law, if the cube of varied stress is in inverse proportion to the number of repetitive cycles, then this experiment is equal to a truck wheel loading being imposed 60 million times.

4. CONCLUSION

The corrugated steel web section of a full size box girder test piece was loaded with horizontal shear forces at the same level as an actual bridge and under those conditions oscillating moments due to traffic loads, 222(kN), were repeatedly imposed. The result showed no detectable change up to 60 million cycles. So it is clear that there is little possibility of fatigue of this section becoming a problem.

A STUDY ON DESIGN METHOD OF SHEAR BUCKLING AND BENDING MOMENT FOR PRESTRESSED CONCRETE BRIDGES WITH CORRUGATED STEEL WEBS

Hiroyuki Ikeda, Kenichirou Ashiduka
Japan Highway Public Corporation
JAPAN

Toshimichi Ichinomiya
Kajima Technical Research Institute
JAPAN

Yoshihide Okimi, Toru Yamamoto
Kajima Corporation
JAPAN

Masato Kano
Bridge and Computer Engineering Co., Ltd.
JAPAN

Keywords: shear buckling, bending moment, strain distribution, finite element analysis

1 INTRODUCTION

Prestressed Concrete box girders with corrugated steel webs were put to practical use in France as alternatives with lighter weight to conventional prestressed concrete box girders, and they have recently been used in Japan. Shear and flexural behavior of bridges with prestressed concrete girders with corrugated steel webs has been studied by basic tests and analyses and taken into consideration in actual design.

In this study the applicability of analysis considering both material nonlinearity and geometric was verified for accurately predicting shear buckling strength. Strain distribution on the top and bottom concrete slabs was measured using specimens with sections subject to pure bending, and the validity of the Bernoulli's assumption when bending was predominant was verified.

2 STUDY ON SHEAR BUCKLING

Fig. 1 shows the specimen. The specimen was supported on bearings at both ends which allowing free rotation and longitudinal sliding, and load was applied at midspan by a hydraulic jack. For analyzing the shear buckling of corrugated steel webs, a complicated nonlinear analysis program was used.

It was verified that shear buckling strength and the relationship between load and deformation could be analyzed accurately even in the range under a great influence of geometric nonlinearity. Thus, the validity of the analysis method was verified.

It was revealed that the analysis considering the initial shape of the specimen could analyze the relationship between load and vertical displacement and the relationship between load and out-of-plane deformation more accurately than the analysis without such considerations (Fig. 2 and 3).

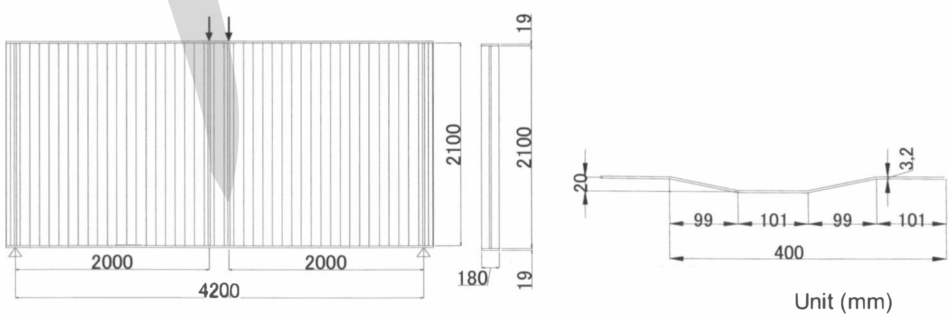

Fig.1 Dimensions of specimen

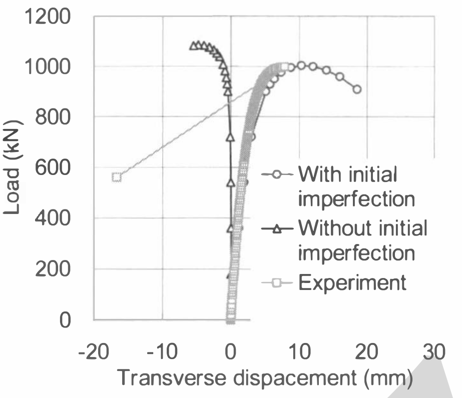

Fig.2 Load-vertical displacement relationship

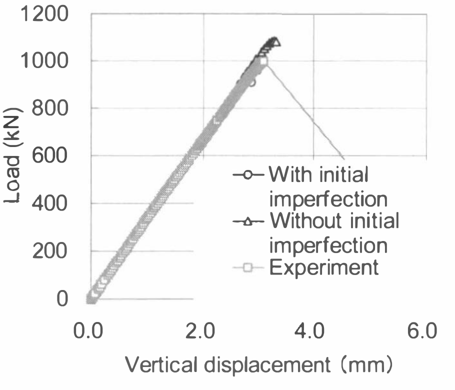

Fig.3 Load-lateral displacement relationship

3 STUDY ON BENDING MOMENTS AND AXIAL FORCES

The dimensions of the specimen and position where strains are measured are shown in Fig. 4. Loads were applied at two points of the specimen simply supported on either end using a 10000-kN loading machine. For analyzing the shear buckling of corrugated steel webs, a complicated nonlinear analysis program was used.

Fig. 5 shows the strain distribution at a load of 50kN. It was found that the Bernoulli's assumption was true in the elastic range in the pure bending section. In cross sections near the position where loads were concentrated, the Bernoulli's assumption did not hold true even in the pure bending section. The analysis, however, could predict the test results accurately.

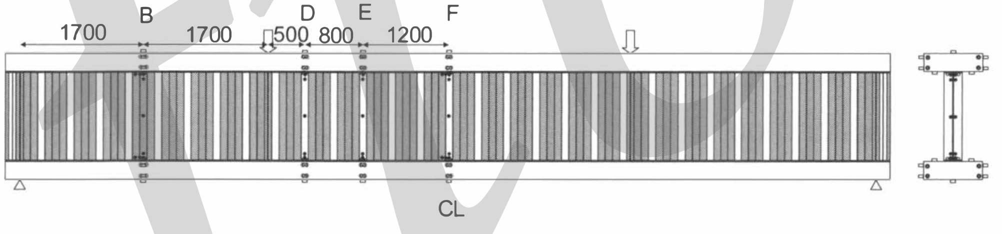

Fig. 4 Position of strain gauge

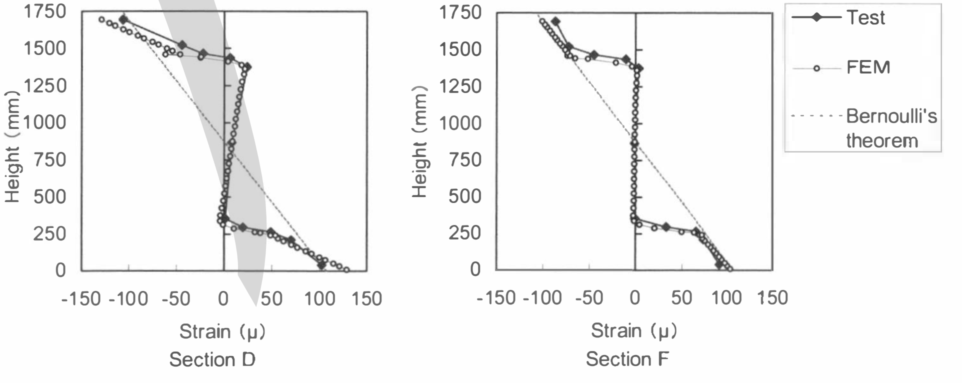

Fig. 5 Strain distribution at load of 50kN

A STUDY OF THE ULTIMATE STRENGTH PRESTRESSED CONCRETE BRIDGES WITH CORRUGATED STEEL PLATE WEBS WITH A ENTIRELY EXTERNAL CABLE STRUCTURE

Tsutomu Kadotani
Japan Highway
Public Corporation,
Kansai branch, Japan

Keiichi Aoki
Japan Highway
Public Corporation
Head office, Japan

Akio Shoji Taku Yoshikawa
Oriental Construction Co., Ltd.,
Head office, Japan

Keywords: external cable, ultimate strength, increased tensile stress, nonlinear analysis

1 INTRODUCTION

The adoption of external cable systems has been increasing recently because this makes the maintenance after excretion easier. The method of calculating the ultimate strength is an important issue in the design of the external cable structure.

To increase the ultimate strength in the calculation, the reinforcing bars are arranged as tensile-resistance material. When design does not include the increased tensile stress caused by the extension of the external cable at the ultimate design load, the volume of the reinforcing bars is increased, leading to uneconomical design. Thus, a study of the application of how the ultimate load affects the increased tensile stress has been undertaken in recent years. There are two International Standard methods of calculating the increased tensile stress, DIN[1)] and AASHTO[2)], and the domestic standard methods include, the Standard for Design and Execution of external cable structure/Precast segment[3)] KOUSA[4)] et al. and KOSAKA[5)] et al.. However, these only concern the simple-girder type and the same girder depth, even if they are included in a continuous girder or continuous rigid-frame structure.

This paper presents the results of a nonlinear analysis (material nonlinear + geometric nonlinear) of the two bridges that were conducted to formulate the increased tensile stress for this type of structure. For the formulation, the calculation method suggested by KOSAKA et al. was adopted as a reference, which indicated that the increased volume of the external cable performs a function between the distance of the external cable fixed by anchors and the effective height.

2 ANALYSIS METHOD

To determine the ultimate strength, a nonlinear-frame analysis is implemented to divide the cross section into fiber elements; at the division should be maintained at about twenty for both upper and lower slabs considering only the shear rigidity of the corrugated steel plate. The reinforcing bars are placed in two-stages for both the upper and lower slab and all the external cables are estimated as member. The external cable should be supported by anchoring parts of rigid member and a deviator which only has rigidity in the vertical direction. This analysis doesn't take the friction in a deviator into account. Fig.1 shows an analysis model of the three-span continuous rigid-frame KATTEGAWA bridge. In another case T-shaped rigid-frame MAETANI bridge was analyzed. These analysis takes structural changes into account to reproduce the initial stress condition.

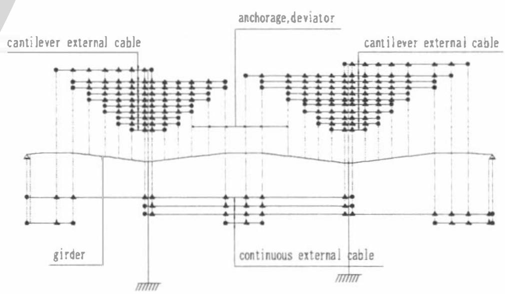

Fig.1 Analysis model of KATTEGAWA bridge

As the cross section of the aimed point at the ultimate design load, there are two cases of cross section, at a intermediate support and at the midspan, and the dead load should be loaded equally after the design load has been established. In addition, the live-load should be applied so that each cross section of the aimed point is under the most strict stress condition.

3 RESULTS

3.1 Ultimate strength

There are two cases as the cross section of the aimed point, at a intermediate support (Case-1) and at the midspan (Case-2) in this analysis. Table 1 shows the results of a nonlinear analysis.

The decision of the flexural braking shall be given when the compressive strain of concrete reaches 3500 μ on a certain cross section. According to the results, both of bridges were found to have efficient strength compared with a coefficient of 1.7, which we multiplied with the combination at the ultimate design load.

Table 1 Load magnifications at the ultimate design load

Bridge	Case-1	Case-2
KATTEGAWA	2.49	3.23
MAETANI	2.18	2.16

For both bridges, the compressive strain of concrete reached 3500 μ near the intermediate supporting point. Accordingly, the MAETANI bridge was not found to differ much between the two cases. The reason why the strength of Case-2 for the KATTEGAWA bridge increased was thought to be because the continuous cable was anchored to the intermediate supporting point without anchoring on the way, providing efficient strength for the cross section.

3.2 Examination of increased tensile stress

Table 2 suggests the simple formulation of the increased tensile stress on a PC bridge with corrugated steel plate webs with a entirely external cable in this study.

However, The cantilever cable of a continuous girder structure showed a less increased tensile stress than that of the rigid-frame structure.

Table 2 Simple formula of the increased tensile stress

The part studied		The formula suggested (N/mm^2)
Cantilever cable	Side span (including the T-shaped rigid-frame structure)studied	$\frac{L}{d_{p1}} \geq 50 : \Delta f_p = 0$ $\frac{L}{d_{p1}} \leq 50 : \Delta f_p = 1000 \times \frac{d_{p1}}{L}, \Delta f_p \leq 200 N/mm^2$
	Midspan studied	$\frac{L}{d_{p1}} \geq 50 : \Delta f_p = 0$ $\frac{L}{d_{p1}} \leq 50 : \Delta f_p = 1500 \times \frac{d_{p1}}{L}, \Delta f_p \leq 400 N/mm^2$
Continuous cable		$\frac{L}{d_{p2}} \geq 50 : \Delta f_p = 0$ $\frac{L}{d_{p2}} \leq 50 : 4000 \times \frac{d_{p2}}{L}, \Delta f_p \leq 400 N/mm^2$

REFERENCES

1) DIN4227, Spannbeton,Bauteil mit Vorspannung ohne Verbund,Teil 6,1980(in Germany)
2) AASHTO LRFD Bridge Design Specifications SI Units First Edition, 1994
3) Prestressed Concrete Engineering Association: Standard of Design and Execution for External cable structure and Precast segment execution method, 1996.3.(in Japanese)
4) A study of the formula of increased stress for external cable at ultimate load working, Concrete Engineering, Annual report, Vol.19, No.2, 1997(in Japanese)
5) A survey of Ultimate bending moment for PC bridge used external cable, The Civil Engineering Society of Japan No.613/V-42, 147-164, 1999.2(in Japanese)
6) Tagawa et al.: A study of Corrugated web girder, NKK, Engineering report, Vol.71, pp25-33, 1976.10(in Japanese)

MECHANICAL CHARACTERISTICS OF CONNECTION BETWEEN CONCRETE SLABS AND CORRUGATED STEEL WEBS

Takayuki Ebina, Senior Research Engineer, DPS Bridge Works Co., Ltd., Tokyo, Japan
Hisao Tategami, Chief Research Engineer, DPS Bridge Works Co., Ltd., Tokyo, Japan
Kenji Uehira, Director, R&D Center, DPS Bridge Works Co., Ltd., Tokyo, Japan
Keiichiro Sonoda, Professor, Osaka Inst. of Technology, Osaka, Japan

Keywords: corrugated steel web, lightweight aggregate, perforbond rib, connection

1. INTRODUCTION

In the recent years, remarkable progress has been made in the construction of composite girder bridges in view of cost-reduction, the current trend in the construction industry. Among the possible solutions, one of them is to replace the concrete web of a conventional prestressed concrete (PC) box girder bridges with corrugated steel webs, so that reduction is self-weight and improvement in the effectiveness of prestressing is achieved. Such bridges are widely constructed in Japan, considering its relative merits. Under these circumstances, if high-performance lightweight aggregate concrete (HLA concrete) is combined with corrugated steel plates, further weight reduction as much as 30-35% could be achieved.

Moreover, with the increase in construction of bridges with corrugated steel webs, an improved type of connection has been proposed that could resist the transverse bending moments at the joints, which is a feature found in these bridges [3]. Connection using perforbond ribs (plate with perforated holes) is considered to be suitable method in view of resisting the transverse bending moments. An extensive research was conducted using normal concrete and HLA concrete to obtain the mechanical characteristics of such joints. Moreover, an improved type of connection consisting of twin perforbond ribs in the form of a channel was proposed as shown in Fig. 1(b). Push-out tests using this new type of connection was experimentally investigated using model specimens. This paper discusses the experimental results and the proposed equation for the shear strength of perforbond ribs.

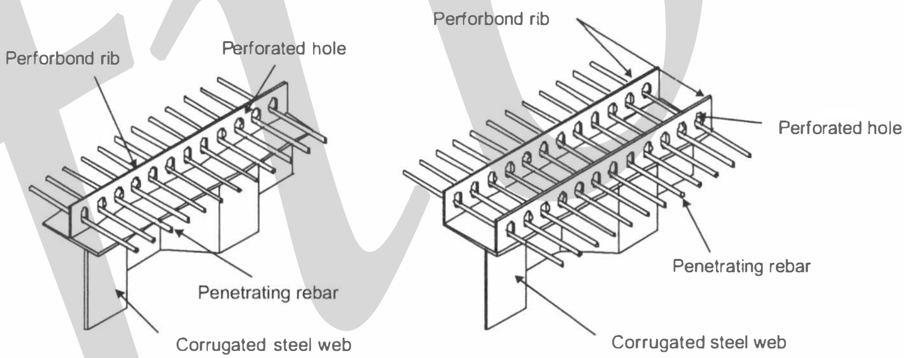

(a) Single perforbond rib

(b) Twin perforbond ribs (channel type)

Fig. 1 Connection method using perforbond ribs

2. EXPERIMENTAL INVESTIGATION

Several parameters such as hole diameter, effect of bonding between plate and concrete, placement of reinforcement and its position, and method of casting were considered in the test Series-1. In Series-2, HLA concrete was used to compare the effect with normal concrete. Details of these tests have been reported elsewhere [2]. In Series-3, Type C-1 through C-8 was made of twin perforbond ribs (channel type) as shown in Fig. 1(b), that are considered to have higher transverse resistance moment. Some of the specimens in this series were made of normal concrete while some were made of HLA concrete. Since this type of twin perforbond connection was to be used only for connecting the upper concrete flange with the steel web, the standard method of casting of concrete was adopted. Push-out tests were carried out on these specimens to obtain the shear strength capacity of perforbond ribs.

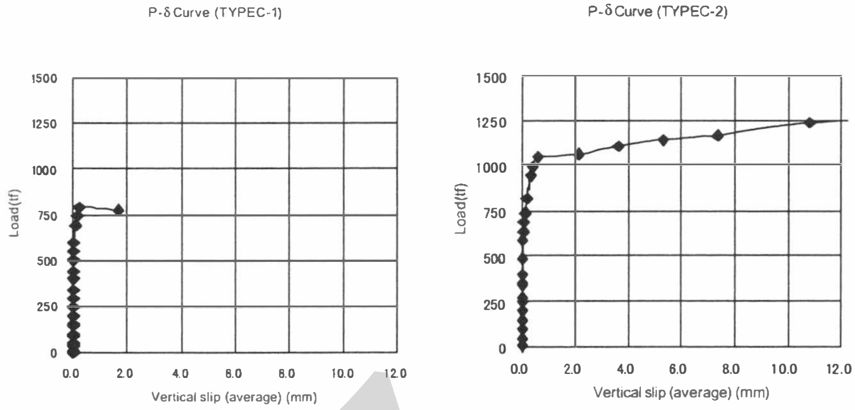

Fig. 2 Variation of vertical relative slip with load for twin perforbond rib specimens

3. TEST RESULTS AND DISCUSSIONS

In order to evaluate the shear strength of each specimen, the proposed equations based on previous studies were used [2]. These equations were used in the evaluation of the strength of perforbond ribs in this investigation. Moreover, these equations incorporate a factor of safety of 0.7, a value similar to that recommended by Leonhardt et.al in their studies [1]. The experimental results were compared with the calculated values, which indicate that the prediction equations are appropriate to evaluate the shear strength of perforbond plates. Moreover, the ratio of experiment to predicted values for specimens with HLA concrete is smaller than those specimens made of the normal concrete. The test results revealed that the shear strength of HLA concrete is slightly lower than that of the normal concrete.

The variation of vertical deformation of a twin perforbond plate with applied load is shown in Fig. 2. It is evident that there is almost no relative slip between the steel flange and concrete for a load up to about one third of the ultimate capacity. Moreover, when comparing the results of Type C-2 and C-1 with and without penetrating reinforcement respectively, it was found that the effect of penetrating reinforcement not only increased the shear capacity, but also the ductile behavior of the joint.

4. APPLICATION OF PERFORBOND RIB CONNECTION IN ACTUAL BRIDGE

Based on these experimental results, the application of twin perforbond plate connection type was applied on the Tanigawa Bridge that is being constructed in Gunma Prefecture, on the Numata-Minakami Route, where this new type of connection is adopted in the upper flange, for the first time in Japan.

5. CONCLUDING REMARKS

The following conclusions are made from this study.

1) There was hardly any slip in the perforbond rib up to the design load level, which is approximately one-third of the ultimate capacity.
2) It was possible to evaluate the capacity of the perforbond rib by the proposed prediction equations.
3) The twin perforbond rib (channel type) connection proposed in this study has sufficient strength to resist the horizontal shear and transverse bending moments acting at the upper flange of the connection.
4) Although it was found that the shear strength of the connection consisting lightweight concrete was smaller than that of the normal type concrete, it was not necessary to apply a reduction coefficient for the strength calculations.

REFERENCES

1) Leonhardt, F., Andra, W., Andra, H. and Harre, W.: Neues, vorteilhaftes Verbundmittel fur Stahlverbund-Tragwerke mit hoher Dauerfestigkeit, BETON-UND STAHIBETONBAU, pp325~331, 1987.
2) Shintani, E., Ebina, T., Uehira, K. and Yagishita, F.: Study for Shear Connector of Corrugated Steel Web and Concrete Slab. Proc. of The 9th Symposium on Developments in Prestressed Concrete, pp.91-96,Oct., 1999(in Japanese).

STRUCTURAL CHARACTERISTICS OF THE PC BOX GIRDER BRIDGE (SHIRASAWA BRIDGE) CONSISTING OF CORRUGATED STEEL WEBS WITH HORIZONTAL CURVATURE

Takeyasu Tezuka
Omachi Construction Office
JAPAN

Yujiro Kobayashi
NGANOGIKEN Co., Ltd.
JAPAN

Hiroshi Yasumori   Takatoshi Fujita
DPS Bridge Works Co., Ltd.
JAPAN

Keywords: corrugates steel web, perforbond rib, PC bridge, horizontal curvature

1. INTRODUCTION

The Shirasawa Bridge was constructed across the Shirasawa River on the "Tateyama-Kurobe Alpine Route", a major local road linking the Omachi city in Nagano prefecture and the Tatayama town in Toyama prefecture, Japan. This bridge is being constructed as part of the rehabilitation project under the disaster prevention measures. The special characteristic of this PC box girder bridge with corrugated steel webs is that, it has a horizontal curvature with a radius of 250 m. Such bridges are very rare in the world, which makes the Shirasawa Bridge a unique one (Photo 1).

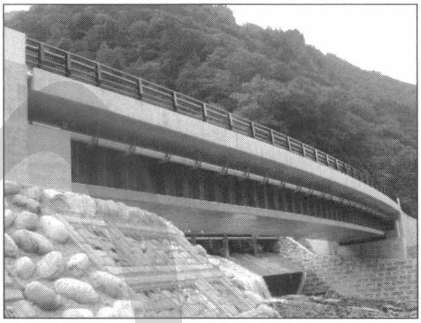

Photo 1 Complete view of the bridge

One of technical aspects of this bridge is the presence of horizontal curvature that would influence the overall behavior and torsional deformation of the structure, about which not much of knowledge is available. As such, a three dimensional FEM analysis was carried out for the full bridge model to have a better understanding of the behavior of such bridges. The analytical results were compared with the results of static and vibration test caused by moving truckloads, on the constructed bridge.

This paper highlights the structural characterizes and design considerations of Shirasawa Bridge. Further, the connections between lower flange of concrete slab and steel webs were of perforbond rib (plate with perforated holes) connection type that was adopted for the first time in Japan. Details of this new type of connection are also discussed in this paper.

2. OUTLINE OF THE BRIDGE

The layout and details of this bridge is shown in Fig. 1. The design details are outlined below.

Concrete	:	σ_{ck}=40 N/mm^2
Steel plate	:	SMA490W
External tendons	:	SWPR7B19S12.7
Internal tendons	:	SWPR7B12S15.2B
Reinforcement	:	SD295A

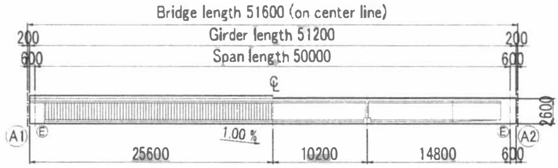

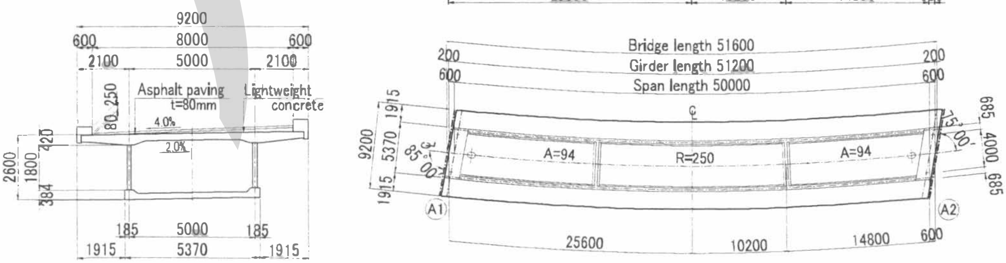

Fig. 1 General layout

3. EVALUATION ON TORSIONAL BEHAVIOR

According to the existing design standards for PC box girder bridges, the shear forces are borne completely by the corrugated steel plates[1]. The evaluation of torsional resistance is based on the pure torsion, considering the torsional shear behavior.

To evaluate the applicability of the existing evaluation method for torsion explained above, the overall torsional behavior of this bridge was verified using FEM analysis. In this FEM analysis a three dimensional model was developed using solid elements and shell elements for concrete slabs and steel webs respectively. The model also incorporated the horizontal curvature of 250 m radius as well as the skew angle at the two ends of the bridge, so that the effect of these would be properly evaluated.

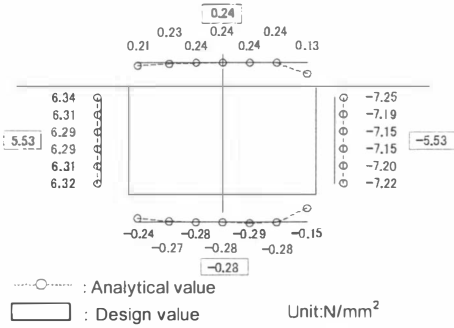

Fig. 2 Shear stress variation

The shear stress variation of the cross section at mid span is plotted in Fig. 2, where the angle of twist varied linearly as well as the shear force is zero in the axial direction of the bridge. It can be seen that there is a good agreement between shear stress values based on the design equations and FEM analysis. As such, it was confirmed that the existing design equation is applicable in the design of this bridge.

4. STATIC LOADING TEST

To observe the behavior of this bridge under imposed loads, a loading test was carried out using loaded dump trucks (Photo 2). Four trucks of 200 kN load each were used for this test. Loading tests were carried out to obtain the flexural and torsional behaviors by appropriate loading conditions.

The shear stresses caused by the torsional test results are compared with the FEM analytical results. In contrast, the support region shows considerably high shear stresses, especially in the steel plate located on the outer perimeter, which is believed to be influenced by the skew angle present in the bridge.

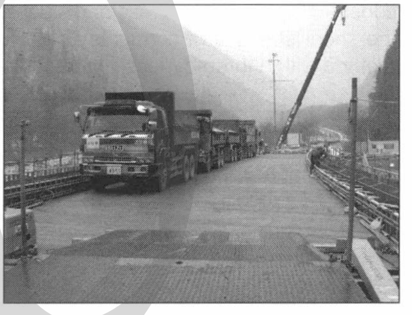

Photo 2 Torsional load test

5. VIBRATION TEST BY MOVING LOADS

Vibration characteristics of this bridge under moving load were investigated by carrying out a moving load test using two trucks. Two types of tests were done, one for flexural test by having the truck run along the center line of the bridge axis and the other for torsional test, by truck running on the cantilever part of the upper flange. In each of these two tests, a single truck and two trucks were used making a total of four cases.

A preliminary analysis was carried out using conventional beam theory and FEM analysis. Moreover, using the beam theory, the shear deformation was taken into consideration in the analysis, and the shear resistance by the corrugates steel plates were assumed to be 100% and 70% that led to a total of four cases to be analyzed where the fundamental natural frequency was computed. It can be seen that there is very good agreement between the measured values and computed frequencies by FEM analysis. For frequencies calculated by beam theory, good agreement is obtained for the case where the shear resistance taken by the corrugated steel plate was assumed to be 70%.

Considering the dynamic natural frequencies, the calculated values also agreed well with the measured values.

REFERENCES:

1. Committee on Composite Structures with Corrugated Steel Web: *Planning Manual for PC Bridges with Corrugated Steel Web (Draft)*, October 1998 *(In Japanese)*
2. Uehira, K., Shintani, E., Ebina, T. and Sonoda, K. : On the Relationship between of the Torsional Behavior and the Cross-beam Interval for the PC Box Girder with Corrugated Steel Plates at Web, *J. of Prestressed Concrete, Japan*, Vol.41, No.1, pp. 38-42, 1999. (*In Japanese*)

CONSTRUCTION OF PRESTRESSED CONCRETE BOX-GIRDER BRIDGE WITH CORRUGATED STEEL WEBS(PART1 OF NAKANO VIADUCT)

Jianping Liu	Oriental Construction Co.,Ltd	Japan
Kunihiko Harata	Oriental Construction Co.,Ltd	Japan
Kazuyuki Tajima	FujiPS Construction Co.,Ltd	Japan
Hirofumi Hadama	Hanshin Expressway Public Corporation	Japan

Keywords: corrugated steel webs, cantilever erection, deformation, stress

1 INTRODUCTION

The prestressed concrete box-girder bridge with corrugated steel webs is attracting more and more attention now in Japan. Steel webs are used instead of concrete webs because they can reduce 10%～30% self-weight of the bridge and provide a more convenient solution to the prestressing. Nakano Viaduct, a bridge of this type with 250m～440m radius curve line, are reported in this paper. It is a 4-span continuous box-girder bridge which is constructed by using cantilever erection method. Internal cables were mainly used to resist dead load in upper and lower concrete slab, and external cables were used to oppose live load. A new connection method was adopted to connect corrugated steel plate with the upper and lower concrete slab. In addition, in order to clarify the mechanics behavior throughout the construction,, concrete stress and steel strain were measured in field measurement. It was also confirmed the shear stresses of corrugated steel webs and the deformations of this bridge by using finite element method with a three-dimensional real scale model.

2 THE OUTLINE OF THE CONSTRUCTION

2.1 View of the bridge

This paper reports the east main lane bridge of Nakano viaduct. The general view of this bridge is illustrated as Fig.1.

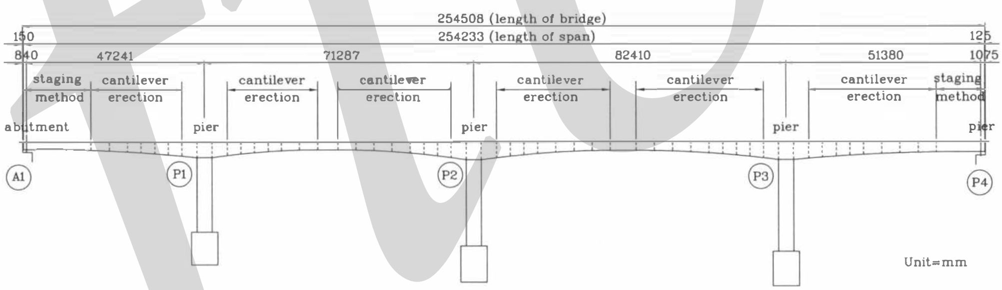

Fig.1 General view of east main lane bridge

2.2 Specification, Production, and Installation of Corrugated steel

The corrugated steel which was used for this bridge was 1200mm in length and 200mm in height and the thickness varied depending on the shear force from 9mm to 19mm. A large press machine was used to produce the corrugated configuration and the size of each piece was divided within 3m on a side because of delivery restrictions. And the installation of corrugated steel was completed by crane.

2.3 Connection of the corrugated steel with the concrete slab

The upper slab side adopted a new connection, using CT shape steel plates combining with stud dowel as shear connection between steel webs and concrete upper slab, as Fig.2 shows. Here, CT shape steel plates were used as perfobond strip to reduce the number of studs. Moreover, it is proposed that the stud dowel resists the bending moment in the transverse direction that occurs at the connection.

Fig.3 shows the connection structure of the lower slab side. In this structure, a hole was drilled in the corrugated steel and the penetrating steel bar was arranged. Two pieces of connection steel bar were welded in the bridge axial direction at the edge of the corrugated steel. This connection method aims for the following; a diagonal panel of the corrugated steel which is buried in the concrete lower slab can efficiently function as an anti-dislocation block; the connection steel bar, and the concrete which is filled with the hole on the corrugated steel as a concrete dowel can resist against the shear force.

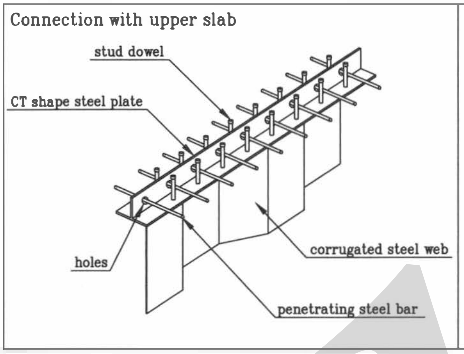

Fig.2 The connection of the corrugated steel with the upper slab

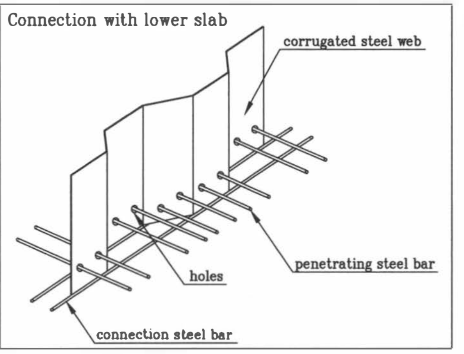

Fig.3 The connection of the corrugated steel with the lower slab

3. FIELD MEASUREMENT

The field measurement was implemented to examine deformation of the girder section. Also, we measured strain of the concrete slab and the corrugated steel webs to confirm the design validity compared with the result of Finite Element Method analysis. The FEM model was illustrated as Fig.4

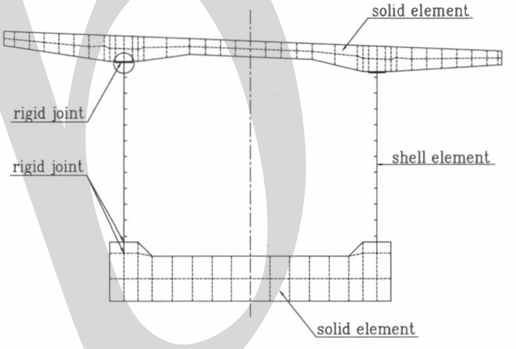

Fig.4 The section of the analysis model

3.1 Shear stress of the corrugated steel webs

About 40% of the shear force was imposed on the upper and lower concrete slab as shown in Table 1. Therefore, it was confirmed that the design method on the shear force was effective for this bridge, to implement only the corrugated steel webs to resist the whole shear force.

Table 1 Share ratio of shear force on the upper and lower slab

Construction procedure	Block7	Block8	Trav.Re	P2-P3	P1-P2	Ext.Ca	Brid.Sur
Designed value (N/mm^2)	19.83	21.64	20.71	24.36	23.58	18.17	22.00
Fem analysis value (N/mm^2)	12.29	13.01	11.55	14.70	14.47	11.53	15.12
Share ratio (%)	38%	40%	44%	40%	39%	37%	31%

3.2 Stress in the axial direction on the upper and lower slab

The design of this bridge only considered the concrete member on the upper and lower slab for the bending rigidity in the bridge axial direction because of accordion effect of corrugated steel webs. And the measured value changed in almost the same way as the designed value and FEM analysis value.

Also, it was found that the bending stress distribution, which was transmitted to the concrete members, always keeps a linear distribution. Based on the above, the validity of design method was confirmed.

[REFERENCES]

[1] Leonhardt,F., Andra,W., Andra,H.P. & Wharre,W.1987. New improved shear connector with high fatigue strength for composite structures. Beton-und Stahlbetonbau 1987.

[2] Ebina,T., Takahashi,K. Uehira,K. & Yagishita,F. 1998. Basic study for shear capacity of perfobond strip. Proceedings of the 8th Symposium on Developments in Prestressed Concrete 1998.

DESIGN OF PC CORRUGATED STEEL WEB BOX GIRDER BRIDGES OF NABETA-WEST PROJECT IN NEW MEISHIN EXPRESS WAY

Hiroyuki Ikeda Japan High Way Public Corporation
Yukihiro Kutsuna Japan High Way Public Corporation
Katsumi Sekii P.S. Corporation
Yuichi Ito P.S. Corporation

Keywords: corrugated steel web, single lap fillet welding, scallop, external cable

SUMMARY

Two PC corrugated steel web box girder bridges of Nabeta-West Project have been completed in March, 2001. The corrugated steel web has a lot of advantages. Concrete web is replaced by steel web, so the weight of superstructure is reduced. Also lots of labor work, such as concrete work, re-bar work, formwork and sheathing work of cables, can be saved. In addition, the corrugated steel doesn't resist axial force; thus prestressing force is effectively introduced into upper and lower slabs.

These bridges are exclusively external prestressing cable structures and constructed with the cantilever erection method. The single lap fillet welding is used to join corrugated steel plates. The joint between concrete and steel is the angle dowel joint method. Shear resistance, shear-buckling resistance and fatigue resistance are considered to decide the thickness of steel webs. Two scallop shapes, which produce smaller intensive stresses in the field fillet welding portion, are selected for these bridges. In order to confirm the safety of welding, several finite element analyses and tests are carried out. To effectively transmit force flow between the upper slab and the lower slab, especially of erection external cables anchored at upper slabs, the vertical prestressed concrete rib is installed at every anchorage of the external erection cable.

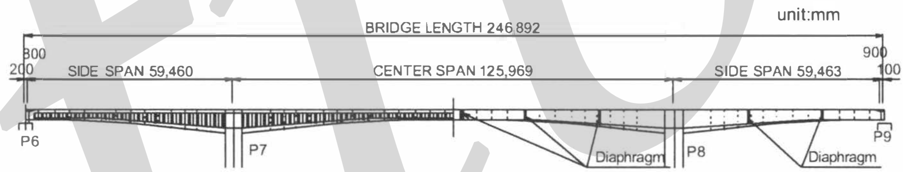

Fig.1 OUTLINE (SIDE VIEW)

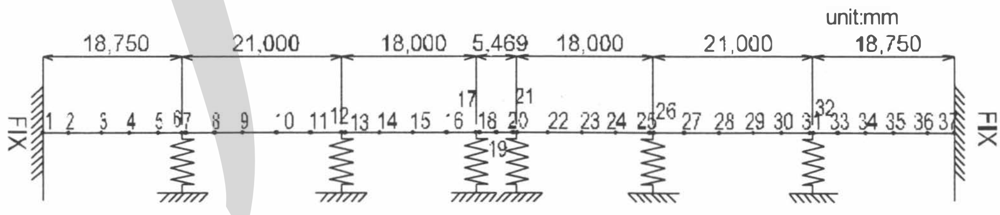

Fig.2 SKELETON OF BEAM ANALOGY MODEL FOR TORSION AND WARPIG

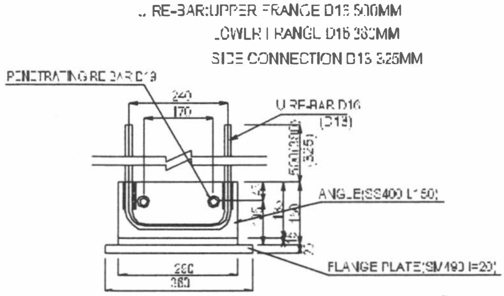

Fig.3 DEATAILS OF ANGLE DOWEL JOINT

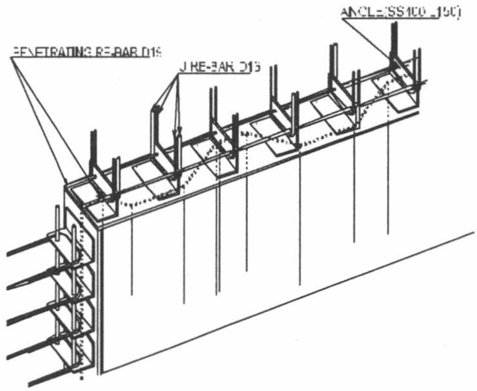

Fig.4 GENERAL VIEW OF ANGLE DOWEL

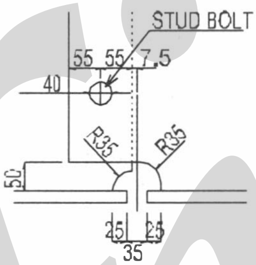

Fig.5 JOINT OF STEEL PLATES (A TYPE)

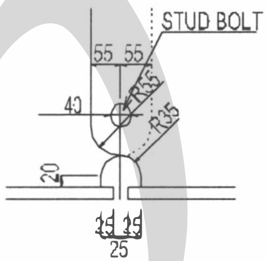

Fig.6 JOINT OF STEEL PLATES (B TYPE)

CONCLUSIONS

① Installation of horizontal ribs and vertical ribs is recommended for large external erection cable to prevent large tensile stress and deformation in corrugated steel webs because the rigidity of corrugated steel web is small.

② The joint method between corrugated steel plates themselves are confirmed to be strong enough by FEM analyses, the shear tests and the fatigue tests. In addition, two adopted scallop shapes cause smaller intensive stress and good enough for construction.

③ Two erection external cables for one construction block is ideal for structure and construction because every block takes same prestressing forces and construction becomes repeating almost same blocks.

REFERENCES

1. Prestress Concrete Technical Association, "Recommendation for design and construction of external prestressing and precast segmental bridges", 1996.3
2. Mizuguti, Ashiduka, Satou and Sakurada, "Study of deformation of Hondani Bridge (PC corrugated steel web box girder bridge with transitional section height)", 9th prestressed concrete symposium 1999.10.
3. The Society of Research for Composite Structure with Corrugated Steel Web, "Manual for planning of corrugated steel web bridges", 1998.12.
4. The Society of Japan Steel Structure. "Specifications of fatigue design for steel structure", 1993.3.

DESIGN AND CONSTRUCTION OF PRESTRESSED CONCRETE BRIDGE WITH CORRUGATED STEEL WEB

Kouhei TAGUCHI Takeshi OGAWA Kiyotaka TOISHI Hidekazu TAKASHIMA
Ojiya Public Engineering Office, Niigata Prefecture,JAPAN
Asia Kousoku Corporation JAPAN
P.S. Corporation JAPAN

Keywords: corrugated steel web, scallop, partially bonded cable method

1. INTRODUCTION

The Chushizawa Bridge is a 2-span continuous prestressed concrete bridge with corrugated steel web, which was constructed in Chushizawa, Hirokami-mura, Kitauonuma-gun, Niigata Prefecture across the Hanegawa River. The Uonuma district of Niigata Prefecture, where the bridge is located, is one of the highest snowfall areas in Japan, where the snowfall measures 2.5 to 4.0 m. Therefore, the period of construction was limited if the bridge was to be built by cast-in-place and using supports. The prestressed composite box girder with corrugated steel web was adopted as main structure, which have advantage in construction period at the construction site than ordinary prestressed concrete structures.

The corrugated steel webs were mutually joined by lapped fillet welding. The corrugated steel webs and the concrete flange were connected by stud dowels for the upper concrete flange and the embedding system for the lower concrete flange. Besides the longitudinal external cables, cables were partially installed within the lower concrete flange at the middle of the bridge. This partially bonded cable method was implemented to increase the ultimate strength. This paper describes the design and construction of the Chushizawa Bridge.

2. OUTLINE OF CONSTRUCTION

A construction plan of the bridge is shown in Fig.1. The materials used are listed in Table 1. An outline of the project is listed as follows.

Name of the project: Urgent construction of the Regional Road Route Chushizawa-Tyuka, construction of bridge superstructure
Project site: Chushizawa, Hirokami-mura, Kitauonuma-gun, Niigata Prefecture
Employer: Ojiya Public Engineering Office, Niigata Prefecture
Construction period: From December 1, 1999 to January 3, 2001
Structure: 2 span continuous prestressed concrete box girder bridge with corrugated steel web
Road class: Type 3, Class 4
Length of the bridge: 97.000 m
Length of the girder: 96.700 m
Spans: 47.800 m + 48.453 m
Width: Roadway : 8.000 m
Sidewalk : 3.500 m
Incline: A1: 90° 00'00"
P1: 90° 00'00"
A2: 60° 00'00"
Gradient: 4.000% to -2.721%
Live load: Live load B

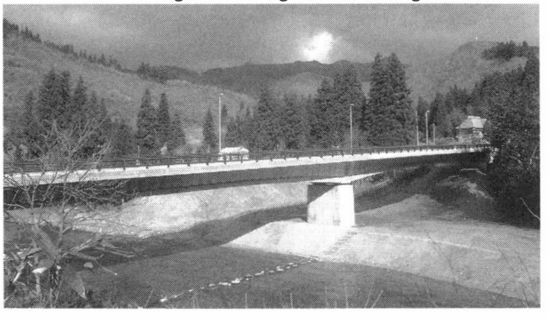

Photo.1 Completed bridge

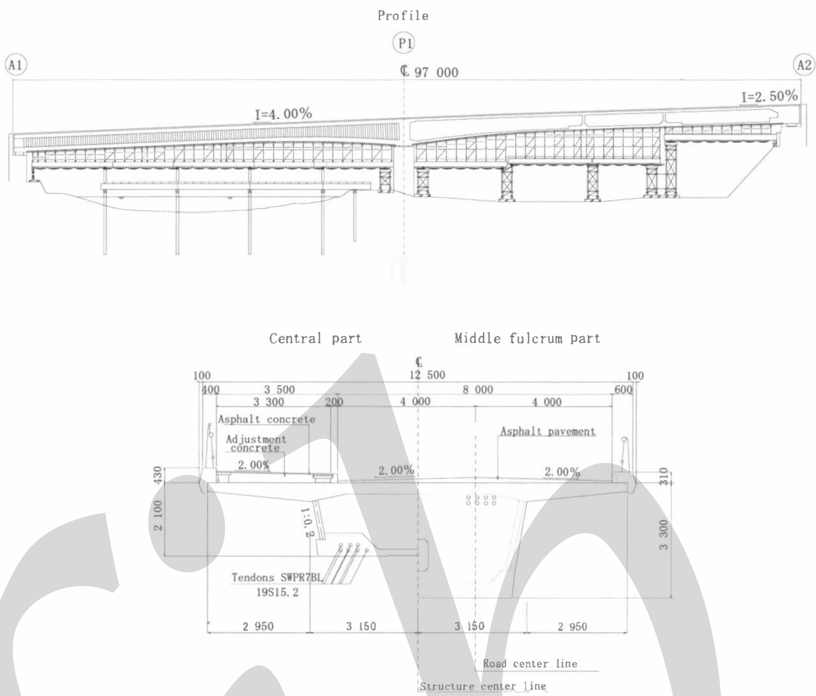

Fig.1 Construction plan

Table 1 Material list

Specifications		Unit	Quantity
Concrete	Design compressive strength σ_{ck}=40 N/mm^2	m^3	721.0
Reinforcement	Main girder SD295A Welding of corrugated steel webs SD345	t	91.6
Prestressing steel	External cable SWPR7B 19S15.2	t	28.5
	Transverse prestressing cable SWPR19 1S28.6	t	11.6
	Vertical prestressing cable SBPR930/1180 ϕ32	t	0.6
Corrugated steel web	SM400, SM490Y, SM570	t	36.1

REFERENCES

[1] Society of Research for Corrugated Web Composite Structure: Design Manual for Prestressed Concrete Bridges with Corrugated Steel Webs (draft) (in Japanese), December 1998.

[2] Japan Road Association: Specifications for Highway bridges: Part I, General (in Japanese), December 1996.

[3] Japan Road Association: Specifications for Highway bridges: Part II, Steel Bridges (in Japanese), December 1996.

[4] Japan Road Association: Specifications for Highway bridges: Part III, Concrete Bridges (in Japanese), December 1996.

THE PRESTRESSED CONCRETE BRIDGE ALTWIPFERGRUND WITH CORRUGATED STEEL WEBS

Helmut Roesler
Leonhardt, Andrä und Partner, Germany

Gundolf Denzer
DEGES, Germany

Keywords: prestressed bridge, corrugated steel webs

1 INTRODUCTION

With the reunification of Germany several road and railway projects were started to improve the infrastructure in East Germany. The authority to organize the motorway projects is DEGES, Deutsche Einheit Fernstrassenplanung- und –bau GmbH. One of these projects is the motorway A71 Erfurt-Schweinfurt , crossing the mountains of the Thüringer Wald. At the northern rim, close to the city of Ilmenau, the motorway has to pass a natural resort, the 100m wide valley Altwipfergrund, an important European Fauna-Flora-Habitat. The bridge crossing the protected area is 279m long, has a main span of 115m and is build with two prestressed box girders with webs from corrugated steel. It is the first time that this hybrid type of bridge construction has been built in Germany. The following gives a description of the special demands for the aesthetics of the bridge , its design , its construction-stages and an outlook on the future of this special type of hybrid bridge type.

2 DESIGN OF BRIDGE

The situation of the bridge within the nature-resort of European importance was deciding for the shape of the bridge. Within the valley no pier was allowed, not even any temporary support. This let to the main span of 115 m and to the free cantilevering construction method. The lovely natural surroundings further require slender dimensions of all structural parts. The solid concrete piers are designed with great slenderness, their top is widened for the bearings and their future exchange. The haunched girder bridge is crossing the valley 35 m above ground. The chosen depth of the superstructure results in the slenderness ratio at the supports of 115m / 6m = 19,2 and in the span of 115m / 2,8m = 41,1.

3 CORRUGATED STEEL WEBS

The web of the box girder consists of folded steel plates and has several advantages compared with the prestressed all-concrete box girder :

- prestressing is very efficient as the web area does not carry any prestressing force;
- the folded web can take the shear forces without additional stiffeners;
- the folded web is very stiff in transverse direction, this makes the shape of the box very robust;
- the web can be used as support for the scaffolding using cantilever construction method;
- scaffolding can be made very light, the construction steps can be made larger;
- large construction steps save time;
- reduced dead load

4 DETAILS OF THE WEB

Manufacturing, transport on road and placing of the web required relatively small pieces with a transport width of 3,30m. This led to joints which were planned to be welded, but finally the contractor used high-strength bolted connections together with splice plates. Material of the web is steel S 355 J2G3-C,the thickness is 10 to 22mm. The steel plates are cold formed into a trapezoidal shape with minimum radius of 240mm. Buckling of the web has been calculated according to DASt-Richtlinie 015, which is suited to the needs of small girders. With changed regulations, actually under discussion, a reduction of the webs by 10-20 % could be achieved.

5 CONNECTION WEB / TOPSLAB

The web in transverse direction is relatively stiff and requires, therefore, a robust connection to the slab for fatigue resistance. At Altwipfergrund this was achieved by means of single V- penetration welds between web and flange as well as by steel-loops between flange and concrete slab in addition to ordinary welded studs. The steel-loops were bolted to the flange after erection of the scaffolding .

6 CONNECTION WEB / BOTTOMSLAB

Several types of this connection have been discussed. To arrange the flange on top of the concrete has the disadvantage of a joint between steel and concrete at the airside. The slab has to be poured underneath the flange. At Altwipfergrund finally the flange was arranged perpendicular to the web below the concrete slab.

7 PRESTRESSING

Due to the long main span of 115m and the need to use the free cantilever method the use of a mix of external and internal prestressing tendons was adequate.

- top slab 2x12 tendons with 2,6 MN each (for construction stage and final stage)
- bottom slab 4 tendons with 2,2 MN each (for continuity at mid span)
- external tendons Suspa-Draht EX-66 2,97 MN each at support 8, end span 20, mid span 20

8 CONSTRUCTION METHOD

The ground of the valley between the piers is a taboo zone, temporary supports for construction are forbidden. Thus the superstructure had to be constructed by the free cantilever method. Steps:

- Pier, temporary support, starting elements including concrete cross frames and 6,6m long beams
- installation of corrugated steel webs 1a,1b
- scaffolding for bottom slab on top of webs, concreting bottom slab1a,1b
- installation of corrugated steel webs 2a, 2b
- concreting top slab 1a, 1b, prestressing top slab 1a, 1b; - concreting bottom slab 2b, 2b
- installation of corrugated steel webs 3a,3b

9 SUMMARY

The new hybrid bridge with prestressed concrete slabs and corrugated steel webs has been built in Germany for the first time. Some details as well as regulations have to be further developed. The bridge has advantages due to reduced dead load, optimised distribution of prestressing, and by using the web elements for construction. Therefore, this bridge type is suitable for special needs and will be applied also in the future.

Elevation

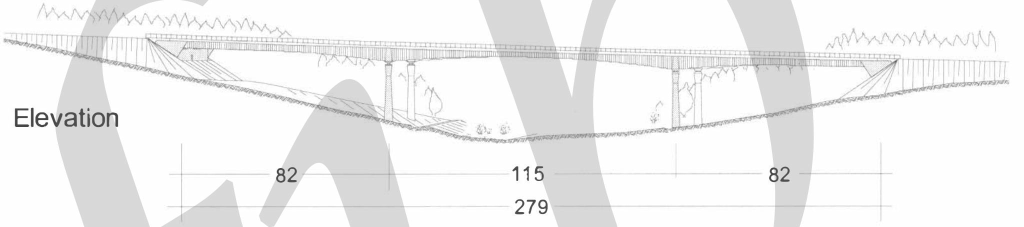

Cross-Section in Midspan

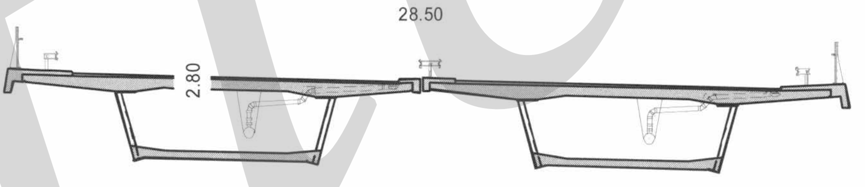

Corrugated Steel Web

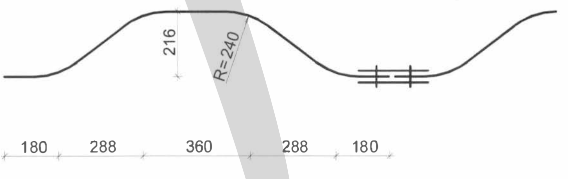

Edge Detail

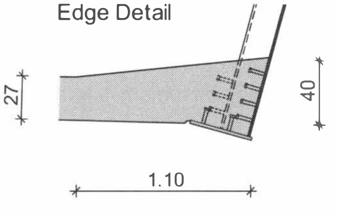

Construction-Stages

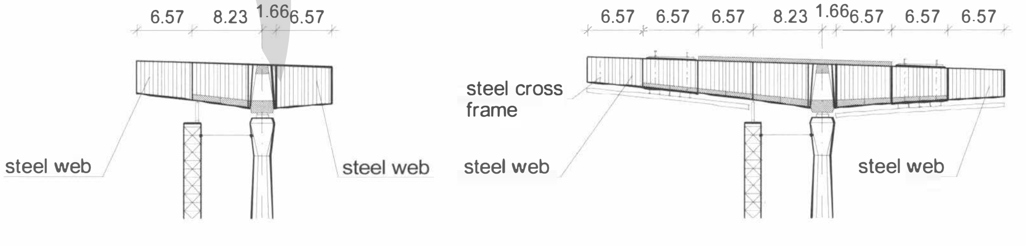

EXPERIMENTAL STUDY ON A JOINT IN PRESTRESSED CONCRETE BRIDGE WITH STEEL TRUSS WEB

Takashi Tsujimura   Akio Shoji   Tadayuki Noro   Shinji Muroi
Oriental Construction Co., Ltd.   Nippon Steel Co., Ltd.
Tokyo, Japan   Tokyo, Japan

Keywords: composite bridge, joint, full-scale model test

1. INTRODUCTION

PC composite bridges with steel truss web, in which concrete web of conventional concrete box girder is replaced with steel trusses, can be so anticipated as to have both the advantages of steel and concrete bridges. This type of bridge is paid much attention as a bridge from now, because of construction cost reduction of whole structures including understructures and footings.

Generally, connections or joints in PC composite truss bridge have to possess high strength and stiffness since the truss diagonals are connected directly to the concrete flanges, and complicated forces are transmitted through connections or joints.

In this paper, a new connection system, which considers the above mentioned features, has been proposed for PC composite truss bridges. As shown in Fig.1, the diagonals consist of steel pipes and end steel plates. Ring-shear-key within the connection is composed of socket type steel flange plate or jack type steel pipe for both ends of compressive and tensile diagonals respectively. The steel pipe diagonals are directly embedded into the slab concrete at both the ends, and axial forces in compression or tension are transferred to each diagonal through the shear key and concrete.

Experiments were performed for a full-scale model specimen of the proposed connection system. In the followings, the experimental results by a fatigue and a static loading tests are described to investigate fatigue and static characteristics of the system.

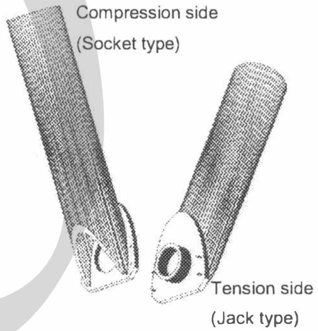

Fig.1 General view of connection

2. OUTLINE OF THE TESTS

2.1 Test specimen

In order to determine dimensions and design load intensity of a specimen, a sample bridge with 119m span was assumed. The specimen is focused to only the connection part of the sample bridge at the span center. The cross section of the specimen was designed in conformity with the conventional highway bridge design standards. The standard design compression strength of concrete was set at 40 N/mm^2.

2.2 Static Loading Test

The test specimen in an assembled condition is shown in Fig.2. Loads were applied statically in the vertical direction using a loading machine with a capacity of 20,000 kN. And loading pattern was adopted four-step loading with gradual increase up to 3.6 times the design load.

2.3 Fatigue Loading Test

Fatigue loading test was conducted by applying the load horizontally to the concrete slab and the specimen shown in

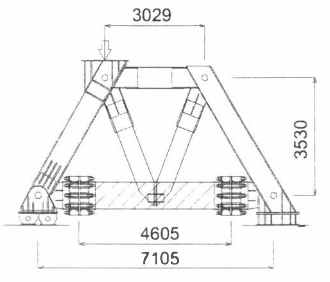

Fig.2 Test appearance (static)

Fig.3. The load was determined so that the axial force of diagonal members, assumed in the trial design, became equal to that of compression diagonal members. Then two million cycles of actuated loading was applied under frequencies of 1~3 Hz. Such loads are equivalent level to the design service load of the sample bridge. As result, the axial force in the compressive steel pipe diagonal varies from 552kN to 1,127kN.

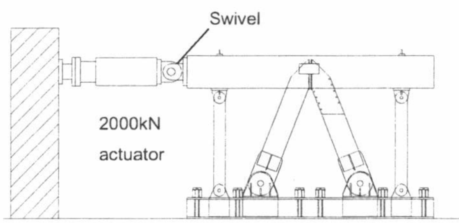

Fig.3 Test appearance (fatigue)

3. THE RESULTS

3.1 Static Loading Test

Fig.4 shows the crack pattern on the surface of concrete slab after the static loading test finished. In the position marked with ①, the first crack occurred in the concrete slab and at this point, the axial force in the diagonal members reached 1.3 times the design load. And then a diagonal crack occurred in the center position of the connection when the axial force in the diagonal members became 1.6 times the design load. This is the position marked with ②. From the angle of occurrence, this crack is judged to be a diagonal tensile crack caused by a shearing force working on a local portion.

Following the occurrence of the diagonal crack in the concrete slab, the occurrence of strains of Ring-shear-key abruptly increased, as shown in Fig. 5.

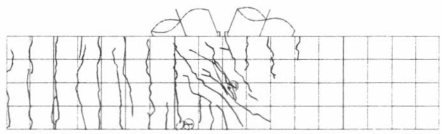

Fig.4 Crack pattern on the surface of concrete slab

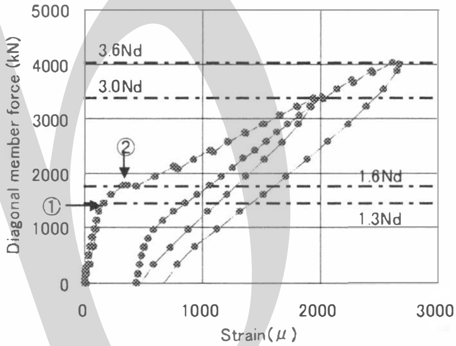

Fig.5 Max principal strains of Ring-shear-key

3.2 Fatigue Loading Test

After a fatigue loading test under two millions cyclic loadings was performed, any unsound phenomenon such as fracture or yielding of steel members was not observed. All measured strains showed constant trends regardless of the number of loading cycles.

4. CONCLUSIONS

The results obtained from the static and fatigue loading tests are as follows.

(1) Static loading test

1) When a load 1.6 times the design load assumed in the trial design was applied, a diagonal tensile crack occurred in the concrete slab of the connection part, which however did not lead to abrupt fracture due to working of the Ring-shear- key.

2) The joint possessed yield strength more than 3.6 times the design load assumed in the trial design.

(2) Fatigue loading test

1) Through the fatigue loading test, no significant damage was found on a concrete flange except a thin crack.

2) Through the fatigue loading test, deformations of the specimen were not affected by cycles of loadings, and no deterioration of the stiffness at the connection was observed.

REFERENCES

[1] Japan Road Association: Specifications for Highway Bridges, December 1996

NEW TYPES OF COMPOSITE BRIDGES ON GERMAN HIGHWAYS

Ulrich Gossla
Dr.-Ing.
Köhler+Seitz Consulting Engineers
Nürnberg, GERMANY

Thorsten Wanzek
Dr.-Ing.
Köhler+Seitz Consulting Engineers
Nürnberg, GERMANY

Keywords: bridge, steel, concrete, composite bridge, deck slab, rehabilitation

1 INTRODUCTION

Along the A71 and A73 highway linking formerly East and West Germany numerous bridges with main spans over 80 meters were designed as composite superstructures. Among these bridges is Wilde Gera Bridge, the longest arch bridge in Germany with an arch span of 252 m and concrete composite superstructure.

The width of the deck slab is around 28 m carrying two traffic lanes for each direction. The slab rests on a single cell steel trough and a diagonal inner and outer truss system.

Most highways in Germany usually consist of 2 to 3 lanes in each direction. Including shoulders the recent design width of a typical cross section is 28.50 m for 2x2 lanes and 36.50 m for 2x3 lanes. In case of rehabilitation works highways traffic cannot be shut down but two closer lanes in each direction must be open for traffic permanently.

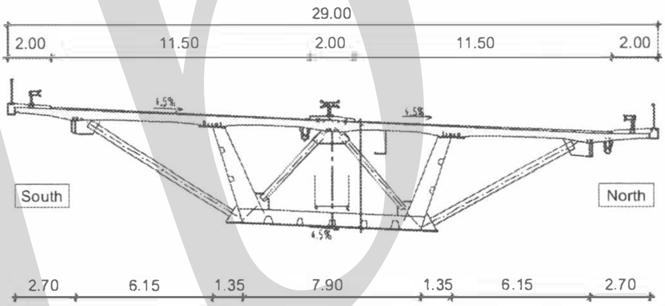

Fig.1: Typical 29.00 m cross section of 4 lane highways on bridges

2 DESIGN

In Germany highway bridges are designed for a minimum of 50 years.

Since the 80s the design principles in Germany foresee separate superstructures (half bridges) for each direction on concrete bridges. Recently new types of full bridges with a single superstructure have been carried out and are currently under construction on the highway A71/73 connection for former East and West part of Germany through the Thuringian mountains around 100 km north of Nürnberg. The superstructure consists of a open steel box and diagonal and transversal struts and longitudinal side beams that support the deck slab. The steel box is assembled on site by welding using large prefabricated element.

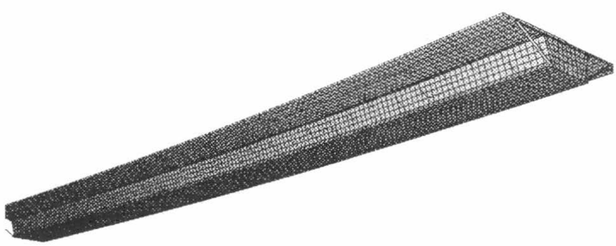

Fig. 2: Three dimensional finite element model of one half of the superstructure

In order to ensure such long life cycle, partial or even full replacement of the concrete slab is taken into account. Possible reasons for such necessary slab replacement are local deterioration of concrete or reinforcing steel caused by fire or contamination with aggressive substances in the unlikely case of vehicle accidents on the bridge. On bridges with separate superstructures for each direction, such kind of maintenance work can be easily carried out. However, taking into account the importance of the new highways, slab replacement has to be planned under full traffic loading conditions, providing 4 lanes on half side of the cross section without additions strengthening.

According to the tender, the structural design has to take into account repair and partial replacement measures on the concrete deck slab under traffic. It had to be verified, that any part of the deck slab can be replaced step under traffic. Theoretically, it is possible to replace the whole concrete deck.

The entire slab is divided into 92 sections for possible slab replacement, 4 over the width. In longitudinal direction, the possible length of the replacement sectors is up to 18.00 m. For the unlikely case of a slab replacement in the future, replacement sectors are already designed. Moment and normal force redistribution and especially the torsion behaviour of the disturbed box section are investigated by spatial finite element analysis. The detailed analysis had proven sufficient torsion stiffness even without additional torsion truss.

For the design of the superstructure an analysis of stress redistribution between deck slab and steel girder was carried out. When parts of the deck slab are cut off, normal forces in the slab and composite forces between steel and concrete cause an increase of deflection under self weight. As those mechanisms are rather complicated and effects on the complex structure difficult to understand, the main effects are explained on a simple model using a two span continuous beam.

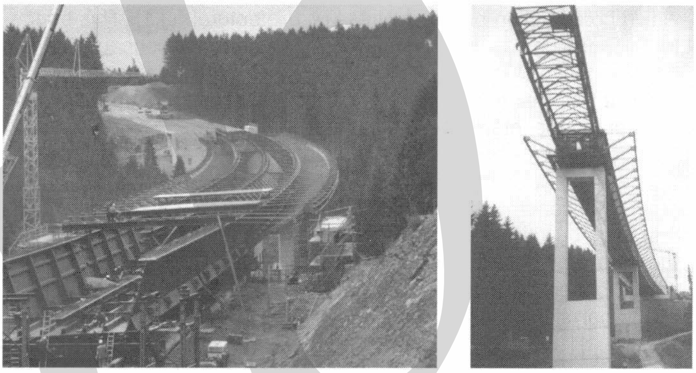

Fig. 3 Launching of the steel girder of Sesslestal Bridge

3 ERECTION

The U-shaped steel girder are assembled on site. Half prefabricated steel segments were transported from the steel manufacturer to the construction site and welded together.

The launching was performed in five stages. According to the calculation, maximum cantilever deflections of 1.30 m were expected during launching. In order to compensate these deflections, a lifting device on the end of the launching girder was arranged.

As in Germany salt is used as de-icing agent in winter times, sealing and crack control are extraordinary important for long life structures. Bridge decks are sealed by epoxy coating and bituminous layers and bridge caps separated from the carrying structure. Nevertheless, crack control must not be neglected. Cracks are controlled to 0.2 mm. Amount, diameter and spacing of re-bars are strictly regulated for composite bridges. The slab is concreted in 15 stages. First, the middle parts will be concreted and secondly the support parts. This method reduces longitudinal tension strains in the deck slab.

DESIGN OF A CONTINUOUS COMPOSITE TRUSS GIRDER BRIDGE STIFFENED WITH EXTERNAL CABLES

Hirokazu IWASAWA
Road Construction
Department of Public Works
Niigata Prefecture,Japan

Mitsuharu KOMURO Masashi KARAKI Satoshi TAKANO
New Structural Engineering,Ltd.
Japan

Masatsugu NAGAI
Nagaoka University
of Technology
Japan

Keywords: composite truss girder bridge, external cable, stud

1 INTRODUCTION

Cost rationalization and labor saving was taken into account recently actively for bridges structures and construction in Japan. One way being explored is the adoption of steel-concrete composite structures with many studies done for a most effective use of steel and concrete materials. Composite truss highway bridges in Japan are built as simple span composite truss girder bridges until now[1]. This allows of simplifying the design of continuous composite structures for truss bridges. This paper describes the design method, especially the detailed design of the slab, of the KOSHIRAKURA Bridge which construction began in NIIGATA Prefecture[Fig.1]. This bridge is a 3 span continuous composite truss bridge using external cables.The fundamental concepts of the design of this bridge are as follows.

- The conventional longitudinal beam and cross beams used as floor structure are omitted.
- The external tendons are prestressed in the longitudinal direction to limit the tensile stress in the slab on the intermediate supports.
- Cross beams and intermediate cross bracing are not installed.

The extermal cables are installed in order to improve the section forces of steel members and to prevent of concrete slab cracks. This point create an extremely simple structure and this bridge is the first to be build in Japan for this structural type. So It was important subjects to establish the design of the slab on the structure for the whole bridge. This paper describes a method for the design of this bridge based on a plane frame structural analysis and accordingly compared the results with a 3-D FEM analysis.

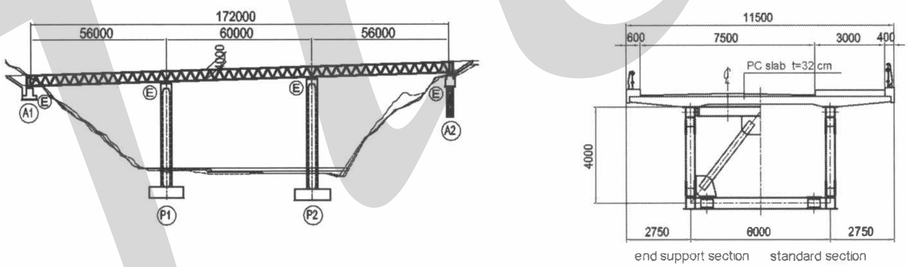

(a) side-view (b) cross section

Fig.1 General view of this bridge

2 SUMMARY OF STUDY

2.1 The section forces of the slab due to global structural action

The design of the slab was carried out by use of a palne frame structural model. As this structure is a composite girder, the design of concrete slabs was carried out considering the slab action and the global structural action. The section forces of the slab due to the global structural action are separated as shown in Fig.2 to carry out the design of the bridge. The section forces are divided as follows:

(a)The axial forces
(b)The bending moment calculated on the structure for the whole bridge structure.
(c)The bending moment due to the rigid frame action on the structures joining global rigid panel points.
(d)The bending moment with the between panel points of the truss considered as support points.

2.2 Evaluation of the stress due to the axial forces

A concentration of normal forces N produced in the slab by the diagonal members occurs in the panel points. One of the objects of the design of this bridge is to grasp how to transmit and distribute these concentrated forces into the slab. In this case, the concept of the stress concentration coefficient α was introduced as follows:

$$\alpha = (\sigma - \sigma') / \Delta\sigma$$

where, σ =the max. value of normal stress, $\Delta\sigma$ =the average stress due to increased nomal force (ΔN), σ'=the stress according to the normal force. The validity of this method is confirmed by comparison with the results of the stress given by the FEM[Fig.4].As the result of analysis, the stress concentretion coefficient can be taken as α =2.0 in design of this bridge.

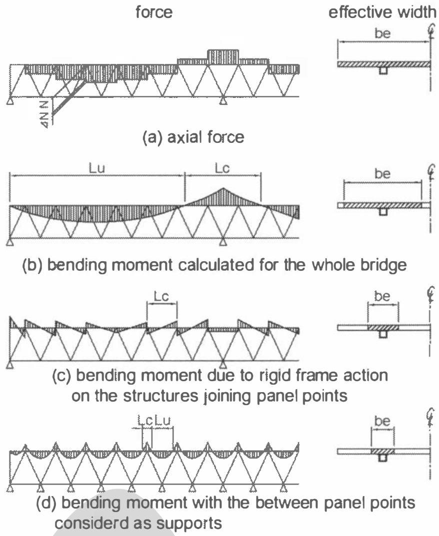

Fig.2 Forces and effective width of the slab

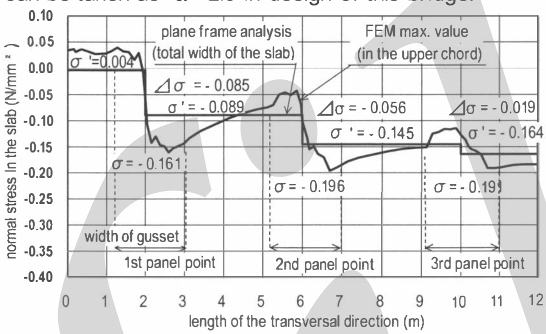

Fig.3 Normal stress due to axial forces

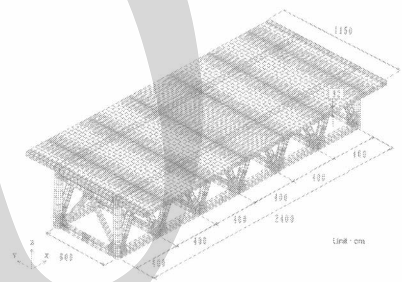

Fig.4 3 -D FEM model (solid and shell)

Table 1 Stress concentration coefficient α

		1st panel	2nd panel	3rd panel
Right edge of the gusset	$\sigma - \sigma'$(N/mm^2)	-0.157	-0.107	-0.046
	$\Delta\sigma$ (N/mm^2)	-0.085	-0.056	-0.019
	α	1.85	1.91	2.42

2.3 Stresses due to the bending moment considering the effective width of the slab

Fig.2 shows the equivalent span lengths Lu and Ls for each case of decomposed bending moment. The bending stress of the slab due to the global structural action needs to be calculated by using the effective width of the slab, which is calculated from the equivqlent span lengths corresponed to the bending moment. The validity of the calculation method by using the effective width of the slab is confirmed by comparison with the results of the stress given by the FEM analysis [Fig.4]. And as the gusset plate supports the panel point widely, the length was examined to be taken into account for reduction of the bending moment on the basis of the result of this FEM analysis. This method of design of a slab by introducing the notion of effective width can be considered to be used on practical way.

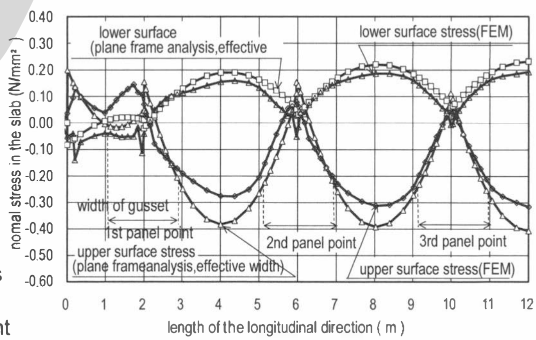

Fig.5 Normal stress due to bending moment

REFERENCES

[1]Takeo Fukuda : As to Composite Truss Girder –Nakajuku Bridge to be constructed in Niigata Prefecture-,Journal of Civil Engineering Technology,pp.24-30,1956

DESIGN OF THE KINOKAWA VIADUCT COMPOSITE TRUSS BRIDGE

Hiroo Minami Masato Yamamura Yohei Taira Kosuke Furuichi
Kajima corporation
JAPAN

Keywords: composite truss bridge, external cables, joint structure, fatigue experiment

1 INTRODUCTION

In recent years, the development of composite-structure bridges introducing the merits of both steel and concrete has been actively performed with the purpose of rationalizing the structure and laborsaving in the construction. One such structural scheme is the steel/concrete composite truss bridge. Such bridges were constructed in only a few cases in France, and this bridge will be the first construction of a composite truss bridge in Japan.

2 COMPOSITE TRUSS BRIDGE

The composite truss bridge is a composite bridge, the objective of which is to achieve a more rational structure by combining the mutual merits of a steel structure and a prestressed concrete structure by replacing the web of the prestressed concrete box girder bridge with steel truss diagonal, and making the upper and lower deck slabs in the remaining pressed concrete structure (see **Fig.1**).

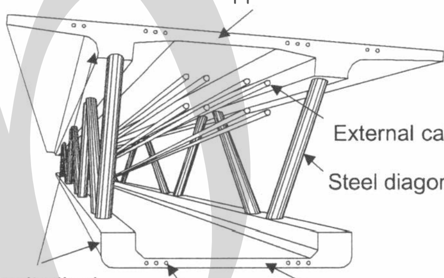

Fig.1 Composite truss bridge

In a prestressed concrete box girder bridge, making the web which occupies 10~30 % of the dead weight of the main girder to be light-weight steel truss diagonal, the dead weight of the main girder can be reduced, thereby reducing the load on not only the superstructure but also to the foundation/pier structure. Also, because the bridge's axial rigidity of the steel truss diagonal is small, other than being able to improve prestress force introduction efficiency, assembling reinforcing bars of concrete web, cable placement, concrete casting, etc. can be omitted, enabling laborsaving in the construction and a reduction of the construction period.

3 OUTLINE OF THE KINOKAWA VIADUCT

3.1 General condition

The general conditions are listed below, and the structural general drawing is shown in **Fig.2**.

Owner	Kinki Regional Development Bureau, Ministry of Land, Infrastructure and Transport
Construction location	Shingu City, Wakayama Prefecture
Structural scheme	Four-span continuous steel/concrete composite truss bridge
Bridge length	268.0 m
Span length	51.85 m + 2 @ 85.0 m + 43.85 m
Width	10.5 m

3.2 Characteristics

(1) Bridge scheme

As a result of comparing and investigating the rigid frame structure and continuous girder structure, the continuous girder structure is adopted. This is because the superstructure can be made simple by making it to be the continuous girder structure using a quake-absorbing bearing, and the bridge

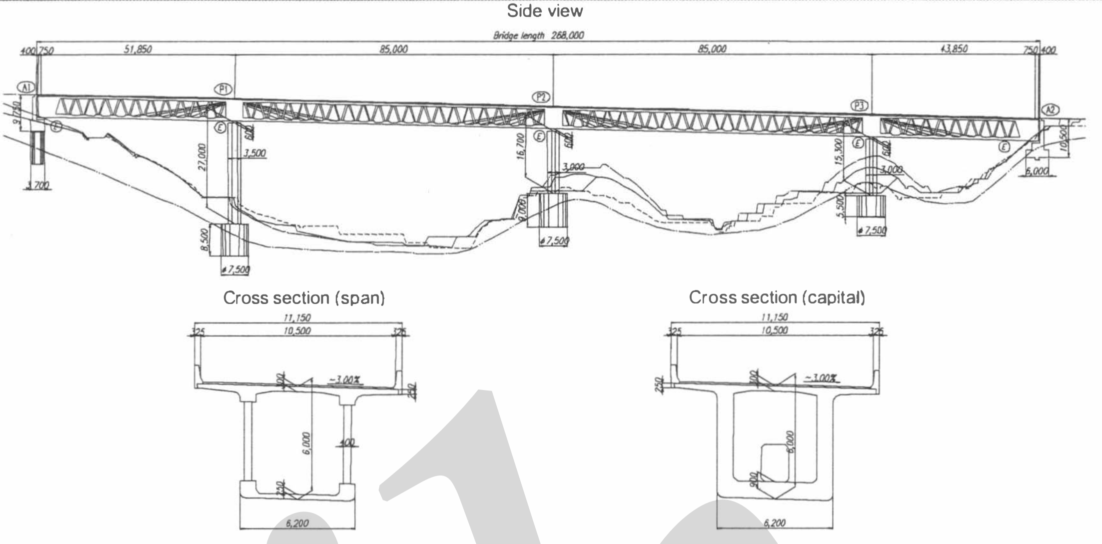

Fig.2 General view

pier/foundation can be shrunk, improving the durability and processibility of the structure system as a whole while being almost equivalent in cost.

(2) Girder cross section

The girder cross section is made to be equal to 6 m in girder height over the entire bridge. In a composite truss bridge, because the web is replaced with steel tubes, even if the girder height is increased, there is almost no increase in the dead weight of the girder. Therefore, the girder height is increased as far as the construction limit of the intersecting roads allow, attempting to increase the cross-sectional rigidity and cross-sectional durability and to reduce the quantity of the used prestressing cables.

(3) Steel truss diagonal

As the steel truss diagonal, steel tube (STK490, ϕ=406.4, t = 9~22 mm) is used. As the steel truss diagonal, a round-shape steel tube instead of a rectangular steel tube is adopted because of the weldability problem in the joint structure and in the interest of economy. By filling the same concrete with the deck slab inside the steel tube where compressive axial force operates, making it a steel/concrete composite structure, an attempt was made to reduce the used steel tube plate thickness.

(4) Joint structure

In this bridge, the joint structure developed by our company (Steel box type joint structure, **Fig.3**) was adopted. Fatigue tests using the actual-size partial models which is one joint of the truss structure taken out is performed with the objective of checking mainly the safety of repeated load to the welded sections. And in order to check the behavior of the joint section at a larger load than in the fatigue test, a static load loading test is performed after the end of the fatigue test.

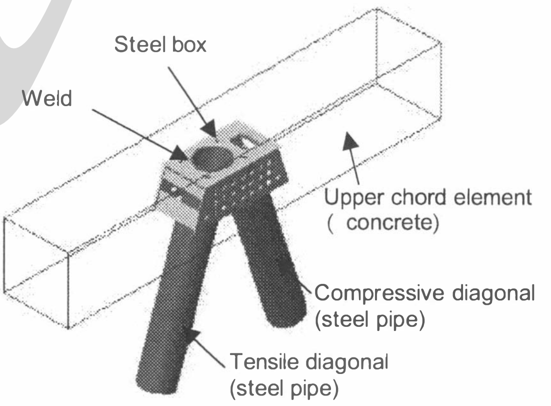

Fig.3 Joint structure

4 CONCLUSION

Presently, the Kinokawa viaduct is under a cantilever erection of its main girder, scheduled to complete the girder construction in March, 2003. The work is the construction of the first composite truss bridge in Japan, adopting new technologies both in its design and construction.

EXPERIMENTAL STUDY FOR COMPOSITE PRESTRESSED CONCRETE GIRDER BRIDGE WITH EXTERNAL TENDONS OF LARGE ECCENTRICITIES

Kosei Ido Naoki Hagiwara Jun Yamazaki
Nihon University College of Science & Technology
JAPAN

Kenji Umezu
Sumitomo Constr. Co., Ltd, JAPAN

Hiroki Kouno
Nihon University
JAPAN

Keywords: External tendon, Large Eccentricity, Composite Girder, Extradosed

INTRODUCTION

The subject of this report is the experiment of a reduced scale structure model, Fig.1, and its reliability for utilization in the design of real scale structures.
In spite of an affinity of the structure form to that of a “self anchored suspension bridge”, the type of the structure for study is expressed as “prestressed concrete (PC) girder bridge with external tendons of large eccentricity”. The effects of prestress on the girder are common in both types in that they exert axial compression and uplift force. The effects can differ if the flexibility of the members connecting the main tendon and the girder is not negligible.

The paper reports the followings.

1. A prototype bridge form as a base for the reduced scale model. The center span length is 180m. (Fig.2)
2. A design rationale, referred as “EL design method” by the authors.
3. Structural characteristic obtained by the “EL design method” for span lengths varying between 130m and 300.
4. Experiment with 1/36 scale model. The center span is 5m. (Fig.1)
5. FEM analysis of 1/36 scale model and check against calculations and assumptions.

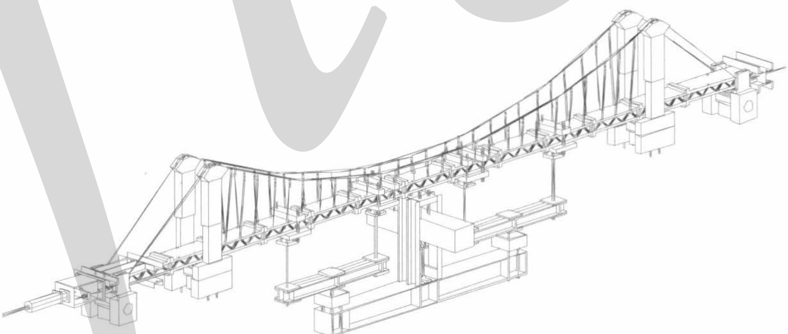

Fig.1 1/36 scale model

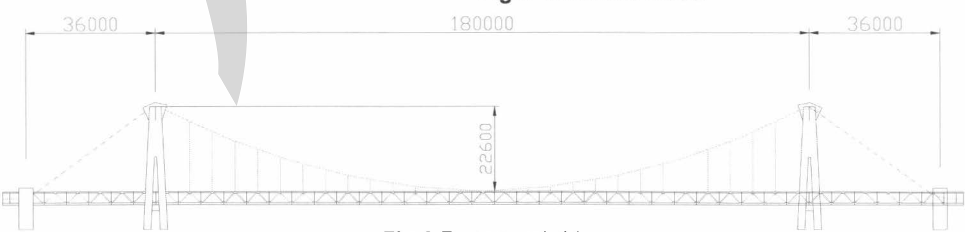

Fig.2 Prototype bridge

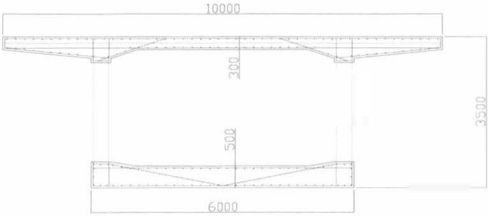

Fig.3 Cross section of girder

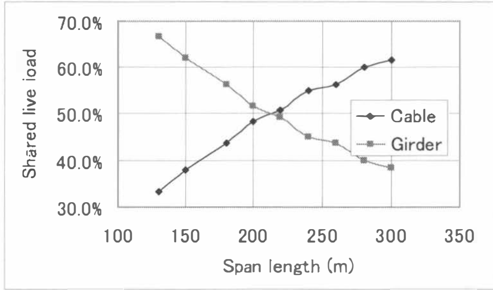

Fig.8 Live load shared by girder and cable

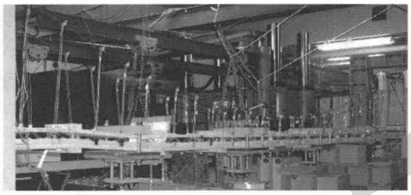

Photo.4 Maximal displacement

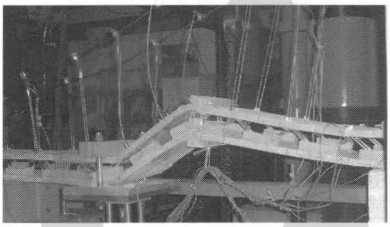

Photo.5 Failure

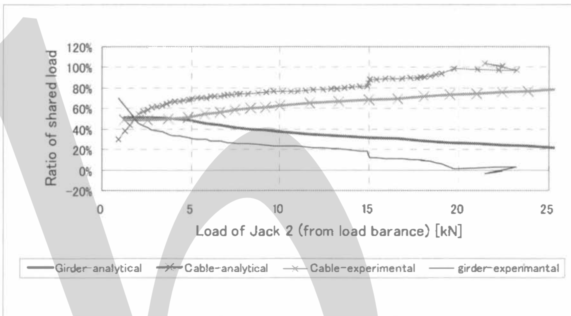

Fig.17 Load shared by girder and cable

CONCLUSION

Based on the report herein it is concluded that the experiment of structure model is a useful means in conceiving the realization of the types of structure lacking in previous experiences.

In view of comparisons made on the experimental results, calculations, its assumptions, and FEM analyses, there were no serious contradictions.

Hence, the structure scheme of the prestressed concrete bridge with external tendons of large eccentricity reported here is considered to be a viable candidate for future construction.

The prestress in the external tendon of the structure studied here exerted axial force and uplift force as expected. These effects are similar to those in St Remy de Maurienne Bridge of France, which is said to be an "extradosed bridge" in SETRA periodical, July, 1997.

Hence, the structure type reported here may be said to belong to the extradosed PC bridge.

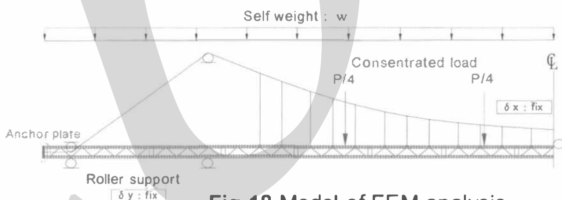

Fig.18 Model of FEM analysis

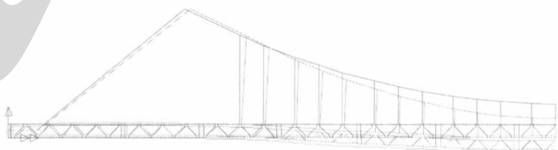

Fig.20 Deformation

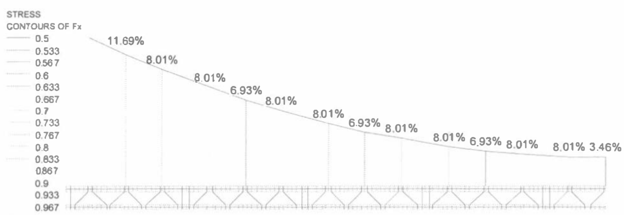

Fig.23 Percentages of tensile force in hanger cable

COMPOSITE BRIDGES – AN OVERVIEW

Mike Schlaich, Dr. sc. techn.
Schlaich Bergermann und Partner, Consulting Structural Engineers
Stuttgart, Germany, www.sbp.de

Keywords: composite structures, composite bridges, typology, connectors, teeth connectors.

SUMMARY

The intention of this paper is to give an overview on selected interesting items regarding composite steel-concrete bridges. Covering the entire field of composite structures is not possible within the scope of such a paper. Therefore, bridges are used as representatives as many trends stem and derive from there.

The paper starts with definitions relating to composite bridges:

composite: combination of two or more materials in one cross-section (most commonly an I-section with a bottom flange and a web of steel and a top flange made of concrete) to improve resistance and deformation properties.
hybrid: combination of two or more structural systems in one structure (usually a primary truss system combined with a secondary girder working in bending).
mixed: combination of two or more materials independently acting in one structure.

Next, all advantages and disadvantages of composite bridges, when compared to concrete-only or steel-only bridges, are listed and a brief historical overview is given. One main section is dedicated to an overview of classic and promising new composite bridge types.

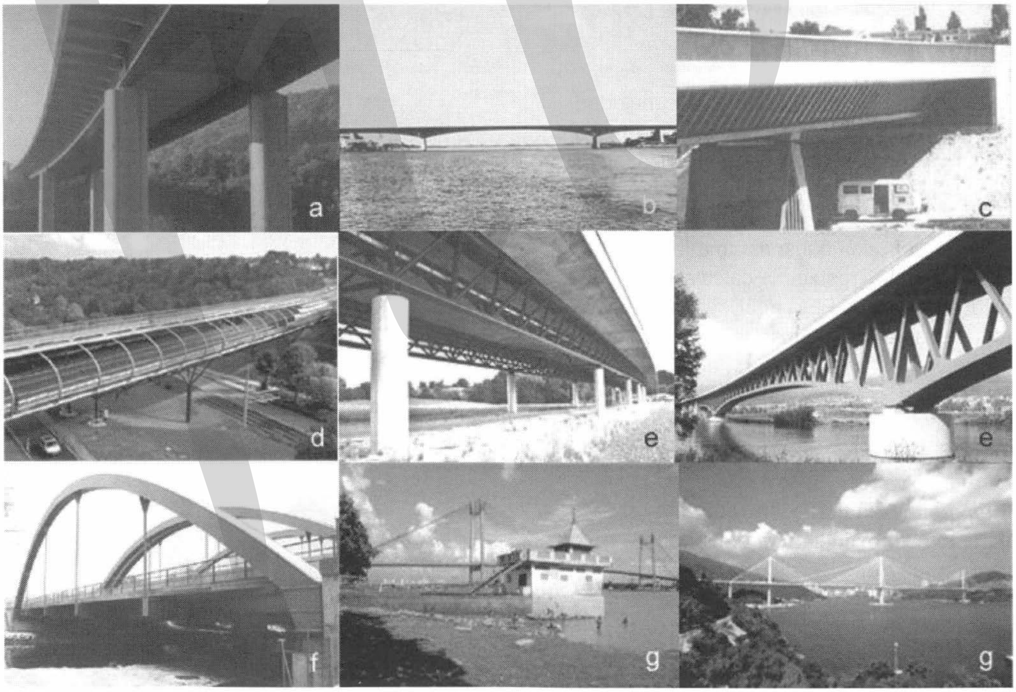

Fig. 1 a) The classic composite deck section consisting of a steel grid made of longitudinal I-beam sections and cross girders with a concrete slab on top; b) Double composite section; c) Composite section with folded webs; d) Steel truss to support the concrete slab (without top chord); e) Steel trusses with top chord; f) Arch bridge with composite decks; g) Cable-stayed bridges.

The second main section is dedicated to connections between steel and concrete. It is shown that the load bearing behaviour of the most common device, the welded steel-headed studs, can easily be explained with strut-and-tie models. For a safe load transfer without making use of the concrete tensile strength (Fig. 2b) the length of the studs should be as shown in Fig. 2a.

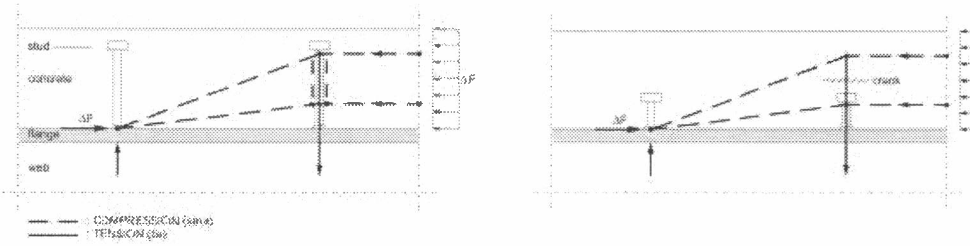

Fig. 2 a) Load bearing behaviour of a welded steel-headed stud; b) Concrete cracking at short studs.

Emphasis, however, is on a new type of connection, the so-called teeth connectors, which have proved to be efficient for the transfer of high concentrated loads between steel and concrete. Their load bearing behaviour is explained and design guidelines are given.

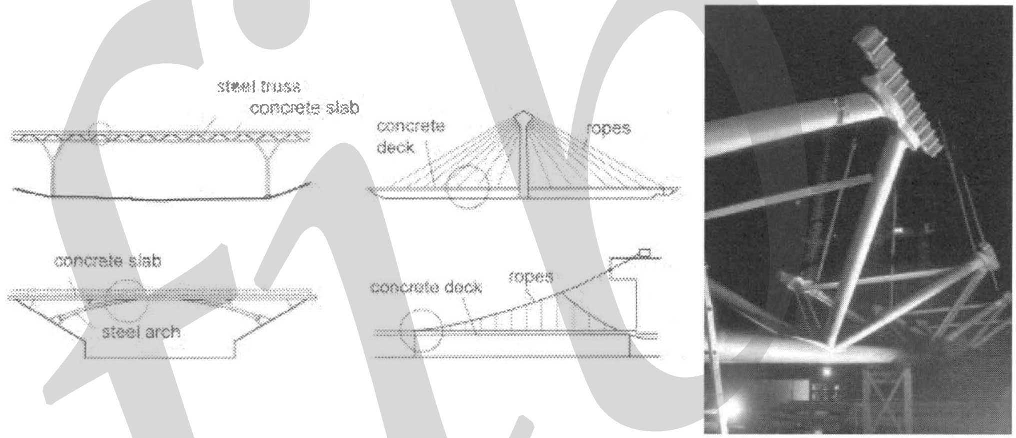

Fig. 3 Examples for transfer of concentrated loads and detail of a bridge under construction.

There is a large variety in the design of steel-concrete composite bridges. Composite sections have been used for almost all types of bridges and often they turn out to be more economic and elegant than pure concrete bridges. Major breakthroughs have taken place in the last two decades regarding structural solutions, connection details and codes. Now, there seems to be a time of consolidation and there are others field where the pace of development is faster. In the context of composites, “Advanced Composites” is one of the keywords. Glass-fibre-reinforced polymer composites have already been used as the principal structural material of several bridges. Hopefully, these developments lead also to new bridge types and not only to copies of existing typology with less weight. Variety is one mean towards more beauty of our structures.

More than 30 references regarding state-of-the-art literature on composite structures are given in order to enable the reader to obtain further details on all the subjects treated here.

A NEW GENERATION OF PRESTRESSED CONCRETE COMPOSITE BRIDGES WITH FRP PANEL WEB

Kyoji Niitani Hiroyuki Abe Ulrich Gossla
Oriental Construction Co., Ltd., JAPAN Koehler+Seitz Beraten und Planen GmbH, GERMANY

Keywords: FRP, composite bridge, prestressed concrete, concrete dowel

1 INTRODUCTION

In seismic active regions like Japan, the reduction of self-weight of the superstructures leads to more economical solution because the earthquake load must be considered when bridges are designed. A new structural type of composite bridge, prestressed concrete bridges with FRP (Fiber Reinforced Plastic) panel web as shown in Fig.1, is proposed as the bridge for the next generation. The heavy concrete web of conventional prestressed concrete box girder is replaced with light and durable FRP panels. It is expected that it can reduce the very costly maintenance burden during the life span of the bridge.

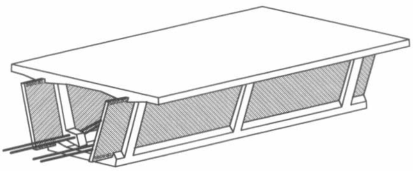

Fig.1 Schematic description of prestressed concrete composite bridge with FRP panel web

2 CONNECTION BETWEEN CONCRETE AND FRP

Connection between two different materials is very important in a composite structure. Concrete dowel is selected as a shear connector between concrete and FRP panels as shown in Fig.2. In this research, five-layered laminated panel reinforced with glass fibers (GFRP) was used.

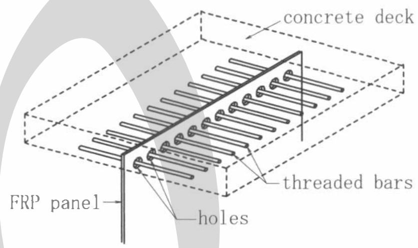

Fig.2 Concrete dowel

Push-out tests were performed to search for possible applications of concrete dowel to connection between concrete and FRP panel. Fig.3 shows the relationship between shear force per hole and relative displacement between concrete and panel. Comparison between specimens with steel and FRP shows that relative displacement between concrete and FRP panel prior to yielding of concrete dowel is little greater than that of steel. However, The shear strength per hole, that is the ultimate strength of the concrete dowel, is almost the same for both specimens. From test results, it can be said that concrete dowel between concrete and FRP panels is also as effective as that between concrete and steel.

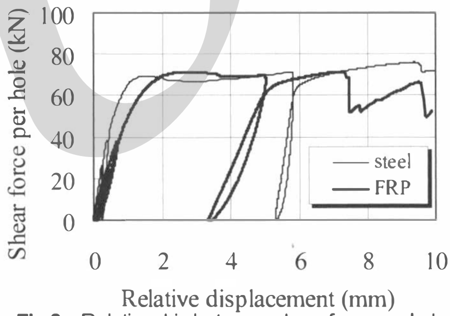

Fig.3 Relationship between shear force per hole and joint slip between concrete and panel

3 CONNECTION BETWEEN ADJACENT FRP PANELS

Regarding prestressed concrete composite bridge with FRP panel web, FRP panel can be relatively big and should be divided into appropriate lengths, considering fabrication and transportation. As a result, connection between adjacent FRP panels can not be avoided at construction sites.

Experiments on bolt joints of laminated FRP members were performed, and properties of strength and failure modes were investigated. Also possibility of friction type connection between laminated FRP members was also investigated. Fig.4 shows relationship between axial force of bolts and strengths of specimens. Axial force of bolts increases the strength of specimens and the relationship between them is linear. Calculated strengths with assumption that the sliding coefficient

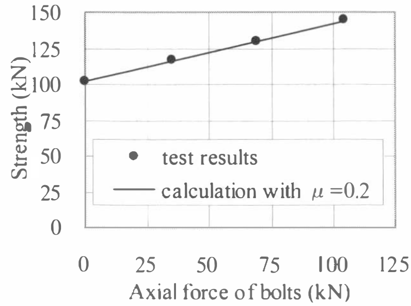

Fig.4 Relationship between axial force and strength

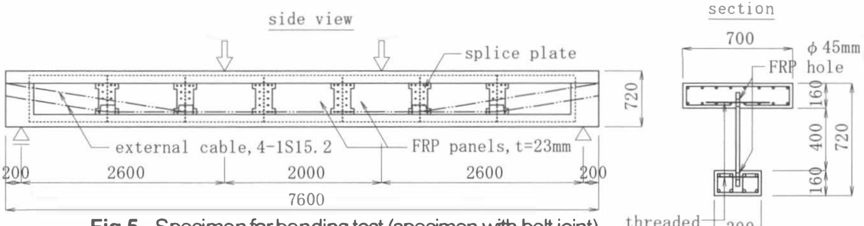

Fig.5 Specimen for bending test (specimen with bolt joint)

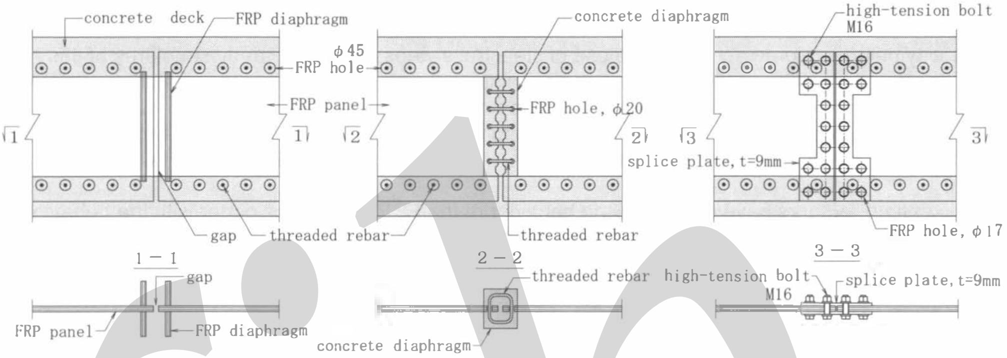

(a) gap (without connection) (b) connection with concrete diaphragm (c) bolt joint

Fig.6 Detail of joints between adjacent FRP panels

between a splice plate and a FRP panel is 0.2, shows good agreement with test results.

4 BENDING TESTS

Static loading tests were performed using three specimens shown in Fig.5. Concrete dowel was applied to the connection between the concrete and the FRP panel the same way as in the push-out tests. FRP web was divided into seven panels. In three specimens, connection between adjacent FRP panels was different as shown in Fig.6. They are gap between two adjacent FRP panels without being connected, connected with concrete diaphragm in which ties were threaded into holes drilled at the both sides of FRP panels and connected with bolt joints using friction type connection. The number of bolts for was decided according to single-bolt tests.

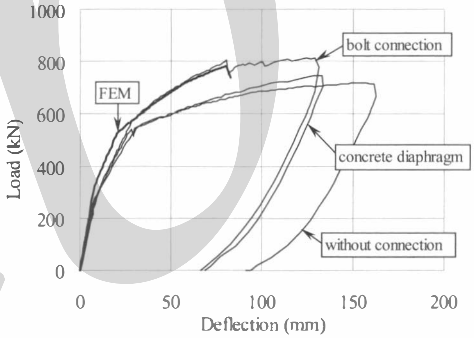

Fig.7 Load-deflection

Fig.7 shows the relationship between load and deflection at the mid-span. From comparison of deflections of three specimens with different joint between adjacent panels, it can be seen that after loading exceed 550kN deflection of a specimen with bolt joint shows higher rigidity than that of two specimens with concrete diaphragm and without joint. Also, ultimate strength of a specimen with bolt joint is about 10% higher than that of rest specimens. These mean that the bolt joint is the most rigid connection in the three types of joint between adjacent FRP panels. Load-deflection curve calculated with FEM considering no-linearity of materials and geometry is also drawn in Fig.7. Load-deflection curve and ultimate strength of a specimen with bolt joint show good agreement with calculated strength and curve. In the FEM analysis, the beam is assumed as a perfect composite beam. Therefore, it can be said that the both connections, one is concrete dowel adopted as a connection between concrete decks and FRP panels, and the other is bolt joint adopted as a connection between adjacent FRP panels, are rigid enough to show composite performance.

5 CONCLUSIONS

A new generation of prestressed concrete composite bridge with FRP panel web is proposed and fundamental experiments were performed. From the experiments it can be said that pultruded and laminated FRP panels are as practical as a composite material in bridge construction.

STUDY OF A FRP TRUSS BRIDGE

Noritaka Sugano Masayuki Okada Makoto Sudo Junji Ogata
FUJI P.S CORPORATION, JAPAN ingerosec corporation, JAPAN

Keywords: FRP, truss bridge, external tendon, highly expansive material

1 INTRODUCTION

Construction and research for composite bridges are recently progressing in Japan in order to obtain an economical efficiency by laborsaving during the bridge construction and by lightening of the superstructure.

One way being explored actively is the use of steel truss webs girder and many structures of this type are in construction in Japan. But another way consists in the use of FRP instead of steel for the truss members, as the FRP material has an excellent weather resistance and doesn't need maintenance.

Authors have studied the use of FRP truss webs for a 3 spans continuous concrete box girder bridge carried out using the segmental balanced cantilever method in order to check the possibility of such a design.

In a first time, authors have compared the behavior of the FRP truss webs girder with the behavior of the same one with replacement of the FRP by steel and have designed a workable FRP truss bridge.

In a second time, authors have examined the methods of connection between FRP truss members and concrete slabs. A connection using expansive admixture has been designed and have been carried out some tests to verify the feasibility of such a method.

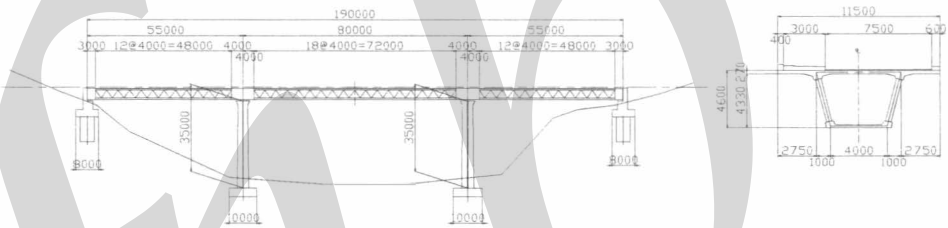

Fig.1 General view

2 COMPARATIVE DESIGNS

2.1 Truss member forces

Under live load, the axial forces in the FRP diagonals represents only 60 to 75 % of the ones in the steel diagonals. Due to the smaller modulus of elasticity of the FRP material, the truss is less rigid and a bigger part of the global shear force will be reported to the concrete slabs and to the tendons, allowing a smaller variation of stress in the FRP truss members.

As the deformations under dead load are very small, the bending moment at permanent state in the diagonals are close to 0 for the two alternatives. But under the live load, the FRP diagonals will have to support a maximum bending moment of 52 kNm compared to a bending moment of 154 kNm for the steel. This interesting result can be explained by the lower modulus of elasticity of the FRP that compensate largely the greater deformability of the girder.

2.2 Upper and lower slabs forces

It is clear that, as the FRP truss is less rigid, bigger bending moments occur in the upper slab on support and smaller at midspan. The compressive forces are similar, but the traction force under live load is smaller for the FRP truss.

For the lower slab, the traction and compression forces are similar, but the bending moment is bigger at midspan for the FRP truss.

2.3 External tendons

Under the live load, the external tendons will support a portion of the global shear force. The calculated variation of tension with the designed tendons is close to 100 MPa.

2.4 Deflection

The deflection for the FRP truss web girder is 3 times larger that the one of the steel web, with a deflection L/1060 for the FRP truss and L/3200 for steel truss.

3 TEST OF THE FRP MEMBERS ANCHORAGE

3.1 Fixation of the FRP members

The method consist in placing an expansive material between the FRP tube and a steel socket in order to ensure the transmission of forces. The steel socket will comprise standard welded studs for the connection inside the concrete.

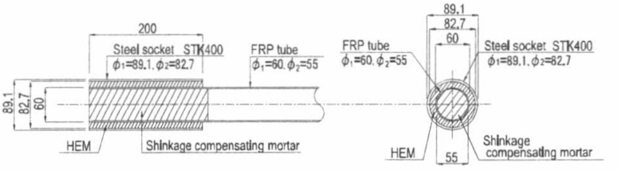

Fig. 2 Details of anchorage

3.2 Test sample and traction test

The figure 2 show the samples used for the tests..

The FRP tube sample number 1 is filled on all its length with a shrinkage compensating mortar and the FRP tube sample number 2 is only filled at each extremity on a length 200 mm with the same shrinkage compensating mortar in order to cover all the socket length.

The sample is put in a central hole jack and anchor plates are placed against the sockets to support the jack force. The jacking force is applied slowly, by step of 10 kN.

3.3 Test results

3.3.1 FRP member

Table 1 presents the main tensile characteristics obtained for the two samples.

The tensile modulus of elasticity is 1.14 times greater for the sample 1 than for the sample 2 and the tensile strength is 1.04 times greater. Compared with the theoretical values, the tensile modulus of elasticity is between 1.10 – 1.26 times greater in the test, but the tensile strength is only 70% of the theoretical value.

Table 1 Main tensile characteristics

	Tensile modulus of elasticity (GPa)	Tensile strength (MPa)
Sample 1	27.7 (1.26)	276 (0.69)
Sample 2	24.2 (1.10)	266 (0.67)
Theoretical (Sample [illegible]	22.0	400

( ) is experiment／Theoretical

3.3.2 Strain of the socket

The figures 3 show the distribution of the stress along the socket during the tests for the sample 1.

The behavior of the sockets is similar for the two samples. At FRP fracture, the anchorage length represents 1/3 of the length of the socket. With a linear interpolation calculated for the first 4 values at maximum load of the 60 mm part of the socket close to the jacking plate, we find an anchorage length of 59.4 mm for sample1 and 59.6 mm for sample 2.

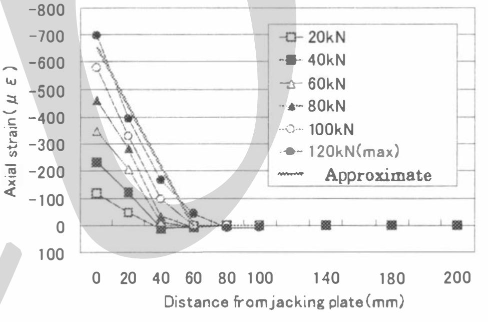

Sample 1

Fig 3 Distribution of the axial strain along the socket

3.4 Conclusion

The conclusions of the experimental tests are the following:

1) The connection of the FRP tubes and Steel sockets can be made with use of a HEM material.
2) The results obtained for the two FRP samples are similar.
3) The friction coefficient obtained by test was 0.46. Taking in account this value, the socket length required for the studied bridge is 300 mm.

The tests carried out allow to check the possibility of use and connect the FRP material. The proposed method is to use a steel socket to transmit the force through concrete. But this new method need some other tests to study parameters like diameter of tube and length of socket.

REFERENCES

[1] JSCE : Guidelines for design and construction of concrete structure using continuous fiber reinforced materials, Concrete library, 1996.9

[2] Harada,T., Soeda,K., Idemitsu,T., Watanabe,A : Characteristics of Expansive Pressure of an Expansive Demolitionagent and the Development of New Pressure Transducers, Journal of Materials Concrete Structures and Pavements, No.478/V-21, pp.91～100, 1993.11

DEVELOPMENT OF PRE-CAST PC-SLABS WITH SHEAR TRANSMISSION JOINT

Hidenori Ishii Masayoshi Higuchi
Kawada Construction Co.,Ltd

Keywords; Shear transmission joints,Durability,Alternating shear force loading test

SUMMARY
Recently, the precast decks and the joints' development intending for labor-saving and high durability are prosperous. The authors are trying to develope a favorable precast deck with a new unique jointing system named as 'ST-Slabs', The precast panels are jointed by using studs and non-shrinkage mortar to transmit only shearing forces between each panel without longitudinal prestressing. For the new type of joint, the shear strength were verified under static loading and fatigue loading of alternating shear force. The results of the joint seemed to be favorable for actual bridge deck.

INTRODUCTION
Precast PC Slabs (hereafter "PCa slab") are often used for labor saving and high durability on newly establishing steel bridges or replacing damaged slabs. However, the joint of PCa slab has various problems on the construction.

Accordingly, we designed our unique PCa slab whose longitudinal prestressing is omitted, the interval of the joint is shortened, and has shear transmission joint for labor saving, shortening construction period, and improving economical efficiency. Fig. 1 shows the structure of PCa slab using steel plate and the headed stud. Transmission of bending moment to the bridge direction is not considered, and the stress transmission at the joint part of PCa slab is mainly considered only for shear force to eliminate the level difference of joints and the load distribution. (hereafter called "ST slab: Precast Slabs with Shear Transmission Joint) On the joint, the headed stud is welded zigzag, two layer of anchor steels are welded on the main body side, and attached on the edge of PCa slab.

This time, in order to simulate the load of running wheels practically, we report the results of fatigue test by wheel load running test machine using full-scale test pieces, static and fatigue durability tests using the test pieces with joint-structure beam.

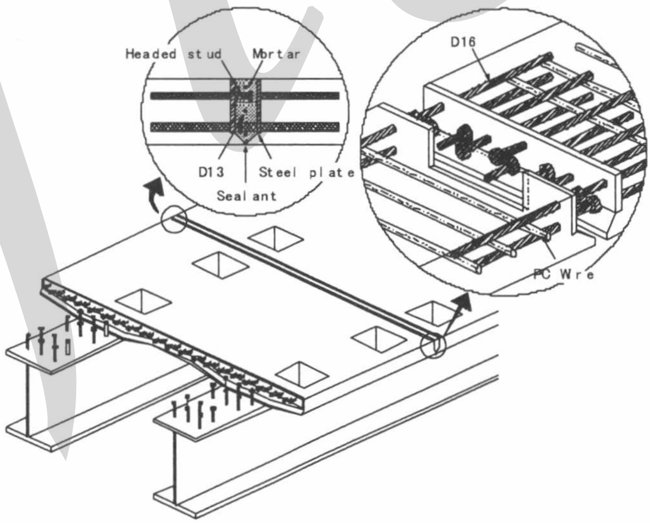

Fig. 1 General structure of ST slab

WHEEL LOAD RUNNING TEST

Wheel load running test using full-scale test piece was carried out to practically simulate running wheel load, and confirmed the continuity and durability of the joint part.

SHEAR LOAD CAPACITY TEST WITH TEST BEAM

Fatigue durability of the joint was confirmed by the test with wheel load running test machine. However, to clearly grasp the load capacity mechanism at the joint part, the structure of joint part was extracted as a beam. Load capacity and durability tests by were carried out with the test beam using the testing device to apply pure shear force.

CONCLUSION

The main results obtained from the tests on continuity and durability using PCa slabs with joint are as below.

1) Fatigue durability and continuity of PCa slabs that have shear transmission joint using stud are secured without no remarkable problem. However, on the joint part, penetrating cracks occur on the joint part and waterproof works need to be executed.
2) Crack pattern on the alternating shear test is the same as wheel load running test.
3) From pure shearing test using test beam, shear capacity and destruction mechanism were examined. Effectiveness of stud and checkered steel plate was confirmed.
4) To improve shear capacity, the following methods were proved to be effective.
a) Place reinforcement steel surrounding the stud to improve cone destruction capacity. However, TYtpe-2 is more favorable than reinforcement 1 since the latter works becomes complicated.
b) Use checkered plate to distribute shear force.

From the viewpoint of structured and economical efficiency, we would like to also examine the combination of checkered plate and penetration reinforcement.

REFERENCE

1) Higuchi, Kajikawa, Arai: Development of Precast Slabs with Shear Joint, Kawada Giho, Vol. 17, 1997
2) Kim, Matsui, Egashira, Miyagawa: Experimental Studies on Load Capacity of Precast Slabs Shear Key Joint, JCI, 1999.7

APPLICATION FOR COMPOSITE GIRDER BRIDGE WITH CHANNEL-SHAPED PRECAST PC DECK SLABS

Shinichi HINO, Kohei YAMAGUCHI, Hiroki GODA, Tadahiko TSUTSUMI, Nobuyuki YOSHIZAKI
Associate Professor, Assistant, Student, Chief Engineer, Chief Engineer
Kyushu Univ., Kyushu Univ., Kyushu Univ., Fuji P.S. Corporation, Fukuoka Kitakyushu Urban Expressway

Keywords: Composite Girder, Bridge, CPC Deck Slab, Wheel Running Test, Push-Out Test

1. INTRODUCTION

A channel-shaped precast PC panel (CPC panel) has been developed for the purpose of an improvement of the durability against to the vehicle load and the fabrication and erection work of deck slabs in steel girder bridges on site. As it is well known, the application of precast panel in constructing the slab of steel girder bridge is easily and useful for the reason that most of middle class bridges are non-composite structures.

A channel-shaped precast PC panel (CPC panel) as shown in Photo 1. Fig. 1 shows general view of CPC panel system applied to steel girder bridges. The principal of composite activity of the structure that CPC panel is applied as the compressive flange is illustrated in Fig.2, and also is described as follows; The horizontal shear force between steel girder (S1) and the filled up mortar that increases in proportion to the flexural deformation of the composite girder is transferred by the proper quantity of studs (S2). The bottom uneven shape of CPC panel acts effectively to transfer horizontal shear force between the filled up mortar and CPC panel (p1, p2). Studs provided at the joint of CPC panels and openings filled with pouring mortar or concrete act effectively to resist the uplift that occurred by slab action (T1, T2).

The purpose of this study is to provide some useful information with respect to the reasonable design for the composite girder bridges with CPC panels as deck slabs. This paper presents experimental and analytical studies and an outline of the practical application for the actual composite box girder bridges with CPC deck slabs.

2. EXPERIMENTAL STUDY

In this paper, shear resistance of CPC-H steel joint as shear connectors (Photo 2), flexural behavior of CPC-H steel composite beams (Photo 3) and fatigue durability of two main steel composite girders (Photo 4) have been investigated for the purpose of practical application of CPC panels to the deck slab in the medium span composite girder bridges. From the test results, it has been confirmed that the bottom uneven shape of

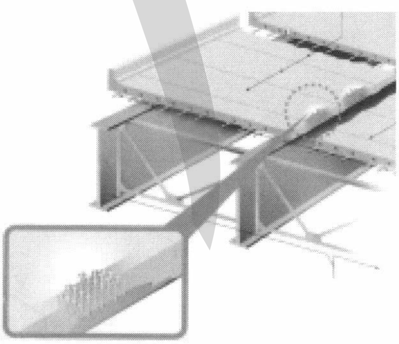

Fig. 1 General View of CPC Panel Systems

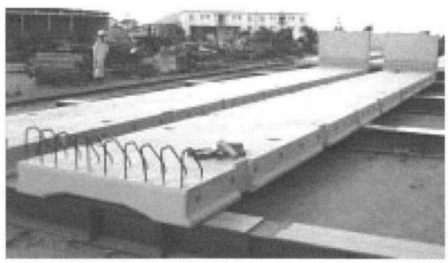

Photo 1 CPC Panels

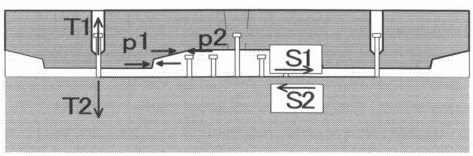

Fig. 2 Principal of Composite Activity

CPC panel acts effectively as shear connectors between CPC panel and the filled-up mortar, and also that such a composite beam behaves full compositely almost up to the ultimate stage, and also that high durability.

3. APPLICATION FOR COMPOSITE BOX -GIRDER BRIDGE

Photo 5 and Fig. 3 show Kaizuka Ramp Bridge that carries the Fukuoka Urban Highway located in Fukuoka city, Japan. This bridge has been first constructed to adopt the composite girder bridge with CPC deck slabs. It is simply supported box-girder bridge with 26.4 m in length and 8.7 – 11.3 m in effective width, completed in 1999.

CPC panels were fabricated by pretensioning system in the factory, and were erected on site by using truck cranes. The on-site construction could be executed with in only 3 weeks, including the erection of CPC panels and the bridge deck work.

4. CONCLUSION

In conclusion, this system to accomplish composite activity is to be effective measure for improvement of workability in the composite girder bridges construction, and also that this composite girder bridge can be practically designed as the full composite girder.

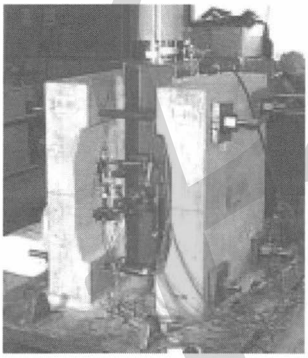

Photo 2 Push-Out Test Specimen

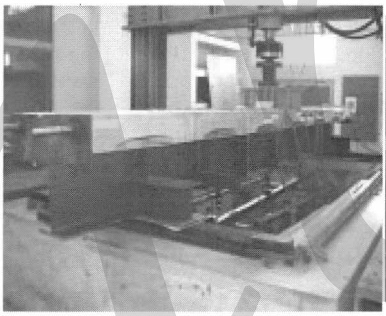

Photo 3 CPC Composite beam

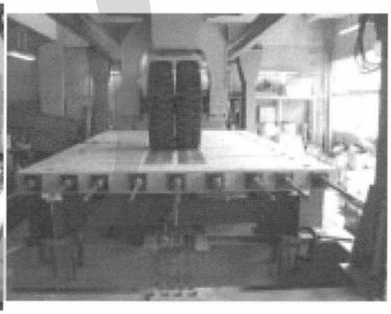

Photo 4 Wheel Running Test

Photo 5 Kaizuka Ramp Bridge

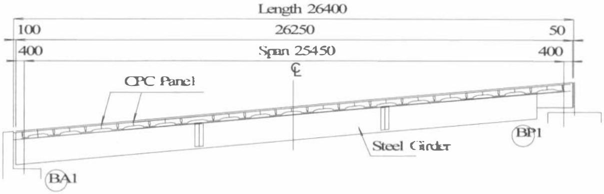

Fig. 3 General View of Kaizuka Ramp Bridge

DEVELOPMENT OF A NEW JOINT STRUCTURE FOR PRECAST RC BRIDGE DECKS

Katashi Fujii[1], Toshio Horikawa[2], Yasunori Nakamo[3], Kunihiko Togawa[4], Noriyuki Chiba[5]

[1, 3, 5]Hiroshima University, Japan [2]Osaka Institute of Technology, Japan [4]Kyokuto Corporation, Japan

Keywords: precast bridge deck, joint structure, fatigue, ultimate strength, wheel loading test

1 INTRODUCTION

In recent years the opportunities to use precast bridge decks have increased with demands to simplify work, reduce labor content, and shorten the duration of construction work. In Japan, loop joints are being used more frequently in the joining of precast decks, however this method presents considerable difficulties in execution for reasons such as the complexity involved in forming the reinforcing steel loops, and the difficulty of inserting the main reinforcing steel in the loops on-site. In an effort to improve the ease of execution of such work, the authors have developed a new joint structure which resembles the conventional lap joint, and has been termed the 'broom joint' for the purposes of this paper. A joint in which the ends of the reinforcing steel in the broom joint are bent upwards (BUP) has also been devised. These joints have proven to be both readily usable on-site and economical, however it is anticipated that introduction into practical use will require a strength at least equal to that of the loop joint. This research has therefore focused on verifying the strength of the new joints using static bending, fixed-point fatigue, and wheel loading tests for the purposes of applying the proposed joint structures to practical bridge decks.

2 JOINT STRUCTURES

This section details the characteristics of the loop joint (see Fig.2.1), and the two joints proposed in this research - the broom joint (see Fig.2.2) and the BUP joint (see Fig.2.3). A test slab without a joint (see Fig.2.4) was also used for the purposes of comparison. Reinforcing bars are D16 (distribution reinforcement) and D19 (main reinforcement).

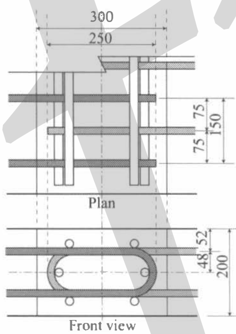

Fig.2.1 Loop Joint

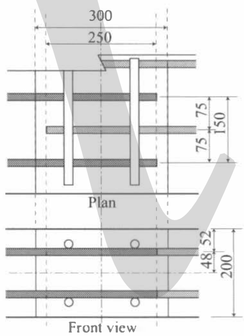

Fig.2.2 Broom Joint

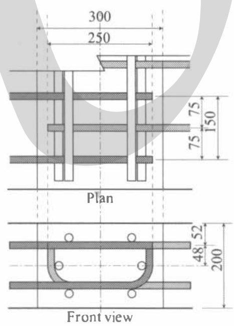

Fig.2.3 BUP Joint

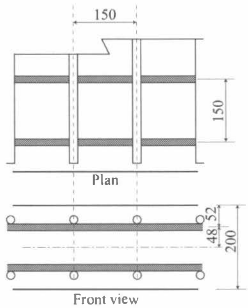

Fig.2.4 Without Joint

3 TESTING

3.1 Static Bending Test

Static bending tests were conducted as shown in Fig.3.1.1 on slabs containing the three types of joint structure as described above, and on a slab without a joint, to investigate the bending strength of the new joints.

Table 3.1.1 shows the list of test slabs and ultimate strength for each test slab. The broom joints noted in the table were constructed with laps of 100mm, 200mm, and 300mm to investigate the necessary lap lengths. As is apparent from the table, the strength of the BUP joint (Type C) is equivalent to that of the loop joint (Type A), and the lap length necessary for the broom joint is approximately 200mm (Type B2).

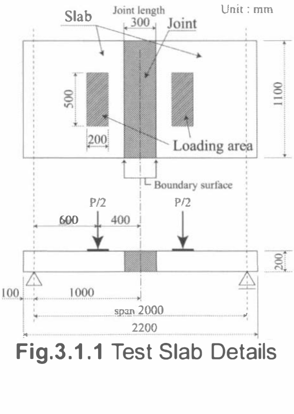

Fig.3.1.1 Test Slab Details

Table 3.1.1 Test Slabs and Ultimate Strength

	Type A	Type B1	Type B2	Type B3	Type C	Type D
Joint Type [Lap length (mm)]	Loop [200]	Broom [100]	Broom [200]	Broom [300]	BUP [200]	No Joint [---]
Maximum Load (kN)	321	217	334	367	320	353

3.2 Fixed-Point Fatigue Test

Test slabs with loop (Type A) and broom (Type B) joints, and a test slab without a joint (Type D) were subjected to fixed-point fatigue tests to investigate fatigue strength of the broom joint. Test slab and load conditions are shown in Fig.3.2.1.

Fig.3.2.2 shows relationship between crack width at the construction joint and cycles. Solid lines indicate crack width at maximum load for each step, and dashed lines indicate crack width of remained cracks when unloaded. The crack width for broom joints is smaller than for the loop joint, and it is therefore concluded that the broom joint has sufficient strength.

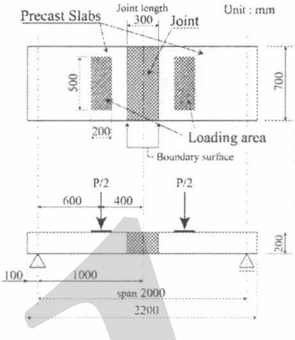

Fig.3.2.1 Test Slab Details

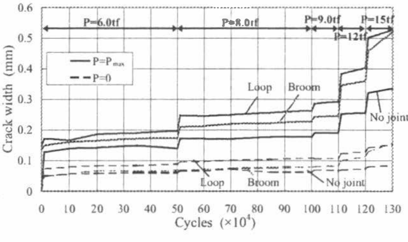

Fig.3.2.2 Cycles vs. Crack Width

3.3 Wheel Loading Test

Wheel loading tests were conducted in order to verify the strength of the new joint under load conditions as close as possible to reality. As shown in Fig.3.3.1, the test slab incorporated four joints - two loop joints, one broom joint, and one BUP joint.

Fig.3.3.2 shows the relationship between cycles and deflection at the center of each joint. The deflection is that obtained when the load is applied statically to the joint. The value for the BUP joint is smaller than that for the loop joint (Loop1) in the corresponding position, and is considered to provide sufficient strength. The value for the broom joint is slightly larger than that for the loop joint (Loop2) in the corresponding position, however it is well within the required range.

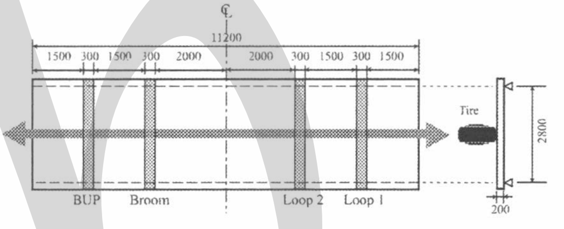

Fig.3.3.1 Test Slab Details

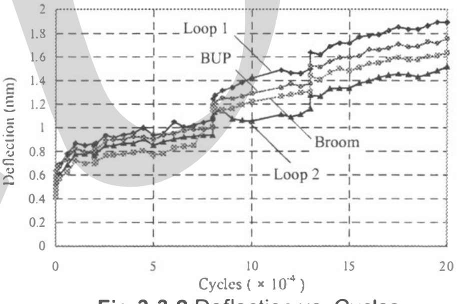

Fig.3.3.2 Deflection vs. Cycles

4 CONCLUSIONS

(1) Both broom and BUP joints presented in this paper are suitable for practical use as joints in precast reinforced concrete slabs. Because of strengths of these joints are almost same as that of a slab without a joint. They have no disadvantage comparing with the loop joint.

(2) Provided that the lap length of the reinforcing bar exceeds 250mm, broom joints provide similar strength to loop joints, and the slip of the reinforcing bars is not observed in the case of D16. Remained strength tests conducted after fatigue tests showed sufficient remained strength in the broom joint.

(3) For deflection, cracking, and strain in reinforcing bar, noticeable damage was not observed during the wheel loading tests.

REFERENCES

[1] Japan Road Association: Japanese Specifications for Highway Bridges, 1996 (in Japanese)

[2 Fujii, K. Nakamo, Y. Togawa, K. : Fatigue durability of a new joint for precast RC slabs, EASEC-8, CD-ROM, Dec. 2001

TIME-DEPENDENT STRESS ANALYSIS FOR CONTINUOUS CONCRETE -STEEL COMPOSITE GIRDER BRIDGES

Takashi Yamane
Kyokuto Corporation,
JAPAN

Makoto Kawakami
Akita University,
JAPAN

Kie Shibata
Sendai City Office,
JAPAN

Keywords: time-dependent stress, composite girder, stiffness matrix method, creep, shrinkage

1 INTRODUCTION

In recent years, research is actively conducted on concrete-steel composite structures with the aim of rationalizing the infrastructure and reducing the related costs. Achievements from the research are finding applications of composite system in various types of structures. Different materials are usually combined in building these structures and, in the majority of cases, concrete and steel are used stage by stage while construction is under way. It follows that accurate evaluation of their behavior is hardly possible as long as traditional way of analysis is made. In order to secure a high degree of their serviceability and safety, prime importance should be placed on the fact that steel restrains the changes in volume of concrete resulting from its creep and shrinkage and on the evaluation of time-dependent stress attributable to structural variations.

This paper describes the findings from the comparative study and discussion on the analyses of time-dependent stress occurring to the concrete-steel composite girder bridges with different installation methods of deck slabs. A displacement method was employed for the analysis. Also used was a stiffness matrix method that could easily be adapted to any changes in the specific structural system. Additionally, an analysis that allows the researcher to find sectional stress re-distribution resulting from time-dependent stress at any reference point was used in order that the positional changes of the centroid of member section attendant on aging may easily be followed.

2 ANALYTICAL METHOD

Time-dependent changes in strain and stress resulting from creep and drying shrinkage during the period from t_0 to t can be derived using the following procedure:

Step 1 Calculate strain and stress at Time t_0 by using an displacement method of analysis.

Step 2 Assuming absence of bond between concrete and steel, calculate the strain and curvature in concrete due to creep and drying shrinkage.

Step 3 Calculate Stress to Restrain Free Strain in Concrete and Corresponding Restraining Force

Step 4 Release member force on age-adjusted member section and calculate corresponding stresses. Since the structure is statistically indeterminate, indeterminate member force should be calculated, and then the resultant change of strain should be added to it.

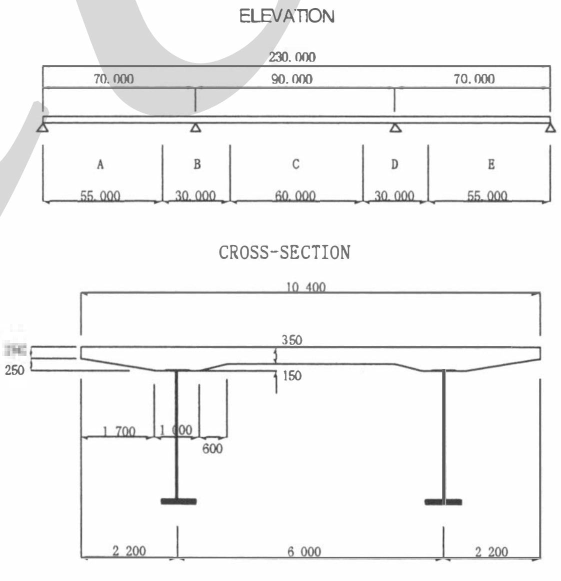

Fig.1 Bridge Profile

Time-dependent stresses are total of stresses calculated in ***Step 3*** and ***Step 4***.

3 ANALYSES

The structure analyzed in this research is a continuous three-span concrete-steel composite bridge having PC deck slabs. Its structural drawing is given in Fig.1, and its construction methods are explained in Fig.2. The results of the analysis are shown in Fig. 3.

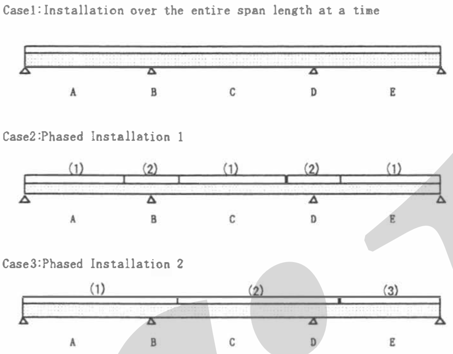

Fig.2 Deck Installation Methods

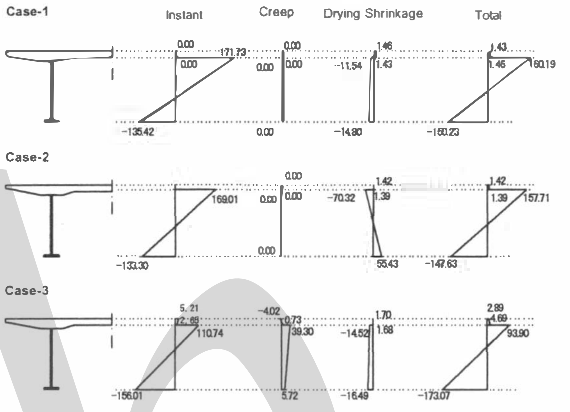

Fig.3 Stresses in Deck Slab at Interior Support

4 SUMMARY

The stiffness matrix method was employed to analyze the time-dependent stress of the continuous concrete-steel composite girder. Findings are recapitulated as follows:

1) The centroid of the composite section moves as the elastic coefficient of concrete changes. Employment of the stiffness matrix that can deal with any desired reference point has successfully taken the effect into consideration.
2) Although the stress of composite girder is analyzed assuming that concrete deck slab is monolithic material, the presented method shows promise of analyzing restrained stress caused by reinforcing bars that are laid in the deck slab.
3) One of the most effective ways of minimizing the tensile stress occurring to deck slabs would be a construction method where the instant stress at the intermediate point of support could be minimized. Even with this method, there remains the possibility of the critical stress leading to cracking being applied in the presence of time-dependent stress.

REFERENCES

[1] Ghali, A. and Favre, R. : Concrete Structures Stresses and Deformations, 1995

[2] Kawakami, M., Matsuzuka, T., Kashifuku, K. and Tokushige, H. : Time-Dependent Stress Analysis of Continuous Composite Girder by Stiffness Matrix Method, Journal of Structural Engineering, JSCE, Vol.43A/1997.3

COMPOSITE ACTIVITY OF INABE RIVER BRIDGE (COMPOSITE BRIDGE WITH PRECAST PRE-STRESSED CONCRETE SLAB)

Yukihiro Kurata Takashi Miyaji Ryouichi Onobe
Ishikawajima-Harima Heavy Industries Co.,Ltd , Japan

Masami Fujita
Japan Highway Public Corporation , japan

Keywords: precast, composite, shrinkage, creep,

1. INTRODUCTION

INABE RIVER BRIDGE is a continuous box girder bridge having a 100m-class span, and its deck adopts precast floor slabs in which prestress is introduced in the direction vertical to the longitudinal bridge axis Since the bridge has a structural feature that floor slabs and the main girders are connected by means of stud dowel joints, floor slabs and the girders exhibit combined behavior, and great tensile force occurs in those floor slabs around the middle fulcrums (see Fig. 1). To cope with this problem, prestress was introduced also in the bridge axis direction using PC steel wires. The prestress technique that uses the bridge-axial PC steel wires was rarely adopted in Japan because this technique, in general, produces high binding force in the steel girders and, in addition, it is low in the construction efficiency due to creep, drying shrinkaoe and other factors.

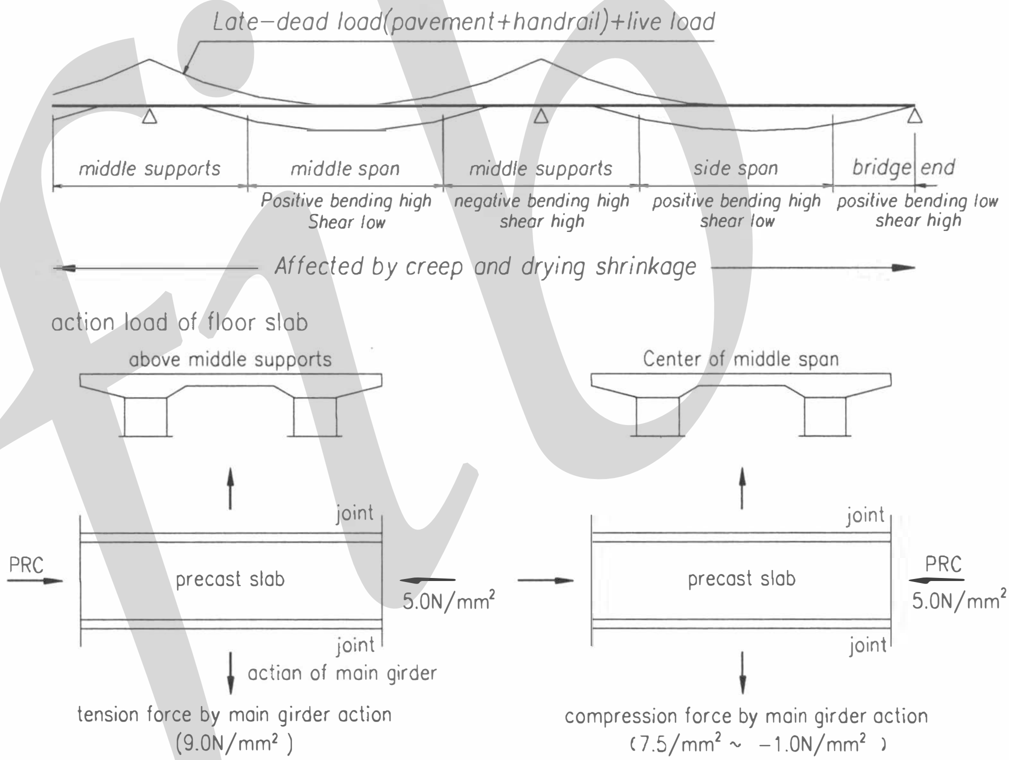

Fig. 1 Behavior of Continuous Combined Girder

The Inabe River Bridge project effectively introduced prestress, making the most of features of precast floor slabs based on the following 1) to 3) design concepts:

1) Install Teflon plus rubber on the underside of the precast PC floor slabs to counteract the binding force of the steel girder, and apply prestress prior to combination with floor slabs (no prestress is introduced in the steel girders).
2) For the problem of creep, combine floor slabs and steel girders one month after application of prestress (to let creep develop free from binding force of steel girders).

3) For the problem of drying shrinkage, leave floor slabs outdoors for 90 days after fabrication for temporary placement, followed by combination of floor slabs and steel girders (let drying shrinkage develop free from binding force).

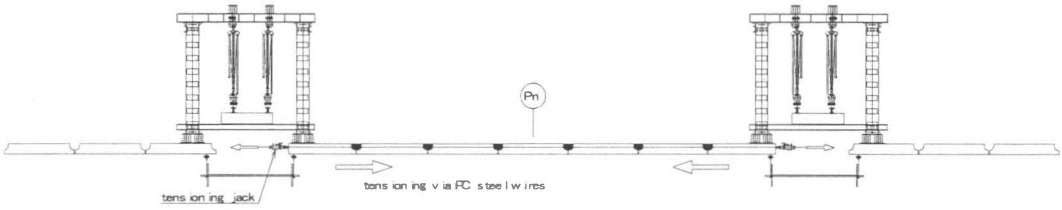

Fig. 2 Schematic Prestress Introduction

PC floor slabs were designed so that crack will not occur in concrete through the adoption of the above construction procedures. For creep strain and drying shrinkage, however, it was considered that there did not always exist good agreement between theoretical values and measurements in practical construction of floor slabs. During the field construction, therefore, strain sensors were installed for measurement of floor slab stress and obtained measurements were compared with design estimation values.
Based on the measurement results, this paper discusses the significance and potential future development of introduction of bridge-axial prestress via PC steel wires to make the most of characteristics of the abovementioned precast floor slabs.

2. MEASUREMENT OF STRAIN IN PRECAST PC FLOOR SLAB

I measure the strain in precast PC floor slabs for an extended period just after the factory fabrication to installment and further on in order to examine the concrete shrinking process due to drying shrinkage, creep and other factors and the effects of degree of prestress application through comparison with design values

3. DISCUSSION

(1) Binding force of steel girder
Measurement result of elastic prestress deformation strain allows us to conjecture that, taking into account no lost prestress, floor slabs and the steel girders were completely disengaged.

(2) Creep
It was confirmed that creep also developed beyond the design value in 30 days. Therefore, it is considered that creep stress that acts on floor slabs and steel girders after combination is not greater than the design values.

(3) Drying shrinkage
It was confirmed that drying shrinkage had advanced beyond the design value in 90days of fabrication. Therefore, it is considered that degree of drying shrinkage that acts on floor slabs and steel girders after combination is not greater than the design values.

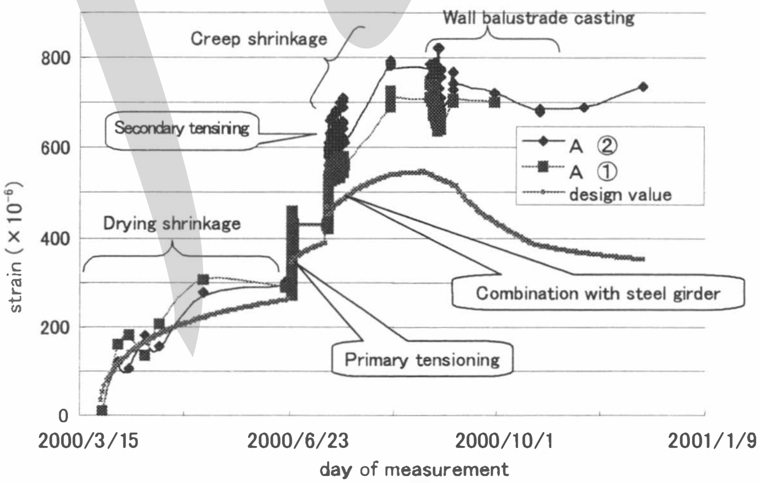

Fig. 3 Strain of Floor slab at middle fulcrum (total strain)

A STUDY ON NEW CONCRETE-WOODEN COMPOSITE BRIDGE USING PRESTRESSING

Hiroshi Watanabe Kazuyoshi Nishina Shinya Saiki
P.C. Bridge Co., Ltd.
JAPAN

Tsutomu Kubota
Nagano-Giken Co., Ltd.
JAPAN

Keywords: composite structure, glulam timber, concrete slab, slab span length, prestressing joint

1 INTRODUCTION

Structural material used in civil work has changed from stone and wood to concrete and steel. And concrete itself has shifted to reinforced concrete and prestressed concrete with improved mechanical characteristics. From the view point of harmonization with the environment, effective utilization of resources, and development of regional industries, on the other hand, glulam timber has also been put into application as structural material and used in greater sizes [1,2]. In the area of bridge construction, where more and more composite structures of steel and concrete, combining the advantages with each other, have come into use so as to attain structure. Wooden bridges using glulam timber is also increased in modern bridge construction.

Under the circumstances as above, the authors have been studying girder bridge, the new type of wooden bridges, using glulam timber and come to an understanding that, for the most rational construction, <1> the glulam timber for the main girder shall be connected by prestressing, <2> the slab shall be concrete, and <3> the slab and main girder shall be put together into a composite structure.

This paper describes an outline of the application of the prestressing to the joint of glulam timber, and the result of our study on the member forces of the concrete slab, the fundamental characteristic of a composite structure girder bridge using concrete and glulam timber.

2 APPLICATION OF PRESTRESSING TO THE JOINT OF GLULAM TIMBER

2.1 Basic Concept of Using Prestressing for Glulam Timber

A conception of using prestressing for glulam timber was invented in Ontario, Canada in 1930s as a "prestressed wooden slab", where the glulam timber were placed in series and prestressing was used in the perpendicular to the fiber direction so as to build up the slab structure [1,2].

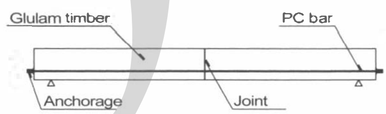

Fig.1 Joint by prestressing in the axial direction of member

When employing the glulam timber as structural member, joint has been a primary issue, and various connecting means of the timber, such as fitting, bonding, and bolting, have been studied and proposed. Up to this date, however, no such means that maintains the same strength on the joint as on the base material and enables to carry out rational joint at a job site has been found.

Such being the case, the authors have proposed a new connecting method using prestressing [3]. It is a means for connecting the glulam timber in series using prestressing (Fig. 1).

2.2 Application to Bridge in Practice

Our proposal on the glulam timber joint using prestressing has been accepted as a new technique for the wooden bridge construction, and has been applied to a bridge in practice. Each Table 1 and Photo 1 shows the outline.

Tab.1 Specification of glulam timber bridge using prestressing joint

Bridge name	Shirahone Promenade Bridge
Erection location	Nagano Prefecture
Structure	Simple girder
Bridge length	19.050m
Width	1.500m
Live load	Side walk live load
Timber used	Larch glulam timber
PC bar used	SBPR930/1180 ϕ32

Photo 1 Glulam timber bridge using prestressing joint

3 CONCRETE SLAB

Authors have come to an understanding that slab of a concrete structure are suited for a composite structure girder bridge using concrete and glulam timber serving as a roadway bridge. The slab of a concrete structure serves as a roof for the glulam timber of the main girder, and contributes to improve the durability since it prevents direct effect of rainwater. According to Specification for Highway Bridges (hereafter the Specification), however, the design force of the slab are specified for concrete structures and steel structures, but no clear definition is given to wooden structures. In our study, we examined the member forces of the slab of the wooden girders, using three-dimensional FEM analysis, and compared the result to that of the concrete girders and steel girders.

3.1 Analysis Model

Fig. 2 is an examination model of a girder bridge comprising the main girders made of glulam timber and concrete slab. This is based on a bridge with its span length of 15.0 m and effective width of 7.0 m. The main girder pitch is set to 1.65 m, which is one of the widest for a girder type wooden bridge in Japan. The slab thickness is set to the minimum overall thickness of 16 cm according to Specification Part III :Concrete Bridge Design. And the load represents the T-load.

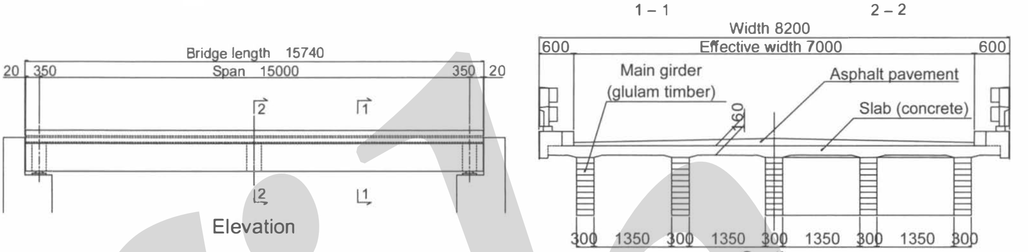

Fig.2 Examination model

3.2 Examination of the Structure in the Perpendicular to Bridge Axis Direction and the Bridge Axis Direction

From the results obtained from the FEM analysis and the Specification (Tab.2,3), it is understood that, for the design bending moment calculation, in the perpendicular to the bridge axis direction, of the slab of a wooden girder bridge, increasing the slab span of the concrete girder bridge mentioned in the Specification by 15% will do. And it is understood that, for the design bending moment calculation, in the bridge axis direction, of the slab of wooden girder bridges, increasing the slab span of the concrete girder mentioned in the Specification by 5% will do.

Tab.2 Comparison of bending moment in the perpendicular to the bridge axis direction (kN-m/m)

		(a) At center of the span		(b) At support (clear span)	(c) At support (span between center of the girders)
FEM analysis	Wooden girder bridge	15.4	(1.12)	-6.8	-2.3
	Concrete girder bridge	13.8	(1.00)	-5.9	-2.6
	Steel girder bridge	15.5	(1.12)	-5.0	-7.6
Specification for Highway Bridges	Concrete girder bridge	18.6	(1.00)	-32.8	-
	Steel girder bridge	21.4	(1.15)	-	-37.3

*Figures in () represents the ratio over the concrete girder bridge

Tab.3 Comparison of bending moment in the bridge axis direction (kN-m/m)

		At center of the span	
FEM analysis	Wooden girder bridge	9.7	(1.05)
	Concrete girder bridge	9.2	(1.00)
	Steel girder bridge	10.6	(1.15)
Specification for Highway Bridges	Concrete girder bridge	14.0	(1.00)
	Steel girder bridge	16.4	(1.17)

*Figures in () represents the ratio over the concrete girder bridge

4 CONCLUSION

Under the present circumstances surrounding to the construction industry where keywords such as energy, carbon dioxide, and environment have drawn people's attention, glulam timber as well as concrete and steel has been put into use as structural members. In connection with our study on the composite bridge of concrete and glulam timber, this paper has described the outline of the joint using prestressing for the glulam timber and the result of our examination on the member forces of the concrete slab. In addition, although a means using studs is employed for connecting the main girder made of glulam timber and the concrete slab, further study is necessary because joint is a very important issue.

REFERENCES

[1] Forestry Agency : Current Trend-Timber Bridges, RYUGENSHA,Inc, Mar., 1995
[2] Bridge Editing Committee : MODERN TIMBER BRIDGE, BRIDGE ENGINEERING, Vol.30, Nos.13, Dec., 1994
[3] Kiyoroku Fukayama, Hiroshi Watanabe, Tsutomu Kubota, Yasuji Mitsui : A Study On New Joint System For Glulam Timber Beams By Prestressing, JSCE Journal, No.616 / VI-42, pp.91-102, Mar., 1999

APPLICATION OF INNOVATIVE COMPOSITE SYSTEM WITH STEEL AND CONCRETE MEMBERS – POST RIGID SYSTEM –

Koji Kitagawa Hiroshi Watanabe Yoshihiro Tachibana
Kawada Industries, Inc., JAPAN

Hirokazu Hiragi
Setsunan University
JAPAN

Akimitsu Kurita
Osaka Institute of Technology, JAPAN

Keywords: PR System, Time-Setting Resin Mortar, PR Stud

1 INTRODUCTION

In the past, no structural system that changes with the progress in time from a non- to a full composite system has been developed, called the PR System. Within the PR System (**Figure 1**), the tensile stress that occurs during drying shrinkage in concrete restrained by steel members can be mitigated and the prestressing force can be introduced into concrete members without restraint of steel members because the PR System is non-composite during prestressing and is composite when live a load is applied later. The PR System will therefore extend the versatility of composite structures.

We have developed a new type of stud called the PR Stud (refer to **Photo 1**) as a shear connector and used the Time-setting resin mortar-A and -B to realize the PR System, which is temporarily flexible but becomes rigid at the serviceability state. In advance of the development of the PR Stud, testing and development had been conducted on both of the resin mortars, which play an important role in the PR System, in regards to the compressive strength and to Young's modulus after the hardening time as well as viscosity and adhesive strength before the hardening time. This paper also describes various actual bridges projects which have adopted the PR System.

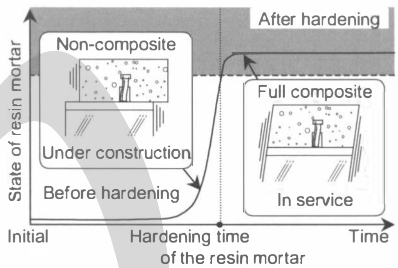

Figure 1 PR System

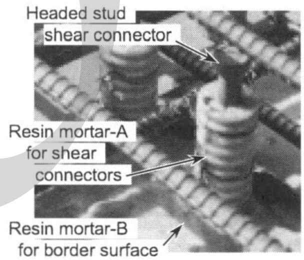

Photo 1 PR Stud

2 CONFIRMED PERFORMANCES

The requirements and remarks regarding each resin mortar and the PR Stud are confirmed. There are constructional requirements on both of the resin mortars before hardening time.

The resin mortar-B should have low viscosity so that it can be plastered via a roller and the resin mortar-A should have high viscosity so that it will not sag. The viscosity of each resin before hardening time was adjusted by changing the amount of filler. After hardening time, both of the resin mortars should be over compressive strength of concrete and the resin mortar-B should be to the same Young's modulus degree in which the PR Stud behaves equivalent to ordinary studs. Through the compression test, compressive strengths of the resins are more than 100 N/mm^2, which far exceeds that of the concrete, and greater values of Young's modulus were obtained the resin mortars with silica sand. The resin mortar-B requires that the bond strength is very low before hardening time, and that it is high after hardening time. Through the adhesion test, the resin mortars are satisfied requirements.

The PR Studs must have a low resistance against horizontal shear for while after construction but have a shear resistance equivalent to that of ordinary studs after hardening time. Through the push-out shear test, the PR Studs are satisfied requirements. In addition, the PR Stud with resin mortar-B (namely the PR System) has extra bond strength in early range of relative slip.

3 APPLICATION EXAMPLES

Some application examples of the PR System are introduced below:

3.1 For composite girder with steel and concrete

The Shiratori-bridge is a pedestrian bridge with a length of 18.7m. In the design stage, the main requirement is a thin girder, maintenance-free and low cost. This new type of composite girder, in which concrete is attached around steel girders with the PR System, was proposed. In conventional composite system, a prestressing force cannot be introduced into only concrete because concrete and steel become rigid as soon as the concrete cured. Using the PR System, in this new girder, concrete and steel could slip freely under prestressing and unite after the resin mortar hardens.

Photo 2 For composite girder

3.2 For girder with prestressed concrete slab

The Meishi-bypass Toyoake CF ramp is steel box girder bridge with concrete slab prestressed on site. A rigid box shaped cross beam is in the middle support where the number of main girders changes according to road width. When introducing prestressing force into concrete slab, the cross beam would resist against compression of concrete slab. Because other cross beams are also shaped rigid, the PR System was applied to all areas. As a result, restraint by steel members can be mitigated until the construction stage of prestressing.

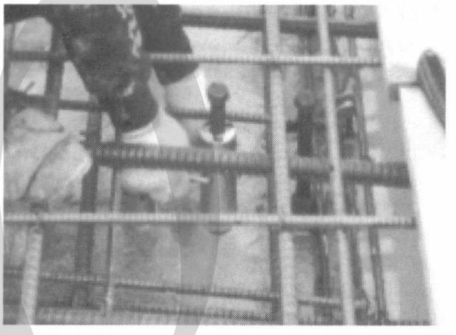

Photo 3 For prestressed concrete slab

3.3 For other concrete members

The Chitose-viaduct is a steel plate deck box girder bridge. Wheel guards, mounted layer under sidewalk and barrier curb of concrete, are connected to the steel plate deck with a slab anchor. After the concrete cures, tensile stress occurs during drying shrinkage in concrete, restrained by steel members. If the tensile stress is greater than the tensile intensity of the concrete, it becomes the cause for cracking. The same condition will often be witnessed in major steel plate deck girder bridges. In this project using the PR System, the quality of concrete improvements has been confirmed.

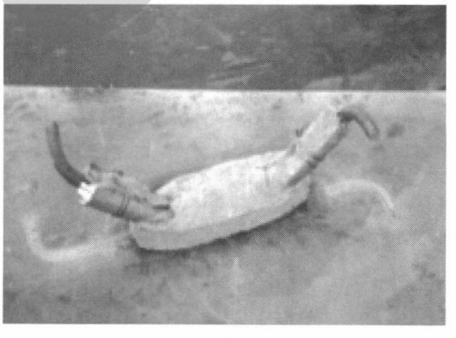

Photo 4 For slab anchor

4 REFERENCES

[1] H. Watanabe, Y. Tachibana, K. Kitagawa, Y. Ushijima, H. Hiragi, and A. Kurita: Development of An Innovative Composite System – Post Rigid System – Between Steel and Concrete Members, Journal of Structural Engineering, Vol.47A, pp1363-1372, 2001

[2] K. Kitagawa, H. Watanabe, Y. Tachibana, H. Hiragi, and A. Kurita: Development of Innovative Composite System – between Steel and Concrete Members, RILEM Proceedings PRO 21, Volume 2, pp1333-1342, 2001

APPLICATION OF DEFORMED H-SHAPES TO COMPOSITE STRUCTURES

Sachito Tanaka, Ph.D.
Kawasaki Steel Corporation
JAPAN

Hiroya Okubo
Kawasaki Steel Corporation
JAPAN

Masakatsu Sato, Dr. Eng.
Chiba Institute of Technology
JAPAN

Keyword: deformed H-shapes, slab bridges, slab decks, bridge peers

1 INTRODUCTION

Steel-concrete composite structures have been widely used as materials for civil engineering and building construction, because of a rational combination of the advantages of the characteristics of steel and concrete; tensile strength and toughness of steel and compressive strength and stiffness of concrete. The advantages of this structure are, moreover, their noise and vibration absorption and high corrosion resistance properties.

It is of primary importance that the steel-concrete composite structure is provided with an effective stress transmission mechanism in the steel-concrete interface. The bond strength between steel and concrete may be increased through either mechanical shear connectors, as used in composite girders, or surface protrusions as in the case of deformed bars [1]. The latter has a great advantage in efficiency and material saving, and therefore, any substantial improvement in steel-concrete bond must be derived from the optimum selection of steel surface protrusions. Deformed flange H-shapes, which bond strength is superior to deformed bars, have newly developed in 1977 and so far applied to various composite structures.

This paper describes properties of the H-shapes, and clarified structural features and behavior on their applied structures.

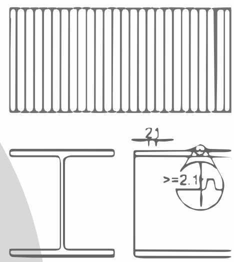

Fig.1 Deformed flange H-shapes

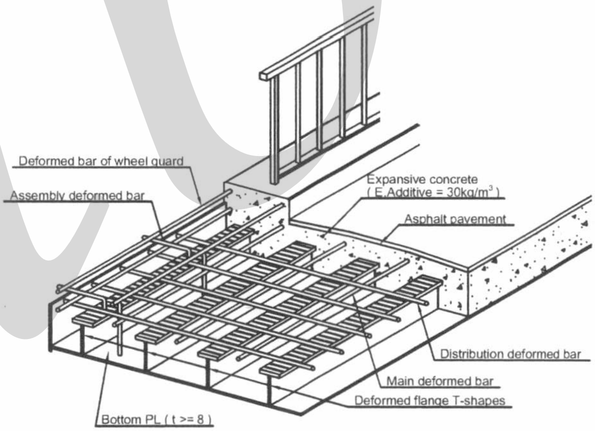

Fig.2 Composite slab bridge

2 NEW DEFORMED FLANGES H-SHAPES

The H-shapes have lateral protrusions on the outside surface of both flanges, as shown in Fig.1. Lateral protrusion height and space on their surface have been determined on the basis of the results of bond strength tests.

If the protrusion of outer flange surfaces is too high on the H-shape, the fatigue strength will be caused to decrease. There are, in addition, limiting factors in the manufacture of the flange protrusions such as pressing capacity and temperature control during the rolling process.

3 APPLICATION TO COMPOSITE SLAB BRIDGES

Composite slab bridge is fabricated by filling up the T-shapes (formed by cutting the H-shapes in half) with expansive concrete, as shown in Fig. 2. In this slab bridge, protrusions on the upper flange act as shear connectors to permit the concrete covering to be reduced in thickness. The depth of this bridge can therefore also be thinner than that of conventional bridges. In addition, the bottom plates can be utilized as permanent forms, thereby making it possible to achieve more accuracy and reduce the construction time.

The mechanical properties of this bridge in the elastic range, as well as the composite characteristics between steel girder and slab concrete at the failure stage, are confirmed by conducting a high-cycle fatigue test and a static bending rupture test on the approximately full-sized slab specimens.

4 APPLICATION TO COMPOSITE BRIDGE PIERS[2]

The composite bridge piers are combined with durable precast forms and the H-shapes columns instead of the conventional main longitudinal reinforcement, as shown in Fig. 3. These piers have superior seismic performance, which is provided by the durable precast forms and H-shapes columns having enhanced bond strength and higher rigidity than conventional reinforcement bars.

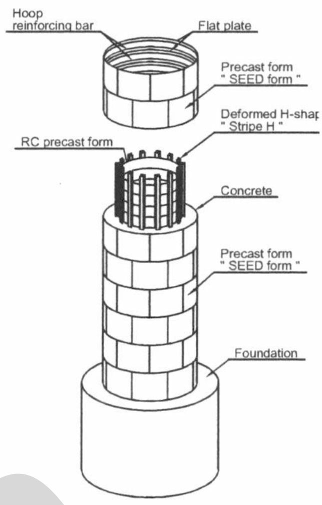

Fig.3 Composite bridge pier

The effects, which limit both the crack dispersion and the widening of cracks, are equivalent to or better than those experienced in reinforced concrete structures, because the precast forms have stainless steel fibers on their surfaces. Moreover, the structure becomes highly resistant against salt attack, frost damage and carbonation with much improved durability, because the durable precast forms protect the surfaces of the structure.

5 FURTHER APPLICATION TO COMPOSITE SLAB DECKS

Fig. 4 shows schematic structure of composite slab deck. The deck is consist of concrete and steel members including bottom plate, deformed bar and deformed flange T-shapes as main members, similarly to composite slab bridge.

Static and fatigue tests were carried out to investigate structural behaviors for ultimate load and fixed repeating load. Moreover, cyclic fatigue test under running wheel load was conducted to verify enough durability.

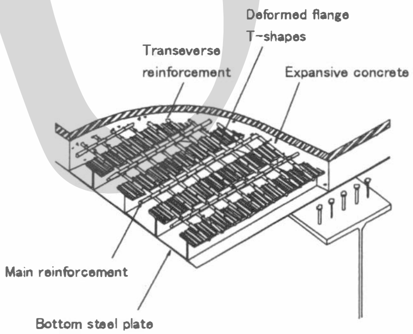

Fig.4 Composite slab deck

6 CONCLUSION

Through various tests such as static bending tests and fatigue tests and horizontal alternating load test, the following results are concluded:

(1) The T-shapes (or the H-shapes) and concrete retain composite action even at the failure stage.
(2) These composite structures can be designed on the basis of conventional RC method.
(3) These composite structures have more excellent fatigue strength to high cycle loadings. Furthermore, higher ductility against cyclic earthquake loads, as compared with those of conventional reinforced structures.

REFRENCE

[1] YAMASAKI T. et al.: Studies on Fatigue Characteristics of Large Diameter Deformed Bar D51 in Axial Loads and Reinforced Concrete Beams, Trans. of JSCE, Vol. 10, pp.301-302, 1978.

[2] Yoshida Y. and Ueda T.: Composite Steel and Concrete Pier Using Durable Precast Form, Proc. of IABSE Conference, pp.22-27, 1997.

ANALYTICAL STUDY OF DRYING SHRINKAGE STRAIN IN COMPOSITE SLAB HAVING STIFFENING RIBS

Yuuichi Watanabe Yuu Moroyama
Ishikawajima-Harima Heavy Industries Co.,Ltd
JAPAN

Keywords: composite slabs, drying shrinkage strain, analysis

1 INTRODUCTION

To rationalize construction the steel rationalized bridge (two-main-girder bridge) has been adopted in Japan. The steel rationalized bridges have a six-meter or longer main girder span. Cases are increasing that adopt composite deck-slab fabricated in a steel form by half-precast system (hereafter referred to as "composite slab") to attain improved bearing capacity of composite slabs, enhanced fatigue durability and reduced maintenance and inspection cost.

Composite slabs have a structural feature that the steel form, which remains as a permanent form, is used as a tensile rebars to the deck-slab, and as a result, fabricated panels have a smaller cross-section and are light-weighted than RC deck-slabs. Those composite slabs developed in recent years, in particular, are often provided with ribs in the span direction as a reinforcing material so that they can stand on a six-meter or longer slab span. For such ribs, various steel shapes are used, such as flat bar, channels and angles, which work as the bracing of steel form when concrete is cast, and after concrete setting, they can work as a tensile stiffener as well as a fixer between concrete and steel members.

However, this type of composite slabs pertain a certain concern that concrete cover becomes thinner in the rib area, easily allowing cracks to occur in concrete in the vicinity of rib members due to drying shrinkage, thermal stress and other factors.

In this study, focus was put on drying shrinkage cracking and analytical study was carried out using a nonlinear temperature stress analysis program. As a result, we have clarified the distribution of shrinkage strain that arise in concrete of composite slab that have reinforcing rib and also obtained useful data that may be reflected in design, which are reported here.

2 ANALYSIS CONDITIONS

2.1 Concept of analysis

Analysis of drying shrinkage strain distribution was performed using a Finite-Element Method (FEM) program for nonlinear concrete temperature stress analysis (ASTEA-MACS for Windows ver.2 by RCCM Inc.). This analysis aimed at determining the relationship between the effects of stiffening ribs of composite floor slab on strain distribution in the concrete and crack occurrence. Here, we assumed that concrete properties do not change but we changed the shape of ribs, the thickness of cover, the quantity of rebars and other factors for comparative study of the effects of binding exclusively.

2.2 Analysis model

To prepare an analysis model, the cross-section in the bridge axis direction (direction of applied force) of a composite floor slab (slab thickness of 300mm) was cut off by the length of 1500 mm to create four types of 2D models. An example is shown in Fig. 1 and study cases are listed in Table 1.

Analysis Model 1 (cover of 50mm, stiffening rib with top flange, with rebars placed)

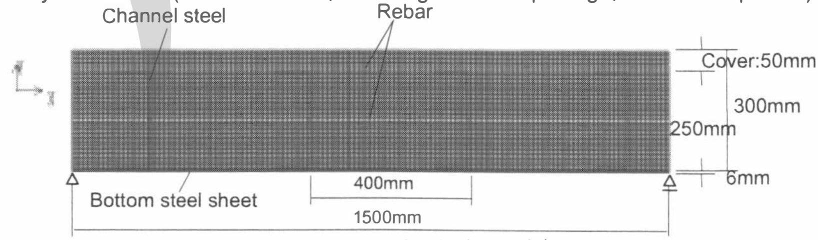

Fig. 1 Analysis Model

2.3 Shrinkage characteristics

We assumed the drying shrinkage strain of concrete in non-binding condition by the following Equation (1) that uses parameters of unit water volume, relative humidity and volume/surface area ratio stated in the "Standard Specification for Concrete" by the Japan Society of Civil Engineers. After a year, the strain values of concrete and expansive concrete were measured to be 136μ and 50μ, respectively.

$$\varepsilon'_{cs}(t)=\varepsilon'_{sh}\times\{1-\exp(-0.108(t-t_0)^{0.56})\ (\times 10^{-5}) \qquad (1)$$

where $\varepsilon'_{sh}=-50+78\{1-\exp(RH/100)\}+38\cdot\log_e W-5E\{\log_e(V/S/10)\}^2$

The history of strain in expansive concrete was calculated using the following Equation (2). Although the Japan Society of Civil Engineers specifies the maximum expansion of expansive additives to be 200 to 250μ, we set the maximum expansion strain in hot atmosphere (i.e., at temperaure of 30°C) to 80μ because lime-based expansive additives show decrement in expansion effects when temperature rise as reported by some previous studies.

Table 1 Study cases

Analysis cases	Analysis models	Cover (mm)	Upper flange	Expansion material	Rebars	Distribution bar
Case 1	Model 1	50	○	×	○	D16-200
Case 2	Model 2	100	○	×	○	D16-200
Case 3	Model 3	50	×	×	○	D16-200
Case 4	Model 4	50	○	○	○	D16-200
Case 5	Model 5	50	○	×	×	-
Case 6	Model 6	50	○	×	○	D16-100

$$\varepsilon'_{ex}(t)=80\times\{1-\exp(-0.7t^{1.5})\}(\times 10^{-5}) \qquad (2)$$

3 RESULT AND CONSIDERATION

Fig.2 shows an example of strain distribution. This indicates that the shrinkage strain around the surface layer between ribs where binding is weak is higher while the shrinkage strain around the top edge of rib subject to the binding of rib is smaller. Table 2 shows the shrinking force calculated from the distribution of shrinkage strain by multiplying the train difference by the Young's modulus of concrete. When this shrinking force exceeds the tensile strength of the concrete, shrinkage cracking occurs. The following section discusses the comparison between cases.

Case 1: Cover of 50 mm, w/ top flange, w/o expansive additive, rebars of D16-200

Case 6: Cover of 50 mm, w/ top flange, w/o expansive additive, rebars of D16-100

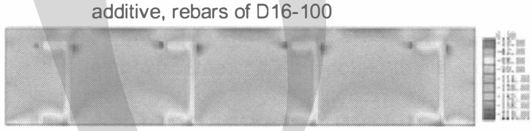

Fig. 2 Distribution of Drying Shrinkage Strain

Table 2 Shrinkage force calculated

	Strain between nbs μ	Strain on nb μ	Strain difference μ	Young's modulus N/mm²	Tensile stress N/mm²	Tensile strength N/mm²
Case 1	169.9	99	70.9	20700	1.47	2.52
Case 2	163.9	103	60.9		1.26	
Case 3	165.9	112.4	53.5		1.1	
Case 4	77.3	52.4	24.9		0.52	
Case 5	174.4	98.6	75.8		1.57	
Case 6	164.2	98.5	65.7		1.36	

1) Effects of cover (comparison between Cases 1 and 2)

When using distribution bars of D16-200, the tensile force arising on the rib top edge decreased from 1.47 N/mm^2 to 1.26 N/mm^2 when the cover was changed from 5 cm to 10 cm. Augmented cover is effective in control of shrinkage cracking, but a 50mm cover can prevent deleterious cracks from occurrence even if a 100mm top flange is provided in the cases drying shrinkage strain is small in the first place like the concrete specified in the above discussion.

2) Effects of top flange of rib (Cases 1 and 3)

As a result of comparison of effects of 100mm-width top flange, shrinking force can be reduced by 30% in the case not furnished with top flange and thus cracking is less likely to occur compared with the case furnished with top flange.

3) Effects of rebars (Cases 1, 5 and 6)

As the quantity of rebars was increased, the shrinkage strain on the surface layer between ribs decreased and the shrinking force was also alleviated. This shows that placing rebars can lessen the difference from the shrinkage strain arising on the rib top edge, and decrease the shrinking strain.

4) Effects of expansive concrete (Case 4 and others)

Mixing of expansive additives decreased both the strain between ribs and the binding by the rib top edge, which was effective in controlling the crack occurrence.

A PROPOSAL OF A STEEL-CONCRETE HYBRID CAISSON WITH PERFOBOND STRIP COMPOSITE MEMBERS

Toyohiko Watanabe Masaru Otsuka
Yokogawa Bridge Corporation

Jun Nagata Hiroshi Yokota
Port and Airport Research Institute
[1-1, 3CHOME, NAGASE, YOKOSUKA, 239-0826 JAPAN]

Keywords: Caisson , hybrid , perfobondrib , design , steel

1 INTRODUCTION

In recent years, caissons with steel-concrete composite members, namely "hybrid caissons", have increasingly been replacing the conventional RC caissons in the construction of large-scale gravity type offshore structures such as breakwaters, quays and revetments. Standards for such hybrid caissons are also gradually put in place [1)]

This paper reports on the preliminary design of the hybrid caisson and the scope of the "preliminary design" here goes beyond design per se but stretches from manufacturability and workability to economical efficiency. Carried out first was the preliminary design of the conventional hybrid caisson using studs as the shear connector. Then, it was compared, in terms of manufacturability, workability and economical efficiency, with a new type of hybrid caisson whose outer wall is made with composite member using perforated steel-plate ribs as the shear connector. This paper is to propose such application of perfobond strip composite members, which was found to be feasible in the study.

2 APPLICATION OF PERFOBOND STRIP COMPOSITE MEMBERS

The result of a preliminary design using the perforated steel-plate ribs shown in Figure 1 as the shear connector between the steel plate and concrete. Note that the preliminary design was carried out based on the design method of perfobond strip composite members that has increasingly been put in use as the composite slab of bridges, such as references 2), 3) and 4), adopting the following criteria:

① Employ the limit state design method
② In the design, use the safety factors set forth in the reference 1)
③ The steel-concrete ratio of Young's modulus n is set at 10[2)]
④ The perforated steel-plate ribs are placed in the vertical direction for ease of concreting workability.

3 COMPARISON BETWEEN PERFOBOND STRIP COMPOSITE MEMBER TYPE AND CONVENTIONAL HYBRID CAISSONS: RESULTS

The characteristics of the hybrid caisson using the perfobond strip composite member as compared to the conventional type are summarized as follows.

(1) When the perfobond strip composite member is applied to the outer wall of a caisson, the connecting mechanism between the perfobond strip composite member and the steel reinforced concrete base or the partition wall was found feasible from both design and manufacturing points of view.

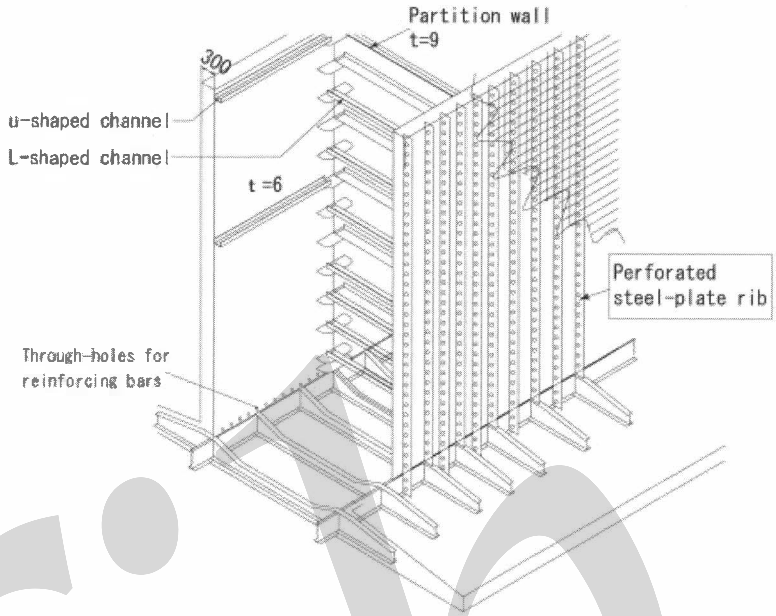

Figure 1 Application of perfobond strip composite member type

(2) The ribbed steel plate is obviously more rigid than the studded steel plate. It was confirmed that use of this advantage brought about the following beneficial effects:

① A great reduction in the amount of stiffeners on the steel plate to bear the temporary dead load of the concrete being placed
② Elimination of bar arrangement work at later work stages, reduction of work stages and improvement of quality control, which is made possible by the fact that the bar arrangements are made on the perfobond strip composite member upon major assembly of the steel shell
③ Elimination of the need for vertical supporting materials, due to the fact that the ribs can function as such

(3) While the manufactured weight is almost the same as that of the conventional type, the area of reinforcement is reduced because the steel ribs behave like the reinforcement.

(4) Because of the high fatigue strength of the steel plate, the perfobond strip composite member type is potentially applicable to offshore structures, for which a load-carrying capacity is required under the fatigue limit state.

(5) Application of perfobond strip composite members to bottom slabs remains as a future issue.

REFERENCE

1) Coastal Development Institute of Technology, Manual on steel-concrete hybrid caissons for port structures, 1999.6

2) Yokogawa Bridge Corp., Design Manual on Power-Slab (Steel-Concrete Hybrid slab), 1999.4

3) Jun Nagata, Yoshiaki Omachi ,Kazuhiko Takata and Renji Kiyota : Experimental Studies on Fatigue Strength of Power Slab Using Wheel Tracking Machine, YOKOGAWA BRIDGE GROUP TECHNICAL REPORT No.27, pp103-109, 1998.10

4) Leonhardt, F.et al.: Neues vorteilhaftes Verbundmittel Für Stahlverbund-Tragwerke mit hoher Dauerfestigkeit, BETON UND STAHLBETONBAU, 1987.12

PRESTRESSED CONCRETE BEAM WITH REINFORCING STEEL PLATE AT COMPRESSIVE ZONE

Tatsuo Arai , Yukie Noda , Koji Osawa
Kawada Construction Co.,Ltd.; Civil Engineering Div., JAPAN

Keywords: prestressed concrete beam, reinforcing steel plate, low beam depth

1 INTRODUCTION [1]

This paper reports on prestressed concrete (hereafter "PC") beam where reinforcing steel plate is used at compressive zone of main beam for lowering beam depth of road bridge.

In Japan's conventional PC beam bridges, the ratio of beam depth and span is generally from 1/18 to 1/24, and some special method have been required to make the beam depth lower than this. Generally, when designing PC beam with low beam depth, larger axial compressive force needs to be applied since the resistance cross section of concrete becomes smaller, and enough eccentricity cannot be secured when placing prestressing steel in the cross section of beam. As a result, in some cases, the stress at main beam's compressive edge may be excessive when prestressing or when live load is affected.

The PC beam with reinforcing steel plate at compressive zone (hereafter "RS beam",Fig.1) was developed to improve the stress condition as above, and the characteristic points are;

①Increasing sectional rigidity by reinforcing steel plate

②Improving the stress at main beam's compressive edge utilizing the stress transfer (restrained effect of reinforcing steel plate) in the cross section by creep and shrinkage of concrete.

Regarding the former, the validity on bending and shearing behavior has been confirmed by static loading test and fatigue test. On the latter, long-period measurement was carried out under the appointed environment (temperature: 20℃, humidity: 70%) using controlled temperature and humidity room to confirm the restrained effect. [3]

In this paper, technical characteristics of the beam, the relation between span and ratio of reinforcing steel plate from trial design, static loading test of full-scale pre-tensioned slab beam, and actual results of two bridges using the beam are reported.

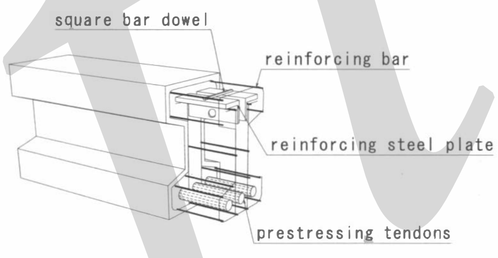

Fig.1 Schematic diagram of RS beam

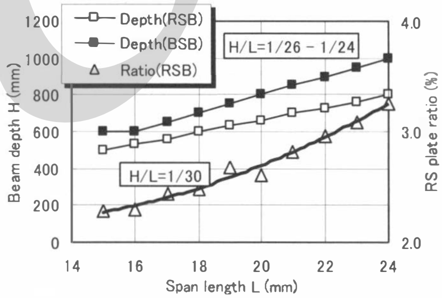

Fig.2 Relation between span and depth , and ratio of reinforcing steel plate

2 TRIAL DESIGN [2]

Reinforcing steel plate is placed on JIS(Japanese Industrial Standards) pre-tensioned PC slab beam (hereafter "BS beam") to reduce the beam depth. Fig.2 shows the relation between beam depth and span on BS beam and RS beam designed as a trial. In addition, Fig.2 also shows the ratio of reinforcing steel plate's cross section. On the depth of RS beam, the ratio between beam depth and span was appointed to be 1/30 equally, and became lower for 100-200mm. For example Fig.3,Table 1 show a case of 24m span.

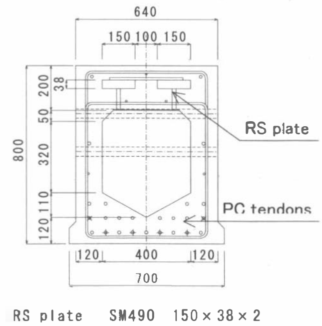

Fig.3 Typical Section(24m span)

Table 1 shows the main beam's stress of span center cross section when design load is affected in the case of considering the effect of steel plate's restraint (CASE-2) and the case of not considering (CASE-1). When considering the effect of steel plate's restraint, concrete upper edge's compressive stress is reduced to about one-half, and the compressive stress of reinforcing steel plate becomes approximately two times.

3 FULL-SCALE TEST

For the purpose of grasping RS beam's dynamic performance until the destruction and design load performance, static load test of full-scale pre-tensioned slab beam was carried out.(Photo 1)

4 ACTUAL RESULTS

We have two actual cases of RS beam bridge, and the two bridges are briefly introduced here. Table 2 shows the actual cases of bridges. Torinome Bridge is a road bridge for river management completed in 1997(Photo 2), and Kaiun Bridge is the bridge constructed in 2000 according to the renewal from old bridge in the city. Both bridges are located above a river and beam depth was limited due to the vertical alignment of the road, and RS beam was adopted. Beam depth of both bridges is 100mm lower than BS beam.

Table 1 Comparison on the effect of steel plate's restraint

	Concrete stress		RS plate stress
	top	bottom	
CASE-1	15.8	-2.3	89.6
CASE-2	8.1	-0.2	175.7
Allowable stress	16.0	-1.8	190.0

(Unit : N/mm^2, Negative figure means tension)

Table 2 Actual cases of bridges

Bridge name	Location	Completion	Span (m)	Beam depth (mm)
Torinome Bridge	Tochigi pref.	1997	18.0	600
Kaiun Bridge	Tochigi pref.	2000	15.3	500

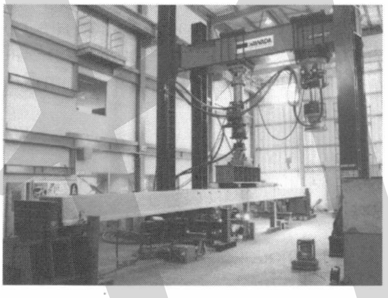

Photo 1 Loading test (Kaiun Bridge)

Photo 2 Completed whole view (Torinome Bridge)

5 CONCLUSION

RS beam bridge has advantageous characteristics such as realizing lower beam depth, good workability with no additional works or management on site, and high bending rigidity. Accordingly, we consider it one of the effective construction methods for rebuilding existing bridges in urban district whose demand will be further increased after this. We would like to make further detailed examinations regarding the application of RS beam to the precast segmental method after this.

REFERENCES

[1] Noda,Y., Osawa,K., Arai,T., Kishi,Y.: Prestressed Concrete Girder with Compression Bars, *Bridge and Foundation*, pp.39-44, Feb. 2000

[2] Arai,T., Kitano,Y., Kobayashi,Y.: Characteristics of Prestressed Concrete Slab Bridge with Reinforcing Steel Plate, Prestressed Concrete Engineering Association, The 8th Symposium Papers, pp.231-234, Oct. 1998

[3] Osawa,K., Kobayashi,Y., Sano,Y., Arai,T.: Creep and Shrinkage Measuring Test of Prestressed Concrete Beam with Steel Plate in Compressive Zone, Prestressed Concrete Engineering Association, The 9th Symposium Papers, pp.473-478, Oct. 1999

A STUDY ON RIGIDITY OF CONCRETE FILLED STEEL SQUARE TUBULAR BEAM-COLUMNS USING HIGH STRENGTH CONCRETE

Takashi Fujinaga Isao Mitani Yasuhiro Ohtani
Department of Architecture and Civil Eng.,
Kobe University, JAPAN

Go Nakamura
Obayashi Corporation
JAPAN

Keywords: CFT beam-columns, axial load ratio, tangent modulus, residual stress, Poissonís ratio

1 INTRODUCTION

Concrete filled steel square tubular (CFT) columns are used as beam-column members of high-rise buildings in Japan recently. There are many researches on CFT beam-columns in Japan. Authors have worked to propose hysteresis models of the members for the elasto-plastic analysis on the earthquake response. Proper evaluation of the horizontal rigidity of structural member is important to estimate the deformation capacity of beam-columns. The objective of this study is to investigate a estimation method for the rigidity of square CFT beam-columns using high strength concrete, subjected to bending under constant compressive load. Fifteen beam-column specimens of square CFT were tested. As test parameters, axial load ratio n, width-to-thickness ratio D/t, and strength of concrete F_c are selected. Based on the test results, the effects of the parameters on the horizontal rigidity of square CFT beam-columns are discussed.

2 INITIAL RIGIDITY OF CFT BEAM-COLUMNS

In calculating the horizontal rigidity of the square CFT beam-columns, bending deformation and shearing deformation are considered. It is assumed that the bending and the shear rigidities are not influenced each other. The bending rigidity is calculated using the slope-deflection equation modified for axial load. The shear rigidity is expressed by next equation. Shape coefficient is quoted from Ref.3 and is taken into account in estimating shear rigidity.

$$K_b = \frac{N \cdot k}{2\left(\tan \frac{kL}{2} - \frac{kL}{2}\right)} \quad , \quad K_s = \frac{{}_sG \cdot {}_sk \cdot {}_sA + {}_cG \cdot {}_ck \cdot {}_cA}{L} \qquad (1)$$

where $k = \sqrt{N/EI}$, $EI = {}_sE\,{}_sI + {}_cE\,{}_cI$, N: axial load, ${}_sE$ and ${}_cE$: Youngis modulus of steel and concrete, ${}_sI$ and ${}_cI$: moment inertia of steel and concreteÇ L: buckling length, ${}_sG$ and ${}_cG$: shear modulus of steel and concrete, ${}_sk$ and ${}_ck$: shape coefficient of steel pipe and concrete, ${}_sA$ and ${}_cA$: area of steel and concrete.

$$_{cal}K_1 = \frac{Q}{\delta} = \frac{1}{1/K_b + 1/K_s} \qquad (2)$$

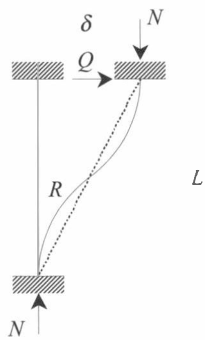

Fig.1 Loading Condition

3 EFFECT OF THE PARAMETER

From the comparison of the rigidities, the axial load ratio and compressive strength of concrete are observed to have distinctive effect on the rigidity. When the strength of filled concrete is high, the steel column is subjected under vertical load with large axial load ratio. In this chapter, the effects of the parameters are discussed, and the method of calculation is modified and refined.

3.1 The rigidity in consideration for the tangent modulus

Because of the nonlinear characteristic of the concrete, the rigidity of the beam-columns is overestimated. And, if there exist residual stresses and imperfection of the section in steel tube, the stiffness of steel tube decreases in the tangent modulus.

In this paper, the stress-strain relationship of concrete and steel are supposed as a quadratic curve. Then, to calculate the rigidity of CFT beam-column, the more accurate horizontal rigidity (${}_{cal}K_2$) is calculated by using tangent modulus stiffness in stead of Youngis modulus, both steel and concrete.

The ratio of the measured rigidity to calculated rigidity ($_{exp}K\,/\,_{cal}K_2$) are in the range of 0.561 - 0.795 (See Table1).

3.2 The rigidity in consideration for the separation between surface of concrete and steel

When the axial load was applied on the CFT column, the bond between concrete and steel is lost due to difference of Poissonís ratio of the two material. The tangent modulus and the separation between surface of concrete and steel are taken consideration. The rigidity of CFT column ($_{cal}K_3$) are calculated by addition the rigidity of steel column and the rigidity of concrete column (Eq.3).

$$_{cal}K_3 = {_{cal}K_s} + {_{cal}K_c} = \frac{1}{\frac{1}{_sK_b} + \frac{1}{_sK_s}} + \frac{1}{\frac{1}{_cK_b} + \frac{1}{_cK_s}} \qquad (3)$$

The ratio of the measured rigidity to calculated rigidity ($_{exp}K\,/\,_{cal}K$) are in the range of 0.596 - 0.844.

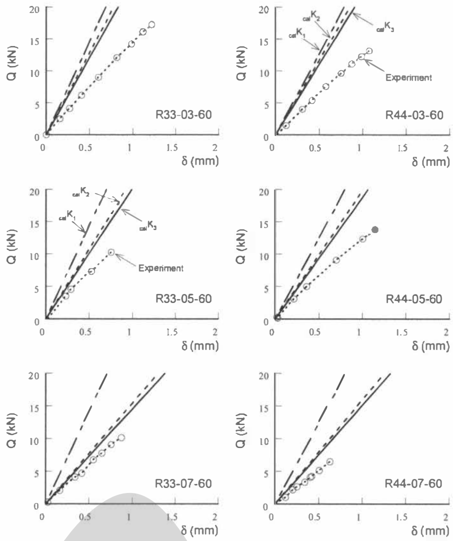

Fig.2 Comparison of the Rigidity

4 CONCLUDING REMARKS

The three calculated horizontal rigidities are shown :

1) Rigidity, which assumes Navieris hypothesis and is calculated by using Youngís modulus, 2) Rigidity, which assumes Navierís hypothesis and is calculated by using tangent modulus, 3) Rigidity calculated by using tangent modulus and take into account the loss of bond between concrete and steel.

From the comparison between measured rigidity and calculated rigidity, it became clear that:

(1) In calculating the horizontal rigidity of the beam-column, the calculated rigidity estimate the experimental very conservative, when Youngis modulus was used.

(2) When the horizontal rigidity is calculated by using tangent modulus stiffness, the ratio of the experimental rigidity to calculated rigidity ($_{exp}K\,/\,_{cal}K_2$) are in the range of 0.561 - 0.795.

(3) In addition to the effect of the tangent modulus, the separation between surface of concrete and steel is take into account . The ratio of the experimental rigidity to calculated rigidity ($_{exp}K\,/\,_{cal}K_3$) are in the range of 0.596 - 0.844.

REFERENCES

[1] Kanda, N., Fujinaga, T., Mitani, I., Ohtani, Y. and Nakamura, G. : An Experimental Study on CFT Square Beam-Columns using High Strength Concrete. Summaries of Technical Papers of Annual Meeting AIJ, Sep., 2000 (in Japanese)

[2] Architectural Institute of Japan: AIJ Standard for Structural Calculation of Reinforced Concrete Structures -Based on Allowable Stress Concept-. Nov., 1999 (in Japanese)

[3] C. L. Dym, I. H. Shames: Solid Mechanics (A Variational Approach). McGraw-Hill, 1973

Table 1 Comparison of the Rigidity

Specimen	n	N (kN)	$_{exp}K$ (kN/mm)	$_sE_0$ (GPa)	$_cE_0$ (GPa)	$_{cal}K_1$ (kN/mm)	$_{exp}K/_{cal}K_1$	$_sE_t$ (GPa)	$_cE_t$ (GPa)	$_{cal}K_2$ (kN/mm)	$_{exp}K/_{cal}K_2$	$_{cal}K_3$ (kN/mm)	$_{exp}K/_{cal}K_3$
R33-03-30	0.3	210	**17.95**	206.0	24.43	**25.38**	**0.707**	176.1	22.47	**22.22**	**0.808**	**20.84**	**0.861**
R33-05-30	0.5	350	**17.47**	206.0	24.43	**25.16**	**0.694**	151.9	17.16	**18.11**	**0.965**	**16.98**	**1.029**
R33-07-30	0.7	490	**16.20**	206.0	24.43	**24.95**	**0.649**	120.6	10.33	**12.86**	**1.260**	**12.06**	**1.344**
R33-02-60	0.25	261	**14.84**	206.0	35.01	**29.12**	**0.510**	175.6	34.72	**26.48**	**0.561**	**24.88**	**0.596**
R33-03-60	0.3	310	**15.14**	206.0	35.01	**29.04**	**0.521**	169.4	33.85	**25.57**	**0.592**	**24.04**	**0.630**
R33-04-60	0.4	413	**14.18**	206.0	35.01	**28.88**	**0.491**	155.8	31.94	**23.60**	**0.601**	**22.18**	**0.639**
R33-05-60	0.5	517	**14.48**	206.0	35.01	**28.72**	**0.504**	141.0	29.86	**21.47**	**0.675**	**20.19**	**0.717**
R33-06-60	0.6	661	**13.96**	206.0	35.01	**28.50**	**0.490**	118.5	26.69	**18.23**	**0.766**	**17.15**	**0.814**
R33-07-60	0.7	771	**12.28**	206.0	35.01	**28.32**	**0.434**	99.0	23.95	**15.44**	**0.795**	**14.55**	**0.844**
R44-02-60	0.2	175	**14.57**	206.0	33.77	**25.57**	**0.570**	184.2	35.94	**24.96**	**0.584**	**23.57**	**0.618**
R44-03-60	0.3	262	**13.33**	206.0	33.77	**25.44**	**0.524**	172.7	34.31	**23.46**	**0.568**	**22.16**	**0.601**
R44-04-60	0.4	350	**14.52**	206.0	33.77	**25.30**	**0.574**	160.3	32.57	**21.87**	**0.664**	**20.67**	**0.703**
R44-05-60	0.5	454	**14.40**	206.0	33.77	**25.13**	**0.573**	144.7	30.37	**19.88**	**0.725**	**18.79**	**0.766**
R44-06-60	0.6	545	**10.34**	206.0	33.77	**24.99**	**0.414**	129.9	28.30	**18.00**	**0.575**	**17.02**	**0.607**
R44-07-60	0.7	636	**10.23**	206.0	33.77	**24.84**	**0.412**	113.8	26.04	**15.96**	**0.641**	**15.11**	**0.677**

FATIGUE TESTS OF A NEW JOINT IN COMPOSITE BRIDGE USING DIAGONAL STEEL TRUSS WEB

Kosuke Furuichi Yohei Taira
Technical Research Institute
Kajima Corporation, Japan

Keita Masumoto Masato Yamamura
Civil Engineering Design Department
Kajima Corporation, Japan

Keywords: fatigue test, composite structure, truss structure

1 INTRODUCTION

Steel-concrete composite truss bridges uses steel tubes for diagonals that replace the web members of the box girder of a prestressed concrete bridge. In this truss structure the axial forces is transmitted via joints where diagonals intersect top or bottom chords. The joint structure is very important and joints exhibit complex mechanical behavior. Various joint structures have been proposed, and research and development of their structures are being carried out.

The authors proposed the "steel box structure", a composite joint structure that uses steel and concrete effectively, and conducted model tests to verify the strength of the joint [1], [2].

In this study, a fatigue test was conducted using a joint specimen to verify the safety of the joint structure, and a static load test was conducted after the fatigue test to verify the strength of the joint. This paper provides the test results.

2 TEST OUTLINE

2.1 Specimens

Fig. 2 shows the shape of the specimen. The steel box made of steel plates by welding is embedded in the top chord. A tension diagonal that carries tensile forces and a compression diagonal that resists compressive forces are connected via concrete in the steel box. The axial force of the tension diagonal is transmitted to the concrete in the steel box via the steel plate on the top surface of the box that is welded to the diagonal. The axial force of the compression diagonal is transmitted to the concrete in the box via the shear connector of circular round steel bars attached at the end of the compression steel tube.

Perforated steel plates are used on both sides of the steel box to ensure better concrete filling and integrate the steel box with surrounding concrete. The shear at the joint is resisted by concrete, the side plates of the steel box and the shear reinforcement arranged around the side plates.

2.2 Test Method

Fig. 2 shows the loading equipment. Loads were applied laterally at the end of the concrete by a 2,000 kN actuator fixed on the reaction sidewall. Thus, tensile and compressive axial forces were applied to the diagonals on the side of the load point and on the other side, respectively to identify the transmission of forces at the joint.

In the fatigue test, the loads which stress of 40-60% of allowable stress (186 MPa) acted on a steel tube were applied repetitively with the minimum and maximum lateral loads set at 640 kN and 910 kN (maximum fatigue load. The frequency for loading in the fatigue test was set at 1.5 Hz and loading and unloading was repeated 2 million times.

At the end of the fatigue test, a static load test was conducted to verify the strength of the joint.

3 RESULTS OF FATIGUE TEST

The relationships between the lateral load and displacement when loading was repeated once, one million

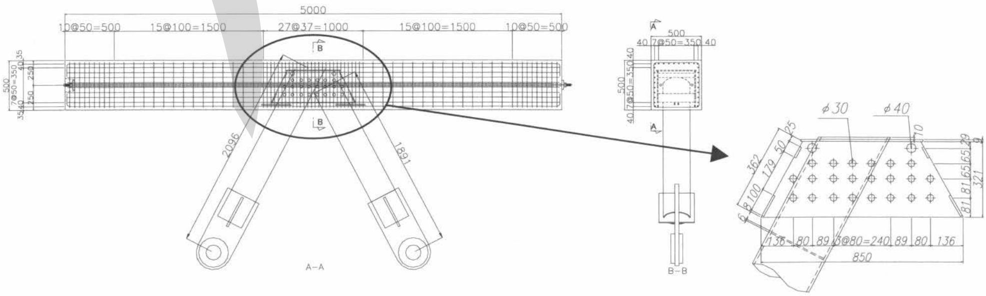

times and two million times are shown in **Fig. 3**. In the initial stages of loading, displacement increased to about 6 mm during the fitting of the specimen to the jig. Then, the load and displacement increased linearly. Displacement slightly increased with the increase of the number of times of loading. The gradients of the curves in **Fig. 3** are almost identical. Thus, changes of stiffness were hardly observed.

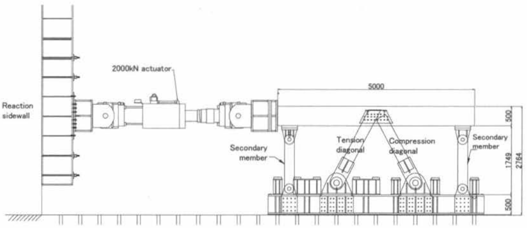

Fig.2 the loading equipment

The relationship between the principal strain around the point where the tensile steel tube was welded to the top steel plate of the steel box are shown in **Fig. 4**. The change of this point was outstanding and the number of times of repetitive loading. The principal strain plate remained constant during the fatigue test. At the end of the test, the value was sufficiently smaller than the yield strain (1,938 x 10^{-6}).

From the result of the fatigue test, no abnormal conditions such as fracture were found in the joint during the fatigue test. Thus, the safety of the joint structure against repetitive loading and unloading was verified.

4 RESULTS OF STATIC LOAD TEST

Fig. 5 shows the relationship between the applied load and lateral displacement of concrete.

In the initial stages of loading, displacement increased during the fitting of the specimen to the jig. Then, the applied load and displacement increased linearly. At 1,743 kN, the yield strain that could be obtained from material tests was reached in some parts of the tension steel tube, and then stiffness decreased gradually. The load reached the maximum level at 4,016 kN and at a displacement of 54.6 mm. Then, buckling occurred at the point where the jig was connected to the compression steel tube at a displacement of 63 mm, and the load decreased. **Photo. 1** shows situation of the steel tube buckled.

No abnormal conditions such as fracture were found in the joint until buckling of the compression steel tube. Thus, the ultimate capacity of the joint had more than 4.4 times the maximum fatigue load of 910 kN

5 SUMMARY

The results of a fatigue test and subsequent static load test on the joint of a steel-concrete composite truss are listed below.

- As a result of two million times of repetitive loading and unloading, stiffness of the joint remained constant and changes in strain of steel tubes and boxes were hardly in the initial stages of the fatigue test through the end of the tests. Thus, it was found the safety of the joint structure against repetitive loading and unloading was verified.
- As a result of having done static load test after fatigue test, no abnormal conditions such as fracture were found in the joint until buckling of the compression steel tube (4,016kN). Thus, it was found the joint of the steel box had high capacity.

REFERENCES

[1] Kentaro Yoshida, et al., : Experimental Study of a New Joint in Prestressed Concrete Composite Bridges with a Steel Truss Web, KaTRI Annual Report, 2000(in Japanese)

[2] Kosuke Furuichi, et al., : Experimental Study on a New Joint for Prestressed Concrete Composite Bridge with Steel Truss Web, International Symposium on Connections between Steel and Concrete, pp.1250-1259.

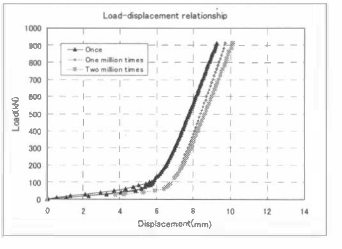

Fig.3 Load –displacement relationship

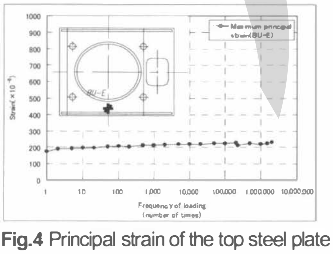

Fig.4 Principal strain of the top steel plate of steel box and number of loading

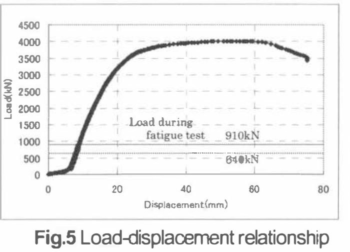

Fig.5 Load-displacement relationship

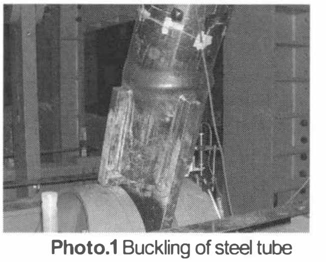

Photo.1 Buckling of steel tube

BEHAVIOUR OF ECCENTRICALLY LOADED CONCRETE-FILLED STEEL TUBES

De Nardin, Silvana
MSc.in Structural Engineering*
snardin@sc.usp.br

El Debs, Ana Lúcia
Prof. of Civil Engineering*
analucia@sc.usp.br

Department of Structural Engineering
University of São Paulo at São Carlos – BRAZIL

Keywords: high strength concrete, composite columns, concrete-filled steel tube, beam-column.

1 INTRODUCTION

By definition, a concrete-filled composite column is a structural element predominantly subjected to normal loading. The steel section is normally composed of one or more sections made of standard structural steel section and filled with concrete. Figure 1 shows some typical examples of filled-in columns.

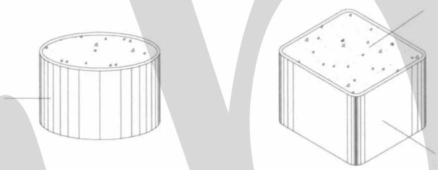

Figure 1- Typical examples of concrete-filled composite columns

The use of composite columns in high rise buildings has witnessed significant increase in the last few decades. Among the various factors that contribute to such increase are factors directly associated to some positive aspects of these elements in service such as: reduction of the dimensions of the structural elements accompanied by economy in material consumption, labour force, and possible ultra-long span, increased capacity, stiffness and ductility (especially with the advent of new high performance building materials).

Presently, the specification concrete-filled columns in building projects are becoming a common design procedure for engineers. This call for the necessity for an increase knowledge of the behaviour of these elements besides developing more simple though rigorous and reliable design procedures for the verification of global structural safety. The urge to attain such goals has led researcher to studying various aspects that influence the behaviour of filled-in composite columns.

The behaviour of structural filled-in composite columns subjected to bending-compression loading is highly influenced by factors such: material strength, steel-concrete boding, confinement and nature of loading. All these aspects exert a certain degree of influence on the load carrying capacity of these elements.

In this like, the prime objective of this paper is to bring to light and make a detailed analysis of the influence of some parameters on the load carrying capacity of filled-in columns under bending-compression loading. The major parameters to be considered are:

- breadth/thickness ratio;
- eccentricity of applied load; and
- the concrete strength (fck)

To estimate the load capacity of the columns, a CFT software program developed by Marques & Marques [1] was used. The results thereof show good agreement with test results given in (De Nardin et al. [2]).

2 THEORETICAL STUDY

During the analysis procedure, the following parameters were considered: the b/t ratio, eccentricity of applied load (e) and the concrete compressive strength. In all, 504 concrete-filled composite columns of both rectangular and circular cross section were tested. Table 1 shows detail geometric characteristics together with loading configuration material properties and the nomenclature adopted for the these columns.

Table 1: some characteristic of concrete-filled composite columns studied

Transverse section	b/t	Element	Eccentricity (mm)	fck (MPa)
150 x 150 x 3	50	CFTS-3	5 to 70 mm, with increments of 5 mm. Total of 15 eccentricities*.	40 to 80 MPa, with increments of 5 MPa. Total of 9 concrete strengths.
150 x 150 x 6, 3	23,8	CFTS-6,3		
100 x 200 x 3	33,3	CFTR-3		
100 x 200 x 6,3	15,9	CFTR-6,3		
* for the rectangular sections, the eccentricity was considered about the minor axis of inertia.				

3 CONCLUSIONS

A study of the influence of parameters such as concrete compressive strength, load eccentricity and the breadth/thickness ratio showed very interesting results.

It was verified that, for concrete-filled columns under loads applied with large values of eccentricity, increases in concrete compressive strength do no lead to any significant increases in strength capacity. This is due to that fact that, the increase in load eccentricity the neutral axis shifts, dividing the transverse section into two distinct regions: one under tension and the other compressed. Since the concrete contribution under tension is neglected, any increase in compressive strength does not have any additional effect.

In the light of carrying out the present study parametrically using parametric relations such as breadth/thickness ratio, it is worth mentioning that great caution should be taken. This is because the transverse section exerts great influence on strength capacity values and it is thus not correct to represent the transverse section by only the b/t ratio.

4 ACKNOWLEDGEMENT

The authors greatly acknowledge the financial support by the State of São Paulo Fund for Research (Fundação de Amparo à Pesquisa do Estado de São Paulo FAPESP) that resulted in the present paper.

REFERENCES

[1] Marques, S. P. C.; Marques, D. C. C. Anàlise não linear de pilares tubulares de aço com núcleo de concreto de alto desempenho. In: XXIX JORNADAS SUDAMERICANAS DE INGENIERIA ESTRUCTURAL . Memorias (CD). Punta del Este - Uruguai, 2000.

[2] De Nardin et al. Comportamento de pilares preenchidos submetidos à flexão normal composta. In: I CICOM CONGRESSO INTERNACIONAL DA CONSTRUÇÃO METÁLICA Proceedings (CD). São Paulo-SP, 2001.

[3] Cederwall, K.; Engstrom, B.; Grauers, M. High-strength concrete used in composite columns. In: HESTER, W. T., ed. High-strength concrete: second international symposium. Detroit, ACI. p.195-214. (ACI SP-121), 1990.

BEHAVIOUR OF REINFORCED CONCRETE COLUMNS CONFINED BY CARBON FIBER-REINFORCED POLYMER (CFRP) WRAPS

Ricardo Carrazedo João Bento de Hanai Adilson Roberto Takeuti
Department of Structural Engineering, University of São Paulo at São Carlos
São Carlos – Brazil

Keywords: confinement, columns, strengthening, reinforced concrete, FRP

1 INTRODUCTION

The strengthening of reinforced concrete structures has been significantly improved by the development of new structural materials such as fiber-reinforced polymers (FRP). These materials show excellent mechanical properties such as high specific strength and modulus of elasticity. Due to their low weight, FRP can easily be applied on the element surface. Moreover, FRP strengthened elements have insignificant dimensional increase. Despite the relatively high cost of these materials, their technological advantages are relevant and a large number of structures have been rehabilitated using FRP during the last years.

This paper presents and discusses the results of a theoretical-experimental analysis on confinement of reinforced concrete columns. Two kinds of passive confinements are analyzed: steel spirals and FRP wraps. The main variables in this study are the transverse steel ratio (ρ_s) and the number of FRP layers (n). Another important effect observed is derived from cross section geometry.

Twelve short columns composed of FRP and steel confinement were subjected to axial compressive loading in a servo-hydraulic testing machine. The tests were conducted at a constant axial strain rate. It was then possible to obtain the stress-strain response of these columns and compressive load capacity. The effect of confinement predicted by analytical models was then compared with test results, considering strength, strain and stress-strain behavior of the confined concrete as the main parameter.

The theoretical analysis was based on the combined effect of the confinement pressure due to the FRP jacket and steel spirals in the concrete core.

2 EXPERIMENTAL PROGRAM

2.1 Specimen characteristics

Twelve concrete columns were loaded in axial compressive with a strain rate of $8{,}8.10^{-6}$/s. Nine of them had circular cross sections with three different transverse steel rates (ρ_s) and number of CFRP layers (n). The diameter of the columns was 190 mm. The remaining three columns were of square cross sections with zero, one and two CFRP layers without any steel reinforcement. Square columns had side length of 150 mm and corners rounded off by 30 mm.

Based on [5], the longitudinal strength and modulus (E_f) of carbon fibers was 2730 MPa and 220 GPa, respectively. The epoxy resin used was a bi-component type. A layer thickness of 0.13 mm was adopted as recommended by the manufacturer. The strength prediction of fibers in the columns was based on failure strains (ε_{fu}) measured.

2.2 Stress-strain behaviour of the confined concrete

FRP wrapped circular columns showed a bi-linear stress-strain curve as suggested by [3] and [4]. Fig. 1 shows the stress-strain curves for FRP confined circular concrete columns tested. Normalized stresses are related to the unconfined strength (f_{co}).

However, square columns did not show perfect bi-linear stress-strain behaviour. It was observed that there is a more pronounced non-linearity in the second branch. Another observation is that the transition zone is more pronounced than in the circular columns.

Some of the columns had both types of confinement: FRP wrapping and steel spirals. In these columns the predicted carrying capacity was calculated by adding confinement pressures in the central core. Observations from the test program showed that at the maximum axial load, the transversal steel reaches yield point. Thus it was concluded that the pressure acting in the central core is given by the sum of the pressures provided by the transverse steel and the FRP wrapping.

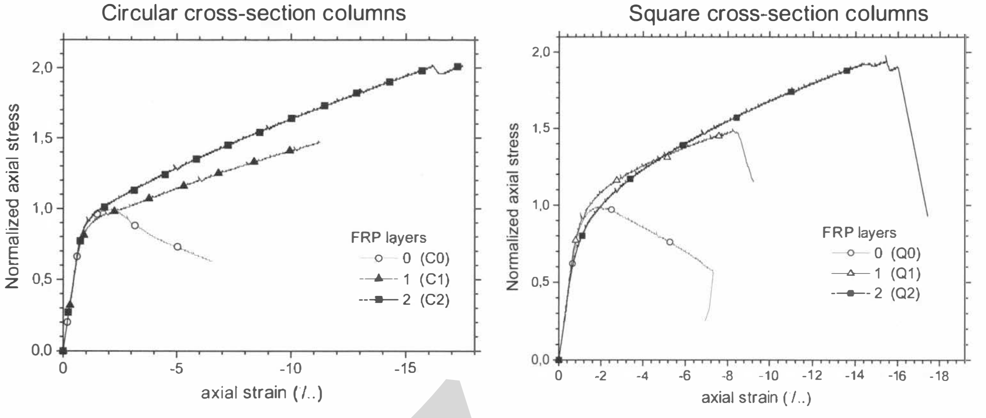

Fig. 1 Stress-strain curves for FRP confined columns

3 CONCLUSIONS

The theoretical confinement models provided good predictions to the behavior of FRP strengthened circular columns. The strength evaluations were very close to the test results. The stress-strain curve suggested by [3] showed a better fit to the data than [4].

Combined confinement effects of FRP and steel reinforcement in circular columns were verified. Theoretical evaluations of the load capacity considering these effects showed a good agreement with test results. This suggests that there are effective contributions of the two types of confinement in the central core.

Square columns showed stress-strain curves near to bi-linear. However a slight non-linearity was observed in the second branch. The effective lateral pressure (f_{le}) showed to be less than the uniform idealized pressure for circular columns (f_{li}), with an effectivity coefficient near to 0.7. The stress-strain curves of square columns were very similar to the circular columns. This is attributed to the similar levels of normalized lateral pressure estimated for the two situations.

The force-displacement curves of reinforced circular columns showed that the ultimate strain and strength of confined concrete were dependent of the transverse steel ratio (ρ_s) and FRP layers (n). This fact shows that these two forms of confinement work together in the central core.

4 ACKNOWLEDGEMENTS

The authors express their gratitude to FAPESP (São Paulo State Research Foundation) and CAPES (Federal Government) for the financial support and scholarship and to Sika S. A. for providing the materials used in the test program.

REFERENCES

[1] Richart, F. E., Bradtzaeg, A. and Brown, R. L. : The failure of plain and spirally reinforced concrete in compression. Bull. No. 190, University of Illinois, Engineering Experimental Station, Urbana, Ill., 1929.

[2] Mander, J. B., Prietsley, M. J. N. and Park, R. J. T. (1988-b). : Theoretical Stress Strain Model for Confined Concrete, J. Struct. Eng., ASCE, v. 114, p. 1804-1827.

[3] Miyauchi, K., Nishibayashi, S. and Inoue, S. (1997). : Estimation of strengthening effects with carbon fiber sheet for concrete column. In: Third International Symposium, Vol. 1, Tokyo, October, Japan Concrete Institute. p. 217-225.

[4] Samaan, M., Mirmiran, A. and Shahawy, M. (1998). : Model of concrete confined by fiber composites. Journal of Structural Engineering, ASCE, v. 124, p. 1025-1031.

[5] American Society For Testing And Materials – ASTM D 3039/ D 3039m - (1995). : Standard Test Method for Tensile Properties of Polymer Matrix Composite Materials.

THE MECHANICAL CHARACTERISTICS OF CIRCULAR RC COLUMNS CONFINED BY THIN STEEL SPIRAL TUBE

Shoko Moroishi
Hiroshima Institute of Technology
Graduate School, JAPAN

Tatsumi Sato
Prof. Hiroshima Institute of Technology
Dr Eng, JAPAN

Keywords: circular RC columns, confined effects, bending strength, shear strength

1. INTRODUCTION

The remarkable damages of RC buildings due to the recent earthquakes are the story failure of the middle floor, and the crushed columns of the 1st story of the pilot's type RC buildings.

It is thought that the cause of crashing the columns is due to the combination of high axial force and high shear force subjected at the same time under the earthquake motion.

If the RC column is failed by shear force, the axial strength is rapidly lost, and brittle failure occurs by expanding shear cracks to the whole section obliquely.

To prevent such crushing, it is important to secure the axial and lateral strength of column and to improve its deformability.

Since 1983, we developed a method to prevent the decline of the axial strength caused by the shear failure, and to improve the strength and deformability. [2)] But, the reduction of the section of columns by the exfoliation of cover concrete outside shear reinforcements cannot be prevented.

Therefore, in this paper, a new system is proposed that restrains the whole section of circular RC column confined by thin steel spiral tube (of the following T.S.S tube), and no spiral hoop is used by the expectation of the hoop tension of T.S.S tube itself.

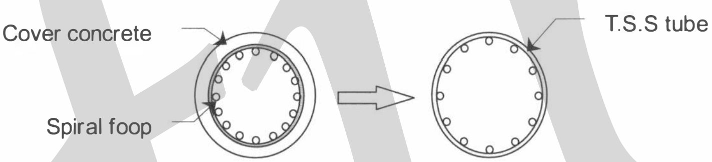

Fig.1 Proposed column

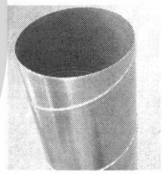

Photo.1 Used T.S.S

2. THE EXPERIMENTAL STUDY OF CIRCULAR RC COLUMNS CONFINED BY T.S.S

2.1 The outline of specimens

Bar arrangements and the strength of used material is shown in Fig.2, Table.1. 10 specimens of RC circular columns, with a diameter of 300mm and numbers of main reinforcements of 16–D13 (SD295), were made and experimented.

The experimental parameters are axial force ratio that varies in 0.3, 0.5, 0.6, and thickness of T.S.S tube or thickness / diameter ratio, and clear-span/diameter ratio.

So the name of specimens is decided as follows,

OC4－40－3

Axial force ratio : n × 10
Clear span/Diameter ratio : $H/\phi \times 10$
Thickness/Diameter ratio : $2t/\phi \times 1000$

N: Axial load　　t: Thickness of T.S.S

A_c: Concrete section　　ϕ : Diameter

$n=N/A_c\sigma_b$: Axial force ratio　　H: Clear span

Table.1 Strength of used material

	Tensile strain	Yield strength		Tensile strength	
	(%)	(kN)	(N/mm^2)	(kN)	(N/mm^2)
D13	21.4	256.9	337.7	368.6	468.1
T.S.S	－	4.49	299	5.53	368

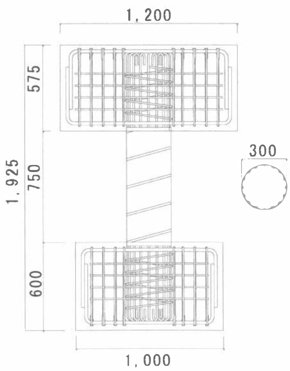

Fig.2 Bar arrangements

2.2 Biaxial experimental program and results

The specimens were set as the rotation of the top and bottom beams are fixed. After, the axial force was applied to the decided axial load ratio. Next, the repeated monotonically increasing of the lateral force was applied until the specimen failed or the drift angle of column is R=5.0%.

The lateral maximum strength of the specimens in the biaxial experiment, the ductility coefficient obtained by the experiment was shown in Table.2, and an example of the lateral load-Drift angle relationship curve (P-R) was shown in Fig.3.

Table.2 Experimental results of biaxial experiments

Specimen	Concrete strength σ_b (kN/mm^2)	Maxium Strength (kN)	Ductility μ
OC4-40-3	25.48	203.8	8.21
OC4-40-6		236.3	3.36
OC8-40-3	33.12	229.0	9.80
OC8-40-6		287.2	5.77
OC4-25-3	35.85	348.5	1.00
OC4-25-5	32.84	381.5	-
OC8-25-3	35.85	396.4	4.58
OC8-25-5	32.43	376.0	3.59
OC11-25-3	35.85	405.0	12.50
OC11-25-5	34.45	444.7	3.90

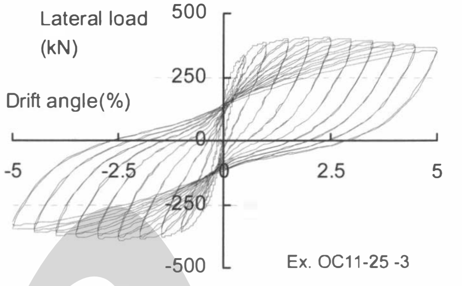

Fig.3 The lateral load-Drift angle (P-R) curve

If the ductility coefficient μ obtained by the experiment, is 5.0 or less, the all specimens confined failed by shear and the accumulation of axial strain of the specimens become very large. So the probability of cut of T.S.S is high.

As the boundary of shear failure type and bending failure type, the expression in equ(1) is obtained for the boundary discriminated equation. And all the columns of the discriminated line bottom are shear failure.

$$H/\phi + 5 \times 2t/\phi - n/0.3 < 4 \cdot\cdot\cdot (1)$$

In the specimens failed by bending, the remaining axial strength after the biaxial experiment is all must equal to the original axial strength, therefore these columns can prevent from the crushing.

From the calculated study, the maximum bending and shearing capacity of circular RC column can be estimated in consideration of all area of main reinforcements and the stress-strain relationships of concrete confined by T.S.S tube.

3. CONCLUSION

1) By reinforcing RC column with T.S.S tube, it confirmed having the shear reinforcement effect and the clear confined effect.

2) Proposed RC column is excellent in the structure performance to failure prevention compared with the conventional column.

3) By the suitable determination of thickness of T.S.S tube, the design of the column with required sufficient strength and deformation performance can be possible.

4) Making thickness-diameter ratio into 0.8% can prevent shearing failure or more with a long column, when axial load ratio is 0.4 or less.

5) In the case of the length of columns becomes short and the axial load ratio is 0.4 or more, it is required for the thickness-diameter ratio to make 1.1% or more, to prevent shearing failure.

REFERENCES

(1) AIJ: Design Guidelines for Earthquake Resistant Reinforced Concrete Buildings Based on Inelastic Displacement Concept (Draft), 1997
(2) T. Sato, B. Wada, K. Minami: Strengthening effects of RC columns using thin steel spiral tube. 12WCEE, Auckland, New Zealand. , 2000
(3) AIJ: Structural Guideline for Reinforced Concrete Buildings, 1994
(4) Sato, T., Moroishi, S.: The mechanical characteristics of circular RC columns confined by thin steel spiral tube. Bulletin of Hiroshima institute of technology., Vol.36., pp61～68, 2001

WORLDWIDE APPLICATION OF ADVANCED COMPOSITE SYSTEMS IN BRIDGE STRENGTHENING

Miklos Basler
Sika AG
Switzerland

Hirofumi Bandoh
Sika Ltd.
Japan

Marco Ammann
Sika Ltd.
Japan

Keywords: Advanced Composites, Bridge Strengthening, CarboDur Composite Systems

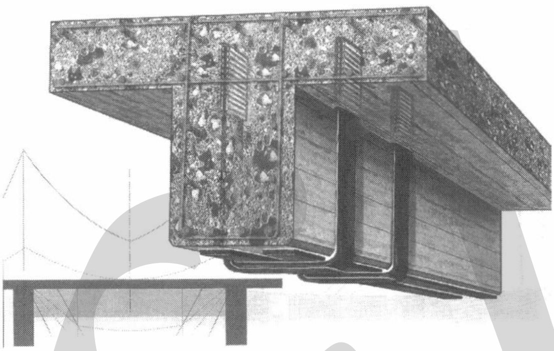

Fig 1 CarboDur CFRP plate systems

ABSTRACT

This paper describes the development and application of the CarboDur Composite Systems in Bridge strengthening. Relevant test reports are presented concerning the Fatigue resistance of the system as well as tests showing that the load-bearing capacity of structures is not affected by the influence of traffic-induced oscillations during the curing of the structural adhesive.

By a new technique and tested Systems it is nowadays possible to pre-stressed CarboDur CFRP plates and to increase the utilisation factor of the high tensile strength of the CFRP. Important projects are presented including use of pre-stressing in order to show the power and the potential of the Systems in Bridge engineering.

1. INTRODUCTION

Demands for high durability, longer service life and reduced maintenance cost have prompted a new look at Advanced Composite Systems for Bridge strengthening. Thanks to intensive research and development projects at the EMPA high strength CarboDur CFRP plate system was applied the first time outside the laboratory in 1991 for strengthening the Ibach bridge at Lucerne, Switzerland.

This Advanced Composite System is composed by

- CarboDur CFRP plates, a long term tested and approved system particularly suitable for flexural strengthening, in-situ rehabilitation as well as for pre-stressing and Sikadur-30 adhesive
- CarboShear L-shaped CFRP plate well appropriate for shear strengthening of reinforced concrete structures and Sikadur-30 adhesive
- SikaWrap FRP uni- and/or bidirectional fabrics with Sikadur impregnation resins

2. RELEVANT TEST REPORTS

Before strengthening of bridges or structures exposed to dynamic load with Advanced Composite Systems, two basic questions have to be answered. They are:

- What is the influence on the load-bearing capacity of structure exposed to dynamic and vibrating loads during curing of the structural adhesive?
- What is the influence on the load-bearing capacity of structure exposed to fatigue loading during the life span of structure?

To answer these questions Sika commissioned the Swiss Federal Laboratories for Material Testing and Research (EMPA), Dübendorf with objective of investigating the above mentioned influences. While tests, see EMPA Test Reports No 170'569e-1, 418931E and 418931E/1, clearly showed that there is no difference in the load-bearing capacity of test specimen without or with oscillating loading during curing of Sikadur adhesive, Fatigue and failure test, see EMPA Test Report No. 402'017E/2 gave a proof of outstanding behaviour of CarboDur CFRP plate system to fatigue.

3. PRE-STRESSED CARBODUR PLATE SYSTEMS

The main reason for develop pre-stressing CarboDur Systems was their advantages comparing to unstressed CarboDur System:

- High utilisation, min. 90% of the tensile strength of CFRP plates in ULS
- Active paricipation of CFRP plates in carrying permanent loads at the time of application
- Reduction of stresses in re-bars and crack widths in Service Limit State (SLS)

Table 1 System Information

	Sika-LEOBA	Sika-StressHead	Sika-Mostogradnja
First application	1999	1999	2000
CarboDur plate type S	50x1.2mm/90x1.4mm	60x2.4mm	50x1.2mm-150x1.2mm
Cross section	60/126mm^2	144mm^2	60-180mm^2
Strain at pre-stressing	6 $^0/_{00}$ / 7.5 $^0/_{00}$	9.5$^0/_{00}$	7$^0/_{00}$
Pre-stressing force	60 / 165 KN	220 KN	70-210 KN

Since 1998 several bridges and buildings were strengthened with the mentioned systems in Germany, Switzerland, Netherlands, Korea and Yugoslavia.

4. BRIDGE STRENGTHENING WITH CARBODUR SYSTEMS

4.1 The Cairo Bridge

The seismic retrofitting of the bridge in Illinois, US was completed by confinement of columns with 4 to 14 layers of SikaWrap FRP fabric system.

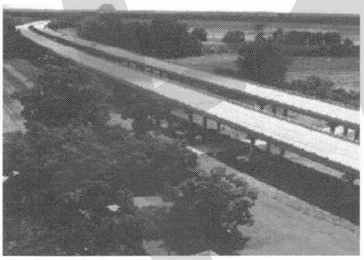

Fig 2 View

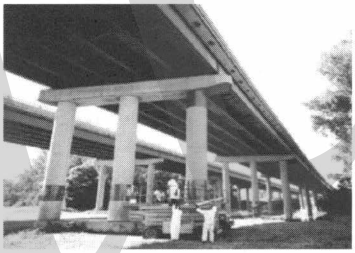

Fig 3 Application in progress

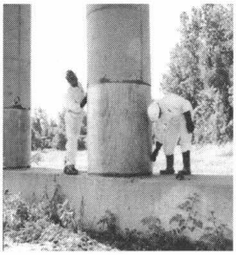

Fig 4 Smooting of SikaWrap

4.2 The Nišava River Bridge

In order to increase the flexural strength of the bridge over support due to increased traffic load the bridge was strengthened with pre-stressed CarboDur CFRP plates, system Sika-Mostogradnja.

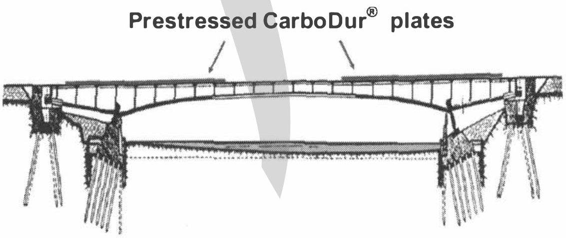

Fig 5 CarboDur strengthening

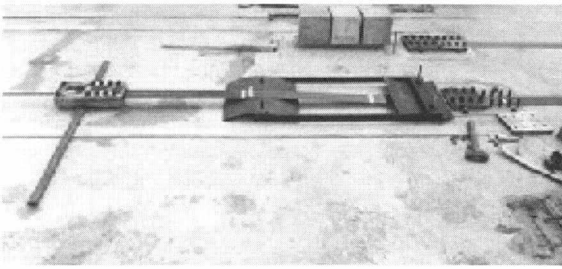

Fig 6 Pre-stressing in progress

DESIGN AND CONSTRUCTION OF THE MATTO PEDESTRIAN OVERPASS

Kaoru Sakamoto Akira Murayama
Japan Highway Public Corporation,Japan

Takeshi Yamagishi
Kawada Industries,Inc,Japan

Kenji Nakata
Ishikawa Pref.Japan

Keywords: Pre-Beam, protect against briny corrosion, concrete scale-off, erection of fully-assembled bridge unit

1. INTRODUCTION

The MATTO Pedestrian Overpass is a simply supported Pre-Beam Composite Bridge with the span of 60m, which is probably the longest one in the world. This overpass crosses over the Hokuriku Motor-Highway and is located in the area where severe deterioration of structure due to salt would be expected. So in order to verify the suitable countermeasures for deterioration due to salt, we have executed several studies and experiments, using the real-size model. On the other hand, with regard to erection method, since the only one night was allowed for the closure of Motor-Highway, we have erected the fully-assembled bridge unit, for which slab concrete work and other necessary works had also been finished, by using super big carrier. Fig. 1 View of the bridge supported to be completed.

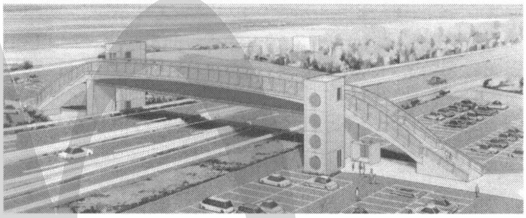

Fig.1 View of completion

2. PRE-BEAM COMPOSITE GIRDER

The Pre-Beam composite girder is made by casting concrete into the lower flange while keeping a tensile force introduced in the lower flange, with the load placed on the steel plate-girder (Pre-flexion). After the concrete has been hardened, the applied load is (Released), the pre-stress is introduced into the concrete. Thus, the steel-concrete composite girder is born to be free from a tensile stress to concrete under the dead load so that the girder depth could be lower. A typical cross section is shown in Fig.2.

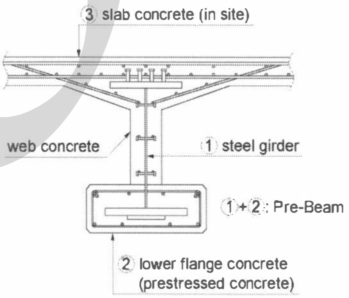

Fig.2 typical cross section

3. PROTECTION AGAINST BRINY CORROSION AND CONCRETE SCALE-OFF

The bridge has a lot of brine brought thereto with the wind. And salt is scattered as anti-freezing agent on the highway in winter. Since it is located over a highway, it is critical to take a concrete scale-off countermeasure, too. And these measures are taken as shown in Fig. 3.

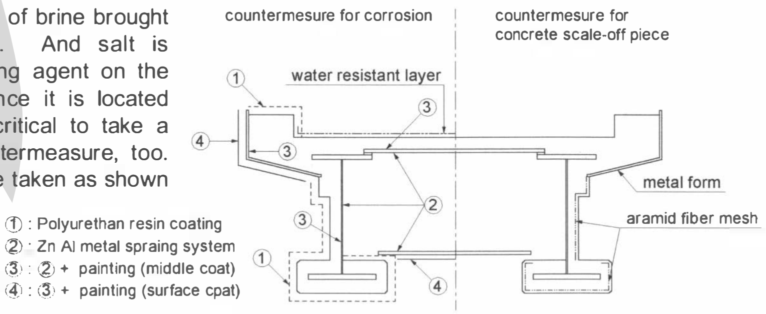

Fig.3 Corrosion and Concrete Scale-off Countermeasures

4. VERIFICATION TESTS

4.1 Testing for Zinc/Aluminum Film to Follow Possible Strains in Zn·Al Spraying System

Indoor testing was carried out with a scale model girder to verify the feasibility of following the steel girder strain during the Pre-flexion and Release of the Zn·Al Spraying System on the steel girder. And the Zn·Al spray-coated film had no change before and after the strain-following test. It could be verified that the Zn·Al spray-coated film could satisfactorily follow a strain upon Pre-flexion/Release.

4.2 Testing Zn·Al Spraying System for Adherence

The Zn·Al film is covered with concrete. Non-adherence between Zn·Al coated film and concrete, however, would have a possibility to lead to a scale-off of concrete. We had verified, therefore, what level of adherence is available between Zn·Al coated film and concrete, including its difference by film thickness, type of coating, concrete strength and casting technique. It could be verified that a design film thickness of 100 μm could be applied problem-freely. The test situation is shown in Photo-1 and 2.

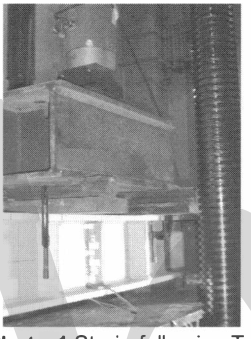

Photo-1 Strain-following Test

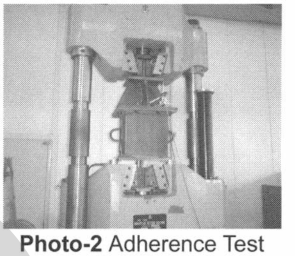

Photo-2 Adherence Test

5. PRE-FLEXION

The bridge reported herein differed from the conventional engineering in terms of size, cross sectional shape and steel material surface treatment. In addition, the bridge adopted an engineering technique different from the conventional pre-flexion. Even in this case, therefore, it must be necessary to make certain that steel and concrete could be unified (composed) through a successful introduction of pre-stressing into the lower flange concrete. In this sense, strain and flexure were really measured. And it could be verified that both flexure and steel girder strain showed a behavior nearly as calculated. Table 1 shows the Pre-flexion measurement results.

Table 1 Pre-flexion Measurements (inter-span center)

item	measuring point	measuring method	unit	design value	control range	measured value	
						G1 girder	G2 girder
steel girder strain	inter-span center upper-flange	strain measurement	μ	-1400 (-280N/mm^2)	-1386～ -1456	-1419	-1450
	inter-span center lower-flange	=ditto=	μ	1250 (250N/mm^2)	1238～ 1300	1290	1299
steel girder deflection	inter-span center	displacement gauge	mm	495	489～ 513	507	513

6. ERECTION

The steel girder fabricated in plant was hauled to a yard at a distance of approximately 250 meters away from the location where the bridge was to be erected. And the Pre-Beam girder was produced in the yard. Subsequently, the floor slab concrete was cast while handrails were installed until the bridge had been nearly accomplished.

The bridge erection work was carried out while suspending the traffic on the Hokuriku Motor-Highway for nine hours in the nighttime. How the bridge was erected is shown in Photo-3.

Photo-3 Haulage

REFERENCE

1) Development Engineering Research Center of Japan, Recommendations for Design and Construction of Pre-Beam Composite Girder Bridges-3rd Edition (1997).

Session 6 | Seismic design of concrete structures

NONLINEAR ANALYSIS BASED VERIFICATION OF STRUCTURAL SEISMIC PERFORMACE FOR PRACTICE

Koichi MAEKAWA
Department of Civil Engineering
University of Tokyo, Japan

Satoshi TSUCHIYA
COMS Engineering Corporation
Japan

Keywords: damage index, nonlinear analysis, performance-based design, RC, shell structures, frame structures

1 INTRODUCTION

For current seismic design, multi-directional responses of structures are not directly quantified and primary ground motion in a single direction is considered. This idealized approach is acceptable for design procedures of 1-DOF structural models. However, difficulty is encountered to treat more general cases. Herein, some equivalent conversion into 1D field has to be made and an advanced judgment is required. For example, when we try to explicitly consider the nonlinearity of soil-structure interaction for practice, simplified ways may bring non-rational design and unreasonably higher cost. There exists great benefit in applying 2D/3D nonlinear analysis for performance check of the targeted structures.

It is currently discussed that 3D finite elements, whose degree of freedom is reduced in terms of transverse shear, should be utilized for flexural-based nonlinear simulation. The material based damage can be brought in quantity that makes judgment of serviceability and function during and after the earthquake possible.

In this paper, the recent degenerated finite element analysis of 3D and application to the practical design are presented. Especially, the main focus is addressed to the indicator to check the limit state of structural members (plate/shell and frames) in terms of mechanical damage of constituent materials.

2 THREE-DIMENSIONAL PLATES AND SHELLS

2.1 Multi-directional constitutive modeling for reinforced concrete

The multi-directional cracking and their interaction are taken into account based on the active crack approach [1]. All microscopic physical states are inherently included in the scheme of stress-strain relation. The stress carrying mechanisms are composed of compression/tension parallel and normal to cracking and shear transfer.

2.2 Verification – member/structural level -

The constitutive models have been verified on several kinds of the member/structural behaviors, such as the shear wall and 3D shells under monotonic as well as cyclic loads, it is recognized that in-plane RC models function well under both static and dynamic excitation.

2.3 Design criterion of seismic limit state

From the parametric study with the verified FE analysis as shown in Fig. 1, the limit state of seismic performance level 2 (no collapse, possible reuse after earthquake without strengthening) is proposed in terms of compression as:

$$\varepsilon'_{p,comp} \leq 2 \cdot \varepsilon'_{u} \tag{1}$$

where, $\varepsilon'_{p,comp}$ is the maximum principal compressive strain of all elements on the extreme outer surfaces and ε'_{u} is defined as the peak strain of concrete under uni-axial compression.

As stress and strain fields are rather uniform than the cases of beam/columns, limit state of constituent elements is closely associated with the structural limit state of seismic performances.

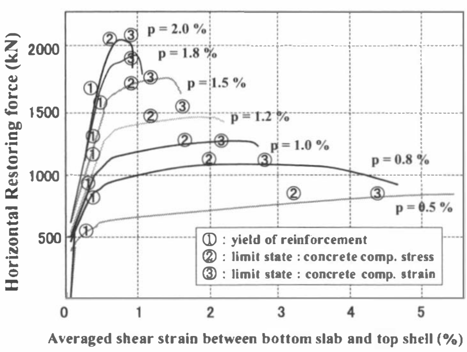

Fig. 1 Parametric study

3 THREE DIMENSIONAL FRAMES

3.1 Fiber modeling

Uni-axial stress field along the lineal member's axis is assumed and Euler-Kirchoff's hypothesis is adopted in fiber modeling. Buckling model of main reinforcing bars is employed here.

3.2 Cross sectional damage index

The authors take notice of fracture parameter of concrete. In the scheme of elasto-plastic fracture model used for concrete compression, the fracture parameter is defined as the reduction rate of unloading stiffness and physically means the volume ratio in which the shear elastic strain energy can be stored. The elasto-plastic fracture model is formulated on full 3D stress and strain fields [2], and it can be simply reduced to uni-axial states [1] as shown in Fig. 2.

The value of fracture parameter represents the mechanical damage of concrete, and usually it is not uniform over the cross-section. Then, the sectional averaged value within a referential section is the indicator of mechanical damage and can be defined as:

$$F = 1 - \overline{K} \equiv \frac{1}{A_c}\int_{A_c}(1-K)dA \approx 1 - \frac{\sum K \cdot \Delta A}{A_c} \qquad (2)$$

where, F is cross-sectional damage index, $\overline{K}$ is average fracture parameter, K is local fracture parameter in each microscopic cell, and A_c is concrete cross-sectional area.

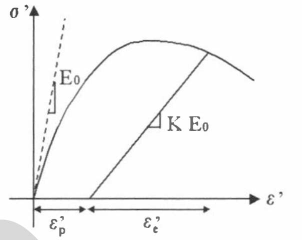

$$\sigma' = E_0 K\{\varepsilon' - \varepsilon'_p\}$$
$$K = \exp[-0.73\varepsilon'_{max}\{1-\exp(-1.25\varepsilon'_{max})\}]$$
$$\varepsilon'_p = \varepsilon'_{max} - 20\{1-\exp(-0.35\varepsilon'_{max})\}/7$$

Fig. 2 Fracture parameter

3.3 Relationship of member displacement and damage index

Through numerical simulations of typically supplied RC columns as Japanese infrastructures under static reversed cyclic loading, it is found that the point in the softening range after the peak capacity approximately coincides with the cross sectional damage index F=0.500 for all columns. It is confirmed at this moment that the average fracture parameter $\overline{K}$ suddenly decreases from about 0.600 after the maximum capacity. Displacement where the damage index reaches 0.500 are different between the reversed cyclic and monotonic loadings as shown in Fig. 3, and the proposed index can reflect the different damage situation according to the loading paths.

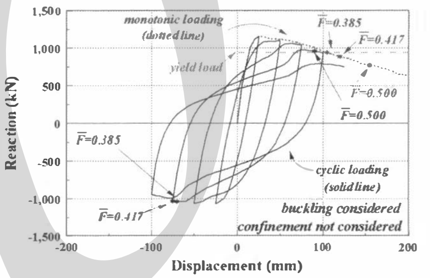

Fig. 3 Sample of numerical simulation

3.4 Applicability of damage index to multi-axes loading

For cyclic loading in skew directions, it can be thought that the horizontal displacement where the damage index reaches 0.500 bears the post-peak yield capacity of member ductility. On the other hand, the local strain and damage around four corners are so large in these cases, although the localized damage of concrete is limited within a narrow area and the rest of concrete was kept less damaged.

3.5 Applicability of damage index to confinement effect by hoop reinforcement

The confinement effect is formulated by changing the evolution rule of fracturing in accordance with the magnitude of lateral confinement. By means of this analytical approach, ductility improvement of column members by confinement and rationality of the cross sectional damage index are investigated. It is found that the displacement where the horizontal restoring force decreases up to the yield load level from the peak capacity corresponds to the cross sectional damage index as 0.500. For analysis of column members in which flexural ductility is brought by the confinement effect, the proposed damage index may be generally used for assessing the seismic performance level 2 as well.

REFERENCES

[1] Okamura, H. and Maekawa, K.: *Nonlinear Analysis and Constitutive Models of Reinforced Concrete*, Gihodo-Shuppan Co. Tokyo, 1991.

[2] Maekawa, K., Takemura, J., Irawan, P. and Irie M.: Continuum fracture in concrete nonlinearity under triaxial confinement, *Proc. of JSCE*, No.460/V-18, pp.113-122, 1993.

FORMULATION OF TRANSMITTING BOUNDARY FOR INFINITELY LONG ELEVATED BRIDGE OF DYNAMIC RESPONSE ANALYSIS

Sanghun Lee Tada-aki Tanabe
Department of Civil Engineering, Nagoya University
JAPAN

Keywords: Energy-Transmitting Boundary, Energy Radiation, Discrete System

1 INTRODUCTION

When seismic analysis was conducted for infinitely long elevated bridges, generally, the boundary condition for joint of the bridge had been considered as free. However, wave energy is transmitted through the interaction between neighboring bridges. Up to now, in the geotechnical engineering field, starting with the Lysmer's study [1] of semi-infinite layered soil structure, every kind of transmitting-boundary has been established. However, about the structure having column, beam and joint like elevated bridge, the simple wave solution cannot be applied although it could be applied to soil structure. For frame structure, Miwa etc. [2] formulated the energy-transmitting boundary, but an obvious explanation and verification of the formulation have not been provided. In this research, the basic feature of the transmitting boundary in discrete system was investigated using the model of continuous mass point and spring with single-degree-of-freedom, and clear verification was conducted. As an application, energy radiation about mass-spring model was calculated using harmonic ground excitation with various frequencies.

2 CONDITION OF ENERGY PROPAGATION

In order to formulate the boundary condition that consider the interaction between structures as continuous elevated RC bridge, it needs to define the condition of energy propagation. In this paper, for obvious understanding, uniformly continuous mass-spring model with no ends is chosen as shown in Fig.1. Equation of motion at arbitrary lumped mass r can be written as

$$-m\frac{d^2x_r}{dt^2}-(x_r-x_{r-1})k+(x_{r+1}-x_r)k=0 \qquad \text{where, } r=-\infty,\dots,-1,0,1,\dots,\infty \tag{1}$$

This equation can be applied to any point of infinite mass-spring system under consideration, by changing the subscript r. Displacement of this equation can be expressed using angular frequency ω [3], then suppose that the wave solution $x_r = u\eta^r e^{i\omega t}$ exists for any frequency ω. Where, u is complex amplitude of horizontal displacement. In the same manner, the solutions $x_{r-1}=u\eta^{r-1}e^{i\omega t}, x_{r+1}=u\eta^{r+1}e^{i\omega t}$ also exist for the r-1th and r+1th lumped mass. Substitution of these solutions into Eq. 1 yields

$$\{\eta^2(-k)+\eta(-m\omega^2+2k)+(-k)\}\cdot u=0 \tag{2}$$

Ignoring the trivial solution, the eigenvalue η to a frequency ω can be obtained, which satisfies the equation $\eta^2(-k)+\eta(-m\omega^2+2k)+(-k)=0$

$$\eta=\frac{(-m\omega^2+2k)\pm\sqrt{(m\omega^2-2k)^2-4k^2}}{2k} \tag{3}$$

Eq.3 can be written by exponential function $\eta = a\cdot e^{\pm i\phi}$, in which $a=\sqrt{(\mathrm{Re}(\eta))^2+\mathrm{Im}(\eta))^2}$, $\phi=\cos^{-1}(\mathrm{Re}(\eta)/a)$. From this, another expression of the solution can be gained

$$x_r = u\cdot a^r e^{\pm ir\phi}\cdot e^{i\omega t}=u\cdot a^r e^{i(\omega t\pm r\phi)} \tag{4}$$

Three types of waves can be determined as follows, according to the relation between ω and k/m.

(1) Case 1: $\omega^2 < 4k/m$, ϕ is real; the wave propagates

(2) Case 2: $\omega^2 = 4k/m$, $\phi = 0$; standing wave

(3) Case 3: $\omega^2 > 4k/m$, ϕ is imaginary; exponential mode

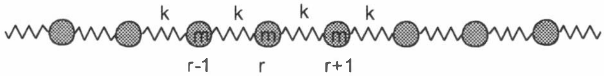

Fig.1 Model of mass-spring system

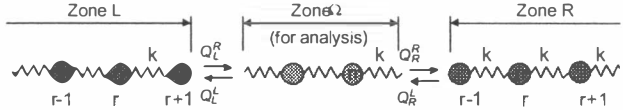

Fig.2 Force on boundary of zone L, R

3 FORMULATION OF BOUNDARY CONDITION

Let us consider reactions of forces to zone Ω for analysis in Fig.2, which are acting on the right-end of zone L or acting on the left-end of zone R. When considering r -1th mass of zone R, the relation of force and displacement in horizontal direction can be written as $f_{r-1} = k(x_{r-1} - x_r)$ (5)

The joint force that is transmitted from the zone Ω to right can be written as follows using complex joint force amplitude. $Q_R^R = f_{r-1} = f_R^R \cdot e^{i\omega t}$ (6)

The upper subscript of complex joint force amplitude shows direction of wave propagation, and the lower one shows zone considered. Substitution into Eq. 5 of the displacement x of Eq.4 and joint force f of Eq.6 gives the follow equation, where $r = 1$. $f_R^R = ku(1 - ae^{-i\phi}) = \left(k - kae^{-i\phi}\right) \cdot u = R_R \cdot u_R^R$ (7)

In the same manner, another boundary conditions can be obtained.

4 FORMULATION CONSIDERING GROUND VIBRATION

In order to consider ground excitation, the case that spring k' is added to the model of Fig.1 will be considered as shown in Fig.3. The detailed content is written in the full paper.

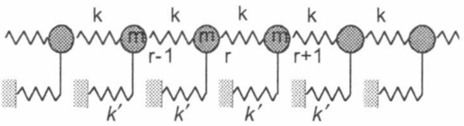

Fig.3 Model considering grounding vibration

5 DAMPING EFFECT OF ENERGY RADIATION

In problems of dynamic unbounded medium-structure-interaction analysis, the damping effect of energy radiation of outgoing waves has already been evaluated [4]. When earthquake partially applies to an infinitely long elevated bridge, e.g. zone Ω shown in Fig.2, zone Ω will be excited. And some energy may radiate to the zone L and R. The radiation of energy results in damping effect. In this section, numerical analyses were carried out with various cases to evaluate that radiation damping. In calculation, the system shown in Fig.3 was considered. The acceleration of ground excitation is cosine wave. That is,

$\{a_0\}_\Omega = 50\cos\omega t$, $(0 \le t \le 10\,\text{sec})$

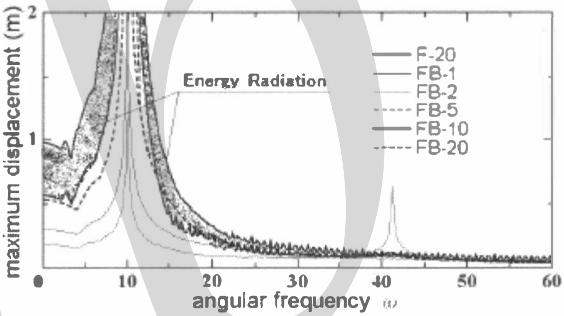

Fig.4 Maximum displacement in frequency domain

Total time increment for analysis is 8192. The maximum displacement by FB-1, FB-2, FB-5, FB-10, FB-20 are plotted as a function of frequency ω in Fig.4. The curves of waves do not show much difference by the increase of number of masses beyond 10. The maximum displacements of FB-20 are about 60% of that of F-20 except near the frequency of 2nd standing wave, where $\omega = 41.23$.

6 CONCLUSIONS

In this paper, using mass-spring model, energy-transmitting boundary conditions were formulated. The relations between ω and k/m, represent the types of waves. Even if the wave does not propagate, it cannot be ignored in formulation. The value of ***a***, has different value even with the same propagating condition. Because of its importance, ***a*** is considered to be inserted to transmitting boundary. In the formulation considering ground vibration, only the ground vibration of zone Ω was taken into account, not the ground vibration of zone L and R. If ground excitation applies to a part of the structure, its energy may be radiated to both infinite zone L and R. The radiation damping was calculated by the analysis of continuous mass-spring models with the transmitting boundary presented herein.

REFERENCES

[1] Lysmer, J. and Wass, G. : Shear wave in plane infinite structures, Journal of the Engineering Mechanics Division. ASCE, Vol.98, No.EM1, Proc. Paper 8716, February, 1972, pp.85-105

[2] Miwa, K. and Tanabe, T. : Study of the transmitting boundary for semi-infinite girder structure, Proceeding of the Japan Concrete Institute, Vol.18, No.2, pp.299-304, 1996 (in Japanese)

[3] Muto, K. : Dynamic Analysis Of Structure, Maruzen, pp.245-248, 1966 (in Japanese)

[4] Wolf, J. : Dynamic soil-structure interaction, Prentice-Hall, Inc., 1985

NUMERICAL EVALUATION ON SEISMIC PERFORMANCE OF REINFORCED CONCRETE BRIDGE PIERS USING DYNAMIC LATTICE MODEL

Tomohiro Miki Manakan Lertsamattiyakul Junichiro Niwa
Department of Civil Engineering, Tokyo Institute of Technology, JAPAN

Keywords: reinforced concrete (RC) bridge piers, dynamic lattice model analysis, seismic performance, carbon fiber reinforced plastic sheet (CFS)

1 INTRODUCTION

In this study, in order to predict the behavior of RC bridge piers subjected to earthquake motion, the dynamic lattice model analysis [1] including the buckling model of the reinforcing bar [2] is carried out. The static lattice model is verified for three RC bridge piers strengthened by the carbon fiber reinforced plastic sheets (CFS) [3]. The comparison of analytical results using the static lattice model with the experimental results of RC bridge piers subjected to static reversed cyclic loading is conducted. Then, the dynamic lattice model analysis is carried out for the same RC bridge piers as the static analysis strengthened by CFS.

2 ANALYTICAL RESULTS AND DISCUSSIONS

2.1 Outlines of the experiment

The experimental work of RC bridge piers subjected to reversed cyclic loading tested by Ogata et al. [3] was adopted for the comparison with analytical predictions. The details and dimensions of piers are shown in **Fig.1**.

The reversed cyclic loading is provided by horizontal cyclic displacement at a height of 2600 mm from the top of the footing under constant axial compression (144kN). The displacement amplitude is stepwisely increased as the magnitude of $n\delta_y$ with 1 cyclic during each step.

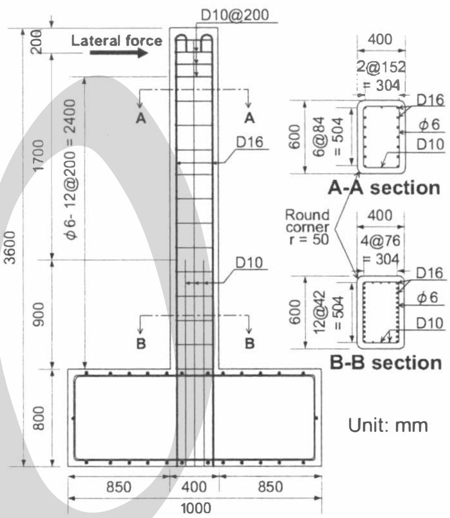

Fig.1 Outlines of the specimen

2.2 Static lattice model analysis

A static lattice model used to analyze the test specimens is shown in **Fig.2**. The relationships of lateral force-lateral displacement at the top of the pier calculated from the static lattice model analysis are shown in **Figs.3 and 4**, in which the experimental results of the C-1 pier (with flexural and shear strengthening by CFS and with cut-off of longitudinal reinforcing bar) and the C-3 pier (with shear strengthening by CFS and without cut-off of longitudinal reinforcing bar) are also exhibited. It can be seen that the response of the C-1 pier from the analysis including the buckling model indicates the slight pinching and the decrease in the energy dissipation capacity. Similarly, as can be understood from the analytical result of C-3 pier shown in **Fig.4**, the ductility of C-3 pier is very close to the experimental one. Therefore, the static lattice model analysis including the buckling model of reinforcing bar can predict the mechanical behavior of a RC pier accurately, even if the buckling occurs.

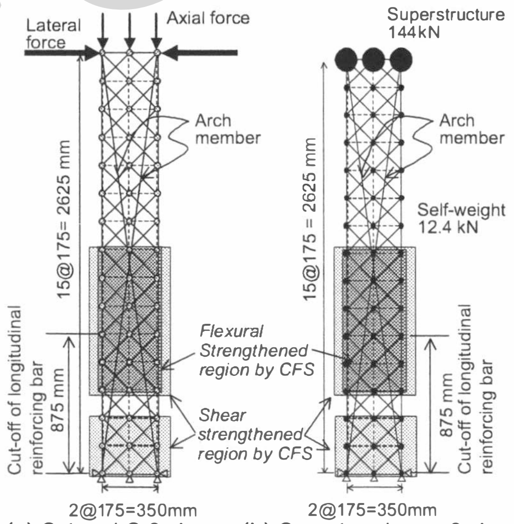

(a) C-1 and C-3 piers **(b)** Case 1 and case 3 piers

Fig.2 Outlines of the static and dynamic lattice models

2.3 Dynamic lattice model analysis

A dynamic lattice model used to analyze the tested specimens is shown in **Fig.2**. The targets for the dynamic lattice model analysis are the RC bridge piers, which are the same dimensions and mechanical properties as the C-1 piers examined in the static analysis. The analytical cases are explained in **Table 1**.

The relationships between the base shear force and the top horizontal displacement of case 1 and case 3 piers are shown in **Fig.5**. It seems that the analytical result of the case 1 pier predicts the large deformation with the slight pinching. In contrast, the response of the case 3 pier indicates the significant energy dissipation capacity after the yielding of longitudinal reinforcing bar. This means the buckling occurs in the case 1 pier, but does not happen in the case 3 pier. The analysis for the case 1 pier without considering the buckling in the dynamic lattice model is also conducted. The comparison of the results with and without including the buckling model in the analysis indicated that the neglect of buckling results in slight underestimation for the response displacement and also residual displacement.

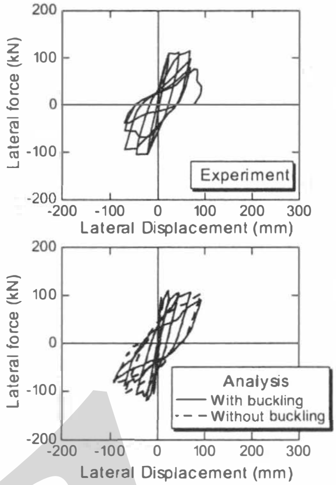

Fig.3 Load-displacement relationship of C-1 pier

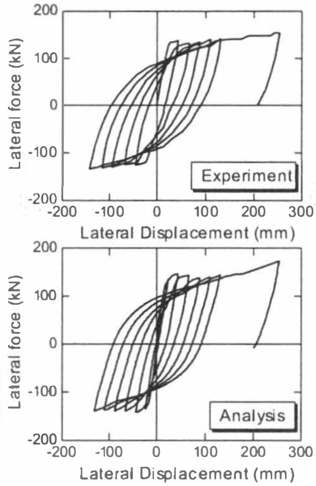

Fig.4 Load-displacement relationship of C-3 pier

Table 1 Analytical cases of the dynamic lattice model

ID	Longitudinal reinforcement	Strengthened region by CFS	
		0 – 500 (mm)	500 – 930 (mm)
Case 1	With cut-off	–	–
Case 3	With cut-off	Transverse	Transverse

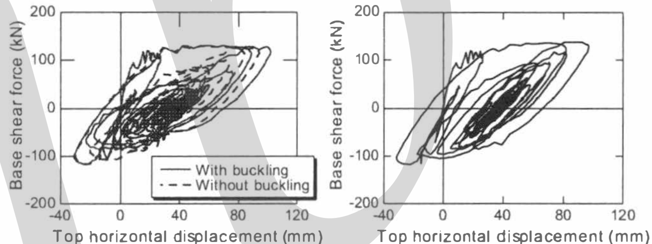

(a) Case 1 pier **(b)** Case 3 pier

Fig.5 Base shear and top horizontal displacement relationship

3 CONCLUSIONS

1. It has been confirmed that the static lattice model analysis including the buckling model of reinforcing bar can predict the overall mechanical behavior of a RC bridge pier strengthened by the carbon fiber reinforced plastic sheet (CFS) very nicely, such as the load-carrying capacity and the post peak behavior.
2. By the dynamic lattice model analysis including the buckling, it is found that the post peak behavior can be captured with an appropriate accuracy as well as the static analysis.
3. It has been found that the buckling affects the post peak behavior when the buckling occurs. Furthermore, it is confirmed that the neglect of the buckling often results in an underestimation of the response displacement and also the residual displacement, which might lead to unsafe design.

REFERENCES

[1] Niwa, J., Choi, I.C., and Tanabe, T.: Analytical Study for Shear Resisting Mechanism Using Lattice Model, Concrete Library of JSCE, No.26, pp.95-109, Dec., 1995.

[2] Dhakal, R. P.: Enhanced Fiber Model in Highly Inelastic Range and Seismic Performance Assessment of Reinforced Concrete, Doctoral thesis, The University of Tokyo, Tokyo Japan, Sep. 2000.

[3] Ogata, N., Andoh, H., Matsuda, T., Kobatake, Y. and Ohno, S.: Seismic Retrofitting Using Carbon Fiber for Existing RC Bridge Piers, Journal of Construction Management and Engineering, JSCE, No.540/VI-31, pp.85-104, Jun., 1996 (in Japanese).

SEISMIC PERFORMANCE OF PRESTRESSED CONCRETE PIERS

Takuya Mori, Dong-kyu Park
P.S.Corporation
JAPAN

Shoji Ikeda
Yokohama National University, JAPAN

Tamio Yoshioka
Oriental Construction Co., LTD. JAPAN

Keywords: seismic performance, prestressed concrete pier, energy absorption, residual displacement, ductility factor, pseudo-dynamic test, nonlinear hysteresis model

1. SUMMARY

In order to investigate the utilization of vertical prestressing in bridge piers, a systematic research has been carried out in Japan Prestressed Concrete Engineering Association (JPCEA). The reversed cyclic loading tests showed that reinforced concrete columns with appropriate prestress have enough ductility and remarkably decrease the residual displacement. The pseudo dynamic tests showed that they have superior seismic performance against the near field earthquake such as the Kobe Earthquake. This paper describes the experimental results and the evaluation of seismic performance achieved by introducing prestress into reinforced concrete columns, and proposes the nonlinear hysteresis model for prestressed concrete piers.

2. TEST SPECIMENS

The specimens were 40cm square in cross section and the loading span was 1.5m from the top of footing. The following factors are selected as experimental variables: (1) cross section shape (solid or hollow), (2) axial stress due to topside load (1 or 4MPa), (3) compressive strength (35 or 60 MPa), (4) level of prestress (0, 2, 4 or 8MPa), (5) bonded or unbonded prestressing tendon and (6) characteristic of precast segmental column.

3. EXPERIMENTAL RESULTS

Figure 5 and 6 compare the accumulated energy absorption and the residual displacement respectively of the individual specimens with the level of prestress. The accumulated energy absorption decreased as the level of prestress increased and this tendency did not largely varied with the displacement. And also the residual displacement decreased in the same way, but the specimens prestressed having 4MPa and 8MPa (S-3 and S-5) didn't change very much.

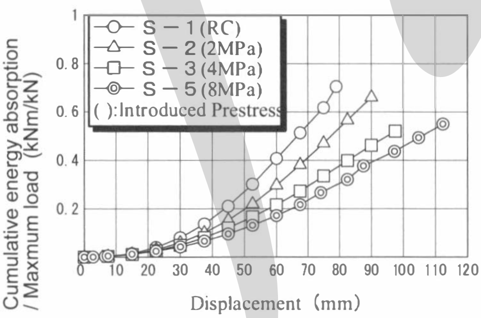

Figure 5: Cumulative energy absorption

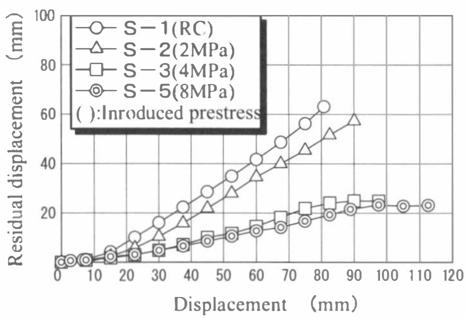

Figure 6: Residual displacement

Figure 7 shows the ductility factors of the specimens. Here, the ductility factor μ is the ratio of the ultimate displacement to the yield displacement. The ductility factor was about 6 or 7 for RC specimens, but it was improved as the introduced prestress was increased.

Therefore, the deformation capacity is improved as the level of prestress. On the other hand increase of the axial stress by the external axial force caused decrease in ductility factor shown in Figure 8. From these results it has been found that the effect of prestressing is different from the external axial force on the deformation capacity, though both introduce compressive stress to the concrete.

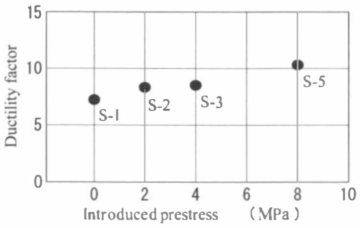

Figure 7: Ductility factor and Introduced prestress

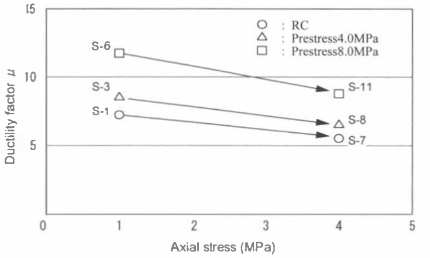

Figure 8: Ductility factor and axial stress

4. NONLINEAR HYSTERESIS MODEL FOR PC PIERS

Based on the experimental results, we studied the nonlinear hysteresis model for PC piers. The behavior of PC piers after the yield of the member is somewhere between the model for RC members and the origin-oriented model. We proposed a nonlinear hysteresis model shown in Figure 11.

Here The sharing factor of prestressing tendon γ means the contribution of the PC tendons to the ultimate flexural strength.

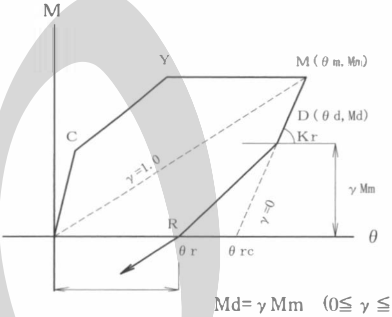

$Md = \gamma Mm \quad (0 \leqq \gamma \leqq 1.0)$

$\theta r = (1-\gamma)\theta rc$

(when $\gamma \geqq 0.8$: $\gamma = 0.8$)

Figure 11: Nonlinear hysteresis model for PC piers

5. CONCLUSIONS

1) Rapid desrease in flexural capacity was not found to the PC specimens, even after the vertical reinforcement buckling, but they showed ductile behavior. While RC specimens showed rapid decrease in load carrying capacity after the vertical reinforcement buckling.

2) The PC specimens had fewer flexural and shear crack in number than the RC specimens.

3) As the level of the introduced prestress increased, the energy absorption decreased. However, the residual displacement gets smaller as the sharing factor of prestressing tendon: γ increases.

4) According to the results of the pseudo-dynamic tests, the response of the RC specimens tended to deviate to one side in the case of the near field earthquake and the residual displacement became larger. However, the response of the PC specimens did not deviate and showed a much smaller residual displacement response than that of the RC specimens because of their high restoration capability. It is considered that the effect of hysteresis damping is small on the response.

5) The proposed nonlinear hysteresis model was verified to have sufficient accuracy from the test results.

6) According to the additional experiments to study the effect of the prestreeing level, it would be recommendable to keep λ ratio relatively higher, being able to yield prior to buckling of longitudinal reinforcement.

References

[1] *Guideline on the seismic design for prestressed concrete piers* : JPCEA, 1999.11

[2] Ikeda S., Mori T. and Yoshioka T.; *The Experimental Study on the Seismic Performance of Prestressed Concrete Piers*, Journal of Prestressed Concrete, Vol. 40, No.5, 1998.9.10

NEW GENERATION OF EARTHQUAKE RESISTING SYSTEMS

José I. Restrepo
Associate Professor
University of California, San Diego
UNITED STATES

Keywords: energy dissipation devices, precast concrete, prestressed concrete, self-centering systems

1 INTRODUCTION

The impact and cost of the consequences of damage caused by earthquakes worldwide during the past two decades have raised serious questions of whether current building seismic design philosophies are satisfying the needs of modern society. Most seismic design standards are based on a life-prevention approach where building structural and non-structural damage is accepted providing that collapse is avoided. No other economic parameters, such as the cost of damage to equipment and stored goods and the cost associated with loss of operation following a moderate/strong earthquake, are currently accounted for in the design process. The rapid advance in technology has meant that often, in many countries, the cost of equipment, of stock and the loss of business operation in the aftermath of a moderately or strong earthquake are higher than that of the building itself. As a result, and in spite of efforts aimed at improving seismic design methodologies and construction practices, economic losses due to earthquakes have increased rather than decreased in the past decades.

This paper describes a number of emerging structural wall systems aimed at minimizing seismically induced structural damage. The design of the system within a displacement-based seismic design procedure is also discussed herein. Finally, the paper describes the results of experimental work performed on these systems.

2 NEED FOR DEVELOPMENT OF NEW STRUCTURAL SYSTEMS

The cost associated with the loss of business operation, damage to equipment and structural damage following a moderately strong earthquake can be significant to modern society, particularly in those centers of advanced technology. Such cost is often comparable, if not greater, to the cost of the building itself. Whilst the concept of inelastic response is very appealing, it has two main drawbacks: First, regions in the principal lateral force resisting system will be sacrificed in moderately strong earthquakes and in need of repair, or damaged beyond repair in strong earthquakes.

Another important issue in seismic design nowadays deals with current societal performance expectations. While the principle of mitigating loss of life in a strong earthquake still prevails, society expects buildings to survive a moderately strong earthquake with no disturbance to business operation. This implies that repairs of incipient structural damage may not be economical and may no longer be tolerated in small and moderately strong events.

A primary objective of the design of these systems is to ensure a self-centering response. These systems are jointed as non-linear deformations occur only at some specific connections. Typical responses of jointed systems are shown in Fig. 1. A rocking-only system behaves essentially non-linearly elastic whereas hybrid systems are explicitly designed for energy dissipation and typically the wall toes and the contacting surface at the foundation are armoured with steel plates to confine the concrete and prevent any cosmetic damage from occurring prematurely. Equivalent viscous damping ratios in hybrid systems can theoretically reach 0.287 due to hysteretic energy dissipation.

3 EXPERIMENTAL WORK

Rahman and Restrepo, Holden et al. and Toranzo et al. have reported testing on a variety of jointed systems. A result of the experimental program showing the self-centering characteristics of a hybrid wall system are shown in Fig. 2.

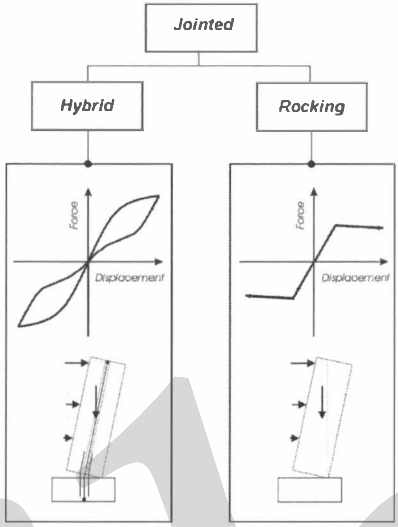

Fig. 1 Reversed cyclic lateral force – lateral displacement response of jointed systems

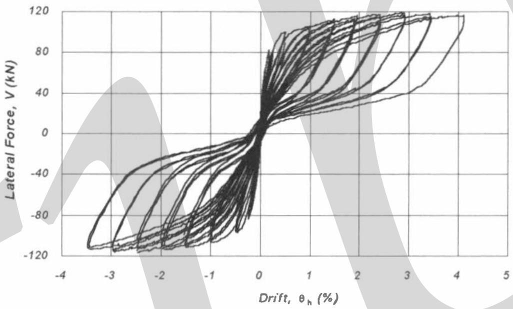

Fig. 2 Hysteretic response of a jointed and a hybrid wall tested by Rahman and Restrepo

4 CONCLUSIONS

1. This paper described the behavioural concepts pertinent to a new generation of structural concrete jointed systems.

2. The main advantages of the jointed systems described are the large lateral displacement capacity, the lack of structural damage associated with large displacements and the ability to return to the original position upon unloading.

3. Jointed systems can be explicitly designed with hysteretic energy dissipation devices to provide energy dissipation with a theoretical equivalent viscous damping up to 0.287.

4. The self-centering response characteristics of jointed systems make them ideal for use with a displacement-based design approach. The equivalent viscous damping is, however, amplitude dependent. This dependence must be considered in design.

5. Results from non-linear time history analyses indicate that the dynamic response of hybrid wall systems, as reflected by the bending moment and shear force envelopes, is similar to that of conventional monolithic wall systems.

6. Quasi-static and shake table experimental work have clearly shown the benefit of jointed systems.

PRECAST PRESTRESSED CONCRETE FRAME WITH BASE ISOLATION SYSTEMS

Kimiya Hamada, Fu Jinhua, Kazunori Osako and Mitsuo Hayashi
P.S.Corporation
JAPAN

Keywords: precast prestressed concrete, base isolation systems, earthquake response

1 INTRODACTION

Since 1995 (happened Hyogoken-ken Nanbu Earthquake), a precast prestressed concretre (PC) frame with base isolation systems was developed gradually as a new structural framing for the building in Japan. The design concept of a precast PC structural systems was considered to be an execution method for less man-power by using precast members, utilizing the mechanical characteristics of PC member, and preventing the damage of constructions under serious earthquake motions. The mechanical characteristics of a normal PC member is to perform the excellent restoring behavior under service loading, so the energy dissipation of a member in the relation of load-deflection was less than that of the other members. Because of the response deformation of PC structure under earthquake motions is performed to be larger than that constructed by the other structural members. However, the response performances of the structure by the less energy dissipation could be supplemented perfectly by the base isolation systems. Therefore, a precast PC structure with base isolation systems was projected often in Japan. The design practices for the structures with base isolation systems was first established due to the Building Standard Enforcement Regulation (No.2009) by Ministry of Construction accompanied by Japanese Building Law Enforcement Order amended in June 2000. The structural design, and the earthquake performances in the existing precast PC housing with base isolation systems are discussed.

2 OUTLINE OF BUILDING EITH BASE ISOLATION SYSTEMS

The existing structure with base isolation systems is a 6-story precast PC housing. The typical floor plan, arrangement of laminated rubber bearings, and structural elevation are shown in Fig.1, 2 and 3.

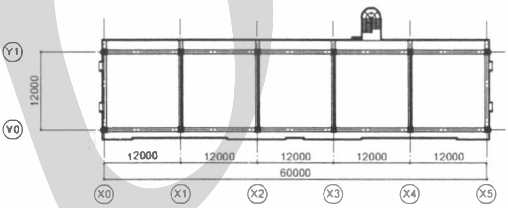

Fig.1 Typical floor plan

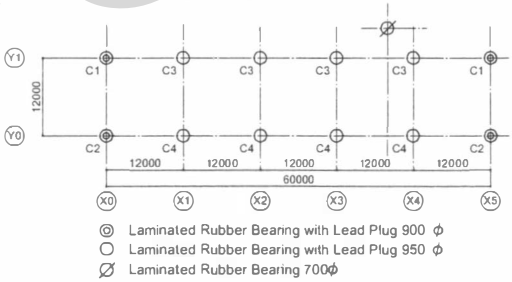

Fig.2 Arrangement of laminated rubber bearings

3 INCREMENTAL LOAD ANALYSIS

Incremental load analysis of structure was carried out to investigate the collapse mechanism of frame, lateral load resisting capacity, the member ductility factors, and nonlinear story lateral load resisting data to make an analytical model of the structure in the earthquake response analysis. In the analysis, the basement of the structural frame was assumed to be fixed on the foundations. Lamped mass models of structure maid up by the relation of story shear force and interstroy drift are listed in Table 3.

4 NONLINEAR EARTHQUAKE RESPONSE ANALYSIS

Nonlinear earthquake response analysis using lamped mass model was carried out to investigate the seismic performances of a precast PC frames with base isolation systems. Analyzing method was as numerical integration by the Newmark's β principle (a vale of β taken to be 1/4). A damping model matrix was assumed to be proportional to the instantaneous stiffness matrix. The first mode

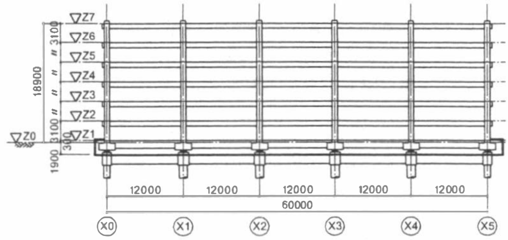

Fig.3 Structural elevation

damping factor was assumed to be 3%, and that for higher models are assumed to be proportional to mofel frequencies.

4.1 Hysteresis Models and Earthquake Motions

A hysteresis model used in earthquake response analysis is nonlinear elastic model for lateral story shear stiffness in the upper structure. That of laminated rubber bearing with lead plug is used as modified bi-linear model. Four earthquake motions of El Centro 1940 (NS), Taft 1952 (EW), Hachinohe 1968 (EW), and simulated record representing the execution site were used in the analysis. Amplitude of the records was scaled to yield the maximum ground velocity of 50 cm/sec.

4.2 Analytical Results

The maximum response lateral shear force and the maximum interstory drift in each direction of the housing structure are shown in Fig.4 and 5.

5 CONCLUSIONS

Nonlinear earthquake response analysis of the precast PC housing with base isolation systems was carried out using four earthquake motions. The analytical results were verified to investigate the effect of base isolation systems used. From verification of those results, the following conclusions may be drawn;

1) Response story drift of the precast prestressed concrete housing with base isolation systems was small significantly comparing with the response of that without one.
2) The maximum response lateral shear forces and interstory drifts of the precast PC housing satisfy the response criteria defined in the normal buildings with large margin.
3) The precast PC housing could be designed effectually by using base isolation systems.

REFERENCES

[1] Kabeyasawa, T., H. Shiohara, and S. Otani, "Analysis of the Full-Scale Seven-Story Reinforced Concrete Test Structure", JOURNAL OF THE FACULTY OF ENGINEERING, UNIVERSITY OF TOKYO, Vol.XXXVII, No.2 (1983).

Table 1 Lamped mass models

Story	Longitudinal direction initial stiffness (kN/mm^2)	Cracking point		Yield point	
		dc(cm)	Qc(kN)	dy(cm)	Qy(kN)
6	750	3.19	2393	15.58	4014
5	1009	3.87	3902	15.19	7723
4	1085	4.49	4868	18.11	10348
3	1142	5.32	6075	20.95	12497
2	1279	5.95	7602	22.16	14046
1	1819	5.03	9153	20.36	14938

Story	Transverse direction initial stiffness (kN/mm^2)	Cracking point		Yield point	
		dc(cm)	Qc(kN)	dy(cm)	Qy(kN)
6	7583	---	---	---	---
5	12393	---	---	---	---
4	14791	1.86	27496	10.84	36593
3	16219	1.70	27508	10.34	37471
2	17037	1.61	27498	10.25	38289
1	15934	1.77	28155	11.31	39813

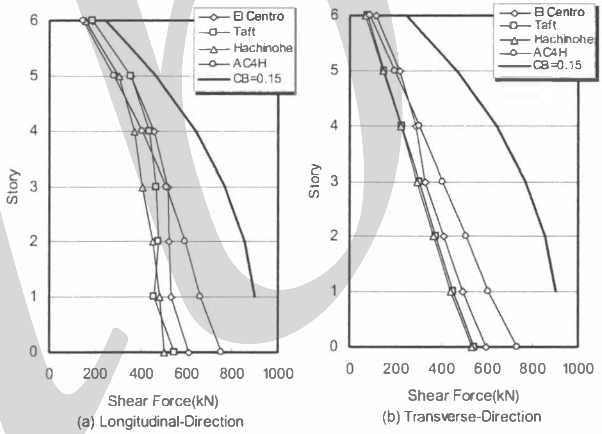

Fig.4 The maximum response lateral shear force

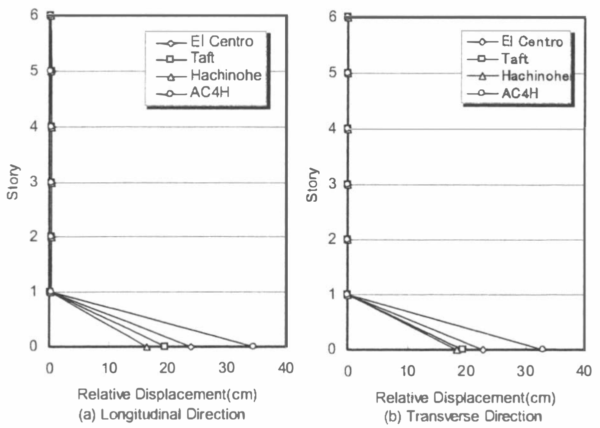

Fig.5 The maximum interstory drift

SEISMIC RESPONSE CHARACTERISTICS OF SEISMICALLY ISOLATED BRIDGE CONSIDERING HARDENING EFFECT OF SEISMIC ISOLATOR

Yukio Adachi
Hanshin Expressway Public Corporation

Shigeki Unjoh
Public Works Research Institute

Keywords: Hardening Effect, Seismically Isolated Bridge, Seismic Isolator, Reliability

1 INTRODUCTION

Seismically isolated bridge shows non-linear response both at seismic isolators and columns where intensive earthquake hits the bridge. Such non-linear response characteristics are influenced by the hardening effect of the seismic isolator and over-strength effect of the bridge column. In order to clarify such non-linear behavior of the seismically isolated bridge, seismic response analyses are conducted considering hardening effect of the seismic isolator and uncertainties of non-linear parameters of the seismic isolator and the bridge column using Monte calro techniques. Based on the result of the analyses, the seismic reliability of isolated bridges are evaluated using safety index β.

2 UNCERTAINTY OF MECHANICAL PROPERTIES OF BRIDGE COLUMN AND ISOLATORS

First of all, in order to clarify the stiffness and strength characteristics and their uncertainty, the strength and the ductility capacity of the rectangular reinforced concrete column commonly used for highway bridges in urban area in Japan are investigated by considering the uncertainty of material strength, elastic modulus, cross sectional area, dimensions, and axial force using Monte calro technique. As the result of the simulation, it is found that the over strength characteristics of material property reduce ductility capacity of the reinforced concrete section because the yield curvature increases due to over strength characteristics and its increase is more than ultimate curvature. On the contrary, the average yield strength increases due to the over strength characteristics of steel reinforcement.

Secondly, in order to investigate the uncertainty of mechanical properties of seismic isolators, results of cyclic loading tests of small-scaled models, large-scaled, and actual bearings are statistically studied using in total of 548 of LRB, 700 of HDR, and 187 of RB data. As the result of the statistical study, it is obtained that the uncertainty of equivalent stiffness and damping ratio of HDR is generally less than that of LRB and RB. The amazing fact that almost the same level of uncertainty of stiffness and damping characteristics of the seismic isolators as the stiffness distribution of the commonly used reinforce concrete columns even though the isolators are manufactured in factory so that the uncertainty of those isolators had been considered smaller than that of bridge column. The average rupture strain of LRB and RB are around 330%. On the contrary, the average rupture strain of HDR is over 500%. The average ultimate shear capacity of LRB and RB is around twice of the shear strength at 250% shear strain and also the distribution shapes of LRB and RB are very similar. These differences might be resulted by the rubber material used for isolators. LRB and RB are made from natural rubber and HDR is made from artificial rubber.

3 SESIMIC RESPONSE ANALYSIS OF SEISMICALLY ISOLATED BRIDGES

As for the seismically isolated bridge subjected to intensive earthquake, the nonlinear response of the seismic isolator and the nonlinear response of the bridge column interact each other so that the seismic behavior of the isolated bridge is greatly influenced by the hardening effect and stiffness and strength uncertainty. In order to investigate this interaction effect induced by over strength and hardening effect, seismic response analyses are conducted considering stiffness and strength uncertainties by Monte calro techniques. The hardening model used in this study is shown in **Figure 1**.

The seismic response analyses are performed by changing natural period of the seismic isolators and bridge columns using 2 DOF model. The input seismic motion is the modified JR Takatori ground motion that is fit to the Japanese design spectra. The distribution of the dynamic parameters used for the isolators and columns were set by considering the results of the study descried above. The parameters are assumed to follow the normal distribution and independent each other. The trial number for the simulation was 20,000.

Figure 2 and **3** shows the summary of the result of the case of LRB. The hardening response reduces the response displacement of the isolator but increases the response force of the isolators and also the response ductility of the column. The ductility change ratio is significantly high where much elongation of natural period by isolator is expected in design. In this way, the hardening effect strongly influences the interacted response between the isolator and the column. Almost the same results are obtained for HDR and RB except that the hardening response of RB only increases the response displacement of the isolator. As for the safety index of the case of LRB with considering hardening effect, the safety index is around 1.0 for displacement and around 1.5 for force. The safety index of the column is varied from 2.0 to 0.0 depending on the period of the isolator.

4 CONCLUSION

It can be concluded that the hardening effect and over strength characteristics are strongly influenced to the seismic response and the seismic safety of the seismically isolated bridge. Especially the hardening effect of seismic isolator increases the ductility response of the column; furthermore, this effect is more significant where much elongation of natural period by isolator is expected in design.

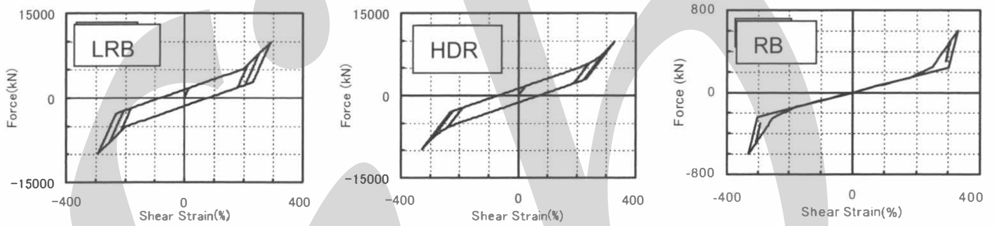

(a)LRB (b)HDR (c)RB

Figure 1. Hysteretic modeling of seismic isolators with hardening effect

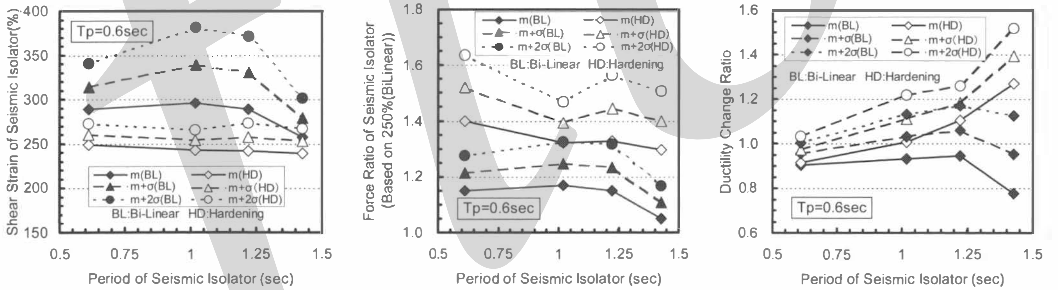

(a) Response shear strain of isolator (b) Response shear force of isolator (c) Response ductility of column

Figure 2. Seismic response characteristics of the seismically isolated bridge –Period dependency (LRB)-

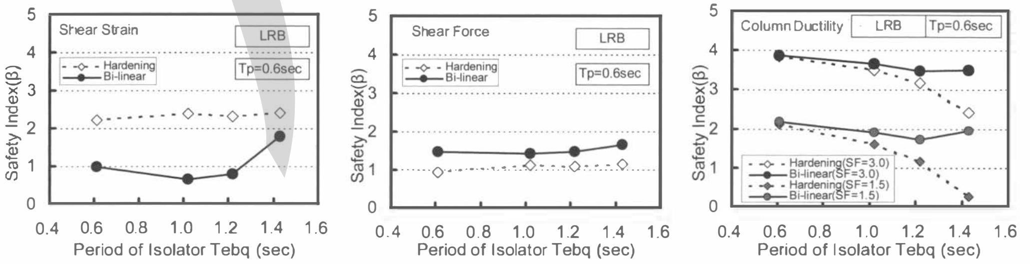

(a) Response shear strain of isolator (b) Response shear force of isolator (c) Response ductility of column

Figure 3. Safety index of the seismically isolated bridge -Period dependency- (LRB)

SEISMIC BEHAVIOR OF PRE-STRESSED CONCRETE CABLE-STAYED BRIDGES SUBJECTED TO FAULT DISPLACEMENT

Keitaro KONUMA
Doctor course, Kyushu University
JAPAN

Junghowan LEE
Daiichifukken
JAPAN

Tatsuo TAKAHARA
Yamaguchi Prefecture
JAPAN

Sanehiro ARIMURA
New Structural Engineering, Ltd.
JAPAN

Hisanori OTSUKA
Kyushu University
JAPAN

Junji OGATA
ingerosec Corporation
JAPAN

Keywords: cable-stayed bridge, extra-dosed bridge, seismic design, nonlinear analysis, fault displacement

SUMMARY

In the seismic country Japan, the effort to improve the earthquake resistant capacity of structures has been done from the experience of earthquake damage up to now. After the 1995 Hyogo-ken Nanbu Earthquake, the seismic motion by the inland direct strike type earthquake is designated in the specifications in Japan in addition to the seismic motion by the plate boundary type large-scale earthquake. However, as observed in the 921 Chi-Chi Earthquake (1999) in Taiwan, the damage to structures inflicted by fault is noticed. It is an urgent topic to make clear the influence of fault displacement because of the existence of bridges extending over active faults in Japan. In this paper, 3 pre-stressed concrete cable-stayed bridges were taken as some examples to verify their behavior subjected to fault displacement.

1 INTRODUCTION

If any fault appears across a bridge, its abutments and piers move in large scale, and the bridge shows different behavior from the case that it is affected by only seismic inertia force.[1][2] In case of cable-stayed bridge and extra-dosed bridge, the girders are suspended with stay cables from pylon, so it is difficult for us to image how the collapse of the members happens under the movement of their substructures. But, even if the member doesn't collapse, it is important for ensuring the seismic safety of the cable-stayed bridges crossing fault by not only seismic inertia force but also fault displacement. Especially, cable-stayed bridges have the small ratio of the height of girder to the length of the span, and its stay cables influence the performance of the bridge structures. Considering them, it is necessary to study about the characteristics of behavior and damage of the cable-stayed bridges due to fault displacement.

2 THE SUBJECT BRIDGES OF ANALYSIS

2-span cable-stayed bridge with rigid connection, 3-span cable-stayed bridge with floating suspension system and 3-span extra-dosed bridge with rubber support were chosen for the subject of this study. They have deferent number of span and supporting type of girder, each other.

3 FAULT DISPLACEMENT ANALYSIS AND STRUCTURAL MODELS

3.1 Fault Displacement Analysis

In this study, on the assumption that the fault appears across the bridge, the displacements were forcibly input at the foundations of the bridge model. And, in order to make clear the relation between the direction of fault displacement and the characteristics of the progress of damages, the directions of displacement were limited to only 5 directions, as shown in Fig.1. Still more, in order to make sure the relation between the scale of fault displacement and the scale of damage, these displacements were input little by little.

3.2 Structural Models

The subject bridges were modeled with the 3-D framework models, considering the material nonlinear characteristics of the members.

For Modeling of concrete members, the material nonlinear characteristics were considered with the relation between bending moment and curvature (ϕ), the M - ϕ curve. Especially for the PC members of the girders, in addition to the above modeling of RC members, elastic limit and yielding of the tendons were considered.

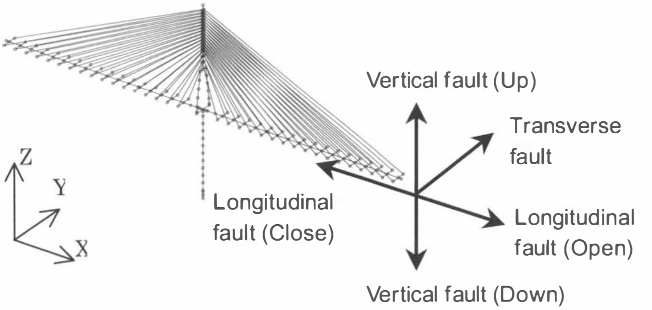

Fig. 1 Direction of fault displacement for the analyses

For modeling of the stay cables, not only the yield of cables but also the characteristics of the cable structure for the compression road was considered. It was that the cables don't resist against the nominal compression force but the tensile force.

4 RESULTS OF ANALYSES

4.1 2-spans cable-stayed bridge with rigid connection

For the vertical displacements and transverse displacement, the damages concentrated into the girder. For the longitudinal displacements, the damages in the pier dominated, because the pier was pushed horizontally and bended at the rigid connection with the girder and the pylon.

4.2 3-spans cable-stayed bridge with floating suspension system

For the fault across the side span, remarkable damages appeared into the P1 and the girder, but didn't into P2. For the fault across the center span, fatal damage didn't appeared into the piers and pylons. Because the girder was suspended only stay cables, for the vertical displacement and the longitudinal displacement, the girder behaves as a beam, and the damage due to bending concentrated into the center of main span. For the transverse displacement, the damage distributed to each side of the fault.

4.3 3-spans extra-dosed bridge with rubber support

The pylons weren't damaged in any cases, and the piers were damaged only longitudinal displacement between P1 and P2. But for these longitudinal displacements, the girder hardly suffered damage, because the girder and the pylons were separated with the piers after that the supports broke.

5 CONCLUSION

In this study, it was confirmed that the 3 cable stayed PC bridges, which were designed in the past, were damaged with yielding of reinforcements by fault displacement of 2.0(m).

ACKNOWLEDGEMENT

This study was done as a part of activity of the committee for the seismic safety of concrete bridges subjected to fault displacement, in Japan Concrete Institute (JCI).

REFERENCES

[1] Otsuka,H., Matsuda,T., Yabuki,W. and Kuriki,S., Damage Investigation report of the 921 Chi-Chi earthquake in Taiwan, Department of civil and structural engineering, Kyushu university, 2/2000
[2] Report of the ductility design subcommittee, The earthquake engineering committee, Japan society of civil engineers, 3/2001

THE INVESTIGATION OF EARTHQUAKE RESISTANCE OF RIGID-FRAME BRIDGES DUE TO FAULT DISPLACEMENT

Wataru Yabuki, Hisanori Otsuka
Kyushu University
JAPAN

Kunio Noguchi, Tsutomu Yoshizawa
Nippon Engineering Consultants Co.,Ltd.
JAPAN

Youzou Masaki, Makoto Shinno
Structure Engineering Center Co.,Ltd.
JAPAN

Daizou Ochi
Sumitomo Construction Co.,Ltd.
JAPAN

Keywords : fault displacement, rigid-frame bridge, earthquake resistance

1 INTRODUCTION

In the chi-chi earthquake that struck in Taiwan on September 21st, 1999, the fault displacement caused much damage to various bridges.
(**Pic 1**) Under such displacement, the damage is also produced in the position which does not consider the plastication in the present seismic design.
However, countermeasures against the fault displacement are hardly discussed in Japan where many faults exist, as in Taiwan.
Therefore, it is important to confirm the safety of bridges designed according to current or old specifications, and to identity the optimum bridge type for fault displacements. In this study, static displacement analysis was carried out for various rigid-frame bridges designed according to Japanese specifications, and the safety against the fault displacement was examined. The degree and direction of fault, spans of the bridge, design specifications of the bridge, bridge pier height, etc. were set as the conditions of the parametric study, and the position where the plastic hinge forms and degree of the damage for each fault were clarified.

2 OUTLINE OF BRIDGES

In this study, three rigid-frame bridges designed according to different specifications were selected. Bridge A is a 3-span continuous rigid frame bridge with bridge piers of different height, which was designed according to the 1980 specifications. This bridge is outlined in **Figs 1**.

3 ANALYTICAL MODEL AND SKELETON CURVE

The superstructure is assumed to be all linear or all nonlinear beam member, and piers are nonlinear beam members. The forced-displacement analysis fot the displacement of the bridge pier and girder edge is carried out assuming that the relative displacement occurs at the center and side spans due to the fault. The following four cases are examined.

1. Case 1 : longitudinal direction (the fault displacement occurs in the center span)

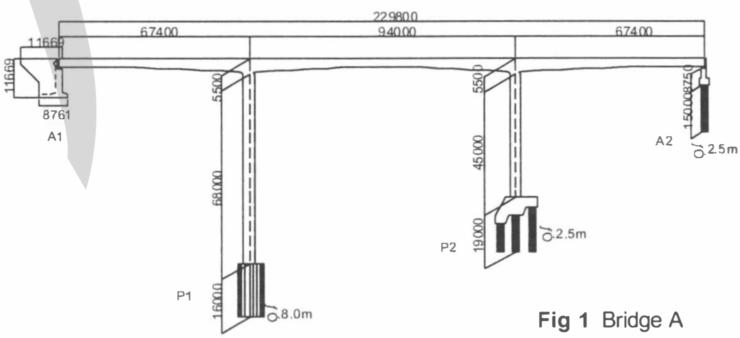

Fig 1 Bridge A

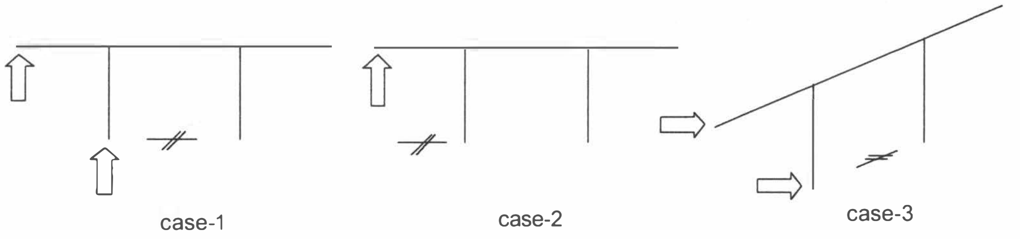

Fig 2 The conceptual scheme of the analysis cases

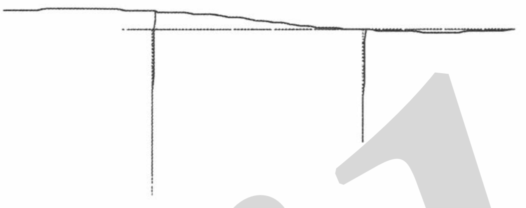

Fig 3 The deformation shape (case-1)

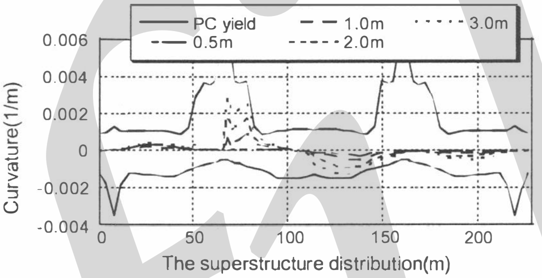

Fig 4 Distribution of curvature at the superstructure (case-1)

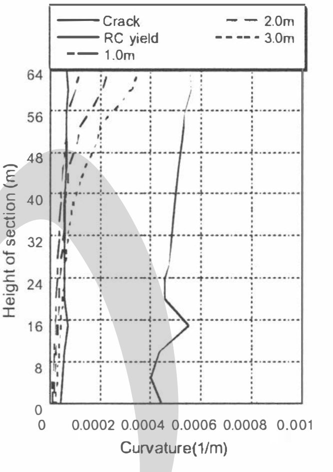

Fig 5 Distribution of curvature at the bridge pier (case-1)

2. Case 2 : longitudinal direction (the fault displacement occurs in the side span)
3. Case 3 : transverse direction (the fault displacement occurs in the center span)
4. Case 4 : transverse direction (the fault displacement occurs in the side span)

The conceptual scheme of the analysis cases are shown in **Fig 2**.

4 ANALYTICAL RESULTS

The analytical result for bridge A is shown in **Fig 3** to **Fig 5**. In this study, the damage of members is shown in the distribution of the response curvature.

5 CONSIDERATION AND CONCLUSION

The results are confirmed that damage occurs in the span where the fault displacement was generated, regardless of the span number. For both vertical and transverse direction displacement, the deformations of the bridge piers are small, and the damage concentrated in the PC girder. Cracks are produced even for the displacement of 0.5 m in the PC girder, and PC steel (for displacement of 3.0 m) of the PC girder quickly yields due to yeild of the reinforcement of the bridge pier.

In new of the fact that seismic design currently assumes that damage occures to the bridge pier base, and that the PC superstructure behaves elastically in the case of fault displacement in an earthquake, new countermeasures are clearly necessary.

BEHAVIOR OF HIGHWAY VIADUCT FRAME STRUCTURES WITH RETROFITTED COLUMNS UNDER CYCLIC LOADING

Wael ZATAR *1, Hiroshi MUTSUYOSHI *2
Yoshito KONISHI *3, and Atsushi MORI *4

*1: D. Eng, Dept. of Civil Engineering, University of Kentucky, Lexington, 40506-0281 KY, USA.
*2: D. Eng, Dept. of Civil and Env. Engineering, Saitama University, Saitama, Japan.
*3: Metropolitan Expressway Public Corporation, Tokyo, Japan.
*4: Ph.D., Japan Engineering Consultants Co. Ltd., Tokyo, Japan.

Keywords: earthquake resistant structures, shear capacity, reversed cyclic loading, shear enhancement, seismic retrofitting.

1 INTRODUCTION

Tremendous damages to bridges in general and to piers in particular were a direct result of the disastrous Hyogo-Ken Nanbu 1995 earthquake in Japan. Many bridges collapsed due to the lack of ductility. Such a catastrophic event led to avenues for questions and research on seismic behavior and possible rehabilitation and/or retrofitting of RC structures, specifically bridges, not only in Japan but worldwide as well. Due to the disastrous event, many RC bridge piers had experienced severe damage and have been retrofitted by the use of steel or concrete jacketing [1].

2 CONCEPT AND PROCEDURES

The operational authority supervising an RC highway viaduct, constructed in Tokyo in 1972, carried out a necessary preliminary assessment of the highway to sustain future earthquakes. It was found that the RC piers lack sufficient ductility because of their inadequate shear reinforcement. Consequently, retrofitting of the RC piers by steel jacketing was employed in response to the first phase of the expressway assessment. Nevertheless, a subsequent assessment of the overall as-built viaducts incorporating the retrofitted piers left doubts that the un-retrofitted parts, including the RC beams and the beam-to-pier connections, may experience undesirable failures thus prohibiting to achieve the overall target ductility during future earthquakes. Accordingly, it was decided to conduct an experimental investigation in the form of two 1/6-scaled models of the viaducts (named S1 and S2) to ascertain the overall behavior, damage propagation, failure mechanism and modes [2]. The main experimental variable was the quantity of shear reinforcement of the RC beams while all details of the other parts were identical. Each specimen consisted of a footing, two identical columns and a beam with two overhanging cantilevers. Analytical investigations declared that it was not expected that the retrofitted columns of the prototypes might experience major damages because of the steel jacketing effect. To simulate the retrofitted columns in the specimens level, columns with an adequate percentage of shear reinforcement (0.38%) were utilized. Strength ratios between the beams and the columns were chosen to represent the as-built ones. The shear reinforcement of specimen S1 represented the least critical quantity (0.05%) of the as-built cases while that of specimen S2 represented the average of many actual cases with comparatively low shear reinforcement ratios (0.1%). Each specimen was tested under statically increasing reversed cyclic horizontal loading and a vertical load at mid-span. Each specimen was subjected to pre-determined displacement excursions. Three repetitions of each cycle were utilized during testing. Concrete and steel strains at various locations, deflections along the beam lengths, axial & lateral displacements and strains were monitored during each test through the use of an extensive instrumentation. Mechanical behavior of the specimens was studied in terms of hysteretic behavior, displacement ductility, damage propagation, and final failure modes. Furthermore, a numerical analysis was then performed to check and/or confirm the applicability of the FE technique to simulate the overall response and behavior. Based on the experimental data, a calibrated base-line FE model was obtained that may serve to identify the parts of each viaduct that requires further retrofitting. Although it was clear that the behavior of specimen S2 was better than that of specimen S1, because of the increased shear reinforcement ratio, the beams of the highway may require additional retrofitting to allow achieving the desired overall structural displacement ductility. Two additional small-scaled specimens (named SR1 and SR2) with retrofitted beams were, then, tested. The specimens had similar dimensions and details to those of specimen S1. The beam of specimen SR1 was retrofitted for shear using two bonded steel plates and anchors while that of specimen SR2 was retrofitted by using U-wrapped laminates of carbon fiber reinforced plastics (CFRP). Although it was observed that the behavior of SR1 was enhanced as a result of the increased shear capacity, the steel plates experienced buckling and de-bonding in the location of the major shear crack in the right side of the beam just prior to failure. Such a de-bonding prevented the beam from attaining further ductility and led to a final shear failure. As for specimen SR2, the use of the CFRP laminates was effective in obtaining a higher ductility and a better overall behavior than those of specimen S1. Nevertheless, peeling of the laminates that resulted in a final shear failure mode took place. Therefore, further precautions, including increasing the anchorage length of the laminates by full wrapping or U-wrapping with wings, should be taken into consideration to prevent, or at least postpone, such peeling.

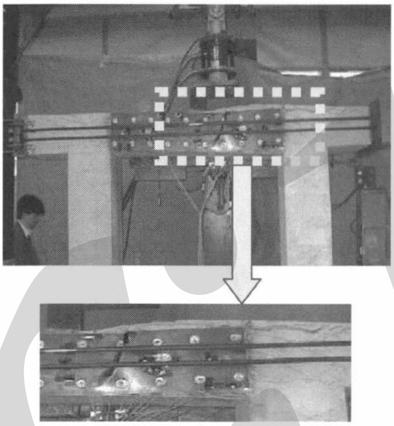

Fig. 1. Photo of final failure mode of SR1

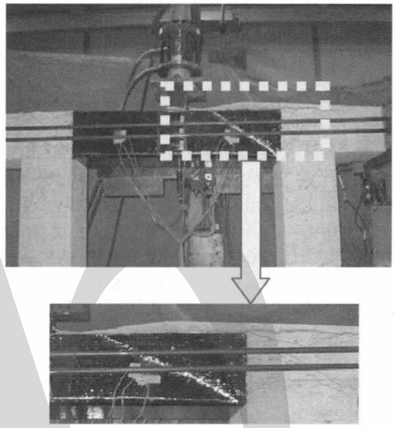

Fig. 2. Photo of final failure mode of SR2

3 SUMMARY AND CONCLUSIONS

The overall assessment of the viaducts of an existing highway with retrofitted columns left doubts that the un-retrofitted parts may experience undesirable failures thus prohibiting to achieve the target ductility during future earthquakes. Consequently, an experimental program was conducted incorporating high ductile columns to simulate the retrofitting effect of the columns. Through investigation of damage propagation, failure mechanism and overall hysteretic behavior of the specimens, the following conclusions were drawn:

1) The expected upper plastic hinges of the simulated retrofitted columns have adequate strength that ensured minimal damages. The lower plastic hinges have enough strength and ductility.
2) The beams suffered considerable damages and failed in a shear mode at a comparatively low displacement ductility. Appropriate retrofitting for the RC beams may be employed to ensure an enhanced overall performance and a full use of the high ductile columns.
3) Retrofitting of the RC beams by bonded steel plates showed an overall enhancement of the behavior and a delay in the failure though a final shear failure was pronounced. The failure may be attributed to the de-bonding and buckling of the steel plates. Therefore, further precautions to prevent, or at least postpone, the de-bonding should be taken into consideration.
4) Attaching U-wrapped CFRP laminates to the beams resulted in an overall enhancement of the behavior and a delay in failure, though a final shear failure was pronounced. This may be attributed to peeling of the laminates due to insufficient anchorage length. Consequently, further precautions including increasing the anchorage length of the laminates by full wrapping or U-wrapping with wings should be taken into consideration to prevent, or postpone, such peeling.

REFERENCES

[1] Kawashima, K., "Seismic Design and Retrofit of Bridges," 12th World Conference of Earthquake Engineering (WCEE), A State of The Art Report, 2000, Paper No. 2828.
[2] Zatar, W., Mutsuyoshi, H., Konishi, Y., and Mori, A., "Seismic Behavior of Beams of Reinforced Concrete Highway Frame Structure" Proceeding of the Japan Concrete Institute, Vol. 23, No. 3, paper No. 3209, pp. 1249-1254, 2001.

SEISMIC RETROFITTING AND STRENGTHENING OF SPHERICAL PRESTRESSED CONCRETE WATER TANK

S.G. Joglekar
Director &
Vice President

U.K. Rajeshirke
Associate Principal
Consultant

STUP Consultants Limited, Mumbai, India

S. Ramanujam
Chief Engineer

R. Patnaik
Addl. Chief Engineer

Architectural & Civil Engg. Division, Bhabha Atomic Research Centre (BARC), Mumbai, India

Keywords: Health / Deterioration of Concrete Structure, Seismic retrofitting, Hydrodynamic Effects, Prestressed Concrete Water Tank.

1 INTRODUCTION

The spherical prestressed concrete tank (called Ball Tank) was constructed around 1959, for storing 3865 m^3 of de-mineralised water which is to be used for emergency cooling and shutdown of nuclear reactor. The geometry of the tank is shown in Fig. 1.

The diameter of the sphere is 21.7 m and it is resting on a conical shaft. A central access shaft with 3.37 m diameter and 11.5 m height with wall thickness of 127mm is springing from spherical R.C.C. dome at bottom. Water container which is of 200mm thickness is prestressed using 104 cables in circumferential direction and 92 cables in meridional directions using 12∅5 Freyssinet system. Rest of the element, viz. supporting shaft, central access shaft, cupola dome are in RCC. The structure is considered as one of first generation pioneering structure in PSC in India. Structural health of the tank has been monitored from time to time and found acceptable in last 40 years.

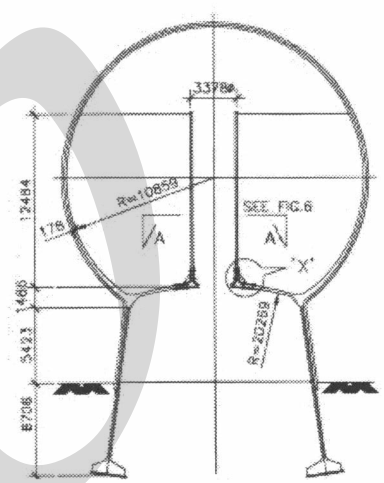

Fig. 1 : Cross Section of Ball Tank

2 EVALUATION OF PERFORMANCE UNDER SSE – DYNAMIC FEM ANALYSIS

In absence of any reference of hydrodynamic effect on spherical container with Inner Shaft a number of analyses were carried out at BARC, Ref. 3, for considering the correct mass distribution of water acting with the mass of the structure in a combined 3-Dimentional Finite Element Model for structural analysis (Fig.2a). Enveloped response spectra Safe Shutdown Earthquake (SSE) for the region is used which is having 0.2g ZPA value.

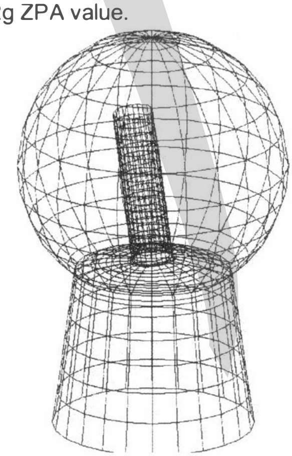

Fig.2a : FEM Model & First Mode of Vibration

It was established that spherical geometry can be considered as an equivalent cylinder with the same volume and height of water. To get impulsive pressure distribution along the cylinder, La place equation has been used with appropriate boundary conditions. The solution gives distribution of impulsive pressure variation along the height of the tank, which can be integrated to get equivalent lump masses. For modelling water mass, the total mass of water is distributed to account for sloshing and impulsive pressure for horizontal excitation. For vertical excitation, the total mass is taken as impulsive mass only. For horizontal excitation mass corresponding to first sloshing mode and second sloshing mode was established as 0.37 M and 0.05 M respectively, where M is total mass of water. Corresponding frequencies were calculated as 0.2 Hz and 0.235 Hz respectively. Masses corresponding to first and second mode can be lumped at height h_1= (-)0.227 h and + 0.373 h when h is total height of water and h_1 is distance from centre of gravity of water mass. These single (lumped) sloshing masses have been divided into three masses at each level and corresponding spring constants for attaching the same to the structural elements have been calculated, (Fig.2b).

In the direction of horizontal excitation a certain portion of mass (1183 T) moves along with the central shaft. The remaining mass which moves along with outside sphere is given by subtracting this mass from total mass.

At each height, the distribution along the periphery has been done by following the cosine and sine variation for two directions of excitation. For vertical motion total impulsive mass was distributed along the bottom dome and walls of spherical container.

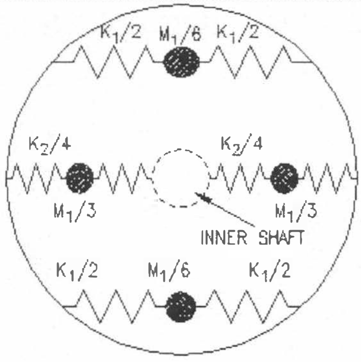

Fig.2b : Liquid Sloshing Mass & Spring

3 RESULTS OF ANALYSIS AND CONCLUSIONS

The results were used to check stress resultants in concrete, steel, prestressing steel etc. It showed that :

a) The structure as a whole is meeting all the requirements of the safety standards. Thus, the stress levels are qualified for OBE level of earthquake and the structure is also safe under SSE conditions.
b) At a few locations, viz. base connection of the RCC access shaft, with cupola dome and a part of dome at the junction need strengthening, as well as repair to stop leakage of water.
c) Since upper portion of access tower is a thin walled RCC structure, improved protection from leakages and attack on concrete by water is considered useful to limit future deterioration.

4 STRENGTHENING MEASURES

Two main alternatives were either to provide radial supports from tank walls to top of shaft, which was not favoured, or to strengthen the shaft without changing the overall structural arrangement. This was possible by any of the three alternatives :

1. Using carbon reinforced plastic plates,
2. By fixing 3.15 mm thick M.S. plates on both sides of RCC shaft and add stiffeners at the base using through bolting and epoxy (Fig.3).

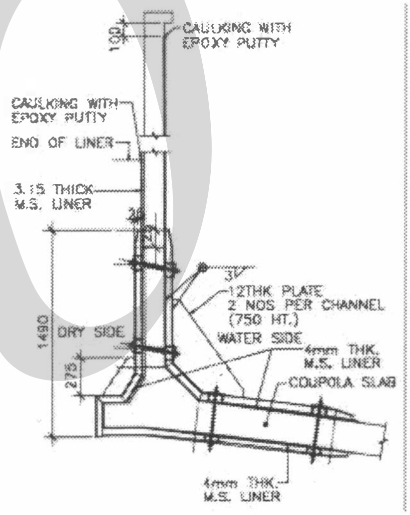

Fig.3 : Strengthening Arrangement

5 CONCLUSION

A Heritage Prestressed Concrete Structure of early years is found to be in good serviceable condition after over 40 years of use. It needed to be reassessed and retrofitted to ascertain its continued use for next 15-20 years period at least in light of the stringent requirements for nuclear safety related structure.

This was successfully done through a complex process of health/ageing effect studies, difficult and advanced analytical methods and a simple but effective strengthening / rehabilitation method is a tribute to many working teams from different organisations.

REFERENCES

[1] IAEA TECDOC-348 : Earthquake Resistant Design of Nuclear Facilities with Limited Radio-acting Inventory, Vienna 1985.
[2] Abraham. H. N. : The Dynamic Behaviour of Liquid in Moving Containers, NASA SP:106, 1966.
[3] Basha et.al : BARC's Report on Seismic Re-valuation of Ball Tank of CIRUS, BARC, April 1999.

SEISMIC STRENGTHENING OF REINFORCED CONCRETE WALLS BY SR-CF SYSTEM

-Methods and Effects of Shear Strengthening by Carbon Fiber Sheets and CF-anchors-

Yasuo Jinno Hideo Tsukagoshi
Shimizu Corporation, JAPAN

Keywords: strengthening, reinforced concrete wall, carbon fiber sheet, CF-anchor, shear

1 INTRODUCTION

The SR-CF system[1] is effective to retrofit columns with side walls[2], beams[3], and walls[4], around which hoops of carbon fiber sheets are difficult to form. This system uses special devices called CF-anchors to fix carbon fiber sheets to reinforced concrete building frames. This paper describes the shear strengthening of a wall by the SR-CF system and shear tests of the reinforced wall, and proposes methods for assessing the shear resistance.

2 TEST PROGRAM

The SR-CF system strengthens a wall by diagonally gluing a carbon fiber sheet on the surface of the wall and fixing its edges to the peripheral column, beam, and floor using CF-anchors. The CF-anchor is a bundle of carbon fiber strands, and is immersed into epoxy resin and hardened before use as in carbon fiber sheets. One end of the CF-anchor bundle is spread like a fan and glued to a carbon fiber sheet. The other end is inserted into a hole drilled on the concrete wall and is fixed with replenished epoxy resin. The anchors fix the edges of a carbon fiber sheet on a concrete wall. This method gives the carbon fiber sheet the performance of a tensile brace, and increases the shear resistance of the wall.

To examine the shear strengthening effect of the SR-CF system on existing reinforced concrete walls, the authors tested the shear resistance of wall specimens that were strengthened by the SR-CF system.

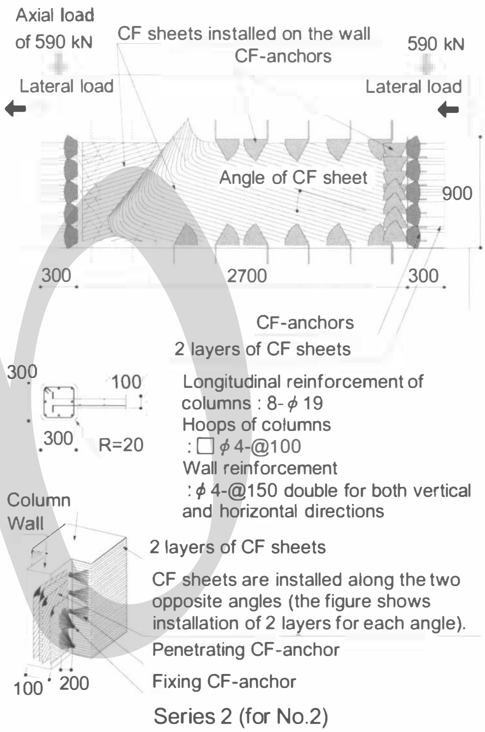

Fig.1 Configuration of specimens and strengthening methods

Table 1 List of specimens

Series	Specimen	Strengthening of the wall		Strengthening of columns	Notes
1	W-N	No strengthening			With finishing mortar
	W-B-C1	Vertically and horizontally	Front:1 layer, rear:1 layer	2 layers	
	WM-N	No strengthening			
	WM-D-C1	Diagonally	Front:1 layer, rear:1 layer	2 layers	
2	No.1	No strengthening			
	No.2	Diagonally	Front:2 layers	2 layers	
	No.3	Diagonally	Front:4 layers		
	No.4	Diagonally	Front:3 layers, rear:3 layers		
	No.5	Diagonally (2 layers of PAN sheets and 2 layers of pitch sheets)	Front:4 layers		
	No.6	±45 degrees (2 layers of PAN sheets and 2 layers of pitch sheets)	Front:4 layers		
	No.7	Diagonally	Front:4 layers		No CF-anchors
	No.8	Diagonally	Front:2 layers, rear:2 layers		

3 TEST RESULTS AND DISCUSSION

All of the specimens that were strengthened with diagonally installed carbon fiber sheets showed maximum resistance values larger than the non-reinforced specimen. The shear resistance was more significantly increased with higher degrees of strengthening.

To estimate the shear force that acts on the carbon fiber sheets, the authors assumed that the shear deformation was dominant and the walls deformed into parallelograms. The carbon fiber sheets that were diagonally laminated on the walls were regarded as tensile braces installed along existing walls. Assuming that the strain on the carbon fiber sheets is uniform for the entire wall surface, the shear force that is imposed to the sheets is expressed with Equation (1). Here, σcf and Ecf are the apparent tensile strength and the apparent Young s modulus of the carbon fiber sheets, which are used to estimate the strengthening effect of the sheets. These values are different from the mechanical properties, and should be determined from experiments.

$$Qcf = L \cdot tcf \cdot \sigma cf \cdot \sin\theta \cdot \cos\theta \qquad (1)$$

where, Qcf: shear force imposed on the carbon fiber sheets, L: internal length of the wall, h: height of the wall, tcf: thickness of the carbon fiber sheets, σcf: apparent strength of the carbon fiber sheets determined from experiments (=680MPa), θ : offset angle of the carbon fiber sheets.

Figure 2 shows the experimental shear forces at drift angles of 1/400 and 1/200 rad as a function of the amount of carbon fiber sheets, and the linear regression equations as well. The factor of the second term in the regression equation corresponds to the apparent strength of the carbon fiber sheets σcf of Equation (1). The σcf value for a drift angle of 1/400 rad was 680 MPa.

The ultimate strength of a wall is determined as the sum of the strength of the wall prior to strengthening and the shear force Qcf derived by Equation (1).

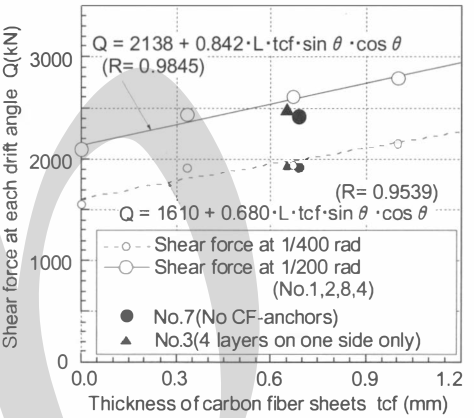

Fig.2 Relationship between shear force and amount of strengthening

4 CONCLUSION

The authors proposed a method for shear strengthening of reinforced concrete walls using carbon fiber sheets and CF-anchors, and tested their effects.

The shear strength of a wall is improved by diagonally laminating carbon fiber sheets and fixing the edges to the peripheral frame with CF-anchors so that the carbon fiber sheets act as tensile braces. The shear force contribution of the carbon fiber sheets can be calculated from Eq.(1).

ACKNOWLEDGMENTS

This report includes some of the results obtained in a project of the Petroleum Energy Center, entitled "Development of pitch carbon fiber reinforcement materials for concrete structures."

REFERENCES

[1] SR-CF System Research Association : Design Guidelines for SR-CF System, Feb. 2002 (in Japanese)

[2] K.Masuo, S.Morita, Y.Jinno, H.Watanabe : Advanced Wrapping System with CF-anchor -- Seismic Strengthening of RC Columns with Wing Walls, FRPRCS-5, Vol.1, pp.299-308, May 2001

[3] Y.Jinno, H.Tsukagoshi, Y.Yabe : RC Beams with Slabs Strengthened by CF Sheets and Bundles of CF Strands, FRPRCS-5, Vol.2, pp.981-988, May 2001

[4] Y.Jinno, H.Tsukagoshi : Structural Properties of RC Walls Strengthened by Carbon Fiber Sheets and CF-anchors, Summaries of Technical Papers of Annual Meeting -Architectural Institute of Japan, Structures IV, pp.67-68, Sep.1999, (in Japanese)

DAMAGE CONTROLLED SEISMIC DESIGN BY PRECAST PRESTRESSED CONCRETE STRUCTURE WITH MILD - PRESS- JOINT (PART 1) BASIC CONCEPT OF DESIGN

Kiyoshi Nakano
Professor Emeritus
Tokyo Denki University
JAPAN

Keizo Tanabe
Kurosawa Construction Company
JAPAN

Shigemi Machida
Tokyo Kenchiku Structural Engineers
JAPAN

Akira Wada
Professor, Tokyo Industrial University
JAPAN

Keywords: damage control, ductile connection, energy dissipation

1 INTRODUCTION

Final target in structural design against severe earthquakes has been to avoid collapse of structures so as to save human life, so far. Consequently, estimation of the amount of monetary and functional losses, which might be caused by severe earthquakes, has scarcely been considered in design practices. However, functions of society are becoming more and more complicated, and waste with natural resources and energy is not permitted ecologically. So that, damage control design procedure will become the main current in structural design, in the near future. The present paper proposes a new structural system to meet with the above current.

2 OUTLINE OF MILD-PRESS-JOINT SYSTEM

Principal features of the proposed new structural system are as follows:

1) Structural members, beams and columns are precast-prestressed components. Structural frames are realized by connecting the beam and the column using prestressing tendons. The frames behave as full-prestressing structures under design vertical load and under Level 1 earthquake load provided for by the Japanese Building Law. Under Level 2 earthquake load (recurrent period of 500 years) and Level 3 earthquake load (recurrent period of 1000 years), the connections rotate elastically to prevent damage to beams and columns. Seismic energy dissipation devices, such as damper and damping wall, are installed as needed.
2) Prestressing tendons are classified into primary tendons and secondary tendons. The primary tendons are stretched up to 85% of nominal yielding load, and then are anchored at the end surface of each component. The secondary tendons are playing the role to connect beams and columns or columns and foundations. The effective prestressing force of the secondary tendons is limited to 50% of nominal yielding load. It is because the secondary tendons should not be entered in plastic range under Level 2 or Level 3 design earthquake loads.
3) Shearing stresses in the connection among beams and columns are transmitted through corbel integrated into columns. In the connection among columns and foundations, shearing stresses are transmitted through the pedestal blocks.

3 MERIT OF MILD-PRESS-JOINT SYSTEM

Principal merits of the new system are summarized as follows:

(i) High grade of durability is assured.
(ii) Energy absorbing capacity was improved.
(iii)Residual horizontal drift is negligibly small.

4 PROCEDURE OF LOSS CONTROL DESIGN

Procedure of loss control design is shown in Fig. 1.

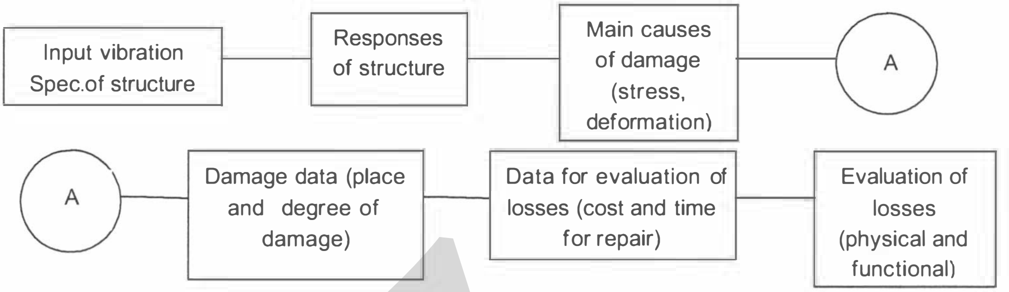

Fig. 1 Procedure of Loss Control Design

5 DESIGN DETAILS

Typical connection details are shown in Fig. 2& 3.

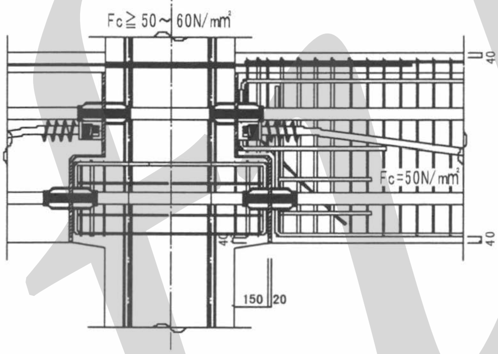

Fig. 2 Beam-column connection

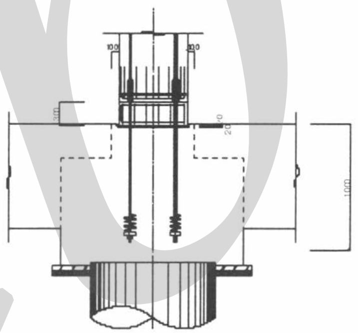

Fig. 3 Column-foundation connection

6 CONCLUDING REMARKS

1) The proposed structural system shows a practical solution for damage control design procedure. That procedure would improve a mutual understanding among engineers and clients, and would be effective to meet with ecological requirement.

2) It is evidenced that prestressing technology gives a superb engineering solution for structures under seismic loading as well as under gravity loading.

REFERENCES

1. K. Nakano et al., Damage control design by precast-prestressed structure with MILD-PRESS-JOINT (part 1. Basic concept of design), Summaries of technical papers of annual meeting, ARCHITECTIRAL INSTITUTE OF JAPAN, September 2001. pp. 893-894.

2. Keizo Tanabe, Mechanical properties and seismic resistance of a rigid frame composed of corbel-style precast-prestressed concrete components assembled by prestressing tendons, doctoral thesis, Tohoku University, May 1996.

DAMAGE CONTROLLED SEISMIC DESIGN BY PRECAST PRESTRESSED CONCRETE STRUCTURE WITH MILD-PRESS-JOINT

PART 2 KERNEL OF STRUCTURAL DESIGN AND EXAMPLES

Keizo Tanabe
Kurosawa Construction Co.
Doctor of Engineering
JAPAN

Yasuhiro Matuzaki
Professor, Tokyo
Science University
JAPAN

Motohiko Yamada
Professor,
Tohoku University
JAPAN

Keywords: resisting moment, ultimate strength, imaginary rotation angle, hysteresis loop

1 INTRODUCTION

Many buildings designed in accordance with the concept introduced in part (1) have been constructed in Japan. Those buildings satisfy design requirements provided for in the Japanese Building Law and related regulations. However, specific structural characteristics, such as robustness under seismic loads, minimal residual lateral deformation, and easiness of repair works, have never been openly described in design documents. The reasons of the above situation are as follows, firstly the specific characteristics are out of official requirements, and secondly quantitative expression of the characteristics is rather difficult. In this paper, authors present a method for the quantitative expression referring some experimental data[2)].

2 EXPERIMENTAL STUDY OF MILD-PRESS-JOINT SYSTEM

Based on an experiment[2)], behavior of strains in tendons under cyclic loading has been revealed. It is found that strains in the upper and lower tendons do not change independently. Strains in tendons change in proportion to distance from a certain center. The center is named as "rotation center of tensile strain", and is denoted by "**Or**" in Fig.1. The finding of concept of the center makes it quite clear to understand behavior strains in tendons. As shown in Fig.2, location of center, **Or**, moves smoothly toward the center of gravity of cables in accordance with in crease of drift angle.

There is also an important finding in the experiment that stresses in tendons are able to express as a function of imaginary tensile strain, ε_o, and imaginary rotation angle, Φ_s.

Trajectories of the imaginary tensile strains and the imaginary rotation angle are able to express as function of drift angle, **R**, as shown in Fig.3 and Fig.4.

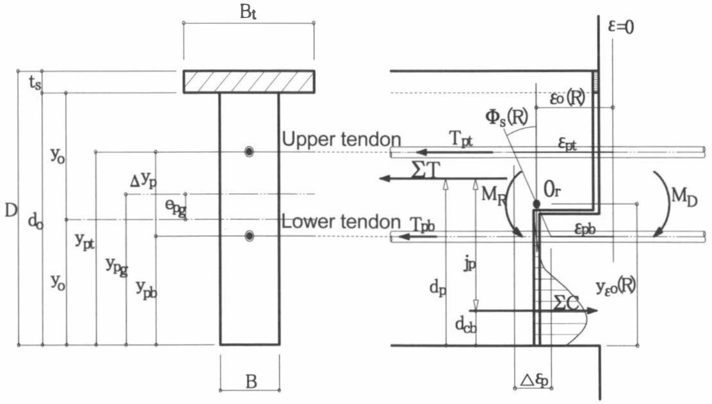

Fig.1 Behavior of strain in prestressing tendons

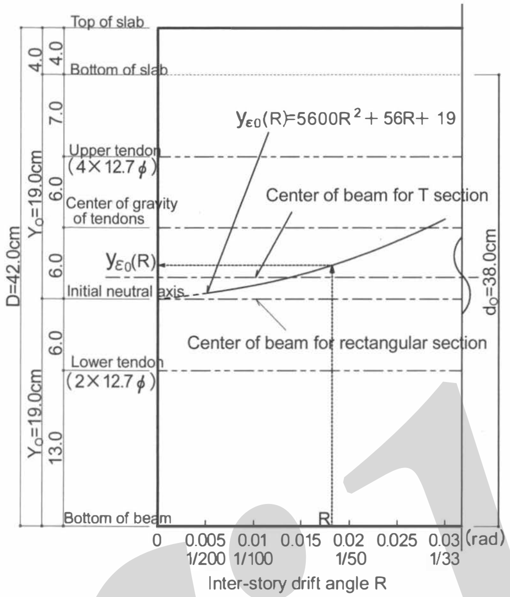

Fig.2 Trajectory of $y_{\varepsilon o}(R)$

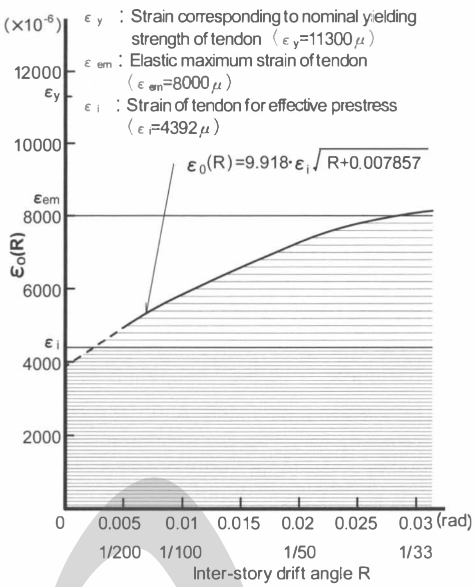

Fig.3 Trajectory of $\varepsilon_o(R)$

3 ANALYTICAL EXPRESSION

With the help of the concept, "rotation center of tensile strain", and two parameters, the imaginary tensile strain and imaginary rotation angle, behavior of connection can be expressed analytically. For the purpose of validating the analytical expressions the next assumption should be accepted.

(i)The distance between upper tendon and lower tendon should not be greater than 1/2 of beam depth, and be arranged within 3/8 of beam depth from centroid of the beam.

( ) Effective prestresing force of tendons should not be greater than 50% of nominal yielding strength of tendons.

( ) Strain of tendons attains to the maximum value when story drift angle reaches to 1/50, and maintains the same value for drift angle greater than 1/50.

The maximum value is assumed tentatively to around 80% of strain corresponding to nominal yielding strength of tendons.

( ) Prestresing strands should be used as tendons. Bond characteristics of strand are suitable in using under cyclic loadings.

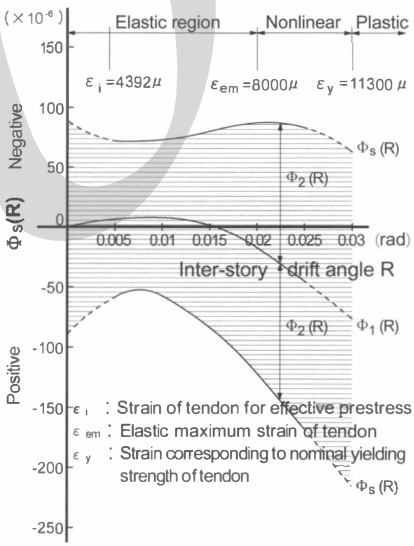

Fig.4 Trajectory of $\Phi_s(R)$

REFERENCE

[1] Keizo Tanabe et al.:Damage control design by precast-prestressed structure with MILD-PRESS-JOINT (part 1 — 4), Summaries of technical papers of annual meeting, ARCHITECTIRAL INSTITUTE OF JAPAN, pp. 893-900. September 2001. 9,

[2] Keizo Tanabe: Mechanical properties and seismic resistance of a rigid frame composed of corbel-style precast-prestressed concrete components assembled by prestressing tendons, doctoral thesis, Tohoku University, May 1996.

EFFECTS OF BEAM PRESTRESSING FORCE ON THE STRENGTH AND FAILURE MODE OF R/C EXTERIOR BEAM-COLUMN JOINTS

Hitoshi Shiohara Afonso Toshiiti Sato Shunsuke Otani Taizo Matsumori
The University of Tokyo, Graduate School of Engineering, Department of Architecture

Keywords: reinforced concrete, beam-column joint, prestressing force, failure mode.

1 INTRODUCTION

The number of past experimental investigation on reinforced concrete exterior beam-column joints with prestressing is limited, and more limited is the number of studies related specifically to evaluate the joint strength [1]. Six reinforced concrete exterior beam-column joints with and without post tensioning in the beam were tested under static lateral load reversals. The objectives of this study are to study the effects of (a) post tensioning force in the beam, (b) location of anchorage plates for beam longitudinal bars and/or post tensioning steel bars, (c) amount of lateral reinforcement in beam-column joint, and (d) mid layer longitudinal bars in column on the joint failure.

2 OUTLINES OF TESTS

The test specimens were half-scale reinforced concrete (RC) and post tensioned (PC) plane frame exterior beam-column joint sub-assemblages without slabs.

In total, six test specimens were tested. The parameters were: (1) existence of post tensioning force on the beam (PC or RC); (2) location of the anchorage plate for the beam longitudinal bars and post tensioning bars (inside or outside of joint core); (3) amount of lateral reinforcement in the joint (zero or minimum reinforcement); and (4) existence of intermediate longitudinal reinforcement in the column. The dimensions of a beam were common in all six specimens and were 200 mm by 300 mm. Column dimensions were either 250 mm square or 250 x 300 mm, varied in reinforced concrete specimens. The reinforcement details are shown in Fig. 1.

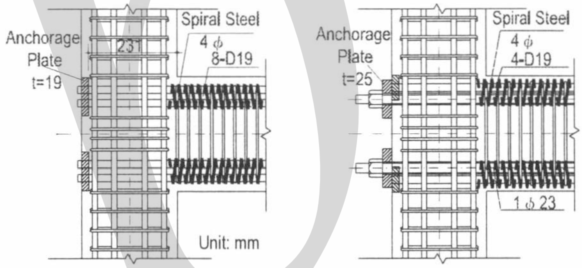

(a) RCJ-1 elevation (b) PCJ-4 elevation

Fig.1 Reinforcement detail of test specimen

Figure 2 shows the loading setup. Pins at the column top and bottom, and a roller at the beam end supported the test specimen. The loads were applied to the specimen through a universal pin attached to the column top. A constant axial load of 250 kN was applied using the vertical actuator, while reversed cyclically increasing lateral load, using horizontal actuator, was applied by displacement control.

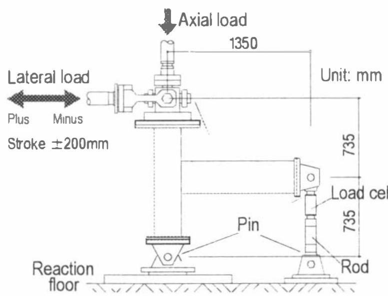

Fig.2 Loading setup

3 TEST RESULTS

The test results are summarized in Table 1. The relationships of story shear and story drift are shown in Fig. 3. All the specimens failed in joint shear failure mode.

Table 1 Summary of test results

Test specimen	RCJ-1	RCJ-2	RCJ-3	PCJ-4	PCJ-5	PCJ-6
Maximum story shear (+) (kN)	107	111	108	122	117	121
Story drift (% rad)	2.7	2.7	2.7	2.7	2.7	4.0
Minimum story shear (–) (kN)	110	109	105	117	107	117
Story drift (% rad)	2.7	2.7	2.7	2.7	2.7	4.0
Maximum joint shear* (+) (kN)	706	748	690	722	694	781
Minimum joint shear* (–) (kN)	678	669	635	709	648	743
Failure mode**	A	A	A	A	A	A
Story shear at beam flexural yielding (kN)***	142	145	145	126	126	131
Story shear at column yielding (kN)***	181	225	201	181	181	181

* Occurred at story drift 2.7% rad; ** Failure mode: A - joint shear failure;
*** Calculated values based on bending theory.

4 CONCLUDING REMARKS

From this study, it was concluded as follows:

(1) All specimens showed joint shear failure initiated after beam bar reached yielding strength. The story shear capacity of the beam-column sub-assemblage was much smaller than that calculated based on the flexural strength of beam section or column section using bending theory;

(2) In post tensioned specimens the story shear, joint shear force and column bar stress were higher than that of the normal reinforced concrete test specimens;

(3) In the case that the end plates of beam bars and/or post tensioning were anchored outside of the outer column reinforcing bar, bond condition is improved due to the confinement by the anchorage plate, and consequently the column bar stress and bond stress were increased;

(4) In the test specimen, which did not have joint lateral reinforcement, the story shear-story drift relation was almost the same until the maximum story shear was reached, it showed severe strength deterioration at larger deflection;

(5) In the test specimen, which did not have intermediate column reinforcing bar, maximum story shear, the joint shear force and column outer reinforcing bar bond stress was lower than that of the specimens with intermediate column bars.

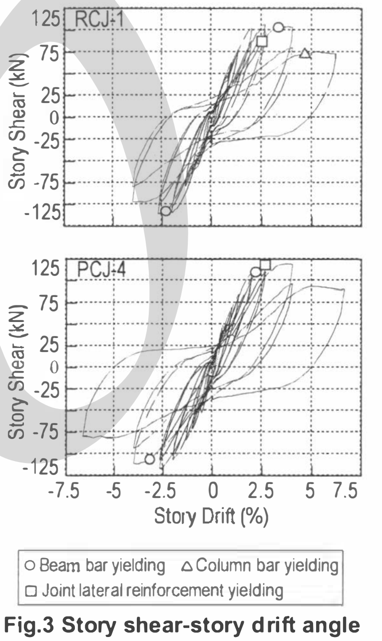

Fig.3 Story shear-story drift angle relation

REFERENCES

[1] Sato, A. T., Yang, C., Shiohara, H., Otani, S., "Shear resisting mechanism of R/C exterior beam-column connections with post tensioned beams," Transactions of the JCI, Japan Concrete Institute, Vol.23 (to be published in February 2002).

SHEAR STRENGTH OF INTERIOR BEAM-COLUMN JOINTS UNDER SEISMIC LOADING

Gaetano Russo
Department of Civil Engineering
University of Udine
ITALY

Giuliana Somma
Department of Civil Engineering
University of Udine
ITALY

Beam-column joints are critical regions in reinforced concrete frames subjected to severe seismic attack because their cracking, due to high shear force and bond breakdown within them, can lead to joint stiffness decrease, allowing large overall story drift and consequent structural damage.

A lot of design code recommendations and analytical expressions for computing the interior beam-column joints shear strength under seismic loading exist, but are not able to supply an accurate prediction, mainly because of the several parameters that take part and statically indetermination of the problem. There are different approaches followed by various codes and authors, trying to predict the real shear strength behavior of an interior beam-column joint under earthquake loads. Some authors, provide expressions based on the two separated mechanisms of the truss and diagonal concrete strut, some on a limit value linked to the concrete tensile or compressive strength, and finally some provide an iterative solution procedure based on the interaction between a diagonal, an horizontal and a vertical strength mechanism.

An analytical expression is here proposed allowing for the strength mechanisms which resist to joint expansion always observed in tests. This expansion is due to joint diffuse diagonal cracking in the opposite directions, during severe moment reversals that again and again transform the rectangular joint region in a diamond, by elongating and strengthening both joint diagonals. So it may be stated that, under the load actions which simulate the seismic action, within the joint there is the development of lengthening strains and relative motions in both vertical and horizontal directions.

On the basis of previous considerations, an expression is proposed, which takes into account the following resisting mechanisms to joint expansion: (1) vertical stress transmitted by column, (2) longitudinal beam reinforcement, (3) external constraints to beam free elongation, if the case, and (4) passive confinement due to stirrups, when present. The proposed expression for shear strength of an interior reinforced concrete joint is

$$v_{jh} = 0.41 \cdot f_{ct} \cdot \sqrt{1 + \frac{f_a + f_{V\,lim}}{f_{ct}}} + \left(0.83 + 0.68 \cdot \frac{l_c}{l_b}\right) \cdot \frac{f_{yh} \cdot A_{sh}}{A_g} + 0.05 \cdot \frac{f_{yh,h} \cdot A_{sh,h}}{A_g} \qquad (1)$$

To evaluate the model reliability also shear strength expressions provided by ACI Code, Eurocode and by Paulay and Priestley have been considered.

Theoretical joint shear strength has been computed for all the 262 tested specimens found in literature by means of Eq.(1) and the others considered. The ratios between experimental and computed joint shear strength are shown in Fig.1 versus the concrete compressive strength. The coefficients of variation and average values, relative to each expression, are also indicated.

The measure of the prediction uniformity is given by the coefficient of variation, COV: the lower this value is, the greater the uniformity. From the diagrams and COV values it is evident that ACI Code, Eurocode, as far as the expression proposed by [1], lead to very variable experimental to computed beam-column joint shear strength, i.e. to uncertain value of safety factors. Instead the proposed formula [Eq.(1)] shows that the range of safety factor variation is limited, as it is proved by the low COV value.

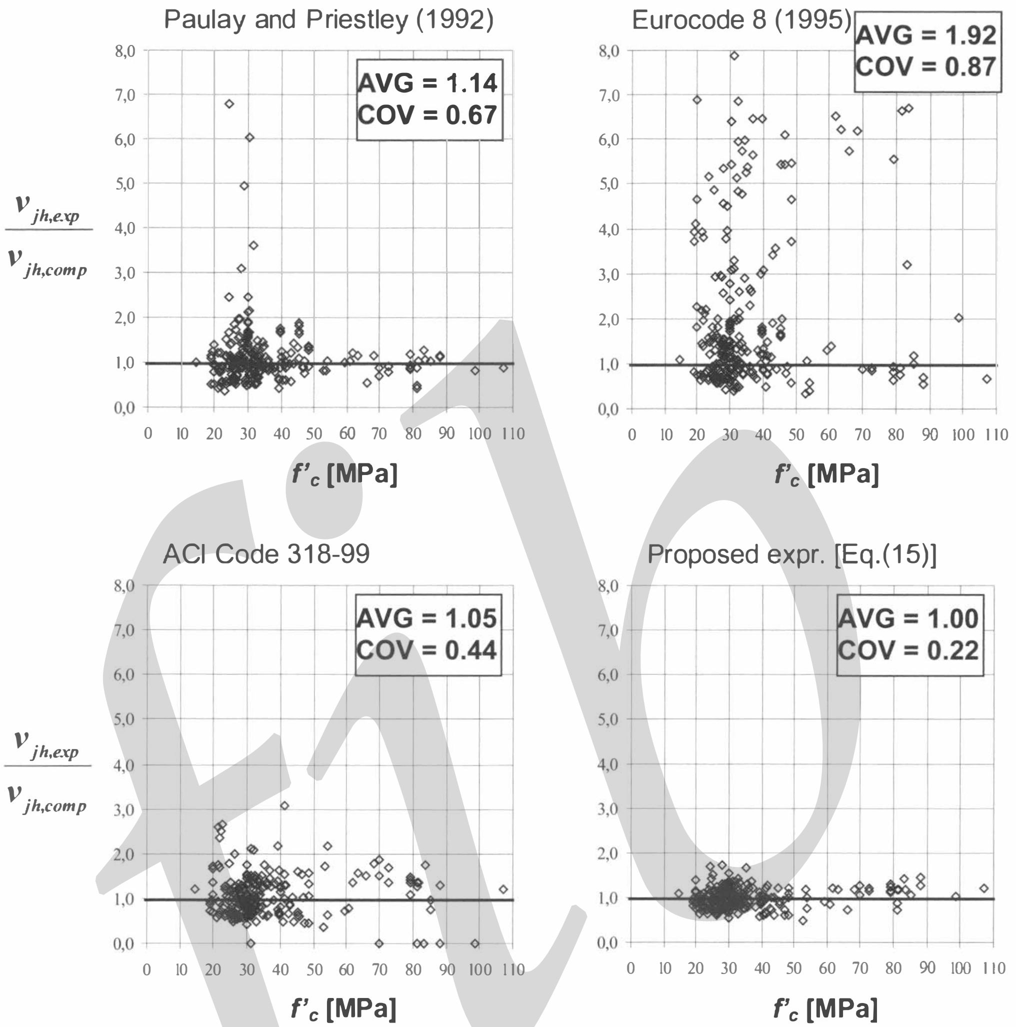

Fig.1 Experimental to computed shear strength ratio versus f'_c, for the 262 joints

REFERENCES

[1] Paulay, T., and Priestley, M.J.M. : Seismic design of reinforced concrete and masonry buildings, John Wiley and Sons, New York, p.744, 1992.

[2] ENV 1998-1-3 Comitè Europeen de Normalization CEN : Eurocode 8 - Design provisions for earthquake resistance of structures – Part 1-3: General rules - Specific rules for various materials and elements, 1995.

[3] American Concrete Institute (ACI) : Building Code Requirements for structural concrete (ACI 318-99) and Commentary (ACI 318R-99). ACI 318-99, Farmington Hills, Mich, 1999.

[4] Russo, G., and Somma, G. : Shear Strength of R/C Beam-Column Joints without Shear Reinforcement under Seismic Loading. Studies and Researches, Vol.23, 2002, p.31, (accepted for publication).

SHEAR PROPERTIES OF PRESTRESSED REINFORCED CONCRETE MEMBERS UNDER REVERSED CYCLIC LOADING

Yasuhiro Mikata, NEWJEC Inc., JAPAN
Susumu Inoue, Kazuo Kobayashi, Tamotsu Nieda, Osaka Institute of Technology, JAPAN

Keywords: prestressed reinforced concrete, reversed cyclic loading, shear force carried by concrete, shear deformation

1 INTRODUCTION

Prestressed concrete (PC) members have some advantages such as small residual displacement and high crack controlling ability, while they have less energy absorption characteristics and ductility compared with reinforced concrete (RC) members. However, Recent report shows that introduction of an appropriate amount of prestress to RC columns decreases seismic damage and residual deformation after severe earthquakes compared with the case without prestressing. [1]

When column members are subjected to reversed cyclic loads during earthquakes, shear force carried by concrete deteriorates remarkably. However, shear capacity of prestressed reinforced concrete (PRC) members under reversed cyclic loading has not been well investigated. Therefore the rational seismic design method, which can evaluate the deterioration mechanism of concrete shear resistance under reversed cyclic loading, should be established for PRC structural members.

In this study, the effects of prestressing on seismic performances, especially on shear capacity of PRC beam members, are investigated focusing on the influences of shear reinforcement ratio, level of introduced prestress and bonding characteristics of prestressing steels. The ratio of shear deformation to the total one is also discussed.

2 TEST RESULTS AND DISCUSSIONS

Specimens used are prestressed reinforced concrete (PRC) simple beams with rectangular section of 100×200mm and total length of 1800mm as shown in Fig.1. They were tested under reversed cyclic loads with gradually increased deflection amplitudes such as, $1\delta_y$, $2\delta_y$, ・・・(δ_y: yield deflection),up to failure. Details of test variables and results of loading tests are shown in Table 1.

In case of ρ_w(shear reinforcement ratio) =0.79%, ultimate flexural capacity calculated by using fiber model are smaller than ultimate shear capacity calculated according to JSCE code irrespective of bond characteristics of prestressing bar. However, almost all the beams except for the beam (B-3-1-1,U-5-1-1), which failed in flexure, showed shear failure after flexural yielding. These facts suggest that shear force carried by concrete deteriorates due to the load reversals at large deflection amplitude.

In case of ρ_w=0.40%, the ultimate deflection of B-0-2-1(non-prestressed specimens) is $-5\delta_y$. On the other hand, the ultimate deflection of B-3-2-1 (σ_{cp}=3.0N/mm^2) was $+7\delta_y$ That became $-7\delta_y$ for B-5-2-1 (σ_{cp}=5.0N/mm^2). From these facts, the ultimate deflection increases with increasing the introduced prestress.

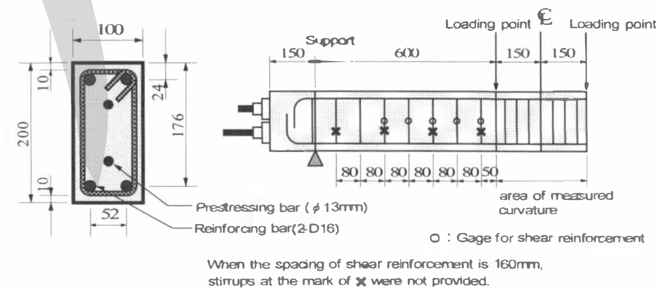

Fig.1 Dimensions of specimens and loading condition (unit: mm)

Table 1 Results of loading tests

*1 Specimens	Concrete Strength f'_c (N/mm²)	Shear reinforcement ratio ρ_w (%)	*2 Introduced prestress σ_{cp} (N/mm²)	*3 Ultimate shear capacity (Cal.) P_{us} (kN)	*4 Ultimate flexural capacity (Cal.) P_{ub} (kN)	Maximum Load (Mea.) P_u (kN)		*5 Ultimate deflection	*6 Failure mode
						Pos.	Neg.		
B-0-1-1	33.5	0.79	0.0	149.7	120.2	127.1	-126.2	$+10\delta_y$	FS
B-0-2-1	32.2	0.40		98.8	120.0	115.6	-111.7	$-5\delta_y$	FS
B-3-1-1	34.3	0.79	3.0	155.8	123.0	132.1	-129.5	$+11\delta_y$	F
B-3-2-1		0.40		105.6	123.0	120.3	-122.1	$+7\delta_y$	FS
B-5-1-1		0.79	5.0	159.5	123.4	133.4	-131.3	$+9\delta_y$	FS
B-5-2-1		0.40		109.3	123.4	128.4	-122.1	$-7\delta_y$	FS
U-0-1-1	37.2	0.79	0.0	151.4	91.7	126.7	-125.6	$-9\delta_y$	FS
U-0-2-1		0.40		101.2	91.7	106.9	-109.0	$-6\delta_y$	FS
U-3-1-1		0.79	3.0	158.6	100.8	119.9	-119.4	$+10\delta_y$	FS
U-3-2-1		0.40		108.4	100.6	117.2	-117.3	$+7\delta_y$	FS
U-5-1-1		0.79	5.0	162.8	105.5	118.7	-126.1	$-8\delta_y$	F
U-5-2-1		0.40		112.6	105.5	123.6	-126.5	$+8\delta_y$	FS
B-0-2-0	32.2	0.40	0.0	98.8	120.0	125.6	—	30.2mm	SC
B-3-2-0	34.3	0.40	3.0	105.6	123.1	135.1	—	76.6mm	SC
B-5-2-0		0.40	5.0	109.3	123.4	133.8	—	90.1mm	F

*1 B-∗-∗-∗: bonded type specimens, U-∗-∗-∗: unbonded type specimens, ∗-∗-∗-1: reversed cyclic loading, ∗-∗-∗-0: monotonous loading
*2 σ_{cp}=0.0 means that prestressing bars are not tensioned.
*3 $P_{us}=2(V_{cd}+V_{sd})$, (V_{cd}, V_{sd} is calculated by JSCE code)
*4 The values calculated by the fiber model.
*5 Yield displacement: (δ_y=5mm), Ultimate displacement is the deflection amplitude where the load carrying capacity is reduced to yield load in measured load-displacement curve.
*6 FS: shear failure after flexural yielding, SC: shear compression failure after flexural yielding, F: flexural failure

The measured shear force carried by concrete at the deflection amplitude of $1\delta_y$ increased with increasing the introduced prestress irrespective of bond characteristics of prestressing bar. Although the concrete shear capacity decreased with increasing the applied deflection amplitude, the introduction of prestress can restrain the deterioration of concrete shear capacity due to the load reversals.

The ratio of shear deformation to the total one decreased with increasing introduced prestress after deflection amplitude of $1\delta_y$. Consequently, the increasing behavior of shear deformation with increasing the deflection is restrained by introduced prestress. Therefore, introduced prestress contributes to the improvement of ductility of prestressed reinforced concrete members.

3 CONCLUSIONS

(1) In both of bonded and unbonded type specimens, the measured shear cracking load and maximum load increased with increasing the introduced prestress even under reversed cyclic loading.
(2) The introduction of prestress can restrain the deterioration of concrete shear capacity due to the load reversals.
(3) The increasing behavior of shear deformation with increasing the deflection is restrained by introduced prestress. Therefore, introduced prestress contributes to the improvement of ductility of prestressed reinforced concrete members.

REFERENCES

[1] Ikeda, S.: Seismic behavior of reinforced concrete columns and improvement by vertical prestressing. Proceeding of The 13th FIP congress on challenges for concrete in the next millennium, vol.2, pp.879-884, 1998.5

STUDIES ON SHEAR BEHAVIOR OF PRECAST JOINT HAVING INCLINED BAR ARRANGEMENT

Keiichi Katori Shizuo Hayashi
Structural Engineering Research Center, Tokyo Institute of Technology, JAPAN

Keywords: Precast Concrete Structure, Shear behavior, Joint, Connecting bars, Inclined arrangement

1 INTRODUCTION

In Japan structural design of the precast member-to-member joint has calculated by the method based on allowable stress concept. But the new design method based on inelastic displacement concept is required.

Reinforcement bars have ductility for shear force better than that of concrete. So shear behavior of connecting bars across the precast joint will have large influence on design method based on inelastic displacement concept. Authors has performed studies on establish of new design method for precast joint under shear force. In this paper authors performed experiment of precast joint under shear force that have connecting bars under inclined arrangement, and investigated the relationship between shear behavior of the joint and inclined angle of connecting bars.

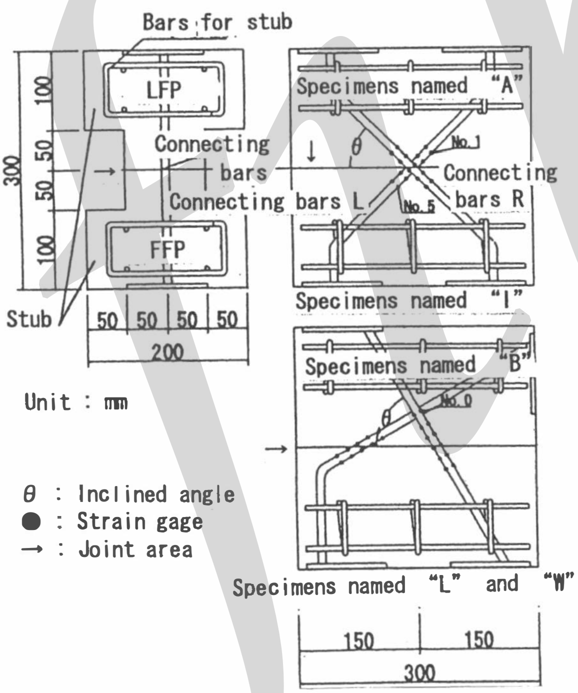

Fig. 1 Detail of specimens

2 OUTLINES OF EXPERIMENT

Specimens were planned as a model of the small element of precast beam-wall joint (horizontal joint). Detail of specimens is shown in Fig.1. Inclined angle between connecting bars and joint, pattern of arrangement of connecting bars and crossing position of connecting bars were selected as parameter of the specimens. 50 specimens were made.

All connecting bars were used by D10 normal strength bar and those bars of specimens named "I" and "L" were made by cutting off from welded mesh bars which was used for connecting bars of specimens named "W". Concrete for specimens had normal strength

Cyclic shear force was subjected to joint area by using S-shape loading frame.

3 RESULTS OF EXPERIMENTS

Results of shear loading experiment in typical specimens are shown in Fig. 2. Shear force born by connecting bars ($_{S}Q$) and axial force of connecting bars($_{N}Q$) when connecting bars became yield were calculated. The ratio of $_{S}Q$ and $_{N}Q$ are shown in Fig. 3. When connecting bars became yield, $_{N}Q$ of right connecting bars became from 52 times to 85 times as large as $_{S}Q$ of right connecting bars. And $_{N}Q$ of left connecting bars became from 192 times to 261 times as large as $_{S}Q$ of left connecting bars. It seems that connecting bars act axially and not seems that connecting bars suffer dowel action.

In well-known calculation formula of shear strength for precast joint these consist of cumulation of shear force born by plural shear resistant mechanisms. Shear resistant mechanisms is consist as follows for example; 1) dowel action of connecting bars, 2) so-called "shear frictional mechanisms", 3)

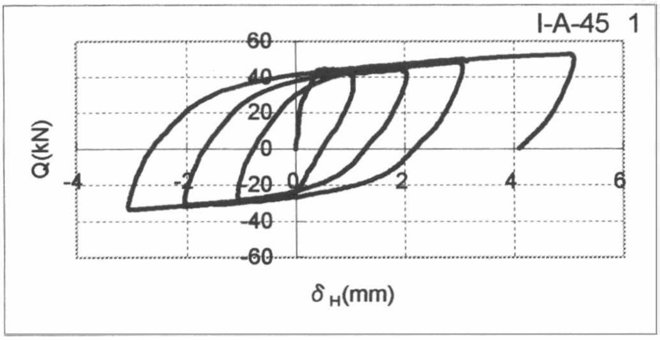

Fig. 2 Q–δ_H relationship of typical specimen

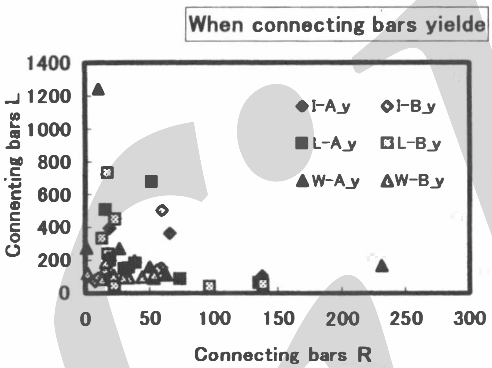

Fig. 3 Axial force-dowel shear force of connecting bars Right and Left

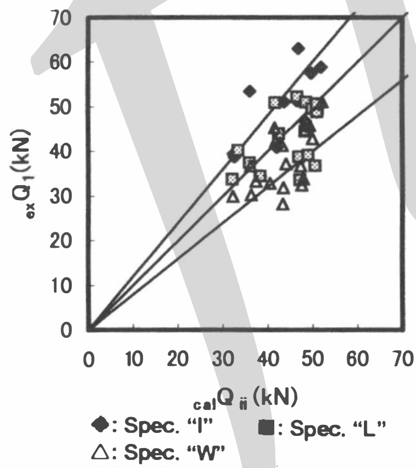

Fig.4 Relationship between ${}_{ex}Q_i$ and ${}_{ex}Q_{ii}$

frictional force caused by compressive force from outside, and so on.

Comparison between ${}_{ex}Q_1$ and cumulative shear force calculated by as follows (${}_{cal}Q_{ii}$) is shown in Fig. 4. ${}_{cal}Q_{ii}$ was calculated as follows; ${}_{cal}Q_{ii}$ is calculated by following formula,

$$ {}_{cal}Q_{ii} = ({}_sQ_h + {}_sN_h) + \mu \cdot ({}_sQ_v + {}_sN_v + N) \quad (1) $$

$$ \mu = 1.73 \cdot (\sqrt{\sigma_B} / 30) \quad (2) $$

where, ${}_sQ_h$ is a horizontal element of ${}_sQ$ and ${}_sN_h$ is a horizontal element of ${}_sN$. ${}_sQ_v$ is a vertical element of ${}_sQ$ and ${}_sN_v$ is a vertical element of ${}_sN$. N is compressive force against joint area led by screw jack. μ is a so-called "shear frictional coefficient" and formula (2) was led by the authors past studies.

From Fig. 4 cumulation of shear force bom by each shear resistant mechanism shown in formula (1) would calculate the strength of the specimens moderately.

4. CONCLUSION

Following knowledge is taken from this study;

1) To incline connecting bars against joint area lead precast joint ductile.
2) Connecting bars which was inclined against joint area acted mainly axially, and not had dowel action.
3) Shear strength of precast joint which had inclined connecting bars was able to calculate by using the cumulative strength method for shear force bom by each shear resistant mechanism.

REFERENCE

1) Katori, K., and Hayashi, S.: Experimental studies on the shear wall-floor slab joint of precast concrete structure using inclined arrangement. J. Struct. Const. Eng., AIJ, No.457, pp.47-59, Mar. 1994
2) Guide for design and prefabrication of precast reinforced concrete structures, AIJ, Oct. 1986
3) Katori, K., and Hayashi, S.: Estimate of the shear strength of construction joint by using its surface roughness and characteristics of slip displacement of joint under shear force. J. Struc. Const. Eng., AIJ, No.507, pp.107-116, May 1998

TOWARDS UNIFYING ULTIMATE LIMIT STATE OF SHEAR FOR PILE CAPS

Masahiro SHIRATO Jiro FUKUI Naoki MASUI Kenji KOSA

Public Works Research Institute, Tsukuba, Japan
Obayashi Corporation, Tokyo, Japan
Kyushu Institute of Technology, Kitakyushu, Japan

Keywords: pile cap, shear strength, deep beam, compression pile, pull-out pile

1 INTRODUCTION

In Hyogo-ken Nanbu Earthquake in 1995 it was clearly found that there is a demand from structural engineers for an appraisal of consistent design methodologies which can provide a realistic description of the behavior of pile caps. This paper describes the behavior of pile caps in following two investigations. First, it introduces a newly established design method of ultimate shear strength of pile caps supported by compression piles. The focus of the second investigation is that in the former design specifications of bridges in Japan the structural design method of pile caps in the cases of such a pull-out pile was not well documented. In addition limited previous work was available. Under this circumstance Public Works Research Institute (PWRI) has conducted experimental and numerical studies to evaluate the shear resisting mechanism of pile caps. Conclusions described in this paper have been introduced into the new version of design specifications of highway bridges in Japan [1].

2 IDENTIFICATION OF LOAD PATHS IN PILE CAPS USING STRUT AND TIE MODEL

Fig. 1 illustrates load (stress) paths in a pile cap where solid lines and dotted lines mean compression struts and tension ties respectively. The right hand side of Fig. 1 explains that the pile load is supported by forming ``force triangle'' consisting of C_3 (compression) and T_2 (tension).

Many experimental studies have confirmed the applicability of strut and tie models for pile caps with compression piles. On the other hand different force equilibrium takes place in the pile cap due to pull-out pile. It seems that a conventional compression strut is not available in this case, which means that point X has to be determined by a complicated and sophisticated load pass. This is the main difference in the design of pile caps in the cases of compression and pull-out piles.

3 REVIEW AND RE-EVALUATION OF SHEAR DESIGN OF PILE CAPS

Since 1996 the design procedure for pile caps have been given in Specifications for Highway Bridges IV; Substructures, Japan.

$$S_d = S_{dc} + S_{ds} = c_{dc} S_c + c_{ds} S_s \qquad (1)$$

where S_d is shear strength as deep beams, S_{dc} is shear resistance carried by concrete in deep beams and S_{ds} is shear resistance carried by transverse reinforcement. S_c is shear resistance carried by concrete in ordinary (slender) beams, S_s is shear resistance carried by transverse reinforcement derived from truss analogy, c_{dc} is the modification coefficient of S_c and c_{ds} is the modification coefficient of S_s, both are dependent upon a/d, where a is shear span and d is effective depth.

Existing experimental data on the shear strength of deep beams were collected and they are summarized in Fig. 2, where S_e is the observed shear strength. Fig. 2 showing that the relation between S_e/S_c and a/d derived from previous load tests except the results of specimens with small b/d ($b/d < 0.4$), where b is the width of the beams, gives the best fit coefficient in Eq. (2).

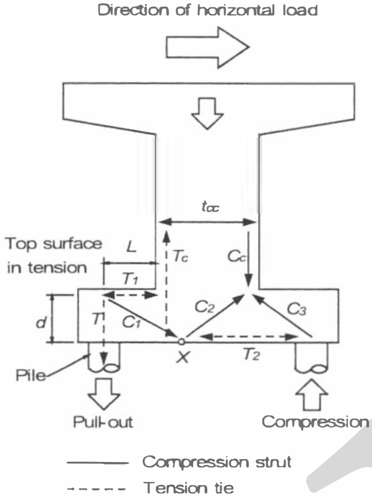

Fig.1 Strut and tie in pile cap

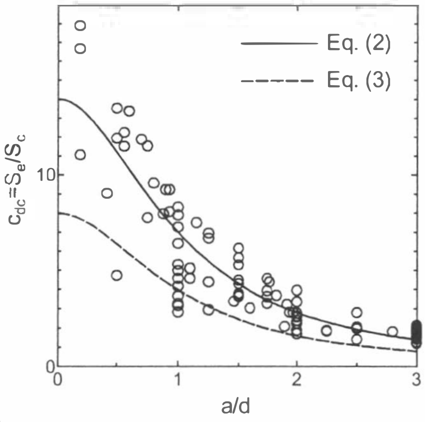

Fig. 2 Effect of shear span to depth ratio on concrete shear strength in the case of $b/d \geq 0.4$

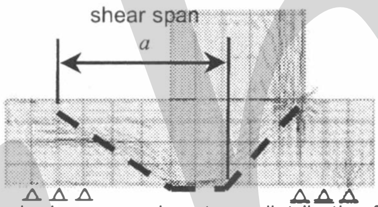

Fig. 3 Principal compression stress distribution from FEM

$$c_{dc} = \frac{14.0}{1+(a/d)^2} \tag{2}$$

A reliability analysis was introduced to re-evaluate the modification coefficient c_{dc} employed in the design provisions. Because design practice requires a safety margin in shear strength, a reliability index, so called β, was set to 2.0, in which only 2.3 % data may fall.

$$c_{dc} = \frac{7.98}{1+(a/d)^2} \tag{3}$$

4 RESEARCH ON SHEAR OF PILE CAP WITH PULL-OUT PILE

The experimental program consisting of three test series involves an investigation on the mechanism and the development of design method for shear of pile caps subject to pull-out load.

The two-dimensional finite element (FE) model described herein represents specimens in the experiment. The nonlinear FE analysis was performed for the test specimens to find compressive stress flow, as shown in Fig. 3.

Finally it is confirmed that Eq. (4) gives the shear span of pile caps with pull-out piles.

$$a = \min(L + t_{cc}/2,\ L + d) \tag{4}$$

where L and t_{cc} are referred to Fig. 1.

REFERENCES

[1] Japan Road Association: Specifications for Highway Bridges IV; Substructures, Maruzen, Tokyo, 2002. (in Japanese)

SHEAR LOADING TEST OF REINFORCED CONCRETE HOLLOW SECTION COLUMN FOR BRIDGE TOWER

Koichi Tanaka Hajime Ohuchi
Obayashi Corporation Technical Research Institution, JAPAN

Keywords: shear, hollow section column, tower, high strength hoop, lightweight concrete

1 INTRODUCTION

Reinforced concrete(RC) can provide more economical solution for long span bridge tower such as a 200-300m height huge suspension bridge. Form economical construction aspect, lightweight and high strength concrete and steel reinforcement are expected to be used as well as unemployment of lateral tie hoops. However, only few studies have been found on ultimate shear strength of hollow RC member with these materials and reinforcing details.
In these back ground, we conducted three points loading test up to shear failure of the beam under high axial stress. Following were focusing aspects;
1) Applicability of design equation for ultimate shear strength for RC beam with high strength reinforcement (700N/mm^2).
2) Less shear strength contribution of lateral tie hoops.
3) Applicability of lightweight aggregate usage concrete for the present structure.

2 OUTLINE OF EXPERIMENTAL TEST AND TEST RESULT

Experimental parameters are shown in **Table 1**. The cross section of test specimen is illustrated in **Fig.1**. Obtained Load - Displacement relationship is shown in **Fig.2**. In case of high strength hoop usage, smaller shear stiffness and shear strength were observed after bending crack appearance. In case of tie hoop usage, more ductile behavior was observed in the post peak. Confinement by tie hoops can provide improvement of concrete ductility. But increase of shear strength does not observed in that case. The

Table 1 Test Specimens and Parameters

Test Specimens	Lateral Reinforcement Details: Reinforcement Ratio : p_w (%)	Yield Strength σ_y (N/mm^2)	Confining Stress $p_w\sigma_y$ (N/mm^2)	Tie Hoop	Concrete Aggregate	Axial Stress (N/mm^2)	longitudinal reinforcment ratio (%)
H04	0.40	774	3.10	-	- (mortar)	9.8	4.59
H04T				exist			
N08	0.79	406	3.21	-			
H04NA	0.40	774	3.10	-	Normal		
H04LA					light-weight		

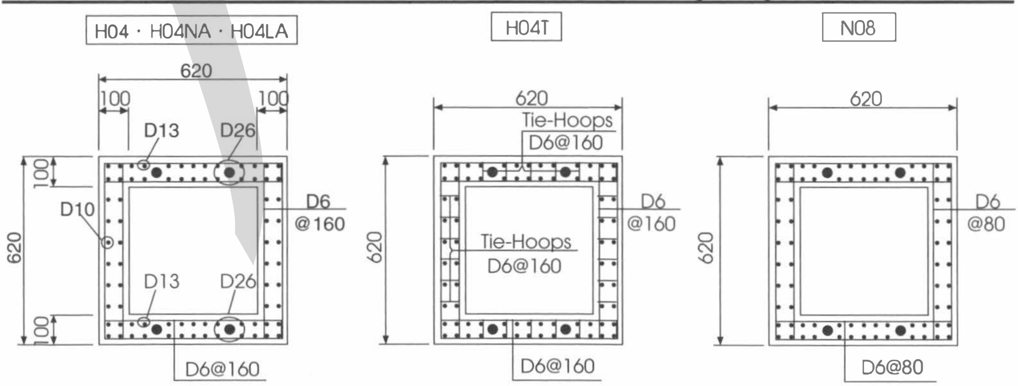

Fig.1 Cross Section Dimention and Reinforcement Detail of Specimens

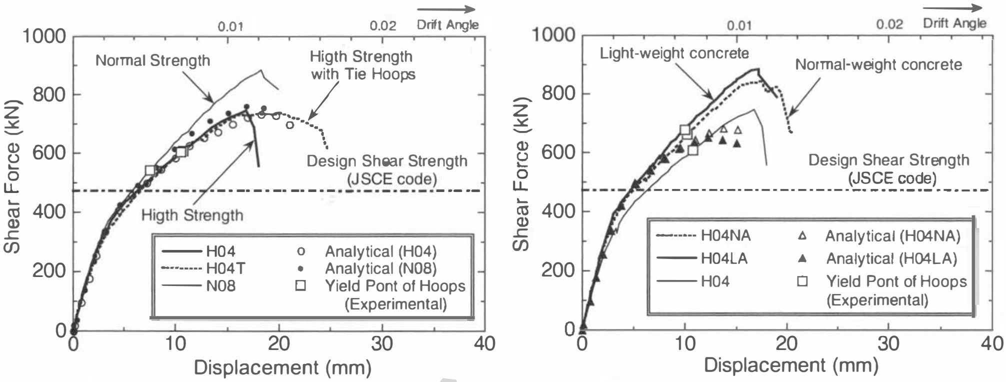

Fig.2 Load-Displacement Relationship(Left:H04,H04T,N08, Right:H04NA, H04LA)

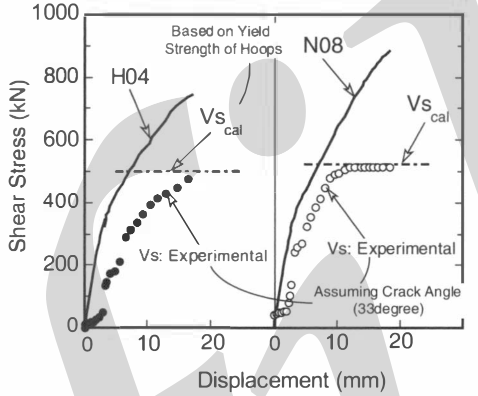

Fig.3 Shear Contribution of Hoop Reinforcement

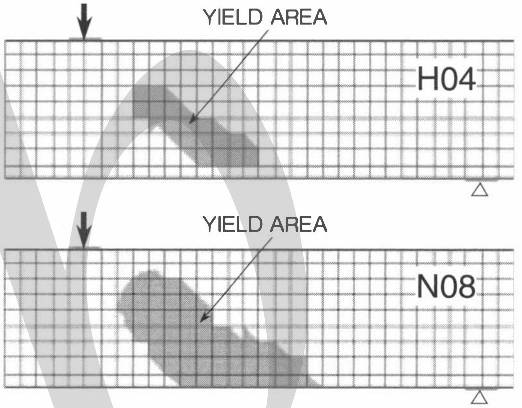

Fig.4 Analytical Yielding Area of Hoop Reinforcement

influence by different aggregate is as follows; larger shear stiffness and strength are provided in case of normal and lightweight aggregate concrete compared with mortar case, that is due to the difference of tensile strength and that of shear crack surface for interlocking. It should be noted that JSCE code provided conservative shear strength against all specimens.

Fig.3 shows shear stress pass of hoops, that was calculated with assuming diagonal shear crack(angle is 33degree). In case of normal strength hoop (N08), the shear contribution (Vs) reached the calculated yield value before peak. On the other hand, in case of high strength hoop (H04), that value (Vs) reached the calculated one at the peak. When high strength hoop is used, shear contribution of hoops becomes smaller, because the yielding area becomes smaller compared with in case of normal hoop usage. **Fig.4** shows analytical yielding area of hoop reinforcement of H04, N08 specimens. The normal strength case provides larger yielding area than high strength one. The narrower yielding band as shown in **Fig.4** can explain the main reason of the less shear strength.

3 CONCLUSION

1) Shear strength can be conservatively evaluated by the JSCE code formula, even for high strength hoop reinforcement usage members.
2) 700N/mm^2 class high strength hoop yields before shear failure.
3) No difference was observed in crack pattern in case of high strength hoops usage.
4) Yielding area becomes smaller in case of high strength hoops usage.
5) Tie hoops is negligibly affects on shear strength.
6) Usage of lightweight aggregate does not affect on the shear strength.
7) It is future work to solve the influence of wall thickness, axial force level and lateral reinforcement.
8) More accuracy is required in the shear strength prediction.

COMPARISON OF STRUCTURAL CHARACTERISTICS, SEISMIC PERFORMANCE AND ECONOMICAL ASPECT OF DIFFERENT PRESTRESSED CONCRETE STRUCTURAL FOR LONG SPAN BRIDGES IN SEISMIC REGION

Hisanori OHTSUKA and WataruYABUKI
Graduate School of Civil Eng., Kyushu Univ.
Japan

Tadao WAKASA*
New Structural Eng., Ltd.
Japan

Junji OGATA
ingerosec
Japan

Keywords: cable-stayed bridge, extradosed bridge, non-linear dynamic analysis, multi-suspended type

1 INTRODUCTION

In recent years, prestressed concrete (PC) bridges, including composite cable-stayed bridges, are developed to be larger with longer spans. However, in a seismic country, it is considered that while assessing the economical and structural rationality of different types of PC bridges with long spans, it is important to assess them quantitively treating the superstructure and substructure as a whole system. Generally, the structural types suitable for long span PC bridges may be classified into the cantilever bridge, cable-stayed bridge and extradosed bridge considering historical development of PC bridges. In a seismic country, it is thought that there is an adaptable scope for each above-mentioned type of structure when considering the dynamic interaction between the superstructure and substructure and treating them as a whole system.

In this paper, authors tried to work out the preferable span for each type of structure, where for the cantilever bridges the past examples were quoted, and for the PC cable-stayed bridges and extradosed bridges. 3 cases with span L=150, 200, 250m, including the data basing on the actual bridges by present, were studied by comparing their structural, seismic and economical characteristics during earthquake.

In the case of L=250m for extradosed bridge, the superstructure are used composite structure using steel structure in the center span, in order to lighten the weight of superstructure .

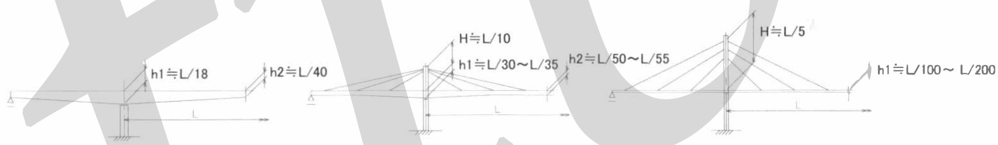

PC cantilever bridge　　Extradosed bridge　　PC cable-stayed bridge

Fig. 1 Relation of the structure and depth of girder

2 NON-LINEAR DYNAMIC ANALYSIS AND THE RESPONSE OF SECTIONAL FORCES AT THE PYLON AND PIER

Dynamic analyses have been carried out considering the non-linearity of the pylons, main girder and piers for the structures . For these analyses, the Newmark's β method ($\beta = 0.25$) with a step of 0.002 s had been used in order to calculate the response of the structure for the first 20 seconds of the seismic records. Takeda's model had been adopted for the RC material.

These results show that:

① In the longitudinal direction and in all conditions of structural types and spans, the suspended cable-stayed bridge type allows a saving of 20 to 30 % on the bending moment and of 50 to 60 % on the shear force.

② In the transversal direction and in all conditions of structural types and spans, the suspended cable-stayed bridge type is similar as the extradosed bridge for the bending moment and allows a saving of 20 to 30 % on the shear force.

These results may be considered as the effect of a lower weight of the deck girder of the cable-stayed bridge, which can explain a reduction of the forces of about 20 %, as a structural damping effect of the suspended structure.

3 CONCLUSION

The suspended structure, which is generally used for a PC cable-stayed bridge, can decrease the seismic forces acting on the substructure due to the larger damping effect of stay cables.

Further, the structure of rigid frame is used well in a cantilever bridge and an extradosed bridge. For this type of structure, though the girder is rigidly connected to the pier, the sectional forces of seismic response may not be so small as that of a suspended structure because of a less structural damping.

As a result of comparison on PC cantilever bridges, PC cable-stayed bridges and extradosed bridges with spans of 100～250m, it has been shown that the economical boundary between the extradosed bridge and the cable-stayed bridge is about L=150m from the cost comparison of superstructure. Further, the ratio (PC cable-stayed bridges / extradosed bridges) including both the superstructure and the substructure are 0.84 ～0.86 , meaning that the cable-stayed bridges are 14% ～16% cheaper than the extradosed bridges for all cases treated in this paper . And it is clear that the cable-stayed bridge is advantageous for a span over 150m when assessing the whole system with both the superstructure and substructure.

While, for a span of about 80～150m, the extradosed bridge may be considered excellent in structure and landscape, because the girder can be designed much lower than that of the cantilever bridge.

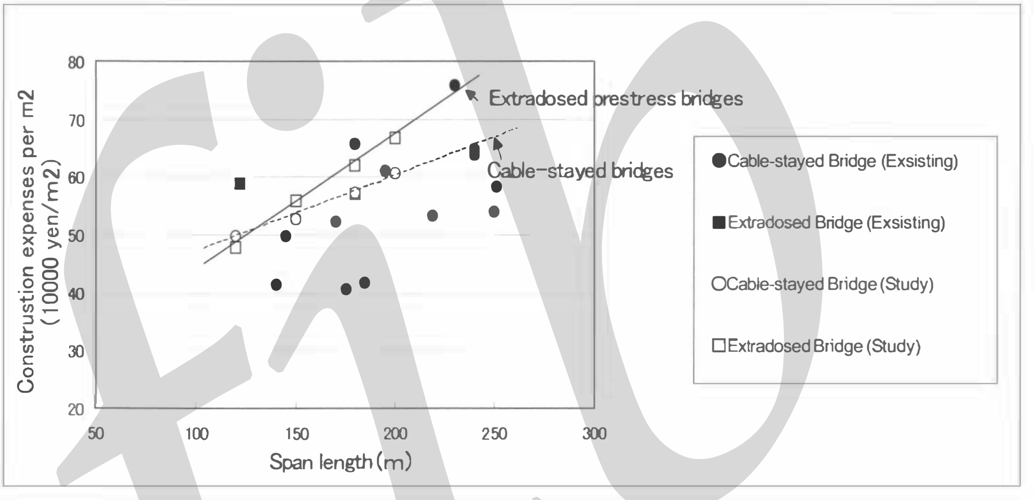

Fig. 2 Global Cost Ratio without Foundations

REFERENCE

[1] Jun Yamasaki, et al. "The Structural Characteristics of PC Bridges with Large Eccentic Tendons", Prestressed Concrete, Vol. 39, No.2, Mar. 1997

[2] Hisanori Otsuka, et al. "Rationality with Different Types of Prestressed Concrete Long Span Bridges in a Seismic Country", Proceeding of the 55th Annual Conference of JSCE, (September, 2000) V-544

PROBABILISTIC PARAMETERS OF THE SEISMIC PERFORMANCE OF REINFORCED CONCRETE FRAMES

Fabio Biondini, Giandomenico Toniolo
Department of Structural Engineering, Technical University of Milan

Keywords: seismic response, design reliability, concrete structures, simulated earthquakes.

1. INTRODUCTION

The paper gives a contribution to the reliability assessment of the design methods of Eurocode 8 (EC8) with reference to r.c. frame systems. To this aim, the very simple type of structure shown in Fig. 1 in its two arrangements corresponding to a cast-in-situ monolithic solution and a precast hinged solution, is considered. For this structure it is assumed that, under the same seismic force F, the arrangement of Fig. 1.a, with four critical sections dimensioned for a moment $m=Fh/2$, may dissipate the same amount of energy which the arrangement of Fig. 1.b dissipates in its two critical sections, dimensioned as they are for a moment $M=Fh$ double than the first one ($4u \cong 2U$). In other words, the dissipation of energy is not a question of number of dissipation zones, but it is a question of total structural volume involved in dissipation: few larger zones may dissipate the same amount of energy of many smaller zones. Thus, both the structures are intended to belong to the "prized" type of frames, with the same force reduction factor (the behaviour factor of EC8). This deny the discriminations set by the first version 1994 of EC8 to some type of one storey precast structures.

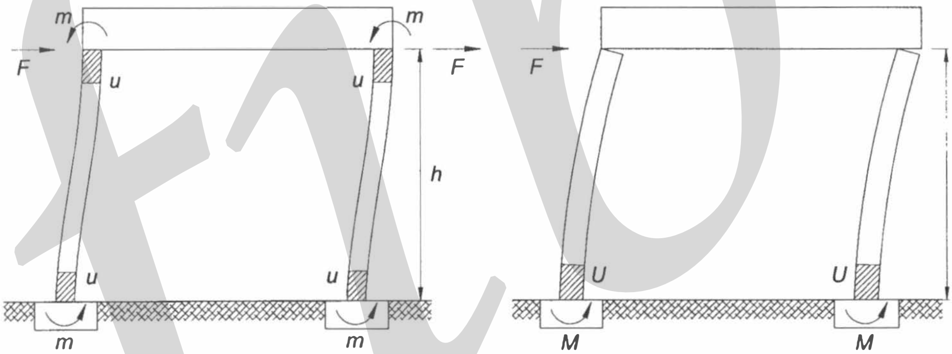

Figure 1. Energy dissipated by the frames: (a) monolithic and (b) hinged arrangement.

The confirmation of the previous assumption and the actual quantification of the reduction factor should come from the results of the analysis. To this purpose a large number of dynamic analyses have been done assuming as many artificial accelerograms.

3. STRUCTURAL ANALYSIS

The dynamic non-linear analysis is based on the motion equation of single degree of freedom systems. The shear force of the columns is directly given as $V(d)=F(d)-N_{ad}d(t)/h$, where d is the top displacement of the structure, $F(d)$ is read on the proper force-displacement model as a function of the preceding load history and the second term represents the second order effect of the vertical load N_{ad} acting on the columns. The F-d function of the degrading elastoplastic stiffness has been derived from Takeda model, completed with a decreasing branch in order to represent the ultimate phase of failure.

The analyses have been repeated 1000 times with artificial seismic actions generated using the programme SIMQKE. For the present application, a "compound" function has been chosen as envelope curve. The shape parameters have been generated as random variables according to an uniform distribution within proper ranges. As regards the frequency content of the accelerograms, the ground motions have been generated according to the response spectra type 1 for subsoil class A of EC8.

The computed responses are represented by the overstrength κ of the structure with respect to the design strength. The overstrength κ is the basic measure of the reliability of the design rules of the Eurocode 8, since it represents the direct comparison between the "actual" experimental strength and the "design" computed strength of the structure.

4. RESULTS OF THE ANALYSIS AND CONCLUDING REMARKS

The results of the analyses are summarised in the correlation diagram of Fig. 2, which shows the correlation between the responses of the two structures in terms of the overstrength κ (correlation factor $\rho_\kappa = 0.884$). Such diagram allows a direct comparison between the seismic behaviour of the two types of frames, showing the substantial equivalence of any couple of values. In statistical terms, a more meaningful comparison of the responses can be deduced from the density distributions of the overstrength ratio κ. Such distributions are shown in Fig. 3, together with their fitting curves drawn according to the lognormal model. The characteristic values of the overstrength deduced by such model ($\kappa_{0.05}$=1.27 for both the monolithic and the hinged frame) are somewhat higher than κ = 1, which is the limit of full reliability of the comparative analysis.

The results clearly show that the precast frame with hinged beams, having critical sections located at the base of the columns and dimensioned for the corresponding clamping moments, is able to dissipate the same quantity of energy which the monolithic frame dissipates in its more numerous critical sections, being dimensioned for halved moments.

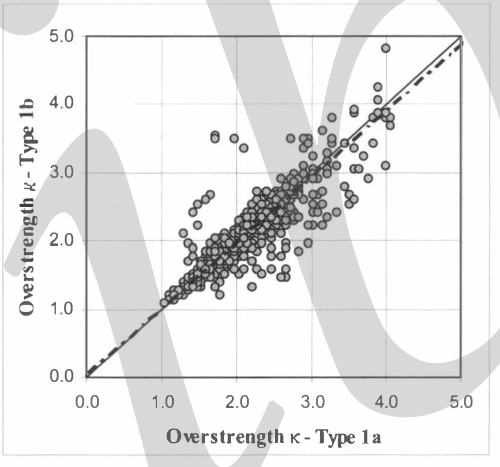

Figure 2. Correlation diagram of the overstrength ratio κ for both the monolithic and the hinged frames (1000 simulations).

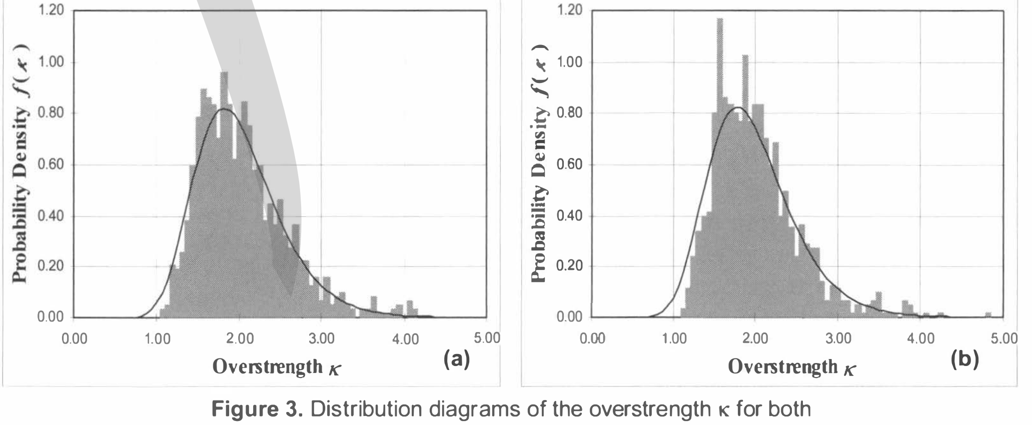

Figure 3. Distribution diagrams of the overstrength κ for both (a) the monolithic and (b) the hinged frames.

EXPERIMENTAL STUDY ON SEISMIC PERFORMANCE OF PRECAST PRESTRESSED CONCRETE BUILDING

Hiroto KATO
Building Research Institute, Tsukuba, JAPAN,
Email: pckato@kenken.go.jp

Yuuhiko ICHISAWA
P.S. Corporation, Tokyo, JAPAN,
Email: ichisawa@psgate.psc.co.jp

Kei TAKAMATSU
Itho-Gumi Construction Co., Ltd., Sapporo, JAPAN,
Email: k-takamatsu@mua.biglobe.ne.jp

Naoto OKAMOTO
Ohmoto-Gumi Co., Ltd., Tokyo, JAPAN,
Email: okamoton@gw.ohmoto.co.jp

Keywords: precast prestressed concrete structure, substructure pseudo dynamic tests, seismic performance, earthquake response behavior, equivalent linearization method

ABSTRACT

A series of seismic loading tests on a precast prestressed concrete (PC) specimen had been carried out, which were consisted of substructure pseudo dynamic (PSD) tests and static loading tests. The objectives of the study were to grasp the earthquake response behaviour of the specimen and evaluate the basic structural performance of it.

The specimen was a 1/2.74 scaled model of a prototype PC building, which was an eleven-story and 45m height moment resisting frame structure and composed of all precast structural members. In the tests, the lower three stories were actually loaded, while upper eight stories were simultaneously calculated in a computer with a numerical restoring characteristics model, and these data were gathered into the computer to reproduce the dynamic response of whole building in earthquake excitation (Fig.1). The *Hachinohe*(1968) EW wave with normalized maximum velocity of 0.25, 0.50 and 0.75m/sec and the *JMA-Kobe*(1995) NS wave were employed in the PSD tests as input accelerations.

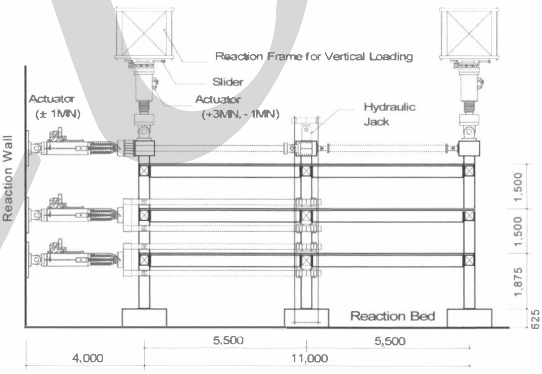

Fig. 1 Overview of Test Set-up

The outcomes from the loading tests are shown in Figs.2 and 3. The restoring characteristics of specimen in the region of small deformation were the particular one of PC structure, which is small residual displacement and less hysteretic loop area. The maximum responses in 0.50m/sec input test were R_{max}=1/86 as the story drift angle and Q_1=2.20MN as the base shear force. And also the maximum values in *JMA-Kobe* test were R_{max}=1/52 and Q_1=2.45MN, which approximately coincided with 0.4 in the standard base shear coefficient. Damages of the specimen occurred mainly at the

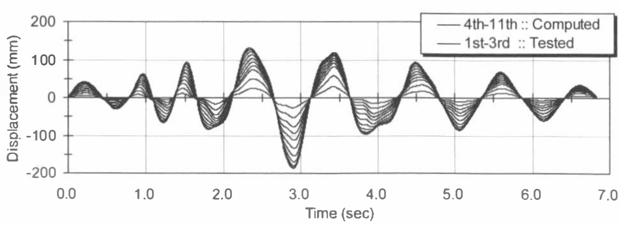

Fig. 2 Dynamic Responses of Specimen in *JMA-Kobe* Test

ends of beams and the bottoms of first story columns, those corresponded to the assumption in the structural design.

The specimen shows the good load carrying capacity even in the large deformation region. And the post dynamic analyses showed the good agreement with the experimental results; the employed restoring characteristics model can adequately reproduce the dynamic behavior of the specimen.

In addition, the maximum displacement responses of the specimen were evaluated by the equivalent linearization method adopted in the Building Standard Law of Japan. Though the estimated values were a little larger than those of the experimental results (Fig.4), it was showed that the design method is valid and practical with some safety margins.

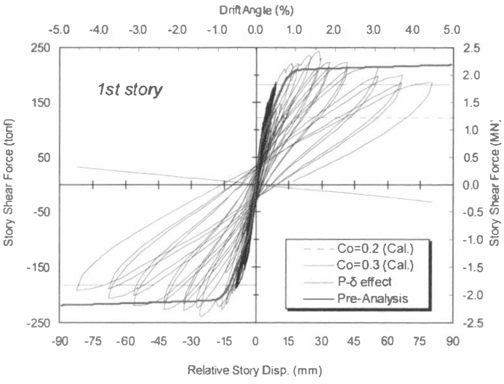

Fig. 3 Story Shear Force and Relative Story Displacement Relationship (First Story)

The major findings obtained from the substructure PSD tests and the static loading tests are summarized as follows:

1) The precast PC specimen had the sufficient seismic property to severe earthquake excitation and showed the good performance in the large deformation region.
2) The cracks of the specimen concentrated near the joint between precast structural members.
3) The equivalent damping factor (*heq*) was small, the value was around 0.08 even in the large deformation such as 1/25 of the story drift angle.
4) The dynamic response analyses using "*PC-model*" could adequately reproduce the elasto-plastic behavior of the specimen.
5) Though the responses of the specimen by the equivalent linearization method were relatively larger than the experimental results, it is confirmed that the method gives the effective results with some safety margins.

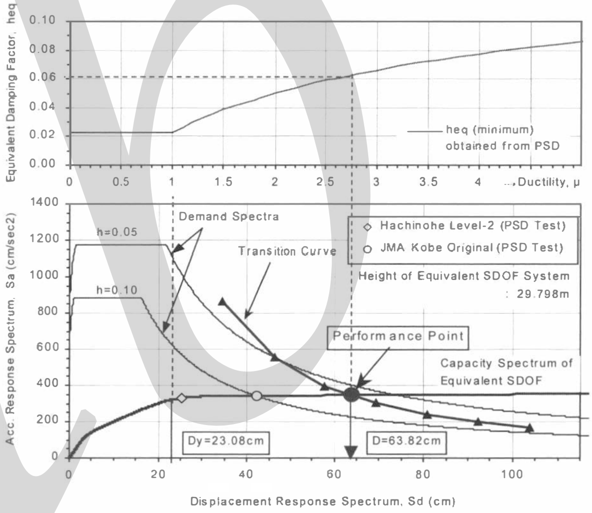

Fig.4 Performance Point by Equivalent Linearization Method

REFERENCES

[1] Kato H, et al., "Earthquake Response of An Eleven-story Precast Prestressed Concrete Building by Substructure Pseudo Dynamic Test", Proceedings of 12th WCEE (New Zealand), January 2000

[2] Nakashima M., et al., "Integration techniques for substructure pseudo dynamic test", Proceedings of 4th U.S. NCEE, 1990, pp.515-524.

[3] Okamoto S. and Kato H., "Earthquake response characteristics of prestressed concrete building structures", Proceedings of 10th WCEE, 1992, pp.4389-4394.

[4] Commentary for The Calculation of Response and Limit Strength, Kenchiku Gijyutu, April 2001, pp.97-168 (in Japanese)

SEISMIC PERFORMANCE OF CONCRETE PIERS PRESTRESSED IN THE CRITICAL SECTION

Shoji Ikeda Satoru Nonaka
Yokohama National University
Japan

Seiji Hirose Takahiro Yamaguchi
Kyokuto Kogen Concrete Shinko Co., Ltd.
Japan

Keywords: pier, vertical prestressing, automatic anchorage, seismic performance

1. INTRODUCTION

With a view to achieving vertical prestressing in actual piers in the most reasonable way, the authors have proposed a new design concept of concrete piers in which vertical prestressing was introduced only in critical sections e.g. the bottom portion of the pier. In this study, in order to investigate the seismic performance of concrete piers prestressed in the bottom portion, reversed cyclic loading tests and a pseudo-dynamic test was carried out using a prestressed concrete column specimen.

Fig. 1 shows a scheme of the vertical prestressing into the pier bottom. The features of proposed design concept is to use of an automatic anchorage, which separates the anchorage point from the tensioning point. This enables it to tension PC strands from the voluntary point such as the sides of a pier in spite of the complicated steel arrangement and to introduce vertical prestressing over a desired range throughout the pier height.

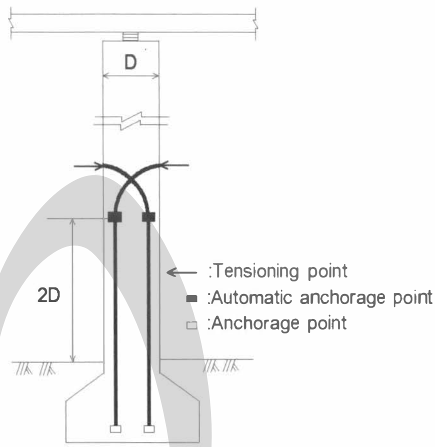

Fig.1 A scheme of vertical prestressing in the bottom portion

2. TEST SPECIMENS

Table 1 shows main characteristics of the test specimens and Fig. 2 shows an example of their configurations. The axial stress given by prestressing was 4MPa and was common to all test specimens. The concrete strength was designed to be 35MPa. Among the total five pier test specimens prepared, two specimen (P-N10 and P-N13) were prestressed over their entire height and the remaining three specimens (P-NH-C, P-NH-A1 and P-NH-A2) were only prestressed within a range up to 2D (D is the height of the cross section) height from the footing top surface. It was the specimen P-NH-A2 that PC strands had been anchored to by means of automatic anchorage. In the three test specimens where PC strands were anchored at 2D, high-strength rebars SD785D16 (hereinafter referred to as the additional rebars) rising from the top surface of their footing were added in order to smooth the force transmission at 2D anchorage points.

Table 1 Characteristics of specimens

Specimen	Area ratio of longi. rebar (%)	Area ratio of PC strand (%)	Vertical prestressing range	ν *1	Calculated flexural capacity (kN)
P-N10	0.71	0.49	Whole	0.80	216
P-N13	1.27	0.49	Whole	0.63	249
P-NH-C	0.63	0.49	2D	0.77	208
P-NH-A1	0.71	0.49	2D	0.80	216
P-NH-A2*2	1.27	0.49	2D	0.63	249

*1:Sharing ratio of PC strand in flexural capacity
*2:Automatic anchorage used D: Height of cross section

3. TEST RESULTS AND DISCUSSION

Fig. 3 shows a comparison of the load-displacement envelopes. The envelope of load-displacement of specimen P-NH-A2 where prestressing was applied only to the bottom portion was coincide well with that of specimen P-N13 where it was applied throughout the whole height. Similarly, in the case of a comparison between specimen P-NH-A1 and P-N10 in which the calculated flexural capacity was about 20% smaller than the above two specimens, no significant influence by the cut-off of PC strand was shown. These results clarified that the specimens prestressed in the bottom portion have an inherent flexural performance which is comparable to that of specimen prestressed in the whole height of the column, provided that the cut-off portion of PC strands is reinforced with additional rebars.

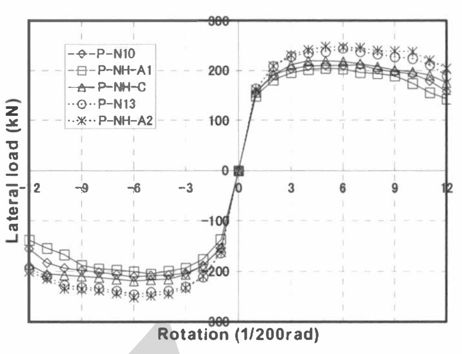

Fig.3 Envelops of lateral load-displacement curves

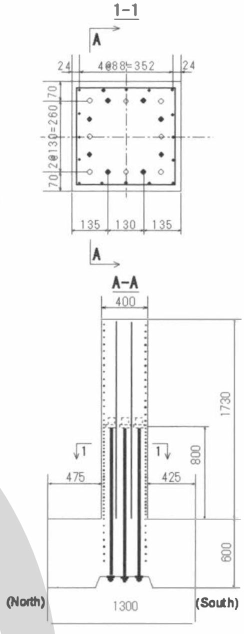

P-NH-A1,P-NH-A2
Fig.2 Shape of specimen

A pseudo-dynamic test using a specimen corresponding to specimen P-N13 was carried out to confirm the seismic performance of PC piers under an actual earthquake. The used acceleration motion was N-S wave of JR Takatori Station (maximum acceleration: 642 gal) recorded during the 1995 Hyogo-ken Nanbu Earthquakes. Figs. 4 shows the lateral load-response displacement relationship. The residual displacement at 15 seconds when the pseudo-dynamic test finished loading was about 5mm, which was less than 1/200rad, and no declining restoring force was observed. The excellent seismic performance of PC piers could be verified under the actual near field earthquake wave.

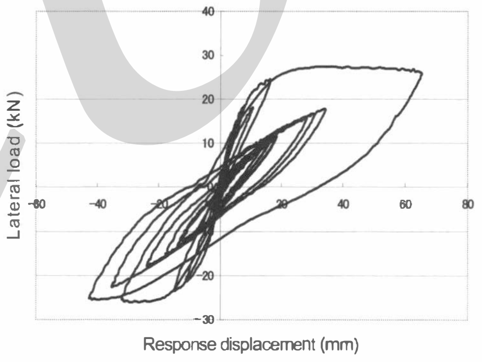

Fig.4 Lateral load–response displacement curve

4. CONCLUSION

The results obtained within the scope of this experimental study are summarized below:

(1) The combination of introducing vertical prestressing only in the bottom portions and additional rebars arranged was quite effective for enhancing the ductility and the restoration capability of concrete piers as well as for prestressing the whole height.

(2) By adopting the idea to arrange PC strands only at the pier bottom portion, and using automatic anchorage, the construction of economical PC piers in which the volume of PC strands could be minimized, and tensioning works could be done at an easy position were shown.

(3) From the results of the pseudo-dynamic test, it was verified that PC piers can exhibit excellent seismic performance with advanced restoration capabilities against near field earthquakes in the 1995 Hyogo-ken Nanbu region.

SEISMIC PROPERTIES OF PPRC PIER

Masahiro Nakai
P.S.Mitsubishi Construction Co.,Ltd.
Civil Engineering & Development Dept
JAPAN

Yukitake Shioi , Akira Hasegawa
Hachinohe Institute of Technology
Civil Engineering Division
JAPAN

Keywords : PPRC, seismic performance, high strength non bleeding mortar

1 INTRODUCTION

In the 1966 (36 years ago) Precast RC pier which was substructure of railway bridge was constructed at IWATE prefecture (see Photo- 1). Till now, this pier have experienced of the great earthquake. But there were not any damage at the surface. PPRC pier is advantageous in many respects when constructed on-site but should have their performance with respect to seismic load, which is the major load after completion. The results of horizontal loading tests for this type of pier were reported by Nakano and others in the 1996 committee. The condition reported at that time were such those:

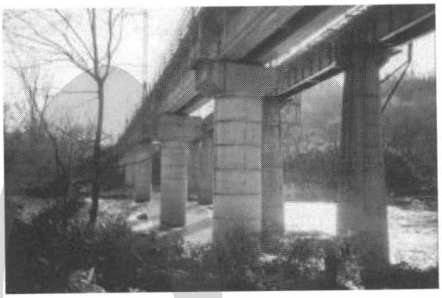

Photo.1 Mabechi river bridge

(1)Frame bodies were hollow cylinders.
(2)No adhesive was used between precast blocks and the effects
of shear keys were investigated.
(3)There was a great amount of prestress induced.
(4)The effects of the layouts hoop ties were investigated.

The following conditions were reached according to loading tests with four specimens:

(1) The maximum loading capacity and ductility of PPRC piers are equal to those of RC piers.
(2)Doubly provided hoop ties contribute to improvement of ductility.
(3)Prestress induced with reinforcement increases restoring force characteristics but decreases the amount of energy absorption.
(4)The existence of shear key at joint faces restricts to the displacement of joints.

Based on these results, PPRC piers have been found to demonstrate the same performance as RC piers. However, since they were disadvantageous in term of construction cost, further investigations were needed. Therefore, comparison studies were made by horizontal loading tests for the seismic performance of several improved prestressing methods that would significantly affect construction efficiency.

2 OUTLINE OF THE TESTING

2.1Specimen

Fig. 1 indicates the dimensions of a specimen. Epoxy was applied to the joint faces of specimens and prestressing steel bars were used in the center with stress of 1N/mm^2 for connection of the footing and precast body. The T series has five specimens with axial sheaths for reinforcement and grout in addition to one (TC:RC cast-in-place). The Y series has prestressing stands instead of reinforcement and YC corresponds to TC without sheath. The difference in behavior are studied according to respective fixing methods .

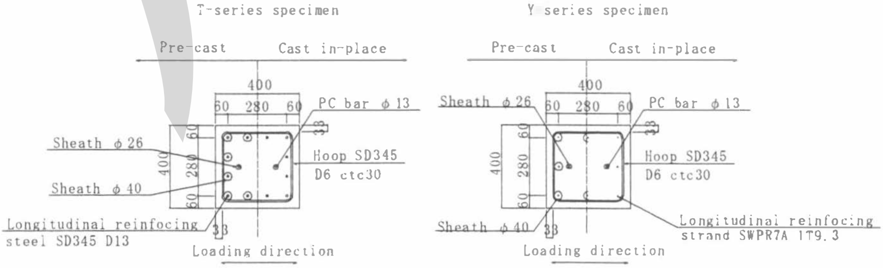

Fig.1 Cross section of specimen

Table 1 indicates the type of specimen.

Table1 Type of specimem

Type	Specimen	Type of longitudinal steel	Fixing material	Type of anchoring	Anchorage of prestressing steel bar
T-series	TC	Reinforcement (SD345,D13)	Concrete		Unbond
	TMKK		Mortar	Anchored1)	
	TMFK			Non-anchored2)	
	TMSK			Non-anchored3)	
	TSKK		Cement paste	Anchored1)	
	TMKB		Mortar		Bond
Y-series	YC	PC strand wire (SWPR7A, 1S9.3)	Concrete		Unbond
	YMKK		Mortar	Anchored1)	
	YSKK		Cement paste	Anchored1)	

3 CONCLUSION

The findings of these tests indicated that:

(1)PPRC piers have the same maximum load in comparison to RC piers but better ductility.

(2)The design of PPRC piers should be based mainly on bending moment but not shear force due to bending moment.

(3)Damage of PPRC piers by earthquakes can be easily repaired and they can become useful for emergency traffic immediately after earthquakes.

(4)The design of PPRC piers with reinforcement inserted in sheaths (T series) should follow the design of RC structures.

(5)The design of PPRC piers with prestressing strands(Y series)requires the proposal of other calculation methods with an emphasis on bending moment.

(6)In order to ensure proper construction, the steel anchoring should be firmly secured.

(7)Results confirmed that PPRC piers can substantially reduce overall construction costs through the adoption of both methods with such advantages of tight work space, area, extremely short construction period and so on.

REFERENCES

[1] Shioi,Y.,Hasegawa,A.,Nakai,M.,and Tsuda,Y.,:Seismic performance tests of joint method of precast prestressed reinforced concrete members.JCI,Vol.38,No.8,2000.8,pp33-39.(in Japanese)

[2]Nakai,M.,Okuyama,K.,Umeda,J.,and Tuda,K.,:Study of the primary factors which improve ductility,JCI Annual ,Vol.23,No.3,2001,pp1159-1164.(in Japanese)

[3]Tada,K.,Shima,H.,and Kuno K.,:Bond characteristic of reinfocement fixed by mortar in the sheath, JCI Annual ,Vol.18,No.2,2001,pp154-59.(in Japanese)

LIMIT ANALYSIS OF PRESTRESSED CONCRETE PILES BY THE YIELD LINE THEORY CONSIDERING INTERACTION OF COMBINED FORCES

UEHARA Shuichi
Ariake National College of Tech.
JAPAN
uehara@ariake-nct.ac.jp

SAKINO Kenji
Kyushu University
JAPAN

ESAKI Fumiya
Kyushu Kyoritsu University
JAPAN

Keyword: limit analysis, yield line theory, shear, pile

1 INTRODUCTION

A limit analysis method of reinforced concrete columns with rectangular sections has been proposed by the authors[1]. The method is based on the generalized yield line theory and takes account of the interaction of bending moment, axial force and shear force. In the present paper, the method is applied to prestressed concrete (referred to as PC hereafter) piles with hollow circular sections.

2 ANALYTICAL METHOD

2.1 Summary of analytical method

Fig. 1 shows a PC pile subjected to bending moment, axial force and shear force antisymmetrically. As already proposed[1], yield lines are assumed as planes which cross the extreme compressive corner of member ends. The pile fails when the yield lines reach at their yield strength. Fig. 2 shows a failure mechanism. The middle element may move and rotate. Horizontal shear capacity Q can be calculated by the equilibrium condition with internal forces at the yield line. As a failure mechanism (or kinematically admissible state) is assumed, the obtained value is considered to be an upper-bound value. Hence the minimum value would be the horizontal shear capacity when the inclination angle θ_f of yield line is varied.

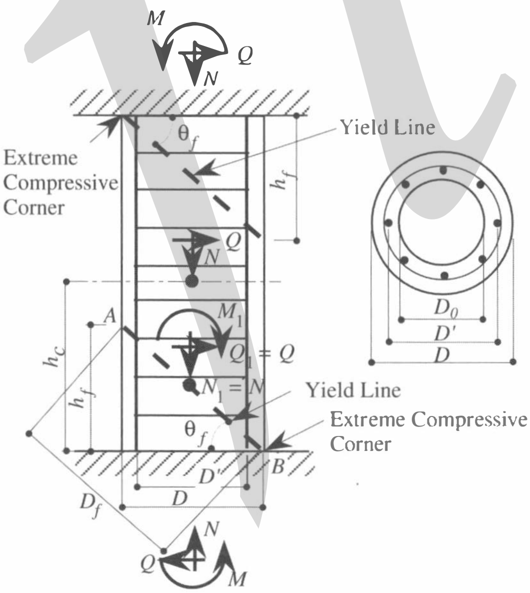

Fig. 1 PC pile with a hollow circular section subjected to bending moment, axial force and shear force

2.2 YIELD CRITERION

The yield criterion of pile sections is evaluated by the superposition theory. However an approximate yield criterion of reinforced concrete sections is used in the present paper as used in Ref.[1]. The curved surface of the yield criterion is obtained by expanding the yield criterion of concrete as much as the effect of reinforcements on every axis.

2.3 EFFECTIVENESS FACTOR

The horizontal shear capacity is greatly influenced by the effectiveness factor ν, when longitudinal reinforcing bars are elastic[2]. Therefore ν was examined by using experimental values of employed specimens. It is clarified that ν is influenced by composite axial stress ratio σ_{c1} and a formula is proposed.

3 ANALYSES OF 82 SPECIMENS

To estimate the horizontal shear capacity of PC piles two equations are

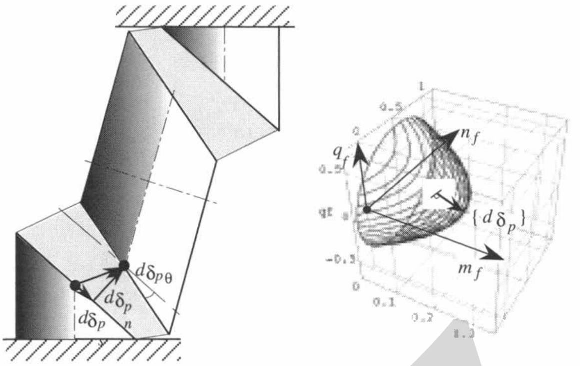

Fig. 2 Failure mechanism of a PC pile following the associated plastic flow rule

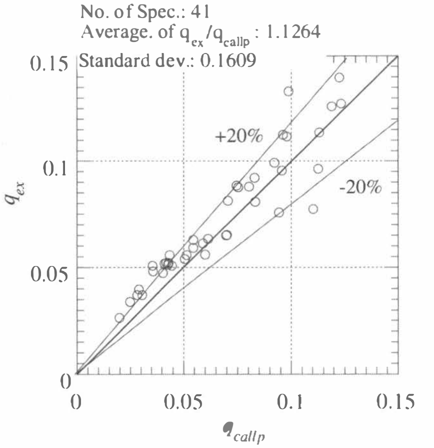

Fig.3 Analysis of specimens controlled by longitudinal reinforcement yielding

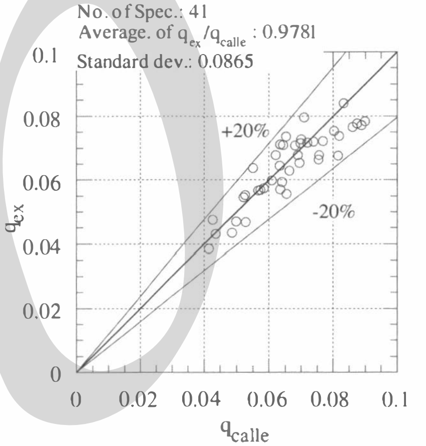

Fig.4 Analysis of specimens controlled by elastic longitudinal reinforcement

used. One is an equation controlled by longitudinal reinforcing bars yielding, in which $\nu = 1.0$ is used. The other is an equation controlled by elastic longitudinal reinforcing bars, in which ν is estimated by the proposed formula. The smaller value is considered as analytical value.

Fig. 3 shows the comparison between analysis and observed on horizontal shear capacity of the specimens controlled by longitudinal reinforcing bars yielding. The average of q_{ex}/q_{cal} is a little large and the standard deviation is also a little large.

Fig. 4 shows the comparison between analysis and observed on horizontal shear capacity of the specimens controlled by elastic longitudinal reinforcing bars. The shear capacity is predicted very well.

4 CONCLUSIONS

From the study in the present paper, following conclusions can be drawn:

(1) The effectiveness factor is influenced by composite axial stress ratio σ_{c1}.

(2) The horizontal shear capacity of PC piles can be estimated well by the proposed method when longitudinal reinforcing bars are elastic, i.e. controlled by shear failure.

(3) The horizontal shear capacity of PC piles are underestimated a little by the proposed method when longitudinal reinforcing bars are plastic, i.e. controlled by flexural failure,

REFERENCES

[1] Uehara, S., Sakino, K., Fumiya F. : Limit analysis of reinforced concrete columns by the yield line theory considering interaction of combined forces, Transactions of JCI, Vol.22, pp.413-426, 2000

[2] Uehara, S., Sakino, K., Fumiya F. : Limit analysis of 142 shear walls with a barbell section by the yield line theory considering interaction of combined forces, Journal of structural engineering, AIJ, vol. 46B, pp.547-560, March 2000 (in Japanese)

PROPOSAL OF THE HYSTERESIS LOOP FOR THE PRE-STRESSED CONCRETE BOX GIRDERS WITH ECCENTRICALLY LOCATED PC CABLES

Hisanori Otsuka, Wataru Yabuki,
Kyushu University, JAPAN
Meguru Tsunomoto, Yousuke Urakawa
Oriental Construction Co.,Ltd. JAPAN

Shin-ichi Ishihara
Kozo Keikaku Engineering, Inc., JAPAN
Tadahiko Tsutsumi
Corporation of Fuji P.S. JAPAN

keywords: PC box girders, hysteresis loop, eccentrically located PC cables

1 INTRODUCTION

Skelton curve and hysteresis loop are necessary in the nonlinear time history analysis of bridges. These curves for the RC members already have been proposed, but hysteresis loop for PC girders with eccentrically located tendons has not obtained . According to the experimental works, a formulation of hysteresis loop are proposed.

2 OUTLINE OF EXPERIMENTAL WORKS

The specimens are one box girder, and are scaled down into about 1/8.5 for ordinary existing girders. The strength of concrete is 40N/mm², the type of reinforcement are SD295(D13), and the type of PC tendons are SWPR7A15.2. Cyclic increasing loads are applied for simple girder subjected to pure moment in center part of girder(**Fig 1**). The degree of eccentricity of PC tendons is a parameter for this study, and the specimen of L02, L03 L04, and L23 are symetric, lower eccentric, upper eccentric, and moderate lower eccentric location of PC tendons(**Fig 2**).

3 EXPERIMENTAL RESULTS AND PROPOSED EQUATION

Fig 3 shows the hysteresis loops for L03 and L04 models. The bending capacities are different in positive and negative moments because of eccentric locations of PC tendons. **Fig 4** shows the sketch of proposed curve in unloading stage. This curve Y is expressed by the combination of two equations y_1 and y_2 as shown in below.

$Y = C \cdot y_1 + (1-C) \cdot y_2$ in which $y_1 = \sin(-1.5\pi \cdot x^p)$ $y_2 = 1 - e^{-qx}$

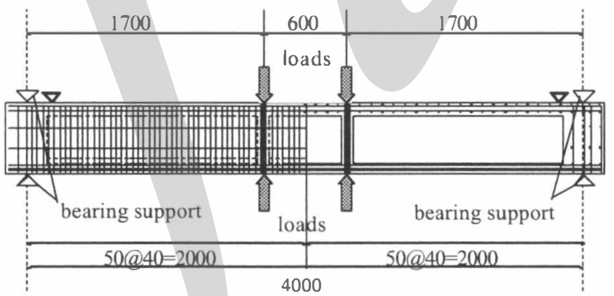

Fig 1 Ttest specimen (unit mm)

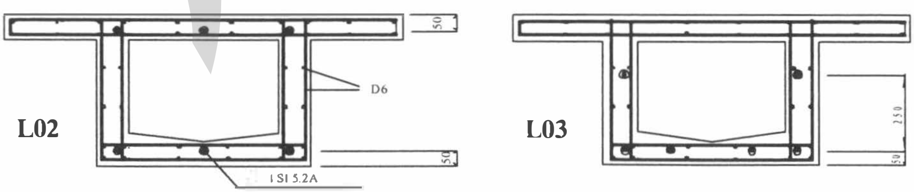

Fig 2 A cross section of L02 and L03(unit mm) (● : PC tendon)

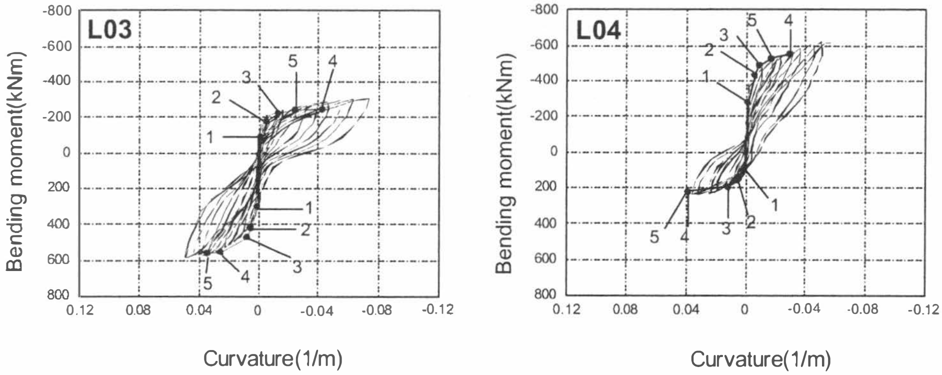

Fig. 3 Bending moments - curvature relation and analytical skelton (1:crack , 2:yield of reinforcement, 3: elasic limit of PC tendon, 4: yield of PC tendon, 5: failure of compressive concrete)

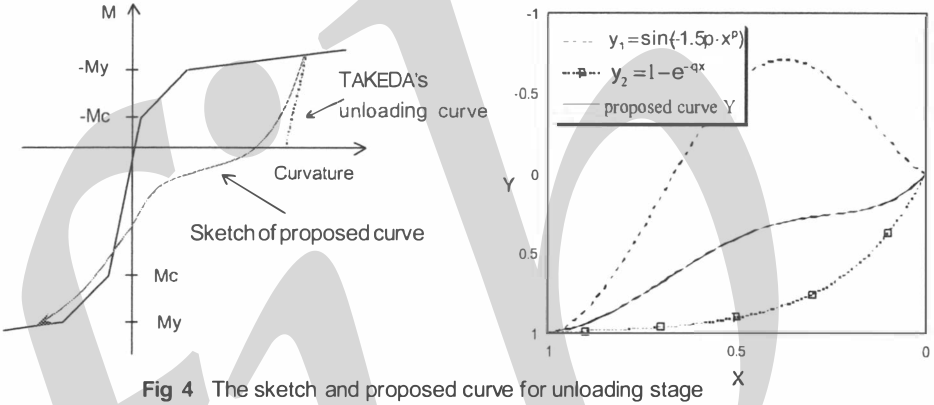

Fig 4 The sketch and proposed curve for unloading stage

The coefficients p and q in equations y_1 and y_2 are determined by the degree of excentricity of PC tendon.The coefficient C is detemined by the following equation derived by the definition of damping ratio. γ_1 and γ_2 are defined as the bending capacities for positive and negative moments to sum of both capacities in the absolute values, respectively. Therefore $\gamma_1 + \gamma_2 = 1$. α and β are obtained by proposed formula.

$$C = \frac{\beta_1 + \beta_2 + 1 - \pi \cdot h \cdot (\gamma_1^2 + \gamma_2^2)}{\alpha_1 + \alpha_2 + \beta_1 + \beta_2 + 2}$$

The damping ratio is calculated by the ductility ratio, amount of prestressing, and bending capacity ratio $\gamma = \gamma_1 / \gamma_2$.

$$h = A(1 - e^{-B\mu})$$

Fig 5 shows the comparison of damping ratio between experimental results and the above mentioned equation.

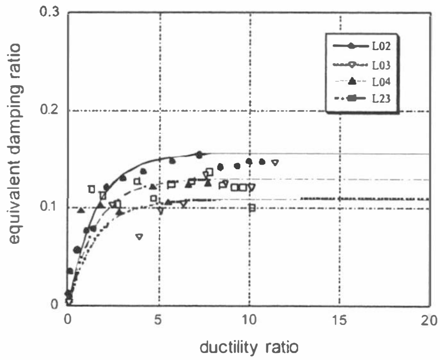

Fig 5 Comparison of the equivalent damping ratio

By the comparison of the hysteresis loops, damping ratios and residual bending curvatures obtained by experiments and proposed formulas, it is clear that the proposed formulas can simulate these loop and values of any PC girders with or without eccentrically located PC tendons with sufficient accuracy.

REFERENCES

[1]H.Otsuka, W.Yabuki, S.Ishihara, Y.Urakawa, and M. Tsunomoto: Study on the of Hysteresis loops of Prestressed Concrete Box Girderrs with Eccentrically Located Tendon, Journal of Prestressed Concrete, Japan,Vol.44,No.1, pp.65-72,Jan-Feb., 2002.(in Japanese)

BOND STRENGTH OF REINFORCED CONCRETE MEMBERS CONFINED WITH FIBER REINFORCED POLYMER SHEET

Tetsuzo KAKU
Toyohashi University of Technology, Japan

Susumu KONO
Kyoto University
Japan

Kazunari MATSUNO
Kure National College of Technology, Japan

Keywords: FRP sheet, carbon, bond strength, cantilever type bond test

1 INTRODUCTION

It is well known that the confinement by FRP sheets greatly increases the shear capacity of reinforced concrete beam and column. The increase in shear capacity due to FRP sheets has been experimentally evaluated and incorporated in design equations. According to a truss analogy, the increase in shear capacity should be guaranteed by also increase of bond stress. However, the increase in bond strength for RC members confined with FRP sheet has not been fully quantified.

Sixty cantilever type bond tests and seventeen anti-symmetric loading beam tests were carried out in order to investigate the effectiveness of the FRP sheet for the increase of the bond strength of longitudinal bars in the existing RC members

2 CANTILEVER TYPE BOND TEST.

Shown in Fig1. is the cantilever type specimen used in this study. FRP sheet was rolled and attached to the surface of the specimens with stripe manner for easier searching the concrete cracking. Main test variables were the type of FRP sheet (carbon, aramid and glass), the amount of FRP sheet (p_{wf}= 0,0.08,0.16 0.25,0.32%), the location of tested bar at concrete casting (top or bottom bar), the diameter (D19,D25) and numbers (2,3 or 4) of the tested bars.

Defining the bond stress as the tensile force of tested bar divided by bond length and bar perimeter, the relationship of bond stress and slip at loaded end are shown in Fig.2, where, it can be seen that the bond strength increased and the slope of falling branch after peak load became more gentle as p_{wf} increased.

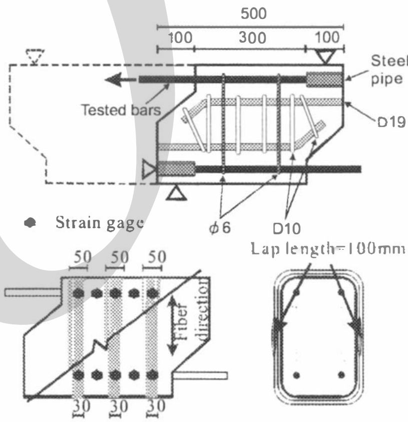

Fig.1 Specimen dimensions

3 PROPOSAL OF BOND STRENGTH EQUATION

The bond strength of the longitudinal bars in the RC members were assumed to be the summation the bond stress carried by concrete τ_{co}, transverse reinforcement τ_{st}, and FRP sheet τ_{wf} as shown in Eq.1

$$\tau_u = \tau_{co} + \tau_{st} + \tau_{wf} \tag{1}$$

Considering the result of the cantilever type bond test, the following bond strength equation was derived.

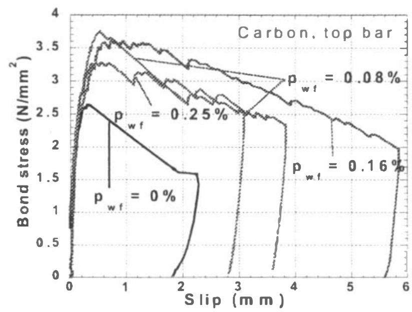

Fig.2 Tensile force-Displacement relation

$$\tau_{wf} = \frac{1}{6} \cdot \left(\frac{E_{wf}}{E_0} + 0.5 \right) \cdot \left\{ 1 - \left(\frac{p_{wf}}{0.0035} - 1 \right)^2 \right\} \cdot \sqrt{\sigma_b} \quad (\mathrm{N/mm^2}) \quad (2)$$

where the E_{wf} is the elastic modulus of the FRP sheet and E_0 is that of the some basic sheet.

Figure 3 shows the comparison of test results and calculated values obtained from Eq.1,3. It can be seen that design equation predicts the bond strength very well and rather conservatively

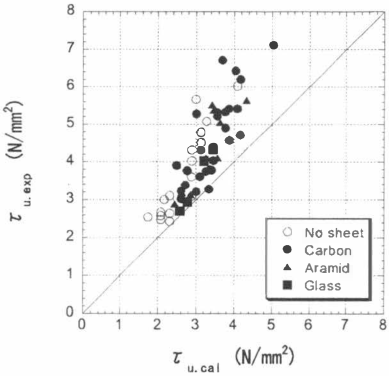

Fig.3 Bond strength experiment-calculated

4 ANTI-SYMMETRIC LOADING BEAM TEST

For the practical application of the proposed equation (Eq.1,2), it must be necessary to verify its applicability. Seventeen anti-symmetric loading beam tests simulated the stress state of the members in RC building under earthquake loading were carried out for that. The details of test specimens were shown in Fig.4

Figure5 shows the shear force-drift angle relation in the clear span for Batch1,2 specimens with no sheet (p_{wf}=0%) and with carbon sheet(p_{wf}=0.08,0.16,0.32%). Every specimen fell in bond splitting failure of outer longitudinal bars in clear span. The sheet confinement increased greatly the bond strength and ductility of beam.

The shear force at the bond splitting failure of RC member Q_{bu} was derived by the similar manner adopted in "Design Guideline for Earthquake Resistant RC Building Based on Ultimate Strength Concept" published by AIJ. Figure6 shows the comparison the experimental values including other investigator's data in Japan and calculated ones obtained from Eq.1,3. It should be noticed that some data showed over estimation. The deterioration of bond strength due to repeated reversed loading must be considered in future.

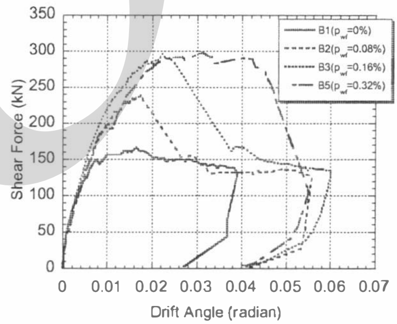

Fig.5 Shear force-drift angle relation

REFERENCES

[1] S.Kono, K.Matsuno, T.Kaku "Experimental Study on Bond –Slip Behavior of Longitudinal Bars in Concrete Beams Confined with Fiber Reinforced Polymer Sheets" ACI, SP-188-31,pp333-345,1999

[2] S.Kono, K.Matsuno, T.Kaku "Bond–Slip Behavior of Longitudinal Reinforcing Bars Confined with FRP Sheets" Proc. of 12WCEE, Aukland,New Zealand, 2000 Fiber Reinforced Polymer

[3] Fujii,S. and Morita,S., "Splitting Bond Capacities of Deformed Bars, Part 2 Proposed Ultimate Strength Equation for Splitting Bond Failure" Transactions of AIJ, Vol.319, pp.47-55,Nov.1982

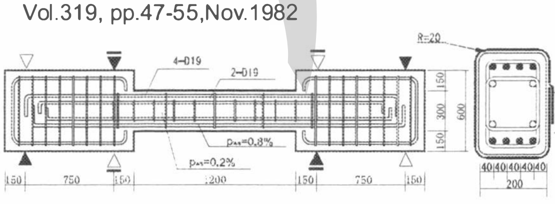

Fig.4 Outline of anti-symmetric lading beam test

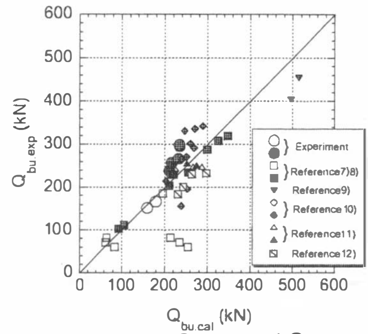

Fig.6 Comparison between $Q_{bu.exp.}$ and $Q_{bu.cal.}$

BONDING PROPERTIES BETWEEN FRP SHEET AND CONCRETE IN CLEAVAGE

Masakazu MITSUI Kimio FUKUZAWA Tatsuya NUMAO
Dept. of Urban and Civil Engineering
Ibaraki Univ., JAPAN

Isao FUNAKAWA
Technical Research Institute
Aoki Co., JAPAN

Keywords: FRP sheet, bonding property in cleavage, bond softening diagram

1 INTRODUCTION

Recently, the strengthening method of concrete structures by bonding FRP sheets using carbon, glass or aramid continuous fibers has gained a great interest. The bonding properties between FRP sheet and concrete influence the structural behavior of concrete member which is strengthened by the FRP bonding method. The bonding properties may be classified into three types according to the direction of interfacial debonding force: the bonding properties in shear, in tension and in cleavage. This paper concerns the bonding properties in cleavage between FRP sheet and concrete. It is well known that the roughness of the bonding surface affects the bonding strength between concrete and FRP sheet. However, only few papers describe the relationship between the roughness of concrete surface and the bonding properties in cleavage. In the study, compact tension tests (CT tests) were conducted in order to obtain the bonding properties in cleavage, varying the treatment method of the concrete surface and the strength of concrete. The bond softening diagram and the fracture energy Gf are derived from the CT test results as the bonding properties in cleavage.

2 EXPERIMENTS

2.1 Specimen

The specimen for the CT test is shown in Fig. 1. The specimens were made by bonding an upper and a lower concrete blocks, setting carbon continuous fiber sheets (CFSs) applied an epoxy resin between two blocks. The bonding surfaces were roughened by four treatment methods: disk-grinding, sandpaper polishing, sandblasting and chipping (see Table 1). The CFSs, which have a tensile strength of 4.9kN/mm^2, an elastic modulus of 230kN/mm^2 and a fiber areal weight of 200g/m^2, were used in the experiments. The compressive strength of concrete were 34.5N/mm^2 (low), 51.2N/mm^2 (middle) and 78.1N/mm^2 (high) at 28 days. The experiments were done combining the factors as shown in Table 1.

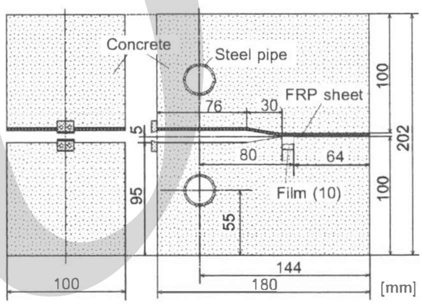

Fig. 1 CT specimen

Table 1 Test program

Test No.	Surface treatment	Superficial area ratio	Comp. strength [N/mm^2]
1	Disk-grinding	1.02	34.5
2			51.2
3			78.1
4	Sandpaper polishing	1.00	51.2
5	Sandblasting	1.18	
6	Chipping	1.17	

2.2 Testing procedures

The tensile load P and opening displacement at a notch tip of specimen (CMOD) were measured by using a load cell (capacity of 10kN) and clip gage (sensitivity of 1000 μ/mm), respectively. Measurement of P and CMOD were done about 150 times/min, using a high-performance data logger in order to grasp the peak in the P-CMOD curves.

3 INFLUENCE OF VARIOUS FACTORS ON BOND PROPERTIES IN CLEAVAGE

3.1 Estimation method of bond softening diagram

Tension softening diagram of concrete is shown as a relationship between tensile stress and the crack width at the descending region. The multi linear approximation method, proposed by Kittaka et al. is generally used as the method to obtain the bond softening diagram.

3.2 Influence of surface treatment method on bond properties in cleavage

P-CMOD curves/bond softening diagrams of various surface treatment method using a concrete whose compressive strength is 51.2MPa are shown in Fig. 2(a) and (b). It is shown from the figure that the P-CMOD curve and bond softening diagram of sandpaper polished specimen shows a good agreement with that of disk-grinded specimen. The maximum stress of the sandblasted specimen is higher than that of the sandpaper polished or the disk-grinded specimen, and this means that the bond behavior between FRP sheet and sandblasted concrete is superior to the other. It is shown in Table 1 that the superficial area ratio of sandpaper polished and disk-grinded specimens are nearly equal and that the superficial area ratio of sandblasted specimen is larger than that of both specimens. This means that the P-CMOD curve and bond softening diagram are influenced by the surface roughening method. On the contrary, those of chipped specimen is inferior to that of sandblasted specimen, although the superficial area ratio of them are nearly equal. This shows that the bond between the coarse aggregate and the mortar matrix at the concrete surface vicinity has been destroyed by the chipping.

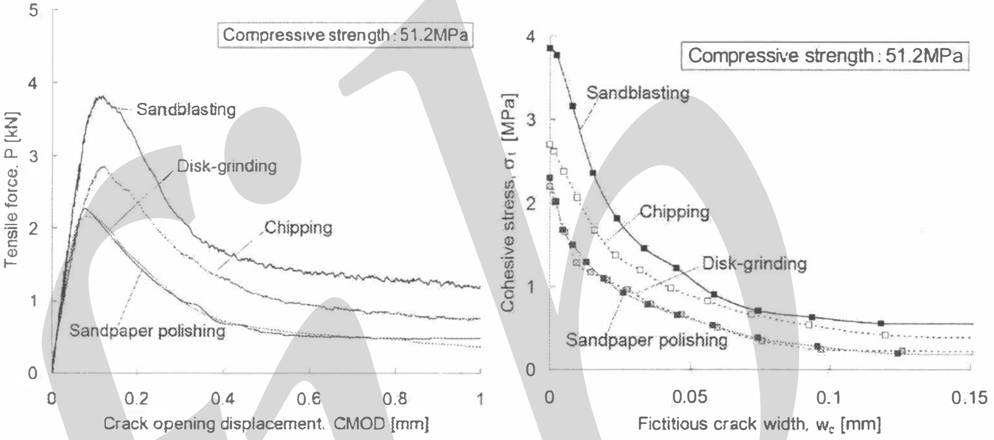

(a) P-CMOD curves (b) Bond softening diagrams

Fig. 2 Influence of surface treatments on bond properties in cleavage

3.3 Influence of concrete strength on bond properties in cleavage

The gradient at the initial part of the P-CMOD curve and the maximum tensile load increase with the increase of the compressive strength of concrete. The fracture energy G_f which calculated from the bond softening diagram and the maximum cohesive stress s_{max} increases almost linearly as the compressive strength of concrete increases.

4 CONCLUSIONS

The compact tension tests were carried out in order to obtain the bond properties in cleavage between FRP sheet and concrete. The influence of the surface treatment method and the compressive strength of concrete on the cleavage bond properties was examined. The following conclusions may be drawn from the experiments and analysis.

(1) We propose a method for obtaining the bond softening diagram between the FRP sheet and the concrete in cleavage by FEM analysis programed the multi linear approximation method.
(2) The surface treatment method of concrete has a large influence on the bond properties. It is confirmed that the highest bonding properties are obtained by sandblasting and that the maximum cohesive stress and the fracture energy of sandblasted specimen are about the double to those of sandpaper polished or disk-grinded specimen.
(3) The chipping greatly lowers the bond properties between FRP sheet and concrete, since the damages at the vicinity of the concrete surface are given through chipping.
(4) The fracture energy and the maximum cohesive stress increase almost linearly with the increase of the compressive strength of concrete.

FASTENINGS TO CONCRETE FOR USE IN SEISMICALLY ACTIVE REGIONS

Matthew Hoehler and Rolf Eligehausen
Institute of Construction Materials, University of Stuttgart, GERMANY

Keywords: anchors, fastenings, seismic, crack behavior

ABSTRACT

Post-installed anchors, which have been designed and tested for use in non-seismic environments, are commonly used for the fastening of structural and non-structural components in reinforced concrete structures located in seismic regions. Inadequately tested or inappropriately used anchors can lead to unanticipated behavior that can compromise overall structural performance and endanger human life. This paper emphasizes the need to account for the condition of the anchorage material, especially cracking in the global structure, when developing testing and design guidelines for post-installed anchors for use in seismic regions. A method for approximating crack width, spacing and opening and closing of cracks in reinforced concrete flexural members over the entire range of member deformation is suggested.

1 TESTING STANDARDS AND DESIGN GUIDELINES

To discuss a comprehensive approach to the development of testing standards and design guidelines for post-installed anchors, it is useful to make distinctions between: *Environment*, *Structure* and *Anchorage* (Fig. 1). Only once the loading to be applied to the anchor (Fig. 1; Anchorage (1)) and the condition of the anchorage material (Fig. 1; Anchorage (2)) have been determined, can one develop realistic protocols for seismic testing of anchors. The majority of work toward developing seismic testing standards for post-installed anchors up to the present has been focused on establishing cyclic loading patterns for anchors representative of the dynamic loading caused by a sub-structure [1]. Testing procedures, loadings and acceptance criteria for seismic testing of anchors in cycled cracks, are areas of ongoing research and are the focus of the present work.

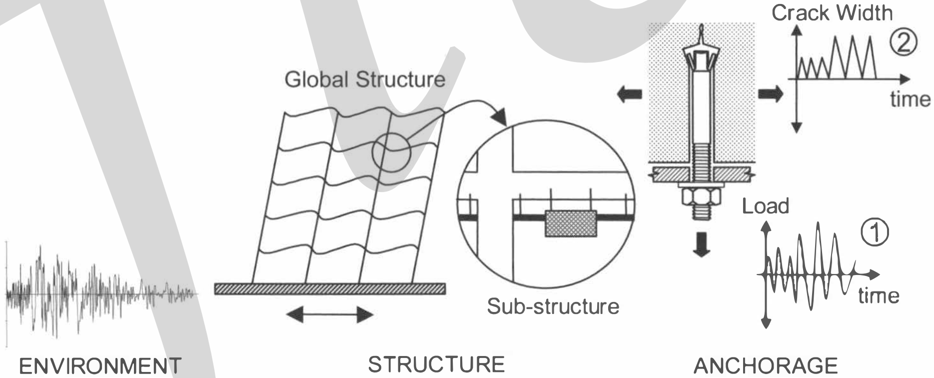

Fig. 1 Distinctions for discussion of seismic testing and design guidelines for anchors.

1.1 Post-installed anchor behavior in cracked concrete

Numerous investigations have shown that the behavior of post-installed anchors in cracked concrete can differ significantly from the behavior in uncracked concrete [2]. Tests on a variety of anchors loaded in tension in a stable crack width show reductions of the load bearing capacity of 30% and more even at relatively small crack widths (0.3 mm) (see Fig. 2). Many anchors designed for use in uncracked concrete are not suitable for use in cracked concrete.

2 PREDICTING CRACK BEHAVIOR THROUGH DISTRIBUTION OF DEFORMATION

As a building responds to earthquake ground motion, it experiences lateral displacements, and consequently, deformations of its individual elements. Assuming a strong column - weak girder design, one can visualize the transverse motion of a building being accounted for as shown in Fig. 3. The goal is to obtain an estimate of the location, width and number of opening and closing cycles of cracks in a reinforced concrete structure during an earthquake. This can be achieved using a distribution of rotations through discrete cracking. The concept was motivated by work performed by Bachmann [3]. By taking rotational deformation as a starting point, one can predict cracking in a reinforced concrete member as a function of a given rotation demand.

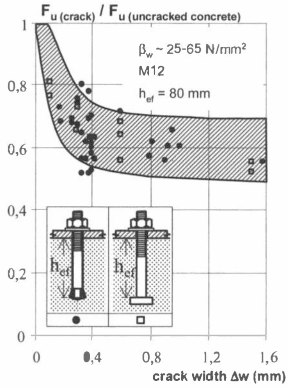

Fig. 2 Bearing capacity of undercut anchors and headed studs in cracks under tension loading (after [2]).

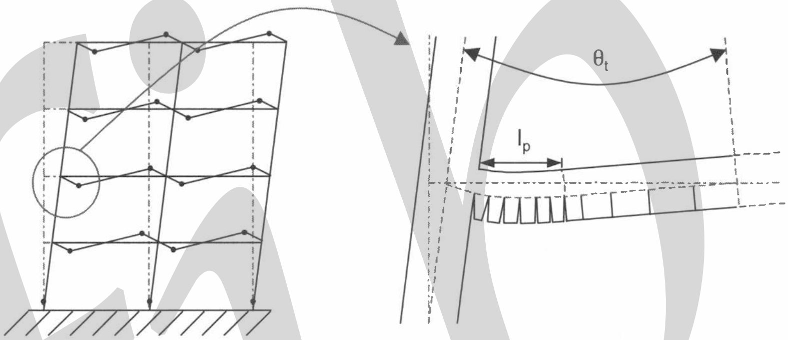

Fig. 3 Accommodating transverse motion through cracking (θ_t = member rotation, l_p = hinge length).

3 CONCLUSIONS

(1) Realistic seismic testing standards and design guidelines for post-installed anchors must account for cycled crack widths in the anchorage material.

(2) Crack width and crack opening and closing behavior can be estimated for reinforced concrete flexural members by accounting for rotational deformation through discrete cracking.

(3) Preliminary studies indicate that at an "Immediate Occupancy" performance state (peak member rotation of 0.005 radians) most members will remain in the elastic range and *maximum* crack widths below about 0.45 mm to 0.63 mm are typically observed.

(4) At a "Life Safety" performance state (peak member rotation of 0.02 radians) members are likely to form plastic hinges. *Maximum* crack widths outside of the plastic hinge region may exceed 0.63 mm and very large crack widths (> 1 mm) are observed inside the plastic hinge.

REFERENCES

[1] ICBO ES : *AC01 – Acceptance Criteria for Expansion Anchors in Concrete and Masonry Elements*, ICBO Evaluation Service, Inc., Whittier, California, January, 1999

[2] Eligehausen, R.; Balogh, T. : "Behavior of Fasteners Loaded in Tension in Cracked Reinforced Concrete", *ACI Structural Journal*, Vol. 92, No. 3, May-Jun. 1995, pp. 365-379

[3] Bachmann, H. : *Zur plastizitätstheoretischen Berechnung statisch unbestimmter Stahlbetonbalken (Plasticity Theory Calculations for Statically Indeterminate Reinforced Concrete Beams)*, Report Nr. 13, Dissertation, Institut für Baustatik, Eidgenössische Technische Hochschule (ETH), Zürich, 1967, in German

DISPLACEMENT – BASED APPROACHES IN SEISMIC DESIGN OF RC STRUCTURES

Gian Michele Calvi, Università degli Studi di Pavia, Italy
gm.calvi@unipv.it

1 INTRODUCTION

Displacement-based approaches to earthquake engineering evaluation and design have been the subject of several proposals in the last years, being considered a more efficient alternative than force-based approaches to provide improved reliability in the engineering process by more directly relating computed response and expected performance.

Within the framework of fib Commission 7, and more specifically of Task Group 7.2, a detailed review of the proposed approaches have been performed, including sample calculations and comparisons of the capability and of the efficiency. This paper is a short summary of some of the material presented in the Bulletin [1] produced by the TG currently being printed.

2 DESIGN APPROACHES

There are several criteria that can be used to organize the various displacement-based design procedures, however, two of them appear to be more fundamental: (a) The role that displacement plays in the design process, (b) The type of analysis used in the design process.

According to the first criterion the various design procedures can be considered to fall into one of three basic categories based on the role that deformation plays in the design process, described as (1) Deformation-Calculation Based (*DCB*), (2) Iterative Deformation-Specification Based (*IDSB*), and (3) Direct Deformation-Specification Based (*DDSB*). The DCB methods involve calculation of the expected maximum displacement for an already designed structural system. Detailing is then provided such that the displacement capacity of the system and its components exceeds the calculated maximum displacement. As a result, no attempt is made to induce a change in the system to alter the maximum displacement demand, but rather, the demand is taken as a design quantity which is dealt with through proper detailing. The IDSB methods are similar to the DCB methods in that they involve analysis of an already designed system to evaluate the expected maximum displacement. However, unlike the DCB methods, a limit to the maximum displacement is enforced, and as a result, changes are made to the structural system such that the analysis displacements are kept below the specified limit, and hence the iterative nature of the process. The DDSB methods utilize as a starting point a pre-defined target displacement. The design of the structure then progresses in a direct manner whereby the end result is the required strength, and hence stiffness, to reach the target displacement under the design level earthquake. These procedures are not iterative, and do not require a preliminary design.

According to the second criterion, i.e. the type of analysis used in the design process, the procedures can be described as: (1) Response spectra - initial stiffness based, (2) Response spectra - secant stiffness based or (3) Time history analysis based. Initial stiffness based procedures utilize elastic stiffness (or a variation thereof) coupled with approximations between elastic and inelastic response, such as the equal displacement approximation or other R-Δ -T relations to evaluate the maximum response. Secant stiffness based procedures utilize the secant stiffness to the maximum response level and the concept of equivalent viscous damping to characterize the non-linear response of structural systems. Time-history methods solve the equations of motion by direct integration for a specific earthquake time history to evaluate the maximum response. The analysis may be elastic or inelastic, although there is little advantage in conducting elastic time history analysis. Time history analysis may be based on frame members where assumptions on section hysteretic characteristics are required. Analysis may also be based on fibre models where individual materials that comprise the structural system follow an assumed non-linear response.

3 APPLICATION AND EVALUATION OF DISPLACEMENT-BASED APPROACHES

Results for five different case studies designed in accordance with eight different displacement based design methods are considered (see table 1).The five case studies included: (1) an 8 storey building with walls of equal dimensions in a regular layout on a rigid foundation; (2) an 8 storey building similar to that of Case Study 1 but with a flexible foundation; (3) an 8 storey building with walls arranged in an irregular layout; (4) a 7 storey regular moment frame building; (5) an 8 storey frame building with a vertically irregular layout.

Several kinds of comparisons between different methods were possible, considering for example flexural and shear strength, shear distribution, required reinforcement and distribution. Since it is not possible to enter here in any detail, due to space constraints, the essence of the results is summarized in table 3, in terms of the base shear design strength required by each method for all case studies; more details can be found in [1] and [2]. It is immediate to note how different can be the strength requirements produced by different methods (in some case more than four times).

Table 1: Design base shear required by each method for all case studies

Method	Case Study 1	Case Study 2	Case Study 3	Case Study 4	Case Study 5
Panagiotakos	9480	7200	10987	13406	7131
Aschheim	3008	5755	4426	3732	4038
Chopra	3416	3750	2434	3077	6307
Freeman	4537	5419	5675	4499	4584
SEAOC	4560	4560	3013	3596	3249
Priestley	2900	3494	3417	6136	7623
Kappos	5400	5562	8672*	9627	4464
Browning	N/A	N/A	N/A	13369	N/A

Three spectrum-compatible time-histories were generated and used to subject each of the structures to the spectrum compatible accelerograms.

The most striking result provided by the assessment of each method's performance is that the design strength has a low influence on displacements. It was seen that despite ratios of strength as great as four between methods, ratios of displacement never exceeded two. In fact, the ratio of displacements between two given methods was always less than or equal to half the ratio of the strengths for the same methods.

Preliminary results for the performance assessment of Case Study 3 indicate that the drift and displacement ductility demands for a serviceability level earthquake ground motion will generally be close to or above the design limits.

It is worth pointing out that no recommendations to account for twist-induced period lengthening were found for any of the methods. This period lengthening occurs in structures such as Case Study 3 because the twist of the structure causes the centre of mass to displace further than the centre of rigidity. For methods that use a target displacement to obtain the required stiffness, it appears that an initial estimate of the twist could be used to increase the target displacement. This larger target displacement would then result in a longer period being designed for. However, neglecting this twist is unlikely to result in non-conservative design since the structure would essentially be given a shorter period and higher strength than what is necessary to maintain the target displacement.

4 CONCLUSIONS

The application of eight different displacement based design procedures to 5 different structural forms has highlighted the strengths and weaknesses of each of the methods. It has been shown that all the methods successfully maintain the target design parameters even though significant variation in design strength exists. It has been shown that the variation in design strengths between methods has a low influence on peak displacements due to the relationship between stiffness and displacement. The influence was observed to reduce with the inclusion of foundation flexibility and in general where the response entered the range of the spectra where the displacement tend to be more uniform, i.e. for more flexible structures. Limitations have been identified for all of the eight displacement based design methods considered. However, it is also considered that all of these limitations can easily be overcome now that they have been identified. This investigation concludes that the future for displacement based design is bright, with a range of design methods available, shown to perform reasonably well in the examples considered.

5 REFERENCES

[1] *fib* TG7.2, (2002), Displacement-based design and assessment, Bulletin in printing

[2] Sullivan, T., M.J. Kowalsky, G.M. Calvi and M.J.N. Priestley, (2002), Limitations and performances of different displacement – based design approaches, Proc. of the 2nd Int. ROSE School Seminar, to be published by the *Journal of Earthquake Engineering*

DISPLACEMENT-BASED SEISMIC ASESSMENT AND RETROFIT OF REINFORCED CONCRETE BUILDINGS

Telemachos B. Panagiotakos, Antonis J. Kosmopoulos and Michael N. Fardis

Department of Civil Engineering,University of Patras, GREECE

Keywords: seismic assessment, concrete buildings, displacement-based assessment

1. INTRODUCTION

The largest part of the seismic threat to human life and property comes from existing substandard buildings. A procedure is proposed and applied for seismic assessment and retrofit of individual reinforced concrete buildings, using as criteria demands and supplies of: a) chord rotations at member ends, and b) shears in members and beam-column joints.

2. ESTIMATION OF SEISMIC CHORD ROTATION AND SHEAR FORCE DEMANDS

Member chord rotations are estimated from a 5%-damped elastic analysis - static with inverted triangular distribution of lateral forces or modal response spectrum (dynamic) – or from a nonlinear static (pushover) analysis, carried to a top (or a work-equivalent) displacement of the building given by the 5%-damped elastic spectrum at the fundamental period of the structure. The elastic rigidity of members should be equal to the secant rigidity at yielding of both ends in antisymmetric bending, i.e. to: $EI=M_yL/6\theta_y$. Yield moment M_y can be computed from first principles; chord-rotation θ_y at yielding is computed through Eq. (1), developed on the basis of 1133 test results:

$$\theta_y = \phi_y \frac{L_s}{3} + 0.0025 + a_{sl}\frac{0.25\varepsilon_y d_b f_y}{(d-d')\sqrt{f_c}} \qquad (1)$$

In Eq. (1) ϕ_y is the yield curvature, computed from first principles or empirically as $\phi_y=1.85f_y/E_sd$, L_s the shear span $\approx L/2$, f_y and f_c (in MPa) the strengths of steel and concrete, d_b the diameter of tension reinforcement, and d, d' the depth to the tension and compression reinforcement respectively. The proposed version of the equal displacement rule was developed from about 1500 nonlinear dynamic analyses of various regular bare RC frame or dual structures; their results are summarized in Table 1.

Table 1 Mean and 95%-fractile building-averages of inelastic-to-elastic chord rotation and drift ratio

	Beam chord rotation				Column or wall chord rotation				Displacement			
	Mean		95%-fractile		Mean		95%-fractile		Mean		95%-fractile	
	Stat.	Dyn.	Stat.	Dyn.	Stat.	Dyn.	Stat.	Dyn.	Stat.	Dyn.	Stat.	Dyn.
roof	1.2	1.25	1.85	1.7	1.15	1.0	1.9	1.65	0.85	1.02	1.04	1.21
base	1.0	1.2	1.35	1.65	0.9	0.85	1.1	1.05	-	-	-	-
mean	1.11	1.22	1.59	1.67	1.04	0.92	1.51	1.35	1.06	1.0	1.35	1.33

Table 2 Inelastic-to-elastic chord rotation ratio in open-ground-storey of partially infilled buildings

Beams		Existing columns (assessment)				Upgraded columns (redesign)			
		Bottom		Top		Bottom		Top	
Mean	95%-fract.	mean	95%-fract.	mean	95%-fract.	mean	95%-fract.	mean	95%-fract.
0.7	1.0	0.95	1.2	1.2	1.8	0.7	0.9	0.8	1.35

Several thousand nonlinear dynamic analyses of open-ground-storey infilled buildings led to the conclusion that peak inelastic chord rotations in ground storey beams and columns may be estimated by applying the modification factors of Table 2 to results of a 5%-damped static analysis of the elastic structure with the infills modelled as rigid diagonal struts. Pushover analysis can also be used with the infills considered as nonlinear diagonal compression struts. The target top displacement can be estimated from the 5%-damped elastic spectrum according to the last four columns of Table 1.

If the analysis is nonlinear static (pushover) the shear force demand $V_{E,max}$ is the value from the analysis, taking into account the simultaneously acting transverse loads, $g+\psi_2q$ (for beams). If the analysis is linear elastic, in the nonlinear regime $V_{E,max}$ at end i is estimated from Eq.(2), with $V_{g+\psi 2q,oi}$: shear force at end i due to loads $g+\psi_2q$ considering the member as simply-supported; l_n: member clear length; M_{yi}^-, M_{yj}^+: yield moments at ends i and j, with tension at the top at end i and at the bottom at j.

$$V_{E,max,i} \approx V_{g+\psi_2 q,oi} + \frac{M_{yi}^{-} + M_{yj}^{+}}{l_n} \tag{2}$$

3. MEMBER ULTIMATE CHORD ROTATION AND SHEAR - THEIR USE IN ASSESSMENT

Member chord rotation demands (mean or 95%-fractile) should be compared to the ultimate chord rotation, θ_u of the member under cyclic loading. Eq (3) was developed for the mean ultimate chord rotation of flexure-controlled RC members from the results of 1048 monotonic or cyclic tests to failure:

$$\theta_u = \alpha_{st,w}(1-0.38a_{cyc})\left(1+\frac{a_{sl}}{1.7}\right)(1-0.375a_{wall})\left(0.3^{\nu}\left[\frac{\max(0.01,\omega')}{\max(0.01,\omega)}f_c\right]^{0.2}\left(\frac{L_s}{h}\right)^{0.425}25^{\left(\alpha\rho_{sx}\frac{f_{yw}}{f_c}\right)}\left(1.45^{100\rho_d}\right) \tag{3}$$

in which: $L_s/h=M/Vh$: shear span ratio at member end; ω, ω': mechanical reinforcement ratios, $\rho f_y/f_c$, of tension and compression longitudinal reinforcement (not including diagonal bars; in shear walls vertical web reinforcement included in ω); f_c: uniaxial concrete strength (MPa); $\nu=N/bh_cf_c$: axial load ratio normalized to width b of compression zone, section depth h and f_c; $\rho_{sx}=(A_{sx}/b_ws_h)$: ratio of transverse steel parallel to the direction (x) of loading (s_h=stirrup spacing); α: confinement effectiveness factor= $(1-s_h/2b_c)(1-s_h/2h_c)\left(1-\sum b_i^2/6b_ch_c\right)$ (b_c, h_c: dimensions of confined concrete core, b_i= distances of restrained longitudinal bars); ρ_d: steel ratio of diagonal reinforcement in each diagonal direction; a_{st}: 0.016 for ductile hot-rolled or heat-treated (tempcore) steel, 0.0105 for brittle cold-worked steel; a_{cyc}: 0 for monotonic loading, 1 for cyclic; a_{sl}: 1 if there is slippage of longitudinal bars from their anchorage zone, or 0 if there is not; a_{wall}: 1 for shear walls, 0 for beams or columns.

Eq. (3) may be applied to flexure-critical members without seismic detailing, applying for cyclic loading an overall multiplicative factor k_u of 0.85 and using α=0 for confinement with 90° stirrup hooks.

On the basis of 15 tests on concrete columns strengthened with RC jackets, it was concluded that if: a) the member is considered monolithic with full composite action; b) the strength of the new concrete is considered to apply for the full section; and c) the longitudinal bars of the jacket are considered as top and bottom reinforcement of the section and those of the old column as vertical web reinforcement, then the modification factors on the values of M_y, θ_y, θ_u, estimated according to these assumptions are: k_m=0.9, k_y=0.9, k_u=1.0. On the basis of 33 tests on specimens repaired with replacement of crushed concrete with epoxy mortar, non-shrink concrete, fibre-reinforced concrete, etc., it was concluded that if the value of f_c of the repair concrete is adopted for the entire specimen, the modification factors on M_y, θ_y from Eq. (1) and θ_u from Eq. (3) are k_m=1.05, k_y=1.15 and k_u=0.9.

The 5%-fractile of chord rotation capacity is 40% of the mean value θ_{um} from Eq. (3). The proposed verification of members at the "Life Safety" performance level is:

$$\gamma\theta_{Ek,0.95} \le \theta_{uk,0.05} = 0.4\theta_{um} \tag{4}$$

with γ: safety factor against exhaustion of member deformation capacity at the "life safety" earthquake. If the demand value θ_E in Eq. (4) is derived from a linear-elastic analysis, the modification factors for 95% chord rotations from Table 1 should be applied to it. If derived from pushover analysis, it needs to correspond to the 95%-fractile value of top or equivalent (mean) drift, obtained by applying to the 5%-damped elastic displacement the multiplicative factors in the last 2 columns of Table 1.

The database from which Eq. (3) was derived includes elements with shear ratio, as low as 1.5, but not shear-critical. Assessment of members in shear is based on the check that maximum shear force during the response, $V_{E,max}$, does not exceed shear capacity, V_R: $V_{E,max} \le V_R$. The expression fitted to V_R as a function of plastic chord rotation ductility demand, $\mu_\theta^{pl}=\theta^{pl}/\theta_y$, ($\theta^{pl}=\theta-\theta_y$) at the member end where shear is checked, is (units: MN, m):

$$V_R = \frac{h-x}{2L_s}N + \max\left(0,\ 1-0.035\mu_\theta^{pl}\right)\left[\rho_w f_{yw} b_w z + 0.018\max\left(5-\frac{7}{8}\frac{L_s}{h},1\right)(1+140\rho_l)\sqrt{f_c}\,b_w d\right] \tag{5}$$

In Eq.(5), fitted to 93 cyclic shear-controlled tests (14 of which with old detailing), b_w is the web width, $z_b=d-d_1\approx0.9d$ the internal lever arm, N the axial load, x the compression zone depth, ρ_w and ρ_l the ratios of transverse and (total) longitudinal reinforcement, and f_{yw} the yield strength of transverse steel.

The procedure was computationally implemented in a user-friendly interactive program and applied for the assessment and retrofit of a 3-storey RC building representative of old construction without engineered earthquake resistant. A full-size frame will be constructed after this building and tested pseudodynamically at the ELSA facility of the JRC in Ispra (I), before and after retrofit.

DAMAGE EVALUATION OF REINFORCED CONCRETE COLUMNS UNDER LARGE AXIAL LOAD AND LATERAL DEFORMATION

Susumu KONO Yusaku ARAI Bechtoula HAKIM Fumio WATANABE
kono@archi.kyoto-u.ac.jp rc.arai@archi.kyoto-u.ac.jp rc.hakim@archi.kyoto-u.ac.jp nabe@archi.kyoto-u.ac.jp
Department of Architecture, Kyoto University, Kyoto, 6068501 Japan

Keywords: Damage evaluation, plastic hinge, axial load, biaxial lateral loading, corner column

1 INTRODUCTION

This study aims to evaluate damage to reinforced concrete columns, that experience large axial load and cyclic reversal bidirectional lateral deformation so that appropriate evaluation procedures can be proposed in future. In an experimental program, four large scale columns were tested under the reversal bidirectional lateral deformation with variation in axial load level in order to study the effects of loading history and intensity on the damage progress. The shear failure was inhibited and the damage gradually progressed with concrete crushing and yielding of reinforcing bars. In an analytical program, a simple fiber model was employed to predict the deterioration of moment capacity and the variation of axial strain at a plastic hinge region. The limit deformation capacity based on the existing models was compared to the test results to see their applicability. Progress of cracking and spalling was observed and compared with each other and with half-size specimens.

2 TEST SETUP

Four specimens are identical as shown in Fig. 1(a). The columns had a square section with 600 mm by 600 mm and shear span to depth ratio was 2.0. Table 1 shows the test variables. Loading system is shown in Fig. 1(b).

3 TEST RESULTS

3.1 Moment-curvature and axial strain-curvature relations

Figures 2 and 3 show moment-curvature and axial strain - curvature relations, respectively, with fiber model predictions. In this fiber model, Popovic's model was used for concrete and Ramberg-Osgood model was used. The peak point of confined concrete was obtained based on the Japanese research [1] as follows.

$$f'_{cc}=f'_c+11.5\alpha\left(\frac{d'}{c}\right)\left(1-\frac{s}{2D_{core}}\right)\rho_h f_{hy} \qquad (1)$$

where f'_{cc} is the strength of confined concrete, f'_c the strength of plain concrete, f_{hy} the yield strength of shear reinforcement, ρ_h the volumetric ratio of shear reinforcement, d' the diameter of the shear reinforcement, c the unsupported length of the shear reinforcement, s the spacing

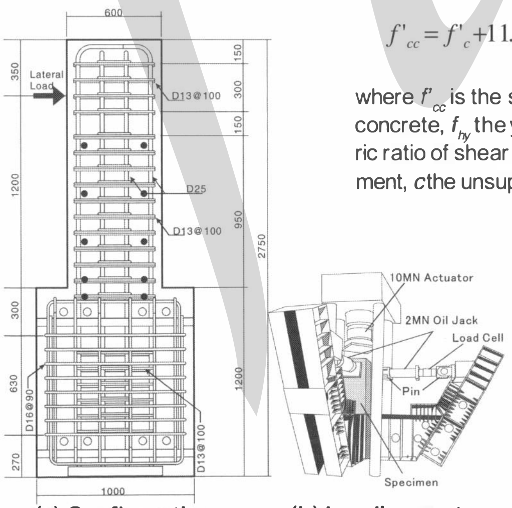

(a) Configurations (b) Loading system

Figure 1 Experimental setup

Table 1 Test variables

Specimen	Variable: Axial load level	Variable: Lateral loading	Comment
L1D60	Constant	Uni	Positive side
L1N60	(0.6)	Bi	Reversal
L1NVA	Varied	Uni	Reversal
L2NVA	(0-0.6)	Bi	Reversal

L1N60 failed due to out-of-plane deformation.

of the shear reinforcement, D_{core} the width of the confined core concrete. Coefficient, α, was inserted to the original equation to increase the effect of confinement based on the authors' previous study due to the strain gradient and high axial load. It can be said that the fiber model predicted the moment-curvature relation and axial strain - curvature relation with a good accuracy. The fiber model was optimized for the small section (250 mm by 250 mm) and it seem to be appropriate for the large section (600 mm by 600 mm), too. The sizes are not be clearly seen in predicting moment and axial strain. This is because the flexural failure mode is ductile since the failure is dominated by concrete compression behavior and steel yielding.

3.2 Limit deformation capacity

The limit rotation angle *Ru* was computed from Inai et al's method [2] and Kato et al's method [3]. Both methods employ the concept of equivalent axial stress ratio to take into account the effect of axial load variation. However, the accuracy of these methods was not sufficient to predict the experimental results.

3.3 Cracking and spalling

New cracks formed and the existing cracked extended up to R=1% (R: member rotation angle). After R=1%, the existing cracks widened and the concrete under compression spalled but new formation of tension cracks was not observed. This observation also applies to other three specimens. Although it is not shown, similar specimens with smaller size (250 mm x 250 mm section) tested by authors showed that the spalling was observed at the lower 250 mm region which equaled the width of the column. Since the spalling spread to the lower 900 mm in Fig. 8, the size effect may have caused the difference. Since the information on cracks and spalling is indispensably to rehabilitate lightly damaged members, it is necessary to make a model to predict its progress by collecting more data.

4 CONCLUSIONS

Four column base model specimens with 600 mm by 600 mm square section and 2.0 shear span to depth ratio were tested to study the effects of variable axial load and bidirectional horizontal deformation on the progress of damage.

1. The employed fiber model predicted the variations of moment and axial strain in a good accuracy although the accuracy needs to be enhanced for bilateral loading cases.
2. Ultimate deformation capacity computed based on an equivalent axial stress level proposed by Inai et al and Kato et al was not able to sufficiently predict the experimental results in this study.
3. Four specimens showed similar progress of cracking and spalling and the extent of damage seems to have size effect. More data need to be collected to predict these behaviors so that the appropriate rehabilitation strategies and their cost can be determined.

REFERENCES

1) Kato, D., Watanabe, F., Nishiyama, M., and Sato, H., "Confined concrete with high strength materials," ACI Special Publication 176, pp. 85-104, 1998. 2) Inai, E. and Hiraishi H., "A method for evaluating deformation capacity of exterior R/C columns after flexural yielding," 12 World Conference of Earthquake Engineering, report 1823, 2000. 3) Kato, D., Shiba, J., and Matsuda, T., "Deformation capacities of r/c columns under varying axial load," Journal of Structural and construction engineering, Architecture Institute of Japan, No. 506, pp. 155-161, April, 1998.

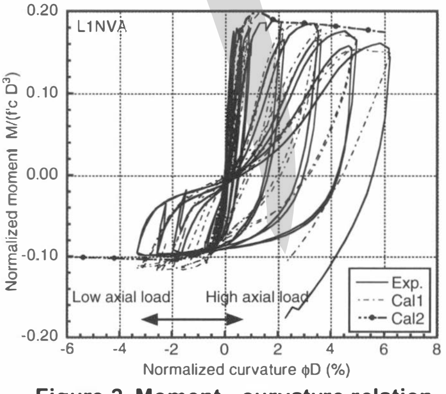

Figure 2 Moment - curvature relation

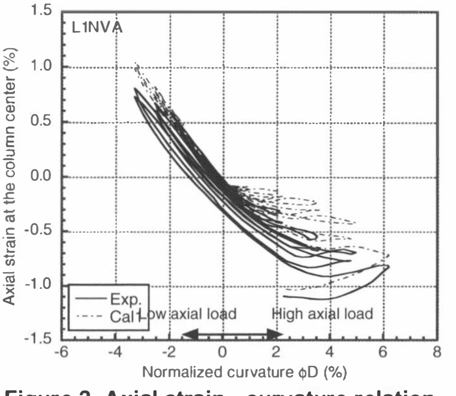

Figure 3 Axial strain - curvature relation

RESIDUAL DISPLACEMENT OF SEISMIC RESISTANT REINFORCED CONCRETE PIERS SUBJECTED TO COUPLED ECCENTRIC AXIAL FORCE AND TORSION

Hisatomo MATSUZAKI, Naoto Mashiko, Hitoshi ICHIKAWA,
Metropolitan Expressway Public
Corporation, JAPAN

Satoshi TSUCHIYA
COMS Engineering
Corporation, JAPAN

Keywords: residual displacement, eccentric axial force, 3D nonlinear FE analysis

1. INTRODUCTION

Structural conditions have become complicated in urban highways because many elevated roads have been constructed under severe ground limitation. If reverse L-shaped RC piers were exposed to the impact of an earthquake in the direction of a bridge axis, pillars would subject to twist moments due to firm application of eccentric axial tension to the piers. However, effects of such twists on quakeproof performance of RC piers have not been fully described in Standard Concrete Manual in 1996 and a more thorough discussion about the effects is yet to be fostered. So in the results of an experiment commissioned by our cooperation in 1997, Ichikawa, et al., showed that effects of twist of piers on behavior in the direction of a bridge axis during earthquakes could be neglected in actual designs[1). However, because large residual deformation to the orthogonal direction and the loading axis was observed, a clarified generation mechanism of this residual deformation is called for in order to find measures to contain the problem. For the purpose of this article, we performed a 3D nonlinear FE analysis and made a summary report of the mechanism of the deformation as well as ways to control it.

2. DETERMINATION OF ANARYSIS MODELS

(1) Target piers

The targets of this analysis are a model of test pieces with application of reversed cyclic loading and a model with a partly modified bar arrangement of the former.

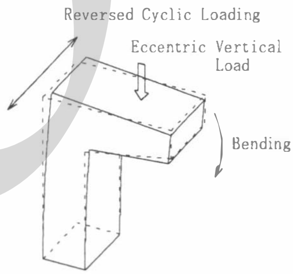

Fig. 1 Residual deformation

(2) Main points of the analysis

The purpose of the analysis is to clarify generation mechanism of residual deformation (see Figure 1). Based on findings of Ichikawa, et al. [1)], we can give the following hypothesis. When there is iterated application of bent or sheared load in the direction of a bridge axis, reinforcing bars with application of strained tension caused by the eccentric axial tension will furthermore subject to force in the direction of the bridge axis, making them more likely to yield. Furthermore, the iterated application of load could lead to damage of the concrete. As a result, rigidity of section of piers in the eccentric direction could weaken, causing deformation in the eccentric direction to develop under eccentric axial tension. In this study, we made an attempt to minimize residual deformation to which plus-and-minus alternating load was applied in the direction of a bridge axis by collecting lateral reinforcing bars to near the center axis. Figure 2 shows the left section of a pier used in the experiment and the right cross section diagram that

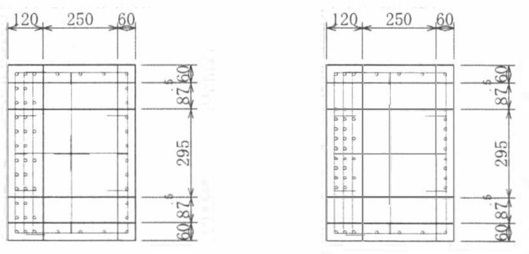

(a)No.3 Reproduced Model (b)New Proposed Model

Fig. 2 Cross section of the pier models used in analyses has a bar arrangement to control residual deformation.

3. ANARYSIS PROGRAM AND ANARYSIS CONDITIONS

As an analysis tool we use a program COM3 being developed in the Concrete Lab of University of Tokyo. The model used in this analysis implemented a 3D solid element and has 20 nodes for each element. In order to shorten the time required for analysis, elastic elements were used in the upper 2/5 of beams as well as in the pillars of the specimens that did not seem to affect residual deformation. RC elements (nonlinear elements) were used in the lower 3/5 of the pillar base part of the rest of the piers.

Loading condition is as follows; static alternating load of an integer times of yield change (δ y) of a section of each model is iterated twice and it is increased up to 5 δ y.

4. ANARYSIS RESULTS

Since analysis of effects of fundamental parameters has already been performed by Ichikawa, et al., we concentrated on the hysteresis curves of load change in the analysis of plus-and-minus alternating load in order to focus mainly on the relevance of the analysis model. As shown in Figure 3, due to changes in the bar arrangements, they showed some signs of weakening in strength. However, the effects were very small and were thus negligible. Figure 4 shows the details of increase in residual deformation in the eccentric direction. When we drew a comparison between the model

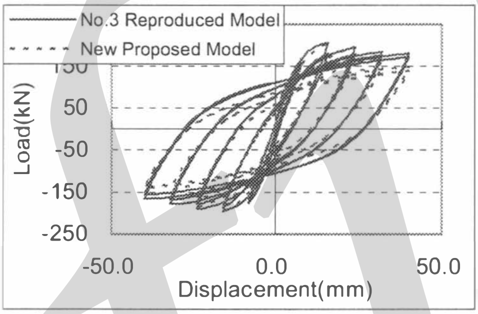

Fig. 3 P-δ relation of alternating load

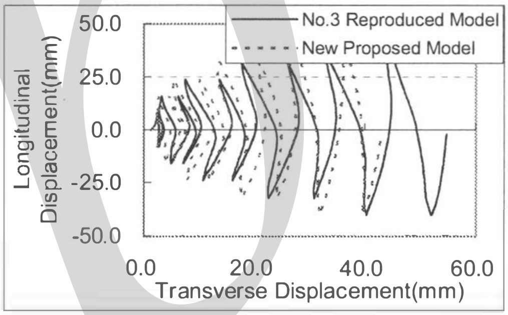

Fig. 4 Residual deformation

used to re-enact the experiment and the deformation suppression model reading the graph, we found residual deformation in the eccentric direction of the deformation suppression model was about 80 % of the experimental model.

5. SUMMARY

Residual deformation in the orthogonal direction to a bridge axis generated from the vibration of RC piers in the direction of the bridge axis due to application of eccentric axial tension is caused by the following mechanism: reinforcing bars exposed to firm tension due to eccentric axial tension yield in the orthogonal direction of the bridge axis can lead to weakened rigidity of the piers in the orthogonal direction.

REFERENCES

1) Ichikawa, et al., "An experiment in quakeproof performance of RC piers with application of eccentric axial tension and twisting moment", JCI, Collected Papers of a symposium for "Iteration Degradation in the plastic region", pp331-336, August 1998 (in Japanese).
2) Ichikawa, et al., "Behavior analysis of iteration of load in the horizontal direction applied to RC piers with eccentric axial tension", Proceeding of the 54th Annual Meeting of JSCE, 5-288, pp576-577, October 1999 (in Japanese)

EFFECT OF TENDON TENSIONING LEVEL ON THE SEISMIC PERFORMANCE OF PRESTRESSED CONCRETE PIERS

Dong kyu Park
P.S. Corporation
JAPAN

Shoji Ikeda
Yokohama National
University, JAPAN

Keywords: tendon tensioning level, flexural capacity ratio, residual displacement modification factor

1 INTRODUCTION

From the test results conducted over the last few years in Japan, it has been confirmed that prestressed concrete piers have great potential to replace conventionally reinforced concrete piers, showing much smaller residual displacement, better property of restoration, and good seismic performance despite of lower energy dissipating ability. In this experimental research, a new approach will be discussed to predict the residual displacement of prestressed concrete piers after a seismic event. Some emphasis will be placed on finding the effect of tendon tensioning level on the behavior of prestressed concrete piers in an effort to pull out of the best possible performance out of such piers.

2 TEST UNITS AND LOADING PROGRAM

The two main parameters are defined as follows by γ and λ ratio in case of symmetric cross-section:

$$\gamma = A_P \sigma_{PY} / (A_P \sigma_{PY} + A_S \sigma_{SY}) \quad (1)$$

$$\lambda = \sigma_P / \sigma_{PY} \quad (2)$$

where, A_P: total area of prestressing steel, σ_{PY}: yield stress of prestressing steel, A_S: total area of longitudinal bar, σ_{SY}: yield stress in longitudinal bar, σ_P: stress in prestressing steel due to prestress

Table 1 Details of test units

Test units	Concrete compressive strength [N/mm²]	Reinforcement ratio [%]		Hoop ratio [%]	SP* (SA*) [N/mm²]	γ ratio	λ ratio
		Nonprestress-ing steel	Prestressing steel				
S1-RH-00	61	5.08	0.00	0.53	0.00 (4.00)	0.00	*
S2-PH-P50	61	0.72	1.04	0.53	8.00 (4.00)	0.87	0.50
S3-PH-P50	61	0.72	1.04	0.53	8.00 (4.00)	0.87	0.50
S4-PH-P50	54	0.72	1.04	0.53	8.00 (4.00)	0.87	0.50
S5-PN-P52	53	0.71	0.49	0.53	4.00 (1.00)	0.76	0.52
R1-PH-P00	58	0.95	0.52	0.53	0.00 (1.00)	0.70	0.00
R1-PH-P25	57	0.95	0.52	0.53	2.10 (1.00)	0.70	0.25
R1-PH-P50	55	0.95	0.52	0.53	4.10 (1.00)	0.70	0.50
R1-PH-P75	57	0.95	0.52	0.53	6.20 (1.00)	0.70	0.75
R2-PH-P25	69	2.87	0.52	0.53	2.10 (1.00)	0.44	0.25
R2-PH-P75	65	2.87	0.52	0.53	6.20 (1.00)	0.44	0.75

SP* : Stress in concrete due to prestress, SA* : Stress in concrete due to axial load

Type-S specimens have been designed to have the same flexural capacity and almost identical λ ratio for prestressed concrete specimens, but have different cross-section and reinforcement configuration, resulting in different γ ratio varying from 0 to 0.87. On the other hand, Type-R specimens have been designed to have the same amount and arrangement of prestressing steel, while having different nonprestressing steel ratio by 1.92%. In addition, tendon tensioning was introduced in the range of 0 to 75% of yield stress of prestressing steel in order to find the proper relationship between the property of restoration and considered parameter λ ratio.

3 TEST RESULTS AND OBSERVED BEHAVIOR OF TEST UNITS

As is designed, Type-S specimens showed little difference in observed peak strength. However, displacement ductility factor differ in the very wide range from 4.9 to 7.8. According to the results, most of test units have been found to have enough displacement ductility factors. The yield of prestressing steel was observed to occur earlier in proportion to λ ratio. However, it have been verified that prestressed concrete piers didn't show abrupt decrease in load carrying capacity even after yield of prestressing steel, showing ductile behavior and good displacement ductility factor even in the specimens having higher tendon tensioning level. From the load-displacement envelopes obtained, it has been found that λ ratio put a notable influence on the ascending branch of the load-displacement relationships. As far as λ ratio remain between 0.5 and 0.75, regardless of the type of specimen, the specimens demonstrated their full flexural strength resulting in nearly identical peak load with the analytical. With higher λ ratio, concrete compressive failure and buckling of longitudinal reinforcement have been found to occur a little earlier. In addition to that, concrete compressive failure has been found to occur irrelevant to γ ratio, contrary to the fact that in general buckling of longitudinal bar and yield of prestressing steel occur earlier as reinforcement ratio decrease.

4 RESIDUAL DISPLACEMENT MODIFICATION FACTOR C_R

The following have been discussed to have more simplified expression for residual displacement modification factor C_R. The peculiarity of prestressed concrete piers, having smaller residual displacement and higher restoring force, was found apparent from γ ratio 0.3 or more. On the top of that, when λ ratio is 0.5 or more, the effect of tendon tensioning level get relatively smaller on its behavior. Therefore C_R could be expressed conveniently as follows for prestressed concrete piers having λ ratio 0.5 or more.

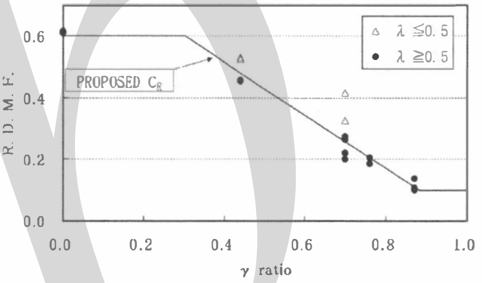

Fig. 1 Proposed R.D.M.F.

$$0.1 \leq C_R = 6(1-\gamma)/7 \leq 0.6 \qquad (3)$$

5 CONCLUSIONS

Based on the analysis of test results and comparisons with the theoretical predictions, the following conclusions were drawn.

1. The behavior of prestressed concrete specimens was affected significantly by the 2 main parameters. Especially the behavior at earlier loading stage gets a notable influence of λ ratio. While γ ratio put an influence especially on the residual displacement and the restoring force.
2. As far as short term behavior is concerned, in order to extract its full performance and capacity out of a given prestressed concrete cross-section, it would be recommendable to keep λ ratio relatively higher, being able to yield prior to buckling of longitudinal reinforcement and keeping better property of restoration at earlier loading stage.
3. According to the analytical results, the peculiarity of prestressed concrete piers, having smaller residual displacement and higher restoring force, was found effective and obvious from γ ratio 0.3 or more. However, considering the test results, γ ratio should be 0.5 or more to keep its outstanding seismic performance and maintain its inherent merits.
4. In comparison of the experimental and analytical results, the proposed expression for displacement modification factor C_R has been verified applicable to the design of prestressed concrete piers.

REFERENCES

[1] Ikeda, S.: "Seismic behavior of reinforced concrete columns and improvement by vertical prestressing", Proc. of FIP, Vol.2, pp.879-884, May, 1998

DUCTILITY ENHANCEMENT OF CONCRETE BY LATERAL CONFINEMENT

Fumio Watanabe
Department of Architecture and Architectural Systems, Kyoto University, Sakyo, Kyoto, JAPAN

Beni Assa
Faculty of Engineering
University of Sam Ratulangi, Manado
INDONESIA

Keywords: confinement, stress-strain curve, ductility, column

1 INTRODUCTION

The application of transverse reinforcement to potential plastic hinge zone is essential to obtain the ductile response of reinforced concrete columns during a major earthquake. Several stress strain idealizations for confined concrete have been proposed and applied to the evaluation of column ductility. However these idealizations are empirical ones to a greater or lesser extent, especially for the configurations of transverse reinforcement. Therefore more general approach is needed to investigate the effects of transverse reinforcement details and to establish the theoretical method for the prediction of stress strain curve of confined concrete.

2 LOADING TESTS ON CONFINED CUIRCULAR COLUMNS

A total of thirty-two 145x300 mm concrete cylinders were tested under monotonic concentric compression. No cover concrete was provided in all specimens. The target strength of concrete ranged from 20 MPa to 90 MPa. Bar diameter of continuous spirals and welded circular hoops were 6.25 mm. Nominal yield strengths of them were 1300 MPa and 800 MPa, respectively. The spacing of continuous spirals or circular hoops was varied from 19 mm to 75 mm in center. The axial deformation of concrete cylinder was measured at the central part of specimens with gage length of 145 mm. From the tests following 4 empirical equations were obtained by regression analysis for all of specimens.

$$f_{cc} = f_c^{'} + 3.36 f_{rp} \quad (1)$$

$$\varepsilon_{cc} = (1 + 21.5 f_{rp} / f_c^{'})\varepsilon_c \quad (2)$$

$$\varepsilon_{80} = (2.74 + 32.8 f_{rp} / f_c^{'})\varepsilon_c \quad (3)$$

$$\varepsilon_{rp} = 0.0021 + 0.016 f_{rp} / f_c^{'} \quad (4)$$

where, $f_c^{'}$, f_{cc}: compressive strengths of unconfined and confined concrete, f_{rp}; lateral pressure at peak, ε_c, ε_{cc}; strain at peak of unconfined and confined concrete, ε_{80} ; strain at 80% of peak load in descending branch, ε_{rp}; lateral strain at peak.

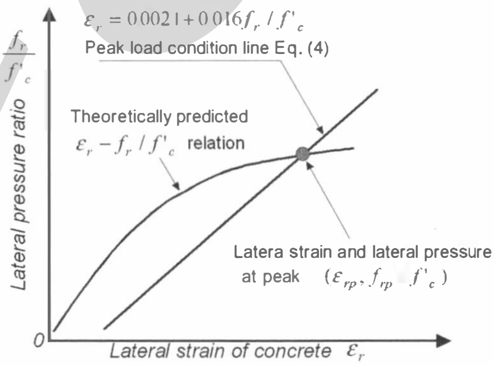

Figure 1 Peak load condition line

The relationship between the lateral strain and the lateral stress at peak load was obtained by a linear curve as given by Eq. 4 regardless of the amount of transverse reinforcement. That is, lateral pressure, $f_r / f_c^{'}$, – lateral expansion, ε_r, curve intersects the line given by Eq. 4 when the stress strain curve of confined concrete reaches the peak load. Therefore the key of the prediction of stress strain curve of confined concrete is how to calculate the lateral pressure and lateral expansion for transverse steel concrete system.

3 THEORETICAL PREDICTION OF S-S CURVE OF TIED CONCRETE SECTION

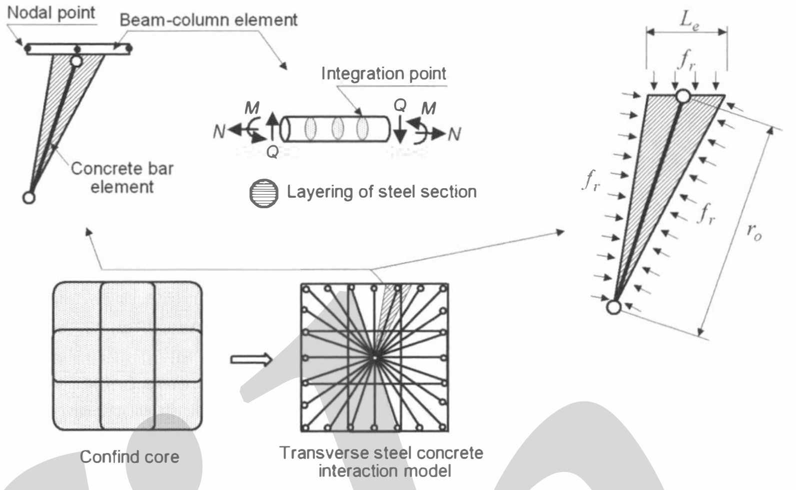

Fig. 2 Analytical model for transverse steel concrete interaction

For square tied column section, f_r-ε_r curve can be predicted by finite element analysis by applying the transverse-steel concrete interaction model indicated in Fig. 2. Figure 3 indicates the process to obtain the stress strain coordinate at peak load and the predicted stress strain curve for Unit-2 specimen (Scott et al 1982) with their observed one. The numerical expression of stress strain curve of confined concrete is given by Popovics proposal.

4 CONCLUSIONS

New analytical method for predicting the stress strain curve of confined concrete gives successful results. The method can be applied to the flexural analysis of tied concrete column.

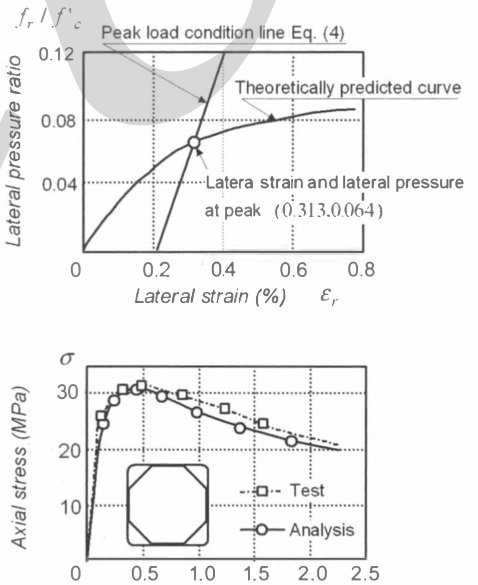

Fig. 3 Comparison between tests and analysis

REFERENCES

1) Richart, F. E. et al., “A Study of the Failure of Concrete under Combined Compressive Stresses”, University of Illinois, Engineering Experimental Station, Bulletin No. 185, 1928.
2) Yokoo, Y. , and Nakamura, T. , "Non-stationary Hysteretic Uniaxial Stress-Strain Relations of Wide-Flange Steel : Part II - Empirical Formulae", Transactions of Architectural Institute of Japan, No.260, Oct 1977, pp.143 - 149.
3) Popovics, S., "A numerical Approach to the Complete Stress-strain Curves of Concrete", Cement and Concrete Research, Vol.3, No.5, September 1973, pp.583-599.
4) Scott, B. D., Park, R., and Priestley, M. J. N., “Stress-Strain Behavior of Concrete Confined by Overlapping Hoops at Low and High Strain Rates”, ACI Journal, January-February 1982, Title No.79-2, pp.13-27.

SEISMIC BEHAVIOR OF HIGH STRENGTH CONCRETE COLUMNS CONFINED BY COLD-ROLLED RIBBED STEEL TIES

Hao Wang and Huiying Zhang
Beijing Institute of Architectural Design & Research, China
Dept. of Civil Engineering, Tsinghua Univ., Beijing, China

Keywords: high strength concrete column, cold-rolled ribbed steel ties, ductility

1 INTRODUCTION

The technology of high-strength concrete (HSC) has been greatly improved over the last decade and it has become the main direction of the current development of concrete technology because HSC has its distinguished advantages compared with ordinary concrete: higher compressive strength, higher stiffness and lower deformation. However, HSC has a marked shortcoming in material performance, whose ductility is worse than that of ordinary one. It is known that concrete's brittleness increases with the increments of its strength, which is disadvantageous for the structure's performance to resist earthquake.

In high buildings, HSC is used mainly in columns, whose safety level determines the safety degree of the whole building directly. Former research showed that adequate lateral confinement is the main measure to guarantee sufficient strength and ductility of columns. Currently in China, the steel used as ties are mainly Grade I, and occasionally Grade II. Grade I steel's strength is not high, thus greater amount is needed, while Grade II steel is not thin enough to be used as ties. In HSC columns, replacing ordinary ties with high strength ones is an effective method to improve their strength and deformation ability, reduce the steel amount and facilitate construction. LL550 cold-rolled ribbed steel, a kind of high-efficient, energy-saved steel developed recently, has higher strength than ordinary hot-rolled steel. In addition, with ribs in the surface, it has stronger adhesive strength with concrete than ordinary cold-rolled wire. Therefore, it became an important choice in the engineering applications.

Between 1999 and 2000, Peng Li[3] did some experimental research on the anti-seismic performance of the compressive bending components of high strength concrete with cold-rolled ribbed ties. Based on that reference, this paper performs further research.

2 TEST PROGRAM

2.1 Test specimens

Six column specimens with square cross sections were tested. Each column had a cross section of 200mm×200mm and a height of 1150mm.

Table 1 gives the designations of all the specimens. Fig. 1 and table 1 show details of the vertical and transverse reinforcement used in construction of the specimens.

2.2 Material properties

In this experiment, LL550 cold-rolled ribbed steel was used as ties and new grade III steel was used as longitudinal reinforcement. The diameters of ties and longitudinal bars were 6mm and 12mm respectively. The yield strength and the yield strain of LL550 cold-rolled ribbed steel were 547.60Mpa and 4773$\mu\varepsilon$. The yield strength of new Grade III steel was 501.87Mpa.

The concrete strength used in the specimens was designed as C60. But the actual strength was different, which was all listed in Table 1.

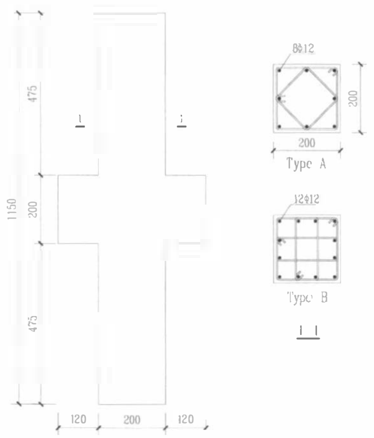

Fig.1 Dimension of test specimens and details of ties

2.3 Instrumentation, loading rules and measurement

The experiment was carried out under the reaction arch of the Structure Laboratory of the Department of Civil Engineering of Tsinghua University.

When set up, each test column was subjected to axial load and cyclic lateral loads. The axial load was applied first and kept constant at a predetermined level during each test. Two levels of axial load were used, which were 27% and 45% of nominal column axial load capacity. Each specimen was subjected to a number of lateral loading cycles while maintaining constant axial loads. The first three loading cycles were controlled by horizontal loads. Max values of two directions were equal and increased every cycle. From the fourth loading cycle, the column was pushed horizontally by displacement. Max values of each cycle were augmented gradually and the increment was 1.5mm or 2mm. Testing was stopped when the specimen could not sustain the vertical load under increasing horizontal displacement.

Several instrument types were used to obtain axial and horizontal load, horizontal displacement, rotational angle of the column top, the strain of longitudinal bars and ties.

Table 1 Details of test specimens and some important test results

Specimen designation (1)	Tie type (2)	Tie spacing (3)	f_c (MPa) (4)	λ_v (5)	n (6)
SLL-1	A	150mm	50.50	0.085	0.27
SLL-2	A	180mm	51.10	0.070	0.27
SZHL	B	100mm	51.22	0.148	0.45
SHL-1	A	70mm	53.26	0.173	0.45
SHL-2	A	100mm	52.06	0.124	0.45
SHL-3	A	150mm	52.78	0.082	0.45

Note: (1) Specimen designation, where S=seismic resistant experiment; 1st L=low axial low ratio; 2nd L=high axial ratio; Z=different longitudinal bars; number=sequence in every group; (2) See Fig. 1 for description of each detail type; (4) f_c=concrete compressive strength; (5) λ_v=the index of ties, defined as $\rho_v \cdot f_y / f_c$, where ρ_v is the volumetric ratio of ties and f_y is the yield strength of ties; (6) n=axial load ratio.

REFERENCES

1. Peng Li, "Experimental Study of the Seismic Behavior of High Strength Concrete Columns With Cold-Rolled Ribbed Confinement", Master's Degree Thesis, Tsinghua University, 2000.
2. Hao Wang, "Experimental Study of HSC Columns With Cold-rolled Ribbed Ties Under Concentric and Seismic Loading", Master's Degree Thesis, Tsinghua University, 2001.
3. National Standard of China, "Technical Specification for High-Strength Concrete Structures (CECS 104:99)", 1999.

FAILURE MECHANISM OF POST-TENSIONED BEAM-COLUMN SUBASSEMBLAGES

Minehiro Nishiyama
Architectural Engineering, Kyoto University, Kyoto 6068501, JAPAN: e-mail:*mn@archi.kyoto-u.ac.jp*

Keywords: prestress, beam-column joint, post-tension, failure mechanism, bond, grout, anchorage

1 INTRODUCTION

Prestress introduced into the beam through the joint of post-tensioned beam-column subassemblages has been considered to increase shear strength of the joint core because of its multi-axial state of stress with column axial load, and larger compressive block in the beam critical section, which results in larger compressive strut in the joint core. However, in some experiments on prestressed beam-column joints it was revealed that prestress was not beneficial on shear strength of the joint core. Effectiveness of prestress on shear strength of post-tensioned beam-column joints is still controversial.

The objectives of this paper are to make failure mechanism of post-tensioned beam-column subassemblages clear in terms of the anchorage location and bond characteristics between prestressing steel and grout mortar. The conclusions obtained in this study would be of importance for the practical design of prestressed concrete beam-column joints.

2 EXPERIMENTAL WORK

The experimental work is divided into two test series; in Series A the test parameters are location of anchorage of prestressing tendon and amount of prestressing force, in Series B the parameter is type of tendon, i.e., bond strength. Each test series consists of four prestressed concrete beam column joints. All test units had the same dimension of beams (200x300mm) and columns (300x300mm). They were beam-external column joint assemblages.

2.1 Series A

The experimental variables were location of anchorage of prestressing tendon (inside and outside the joint core) and amount of prestressing force (axial load level of $0.08f'_cA_b$ and $0.15f'_cA_b$). The test unit is shown in the figure. Two of them are the test units whose prestressing steel bars were anchored to the steel plate (120x120, t=30mm) embedded in the joint core. The steel plate was located at the center of the joint core. In the other two, bars were anchored to the steel plate (300x200, t=30mm) attached to the column face. Two types of bars were used; one was 17mm in diameter round bar, and the other was 23mm in diameter round bar.

The test units were so designed as to fail in shear in the beam-column joint; the shear strength of the joint core calculated according to the AIJ (Architectural Institute of Japan) guidelines was smaller than the input shear derived from the equilibrium of forces at the flexural strength.

2.2 Series B

The variable in Series B was type of prestressing steel; round bars (SBPR1080/1230), deformed bars (SBPDL1080/1230) and strands (SWPR7AL) were used. The diameters of the tendons were 13.0mm, 12.6mm and 12.4mm, respectively.

3 GENERAL BEHAVIOR OF TEST UNITS

3.1 Series A

The test units with the anchorage outside of the joint core were able to be loaded to well beyond the beam rotation angle of 1/20 with little reduction in moment capacity. In the units with the anchorage inside of the joint core, after the maximum moment had been reached at the beam rotation

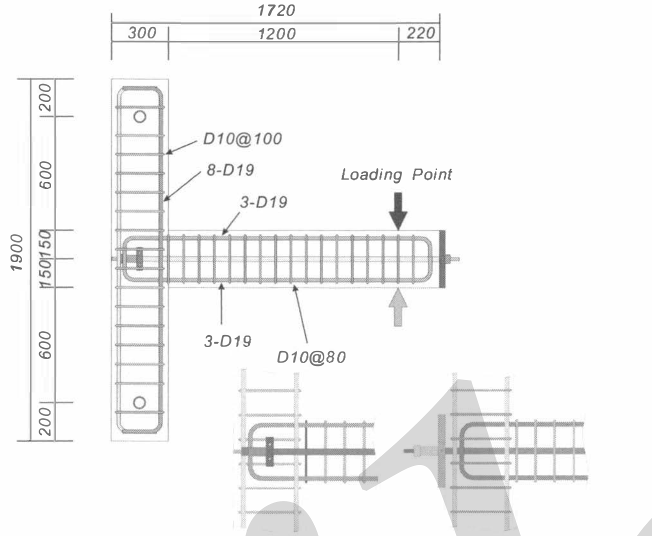

Inside anchorage Outside anchorage

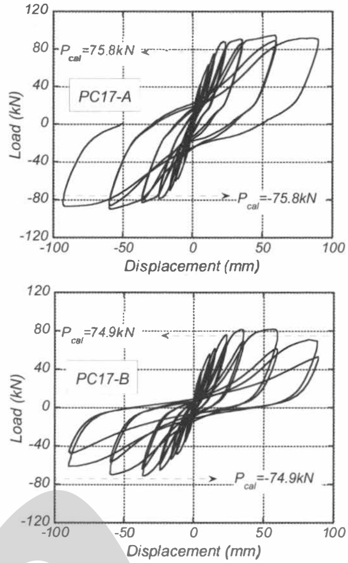

angle of approximately 5% in each direction, the subsequent reduction in stiffness and strength with pinched hysteresis was observed due to damage concentrating in the joint core. In PC17-B, the moment at the beam rotation angle of 1/13 was about 88% of the maximum moment capacity. In PC23-B, 20% reduction was observed at the final stage of loading.

3.2 Series B

Although the test units were designed as to fail in shear in the joint prior to flexural yielding of the beam, stiffness reduction due to flexural yielding was observed before extensive shear cracks appeared in the joint. The ratios of the load capacities to P_{cal}, the load corresponding to the moment capacity calculated by the ACI318 method, are 1.21, 1.22, 1.21 and 1.17 for PC-K1, PC-K2, PC-K3 and PC-KU, respectively. No significant difference is not observed in these load-displacement curves. This is because the contribution of prestressing steel to the load capacity is small; the ratio is approximately 6-7%.

4 CONCLUSIONS

On the basis of the test results described in this paper the following conclusions are derived.

Series A:

(1) The maximum load capacity of the test units with the inside anchorage, PC17-B and PC23-B was smaller than that of the units with the outside anchorage, PC17-A and PC23-A. The ideal strength calculated by the ACI method was not attained in the units with the inside anchorage, PC17-B and PC23-B.

(2) The hysteresis loops obtained from the test units with the inside anchorage, PC17-B and PC23-B indicated reduction in capacity and pinching due to joint shear failure. Conversely, the units with the outside anchorage, PC17-A and PC23-A showed much better hysteresis loops even in the large ductility regions.

Series B:

(1) Bond strength between prestressing steel and grout mortar did not have a significant effect on the behavior of the test units. This is because the amount of prestressing steel was small compared with that of mild steel. Further study is needed.

(2) The proposal by the AIJ guidelines for the joint shear strength underestimated the joint strength of the test units.

DEFORMATIONAL ASSESSMENT OF UNDERGROUND MULTI-WALLED BOX-TYPE REINFORCED CONCRETE STRUCTURES FOR PERFORMANCE BASED DESIGN

Yoshinori Miyagawa Yukio Aoyagi

Central Research Institute of Electric Power Industry(CRIEPI), JAPAN

Keywords: underground, seismic performance, wall, soil-structure interaction

1. INTRODUCTION

In 2002 a seismic performance assessment guideline for reinforced concrete facilities in nuclear power stations was published in Japan. This guideline shows the principle that non-linear dynamic analysis for ground-structure coupled system should be conducted. CRIEPI together with Japanese power companies verified the applicability of existing non-linear FEMs to two-dimensional rigid frame in-/underground reinforced concrete structures, which led to the adoption of the above-mentioned principle. Since the analysis involves complicated interactive systems of soil and embedded RC structures, the verification is limited to the cases in which the structures can be idealized as a two-dimensional problem. In the future we are urged to extend our methodology to the seismic assessment where three-dimensional considerations should be required. The present paper proposes one concept to this direction.

2. TARGET STRUCTURES AND THEIR FEATURES

The reinforced concrete structures in question include ducts for accommodating cooling water pipes, communication cables etc., intake water pits, pump station rooms, intake as well as drainage channels and the like. These structures have a common characteristic that they are constructed in-ground and composed of plane members. **Fig.1** is a schematic illustration of an intake water facility.

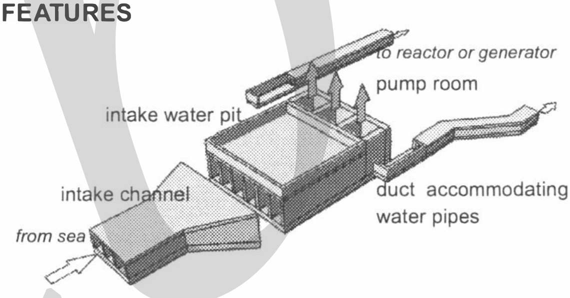

Fig.1 Outline of Underground RC Structures

3. DEFINITION OF SEISMIC PERFORMANCE ASSESSMENT

Seismic performance assessment is tantamount to the checking process whether the results of seismic response analysis satisfy required performance and divided into following three stages.

(i) Quantification of required performance
(ii) Seismic response analysis
(iii) Comparison of response values with limit values

4. PROPOSAL OF ASSESSMENT METHOD OF 3D COUPLED SYSTEM

In this chapter, a seismic performance assessment method is presented. The outline of response analysis that forms nucleus of assessment is shown in **Fig.2**. The proposed method can be regarded as a kind of ground deformation method[1] since the free field ground displacement is calculated independently by the dynamic analysis for soil-column.

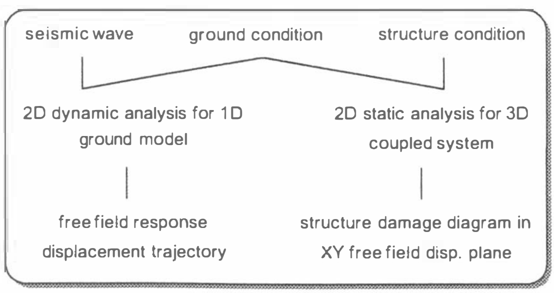

Fig.2 Flow of Proposed Response Analysis

The ground response analysis to be

applied for free field must be what can compute response displacements in two horizontal directions by inputting earthquake waves with corresponding two horizontal components. Constitutive law should be capable of expressing elasto-plastic properties of soil such as estimated by Nishi model[2]. The results are depicted as a trajectory on the XY free ground displacement plane(**Fig.3**).

In the following stage of deformability analysis in ground-structure coupled system the structural damages and/or the reduction in load bearing capacities with respect to the arbitrary free ground

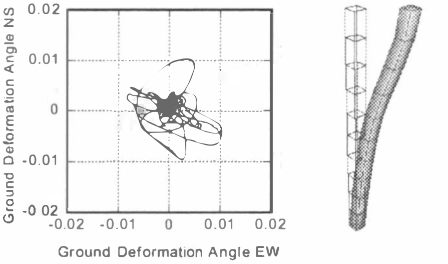

Fig.3 2D Input Response Analysis for 1-D Ground Model

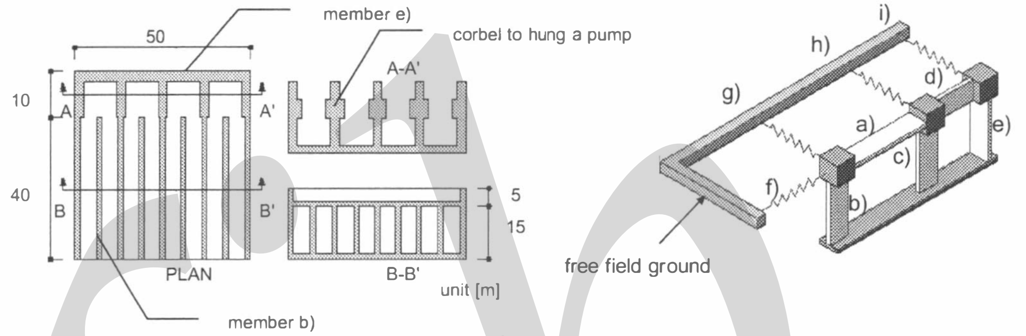

Fig.4 Decomposition of Coupled System into Link Model

displacements are evaluated. This is realized by simplifying the coupled system into a link model(**Fig.4**) and performing analysis with regard to as many directions as possible. The results are also drawn on the same XY displacement plane as shown in **Fig.5**. We call this curve structure damage diagram. In the figure six curves are depicted corresponding to the following items that are provisionally arranged as required performance for member b) and e), respectively.

(A4) Any member should not entirely lose its load capacity.

(A5) Any member should not lose 20% of its load capacity

(B1) Any member does not yield.

(B2) Any member does not cause excessive shear crack.

Based on these two graphs, we can visually grasp the relationship between any seismic wave and structure damages (**Fig.6**).

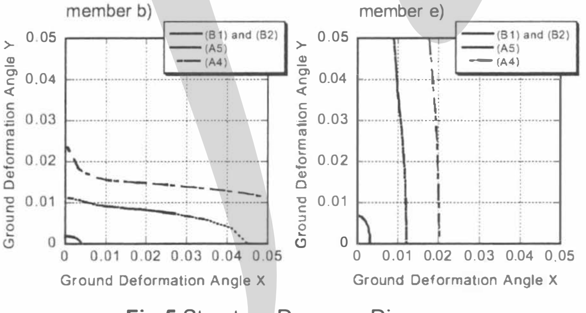

Fig.5 Structure Damage Diagram

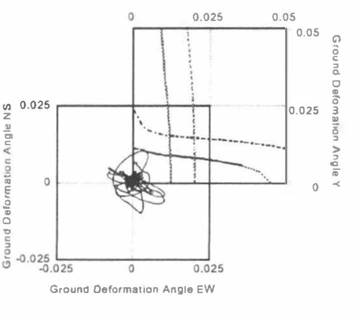

Fig.6 Comparison with Ground Motion

REFERENCES

[1] Japan Road Association : Recommendations for Design and Construction of Underground Parking Space, 1992.(in Japanese)

[2] Nishi,K., Esashi,Y.: Stress-strain Relationship of Sand Based on Elasto-plastic Theory, Proc., JSCE, No.280, pp.111-122,1978.

SEISMIC PERFORMANCE EVALUATION METHOD OF PRESTRESSED CONCRETE FRAMES

Ryuichiro Uchida
Matsui Construction Co.,Ltd, Japan

Masahiro Nakamura
Kurosawa Construction Co,Ltd, Japan

Hiromitsu Suetsugu
Nihon University
Japan

Masayuki Hamahara
Nihon University
Japan

1. INTRODUCTION

The Building Standard Law Enforcement Order in Japan, revised in 2001, adopted the design method based on performance concept. Consequently the seismic design of the building structure is conducted on the basis of the response spectrum and the equivalent linealization method, in which the anti-seismic performance of the frames can be evaluated. In adopting the method, the relationship between the restoring force characteristics of frames and that of their constituent members is indispensable for the structural designers. With respect to prestressed concrete, however, the relationship has not been clarified yet.

In this paper, Elasto-plastic analyses using a displacement method were systematically performed, in order to investigate the hysteretic behavior of multi-story Prestressed Concrete frames. On the basis of the analyses, a restoring force characteristics model was proposed in order to predict the hysteretic behavior of prestressed concrete frames. Furthermore, a design method was proposed to verify the structural performance of the prestressed concrete frames subjected to seismic load.

2 IDEALIZATION OF THE RELATIONSHIP BETWEEN REDUCED DISPLACEMENT AND BASE SHEAR

In constructing the stiffness matrices for Prestressed Concrete frame, the restoring force characteristics model proposed by Hamahara et al. [1] was applied to the moment – rotation angle relationship at the end of their constituent members. The restoring force characteristics was idealized by the hysteresis loop of a degrading stiffness type and a envelope curve which consist of three linear segments. The first break in the envelope was defined by Eq. (1) and the initial stiffness obtained from the analyses.

$$Q_c = \left(2A_y - Q_y \cdot D_y\right) / \left\{D_y - \left(Q_y / K_e\right)\right\} \qquad \text{-----(1)}$$

Eq. (1) was determined so that the energy up to the yielding point calculated by the analyses equal to that obtained from the model (see Fig. 2). Y, Y' point are the yielding point (see Fig. 1).

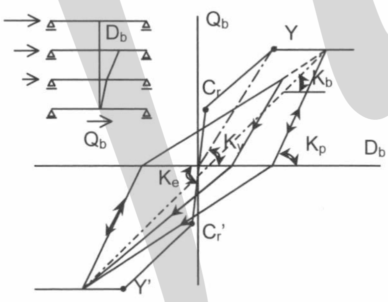

Fig. 1 Db-Qb relationship

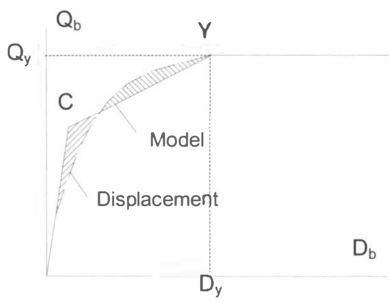

Fig. 2 Idealization of envelope curve

Similar to the constituent members, the gradient of unloading path (K_p) was express by the initial stiffness (Ke) the gradient of the line connecting the negative and positive maximum responses point, and the hysteretic parameter, r, which governs the hysteretic damping (hereinafter abbreviated as the hysteretic parameter). That is,

$$K_p = r \cdot K_e + (1 - r) \cdot K_b \qquad \text{-----(2)}$$

The hysteretic parameter, r, was evaluated as Eq. 3.

$$r = \overline{\mu} \cdot \sum_{i=1}^{N} C_{ri} \cdot M_{yi} / \sum_{i=1}^{N} M_{yi} \quad \text{------(3)}$$

where, $C_r = \alpha_y \cdot a_r \cdot (q_r + 0.5 \cdot q_p{}^2) / (q_r + q_p)$ ------(4)

$$a_r = a/(4D) \text{ but } a_r \le 1, \quad q_p = \text{prestressing force}/(b \cdot D \cdot \sigma_B), \quad q_r = T_{ry}/(b \cdot D \cdot \sigma_B)$$

$$\alpha_y = [0.043(1 + a/D) + 1.67n\{p_t + 3.5 \cdot p_g \cdot (d_g / D)\} + 0.33\eta_o] \cdot (d_r / D)^2 \quad \text{------(5)}$$

where, a/D denotes shear span ratio; n denotes ratio of the modulus of elasticity of reinforcement to that of concrete ; p_t denotes tensile reinforcement ratio and p_g denotes gross reinforcement ratio of tendons.

3 VERIFICATION OF SEISMIC PERFORMANCE OF PRESTRESSED CONCRETE FRAMES

Hamahara et al. [2] conducted a parametric study whose variables were the ratio of the shear force at yield to the building weight; the ratio of shear force at initial crack to that at yield; the period for initial stiffness; the ratio of the period at the yield to that for initial stiffness; the hysteretic parameter and ground motion. In this study following equation was proposed in order to predict the substitute damping factor.

$$h_e = \alpha_2(\mu - \mu_{cr}) / [(\mu - \mu_{cr}) + \alpha_1] + h_o \quad \text{------(6)}$$

where, $\alpha_1 = (T_1 / T_2)\{1/(r + 0.0075)\}$, $\quad \alpha_2 = 0.4 \quad \mu = D_{max} / D_y \quad \mu_{cr} = D_{cr} / D_y$

D_{max}, D_{cr}, D_y denote the maximum, cracking and yielding displacement respectively.
The procedures for evaluating the seismic performance of prestressed concrete frames are as follows.

STEP 1 Determine the dimension and reinforcement arrangement of the frames designed.
STEP 2 Determine the reduced displacement at ultimate limit stage by the push-over analysis.
STEP 3 Idealize the envelope curve.
STEP 4 Determine the ductility factor and base shear. Calculate the period at initial stage, yielding and at ultimate limit stage.
STEP 5 Calculate the hysteretic parameter and substitute damping using Eq. (3),(6).
STEP 6 Calculate the response base shear (Q_{br}) using a response spectrum and verify:
$Q_{bu} \ge Q_{br}$ If this criterion is not satisfied then return to STEP 1.

4 CONCLUSION

Elasto-plastic analyses using a displacement method were systematically performed, in order to investigate the hysteretic behavior of multi-story prestressed concrete frames. On the basis of the analyses, the following conclusion may be stated.

1) The hysteretic behavior of the prestressed concrete frames was governed by that of the yielding constituent members.
2) Taking account of this result the restoring force characteristics model was proposed in order to evaluate the hysteretic behavior of prestressed concrete.
3) The procedures for evaluating the seismic performance of prestressed concrete frames were proposed

REFERENCES

[1] M. Hamahara, H. Suetsugu and M. Okada: "Elasto-plastic hysteretic behavior of prestressed concrete beams, *Transaction of AIJ*, No.410, 1990,pp63-69

[2] M. Hamahara, H. Suetsugu, junjiroh Motooka and M. Okada: "Effect of prestressing force and Mode of mechanism on hysteretic behavior of prestressed concrete frames, *Proceedings of Fip Symposium '93*, Oct. Vol.1 1993,pp.219-226

SEISMIC DESIGN OF CONCRETE BRIDGES

Kazuhiko Kawashima
Tokyo Institute of Technology
Japan

Key Words: seismic design, bridges, reinforced concrete, ductility, strength

The extensive damage to bridges in the 1994 Northridge, USA, the 1995 Kobe, Japan, the 1999 Chi-Chi, Taiwan, and the 1999 Kocaeli and Duzce, Turkey earthquakes revealed the vulnerability of bridges under extreme ground motions. In particular, in the 1995 Kobe earthquake a number of bridges suffered extensive damage as a result of the insufficient shear strength and ductility capacity of reinforced concrete columns. Being located in the monsoon area, the high-rate of erosion developed thick sedimentation in Japan. Because damage of bridges mostly resulted from the instability of ground, it was a principle to construct rigid and massive foundations and piers. Shear capacities were not obviously critical in such rigid and massive piers. Various unique technologies for mitigating damage, such as the unseating prevention devices and countermeasures for soil liquefaction, have been developed and implemented. The static seismic analysis assuming 0.2-0.3 g response acceleration based on the working stress approach contributed significantly to mitigate the damage in past earthquakes prior to the 1995 Kobe earthquake. However the direct implementation of such a design practice to urban viaducts which were constructed since the 1970's involved the lack of ductility and shear capacity of columns.

Based on the lessons from the Kobe earthquake, the seismic design was extensively revised in 1996. The revisions include 1) the design ground motions reflecting the near-field ground accelerations; 2) routine use of inelastic dynamic response analyses for certain types of bridges; 3) extensive use of elastomeric bearings instead of steel bearings; 4) use of seismic isolation; 5) enhancement of strength of unseating prevention devices; and 6) effect of lateral spreading of the surface ground as a result of liquefaction. However the most significant revision was the enhancement of ductility and shear capacities of reinforced concrete columns.

As a result of the limited damage of reinforced concrete columns prior to the Kobe earthquake, few studies accounted for the ductility and shear capacity in Japan. Cyclic loading tests have been extensively conducted for reinforced concrete columns at many institutions and universities after the Kobe earthquake. The tests contributed to provide new design requirements for ductility capacity and shear strength of reinforced concrete columns. Since technical development for the enhancement of reinforced concrete piers/columns was one of the most important aspects in the revision of seismic design codes after the Kobe earthquake, some unique technical developments for reinforced concrete columns with verification by tests are presented in this paper.

1 INTERLOCKING COLUMNS WITH LARGE CROSS SECTIONS

Interlocking spiral columns consisting of 2 spirals with a diameter of 6 m (8.5 m wide and 6 m long in the transverse and the longitudinal directions, respectively) were constructed. Since it was much larger in size than the interlocking columns which were constructed elsewhere, a unique experimental test was conducted by the Japan Highway Public Corporation (JH) in conjunction with the construction of the bridge. Since assemblage of the interlocking spirals requires a special skill, an in situ assemblage test of large diameter interlocking spirals was conducted.

2 UNBONDING OF LONGITUDINAL BARS AT THE PLASTIC HINGE

One of the measures to mitigate the concentration of the deformation of the longitudinal bars at the plastic hinge is to unbond the longitudinal bars from the concrete. By appropriately unbonding the longitudinal bars between a certain interval, the deformation of the longitudinal bars decreases as a result of averaging the strain in the interval. A cyclic loading test for 1.45 m tall square columns with varying the interval of unbonding was conducted to show the effectiveness of enhancing ductility capacity. An important feature of the unbonded column is a rocking response of the column relative to the footing. Since the longitudinal bars are unbonded for a certain length, the longitudinal bars in tension pull out from the column, which results in a dominant rocking response of the column. As a result of small flexural deformation, the flexural failure of the column is limited. It is considered that the unbonding is effective to increase the ductility capacity of columns by properly choosing the unbond length.

3 PRESTRESSED CONCRETE COLUMNS

Prestressed concrete columns have been seldom constructed throughout the world in spite of their various merits. To verify the seismic performance of prestressed concrete columns, an extensive experimental and analytical study was conducted. In the loading test, rectangular prestressed concrete columns with an effective height of 1.5 m and a section of 400 mm by 400 mm were constructed. Cracks of concrete are much fewer in the prestressed columns than the standard reinforced concrete column during the loading and unloading reversals. In the standard reinforced concrete column the restoring force remarkably decreases when longitudinal bars locally buckle, while such a remarkable deterioration of restoring force does not occur in the prestressed columns. Various merits support the implementation of the prestressed concrete columns.

4 ISOLATOR BUILT-IN COLUMN

Since the hysteretic behavior of a reinforced concrete column occurs only at the plastic hinge, it is interesting to replace the concrete in the plastic hinge by an appropriate material that provides enough deformation and energy dissipation so that the flexural deformation at the rest of a column is limited. This type of column was studied using a high damping rubber that is used for a standard high damping rubber bearing for seismic isolation. A series of seismic loading test was conducted to verify the performance of the isolator built-in columns. Failure of concrete is limited in the isolator built-in column until 4% drift. However the longitudinal bars start to rupture in the rubber unit at 4.5% drift. The use of ductile steel is required to mitigate the rupture of the longitudinal bars as a result of concentration of strain at the bars in the rubber unit.

5 SEISMIC PERFORMANCE OF C-BENT COLUMNS

An eccentricity e between the column center and the point where the deck weight applies results in a static eccentric moment in the column. Under a strong excitation which is likely to cause an extensive failure and develop a large residual displacement in the compression side. The performance of C-bent columns was studied based on a cyclic loading test using columns with a rectangular section of 400 mm by 400 mm. The column with 1D eccentricity not only displaces laterally but also rotates around the column axis due to the eccentricity. As a result of rotation, failure of concrete started at the 2 corners in the eccentricity direction, and progressed to the 4 surfaces. The column with 1D eccentricity deteriorates much faster than the column without eccentricity. Another significant feature of the C-bent columns is the drifting of the columns in the transverse direction under the longitudinal and vertical loadings. Since the compression failure of concrete and the longitudinal bars was more destructive in the eccentric compression side than the eccentric tension side, this resulted in residual drifting of the column in the eccentricity compression direction. The residual drift reaches 2.3% and 3.7% in the columns with the eccentricities of 0.5D and 1D, respectively, at 4% lateral drift. Careful analyses are required for the columns with eccentricities for their restoring force and ductility capacities.

6 VERIFICATION OF SEISMIC PERFORMANCE OF RC COLUMNS USING PLOT TYPE MODELS

As a result of the limitation of loading facilities, it is common to use scaled models in the loading tests. However there exist various scale effects in the interpretation of loading test results derived from small scale modes. Hence, the calibration of test results from scale models is important to evaluate the strength and ductility capacities of plottype. A cyclic loading tests for 9.6 m tall rectangular columns with a section of 2.4 m by 2.4 m and a 2.4 m tall rectangular column with a section of 0.6 m by 0.6 m was conducted. The smaller column is a 1/4-scale model of the prototype. Failure of the prototype column was initiated by buckling of longitudinal bars and spall-off of the covering concrete at 2.5% drift, and proceeded to outward deformation of the tie bars and failure of the core concrete at 3% drift. Rupture of the longitudinal bars at 3-3.5% drift resulted in a significant decrease of the lateral restoring force. The failure progressed in a similar manner in the 1/4-scale column although it progressed slightly later than the plottype column

REFERENCES

[1] Hoshikuma, J., Unjoh, S. and Nagaya, K.: Flexural ductility of full-scale bridge columns subjected to cyclic loading, First fib Congress, Osaka, Japan, 2002
[2] Ikeda, S., Mori, T., and Yoshioka, T.: Seismic performance of prestressed concrete columns, Prestressed Concrete, 40-5, pp. 40-47, 1998 (in Japanese)
[3] Shito,K. Igase,Y., Mizugami,Y., Ohasi,G., Miyagi,T. and Kuroiwa, T.: Seismic performance of bridge columns with interlocking spiral/hoop reinforcements, First fib Congress, Osaka, Japan, 2002

PRACTICAL SEISMIC DESIGN FOR PRESTRESSED CONCRETE PIERS

Hiroshi Takemura
P.S. Corporation, JAPAN

Mikio Kato Toshiaki Goto
Nagoya Expressway, JAPAN

Keywords: prestressed concrete pier, seismic design, nonlinear dynamic analysis

1 INTRODUCTION

Prestressed concrete (PC) pier is that vertical prestress is introducing, which has an advantage for restoration capability at unloading. Many studies about PC pier were conducted, and these results were arranged by Japan Prestressed Concrete Engineering Association as " Guideline for Seismic Design of Prestressed Concrete Piers " in 1999. As Nagoya Expressway decided that one of the piers of four continuous steel girder bridge changes from RC pier to PC pier, it was necessary to consider entire bridge system. This paper describes the practical seismic design, considering entire bridge system, for PC pier that will be constructed first in Japan.

2 FEATURES OF PRESTRESSED CONCRETE PIER

Nagoya Expressway has new projects constructing viaducts. One of these projects, there is four continuous steel girder bridge. Nagoya Expressway decided that one of the pier is changed to PC pier. This is why there are some structural advantages as follows.
1) It has high ductility because PC tendons are not buckling even if the earthquake occurs.
2) It has high serviceability because residual displacement is small after the earthquake.
3) It is enable that the section area is small because PC tendons have high strength.
4) It has high durability because the crack is controlled by prestressing.
5) It is enable that the amount of reinforcement is decreased largely, so construction speed improves.

3 SUITABLE PARAMETERS FOR PRESTRESSED CONCRETE PIER

The authors conducted parameter studies and clarified the suitable parameters as follows.
1) It is desirable that the horizontal capacity of PC pier is equal to that of RC pier.
2) The compressive stress by prestressing is 2 to 4 MPa.
3) The most suitable value of the ratio between PC tendons and reinforcements is about 0.5.
4) It is desirable that the yield stiffness of PC pier is equal to that of RC pier.
Fig.1 shows the PC pier which satisfies these conditions and RC pier before changing to PC pier.

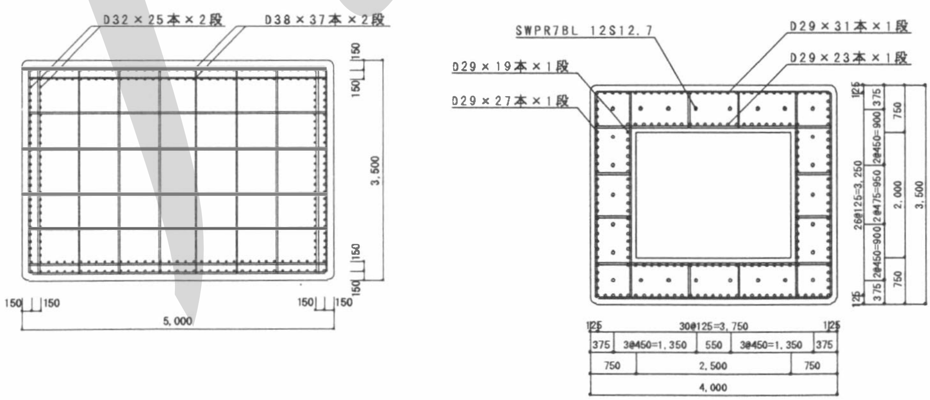

(1) reinforced concrete (2) prestresed concrete

Fig.1 Comparison between PC and RC pier

4 SEISMIC DESIGN BASED ON DUCTILITY DESIGN METHOD

Seismic design based on ductility design method is performed. As a result of this design, it enables to design PC pier without any problems if the lateral restraining reinforcement ratio is about 1%. It can reduce amount of section area and reinforcement largely. However, in case of having high lateral restraining reinforcement ratio, we have to pay attention to the difference of the allowable ductility factor and the equivalent lateral force coefficient between PC pier and RC pier. This is because the ultimate displacement of PC pier is smaller than that of RC pier shown in Fig.2. This means that PC pier has to be designed with great force, and other piers also have to be designed with it if PC pier's equivalent lateral force coefficient is the greatest in all piers. In this design, it has no influence on other piers although PC pier's equivalent lateral force coefficient is the greatest in all piers.

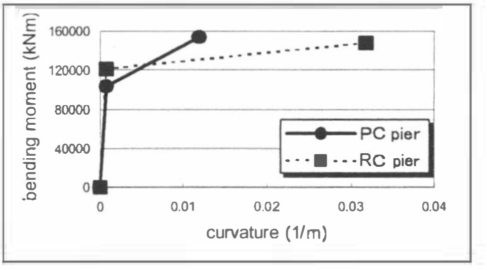

Fig.2 Relation between bending moment and curvature

5 SEISMIC DESIGN BASED ON NONLINEAR DYNAMIC ANALYSIS

The nonlinear time-history response analysis is performed. As a result of the nonlinear dynamic analysis, it enables to design PC pier without any problems. However, in case of having high lateral restraining reinforcement ratio, we have to pay attention to the difference of the second stiffness after yielding between PC pier and RC pier. In case of PC pier, the stiffness after yielding keeps yet, so response force is conveyed from the plastic hinge area to upper members. So, the response curvature of PC pier is greater than that of RC pier. Therefore, we have to investigate how to calculate the ultimate displacement in case of having high lateral restraining reinforcement ratio, in future.

6 CONCLUSIONS

The conclusions of this paper are given below.

1) The authors show that the suitable parameter of PC pier is that the compressive stress by prestressing is 2 to 4 MPa, the ratio between PC tendons and reinforcements is about 0.5, and the horizontal capacity and yield stiffness of PC pier is equal to those of RC pier in case of changing from RC pier to PC pier.

2) It enables to design PC pier a part of continuous girder bridge without any problems if the lateral restraining reinforcement ratio is about 1%. It can reduce amount of section area and reinforcement largely.

3) In case of having high lateral restraining reinforcement ratio, the PC pier's ultimate displacement calculated by the Guideline is less than that of RC pier. It brings that it has to design with great equivalent lateral force seismic coefficient, and it influences to the upper members of plastic hinge area in nonlinear dynamic analysis because of the second stiffness after yielding. Therefore, we have to investigate more about this point in future.

4) The PC pier is more effective for residual displacement than RC pier according to the results of ductility design method and nonlinear dynamic analysis.

REFERENCES

1) Design Specifications for Highway Bridges Part V : Japan Road Association, 1996.12
2) Guideline for Seismic Design of Prestressed Concrete Piers: Japan Prestressed Concrete Engineering Association, 1999.11
3) Proceedings of Prestressed Concrete Pier: Japan Prestressed Concrete Engineering Association, 1999.11

A STUDY ON THE SEISMIC PERFORMANCE OF PC RIGID FRAME BRIDGE WITH NONLINEARITY OF SPREAD FOUNDATION

Taku Yoshikawa Tsutomu Machi Meguru Tsunomoto
Oriental Construction Co., Ltd.,
Japan

Keywords: PC rigid frame bridge, spread foundation, seismic performance, nonlinear analysis

1 INTRODUCTION

For the seismic design of a bridge, the spread foundation system which is installed on the base rock generally fixes its footing assuming the deformation of the ground does not influence so much or the linear ground spring is estimated if we take account of the deformation. Because it is considered that general bridge has principal nonlinearity at the structural member of the pier base. However, when the Level 2 Earthquake Motion acts, floating of the spread foundation and yielding of the base ground may cause the spread foundation to show the nonlinear behavior. Considering such behavior of the spread foundation should enable us to implement the seismic design of the pier and the superstructure rationally. Thus, this study aimed at the longitudinal direction of a Prestressed concrete (hereinafter called "PC") continuous rigid frame bridge which was seismic-designed with fixed foundation to conduct nonlinear-static analysis and the nonlinear-dynamic analysis, taking account of the nonlinearity effected by the yielding of the base ground and floating of the spread foundation and to examine the influence of nonlinearity of the spread foundation on the seismic performance of bridge. In addition, this analysis used the kind of base ground, model and nonlinearity of the ground spring as parameter.

2 AIMED BRIDGE AND ANALYSIS MODEL

The PC three-span continuous rigid frame bridge with center span of 100m was examined as shown in **Fig.1**. The pier height was set in the range of 30m or 60m which the dynamic analysis for the seismic design might be desirable. The analysis model was settled as two-dimensional frame model and the superstructure had linear-beam element. Considering the plastic hinge, the nonlinear rotating spring was installed on the upper and lower ends of pier and the place outside of plastic hinge area was modeled as nonlinear beam element. The analysis models of spread foundation applied for this study were the following three models as shown in **Fig.2**; (1) Model that fixes the foundation. (2) Rotating spring model installed by the nonlinear rotating spring at the bottom of foundation which takes account of ground yielding and the floating of the spread foundation, and (3) Distributed-spring model that places vertical nonlinear spring at the bottom of foundation. The nonlinearity of spread foundation was established for each model as below. (1) Rotating model

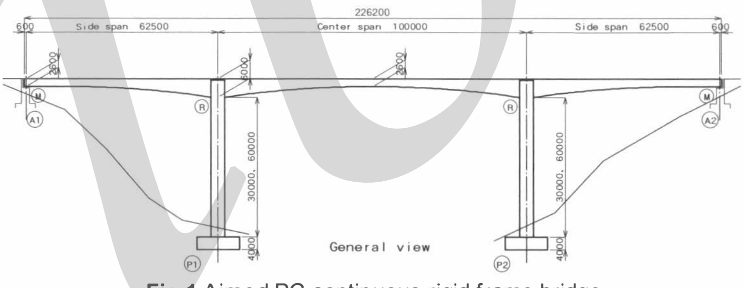

Fig.1 Aimed PC continuous rigid frame bridge

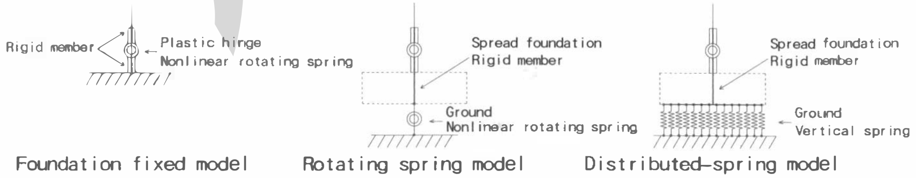

Fig.2 Analysis mode of spread foundation

(Highway model) : Curve model considering the floating foundation and the upper limit of reaction force described in “Specifications for Highway Bridges Part IV”. (2) Rotating model (Railway model) : Tri-linear model described in “Design Standards for Railway Structures”. (3) Distributed-spring model : This “Bi-linear model” sets the stiffness on the tensile side of nonlinear spring which was placed vertically as zero to consider the floating, and also sets the ground yielding point on the compression side.

3 NONLINEAR STATIC ANALYSIS

Fig.3 shows the relationship between horizontal seismic force and horizontal displacement at the superstructure when we applied the rotating spring model (Highway model). When the foundation was fixed, both cases of pier height of 30m and 60m showed same linear behavior till the yielding of the plastic hinge at the lower end of pier and the lower end of pier reached the ultimate after the upper end of pier yielded. On the other hand, when we considered the nonlinearity of spread foundation, the case of pier height of 30m showed similar behavior to that of foundation-fixed type till the ground yielding limit of horizontal seismic force 0.4 and then the lower end of pier did not yield while the upper end of pier indicated a behavior from yielding point to ultimate. In this case, to consider the nonlinearity of spread foundation decreased the horizontal seismic force about 0.1 at the ultimate. The case of pier height of 60m showed same behavior as the case of 30m which decreased the slope of the relation of horizontal seismic force-horizontal displacement from the ground yielding limit and only the upper end of pier reached the yielding and ultimate. Also, however this case reduced the horizontal seismic force at the ultimate about 0.1, the reduction ratio of the higher pier height was larger than that of lower pier height.

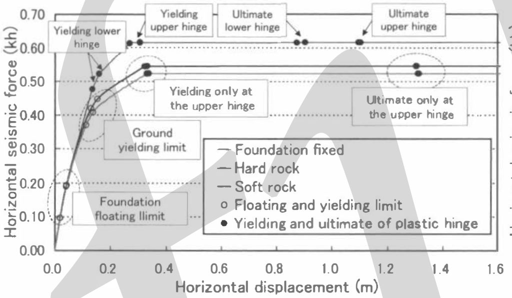

(a) Pier height H=30m

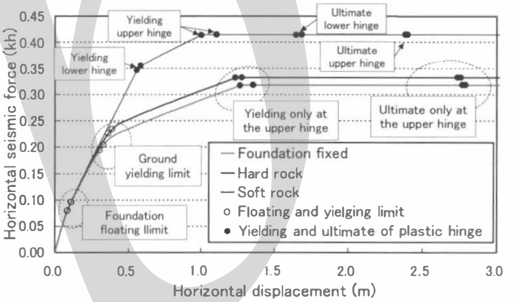

(b) Pier height H=60m

Fig.3 Relation between horizontal seismic force and horizontal displacement

4 NONLINEAR DYNAMIC ANALYSIS

In the static analysis that considered nonlinearity of spread foundation, the upper end of pier only yielded not the lower end of pier after the foundation yielded. On the other hand, in the dynamic analysis that took account of nonlinearity, the foundation and the lower end of pier yielded together at the pier height of 30m and the upper end of pier did not yield. In the case of pier height of 60m, the plastic hinge at the upper and lower ends of pier did not yield and only the foundation spring reached at the yielding. Regardless of pier height, the response ductility factor of the lower end of pier was increased in the order of soft rock, hard rock, fixed-type.

5 CONCLUSION

The following shows the results of the static analysis.

When the nonlinearity of spread foundation is considered, the ground yielding does not cause the yielding of the plastic hinge at the lower end of pier, however the plastic hinge at the upper end only yields and reaches the ultimate state.

The following shows the results of the dynamic analysis.

Taking the nonlinearity of spread foundation for the static analysis, the plastic hinge at the lower end of pier did not yield, but both of the spread foundation and the lower end of pier yielded for the dynamic analysis.

SEISMIC DESIGN OF PRESTRESSED CONCRETE FRAMES

Jin Xu Zuhua Wang
South China University of Technology, **P.R.China**

Keywords: prestressed concrete, frame structure, seismic design, ductility, earthquake response

1 INTRODUCTION

Prestressed concrete frames, used to resist vertical load widely, which are made of high-strength tendons or strands, middle-strength steel and high-strength concrete, are used to resist seismic action growing with each passing day. The anti-seismic ability about this structure system and how to assure it are very noticed in engineering design. To study them, we may recur to: 1) test and theoretical research
; 2) the anti-seismic experiences of prestressed concrete structure in pervious earthquakes; 3) the articles and suggestions about seismic design enacted by some states and international institutes; 4) the anti-seismic experiences and codes about RC structure.

In the anti-seismic aspect, the major advantages of prestressed concrete frames, compared with RC frames, are greater span; smaller size of frame members; lighter dead weight; smaller linear stiffness of cross beam, more flexible structure, longer vibration period, so smaller imposed seismic force. In the other hand, the disadvantages of them are larger displacement reaction, weaker ductility, lower ability consuming energy in cyclic loading. However, It should be indicated that the above disadvantages are only for a prestressed concrete frame. For a prestressed concrete flat-slab-column structure, it is substantiated by study and experimental that it can bear favorable seismic capability.

In this paper, seismic capabilities of prestressed concrete frames are studied, by reasonable prestressing degree, controlling displacement response, ensuring "a column is stronger than a beam" and controlling crack width, and several suggestions about seismic design are offered in the end.

2 SEISMIC DESIGN METHODS OF PRESTRESSED CONCRETE FRAMES

2.1 Control displacement response

Concerning larger displacement, it can be controlled as reinforced concrete structures by reasonable structural arrangement, suitable size of column and calculation.

2.2 Ensure "a column is stronger than a beam"

The concept of " a column is stronger than a beam" is to ensure that plastic hinges near joints occur in the end of beams and not of columns. It can be guaranteed through increasing bearing capacity of columns and ensuring rotary capability of plastic hinges as reinforced concrete frames.

For prestressed concrete frames, the amplification multiple of bearing capability of column end is the same values as is stipulated in present RC codes.

2.3 Control prestressing degree

Moreover, to guarantee good ductility, ability consuming energy and controlling crack in such frames, a steel index and a ratio of partial prestress, which can control prestressing degree λ ($\lambda = \sigma_{pc}/\sigma_{pcs}$, a ratio between prestress and stress under short-term loads in prestress steel bars), and a coefficient limiting tensile stress are put to rational design. The details are as follows.

1. A steel index ϖ

A steel index ϖ is defined by the following expression:

$$\varpi = \frac{A_P f_{py} + A_s f_y - A_s' f_y'}{b h_0 f_c} = \omega_p + \omega_s - \omega_s' \qquad (1)$$

According to a lot of prestressed concrete beam test [1]. ϖ affects greatly prestressing degree and sectional curvature ductility μ_ϕ. μ_ϕ is decreased extremely while ϖ is increased. In seismic design, ACI318-89, NZS3101-82 and CEB-FIP MC78 can be referred. However, ϖ can't express independent influence of prestressing steer bars.

2. A ratio of partial prestress PPR

A ratio of partial prestress PPR, defined by following expression, is another expression to express presstressing degree:

$$PPR = \frac{A_p f_{py}}{A_p f_{py} + A_s f_y} \qquad (2)$$

According to testing for bending menbers [1], μ_ϕ is decreased while PPR is increased. And it is shown more and sensibly when ϖ is lower. Furthermore, by a series of reasoning, formula (3) can be gotten. It indicates that ϖ and PPR have coincidence influence to prestressed degree under the same non-prestressing bars. In order to ensure ductility and ability consuming energy, the study suggests that PPR should be controlled from 0.5 to 0.7 in seismic design.

$$\varpi = \frac{\omega_p}{PPR} = \frac{\omega_s}{1 - PPR} \qquad (3)$$

2.4 Anti-crack and a coefficient limiting tensile stress α_{ct}

A coefficient limiting tensile stress α_{ct} is a multiplication factor for tensile strength of concrete and used for controlling crack width in China code (GBJ 10-89). In order to ensure ductility and ability consuming energy, λ should not be very high, but this goes against anti-crack. Author had been educed a relation between λ and α_{ct} as follows [2]:

$$\alpha_{ct} = (1-\lambda)\left(\frac{\sigma_{sc}}{\gamma f_{tk}}\right) \qquad (4)$$

By the formula (4), λ and α_{ct} can be changed each other. We can get a λ satisfied with anti-crack. By study, the controlling quantity of λ and α_{ct} are offered in according of the controlling crack width W_{max}[3]. For example, the quantity of W_{max} is less than 0.1mm when λ =0.7, or α_{ct} =1.5 ($\sigma_{sc} \le 5\gamma f_{tk}$).

3 RECOMMENDATION CONTROLLING VALUES USED IN A SEISMIC DESIGN

By the above study, ϖ, PPR and α_{ct} should be controlled to improve anti-seismic ability and controlling crack width of prestressed concrete frames. Some recommendation values are as follows:

1. According to earthquake intensity and high of the building, the building can be divided into two types (Important and Normal) in a seismic design. The controlling values are as follows:

Building Type	Important	Normal
ϖ	⩽0.25	⩽0.35
PPR	⩽0.50	⩽0.70

2. According to the use equirement of building, the requirement to control the crack width W_{max} can be confirmed. For prestressed concrete frames working in normal condition, a coefficient limiting tensile stress α_{ct} should accord with the below requirements.

When the design is for short-term combined load:

$\sigma_{sc} - \sigma_{pc} \le \alpha_{ct}\gamma f_{tk}$ $\quad 1<\alpha_{ct}<1.5$ $\quad$ (W_{max}⩽0.1mm)

$\sigma_{sc} - \sigma_{pc} \le \alpha_{ct}\gamma f_{tk}$ $\quad 1<\alpha_{ct}<3$ $\quad$ (W_{max}⩽0.2mm)

When the design is for long-term combined load:

$$\sigma_{lc} - \sigma_{pc} \le 0.8\gamma f_{tk}$$

For the requirement of λ:

When W_{max}⩽0.1mm: $1 \le \alpha_{ct} \le 1.5; \lambda \ge 0.9 - \gamma f_{tk} / \sigma_{sc}$

When W_{max}⩽0.2mm: $1 \le \alpha_{ct} \le 3; \lambda \ge 0.7 - \gamma f_{tk} / \sigma_{sc}$

REFERENCES

[1] Zhitao Lu and Jiuru Tang: Study of seismic reinforcing steel about high-efficiency prestressed concrete frames. In “Engineering practice of high-efficiency prestressed concrete structure”, Building Industrial Publishing Company of China, 1993.10

[2] Zuhua Wang, and Shitong Wang: Unbonded prestressed concrete structures. Space Structure Institute of Guangdong (China), 1997.3

[3] Huiling Chen. Application handbook about high-efficiency prestressed concrete structures , Building Industrial Publishing Company of China, 1998.6

VERIFICATION OF THE FAILURE OF REINFORCED CONCRETE PIERS UNDER THE NEAR-FIELD EARTHQUAKE

Yukio Adachi
Hanshin Expressway Public Corp.

Hiroshi Ishizaki
Hanshin Expressway Public Corp.

Shinya Ikehata
Japan Highway Public Corp.

Shoji Ikeda
Yokohama National University

Keywords: reinforced concrete pier, shear, cut-off, near field earthquake, pseudo dynamic test

1 INTORDUCTION

Lots of infrastructure including expressway bridges were severely damaged due to 1995 Hyogoken Nanbu earthquake and some of them were resulted to collapse. There was a case that a bridge pier was completely collapsed but its adjacent pier was almost no damage or had relatively minor damage even though the two piers were almost the same size, carrying slightly different dead load, and provided with the same reinforcement arrangement except the amount of longitudinal reinforcement at the bottom of the piers. The pier with more reinforcement was completely collapsed due to the earthquake by shear failure at the longitudinal reinforcement cut-off; the other was slightly damaged at the bottom by flexure even though the longitudinal reinforcement cut-off was also existed at the mid height of the pier. The two piers were designed in accordance with the same highway design specification so that it is considered to be very important to clarify the reason why the damage of the two piers was so different. In order to clarify the difference of the seismic damage described above, cyclic loading tests and pseudo dynamic tests were carried out to clarify the damage and collapse mechanism and its process of the two piers.

2 EXPERIMENT

The experiment cases were shown in **Table 1**. The specimens, Type A and Type B, used in the tests were exact 1/7-scale models of the two piers described above. The size and the rebar arrangements of the two specimens are shown in **Figure 1**.The specimens were cantilever circular solid pier with spread footing. The diameter was 400mm. The height from the bottom of the pier to the loading point was 1680mm. Type A specimen had a one cut off at the mid height of the pier in the longitudinal reinforcement arrangement whereas type B specimen had two cut-offs. The important difference between type A and type B specimen was the amount of the longitudinal rebar at the bottom of the pier.

In order to clarify the fundamental ductility characteristics of the tested specimens, Type A and Type B, static cyclic loading tests, one cycle of each loading step, under constant axial load were performed. The loading displacement of each step was 8.4mm that was calculated from 1/200 rotation angle. In order to clarify the difference of the damage of the two specimens subjected to seismic loading, pseudo dynamic tests were performed. Three ground motions, T. sta. ground motion, A. ground motion, and T. ground motion, which had the same peak acceleration, 600 gals, were employed for the tests. T. sta. ground motion and A. ground motion are observed ground motions measued at JR Takatori station and the Amagasaki viaduct at the 1995 Hyogoken Nanbu earthquake respectively, which contain relatively strong low frequency component. T. ground motion is a generated ground motion which contains relatively strong high frequency component.

3 RESULTS

According to the results of the cyclic loading test, less ductile force-displacement relationship was observed for Type B specimen that had more longitudinal reinforcement. The photos of the damage of the specimens are also shown in **Figure 1**. The type A and type B specimen satisfy the seismic demand at the time of the construction but the strength of each specimen the type B specimen is greater than that of the type A specimen. However, this greater flexural strength demands the more shear strength and this resulted in concentration of deformation and the damage and reduction of ductility capacity at the longitudinal bar cut-off where the smallest shear capacity in the specimen. Contrarily, less flexural strength resulted in less demand for the shear capacity and less damage at the longitudinal bar cut-off in the case of the type A specimen. The shear strength demand is larger for the pier with more reinforcement so that the more reinforcement resulted in less ductility I this case.

According to the results of the pseudo dynamic test, the degree of the seismic damage of each specimen was recognized to depend greatly on the ground motion characteristics even though the employed ground motions had the same peak acceleration. The severe damage was observed when the test employed T. sta. wave that had strong low frequency component.

4 CONCLUSION

The difference of the damage of the two adjacent piers that are almost the same size, carrying slightly different dead load, and provided with the same reinforcement arrangement except the amount of longitudinal reinforcement at the bottom of the piers is clarified by performing static cyclic loading tests and pseudo dynamic tests.

According to the experiments, the reason of the difference of the damage of the two piers was clarified by the difference of the flexural capacity and difference of the shear capacity demand. The pier that had slightly stronger flexural capacity and had more shear capacity demand resulted in suffering completely shear failure and the pier that had less flexural capacity and had less shear capacity demand resulted in suffering minor shear damage.

Table 1. Experiment cases

Case	A-ST	B-ST	B-PD-T	A-PD-A	B-PD-A	A-PD-T.sta.	B-PD-T.sta.
Loading method	Static cyclic loading		Pseudo dynamic				
Input motion	-	-	T. wave	A. wave	A. wave	T.sta. wave	T.sta. wave

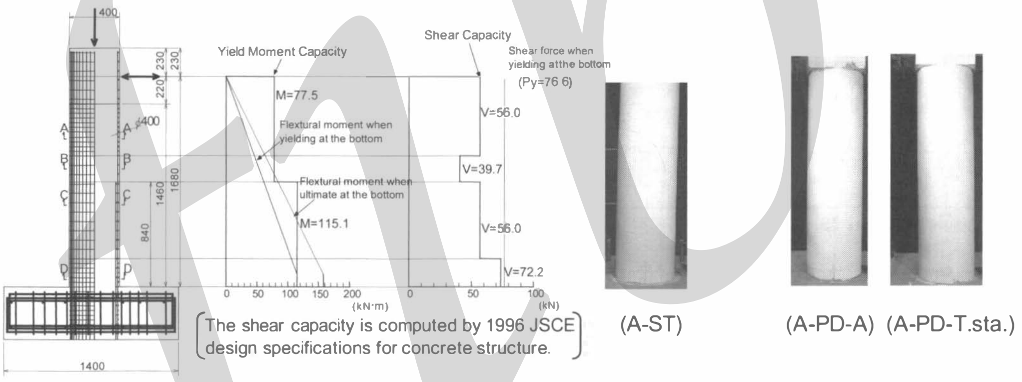

(a) Type A specimen

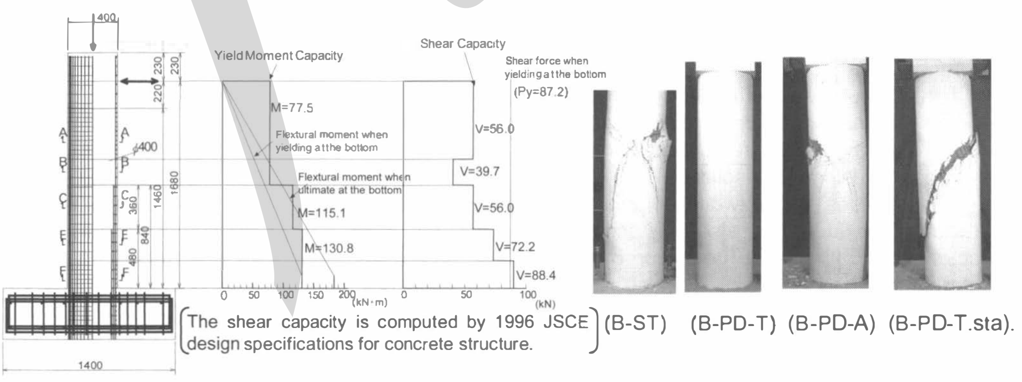

(b) Type B specimen

Figure 1. Rebar arrangement and the damage after the experiments

EUROPEAN DEVELOPMENTS IN CODIFIED SEISMIC DESIGN OF CONCRETE STRUCTURES

Michael Fardis

University of Patras, Department of Civil Engineering, Patras, GR

1 DEVELOPMENT OF THE EN EUROCODES AND THE OUTLOOK FOR EC8

The most important development in codified seismic design in Europe in the past 20 years was that of a single design code for the European area, namely Eurocode 8 (EC8), within the framework of the series of Eurocodes covering structural design of practically all types of civil engineering works with any structural material. The parts of EC8 are listed in Table 1. In June 2002 Parts 1 and 5 are close to finalisation and approval. All others are far from their final form. The key points of EC8-Part 1 relevant to concrete structures – mainly buildings – are overviewed, per the "final" draft of May 2002.

The EN Eurocodes provide for national choice in all parameters controling safety, durability, serviceability and economy, through "Nationally Determined Parameters" (NDPs) which may include: a) symbols (e.g. safety factors, the mean return period of the design seismic action, etc.); b) technical classes (e.g. ductility classes); and c) methods (e.g. alternative models of calculation). For symbols, the EN Eurocode may give an acceptable range of values and will recommend in a note a value. It will also recommend a class or a procedure/method among the alternatives identified as NDPs.

National choice will be exercised through the National Annex, which may also contain country-specific data (e.g. a seismic zonation map, spectral shapes for the various types of soil profiles provided in EC8, etc.), which will constitute also NDPs. A National Annex may provide supplementary information, non-contradictory to any of the rules of the EN Eurocode. Examples for Eurocode 8 may be: a) Acceptable values of member plastic hinge or chord rotations for design on the basis of nonlinear analysis with direct verification of deformations; or b) models for masonry infill panels. A National Annex for Eurocode 8 may not be required in non-seismic EU countries.

Table 1: Eurocode 8 parts and key target dates (as of June 2002)

EC8 Part	Title	Final draft	Approval for formal vote	National publication	Withdrawal of nat. standards
1:	General rules, seismic action, buildings	Dec.01	July 02	Sept. 05	Nov. 08
2:	Bridges	Jan. 03	July 03	July 06	Sept. 09
3:	Strengthening and repair of buildings	Sept. 02	Feb. 03	March 06	Nov. 08
4:	Silos, tanks, pipelines	June 03	Dec. 03	Jan. 07	Dec. 09
5:	Foundations, retaining structures, geotechnical aspects	Nov.01	July 02	Sept. 05	Nov. 08
6:	Towers, masts, chimneys	Sept. 02	Feb. 03	March 06	Nov. 09

2 THE PROVISIONS OF EC 8 - PART 1 APPLICABLE TO CONCRETE BUILDINGS

Although its main object is buildings, Part 1 of EC8 includes also the general provisions for the other parts to build on: performance requirements, seismic action, analysis procedures, and general concepts and rules applicable to structures beyond buildings. For buildings, it covers the main structural materials – concrete, steel, composite (steel-concrete), timber and masonry. It also covers seismic design using base isolation.

EC8 provides for a two-level seismic design, with the following performance objective: a) protection of life under a rare seismic action ("design seismic action"), by prevention of collapse of the structure or parts thereof; b) reduction of property loss due to a frequent event, through limitation of structural and non-structural damage. The no-local-collapse performance level is achieved by dimensioning and detailing structural elements for a combination of strength and ductility that provides a safety factor between 1.5 and 2 against loss of gravity load capacity and lateral load resistance. The damage limitation performance level is achieved mainly by limiting storey drifts to levels acceptable for the integrity of all its parts. Another objective is to prevent global collapse in an extremely strong earthquake, like the "Maximum Considered Earthquake" (MCE) of US codes, through across-the-board application of the capacity design concept, to control the inelastic response mechanism.

Hazard levels are left for national determination. For structures of ordinary importance the recommendation of EC8 is for: a) a 10% exceedance probability in 50 years for collapse prevention and b) a 10% in 10 years seismic action for damage limitation. The elastic response spectrum of the "design" seismic action is anchored to the ground acceleration on rock, to be mapped in national zoning maps. The spectrum includes regions of constant spectral acceleration, pseudovelocity or displacement. Definition of the exact spectral shape for the standard soil types in EC8 is left to National Annexes, depending on the earthquake magnitude contributing most to hazard. EC8 recommends two standard spectral shapes per soil type: for earthquakes with M_s above or below 5.5.

EC8 allows neglecting the seismic action in design, if it is considered so low that earthquake resistance is provided by design for other actions. The recommended (as NDP) threshold is a value of the design ground acceleration for the specific site and structure of 0.05g. EC8 also allows providing earthquake resistance by just dimensioning members according to the other Eurocodes, for internal forces from analysis for the seismic action with a force reduction or behaviour factor (q) of 1.5 – available due to overstrength – without any measures for local or global ductility ("low-dissipative", or of Ductility Class (DC) low (L)). For non-base-isolated structures this simplification is recommended only if the design ground acceleration for the specific soil type and structure is less than 0.1g.

The majority of structures designed with EC8 will be designed for "energy dissipation". Two ductility classes (DCs) are provided for "dissipative" structures: Medium (M) and High (H) ductility. Availability of the global energy dissipation and ductility capacity needed for values of q higher than 1.5 is ensured through: a) measures to control the inelastic response mechanism, so that concentration of inelastic deformations in a part of the structure (soft storey mechanism) and brittle failure modes are avoided; b) detailing of plastic hinge regions for inelastic deformations. Soft storey mechanisms are avoided by promoting concrete wall (or dual) systems with walls (capacity-)designed to ensure that they remain elastic above the base. If frames resist more than 50% of the base shear, columns are (capacity-)designed to be stronger than beams, with an overstrength factor of 1.3 on beam design flexural capacities. Beams and columns are capacity-designed against pre-emptive shear failure. Once the global inelastic response mechanism is controlled, the behaviour factor q can be ultimately related to the local deformation demands on structural elements; e.g. through the local curvature ductility factor and global displacement ductility factor, μ, and a q-μ-T relation. Detailing rules for elements aim at providing the required local deformation capacity.

The analysis options provided for design of buildings are: a) linear static ("lateral force" method); b) linear modal response spectrum analysis; c) nonlinear static analysis ("pushover"); and d) nonlinear dynamic (time-history). Options c) and d) go with direct check of deformations. The standard is the linear modal response spectrum method, applying to all building types. The lateral force method may be applied if the effects of higher modes are not significant. In buildings which are regular in plan, two independent 2D models may be used for the two horizontal components of the seismic action.

The elastic stiffness in linear or nonlinear analysis should be the secant stiffness to yielding; it may be taken as half of the uncracked stiffness of the gross concrete section.

Displacements from linear analysis are calculated in general on the basis of the equal displacement rule, i.e. by multiplying elastic analysis results by the q-factor.

Non-engineered masonry infills producing irregularities in plan or elevation should be taken into account in the analysis of buildings of DC H, unless walls provide at least 50% of the lateral force resistance. For irregularities in plan, this may require explicit modeling of infills and sensitivity studies.

For DC M or H buildings the behaviour factor, q, by which the elastic spectrum for use in linear analysis is reduced, explicitly includes system overstrength through the ratio α_R of the seismic action at development of a full plastic mechanism to that at the first plastic hinge in the system. Default values for it in EC8 are: a) 1.1 for one-storey frames and wall systems with more than two uncoupled walls per direction; b) 1.2 for one-bay multistorey frames, or dual systems with walls providing 50% to 65% of lateral force resistance or coupled wall systems; c) 1.3 for multistorey multi-bay frames. Higher values may be used up to a maximum 1.5, if confirmed through pushover analysis of the structure.

The q-factors for frames, dual systems with walls providing up to 65% of lateral force resistance) and coupled-wall systems (with at least 65% of the lateral force resistance provided by walls with coupling reducing individual base moments by at least 25%) are: $q=3\alpha_R$ for DC M and $4.5\alpha_R$ for DC H. Systems with uncoupled walls resisting at least 65% of the seismic base shear have q=3 for DCM and $q=4\alpha_R$ for DC H. Torsionally sensitive buildings are penalized with q=2 for DC M, or 3 for DC H. In buildings with vertical irregularities, the q-factor value is reduced by 20%.

The paper summarizes in tabular form the detailing and dimensioning rules for beams, columns and walls of the three ductility classes (DC L, M and H).

SEISMIC DESIGN OF LARGE COMPLEX-SHAPE FLAT SLAB FOR VERTICAL MOTION

Kazuhiko Yamada
Kobori Research Complex

Masahiro Ikezaki
Kansai Branch

Arinori Nimura
IT Solution Department

Kajima Corporation, Japan

Keywords: seismic design, vertical motion, flat slab, nonlinear FEM analysis, dynamic response

1 INTRODUCTION

A practically applied seismic design procedure for a vertical motion is introduced for a structure comprising an octagonal tube frame and internal large complex-shape flat slabs, as shown in Fig.1. The structure will be under construction near Shiten-noji temple, Osaka when the conference is held.

2 METHODS

A substructure method is applied to obtain slab responses to a vertical seismic excitation, as shown in Fig. 2. The structure is modeled as one stick with plural branches (OSPB), as shown in Fig. 3. That is, stick springs express axial stiffness of the tube frame columns while the branches express vertical motions of the flat slabs at each floor. Because the flat slabs at each floor do not have simple shapes, their vertical motions, i.e., the branch dynamics are approximated as those of SDOF systems, whose springs and masses are estimated by nonlinear pushover analyses for a FEM model (Fig.4). The mass of each branch is determined, equating the first natural frequency of the FEM model to that of the SDOF system. The spring characteristics are adjusted, letting the first natural period of the OSPB model be equal to that of the FEM model. Because the peak branch deflection of the OSPB model for dynamic analyses multiplied by the first-mode participation factor corresponds to the largest deflection of the flat slab by the nonlinear FEM analysis, the stress states of the flat slab can be traced for the vertical seismic excitation.

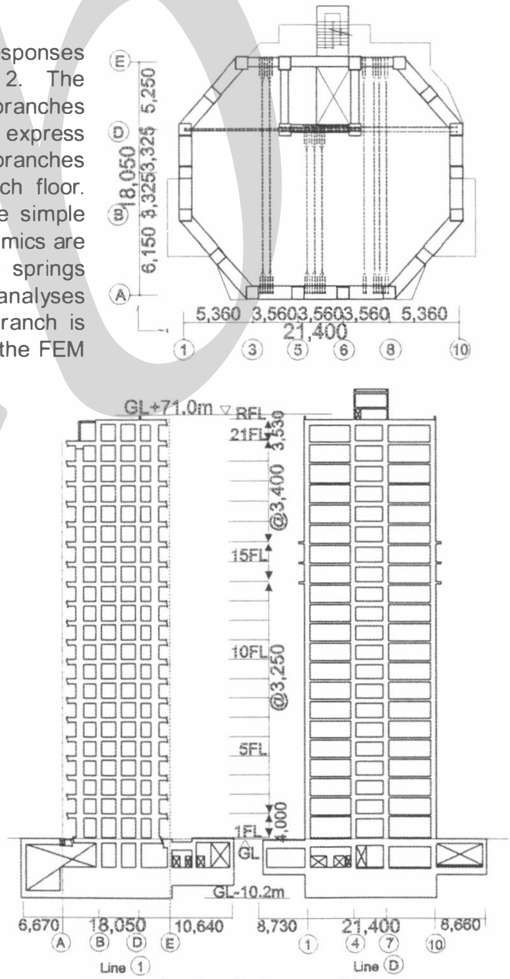

Fig.1 Structural plans and frames

3 RESULTS

The first natural period of a slab is 0.113s (Fig.5). The pushover analyses show that almost linear states are kept in 1.0cm deflection (Fig.6). A vertical excitation shown in Fig. 7 is assumed for calculating seismic responses. Fig. 8 shows vibration modes, periods T_i and participation factors β_i of the OSPB model. Stick and branch nodes move with the same phase on the first mode while branch nodes mainly move on the second mode. Fig. 9 shows that peak vertical acceleration of nodes and branch deflections of the OSBP model for the assumed seismic excitation. The peak branch deflection δ^b_{max} is 0.172cm, which occurs at the top floor. The obtained peak branch deflection δ^b_{max} can be converted to the maximum deflection of the slab δ^s_{max}, multiplied by the first mode participation factor of the FEM model β_1. That is, $\delta^s_{max} = \beta_1\delta^b_{max} = 1.720 \times 0.172 = 0.296$cm. Then, we can estimate stress and crack states when the maximum deflection δ^s_{max} occurs, using the results of the nonlinear pushover FEM analyses. As shown in Fig. 10, no crack occurs for the pre-stressed case while the non-pre-stress case must allow cracks at slab center and edges for vertical motions.

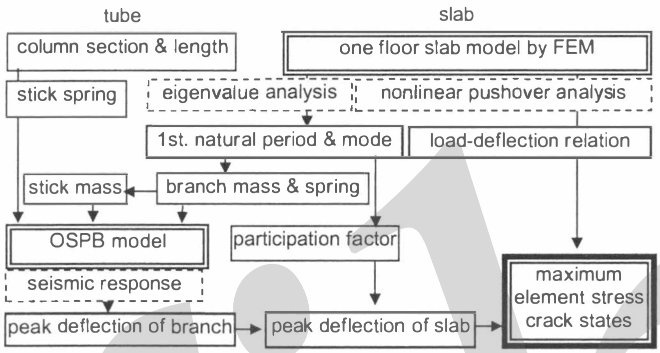

Fig. 2 Verification flow

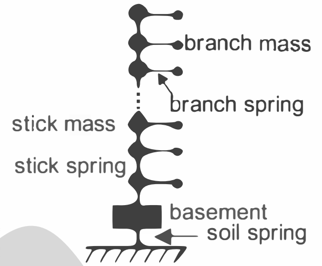

Fig. 3 OSPB model

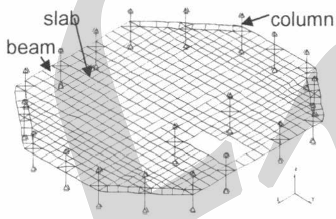

Fig. 4 FEM model

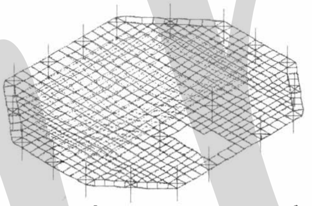

period:T_1^s=0.113s; part. fact.: β_1^s=1.72

Fig. 5 First mode of slab

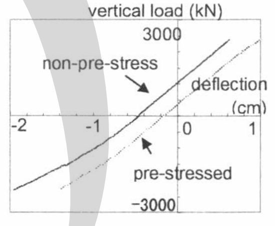

Fig.6 Total vertical loads vs. maximum deflection

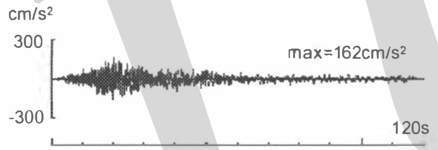

Fig. 7 Vertical seismic excitation acceleration

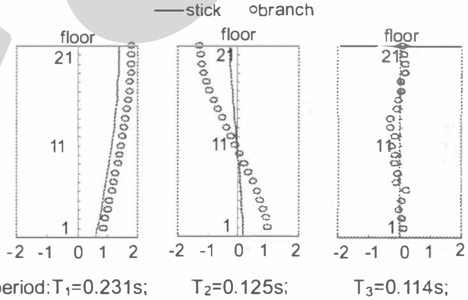

period:T_1=0.231s; part. fact.: β_1=1.83 T_2=0.125s; β_2=1.26 T_3=0.114s; β_3=0.29

Fig. 8 Vibration mode of OSBP model

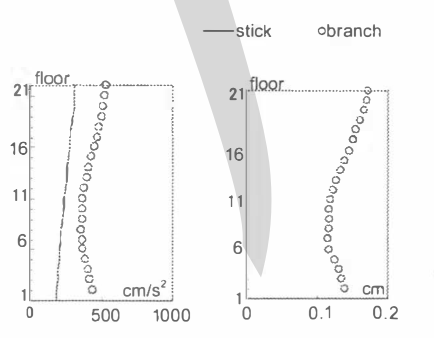

(a) vertical acceleration (b) branch deflection

Fig. 9 Maximum responses on OSPB

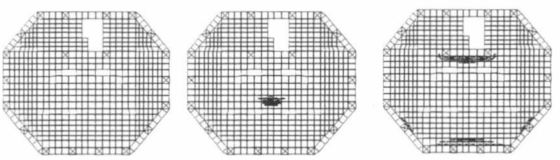

(i) top & bottom (ii) bottom (iii) top
(a) pre-stressed (b) non pre-stress

Fig. 10 Induced crack by vertical motions

THE COMPARATIVE RESEARCH ON ANTI-SEISMIC DESIGN BETWEEN EBF AND FRAMED SHEAR-WALL STRUCTURE AND EBF DESIGN RECOMMENDATIONS

Ziyi Chen
Beijing Municipal Institute of City Planning and Design, P.R. China

Wentao Liu
Beijing Science University

Keywords: Eccentrically braced frame(EBF), Frame shear-wall structure, Design recommendation

1 INTRODUCTION

Framed shear-wall structure is widely used in high-rise building [1], but the frame structure is different from the shear-wall structure in subjecting force and deformation. The deformation of shear-wall structure is of bending type, while the framed structure is of shearing type. When the two structures are combined force and deformation are not compatible since the horizontal shear-force in shear wall is large on the bottom of wall and small on the top of the wall, whereas the distribution in the frame is on the contrary. In the design of actual projects some structures have large earthquake force because of the large stiffness of the shear-wall. Raising yield strength of the structure can only postpone the stage of structure plastic state; but by raising the deformation capability of the structure, the capability of subjecting earthquake force will be improved greatly and thus enables the structure to survive earthquakes. It is found from the experiment [2] that EBF structure made of eccentricity braced instead of shear-wall in tall building can raise the capability of deformation, and is better in energy consumption, lateral stiffness, durability and the capacity of subjecting force. This paper compares and analyzes the features of deformation and subjecting force of EBF and framed shear wall structure by actual project design, the plan drawing of structure is shown in Fig.1 and Fig.2. Based on the tests and analysis, recommendations for design of the EBF structure are presented.

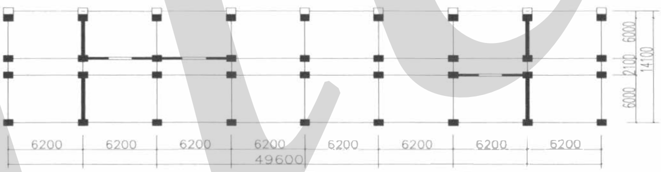

Fig. 1 The plane drawing of frame-shearwall structure (mm)

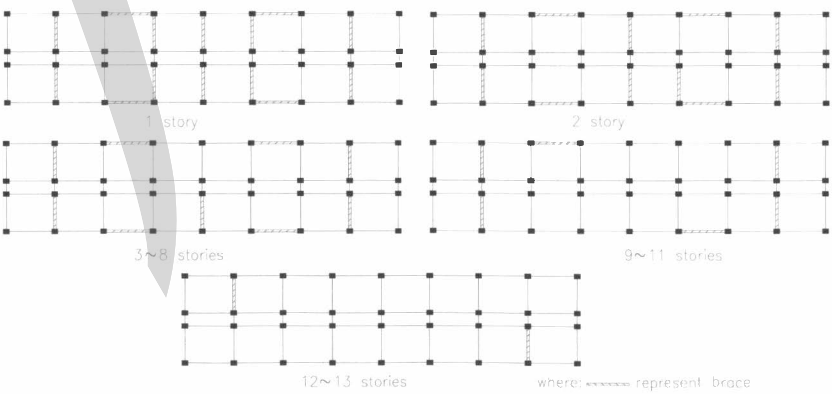

Fig. 2 Arrangement of brace in plane

2 CONCLUSIONS

By comparing the two scheme, we find that the EBF is better in high rise building and it has good property under the seismic action.

We have come to the following conclusions:

(1) The EBF has larger flexibility in arrangement plane in comparison with framed shear wall structure. It can reduce the contradiction between architecture and structure, and can provide the space for pipeline equipment.

(2) The weight of EBF is smaller than that of framed shear wall. Which reduces earthquake force by 15-30%.

(3) The stiffness can be easily regulated in EBF, difference between transverse and longitudinal can be reduced and the lateral displacement can be controlled to a satisfied limited value.

(4) EBF can raise the capability of earthquake resistance by raising the ability of deformation, while the framed shear-wall by raising structure yield strength. So the former is better.

(5) EBF reduce the amount of material(R.C. and steel) and has fine economic effects.

3 DESIGN RECOMMENDATIONS

(1) Braces should be arranged symmetrically in structure. Structure stiffness of two direction have great deference if the braces are unsymmetrical, the deference of stiffness can cause the structure incline under the cyclic loading action.

(2) Stiffness of EBF frame is smaller than shear-wall, and the ratio with frame is relatively stable. The braces can be arranged according to design, and the sudden change of stiffness can be avoided.

(3) Stiffness of EBF frame is adjustable. By changing the section and style of the brace, the stiffness of EBF structure can be easily adjusted in design to optimize the structural scheme.

(4) The strength and stiffness of brace influence the behavior of EBF structure greatly, especially the joint which connecting brace, beam and column. So the joint should be strengthened.

(5) Because the brace is connected to beam, some beams are divided into short beams. To subject to the large shear force (which is caused by push load of brace), these short beams should be designed as ductile short beam by these details:

a. Suitably reduce the shear-compression ratio[3].

b. Put internal crossed reinforcement in the short beam.

c. Reduce the distance of the stirrups in beam.

In summary , EBF has advantages in high rise building, the property is good in elastic stage under the seismic action, and the property in plastic stage would be studied further.

REFERENCES

[1] Zhao Xi-an, "Reinforce concrete structure design on tall building", Printed press by P. R. China building industry, September, 1995.

[2] Shi Jian-guang, and Chen Zi-yi, "Seismic behavior of the new type R.C. frame: EBF", The Fifth International conference on Tall Buildings, Vol.1 , December, 1998 Hong Kong, PP416-428.

[3] Zhu Zhida, and Zheng Yulun, "Design Method on Resistance to Seism of the Ductile Short Reinforced Concrete Beams", Building Structures, No.8(Total 164), August 1997, PP19-26.

SIMPLIFIED ULTIMATE ASEISMIC DESIGN OF REINFORCED CONCRETE BUILDINGS

Minoru Yamada
Prof.em.Kobe Univ.,
Iwakura, Chuzaiji-cho, 156
(606-0021) Sakyo-ku,Kyoto
JAPAN

Keywords : aseismic design, shear span ratio, short column, shear wall, wall ratio

1 INTRODUCTION

In order to popularize the anti-seismic designed medium or low rise reinforced concrete buildings, a simple structural design system [1] is proposed here, based upon the synthetical research on the ultimate behaviors of composing structural elements, long column (LC), short column (SC) and shear wall (SW).

2 ULTIMATE RESISTANCE AND DEFORMATION PROCESS OF ANTI-SEISMIC ELEMENTS IN REINFORCED CONCRETE BUILDING

2.1 Long column element (LC) : bending yield, (cf. Fig.1, Fig.3)

$$V_y^B = \frac{2}{H}M_y = \frac{2}{H} f_c' bD^2 \left(\frac{N}{f_c' bD} + 2\omega\right) e_1 \qquad (1),$$

$$\delta_y^B = \frac{H^2}{6}\Phi_y = \frac{H^2}{6}\frac{\varepsilon_y}{2e_1}\frac{1}{D}\left\{\left(\frac{N}{f_c' bD}+\omega\right)\frac{1}{\alpha+\omega}+1\right\} \qquad (2),$$

where

$\omega = \rho \frac{f_y}{f_c'}$: reinforcement index (3),

$\rho = \frac{a_s}{bD}$: ratio of reinforcement (4).

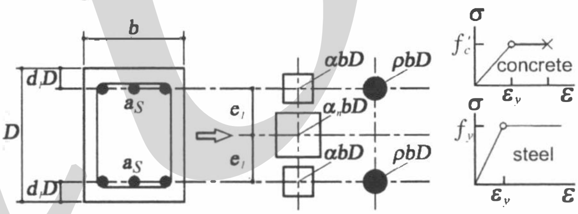

Fig.1 Modeled RC cross section [2]

2.2 Short column element (SC) : shear explosion

$$V_u^S = \frac{7}{8}(1-d_1) f_c' bD\sqrt{-0.10X^2+0.09X+0.01} \qquad (5),$$

$$\delta_u^S = \frac{\tau_u}{G_c}H = \frac{2(1+\mu)}{E_c} H f_c' \sqrt{-0.10X^2+0.09X+0.01} \qquad (6),$$

where

$X = \frac{N}{N_0}$: axial load level ratio (7),

$N_0 = (1+2\omega) f_c' bD$: ultimate axial resistance (8).

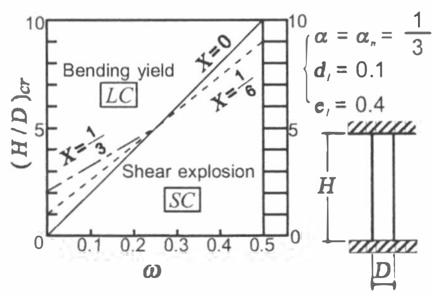

Fig.2 Critical shear span ratio $\left(\frac{H}{D}\right)_{cr}$

2.3 Critical shear span ratio $\left(\frac{H}{D}\right)_{cr}$

between long column (LC), and short column (SC) (cf. Fig.2)

$$\left(\frac{H}{D}\right)_{cr} = \frac{2\left(\frac{N}{f_c{}'bD}+2\omega\right)e_1}{\frac{7}{8}(1-d_1)\sqrt{-0.10X^2+0.09X+0.01}} \quad (9).$$

2.4 Shear wall element (*SW*) : diagonal compression

$$_wV_u = \frac{2}{3}f_c{}'Lt\sin\theta\cos\theta \quad (10),$$

$$_w\delta_u = \frac{0.002}{\sin\theta\cos\theta}H \quad (11)$$

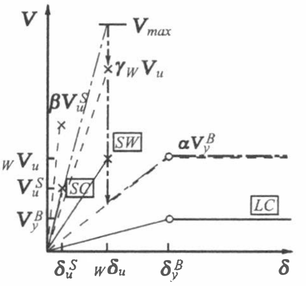

Fig.3 Holizontal load-sway displacements.

3 OVERALL RESISTING PROCESS OF REINFORED CONCRETE FRAMES

Overall horizontal resisting prcess of reinforced concrete frame with α-pieces of LC, β-pieces of SC, and γ-pieces of SW, may be composed as the summing up of resistances of each elements at the same sway value δ, such as shown in Fig.3.

In the $\frac{\alpha}{\gamma}$-$\frac{\beta}{\gamma}$ plane three francture modes, i.e. LC-, SC-,and SW fracture modes, are clearly classified in Fig.4 and in this coordinate system, wall ratios w, periods T, and feasible number of stories of medium or low rise reinforced concrete buildings agaist earthquake are indicated too.

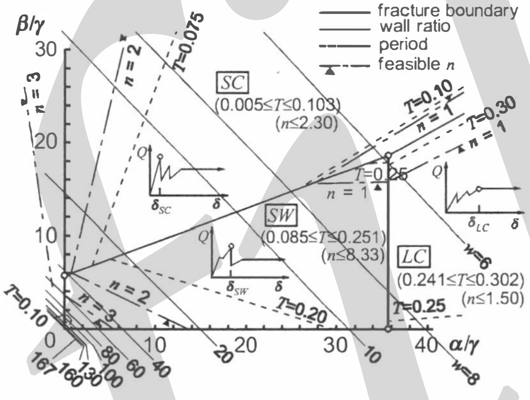

Fig.4 Classification of frature modes

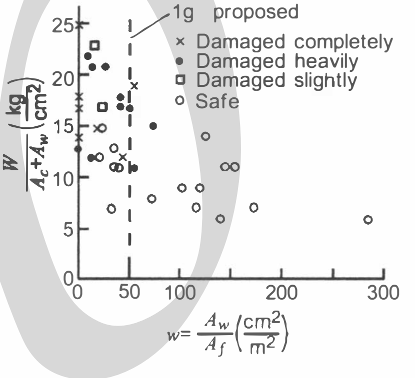

Fig.5 Real damage and wall ratio [3]

4 VERIFICATION OF PROPOSED CALCULATED NUMBER OF STORIES THROUGH REAL DAMAGE UNDER EARTHQUAKE

Statistics of the relationships between wall ratios w and the grade of damage of reinforced concrete school buildings with 3 stories at the Tokachi-Oki-Earthquake 1968, Japan [3] shows clearly the validity of this proposed wall ratio w=50 (cf.Fig5).

5 CONCLUDING REMARKS

A simplified ati-seismic design mothod of medium or low rise reinforced concrete buildings is proposed and verified by the damage statistics at the Tokachi-Oki-Earthquake 1968, Japan. One of the objectives of this research is to Popularize safe medium or low reise reinforced concrete buildings in many earthquake hazadous countries.

REFERENCES

[1] Yamada, M. Ed. : Aseismic Safety of Reinforced Concrete Structures, 1976, Gihodo-Shuppan, Tokyo, Japan (in Japanese).

[2] Yamada, M. : Mass Point Model of RC Members for the Deformation and Fracture Analysis, Proc., *fib* Symp. 1999, Prague, Vol.2, pp.365-370.

[3] Shiga, T., Shibata, A. and Takahashi, T. : Relationships between Earthquake Damage and Wall Ratios of Reinfored Concrete Buildings, Rep., Architectural Institute of Japan-Tohoku Branch, No.12, Dec., 1968, pp.29-32 (in Japanese).

SEISMICITY IN UKRAINE AND EVALUATION OF SEISMIC RESISTANCE OF BUILDING STRUCTURES OF CHORNOBYL NPP SHELTER OBJECT

Nemchynov Yu.I.
D.Sc., professor
Deputy Director

Maryenkov N.G.
D.Sc.
Head of laboratory

Bambura A.N.
D.Sc.
Head of department

The State Research Institute of Building Structures (NIISK)
at the State Committee of Ukraine for Construction,
UKRAINE

Bazhenov V.A.
D.Sc., professor
First pro-rector

Kyiv National University of
Construction and Architecture,
UKRAINE

Keywords: seismic areas, design standards, Chornobyl NPP, seismic resistance of structures, risks of failure

1 SEISMIC ZONES OF UKRAINE

More than 120 thousand square kilometers of the territory of Ukraine (about 20 %) belong to seismically dangerous areas [1]. In these territories, earthquakes with 6 to 9-grade intensity on MSK-64 scale occur, and their population comprises more than 10 million people (21 % of all population of the country). The conditions of construction are complicated by presence of dangerous geological processes, including floods, landslides, hurricanes and tornadoes, karsts and earthquakes.

2 REGULATORY BASIS OF EARTHQUAKE-RESISTANT CONSTRUCTION IN UKRAINE

Effective in Ukraine is the former USSR standard (SNiP II-7-81*) of 1991 issuance with additions to the Russian edition of 1996 introduced since August 15, 1997.

At present, draft standards for earthquake-resistant construction have been developed in Ukraine: the Standards for general-purpose construction and the Standards for design of nuclear plants and nuclear power facilities [2].

For the territory of Crimea, consideration of anti-landslide measures is an important problem in the design. Other regions (Odesa, Mykolaiv and other oblasts) need simultaneous consideration of ground subsidence properties and seismic impacts.

3 CHORNOBYL NPP SHELTER OBJECT. EVALUATION OF SEISMIC RESISTANCE

Chornobyl NPP is located 150 km away from Kyiv City, the capital of Ukraine. After 15 years following the largest accident at the fourth generating unit of Chornobyl NPP (in April 1986) and erection of a protective structure (in November 1986) the Shelter Object (ShO) remains radiation- and nuclear-dangerous. Under the reactor wreckage and in the nearby territory there is about 200 metric tons of irradiated nuclear fuel. According to NIISK data [3], the durability of individual structures does not exceed 5 to 10 years. The international TACIS program of cooperation under the Shelter Implementation Plan (SIP) provides for implementation of a set of measures for strengthening (stabilization) of structures and erection of a new protective shell (Safe Confinement) above the existing Shelter, which will ensure the ShO safety for a longer period (up to 100 years).

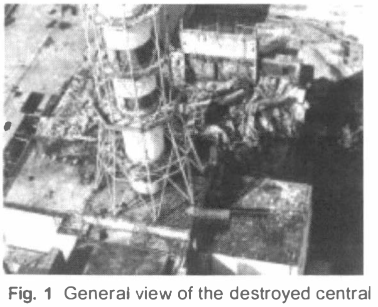

Fig. 1 General view of the destroyed central hall of the 4th generating unit (1986)

The structures of the unit were strongly damaged (Fig. 1). As a result of an explosion, the reactor core region, building structures of the deaerator stack (a gap of the reinforcement in columns, deviation of columns southwards from 0,7 up to 1,5 m) and of the western zone (the ferroconcrete wall at axis 50 deviated westwards up to 115 cm) were destroyed [4].

The seismic danger of the ShO site is determined by earthquakes occurring in the Carpathian and Crimean regions, as well as by local earthquakes. The seismic impact intensity on MSK-64 scale at the site constitutes 5 grades for a design earthquake (DE), 6 grades for a maximum planned earthquake (MPE).

Experimental vibrometric measurements have shown that the ShO oscillation periods under the first form lie in the range from 0,3 to 0,5 seconds. Taking into account the results of examination of the condition of building structures, a 3-D model of the Shelter Object has been developed, and destruction risk calculations have been carried out pursuant to the guidelines [5]. The structure destruction risks in the ShO "dangerous" zones have been found to be (1,3 to 1,6)$\cdot 10^{-1}$ for the southern zone and 810^{-4} for the western zone.

4 TRANSFORMATION OF THE SHELTER OBJECT. NEW SAFE CONFINEMENT. CONCEPTUAL SOLUTIONS

The Ukrainian Government has considered the ShO transformation strategy that was developed with support from the TACIS International Group of Experts with participation of Ukrainian and Russian organizations (1996). The strategy provides for a number of consecutive steps to transform the ShO into an ecologically safe system (ESS).

In compliance with the SIP "*Recommended course of actions*" the Safe Confinement (SC) should be build above the existing Shelter (new protective shell).

The SC should be erected as soon as possible, but not later than in 2007.

Three SC versions have been developed:

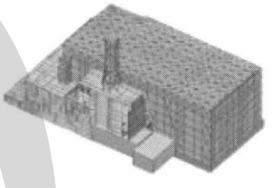

- **"FRAMEWORK"** - confinement from metal structures to be constructed immediately above the existing Shelter. It represents a spatial lattice structure with overall dimensions of 210x99 m and a height of 89,5 m.

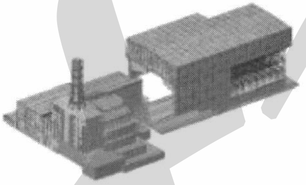

- **"CONSOLE"** - confinement to be constructed near the ShO and then moved into the design position. The CONSOLE consists of two units having different purposes: the industrial unit and the crane unit. The overall dimensions of the confinement constitute 114x246x97 m. The framed structures are load-carrying members.
- **"DOME"** - confinement to be constructed near the ShO and then moved by individual modules. The arched structure consists of four segments with a length of 36 m, a span in axes of 257 m and a height of 100 m. The height of the arch working cross-section is 12 m.

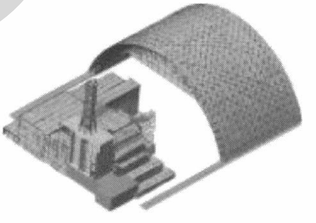

The executed analysis has shown that all three confinement versions have comparable parameters as regards the cost, labor input and collective equivalent radiation doses during construction.

REFERENCES:

[1] Kharitonov O.M., Kostiuk O.P., Kutas V.V., Pronishin R.S., Rudenskaya I.M.: Seismicity of the Ukrainian Territory. – NASU Geodetic Journal, 1996, No. 1, pp. 3-15.
[2] Report of NIISK: "To Conduct a Comparative Analysis of Standards and Rules of Construction in Seismic Areas and to Develop Proposals for Their Application Taking into Account the Specificity of Engineering-geological Conditions of Ukraine"/ Nemchynov Yu.I., Maryenkov N.G. – Kyiv, 1994. – 100 pages.
[3] Findings of Researches of the Condition of ChNPP Shelter Object Building Structures. General Summary on the State of Studies at the beginning of 2001 / NIISK, Kyiv, 2001. – 56 pages.
[4] Kupny V.I.: "Shelter Object: Yesterday, Today, and Tomorrow". – In the collection: Shelter Object – 10 Years. "Main Results of Scientific Researches", Chornobyl, 1996, pp. 57-77.
[5] United States Nuclear Regulatory Commission. Probabilistic Reliability Procedures Guide. Rep. NUREG /GR-2300/2 Vols, NRC, Washington, DC, 1983.

SHAKING TABLE TESTS ON UNDERGROUND RC STRUCTURE DURING SEVERE EARTHQUAKES

TAKEDA Atsushi HIGUCHI Shunichi OHUCHI Hajime
Obayashi Corporation, Japan

Keywords: Dynamic Interaction between Soil and Structure, Underground Structure, Shaking Table Test

1 INTRODUCTION

In this study, the shaking table tests on underground RC structure were carried out to investigate the characteristics of external force acting on the structure, the ground response and dynamic interaction between soil and the structure.

2 TESTS MODEL

As shown in **Fig.1**, the wall shape RC structure models imitating a canal road were installed into the ground model built in a large laminar shear box (H=2000mm, L=4350mm, B=2850mm), and the model was shaken by the shaking table. The RC structures were fixed to the bottom plate of the laminar box with using the truss form load transducer installed between them.

For the ground model, the air dried Gifu Sand is used. The sand is compacted elaborately .

The RC specimens are wall shaped structure with footing. The tension reinforcement ratio is 0.67% and shear reinforcement ratio is 0%.

3. TESTS RESULTS

In this section, the results of the test used sine motion, which has frequency of 5Hz, 20 cycles and maximum acceleration of 700gal will be discussed. In this test, the RC specimens yielded.

3.1 Maximum Values Obtained by Various Instrumentations at the Tests

The maximum values obtained by various instrumentations at the tests are shown in **Tab.1**. Relative displacement, strain of rebar and soil pressure are accumulated values of the static components at the time of ground model preparation, residual components resulted from the previous shaking events, and dynamic components of this test. In **Tab.1**, the relative displacement of RC specimens is different from that of the laminar box very much. Because the residual displacement of RC specimens by the past tests is 12mm, although the residual displacement of laminar box is almost 0mm after the each tests. At the top of the RC specimens and the surface of the ground, the magnitude of acceleration is amplified about twice as large as that of input motion.

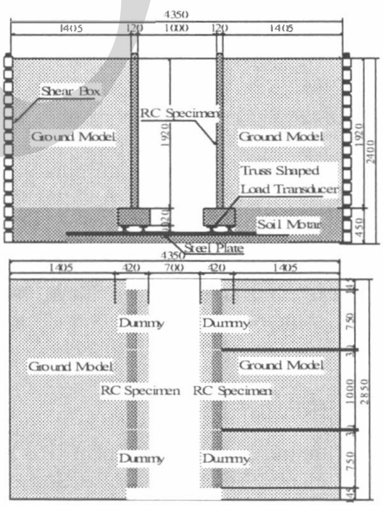

Fig.1 Whole Model

Tab.1 Maximum Value

Acceleration (gal)	Shaking Table	717
	Surface of Ground	1375
	Top of RC Specimen	1547
Relative Displacement (mm)	Top of Shear Box	12.8
	Top of RC Specimen	27.2
Strain of Rebar (μ)	Ground Side	2900
	Trench Side	117
Soil Pressure (N/cm^2)		3.73

3.2 The Behavior of RC Specimens

Moment-curvature (here after, M-ϕ) relation observed at the base of RC specimen is shown in **Fig.2**. The bending moment is measured by truss shaped load transducer. The positive directions of the bending moment and curvature are the direction that the ground pushed RC specimen toward the trench.

According to the shape of M-ϕ relation, it is cleared that the RC specimen is yielded at the first cycle (thick line part in the figure).

As shown in **Fig.3**, the strain of rebar is very large and is accumulating whenever the cyclic loading directs towards the ground side, although that is very small in trench side. Then the deflection of the RC specimen to the trench side increased cycle to cycle. This is due to the mechanism mentioned below. (1)When there is large acceleration occurs in the direction from the RC specimen to the ground, the ground deflected greatly compared to the RC specimens, because the ground had much larger mass than the RC specimens. (2)Then the sand near the RC specimens became loose, and the dense sand at the surface of the ground settled into the part of loose sand. (3)When the deflection of the ground returned to the initial position, RC specimens are pushed by the settled sand to the direction of the trench side. (4)Then the deflection due to the settled sand became the residual deflection. Actually, the remarkable settlement of the ground surface near the RC specimens was observed at the tests.

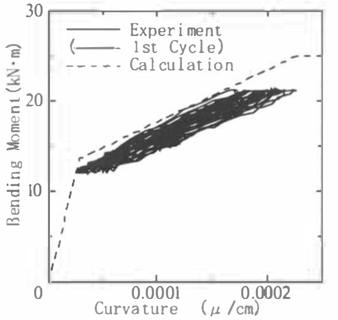

Fig.2 M-ϕ Relation

3.3 Deflection Mode

Fig.4 shows the deformation shapes of RC specimen and the free field ground at the moment which the maximum displacement of top of the RC specimen was observed. In this figure, only the dynamic displacement components are indicated but the residual components accumulated in past test exist.

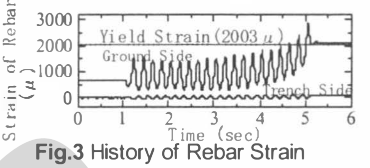

Fig.3 History of Rebar Strain

Fig.4 shows that the ground deform in shear mode although the RC specimens deform in bending mode.

4. NON-LINIER FRAME ANALYSIS CONCERNING THE GROUND DEFORMATION RESPONSE DURING THE EARTHQUAKE

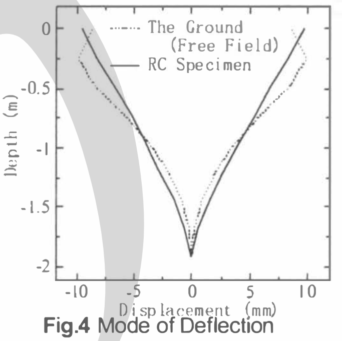

Fig.4 Mode of Deflection

4.1 Calculation Method and Procedure

The calculation model consists of non-linear beam elements as the RC structure and linear springs as the ground (ground springs, here after). The free field ground deformation is applied to the RC structure through ground springs.

The displacements of the ground at t=4.1sec (at 15th cycles of the event) of the shake event mentioned above are applied free nodes of ground springs. Earth pressure at rest and effect of residual displacement induced prior shake events are concerned as pre-load acting on the RC structure.

4.2 Calculation Result

Fig.5 shows both calculated and measured deformation of the RC structure. Although deformation shapes show good matching, calculated displacements are about 10% smaller than measured displacement. This is due to the difference of the initial deformation shape of the RC structure.

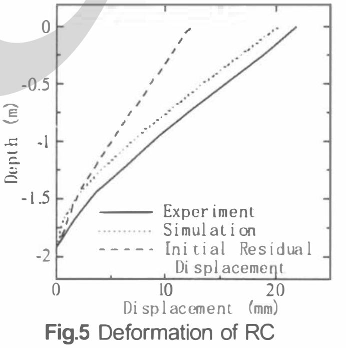

Fig.5 Deformation of RC specimen

5. CONCLUSION

(1)The shaking table tests using the RC specimens were carried out. As the results, the non-linear behavior of the RC specimens and the ground were clarified, and the clue to clarify the dynamic interaction between ground and RC structure involving the non-linear behavior was obtained. (2)With using the truss shaped load transducer installed between the bottom plate of the laminar box and bottom of the RC specimen, the external force(moment and shear force) acting on the RC specimen was measured. (3)It is found out that, the sand near the RC specimen may settle during shake event and that causes the accumulation of the residual deflection of RC specimen. (4)It is found out that, deformation mode of the ground and the RC specimens were different and that causes the deflection of the RC specimens concentrated on the base. (5)The simulation of the test using non-linear frame analyses concerning the ground deformation response was carried out. It is found out that the residual deformation accumulated in the ground must be considered suitably as well as the dynamic response of the ground.

ANALYTICAL EVALUATION ON SHAKING TABLE TEST FOR REINFORCED CONCRETE BUILDING MODEL

YE Xianguo[1], LI Kangning[2], XU Qin[1] and ZHONG Xun[1]

1 Hefei University of Technology, Hefei 230009, P. R. China
2 Earthquake Disaster Mitigation Research Center (EDM), Miki, Hyogo, Japan

Keywords: RC building; shaking table test; seismic response; inelastic dynamic analysis.

1 INTRODUCTION

Both shaking table test and nonlinear analysis are important approach in earthquake engineering research and design. The results of shaking table test are affected by the size and similitude design of test model, the properties of model materials, the input and control of vibration, and the data acquisition and treatment, etc. So far, some aspects in developing inelastic dynamic tools are still under investigation. The reliability of the analysis technology and computer program needs to be evaluated carefully, by means of comparison with real structural seismic response.

This paper presents the analytical evaluation on the results from a three-directional shaking table test of a building model. The original three-directional records near the site of the building during the Mexico earthquake are used as the input excitation.

Inelastic dynamic analysis is conducted, using a sophisticated 3-D frame model, which is based on the nonlinear force-deformation relation of individual structural members. The simulated responses are compared with corresponding test records. It shows that tuning the hysteresis model by using appropriate parameters, the simulated results are comparable with the recorded responses.

2 OUTLINE OF THE TEST

The main objectives of the test are (1) to simulate the seismic damage of a RC frame building and so to testify the validness of current shaking table test technology; (2) to comprehensively understand the nonlinear dynamic response characteristics of R/C structures; (3) to obtain the first-hand test data to verify the performance and reliability of analytical simulation methods and tools.

The structural prototype of the model is a 10-story RC frame building, which was damaged in the 1985 Mexico Michoaca'n Great Earthquake [1]. It has a regular rectangle shape consisting of five frames with the bays of 9.0 m in the longitudinal direction, and four frames with the bays of 6.0 m in the transverse direction. In the transverse direction four shear-walls were placed in the two end-frames. The total height of the structure was 39.05 m. The test model is made in one-tenth scale. It was cast using fine gravel concrete and galvanized steel wires and designed according to the general similitude law [2] that considered the effect of the short of artificial mass. The test model total weight is 15 ton including the base plate weight and the artificial mass loaded on each floor slab. The view of the specimen mounted on the test table was shown in the Photo 1, and the specimen floor plan and the location of the acceleration/displacement sensors were given in Fig. 1. The test was carried out on the 4×4 m^2 MTS shaking table in Tongji University, China, in 1998. The input earthquake motions are the original three-directional acceleration records SCT85 and SCT95, obtained near the prototype building site during the 1985 and 1995 Mexico earthquakes. The SCT85 input was repeated, increasing the acceleration peak value gradually. White noise waves were inputted among the earthquake excitations to monitor the change of the model's dynamic properties.

3 ANALYTICAL SIMULATIONS

The analytical simulation by nonlinear dynamic responses was carried out on the prototype building to gain the responses for the comparison with the shaking table test results. The simulation was executed using the computer program CANNY, which was proved reliable performance in predicting earthquake responses and damage of building structures. Detail of the structural modeling for the analysis and the numerical methods can be found in the reference literature [3].

In order to compare on the same base the results of inelastic dynamic analysis with that obtained from the shaking table test, the input for the dynamic analysis makes use of the acceleration time history observed on the shaking table surface. Furthermore, the observation results from the 11-run shaking table tests were jointed together to form the input acceleration waves in a long duration of 2048 seconds. Therefore, the dynamic analysis on the building could be carried out once to cover the all 11 runs of the shaking test. By this way, the accumulation affect of nonlinear structural damage can be reproduced by the analysis. The equations of motion are solved by step-by step integration in Newmark-β method, under a time interval of 1/200 second. Raylaigh's damping is used assuming mass and stiffness matrix proportional damping (damping constant 5%).

4 CONCLUSIONS

- Shaking table test results are greatly affected by the specimen size, the similitude design, the input and excitation control, and the precision of the data acquisition system. By careful design of reduced- scale specimen, the responses and damage development of the specimen by shaking table test can be reproduce the real building earthquake damage.
- By current 3-D nonlinear analysis models and methods, the numerical simulation have obtained agreeable results with the test when the structural model responses in elastic or minor damage stage. During strong motion excitation and severe structural damage, it may result in considerable difference with the results between the analytical simulation and the reduced-scale specimen test. The difference could be attributed to the error of the similarity between the reduced-scale specimen and the prototype building in nonlinear status. It demands further investigations on both the analytical simulation and the shaking table test. In the analytical simulation it deserves to perform the analysis on the test model for direct comparison. In the shaking table test, it is greatly expected conducting full-scale structure test by accurate data acquisition and vibration control for high reliable results.

The investigation of the paper is funded by the State Key Laboratory at Tongji University, Shanghai, and by the National Natural Science Foundation of China (No. 59978013). The graduate students Liu Tao, Ge Yingyu and Jiang Xin also jointed the research project and contributed to the paper.

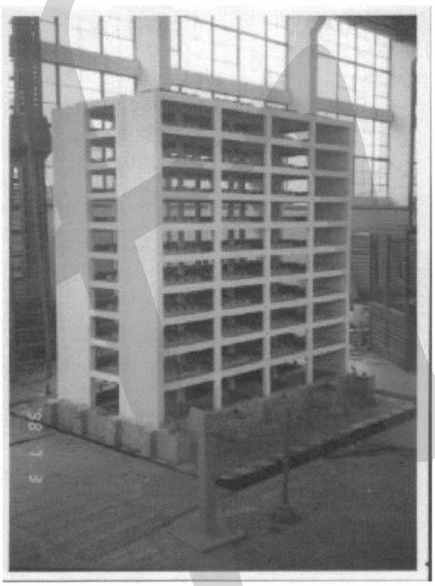

Photo 1 The View of the Specimen On the Table

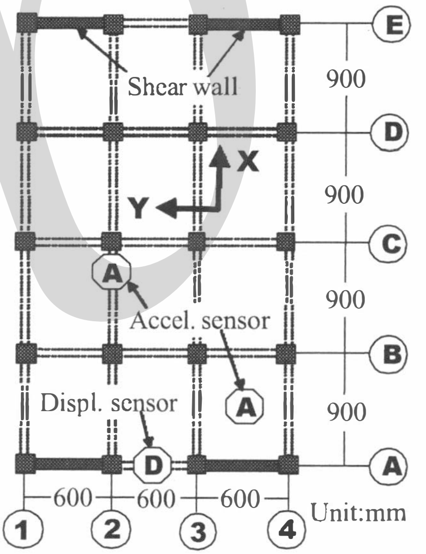

Fig. 1 Specimen Floor Plan and Sensor Location (1/10 reduced-scale from prototype building)

REFERENCES

[1] Meli R., Code-prescribed seismic actions and performance of buildings, Proc. of 11th WCEE, Madrid, Spain, 1992

[2] Zhang Minzhen, Study on similitude laws for shaking table test, Earthquake Engineering and Engineering Vibration, Vol.17, No.2, 1997

[3] K.N. Li, T. Kubo and C.E., Ventura, "3-D Analysis of Building Model and Reliability of Simulated Structural Earthquake Responses," Proceedings of the International Seminar on New Seismic Design Methodologies for Tall Buildings, Oct. 15-16, 1999, Beijing China, pp.34-41.

STUDY ON THE ELASTO-PLASTIC BEHAVIOR OF FULL SCALE RC COLUMNS SUBJECTED TO VARYING AXIAL LOADING

Masakazu TERAI Yasuhiro NAGATOMI Koichi MINAMI
Fukuyama University
JAPAN

Key words: varying axial loading, full scale, size effect, RC Column, ultimate strength

1 INTRODUCTION

Many experimental researches about the size effect of Reinforced Concrete (RC) structures have so far been carried out.[1] However,since load devices have little capacity for testing large-scale specimens, no experiment of large dimension RC columns similar to actual load conditions have been carried out.

This paper presents the experimental work on elasto-plastic behavior of the full scale RC column, which have the cross-section size of 600*600mm subjected to cyclic horizontal load and varying axial load. Moreover, it compares this experimental results with the experimental ones of the scaled model, which have the cross-section size 300*300mm, and the size effect on the ultimate strength of RC column is studied.

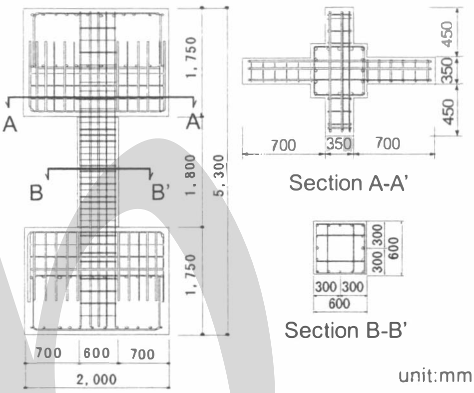

Figure 1 Detail of specimen

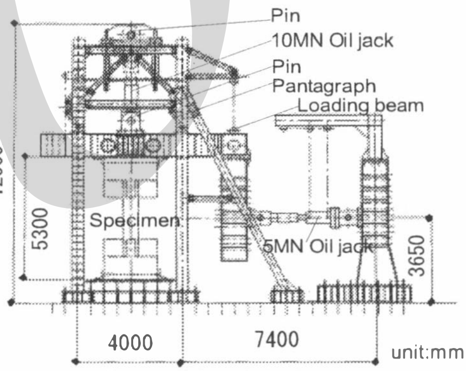

Figure 2 Load device

2 EXPERIMENTAL METHODS

2.1 Test specimen and parameters

The specimen assuming side columns with large axial force fluctuation was planned. The mechanical properties of steel and compressive strength of concrete cylinder are shown in Table 1, and the bar arrengements and dimentions are in Figure 1.

2.2 Loading method

The loading system is outlined in Figure 2. This experiment is tested under cyclic lateral loading and varying axial loading. In the test, a conpressive axial force ${}_{M}N_{max}$ is $0.6{*}{}_{c}N_{u}$(${}_{c}N_{u}$: maximum yield strength of concrete member against compressive axial force) and a tensile axial force ${}_{p}N_{max}$ of $0.16{*}{}_{c}N_{u}$ is applied. The method of varying axial loading is shown in Figure 3.

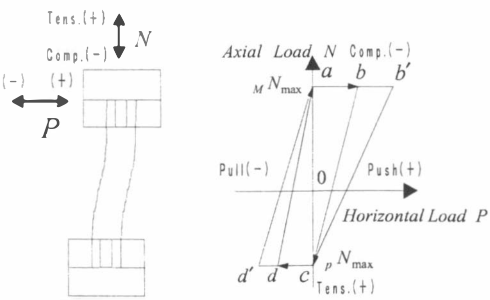

Figure 3 Method of varying axial loading

3 TEST RESULTS

Figure 4 shows the observed crack pattern(a) at 1/100rad. of drift angle and (b) at 1/25rad., and Figure 5 shows the relationship between shear force and deformation of the test section.

The maximum strength(1540kN) is recorded at the same time as shear failure occured between 1/

Table1 Material properties of concrete and steel

Concrete	Main Bar	Hoop	Axial Loading
Compresive strength $\sigma_{B0} = 27.2 N/mm^2$ Young's modulus $E_c = 25600 N/mm^2$	16-D25 (SD345) Yield stress $\sigma_y = 385 N/mm^2$	4-S10@100 (KSS785) (welded) Yield stress $\sigma_y = 904 N/mm^2$	Compression $-0.6bD\sigma_B = -5500kN$ Tension $0.16bD\sigma_B = 1500kN$

σ_B: *Compressive Strength* $(=\lambda \cdot \sigma_{B0})$ λ : *reduction coefficient*$(=0.85)$
σ_{B0}: *Compressive strength of concrete sylinder*$(\phi 100 \times 200mm)$

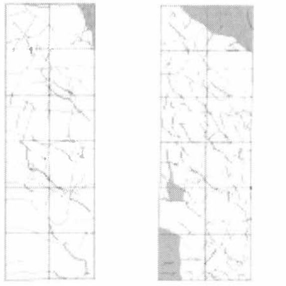

(a)R=+1/100rad. (b)R=+1/25rad.(final)

Figure 4 Crack patterns

100rad. and 1/66rad. of drift angle bacause the shear cracks extend from the top-end of column to the bottom-end. On the other negative direction(tensile axial loading side), the maximum strength(820kN) is recorded as flexural failure occured between 3/100rad. and 1/25rad. of drift angle.

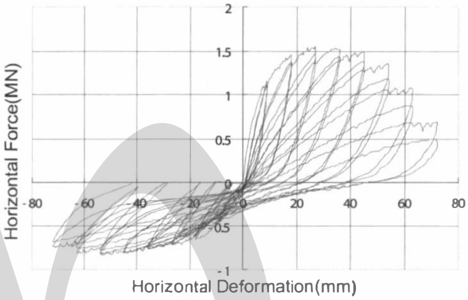

Figure 5 History curves

4 DISCUSSIONS

4.1 Examination of strength

The ultimate flexural strength can be estimated by the superposed strength. The ratio of experiment value/calculation value becomes 0.89 in the full scale RC column.

The ultimate shear strength is calculated based on the theory of the arch-truss mechanisum. For the full scale RC column of the section size 600mm*600mm, it is necessary to consider the size effect as well as the flexural strength, though the ratio of experiment value/calculation value becomes 1.12 and evaluates the experiment value to the safety side a little.

Table 2 Maximum strength unit:MN

reduction coefficient	Loading Direction	Test value①	Fluxural Strength②	Shear Strength③	①/②	①/③
1.00	+	1.54	1.73	1.38	0.89	1.12
	−	-0.82	-0.72	-1.38	1.13	0.59
0.85	+	1.54	1.50	1.48	1.04	1.04
	−	-0.82	-0.61	-1.48	1.34	0.55

4.2 Examination of Size Effect

The ultimate strength considering the size effect in compressive strength of concrete, reduction coefficient is 0.85 as thought in ACI Standard 318[2] etc., is shown in Table 2 and Figure 6. In the comparison between the experiment value and the calculation value, by taking into account the size effect of compressive strength of concrete, the maximum strength of the full scale RC column can be almost evaluated.

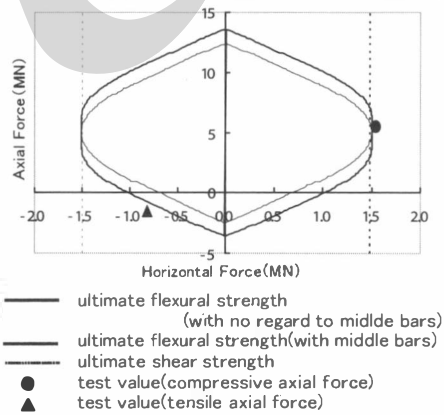

Figure 6 Maximum strength

5 CONCLUSIONS

Through the experiment conducted in this study, the following can be assumed:

1)The maximum strength of the full scale RC column is recorded at the same time as shear failure occured between 1/100 rad. and 1/66 rad. of drift angle.

2)As a results of calculating the ultimate strength, It turned out that calculating with decreasing of concrete compressive strength was necessary in order to evaluate the ultimate strength of the RC column with full scale adequately.

REFERENCES

[1]Japan Concrete Institute, Applications of Fracture Mechanics to Concrete Structures, 1993

[2] ACI Committee 318, Building Code Requirements for Structural Concrete and Commentary,1999

THE RELATIONSHIP BETWEEN FLEXURAL STRENGTH AND DEFORMATION OF UNBONDED POST-TENSIOND CONCRETE BEAMS SUBJECTED TO EARTHQUAKE LOAD

Yoshihiro Ohta Haruhiko Okamoto
TAKENAKA CORPORATION,JAPAN

Keywords : Unbonded prestressing tendons, beam-column connection

1 INTRODUCTION

There are many studies of unbonded post-tensioned concrete beam under earthquake motion, but researches reported the behavior of beam-column connections as part of an indeterminate system subjected to lateral load are very little [1].

The purpose of this paper was to clarify the behavior of unbonded post-tensioned concrete beam in an indeterminate system under earthquake motion. Specimens modeled a single story of a one-bay frame with unbonded post-tensioned concrete beam were tested.

This report describes the variation of the stress in the prestressing tendon and the relations between the moment and the rotation angle at the end of beams during testing. On the variation of the stress in the prestressing tendon, the measured variation of the stress in the prestressing tendon on this test was compared with the calculated variation of them by the proposed experimental equations. To clarify the behavior on the end of the beam in this indeterminate system, the relations of the moment and the rotation angle on the end of the beam were investigated analytically.

2 TEST PROGRAM

The general descriptions of the specimens are listed in Table 1. The geometrical configuration of the specimen and the arrangement of reinforcements and presstressing tendons of specimen UPC-1, UPC-2 is shown in Fig.1. The loading apparatus are shown in Fig.2.

Table 1 Descriptions of the specimens

Spec.	The ratio of the initial tensile stress to the yield strength	The ratio of the depth to the length of the beam
UPC-1	0.80	12.9
UPC-2	0.60	12.9
UPC-3	0.80	16.4

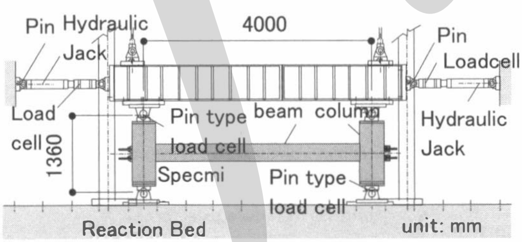

Fig.2 Loading apparatus

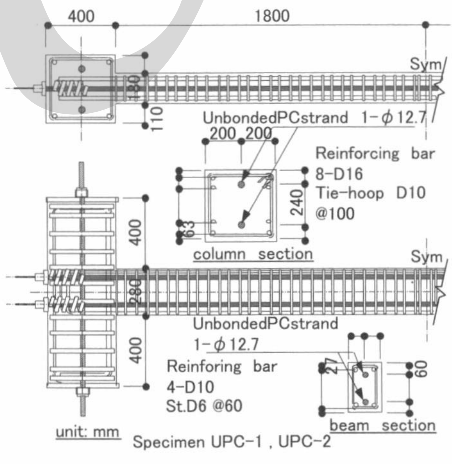

Fig.1 Configuration of the specimen

3 DISCUSSION OF TEST RESULT

3.1 GENERAL SPECIMEN RESPONSE

The overall horizontal load –versus- drift relationships of the specimen UPC-1 is shown in Fig.3. Observed behavior of the three specimens during the tests was almost identical among specimens and can be summarized as below.

After the initial flexural crack of the beam at 0.1-0.2 % drifts, the yield of the longitudinal reinforcements of the beam occurred at 0.4-0.7 % drifts. The crush of concrete at the end of the beam approximately occurred at 2.0 % drifts and the horizontal load reached peak load at 2.0-3.0 % drifts. The ultimate failure was caused due to the compression concrete failure for flexure on the end of the beam.

3.2 TENSILE STRESS OF PRESTRSSING TENDONS

To understand the variation of the stress in the unbonded prestressing tendons of the prestressed beam on this test, the measured variation of the stress in the unbonded prestressing tendons was compared with the calculated variation of them by the proposed experimental equations. The comparison between measured variation of tensile stress in the prestressing tendons at the maximum of horizontal load and the variation of tensile stress at the ultimate flexural strength calculated by proposed equations [2], [3] is shown in Table 2. It tends that the variations of stress in the prestressing tendons calculated by the equation proposed by A.H.Mattock overestimate test results and the variations of stress by the equation proposed by Y.Takemoto underestimate them.

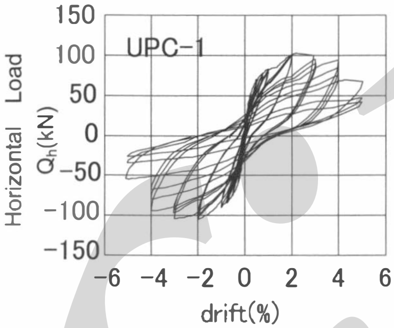

Fig.3 Horizontal load –versus- drift relationships of specimen UPC-1

Table 2 Comparison between measured and calculated variation of stress in the PC tendons

Spec.	R at Qmax 1) %	$D_p\sigma_{exp}$ 2) N/mm² ①	$D_p\sigma_{cal\text{-}m}$ 3) N/mm² ②	$D_p\sigma_{cal\text{-}t}$ 4) N/mm² ③	①/②	①/③
UPC-1	2.18	146	201	104	0.73	1.41
	-1.98	150			0.75	1.44
UPC-2	2.93	214	205	105	1.04	2.04
	-2.78	225			1.09	2.14
UPC-3	1.99	65.1	178	67.2	0.37	0.97
	-1.99	85.4			0.48	1.27

1)R at Qmax : Drift at the maximum of horizontal load
2)$D_p\sigma_{exp}$: Average variation of stress in pc tendons at the maximum of horizontal load measured by load cells set up on the column side
3)$D_p\sigma_{cal\text{-}m}$: Variation of stress in pc tendons calculated by the equation proposed by A.H.Mattock [2]
4)$D_p\sigma_{cal\text{-}t}$: Variation of stress in pc tendons calculated by the equation proposed by Y. Takemoto [3]

3.3 THE RELATION BETWEEN MOMENT AND ROTATION ANGLE AT THE END OF BEAMS

To clarify the behavior on the end of the beam in this indeterminate system, the relations of the moment and the rotation angle on the end of the beam were investigated analytically

The comparison between the relations of the measured moment M_{ex} and the measured rotation angle θ_{ex} at the end of beam with the relations of calculated moment M_{in} and calculated rotation angle θ_{in} to the result for the envelop of the positive loading of specimen UPC-1 is shown in Fig.4.Good agreement was obtained between the relations of M_{ex} and θ_{ex} with the relations of M_{in} and θ_{in} except for a few cases.

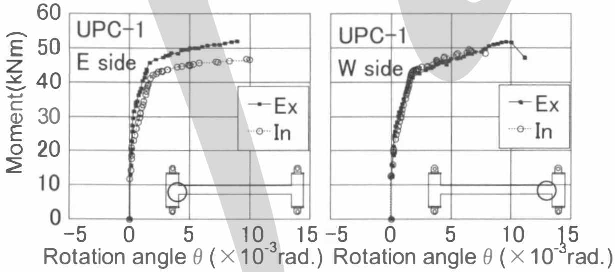

Ex : the relations of the moment M_{ex} and rotation angle θ_{ex}
In : the relations of the moment M_{in} and rotation angle θ_{in}

Fig.4 Comparison between the relations of M_{ex} and θ_{ex} with the relations of M_{in} and θ_{in}

REFERENCES

[1] Hiroshi Muguruma, Fumio Watanabe, Minehiro Nishiyama : The Study of Behavior about Unbonded Prestressed Concrete Beam in an Indeterminate System, Prestressed Concrete,March 1985,pp66-73.
[2]Alan H .Mattock, Jun Yamazaki, Basil T. Kattula : Comparative Study of Prestressed Concrete Beams, With and Without Bond, ACI Journal, February 1971,pp116-125.
[3]Yasushi Takemoto : Ultimate Tendon Stresses in Unbonded Partially Prestressed Concrete Members, Report Obayashi Corporation Technical Research Institute, February 1984,pp49-54.

EXPERIMENTAL STUDY ON THE SEISMIC RESPONSE OF REINFORCED CONCRETE BUILDINGS WITH PRECAST FLOOR SYSTEM

Oscar Lopez-Batiz
National Center for Disaster Prevention, Mexico

Keywords: precast floor system, seismic behavior, torsional stiffness

1 INTRODUCTION AND SIGNIFICANCE OF THE STUDY

The use of prefabricated floor systems is more commonly used each day in Latin American construction of reinforced concrete buildings. This system is not clearly mentioned in the design and construction recommendations or guides for reinforced concrete structures in this region, which causes uncertainty in the structural design and, in some cases, leads to selection of design parameters that are not fully based on theoretical or experimental developments. Design procedures of this type of structures are based on the traditional method of reinforced concrete building design. The only difference is the consideration of a hypothesis of less deformation capacity and rigidity of the whole structure due to the prefabricated floor frame behavior characteristics.

The experimental results on two structural models full-scaled reinforced concrete structures built and tested in the Large-scale Structures Laboratory of CENAPRED are shown. The models were subjected to lateral translational and torsional reversal cyclic loading. One of them was cast *in situ* (CR model) and the other consists of cast *in situ* frame and precasted floor system (PCR model).

The aim of this study was to establish a direct comparison between the behavior to lateral forces of a traditional monolithic reinforced concrete structure and a reinforced concrete structure with a prefabricated floor system. The only variable considered was the type of floor system, while all the other parameters and characteristics were kept constant.

2 PRINCIPAL FINDINGS FROM EXPERIMENTAL TEST

The models had the same dimensions, one level, one span in each direction, story height of 2 m, and the distance between the columns of 4.5 m in both directions. The structural elements of the frame are: beams of 400x250 mm and columns of 400x300 mm. The orientation of the columns was decided in the way that the larger moment of inertia would be parallel to the direction of lateral force. The slab had a total thickness of 120 mm in the CR model and 170 mm in the PCR model, in which a concrete topping layer of 40 mm was included. Fig.1 shows a general view of the test model.

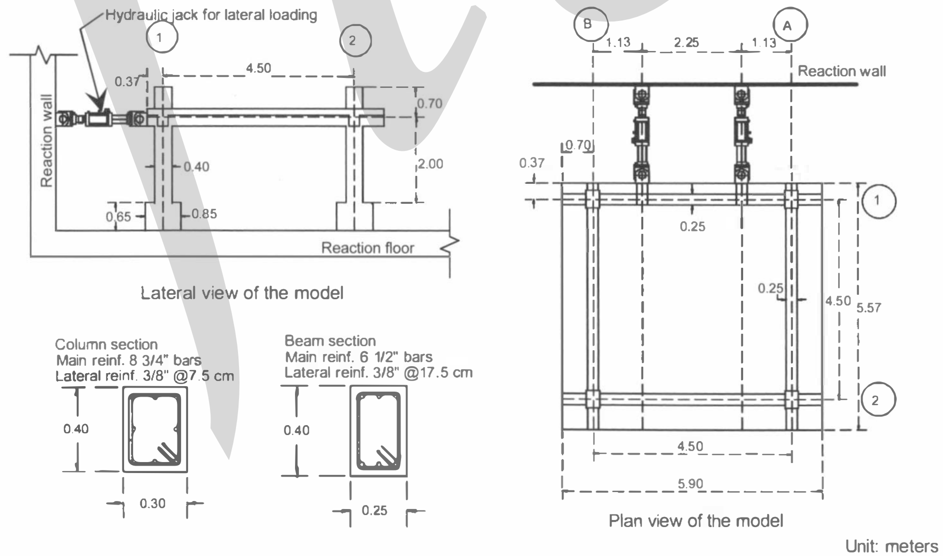

Fig. 1 General view of the test model

The models were designed according to the Mexico City Building Code (abbreviated as RCDF-NTC), so that its intended failure mechanism followed a "strong column – week beam" type.

The instrumentation for both models was the same, so that the effect of the floor structural systems in the general behavior of the specimens could be directly compared. The models were subjected to lateral forces only to simulate the seismic effect. Lateral displacements were applied to the models by two hydraulic jacks of 500 kN maximum capacity. It was applied symmetrically (for translational loading pattern, for torsional loading it was eliminated the jack parallel to axis B) to the model in points located along the axes parallel to frames A and B (Fig.1).

General behavior of the models

In general, the behavior of both models allowed the "weak beam–strong columns" concept, without any significant influence of the type of the floor system on the formation of the failure mechanism. The crack pattern of the slabs showed that the width of the contributing slab is practically equal to half span in the perpendicular direction to the applied load direction.

Analysis of results

There was not significant difference on the lateral load-displacement curves between both models.

For torsional load–displacement curves of the models the general tendency of the curves for both models is similar. The peak to peak stiffness of the models during the torsional demand were computed; the results are shown in Fig.2. There is a slight difference between the torsional stiffness of the models, the stiffness for the model CR was 8% larger for the first two torsional cycles, and 5% larger for the following torsional loading cycles.

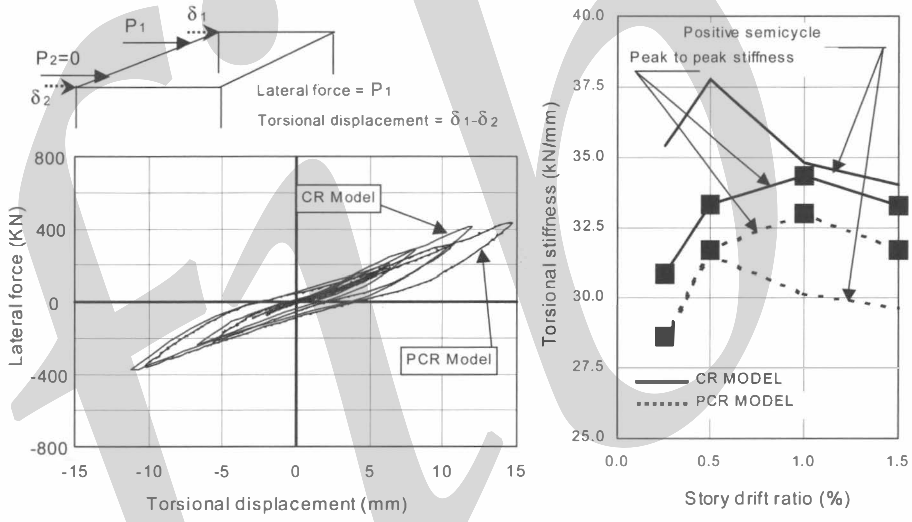

Fig. 2 Torsional load – displacement curves for the models, and torsional stiffness

Regarding the elongation of the floor system, from the experimental results it can be seen that the models, after being subjected to a maximum lateral displacement of 80.0 mm, had a residual elongation of the floor system of approximately 9.75 and 7.61 mm for models CR and PCR, respectively. This final residual elongation of the floor system, is about 12.2% and 9.5% of the maximum lateral displacement applied on the model, for the CR and PCR models, respectively. The elongation pattern of the floor system under successively increasing lateral displacements turned out to be similar for both models, the inelastic elongation on the floor system was about 16.6% of the value of the lateral displacement applied.

3 PRINCIPAL CONCLUSIONS

The most relevant conclusions can be summarized as follows:

1) The crack patterns and the configuration of the yielding mechanism did not vary significantly between the models; 2) The lateral load-lateral displacement behaviour of the models, when only the translational displacement is considered, were practically equal on both models up to a drift ratio of 2.0%; 3) When the models were subjected to representative torsion loads, CR model presented larger stiffness than PCR model, with a difference of 8%; 4) Instability was not observed, nor were indications of loosed small vaults on the PCR model. No observed slippage of the prestress joist over the main beam occurred.

RIBBED MAT FOUNDATION FOR TWO SEISMIC RESISTANT BUILDINGS

Agustin A. Mazzeo, Dr.Ing°
Facultad de Arquitectura y Urbanismo
Facultad de Ingenieria
Universidad Central de Venezuela. Caracas, Venezuela

Keywords: mat foundations, tall buildings, seismic resistant

1 INTRODUCTION

The two reinforced concrete celular ribbed mats described in this paper were used as solution for the foundations of two seismic resistant reinforced concrete tall buildings built in heavy seismic zones of Venezuela. Both structures were designed by the author to withstand the seismic provisions prescribed by Venezuelan Seismic Regulations [1]. In both cases, mats were selected as foundation system for those buildings as the best choice to accomplish the structural design with resistant soil conditions, dynamic responses and economical advantages. Buildings shown in Fig. 1 and Fig. 2. had overcome minor and medium earthquakes events without any damages.

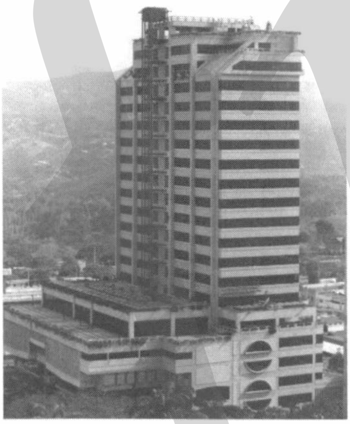

Fig. 1. View of Building 80m. high
Architect Paolo Donghia.

Fig. 2. View of Building 60m. high
Architect Ralph A. Brewer.

2 MAT BUILT EXAMPLES

2.1 First example

Corresponds to the 80 meter high building shown in Fig. 1. It has a reinforced concrete seismic resistant ductile structure, founded on a *rectangular* celular ribbed mat of 21,60 meters x 50,75 meters. Stiff inverted rectangular ribs of 2,50 meters wide by 2,60 meters high were placed in a rectangular grid of 8,10 meters by 9,07 meters. Bottom slab in direct contact with soil resistant stratum is 55 centimeters thick.

2.2 Second example

Corresponds to the 60 meters high building shown in Fig. 2. It also has a reinforced concrete seismic resistant ductile structure, founded on an almost *square* celular ribbed mat of 47,40 meters by 45,40 meters. Stiff inverted rectangular ribs of 2,75 meters wide by 3,50 meters high were placed in a square grid of 10,60 meters by 10,60 meters. Bottom slab in direct contact with soil resistant stratum is 60 centimeters thick.

3 MAT ANALYSIS, DESIGN AND CONSTRUCTION

3.1 Rigidity Conditions

The analysis of both mats were carried out assuming linear distribution of the soil reaction pressure, assumption justified in both cases by the high value of the soil coefficient of subgrade reaction (soil reaction modulus) of more than 20.000 metric ton per cubic meter. (1250 kips per cubic foot) and by the mat´s structural stiffness.

3.2 Structural Analysis

The conditions of equilibrium and geometrical compatibility of the entire mat were taken into consideration by means of a mathematical model that represented the grid formed by the orthogonal inverted ribs supported at the points of intersections with column vertical axes. Model considered full structural interaction in both directions between orthogonal inverted stiff ribs.

3.3 Construction Provisions

Mats dimensions called for special specifications regarding inevitable construction joints. In both mats the concrete of thick bottom slabs were poured doing upside-down shear-keys at center of panels at each construction joint. Construction joints at inverted ribs, were also selected at the center of some spans, using upside-down shear-keys of half depth of the transverse section of the ribs. Fig. 3 shows executed joints. Upside-down shear-keys are needed in mat construction joints, because soil reactions acts in up direction, and because ribs continuity requires that the second concrete pour in the construction joint goes downward the first concrete pour. In this way, the second poured part when it hards, results really supported by the first one.

Fig. 3. Detail of inverted Shear-key construction joints.

REFERENCES

[1] Venezuelan Seismic Code. *Edificaciones Antisísmicas.* Covenín 1756-87. Caracas. 1988.

NEW APPROACH FOR ADDING RESTRAINERS ON EXISTING STRUCTURES

Shinji Izumi Akihiko Iizuka Yoh Takebe
PC Bridge Co., Ltd. Osaka Branch, JAPAN
Design & Engineering. Engineering Management & Purchase

Keywords: seismic, restrainer, epoxy bond, impact load

1 INTRODUCTION

After Hyogo Kobe earthquake, the local Government has planed for the prestressed concrete simply supported T-girder bridges to enforce the resistance to the seismic actions under the new Japanese seismic codes. To satisfy the new codes, the diaphragms were needed to be reinforced. At the planning stages, it was targeted that the damages on existing girders, caused by the seismic forces and the construction processes such as drilling holes and so on, should be minimized. It is expecting that the failure mode shall be the shear failure at diaphragm side boundary between main girder and diaphragm.

The characteristic of the proposed method is that the bond between existing girders and cast-in-place diaphragms is made only by bonding agents. For that purpose, specially arranged bonding agent is developed. In Figure.1, the Original Plan and the Adopted Plan are shown.

This paper is presenting the test results of the basic tests for epoxy bonds themselves, and the 1/2 sized model restrainer system tests for static and impact loads.

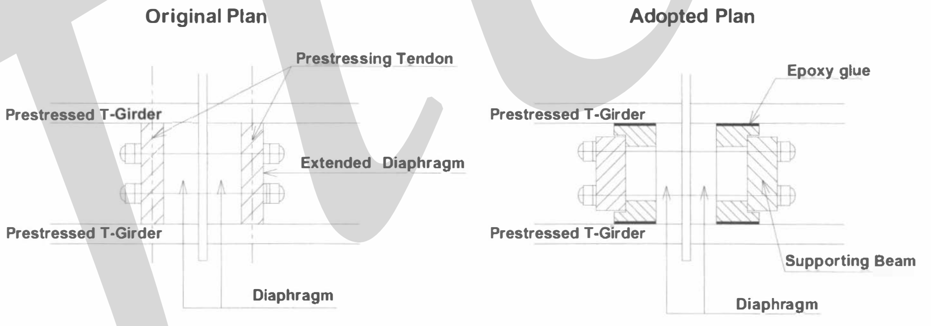

Figure.1 General View of Original and Adopted Restrainers

2 CHOICE OF BONDING AGENTS

2.1 Requirements of Bonding Agents

Six types of bonding agents "five epoxy type bonds and one polymer cement type bond" are compared prior to the tests. The following requirements need to be satisfied for bonding agents.

1. Required workable periods are at least 5 hours.
2. Long term durability is required.
3. Strong bonding performance between new and old concrete is required even at wet condition.
4. Even thickness is preferred.

2.2 Choice of Bonding Agents

Two types of epoxy bonds and a polymer cement type bond were chosen for bonding strength test based on the workable period requirement. Based on the test performance, one type of epoxy bond has been decided to use for the farther 1/2 size model tests.

3 SHAPE OF CAST-IN-PLACE NON-SHRINK-MORTAR BRACKET

Because of the strong bonding effect, and the expected type of failure. The shape of the cast-in-place non-shrink-mortar bracket was determined by the 3-D solid finite element analysis. In Figure.2, the general shape and 3-D analytic model of bracket are shown. Analytic results are summarized on Table.1.

Table.1 Analytic Results at A & B

(N/mm^2)

	Case-1	Case-2	Case-3
H	50mm	100mm	150mm
A	4.4	3.3	1.8
B	2.9	5.2	6.1

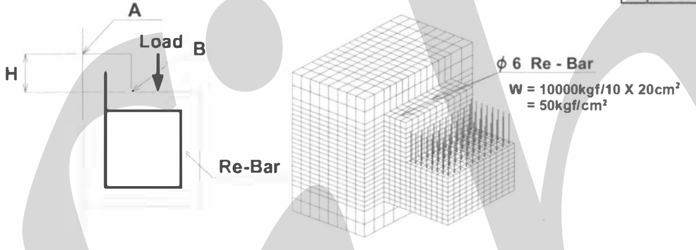

Figure.2 General Shape and 3-D Analytic Model

4 CONCLUSION

Based on the bonding agent effects and the 3-D solid finite element analytic results, the 1/2 scale model static and impact tests were performed. The following conclusions are drawn:

1. At the static loading test stage, the failure loads were approximately 2 times design load value.
2. At the impact loading test stage, the failure loads were approximately 1.7 times static failure loads and well over design load.
3. The failure occurred at the non-shrink-mortar brackets as expected.

REFERENCES

(1) Products Catalogue of Nihon Kasei Co., Ltd.
(2) Products Catalogue of Nichibei Resin Co., Ltd.
(3) Japan Road Association, "Specifications For Highway Bridges Part V : Seismic Design," December 1996.

THE STUDY ON SEISMICS SAFETY ANALYSIS OF ARCH BRIDGES DUE TO FAULT DISPLACEMENT

Hisanori Otsuka, Wataru Yabuki
Kyushu University
JAPAN

Shogo Matsunaga
CTI Engineering Co.,Ltd.
JAPAN

Hiroyuki Murai, Yusuke Ogura
Yachiyo Engineering Co.,Ltd.
JAPAN

Keywords:fault displacement, concrete arch bridge, earthquake resistance

1 INTRODUCTION

In this study, resistance to fault displacement, what members suffer damage, whether structural improvements to withstand fault displacement can be made, etc., were examined for arch bridges. In the numerical calculations, the degree and direction of fault movement, the span length and rise height of the arch, the rigidity ratio of the superstructure and arch ring, and the design specifications of the bridge, are considered as parameters.

2 BRIDGE TYPES STUDIED AND ANALYSIS CONDITIONS

2.1 Bridge Types

In this study three types of concrete arch highway bridges are considered. The selected types are shown in **Figs 1** and outlined in **Table 1**.

2.2 Condition of analysis

In this study, the material non-linear static analysis method is used. Forced displacement due to fault displacement is applied to each of the base of the arch rib, the end posts and the end of stiffening girders. The conditions of analysis and their cases are summarized in **Table 2**.

Assuming that relative displacement due to a fault occurs at the mid span, the following three cases are examined:

Case 1: arch rib moves horizontally toward both sides in the longitudinal direction
Case 2: vertical direction
Case 3: horizontal fault displacement occurs in the transverse direction

As an example, the concept of analysis for bridge B is given in **Table 2**. The analysis is carried out for each of the three cases mentioned above for fault displacements of 0.5 m, 1.0 m and 2.0 m (7.0 m: bridge A) respectively taking into consideration the fault displacement already measured.

3 RESULT OF ANALYSIS ON BRIDGE C

The result of bridge C is shown only.

3.1 Vertical direction (Case 2)

As in Case 1, damage develops in the springing, but in Case 2 damage progresses a little earlier than in Case 1.

3.2 Horizontal transverce direction (Case 3)

The damage developed in four arch rib positions connected by cross members, which was a very different result than for the other two types bridges. The cross members of this bridge have such a large sectional area as the arch rib,

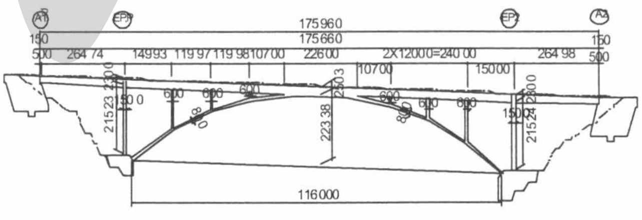

Fig 1 Bridge type B (Langer arch bridge)

Table 1 Bridge types

	BRIDGE A	BRIDGE B	BRIDGE C
Bridge type	lohse arch bridge	langer arch bridge	halfthrough suspension arch bridge
Length of bridge	270.0 m	176.0 m	105.0 m
arch span / rise (span rise ratios)	180.0m／27.5m (6.5)	116.0m／22.338m (5.2)	92.0m／ 17.0m (5.4)
Specification	1990	1996	1980

Table 2 Condition of analysis and Analysis cases

MODEL	BRIDGE A	BRIDGE B	BRIDGE C
Component in consideration of non linear behavier	arch rib, stiffing girders, vertical members, end posts, piers	arch rib, stiffing girders, vertical members, end posts	arch rib cross member
Direction of fault displacement (Analysis case)	The case where the fault moved in the direction of the following was set up. (1) arch rib moves horizontally toward both sides in longitudinal direction :Case-1 (2) vertical direction:Case-2 (3) horizontal fault displacement occurs in transverse direction : Case-3 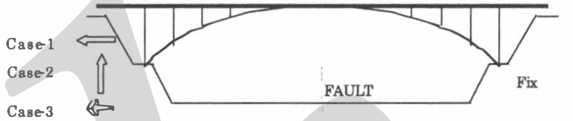		
Fault Displacement	0.5m,1.0m,2.0m		

so the effect of the deformation on the whole bridge is big. The ultimate ductility factor was 8.97, and it was proven that the ductility factor did not reach the ultimate curvature for a displacement of 2.0 m.

4 DISCUSSIONS AND CONCLUSIONS

1. The damage is concentrated in the springing and the crown of each bridge.
2. For the horizontal transverse displacement, care is required at the springing in the Langer arch bridge, and at the crown in the Lohse bridge.
3. The Langer arch bridge had a greater allowance for the ultimate state compared with the half-through suspension bridge. Ductility has been improved according to the specifications of 1996, and the degree of allowable damage has increased.
4. In the half-through suspension arch bridge, the damage develops at cross members. It is shown that damage in the arch rib can be pre vented by introducing damage to cross members by installing a pin, etc.

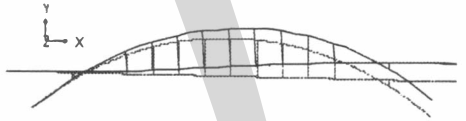

Case-2

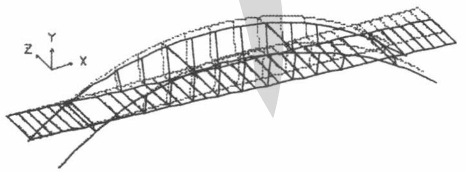

Case-3

Fig 2 The deformation shapes

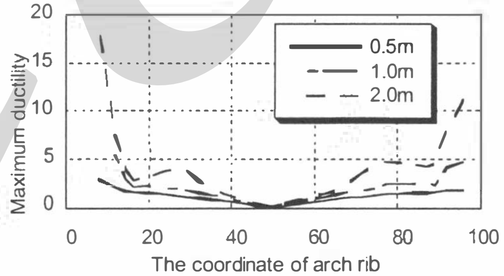

Case-2

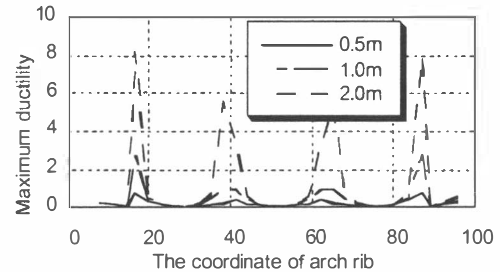

Case-3

Fig 3 Distribution of ductility factar (arch component)

STUDY ON SEISMIC RETROFIT FOR EXISTING R/C BUILDINGS BY USING CHS BRACING

Ryoji Kinoshita Kazuaki Miyagawa Manabu Haginoya — Kawasaki Steel Civil Eng.&Const.
Kazuyoshi Fujisawa — Kawasaki Steel
Katsuhiko Imai — Osaka Univ.
Yasuhiro Ohtani Isao Mitani — Kobe Univ.

Keywords: seismic rehabilitation, hysteretic damper, energy dissipation, seismic index

1 INTRODUCTION

In 1995, a destructive earthquake (Hyogoken-Nanbu Earthquake) hit the urban restricted area along Osaka Bay and Awaji Island. This earthquake revealed that many existing R/C buildings have insufficient seismic capacity and may suffer serious damage due to earthquake. Therefore engineers have begun to develop the new retrofitting techniques to mitigate damage of vulnerable buildings against future earthquakes. To find or develop a good solution for seismic rehabilitation is very significant and urgent problem in Japan. In this paper, authors propose new retrofitting method illustrated in Fig.1. Typical conventional method is H-section braces that are installed in plane of R/C frame after removal of wall, which require reinstallation of wall. In proposed method, reinforcing frames with CHS(circular hollow section) bracings are placed on outer surface of R/C frames and connected to them by mechanical connectors with high strength mortar. As a result, elimination of removal and reinstallation can lead to lower cost and shorter time for completion.

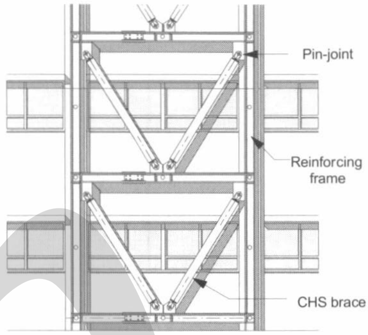

Fig.1 Proposed method

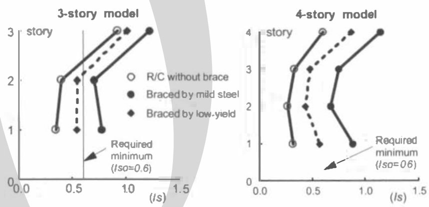

Fig.2 Seismic Indices(*Is*)

2 EVALUATION AND DYNAMIC ANALYSIS

Evaluation and rehabilitation of existing R/C buildings by using CHS braces are simulated for two model structures. One is 3-story building of which R/C frame is consisted of ductile columns. The other model is 4-story building composed mainly by brittle columns. Seismic capacity index (*Is*) defined by ref.1 is calculated for both models (see Fig.2). Results of dynamic response analysis of revel 2 acceleration(50 kine) for same model structures show good energy dissipation characteristic by hysteretic damper(FLD) on reduction of story-drift angle (see Fig.3).

Trough evaluation and analysis carried out, it is concluded that energy dissipation effect by the hysteretic damper cannot be explicitly estimated by seismic index, though seismic index method is applicable to the model structures.

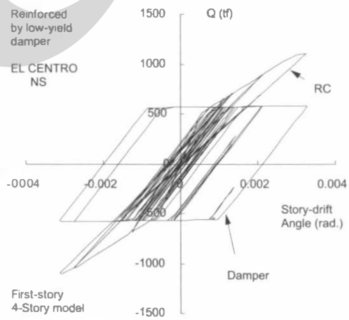

Fig.3 Analytical Result

3 EXPERIMENT OF SHEAR CONNECTION

Full-scale monotonic and cyclic tests are executed to confirm strength and ductility of connection. Figs.4 and 5 show a cy-

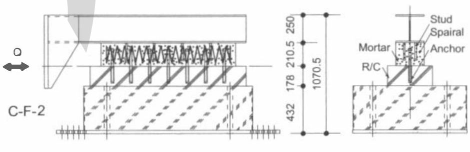

Fig.4 Cyclic Test Specimen

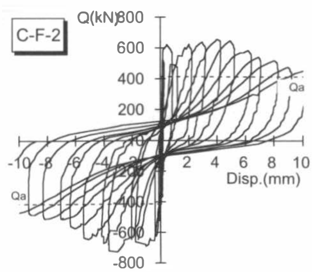

Fig.5 Load-Slip Relationship

clic test specimen and a test result of load-slip relationship, respectively. Proposed connection can sustain the design shear load(Qa) calculated by ref.2 and exhibit ductile behavior.

4 EXPERIMENT OF RETROFITTED FRAME

Eleven test specimens of 1/3-scaled portal frame are carried out to evaluate effects of reinforcing frame including single tube brace or tube-in-tube FLD brace. Figs.6 and 7 show a configuration of specimen (No7,8) and test results of horizontal shear(Q) to story-drift(R) relationship, respectively. The connection can transfer shear force caused by braces to existing R/C frame (see Fig.8).

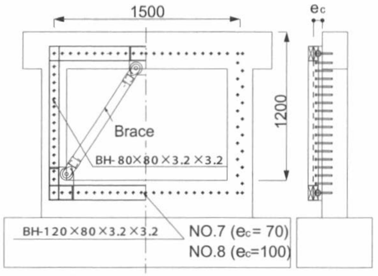

Fig.6 1/3 Scale Test Specimen (Reinforcing frame with braces is placed on outer surface of R/C frame. *e_c : denote distance of eccentricity)

5 APPLICATION

Standard tube-in-tube brace configuration and sizes are showed in Fig.9 and Table 1, respectively. Fig.10 represents a typical building retrofitted by the proposed method.

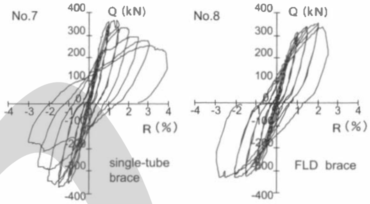

Fig.7 1/3 Scale Test Results

6 CONCLUSION

Through analytical and experimental approaches, the following conclusions are obtained.
(1) The proposed method is capable of mitigating damage caused by future earthquakes.
(2) Basic design method described in refs.1 and 2 is applicable to the proposed retrofitting method.
(3) Low-yield point steel damper is effective to reduce dynamic story-drift response of a R/C building.

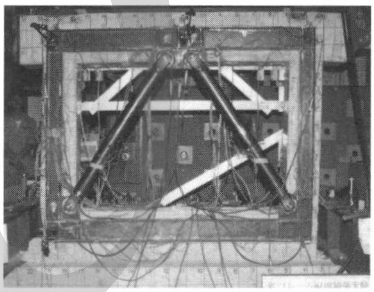

Fig.8 No8 Specimen at R= -2.5% (FLD braces are used)

REFERENCES

[1] Japan Building Disaster Prevention Associations: Standards for Seismic Capacity Evaluation of Existing Reinforced Concrete Buildings, 1990. (In Japanese)
[2] Japan Building Disaster Prevention Associations: Guidelines for Seismic Rehabilitation of Existing Reinforced Concrete Buildings, 1990. (In Japanese)
[3] Katsuhiko Imai, Nobuyuki Yasui, Yasuyoshi Umezu: Development of Tube-in-tube Type Bracing Member (Force Limiting Device) and It's Impulsive Analysis, Proceedings of SSRC 1997 Annual Technical Session and Meeting, Toronto, Canada, vol1.1, pp.515-534, 1997.

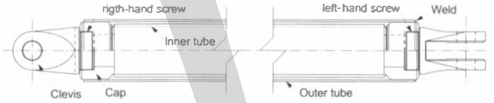

Fig.9 Tube-In-Tube FLD Brace

Table 1 Standard CHS Sizes

FLD type	Brace size diameter mm	Brace size thickness mm	Axial strength kN
mild steel YP=240 kN/mm²	135.0	7	661
	190.7	7,8	949,1070
	244.5	10,12	1730,2050
	273.1	12,15	2310,2850
low yield steel YP=80~ 120 kN/mm²	165.2	8.3	327
	177.8	9.5,12	401,500
	216.3	11.7	601
	241.8	12.2,14	703,801
	273.1	13.9~ 18.8	900~ 1200

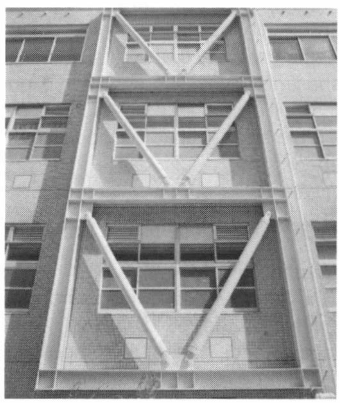

Fig.10 Shimane Univ.

STUDY ON A STRUCTURAL CONTROL SYSTEM USING R/C NON-STRUCTURAL WALLS

Takashi Taguchi
Yahagi Construction Co.,Ltd., Japan

Akira Tasail
Yokohama National University, Japan

Keywords: structural control system, R/C non-structural wall, steel plate, structural experiment, earthquake response analysis

1 INTRODUCTION

Recently, many structural control systems that reduce the response during an earthquake have been used to the practical application [1]. However, some kind of the method reduces the performance in the occupancy by installing to the opening. The authors proposed a structural control system using R/C non-structural walls [2]. This system is composed of X-shaped steel plates embedded into the R/C non-structural wall, as shown in Figure 1. The steel plates deform into plastic range proportionally to the story drift. That is, this wall as hysteretic dampers absorbs vibration energy by their hysteretic performance.

In the previous researches, capacity and restoring force characteristics of the R/C non-structural wall were confirmed by the real scale structural experiment [2]. In addition, the earthquake responses of R/C buildings with this system were analyzed based on the experimental results [3]. In this paper, the real scale structural experiment is summarized and the effectiveness of this system on the change of the building height is discussed by the earthquake response analysis.

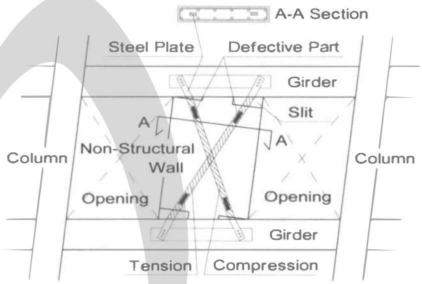

Figure 1 Outline of this system

2 STUDY ON THE REAL SCALE EXPERIMENT

2.1 Outline of the experiment

Three real scale R/C non-structural wall specimens were experimented. The specimen SD-21 is shown in Figure 2. In the specimen SD-21, the steel plates with defective parts of ellipse shape in the vicinity of the slit were used to control the yielding of the plates. The sectional area of the defective part was half of the total sectional area of the plate and its length was 150 mm. The specimens were subjected to lateral shear reversals statically by the loading apparatus.

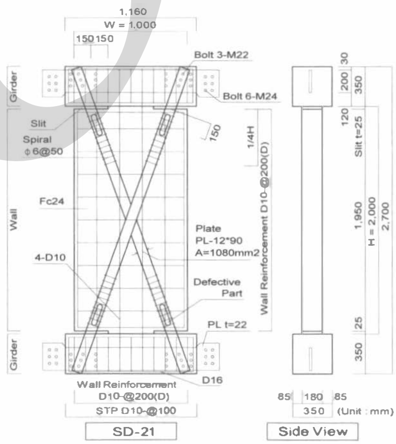

Figure 2 Specimen SD-21

2.2 Experimental results

In the all specimens, the cracks were observed only in the immediate vicinity of the slits. The restoring force characteristic of specimen SD-21 is shown in Figure 3. Marks in the figure indicate the yielding at each location of the steel plates. Desirable energy absorbing performance was developed in the all specimens.

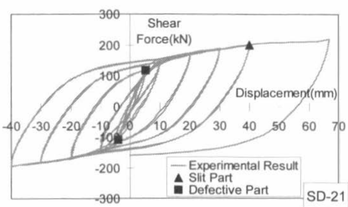

Figure 3 Restoring force characteristic

3 STUDY ON THE EARTHQUAKE RESPONSE ANALYSIS

3.1 Outline of the analysis

The effectiveness of the proposed system on the earthquake response of the building was analyzed. Responses of the R/C building with or without the proposed system were compared. As an analytical model of the R/C building, the lumped-mass model was adopted. Four earthquake records and two simulated earthquake motions were used.

3.2 Analytical models

4 stories, 8 stories and 12 stories R/C buildings (frame models) were chosen as the analytical models. In those models, the floor height and the weight of all stories were assumed to be 3000mm and 4900kN, respectively. The damping of the frame models was assumed to be proportional to the stiffness of the structure and assumed to be 3% for the first natural frequency. The tri-linear type TAKEDA model was adopted as the hysteretic characteristics of each story.

The installation quantity of the R/C non-structural walls was changed as the ratio of the initial stiffness ${}_2K_i$ or the yield shear force ${}_2Q_{yi}$ of the walls for the initial stiffness K_{1i} or the yield shear force Q_{yi} of each layer of the frame models. The analytical models are shown in Table 1. The model M-00 indicates the frame model without the walls. In the earthquake response analysis, the wall model was represented as an additional shear spring as shown in Figure 4. As the damping of the walls, only the hysteretic damping was considered.

Table 1 Variables of the analysis

Analytical Model	Ratio of the Initial Stiffness ${}_2K_i/K_{1i}$	Ratio of the Yield Shear Force ${}_2Q_{yi}/Q_{yi}$
M-00	0.	0.
M-21	0.2	0.1
M-22	0.2	0.2
M-41	0.4	0.1
M-42	0.4	0.2

symbol description in the table
K_{1i} initial stiffness of the frame model (kN/mm)
Q_{yi} story shear force at yield point of the frame model (kN)
${}_2K_i$ initial stiffness of wall (kN/mm)
${}_2Q_{yi}$ story shear force at yield point of wall (kN)

3.3 Analytical results (8 stories model)

The analytical results of the 8 stories models are shown in Figure 5. The maximum response of story drift was reduced most effectively in the model M8-42, in which both initial stiffness and yield shear force were increased as twofold those of the model M8-21. The response of the model M8-41 with twofold initial stiffness of the model M8-21 was reduced from the model M8-00. However, the response of the model M8-22 with twofold yield shear force of the model M8-21 was lager than that of the model M8-21 in many analytical cases. It should be noted that the quantity of R/C non-structural walls assumed in the model M8-21 was enough to make the response story drift smaller than about 1/100 radian under large earthquakes with the velocity of 50 cm/sec, except for the JMA Kobe record.

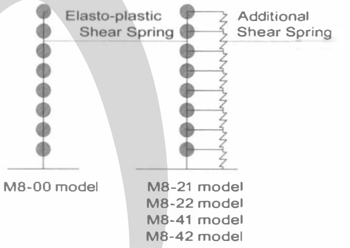

Figure 4 Analytical models

4 CONCLUSIONS

A structural control system using the R/C non-structural walls with X-shape steel plates was proposed. From the real scale structural experiment and the earthquake response analysis, the following conclusions were obtained.

Desirable energy absorbing performance was confirmed in all specimens. Buckling of the steel plates was not observed during the loading. Moreover, the damage was not observed, except for immediate vicinity of the slits.

This structural control system reduced the response of story drift. The R/C non-structural walls with relatively large initial stiffness and yield shear force were effective to reduce the maximum response.

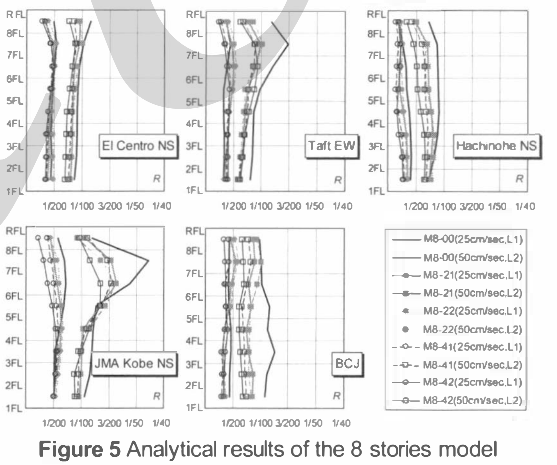

Figure 5 Analytical results of the 8 stories model (maximum story drift)

REFERRENCES

[1] Japanese Society of Steel Construction and The Kozai Club, Seismic Design for Moment Resistant Frames with hysteretic damper, 1998 (in Japanese)

[2] T.Taguchi and A.Tasai, Experimental Study on R/C Non-Structural Walls with a Role of Vibration Control, Journal of Structural Engineering, Architectural Institute of Japan, Vol.47B, pp.105-115, 2001 (in Japanese)

[3] T.Taguchi and A.Tasai, Earthquake Response of Buildings Added with R/C Non-Structural Walls of Energy Absorbing Device, Transactions of the Japan Concrete Institute, Vol.23, pp.247-254, 2002

PROPOSAL OF PARTIAL SAFETY FACTORS FOR SEISMIC DESIGN OF CONCRETE STRUCTURES IN CONSIDERATION OF RELIABILITY THEORY AND OPTIMIZATION OF STRUCTURAL SYSTEMS

Mitsuyoshi Akiyama Motoyuki Suzuki Daisuke Maruyama Hong Kee Nam
Graduate School of Eng., Tohoku University, JAPAN

Keywords: system reliability theory, safety factor, RC bridge pier, seismic design

1 INTRODUCTION

ISO 2394 [1] is to be revised so as to incorporate the limit state design method which introduces probabilistic concepts. Against this background, a reliability-based optimal design method which takes the structural system into consideration [2] was proposed by the authors. This proposed method, however, complicates design for engineers unfamiliar with reliability analysis because requires difficult probabilistic calculation. In this paper, an attempt is made to systematize the optimization method of partial safety factors, so as to meet the required reliability level. Secondly, the proposed method is applied to seismic design of RC bridge piers, and a set of partial safety factors for use in seismic design of RC bridge piers, is estimated.

2 ANALYTICAL METHOD

Figure 1 shows the evaluation flow of basic safety factors for seismic-design of a RC bridge pier. The following is a summary of this evaluation flow:

(a) Set target safety index β_t, objective function W and limiting conditions

(b) Conduce seismic-design of RC bridge piers based on the following criterion equations and the estimated basic safety factors by optimization analysis. The specific evaluation method of strength and response in Eq. (1) – (3) is the same as in reference [2].

Check for shear failure:

$$\gamma_{s0,s} \cdot \frac{V_{act}}{V_c/1.3 + V_s/1.15} \le 1.0 \tag{1}$$

Check for ductility:

$$\gamma_{s0,d} \cdot \frac{\delta_p}{\delta_y + (\delta_u - \delta_y)/1.5} \le 1.0 \tag{2}$$

Check for residual displacement:

$$\gamma_{s0,r} \cdot \frac{C_R(\delta_p - \delta_y)}{\delta_{Ra}} \le 1.0, \tag{3}$$

where, $\gamma_{s0,s}$, $\gamma_{s0,d}$, $\gamma_{s0,r}$: basic safety factors to ensure the prescribed reliability, V_{act}, V_c, V_s : applied shear force, shear strength without ties and contributed by ties, δ_y, δ_u, δ_{Ra}, δ_p : yield displacement, ultimate displacement, allowable residual displacement and seismic response displacement based on the equal energy assumption and C_R : residual displacement response spectrum.

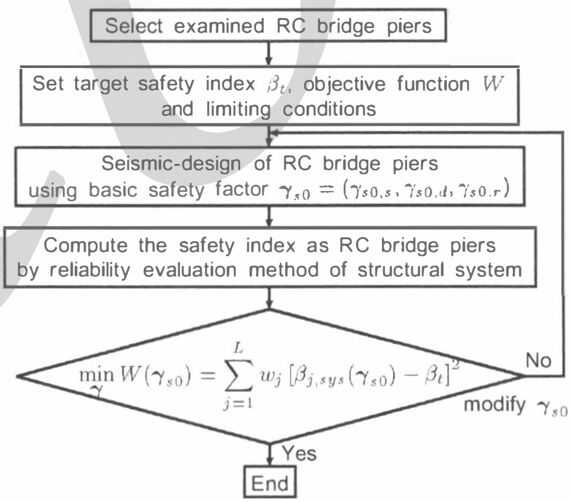

Fig.1 Flowchart

(c) Estimate the safety index β_{sys} as a cluster of RC bridge piers, seismic-designed based on Eq. (1) – (3), from the limit state equations shown in Eq. (4) – (6) based on the reliability evaluation method of the structural system.

Limit state equation for shear failure	: $g_i = \alpha_1 V_c + \alpha_2 V_s - \alpha_3 V_{act}$ $(i = 1, 4)$	(4)
Limit state equation for ductility	: $g_i = \alpha_4 \delta_u - \delta$ $(i = 2, 5)$	(5)
Limit state equation for residual displacement	: $g_i = \delta_{Ra} - C_R(\delta - \delta_y)$ $(i = 3, 6)$	(6)

where α_1, α_2, α_3 : coefficient to take the variation at the estimated V_c, V_s and V_{act} into account, α_4 : coefficient to take the variation at the estimated ultimate displacement into account and δ : seismic

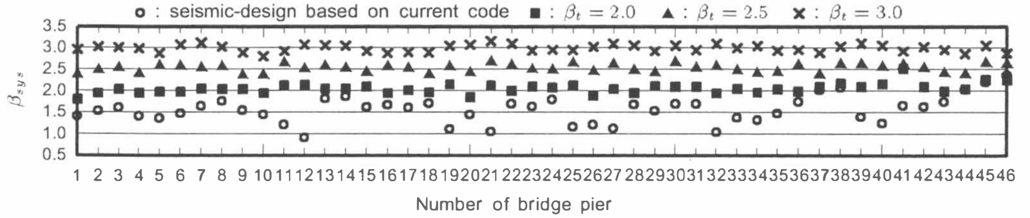

Fig.2 Safety index β_{sys} for RC bridge piers

response displacement depending on the natural period and the yield strength ratio R_u of RC bridge piers. In Eq. (4)–(6), $i = 1 \sim 3$ are expressive of checking for the longitudinal direction and $i = 4 \sim 6$ are expressive of checking for the transverse direction.
(d) Minimize the aggregate of deviation between the safety index $\beta_{j,sys}$ of seismic-designed RC bridge piers used by evaluated partial safety factors γ_{s0} and the target safety index β_t based on sequential quadratic programming method (SQP method).

3 RESULTS

This paper assumes 46 RC bridge piers of differing design conditions, for example, the size of sections, natural period and so on, as the examined RC bridge piers. These RC bridge piers where test-designed based on the current design code [3]. In all cases, ground classifications were the Type I ground model and all of these fulfilled safety checking equations for Type II earthquake ground motion. The failure mode for all designed sections was the flexure failure mode. Table 1 lists the evaluated basic safety factors for each target safety index β_t based on the flow shown in Fig.1. In this paper, the target safety index is assumed to be $\beta_t = 2.0, 2.5, 3.0$. Figure 2 shows the safety index β_{sys} for a cluster of RC bridge piers at these basic computed safety factors. The seismic-designed RC bridge piers based on the current design code ensure high safety index values of β_{sys} which range from 0.9 to 2.4. On the other hand, as shown in Fig.2, the safety index β_{sys} for RC bridge piers for which the basic safety factors shown in Table 1, were used is close to the target safety index β_t. Table 2 shows the average increasing rate of strength of seismic-designed RC bridge piers based on the current design code for the target safety index $\beta_t = 2.0$. There is little difference between the strength of seismic-designed RC bridge piers based on estimated basic safety factors and the strength of test-designed RC bridge piers based on the current design code.

Table 1 Basic safety factors for each target safety index β_t

target safety index	$\gamma_{s0,s}$	$\gamma_{s0,d}$	$\gamma_{s0,r}$
$\beta_t = 2.0$	1.53	1.22	1.30
$\beta_t = 2.5$	1.71	1.64	1.75
$\beta_t = 3.0$	2.05	2.21	2.23

Table 2 Average increasing rate of strength ($\beta_t = 2.0$)

	Average increasing rate of strength (%)
Flexure strength (LG)	117
Shear strength (LG)	117

4 CONCLUSION

This paper has shown necessity of system method procedure which attains the required reliability level. The optimization method of partial safety factors, in which the required reliability level is attained without reliability analysis, was systematized based on our previous study. Based on the proposed method, basic safety factors to be applied to the seismic-design of RC bridge piers were estimated from 46 RC bridge piers differing in design conditions.

REFERENCES

[1] ISO: International Standard ISO/DIN 2394, General Principles on Reliability for Structures, 1998
[2] Mitsuyoshi AKIYAMA, Ryoji MATSUNAKA, Mitsuru DOI and Motoyuki SUZUKI: Reliability-based Optimal Design Considering Structural System and Its Application to Evaluation of Seismic Performance of RC Bridge Pier, J.Struct. Mech., JSCE, No.662/V-49, pp.185-204, 2000 (in Japanese)
[3] Japan Road Association: Design Specifications of Highway Bridges V Seismic Design Stitch, 1996 (in Japanese)

DUCTILITY DESIGN OF CONCRETE ENCASED STEEL PIERS

Hideki Naito Mitsuyoshi Akiyama Motoyuki Suzuki
Graduate School of Eng., Tohoku University, JAPAN

Keywords: instability of longitudinal bars, ductility evaluation, concrete encased steel columns

1 INTRODUCTION

Concrete encased steel (SRC) piers make it possible to maintain high ductility without over-reinforcement, and many such piers are constructed nowadays in Japan. However, as there have been few studies on SRC piers, SRC codes have been formulated based on RC codes. But the dynamic properties of SRC piers are far different from those of RC piers.

Therefore, the method of ductility evaluation of SRC piers is herein examined. The ultimate displacement is defined as the buckling of longitudinal bars inside the reinforced cross section, because the buckling of bars may also cause the collapse of SRC columns as well as of RC piers, both of which have heavy longitudinal reinforcement. Repairs necessitated by such collapse entail considerable work. The method herein proposed can be applied to both RC and SRC columns and makes possible to design piers taking the details of the quantity and arrangement of the longitudinal and transverse reinforcement, into consideration.

2 CALCULATION OF ULTIMATE CURVATURE

2.1 Buckling analysis

In RC and SRC columns, the longitudinal bars are prevented from buckling by the cover and the ties. Thus, buckling analysis is introduced, in which the plasticity of longitudinal bars in the case of reversed loading and the prevention of buckling by the cover and the ties are taken into account. Comparison with the ultimate curvatures from experimental trials using RC columns [1][2] and buckling analysis is shown in Table 1, where the ultimate state is defined by the buckling of bars. It is observed that the values of the experimental trials are accurately evaluated by buckling analysis of longitudinal bars.

Table 1 Ultimate curvature

Speci-men	Buckling mode Experiments / Analysis	Ultimate curvature ($\times 10^{-5}$/mm)	
		Experi-ments	Analysis
No.1	4 / 3	4.90	3.96
No.2	6 / 3	5.03	4.54
No.3	2 / 1	4.61	4.42
No.4	4 / 3	3.65	4.85
No.5	4 / 2	2.08	2.05
No.6	4 / 3	1.91	2.69
No.7	5 / 3	3.94	2.27
No.8	7 / 5	2.55	1.93
No.9	4 / 2	1.15	1.22
No.10	4 / 3	1.39	1.34
No.11	4 / 3	4.62	5.73
No.12	3 / 3	3.32	3.87
No.13	4 / 3	4.29	4.75

2.2 Simple method

The ultimate curvature can be obtained by buckling analysis. However, it is difficult to introduce non-linear buckling analysis into seismic design. Thus, a simple method is devised based on the results of bucking analysis. A comparison of the values obtained by the simple method and those of buckling analysis is shown in Fig. 1. The proposed method makes it possible to obtain the ultimate curvature accurately, without the use of buckling analysis.

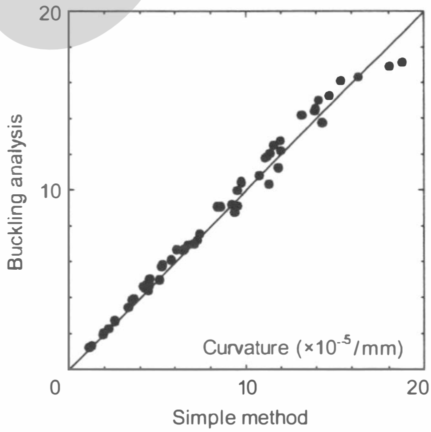

Fig.1 Comparison between simple method and buckling analysis

3 DUCTILITY EVALUATION OF RC AND SRC COLUMNS

3.1 Plastic Hinge Length

The plastic hinge length responding to the ultimate curvature is examined. As a result, the plastic hinge length in Mattock [3] is valid. It is possible to calculate the ultimate displacement by the plastic hinge length in Mattock and the ultimate curvature obtained by use of the simple method.

3.2 Comparison with RC columns

A comparison is made between the values from the proposed method and the values from the 57 experimental trials described by other authors, including the 13 specimens shown in Table 1. From the comparison shown in Fig. 2, it is observed that the results from experimental trials, conservative in the most of the specimens, can be evaluated by the proposed method.

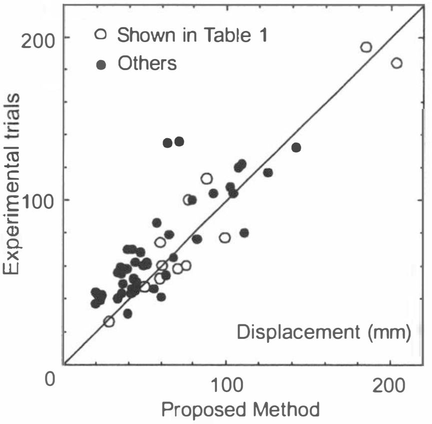

Fig.2 Comparison with RC columns

3.3 Comparison with SRC columns

In the case that the transverse bars are arranged on the outside of longitudinal bars in the cross section of SRC columns, the proposed method may be applied as well as RC columns in Fig. 2. A comparison with the values from experimental trials of SRC columns [4] is examined. The cross sections are shown in Fig. 3, and the results are shown in Table 2. It appears that the proposed method is valid, not only for RC columns but also for SRC columns. Thus, it is possible to calculate the ultimate displacement between RC and SRC columns with same method.

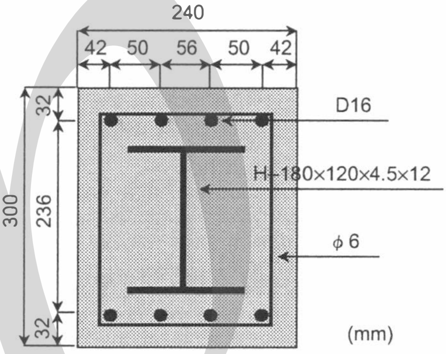

Shear span = 900 mm; Axial loads = 6.8 MPa

Fig.3 Cross section of SRC columns

Table 2 Comparison with SRC columns

Speci-men	Spacing of ties (mm)	Buckling Mode N_B	Results (mm)	
			Proposed method	Experi-ments
N100	100	2	25	27
N150	150	1	28	29
N200	200	1	26	25

4 CONCLUSION

Comparison with the experimental results shows that the proposed buckling model is valid. It can simulate the buckling of bars while taking the plasticity of bars and the prevention of bucking by the cover and the ties into account.

The simple method is proposed based on the buckling analysis. The proposed method makes it possible to calculate the ultimate curvature accurately without the use of the buckling analysis.

It also makes it possible to calculate the ultimate displacement accurately for both RC and SRC columns by use of the same method.

REFERENCES

[1] Asazu, N., Unjoh S.,Hoshikuma, J. and Kondoh, M.: Plastic Hinge Length of Reinforced Concrete Columns Based on the Buckling Characteristics of Longitudinal Reinforcement. Journal of Structural Mechanics and Earthquake Engineering, No.681, I-56, pp.177-194, Jul., 2001 (in Japanese)

[2] Hoshikuma, J.,Nagaya, K. and Unjoh, S.: Plastic Curvature Profiles and Plastic Hinge Length in Reinforced Concrete Columns under Cyclic Loading. Journal of Structural Engineering, Vol.47A, pp.1461-1468, Mar., 2000 (in Japanese)

[3] Mattock,A.H.: Discussion of Rotational Capacity of Reinforced Concrete Beam by W.G.Corley. Structure Div., ASCE, pp.519-522, Aug., 1967

[4] Naka, T., Morita, K. and Tachibana, M.: Strength and Hysteretic Characteristics of Steel-Reinforced Concrete Columns (Part II). Journal of Struct.Constr. Engineering, AIJ, Vol.260, pp.47-58, Oct., 1977 (in Japanese)

SEISMIC SAFETY EVALUATION OF PRESTRESSED CONCRETE TANKS IN CONSIDERATION OF LEVEL II EARTHQUAKE MOTIONS

Motoyuki Suzuki Hiroshi Nishio Kazuma Omura Mitsuyoshi Akiyama Shinya Esumi
Graduate School of Eng., Tohoku University, JAPAN
Abe Kogyosho Co.Ltd., JAPAN
Graduate School of Eng., Tohoku University, JAPAN

Keyword: prestressed concrete tank, seismic design, seismic response analysis, hydrodynamic pressure

1 INTRODUCTION

After the Hyogo-ken Nanbu Earthquake, level II earthquake motions were taken into consideration in formulation of the current Japan design code for prestressed concrete tanks for water supply [1]. In this study, seismic performance of the tank walls of a prestressed concrete circular tank for water supply designed according to the current code is evaluated using elasto-plastic seismic response analysis in conjunction with the FEM model in which the internal water is directly modeled using three-dimensional fluid elements. Then, to devise a simple analytical method for seismic performance evaluation of the tank wall, the accuracy of the responses based on the dynamic analysis in which the effect of the hydrodynamic pressure is converted to mass elements and the accuracy of the equal-energy assumption provided in the current code are verified.

2 ELASTO-PLASTIC SEISMIC RESPONSE ANALYSIS

2.1 Analytical method

This research focuses on a prestressed concrete circular tank for water supply designed according to the Japanese design code as shown in Fig. 1, the capacity of which is about 10,000 m^3. The ratio of the diameter to the wall height is 3.5 and the wall is assumed to be rigidly fixed to a concrete base. The tank wall is prestressed in both of the circumferential and vertical directions, and the dome ring is prestressed in the circumferential direction only. The prestressing force of the tank wall in the circumferential direction is the additional compression force (1.0 MPa) provided in the code plus the hoop tension induced by hydrostatic pressure. The number of reinforcing bars in the circumferential and vertical directions is about the minimum specified in the code. As a result, the seismic performance of the tank meets the requirement for level II earthquake motions specified in the code. In this paper, we call this tank the standard tank.

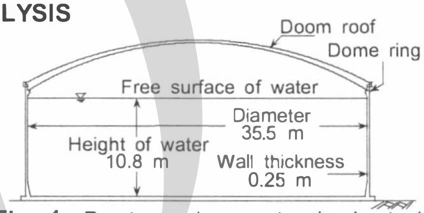

Fig. 1 Prestressed concrete circular tank

Table 1 Material properties

Concrete	Young's modulus	2.98×10^4 MPa
	Poisson ratio	0.2
	Density	2450 kg/m^3
Reinforcing bar	Young's modulus	2.10×10^5 MPa
	Poisson ratio	0.3
Prestressed steel cable	Young's modulus	2.00×10^5 MPa
	Poisson ratio	0.3

Numerical analysis is carried out using the finite element method. Due to symmetry, it is sufficient to model only one half of the tank. Curved shell elements are used to model the tank wall and roof. The internal liquid is modeled using three-dimensional fluid elements. Reinforcing bars and prestressed steel cables are modeled as the layer, in which bars and cables are embedded. In addition, fluid-tank interface elements are used in dynamic fluid-tank interaction analysis to couple the fluid to the structural domain.

The stress-strain curve for concrete is assumed to be elasto-perfectly plastic. The yield condition of Drucker-Prager and smeared crack modeling are used for concrete. The tension stiffening effect is considered after cracking. The stiffness in the unloading process consists of the initial stiffness for compression and the origin-oriented stiffness for tension. The stress-strain curve for a reinforcing bar is assumed to be elasto-perfectly plastic, whereas it is assumed to be a tri-linear for a prestressed steel cable. The material properties used for analysis are shown in Table 1.

Time-history responses are obtained by direct time integration, in which Newmark's β method with the assumption β = 1/4 is used as the numerical integration scheme and the calculation time increment is 1/500 second. As horizontal ground excitation, the waveform observed at the Kushiro Meteorologic Observatory during the Kushiro-oki Earthquake, whose acceleration spectrum at the natural period region of the standard tank is about 2.5 times larger than the corresponding design spectrum, is used.

2.2 Analytical results

The time-history response of the hoop tension at the intermediate part of the tank wall, which has a great influence on seismic safety, is shown in Fig. 2. As a result, cracking takes place in the tank wall at 0.08 seconds after the acceleration input, but the hoop strain is much less than the yield strain of the reinforcement, which is specified in the design code as the allowable strain for maintaining watertightness. Consequently, it is confirmed that the standard tank is able to maintain the level of seismic performance specified in the current code even for a seismic force about 2.5 times greater than the design seismic force.

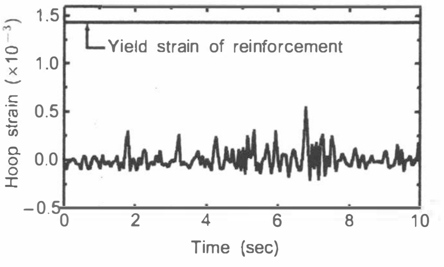

Fig. 2 Time-history response of hoop strain

3 SIMPLE ANALYTICAL METHODS FOR SEISMIC PERFORMANCE EVALUATION

3.1 Elasto-plastic seismic response analysis using added mass modeling

We simplify the FEM model by assigning added mass elements, which have equivalent inertia effect on hydrodynamic pressure as calculated by the velocity potential method [1], to each node on the tank wall.

We input a twofold amplitude of the acceleration record to the standard tank, and compare the responses obtained from fluid element modeling and added mass modeling when the standard tank shows more significant nonlinearity. The comparative time-history response of the hoop strain at the intermediate part of the tank wall for both models are presented in Fig. 3. The reinforcing bars arranged in the circumferential and vertical directions yield. By comparing two plots in Fig. 3, the added mass model is seen to be able to yield reasonably accurate predictions even where the standard tank shows nonlinearity of the degree of yielding of the reinforcing bars. Considering that the original acceleration record of the Kushiro-oki Earthquake is much larger than that of the design seismic wave, it is thought that the added mass model is sufficiently useful to evaluate the seismic safety of a prestressed concrete tank.

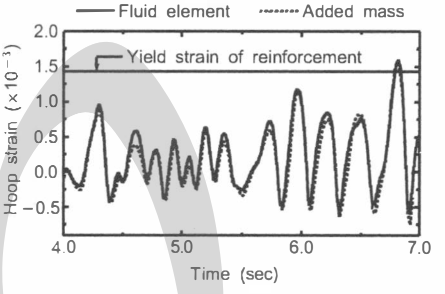

Fig. 3 Comparative time-history response of hoop strain for two modeling

3.2 Estimation of hoop strain based on equal-energy assumption

Here, hoop strain ε_r, based on the equal-energy assumption provided in the current code [1], is compared with hoop strain ε_d, obtained from elasto-plastic seismic response analysis.

Hoop strain ε_r is 1760 μ, whereas hoop strain ε_d is 556 μ. Thus, hoop strain ε_d is less than the allowable strain, but hoop strain ε_r is larger than the allowable one. Therefore, as far as this study goes, the hoop strain obtained by the equal-energy assumption is estimated to be considerably on the safe side. Therefore, it is thought that the prestressed concrete tank may be designed more rationally by applying dynamic analysis in conjunction with the use of added mass model to seismic performance estimation.

4 CONCLUSIONS

Firstly, it was confirmed that the wall of the prestressed concrete tank designed according to the Japanese design code was able to maintain the seismic performance specified in the current code, even for a seismic force about 2.5 times greater than the design seismic force.

Secondly, we simplified the FEM model by assigning additional masses, which have an equivalent inertia effect on hydrodynamic pressure, to each node on the tank wall. As the result, the response obtained from the model with the use of added masses was able to yield reasonably accurate predictions.

Finally, it was confirmed that the hoop strain based on the equal-energy assumption was larger than that obtained from dynamic analysis but was estimated on the safe side.

REFERENCES

[1] Japan Water Works Association: Design and Construction Criteria on Prestressed Concrete Tank for Water Supply, May, 1998 (in Japanese)

SEISMIC SAFETY ANALYSIS OF CONNECTED GIRDER BRIDGE DUE TO FAULT DISPLACEMENT

Masaru NARITOMI
Kyushu Kyoritsu University, JAPAN
Shuichi KITADAI
Japan Engineering Consultants Co.,ltd, JAPAN
Hisanori OTSUKA
Kyushu University, JAPAN
Kazuhiko TAKEBAYASHI
Chuoh Consultants Co.,ltd, JAPAN
Kinji MITUI
Fuji-ps Co.,ltd, JAPAN

Keywords: fault displacement, PC connected girder-bridge, nonlinear static analysis, enforcement displacement input

1 INTRODUCTION

The design method of bridges in Japan was improved after the Great Hanshin Earthquake of 1995 to secure its earthquake performance. However, there is quite few experimental data to estimate damage mechanism of bridge caused by fault displacement. Thus, the authors evaluated the safety of bridges that suffered fault displacement using forced displacement nonlinear static analysis due to various cases of fault movements. The target bridges are reinforced concrete bridges and prestressed concrete bridges designed according to 1980 and 1996 design codes, respectively.

Two different types of bridges were investigated; specifications are shown in table 1.

Table1. Specifications of bridges investigated

	Bridge A	Bridge B
Structural type	6 spans continuous PC composite girder bridge	3 span combination pretension system PC floor system bridge
Application specification	1980 specifications for highway bridges.	1996 specifications for highway bridges
Span length	29.5 m+ 4 X 30.0 m + 25.0 m	19.2 m +20.2 m + 19.2 m
Effective width	9.60 m	4.0 m
Pier height	19.0 m ~ 32.0 m	10.1m

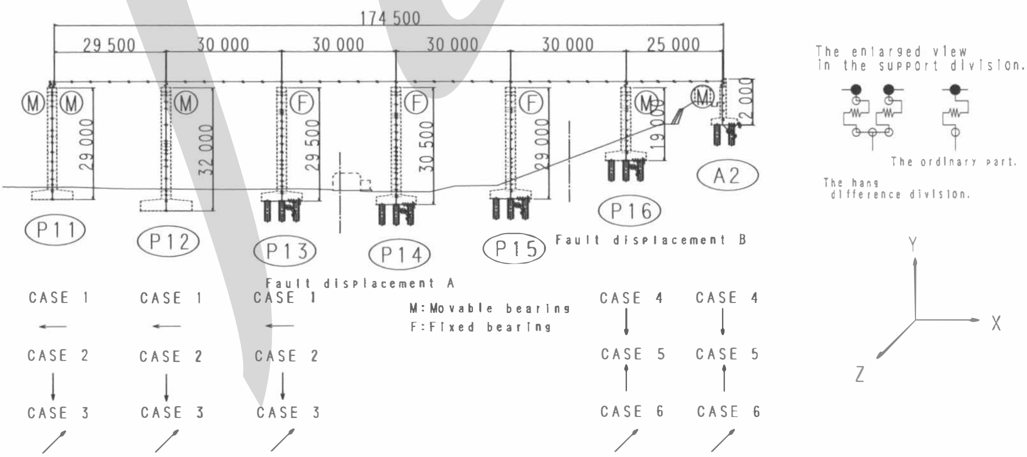

Fig. 1 Analytical model and analysis case (bridge A)

2 ANALYTICAL MODEL AND ANALYSIS CASE

In fig. 1, firstly case of the bridge A and secondly analytical model is described.

Analyses were carried out with fault displacement magnitude lies between the range of 0.01 to 2.0 m and 0.01 to 0.1 m with the serration of 0.01m and 0.05 m respectively. Direction of the fault displacement gave the enforcement displacement to the lower end of the footing of each pier and abutment on the assumption of bridge axial direction, bridge axis cross and vertical direction.

3 THE ANALYTICAL RESULTS

Fig. 2 shows the relationship of generated bending moment and its capacity of P13 (bridge A).

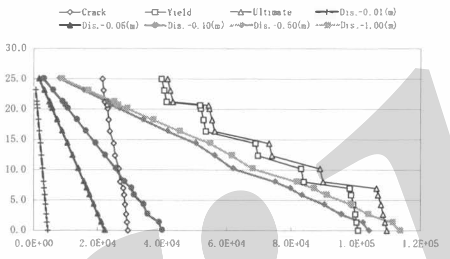

Fig. 2 P13 generation bending moment

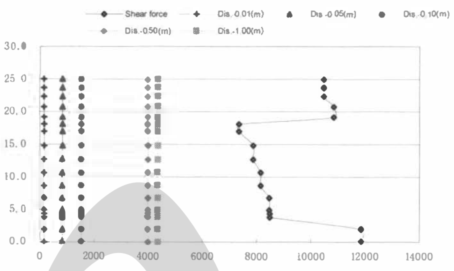

Fig. 3 P13 generation shear force

Bending moment shows stress and generation of the bending moment in the superstructure as in case 2 (the vertical displacement downward) is shown in fig. 4. The yield resistance exceeds at P13 pier at vertical displacement of 0.50 m in main girder sill side in the position of P14 pier side 5.00m however, threshold values of yield strength hasn't increased even though with a vertical displacement of as high as 2.0 m.

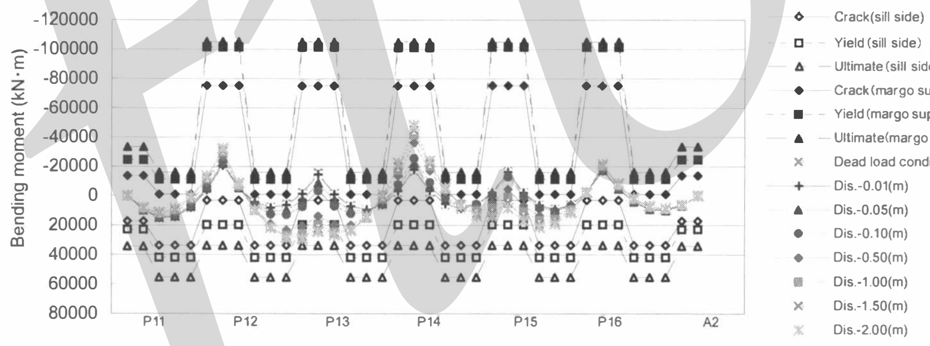

Fig. 4 Relationship between bending moment proof stress and generation bending moment of the superstructure

4 THE SUMMARY

It was concluded that faults tended to generate the damage in a case in which the faults were generated in vertical direction; bridge axial direction and bridge axis cross at the pier for super structures.

PEFERENCES

[1] Japan Road Association: Specification of highway bridge, III-concrete bridge design edition, 1996.12

[2] Japan Road Association: Specification of highway bridge, V-seismic design edition, 1996.12

SEISMIC PERFORMANCE OF BRIDGE COLUMNS WITH INTERLOCKING SPIRAL/HOOP REINFORCEMENT

Koichiro Shito, Yoshinori Igase, , Gaku Ohashi
Research Institute Japan Highway Public Corporation
Yoshiharu Mizugami
Sendai Engineering Office Tohoku Regional Bureaus Japan Highway Public Corporation
Toshiaki Miyagi, Toshiyuki Kuroiwa
Institute of Technology Tokyu Construction Co., Ltd.

Keywords: Interlocking spiral/hoop reinforcement, flexural, shear, seismic performance

1. INTRODUCTION

Transverse reinforcement using interlocking spirals/hoops is one of the rational transverse reinforcing methods for reinforced concrete columns with rectangular cross section because of its easy construction procedure and effective lateral confinement.

The previous test results showed that the performance of interlocking columns was satisfactory and the flexural and shear capacities can be conservatively calculated using current procedures. However, the response of interlocking columns under seismic loading has not been fully studied yet and few relevant experimental data are available for the design purpose in Japan.

The objectives of this study were to experimentally investigate the performance of columns with interlocking spirals/hoops under flexural and shear loading. Three columns with interlocking spirals were tested under cyclic lateral loading in longitudinal direction in order to study the flexural behavior. A conventional column with rectangular hoops and cross ties was tested to assess the performance of the flexural test units. Shear behavior of the columns with interlocking hoops was demonstrated using three test units subjected to cyclic lateral loading in transverse direction.

2. EXPERIMENTAL PROGRAM

The details of the test columns and the measured material strengths are shown in Fig.1. The columns were tested under constant axial compression load and cyclic lateral load in single bending. Flexural test units were loaded on the weak axis of the cross section and the shear units were on the strong axis. Based on the axial force levels of the prototype structures, the axial stresses of 0.8MPa and 1.5MPa were applied to the flexural and shear test units respectively by a load beam and a pair of high strength steel rods. After the axial force was attained, the columns were subjected to lateral force increasing cyclically, under force control, to the shear force of $0.75V_{JRA}$, where V_{JRA} was the flexural strength computed from Specifications for Highway Bridges (JRA code) approach using the measured material strengths. Subsequently, the specimens were subjected to increasing displacement ductility levels with three cycles at every stage.

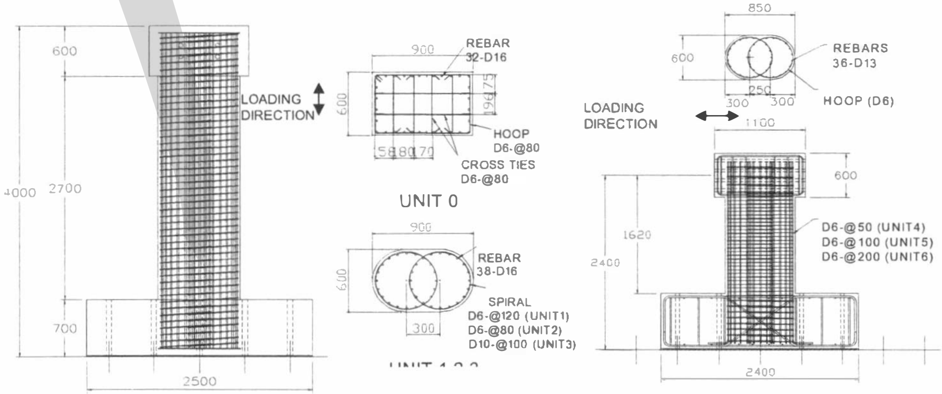

(a) UNIT 0,1,2,3 (b) UNIT 4.5.6

Fig.1 Reinforcement Details of Test Columns

3. TEST RESULTS

3.1. Flexural Test

Measured lateral force-displacement hysteresis loops for Unit 0 through 3 are plotted together with the theoretical flexural responses in Fig.2.

All units exhibited ductile flexural responses with good energy absorption capacity.

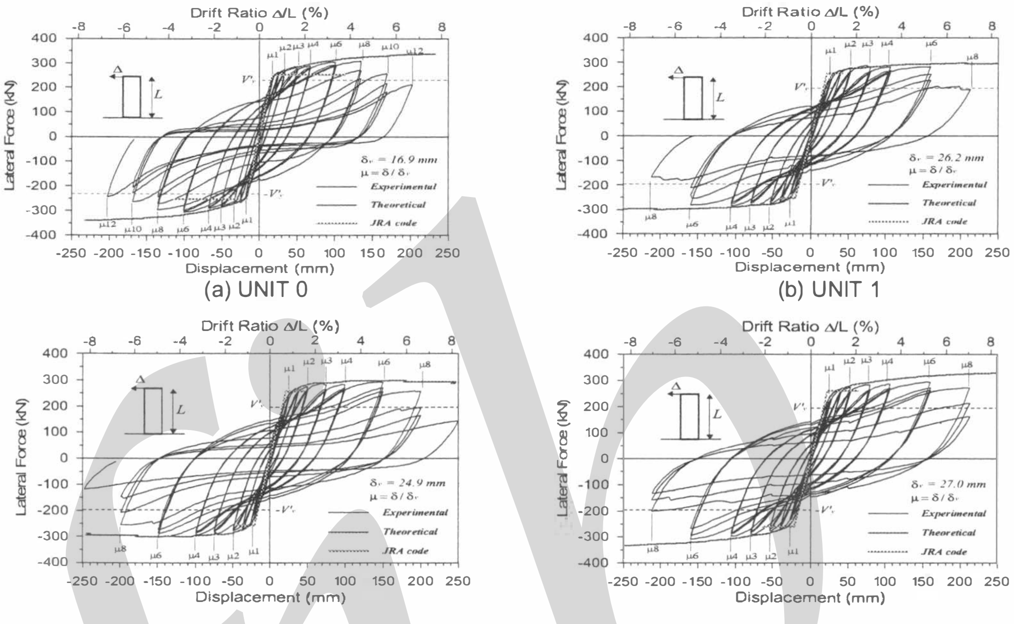

(a) UNIT 0 (b) UNIT 1

(c) UNIT 2 (d) UNIT 3

Fig.2 Lateral Force Displacement Response

3.2. Shear Test

The failure mode was categorized by a shear failure after flexural yielding. The shear test units with different reinforcement ratio showed different failure mode corresponding to the amount of the reinforcement. However, no test units exhibited brittle shear failure, even though the transverse reinforcement ratio was only 1/4 (UNIT6) of an existing bridge column.

4. CONCLUSIONS

The test results showed that the flexural strength and the deformation capacity of the interlocking spiral columns were quite comparable to those of the conventional rectangular column even though the volumetric confinement ratio of the interlocking column was about 34% (UNIT2) of that in the rectangular column. The shear test units with different reinforcement ratio showed different failure mode corresponding to the amount of the reinforcement. However, no test units exhibited brittle shear failure, even though the transverse reinforcement ratio was only 1/4 (UNIT6) of an existing bridge column. For the design purpose, flexural strength and deformation capacity of interlocking columns can be accurately predicted using conventional procedures. Also, taking the core area of the cross section as an effective shear area and taking the shear resistance of two spirals into account, current design equations for shear strength can be used to conservatively estimate the shear strength of the interlocking columns.

REFERENCES

1) ACI. 1995. *Building Code Requirements for Reinforced Concrete and Commentary*. ACI Committee 318, American Concrete Institute, Detroit, MI. revised 1995.
2) JRA. 1996. *Specification for Highway Bridges Part V Seismic Design.* (in Japanese) Japan Road Association, 228pp.

ASEISMIC BEHAVIOR ASSESSMENT OF A LONG-SPAN COMPOSITE EXTRADOSED BRIDGE (KISO RIVER BRIDGE)

Makoto Nakasu Makoto Yanaka
Japan Highway Public Corporation
Japan

Shinichi Yamanobe Hiroaki Okamoto
Kajima Corporation
Japan

Keyword: aseismic design, composite extradosed bridge, dynamic interaction, Level 2 earthquake

1 INTRODUCTION

This paper presents a methodology to assess the aseismic behavior of a composite extradosed bridge assuming active faults. The objective bridge is Kiso River bridge, which is a 5-span composite extradosed bridge with length of 1,145m. The general view of the bridge is shown in Fig. 1.

The purposes of this study are to classify problems related to the safety of the bridge and to establish a new seismic design method. In the study, the behaviors during earthquakes were analyzed taking into consideration the structural characteristics of PC-steel composite continuous extradosed bridges, topography and geology of the construction site, and past earthquake disasters. Fig. 2 shows the flow of the analysis.

2 INPUT MOTIONS FOR DESIGN BY ANALYSIS ON WHOLE-STRUCTURE MODELS

In this study, ground motions at stiff diluvial deposits assuming the Ansei-Tokai and Yoro-Isewan Fault earthquakes, which would cause the heaviest possible damage to the Kiso River Bridge, were first prepared as the strong ground motions for design. The seismic activity evaluation method which took into account the extent of earthquake-causing faults was used and the previous historical earthquakes and active faults near the construction site were taken into consideration[1].

Based on the above strong ground motions for design, the input motions for aseismic design at the top of the bridge foundation were then created by a dynamic interactive response analysis on a two-dimensional whole-structure model. The model consisted of the surrounding ground, foundation, pier and superstructure portions. The analysis took into consideration the characteristics of the surrounding ground and foundation, and the dynamic interaction between the ground and foundation.

The concept of effective ground width is shown in Fig. 3. Fig. 4 compares the results between the two-dimensional and the three-dimensional analyses. In the two-dimensional analysis, a model with an effective width of 1B and fitted with dampers was selected, since it yielded the closest results to the three-dimensional analytical results.

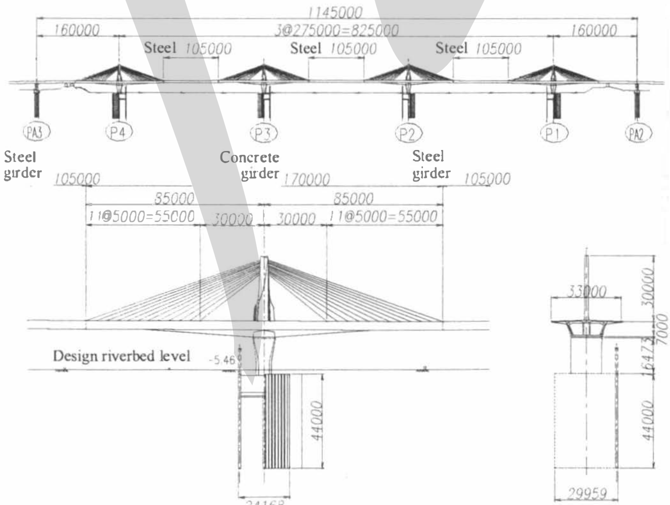

Fig. 1 General view of the Kiso River Bridge

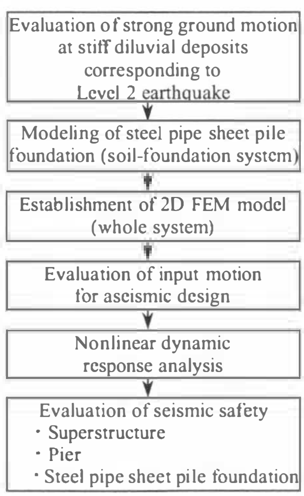

Fig. 2 Analysis flow

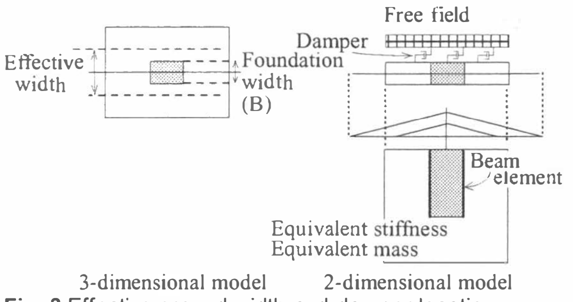

Fig. 3 Effective ground width and damper location

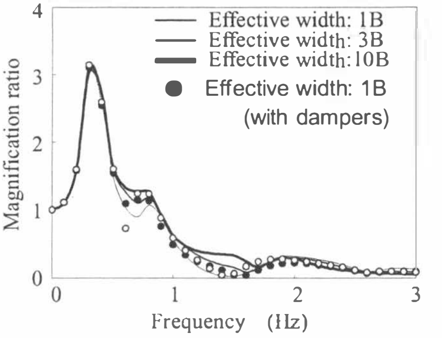

Fig. 4 Comparison of transfer function at the pier bottom

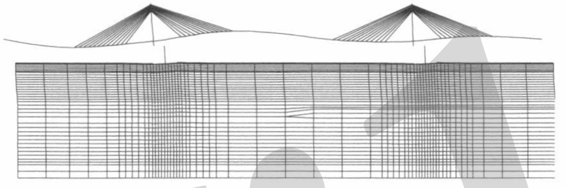

Fig. 5 Natural vibration modes of two-dimensional whole-structure analysis model

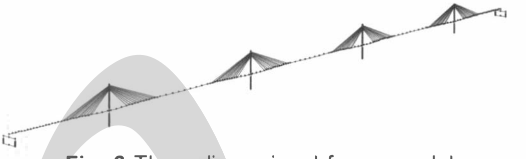

Fig. 6 Three-dimensional frame model

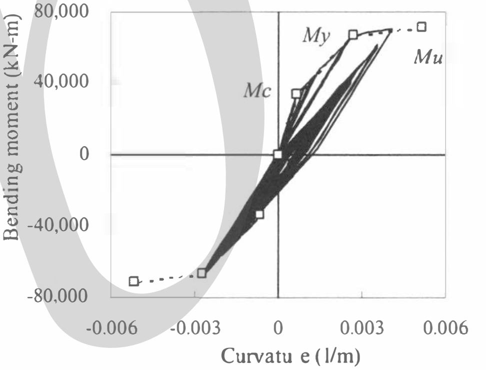

Fig. 7 M-ϕ curve for bottom of tower

One of the representative natural modes of the two-dimensional whole-structure model is shown in Fig. 5.

3 EVALUATION OF SEISMIC SAFETY BY DYNAMIC ELASTO-PLASTIC ANALYSIS

Finally, the seismic safety of bridge members was checked by performing a dynamic elasto-plastic analysis on a three-dimensional pier-superstructure frame model, using the input seismic motions. The three-dimensional frame model is shown in Fig. 6.

The analysis revealed that none of the members would sustain serious damage from possible earthquakes. Fig. 7 shows the bending moment-curvature path at the bottom of the main tower when subjected to the simulated Ansei-Tokai earthquake in the transverse direction. Although the bending moments at the bottom of the towers were smaller than the ultimate moment, they were considerably larger than the yield moment. Since the main towers are the most important members in terms of seismic safety, the cross-sectional shape of the main towers was therefore modified.

This reasurch was conducted under the guidance of the Committee on the Technical Studies and Seismic Design for the Kiso River Bridge on the New Meishin Expressway (chairman: Professor Kenzo Toki, Kyoto University).

REFERENCES

[1] Nakasu M., Yanaka M., Ikeura T. and Ohbo N.: Assessment of strong ground motion for seismic design of The Kiso River Bridge assuming active fault, Proceedings of the 1st fib Congress Osaka, 2002.

[2] Japan Road Association: Specifications for Highway Bridges: Parts I-V, Dec., 1996 (in Japanese)

ASSESSMENT OF STRONG GROUND MOTION FOR ASEISMIC DESIGN OF THE KISO-RIVER-BRIDGE ASSUMING ACTIVE FAULT

Makoto Nakasu Shin Yanaka
Japan Highway Public Corporation

Naoto Ohbo Tomonori Ikeura Masanori Niwa
Kajima Corporation

Keywords: seismic design, strong ground motion, active fault, bridge

1. INTRODUCTION

The concept of a evaluation of strong ground motion level 2, historical earthquakes and active faults near the objective site is firstly investigated. Then, the fault parameters are determined for these subject earthquakes. To consider the rupture spreading of active faults, the following three methods are adopted to evaluate the strong ground motion at engineering base layer: 1) Attenuation formula using equivalent hypocentral distance; 2) Semi-empirical method using a hybrid of stochastic and deterministic model; and 3) Normal mode method.

In this study, the active faults and historical earthquakes near the construction site of the bridges are determined, and the seismic motions of level 2 are evaluated using various methods.

2. DETERMINATION OF SUBJECT EARTHQUEAKES AND FALUT PARAMETERS

In this study, basically, historical earthquake selection is based on 'Japan Damaging Earthquakes'[1], and active fault selection is according to 'Japan Active Fault'[2]. Yoro-Isewan-Fault earthquake is also adopted as subject earthquakes. Figure 1 shows the location of objective site and subject earthquakes. As a fault parameters of historical earthquakes, those proposed in the past researches are adopted.

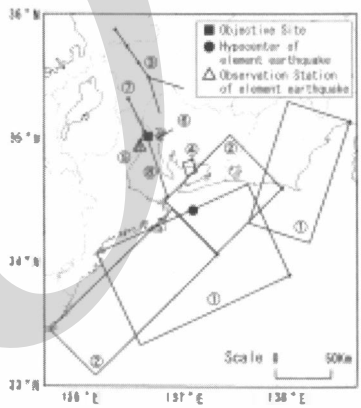

Fig.1 Selection of the subject earthquakes for evaluation

3. EVALUATION OF STRONG GROUND MOTION

Nine determined subject earthquakes are shown in Fig. 2. First, for six inland subject earthquakes (see Fig. 1), the attenuation formula using equivalent hypocentral distance are used. Then for three large earthquakes, Ansei-Tokai-, Tonankai- and Yoro- Isewan- earthquakes, semi-empirical method has been applied.

3.1 Evaluation of strong ground motions due to six inland earthquakes using attenuation formula[3]

For the period range of 1-2 seconds which is around the fundamental period of structure, the amplitude becomes smaller according to the following order: Yoro, Kuwana, Isewan, Nobi, Tenpaku-Kakou, Mikawa. Yoro fault has the largest effects on the ground motion at the objective site.

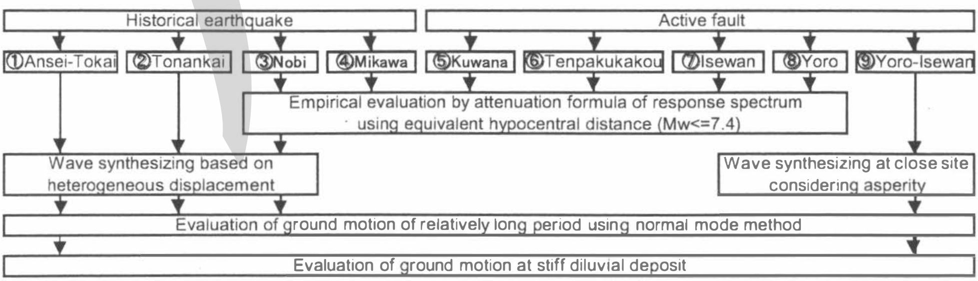

Fig.2 Flowchart of the evaluation of ground motion

3.2 Evaluation of the strong ground motion using semi-empirical method

In the cases of the evaluation of the strong ground motion due to the plate boundary earthquakes, which are Tokai-Earthquake and Tonankai-Earthquake, the recorded ground motions at Yokkaichi-harbor due to the small earthquake are used as element earthquakes. The maximum acceleration and acceleration response spectrum are larger in the case of Ansei-Tokai-Earthquake.

In the case of the evaluation of the strong ground motion due to a large inland earthquakes, Yoro-Isewan-Earthquake which is large and close, to the ground motions are synthesized assuming the existence of the asperity. The spectra due to the small earthquakes computed by attenuation formula of average spectrum of California described previously, is used to generate fitting waveforms.

3.3 Evaluation of the surface waves of long period by normal mode method[4]

In the evaluation of the ground motions of relatively long period by normal mode method, Ansei-Tokai-Earthquake is slightly larger than those due to other Tonankai, Nobi, and Yoro-Isewan earthquake.

4. SYNTHETIC STUDY

Figure 3 shows the acceleration waveforms and response spectra of the ground motion for level 2 at the supporting layer due to Ansei-Tokai-Earthquake and Yoro-Isewan-Earthquake. For comparison of the spectrum, the spectra of type I and type II for Group I soil condition suggested in Specifications for Highway Bridges[5] are also shown in the same figure.

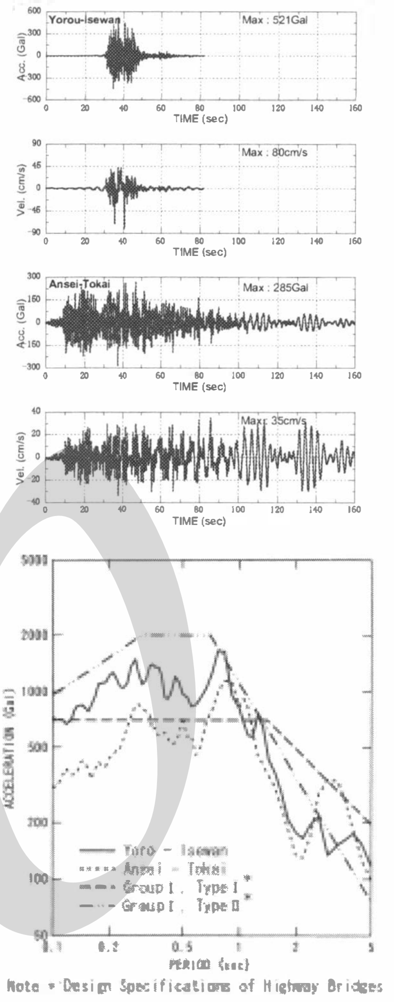

Fig.3 Ground motions and spectra of level 2 design

5. CONCLUSIONS

It is found that the ground motion due to the Yoro-Isewan-Earthquake has the largest effects in short period range, and the ground motion caused by Ansei-Tokai-Earthquake has the most significant effects in relatively long period range.

Acknowledgements:
This study is performed under the guidance of Aseismic design committee (Chairman: Prof. Toki) for study on design and construction of Kiso-sansen-Bridge of New Meishin Expressway(1999).

REFERENCES

[1] Usami, T., :Damaging earthquakes in Japan, newly edited, Publishing House of University of Tokyo, 1996(in Japanese).

[2] Research committee on active faults, :Distribution map of Japan's active faults and materials, newly edited, Publishing House of University of Tokyo, 1991(in Japanese).

[3] Ohno, S. et al., :Intensity of strong ground motion on Pre-Quaternary stratum and surface soil amplifications during the 1995 Hyogo-ken Nanbu earthquake, Japan, J. Phys. Earth, 44, 623-648, 1996.

[4] Kudo, K., :Prediction of ground motion of relatively long period and related problems, Pro. 10th Symposium on ground vibrations, JSAE, pp57-64, 1982(in Japanese).

[5] Road Association, :Specifications for highway bridges, Japan Road Associations, Part V, 1996(in Japanese).

SEISMIC BEHAVIOR OF REINFORCED CONCRETE MEMBERS WHICH USED COAL ASH

Hideo Araki Shunsuke Sugano Kenji Kabayama
Graduate School of Engineering, Hiroshima University
1-4-1 Kagamiyama, Higashi-hiroshima, 739-8527 JAPAN

Keywords: reinforced concrete, coal ash, utilization, seismic behavior

1 INTRODUCTION

The amount of industrial by-products, such as coal ash produced by coal-fired power plants, continues to increase with the demand for more electricity. It is said that total quantities of coal ash produced in Japan will be more than 10,000,000 tons in a couple of years as described in [1]. Utilization of coal ash is a very urgent objective for the environment conservation. In order to consume a large quantity of coal ash, the characteristics of concrete containing high volume coal ash have been investigated recently through the small size cylinder tests as reported in [2] and [3]. The mechanical characteristics of reinforced concrete, RC, members containing high volume coal ash should be investigated in order to utilize coal ash to building structural members. Three series of static loading tests which were carried out to investigate the seismic performance of RC members containing high volume coal ash were reported in this paper.

2 GENERAL TEST PROCEDURES

Three types of RC members were prepared in this experimental study. One of them was a beam type which was designed as the flexural failure type, and the others were column types which were designed as the shear-flexural failure type and the shear failure type. Tests of those specimens were named '**Beam Test**', '**SFCol Test**' and '**ShCol Test**', respectively. One of the parameters was a mix property for concrete containing coal ash. Three types, normal concrete, '**NC**', concrete containing coal ash as a partial replacement of fine aggregate, '**CA**', and high fluidity concrete containing coal ash as a partial replacement of cement, '**HF**' were assigned in each test series. F_C, designed compressive strength at 28 day, was 26N/mm^2 (MPa) for Beam Test and SFCol Test, and 36N/mm^2 for ShCol Test. Table 1 shows summaries of mix properties for concrete. Coal ash used in this study consisted fly ash and cinder ash. The physical properties of coal ash were corresponded to II class of JIS for fly ash.

The test beams, whose section was 600×300mm and length was 4,000mm, were loaded at two points symmetrically in Beam Test. The test column was a cantilevered type with a large footing in SFCol Test. The section of the column was 400×400mm and the height was 1,000mm. Test columns had stiffened stubs on their top and bottom in ShCol Test. The section of the column was 200×200mm and the height was 400mm. Test columns were subjected to cyclic lateral loadings under the constant axial load substituted for the gravity load in SFCol Test and ShCol Test.

3 TEST RESULTS AND DISCUSSIONS

All specimens in each test series had almost similar crack propagations and damaged area during the cyclic loadings. There was no influence of coal ash content on the crack patterns. Crack patterns at the failure stage of each test series are shown in Fig. 1. Load-displacement hysteresis loops were similar regardless of coal ash content in Beam Test and SFCol Test. Hysteresis loops of ShCol Test showed possibility that coal ash content improved the ductility of shear members. Maximum strength of each test series indicated that equations of ultimate flexural strength and shear strength for normal concrete were applicable to RC members containing high volume coal ash.

4 CONCLUSIONS

Seismic loading tests of three types of RC members containing high volume coal ash were performed. From test results, it is anticipated that there is strong possibility of utilizing concrete containing high volume coal ash for building structural members.

REFERENCES

[1] Japan Coal Ash Association (JCAA): Coal Ash Hand-book (2nd Edition), JCAA, 1995 (in Japanese)
[2] Malhotra, V. M.: Investigations of High-Volume Fly Ash Concrete Systems, EPRI TR-10315 Project 3176-66 Final Report, Oct. 1993.
[3] Tanigawa, T., et al.: Characteristics of Concrete Containing a Large Amount of Coal-Ash, Proc. of Japan Concrete Institute, Vol.17, No.1, 331-336, 1995

Table 1 Summaries of mix properties for concrete

Test series	Mix type	W/(C+Ca) Ratio (%)	W/C ratio (%)	Unit (kg/m^3)					
				Water	Bulk material		Fine aggregate		Coarse aggregate
					C	Ca	Sand	Ca	
Beam & SFCol Test	NC	52	52	186	358		810		927
	CA	42	60	180	300		569	124	1,062
	HF	32	70	175	250	300	697		791
ShCol Test	NC	43	43	187	435		748		921
	CA	37	50	180	360		591	121	1,022
	HF	31	61	175	285	285	698		785

W; Water, C; Cement, Ca; Coal ash

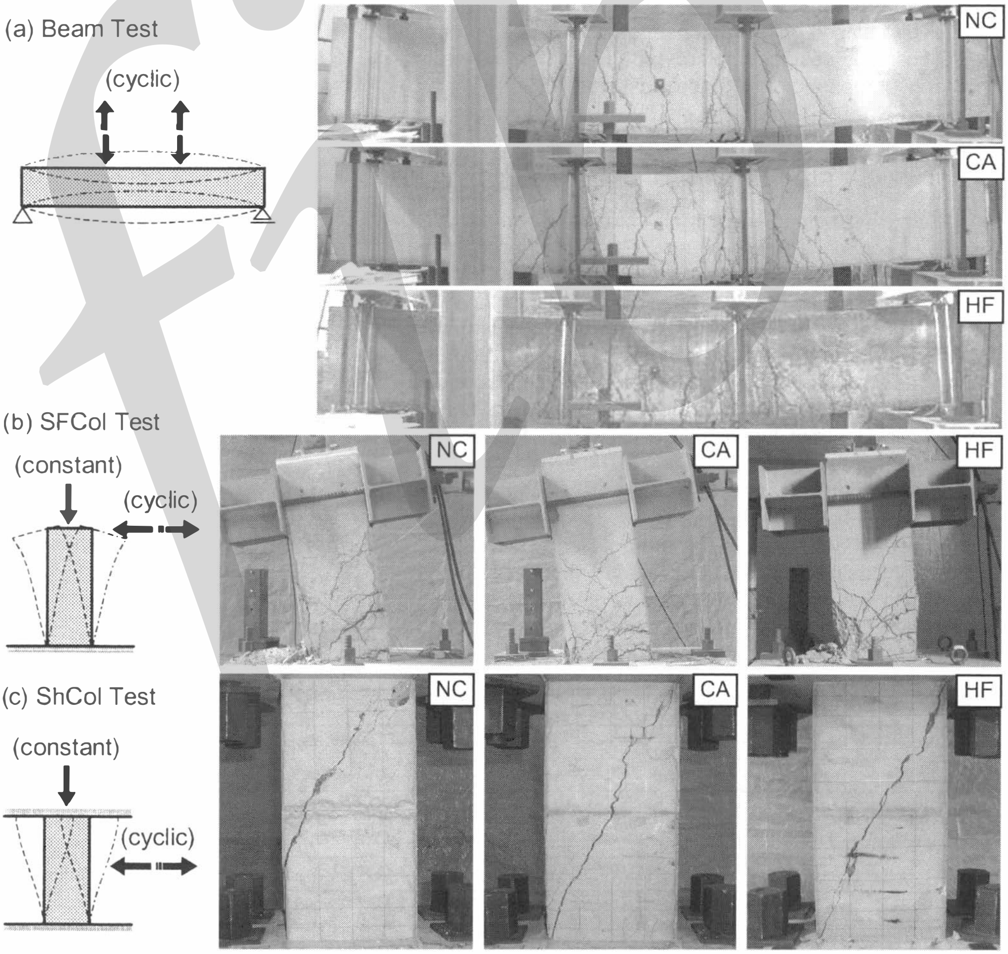

Fig. 1 Crack patterns at the failure stage of each test series

CONSTRUCTION OF SEISMIC RETROFITTING OF UNIVERSITY BUILDING BY USING CHS BRACES AND EXTERNAL PC-BARS FOR SHEAR REINFORCEMENT OF R/C COLUMN

Akihiro Sakaguchi[1)], Tadatoshi Furukawa[1)], Hisao Endo[2)], Ryoji Kinoshita[3)], Kazuaki Miyagawa[3)], Masayoshi Kurashige[4)], Isao Mitani[5)], Katsuhiko Imai[1)]

1) Dept. of Global Architecture, Osaka Univ.
2) Dept. of Facilities, Osaka Univ.
3) Kawasaki Steel Civil Eng. & Const. Corp
4) Koshuha-Netsuren Corp.
5) Dept., of Architectural and Civil Eng., Kobe Univ., Dr. Eng.

Key wards: Seismic Retrofit, CHS Braces, PC-bars, Dry-Process, Reduction of Cost

Many existing reinforced concrete (R/C) buildings designed before 1981 have poor seismic performance in Japan, because they had been designed in accordance with the old Japanese seismic design code, which was extensively revised in 1981. Consequently, a large number of R/C buildings designed before 1981 were more severely damaged comparing with those designed after 1981, by Hyogoken-Nanbu Earthquake, in 1995[1)].

In this paper, authors present the construction report of renewal project of 5-stories R/C building of Graduate School of Engineering Science, Osaka University, including the seismic retrofitting using CHS braces including FLD (Force Limited Device) and PC-bars for shear reinforcement of R/C columns.

The building was constructed in 1960. Seismic index of structure Is[6)] of original building is lower than the required capacity Iso in the first and second stories. The required value of seismic index of structure after retrofitting Iso is set to be more than 0.70. Since the index of story ductility F is relatively low, retrofit techniques to increase strength are employed as a basic strategy. To leave the existing opening section, steel flames with CHS bracing are placed on outer surface of R/C frame. In the first and second stories whose Is are lower than Iso, both the strength and ductility are improved by using FLD as CHS braces. The inner columns assumed to fail by shear stress are reinforced to improve ductility by PC-bars with small diameter that more attached for shear reinforcement to outer to surface of the columns

Photo. 1 Exterior of Existing Building

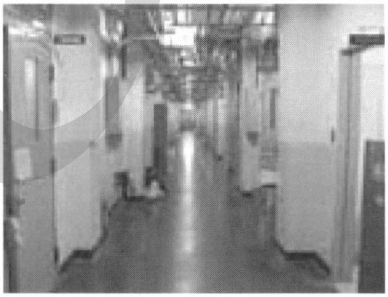

Photo. 2 Interior of Existing Building

Table 1 Seismic Evaluations in Longitudinal Direction

story	breaking type	C	F	Eo	Is
	CS	2.712	1.00	1.72	1.26
	CB	0.215	1.27	after reinforce	
5	reinforcement	0.000	1.00	1.72	1.26
	CS	1.697	1.00	1.22	1.00
	CB	0.180	1.27	after reinforce	
4	reinforcement	0.000	1.00	1.22	1.00
	CS	0.818	1.00	0.74	0.61
	CB	0.238	1.27	after reinforce	
3	reinforcement	0.199	1.00	0.89	0.73
	CS	0.478	1.00	0.62	0.51
	CB	0.352	2.27	after reinforce	
2	reinforcement	0.293	1.00	0.87	0.72
	CS	0.587	1.00	0.69	0.56
	CB	0.143	1.27	after reinforce	
1	reinforcement	0.228	1.00	0.92	0.75

Table 2 Seismic Evaluations in Span Direction

story	breaking type	C	F	Eo	Is
	CS	2.359	1.00	1.44	1.06
	CB	0.046	1.27	after reinforce	
5	reinforcement	0.000	1.00	1.44	1.06
	CS	1.479	1.00	1.05	0.87
	CB	0.140	1.27	after reinforce	
4	reinforcement	0.000	1.00	1.05	0.87
	CS	1.052	1.00	0.80	0.65
	CB	0.012	1.27	after reinforce	
3	reinforcement	0.111	1.00	0.88	0.72
	CS	0.853	1.00	0.80	0.66
	CB	0.113	2.27	after reinforce	
2	reinforcement	0.114	1.00	0.90	0.74
	CS	0.746	1.00	0.82	0.67
	CB	0.104	1.27	after reinforce	
1	reinforcement	0.089	1.00	0.91	0.74

by using specially designed corner blocks. The space between R/C frame and steel frame is used for the catwalk to install air conditioner and airing pipes ducts, and other piping for facilities. The catwalk and the cover-plate of these facilities are arranged to realize the aesthetic appearance of the facade design.

The work started at November 1st, 2000, and finished at March 29th, 2001. The term of work was 5 months. Comparing this method with conventional strengthening method, this method could shorten the term of work dramatically. The reason is that removing outer walls is not required because of placing steel braces on outer surface of the building. It was also greatly effective to shorter the term of work that installation of PC-bars required only small holes penetrating the sidewall of interior columns. Conventional method required dismantling outer walls and windows.

The full application of dry construction process and parallel construction of inner and outer work make it possible to shorten the period of construction and reduce the cost drastically. The construction cost regarding structural reinforcement is reduced to about 60% compared with the conventional method. Moreover, the use of the slender CHS braces with elegant joint details realizes the aesthetic appearance of the facade design.

Photo. 3 Steel Frame with CHS

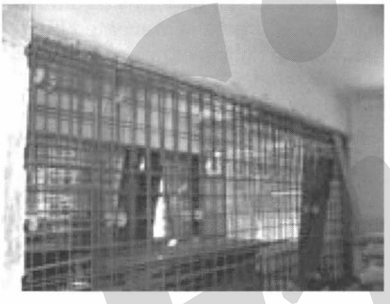

Photo. 5 Thickening Bearing

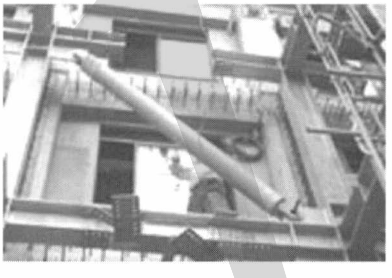

Photo. 7 Installation of Braces

Photo. 8 After Renewal

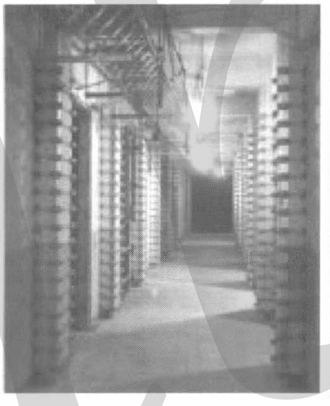

Photo. 4 Installation PC-bar

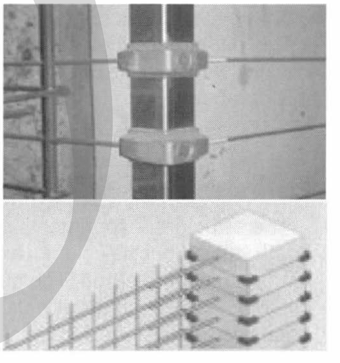

Fig 4 corner blocks

REFFRENCE

1. Okada, T. et. al., " Improvement of Seismic Performance of Reinforced Concrete School Buildings in Japan –Part 1 Damage Survey and Performance Evaluation after Hyogo-Ken Nanbu Earthquake", *Proc. 12th World Conf. Of Earthquake Engrg.*, Auckland, New Zealand, No2421, CD-ROM, 2000.1
2. JBDPA, "The Examples of Seismic Retrofitting of Existing R/C Building", JBDPA, 1997, (In Japanese)
3. Nikkei Architecture, "Earthquake Resistant Building -Learning from the Great Hanshin Earthquake", Nikkei BP, 1995, (In Japanese)
4. Nikkei Architecture, "Guidebook for Seismic Retrofitting", Nikkei BP, 1997, (In Japanese)
5. Ryoji Kinoshita, Kazuaki Miyagawa, Manabu Haginoya, Kazuyoshi Fujisawa, Katsuhiko Imai, Yasuhiro Ohtani, Isao Mitani, "Study on seismic Retrofit for Existing R/C Buildings by using CHS Bracing", *Proc. The First fib Cong. 2002*, CD-ROM, 2002.10, (Submitted)
6. JBDPA / The Japan Building Disaster Prevention Association, "Guideline for Seismic Capacity Evaluation of Existing Reinforced Concrete Buildings", JBDPA, 1990, (in Japanese)

DEVELOPMENT OF REINFORCED CONCRETE HYSTERETIC DAMPER

Yasuhiko Masuda Kuniyoshi Sugimoto Hidekatsu Asai Hiroaki Eto
Obayashi Corporation, JAPAN

Keywords: hysteretic damper, ductility, shear-flexural experiment, response analysis

1 INTRODUCTION

Reinforced concrete hysteretic damper (R/C-damper)[1] is developed. It is used for the pourpose of improving the seismic resistance of building, and is installed in mainly R/C structures. Photo-1 shows the R/C-damper and its name of each part. The R/C-damper is a seismic element, and consists of ductile columns and rigid panels, i.e. ductile columns are installed between rigid panels and the column height is about 1/3 of story height. Against small earthquake or wind vibration, the R/C-damper performs as a wall, thus maintaining comfort for residents. Against severe earthquakes, the main frame is prevented from heavy damage by the hysteresis damping of the R/C-damper. Fig-1 shows the outline of this system. As the deformation on each story drift concentrates to the ductile columns, the R/C-damper shows the efficiency as a hysteretric damper from small deformation level of the main frame.

This paper describes about the result of shear-flexural experiments on the R/C-damper to confirm the ductility of the ductile column and the response analysis on a high-rise reinforced concrete building using this damper.

2 EXPERIMENTS

The structural experiments consist of 3 series. The parameters of experiment were mainly height-depth ratio of ductile column, axial force, reinforcement of ductile column and rigid panel, and difference of construction method. The purposes of each series are as follows. Series-1 is to confirm the ductile column keeping the ductility until 1/50 radian of main frame's deformation, and to investigate the difference of structural performance under two types of precast method. Seres-2 is to increase the yield strength of ductile column and to make yielding at smaller story drift than series-1. And series-3 is to investigate the relation between ductility and axial load of R/C-damper. Fig.-2 shows the dimensions and reinforcement of the test specimens of series-2. Fig.-3 shows the typical load (Q)-story drift (δ) relationships of specimen.

From these three series of experiments, it was confirmed that the R/C-damper behaved as ductile member under cyclic loading, and its energy dissipation capacity was very high under low axial force ($\eta <$ 0.2). Ultimate deformation of the R/C-damper was also estimated by the method on reference [2] in good accuracy.

3 RESPONSE ANALYSIS

Non-linear dynamic analysis was carried out for an R/C 26 story building. Fig.-4 shows the frame of building and analytical model. The structural behavior was simulated by multi-mass model with parallel shear springs at each story. One was main frame's spring and the other was R/C-damper's. The characteristic of these springs under non-linear cyclic loading was used for the model from reference[3].

The response of each case of models to El-Centro-NS, Taft-EW, and Hachinohe-NS were analyzed. Fig.-5 shows the examples of maximum response on story drift. The response for Hachinohe was suitably decreased to about 70% of ordinary case by the hysteretic damper.

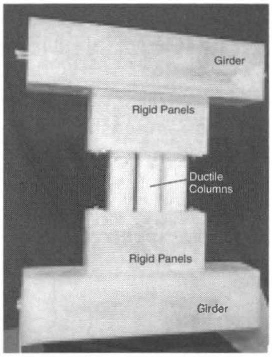

Photo-1 R/C-damper

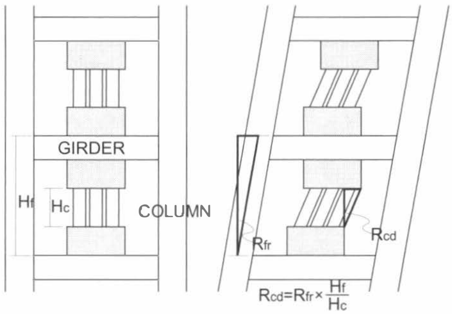

Fig.-1 The outline of damping system

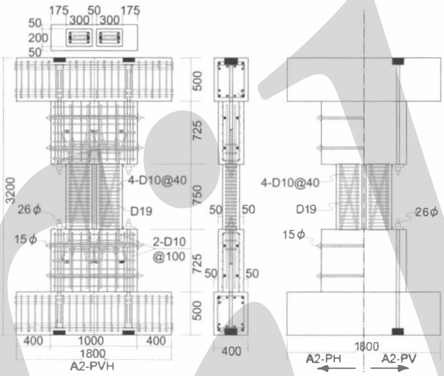

Fig.-2 The dimensions and reinforcement of the test specimens (series-2)

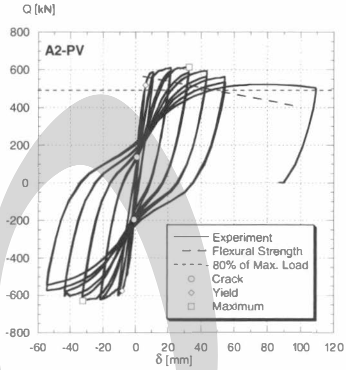

Fig.-3 Load (Q)-story drift (δ) relationships

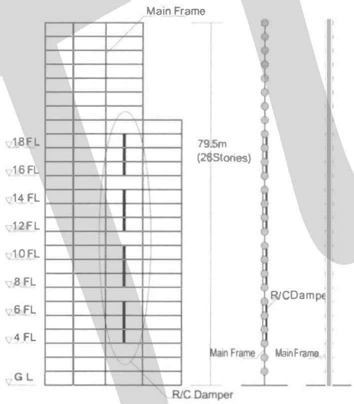

Fig.-4 Frame of building and analytical model

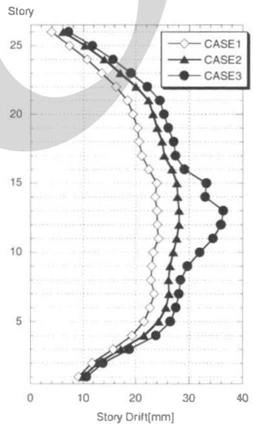

Fig.-5 Examples of maximum response on story drift

REFERENCES

[1] Kuniyoshi Sugimoto, Yasuhiko Masuda and Hiroaki Eto : Development of a Seismic Vibration Control System using Reinforced Concrete Member. Proceedings of the Japan Concrete Institute Vol.23, No.3, pp.1075-1080, 2001 (JAPANESE)

[2] Hiroshi Kuramoto and Koichi Minami : Utility Shear Design of Reinforced Concrete Member for Ductile Earthquake Performance. Proceedings of the Japan Concrete Institute Vol.10, No.3, pp.651-656, 1988 (JAPANESE)

[3] Takeda T, Sozen M A, Nielsen N N : Reinforced concrete response to simulated earthquakes. ASCE Journal, Structural Division 96(ST12), pp.2557-2573, 1970

TEST FOR SEISMIC PERFORMANCE OF CONCRETE COLUMNS MODEL DAMAGED BY ALKALI-SILICA REACTION AND PC CONFINED REINFORCEMENT METHOD

Kazutoshi Okuyama, P.S.Corporation, JAPAN
Kazuyuki Torii, Kanazawa University, JAPAN
Hiroshi Yokota, Mitsuyasu Iwanami, Port and Airport Research Institute Independent Administrative Institution, JAPAN

Keywords
Alkali-silica reaction (ASR), PC confined reinforcement method, outdoor exposure test, Alternating loading test

1. INTRODUCTION

In recent years, the deterioration of concrete structures due to the alkali-silica reaction (ASR) has been reported, and the repair and reinforcement of such structures has become a pressing issue. In the past, many studies have been conducted regarding the mechanism of ASR, the aggregate response, the problem of concrete deterioration caused by ASR and so on. However, the relationship between the damage caused by ASR and the load carrying capacity and ductility of members is not always clear. For this reason, the authors studied the PC confined reinforcement method as one method for repairing bridge piers damaged by ASR, with concrete bridge piers as the target structures.This method involves prestressing the bridge pier using lining PC tendons, in order to increase the lateral binding effect of the ASR-damaged bridge pier and prevent spalling of the covering concrete. The result is a bridge pier with excellent toughness. The purpose of this study was to confirm the impact of ASR damage on the dynamic behavior of concrete bridge piers in the event of an earthquake and confirm the reinforcing effectiveness of the PC confined reinforcement method. To accomplish these goals, outdoor exposure tests and alternating loading test conducted using ASR-damaged model concrete column test specimens.

2. TYPES OF TEST SPECIMENS

The test specimens were single stand-alone columns with footings. Starting in June 1997, the test specimens were exposed outdoors on the premises of the engineering department at Kanazawa University. There were five test specimens in all. Of these, one test specimen was a healthy test specimen in which no ASR had occurred, used for comparison purposes (N). The other four test specimens (A1, A2, S1 and S2) were test specimens in which the inducement of ASR was planned. Moreover, of these four ASR-generated test specimens, S1 and S2 were reinforced with PC confined reinforcement method after they had passed through the requisite exposure period. Table 1 shows a table of test specimens. Table 2 shows the concrete mix.

Table 1 Types of Test Specimen

Name	Type of Mix	Exposure Period	Reinforcement
N	N mix	1.5 years	None
A1	A mix	1.5 years	None
A2	A mix	3.5 years	None
S1	A mix	1.5 years	Done
S2	A mix	3.5 years	Done

Table 2 Concrete Mixes

Type	Unit Quantity (kg/m^3)				
	W	C	S	G1	G2
N	164	308	784	1125	0
A	164	308	784	563	562

G1:Non-reactive aggregate
G2:Reactive aggregate

3. STATUA OF TEST SPECIMEN DAMAGE CAUSED BY ASR (expansion coefficient)

The changes in the expansion coefficient over time were calculated by the changes in distance between contact chips attached in a total of 12 locations — three points each on the east, west, south and north sides — in the height direction of the test specimen. Fig.1 shows an example of the measurement

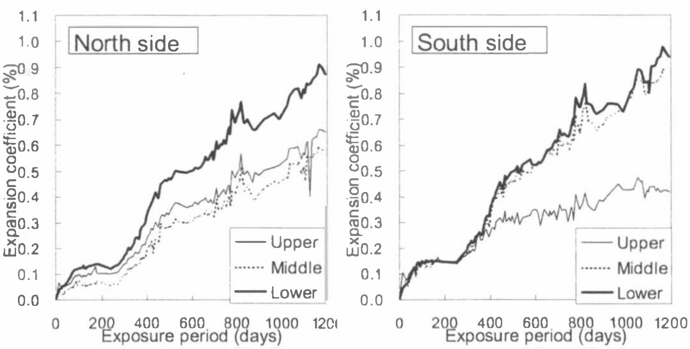

Fig. 1 Changes in Concrete Expansion Coefficient Over Time (A2)

results, for the A2 test specimen.

A year and a half after exposure was begun, the expansion coefficient was 0.3-0.4%. After three and a half years, it had reached a maximum of 1%. In addition, the south side had expanded more than the north side. This was because the damage was affected by the amount of sunlight.

4. RESULTS OF ALTEMATING LOADING TEST

Fig.2 show the load-displacement curves for each test specimen, respectively.

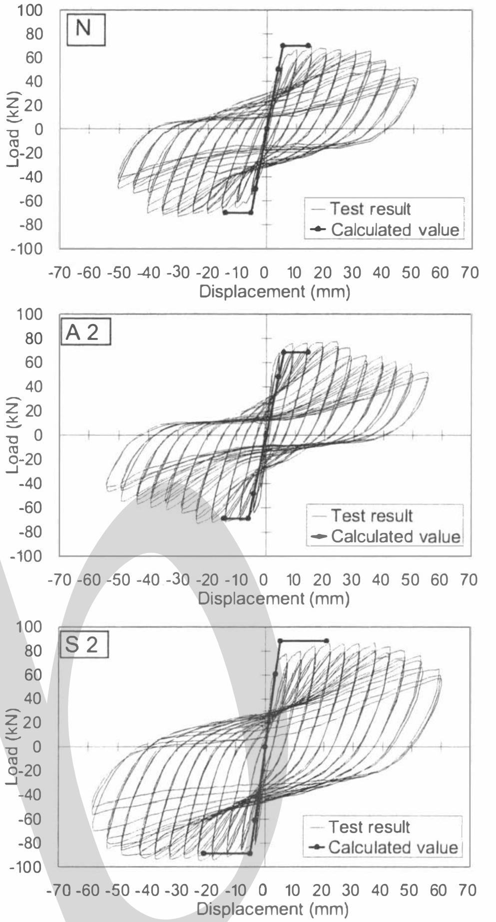

Fig. 2 Load-Displacement Curve

4-1 Effect of ASR damage

The maximum load was almost the same degree for test specimen N and test specimens A2. In other words, ASR damage of approximately 1.0% thickness for the concrete expansion coefficient had almost no effect on the load-carrying capacity of the reinforced concrete members. Nevertheless, the loading steps at which (1) maximum load was reached, (2) stripping of the covering concrete began, and (3) spalling of the covering concrete began occurred earlier for the A2 test specimens. This is thought to have resulted in part because the effect of cracking caused by ASR damage reduced the strength of the concrete in covered sections, and because the honeycomb-like cracking that occurred in the surface as a result of ASR damage caused a drop in bond with the reinforcements.

4-2 Reinforcing effect of PC confined reinforcement method

With test specimens S2, which had been reinforced by means of PC confined reinforcement method, the maximum load was greatly increased, becoming 1.2-1.3 times that for the A2 test specimens. Moreover, even after spalling of the covering concrete occurred, there was no sudden drop in the loading weight as seen in the N, A2 test specimens. This is thought to be because the binding effect of the prestressing PC tendons was able to prevent buckling of the axial bars, so the axial bars were able to resist the compressive force even when subjected to excessive displacement. it was learned that ASR damage of approximately 1.0% for the concrete expansion coefficient would have almost no effect on the reinforcing effectiveness of PC confined reinforcement method.

5. CONCLUSION

Through outdoor exposure tests and Alternating loading tests, the following was learned.

(1) After outdoor exposure over three and a half years, the concrete expansion coefficient was max. 1.0%.

(2) ASR damage of about 1.0% for the concrete expansion coefficient did not significantly decrease the aseismic performance of the reinforced concrete bridge pier model test specimens.

(3) With test specimens reinforced using the PC confined reinforcement method, an improvement in load carrying capacity, ductility and energy absorbing performance was noted. This indicates that, up to a concrete expansion coefficient of 1.0%, PC confined reinforcement method is an effective method of reinforcing ASR-damaged bridge piers.

REFERENCE

[1] Torii, Okuda, Ishii, and Sato, "Repeated Loading Test for ASR Damaged Concrete Colums Strengthened by PC Confined Method." Proceedings of Japan Concrete Institute (in Japanese), Vol.21, No.2, 1999, pp.1051-1056.

SHEAR PERFORMANCE OF VINYL-FIBER REINFORCED CONCRETE COLUMN

Hideo Kosaka
Taisei Corporation
JAPAN

Kazuhiro Kitayama
Tokyo Metropolitan University
JAPAN

Shinji Kishida
Tokyo Metropolitan University
JAPAN

Keywords: Fiber reinforced concrete, Shear, Column

1 INTRODUCTION

It is known that the mixture of polyvinyl alcohol (called PVA) fibers in concrete is effective to enhance the ductility and fracture parameter [1,2]. Then development of PVA fiber reinforced concrete (called PVA-FRC) is expected. On the other hand, same studies on high performance fiber reinforced cementitious composites (called HPFRCC) similar to PVA-FRC are carried out[3]. However, ductility and deformation capacity of PVA-FRC members containing coarse aggregate is not the same as those of HPFRCC members. Therefore it is necessary to grasp basical structural performance and deformation capacity of PVA-FRC members, so we executed tests of PVA-FRC columns providing anti-symmetric bending moment at the top and bottom of a column. Moreover PVA fiber reinforced light-weight cementitious composites (called PVA-FRLCC) column was also tested.

2 OUTLINE OF TEST(SPECIMENS)

Specimen configuration and reinforcing details are shown in Fig. 1. Properties of specimens and material properties of concrete and steel are summarized in Table 1. Six column specimens with one-third scale to actual frames were tested. Square column section (250x250 mm), shear span ratio of 1.5, the amount of longitudinal bars (16 deformed bars with 13 mm diameter) were common for all specimens. High-strength column longitudinal bars were arranged to cause shear failure prior to flexural yielding. Kind of concrete (plain concrete, concrete contained PVA fiber, and light weight cementitious composites contained PVA fiber), specified concrete compressive strength (35 MPa and 72 MPa), column axial load (compression and tension) and the amount of shear reinforcement (none and 0.26 percent) were selected as test parameters. PVA fiber with 30 mm length and 0.66 mm diameter, whose fracture strength and Young•fs modulus was 880 MPa and 29.4 GPa respectively, were used. The ratio of volume of PVA fibers to concrete was 1 percent taking account of workability of concrete mixing and casting. Compressive strength of PVA fiber concrete was 1.07 times greater than that of plain concrete, while tensile strength by splitting test using cylinders with 100 mm diameter and 200 mm height was enhanced by PVA fiber mixture to 1.21 times that of plain concrete. Weight of unit volume was 2.3 g/cm^3 for normal PVA fiber concrete and plain concrete, and 1.5 g/cm^3 for PVA-FRLCC. All kind of concrete was cast in horizontal position using wood form. Control specimen No.1 was made of PVA fiber concrete with specified concrete compressive strength of 35 MPa, had shear reinforcement ratio of 0.26 percent and was subjected to constant compressive axial stress of which ratio to concrete compressive strength was 0.32.

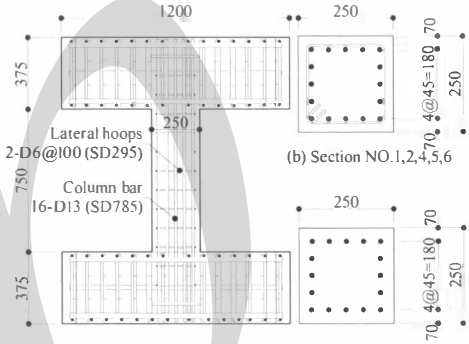

Fig. 1 Configuration and reinforcing details

3 TEST RESULTS AND DISCUSSION

Crack patterns were shown in Fig. 2. Spall-off of shell concrete was prevented in specimens containing PVA fibers. More diagonal cracks were observed in No.1 than No.5. Test results were summarized in Table

Table 1 Properties of specimens and material properties

Specimen Number		1	2	3	4	5	6
Concrete	Kind of concrete	PVA-FRC F35N	PVA-FRC F72N	PVA-FRC F35N	PVA-FRC F35N	*RC 35N*	*PVA-FRLCC LF35N*
	Compressive strength [MPa]	39.7	*76.8*	40.5	40.5	37.1	42.1
Longitudinal Bar	Arrangement	16-D13					
	Yield strength [MPa]	885					
	Gross ratio [%]	1.016					
Shear Reinforcement	Arrangement	2-D6@100		*none*	2-D6@100		
	Yield strength [MPa]	343.4		*none*	343.4		
	Ratio [%]	0.260		*none*	0.260		
Axial Load	Axial stress ratio	0.32	0.15	0.31	*-0.15*	0.32	0.32

2. All specimens failed in shear without yielding of longitudinal bars. Shear strength was attained between drift angle of 0.5% and 1% immediately after development of primary diagonal shear crack except for No.4 subjected to tensile axial load at drift angle of 1.5%. Shear strength for No.1 was enhanced to 1.1 times that for No.5 by the effect of PVA fibers. Shear resistant capacity for No.1 decreased moderately after shear strength comparing with No.5. Stress distribution of hoops was similar for specimens No.1 and No.5. However hoops strain of No.5 was higher than that of No.1. Shear crack width and principal tensile strain of concrete for No.1 were more restrained by PVA fibers than for No.5. For specimes except No.4, hoops yielded immediately after primary diagonal shear crack occurred extending from the top to bottom compressive zone at both ends. Simultaneously shear capacity decreased because tensile stress developed in web concrete was too large to substitute concrete contribution for hoops contribution. This means that shear strength was dominated by concrete tensile strength. For No.4 subjected to tensile axial load, shear crack occurred at drift angle of 0.5%. Hoops yielded gradulally at drift angle of 1% to 2%, and reached the maximum shear capacity. Comparing with No.1 and No.5, truss contribution was almost same even after shear strength at drift angle of 1%. This caused the difference of arch contribution between two specimens after shear strength, exhibiting that arch contribution for No.1 decreased more moderately than for No.5. PVA fibers appeared to be efficient to enhance shear strength and to maintain arch mechanism since reduction of concrete compressive strength due to tensile strain orthogonal to diagonal compressive strut may be prevented.

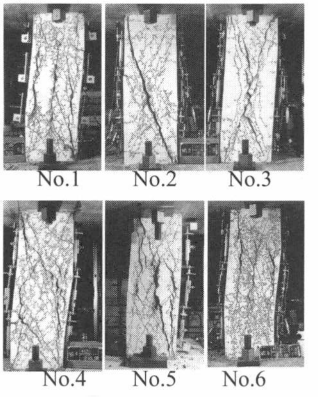

Fig.2 Crack patterns

Truss contribution in PVA fiber was computed by follows;

$$Q_{truss}=b \cdot j_t \cdot \cot\phi \cdot (p_w\,\sigma_{ws}+\sigma_{ct} \cdot \cos^2\phi)$$

In calculation of right-hand side, the inclination of diagonal uniform struts in web concrete was chosen from primary crack inclination observed in test. Concrete tensile stress carried by PVA fibers reached the maximum value of 1.8 MPa for No.4 at drift angle of 0.5%. PVA fibers contained in concrete contributed to truss action in the column. However the point that PVA fibers developed the full effectiveness to transfer of tensile stress was not coincident with the point that lateral shear reinforcement developed full capacity, i.e., yielding.

Table 2 Tesut results

Specimen Number			1	2	3	4	5	6
Flexural crack	Qmc	[kN]	159.6	107.5	158.7	-	134.3	143.2
Shear crack	Qsc	[kN]	246.3	264.4	232.9	-	206.2	143.2
Shear at hoop yielding	Qy	[kN]	247.2	294.5	-	141.3	223.0	185.7
	δy	[%]	0.77	0.80	-	1.00	0.65	0.50
Shear strength	Qmax	[kN]	247.5	299.7	238.9	166.8	225.3	185.7
	δmax	[%]	0.50	0.85	0.45	1.50	0.50	0.50

4 CONCLUSIONS

(1)Since shear cracking along main diagonal in a column was dominated shear strength, shear strength increased proportional to concrete tensile strength. Therefore PVA fibers enhanced shear strength in this test because concrete tensile strength for PVA fiber concrete was greater than that for plain concrete.
(2)PVA fibers prevented spall-off of shell concrete and restrained crack opening and principal tensile strain. Therefore it seemed that PVA fibers confined core concrete. This effect resulted in enhancement of shear strength and the improvement of ductility after shear strength.
(3)The bridging action of PVA fibers carried tensile force across crack corresponding to the half of concrete tensile strength. Hence this tensile stress flow distributed uniformly in web concrete contributed to form truss mechanism, causing the increase in shear strength.

REFERENCES

[1]Oh-oka, T., Kitsutaka, Y. and Watabe, K. : Influence of short cut fiber mixing and curing time on the fracture parameters of concrete, J. Struct. Eng., AIJ, No.529, pp.1-6, Mar., 2000 (in Japanese)
[2]Kamiyama, C., Kitsutaka, Y. and Tamura, M. : A study on test methods of fracture toughness in Various concrete, Proceedings of the Japan Concrete Institute, Vol.23, No.3, pp.91-96, June,2001(in Japanese)
[3]kanda, T., Watanabe, S., and Li, Victor C. : Experimental study on shear behavior of short span beam using PVA-ECC, Proceedings of the Japan Concrete Institute, Vol.22, No.3, pp.193-198, June, 2000 (in Japanese)

MECHANISM OF DAMAGE TO A TAIWAN BRIDGE CAUSED BY THE 1999 CHI-CHI EARTHQUAKE

Kenji KOSA (Assoc. Prof., Kyushu Institute of Technology, Japan)
Kenji TASAKI (Senior Engineer, Dai-Nippon Engineering Consultants, Co., Ltd, Japan)
Yukio ADACHI (Senior Engineer, Hanshin Expressway Public Corporation)
Eiki YAMAGUCHI (Assoc. Prof., Kyushu Institute of Technology, Japan)

KEYWORDS: collision, abutment, earth pressure, frame analysis

1. INTRODUCTION

The Chi-Chi Earthquake that hit the central Taiwan region in September 1999 with a magnitude of 7.7 caused severe damage to the bridge structures in the region. The authors visited the damage sites twice in 1999 and conducted a detailed damage survey, including extensive measurements.

The Chag-Geng Bridge, one of bridges surveyed by us, showed a unique damage in that two adjoining girders fell off the piers despite the fact that no fault displacement was found in the vicinity. The damage mechanism of this bridge was investigated analytically using the results of field measurements and the bridge's design drawing obtained from a Taiwanese authority.

2. DAMAGE TO THE CHAG-GENG BRIDGE

The Chag-Geng Bridge is a simple girder bridge with 13 spans that is situated 1 km east of the Shi-Kan Dam on the Da-Jia River. The 11 spans excluding the both end spans have a length of 34.7 m and a width of 13.1 m each. The bridge is made of five PC main girders. The small girders on both ends are simple girders with a length of 12 m. The piers with a height of 5～8m are RC-made and the foundations are the caisson type. Sufficient reinforcement was found arranged in the oval-shaped cross section of the piers, with the main reinforcement ratio 1.1 %, hoop tie ratio 0.2% plus six intermediate hoops. The abutments are the gravity type. The fixed type shoe is made of a six layer of thin rubber.

Figure 1 shows damage to this bridge. No damage was found on the columns of all piers, but adjoining two girders, D2 and D3, on the left bank side fell off the piers and the end girder D1 stuck into the abutment. But, no clear fault line was found in the vicinity of the bridge. As the causes for girder fall, the following four factors are considered: 1) simple girder structure; 2) relatively small seating length (100 cm) for girders; 3) a device to prevent girder fall was not installed in the bridge axial direction, though a shear key is installed in the opposite direction; and 4) the main reinforcement ratio of the parapet was not sufficient.

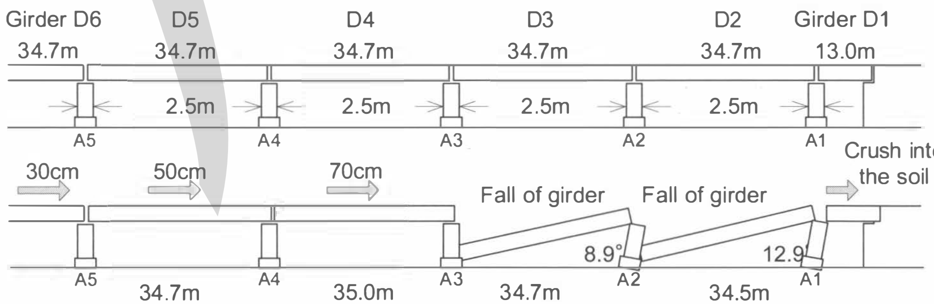

Fig.1 Chang-Geng Bridge and its damage

3. CHECK OF THE PIER STRENGTH

Though the Chag Geng Bridge is constructed by the AASHTO design standard, check was conducted in accordance with the Specifications for Highway Bridges of Japan (1996) to evaluate the strength of piers with the Japanese seismic design standard. Two wave profiles were used for check: one is that recorded around the Chag-Geng Bridge; the other is that recorded at the JR Takatori Station in Kobe because the ground around the bridge was found equivalent to the Type II ground. The design horizontal seismic coefficient used was K_{hc} = 1.53 that was derived from the response spectrum of the Chi-Chi Earthquake. According to the check results, the piers of this bridge were constructed with sufficient considerations for seismic design.

4. NONLINEAR DYNAMIC ANALYSIS

Figure 2 shows the frame model used for dynamic analysis. A simple model was selected to avoid complication of analysis that is usual with a multi-span bridge. The model was formulated in as way that Girder D2 collides with the abutment directly,

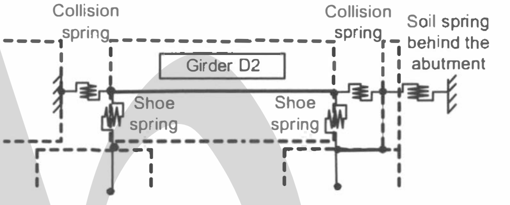

Fig.2 Analysis model

As to the effect of the shoe spring, it was found that the shoe begins to fracture when it is displaced 14 cm horizontally and its strength (2009 KN) is exceeded. This means it is highly likely that a girder-abutment collision and/or a girder-girder collision are triggered when seismic force exceeding the shoe strength is activated. As to the effect of the abutment, it was found that the parapet gradually sinks into the soil behind the abutment, if a collision exceeding the yield strength of the soil is repeatedly caused between the girder and the abutment.

5. CONCLUSIONS

From the analysis using the results of a detailed survey conducted on the Chag-Geng Bridge that suffered severe damage by the 1999 Chi-Chi Earthquake, the following conclusions can be drawn:

① According to the check by the ultimate lateral strength method, the pier of this bridge satisfies the design requirements specified in the 1996 Specifications for Highway Bridges of Japan.

② According to the analysis in which a rubber pad shoe was modeled as the nonlinear spring model, deformation of the pier was negligible, but the shoe got fractured and the girder displaced as much as 77 cm. This means the effect of collision needs to be taken into account when conducting dynamic analysis.

③ According to the analysis in which the soil behind the abutment was modeled as the nonlinear spring model, repeated collision of the girder and the abutment and sinking of the parapet into the soil were reproduced. As the degree of sinking of the parapet differs largely depending on the soil spring model and the constants used, adequate evaluation of the soil behind the abutment is needed.

Reference

[1] Road Association of Japan: Specifications for Highway Bridges and Commentary – IV: Substructure and V: Seismic Design, Dec. 1996.

HYSTERESIS CHARACTERISTICS AND FAILURE MECHANISM OF PRECAST PRESTRESSED CONCRETE BEAM-COLUMN JOINTS ASSEMBLED BY POST-TENSIONING STEEL

Shinji Kishida Kazuhiro Kitayama
Tokyo Metolopolitan Univercity
JAPAN

Makoto Maruta Akiko Kimura
Kajima Technical Research Institute
JAPAN

Keywords: beam-column joints, prestressed concrete, post-tensioning steel bar, joint shear

1 INTRODUCTION

Shear strength in reinforced concrete (RC) beam-column joints can be obtained by Design Guidelines of Architectural Institute of Japan [1], which depends on both the joint shapes as interior, exterior or knee joint and the concrete compressive strength. Whereas, the strength in precast prestressed concrete beam-column joints assembled by post-tensioning steel bars called as PCaPC has not been estimated quantitatively. There are few test data on joint failure of PCaPC beam-column subassemblages [2]. Therefore PCaPC beam-column joint specimens were tested under reversed cyclic lateral loading and column axial loading to study the joint failure mechanism.

2 OUTLINE OF TEST

Section dimensions and reinforcement details are shown in Fig.1. Beam and column elements were precast separately. Post-tensioning steel bars with deformed surface were used to connect precast RC beams and column for all specimens. Therefore beam longitudinal bars were terminated at column face. Interface mortal with the width of 20mm was set between precast beam and column. Bond along post-tensioning steel bars were provided by injecting grout mortal into the sheath except for Specimen BNU. Unbonded post-tensioning steel bars were used for Specimen BNU. High strength mortal was used for grout into the sheath and vertical joint adjacent to column face for Specimens BHH1,BHH2 and BHH3. Specimens BNU and BHH1 were designed to develop beam yielding. Concrete compressive strength of 30MPa for a column and the diameter of 36mm for a post-tensioning steel bar were chosen to cause joint shear failure for Specimens BHH2 and BHH3. Specimen BHH3 is the exterior beam-column joint. The beam ends were supported by horizontal rollers, while the bottom of the column was supported by a mechanical hinge. The reversed horizontal load and the constant axial load in compression were applied at the top of the column.

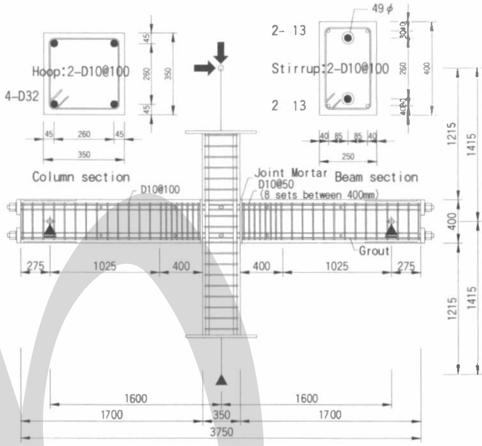

Fig.1 Section dimensions and reinforcement details

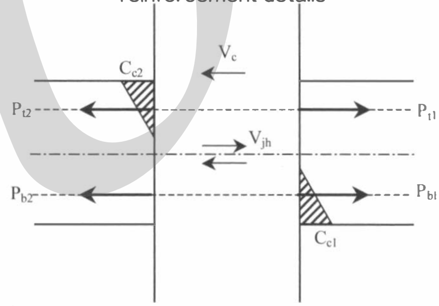

(a) In case that depth of compressive stress block is less than the half of beam depth

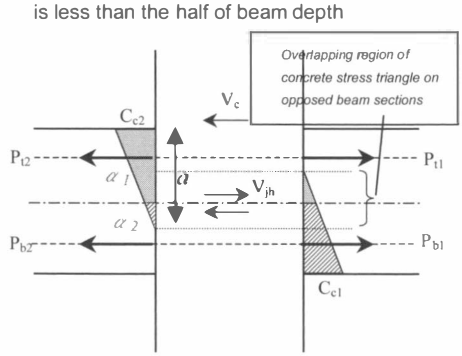

(b) In case that depth of compressive stress block is greater than the half of beam depth

Fig.2 Stress acting on joint panel

3 TEST RESULTS

It was concluded that Specimens BHH2 and BHH3 failed in joint shear, Specimen BNU failed by concrete compression at beam ends in bending moment and Specimen BHH1 failed eventually in joint shear after the post-tensioning steel bars yielded.

4 DISCUSSION OF TEST RESULTS

The neutral axis at first loading cycle was located at a position exceeding 200mm (D/2, D: beam depth) from the extreme compression fiber. In other words the both concrete compressive stress blocks on opposed beam critical sections overlapped at center region across the joint panel as shown in Fig.2 (b). The neutral axis approached to the extreme compression fiber with the increase in deformation.

4.1 Joint input shear force

The joint shear strength calculated by Reference [1] is also shown. Joint input shear force denoted as V_{jh} was computed from post-tensioning steel bar stresses by Equations (1) or (2) according to the definition shown in Fig.2. It is necessary to consider two cases which one is 1) that the distance from the extreme compression fiber to neutral axis (depth of compressive stress distribution) is less than the half of beam depth as illustrated in Fig.2 (a), the other is 2) that it is greater than the half of beam depth as illustrated in Fig.2 (b). In the second case, the maximum joint shear input force can be obtained mathematically in the section on beam center axis. Therefore joint input shear force was computed as Equation (2).

1) In case that depth of compressive stress block is less than the half of beam depth;

$$V_{jh}=P_{t1}+P_{b2}-V_c \qquad (1)$$

2) In case that depth of compressive stress block denoted as a in Fig.2 (b) is greater than the half of beam depth;

$$V_{jh}=\alpha_1 C_{c2}-P_{t2}+P_{t1}-\alpha_2 C_{c1}-V_c \qquad (2)$$

where P_{t1} and P_{t2} are the tensile forces of the top post-tensioning steel bar, P_{b1} and P_{b2} are the tensile forces of the bottom post-tensioning steel bar, C_{c1} and C_{c2} are concrete compressive resultant forces and V_c is the story shear force. Joint shear strength for Specimens BHH2 and BHH3 agreed well with computed strength according to the provisions by Architectural Institute of Japan [1].

4.2 Deformation in joint panel

Mohr's strain circles are shown in Fig.3 to the story drift angle of 2% to investigate deformation characteristics of a joint panel in more detail. The strain circles of Specimens BHH2 which failed in joint shear were larger than that for Specimen BNU. Centers of circle shifted largely to the tensile side. This indicates that the concrete is a joint panel expanded isotropically with the increase in a story drift. Joint shear failure for specimen was caused by the concrete expansion. The strain circle for Specimen BNU that did not fail in joint shear was small. Center of circle was located at the origin and the Mohr's strain circle became large as concentric circles.

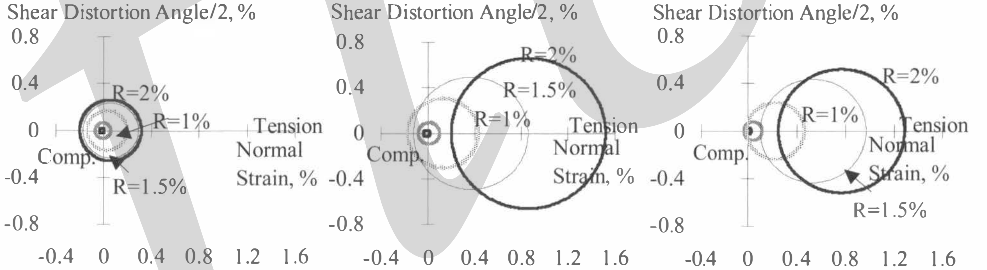

(a)Specimen BNU (b)Specimen BHH2 (c)Specimen BHH3

Fig.3 Mohr's strain circles for joint panel

5 Concluding remarks

(1) Interior and exterior beam-column joints which were made of assembling precast RC beams and column through post-tensioning steel bars failed in shear. (2) The depth of compressive stress block computed by the concrete strains at beam critical section was larger than the half of beam depth. This indicates that the compressive stress block on both beam critical sections overlapped across the joint panel. (3) The joint input shear force was computed by using the measured tensile forces of post-tensioning steel bars and considering that concrete compressive stress block overlapped as mentioned above. (a) The joint shear forces deteriorated with the story shear force after the joint panel failed by shear. (b) Shear strength of PCaPC beam-column joints can be estimated by the prediction method for usual RC beam-column joints.

REFERANCES

[1] Architectural Institute of Japan, Design Guideline for Earthquake Resistant Reinforced Concrete Buildings Based on Inelastic Displacement Concept,1999. [2]Beniya, N., Kashiwazaki, T. and Noguchi, H. : An Experimental Study on Shear Behavior of Prestressed Concrete Beam-Column Connection, Proceedings of JCI, Vol.19, No.2, pp.1179-1184, 1997

THE STRENGTHENING TECHNOLOGY OF THE RC PIER USING PRECAST PANELS IN WATER

Yasushi Fujioka Masaharu Doi Yukinori Kawamura Toshihiro Iwai
P. S. Corporation Hiroshima branch office JAPAN

Keywords: the strengthening of the RC pier, PC confined method, underwater execution, precast panels

SUMMARY

Since the earthquake in the southern part of Hyogo prefecture, the seismic strengthening of the structures has started in earnest. Seismic strengthening, whose immediate treatment are necessary and also easy, has almost finished. Recently the target of strengthening has shifted to the difficult one such as in water or under ground construction. Among them, especially as for the RC piers situated in water, their strengthening requires huge temporary construction works to keep the piers dry by shutting out of other surroundings. Because of the reason above, Authors haven't seen such examples yet. And another reason must be the fear of the environmental effect of surrounding river.

This report explains the strengthening of the RC piers of Sakai Bridge under water whose execution was seemed impossible.

1. OUTLINE OF SAKAI BRIDGE

Sakai Bridge is 27.8 meters long and 25.0 meters wide. This bridge is important for connecting to the main roads of Matsue-shi in Shimane. Seismic strengthening of piers was planned according to the specification of highway bridges revived in 1996. Traditional way of strengthening of piers needs temporary cofferdam by using sheet piles around piers. After execution parts were dried, steel bars were arranged and concrete was poured. The Tenjin River, spanned by Sakai Bridge, flows to the Lake Shinji and it is famous for shijimi clams fishing, so the river is used for the route of their fishing boats. As its water level is high and the girder is only 1.0 meter high, the underwater execution method was selected as the first trial considering the difficulty of temporary cofferdam method to use sheet piles.
The Fig.1 shows the structure of Sakai Bridge.

2. LATERAL CONFINEMENT BY EXTERNAL PC PANELS

As strengthening method of construction of this pier, PC confined method was adopted.

The followings are the characteristics of lateral confinement by external PC panels.

①Underwater execution made it possible by using the precast panels of approximately 120 millimeters thick concrete, which is manufactured in advance, instead of using forms. The precast panels can save the construction of forms at site or the temporary cofferdam using sheet piles.

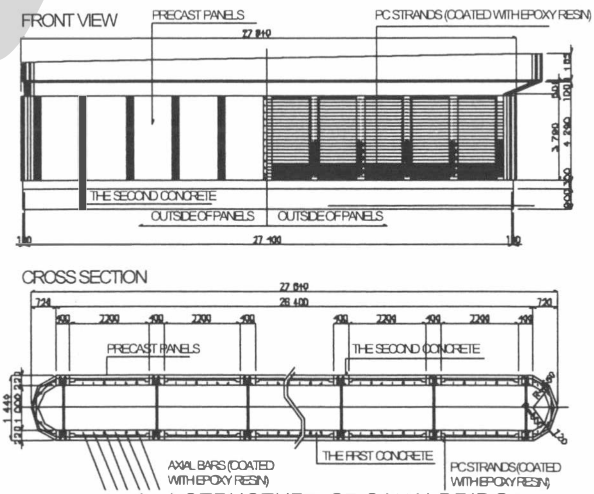

Fig.1 STRUCTURE OF SAKAI BRIDGE

②The improvement of durability was enabled by using the good quality precast panels produced in the factory.

③ The improvement of toughness was enabled by spirally arranging the strong PC strands to the transverse confining, because it works as tie hoops.

④Existing piers was tightened by the precast panels and the new concrete was combined with the old one through tensing transverse prestressing. It is not necessary to use dowel bars.

3. EXECUTION PRODURE

First of all, the execution, in short, is to set axial bars and to encircle precast panels around them. We use them as forms and arrange underwater concrete between panels and existing piers of approximately 100 millimeters thick. (We call the concrete of this point the first concrete). We pass PC strands through the duct that had already been settled to wind piers around the precast panel spirally and tense them. We pierced the high strength bars through pier and arrange concrete between the two precast panels, the span of each panel is approximately 400 millimeters (We call the concrete of this point the second concrete). The main work will have finished. The series of construction works were done by divers. Fig.2 shows the flow of execution. And it shows the details of each flow of execution work as follows.

CONSTRUCTION OF WORKBENCH

①DRILLING CONCRETE OF FOOTING AND PIER

②SETTING UP AND ANCHOR OF AXIAL BAR

③SETTING UP THE PRECAST PANELS

④CONSTRUCTION FORMS AND POURING OF THE FIRST CONCRETE

⑤INSERT OF PC STRANDS FOR TRANSVERSE CONFINING

⑥INSERT OF HIGH STRENGTH STEEL BAR PIERCED THROUGH PIERS

⑦CONSTRUCTION FORMS AND POURING OF THE SECOND CONCRETE

⑧ PC GROUTING OF PC STRANDS FOR TRANSVERSE CONFINING

DEMOLITION AND REMOVAL OF TEMPORARY FACILITIES

Fig.2 FLOW OF EXECUTION

4. CONCLUSION

With various examinations of this construction, the followings were proved.

- Even if the axial direction steel rod epoxy painted were anchored into the hole drilled with the fixing length, as 25 times as the diameter of a steel rod, we didn't find any problems of the construction design.
- It is satisfied that even if underwater concrete were placed in narrow space in the water at 5℃ temperature, the intensity and filling efficiency would satisfactory.

The above various examinations showed that reinforcement of the bridge pier, which has a reinforcement part underwater, was enabled by lateral confinement by external PC panels. It wished that these experiments and data lead to the further construction cost reduction, laborsaving, and shortening the construction term of bridge pier reinforcement.

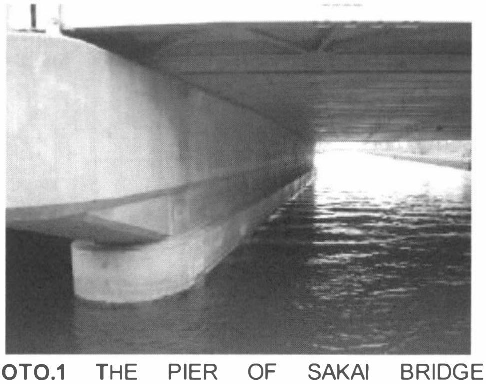

PHOTO.1 THE PIER OF SAKAI BRIDGE STRENGTHENED

THE PROPOSAL OF MAXIMUM STRENGTH FORMULA OF PCA·PC FRAMED SHEAR WALLS AND ITS PRACTICAL APPLICATION

Takashi Toriya Norikazu Onozato Makoto Mochizuki Yukichi Kanehira
DPS Bridge Works Co.,LTD. KOGAKUIN University
JAPAN JAPAN

Keywords: prestressed concrete, framed shear wall, macroscopic model, maximum strength formula

1 OBJECT

In the previous papers [1],[2] the authors cleared the failure behaviors of the reinforced concrete framed shear walls and the precast-prestressed concrete framed shear walls (hereafter, referred to as RC shear walls and PCa·PC shear walls, respectively), based on numerous experimental results executed by the authors. The fundamental distinctions between both failure behaviors are as follows,

1) In PCa·PC shear walls, the sliding occurs along the horizontal and vertical joints of the wall panel and along the bottom joint of the column in compression.
2) The sliding along the bottom joint of the column in compression is an important factor which determines the maximum strength of PCa·PC shear walls.

The objectives of this paper are firstly to propose the maximum strength formula of PCa·PC shear walls in consideration of the above mentioned distinctions, and secondly to investigate the analytical accuracy of the proposed maximum strength formula by analyzing fifty specimens of PCa·PC shear walls.

2 MAXIMUM STRENGTH FORMULA OF PCa·PC SHEAR WALLS

2.1 Macroscopic model

Fig.1 shows the proposed macroscopic model for evaluating the maximum strength of PCa·PC shear walls. The model consists of the upper and lower beams, two columns, and compressive struts *a* and ***c***, which are transposed from the wall panel and are subjected to only compressive stress, and connections at the horizontal and vertical joints of the wall panel.

At the maximum strength, each member of the model is assumed to be under the following properties and stress conditions as shown in Fig.1.

1) Upper and lower beams are rigid, and they do not fall in any failure.
2) Bottom joints of the columns in compression and in tension are under flexural and tensile yielding, respectively.

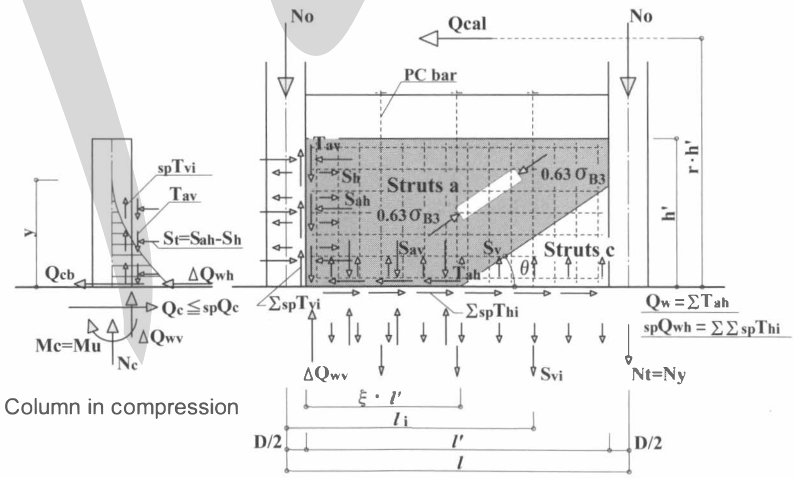

Fig.1 Macroscopic model of PCa·PC shear wall

3) Compressive struts *a* are under yielding at stress of $0.63\,\sigma_{B3}$ (where, σ_{B3} is compressive strength of concrete of wall panel), which is based on the proposal by the authors [3]. Compressive struts *c* are removed, because the part of the column in tension crossing the struts *c* are under tensile yielding. Both struts *a* and *c* have the same inclination angle of θ deg..
4) PC bars, connecting bars, and anchor bars of matching plates at the horizontal and vertical joints are under tensile yielding.
5) The differences between the shear stress component of the compressive struts along the horizontal or vertical joints and the sliding strength of the corresponding joints are directly transmitted to the columns or the beams, respectively.

The stress distribution of Fig.1 shows the simplest yielding mechanism of PCa･PC shear wall. From this stress distribution, the maximum strength formula was derived in consideration of the equilibrium conditions based on the lower bound theorem of the limit analysis and the restriction conditions on slide strengths of the horizontal joint of the wall panel and the bottom joint of the column in compression.

2.2 Analytical results

The analyses using the proposed maximum strength formula were executed on fifty specimens conducted by the authors. The ranges of main parameters of the specimens are as follows,

1) Aspect ratio of wall panel h'/ℓ' : $0.41 \sim 1.38$
2) Dimension of column $b \times D$: $150\times150 \sim 260\times260cm$
3) Ratio of gross reinforcement of column: $0.49 \sim 1.63\%$
4) Compressive strength of wall panel: $24 \sim 68N/mm^2$

Fig.2 shows the relationship of the analytical values $Qcal$ and observed values $Qexp$. The values of mean, standard deviation, and coefficient of variation of analytical accuracy are 0.991, 0.126, and 0.127, respectively. The numbers of the sample points of which $Qexp/Qcal$ is smaller than 0.8, and $Qexp/Qcal$ is larger than 1.2 are 3 and 6, respectively. These results show that the proposed maximum strength formula of PCa･PC shear walls is well adequate.

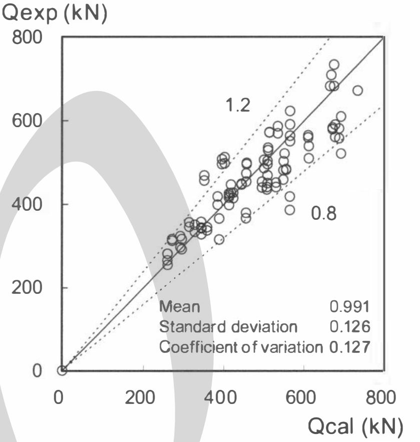

Fig.2 Relationship between $Qcal$ and $Qexp$

3 CONCLUSION

In this paper the macroscopic model and the maximum strength formula of PCa･PC shear walls were proposed, and the analyses using the proposed maximum strength formula were executed on fifty specimens conducted by the authors. The analytical results show that the proposed macroscopic model and the maximum strength formula are well adequate to evaluate the maximum strength of PCa･PC shear walls.

REFERENCES

[1] Mochizuki, M., Onozato, N., Nakamura, M., Kuramochi, H., and Yaginuma, H. :Simplified maximum strength formula of precast prestressed concrete shear walls in consideration of sliding resistance. Jounal of Prestressed Concrete, Japan, Vol.35, No.4, pp.71-79, Jul., 1993 (in Japanese)

[2] Mochizuki, M., Kuramochi, H., Toriya, T., and Takami,T. :Failure behaviors and strength estimation of precast-prestressed framed shear walls with perfect constraint for sliding of side columns. Jounal of Prestressed Concrete, Japan, Vol.37, No.4, pp.68-77, Jul., 1995 (in Japanese)

[3] Mochizuki, M. and Onozato, N.: Macro model of multistory framed shear walls and its analytical method, Concrete research and technology, Vol.1, No.1, pp.121-132, Jan., 1990 (in Japanese)

BASE-ISOLATED BUILDING USING PRECAST PRESTRESSED CONCRETE BY COMPRESSION JOINT METHOD

Hiroyuki Ueda Hidemi Ikeda Kunio Fukuyama Akira Sumi
Building Design Department, Osaka Main Office, TAKENAKA CORPORATION
JAPAN

Keywords: Seismic isolation building, Precast, Prestressed, Compression joint method

1. INTRODUCTION

The design of this building started in 1997 when two years passed from the Great Hanshin Earthquake which brought unprecedented large damage. Afterwards, the concern for the building performance of the society has been rising.

The Koa Fire & Marine Insurance Co., Ltd. Kobe Center (The architectural outline and the panorama photograph are shown in Fig.1) which reported in this paper was planned as a computer center which became the central base of this company. Therefore, some severe demands were presented by the client for this building's performance.

To answer these high level demands for this building's performance, we adopted the system which is composed of the prestressed concrete structure (Hereafter called PS structure) which built up by industrial precast method (Hereafter called PCa method) and the seismic isolator in this building.

We will report on the outline of structural design.

Construction name	The Koa Fire Insurance Co., Ltd. Kobe center
Architectural ground	Kobe City
Design	Takenaka Corporation
Construction	Takenaka and others
Building usage	Computer center and office
Architectural area	12,110.07 m²
Building scale	Three stories on the ground
Structural type	Prestressed concrete structure
Superstructure	Rahmen by PS structure
Isolation structure	Seismic isolation rubber
Basic structure	Spread foundation

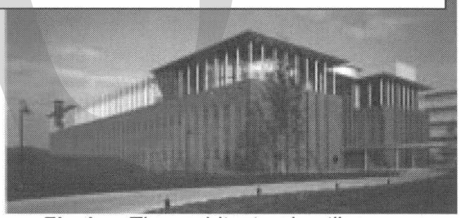

Fig.1 The architectural outline and the panorama photograph

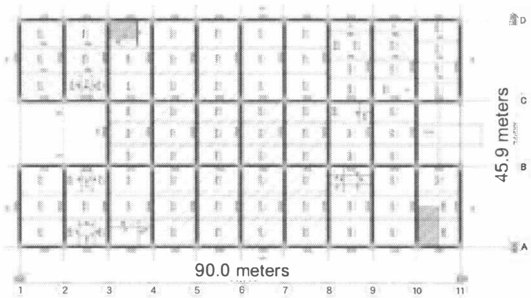

Fig.2 Typical structural plan

2. THE OUTLINE OF STRUCTURAL DESIGN

The demanded performance of structural frame for the computer center which planned as important base of the insurance company is very highly developed. So, severe demands for structural frame were shown from the client as following.

[demand-1] Feature computer center which makes advertising effects
[demand-2] Wide computer room space which has flexibility
[demand-3] Facilities having high earthquake-proof safety
[demand-4] Operation within one year from starting of construction
[demand-5] Proper cost compared with obtained performance

In a past structural design, it is extremely difficult to satisfy these all. However, we answered client's demand according to Fig.3.

To satisfy [demand-2] and to enable a free layout change in the future, it's necessary to secure the long span by the structural design under big live load (1tonf/m^2) in which the quake resisting wall and the brace do not exist.

In this building, considering a floor vibration performance for the computer center, as shown in Fig.2, there are ten X direction span every 9.0m, and Y direction span is 16.2, 13.5, and 16.2m.

At present there is no one that it can answer [demand-3] at the highest level except the seismic isolation building. Then, in this building it was assumed the structural design which supported the 3 stories building over the seismic isolator on the basement.

All members were assumed to be precast elements to satisfy [demand-4], and we planned to shorten the period of construction term rapidly. In addition, the joints of columns and beams were connected by compression joint method. This respect is described later.

And, we positively tend to appeal the performance for the earthquake to the visitor by showing the seismic isolator from the window, or by making the room where can look around the seismic isolators; It was assumed the answer of [demand-1].

The outline and the merit of the PS structure by using compression joint method are brought together in Fig.4.

We designed this building aiming at "The equipment does not fall even against the large earthquake". So, the decrease of the response acceleration was assumed to be the main target. The earthquake performance target value based on mutual agreement with the client and the seismic response analysis result are shown in Table 3 .

We reported on the outline of the seismic isolation building constructed by assembly industrial method using compression joint method.

This structural system has an extremely high performance in flexibility, the earthquake-proof safety, durability, and the term of works.

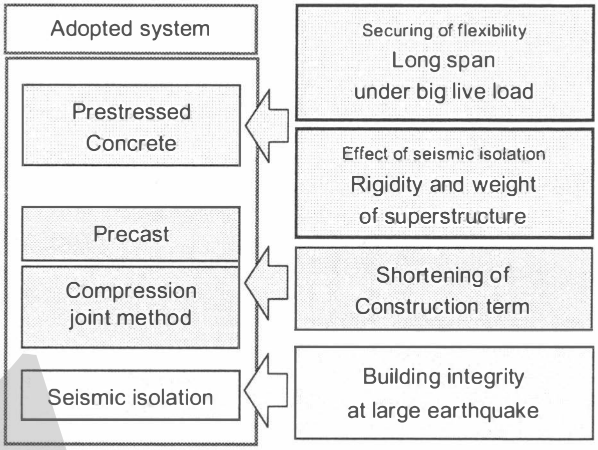

Fig.3 Point of structural design

Outline Assembly industrial method, by which pre-cast structural member is constructed with the tension of pre-stressing wire in the construction site.

Merit

1. **High structural safety :** Because of high strength at joint, an excellent isolation performance and the earthquake-proof safety are secured.
2. **Short term of works:** The amount of field-work can be remarkably decreased, and the term of structural body works shortening can be achieved.
3. **Excellent durability:** The durability of a structural body rises because the high-strength concrete is cast with few unit volume of waters at the factory.
4. **Gentle environmental:** The industrial waste scraps generated in the work place can be extremely few, and the earth environment be considered.
5. **Cost merit:** Some structural body costs rise but there is cost merit in total because the temporary work can be decreased and the term of works can be shortened.

Fig. 4 The outline and the merit of the PS structure by using compression joint method

Table 3 The seismic performance target and the seismic response analysis result

	Performance target	Response result
The maximum acceleration	200cm/s^2 or less	115
Drift angle	1/500 or less	1/1700
The maximum displacement	40cm or less	22

FLEXURAL DUCTILITY OF FULL-SCALE RC BRIDGE COLUMNS SUBJECTED TO CYCLIC LOADING

Jun-ichi Hoshikuma[1] Shigeki Unjoh[2]
Public Works Research Institute, Japan,
Kazuhiro Nagaya[3]
Ministry of Land, Infrastructure and Transport, Japan

Keywords: size effect, ductility, reinforced concrete columns, full-scale test

1 INTRODUCTION

Many researchers previously proposed the ductility assessment procedures for flexural reinforced concrete columns subjected to seismic action. These are established based on mainly experimental results and statistical studies for their data. It should be suggested that such empirical approaches have a limit for application. Some existing ductility assessment procedures note the applicable limits in terms of the flexure-shear strength ratio, longitudinal steel ratio, transverse steel ratio, axial force ratio, aspect ratio, etc. However, the limit of cross sectional size is unclear in the previous proposals, and the size effect on the inelastic behavior of reinforced concrete columns is also unknown.

This research program was initiated with motivation to investigate the size effect on inelastic behavior of reinforced concrete columns with big square cross section that never tested. Full-scale columns with 2400mm square section and 9600mm height were loaded until the columns were completely failed, and inelastic behavior of the plastic hinge region was studied. Furthermore, a 1/4-scale replica model was also tested for comparison with the full-scale column behavior, and the size effect was discussed based on test results.

2 CYCLIC LOADING TEST PROGRAM

Two full-scale columns (called herein L1 and L2, 2400mm square section) and one replica column (called herein S1, 600mm square section) were tested in the program. The unit L2 is a reference column and the unit S1 is a 1/4-scale replica model of the L2. The unit L1 is a model with the same size and longitudinal steel ratio as the L2 but the transverse steel ratio reduced.

The columns were loaded quasi-statically and subjected to cycles of force reversals under the force control until yielding of the extreme longitudinal reinforcement. Subsequently, the lateral displacement was applied with stepwise increasing amplitude ($\pm 1\delta_y$, $\pm 2\delta_y$, $\pm 3\delta_y$, $\cdots$) under the displacement control. The cyclic number in each loading step was three.

3 INELASTIC COLUMN BEHAVIOR

3.1 Lateral Strength and Ductility

Fig. 1 compares the contour of the lateral force and drift hysteresis loops between the unit L2 and S1. The lateral force measured for the unit S1 was modified based on Eq. (1) so as to make a relative comparison the test results.

$$P_{se} = P_s s_e^2 \qquad (1)$$

where, P_{se} : modified lateral force of unit S1
P_s : lateral force measured for unit S1
s_e : scale factor (=4.0)

Fig. 1 indicated that the contours of the unit L2 and S1 exhibited similar response. The maximum lateral force of the unit L2 was slightly larger than that of the unit S1. This difference arises from the difference of yield strength of longitudinal reinforcement between both units. Though the longitudinal reinforcement ratio was equivalent as 0.012, the yield strength of longitudinal reinforcement in the unit L2 was 7% larger than that in the unit S1.

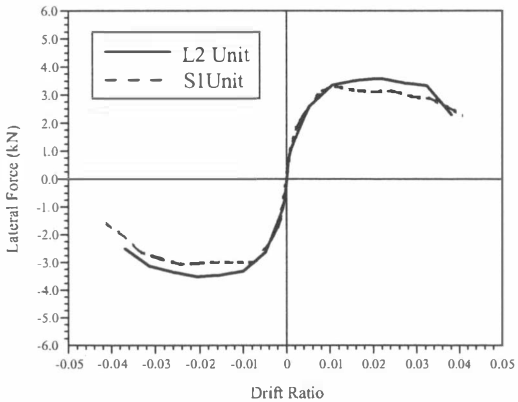

Fig. 1 Contour of Hysteresis Loops

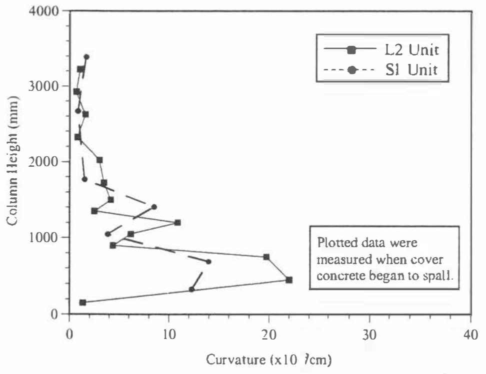

Fig. 2 Comparison of Curvature Profiles between L2 and S1 Units

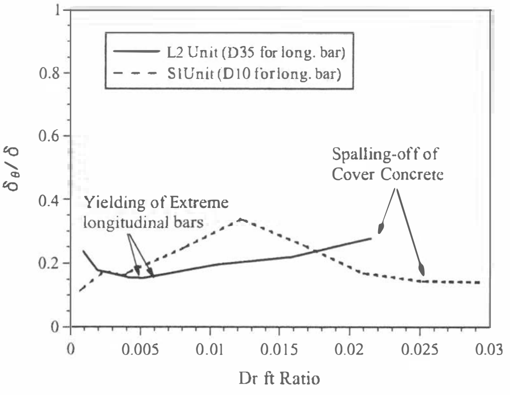

Fig. 3 Lateral Displacement due to Bond Slip of Longitudinal Bars

3.2 Plastic Curvature Profiles

Fig. 2 compares the curvature profiles measured when cover concrete began to spall-off between the units of L2 and S1. Column height and the measured curvatures for the S1 unit were modified based on similitude relationships for relative comparison with the L2. It can be noted that the both units exhibit similar curvature profiles when the columns suffer from the damage as cover concrete spall resulting from buckling of the longitudinal reinforcement. This fact indicates that the size effect on the curvature profiles around the plastic hinge region is not so significant as long as structural details of a replica model is well-scaled down based on a prototype column.

3.3 Base Rotation due to Bond Slip of Developed Bars

In this study, measured lateral displacements were divided into flexure/ shear component and bond slip component. Then lateral displacement at loading point due to bond slip of developed bars was estimated through Eq. (2).

$$\delta_\theta = \theta \times L \qquad (2)$$

where, δ_θ : lateral displacement at loading point due to bond slip of developed bars
θ : measured base rotation
L : column shear span

Fig. 3 compares the ratio of δ_θ to the measured total lateral displacement δ between the units L2 and S1. The value of δ_θ / δ would be affected by longitudinal bar diameter, bond strength, deterioration in flexural stiffness of the critical section due to inelastic cyclic loading and longitudinal tensile strain profiles of the developed bars in footing. For the unit L2, the value of δ_θ / δ is around 0.2 but it slightly increases with increasing the drift ratio of the column. On the other hand, the value of δ_θ / δ in the unit S1 was 0.15 to 0.35, which exhibited larger change than the result of the unit L2. It increases up to 0.012 of drift ratio, and subsequently decreases as the drift ratio increases. However, it should be noted that the lateral displacement due to bond slip of longitudinal bars was observed clearly in the full-scale column as well as the replica model. Furthermore, with viewing overall behavior shown in Fig. 9, the value of δ_θ / δ is roughly equivalent to that for the replica model.

4 CONCULUSIONS

The contour of lateral force and drift hysteresis loop for the full-scale column was relatively similar to that for its replica model. Curvature profiles measured when cover concrete spalled corresponded well for both columns. Furthermore, the base rotation resulting from bond slip of the longitudinal bars was not affected significantly by the size of column section. Therefore, it could be concluded that the size effect on the inelastic ductile behavior of reinforced concrete bridge columns would not be significant as long as we tested. It is, however, important in designing of replica model to determine not only the longitudinal/transverse reinforcement ratio but also the diameter of longitudinal reinforcement and vertical hoop spacing based on the scale factor. These details should be scaled down as precisely as possible, otherwise the size effect would develop in the inelastic behavior and ductility capacity of reinforced concrete columns.

THE EFFECTS OF AMOUNT OF PRESTRESSING STEELS AND BOND-SLIP CHARACTERISTIC BETWEEN PRESTRESSING STEEL AND GROUT ON RESPONSE OF PRESTRESSED CONCRETE FRAME STRUCTURE

Ichizo Kishimoto, Yoshiteru Ohono

Architectural Engineering Graduate School of Eng. Osaka University JAPAN

Keywords: prestressed concrete structure, dynamic response analysis, amount of prestressing steel, bond-slip characteristic between prestressing steels and grout

INTRODUCTION

As a particular feature of prestressed concrete (PC) members in the flexural behavior, the performance of pointing to original position in force reduction stage is pointed out and it indicates PC member is inferior to reinforced concrete (RC) member in energy absorption under seismic loading. So generally the response deformation of frame structures constructed with PC members is larger than that of buildings with only RC members in the earthquake.

On the other hand, some paper report that the additional longitudinal reinforcement bar in PC member sections make possible more energy absorption in plastic hinge region and the response deformation of the buildings subjected seismic force is decreased[1]. These results were derived by the dynamic response analysis in which the idealized hysteresis loop of PC member or story with PC member was employed. Presently, some hysteresis loop models of PC member and of the story of building constructed with PC members are proposed[2] and some of them include ranging between fully prestressed and reinforced concrete members. However, there are many other factors which characterized the flexural behavior of PC members such as located position of prestressing steels, bond-slip characteristic between prestressing steels and grout and so on. No idealized models include these all influences on their features adequately. Especially bond-slip characteristics between prestressing steels and grout have significant influence on the flexural behavior of PC members .

To dissolve this problem, adoption of fiber-models is effective as a model which express the flexural behavior of PC sections. The dynamic response analyses program combined with the fiber-model method requires more time for computation. On the other hand the hysteresis loop of the PC sections are specified automatically by joining the stress-strain relationships of materials, concrete and steels and it is ease to include a bond-slip performance between prestressing steels and grout in the analyses by controlling the stress of prestressing steel directly.

In this paper the dynamic response behavior of PC frame structures are reported. In accordance with the results of dynamic analysis combined with the fiber-model method, the influence of the amount of prestressing steel and the bond-slip characteristic between prestressing steels and grout to the dynamic behavior of PC frame structures are described.

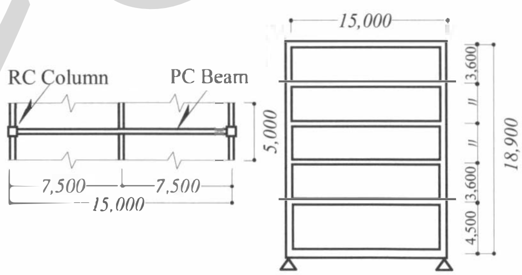

Fig.1 Structural layout of the frame to be design

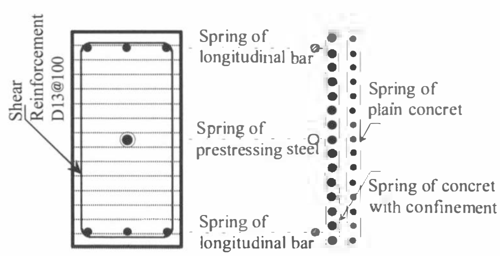

Fig. 2 Idialized section (Fiber model)

CONCLUSIONS

1) The results of fiber model analyses of the

sections of the prestressed concrete beam showed that the bending stiffness were decreased on route in reduction stage of the moment-curvature relationship and the figure of the relationships became a typical S-shaped curve when the deterioration of bonding between prestressing steel and grout was severe. Even in such a case, there was no different in the equivalent viscous damping with different bonding level(Fig. 3).

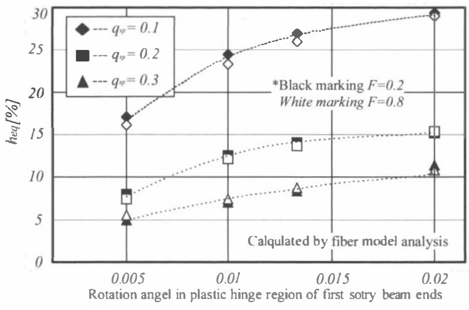

Fig.3 Comparios of equivalent viscous damping coefficient (heq)

2) In Fig. 4 which shows the maximum interstory drift computed by the dynamic response frame analyses the maximum interstory drift was increased with the amount prestressing steel arranged in the beam sections which ultimate flexural strength are equal. The ratio of the average of maximum interstory drift in the left and right to the value of standard model (q_{sp}=0.1, F=0.8) was greater than the ratio of the larger values in the left and right to that. It indicates the possibility that the total deformation of beams, i.e. total rotation angle in plastic hinge region, during the earthquake motion will be greater than that expected by the comparison of the maximum deformation (larger value in the left and right) and the damage of the member will be underestimated with the judgment based on the comparison of larger one of interstory drift in right and left.

3) The comparison of the rotation angle in the plastic hinge region increased with the amount of prestressing steel and the ratio to that of standard mode was 10-20 and 10-40 percent in q_{sp}=0.2 model and q_{sp}=0.3 model respectively. There is no remarkable tendency of inequality about the rotation angle in plastic hinge region with the deterioration level of bonding between prestressing steel and grout. If the accumulated rotation angle is a more suitable for an index to estimate the damage of concrete members than the rotation angle, in case of the member with much prestressing steel, it should be noted that the real damage would be greater than that estimated by the rotation angle (Fig.5).

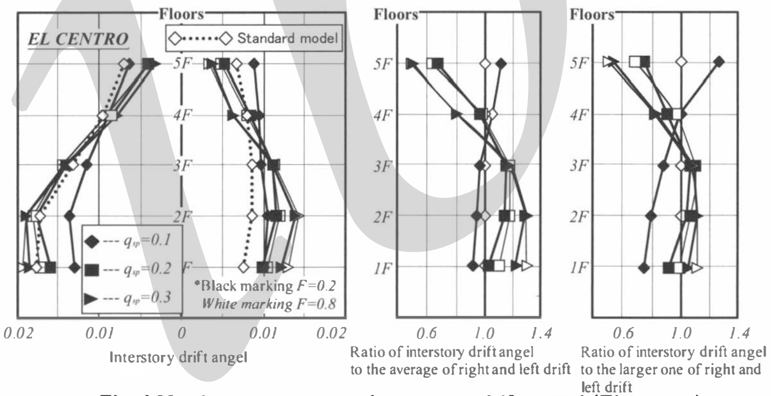

Fig.4 Maximum response interstory drift angel (El centro)

In the present paper we examined the limited models under the limited earthquake level and it is necessary to study the data covering broader fields.

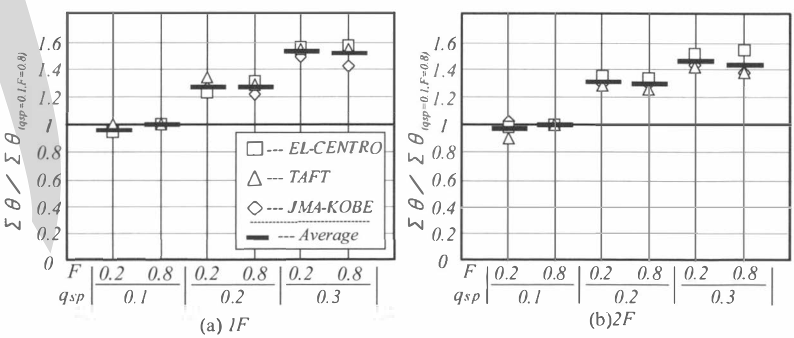

Fig. 5 Ratio of accumulated rotation angle of all models to that of standard model(qsp=0.1,F=0.8)

INELASTIC BEHAVIOR OF REINFORCED CONCRETE SPACE FRAME STRUCTURE WITH STRUCTURAL WALLS UNDER SEISMIC LOAD

Tatsuya Imanishi
MATSUMURA-GUMI Corporation
JAPAN

Toshiyuki Kubota
Kinki University
JAPAN

Keywords: structural wall, boundary column, space frame structure, inelastic dynamic analysis, bi-lateral earthquake load

1 INTRODUCTION

Reinforced concrete structural walls are usually used in buildings to provide lateral strength and stiffness against earthquake forces. Because of the multi-direction behavior of ground motions, structural walls are subjected to vertical load and lateral in-plane and out-of-plane loads simultaneously. This effect should be considered particularly in the seismic design of ductile frames.

However, the inelastic bi-lateral deformation interactions are generally neglected in structural design. And, there is no established guideline for the seismic design of reinforced concrete walls under bi-lateral earthquake loads. Out-of-plane shear capacities of the boundary columns with multistory structural wall are generally neglected in the space frame analysis subjected to bi-lateral earthquake load. There are few research works about reinforced concrete structural walls subjected to bi-lateral deformations under axial loading.

In order to understand the effect of bi-lateral earthquake load in inelastic response, a reinforced concrete space frame structure with structural walls was analyzed. Multi-story reinforced concrete structural walls subjected to bi-lateral earthquake load were discussed focusing on out-of-plane load carrying capacity of boundary columns.

2 FRAME MODEL AND ANALYTICAL METHODS

2.1 FRAME MODEL

Static nonlinear analysis and dynamic nonlinear analysis is executed about a symmetrical 7-story reinforced concrete space frame structure with structural walls shown in Figured 1[1]. The walls, the columns and the beams were so designed that the mechanism of the structure became the beam yield type.

2.2 ANALYTICAL METHODS

The structural members of the frame are replaced by bar elements (columns, beams and braces).

Columns were idealized as an elastic linear element with inelastic rotation springs at both ends considering the fluctuation of axial forces. Beams were similarly idealized as columns besides the consideration of axial force.

The deformation of multi-story structural wall shows bending yield type behavior when deformation was mainly governed by the rotation due to elongation of the tension side column. The truss model can give such deformation mechanism of a structural wall [2][3]. A wall was idealized as a truss model with inelastic column and inelastic brace.

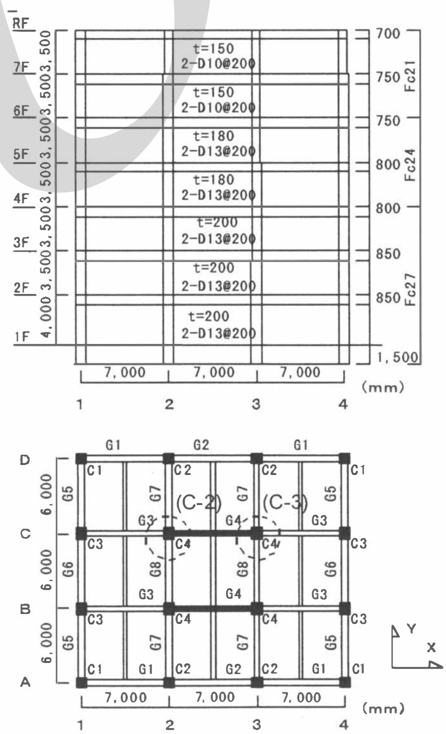

Fig. 1 Seven-Story Building

2.3 DYNAMIC ANALYSIS

In order to understand the effect of bi-lateral earthquake load, inelastic dynamic response analysis of RC space frame structures with structural walls subjected to bi-lateral earthquake load was executed. The analysis was carried out for three loading cases which are X directional horizontal load alone, Y directional horizontal load alone and X and Y directional horizontal load simultaneously.

2.4 BOUNDARY COLUMN RESPONSE

Interior axial force and out-of-plane (Y-directional) bending moment in the boundary column subjected to bi-lateral load are shown in Figure 2. Out-of-plane shear force and out-of-plane deformation in the boundary column subjected to bi-lateral load are shown in Figure 3.

When a space frame structure with structural walls is subjected to bi-lateral earthquake load, the out-of-plane flexural strength of compression-side boundary column becomes larger than that subjected to one-directional static load.

In Figure 4 the out-of-plane lateral deformations of tension-side column and compression-side column are compared. The analyzed results show significant torsional deformation behavior of the geometrically symmetrical space frame structure with structural walls, when subjected to simultaneous bi-lateral earthquake load.

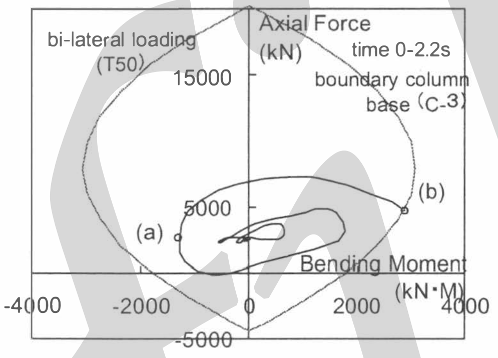

Fig. 2 Axial Force and Out-of-plane Bending Moment

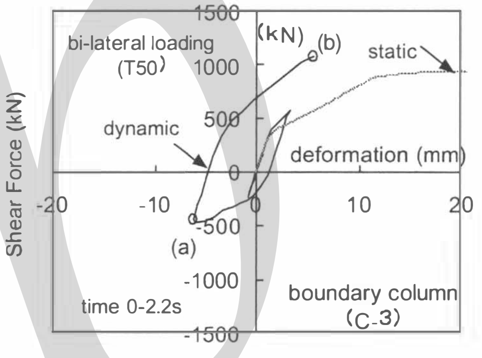

Fig. 3 Out-of-plane Shear Force and Out-of-plane Deformation

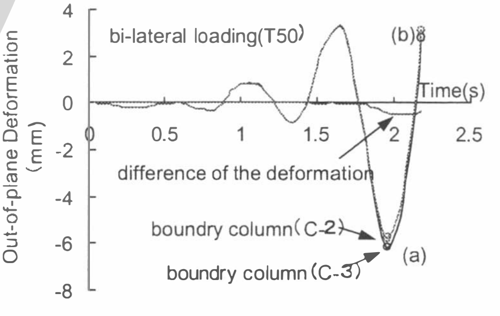

Fig. 4 Comparison of the deformation of the boundary column

REFERENCES

[1] Imanishi, T., Nakagawa, Y., Kubota, T.: Comparison Of Various Static RC Structural Computation Programs For Seismic Performance Evaluation, J. Struc. Constr. Eng., AIJ, No.545, pp.127-134, 2001 (in Japanese)

[2] Imanishi, T., Itakura, Y., Morita, S.: Static Inelastic Response of Reinforced Concrete Space frame Structure with Structural Walls, AIJ, pp.543-544, 1996 (in Japanese)

[3] Imanishi, T.: Inelastic Behavior of Reinforced Concrete Space Frame Structure with Structural Walls under Seismic Load, Thesis submitted to fulfill the requirements of Ph.D. degree, University of Kyoto, 1997, (in Japanese)

A STUDY ON THE DYNAMIC RESPONSE IN THE EARTHQUAKE AND SEISMIC DESIGN OF COMPOSITE ARCH BRIDGE

Y.Yamahana
Headquarters of Civil Engineering
The Zenitaka Corp., Japan

H.Otsuka
Department of Civil Engineering
Faculty of Engineering, Kyushu University,Japan

Y.Tanino
Headquarters of Civil Engineering
The Zenitaka Corp., Japan

H.Nunosita
Headquarters of Civil Engineering
The Zenitaka Corp., Japan

Keywords: composite arch, seismic design, nonlinear analysis

1. INTRODUCTION

Recently in Japan, some concrete arch bridges have been constructed by the concrete lapping method with pre-erected composite arches. By this method, which is called for short CLCA, at first, tubular steel arches are erected, then these tubular arches are filled by concrete to stiffen the members. After that concrete filled tubes are lapped by concrete from the springing to the crown. By this procedure composite arch rib is formed. In this type of bridge arch span length has being larger. Yumenohashi Bridge has 124m arch span length, Shimotabaru-Ohashi Bridge has 125m arch span length, and Kunimi-Ohashi Bridge has 181m arch span length.

Generally, this tubular steel arch rib has hinges at the springings, because of its erection method and erection accuracy. This member is evaluated only for erection, therefore increase of bending deformation ability and the load bearing capacity according to the composite effect can not be quantitatively evaluated in the design. After the revision (in 1996) of the specification of seismic design for highway bridges in Japan, reinforcement with large diameter must be arranged in the concrete arch rib.

From such fact, in this study, by changing the hinge type into the rigid type of tubular steel arch at the springing, it is shown that tubular steel can be evaluated as the member after bridge completing. It is aimed to establish composite arch structure that is excellent in cost and construction.

In this paper, the result of the analytical investigation for composite arch bridges which have medium large span length on seismic performance in the level 1 earthquake (it is to say L1 earthquake :medium-scale earthquake whose outbreak frequency is comparatively high), and in the level 2 earthquake (it is to say L2 earthquake :large-scale earthquake whose outbreak frequency is very small) is mainly described.

2. STRUCTURAL MODEL

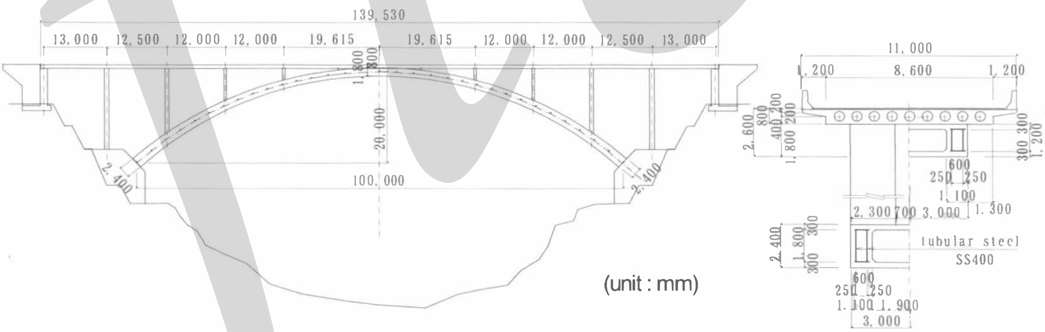

Fig.1 General view of the composite arch model with 100m arch span length (basic model)

Fig.1 shows general view of composite arch bridge which has 100m arch span length. In order to observe the effect by the difference of arch span length, analysis is also carried out for the models of arch span length of 150m and 200m of which the rib height and arch rise, etc differs from the basic model (100m arch span).

3. ANALYTICAL MODEL

The M-ϕ model (the Takeda model: degrading tri-linear type: Fig.2) is used in this study for the elasto-plastic seismic response analysis. Since the axial force of the arch rib member largely fluctuates by the longitudinal motion, the analysis is carried out using asymmetric degrading tri-linear type which can respond to axial force fluctuation (the modified Takeda model) in respect of the restoring force characteristics of arch rib members. The analysis is carried out using the fiber model for the arch members in order to observe as well the difference between the stress of main reinforcement and the stress of the steel plate, as the difference from the result by modified Takeda model.

Support conditions of the model are rigid at the springing, hinge at the top of piers and pin-roller at both ends of the stiffening girder. The damping coefficient is adopted 0.03 for arch and pier members, and 0.02 for the stiffening girder in these analyses. The seismic motions used in these analyses are Kobe marine meteorological observatory wave (T2-1-1), and Kaihoku kyou wave (T1-1-1). Time step for analysis is 0.002 second, and dynamic analysis is conducted for 40 seconds. As the restoring force characteristics are considered by three following models.

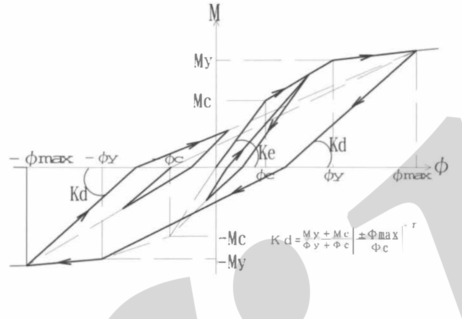

Fig.2 Restoring force characteristics (The Takeda model)

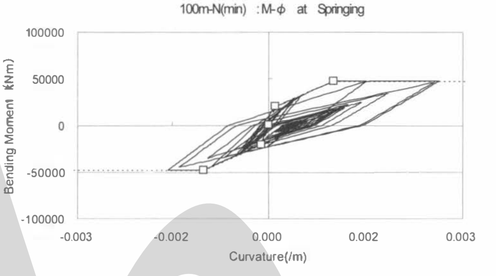

Fig.3 M-φ hysteresis loop(case3:axial force minimum)

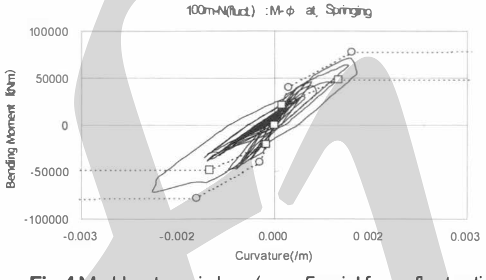

Fig.4 M-φ hysteresis loop(case5:axial force fluctuation)

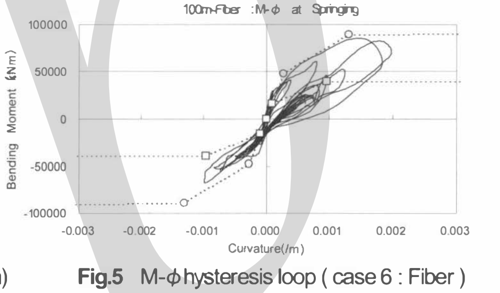

Fig.5 M-φ hysteresis loop (case 6 : Fiber)

4. RESULT

We studied on the construction stage and L1 level earthquake ,and on seismic performance in the L2 level earthquake of the composite arch bridge with the middle and long span(100m～200m arch span) ,which is built by CLCA method. The following was clarified as the result.

①Since the bending moment increases during construction of the arch rib by lapping with concrete, and the concrete filled tubular steel member is burdened by axial force, the axial force which affects concrete member does not increase so much. Necessary reinforcement content can not be decreased. The reduction of reinforcement content during construction is possible by effectively handling the flange plate, and it becomes the rational structure.

② In the longitudinal direction of the composite arch deck bridge with 100m arch span length, the seismic performance after completion of the bridge is improved and it becomes economical, if the flange plate is handled as an effective reinforcement by making the springing of tubular arch into rigid type. For the over 150m span length, the axial force increases, and the effect of the tubular steel becomes smaller concerning the seismic performance.

③On the other hand for the transversal direction of the bridge, it was proven to be also effective on arch span length of 150m and 200m for the seismic performance, if the web plate is handled effectively.

④ In the analysis according to the M-φ (the Takeda) model, which is constant in respect of the axial force, it becomes that the plastication of the member is excessively evaluated, and the design stands on the safety side.

⑤ In case of the fiber model, the stress history of the main reinforcement and the flange plate can be evaluated, and it has reached almost at the same time to the yield point in case of both longitudinal and transversal direction of the bridge for the 100m arch span model.

EFFECTS OF LATERAL PRESTRESS AND ITS MECHANISM ON REINFORCED CONCRETE COLUMNS UNDER COMPRESSIVE AND FLEXURAL STRESSES

Hiroshi Watanabe
Graduate School,
Tokyo Institute of Technology,
JAPAN

Morio Minemura
Central Japan Railway Company,
JAPAN

Keiichi Katori Shizuo Hayashi
Structural Engineering Research Center,
Tokyo Institute of Technology,
JAPAN

Keywords: laterally prestressing, columns, high strength transverse hoops

1. INTRODUCTION

It has been recognized that seismic performance of the reinforced concrete column can be improved when using high strength steels for transverse hoops of the column. Generally in many cases, higher strength were not enough available, because concrete collapse faster than steel's yielding. It is considered that following columns are rational, be expectable full exhibition of high strength steel's performance and active confined effect for concrete with introducing lateral prestress by using high strength transverse hoops. In order to consider effects of the lateral prestress on the concrete columns, eccentric compression tests of such columns were performed. On the other hand, very few attempts have been made at internal stress condition of active confined concrete. Internal strain distribution of the confined concrete column by performing the elemental tests which modeled minute element of the column shall be measured directly, and mechanism of the active confined effect shall be investigated.

2. MECHANICAL BEHAVIOR OF THE LPRC COLUMNS UNDER COMPRESSIVE AND FLEXURAL STRESSES

2.1 Outline of eccentric compressive test

Eight specimens with 120mm×120mm cross section, 270mm length, and about one fifth scale were constructed for the test. The alternating factors are σ'_{wp}=initial tensile stress introduced into a transverse hoop (0 or 0.3 σ_{wy} or 0.6 σ_{wy}), e=eccentric loading distance (0 or 15 or 35mm), and s=pitch of the transverse hoops (30 or 60mm). The fixed factors are quantity of the longitudinal steel bars, bar arrangement (expect No.8), and the concrete mixture. The transverse hoops were made by 2.0mm dia. high strength piano wire with square shaped and welded. Fig.1 shows the loading and measuring apparatus. Arrow shows the eccentric compressive loading. The strain of the longitudinal steel bars and the transverse hoops were measured by using strain gauges. It was pre-tension method that introduced the tensile forces into the transverse hoops before concrete was placed. The initial stress value was controlled by strain gauges of all transverse hoop. The test specimens were listed in Table 1.

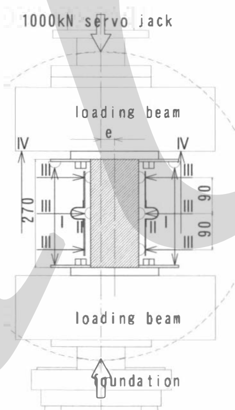

Fig.1 Loading and measuring method

Table 1 List of test specimens

No.	σ_{wp}/σ_{wy}	e (mm)	S (mm)
1	0.0	0	30
2	0.6		
3	0.0	15	
4	0.6		
5	0.0	35	
6	0.6		
7	0.3		
8	0.6		60

2.2 Tests results and consideration

The Laterally Prestressed Reinforced Concrete (LPRC) specimen's maximum bending strength exceeded the Reinforced Concrete (RC) specimen's one. The increase ratio was 6% in e=15mm, and 10% in e=35mm. Fig.2 shows the relation between the transverse hoop strain and the column strain in the longitudinal direction. Vertical axis indicates the transverse hoop strain and horizontal axis indicates the coefficient of the column strain divided by the measured strain when the load in maximum. The RC specimen's ε_w was larger than the LPRC specimen's one. The difference became more remarkable especially after maximum load. ε_{wp} of the LPRC specimen was more than double ε_w of the RC specimen at maximum load. ε_w of the RC specimen and ε_{wp} of the LPRC specimen were defined as the confining force be acting core concrete, ε_w of both specimen were defined as volumetric expansion on the core concrete. The volumetric expansion of the LPRC specimen's core concrete were smaller than the RC specimen's one, because already had been subjected larger confining force before maximum load. Active confining forces prevent volumetric expansion after maximum load, and affects especially on negative slope of the strength softening zone of the LPRC specimen.

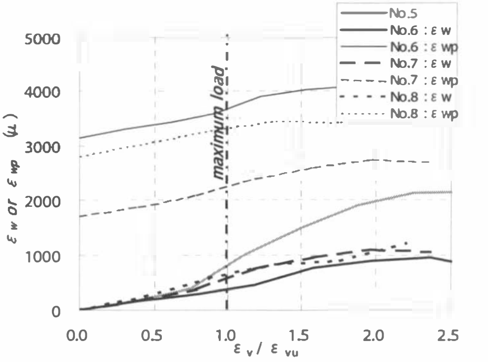

Fig.2 Strain of transverse hoops

3. MECHANISM OF ACTIVE CONFINEMENT

3.1 Outline of elemental test

In this chapter, in order to verify the confinement mechanism, the small segment of the LPRC tests were developed as follows. There were 5 kinds and 3 pieces each of test specimen, totally 15 pieces were prepared for these tests. No.9 to 13 tests carried to make active confinement on each specimen, by using turn buckles to give tension on the hoops, in Fig.3. The tensile force was measured by using strain gauge attached to hoops, and the strain of concrete were measured by this confining force using 1 axis or 3 axis 10mm strain gauges.

3.2 Test results and consideration

The authors tried to investigate correspondence between the experimental elastic strain distributions and the analytical strain distributions, which was analyzed by 3-dimensional finite element method. Specimens No.10 to 13 are made into the candidate for this elastic analysis. Good correspondence is shown, therefore this examination limited within elastic range. Approximately, it became clear that the strain of the elastic range of active confined concrete could be evaluated by 3-dimensional finite element method. A maximum principal stress distribution of No.11's cross section at the transverse hoop position obtained from the analysis result is shown in Fig.4. Since specimen was modeled faithfully, the vertical side was not restrained. On the other hand, since actual column is faithfully modeled in the examination of internal stress, the vertical side is restrained in the longitudinal direction in subsequent examination. The stress produced in concrete becomes the maximum near the longitudinal bars, and becomes small near the center. The active confinement is acting especially on the high domain of stress shown in the figure. It was pointed out in the previous chapter that the seismic performance of column improved by laterally prestressing in the eccentric compression tests. Large active confinement is working to the area of the column section which receives large stresses in compression and flexure. It is thought that active confined effect is expectable under compression and flexure.

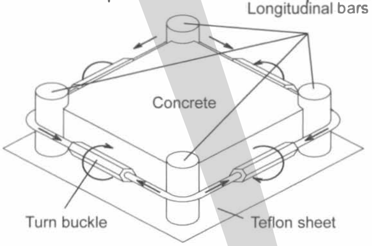

Fig.3 Loading methods for No.10-13

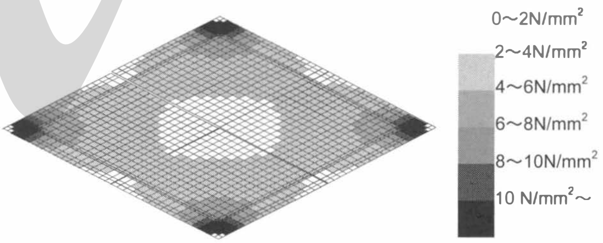

Fig.4 Maximum principal stresses distribution at *T*=5kN

REFERENCES

[1] Watanabe, H. et al.: Experimental Research on Shear Strength of Short Reinforced Concrete Columns with Prestressed Hoops, 12th World Conference on Earthquake Engineering, New Zealand, 2000

[2] ---.: Internal Stress Conditions of Active Confined Concrete Column Element by Lateral Prestressing (Part 1, 2), Summaries of Technical Papers of Annual Meeting Architectural Institute of Japan C-2, pp.487-490, 2001.9

[3] Minemura, M. et al: Mechanical Behaviors of Reinforced Concrete Member under Eccentric Load, Proceedings of the Japan Concrete Institute Vol.23, No.3, pp.637-642, 2001

[4] Architectural Institute of Japan: Design Guidelines for Earthquake Resistant Reinforced Concrete Buildings Based on Inelastic Displacement Concept, 1999

SEISMIC UPGRADING BY PRECAST CONCRETE BRACE WITH ENERGY DISSIPATING FRICTION JOINT

Kishihiko Moriyama, Technical division1, Yutaka Osanai, Osaka Brunch, Kenji Tabata, Construction Branch, Oriental Construction, Japan

Fumio Watanabe, Professor, Department of Architecture and Architectural Systems, Kyoto University, Japan

Keyword : seismic upgrading, external brace system, precast prestressed concrete, friction joint

1 INTRODUCTION

Many of existing reinforced concrete buildings built before 1980 don't meet the structural seismic performance required by the current regulations in Japan. After the Kobe Earthquake, seismic upgrading of existing building structures has been put into force, especially for public buildings such as schools and hospitals. However, the bracing method by precast concrete elements is not well established. This report proposes the seismic upgrading method by the external precast concrete brace which has friction joints with performance of energy dissipating. Further, 3 test results to establish the design and examples of building adopted the proposed bracing system are reported.

2 FEATURES OF PROPOSED METHOD

Outline of proposed method is indicated in Fig.1.In order to solve these problems and requirements, the proposed bracing system has some features as follows. 1) This bracing system consists of two precast concrete diagonal elements. 2) These diagonal elements are attached to the outside of a frame by binding joint. 3) This system has the friction control joint. The friction control joint is realized to dissipate seismic energy and to control the input axial forces to diagonal elements in order to avoid the stiffness change due to tension cracking and the brittle failure of diagonal elements. 4) These diagonal elements are prestressed by post tensioning in order to raise the tension cracking strength.

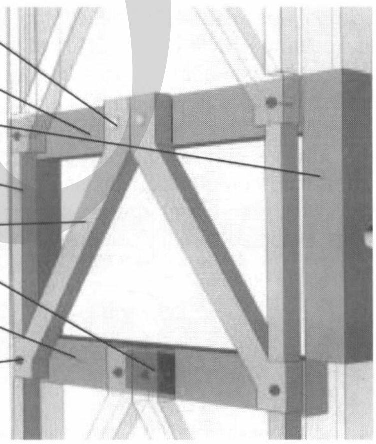

Fig.1 Seismic upgrading by the brace system

3 TESTS OF FRICTION MATERIALS AND BRACED FRAMES

3. 1 Friction tests of granite plate

By push-off shear tests, the design values of friction coefficient for seismic design were determined as follows.

(1) Friction coefficient of first slip = 0.40

(2) Friction coefficient for ensuring resistance of brace system. (Beyond 10mm slip) = 0.65

3. 2 Static loading test on a reinforced concrete frame with brace system

Static loading test was performed using the testing frame of 1/2 scale of the assumed structure. Obtained load deflection curve by test and calculated load deflection curve by non-linear two-dimensional analysis is indicated in Fig.2. Many of the calculated values were identical to the values obtained by the experiment, and the effect of seismic upgrading by brace system has been confirmed.

3.3 Shaking table tests of brace system

Shaking tests were performed using the 2 specimens for the purpose of investigating the dynamic behavior of the brace system. Design friction coefficient based on the static tests and observed friction coefficients by shaking tests was compared in Fig.3. The established friction coefficient in order to calculate the shear strength is appropriate also in shaking tests.

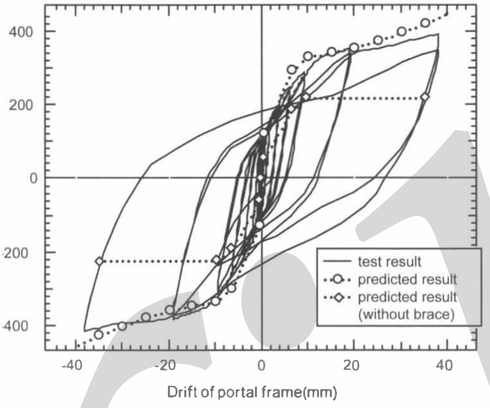

Fig.2 Load deflection curve

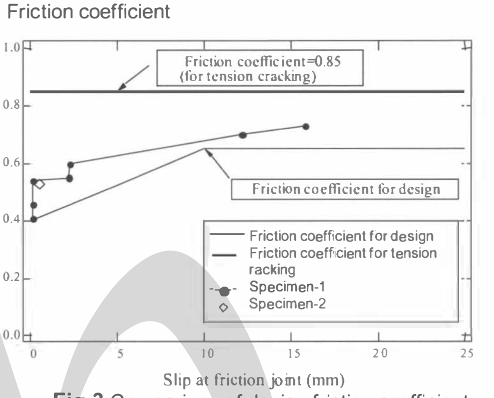

Fig.3 Comparison of design friction coefficient and observed friction coefficients

4 EXAMPLE OF BUILDING ADOPTED BRACE SYSTEM

This chapter introduces seismic upgrading work of a certain junior high school building that adopted a proposed bracing system. A photograph before and after upgrading is indicated in Fig.4, Fig.5. Construction works could be completed during a short period and without interrupting the use of buildings because this bracing system consists of two precast concrete diagonal elements and is installed in perimeter of building. Attaching of the brace systems took the 15th day at construction of this junior high school building. (The number of Installation of the bracing system is 15).

Fig.4 Photograph before upgrading

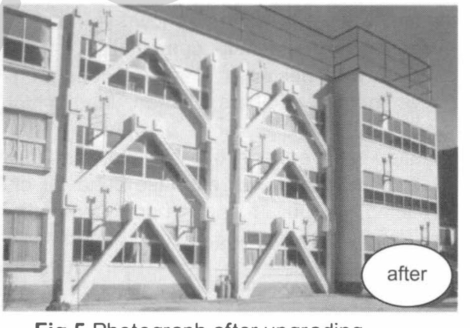

Fig.5 Photograph after upgrading

REFERENCES

[1] Standard for Structural Design and Construction of Prestressed Concrete Structures : November, 1998, Architectural Institute of Japan
[2] The assessment of seismic performance and the seismic retrofitting of the existing building, The kenchiku gijutu, No571, pp88-197, October, 1997 (In Japanese)

DESIGN FOR A HIGH-RISE RC STRUCTURE BUILDING USING A SEISMIC ISOLATION SYSTEM

Hisato OKUDE Akira SUMI Hiroyuki UEDA Yuuji ISHIKAWA
Takenaka Corporation, JAPAN

Keywords: High-rise RC structure, Seismic isolation system, High-strength concrete, Pre-cast

SUMMARY

The building we present in this paper has 25 stories and the main structure is made of reinforced concrete using a seismic isolation system. It has a rectangular plan of 39.8m by 19.6m and a height of 75.15m (cf. Fig. 1). Since high-strength concrete of 80N/mm^2 was applied to reduce the number of columns, a design of free plan rooms became possible. This paper shows an outline of the structural design and illustrates a detail of the isolation system and pre-cast construction system.

In a high-rise building using a seismic isolation system it is important that the vertical stress of the laminated rubber isolator keeps compression at all times because the tensile strength of the rubber is rather weak. As the seismic over-turning moment (O.T.M.) is very large in a high-rise building, isolators located under end-columns have to receive a large amount of pulling force during an earthquake. The biggest problem on a structural design is to diminish the O.T.M. with an optimum isolation system.

Numerical analysis on four kinds of combinations were performed shown in Table 1 and selected the best combination. The combination we selected is "Case-C"; consisting of: five natural rubbers, fifteen lead plug rubbers, and five steel dampers. This combination was very effective in diminishing the O.T.M. and improving the response behavior of the building. Our results from computer analysis show that all laminated rubbers will keep their compression on level-2 earthquakes that have a grand velocity of 50cm/sec.

A construction system using pre-cast concrete pieces was adopted for standard floors of the building. The characteristic of our system is in using a pre-cast piece with which the beam-column connection and the beam are united. There are holes that let the main reinforcement of a column pass in a connection, and inserting the main reinforcement of pre-cast column piece into the hole connects two pre-cast pieces.

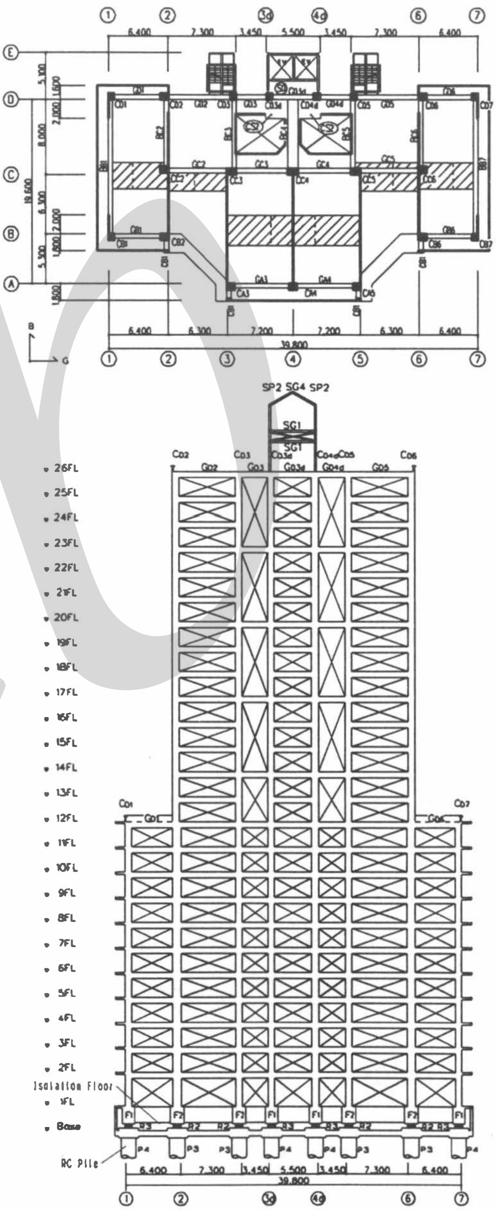

Fig. 1 Structural plan and framing elevation

Then a special high-strength mortar is poured in-between the main reinforcement and the hole in order to secure the adhesion of the main reinforcement in the beam-column connection. It was confirmed that the performance of the beam-column connection using this joint system is equal to the performance without joint by one half model experiment.

Table 1 Simulation Case

Case	Number of devices		
	Natural rubber	lead plug rubber	Steel damper
A	0	20	0
B	3	17	0
C	5	15	5
D	9	11	7

Legend of Waves

- EL CENTRO NS (Observed wave)
- TAFT EW (Observed wave)
- HACHINOHE NS (Observed wave)
- UEMACHI (Imitated wave)
- KOKUJI-123 (Wave decided by law)
- KOKUJI-200 (Wave decided by law)

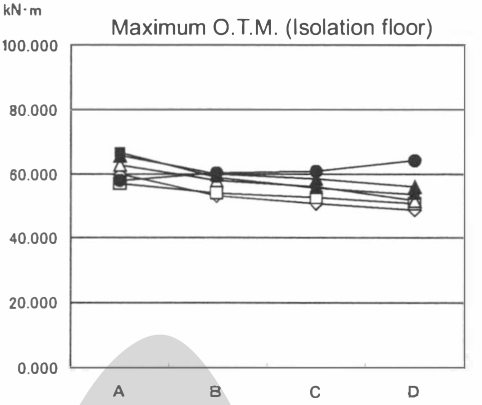

Fig. 3 Comparison of response analysis

Step.1 Building the pre-cast columns

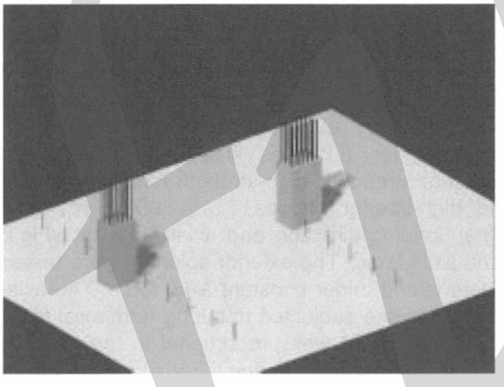

Step.2 Building the pre-cast walls

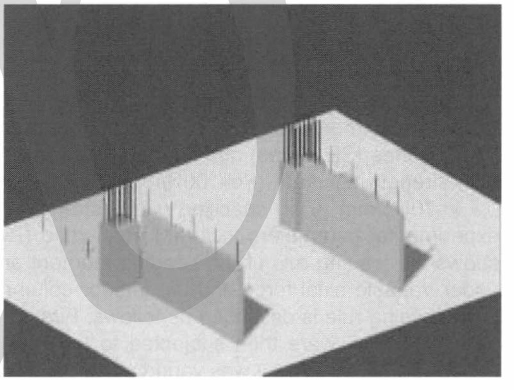

Step.3 Building the connection and beam piece

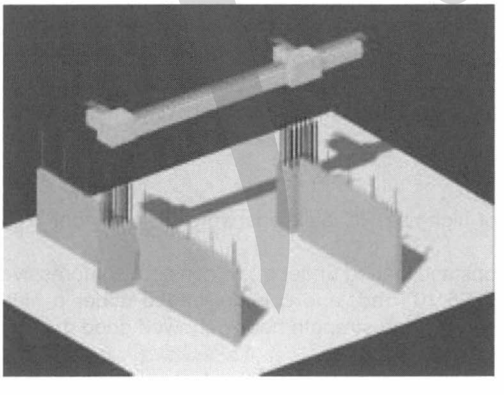

Step.4 Setting up of half pre-cast slabs and pre-cast balcony slabs

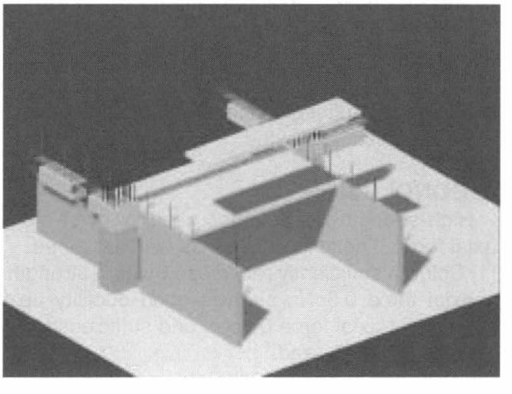

Fig. 3 Construction procedure

STRUCTURAL PERFORMANCE OF HIGH STRENGTH RC COLUMNS WITH 100N/mm^2 STRENGTH CONCRETE

Akiko Kimura Makoto Maruta
Kajima Technical Research Institute
Japan

Keywords: high strength material, variable axial force, bending, shear, column

1. OUTLINE

In Japan, high-rise RC building technology has been developing since the first high-rise RC building was built in 1974. Recently, high-rise RC buildings of over 50 stories have been planned. Columns in the lower stories of high-rise RC buildings are subjected to high long-term compressive axial forces, and the exterior columns are also subjected to high variable axial forces due to overturning moments under earthquake. Therefore, high axial strength columns using high-strength materials have been required to resist earthquake forces.

However, the structural performance of high-strength columns subjected to simultaneous high constant axial forces and high variable axial forces is not clear. The lowest story is normally higher than the upper and yielding hinges are designed to form at the lowest column base under severe earthquake. Therefore, it is necessary to know the structural performance of the lowest-story columns after yielding hinges form. Lower columns from the 2nd~5th stories also need to be of high-strength materials for axial resistance.

This experimental study was carried out to investigate the structural performance of high-strength columns in the lower portion of a high-rise RC building of over 50 stories. Table 1 lists the seven specimens used and their material properties. The scale of the specimens was 1/2.7. The tests were carried out using the test setup shown in Photo 1. Details of the exterior column in the lowest story (LE7) and a section of the 45-degree loading direction column (LE10-45) are shown in Fig.1.Three types of specimens were used: exterior columns in the lowest story (LE series), exterior columns in the lower stories (SE series) and interior columns in the lowest story (LI series). These specimens used high-strength concrete (Fc=100N/mm^2 Fc: design concrete strength), high-strength longitudinal bars (σ y=700N/mm^2 σ y: specified yield strength) and high-strength hoops (σ y=800N/mm^2). The experimental parameters included hoop ratio (Pw (%)), loading direction and axial force ratio.Fig.2 shows the loading rule of the bending moment and the axial force. The exterior columns were tested under variable axial force and the interior columns were tested under constant axial force. The axial force-loading rule is described as follows. First, the columns were subjected to a long-term axial force (0.2cNu). They were then subjected to a variable axial force that was proportional to the bending moment. The axial force was varied up to 0.7cNu on the compressive side and 0.75tNu on the tensile side. When the predicted bending moment of the column was reached, the axial force reached the maximum value: 0.75tNu or 0.7cNu.

The maximum bending strength of high strength RC column under high axial force was not clear. Therefore, the maximum strength obtained from the test results was compared with bending strength obtained from ACI [1] stress block method, which was useful in design of columns, and the maximum strength of the tests was quite higher than the calculations. Then, a particular bending analysis considering confined concrete was conducted and the tri-linier skeleton curve considering variable axial force was also suggested.

2. CONCLUSION

High-strength RC columns used in lower stories of high-rise RC buildings were tested under high axial force. The following results were obtained.

[1] Column sufficiently reinforced by high-strength hoops and loaded under a low constant compressive axial force 0.3cNu showed good ductility up to R=95*10^{-3} rad, and column loaded under a high constant axial force 0.6cNu and sufficiently reinforced by high-strength hoops showed good ductility up to R=20*10^{-3} rad.

[2] The maximum strengths obtained from the test results exceeded the ultimate bending strengths quantified by the ACI [1] stress block method. Thus, a particular bending analysis considering confined concrete was conducted to figure out the bending strength, and the bending strength of the

analysis showed good correspondence with the maximum strength of the test results.
[3] The skeleton curve considering variable axial force showed good correspondence with the restoring force characteristics obtained from the test.

REFERENCES

[1] American Concrete Institute: Building Code and Commentary ACI 318-95/318R-95, 1995
[2] Architectural Institute of Japan: Design Guidelines for Earthquake Resistant Reinforced Concrete Building Based on Ultimate Strength Concept, 1990 (In Japanese)
[3] Architectural Institute of Japan: AIJ Structural Design Guidelines for Reinforced Concrete Buildings, 1994.

Table 1 List of Specimens

Location	Series	Specimen	Cross Section	M/QD	Axial Force	Pw (%)	Material Properties (MPa)	σ_B (MPa)	Ec (kN/mm²)
Exterior Column	LE	LE7	300 × 300	2.5 Lowest Story	0.75tNu ~ 0.7cNu	0.7	Concrete Fc=100 Reinforcement Longitudinal D19-SD685: σ_y=722 Transverse D6-SD785: σ_y=1053*2	112	36.6
		LE10				1.0		114	37.8
		LE10-45*1				1.0		113	38.1
	SE	SE7		1.5 Lower Story		0.7		116	37.4
		SE10				1.0		119	37.9
Interior Column	LI	LI9	300 × 300	2.5 Lowest Story	0.3cNu	0.9		106	35.2
		LI12			0.6cNu	1.2		115	37.4

cNu=0.85Fc(bD-ΣAg)+ ΣAg·σy tNu= ΣAg·σy
Ag: Sectional Area of Longitudinal Bar σy: Yielding Strength of Longitudinal bar M/QD: Shear Span Ratio Pw: Hoop Ratio
σ_B: Compressive Strength of Concrete Ec: Young's Module of Concrete *1: 45-degree loading direction *2: 0.2% Offset Value

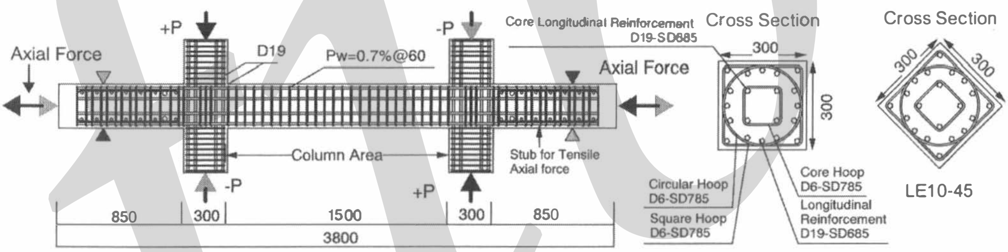

Fig.1 Outline of Specimen

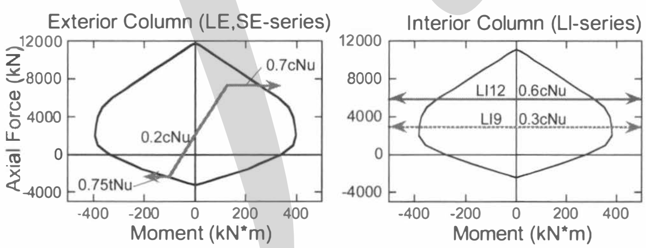

Fig.2 Loading Rule of Bending Moment and Axial Force

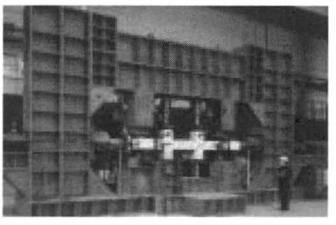

Photo1 Outline of Loading

EARTHQUAKE PERFORMANCES OF PRESTRESSED CONCRETE FRAME WITH DANMPING SYSTEMS

Fu Jinhua, Kimiya Hamada, Kazunori Osako and Mitsuo Hayashi
P.S. Corporation
JAPAN

Keywords: high-rise precast PC building, earthquake response, damping system

SUMMARY: In this paper, a high-rise precast prstressed concrete housing (precast PC) was designed using damping systems to dissipate the earthquake energy. Two cases of earthquake response analyses for the precast PC buildings with and without damping systems were carried out under four typical earthquake motions.

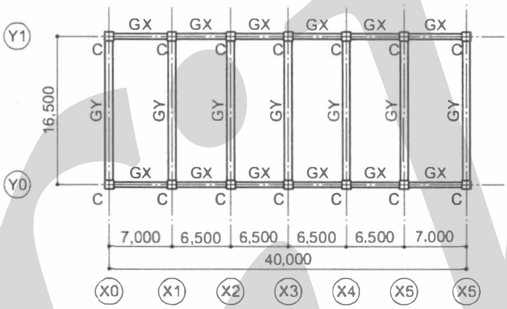

Fig.1 Typical Floor Plan

1 INTRODUCTION

As the precast PC frame was considered generally to perform large response comparing with the other structural systems under earthquake motions, the high-rise frame using PC members was not designed and planned. However, the prestressed concrete member performs excellent restoring behavior and good durability under service loading. In this study, a 22-story precast PC moment resisting frame housing with one long span was produced to design using damping systems to dissipate the earthquake energy. The damping systems were used as hydraulic oil damping systems, and that were set within the frame in two-ten stories.

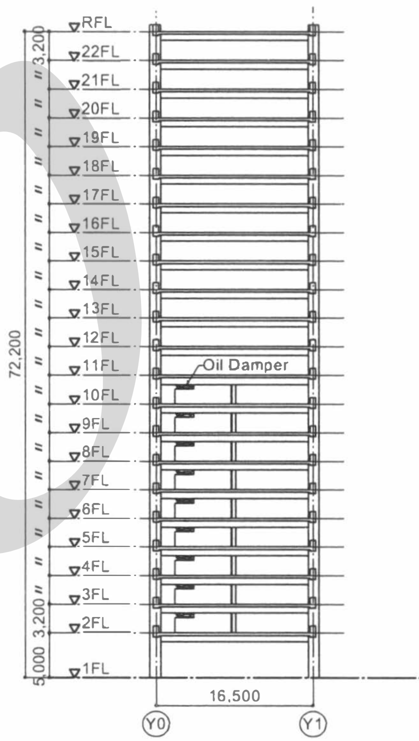

Fig.2 Structural Elevation

2 OUTLINE OF BUILDING PLANNED

The typical floor plan and structural elevation are shown in Fig.1 and Fig.2. The compressive strength of cast-in-situ normal concrete is 30 N/mm². That of precast concrete are 80 N/mm² for first to eighth story columns, 70 N/mm² for ninth to sixteenth story columns, 60 N/mm² for seventeenth to upper story columns and all beams. The yield strength of PC bars for prestressing for columns is 1080 N/mm², and that of PC strands in beams is 1570 N/mm².

3 NONLINEAR EARTHQUAKE RESPONSE ANALYSIS

Nonlinear earthquake response analyses were carried out to investigate the seismic performances of the high-rise precast PC building with damping systems and without ones in the transverse direction under four typical simulated earthquake motions of BCJ-L2, EQ-1, EQ-2 and EQ-3. Analyzing method was as numerical integration by the Newmark's β method (β=1/4). The damping factor for first mode was assumed to be 3%. For structural PC members, the PC hysteresis model shown in Fig.3 was used [1]. The damping systems used as hydraulic oil dampers in two-ten stories of the building are all same. The force of dampers is assumed to be proportional to the velocity. As shown in Fig.4, the yield force Fy=3528kN, the initial stiffness C1=1568kN/cm, and the second stiffness C2=627kN/cm.

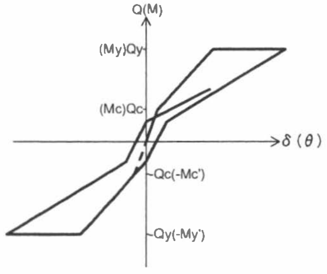

Fig.3 PC Hysteresis Model

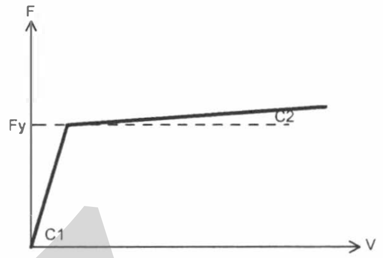

Fig.4 Model of Oil Dampers

4 RESULTS

The elastic periods of the frame for the three modes in transverse direction are 2.10sec, 0.67sec and 0.37sec. The maximum drift angles for two cases of frame with damping systems and without ones are shown in Fig.5 and Fig.6, in which the maximum drift angles were compared for four simulated earthquake motions. From Fig.5 and Fig.6, it is observed that earthquake response in the frame without damping systems was large significantly to compare with that in the frame without ones.

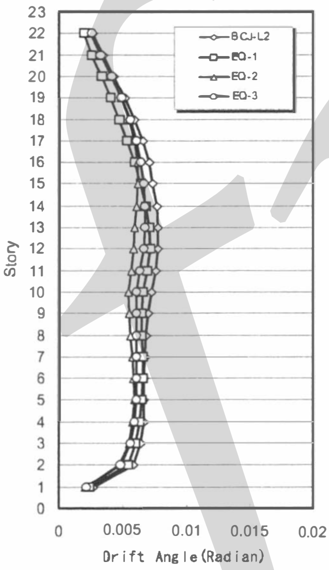

Fig.5 Maximum Drift Angle
(with Damping System)

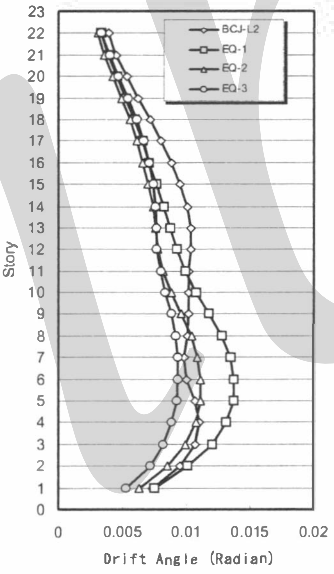

Fig.6 Maximum Drift Angle
(without Damping System)

5 CONCLUSIONS

The nonlinear earthquake response analysis of the precast PC frames with and without damping systems was carried out using four typical simulated earthquake motions. These analytical results were compared to investigate response characteristics in each frame. From comparison of those results in the two cases of PC frames, the following conclusions may be drawn:

1) Response of PC frame with damping systems is much smaller than that for PC frame without ones.
2) Ratios of the maximum response drift angle for PC frame with damping systems : PC frame without ones was shown as 1.00 : 1.73 in the transverse direction frames.
3) Earthquake response in precast PC frame could be reduced significantly by using damping systems.
4) Earthquake response of the frame with damping systems satisfies design criteria for severe earthquake motions favorably.

REFERENCES

[1] Hayashi, M., S. Okamoto, S. Otani, H. Kato, and J. Fu, "Hysteresis Model for Prestressed Concrete Members and Its Effect on Earthquake Response", JOURNAL OF PRESTRESSED CONCRETE, JAPAN, pp57-pp67, Vol.37, NO.4, July 1995.

PERFORMANCE OF STATICALLY INDETERMINATE FORCE IN THE ULTIMATE STATE

Kazunori Osako Takashi Toma
P.S.Corporation
JAPAN

Hideo Moritaka
YASUI Architects & Engineers
Inc.,JAPAN

Yoshiteru Ohno
Osaka Univ.
JAPAN

Keywords: statically indeterminate force, nonlinear analysis, reduction factor, ultimate state

1.INTRODUCTION

This study was carried out by working group (chairman: H. Watanabe) for evaluation on structural characteristics and capacity of the member in Joint Coordinating Committee (chairman: S. Okamoto) on High-rise Prestressed Concrete Building organized by Building Research Institute, Ministry of Construction. Statically indeterminate force of frame member in the service state was calculated commonly by elastic analysis. Similarly, member stress under seismic loading was calculated by elastic or linear stiffness analyses in a normal-rise building. Then, ultimate strength design of the prestressed concrete members was carried out due to sum of these forces using load factors for the ultimate state. Also, statically indeterminate force of each member accompanied by dry-shrinkage, creep, axial deformation, and the deflection due to prestressing of tendons were calculated based on elastic stiffness. However, such a design to sum the forces is very severe in high-rise building to consider economical structural design. A cause to arise the statically indeterminate force is originated by restraining the rotational angle, displacement, and axial deformation at the free ends of the member. Therefore, a value of the statically indeterminate force is varied accompanied by fixing condition at the end of a member. Excessive flexural moment corresponding to the ultimate flexural capacity may be undergone at the both ends of a member in the ultimate state under seismic lateral load, the rotational stiffness at the end of a member was reduced significantly. Also, the statically indeterminate force at the end of a member undergoing at the initial elastic stage was reduced accompanied by reducing level of rotational stiffness at the end of a member. The reduction of rotational stiffness from flexural cracking to yielding in the member undergoing the anti-symmetric moment was represented generally as a relation factor α_y at yielding. A common relation factor α_y at yielding in the prestressed concrete member is distributed from 0.25 to 0.35. The reduction factor α_y at yielding is shown as Fig.1.

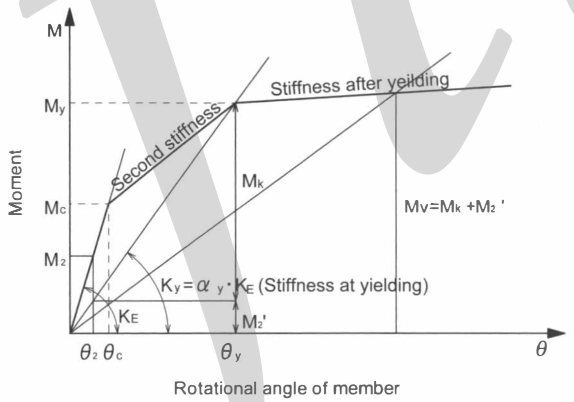

where, K_E: Initial elastic stiffness,
M_y: Flexural yielding moment,
M_c: Flexural cracking moment,
M_k: Flexural moment by seismic lateral loading,
θ_2: Rotational angle restrained by fixing condition,
M_2': $\alpha_y \cdot M_2$ (equivalent statically indeterminate moment at yielding)

Fig.1 Reduction factor α_y at flexural yielding

The reduction factor α_y at yielding is used commonly as varying model of the rotational member stiffness in the nonlinear frame analysis. Therefore, from the nonlinear rotational stiffness model of member, equivalent statically indeterminate forces could be estimated favorably. Beside, the rotational angle restraining at the initial elastic stage is not varied favorably. The performances of the statically indeterminate force accompanied by varying of the rotational member stiffness are below;

1) In the initial elastic stage, all member forces are summed up involving the forces by seismic lateral loading completely. The statically indeterminate forces are not varied.
2) In the stage after flexural cracking to flexural yielding, Initial statically indeterminate force is reduced to be the ratio of equivalent rotational stiffness to the initial rotational stiffness. Also, the effective statically indeterminate moment M_{2e} may be assumed to be $\alpha_y \times M_2$ (about 0.25 to $0.35 \times M_2$) favorably at yielding.
3) The statically indeterminate force was reduced significantly under the ultimate state after yielding, and the effective stress M_{2e} is assumed as $(\alpha_y / \mu) M_2$ favorably.

where, μ : member ductility factor (θ / θ_y), θ : rotational angle of member, and θ_y: rotational angle at yielding.

From the above estimation, the performance of statically indeterminate force in each state may be assumed using the nonlinear characteristics of member favorably. Thereupon, in the cases that the elastic statically indeterminate force was equal to less than about 0.3 times the yield flexural capacity at the ends of a normal concrete member, the effective force was assumed to be about 0.1 times the yield flexural moment. Such an effective statically indeterminate force could be taken no account favorably under the ultimate state. Thereupon, five story prestressed concrete frame building was planed to study performance of the statically indeterminate force under the ultimate state by nonlinear analysis. The member force of the frame under service loading was first calculated using elastic stiffness. To investigate member force and ductility factor of each frame member at seismic loading stage were carried out using two cases of incremental load analyses under loading and unloading the statically indeterminate forces. From the results of two analyses, it's clarified that statically indeterminate forces in the ends of member by service loads are not remained favorably under the ultimate state. Performances of the statically indeterminate force in each stage of seismic loading are discussed.

2. ANALYTICAL RESULTS

Two cases of incremental load analysis were carried out as a push over method. A case 1 was to undergo the statically indeterminate force at the ends of a member, and another Case 2 was analyzed unloading the statically indeterminate force before incremental load analysis. Member force of each case in a loading stage of 0.3 are shown in terms of a base shear coefficient C_B in Fig. 2.

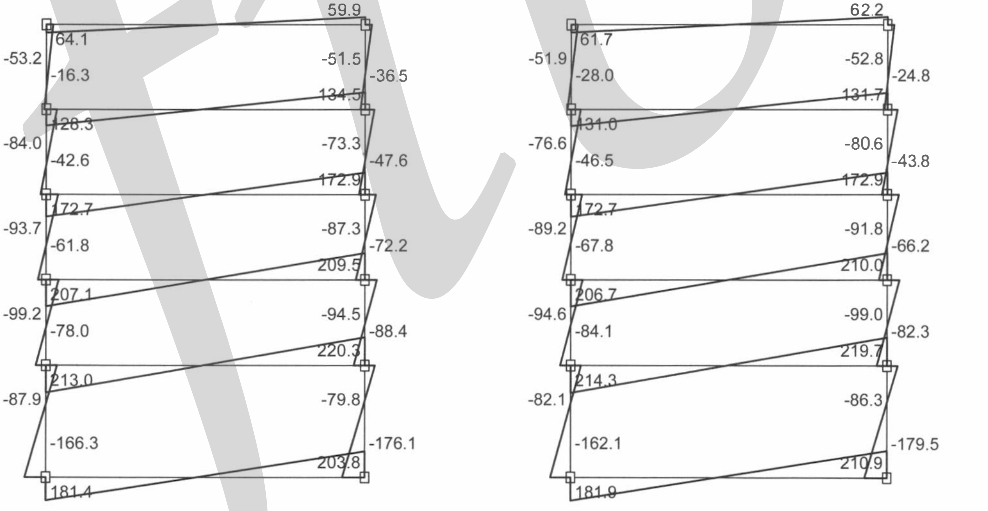

(a) C_B=0.3 <Case-1> (b) C_B=0.3 <Case-2>

Fig.2 Member Force of Each Case

REFERENCE

[1] Toma T., Ohno Y.,Moritaka H., and Hayashi M. "Statically Indetermination Force of Prestressed Concrete Frame at Ultimate State", Proceedings of The 8th Symposium on Development in Prestressed Concrete, 1998.

EXPERIMENTAL STUDY ON PRECAST REINFORCED CONCRETE FRAMES FOR HIGH-RISE BUILDINGS

Makoto MARUTA
Kajima Technical Research Institute
JAPAN

Haruhiko SAKAI
Kansai Branch, Kajima Corporation
JAPAN

Keywords: high-rise building, high strength concrete, structural test, precast, beam-column joint

1 BACKGROUND AND OBJECTIVES

Many high-rise reinforced concrete (RC) structures were constructed as cast-in-situ in Japan. Recently, precast (PCa) method have been developed and adopted for those buldings. Use of precast members speeds up construction and saves labor cost.

Beams and columns are often precast, while beam-column subasseblages (referred to hereafter as Panel) are normally cast-in-situ. Panels for high-rise buildings have heavy reinforcement in beams, columns, orthogonal beams and transverse members. It is difficult in PCa to arrange and set those rebars in panel as same as cast-in-situ. Therefore, new precasting methods are proposed as shown Fig.1. This paper describes the proposed PCa methods and the seismic test to know their structural capacities.

2 SPECIMENS AND TEST

The parameters of this test were the new PCa methods, as shown in Fig.1. **(A)**: separated hoop is adopted in a panel zone, which was cast-in-situ, as a rational reinforcement. Rational reinforcement of panel is the separated hoop of the cast-in-situ panels. **(B):** sleeve joints are embedded in a panel zone. Longitudinal rebars of upper columns and lower columns were connected in the sleeve joints. **(C):** winding pipes are embedded in the panel zone. Bored sleeves in the panel formed by winding pipes. The longitudinal bars of the lower column go through the panel to the joint in the upper column. **(D):** PCa beam bar is jointed extending 0.5D from the column surface. Column is the full PCa. The beam bar is jointed using the mechanical joints in the beam hinge zone. 0.5D is used in **(D)** because it is a more rational length than 1.5D. However, if the beam bar joints are attached to or inserted into the column, the beam's bending strength is high, which would be contrary to the design philosophy. **(E):** the unified casting specimens are compared with the other PCa specimens. Twelve 1/2 (Series 1: 1/2.5) scaled

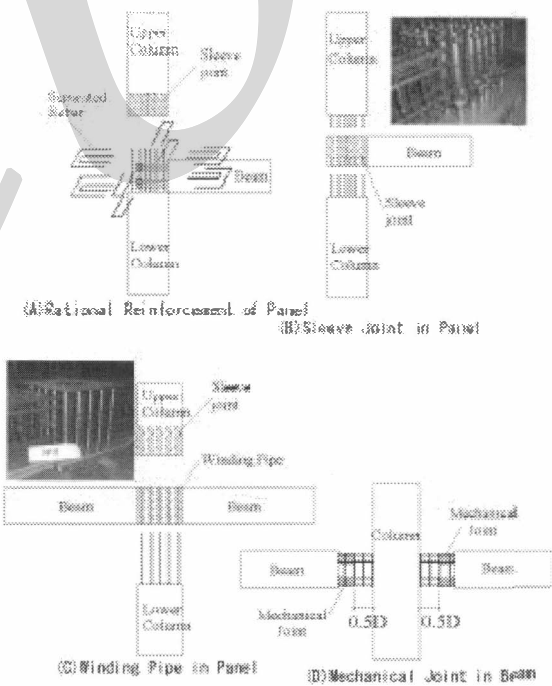

Fig.1 Precast Methods

Table 1 List of Specimens

	Specimen	Series	Failure Type	Joint or Bonding Method		Panel Transverse Rebar	PreCast	Scale
				Beam Rebar	Column Rebar	Type	Method	
	OND			PlateNut	Through	Cosed Welding	(E)Unified Casting	
Exterior	OPUD	1	Beam Yeild	PlateNut	Column Bottom (Upper Column)	Separated Rebar	(A)	1/2.5
	OPSD			PlateNut	Sleeve Joint(Panel)	Cosed Welding	(B)	
	ONS			PlateNut	Through	Cosed Welding	(E)Unified Casting	
	OPUS	2	Panel Sear Failure	PlateNut	Through	Separated Rebar	(A)	
	OPSS			PlateNut	Sleeve Joint(Panel)	Cosed Welding	(B)	
	IND			Through	Through	Cosed Welding	(E)Unified Casting	
Interior	IPHD	3	Beam Yeild	Mechanical	Through	Cosed Welding	(D)	1/2
	IPWD			Through	Winding Pipe(Panel) +Sleeve Joint(Column Bottom)	Cosed Welding	(C)	
	INS			Through	Through	Cosed Welding	(E)Unified Casting	
	IPSS	4	Panel Sear Failure	Through	Sleeve Joint(Panel)	Cosed Welding	(B)	
	IPWS			Through	Winding Pipe(Panel) +Sleeve Joint(Column Bottom)	Cosed Welding	(C)	

specimens were tested, as listed in Table 1. Six were for the exterior frames and six were for the interior frames. The experiments were divided into 4 Series as the failure modes and exterior or interior frames. Each series tested 3 specimens. Series 1 comprised the exterior frames, which were designed to reach flexural beam yield before panel shear failure. Series 2 comprised the exterior frames, which were designed to reach panel shear failure before beam yield. Series 3 comprised the interior frame of the beam yield type, and series 4 comprised the interior frames of the panel shear failure type.

Earthquake-type reversed cyclic lateral loads were applied at the beam ends.

Series 1,2 are exterior frames that the axial forces were linked with lateral forces. In Series 1, the variable axial force ranged from 0.75 tNu (tNu: ACI's maximum tensile axial force of column) to 0.7 cNu (cNu: ACI's maximum compressive axial force of column). It is one of characteristics of this paper that exterior specimens were applied the high axial load.

From the test results, the proposed PCa had roughly the same relationship between load and displacement compared with a unified casting frame. The bending capacities of beam and the shear capacities of panel are all the same between the proposed PCa and a unified casting frame. It was confirmed that the previous method for calculating the panel's shear strength and the beam yield strength could be applied to these PCa frames. However, the panel's shear strength with separated hoop couldn't work under high displacement region, when shear cracks were wide.

3 CONCLUSIONS

Through these tests and discussions, the following conclusions were obtained:

1) All new PCa frames had good structural capacities compared with a unified casting frame. The strength and ductility of the PCa frames were equivalent to or exceeded those of the unified casting frame.
2) Exterior frames under high variable axial force were investigated to determine their cracking strength, maximum strength and ductility. The exterior frame's behavior under severe earthquakes load can be predicted. However, the separated hoops in the panel didn't work when shear cracks became wider.
3) The connection between PCa members didn't slip under high tensile axial force. Its behavior was like that of the unified casting frame.
4) No shear cracks occurred in the panels under 0.7cNu, high compressive axial force. If the calculated crack strength exceeded the maximum strength, the present panel calculation method couldn't apply. This is a theme for the future.
5) The calculated skeleton curves for the interior and exterior frames corresponded well with the test result. They can thus be applied to practical structural design.

THREE-DIMENSIONAL EARTHQUAKE RESPONSE ANALYSES OF RC STRUCTURES BY USING RESTORING FORCE MODEL BASED ON THE PLASTIC THEORY

Koshiro Nishimura Katsuki Takiguchi
Tokyo Institute of Technology, Japan

Keywords: R/C structure, plastic theory, restoring force model, three dimension

1 INTRODUCTION

In order to grasp response of R/C structure during strong earthquake, it is necessary to formulate restoring force characteristics properly. Modeling of multi-dimensional restoring force characteristics of R/C buildings and members based on the plastic theory has been tried. According to the past study [1], it can be said that this method is useful when you want to grasp behaviors of the structures under lateral two-dimensional earthquake excitation macroscopically. However, in case of three-dimensions, restoring force model based on the plastic theory that is adapted to R/C structures and members under cyclic loading cannot be achieved because it is difficult to describe behaviors of axial deformation on unloading that is headed to compressive side. In this paper, three-dimensional restoring force model of R/C structures is proposed that can describe the behavior on unloading. Then earthquake response analysis on one-mass-system with this restoring force model is carried out to examine effects of consideration of axial direction in modeling and input of ground motion of axial direction to the system.

2 RESTORING FORCE MODEL

The restoring force model for RC structure described in this paper has characteristics of flexural-failure. Feature of the restoring force model in this paper is that the model has three -dimensional part, and two-dimensional part and results of calculation are translated to each other, as shown in Fig.1.

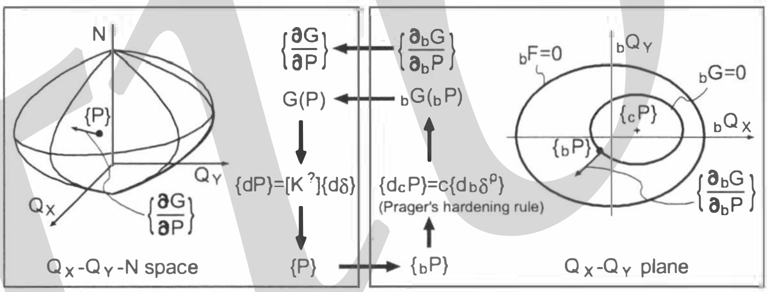

Fig.1 Flow chart of analysis

Yield surface in Q_X-Q_Y-N space, and uni-axial restoring force characteristics of each of two axes, X-axis and Y-axis, is supposed. Relationship between {dP} and {dδ} is formulated by using analogy to the plastic theory on each of four states, which are elastic, elastic and hardening-plastic, elastic and perfectly- plastic, and elastic and hardening-plastic and perfectly-plastic states.

Yield surface and cracking surface is supposed on $_bQ_X$-$_bQ_Y$ plane. The yield surface means perfectly-plastic and cracking surface makes work hardening according to Prager's hardening rule [2].

3 ANALYSIS

In order to confirm appropriateness of the restoring force model, numerical result and static test result of R/C column specimen are compared, as shown in Fig.2.

Earthquake responses of R/C structure are examined by using one-mass-system. Three earthquake accelerograms that is Kobe 1995, Taft 1952, and El Centro 1940 are employed. Three cases of response analyses are carried out to examine effect of consideration of axial direction in modeling and input of axial directional ground motion. Fig.3 shows results of each three cases on each three earthquakes.

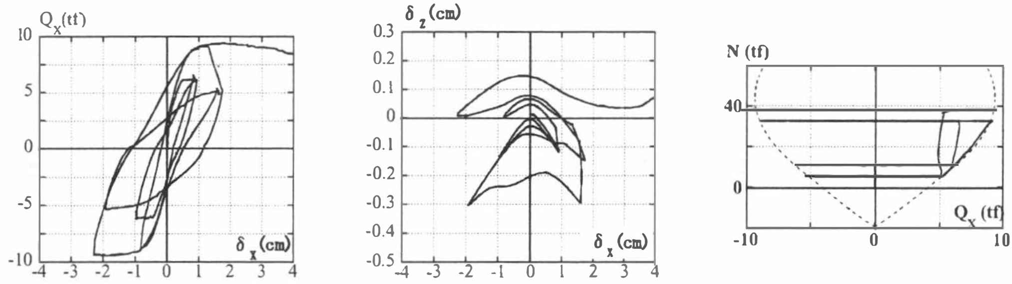

Test result of CBS-V-3-99

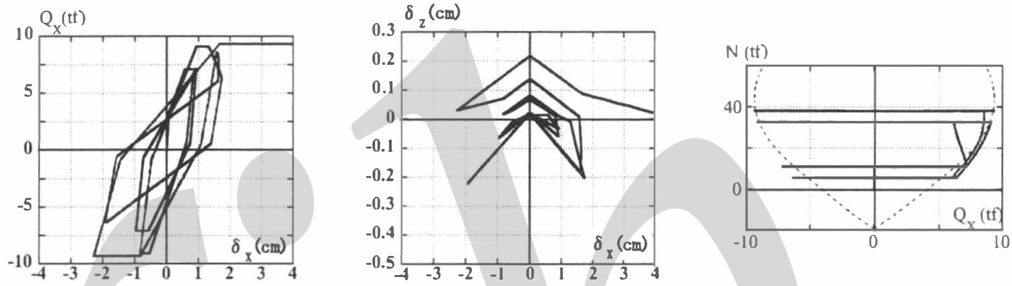

Numerical result

Fig.2 Comparison between test and numerical results

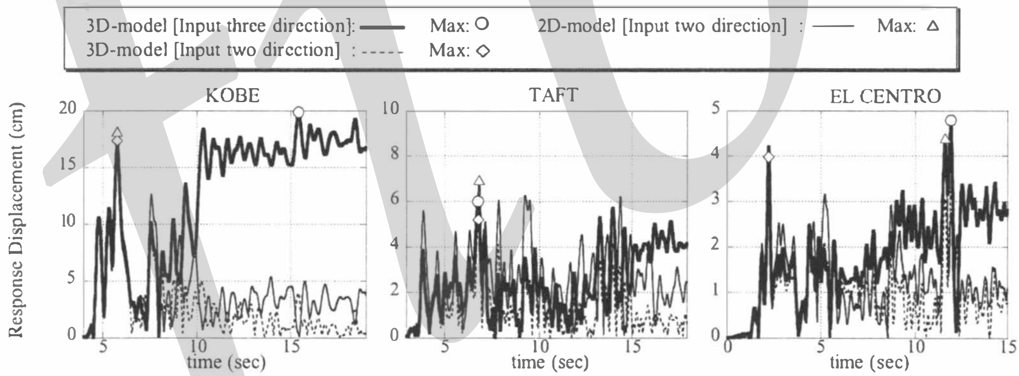

Fig.3 Results of earthquake response analysis

4 CONCLUSION

Three-dimensional restoring force model of R/C structures that can describe behavior of axial deformation on unloading that is headed to compressive side was proposed by using analogy to the plastic theory in this paper. It was confirmed that the model could describe behavior of static test result macroscopically. As a result of dynamic response analysis with the restoring force model, it can be said that to consider effect of axial direction in modeling of restoring force characteristics and to input ground motion of axial direction hardly cause a difference of maximum response displacement in this study.

REFERENCES

[1] H. Takizawa and H. Aoyama: Biaxial Effects in Modeling Earthquake Response of R/C Structures, Earthquake Engineering and Structure Dynamics, Vol.4, pp.523-552, 1976
[2] W.F. Chen, "*Constitutive Equations for Engineering Materials*", Vol.2, Elsevier Science Ltd., 1994

ISSUES ON THE SEISMIC DESIGN OF DUAL STRUCTURAL SYSTEMS IN REINFORCED CONCRETE BUILDINGS

Mario E. Rodriguez John J. Blandon
National University of Mexico, Mexico City, MEXICO

Keywords: Seismic response, dual system, seismic damage, reinforced concrete buildings

1 INTRODUCTION

A dual structural system in RC buildings is the combination of two different concrete structural systems, one being frames and the other structural walls. This type of structural system offers an effective solution for controlling damage during earthquakes. When compared with frame structural systems, a dual system leads to lower lateral displacement demands and consequently lower damage during earthquakes. However, in spite of this appealing feature of dual systems, designers have no specific tools for a rational evaluation of the demand and capacity of lateral displacements in this type of structural systems subjected to earthquakes. This is due to the fact that current design procedures in seismic engineering follow a strength-based approach. Furthermore, since these procedures are based on elastic analyses of structures, results using these procedures might be misleading since it is relevant considering important features of the system in the inelastic range. Among these features compatibility of the frames and walls needs to be considered. In addition, for an adequate evaluation of the expected global ductility capacity of the system, it is necessary to perform a rational evaluation of yield displacements in both frames and structural walls.

This paper evaluates main characteristics of the seismic response of a dual system aimed at developing design recommendations for this system. The evaluation is conducted based on the observed response of a two-story, half scale precast concrete building built with a dual system, which was subjected to simulated seismic loading in a laboratory in Mexico.

2 SIMULATED SEISMIC LOAD TESTS ON A TWO-STORY, HALF SCALE BUILDING BUILT WITH A DUAL SYSTEM

2. 1 Characteristics of the test specimen

The test specimen studied in this research represented at half scale a two-story precast concrete parking structure located in the highest seismic risk zone in Mexico City and designed according to the current Mexico City Building Code [1]. Fig 1 shows typical details of the test specimen, which employed precast frames and cast-in-place structural walls as lateral load resisting system.

2.2 Lateral load testing and observed behavior of the specimen

The specimen was subjected to reverse cyclic lateral loading in the direction shown in Fig 1. Hydraulic actuators applied lateral loads at each level of the specimen and the ratio of the lateral force at the second level (F_2) to that of the first level (F_1) was held constant throughout the test and equal to 2.0. A detailed description of both the lateral loading history and the observed behavior of the specimen is given elsewhere, Rodriguez et al. [2].

3 DESIGN IMPLICATIONS FOR DUAL SYSTEMS FOUND FROM ANALYTICAL AND EXPERIMENTAL RESULTS FOUND IN THIS RESEARCH

The evaluation of the seismic response of dual systems conducted here using both an analytical model and a specimen tested in laboratory indicates the importance of structural walls' participation for controlling lateral displacement demands during earthquakes. The evaluation also showed that the dual system could be designed using a Performance Based Design approach, in which designers could select the levels of walls' participation in the structural response in such a way that this participation is related to an expected building damage for a selected ground motion. In addition, this evaluation emphasizes that in dual systems, it is necessary to take into consideration the compatibility of lateral deformations of frames and walls not only in the elastic range of the building's response but also in the inelastic range of the response.

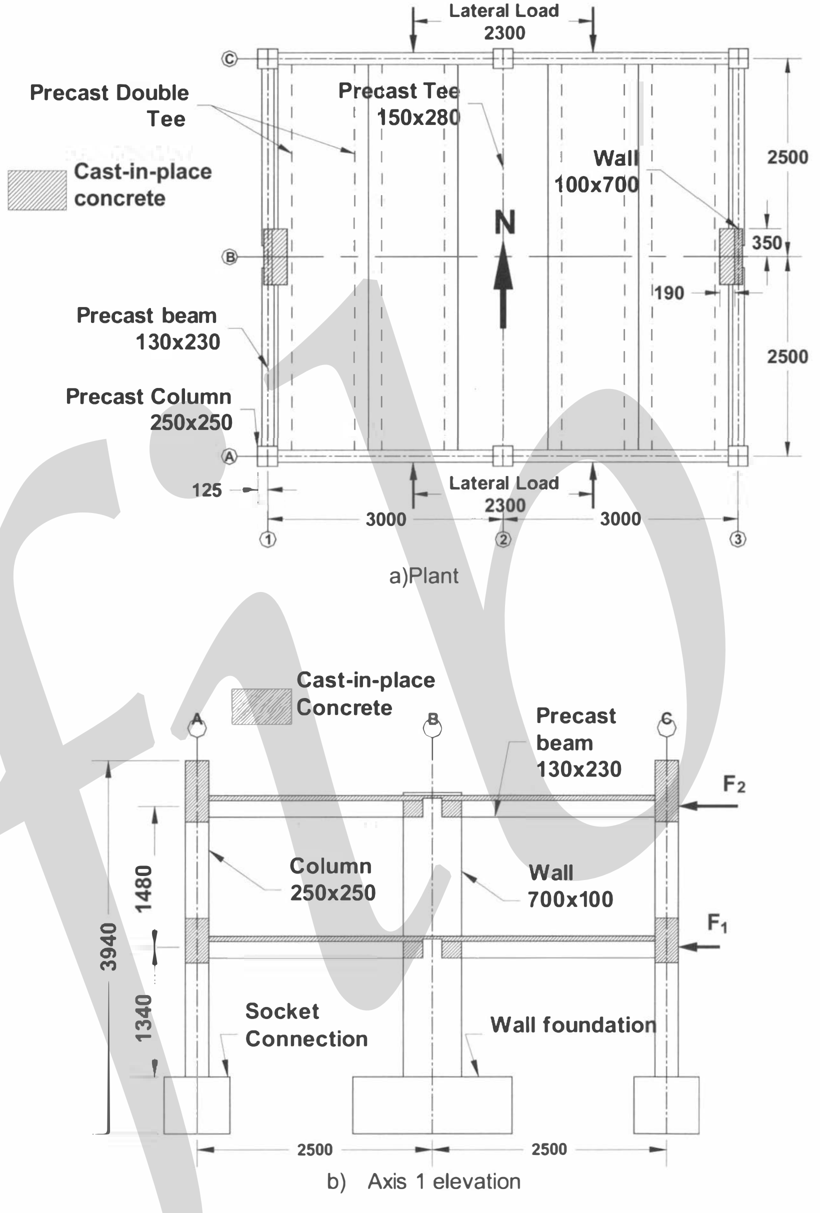

Fig 1 Plant and elevation of a test specimen with a dual system (dimensions in mm)

REFERENCES

[1] Mexico City Building Code, "Reglamento de Construcciones para el Distrito Federal, Diario Oficial", Mexico City, 1993.

[2] Rodriguez, M., and Blandón, J. J., "Seismic Design of Precast Concrete Buildings and Seismic Load Tests of a Two-story Precast Concrete Building" (in Spanish). Serie Azul Report Instituto de Ingenieria, Universidad Nacional Autonoma de Mexico, Mexico, 2002.

BEHAVIOUR OF CONCRETE FILLED HOLLOW STRUCTURAL SECTION BEAM COLUMNS TO SEISMIC SHEAR DISPLACEMENTS

N.J.Gardner
University of Ottawa, Canada.

M.S.Hardika
Udayana University, Bali, Indonesia

Keywords: Concrete, hollow structural section, beam-column, seismic, ductility

1 INTRODUCTION

Describes an extensive experimental program to study the seismic resistance of concrete filled square steel HSS columns, using both normal strength (40 MPa) and high-strength concrete (100 MPa). Twenty-four, concrete filled, 203 mm square, steel hollow structural section (CFSSHSS), beam-column specimens were tested under constant axial compressive load and cyclic horizontal displacement. The lines of action of the horizontal displacements were either square, normal to a conventional axis, or across a diagonal. The experimental investigation included determination of strength capacity, ductility, and flexural stiffness of CFT beam-columns for CSA Class 1 compact (B/t = 21) and Class 4 slender (B/t = 43) HSS sections. Fig.1 shows a column set up for testing. Fig.2 shows the schedule of applied shear displacements. Figs. 3 and 4 show the responses of a square and diagonally loaded specimen respectively.

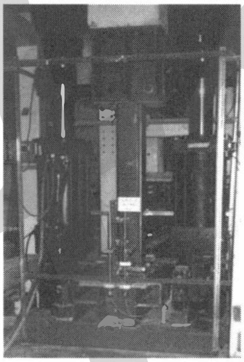

Fig.1 View of Test setup

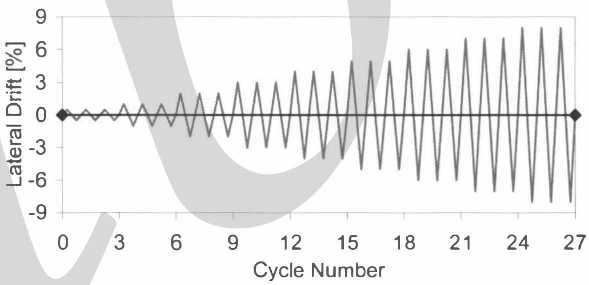

Fig.2 Schedule of applied shear displacements

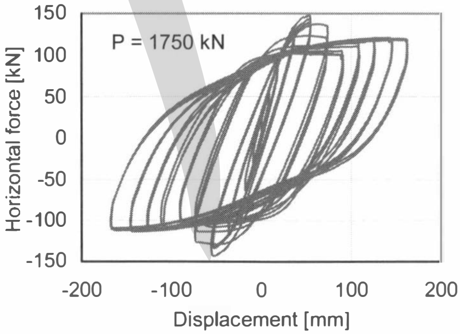

Fig.3 Lateral load v displacement of square section column (SCH-3).

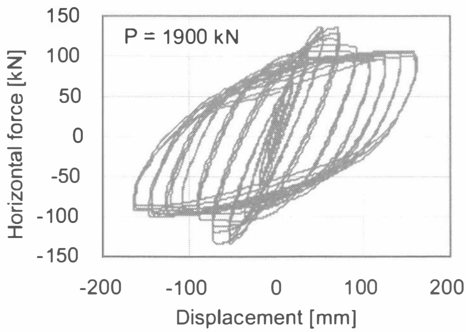

Fig.4 Lateral load v displacement of diagonal section column (DCH-3).

2 PARAMETERS FOR SECTION ANALYSIS

The strength may be calculated using conventional section analysis. The Eurocode 4 rectangular stress block is adopted instead of an assumed stress-strain relationship. In this case, the ultimate stress is α_1 f_{cm}, where α_1 depends on the concrete strength, and the stress block is the full distance from the surface in compression to the neutral axis. The neutral axis is determined from equilibrium. Conventional section analysis of traditional reinforced concrete columns uses $\alpha_1 f_{cm}$ as the concrete strength in the equivalent rectangular stress distribution. However for CFT columns, subjected to axial compressive load and cyclic bending moment, the $\alpha_1 f_{cm}$ can be modified to $\alpha_1\alpha_2\alpha_3 f_{cm}$.

The parameter α_1 maybe summarized mathematically in the following expression

$$\alpha_1 = 1.09 - 0.0025\, f_{cm} \qquad 0.8 \leq \alpha_1 \leq 1.0$$

The parameter α_2 accommodates the effectiveness of the confinement by the steel tube. For Class 1 HSS CFT columns, the wall thickness is appropriate to confine the concrete. Conversely, for Class 4 HSS CFT columns, the wall thickness is not sufficient to significantly confine the concrete.

$$\alpha_2 = 1 - \left(\frac{B}{20t} - 1\right)\left(\frac{P}{3P_o}\right)$$

However, $\alpha_1\alpha_2 \geq 0.8$

Previous investigations have showed that concrete has slightly different behaviour when subjected to the high rates of loading typical of seismic loading. The concrete cylinder strength is increased by 10% for CFT columns subjected to combined axial compressive load and seismic bending moment. ie α_3 = 1.1 for seismic response and α_3 = 1.0 for conventional design.

Figs. 5 and 6 compare the experimental results and predictions as non-dimensional interaction diagrams for square and diagonally loaded CFT beam columns respectively. It must be noted that all the beam columns maintained shear displacements greater than 7% of column height.

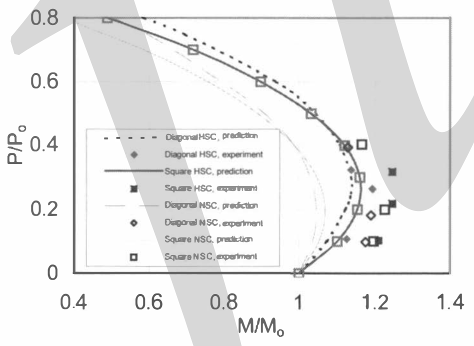

Fig.5 Interaction diagram for Class 1 sections

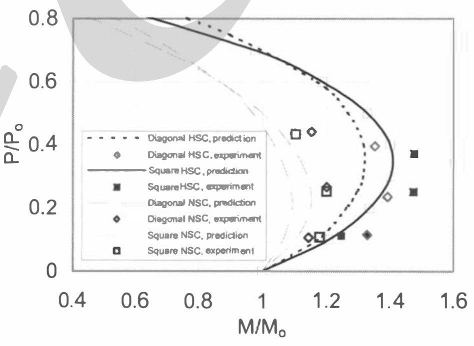

Fig.6 Interaction diagram for Class 4 sections

3 CONCLUSIONS

Tests showed that thin wall and thick wall CFT columns, with either normal strength or high strength concrete, behave in a ductile manner and can sustain drift ratios of 7% with minimum strength degradation. Consequently CFT beam columns are appropriate for structural columns in seismic regions regardless of section wall thickness or strength of concrete.

The modified section analysis proposed to predict the seismic strength capacity of CFSSHSS columns subjected to combined axial compressive load and uniaxial or diagonal bending moment shows good agreement to the test results.

SHEAR CAPACITY OF DUCTILE WALL WITH HIGH PERFORMANCE FIBER REINFORCED CEMENT COMPOSITE

Satoru Nagai Tetushi Kanda Makoto Maruta Takashi Miyashita
Kajima Technical Research Institute IT Solution Department
Kajima Corporation, JAPAN

Keywords: High Performance Fiber Cement Composite, Shear Wall, Ultimate Shear Strength

1 INTRODUCTION

High performance fiber reinforced cement composite (HPFRCC) has recently been developed. Compared to Normal Concrete (NC), this material has some different material characteristics such as strain hardening and multiple cracking under uniaxial tensile stress. As shown in Fig.1, these characteristics are expected to improve reinforced concrete member capacities under earthquakes. The authors have been developing a kind of Engineered Cementitious Composites (ECC) for inclusion in HPFRCC. ECC incorporating Poly Vinyl Alcohol fibers (PVA-ECC) is expected to achieve high seismic resistant performance [1]. To clarify this problem, structural tests on PVA-ECC walls and FEM analysis have been conducted, and these are discussed in this paper.

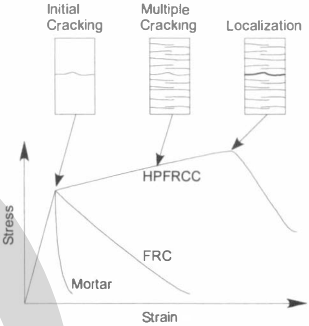

Fig.1 Tensile Stress-Strain of HPFRCC

2 OUTLINE OF EXPERIMENT

The specimens comprised a PVA-ECC wall, columns, a top slab and a base mat of NC as shown in Fig.2. The walls and both side columns were 1100mm high, the loading point was 1300mm from the bottom of the wall and the shear span to depth ratio was 0.58. Three specimens were designed to fail in shear before bending failure. The parameters of this test were wall reinforcement ratio from 0.21% to 0.64%, wall thickness of 50mm or 75mm and method of anchoring wall reinforcement. PVA-ECC incorporates two percent by volume of PVA fibers (0.04 mm diameter, 12 mm long). Maximum aggregate diameter for NC was 10 mm. Cantilever type reversed cyclic loading was applied to the top slab under constant axial load of 900 kN.

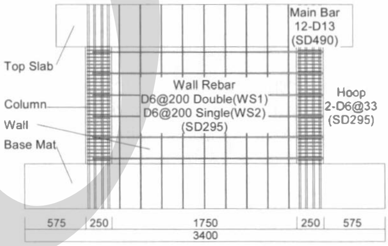

Fig.2 Detail of Walls

3 RESULTS OF EXPERIMENTAL

Fig.3 shows the relationships between shear force and rotation angle R. The calculated flexural and ultimate shear strengths were calculated using a equation for the ultimate flexural strength [2] and the shear strength equation shown in the Architectural Institute of Japan [3]. All specimens were judged to have failed in shear, because the shear force dropped gradually after shear crack expansions with yielding of lateral wall reinforcement. The inclination of the expanded shear crack was about 45 degrees. The maximum strengths of all specimens were from 1.15 to 1.2 times bigger than the calculated ultimate shear strengths.

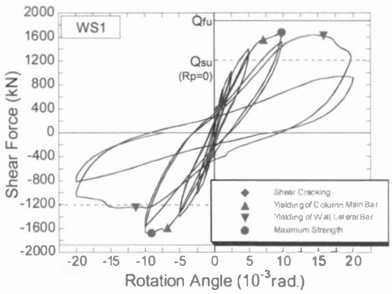

Fig. 3 Shear Force-Rotation angle

Fig.4 shows the cracking patterns of WS1 after the test. Fig.5 represents the maximum shear crack width at peaks of each cycle and the maximum residual shear crack width at unloading. Though numerous cracks were observed, the maximum shear crack width was about 1 mm and the maximum residual shear crack width was less than 0.2 mm

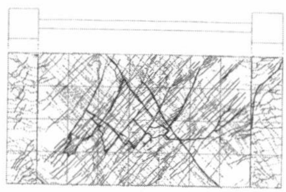

Fig.4 Cracking Pattern

before maximum strength. Application of PVA-ECC resulted in numerous fine cracks in the structural element under loading, and the maximum residual shear crack width was small.

4 DISCUSSION OF TEST RESULTS

4.1 Estimation of Ultimate Shear Strength

To take into account the effects of PVA-ECC, an equation was suggested in this paper. According to the aforementioned investigation, two kind of the tensile strength of PVA-ECC were assumed. As a result, a predicted strength agrees with the experimental maximum strength.

4.2 FEM Analysis

To grasp the shear behavior of walls with PVA-ECC, three types of monotonic parametric analyses using FEM were conducted. Because the elastic-plastic characteristics and the effective compressive strength weren't clarified, some material characteristics of PVA-ECC were assumed. Parameters were stress-strain characteristics in compression and in tension of PVA-ECC.

Fig.7 shows the envelope curves of the experimental and analytical shear force – rotation angle relationships for WS2. The maximum strength obtained from FEM analysis depended mainly on the assumed effective strength of PVA-ECC. In addition, the behavior in the assumed descent region after the maximum strength of PVA-ECC affected mainly the structural behavior of the wall after maximum strength. On the other hand, the experimental and analytical initial stiffness showed good agreement for both specimens. The analytical maximum strengths were slightly bigger than the experimental values. Additionally, the analytical rotation angle up to the maximum strength of WS2 approximately corresponded to the experimental rotation.

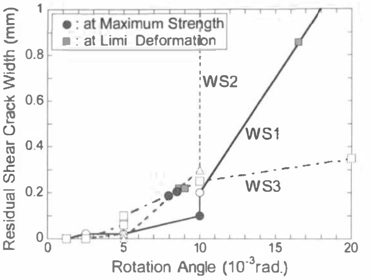

Fig.5 Residual Shear Crack Width - Rotation Angle Relationship

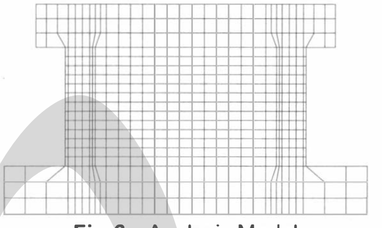

Fig.6 Analysis Model

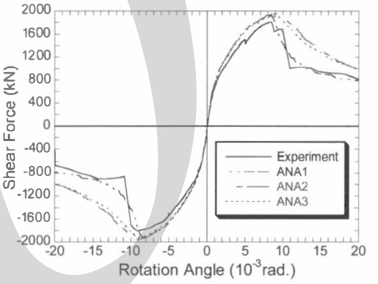

Fig.7 Envelope Curves of the Experiment and the Analyses

5 CONCLUSION

A structural experiment and FEM analyses were conducted on reinforced walls using PVA-ECC. The results obtained from this study as follows:

(1) Walls using PVA-ECC instead of NC had improved ultimate shear strength.
(2) While numerous fine cracks were obtained in walls using PVA-ECC, the width of the maximum shear crack was small and shear crack almost closed after loading.
(3) The modified equation for estimating maximum shear strength for walls using PVA-ECC can predict the maximum shear strength.
(4) FEM analysis can simulate the initial test stiffness, but the maximum shear strength is slightly bigger. The analytical behavior after maximum strength does not corresponded to the test behavior. This is a future theme for a deeper study of PVA-ECC. To clarify the effective strength of RVA-ECC is a most significant issue.

REFERENCES

[1] Kanda, T. : Material design technology for high performance fiber reinforced cementitious composite, JCI Concrete Journal, Vol.38, No.6, pp.9-16, Jun., 2000 (in Japanese)
[2] Hirosawa, M. : Experimental data and its analysis regarding reinforced concrete shear walls in the past, BRI report, No.6, pp.42, March 1975 (in Japanese)
[3] Architectural Institute of Japan : Design guideline for earthquake resistant reinforced concrete buildings based on inelastic displacement concept, 1999 (in Japanese)

THE HORIZONTAL FORCE DISTRIBUTIONS FOR EARTHQUAKE RESPONSES OF REINFORCED CONCRETE UNIFORM FRAMES IN CONSIDERATION OF THE STRUCTURAL DISTRIBUTIONS ALONG THE HEIGHTS

Seiichi Katoh
Oriental Construction Corporation
JAPAN

Toshiharu Arakawa
Department of Architecture,
School of Science and Technology, Meiji Univ.
JAPAN

Keywords: Uniform Frame, Earthquake Response, Elasto-plastic Analysis, Horizontal Force Distribution, Ratio of Stiffness and Weight

1 INTRODUCTION

This paper examines the elastic and the elasto-plastic earthquake response characteristics of reinforced concrete uniform frames with the unbalanced distributions of weight, stiffness, ratio of stiffness and weight along the heights. Those frames are designed using guidelines based on ultimate strength concept and are analyzed on the eigenvalue characteristics. It is additionally discussed the relation of responses and codes for horizontal force distributions. Those codes are based on Ai distribution in Japanese Structural Design Code and on CEB-FIP Model Code 1980. Analytical parameters are 1) varied story and varied amount of structural characteristics, 2) story number of frames, 3) kind and level of input waves.

2 ANALYTICAL MODELS AND INPUT WAVES

Analytical Models are reinforced concrete uniform frames that the story numbers are 5, 10 and 15. Those frames shown in Fig.1 are designed using guidelines based on ultimate strength concept. The natural periods and the lateral load capacities (C_B) of those frames are shown (one span frame model) in Table 1. Input waves used in earthquake response analyses are El Centro 1940 NS (Elce), Hachinohe Harbors 1968 NS (Hach) and Tohoku University 1978 NS (Toho). The response spectra of acceleration on the input waves are shown in Fig.2.

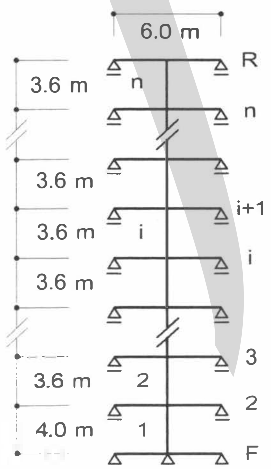

Fig.1 One Span Frame Model

Table 1 Natural Periods [sec] and Lateral Load Capacities

Model	1st Mode	2nd Mode	3rd Mode	C_B
5 Stories	0.444	0.154	0.085	0.37
10 Stories	0.814	0.283	0.167	0.30
15 Stories	1.047	0.381	0.229	0.26

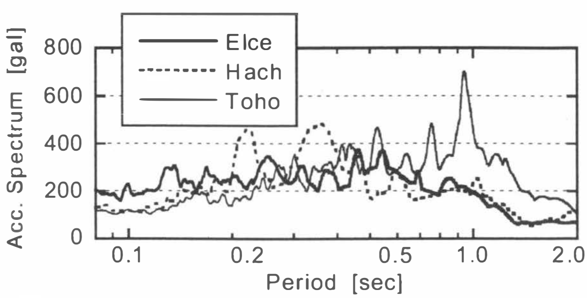

Fig.2 Response Spectra of Acceleration on the Input Waves

3 STRUCTURAL DISTRIBUTIONS ALONG THE HEIGHTS

The parameters for structural distributions along the heights are the weight (Weight Models), the stiffness (Stiffness Models) and the ratio of stiffness and weight (KW Models). As the KW Models are set up, 5, 10 and 15 stories models are respectively divided into five units. The examples of each model are shown in Fig.3.

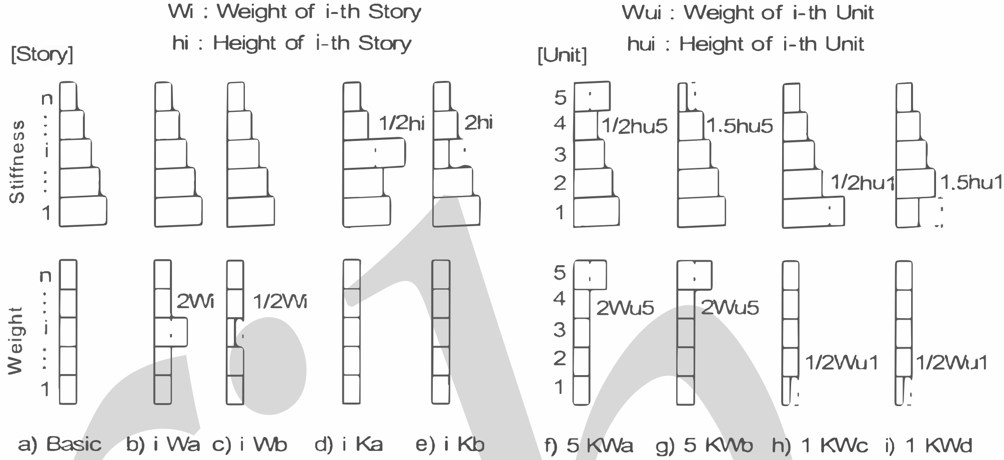

Fig.3 Examples of Weight Models, Stiffness Models and KW Models

4 EARTHQUAKE RESPONSE AND STRUCTURAL DESIGN CODES

The relations of earthquake responses and structural codes, which are based on Ai distribution (Ai distri.) and CEB-FIP, for the horizontal force distributions normalized by the base shear force are shown in Fig.4 restricted to 3KWa. In Fig.4, the vertical axes are shown by the ratio (NH_i) of the height up to i-th story and the frame height.

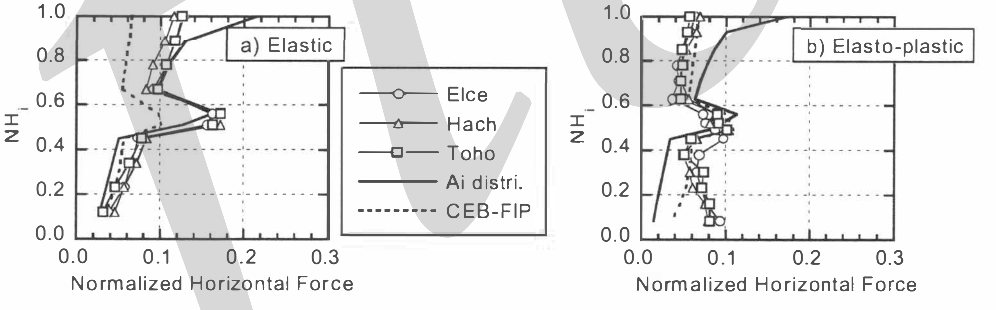

Fig.4 Responses and codes for Normalized Horizontal Force Distributions (3KWa)

5 CONCLUSIONS

1) As the weight on the story of the loop and the stiffness on the story of the node for the modes of the frames were varied, the natural periods of the frames were obviously changed.
2) On the frames with the unbalanced structural distributions along the heights, the inter-story displacements were affected by the stiffness distributions and the horizontal forces were influenced by the weight distributions, even if those frames were varied the ratio of stiffness and weight.
3) The change of the horizontal forces could be roughly represented by both codes of Ai distribution and CEB-FIP. On the normalized horizontal force distributions, those distributions based on Ai distribution appraised accurately the distributions of the elastic responses and those distributions based on CEB-FIP appraised accurately the distributions of the elasto-plastic responses.

Volume 1	**Plenary papers, Primary papers, Condensed papers(1)**
Volume 2	**Condensed papers(2)**
Volume 3～8	**Keynote papers, Contributed papers**